USMCA 2009

(SEIKEN SYMPOSIUM 57)

8th International Symposium on

NEW TECHNOLOGIES FOR URBAN SAFETY OF MEGA CITIES IN ASIA

October 15-16, 2009
Incheon, Korea

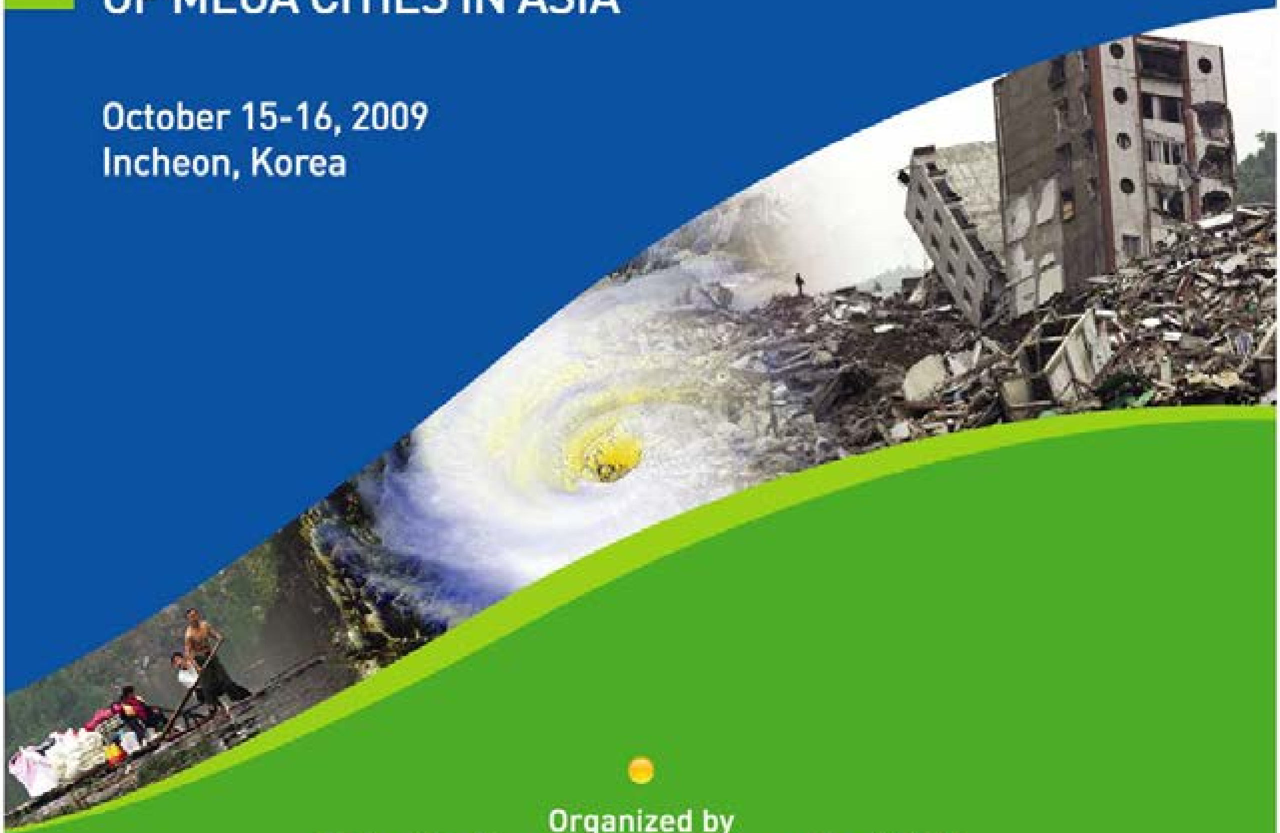

Organized by

National Institute for Disaster Prevention (NIDP),
Seoul, Korea

Korea Disaster Prevention Association (KDPA),
Seoul, Korea

International Center for Urban Safety Engineering (ICUS),
Institute of Industrial Science (IIS),
The University of Tokyo, Japan

Sponsored by

Incheon Metropolitan City Government,
Incheon, Korea

The Foundation for the Promotion of Industrial Science,
Japan

At

Ramada Songdo Hotel, Incheon, Korea

CONTENTS

OPENING SESSION:

CLOSING SESSION:

PARALLEL SESSION 1:

PARALLEL SESSION 2:

PARALLEL SESSION 3:

PARALLEL SESSION 4:

PARALLEL SESSION 5:

PARALLEL SESSION 8:

PARALLEL SESSION 9:

PARALLEL SESSION 10:

PARALLEL SESSION 11:

PARALLEL SESSION 12:

OPENING SESSION

ADVANCED DISASTER MANAGEMENT BASED ON GREEN GROWTH PARADIGM IN KOREA

Park, Yeon-Soo
Vice Administrator
National Emergency Management Agency

ABSTRACT

Global warming changes in rainfall patterns, a rise in sea level, and a wide range of impacts on plants, wildlife which effects on the typhoon, the torrential rain, and the drought expecting to be continuing in the future with ever-increasing size and scope. These changes make the natural and human-made disasters caused by combined effects of the aging society and changing social structure which poses an unprecedented level of destruction and damage. Also, there is a great need for national safety management system on the epoch-making improvement of scientific disaster management which appears new types of disasters through the exchange of traditional disaster environment and responds actively to the rapid exchange of social environment based on u-IT. To reduce the green gas and achieve sustainable economic growth by developing low-carbon, eco-friendly industries, the Korean government makes a plan a "green growth" as a platform of river refurbishment project, in which four rivers will be upgraded. The plans are for creating green belts, surrounding four main rivers in Korea with trees and bicycle paths. The project to develop the Han, Nakdong, Geum and Yeongsan Rivers flowing through the country's major urban, industrial and farming areas and to reduce the damages from flood related disasters around the rivers. The new paradigm is needed to manage the damages regarding on the global warming or climate changes. The new advanced disaster management based on green growth paradigm developed in this study provides the systematical information sharing networking system and sharing real-time monitoring and simulating data amongst government, local authorities and related organizations under both safety management in normal times and circumstance management in disaster times. In this study, the establishment of national safety strategy is also reported to strengthen the functions such as prevention and preparation of disasters.

1. INTRODUCTION

Recently, localized heavy rain, typhoons have been increasing and intensity of them also increasing owing to climate change in the world. Korea had major disasters for ten years such as flood on north part of Kyunggi-Do in 1998 and 1999, Typhoon Saomai in 2001, Typhoon Rusa in

2002, Typhoon Maemi in 2003, heavy rain on Kangwon-Do in 2006, Typhoon Nari in 2007 and heavy rain on Bonghwa, Kyungbook in 2008 which disasters placed within the top ten made flood related damages almost every year in recent.

IPCC reported on the 4th report that disasters regarding on extreme events such as heat wave, drought and flood will be increased at the near future. In the case of flood, increased intensity and frequency can be made large scaled damages at any time. Thus it is needed for reducing flood related damages to prepare the disasters. However, changing of society structures such as old-aged, information-oriented, urbanization and globalized society changed life pattern which made centralization of population and infra structure in the urban area and also increased possibility of disasters. Thus, the central government derives a policy to reduce the damages regarding on these natural and changed society structure based disasters and make a long term roadmap for master plan to prepare and reduce the damages regarding on extreme events.

In this study, concept of green disaster management was defined from reviewing and analyzing of the factors to lead to disasters and advanced disaster prevention and preparedness based on the green growth was also reported from analyzing on various countermeasures collected from various countries coping to climate changes.

2. GREEN GROWTH AND DISASTER MANAGEMENT

2.1 Concept of Green Growth

Now days, advanced countries concentrations their all effort to take a part a main role for leading market regarding on green growth. Although the concept of green growth is not defined but green growth is new paradigm to increase economics based on realizing the low carbon development and the green industry.

Here, low carbonized development means to realize the low carbon economy development route through the low carbonization process. The purpose of low carbon is the low carbon emission and advanced humanistic development. With the low carbonization process, the industrial and energy structures will be adjusted, which will affect the industrial employment structure and the regional employment structure to some extent. It should be noted that the low carbon development does not mean to restrict or eliminate the high carbon industry, but mean to eliminate the lag-behind production capacity, develop policies and methods for new technology, new energies, etc. and realize the dual objectives of sustainable development and handling of climate change.

Green industry means the industry which can promote the improvement of ecological environment, with low energy consumption, low pollution, high carbon efficiency and less rejects, such as Forestry. The low carbon industry is not certainly the green industry, such as the service for finance and insurance. Some environmentally friendly industries may be presented as the industries with high emission and high pollution in a certain period due to outdated technology; some industries can also become the green industry by improving the carbon efficiency and the low carbon technology, such as the resource recovery and processing industry

2.2 Concept of Green Disaster Management

The Green Growth undertaken in the Republic of Korea show that Green Growth can be a pioneering and concrete sustainable economic development model which approach is spurring creativity and innovation for green markets and investments through new policies for greening the industries and jobs.

The example of the policies undertaken in the Republic of Korea show that Green Growth can be a pioneering and concrete sustainable economic development model. Green Growth is also becoming the fundament for joint action between the UN agencies in the region, as advocated by ESCAP, to assist countries to build low carbon and climate change resilient societies.

For this Presidential Committee on Green Growth formed Green Growth Underwriting Project Team which team established five years load map for low carbon and greening the industries. There are three strategies and ten policies in this load map shown in Figure 1 where basic strategy plan for disaster management was included in the project of strengthen for the disaster management abilities.

Figure 1: Three strategies and ten policies developed by the Green Growth Underwriting Project Team

To follow up this national strategy of Republic of Korea, National Emergency Management Agency (NEMA) introduces the Green Disaster Management which means all activities to reduce or prevent the risks having influence on the human society without harm to the environment. Through the Green Disaster Management, we reduce the risks of the disasters increasing by growth oriented development and establish the base for coexistence and harmony between human and nature on the all phages of disaster management such as the prevention, the preparedness, the response and the recovery.

For successful of the Green Disaster Management, the establishment of foundations such as database and technology for the Green Disaster Management is needed at the first stage. Namely, the database and the technologies for estimating size and aspects of the disasters and minimize the damages from disasters such as typhoon, drought, flood and flash flood are needed to manage disasters. Furthermore establishment of eco-friendly countermeasures for disasters are also needed.

Accordingly, it is needed to develop the environmental friendly technology for construction to prevent disasters or restoration technology to recover from disasters. Low carbonization technology and enhanced management technology are needed to take a part on the national effort to reduce greenhouse gases and secure safe and green industries through the extending of research and development support and supporting on the green growth. These policies can make a green disaster management.

3. CHANGE OF RISK FACTORS DUE TO CLIMATE CHANGE

Now days, disaster events have been increasing and this trend is surprisingly increased from later half of 1990s. Especially, various risks created from artificial urbanization, destruction of the environment, estate development make a increasing of vulnerabilities due to floods, landslide and inundation on the sea side and also change a risk pattern as follows:

First, frequency and intensity of extreme events such as cold wave, hot wave, typhoon, floods and drought will be increased. In the case of Korea, rainy days was decreased but total amounts of rainfall and rainfall intensity were increased (National Metrological Institute, 2007)

Second, a new disaster appear or disaster size is bigger on some area because these areas are not undertaken the disaster before but are included in the overlapping area of climate change now. It is expected to more rain on Korea but more dry on China which no rain can make desertification on 2/3 of area of South Korea and yellow send. Because the yellow send from China make a big problems on spring season in Korea, it is needed countermeasures to manage new or bigger disasters due to climate changes.

Third, the vulnerabilities from risks due to sea surface level increasing and melting of ice is increasing. Recent, Tuvalu shown in Figure 2 on the Oceania has suffering from unsufficient drinking water form high salinity on the ground water and unsurfficient useful land from land contaminated by much salt due to high sea surface level. From 2002, the project to emigrate refugees from Tuvalu to New Zealand has been performing. However, 10,000 persons remaining on Tuvalu have insecurity to unexpected disasters.

Figure 2: Scene of Funafuti of Tuvalu' capital city and Nukufetau

4. COPING TO CLIMATE CHANGE AND COUNTERMEASURES FOR DISASTER MANAGEMENT ON FOREIGN COUNTRIES

Although, the policies for reducing on greenhouse gases are performing to cope with climate changes, a new strategies and policies are needed to reduce the damages expected continuous or increasing for a while. In this study, the strategy of USA to cope with climate changes and detailed sub framework of Japan to adapt on climate changes were collected and analyzed to derive the guideline for establishment of strategies on National Emergency Management Agency and other related organizations.

4.1 The Strategy to Cope with Climate Changes in USA

4.1.1 *Change Environmental Monitoring*

The policy makers have to understand the effects on climate changes specifically. Especially, monitoring on system for climate change and natural phenomenon is important to establish the adaptable strategies to cope with climate changes.

Thus, NEMA has to collect data for natural phenomenon from Ministry of Land, Transport and Maritime Affairs (MLTMA) to analysis of relationship between data and disasters and establish the organ an administrative structures to monitor and analyze the metrological data and data regarding on river system such as depth, discharges on the small and middle size river basin in which date are not collected from any organization.

4.1.2 *Analyze Reason of Vulnerability and Finding Countermeasures*

The policy makers can make a change and rise the effects with monitoring on public factors to restrict ability of local government to produce and cope with disasters and concrete coping policies.

Now, because economical indecency of local government and prevent oriented disaster management were not enough, NEMA has to establish the policies to analysis vulnerabilities of each local government and to lead coping policy of local government based on long-term plan. The basic law to drive these policies is the Total Countermeasures for Flood Related Disasters on the Law on Countermeasures for Natural Disasters and it is needed to establish a policy to develop long-term plan to define the vulnerabilities of risk and reduce the risk under local government area through this basic law.

4.1.3 *Prepare long-Term Countermeasures*

The effects on climate changes are should be considered to establish or decide for policy such as investment for infra-structures and economic intensive structures and land development, which have long-term effects on the disaster management.

Thus the construction code for waste and rainfall channels and rivers on urban areas considered future rainfall change aspects is should be considered and the research and development projects are should be developed to establish the concrete construction code.

4.1.4 *Prepare Countermeasures for Weak Point*

The weak point such as infra-structure, eco-system, industry and local government which these are sensitively changed by climate change and society structure changes are should be considered for top policy priority.

Especially, multi-purpose dams and rivers are should be recovered and reinforced for considering on climate change effects. NEMA has to develop the codes or guidelines to add on the rule of disaster assessment for urban plan and land use plan to cope with climate change on the small and middle size urban area.

The new model adapted on Korea is should be developed to determine or estimate the most dangerous area on each local government under low of the Total Countermeasures for Flood Related Disasters and master plan is also should be considered to develop the new model in phases.

4.1.5 *Form and Reinforce Community Network*

Strong relationship between confidential persons or companies is big property to cope with climate change for person or company. Strong readers inspire to the organizations at the hard time and well organized and trained persons spread information to the public persons for well adapting on climate changes.

Thus MEMA have to make effort to build well organized community network instead of government oriented disaster management. For this, NEMA organizes system or supports to revitalize the panel on countermeasures reducing disasters and the self control panel on disaster prevention.

4.1.6 *Use Resources and Capacity of Local Governments*

For development of countermeasures or method for coping method to climate changes, NEMA has to consider cooperation works with local universities and related companies which have professionalized knowledge and technologies.

The capacity of local government are divided by disasters management capacities of persons and local government in which system for education and public relation is necessary for teaching on importance of disaster management and raising disaster management capacities. Central government have to reinforcement relating laws and budget system to support local government to establishment disaster management system which system is not for waiting from central government but prevent and community based network oriented system.

Furthermore, because self disaster management of company is also important, NEMA study and organize system to revitalize the law for supporting on private companies.

4,2 The Strategy to Cope with Climate Changes in Japan

Since 1984 Japan has operating the panel on total policy investigation for countermeasures according to necessary for finding of basic solutions on flood related disasters which are formed by 13 experts working for university and institutes. This panel made basic paradigms and urgent action plans for disaster management and monitoring on results from management every year. The main enhanced paradigms and action plans are following as:

4.2.1 *Transform from Information Receiving to Information Sending*

To escape from disasters, it is needed to reproduce the information sending method and the information for escaping and reducing damages are supported with estimated and monitored information which information produced by system adapted on local area.

4.2.2 *Transform to Society Knowing Guideline for Disaster Management*

The persons and local government who didn't experience on any disasters should learn the possible various disasters and the manual for action.

4.2.3 *Operating the Utilities for Disaster Prevention*

Local government built managing system for disaster prevention and high level construction code to prevent disasters of natural disasters over design based on knowing of capacity for coping with disasters are weakening and urban structure are changing.

4.2.4 *Import New Improvement Technology*

Recent, because natural disasters over construction code and concentrated rainfall are being frequently it is needed to provide effective safety standard before the disasters. For this, the new improvement technology such as safety standard for land use and operating rules for utilities are needed.

4.2.5 *Strengthen Capacity for Disaster Management on Local Region*

To cope with society structure changes such as lower population, old ages, local society decline, urban structure changing, disaster prevention system to attend many related participants, disaster prevention activities to attend residents and wide supporting system are prepared to strengthen the capacity of local disaster management.

5. ESTABLISHMENT OF STRATEGY FOR THE GREEN DISASTER MANAGEMENT SYSTEM

As shown the above, establishment of green disasters management system is known as environmental friendly disaster management system to cope with climate change. These green disasters management system shares its context with recent disasters management paradigms focused on prevention in the disaster management phases.

After all, preliminary activities for minimizing damage, grasping of mechanism on disaster occurrence and development of prevention technologies are should be performed based on a scenario of climate changes, and the most important point in establishing green disaster management system is how to confront to meteorological disasters such as extreme flood having renewed recent records. This study suggested 8 driving assignments focusing on prevention, preparation, response and rehabilitation in disaster management phases for establishing green disasters management system shown in Fig. 3.

Figure 3 Specific Plan of the Green Growth

First, strengthening of early warning ability on the damages of storm and flood according to climate change is required for establishing preliminary prevention system on disasters, and simultaneously a resetting plan on disasters management standard with reasonable level responding to severe meteorological phenomena should be carried out.

Second, weakness factor on disasters according to climate change for propelling disaster prevention project vs. climate change shall be discovered, and then natural prevention project toward dangerous disaster district and small stream etc should be performed based on the results of weakness findings. Specially, water environment including water control should be created through management of small stream and maintenance project for considering ecological environment.

Third, strengthening of emergency rescue and relief system through establishing emergent response system on the vulnerable class should be executed for emergency response system and enhancement of emergency response ability, and establishment of responding system after resetting vulnerable class to climate change such as the aged population and city poor is required. Also, development of training model with national participation is needed and voluntary participation of citizens is induced so as to be spread widely through promoting consciousness on disasters. Specially, insurance should be activated promptly to prevent the disaster by self-help efforts on nature disaster which has been increasing rapidly according to climate change.

Finally, environmental project should be performed by developing construction material of environment and rehabilitation method which is harmonized with natural environment to transfer from function oriented recovery to make successful environmental recovery. Also, development of environmental rescue goods and management of relief materials should be executed.

Through structural and unstructured tasks explained before, the green disaster management could be a basement in making green safety nation where nature and human are coexisting by executing low-carbonate and environmental friendly prevention.

6. RESEARCH S FOR GREEN DISASTER MANAGEMENT

6.1 Forecasting system establishment on flash flood in preparing for climate change

Recent phenomena of abnormal climate is causing a lot of damages owing to severe rain storm, and many damages are occurring annually by Flash flood stemming from abrupt rain storm. Specially, the Flash flood causes a lot of personnel injury because the arrival time is too short and evacuation time is short, and thus forecasting system on the flood is very necessary. For this purpose, NIDP is developing a system to estimate flash flood effects from data receiving ultra-short term rainfall data by cooperation with National Institute of Meteorological Research. The system can respond to abrupt severe storms owing to meteorological extraordinary phenomenon.

6.2 Development on guideline for installation of reduction facilities

Recently, various cases experiments for rainfall-runoff phenomenon were performed to test inducing rainfall's penetration into the ground and its storage. NIDP is installing and managing experiment facilities for reducing rainfall runoff on laboratory located in Daejeon to develop installation standard on rainfall penetration and rainfall storage facilities for flood control.

Currently experiment on the footpath block with water permeability and permeable trench and endeavoring were performed to develop installation standard and to define the food control's effect in reduction facilities of rainfall runoff in case of designing flood-defense facilities for protecting city from penetration.

6.3 New technology for levee repair of small stream

In our country the repair rate rose to a considerable level through repair projects focusing on current national rivers, but relatively that of small streams is low, and thus a lot of damages from recent severe rain storm are occurring in the small streams. Specially, passive repair method for small streams is widely supplied and encouraged actually. In this regard, the NIDP applies passive sea defense method centering on areas having executed repair project for small streams, and intends to present a guideline on proper sea defense method in relation with water quality and flood control by monitoring.

6.4 Automated damage estimation system

Korea has performing damage estimation survey and then analysis for cause and damage amount before establishing rehabilitation plan. This analysis for cause of damages and damage amount are used for establishing rough rehabilitation plan, and for suggesting the improvement rehabilitation for coping with climate changes. Therefore, damage survey is one of most important factors for rehabilitating activities, because there are some problems to estimate damage amount because judging factor of survey's subject is effecting strongly. In this regarding, the NIDP developed a technology which can get subjective damage information from survey by utilizing spacing images on damaged areas. Especially, this image information can be used not only for damage survey but also for assistance to field situation in case of large damage afterwards along with research materials related to disasters.

7. CONCLUSION

This study reported a new disaster management system based on green growth policies. The study also defined the green disaster prevention system focused on necessities of establishment to countermeasures for disaster management for coexisting with nature along with responding efforts on climate change. Also, disaster management policies and systems of the United States and Japan to respond to extreme events in recent were analyzed, and then the detailed strategy for propelling green disaster prevention fit to Korea was suggested. Finally, the NEMA can take a main role in establishing green disaster management system, and further the green disaster management system will be a foundation for a safe country based on the green growth.

Even though many researches are progressing to cope with climate change, extreme events owing to climate change is become and natural disaster according to climate change is also occurring differently with past disasters with bigger size and stronger intensive such as floods of typhoon Nari at Jeju Island in 2007, heavy rain at Bongwha-Gun and North Gyeongsang Province at 2008. Thus it is needed to establish the positive countermeasure for disaster management system adapted in Korea.

German philosopher, Geothe said that positive activities is important such like applying knowledge to real problems and acting according to willingness, rather than our knowledge and intentions to do something. Thus, only positive responding for disasters regarding on climate change will give us safe society and economy at the future. Therefore, a fact that desirable future could be achieved through actions and practices of our generation should not be forgotten.

REFERENCES

Borga, M., Gaume, E., Martina, M. and Thielen, J., 2008. Realtime Guidance for

flash flood risk management, *FLOODsite Consortium*.
Hey, D., Kostel, J., MonTgomery, D., 2009. An Ecological Solution to the Flood Damage Problem.
Federal Emergency Management Agency, The Great Midwest Flood: Voices 10 Years Later, *FEMA Report*.

FRAMEWORK / MECHANISM OF INTERNATIONAL COOPERATION FOR DISASTER RISK REDUCTION AND JAPAN'S CONTRIBUTION

Yasuyoshi Ichihashi
Visiting Professor, ICUS, IIS, University of Tokyo, Japan
ysich555@iis.u-tokyo.ac.jp

ABSTRACT

In recent years, there has been increased international recognition that damages caused by disasters seriously interfere with "human security" by hindering development efforts and the accomplishment of "sustainable development." Furthermore, more recently, there is also growing alarm about global climate change and increasing disaster risks.

Japan, as one of the countries that suffered from frequent natural disasters including earthquakes, tsunamis, typhoons, volcanic eruptions, etc., has accumulated its own knowledge and culture to cope with large scale natural disasters, promoted scientific approaches and developed technologies in related areas. Japan has also developed its own domestic system of early warning and training, immediate rescues, and policies for reconstruction and long term development.

Against such background, Japan has been actively promoting, often by taking initiatives, international efforts to strengthen effective cooperation in the area of disaster risk reduction.

Central to the issue of setting up international framework and mechanism and securing a wide ranging international cooperation was the adoption of "Hyogo Framework for Action" (HFA) at the UN World Conference on Disaster Reduction held in 2005 in Kobe, Japan. Since then the HFA already became an international norm and standard document in the context of disaster risk reduction.

This paper briefly reviews the process and accomplishments so far in the setting up of framework and mechanism of international cooperation on disaster risk reduction, reviews also Japan's contribution in the same area, and calls for a renewed attention to integrate various efforts into a concerted international cooperation.

1. BRIEF REVIEW: SETTING UP OF FRAMEWORK AND MECHANISM OF INTERNATIONAL COOPERATION ON DISASTER REDUCTION

(1) To mitigate damages caused by disasters, it is necessary to coordinate pre-disaster measures and post-disaster efforts of emergency relief and

recovery/reconstruction. Traditionally, international cooperation during large scale disasters has been centered on humanitarian assistance either bilaterally between the governments, or through UN organizations and/or International Federation of Red Cross and Red Crescent Societies. Currently, UN Office for the Coordination of Humanitarian Affairs (OCHA) coordinates search and rescue activities in emergency situations. (The UNDRO, established in 1971 by the UN General Assembly resolution, was incorporated into the UN Department of Humanitarian Affairs (DHA) in 1992. This Department was reorganized into OCHA as part of Headquarter of the United Nations. One of OCHA offices is located in Kobe.) (http://ochaonline.un.org)

(2) On the other hand, pre-disaster measures have not necessarily been given priority in many country's development strategies, and it has become recognized that such efforts are essential in achieving sustainable development. In 1987, following a joint submission from 155 countries led by Japan, UN General Assembly decided that 1990s be the "International Decade for Natural Disaster Reduction." (IDNDR)

(3) In the mid-decade year of 1994, Japan hosted World Conference on Natural Disaster Reduction in Yokohama, the first international conference on disaster risk reduction, and contributed in the adoption of Yokohama Strategy and Plan of Action for a Safer World.

(4) Towards the end of the decade, UN General Assembly adopted "International Strategy for Disaster Reduction." (ISDR) in1999 to succeed IDNDR. UN placed secretariat in Geneva. (http://www.unisdr.org) Thereafter in 2003, UNGA adopted that Japan hosts the next World Conference on Disaster Reduction.

(5) In January 2005, Japan hosted the UN World Conference on Disaster Reduction (WCDR) in Kobe, Hyogo Prefecture. Along with the review of "Yokohama Strategy" implemented for 10 years, the participants of the conference examined a guiding framework in disaster risk reduction and adopted the "Hyogo Framework for Action 2005-2015" (HFA) that gathered up priorities of the disaster risk reduction measures that each country and international organization should carry out for the coming ten years.

(6) It was also decided that the UN/ISDR plays a key role in following up the implementation of HFA, and the result to be reviewed in the United Nations Commission on Sustainable Development 2014/2015. "Hyogo Declaration" was adopted at the same time, which advocated the importance of consolidating sustainable development and disaster risk reduction, and spreading the culture of disaster risk reduction. Furthermore, the Special Session on Indian Ocean Tsunami of December 2004, just before the Conference was held on the initiative of Japan. At this session, Common Statement was released calling for the establishment of an effective and durable tsunami early warning system for the Indian Ocean.

(7) At the WCDR, Japan's Prime Minister (then) Koizumi announced Japan's Initiative for Disaster Reduction through ODA for the comprehensive and consistent cooperation strategy corresponding to each stage of disaster prevention, emergency relief and reconstruction.

Thereafter at the Asia-Africa summit meeting held in April 2005, Japan announced that it will be providing more than US$ 2.5 billion (including more than US$ 1.5 billion of grant aid) over the next five years in assistance for disaster prevention and mitigation, and reconstruction measures in Asia, Africa and other regions.

(8) One of the strategic goals of the "Hyogo Framework of Action" is to integrate risk reduction approach into post disaster recovery. To translate this policy into practice, the International Recovery Platform ("IRP") was established in 2005 as a network of organizations such as ISDR, UNDP, ILO, the World Bank, ADRC (Asian Disaster Reduction Center), and several countries including Japan. Having its secretariat in Kobe, IRP is promoting knowledge sharing, capacity building and supports of the disaster recovery programs. (http://www.recoveryplatform.org/jp/)

(9) Considering the disaster risk reduction as an important part of the agenda for poverty reduction, the World Bank established the "Global Facility for Disaster Reduction and Recovery" ("GFDRR"), in 2006, to support each country to mainstream the disaster reduction into national development plans and policies in line with the HFA. Japan supports effective implementation of this facility and pledged US$ 6 million contribution. Japan also acts as a member of the donor meetings and participates in the Result Management Committee (RMC). (http://www.worldbank.org/japan/jp)

(10) To follow up and to secure implementation of the HFA, UNGA in 2006 decided to establish the Global Platform for Disaster Reduction as a forum to discuss matters related to HFA implementation at country, regional and international level. The 1st meeting of the Global Platform was held in January 2007, and the 2nd in June 2009, in Geneva. (http://www.preventionweb.net/globalplatform/2009)

(11) Thus the current international framework has the HFA as its guiding principles, the global platform as the international forum to review and promote the implementation of the HFA, and ISDR as the central secretariat body of the coordination. National progress reports are being submitted every two years.

(12) Table 1 shows evolution of the international framework on disaster reduction since late 1980's.

Table1:

		UN and the world	Japan
1987		"International Decade for Natural Disaster Reduction" (IDNDR) adopted at UN General Assembly	
1990	International Decade for Natural Disaster Reduction (IDNDR)		IDNDR Promotion Head Office was Created by Cabinet decision
1994		UN World Conference on Disaster Reduction (City of Yokohama) was held. "Yokohama Strategy and Plan of Action for a Safer World" was adopted.	
1995			Great Hanshin Earthquake
1998			Contribution to the promotion of international disaster reduction - Establishment of Asian Disaster Reduction Center in 1998
1999		International Strategy for Disaster Reduction(ISDR) was adopted at UN General Assembly	- Asian Natural Disaster Reduction Conference 2002 - Asian Natural Disaster Reduction Conference 2003
2000		Examination of Yokohama Strategy was adopted at the UN General Assembly	- Asian Natural Disaster Reduction Conference 2004 etc.

Year	ISDR		
2003	↑ International Strategy for Disaster Reduction (ISDR)	World Conference on Disaster Reduction	
		UN General Assembly adopts Japan to host the conference (Dec. 2003) Date: Jan.18-22,2005 Venue: Kobe City, Hyogo Participants: 168 UN member states, international organizations, NGOs, etc.	Central Disaster Management Council decided (May) Affirmed at the Cabinet Meeting (July)
2005		"Hyogo Framework for Action 2005-2015", "Hyogo Declaration", "G8 Response to the Indian Ocean Disaster" adopted at WCDR.	
			"Initiative for Disaster Reduction through ODA" announced Announcement of more than US$ 2.5billion in disaster reduction over FY2005-2009 at the Asia-African Summit
2006		World Bank Global Facility for Disaster Reduction and Recovery (GFDRR) was established	"Grant Aid for Disaster Prevention and Reconstruction" started
2007		"International Forum on Tsunami and earthquake" was held in Kobe.	
	↓	1st session of the Global Platform for Disaster Risk Reduction	
2009		2nd session of the Global Platform for Disaster Risk Reduction	

2. PROMOTING COOPERATION IN ASIA

(1) It is crucial to promote cooperation on disaster risk reduction at regional level where countries share the meteorological, geographical and topographical characteristics. Especially in Asia, a number of natural disasters occurred as represented by the Sumatra Earthquake and the subsequent Great Indian Ocean Tsunami in December 2004, Pakistan Earthquake in October 2005, Sichuan Earthquake in May 2008 and others. Such disasters take a heavy toll of lives and damage the sustainable development of the affected countries. Japan has been promoting regional cooperation including information sharing, human resources development through the activities of Asian Disaster

Reduction Center (ADRC).

(2) ADRC was established in July 1998 in Kobe, Hyogo Prefecture, as a result of Asian Disaster Reduction Experts Meeting in 1996 and Asian Disaster Reduction Cooperation meeting in 1997. Currently it has 27 member countries and 5 advisory countries and organizations, and the main activities cover the following areas: (a) accumulation and provision of information on natural disasters and disaster risk reduction, (b) studies on the promotion of disaster reduction cooperation, (c) gathering of information on emergency relief during times of disaster, (d) developing materials for dissemination of knowledge and raising disaster risk reduction awareness, (e) developing education and training programs dealing with disaster risk reduction information. (http://www.adrc.asia)

(3) In November 2008, Asian Conference on Disaster Reduction 2008 was co-organized in Bali by the Government of the Republic of Indonesia, the Government of Japan, the United Nations Secretariat of the International Strategy for Disaster Reduction (UN/ISDR) and the Asian Disaster Reduction Center (ADRC), and discussed current status of the HFA implementation in each country and ways for its further promotion.

(4) Apart from the ADRC, multilateral cooperation on disaster risk reduction in Asia-Pacific region has been formed in the following manner:

(a) Asian Ministerial Conference on Disaster Reduction was first hosted by China in September 2005, and subsequently hosted by India in November 2007 and by Malaysia in December 2008, and discussed ways to promote regional cooperation.

(b) In December 2005, at the 9th ASEAN-Japan Summit in Kuala Lumpur, the collaboration between ASEAN and Japan in the field of disaster management was reaffirmed on the Joint Statement, and at the 10th ASEAN-Japan Summit in Cebu, Prime Minister (then) Abe declared that Japan would contribute about US$ 5.6 million to provide to ASEAN countries materials for disaster risk reduction.

(c) In January 2007, at the 2nd East Asia Summit meeting in Cebu, Philippines, Japan announced to provide, by making use of Japan-ASEAN Integration Fund (JAIF), US$ 3million in total to support ADRC projects on disaster risk reduction in ASEAN member countries. The projects were: (i) Promotion of Disaster Education in Schools, (ii) Capacity building of Local Government Officials on Disaster Management, (iii) Utilization of satellite image on disaster management, and (iv) Development of web-based GLIDE associated disaster event databases for ASEAN countries. These projects started in 2008.

(d) In April 2009, Japan also announced the following additional contributions in disaster reduction area as one of the measures to help Asian countries to cope with global economic and financial crisis: (i) To provide additional fund of US$ 13 million to JAIF in order to assist ASEAN countries to stockpile emergency supplies for their mutual assistance use, (ii) To develop human resources in

ASEAN countries to evaluate and analyze disaster risks, (iii) To provide US$ 6 million in total, by making use of JAIF, to establish information and communication system in ASEAN countries during times of disaster, (iv) To carry out trainings for about 300 personnel from EAS countries over 5 years time in the field of disaster risk reduction, including those from ASEAN countries mentioned in (ii) above, and also to provide opportunities for the students and youths who visit Japan under the "Japan-East Asia Network of Exchange for Students and Youths (JENESYS) Program to experience disaster risk management in Japan.

(e) Japan-US-Australia
In June 2008, at the Japan-US-Australia trilateral strategic dialogue at the ministerial level, a joint statement was issued in which it was stated that the three countries committed to strengthen cooperation on disaster management and emergency response, and to develop guidelines to facilitate this trilateral cooperation and information sharing on humanitarian assistance and disaster relief.

(f) Japan-China-South Korea
In December 2008, at the Japan-China-ROK trilateral summit, a Trilateral Joint Announcement on Disaster Management Cooperation was issued, in which the leaders of the three countries shared that it is crucial for the three countries to share information on projects, initiatives, good practices, lessons learned and science and technologies to strengthen disaster management capability. It was also stated that the three countries will enhance cooperation in (i) developing comprehensive disaster management framework, (ii) developing measures and systems to reduce vulnerability to disasters and to minimize damage from disasters, (iii) strengthen effective disaster management at the national, local and community levels. Moreover, in order to implement the above cooperation, the three leaders shared the view to hold trilateral heads of government agency and expert level meetings on disaster management in rotation, and to consider the first meeting to be hosted by Japan in 2009.

(g) ARF
ASEAN Regional Forum (ARF) has also been active in disaster relief. It places disaster relief as one of the priority areas of activities, and has been promoting regional cooperation in the Asia-Pacific region. As one of such activities of the ARF, in May 2008, a multi-national disaster relief desk top exercise was conducted in Indonesia, and in May 2009, a multinational disaster relief field exercise was carried out for the first time in the Philippines. The concept of the field exercise was a search and rescue activity for a large scale damages caused by a typhoon in Luzon, to which civilians take the lead with the military assist. 25 countries and the EU participated in this field exercise and relevant events that coincided with the exercise and Japan also participated in a large scale, combining personnel/equipments/aircrafts of Ministry of Foreign Affairs, JICA, Ministry of Defense and Ground/Air/Maritime Self Defense Force.

3. JAPAN'S CONTRIBUTION

Since the initiatives that Japan has been taking in the field of multilateral cooperation for disaster reduction are already described in the above sections, this section mainly focuses on a brief look at Japan's bilateral assistance through ODA.

(1) As mentioned in 1. (7) in the above, Japan announced Initiative for Disaster Reduction through ODA for the comprehensive and consistent cooperation strategy corresponding to each stage of disaster prevention, emergency relief and reconstruction. Thereafter at the Asia-Africa summit meeting held in April 2005, Japan announced that it will be providing more than US$ 2.5 billion (including more than US$ 1.5 billion of grant aid) over the next five years in assistance for disaster prevention and mitigation, and reconstruction measures in Asia, Africa and other regions.

(2) By 2007, the third year of the pledged US$ 2.5 billion over 5 years, total expenditure of the Japanese ODA in the field of disaster risk reduction during 2005-2007 achieved US$ 2.53 billion, and the target was already met in advance. Break-downs by each year are as follows: (Figures include both bilateral ODA and contribution through multilateral organizations)

FY	US$	J\
2005	approx. 840 mil.	approx. 89.8 bil.
2006	approx. 820 mil.	approx. 90.9 bil.
2007	approx. 870 mil.	approx. 100.7 bil.

(3) Break-downs of Japan's bilateral ODA for disaster risk reduction during 2005-2007 by forms of assistance are as follows:

FY	Grant	Loan	Total
2005	J\ 22.6 bil	J\ 55.9 bil	J\ 78.5 bil
2006	J\ 16.2 bil	J\ 67.7 bil	J\ 83.9 bil
2007	J\ 22.6 bil	J\ 60.4 bil	J\ 83.0 bil

(4) Break-downs of bilateral ODA by types of disaster in FY 2007 are as follows:

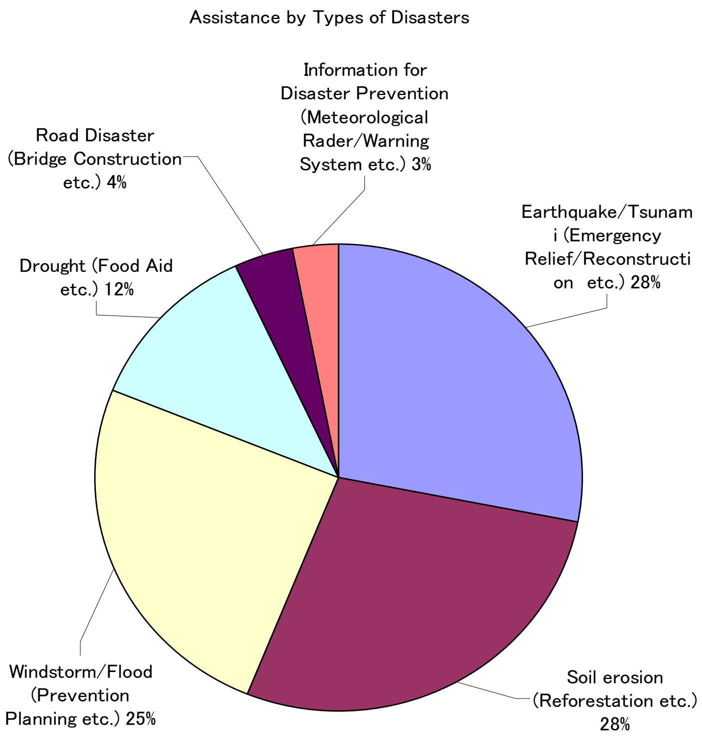

(5) Initiative for Disaster Reduction through ODA divides the types of cooperation by different phases of disaster. (a) Integration of disaster prevention into development policies, (b) Rapid and appropriate assistance in the immediate aftermath of disaster, and (c) Cooperation that extend from reconstruction to sustainable development.

(a) Integration of disaster prevention into development policies

In order to minimize the escalation of damage caused by natural disasters in developing countries, it is essential to take into account the preparedness for possible disasters. In order to introduce the "culture of prevention" into long term national policy, city planning, regional planning, regulations and standards, Japan will provide assistance relating to policy recommendations, institution–building and human resources development. It includes as elements:

- Institution building that incorporates the perspectives of disaster prevention,
- Training of experts and developing capacity for disaster prevention,
- Raising awareness and building capacity of local communities on disaster risk reduction.

<Case File 1> Rising Capacity to Respond and Enhancing Disaster Prevention Framework of Administration Institutions (Turkey)

In 1999, Turkey was hit by two large earthquakes that exceeded magnitude of seven on the Richter scale, causing heavy damages leaving more than 25,000 dead. The Government of Japan extended assistance through Loan Aid, namely "Emergency Measures for Rehabilitation of Earthquake Damage" (FY 1999, J\ 23.6 billon) and "The Seismic Reinforcement Project for Large Scale Bridge in Istanbul" (FY 2001, J\12.0 billion). Reflecting that government bodies' inability to adequately respond may have led to far larger scale of damages than estimated, the Government of Turkey requested the Government of Japan for technical assistance in raising its administrative capacity to respond to disasters, and enhancing its disaster prevention framework.

Technical assistance that began in 2001 emphasized disaster prevention trainings of administrative officials. First, Vice-governors and district governors of Turkey received trainings on the efforts of reconstruction after Hanshin/Awaji Earthquake. From 2003, using the training curriculum developed by returned-trainees, "Disaster Prevention Measure Training Project" was conducted to 260 Vice-governors and district governors. From 2005, "Earthquake Damage Mitigation Project" was carried out which also included trainings to mayors and urban-planning directors.

These efforts are furthering the city planning that would not repeat the disaster tragedy and enhancement of administrative institutions' capabilities to cope with disasters.

(b) Rapid and appropriate assistance in the immediate aftermath of disaster

In the immediate aftermath of a disaster, Japan will provide rapid assistance such as dispatching the Japan Disaster Relief Team for lifesaving, providing basic necessities and food aid, and restoration of basic human economic and social infrastructure. In addition, Japan will dispatch experts specializing in such field as training, risk assessment of buildings and flood control to assist in the human capacity development which will enable an emergency response. The contents are:

- Prompt and appropriate emergency assistance,
- Training of experts and transfer of expertise for emergency response,
- Food aid in response to food shortage caused by disasters,
- Coherent cooperation corresponding to each phase of disaster.

<Case File 2> Seamless Assistance after the Occurrence of Disaster (Indonesia)

In May 2006, heavy damage was caused by a large-scale earthquake that generated in the Central Java in the Republic of Indonesia with more than 5,700 death casualties. Utilizing learned lessons from the past experiences in post-disaster assistance and recognizing the importance of seamlessly connecting emergency response to recovery and reconstruction phase, the Government of Japan carried out assistance in close coordination of various schemes.

Directly after the earthquake, dispatch of Japan Disaster Relief Team (JDR: Medical Team and Unit of the Self-Defense Force), and distribution of emergency relief goods and assistance of goods through emergency grant aid cooperation were conducted. For example, distribution of tents, blankets and other goods necessary for the period of evacuation, emergency treatment of the injured, and establishment of temporary classrooms for the resumption of school education were implemented.

After the emergency phase, recovery and reconstruction assistance were conducted seamlessly through utilization of Grant Aid for Disaster Prevention and Reconstruction as well as technical assistance. For example, official resumption of school education was assisted through distribution of textbooks and other goods upon reconstruction of school buildings and training of teachers. In addition, upon reconstruction of health center, technical assistance such as treatment of trauma and rehabilitation assistance were conducted to enhance medical service.

Such seamless assistance conducted directly after the disaster has facilitated steady progress of reconstruction in Bantur Province of Central Java.

(c) Cooperation that extend from reconstruction to sustainable development

Japan will support actions by developing countries to end the vicious circle of disaster in the reconstruction phase towards developing a disaster-resilient community and sustainable development, targeting areas where severe damage from earthquakes, tsunamis, storms, and floods is widely spread and frequent occurrence of natural disaster is hindering economic growth. For this purpose, Japan will provide cooperation with an emphasis on economic and social infrastructure, building, and systems that are disaster-resilient. The contents are:

- Assistance for developing disaster-resilient economic and social infrastructure and architecture,
- Dissemination of disaster resilient systems and technology,
- Provision of financial assistance necessary for reconstruction and development.

<Case File 3> Prevention of Water Disasters caused by Intensive Rainfall in the Urban Area (Tunisia)

While majority of Tunisia's urban area is within sub-arid area, intensive rainfalls in a short period of time cause floods that could lead to extensive damages. To prevent such damages, the Government of Japan decided to extend its assistance to "Inundation Protection Project" (FY 1997, approximately J\ 9,100 million) through Loan Aid in response to a request from the Government of Tunisia.

This project is a counter-flood measure plan in Ariana situated in the northern Tunis, the capital, and Kairoan which is the hub of the country's central region. In Ariana, rehabilitation of drainage and reservoirs as well as rehabilitation of existing channels are in progress along the Enkhit River. In Kairoan, flood control channels and river dikes are being constructed for Merguellil River and the Zeroud River, which flow into the Kairouan Plain that surrounds the city.

These efforts have mitigated flood damages and have promoted economic and social development in the targeted areas. In particular, in Kairouan, the project will make it possible for a large area of land that has not been utilized because of floodi ng to be used effectively for agricultural purposes.

(6) Apart from the ODA program as described in the above, Japan has experienced extensive devastation caused by a multitude of disasters including earthquakes, tsunamis, typhoons, floods, and volcanic eruptions. Based on harsh experiences, Japan developed disaster management system, and takes full advantages of its experience, knowledge, and technologies to contribute to the improvement of disaster management capabilities in the developing countries. Some examples are as follows:

(a) Early Warning System and Hazard Maps

For early warning systems to be useful in mitigating natural disasters, it is necessary:

(i) to enable the issuance of prompt and accurate early warning information based on accurate, real-time measurements of various natural phenomena and scientific data analysis.

(ii) to incorporate systems for sharing warning information among relevant organizations and disseminating it to people, and

(iii) to raise awareness on disaster reduction to ensure that more timely and appropriate disaster risk reduction actions are taken based on the warning information issued.

In Japan, such early warning systems are established throughout the country.

Also, Japanese municipalities generally create and distribute hazard maps that show the areas vulnerable to earthquakes, tsunamis, volcanic eruptions, floods, and landslides, as well as evacuation information.

Throughout the country, in particular on September 1, Disaster Reduction Day, many disaster reduction drills and outreach activities are conducted to prepare for future disasters.

(b) Community-based Disaster Reduction Activities and Disaster Reduction Education

It is important to improve the general public's awareness of disaster risks and disaster reduction at the community level so that everyone can take the appropriate actions when a disaster strikes. Some communities organize activities designed to increase public understanding of hazard maps and activities to create community-based disaster risk reduction maps. These include "town watching" activities in which people actually go around the town they live in and identify its disaster risks, and hold workshops on disaster risk reduction. Such activities raise local residents' awareness of disasters and disaster reduction, lead to suggestions for improving the community's vulnerabilities, and contribute significantly to improving the disaster reduction capabilities of the community.

To promote disaster reduction education, education materials were created and distributed in 8 Asian countries, in which the tale of "Inamura no Hi" ("Fire of Rice Sheaves") based on an actual disaster experience in Wakayama Prefecture was translated into local languages.

<Case file 4> Flood Hazard Mapping in 8 Asian Countries

Asian Monsoon areas, especially East and Southeast Asian areas experience numbers of floods each year. Many human lives and properties are lost due to the floods. In order to reduce damage caused by floods, built infrastructures like river dikes or reservoirs are very effective. On the other hand, non-built infrastructures such as “Flood Hazard Map”, which can offer information on past flood track records, flood estimation, evacuation route, evacuation place, etc. to the residents, are also important. Effectiveness is higher and quicker especially in areas where built measures are not yet in place.

From such viewpoint, in 2006, the Government of Japan implemented a training course called “Food Hazard Mapping” to technical managers and engineers involved in flood or river management in the public sector from 8 countries in East and Southeast Asia (Cambodia, China, Indonesia, Laos, Malaysia, Philippines, Thailand, and Vietnam). It is expected that after the training, knowledge and technique will be spread in each country, and flood damages in each areas are mitigated through development of flood hazard map.

(7) Some information on Japanese government offices and institutions related to disaster reduction are as follows:

Cabinet Office; http://www.cao.go.jp/index.html (Japanese)
http://www.cao.go.jp/index-e.html (English)
Ministry of Land, Infrastructure, Transport and Tourism;
http://www.mlit.go.jp/ (Japanese)
http://www.mlit.go.jp/index_e.html (English)
National Research Institute for Earth Science and Disaster Prevention;
http://www.bosai.go.jp/index.html (Japanese)
http://www.bosai.go.jp/e/index.html (English)

4. CONCLUSIONS

In the above sections, the author tried to have an overview of overall framework of international cooperation for disaster risk reduction and the related process that has been taken, regional cooperation mechanism particularly in the Asian region, as well as the efforts so far undertaken by Japan. Next year, 2010, will be the mid- term year of the HFA, and at this juncture, the author sincerely hopes that there will be a renewed attention to integrate efforts at various levels into a concerted international and regional cooperation.

DESIGNING RC STRUCTURES FOR FIRE

SAMARTH P. RAMDASI
Former Graduate Student, Dept. of Civil Engineering, IIT, Kanpur, India
imsaneth@gmailcom
SUDHIR MISRA
Professor, Dept. of Civil Engineering, IIT, Kanpur, India
sud@iitk.ac.in
P.S. GHOSHDASTIDAR
Professor, Dept. of Mechanical Engineering, IIT, Kanpur, India
psg@iitk.ac.in

ABSTRACT

Reinforcing bars within concrete need to be protected from high temperatures that may occur outside in the event of a fire, etc. and the cover concrete serves that purpose. Design codes usually place an empirical limit on minimum cover thickness for a certain level of fire resistance.

In order to establish a rational basis for determining the concrete cover thickness, an effort has been made in this study to estimate the temperature variations within concrete for different fires in a model reinforced concrete (RC) chamber using MATLAB. The analysis has carried out in two steps – (a) determination of the environmental (gas) and surface temperature of concrete using the compartment fire model proposed by Pettersson et al. (1976), and, (b) studying the temperature variation within concrete based on 1-d transient heat conduction using the explicit finite difference method. The geometric and material properties of the RC chamber were varied, and the required cover obtained for different 'permissible' levels of temperature at the reinforcement level.

Results showed that the parameters like openings area, room size, and material properties significantly affect the temperatures in the chamber and also within concrete. For example, increasing the compartment size from 4x5x3.1 (A_t=95.8 m^2) to 5x6x3.1 (A_t=128.2 m^2), can reduce the fire temperature by 164^0 C (about 11%). Similarly, lowering of compartment openings can reduce the fire temperature by 125^0C though it also has the effect of increasing the duration of fire by about 8 minutes. Thus, attention to these parameters can help reduce the cover thickness requirement.

1. INTRODUCTION

Concrete is a composite material widely used material in the construction of various kinds of structures. It acts as a load bearing material in building components and the cover concrete protects the reinforcement within from the harmful effects of environmental action such as chloride attack and fire. It has been reported that reinforced concrete (RC) structures lose their ability to carry loads after exposure to higher temperatures due to the effect of high temperatures on both – steel and concrete (Harmathy, 1970; Takeuchi, 1993). Though concrete is poorer conductor than steel, sustained high temperature at the surface, as can be expected in a fire, leads to progressive heating of the inner layers of concrete, and also exposes reinforcing bars to elevated temperature, depending upon factors such as the duration of fire, thickness and properties of the cover concrete, etc. Indeed the properties of concrete are also known to undergo significant changes upon exposure to high temperatures. Effort in this study is directed to study the effect of outbreak of fire in an RC chamber with openings and a certain amount of fuel on the temperature of the environment in the chamber (gas temperature) and the variation of temperature within the concrete.

2. MODEL DESCRIPTION

2.1 Basic description

Figure 1 gives a diagrammatic representation of the RC chamber used in the model here. It can be understood that in the event of a fire in the chamber, the temperature (of the air) within the chamber will increase, which, in turn, will cause the surface temperature of concrete to also increase, depending upon the fire temperature and surface heat transfer coefficient. Further, an increase in the surface temperature will have the effect of increase in the temperatures within the concrete depending upon the properties of the concrete, including conductivity, etc.

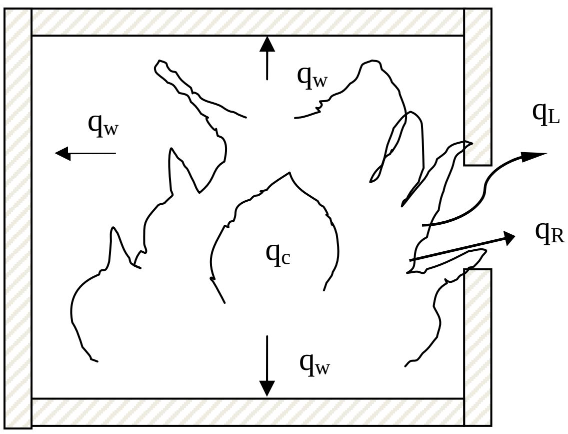

q_c: heat released due to combustion
q_L: convection heat loss
q_w: heat loss by conduction through all the walls of the chamber
q_R: radiation heat loss
q_B: heat stored in the gas volume (neglected, not shown in this figure)

Figure 1: Compartment fire heat balance

In present study, for the first part, i.e. computation of the time-temperature variation of the gas within the chamber and subsequently the surface temperature of concrete, the compartment theory concepts and a mathematical model available in the literature have been used (Harmathy

1972; Pettersson, 1976) have been used. The model discussed takes into account the affect of parameters such as the dimensions of the chamber, fuel load within the chamber, size and location of openings and thermal characteristics of the compartment boundaries (Kawagoe, 1958). It may be noted that all walls of the chamber have been assumed to be made of concrete and have the same thickness. For the second part, the formulation is based on the explicit finite difference method using 1-d heat conduction.

2.2 Problem formulation

As mentioned above the basic mathematical formulation adopted is that developed by Pettersson et al (1976). The heat balance in the event of fire in the RC chamber shown in Figure 1, can be represented as:

$$q_c = q_L + q_w + q_R + q_B \qquad \text{..........(1)}$$

In this study, while q_B has been assumed to be small and neglected, other terms have been evaluated and finally the gas temperature in the chamber calculated using the following equation (Patterson, 1976).

$$T_g = \frac{q_c + 0.52 C_p . T_o . A_w . H^{0.5} + (A_t - A_w) h_i . T_i - A_w . \varepsilon_f . \sigma . T_g^4}{0.52 C_p . A_w . H^{0.5} + (A_t - A_w) h_i} \qquad \text{..........(2)}$$

where,
C_p = Specific heat of the gas in KJ/(Kg.K)
T_o = Outside temperature in K
A_w = Area of the opening in m^2
H = Height of the opening in m
A_t = Total surface area of the room in m^2
h_i = Heat transfer coefficient of the wall in KW/m^2K
T_i = Inside wall surface in K
σ = Stefan-Boltzmann constant KW/m^2K^4
ε_f =Emissivity
T_g =Gas Temperature in K

In the next step, 1-d transient heat conduction equation $\left(\frac{\partial T}{\partial t} = \alpha \frac{\partial^2 T}{\partial x^2}\right)$ has been used to calculate the temperature variation within the chamber walls using a formulation based on explicit finite difference method'. The approach divides the wall into several slices, each measuring Δx, and calculates the temperature at each grid point lying at the interface of the slices at time 'P+1', for the given thermal conductivity K, specific heat C and density ρ using the following relationship.

$$T_i^{P+1} = T_i^P (1 - 2\lambda) + \lambda [T_{i+1}^P + T_{i-1}^P] \qquad \text{..........(3)}$$

where, $\lambda = \frac{\alpha \Delta t}{(\Delta x)^2}$, $\alpha = \frac{K}{\rho C}$, Δt and Δx are the time and distance intervals

At the inside and outside surfaces of the compartment boundaries, surface temperature at point '1' and 'N' is obtained using convection boundary condition and using the image point technique.

$$T_1^{P+1} = T_1^P(1 - 2\lambda - \beta\lambda) + 2\lambda T_2^P + \lambda\beta T_g^P \qquad \text{.........(4)}$$

$$T_N^{P+1} = T_N^P(1 - 2\lambda - \lambda\beta') + 2\lambda T_{N-1}^P + \lambda\beta' T_\infty \qquad \text{.........(5)}$$

where, β and β' are given by as follows:

$$\beta = \frac{2h\Delta x}{K}, \qquad \beta' = \frac{2h'\Delta x}{K}$$

h and h' are the surface heat transfer coefficients (Pettersson, 1976). The time step, Δt, has been so chosen as to ensure that the coefficients of T_i^P, T_1^P and T_N^P are always positive to ensure numerical stability.

3. RESULTS AND DISCUSSION

3.1 Compartment used

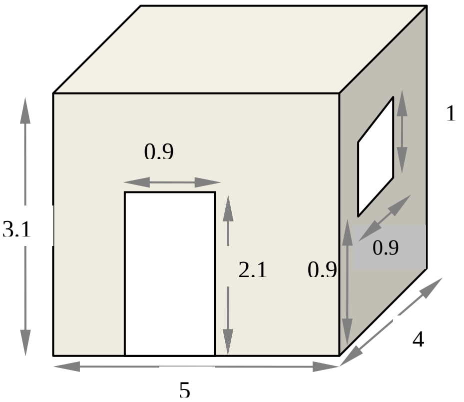

Notes:

i. All dimensions in meter
ii. Thickness of all chamber wall/slabs taken to be 160mm
iii. Ambient temperature outside chamber: 25 ^{0}C

Figure 2: Model chamber used for calculations

Figure 2 shows the details of the model chamber used in the study, including the dimensions, locations of openings, etc. Table 1 gives the details for the different relevant parameters. The results obtained using the model described above are given in the following paragraphs.

3.2 Variation of T_g with time

Effect of total area of the compartment (A_t): Effect of room size, in terms of the total inside surface area of concrete walls on maximum gas temperature (T_{gmax}) has been shown in Figure 3, keeping the opening size and height constant at 2.79m^2 and 1.75m, respectively. The gas temperature has been calculated at three levels of fuel in the room – 300 kg, 500kg and 1000 kg, and varying the total surface area A_t from 10 m^2 to 1000 m^2.

Table 1: Assumed parameters

Parameter	Unit	Value	Remarks
C_P	KJ/Kg	1.01	Specific heat of air
σ	KW/m^2	$5.67x10^{-11}$	Stefan-Boltzmann constant
K	KW/m K	$1.7x10^{-3}$	Conductivity of concrete in the walls of the chamber
C	KJ/Kg	0.836	Specific heat of concrete
ρ	Kg/m^3	2300	Density of concrete
Δx	m	0.010	Grid spacing
Δt	sec	0.4	Time step

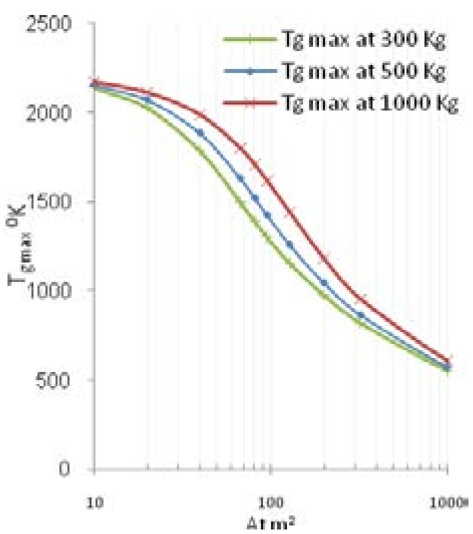

Figure 3: Variation of T_g max with total surface area 'At' for a constant ventilation factor

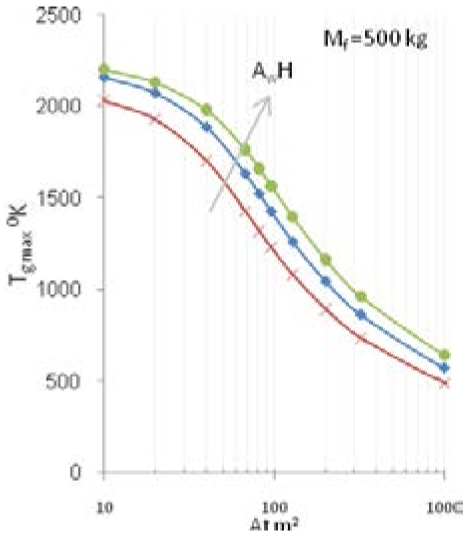

Figure 4: Variation of T_g with At for different $A_wH^{1/2}$ for a constant fuel load

It can be seen from Figure 3 that T_{gmax} decreases as size of room increases with a relatively small impact of the amount of fuel in the room. The result can be attributed to the fact that the ventilation factor $A_wH^{1/2}$ has been kept constant in this study, i.e., flow of fresh air into the room is highly restricted. Thus, for an increase in the size of the room, the effect is simply the lowering of the maximum temperature reached in the event of fire. It is also interesting to note that the effect of the fuel load is reduced at both extremes – for small and large values of A_t. Figure 4 shows the variation of T_{gmax} with A_t for a fixed fuel load of 500 Kg for different ventilation factors. It can be seen that the trend is almost similar to Figure 3 and the variation can be taken as linear except at very high or very low values of A_t.

Effect of varying area (A_w) and the height (H) of opening: The opening size is an important parameter in determining the gas temperature, as an opening serves the dual role of (i) facilitating inflow of fresh air and oxygen, which are required to sustain a fire, and, (ii) serving as an exit for the hot gases resulting in heat loss through convection. In this study, the opening size (A_w) has been varied from 0.5 m^2 to 5 m^2, keeping all other parameters constant, and Figure 5 shows the results obtained. The height of the opening

H, the total surface area A_t of the compartment and the fuel load has also kept constant at 1.75m, 95.8 m^2 and 500kg, respectively.

Now, as opening area increase from about 0.5 to $5m^2$, it can be seen that the T_g increases by about 600ºC. This increase can be justified on account of the fact that for larger openings, there is ample flow of fresh air (along with oxygen) aiding the burning and heat release. It may also be mentioned that larger openings also lead to greater heat loss through them. It should also be noted that the opening size also has an impact on the duration of the fire, and this aspect has dealt with elsewhere (Ramdasi, 2009).

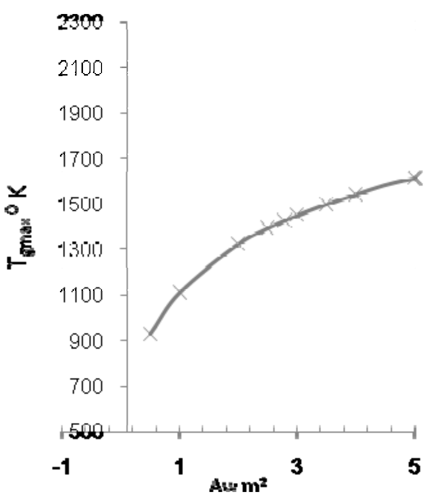

Figure 5: Variation in T_{gmax} with respect to opening size A_w

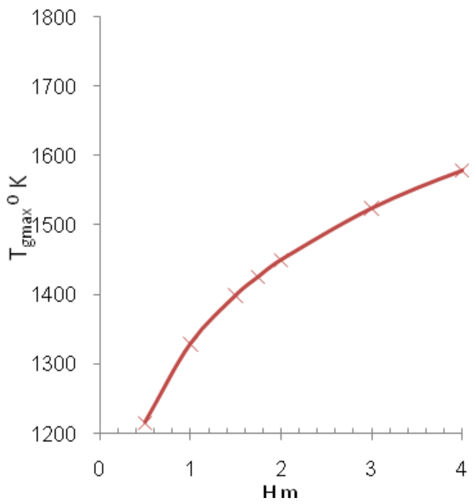

Figure 6: Variation in T_{gmax} with respect to height of the opening H

Similarly, the height of the opening is also an important parameter, and the results obtained by varying the height between 0.5m and 4m are shown in Figure 6. It can be seen that increasing height of ventilation opening, could cause significantly higher values T_g.

3.3 Variation of temperature within concrete

From an engineering point of view it is important to know the temperatures reached at the location of the reinforcing bars to decide the residual strength of the steel bars and the repair strategy (Hemraj, 2009). Though largely related to issues such as the amount of fuel, duration of fire, etc. the variation of temperature within concrete is also affected by the thermal properties of concrete – conductivity and specific heat. Though more rigorous analysis should take into account changes in these properties as the temperature within rises, in the present analysis, these values have been taken to be constant (temperature invariant).

Thermal conductivity of concrete (K): Thermal conductivity of concrete is known to vary between 1.2 and 1.9 W/m K (Lie, 1978), and affects the variation of temperature within concrete. The effect of conductivity on the maximum temperature profile within the concrete wall is shown in Figure 7 for a constant specific heat and density. The results for two durations of fire show that as the K, the maximum surface temperature increases. As the conductivity goes down, dissipation of heat through conduction decreases, increasing the gas temperature and surface temperature within the compartment (Harmathy, 1972). In other words, though the maximum surface temperature of low conductivity concrete increases, the maximum temperature within the concrete decreases. Similarly, in cases when the K is high, the concrete absorbs more energy from the environment, and though the gas temperature (and the surface temperature) goes down, the maximum temperature within concrete tends to increase (Ramdasi, 2009).

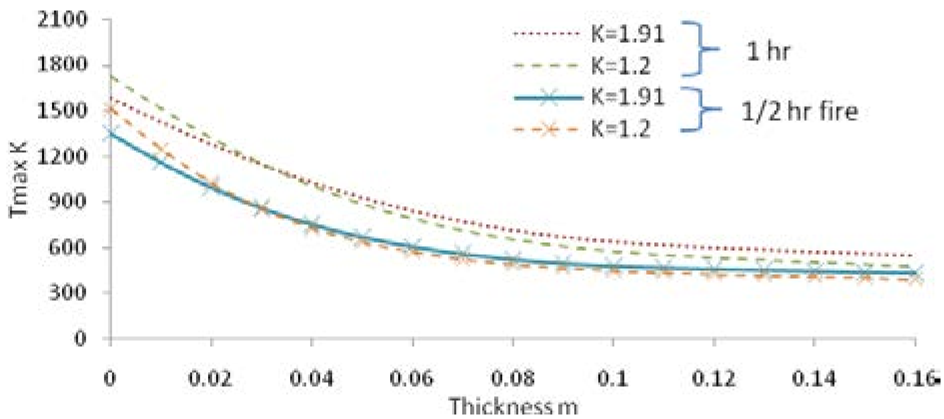

Figure 7: Maximum temperature profile for different conductivity value for different durations.

Specific heat (C): Specific heat of the material is amount of heat required to raise temperature of unit quantity of material by a unit degree of temperature. Thus, for the same amount of heat, a higher rise in temperature may be expected in materials with a lower specific heat, than in a material with higher specific heat. Figure 8 shows the variation in maximum temperature profile within concrete for different values of specific heat taken from the literature. It can be seen that there is a steady increase in maximum temperature values for decreasing specific heat.

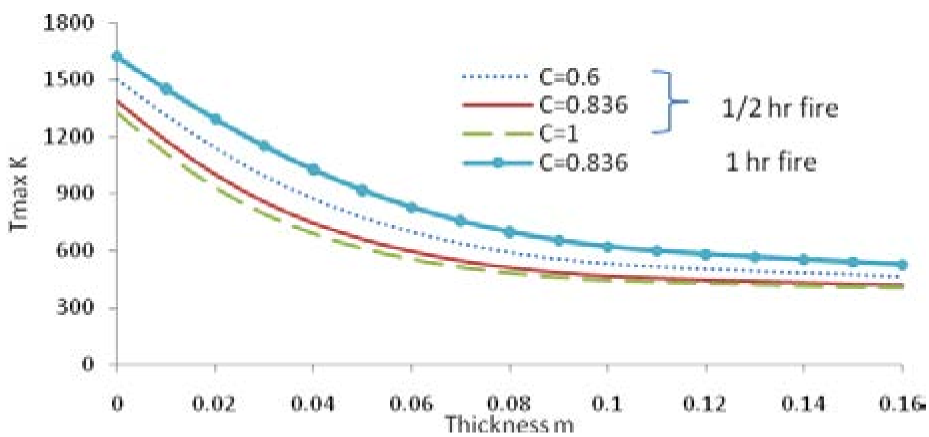

Figure 8: Maximum temperature profile within concrete wall for different specific heat value for full duration.

4. DETERMINATION OF CONCRETE COVER THICKNESS

Codes generally ‘prescribe’ different levels of concrete cover for varying durations of fire (IS 456, 2000). However, more than such an empirical value, a rational design approach should be based on fixing a critical temperature at the reinforcement level, which should not be exceeded in the event of fire, and then determining the required cover based on the properties of concrete, duration of fire, etc. Now on the basis of the analysis discussed above, Table 2 presents the results for the required levels of cover thickness for the model structure given in Figure 1 for different critical temperature at the reinforcement location, depending on the characteristics of compartment.

Table 2: Estimates of required cover thickness for the model structure

Fire duration (hours)	Required cover (in mm) for different critical temperatures		
	400ºC	500ºC	600ºC
1	44	37	32
2	68	59	51
3	88	76	67
4	106	92	80

5. CONCLUDING REMARKS

With special concretes with properties quite different from conventional concrete being used often in very critical structures susceptible to fire, it is important that rational methods be adopted to determine the cover required based on the design fire, the actual geometric design and material properties, and the ‘permissible’ critical temperature at the reinforcement level. The computations presented highlight the importance of these parameters and show that the present specifications need to be re-evaluated.

REFERENCES

Harmathy, T.Z. (1972); *A New Look at Compartment Fires, Part II*. Fire Technology,Vol. *8 (4)*, 326-351.

Harmathy, T.Z. (1970); *Thermal properties of concrete at elevated temperature.* ASTM Journals of Materials, 47-74.

IS:456 (2000); *Indian Standard for plain and reinforced concrete -Code of practice (fourth revision).* Bureau of Indian Standards, New Delhi.

Hemraj, B. (2009*);* Effect of heat on thermo-Mechanically treated reinforcing steel bars. M Tech Thesis submitted to IIT Kanpur

Kawagoe, K. (1958); *Fire Behaviour in Rooms.* BRI Report No.27, Building Research Institute, Ibaraki-Ken, Japan.

Lie, T.T. (1978); *Calculation of the Fire Resistance of Composite Concrete Floor and Roof Slabs.* Fire Technology Vol.14 (1), 28-45.

Pettersson, O., S. Magnussen, and J. Thor. (1976); *Fire Engineering Design of Steel Structures.* Swedish Institute of Steel Construction, Stockholm.

Ramdasi, S.P. (2009); Modeling reinforcement temperatures in RC structures susceptible to fires. M Tech Thesis submitted to IIT Kanpur

Takeuchi, M., M. Hiramoto, N. Kumaga, N. Yamazaki, A. Kodaira, and K. Sugiyama. (1993); Material properties of concrete and steel bars at elevated temperatures. Elsevier Science publishers.

CLOSING SESSION

ALOS AND SENTINEL ASIA FOR DISASTER MONITORING

Prof. Haruhisa Shimoda
Director, Tokai University Space Information Center
Deputy Director, Tokai University Research & Information Center
President of Commission 8 (Remote Sensing Application),
International Society for Photogrammetry and Remote Sensing
smd@keyaki.cc.u-tokai.ac.jp

ABSTRACT

ALOS was launched on 24th Jan. 2006 from Tanegashima Space Center by H2-A launcher. Satellite is operating well and all 3 sensors on-board are also operating well. Commissioning phase ended at the beginning of May 2006, calibration and validation phase ended at October 2006 and ALOS has been full operational from the middle of October 2006.

The mission of ALOS is to provide sufficient data, which enable to generate 1 to 25,000 scale base maps all over the world as well as disaster monitoring. ALOS carries 3 sensors. One is an L band synthetic aperture radar called PALSAR (Phased Array L band Synthetic Aperture Radar). PALSAR has an active phased array antenna, and has many capabilities, like variable incidence angle, variable resolution, scan SAR capability and multi polarization capability.

ALOS has two optical sensors, i.e., AVNIR-2 and PRISM. AVNIR-2 (Advanced Visible and Near Infrared Radiometer) is a follow on of AVNIR on ADEOS and has 4 bands with 10 m resolution. PRISM is a panchromatic sensor with 3 telescopes, which will enable PRISM to take 3 direction (nadir, fore and aft) stereo pairs simultaneously. The resolution of PRISM is very high (2.5m) with rather narrow swath (35km). In addition to the stereo capability which will provide global DEM data, PALSAR will be also useful for the evaluation of global tree stand biomass.

For the disaster monitoring, ALOS is a part of two international projects, i.e. the International Charter "Space and Major Disasters", and Sentinel Asia. International Charter aims at providing a unified system of space data acquisition and delivery to those affected by natural or man-made disasters through Authorized Users. Each member agency has committed resources to support the provisions of the Charter and thus is helping to mitigate the effects of disasters on human life and property.

Sentinel Asia is a "voluntary and best-efforts-basis initiatives" led by the APRSAF (Asia-Pacific Regional Space Agency Forum) to share disaster information in the Asia-Pacific region on the Digital Asia (Web-GIS) platform and to make the best use of earth observation satellites data for disaster management in the Asia-Pacific region.

ALOS has been contributing to these two projects many times during its operational phase.

ALOS follow on is now planned in JAXA. They are ALOS2 and ALOS3. ALOS2 will carry an improved L-band SAR with high spatial resolution (up to 1x3m GSD), while ALOS3 will carry also high resolution optical sensor (0.8m PAN and 2.4m XS GSD).

EARTHQUAKE COUNTERMEASURES FOR SAFER FUTURE IN KOREA

WAON-HO YI
Director, National Institute for Disaster Prevention, Korea
whyi1208@nema.go.kr

ABSTRACT

Due to the great earthquakes which occurred recently in neighboring countries, such as the 1995 Hyogoken-Nambu Earthquake with more than 6,500 fatalities in Japan, the 1999 Chi-Chi Earthquake with more than 2,500 fatalities in Taiwan, and the 2008 Sichuan Earthquake with more than 69,000 fatalities in China, the importance of the future earthquake preparedness measures is highly recognized in Korea. Lesson from the Hyogoken-Nambu Earthquake in 1995, Korea Government has added earthquake as the disaster items in the revised "National Disaster Countermeasures Act" and established 1st Earthquake Disaster Countermeasure Plan. And Korea Government has made the efforts for earthquake hazard mitigation including 1st~3rd Earthquake Disaster Countermeasures Plan focused on setting the seismic performance level, legal system maintenance, prevention, preparation, response, recovery and Earthquake Disaster Countermeasure Act enacted in Mar. 28, 2008. In this paper, proceedings of Earthquake Disaster Countermeasure Plan in Korea from 1995 to 2009 is introduced and discussed.

1. INTRODUCTION

The devastating 1995 Hyogo-Nambu Earthquake occurred in Japan with more than 6,500 fatalities, 1999 Chichi Earthquake occurred in Taiwan with more than 2,500 fatalities and 2008 Sichuan Earthquake occurred recently in China with more than 69,000 fatalities in China awakened the public concern about the possible earthquake disaster in Korea.

Many seismologists pointed out that a disastrous earthquake could occur at any time. After the Hyogoken-Nambu Earthquake in 1995, Korea Government has added earthquake as the disaster items in the revised "National Disaster Countermeasures Act" and established 1st Earthquake Disaster Countermeasure Plan. And Korea Government has made the efforts for earthquake hazard mitigation including 1st ~ 3rd Earthquake Disaster Countermeasures Plan and Earthquake Disaster Countermeasure Act enacted in Mar. 28, 2008.

A comprehensive earthquake disaster countermeasures plan was drawn up to establish the mitigation countermeasures, emergency response countermeasures, and rehabilitation countermeasures of related agencies in 1998.

In this paper, historical and recent earthquakes mainly occurred in Korea and 1st ~ 3rd phase of Earthquake Disaster Countermeasure Plan are introduced. Also, main research and development project plans regarding to the Earthquake Disaster Countermeasure Plan are discussed.

2. STATUS OF THE EARTHQUAKE OCCURRENCE IN KOREA

It is well known that Korea for the earthquake is relatively safer than neighboring countries located in circum Pacific zone such as Japan and China as shown in Fig. 1 (http://www.seismo.ethz.ch/gshap/eastasia). Furthermore, recent hazardous natural disasters occurred in Korea have been mainly caused and governed by meteorological and hydrological phenomena.

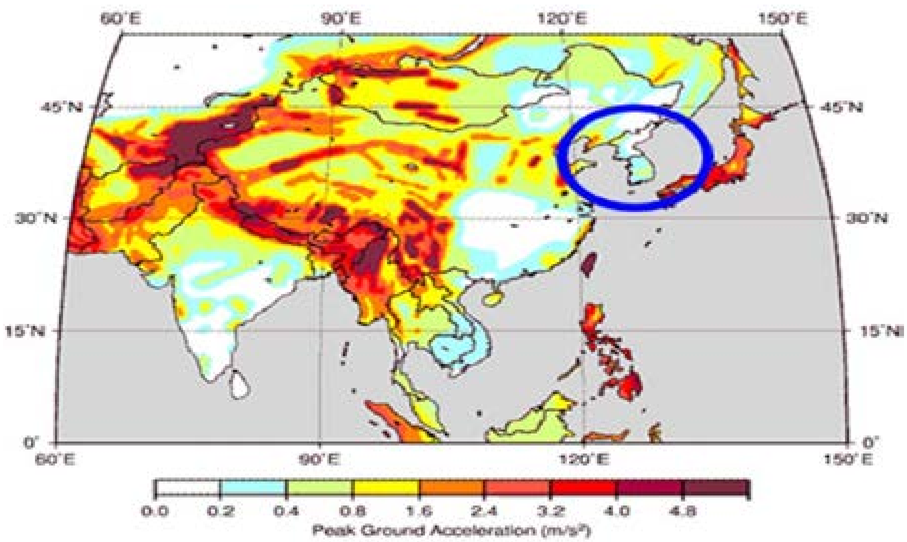

Figure 1: Seismic Hazard Map for Eastern Asia

However, it is pointed out that the Korean peninsula is not free from the destructive earthquakes according to the historical earthquake records. Historical earthquake records from the historical literatures shown in Fig. 2 indicate that a number of earthquakes occurred during the 15-18th centuries and the seismicity in 20th century increased.

In addition, frequency of earthquakes is increased steadily as shown in Fig. 3, although a felt earthquake more than 4.0 of earthquake magnitude is not increased. And also, due to the reason regarding to the Korean peninsula located in border line of Pacific Plate and records of historical earthquake damage, it is needed to prepare the future earthquake.

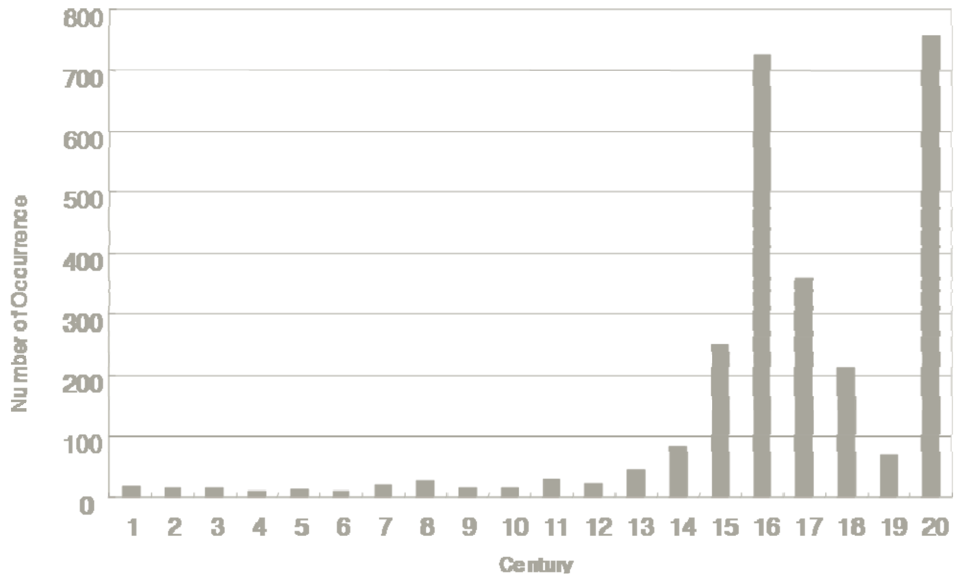

Figure 2: Time Distribution of Earthquake Occurrence in Korea

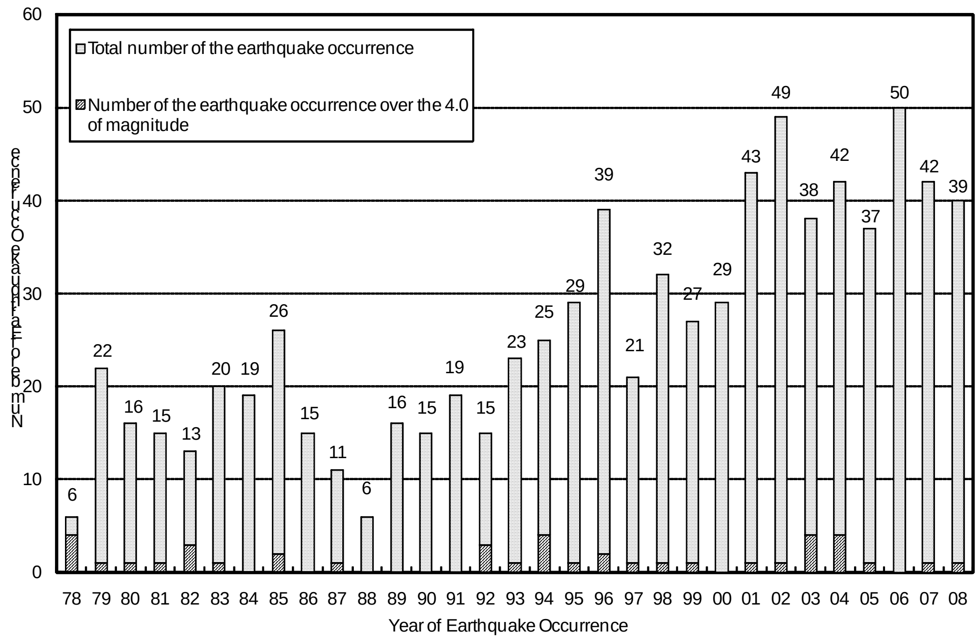

Figure 3: Earthquake Activities (1978~2007)

Table 1 shows the list of representative earthquakes and tsunami affected damages in Korea in 20th Century.

As shown in Table 1, it is found that most of economic losses are caused by tsunamis. However, casualties from earthquake are relatively less than economic losses, because of the earthquake characteristics with short period and sustained time. However, based on the fact that the Tangshan earthquake in 1976 showed that the intraplate seismicity can cause the large disasters, and also several faults are founded in Korea. So that reasons, many researchers carefully attempt to propose that the Korea is not the safe area from the earthquake disaster.

Table 1: Earthquakes and Tsunamis affected damages in Korea

Earthquake/ Tsunami	Mag.	Casualties				Economic Losses
		Total	Death	Injured	Missing	
Ssanggyesa Earthquake (1936.7.4)	5.1	4	0	4	0	- Damages in Building : 113 (Collapse : 3) - Damages in Cultural Buildings including Ssanggyesa
Tsunami Caused by Niigata Earthquake (1964.6.16)	7.5	0	0 (473 in Japan)	0	0	- Wave Height : 32cm(Pusan), 39cm (Ulsan)
Mt. Songni Earthquake (1978.9.16)	5.2	0	0	0	0	-
Hongseong Earthquake (1978.10.7)	5.0	2	0	2	0	- Economic Losses : 301million won - Damages in Building : 100 (Cracks in 1,000 buildings) - Hongju Castle was collapsed - Broken Windows : 500 windows in Official Building
Tsunami Caused by Earthquake in Middle East Sea (1983.5.26)	7.7	5	1	2	2	-Economic Losses : 370million won(Wondeok Port : 243, Samcheok Port 93, Ulleungdo 21, Uljin 6million won) - Damages in Building : 44(Collapse : 1, Flood : 21) - Damages in Ship : 81
Tsunami Caused by Earthquake in Southwestern Seaway of Hokkaido (1993.7.12)	7.8	0	0	0	0	- Economic Losses : 390million won - Damages in Ship : 35 - Fishing-nets : 3,000
Yeongwol Earthquake (1996.12.13)	4.5	0	0	0	0	
Uljin Offshore Earthquake (2004.5.29)	5.2	0	0	0	0	
Fukuoka Earthquake (2005.3.20)	7.0	0	0	0	0	-The elevator was temporarily stopped in Pusan -Unloading operations stopped 30 minutes in Pusan port
Mt. Odae Earthquake (2007.1.20)	4.8	0	0	0	0	- Damages in Building : Cracks were appeared in old URM buildings

3. EARTHQUAKE DISASTER COUNTERMEASURE PLAN

Destructive Hyogoken-Nambu Earthquake in Japan affected huge transition of recognition for the earthquake countermeasures in Korea. With this as a momentum, Korea Government has added earthquake as the disaster items in the revised "National Disaster Countermeasures Act" and established 1st Earthquake Disaster Countermeasure Plan. In this chapter, process of 1st ~ 3rd Earthquake Disaster Countermeasures Plan is discussed.

3.1 The first phase of earthquake disaster countermeasure plan

In January 27, 1995, the 1st Earthquake Disaster Countermeasure Plan of Korea Government is established through the conference participated relevant ministries and experts. In this 1st Earthquake Disaster Countermeasures Plan, setting the seismic performance level, legal system maintenance, and preparing of Earthquake Disaster Countermeasure Act were mainly focused on. As a consequence, direction of the propelled goal is planned as follows.

- Propelling the ACT for the Earthquake Prevention Countermeasures
- Establishment of practical plan for the earthquake disaster mitigation
- Reducing casualties from system maintenance of rescue and relief
- Strengthening the relationship of each ministry and expert group
- Promotion the PR for the consciousness of earthquake disasters
- Strengthening and developing the seismic design code and provision
- Encouragement the R&D for earthquake damage mitigation

From the 1st phase of Earthquake Disaster Countermeasure Plan, adaptation of the seismic design is widened for the 20 kinds of facilities. And seismic design provisions are re-established and applied. Through the evaluation of the 1st phase of Earthquake Disaster Countermeasure, the 2nd phase is established with modification and complement on December 2005.

3.2 The second phase of earthquake disaster countermeasure plan

It is highly recognized for the consciousness of the earthquake and tsunami damages from the Fukuoka earthquake which are occurred on March 20, 2005. After the Fukuoka earthquake, Prime Minister Council decided to establish the 2nd phase of Earthquake Disaster Countermeasure Plan. And 2nd phase of Earthquake Disaster Countermeasure Plan (tentative) is reported on April 12, 2005. As consequences, a special committee regarding to the earthquake disaster prevention for the various improvements is set up. After building the road map for 5 years R&D and policy plan, propelling of the 2nd phase is started. Directions of the propelled goals as shown in Fig. 4 are planned as follows.

- Enactment and maintenance of ACT for the earthquake disaster mitigation.

- Complementation for the early response system of improvement of the observation and alert system for the earthquake and tsunami.

- Developing and strengthening the education and training program for rapid response of the earthquake disaster.

- Building the earthquake disaster mitigation-based foothold including strengthening the seismic provision and developing the earthquake hazard map.

From the 2nd phase of Earthquake Disaster Countermeasure Plan, the Alert System for the earthquake/tsunami and the Earthquake Disaster Management System were successfully developed.

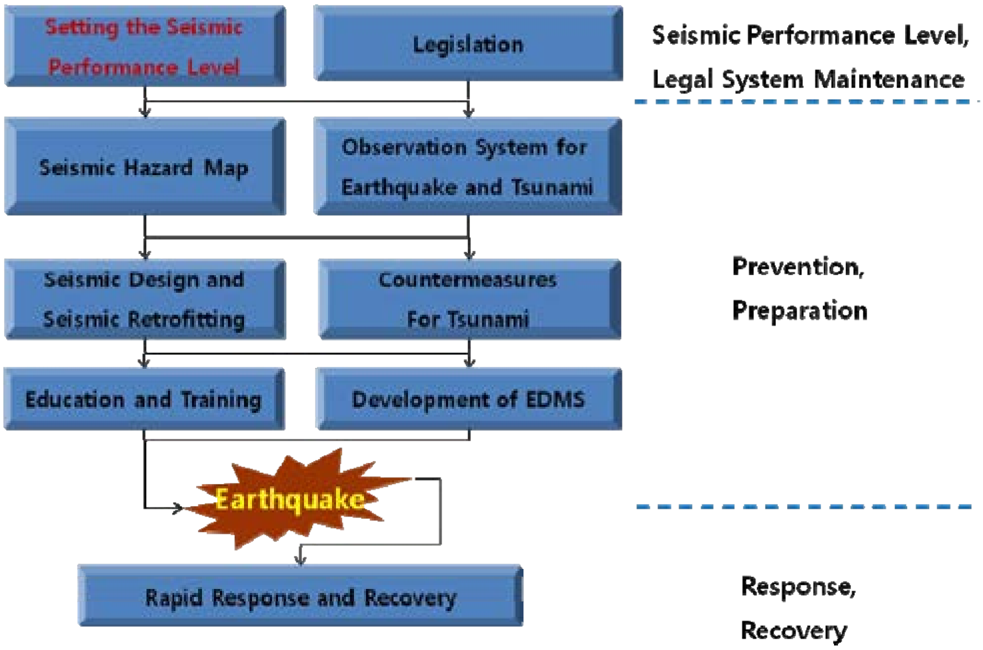

Figure 4: 2nd Phase of Earthquake Disaster Countermeasure Plan

In addition, Earthquake Disaster Countermeasure Act (Act No. 9001) that consists of 8 chapters and 29 articles enacted in Mar. 28, 2008 and enforced in Mar. 25, 2009. From the promulgation of Earthquake Disaster Countermeasure Act, related enforcement decree (Presidential Decree No. 21362) that consists of 8 chapters and 16 articles were enacted and enforced in Mar. 25, 2009. And Enforcement ordinance (Ordinance of Ministry Public Administration and Security No. 72) that consists of 5 articles were enacted and enforced in Mar. 26, 2009.

3.3 The third phase of earthquake disaster countermeasure plan

To keep and make safer Korea for the future earthquake disaster, the 3rd Earthquake Disaster Countermeasure Plan is propelled from 2009. In this 3rd phase from 2009 to 2013, it is mainly focused on the 6 kinds of subject including (1) the seismic retrofitting for the existing structures adopted non-seismic design, (2) development and application of seismic hazard map, (3) development of earthquake notification and response system for the rapid response, (4) development of tsunami countermeasures, (5) strengthening the public education and training related to the earthquake disaster prevention and (6) strengthening and maintenance for the legislation and the organization dedicated to the earthquake will be mainly propelled. In this Earthquake Disaster Countermeasure Plan, it is established by 3 kinds of main tasks these are divided by 8 kinds of subsidiary tasks. And 8 kinds of subsidiary tasks are divided by total 24 kinds of tasks. From 8 kinds of subsidiary tasks, R&D project are being partially implemented in this year 2009 with 58 detailed projects. The 3 kinds of main tasks including 8 kinds of subsidiary tasks are as follows.

(1) Seismic Performance Level and Legal System Maintenance
- Establishment of integrated seismic performance level
- Maintenance of Institutionalized organization for effective promotion regarding to the propelling of Earthquake Disaster Countermeasure Plan

(2) Prevention and Preparation
- Advancement of observation system for the earthquake/tsunami
- Development and utilization of the earthquake hazard map and active faults map
- Re-establishment of seismic design provision and propelling of seismic retrofitting for existing facilities
- Establishment of tsunami disaster countermeasure
- Strengthening of the public education and training program to the nation related to the earthquake disaster prevention

(3) Response and Recovery
- Development of rapid response system for earthquake occurrence

4. Earthquake Disaster Management System

For the prompt damage estimation according to the earthquake occurrence, Earthquake Disaster Management System (EDMS) was developed in 2006. As development of EDMS shown in Fig. 5~6, it is possible to inform the National-wide intensity map, estimation results of the casualties and damages in structures.

Figure 5: Precedence and Advanced Research on EDMS

Fig. 5 shows the development process including the precedence researches which was established and advanced research which will be establishing on EDMS. In 2008 research and development, further development of damage estimation of lifelines and support system concerning with emergency response was surveyed and applied to the EDMS. And 3rd phase of Earthquake Disaster Countermeasures Plan, additional implementation of the system's advancing including the improvement of accuracy and extending the items to damage estimation shown in Fig. 6 will be propelled.

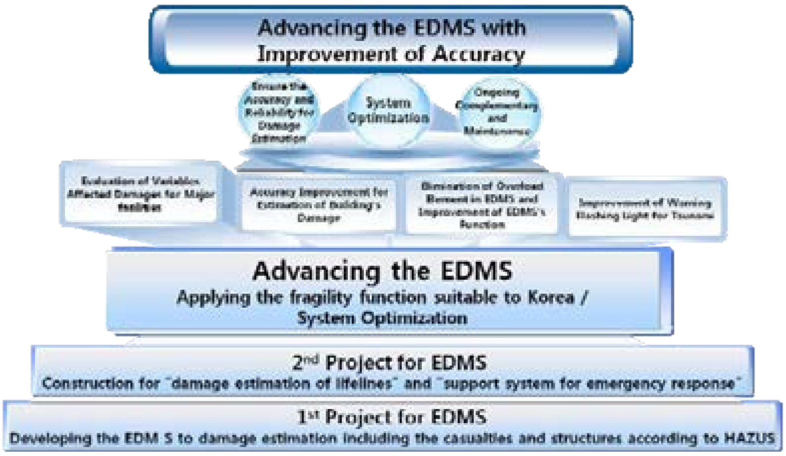

Figure 6: Advancing the EDMS

6. CONCLUSION

It is true that Korea is relatively safer than neighboring countries for the disastrous earthquake and also recent hazardous natural disasters occurred in Korea have been mainly caused by meteorological and hydrological phenomena. However, frequency of earthquakes is increased steadily, and also, Korean peninsula located in border line of Pacific Plate. For that reason, it is urgently needed to prepare the future earthquake. Lessons from disastrous earthquakes cases, all passions and efforts for earthquake disaster mitigation will be devoted with Earthquake Disaster Countermeasures Plan.

REFERENCES

Yi, W. H., 2009, Earthquake Disaster Management Policies in Korea, International Seminar on Disaster Prevention Technology 2009, 57-95

National Emergency Management Agency, 2009. Earthquake Disaster Countermeasure Plan, 204.

National Emergency Management Agency, 2009. Disaster Management for 60 years, 580.

PARALLEL SESSION 1

RESEARCH ON DIGITIZED EMERGENCY RESPONSE PREPLAN FOR PUBLIC SAFETY IN CHINA

WEICHENG FAN
Center for Public Safety Research, Tsinghua University, Beijing, China
State Key Laboratory of Fire Science,
University of Science and Technology of China, Hefei, China
wfan@tsinghua.edu.cn
GUOFENG SU
Center for Public Safety Research, Tsinghua University, Beijing, China
sugf@tsinghua.edu.cn
HONG HUANG
Center for Public Safety Research, Tsinghua University, Beijing, China
hhong@tsinghua.edu.cn

ABSTRACT

Public safety is threatened by numerous disasters and accidents which lead to tremendous loss of life, damaged infrastructures and lifelines, collapsed buildings and houses, and unstable society, etc. It is the responsibility of government and related departments to give a fast and efficient response to this kind of public accidents. Emergency response preplan is the accident control and disaster relief plan which is made by the government or companies beforehand to reduce the unexpected consequence of the public safety related accidents based on the hazard source assessment and disaster forecast analysis. The preplan is the guideline for the emergency response and rescue activity. In this paper, the concept of the emergency response preplan is introduced. Especially the research on digitized emergency response preplan in China is presented. As an example, the digitized emergency response preplan for fire safety of Beijing Olympic venues is shown here. It can give the strong support for arrangement of action and rescue of extinguishing activity, and provide an advanced means of strategy, technical and psychologist training for firefighters, and enhance the comprehensive management of fire emergency response.

1. INTRODUCTION

In recent years, public emergency accidents occur frequently due to urbanization, globe climate change, informationized society, etc. Such as, recent H1N1 influenza, Wenchuan Earthquake in China, Cyclone Nargis in Myanmar, SARS rampant in China, Sumatran earthquake and its resultant tsunami, Hurricane Katrina in USA and 911 terrorism in USA, etc. These accidents all lead to tremendous loss of life, damaged infrastructures and lifelines, collapsed buildings and houses, and unstable society. It is the responsibility of government and related departments to give a fast and efficient response to this kind of public accidents.

After suffered many public accidents, China government recognized the importance of emergency response to public accidents and contributes great effort to promote emergency management. On January 8, 2006, The China State Council issued the national plan on emergency response (China State Council, 2006). The National Emergency Response Preplan aims to increase the government's capability to protect public safety, deal with unexpected accidents, minimize the losses of the accidents, maintain social stability, and promote the harmonious and sustainable development of the country. When the National Emergency Response Preplan is announced, all provinces, autonomous regions and municipalities begin to make their own emergency response preplans, indicating a basic emergency response framework has been set up in China.

In this paper, the concept of the emergency response preplan is introduced. Especially the research on digitized emergency response preplan in China is presented. As an example, the digitized emergency response preplan for fire safety of Beijing Olympic venues is shown here.

2. CONCEPT OF EMERGENCY RESPONSE PREPLAN

2.1 Text and digitized emergency response preplan

Emergency response preplan is the accident control and disaster relief plan which is made by the government or companies beforehand to reduce the unexpected consequence of the public safety related accidents based on the hazard source assessment and disaster forecast analysis. The preplan is the guideline for the emergency response and rescue activity (Fan and Su, 2005).

Usually, these preplans are in the form of text saved in security boxes or electronic medium. Once public accident occurs, the procedure and treatment formulated by these preplans are the major base of the first action. Generally, the hypotheses of the progress process and consequences of the accidents are used when making these preplans. However, because the actual situation usually is very complex, it is impossible that the hypotheses are consistent with the actual accident progress. Therefore, the emergency response preplan cannot be directly used to deal with the public accidents. The text preplan must be revised and amended based on the past experiences, the past cases, on-site situation and theory models to form the actual response action plan for dealing with the public accidents. Because coupled with the science model, decision-making technology and case analysis result, the actual response action plan is called intelligent plan.

Series analysis processes, including the introduction of the past cases, experiences, models, on-site information and database, etc, are needed for the generation from the text preplan to the intelligent plan. If we make the key points in the text preplan structured, and associate, link and embed the required past case libraries, knowledge database, model database to the preplan through some specific ways, then we can establish a new type of preplan based on the computer information system (Yuan et al, 2007).

This preplan includes not only the procedures and methods regularized by the text preplan, but also the required information in the generation process from the text preplan to the intelligent plan. The information include the spatial structure, experts, models, cases libraries, knowledge, emergency resources and other information based on the response platform. This preplan can shorten the generation time from the emergency response preplan to emergency response plan, it is more efficient to play a role of the preplan and implement training exercises and update of the preplan. This new type preplan is called digitized preplan. When public accident occurred, based on the accident information and other related data information, the digitized preplan system will rapidly provide a direct and efficient action plan (intelligent plan) and adjust the action plan in real time. Figure 1 shows the differences between the text and digitized preplan.

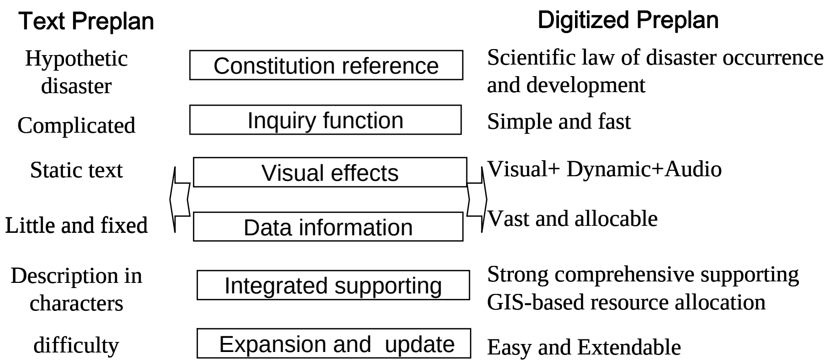

Figure 1. The comparison between text preplan and digitized preplan for emergency response

2.2 Functions of digital emergency preplan

Digitized preplan system is established to satisfy the emergency response to the public accidents. The aim is to rapidly and efficiently accomplish the emergency rescue actions. Digital emergency preplan has following functions.

1) Emergency response information management

Emergency response information is the all data related to the public accident emergency response including preplan information, space environment information, emergency response resource information, on-site situation information and past cases information. These information are very important for emergency response, management of these information is the base function of the preplan.

2) Accident situation analysis and simulation

Accident situation analysis is the analysis by the emergency response personnel. Such as, analysis of the influence area of the accident, statistics analysis of the environment in the emergency area, population, facilities, hazard source and emergency resources, and risk and loss analysis, etc. These analyses will provide emergency response personnel a comprehensive and detailed understanding of the process of the accident and emergency situation. Simulation includes event simulation and emergency response process simulation. Event simulation refers to the simulation of the event of the accident and the prediction of the progress tendency, influence area, damage degree, etc. For example, fire spreading simulation, pollution simulation, hazardous chemical leak prediction, explosion analysis, social stability analysis, meteorological disasters analysis, typhoon track forecasts, landslide and debris flow forecast, a large-scale epidemic spread of the disease prediction, evacuation simulation. These analyses can help emergency response personnel understand the trend of accidents, and make the proper emergency decisions.

3) Emergency response action plan generation and adjustment

Generation and adjustment of emergency response action plan is an auxiliary decision-making function. The emergency response action plan can be generated by the application of the digitized preplan with model database, knowledge database, case libraries, on-site situation and other information, and emergency information, accident situation analysis and simulation results of the current public accident. Emergency response action plan should not be static, but should change as circumstances change in order to better adapt to the actual situation. Therefore, digitized preplan system should adjust the generated action plan according to the accident information and simulation results.

4) Good human-machine interaction and presentation features

A good human-machine interaction capability for managing emergency information is necessary (Elizabeth, 2007) . A good presentation capability can show the accident analysis and simulation results and response process visually and directly, which will help emergency response personnel to better understand the situation more quickly and efficiently and make decision-making plans.

5) Emergency response effect assessment

Emergency response effect assessment refers to assess the emergency response steps, methods and results at the different stages of the emergency response and at the end of the emergency response to confirm if the steps and methods are correct. After the assessment, the system will be revised and improved based on the assessment results. After the emergency response, the emergency process will be compiled into a part of the case libraries.

6) Emergency response exercise

Emergency response exercise is to carry out the accident response exercise using the digitized preplan system in accordance with the virtual events and environmental information when no public accidents occur. The role of the emergency response exercise is to test and improve the digitized system so that emergency response personnel can become familiar with the emergency response procedures, while revise the imperfect parts of the system.

2.3 Structures of digital emergency response preplan

As a software system, the digitized preplan system needs corresponding software modules.

1) System operating interface

In order to make the digitized preplan system has a good human-machine interaction and presentation capabilities, the system interface should be intuitive and clear, easy to use, beautiful and generous.

2) Database system

Database system manages all data information of the digitized preplan system, including knowledge database, model database and case libraries.

Knowledge database includes related general and professional knowledge applied in the emergency response decision-making process. Model database includes all model data for accident analysis and simulation, such as the evolution and impact models, crowd evacuation and early warning classification model. Case libraries include the information of the past cases.

3) Analysis and simulation system

Analysis and Simulation system conducts the accident situation analysis and simulations. Speed and accuracy are necessary. Usually, it is difficult to satisfy both speed and accuracy. Fast model is not too accurate and the simulation speed of the relative accurate model is not satisfied. Therefore, it requires trade-off consideration. Usually, high accuracy model is used for preplan and a faster model is used for on-site simulation. For practical applications, a compromise plan will be applied to try to meet the requirements.

4) Decision-making support system

Decision-making support system helps emergency response command personnel to complete the generation and adjustment of the emergency response plan. The system operates throughout the emergency response process from the beginning to the end, which is the core of digitized system. Decision-making support system integrate the preplan information, database systems and on-site information to provide emergency response resources management and ensure the necessary resources through the master of the main rescue teams, emergency response reservation supplies and rescue equipments, emergency response communication systems, medical emergency response agencies, and emergency response financial reservation, etc. If necessary, it can rapidly provide new resources arrangement plan and achieve interactive, dynamic decision-making command.

5) Assessment system

Assessment system accomplishes the emergency response effect assessment by automatically recording of the accident response process, determination of the assessment index in accordance with the provisions of the emergency preplans and the integrate evaluation of timelines and efficiency of various measures in the emergency response and the evaluation of the emergency response ability combined with early warning system.

6) Geographic information system

Geographic information system is the support system of the digitized system to complete various functions. It can achieve the functions, such as spatial location, inquiry, spatial analysis. GIS can provide data support and spatial decision support for emergency response decision making with the powerful spatial inquiry and spatial analysis capabilities.

3. DIGITIZED EMERGENCY PREPLAN FOR FIRE SAFETY OF BEIJING OLYMPIC VENUES

The emergency response preplan for fire safety focuses on those activities which are directly related to an evolving firefighting or response of the potential incident. For the Olympic venue fire safety, it is the most important to direct based on the emergency response plan of the firefighting. To meet the demand of firefighting in the Olympic projects, Beijing Fire Bureau joined Tsinghua University and other agencies in researching and developing the digital firefighting project and the synchronized training system.

The Olympic venue fire safety preplan for emergency response provides a framework to enable the management of fire protection and firefighting as well as the prevention of and preparation for subsequent events. The main elements that should be included are: basic information about the venue and important units, combustible material and fire load, firefighting force distribution, put-out and rescue tactics, water supply methods, etc. The preplan is named as Fire Emergency Response Information System.

3.1 Fire emergency response information system design

The fire emergency response actions include from initial notification to early coordination efforts to assess and disrupt the incident, to preparatory activation of the response preplan, to deployment of city resources in support of firefighting and rescue operations. Fire brigade, police, public health and medical, emergency management, and other personnel are responsible for Olympic venue fire at the city level (Sun et al, 2006).

The fire brigade moves quickly to coordinate multiple department (police, public health and medical, etc.) activities which include the following: information-sharing (Jackson, 2006), integration of the resources, analysis and forecasting, alert and decision-making (Fredholm, 1997, Danielsson, 1998), interagency course of action development, operational coordination, and other assistance. In order to implement the firefighting and realize the purpose to fire response plan, all of these need a comprehensive information system for fire safety to bring together and make use of all necessary response resources quickly and effectively.

Figure 2. The fire emergency response information system

After being classified, the elements needed to be considered of the fire emergency response information system, as shown in Figure 2, include:

(1) Basic information of venue and its important parts

Such as venue name, address, unit layout, fire prevention zone, evacuation route, main combustible material type and quantity, fire hydrant and locations of firefighting forces, etc.

(2) To design and set fire

Original point of the fire, type of combustive material, fire power curve, type of the fire, possible serious consequence; temperature and concentration change of smoke, evacuation route, etc. are necessary.

(3) Task for fire fighting, control, search, rescue, evacuation

Such as arriving time and parking location of fire fighting vehicles, assigned tasks and resources, attack and back route, real time alarms, new resource requests and resource allocation, co-operation of multiple departments, etc.

(4) Firefighting tactics

Such as different material, different units, different buildings, different regions, different stages of the fire, different technical measures, different games, and different crowd, different water supply methods, etc.

(5) The others

Such as personal protective measures, information on casualties and losses, notes for special type of fires, environment conditions and information of adjacent buildings, etc.

The fire emergency response system is designed to improve the response operations more scientific, effective, and efficient. It is a centralized solution for firefighting correlation, information sharing, resources aggregation, fire development analysis, firefighting and rescue, evacuation and investigation of fire events with the networked matrix mode.

Using simulation and GIS technology, the information system combines hazard layers with city databases, and then applies standardized loss estimation and risk assessment methodology. The platform environment allows users to create graphic presentations, helping users visualize and understand their fire risks and solutions.

The information system gives decision-makers the tools to make better decisions. It establishes a mechanism for sharing the information all cross city including basic geographical information and public safety information, enhances the analysis of available options for rescue operation, optimizes the decision-making process, and can greatly improve the ability to select the best course of response plan.

3.2 General frame and functional modules of the information system

The general frame of the fire emergency response information system is shown in Figure 3:

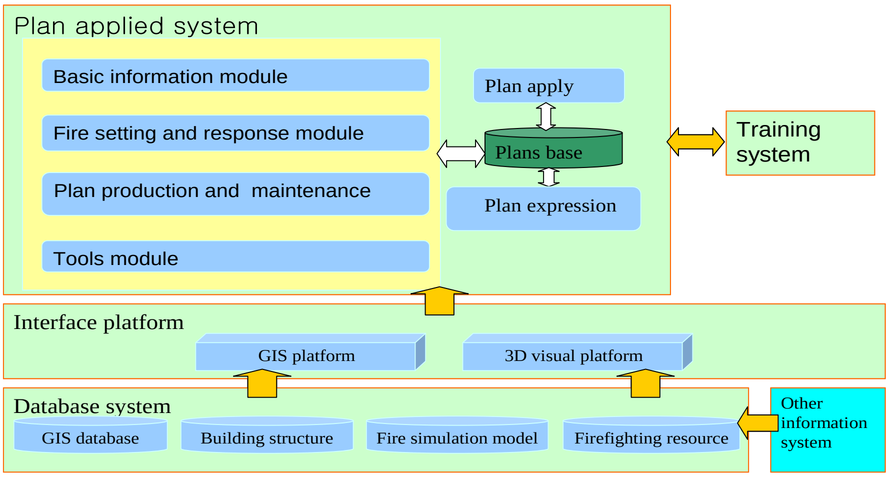

Figure 3. The general frame of the fire emergency response information system

The database of information system includes five parts: GIS database, building structure data, fire simulation models data, firefighting resource data, and plan database. In order to fulfill the fire emergency response plans, it is necessary to obtain the full and accurate geographical information and fire safety related information. The fire emergency response information system has already included a large amount of relevant basic information, such as topographical data of the city, pipe network data of the urban lifeline, information of the dangerous source, key place and infrastructure, rescue force, population distribution and layout of refuge area, etc. The data involved are extensive and complicated in space distribution to meet an urgent need for fire safety.

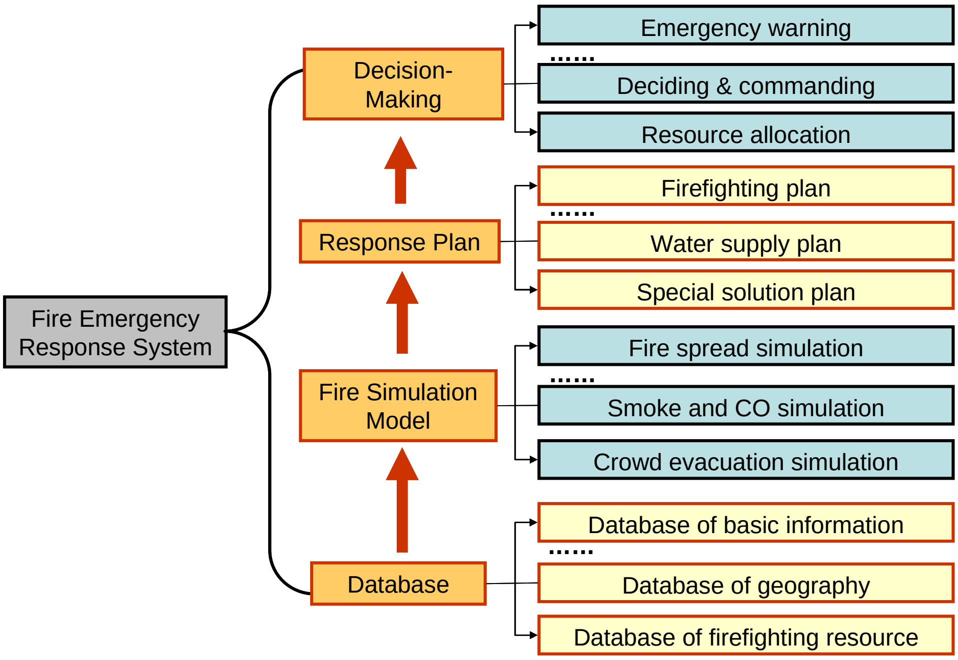

Figure 4. The function flow of the fire emergency response information system

Figure 4 describes the procedure how to get the executable action plan. We can obtain venue information from the monitoring system with the aid of GIS system, use the information in the fire response information system database, then choose the model which accords with present terms from the fire model database, input the data to forecast fire spread and analyze its risk. The results of calculation of these models can offer scientific basis for the firefighting and rescuing. Namely, according to the prediction result and firefighting resource distribution, the response plan is selected from the plan database, to optimize decision-making, and form series implementing commands and actions.

Figure 5 and Figure 6 give some examples about the visual interface in information system. Figure 7 illustrates that the system can provide valuable decision making support for fire emergency response. The interface shows the overall comprehension picture corresponding to the surround information of a venue fire incident. It displays information about venue, related buildings, outside hazards, supporting fire station, hospitals and police stations near to the vicinity of the incident. All on-site and on-road resources are given to plan overall consideration and arrangement according to the risk assessment. The on-going actions and the next tasks are adjusted according to response development.

Figure 5. The photo of Fengtai softball venue and the visual interface in information system

Figure 6. The fire emergency response preplan layout with RS picture

Figure 7. The firefighting force and resource analysis of the information system

4. CONCLUSIONS

The research on digitized emergency response preplan for public safety in China is presented in this paper. Many emergency response preplans are made to increase the government's capability to protect public safety, deal with unexpected accidents, minimize the losses of the accidents, maintain social stability, and promote the harmonious and sustainable development of the country. Digitized emergency response preplan is a new type computer information system based preplan which coupled with past case libraries, experiences, knowledge database, science model database and on-site information, etc. It will rapidly provide a direct and efficient action plan (intelligent plan) and adjust the action plan in real time.

As an example, the digitized emergency preplan for fire safety of Beijing Olympic venues is shown here. It can give the strong support for arrangement of action and rescue of extinguishing activity, and provide an advanced means of strategy, technical and psychologist training for firefighters, and enhance the comprehensive management of fire emergency response. The information system has been proven to be not only useful and rapid during firefighting venue fire, but also economical in firefighting exercise.

REFERENCES

China State Council, 2006. National Emergency Response Preplan.

Danielsson, M., 1998. The cognitive structure of decision making tasks in major versus minor emergency responses. In Scott PA, Bridges RS, Chasterrs J (eds.): *Proceedings of the Global Ergonomics. Cape Town, South Africa*, 627-632.

Elizabeth, C., Murray, T., 2007. Human-Computer Interaction: The Human and Computer as a Team in Emergency Management Information Systems. *Communications of the ACM*, 50, 3, 33-38.

Fan, W.C. Su, G.F., 2005. Progress in emergency management research for a Mega-city in China, *4th USMCA International Symposium. Singapore*, 31-39.

Fredholm, L., 1997. Decision making patterns in major fire-fighting and rescue operations. In R. Flin, E. Salas, M. Strub & L. Martin (eds.): Decision Making under Stress. Aldershot: Ashgate, Bookfield USA.

Jackson, B.A., 2006. Information sharing and emergency responder safety management. Available at: http://www.rand.org/pubs/testimonies/2006/RAND_CT 258.pdf.

Sun, Z.H., Su, G.F. et al. 2006. Fire hazard analysis and digital fire emergency response plan, *Journal of Basic Science and Engineering* 14, 205-211.

Yuan, H.Y., Su, G.F., et al, 2007. Discussion of text preplan, digital preplan and intelligence preplan in emergency management, *China Emergency Management* 4, 4, 20-23.

BEHAVIOR OF LEVEE MODELS REINFORCED WITH CUTOFF STEEL SHEET-PILES DURING EARTHQUAKE

MASARU KANEKO
The University of Tokyo, Japan
masaru3@iis.u-tokyo.ac.jp
JUNICHI KOSEKI
Institute of Industrial Science, The University of Tokyo, Japan
koseki@iis.u-tokyo.ac.jp

ABSTRACT

The number of local downpour that causes damage to levee is increasing recently in Japan. Furthermore, we have tremendous losses due to the breach of levees all over the world, and this was the exact real case in the 2005 Hurricane Katrina in USA. Therefore, the role of levee has become more important than before, in particular with urban areas.

In view of the above, we analyzed results from a series of relevant shaking table model tests, in which an embankment model resting on a liquefiable sandy soil layer was reinforced with steel sheet-piles. Existence of sheet-piles affected the response acceleration characteristics and properties of the excess pore water pressure generation. Bending strains induced in the cutoff sheet-piles were larger in the deeper part, especially at the embedded regions. Sheet-piles installed at the foot of the embankment suffered from larger bending strains than those installed at the shoulder of the embankment.

1. INTRODUCTION

Figure 1: Breached levee in USA

Figure 2: Subsided levee in Japan

Fig.1 shows a photograph of breached I-type flood walls in the 2005 Hurricane Katrina, USA (US Army Corps of Engineers, 2006). During the Hurricane Katrina, collapse of Hurricane Protection System (HPS) triggered catastrophic damages in southeast Louisiana. Sasanakul et al (2008) reported that the cause of I-wall's breaching was composed of two factors; one is the misinterpretation of geologic conditions and the other is the lack of the penetration depth of the sheet-pile into clay layer.

Fig.2 shows an example of earthquake-induced damage to non-reinforced levee during the 1995 Hyogoken-Numbu earthquake, Japan. This levee was located along Yodogawa-river, which separates Osaka and Hyogo prefectures, and the crest of this levee settled down by 2 or 3 m, due to the influence of liquefaction in the foundation layer. If a typhoon or heavy rainfall attacked these areas just after the earthquake, the river water would overflow easily because of the lack of the levee height, and tremendous losses would be induced.

These case histories suggest that some of the levees should be reinforced properly in order to protect our lives and properties from floods. As one of the methods to reinforce levees, use of steel sheet-piles has been considered widely in Japan. For example, the sheet-piles have been used for the revetments along urban rivers. Nowadays, they are also used as the reinforcement for foundation soils against liquefaction.

In view of the above, we set two main targets for our research; the first one is to examine whether subsidence of a levee could be reduced by means of reinforcement with steel sheet-piles after liquefaction occurs in foundation soils, and the second one is to check whether the reinforced levee could keep its required performance to protect our lives and properties, when floods break out. In this paper, regarding the first target, analysis of test results from a series of relevant shaking table model tests (JASPP 2002) is conducted, in which reinforcement of the levee resting on a liquefiable sandy soil layer with steel sheet-piles was made, focusing especially on response characteristics and bending strains of sheet-piles.

2. MODEL CONTAINER AND TEST CONDITIONS

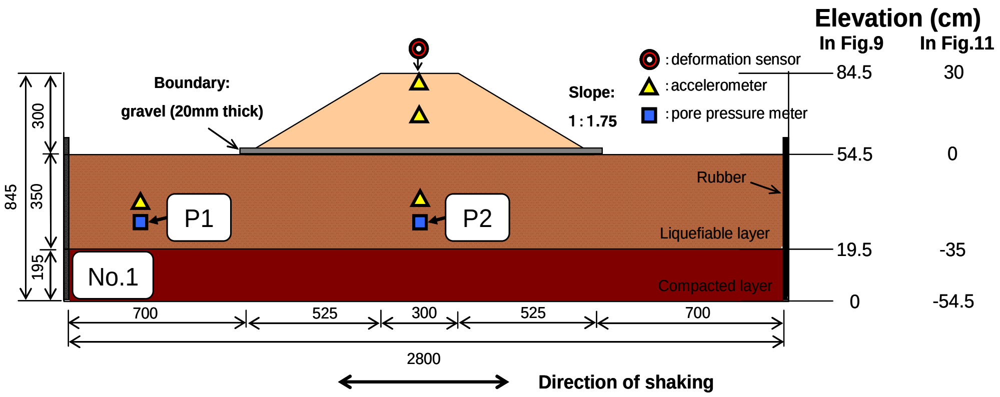

Figure 3: Model container and the definition of elevation

Fig.3 illustrates the configuration of a soil container which measures 2800 mm in length, 340 mm in width, 845 mm in depth. The model ground and levee were made of silica sand No.7 (G_s=2.648, D_{50}=0.177 mm, F_c=1.4 %). The model ground consisted of 2 layers; the lower one named as "compacted layer" having a relative density D_r of approximately 90%, and the upper one was named as "liquefiable layer" having a D_r value of approximately 40%. During shaking, the ground water level was maintained at the surface of the liquefiable layer. The model levee had a height of 300 mm with the slope of 1.75 horizontal to 1 vertical. Five models with different patterns of sheet-piles installation, named as No.1 through No.5 as shown in Fig.3 and Fig.4, were prepared. Fig.5 shows two types of input waves, the one named "a" is the sinusoidal wave (5Hz) with tapered amplitudes, and the other one named "b" is the sinusoidal wave with constant amplitude (5Hz). Each model was subjected to horizontal excitations by following the 4 steps of excitation events step by step.

Step 1 a-300gal
Step 2 a-500gal
Step 3 b-300gal
Step 4 b-500gal

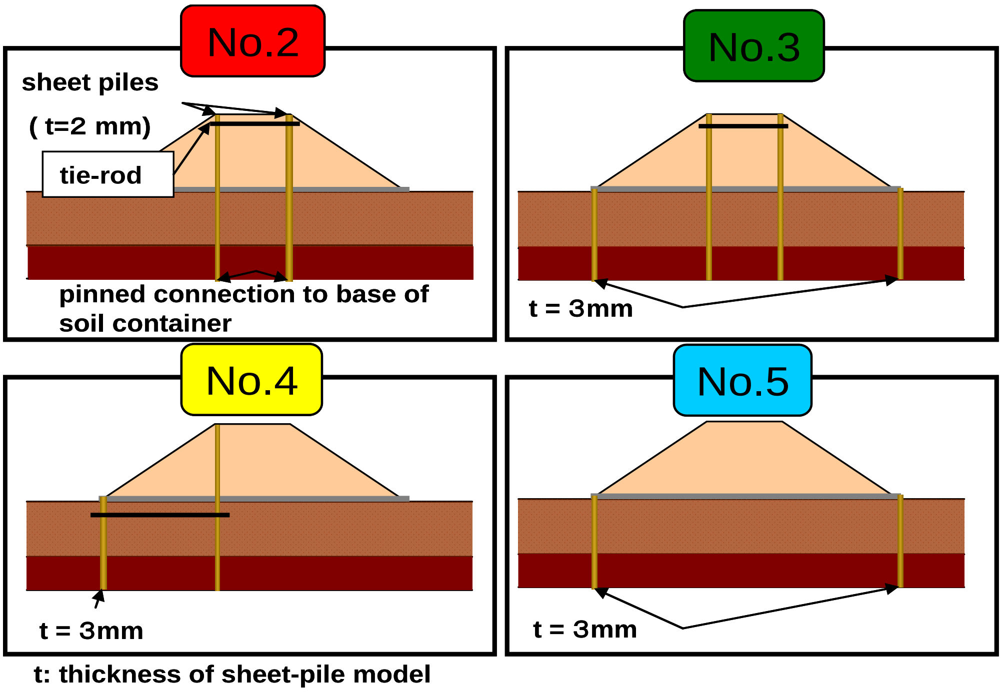

Figure 4: Illustrates of each case

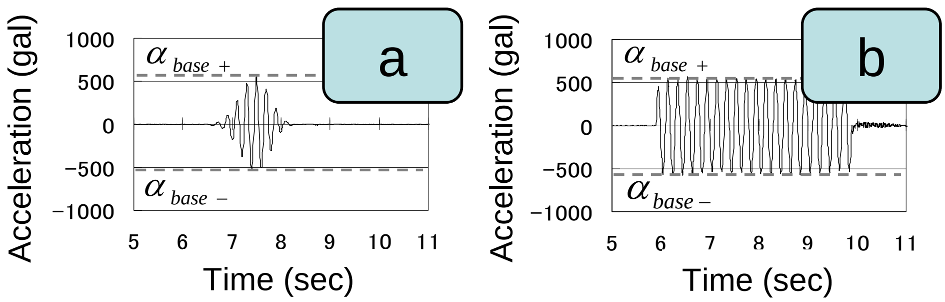

Figure 5: Input waves

3. ANALISIS OF TEST RESULTS

3.1 Residual Subsidence

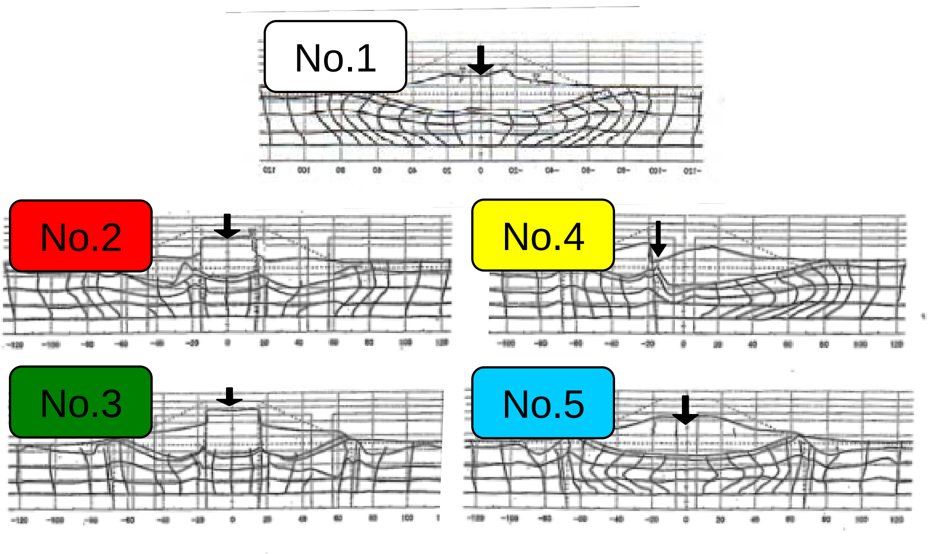

Figure 6: Residual deformation

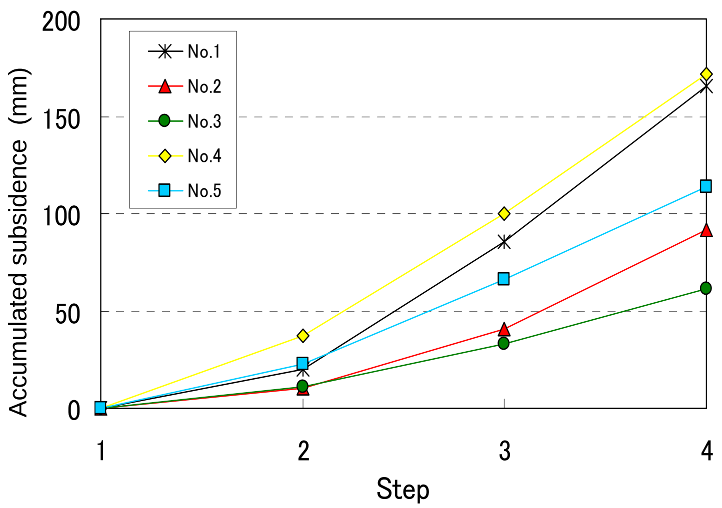

Figure 7: Accumulated subsidence

Fig.6 shows the illustrations of the residual deformation observed after the Step 4 excitation, and Fig.7 shows the accumulated residual subsidence at the crest of the model. It is noteworthy that, though the lateral flow of liquefied subsoil was observed in every case, it could be mitigated to some extents due to the installation of sheet-piles except for case No.1. The levee models with cases No.1 & No.4 remarkably settled down because of no or lack of reinforcement. On the other hand, those of cases No.2 & No.3 did not subside so largely. These results reveal that sheet-piles that are installed in both shoulders of the levee can exhibit the greatest effects in mitigating the subsidence of the levee.

3.2 Response Acceleration of Levee

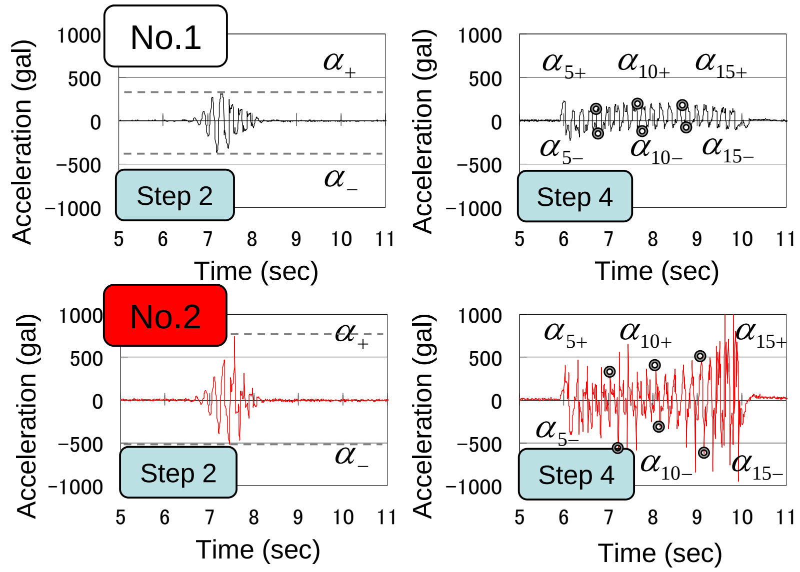

Figure 8: Response accelerations at the crest of the levee model

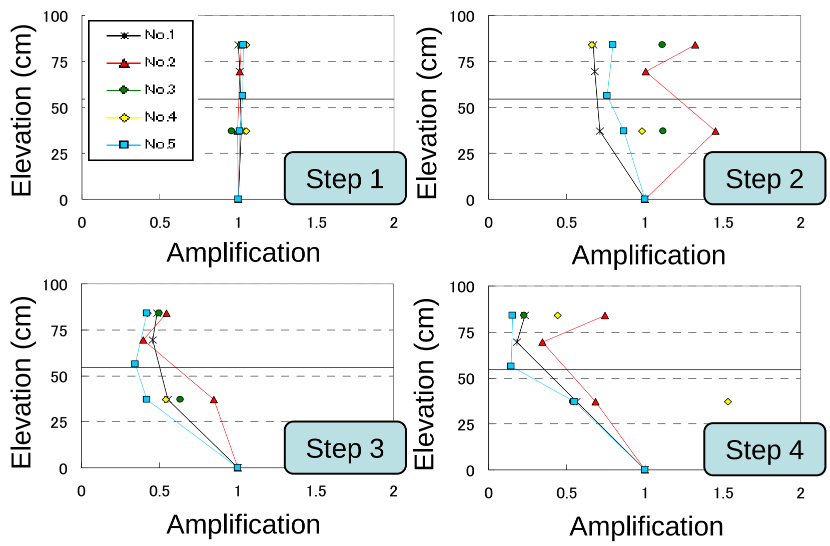

Figure 9: Amplification factors in each case

Typical time histories of response accelerations at the crest of the levee model are presented in Fig.8. The maximum amplitudes of responses acceleration in case No.2 were larger than those in case No.1. The levee model in case No.1 did not respond considerably due possibly to the effect of base isolation by the liquefiable subsoil under the levee. On the other hand, the levee model in case No.2 was larger due to the confinement by the pair of sheet-piles and the tie-rod. Fig.9 shows the distribution of the amplification factors of response acceleration measured at the central axis of the levee model and its underlying liquefiable layer. The elevation is measured from the bottom of the compacted layer (Fig.3). The amplification factors are defined as follows:

$$\text{Amplification factor} = \alpha_{max} / \alpha_{base} \quad \text{(Step1, Step2)}$$
$$= \alpha_{ave} / \alpha_{base} \quad \text{(Step3,Step4)} \qquad (1)$$
$$\alpha_{max} = \max(\alpha_{+},\ \alpha_{-}) \qquad (2)$$
$$\alpha_{base} = \max(\alpha_{base+},\ \alpha_{base-}) \qquad (3)$$
$$\alpha_{ave} = \frac{1}{3}\left(\sum_{i=5,10,15} \frac{1}{2}\left|\alpha_{i+} - \alpha_{i-}\right|\right) \qquad (4)$$

α_{+} & α_{-} are shown in Fig.8, and α_{base+} & α_{base-} in Fig.5. In this paper, α_{ave} is defined as the average of the amplitudes of response acceleration in the 5th, 10th, and 15th cycles. No significant difference between the four cases was seen in Step 1, while clearly different behaviors of response acceleration were observed in Step 2. In Step 2, the values of the amplification factors in cases No.2 and No.3 were over 1.0 due possibly to the effect of confinement by the sheet-piles and the tie-rod, while those in other cases were under 1.0 due to the effect of base isolation as explained above. In contrast, in Step 3 and Step 4, every case showed a reduced value of the amplification factor. These results indicate that the influence of liquefaction appeared in every case, though the extents of liquefaction were different among the different cases.

3.3 Pore Water Pressure and Response Acceleration of Liquefiable Layer

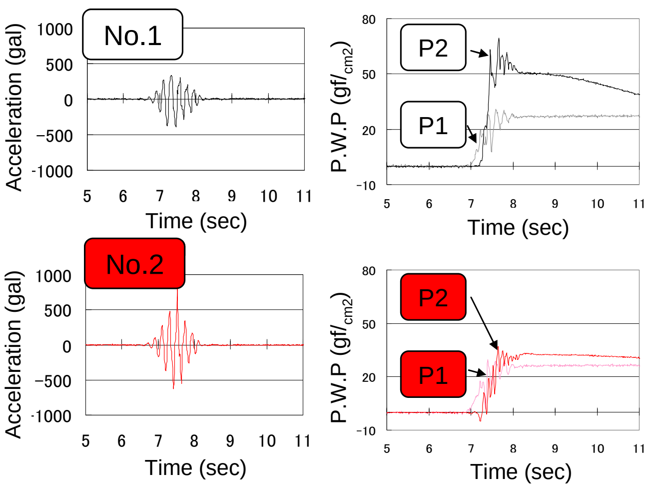

Figure 10: Pore water pressures and response accelerations

In order to investigate more in detail, the difference in the amplification factors between cases No.1 and No.2 in Step 2, the recorded time histories of response acceleration of the liquefiable layer under the levee model and excess pore water pressures measured at P1 and P2 (see Fig.3) are shown in Fig.10. In terms of the response accelerations, the underlying liquefiable layer showed a behavior that was similar to that of the levee itself, as stated in 3.2. The excess pore water pressures, measured at P1 were almost the same behaviors in both cases. However, the excess pore water pressure, measured at P2 below the levee was higher and more rapidly increased after 7sec in case No.1 than in case No.2. Such rapid increase of excess pore water pressure in case No.1 lead to the reduction of effective stress in the liquefiable layer below the levee, and thus affected the response accelerations as well.

3.4 Residual Bending Strain of Sheet-piles

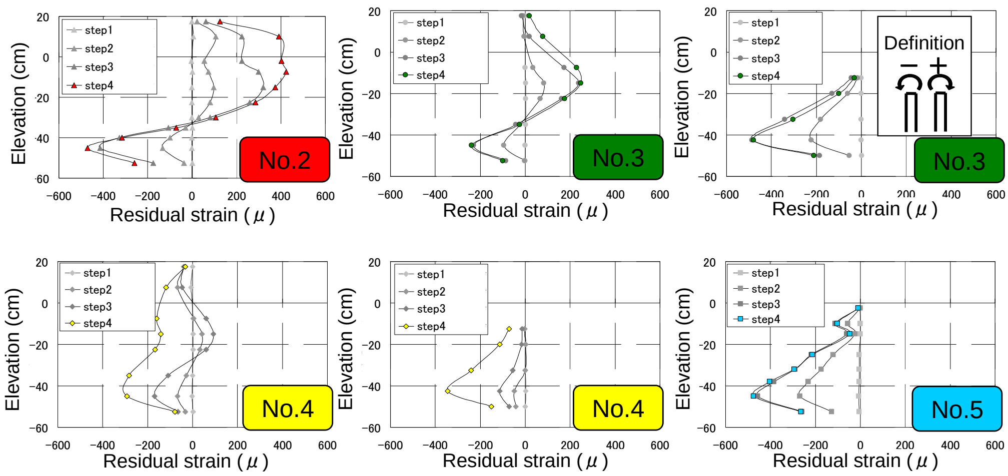

Figure 11: Distribution of residual strain of sheet-piles

Fig.11 presents the distribution of residual bending strain of sheet-pile obtained after each shaking step. The vertical axis shows the elevation which is measured from the surface of the liquefiable layer (Fig.3), and the direction of positive bending strain is defined as shown in Fig.11. The strain was defined to be zero immediately before applying the step 1 shaking. In all cases on the whole, positive strains appeared from the top of levee to the middle of liquefiable layer, and negative strains appeared at the deeper positions. They are influenced by increased earth pressure acting from the levee and the liquefied subsoil, and the tensile load mobilized in the tie-rod. In cases No.3 and No.4 which have two kinds of sheet-piles, one installed at the shoulder of the levee model and the other at its toe, the negative bending strains after shaking become maximum at the lower part of the sheet-pile at the toe.

3.5 Maximum Bending Strain during Shaking

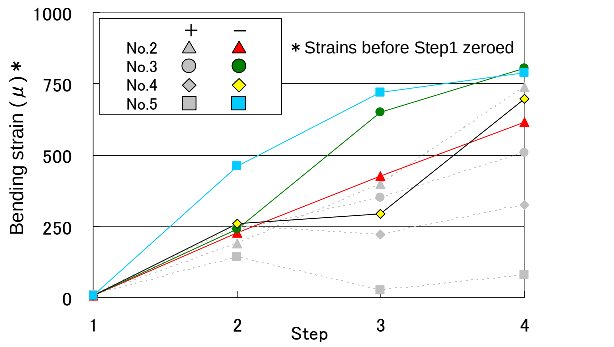

Figure 12: Maximum bending strains during shaking

Fig.12 shows the maximum values of both positive and negative bending strains of sheet-piles during each shaking step. As a whole, negative strains were larger than positive ones except for Step 4 in case No.2, and this tendency was more significantly observed in cases No.3 & No.5, as compared to the other cases.

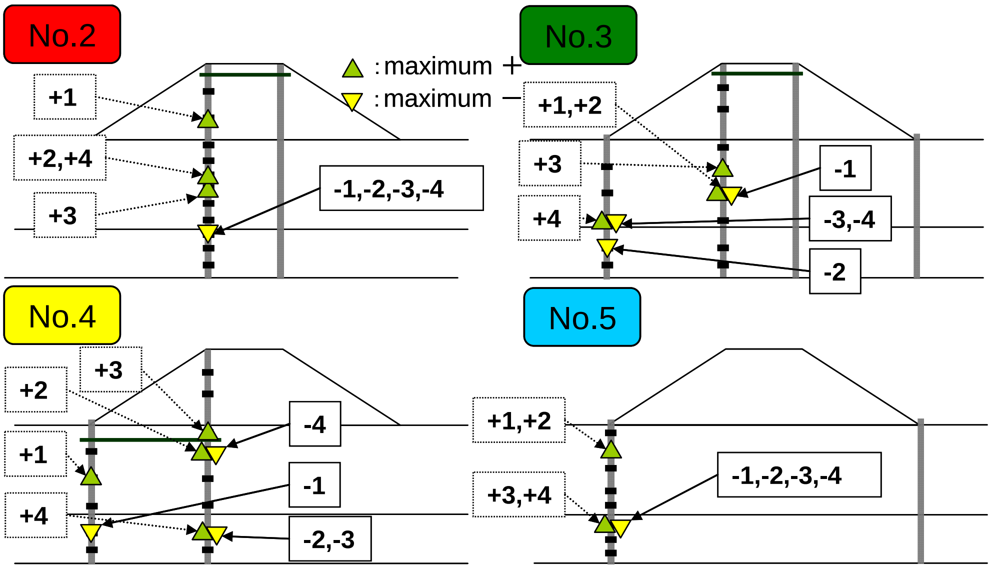

Figure 13: Positions of maximum bending strain

The positions where the maximum bending strain was observed are illustrated in Fig.13 (the numbers in each box indicates the step number). Almost all the maximum negative bending strains in cases No.3 & No.5 were recorded at the lower part, i.e., at the boundary between the liquefiable and compacted layers, of the toe sheet-pile that was not connected by the tie-rod. Generally, the maximum bending strains during shaking were recorded at nearly the same position as the residual bending strain (Fig.11).

4. CONCLUSIONS

In this paper, analysis of results from a series of relevant shaking table model tests on levees reinforced with cutoff steel sheet-piles is made. Test results revealed that sheet-piles contributed to reduce the subsidence of the crest of levee, while the extent of the mitigative effect depended on the locations of their installation. Moreover, sheet-piles affected the response accelerations and the excess pore water pressures, and they were closely related with each other. As for bending strains of sheet-piles, they were larger in the deeper part, especially at the boundary between liquefiable and compacted layers, and those of the sheet-piles at the toe of the levee model tended to be larger than those at its shoulder, when two pairs of cutoff sheet-piles were installed.

REFERENCES

Japan Association for Steel Pipe Piles (2002) *"Technical report on levees reinforced with steel sheet-piles" 33p. (in Japanese)*

Sasanakul , I. et al. (2008) *"New Orleans System Performance during Hurricane Katrina: 17th Street Canal and Orleans Canal North". Journal of Geotechnical and Geoenvironmental Eng., ASCE, 657-667.*

US Army Corps of Engineers (2006) *"Performance Evaluation of the New Orleans and Southeast Louisiana Hurricane Protection System, Draft Final Report of the Interagency Performance Evaluation Task Force", V-9.*

PERSPECTIVES ON SUSTAINABLE PRACTICES AND MATERIALS IN THE JAPANESE CONCRETE INDUSTRY

MICHAEL HENRY
Department of Civil Engineering, The University of Tokyo
mwhenry@iis.u-tokyo.ac.jp
YOSHITAKA KATO
ICUS, Institute of Industrial Science, The University of Tokyo
katoyosh@iis.u-tokyo.ac.jp

ABSTRACT

One of the difficulties in adopting sustainable practices is the wide variety of perspectives on what exactly constitutes sustainability. For the concrete industry, people have focused primarily on the environmental aspect of concrete, which typically includes CO_2 emissions, resource consumption, and waste generation. However, the concrete industry itself is composed of a large collection of separate social groups, each of which has their own perspective and goals regarding the usage of concrete and how sustainability should be achieved. In order to take a step forward towards resolving a unified approach to sustainable practice in the concrete industry, it is necessary to understand how these social groups view concrete as a technology – looking specifically at their relationship to concrete as well as their knowledge level of sustainability. By evaluating these perspectives, a picture of contrasting problems and solutions can be formed, which will then allow for progress towards a common goal of sustainable practice by negotiating the differences between these social groups.

1. INTRODUCTION

The increasing frequency of environmental disasters, such as hurricanes and floods, has emphasized the importance of considering global climate change as a danger to public safety. Climate change has been attributed to rapid growth, urbanization, and industrialization over the past hundred years and, if such unsustainable development continues and deterioration of the global climate goes unchecked, may lead to more disasters due to rising sea levels and changes in wind and temperature patterns (IPCC, 2007).

In order to prevent or mitigate these future disasters, modern societies are attempting to adopt sustainable practices by considering the effects of their actions on the development of future societies. However, even though sustainable development was proposed by the United Nations in 1987, the term was defined in at least 57 different ways from 1979 to 1997 (Murcott, 1997), demonstrating that there still remains much debate regarding what constitutes sustainability. One modern means of visualizing sustainability is given in Figure 1, where it is shown as the integration of the three “pillars”: the environment, society, and the economy. This image captures the idea that the three pillars are not separate but, rather, there exists a co-dependency between them; for example, the well-being of society depends on the well-being of the environment.

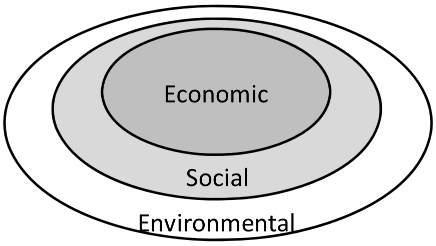

Figure 1 Visualization of sustainability (Cornell, 2009)

The concrete industry contributes both positively and negatively to all three of the areas shown in Figure 1. The concrete industry is a massive employer world-wide, and concrete material is a fundamental component of the infrastructure necessary to support human society. However, concrete also carries with it a significant environmental impact, from emissions due to manufacturing and transport to resource consumption and land use for material production. Furthermore, the production of concrete infrastructure is not a simple process, but involves the labor and cooperation from many different stakeholder groups, such as general contractors, ready-mix plants, cement manufacturers, researchers, government agencies, and so forth. Each of these groups has a unique role, and thus different perspectives and goals. Furthermore, different stakeholders are going to be affected by sustainable practice in different ways, and they may have to compromise their individual goals in order to meet social or environmental requirements.

It is necessary to consider these different perspectives in order to develop a unified approach to sustainable practice in the concrete industry. This paper takes the first step in this process by dividing the concrete industry into different social groups and evaluating their perspectives on topics relating to concrete, sustainability, and sustainable practice and materials in the concrete industry.

2. METHODOLOGY

2.1 Selected social groups

For this study, the Japanese concrete industry was selected due to the authors’ access to experts through domestic industry contacts. The industry itself was divided into four categories: academic, government, contractor, and manufacturer. These categories were selected based upon the structure of the Japanese industry and consideration of the social groups relevant to concrete construction, as described in Figure 2. For civil structures, the government is typically the owner. These groups may also be composed of sub-groups; the government has research institutes as well as construction bureaus, contractors have internal divisions and research groups, and manufacturers include cement producers, aggregate quarries, ready-mix concrete plants, chemical admixture companies, and so forth.

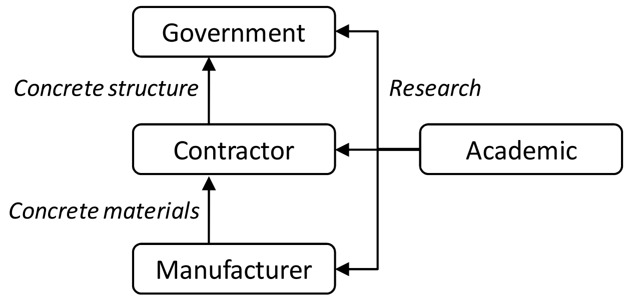

Figure 2 Conceptual structure of concrete industry (civil structures)

2.2 Semi-structured interviews

The social groups' perspectives were evaluated using semi-structured interviews. Semi-structured interviews fall between structured and unstructured interviews, as shown in Figure 3, where the dimensions are degree of structure and depth. Structured interviews are rigid and standardized, with precoded categories for responses, and do not investigate in great depth; unstructured interviews are flexible, following a general set of questions which guide the overall direction of the interview but allow for areas of interest to be investigated in further detail (Punch, 2005).

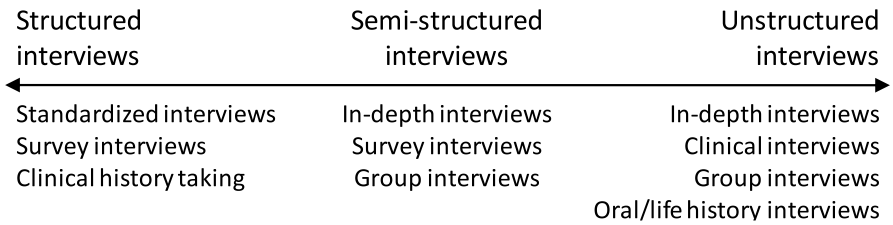

Figure 3 Continuum model for interviews (Minichiello et al., 1990)

After contact was made with the interview subjects, they were provided with an interview summary which contained an overview of the primary questions to be asked. The interview was then conducted following the primary questions, but deviating as necessary to provide clarification on topics of interest. In some cases, the interviewee provided answers to the summary before the interview, in which case the interview was conducted to clarify or expand upon the interviewee's response in greater detail. The interviews were generally conducted in English, but when Japanese was used interview results were translated to English before analysis.

2.3 Research hypotheses & interview topics

This research was conducted in order to understand the perspectives held by different social groups within the concrete industry on the adoption of sustainable practice. Therefore, two main hypotheses were proposed:

(1) The social group's perspective on sustainable practice is affected by their relationship with concrete.
(2) The social group's perspective on sustainable practice is affected by their concept or definition of sustainability.

Based upon these hypotheses, a general outline of the interview topics is given in Figure 4. Sustainable practice in the concrete industry was broken into three different categories based on the authors' research interests.

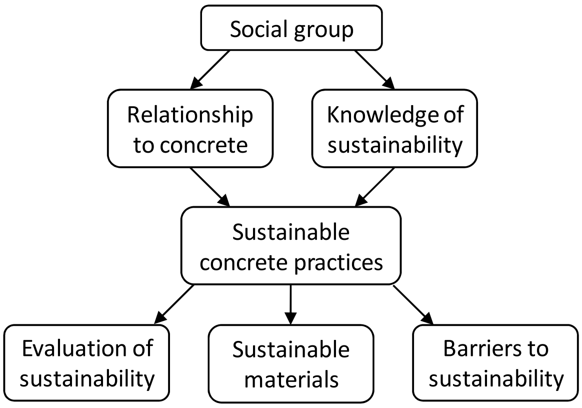

Figure 4 Outline of interview topics

2.4 Coding

Interview results were organized and analyzed by coding. Codes are tags or labels used to give meaning and are attached to data, such as words, sentences, or paragraphs, in order to facilitate retrieval and organization of data for clustering and drawing conclusions (Miles & Huberman, 1994). After conducting the interviews an initial list of codes was constructed to begin analysis and refine the interviewing process for future interviews. Some examples of codes and their definitions are given in Table 1. These codes describe the social groups' perspectives by identifying goals, relationships, indicators, definitions, conflicts, problems, and actions.

Table 1 Examples of codes and definitions

Code	Definition
GOAL	The social group's goals or targets
REL	Relationship between the social group and another social group
IND	Indicators used for evaluating concrete, sustainability, etc.
DEF	The social group's definition of a term or concept
CONF	Conflict between the social group and another social group
PROB	Problem as viewed by the social group
ACT	Action the social group should take or believes should be taken

3. INTERVIEW RESULTS & DISCUSSION

3.1 Distribution and description of interviewees

The distribution of interviewees is shown in Figure 5 and described in Table 2. Six people were interviewed: five of them are involved in research and/or technology development; four of them have worked in an academic setting and have doctoral degrees; three of them are directors or managers; half of the interviewees belong to material manufacturing companies; one is a CEO and one is a professor.

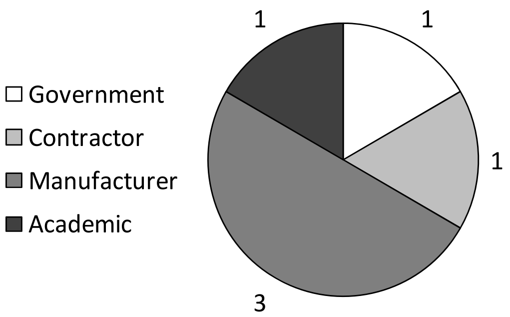

Figure 5 Distribution of interviewees

Table 2 Interviewee descriptions

Interviewee	Description
Government	Director, independent government research center
Contractor	Chief researcher, general contractor
Manufacturer	Technology and Development director, cement company Development center manager, chemical admixture company CEO, concrete ready-mix plant and aggregate quarry
Academic	University professor

3.2 Relationship to concrete

The conceptual structure of the concrete industry shown in Figure 2 illustrates that each social group interacts with concrete differently. The relationship of these groups to concrete is also dependent on the relationship between social groups, depending on their role in the construction process. Within the manufacturer group, the cement and chemical admixture companies are providing a product to the ready-mix plant which produces the actual concrete material for construction. Since the ready-mix plant is the customer of the cement and chemical admixture companies, these companies develop and evaluate their products considering the criteria which the ready-mix plant uses to evaluate its products (Table 3). Concrete is typically specified by compressive strength, slump, and aggregate gradation, so the ready-mix plant evaluates their product based on these criteria. However, since anyone can produce concrete which meets these specifications, concrete quality becomes an important criterion for customer satisfaction. Although ready-mix plants do not have the means for evaluating durability, it may be specified by the owner, so cement and admixture companies need to consider this performance as well.

Table 3 Evaluation criteria for concrete materials

Interviewee	**Indicators**
Government	Hardened (strength, durability), cost
Contractor	Cost, quality
Cement company	Hardened (strength, durability), cost, quality
Admixture company	Fresh (viscosity, fluidity, pumpability, slump retention), hardened (strength, durability)
Ready-mix	Fresh (slump, air content), hardened (strength)
Academic	All criteria

The contractor's role is to construct infrastructure using the concrete produced by the ready-mix plant. Construction is performed according to contract between the contractor and the owner, so the contractors wants to utilize concrete materials with low cost and high quality to meet budget requirements and ensure structural performance. The owner, in turn, is focused on the cost and performance (strength and, in some cases, durability). The academic institution supports all levels of this process by providing research for solving problems found in practice or developing new technologies, techniques, or standards from basic on-going research. However, researchers may not consider cost even though it is important throughout the construction process and used by the other social groups.

3.3 Knowledge of sustainability

Although the relationship of a given social group to concrete may be the same when considering different individuals or organizations within the same social group, knowledge of sustainability is largely dependent on individuals, so that even within the same organization or social group there may be widely varying ideas regarding sustainability. For this research work it is assumed that, since the selected interviewees occupy positions whereby their ideas affect the development or direction of their organization, their individual ideas can be representative of their organization.

The visualization of sustainability shown in Figure 1 emphasizes the dependency between the environment, society, and the economy. This dependency is also shown in the perspectives on sustainability held by the interviewees, which are summarized in Table 4. The common theme between the interviewees is the importance of reducing CO_2 and CO_2 as an indicator for sustainability. The environment is frequently referred to in both concept and indicators, including CO_2, resource consumption, waste usage, recycling, and others. Societal issues are also referenced, such as human activity, safety, community, health, and social merit. Economic issues are mentioned the least, with economic merit and cost/benefit suggested as two means of evaluation. It can be clearly seen that most of the definitions and indicators are focused on the environmental impact, followed by social and economic issues, which reinforces the hierarchy in Figure 1.

Table 4 Perspectives on sustainability

Interviewee	Concept	Indicators
Government	Maintain current level of life while developing human activities, but environment affects all activities	Environmental impact, CO_2, natural resource consumption
Contractor	What everyone can use or do safely from now	Safety
Cement company	Maintaining and improving built and natural environment	CO_2, recycling, land use management, resource consumption, waste materials
Admixture company	Society will define based on environmental issues and economic merit	Environmental impact, CO_2, clean air and water, contamination and pollution, social and economic merit
Ready-mix	Reduction of CO_2	CO_2
Academic	Reduction of CO_2	Resources, air, CO_2, water, soil, noise, waste, economic effect (cost/benefit), community, land systems, population statistics, safety, health, comfort, biodiversity

3.4 Sustainable concrete practice

The final part of the interview focused on the interviewees' perspectives on sustainable practice in the concrete industry, considering in particular how to evaluate sustainability, sustainable materials, and barriers to sustainable practices. The proposed indicators or methods for evaluating sustainable concrete practice are given in Table 5. From these results it can be seen that durability, LCC, and CO_2 are the most common indicators proposed. Durability and LCC are the main engineering-based indicators, whereas several different sustainability-based indicators were also mentioned, including recyclability, environmental preservation, and social benefit. However, most of the interviewees agree that considering cost and CO_2 emissions over the life cycle are the most important means for evaluating sustainability.

Table 5 Sustainable concrete practice indicators

Interviewee	Indicators
Government	LCC, life cycle CO_2, durability, recyclability, use of waste and recycled materials, preservation of natural environment
Contractor	LCC, durability, recyclability, use of inorganic materials
Cement company	LCC, life cycle CO_2, environmental impact, durability
Admixture company	LCC, life cycle CO_2, environmental impact, durability, social benefit
Ready-mix	Durability, workability, reliability, constructability, LCA
Academic	CO_2, other criteria dependent on project

Given these indicators, sustainable concrete materials should be designed considering durability of the material in both the fresh and hardened states, and selection of materials should be conducted based upon evaluation of LCC and life cycle CO_2. Waste and recycled materials should also be used if possible, but it is important to maintain durability and quality since these materials are of inferior quality. Since cement is the primary contributor of CO_2, the use of admixtures or alternative cementitious materials is necessary to reduce the volume of cement as much as possible.

The results in Table 5 showed a general consensus among the social groups regarding what indicators should be used for evaluating sustainable practice, and criteria for sustainable materials could be proposed based upon this consensus. However, there exist many barriers to the adoption of those indicators and the practical application of such materials, as summarized in Table 6. Among these, the problem of establishing an evaluation system is the most prominent. To ensure transparency, official inventory data and a standardized code are necessary. Furthermore, current evaluation systems focus on initial cost, so environmental impact evaluation needs to be integrated with the current system, as well as means for evaluating additional value other than reduced environmental impact. Finally, there are problems of perception. Since recycled materials are inferior in quality, concrete with recycled materials is avoided because people believe that quality cannot be assured. However, the greater problem is the perception that concrete as a construction material is not environmentally friendly.

Table 6 Barriers to sustainable concrete practice

Interviewee	**Barriers**
Government	Lack of inventory data, lack of standardized code, government focus on cost-benefit ratio which doesn't include environmental cost, CO_2 specification relative not absolute, reluctance to use new or unfamiliar materials
Contractor	Focus on initial cost, government doesn't consider long-term usage of infrastructure
Cement company	Lack of standardized code, gap between specifications and actual quality, ready-mix cannot evaluate durability, lack of vertical integration, over-design of structures, gap between high compressive strength and high durability, perception of concrete as not environmentally friendly
Admixture company	Loose environmental codes, balance between company and social benefit, perception of concrete as not environmentally friendly
Ready-mix	Lack of inventory data, lack of standardized code, transparency in calculating CO_2, balance between different evaluation criteria, perception of recycled materials
Academic	Lack of standardized code, transparency in calculating CO_2, focus on initial cost, can't evaluate additional value, balance between different evaluation criteria, sustainability knowledge gap among people

3.5 Relating concrete use and sustainability to sustainable practice

In Section 2.3 two hypotheses were proposed: that sustainable practice was affected by the relationship to concrete, and that sustainable practice was affected by the knowledge of sustainability. From the results presented in Section 3.2, it was found that the social groups' relationship with concrete was tied to the interaction between the social groups and their role in the concrete production and construction process. However, although durability was specified as an evaluation criterion by several groups, demand for durability derives from the owner, who typically only specifies strength. The perspectives on sustainability found in Section 3.3 followed the general hierarchy presented in Figure 1 and most of the emphasis was placed on environmental indicators – primarily CO_2 – although social and economic merit were also mentioned. The results of Section 3.4 showed that evaluation of sustainable practices and materials should be conducted using durability, LCC, and life cycle CO_2. The selection of CO_2 as a sustainability indicator for the concrete industry can be derived directly from the emphasis placed on CO_2 as a general environmental indicator; however, durability and LCC are not currently used to evaluate materials in practice (although durability may be specified in some cases). This follows directly from the barriers identified in Table 6, which showed that there is a lack of standardized code for evaluating LCC, emphasis is placed on initial cost rather than LCC, lack of consideration for long-term usage in some government officials, and lack of method for ready-mix plants to evaluate durability. Furthermore, although there is consensus on the importance of life cycle CO_2 as an indicator, a standardized method for evaluation and ensuring transparency has not yet been established. Figure 6 shows the relationship between these issues.

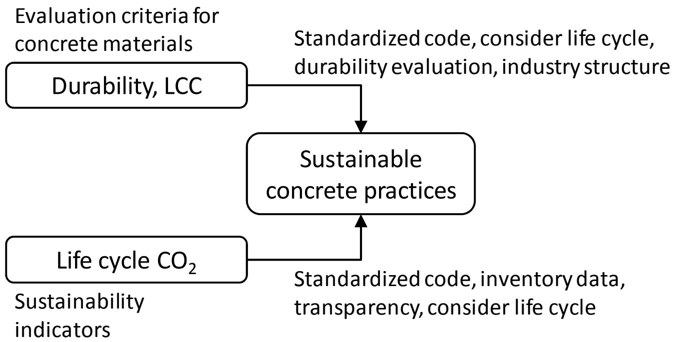

Figure 6 Deriving sustainable concrete practices from relation to concrete and sustainable knowledge

Finally, the importance of each social group's role in the production and construction process (the industry structure) is a key point for developing sustainable practice. The additional value of utilizing sustainable materials needs to be evaluated at each stage of the production and construction process, so the role each group plays needs to be considered when developing codes and boundary conditions for the evaluation of life cycle costs and CO_2 emissions.

4. CONCLUSION

In this paper, the perspectives on concrete, sustainability, and sustainable concrete practice were presented for different social groups in the Japanese concrete industry. It was found that the relationship each group has with concrete is dependent upon their relationship with other social groups due to the structure of the Japanese industry, and that different evaluation criteria are applied at different stages of the construction process. The ultimate product of the manufacturing stage is fresh concrete from the ready-mix plant, so cement and admixture companies focus on assuring the quality and improving the performance of criteria which the ready-mix plant has to satisfy – usually slump and compressive strength. However, the ready-mix plant is more concerned with providing quality concrete to satisfy the requirements of the contractor, whose contract with the owner requires that the contractor provide a certain level of quality at a specified price. Even though each social group relates differently to concrete, the interviewees generally gave similar responses when asked to define and evaluate sustainability. Environmental impact, such as CO_2, received the greatest emphasis, with less emphasis on social and economic concerns. This result reinforces the hierarchy shown in the visualization of sustainability in Figure 1. When considering the development of sustainable practice for the concrete industry, boundaries need to be overcome in order to implement the practices which are considered necessary. The current specification process for concrete emphasizes strength and initial cost; however, evaluation methods and standardized codes should be developed which can provide the means for considering durability and life cycle cost in the evaluation process. CO_2 is clearly a vital indicator for understanding the environmental impact, but standardized evaluation methods, inventory data, and transparency need to be established and considered along with durability and life cycle cost. Finally, boundary conditions for these evaluations need to be set considering the industry structure.

REFERENCES

Cornell, 2009. Cornell University Sustainable Campus (online). Available from: http://sustainablecampus.cornell.edu/csi.cfm (28 August 2009)

IPCC, 2007. *Climate Change 2007: Synthesis Report*. Intergovernmental Panel for Climate Change, Geneva.

Miles, M.B and Huberman, A.M., 1994. *Qualitative Data Analysis*. SAGE Publications, London.

Minichiello, V., Aroni, R., Timewell, E., Alexander, L., 1990. *In-Depth Interviewing: Researching people*. Longman Cheshire, Melbourne.

Murcott, S., 1997. *What is sustainability?* AAAS Annual Conference/IIASA Sustainability Indicators Symposium, Seattle, USA.

Punch, K.F., 2005. *Introduction to Social Research*. SAGE Publications, London.

LANDSLIDE MOVEMENT AND DEFORMATION FOR DIFFERENT LENGTH AND WIDTH OF LANDSLIDE MASS

MUNEYOSHI NUMADA
International Center for Urban Safety Engineering
Institute of Industrial Science, University of Tokyo, Japan
numa@iis.u-tokyo.ac.jp
Kazuo KONAGAI
Institute of Industrial Science, University of Tokyo, Japan
konagai@iis.u-tokyo.ac.jp

ABSTRACT

It is important to forecast the run out-distance of landslides mass to reduce the landslide disaster. This research aims to analyze the key parameter that control the run out-distance of landslides mass. The numerical analysis is an effective approach to analyze the dynamic mechanism of the landslide. For numerical analysis, Material Point Method (MPM) is used in this research.

The condition requested from the numerical analysis includes two following elements: 1. Large deformation of soil; and 2. Input parameters composed of information which can be measured. Input parameters applied in MPM model are slope form (geographical features and slide surface), physical properties of deformation of sliding mass (geological features) and physical properties of sliding surface

The parameters that control the run out-distance of landslides mass are geometry, physical property and frictional coefficients to observe the contribution to run out-distance. For different lengths of the landslide mass (L), the mass movement is examined in the time-marching calculation of MPM. Lengths of the landslide mass segments L_1 and L_2 on the level and inclined sliding surfaces are obtained respectively at every time step. Also width of a landslide mass can be analyzed. As the width increases, the curve converges on the plane-strain solution, and it is rather closer to plane-stress solution for thinner soil cases. The ultimate load capacity F would be more crucial in determining its distal reach.

This research introduced some results for extracting important pieces of information for landslide risk assessment from numerical model and real landslide masses. For coherent mass movements, numerical simulation of landslide mass movements using MPM did hint an idea for extracting parameters from real landslide masses. This knowledge will provide a good perspective for landslide risk assessments.

1. INTRODUCTION

Landslides can range in size from small movements of loose debris to massive collapses of entire summits. For short to medium-length slopes, installing preventive drainage works, anchoring and/or reinforcing slopes will be effective for assessing and mitigating landslide hazards. However for extremely large slope failures, it is very difficult to mitigate and thus the importance of run out analysis emerges. Many landslides with limited internal deformation will move as coherent masses on thin mobile basal layers. However, others will become flow-like in character after running some long distances, though exhibiting some solid features at their early stages of failure. It is important to forecast the run out distance of landslides mass to reduce the landslide disaster.

This research is aim to analyze the key parameter that control the run out distance of landslides mass. The numerical analysis is an effective approach to analyze the dynamic mechanism of the landslide. For numerical analysis, Material Point Method (MPM) is used in this research.

2. NUMERICAL PROCEDURES IN MPM ANALYSIS

2.1 Overview of MPM

The MPM is categorized as one of the mesh-less methods formulated in an arbitrary Lagrangian-Eulerian description of motion. In MPM, a body is to be analyzed as a cluster of material points. Material Point has information of physical properties on a peculiar position and the stress, etc. The material points, which carry all Lagrangian parameters, can move freely across cell boundaries of a stationary Eulerian lattice, and the information is distributed to each node of belonging cells. This mesh is called as computational mesh, should cover the virtual position of the analyzed body. The computational mesh can remain constant for the entire computation, thus the main disadvantage of the conventional finite element method related to the problem of mesh distortions is eliminated for large deformation of soils (Figure 1).

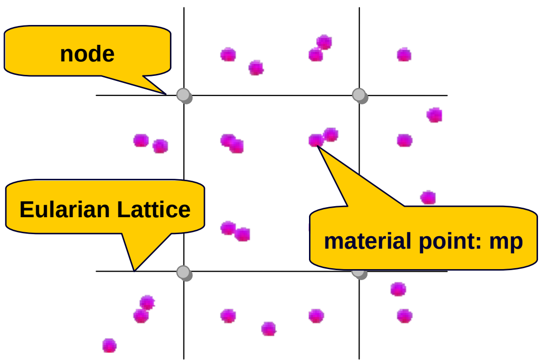

Figure 1: Eularian lattice and material points

2.2 Modeling of landslide mass

All Lagrangian parameters for the entire landslide mass are hardly obtained. For example, it is often that the plants growing on a landslide mass shoot their roots all through the soil mass. In such a way that overall characteristics of the soil mass is largely different from those obtained through test of soil samples taken point-wise from the landslide mass.

The condition requested for the numerical analysis includes two following elements: 1. Large deformation of soil; and 2. Input parameters composed of information which can be measured. Input parameters applied in MPM model are slope form (geographical features and slide surface), physical properties of deformation of sliding mass (geological features) and physical properties of sliding surface.

A lot of parameters that constitute physical properties of landslide are taken into real landslide phenomenon, but the pseudo-three dimensional model can reduce the number of complex parameters as much as possible. The landslide mass is considered to be equivalent fluid in this model and modeling it as assemble of soil columns. In such a model, complex landslide model can be expressed by the interactive force between soil columns, basal force and reducing necessary parameters. Therefore, there is an advantage that the computational complexity can be decreased at the computing lead time (Figure 2).

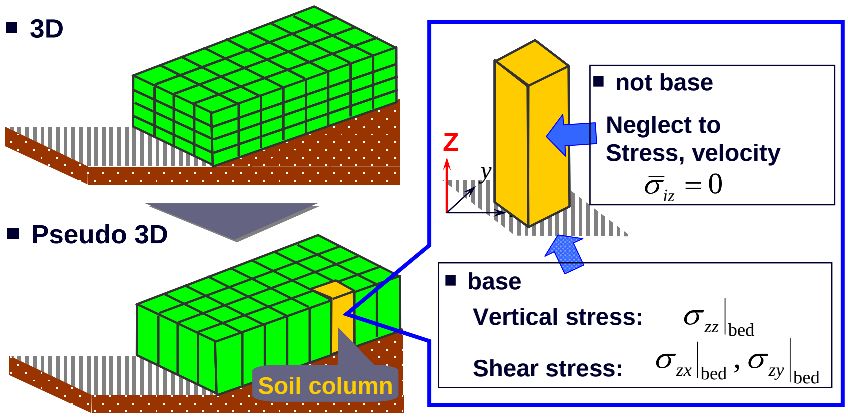

Figure 2: Pseudo three dimensional model of landslide mass

3. NUMERICAL SIMULATION FOR DIFFERENT LENGTH AND WIDTH OF LANDSLIDE MASS

3.1 Modeling of landslide mass

For landslide mass is modeled in MPM, width of the landslide W and depth H are made constant, the landslide length is set different six pattern from 20 to 100m length (Figure 3). The initial thickness H of the landslide mass is set to 1m. A rectangular-planner soil mass of 1m thick is assumed to be resting on a flat slope dipping to a level ground, which spreads in immediately front of the toe of the landslide mass. The slope angle of MPM model is set uniformly to 20 degrees. The coefficient of friction is set separately on the slope side and flat surface side, and the coefficient of flat surface side μ_1 and slope side μ_2 are 0.8 and 0.2 respectively (Table 1). The Young's modulus of the landslide mass E is taken as 2×10^6 Pa, poisson's ratio is 0.3, internal frictional angle ϕ is set to 30 degrees, cohesion c is derived from Rankin's earth pressure model to stand upright 1m height in the gravity. The constitutive law of landslide mass is used Drager-Prager model. The initial material point for one cell arranges to be 2×2 for 0.2m×0.2m size cell.

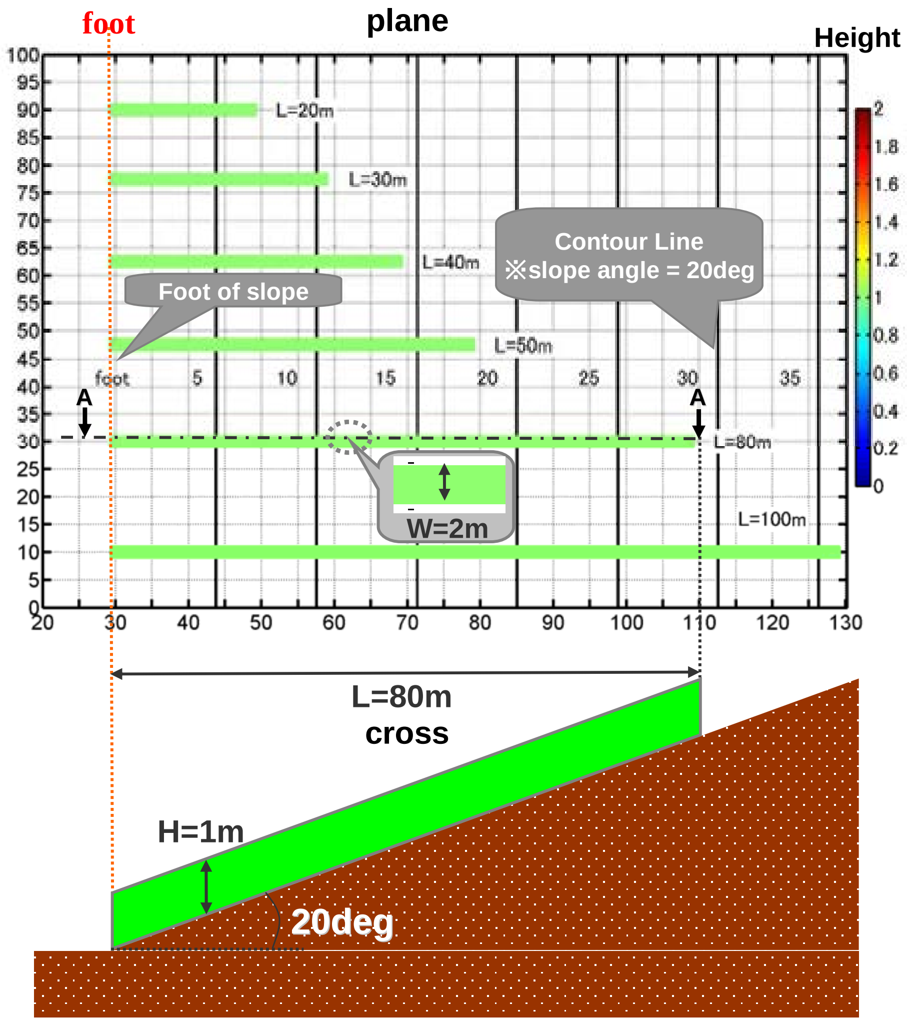

Figure 3: MPM model for different length of landslide mass (upper: plane view, lower: cross)

Table 1: Parameter of landslide mass and MPM setting

Topic	Comment
Sliding surface dip	20 deg
μ_1 (flat surface)	0.8
μ_2 (slope surface)	0.2
ϕ(soil mass)	30 deg
Young's modulus	2×106 Pa
Possson's ratio	0.3
Density	1600 kg/m3
Cell size	0.2m × 0.2m
Initial arrangement of particles in a cell	2 × 2
Time increment	5 × 10-4

3.2 Numerical result of different length of landslide mass

For different lengths of the landslide mass L, the mass movement is examined in the time-marching calculation of MPM (Figure 4). The run out-distance L_1 is defined as the distance from boundary of slope-flat surface zone to head of the landslide mass, and L_2 is the distance of the landslide mass that remains of a slope side (length of the remaining on the slope). These are obtained at every time step. The average stress σ_a is the average value of the stress that acts upon the boundary on a slope and flat side. The average stress σ_a is calculated the average value of the stress of node on the boundary between a slope and a flat surface side. Initially landslide mass keeps $L_1 + L_2$ to be completely identical to the entire length of the landslide mass L. to be exact, the entire length is kept unchanged (Figure 5).

However, as the landslide mass runs further forward over the level ground (deposition zone), its movement slows down due to larger frictional coefficient and with no driving force induced on the level ground. Eventually the following segment of the landslide mass pushes the soil from behind, and immediately after the ultimate load capacity F, the average stress σ_a reaches peak strength σ_p, that the limit landslide mass can sustain is reached and $L_1 + L_2$ value is starts shrinking ($L_1 + L_2 < L$).

For long landslide masses, L_1 converges on a constant value, ultimate L_{1y}, suggesting that the entire length of the landslide mass has little or nothing to do with the ultimate load capacity. In the other word, there is the upper bound of distal reach of the landslide mass. It will be also a matter of course that L_2 can converge likewise on a particular value, ultimate L_{2y}, with the presence of the ultimate load F.

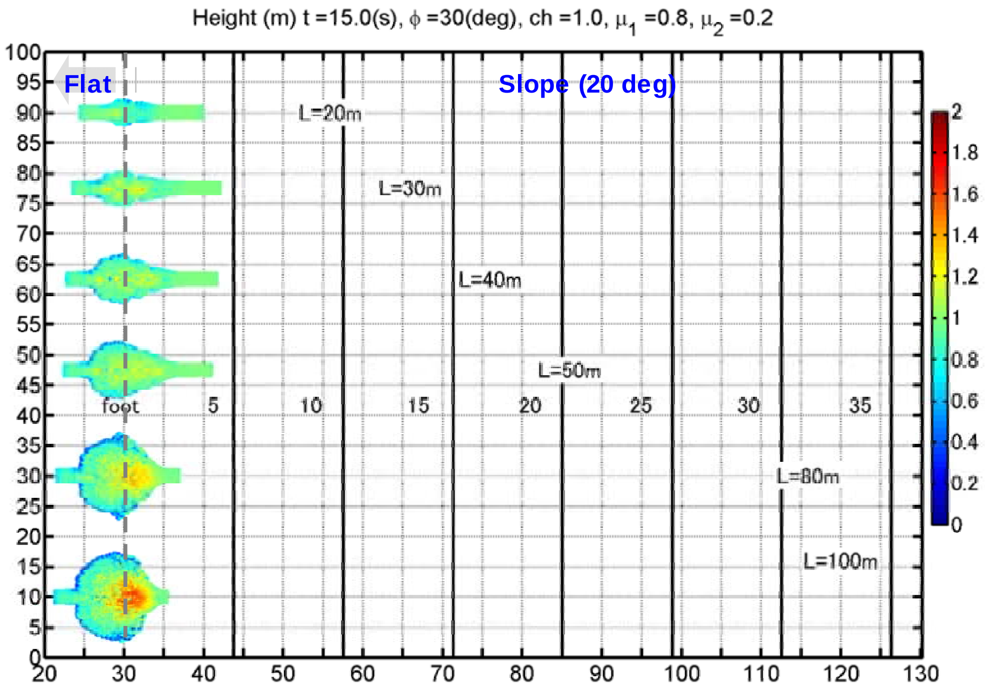

Figure 4: Plane view of height of landslide mass for different length (Time = 15s)

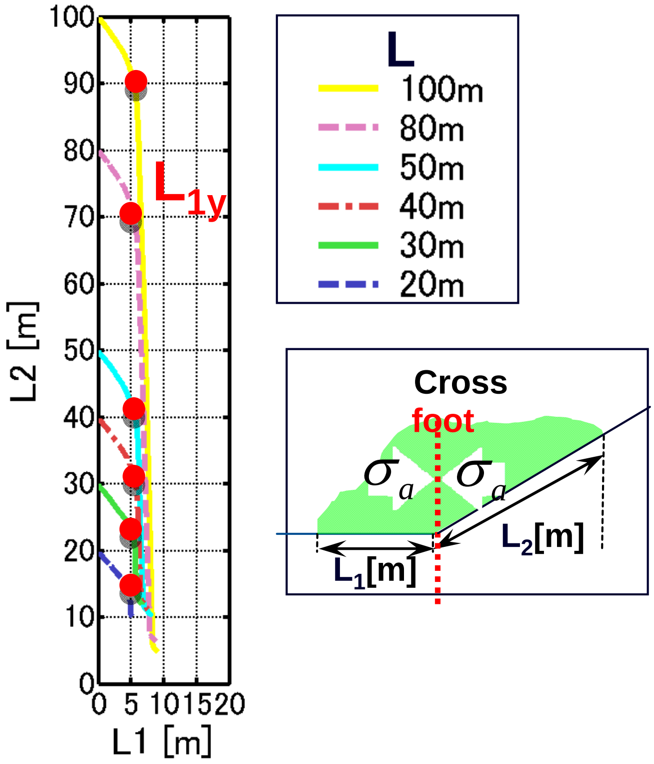

Figure 5:Relationship between L1 and L2 for different length of landslide mass

3.3 Numerical result of different width of landslide mass

Width of a landslide mass can also affect F and therefore L_{1y} and L_{2y}, as the width increases, the curve converges on the plane-stress solution for thinner soil cases (Figure 6). In Figure 7, after the landslide mass starts yielding, dL_2/dL_1 becomes less steep for wider soil masses. This can be explained as follows: This dL_2/dL_1, when multiplied by the cross-sectional area of the landslide mass, is identical to $-dV_2/dV_1$, where dV_2 and dV_1 are soil volumes which pass through the cross section per unit time for segments L_2 and L_1, respectively.

The soil volume dV_1 will be pushed forward over the deposition zone by the following soil volume dV_1, while the volume of $dV_2 - dV_1$ is pushed up and/or sideways making a bulge at around the toe of the slope. It is thus clear that, less steep dL_2/dL_1 indicates larger confinement of $dV_2 - dV_1$ causing slight increase of F even after the initial ultimate capacity F was reached. In other words, the effect of confinement can be quantitatively estimated from geometry of the deformed landslide mass. Width of a landslide mass can also affect F.

As the width increases, the curve converges on the plane-strain solution, while it is rather closer to plane-stress solution for thinner soil cases. The ultimate load capacity F would be more crucial in determining its distal reach. In this research, by analysis on different width of the landslide, as the confining pressure is increasing, peak stress is increasing; it becomes a phenomenon similar to tri-axial compression tests.

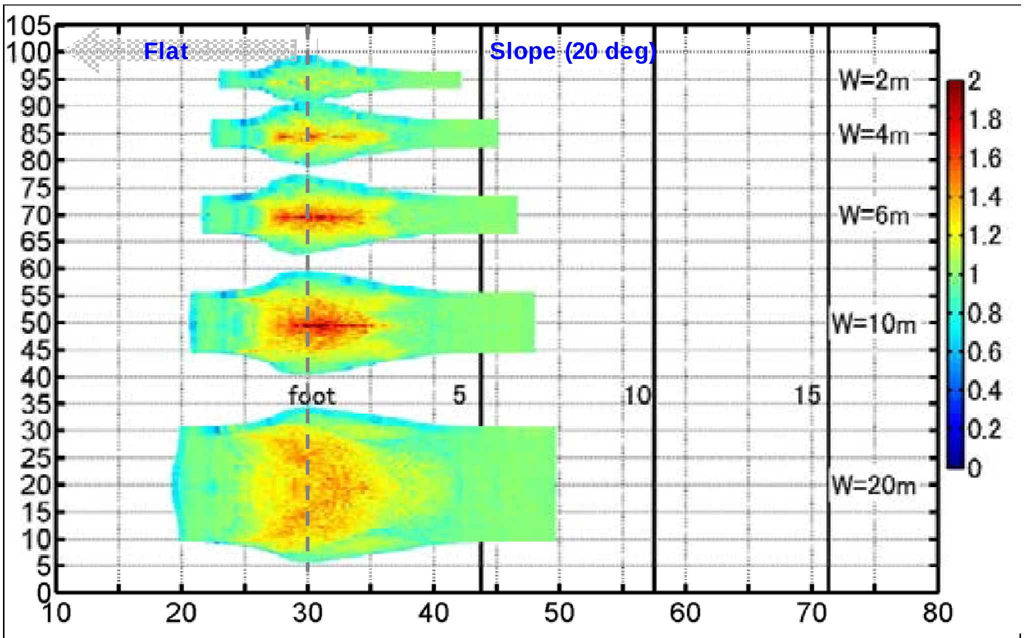

Figure 6:Plane view of height of landslide mass for different width (time = 15s)

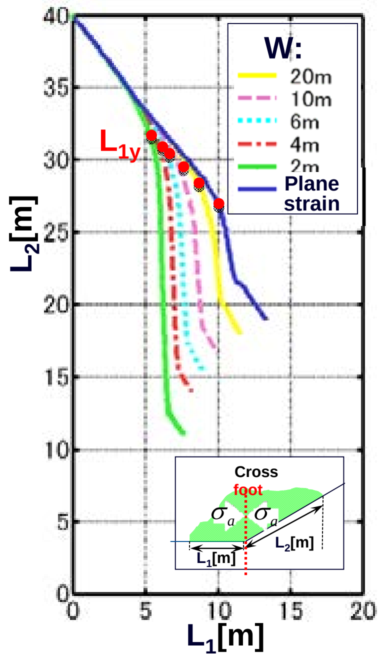

Figure 7: L_1 and L_2 for different width of landslide mass

4. CONCLUSION

This research introduced some results for extracting important pieces of information for landslide risk assessment from numerical model and real landslide masses. For coherent mass movements, numerical simulation of landslide mass movements using Material Point Method (MPM) gave an idea for extracting parameters from real land slide masses. A real cohesive landslide can be viewed as a large-scale specimen of a monotonic loading test for obtaining its ultimate load capacity F, which can be greatly responsible for distal reach of the landslide mass. And also, the coefficient of sliding surface that is one of the important parameter to define run-out distance on the deposit zone is difficult to be evaluated from real site. For that one possible approach is proposed in this research. This knowledge will provide a good perspective for landslide risk assessments.

REFERENCE

Sulky, D., Chen, Z. and Schreyer, H.L. (1994): *A particle method for history dependent materials*, Computer methods in applied mechanics and engineering, 118, pp. 179-196.

Konagai, K. and Numada, M. (2002): *Pseudo-three dimensional lagrangian particle finite difference method for modeling long-traveling soil flows*, Journal of Dam enginnering, 12(2), pp. 123-128.

Numada, M., Konagai, K., Ito, H. and Johansson, J. (2003): *Material point method for run out analysis of earthquake-induced long-traveling soil flows*, Journal of Earthquake Engineering, 27.

CASE STUDIES OF COASTAL EROSION CONTROL BY GEOTEXTILE TUBE

[1]Eun Chul Shin, [1]Sung Hwan Kim and [2]Young Keun Lim
[1]Department of Civil and Environmental Engineering, University of Incheon, Korea, ecshin@incheon.ac.kr, sherikim315@naver.com
[2]Department of Geomarrine Systems, Korea, limyg2005@empal.com

ABSTRACT

Recently, because of the shortage of natural rock, traditional forms of river and coastal structures have become very expensive to built and to be maintained. Therefore, the materials used in hydraulic and coastal structures are changing from the traditional rubble and concrete systems to the cheaper materials and systems. Also, geotextile tube technology has changed from being an alternative construction technique and, in fact, has advanced to become the prime solution of choice. This paper presents the stability analysis and field monitoring results of stacked geotextile tube structure for temporary construction platform, the various issues related to the geotextile tube technology and case history of shore protection of Korea, Republic of Korea. Geotextile tube was proposed for desired crest height, and the stability analysis against external force was conducted to the each cross section of stacked geotextile tube. The considered external forces are wave force, tidal force and lateral earth pressure by reclamation.

1. INTRODUCTION

Erosion problems in coastal zones are become increasingly serious due to the development of artificial activities related to the expansion of city functions, industrial complexes and harbor facilities, as well as the removal of sea sand for use in aggregate resources at the construction sites, which is a major factor in the inflow and outflow of sea sand. In addition, the environmental and economical importance of the coastal beach zones is increased. However, coastal beach zones are constantly eroded by waves accompanied with the rising water level due to storm surges, hurricanes, winter storm impact, and high tide. This erosion motion accelerates the regression of the coastal cliff due to the regression of the dunes or the shoreline. In addition, the regression leads to loss of real estate in the hinterland and ruins the shock-absorbing zone between land and sea. Therefore, the destruction of the dunes may lead to a loss of the habitat or egglaying grounds of living creatures. In addition, the erosion motion of coastal beach zones destroys the living sites of inhabitants who live in coastal beach zones, and the erosion problem harms the local economy by decreasing the number of visitors. For these reasons, concern is increasing for the protection of coastal beach zones. Many nations are striving to prevent damage to such zones, as are private organizations and local selfgovernments. One such preventive effort is beach nourishment or construction of the coast structures. Geotextile containment such as small sand bag has been adopted for the construction of civil structures in the past, large volume geotextile containers are being applied widely in consideration of economical and easy installation, and also for the minimization of environmental effects. Especially, contaminated soil and sediments dredged from port area are utilized to fill in geotextile containment for reclamation. Geotextile containment is widely classified into geotextile bag, geotextile tube and geotextile containment, and they are filled with soil to be shaped of structure. The filling method is normally hydraulic filling by means of pumping, and also mechanical method can be applied according to the site condition. This technology can be applied for the sea shore embankment, embankment core material, embankment enforcement and disaster recovery construction. For environmental application, it can be used for embankment construction to recover and preserve swampy land and dredging reclamation of deep sea contaminated accumulated earth sand. In case of conventional stone and concrete sea shore structures, they accompany large scale environment destruction. However, the construction using this technology does not accompany environment destruction. In particular the materials that may contaminate the environments in sea shore, recovered swampy land and embankment can be used as a filter. Therefore, it is an excellent technology that can bring dual advantages to the environment. Additionally, as it uses the deep sea sand on the site rather than the expensive good quality sand, this technology saves a lot of money. Furthermore it will bring the additional cost saving through shortening the construction period because of the easy application.

2. CONSIDERATED CONTENT FOR CROSS-SECTION DECISION

Formulation of a geosynthetic tube, filled with pressurized slurry or fluid, is based on the equilibrium of the encapsulating flexible shell. The results of this formulation provide both the circumferential tensile force in and the cylindrical geometry of the encapsulating shell material. It should be pointed out that the formulation appears in numerous articles (e.g., Liu 1981, Kazimierowicz 1994, Carroll 1994). For the sake of completeness, only an overview of the basic formulation is reproduced later. Refer to Figure 1 for notation and convention. For clarity of presentation, the tube considered is surrounded by air and is filled with only one type of slurry. However, extension of the formulation to include layers of slurry inside and layers of fluid outside, is straightforward. Note that the cross section is symmetrical, having a maximum height of h at the centerline, maximum width B, and a flat base that is in contact with the foundation soil and is b wide. The pumping pressure of the slurry into the tube is p_0. The average unit weight (density) of the slurry is γ. Hence, the hydrostatic pressure of the slurry at any depth x, as measured from point O, is $p(x) = p_0 + \gamma x$.

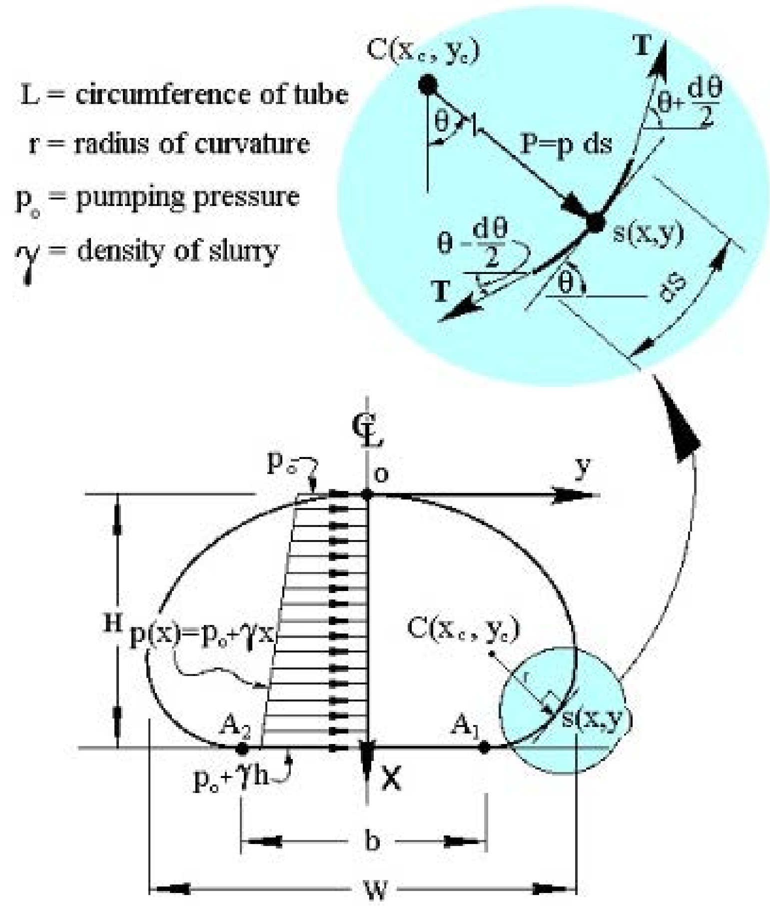

Figure 1:Cross-Sectional View of Geosynthetic Tube

The geometry of the geosynthetic shell is defined by an unknown function y=f(x). At a point of contact S(x,y), the radius of curvature of the geosynthetic is r. The center of this curvature is at point $C(x_c,y_c)$. Both r and C vary along y(x). Consider the forces on an infinitesimal arc length, d_s, of the geosynthetic at S. Since it is assumed that the problem is two-dimensional and that no shear stresses develop between the slurry and the geosynthetic, it follows that the geosynthetic tensile force, T, must be constant along the circumference. Assembling the force equilibrium equation in either x or y direction leads to the following relationship:

$$\gamma(x) = \frac{T}{p(x)} \tag{1}$$

Equation 1 is valid at any point along A_1OA_2. To simplify the analysis, it is assumed that the calculated T from Equation 1 is carried solely by the geosynthetic along the flat base b. That is, no portion of T is transferred to the foundation soil due to shear along the interface between the geosynthetic and soil. The tube in the z-direction(i.e., axial direction) carries the force P. The force T_{axial} per unit length then is P divided by the circumference, L, of the tube. That is:

$$T_{axial} = \frac{2}{L} \bullet \int_0^k (p_0 + \gamma \bullet x) \bullet y(x)dx \tag{2}$$

Typically, the circumferential force T is larger than T_{axial}. Hence, if the geosynthetic having isotropic strength is considered, the value of T_{axial} is not needed in design. However, frequently geosynthetics are anisotropic; i.e., their strength in the warp direction (usually corresponds to the tube's circumferential direction) is different than that in the fill direction (usually corresponds to the tube's axial direction). This anisotropy is particularly common in medium to high strength geotextiles, where different types and number of yarns per unit width are used in each of the principal directions in the fabrication process. The end product may have either significantly higher or worse, lower strength in the axial direction as compared to the circumferential one. Consequently, to assure economical selection of a geosynthetic, producing a safe structure, the value of T_{axial} should always be considered. Program GeoCoPS provides the values of both T and T_{axial}. These values are adjusted by user-prescribed reduction factors that account for the reduction in geosynthetic strength due to seams and possible construction damage. The end result allows for the selection of an adequate geosynthetic.

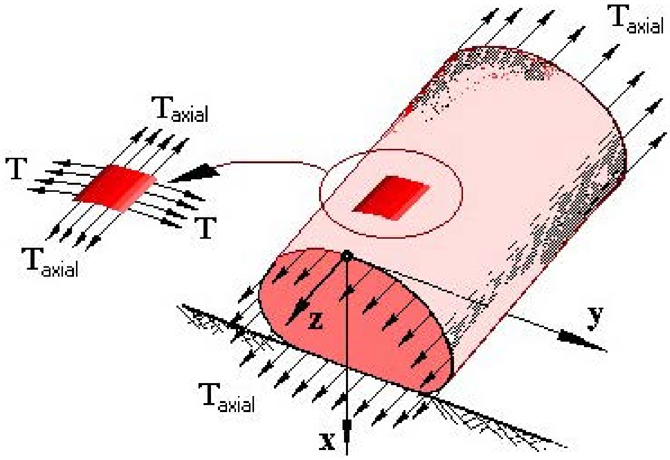

Figure 2: Axial Tensile Force in Geosynthetic Tube

Figure 3: Geosynthetic Tube Install Procedure

3. PARAMETRIC STUDY ANALYSIS AND RESULT

To realize how sensitive the solution for the geosynthetic tube is with respect to the design parameters, a parametric study was conducted. This instructive study was conducted using program GeoCoPS. For all cases, the circumference of the tube was chosen as L= 9.4m(GTD 300), the unit weight of slurry relative to water was taken as 1.2, no water, 1.0m, 1.5m, 2.0m, 2.5m outside the tube was considered, and all safety factors on geosynthetic strength were set to default value.

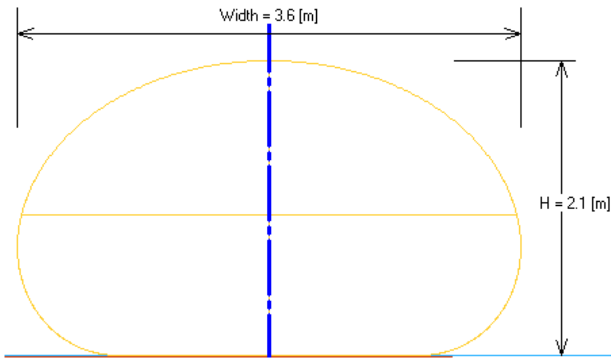

Figure 4: Effects of T_{ult}, on Geometry of Tube (outside water = 2.5m)

Figure 4 shows the effects of the specified tensile force of the geosynthetic on the geometry of the tube. To get a perfect circular cross section, having a diameter equal to D=L/π=9.42m(GTD=300), the required T must approach infinity. Figure 5 illustrates the effects of a designed height h on the geometry of the tube. For a desired height of 1.65m (about 55% of D), the required pumping pressure is nearly zero, and required circumferential force is only 8.9kN/m. however, for a desired height of about 90% of D (h=2.7m), the required pumping pressure is about 13.3kPa, and the required circumferential force is substantially larger, approximately 98.3kN/m.

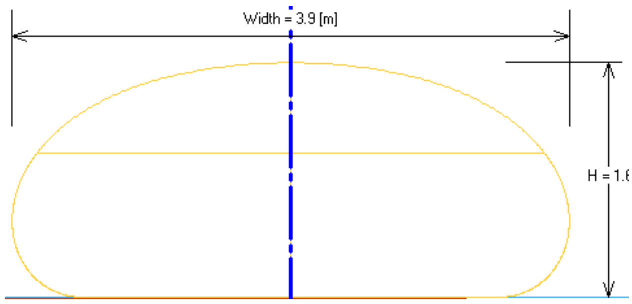

Figure 5: Effects of h on Geometry of Tube (outside water = 2.5m)

Figure 6 demonstrates the relationship between the height of the tube and the pumping pressure. It can be seen that p_0 is most significant at low pressures; as the pressure increases, its effect on h becomes negligible. At a pumping pressure of 20kPa, 90% of the theoretical height is achieved. In fact, the relationship approaches an asymptote of h=D that will be metonly when p_0 is at infinity

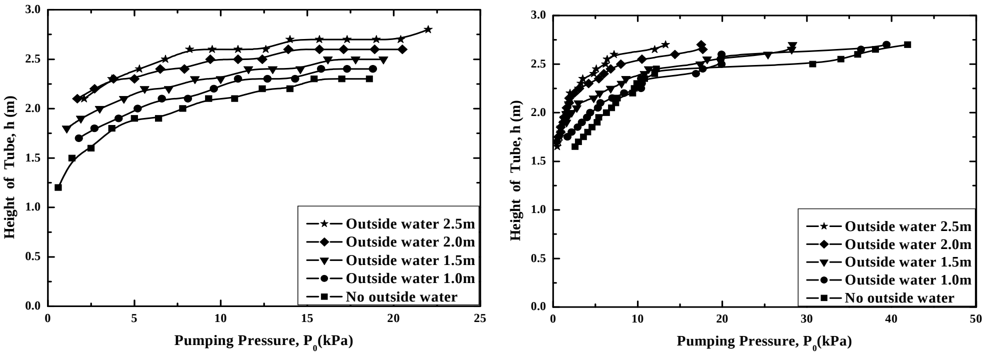

(a) At design tensile strength *(b) At design height*

Figure 6: Height of Tube versus Pumping Pressure

Figure 7 illustrates between ultimate tensile strength and the pumping pressure. For the selected parameters in the parametric study, it can be seen that as p, decreases, the ultimate tensile strength approaches the value of zero. This figure is particularly instructive in the context of design; it illustrates the potential economy when selecting a geosynthetic having an anisotropic strength that corresponds to both tensile forces T and T_{axial} when those are significantly different. Since these strengths must develop through the seams, one can also realize the critical importance of seam strength and efficiency.

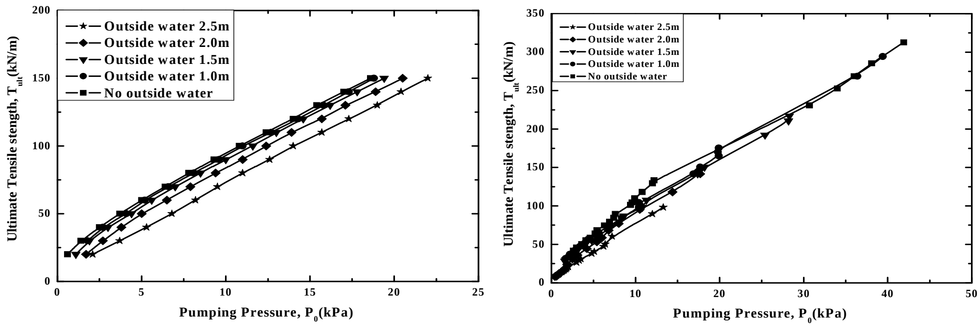

(a) At design tensile strength *(b) At design height*

Figure 7: T_{ult} versus Pumping Pressure

Finally, Figures 8 show the relationship after consolidated height of tube the pumping pressure. At a pumping pressure of 15kPa, for a desired height of 1.2m (about 40% of D), the required pumping pressure is nearly zero. A flat top geometry will render the mathematical solution of the problem of pressurized slurry tube invalid. As reduced slurry unit weight decreased after consolidated height of tube H_f. This approximate procedure allows for a rough estimate of the average drop in height, once a supposed density of fill material is achieved. Also, if the filling ratio is at least up to 80%, the immediate settlement is negligible because geotextile confined the fill material by highly developed tension in geotextile. However, the long-term consolidation of whole geotextile containment bund is more complicated phenomena, there has a single unit behavior and stacked surcharge loading relationship. Therefore, the long-term deformation of geotextile containment bund was need more strict quality control during and after bund construction by field monitoring such as settlement cell, pore pressure transducer and other sea bed scanning systems.

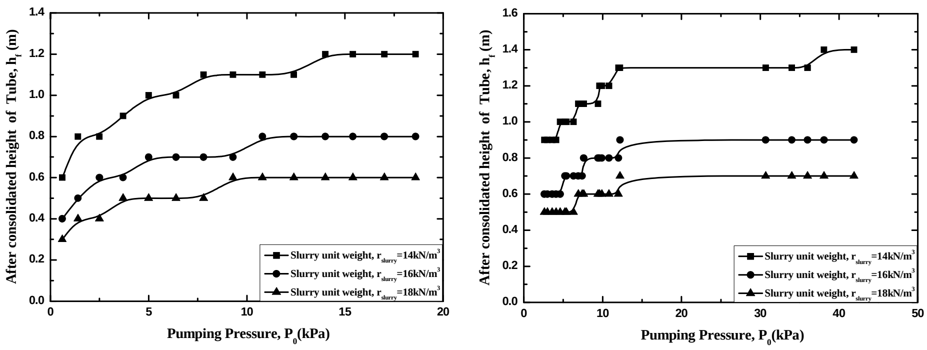

(a) At design tensile strength *(b) At design height*

Figure 8: After Consolidated Height of Tube at Given Pumping Pressure

4. MONITORING OF DEFORMATION

To check variation of shape, deformation, and other condition of the geotextile tube, it shall be surveyed a right angle to the shoreline from datum point of location of geotextile tube. The survey of water shape, deformation, and other condition shall be carried out by diver inspection (video camera), hydrographic method, side scan sonar apparatus on monitoring boat, and it shall be repeated to reduce the scope of error for correct location. 3-D Echo Sounder and GPS system is recommendable as sounding apparatus which has capacity to survey up to 100 meter's deep and the distance of movement(See Figure 9). Also, the pneumatic settlement cell shall be used.

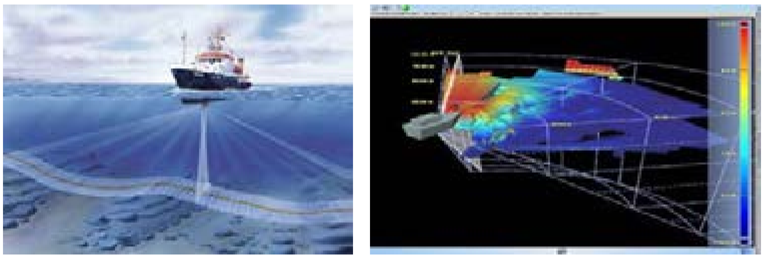

Figure 9: Illustrate Echo-Sounder Apparatus and Surveying Scene

5. CONCLUSION REMARK

An overview of analysis to calculate the geometry and stresses of a geosynthetic encapsulating pressurized slurry has been presented. The validity of the resulting equations was verified against the numerical and experimental results obtained by other investigators. Parametric studies indicate that stresses in the encapsulating geosynthetic are very sensitive at the pumping construction stage, it is extremely important to safeguard against accidental increase in the slurry pumping pressure. The parametric studies also reveal that a significant increase in pumping pressure will only slightly increase the tube’s cross-sectional area and, hence, its storage capacity. A guide to selecting a geosynthetic is provided. It is based on partial safety factors. These safety factors address the seam strength, potential installation damage.(i.e., accidental increase in pumping pressure), accelerating creep, and possible chemical and biological degradation. Also addressed is the required permeability of particles. Finally, a simple procedure to assess the final height of a tube filled up with clayey slurry is proposed. It should be pointed out that complete design of geosynthetic tubes has to also include the head loss occurring as the slurry flows away from the inlet. This aspect of design that will determine either the maximum length of a tube of the distance between inlets along that determine either the maximum length of a tube or the distance between inlets along the tube has not been addressed. Thought empirical rules dealing with this aspect exist, a rational analytical procedure is needed. Also, the measurement during construction for geotextile Tube is classified by 3 items. The first item is monitoring of individual geotextile tube unit for management of filling and dumping process, the second item is deformation monitoring of lumped geotextile tube for local stability, the last item is monitoring of geotextile tube bund for overall stability.

REFERENCES

Shin, E. C., Oh, Y. I. 2004, Consolidation Process of Geotextile Tube Filled with Fine-grained Material, *International Journal of Offshore and Polar Engineering*, Vol. 14, No. 2, pp. 120-158

Shin, E. C., Oh, Y. I. 2004, Using Submerged Geotextile Tube in the Protection of E. Korean Shore, *International Journal for Harbour and Offshore Engineers*, Volume 53, No. 11, pp. 879-895

Shin, E. C., Oh, Y. I. 2007, Coastal Erosion Prevention by Geotextile Tube Technology, *Geotextiles and Geomembranes*, Vol. 25, No. 4, pp. 264-277

Horace, M. Y., Meyers, T., Townsend, D. 1998, Evaluation of Geosynthetic Fabric Containers to Contain Contaminated Dredged Sediment, *Proceedings of Sixth International Conference on Geosynthetics*, Atlanta, Georgia, USA, Vol. 2, pp. 1173-1176.

Gibson, R. E., England, G. L., Hussey, J. L. 1967, The Theory of One-Dimentional Consolidation of Saturated Clay, Finite Non-Linear Consolidation of Thin Homogeneous Layers, *Geotechnique*, Vol. 17, pp. 261-273.

Koerner, R. M., and Koerner, G. R. 1996, Geotextiles Used as Flexible Forms, *Geotextiles and Geomembranes*, Vol. 14, No. 6, pp. 301-311.

Koerner. R. M. 2000, Emergind and Future Developments of Selected Geosynthetics Applications(The thirty second Terzaghi Lecture), *Journal of Geotechnical and Geoenvironmental Engineering*, ASCE, Vol. 126, No. 4, pp. 291-306.

Leshchinsky, D., Leshchinsky, O., Ling H. I., Gilbert, P. A. 1996, Geosynthetics Tubes for Confining Pressurized Slurry: Some Design Aspect, *Journal of Geotechnical Engineering, ASCE*, Vol. 122, No. 8, pp. 682-690.

Pilarczyk, K. W. 1997, Application and Design Asptects of Goecontiners, *Proceedings of Geosynthetics '97 Conference*, Long Beach, CA, IFAI, St. Paul, MN, pp. 147-160.

Pilarczyk. K. W., Breteler, M. K., Stoutjestijk, T. 1998, Stability Criteria for Geosystems -an Overview-, *Proceedings of Sixth International Conference on Geosynthetics*, Atlanta, Georgia, USA, Vol. 2, pp. 1165-1172.

Welsh, J. P., Koerner, R. M. 1979, Innovation Use of Synthetic Fabric in Coastal Construction, Coastal structures, *Journal of Geotechnical Engineering, ASCE* , Vol. 1, pp. 364-372.

Cross-boundary Water Resources Adaptation: Comparing a watershed approach and a political unit approach

AKIYUKI KAWASAKI[1], PETER ROGERS[2]
SRIKANTHA HERATH[3] and KIMIRO MEGURO[1]
[1] IIS, The University of Tokyo, Japan
[2] Harvard University, USA
[3] United Nations University, Japan
akiyuki@iis.u-tokyo.ac.jp

ABSTRACT

The Man-made boundaries such as national borders are typically used as the unit for considering river-basin management and policy, while natural boundaries such as watersheds are propounded as a promising approach for environmental management. However, few studies have proven the latter's utility by comparing the two approaches based on practical analysis with local data. This study investigated the utility of two approaches, a "watershed" and a "political unit (a national or provincial boundary)" approach, for water resources adaptation in cross-boundary sub-basins by investigating a range of climate-adaptation strategies for cooperation among the riparian nations. By investigating the results of each approach, a suitable adaptation strategy for a specific area was assessed and the general advantages and disadvantages of each approach in likely scenarios were demonstrated. The Mekong River basin, fed by the longest international river in the Asia, is the study area. We will show by the use of geospatial technology and hydrological simulation how conflict and cooperation for climate adaptation in a cross-boundary river-basin would be viewed in the light of game theory, and then use this technique to compare the watershed approach and the political unit approach.

This study's innovative, robust methodology for solving complex cross-boundary river-basin issues would be a basis for local policy decision-making and research for climate adaptation and urban and regional planning in the Mekong River and beyond. The characteristics of study areas and initial discussion of this study as well as analysis process are described in this paper.

1. INTRODUCTION

Developing a scientific framework for cross-boundary water resources management is urgently required as available fresh water becomes competitive, and thus causes more conflicts over water, due to both population growth and climate change. Conventionally, river-basin policy is divided by man-made boundaries such as national borders (Beach 2000;

Rogers 1969; Rogers 1993; Rogers and Kung 1985), although many have called for better environmental management through natural boundaries such as watersheds, the area of land where all of the water that is under it or drains off of it goes into the same place (Millennium Ecosystem Assessment 2005; US EPA 2009). This approach would capture most externalities in the river basin, but it is politically problematic, since all of the riparian nations must agree on those externalities. Solid research should inform the policy makers, however, few studies, have proven the utility of the watershed approach by comparing it to the traditional national border approach through practical analysis based on local data. This research will investigate the use of the watershed and political unit approach, for water resources adaptation in cross-boundary sub-basins by investigating a range of climate-adaptation for cooperation among the riparian nations. By investigating the results of each approach, we hope to demonstrate their advantages and disadvantages in likely scenarios, and discuss how a desirable solution can be derived.

The main tool we used for this study is a Geographic Information System (GIS), which is a promising tool for integrated river-basin analysis and management. In particular, we will use the Arc Hydro data model (Maidment 2002), a spatial and temporal data model for water resources, to model the water flow from upstream to downstream. We will show by the use of geospatial technology and hydrological simulation how conflict and cooperation for climate adaptation in an international river-basin may be viewed in the light of game theory, and then use this technique to compare the watershed approach with the political unit approach. The characteristics of study areas and initial discussion of this study as well as analysis process are described in this paper.

2. STUDY AREA

2.1 Overview of the 3S basin

The 3S basin, named after the three sub-basins it contains (the Sekong, Sesan and Srepok), is part of the Lower Mekong River Basin on the Indochinese Peninsula and includes land in Cambodia, Lao People's Democratic Republic (Lao PDR), and Vietnam (Fig. 1). The 3S area is the largest tributary system of the Mekong River Basin (Mekong River Commission 2007). It covers about 10% of the area of the entire Mekong Basin and contributes 17% of the total run-off (World Bank 2006). The Mekong River Commission (MRC)'s Basin Development Planning project (2009) identified the area as a region where considerable development potential exists and as a result, multilateral development banks have been investigating it. World Bank (2006) studied the water resources assistance strategy for integrated development and management. The Asian Development Bank has been supporting arrangements to strengthen regional cross-border collaboration at the request of the National Mekong Committees (NMC) of the governments of Cambodia, Lao PDR, and Viet Nam since April 2006.

The precipitation varies regionally across the 3S, ranging from about 1,500mm in the downstream areas and middle reaches of the Srepok to greater than 3,000mm in the upstream portions of the Sekong and Sesan sub-basins.

Much of the development in the 3S area is related to the design and construction of hydropower plants. As of February 2009, 9 hydropower plants were in operation, 8 were under construction and 24 were still in design or planning stages (Asian Development Bank 2009). The 78,650km^2 study area is divided between the three countries, with 29% of the area in Laos, 33% in Cambodia and 38% in Vietnam. In relation to its large area the total population is low, about 2,700,000 in 2000 and 2,900,000 in 2004, but the population growth rate is much higher than average in each country. The values of area and population by countries within the entire Mekong River basin and within the 3S area are shown in table 1. The social and economic development and resulting environmental pressures are higher in the upstream than the downstream regions. Detailed characterizations of each sub-basin are given in following section.

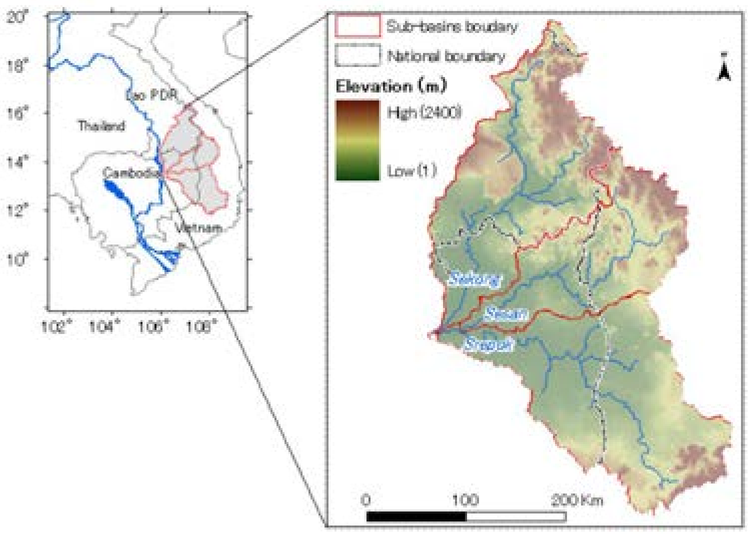

Figure 1: Three cross-boundary sub-basins in the Lower Mekong River Basin, Sekong, Sesan and Srepok (the 3S), cover the three national borders of Lao PDR, Cambodia, and Vietnam in the Indochina Peninsula.

2.2 Characteristics of individual sub-basins

2.1.1 *The Sekong River s*

The Sekong is the only sub-basin of the Mekong including lands from three countries. Seventy eight percent of the area is in Laos, 19% in Cambodia, and 2% in Vietnam. The basin area in Laos, despite covering a majority of the area, have very few population, though the Vietnamese territory is very small it accounts for 18% of the population in the basin. As a whole, population density in the Sekong basin is by far lowest of the three: 11.5 persons/km^2 in 2000.

Hydropower dam development is not very active in comparison to the other two sub-basins; only one plant, located in Laos in the middle of the sub-basin, is currently in operation. However, three relatively large scale hydropower plants (total 572MW) are under construction, and if all the plants now in design or master plans stages are actually built this sub-basin will be the most developed in the 3S, in terms of both number of hydropower plants (20) and installed capacity (total 2,688MW). The planned developments are all located in Lao territory in the middle and upstream region of the sub-basin. If all of these plants are constructed this part of the sub-basin will hold the largest active storage (total 11,067MCM) in the 3S. This development, in combination with changing land-use patterns upstream, may threaten the water use in the downstream Cambodian territory.

Table 1: Area and population by countries within the entire Mekong River basin and within the 3S area.

	Area ($10^3 km^2$)	Current population (million)	Annual Growth Rate (%)	Population in 2020 (million)
Cambodia	155/ 25	14.6 (2007) / 0.28 (2004)	2.5 / 2.99	20.1 /0.34
Lao PDR	202/ 22	6.2 (2007) / 0.22 (2004)	2.9 / N/A	7.7 / N/A
Vietnam	65/ 30	22.2 (2006) / 2.4 (2004)	1.3 / 1.95	25.6 / N/A
Total	**422 / 77**	**65.7 / 2.9**	**2 / N/A**	**77.8 / N/A**

2.1.2 *The Sesan River*

Hydropower plant development is currently most advanced in the Sesan River basin. Five plants, with a total installed capacity of 1,177MW are now in operation. One plant, with a capacity of 360MW, is under construction and five, totaling 1,033MW of installed capacity,, are in the design or master plan stage.. Many reports and documents, especially investigating fishery issues, have been written about this sub-basin, due in part to recent interest in trans-boundary issues (Hirsch 2004; Ian G. Baird 2005; Nam 2006).

The total active storage of existing and planned hydropower plants (5,919 MCM) is small relative to other two sub-basins (11,067 MCM for Sekong, and 9036 for Srepok), which might translate into a relatively small impact on water use in the downstream Cambodian territory. However, since 90% of population of the sub-basin is in Vietnamese territory with a high rate population growth, the corresponding increase of water use might still threaten the downstream areas.

2.1.3 *The Srepok River*

Two small hydropower dams (total installed capacity 28MW) are in operation in the middle of the Vietnamese side of the Srepok basin. Four plants are under construction (total 656MW) and three plants are part of the master plan (total 396MW). Compared to other two sub-basins the total planned installed capacity is small (total 1,080MW), but the total active storage is estimated to achieve over 9,000 MCM. More than 80% of the population lives in the Vietnamese part of the basin and a rapid increase of water use corresponding to population increase and expansion of agriculture on the Vietnamese side are projected in this sub-basin (Kawasaki et al. 2009). This may cause higher pressure on water resources and the environment in the relatively sparsely populated areas on the Cambodian side of the basin.

Poverty remains high in the Central Highlands of Vietnam, particularly the southeastern part of the basin. In the past 25 years, a constant influx of settlers into the sub-basin from other parts of Vietnam has resulted in an increase in transient poverty (World Bank 2006). The climate and hydrological data and documentation available for this sub-basin tends to be relatively abundant and of higher quality, particularly for the Vietnamese side, where the water resources development and management infrastructure is more advanced than in the surrounding areas.

3. METHODOLOGY

We will show by the use of geospatial technology and hydrological simulation how conflict and cooperation for climate adaptation in a cross-boundary river-basin may be viewed in the light of game theory, an analytic method for describing such conflicts and for clarifying the issues at stake. Then, we will use this technique to compare the watershed approach and the political unit approach. The main tool we will use for this study is a Geographic Information System (GIS). Details are described as follows.

3.1 Method

3.1.1 *Analyzing the characteristics of sub-basins.*

To historical trend of land-cover change in this area, comparison of the land-cover area between 1997 and 2002/2005 are described at Table 2. Assumed upstream countries impact on downstream country is analyzed at Table 3 to illustrate the relationships among sub-basins in the 3S area.

3.1.2 *Investigating future available water*

Streamflow in the next several decades, until 2025 and 2050, will be simulated by considering the potential impacts of climate change and socio-economic development on water supply and demand from domestic, agricultural and industrial uses. Various scenarios such as “business as usual”, “minimum” and “maximum” development, and “extreme climate change” will be incorporated for building future land-use and precipitation models by integrating the IPCC (Intergovernmental Panel on Climate Change) climate scenarios (2007).

We have already developed an experimental hydrological model in the Mekong (Kawasaki et al. 2009). By calibrating my simulations to land-use/water-use changes that have occurred in the past, we will sophisticate our model for a policy-making support.

3.1.3 *Considering water resources adaptation strategies*

Possible water resources adaptations will be proposed for each scenario and each sub-basin in light of simulated stream flows and local characteristics. Adaptation involves the following types of activities: investment planning for new or expanded infrastructure (reservoirs, irrigation systems); maintenance and major rehabilitation of existing systems (dam safety, levees); modifications in processes and demands (water conservation, pricing, regulation); and introduction of new efficient technologies (drip irrigation, reuse, recycling). In this process, we will have intensive interviews and discussions about the likely future development scenarios, adaptation strategy and its impact on geopolitics with the experts especially scholars in international politics, environmental politics, public policy and development economics.

Table 2: Comparison of the land-cover area between 1997 and 2002/2005

		Sekong				Seson				Srepok			
		1997		2005		1997		2005		1997		2005	
Laos	Forest	15,841	70%	13,767	61%								
	Agriculture	1,753	8%	1,397	6%								
	Urban area	10	0%	905	4%								
	Grass land	443	2%	0	0%								
	Open land	4,503	20%	6,493	29%								
Cambodia	Forest	5,126	92%	4,369	79%	6,310	83%	4,585	60%	10,620	83%	10,228	80%
	Agriculture	183	3%	175	3%	770	10%	835	11%	486	4%	531	4%
	Urban area	3	0%	5	0%	2	0%	8	0%	0	0%	5	0%
	Grass land	6	0%	104	2%	15	0%	144	2%	69	1%	191	1%
	Open land	187	3%	825	15%	438	6%	1,675	22%	1,514	12%	1,653	13%
Vietnam	Forest	394	57%	407	59%	6,088	54%	5,789	51%	8,991	50%	6,875	38%
	Agriculture	67	10%	39	6%	2,937	26%	2,122	19%	6,116	34%	6,793	37%
	Urban area	0	0%	0	0%	18	0%	0	0%	6	0%	0	0%
	Grass land	34	5%	0	0%	696	6%	0	0%	446	2%	0	0%
	Open land	172	25%	242	35%	3,028	27%	3,268	29%	2,442	13%	4,433	24%

- Area unit is km^2
- Percentage shows the areal portion of each country within the basin.

Table 3: Assumed upstream countries impact on downstream

Assumed impact	Sekong(Viet, Lao-->Cmb)	Sesan (Viet --> Cmb)	Srepok (Viet --> Cmb)
Population increase (Domestic water demand)	×: Very small change in upstream Laos where dominate more than 70% population in the sub-basin	△: Large increase in upstream Vietnam where dominate about 90% population with 0.7 million in the sub-basin	◎: Large increase in upstream Vietnam where dominate about 95% population with 1.7 million in the sub-basin
Land development (agriculture and industry)	○: Rapid change in forest and open land between 97 and 05. Still has the large potential.	×: Small change of land cover in upstream Vietnam between 97 and 05. Not so high potential for large development because of precipitous	○: Rapid change in forest and open land between 97 and 05. Still has the large potential.
HEP storage	◎: Only 1 HEP is operation now, but 11,067MCM active storage HEPs are planned in Laos	○: 2,129MCM active storage are operated and planned in upstream	△: 1,026MCM active storage are operated and planned in upstream

Installed capacity (both in operation and planned)

HEP capacity	◎: 2,688MW HEPs n Laos	◎: 1,736MW in Vietnam 784MW in Cambodia	△: 733MW in Vietnam 347Mw in Cambodia

Then, both a political and a natural boundary approach will be simulated. Water quantity and net benefits (normalized to dollars) will be the criteria for comparison. Several strategies will be considered, such as in this simple two country example:

Case 1: Both Vietnam and Cambodia do nothing;
Case 2: Vietnam optimizes, Cambodia does nothing;
Case 3: Both optimize independently;
Case 4: Regional optimization with distinct sub-regional budgets;
Case 5: Regional optimization with a single regional budget.

3.1.4 *Comparing strategies*

We are faced with the dilemma of how to select the best strategy for the development of the region. For example, choosing case 5 as yielding the highest overall net benefits to the region might not satisfy Vietnam, who would do better in case 3. For Cambodia, however, case 3 is much less attractive than case 5. Luce and Raiffa (1989) would describe these conflicts as a "cooperative two-person nonzero-sum game".

When we have three countries, we use the theory of the core from game theory. Suitable water resources adaptations for the study area will be discussed by comparing various adaptation strategies in both a watershed and a political unit.

3.2 Data

Availability of hydro and climate data in the study area is as follows. 18 hydrological observation data are available in the 3S sub-basins form the Mekong River Commission Secretariat database. All the stations records daily water level in some periods of years such as some records data in 1910-1970 and other records only after 2000. However, only 7stations record daily discharge from 1990's.

Regarding land-cover data, a variety of maps and datasets have been produced showing vegetation types and extent of forest cover in Cambodia however there are discrepancies in the forest cover percentages between these. The wide variety of forest cover figures can be attributed to factors such as incomparable data generation methods, lack of background knowledge on the analyst's past and lack of funds or time (MRC 2003). For more detailed information, please refer to Forest Trends.

The selection of Forest Resource maps in the atlas intends to give an overview o f the forestry sectors in Cambodia including information on vegetation types, trends, non timber forest products and management approaches. Explanations of the methodology used and limitations in regards to data collection are given in the appropriate sections throughout the chapter.

4. FUTURE WORK

In this paper, the characteristics of study areas and initial discussion of this study as well as analysis process are described. The result of this study will be described at another paper in near future. Then, we will visit stakeholders in environmental policy making in the Mekong River Basin to discuss the validity of our research results. The scope of these interviews will be confined to four of the countries in the Lower Mekong: Cambodia, Laos, Thailand and Vietnam (we would like to include China and Myanmar if possible). Their feedback will be taken into account for modifying models and methodologies and refining the proposed adaptation strategies.

Planned organizations to visit include: National and local authorities in the four countries, a joint panel of the regional nations (Mekong River Commission), local offices of multilateral development banks (World Bank, Asian Development Bank), nongovernmental organizations such as the Mekong Watch, and local academic institutes for the Mekong study such as: Asian Institute of Technology, Thailand; National University of Laos, Laos; and Can Tho University, Vietnam.

ACKNOWLEDGEMENT

We are grateful to Ms. Janet He and Ms. Julie Malakie for their dedicated work to conduct the simulations in this study. Also, we appreciate Dr. Masatsugu Takamatsu, for his valuable support for hydrological simulation. This study was supported financially by Research Fellowships of the Japan Society for the Promotion of Science for Young Scientists.

REFERENCES

Asian Development Bank. 2009. *Sesan, Sre Pok and Sekong River Basins Development Study in the Kingdom of Cambodia, Lao People's Democratic Republic and Socialist Republic of Viet Nam, TA6367 (REG): Pilot testing IHA-SGAP in the 3Ss Basins Inception Report*.

Beach, H. L., Hamner, J., Hewitt, J. J., Kaufman, E., Kurki, A., Oppenheimer, J. A., and Wolf, A. T., 2000. *Transboundary Freshwater Dispute Resolution: Theory, Practice, and Annotated References*, United Nations University Press, Tokyo, New York, Paris.

Hirsch, P., A. Wyatt., 2004. Negotiating local livelihoods: scales of conflict in the Se San River basin. *Asia Pacific Viewpoint*, 45 (1), 51-68.

Ian G. Baird, M. M., 2005. *Sesan River Fisheries Monitoring in Ratanakiri Province, Northeast Cambodia: Before and After the Construction of the Yali Falls Dam in the Central Highlands of Viet Nam*. 3S Rivers Protection Network (3SPN), Ratanakiri Province, Cambodia.

Intergovernmental Panel on Climate Change (IPCC), 2007. *Fourth Assessment Report: Climate Change 2007*.
Available at: http://www.ippc.ch/ipccreports/ar4-syr.htm.

Kawasaki, A., Takamatsu, M., He, J., Rogers, P., and Herath, S., 2009. Evaluation of local water resources adaptation to climate change: the Srepok River Basin in Vietnam and Cambodia. *Journal of Water Resources Planning & Management*, in review.

Maidment, D. R., 2002. *Arc Hydro: GIS for Water Resources, ESRI Press*, Redlands, California.

Luce, R., Raiffa, H., 1989. *Games and Decisions: Introduction and critical Survey*, New York: John Wiley, chapter 6.

Mekong River Commission. 2007. *Diagnostic study of water quality in the Lower Mekong Basin: MRC Technical Paper No. 15*. Vientiane, Lao PDR.

Mekong River Commission. 2009. Basin Development Plan, Phase 2 (BDP2): HYDROPOWER SECTOR REVIEW FOR THE JOINT BASIN PLANNING PROCESS (Draft Report). Mekong River Commission, Vientiane, Lao PDR.

Millennium Ecosystem Assessment. 2005. *Ecosystems and Human Well-being: Synthesis*, Island Press, Washington DC.

Nam, E. o. V., 2006. Comprehensive Development Study on Hydropower in Se San River in Cambodia: Summary Report (Draft Volume 1). *Electricity of Viet Nam*, Hanoi, Vietnam.

Rogers, P., 1969. A GAME THEORY APPROACH TO PROBLEMS OF INTERNATIONAL RIVER BASINS. *Water Resources Research*, 5(4), 749-760.

Rogers, P., 1993. THE VALUE OF COOPERATION IN RESOLVING INTERNATIONAL RIVER BASIN DISPUTES. *Natural Resources Forum*, 17(2), 117-131.

Rogers, P., and Kung, S. L., 1985. Decentralized planning for the Ganga basin: Decomposition by river basins. *Sadhana-Academy Proceedings in Engineering Sciences*, 8, 123-134.

US Environmental Protection Agency (EPA). 2009. Watersheds. US Environmental Protection Agency, <epa.gov/watershed/>.

World Bank. 2006. M*ekong Water Resources Assistance Strategy (MWRAS): Options for Integrated Development and Management in the Se Kong - Se San - Sre Pok Catchments of the Mekong in Cambodia, Lao PDR and Vietnam: Main Report*. The World Bank.

COMPARISON BETWEEN LEED® AND CASBEE GREEN BUILDING ASSESSMENT SYSTEM

PRANAB J. BARUAH, KIMIRO MEGURO
International Center for Urban Safety Engineering (ICUS)
The University of Tokyo, 4-6-1 Komaba, Meguro-ku, Tokyo 1538505
{baruah,meguro}@iis.u-tokyo.ac.jp

ABSTRACT

Recently, building and construction sector is gaining increased attention due to their potential in achieving significant energy, water and resource efficiency at minimal or no costs through integrated design approach, which also leads to substantial green house gas reduction towards mitigation of climate change. In order to incorporate various sustainability elements during design, construction and operation of built environment while improving overall building performance, green building assessment systems are being developed around the world. In this review paper, we give a brief overview of presently available building assessment systems around the world before comparing two such systems, namely LEED® (Leadership in Energy and Environmental Design) of USA and CASBEE (Comprehensive Assessment System for Built Environment Efficiency) of Japan. The main reason for comparing them is the difference in their assessment concept, origination country and market transformation strategy. We carried out a descriptive comparison on their effectiveness in addressing sustainability issues, assessment methodology, market maturity, market transformation through leadership, awareness generation & capacity building through education, social transformation through green building advocacy, partnership & outreach, research & development as well as their universality & flexibility for innovation.

Building assessment systems are mainly non-profit initiatives advocating whole building design approach and sustainable design principles, but their pursuance provide considerable economic benefits along with environmental one to stakeholders, which becomes the significant driving factor for their adoption. Thus, these systems are in competition with each other and their business case drives their potential for growth, adoptability and ultimate survival of the vision/principles behind them. Based on our comparison, we analyzed the competitive advantage and found that LEED® system has established a clear competitive advantage in USA and globally over CASBEE, however, CASBEE is the default leader in Japan in terms of adoption. It is inferred that, overall slower adoption of CASBEE in and beyond Japan is not because of weaker assessment effectiveness and/or result delivery potential but because of inability to formulate a strong business case in line with present times.

1. INTRODUCTION

Building and construction sector has been identified as a key sector for sustainable development. The sector provides 5-10% employment in national level and generates about 5-15 % of GDP. If the energy, water and other resources consumed during construction and utilization of the buildings in their entire lifespan is considered, built environment is responsible for about 40% of CO_2e emission, 30% of solid waste generation and about 20% of water effluents. In terms of resources used, about 40% of energy, 20% of water and 10% of land-area are used by the building and construction sector (UNEP-SBCI, 2006). Globally, buildings use about 40% of raw materials (3 billion tons). With business as usual, these figures are projected to go up significantly with increasing population growth, prosperity in emerging countries and rapid urbanization. For example, China is forecasted to add twice the amount of current office space between 2000 to 2020, with roughly 60% of Chinese population living in the city in 2030 from about 40% in 2005. In developed countries, coupled with an inefficient building stock, increasing use of services and appliances, ageing population (in many countries) along with changing lifestyle leading to single-person household, has increased the use of energy and resources use in buildings. At the same time, building and construction sector is a key sector for achieving various efficiency improvements with significant green house gas (GHG) mitigation potential at minimal or negative costs (IPCC, 2007). Sustainable building practices for efficiency improvements and GHG abatements have not been unfamiliar to designers/architects even decades before, however a strong business case for these sustainable designs as well as involvement of various stakeholders and awareness at the customer level (owner and tenant) were lacking. Now, with increasing public concerns about environment, particularly climate change with increasing energy prices and depleting fossil fuel as well other natural resources, a green building (GB) movement is gaining momentum. With the introduction of green building assessment systems around the world, multiple stakeholders in this complex sector with significant inertia to change is gradually recognizing the economic potential and environmental benefits of greening the real estate (Nelson, 2007).

In 1990, UK's Building Research Establishment (BRE) first such building assessment system, BREEAM (BRE Environmental Assessment Method), designed to help the UK building and construction sector incorporate sustainability elements into their designs and construction practices. Last decade and a half have seen development of several green building assessment systems around the world (Baruah et al., 2008) with systems developed in at least 20 countries and the latest one being Germany's DGNB released in 2009. There are hundreds of building evaluation tools available worldwide, however, sustainable or green building assessment systems mentioned here are those that provide a whole-building evaluation (rather than an individual design feature) incorporating an integrated and team approach to design. So, an effective green building assessment system incorporates vast array of best practices and techniques to also provide the framework and strategies to design buildings that are better than the average stock in reducing the overall impact of the built environment on human health and the natural environment by efficiently using energy, water, and other resources, in protecting occupant health and improving employee productivity, and in reducing waste, pollution and environmental degradation in their lifecycle. Some assessments systems also take into account other social, structural and economic elements such as community development, social transformation, durability and affordability. In general, each of these tools reflects social, economic, cultural and climatic backgrounds of the respective country.

In this paper we compare two green building assessment systems, namely LEED® (hereafter, LEED for convenience) from US Green Building Council (USGBC) and CASBEE from Japan GreenBuild Council (JaGBC). Both are voluntary assessment systems. Starting with BREEAM, several well-recognized green building assessment systems including LEED use purely criteria based methodology assigning point values to a selected number of parameters on a scale. On the other end, some systems use rigorous life cycle based approach which is often difficult, laborious and a time-consuming. CASBEE takes an intermediate stance by employing a scheme that promotes life cycle assessment but with an unique methodology to arrive at its rating criteria. In the next section, a brief overview of these two assessment systems is given.

2. USGBC LEED & JAGBC CASBEE ASSESSMENT SYSTEM

Inspired by BREEAM of UK, in order to serve the US building community, non-profit USBGC unveiled LEED in 1998 as a voluntary rating system with a market-driven strategy to accelerate adoption of green building practices. In its website presentation, LEED claims to be a consensus-based “leading edge system for certifying the greenest performing buildings in the world”. Originally developed for new commercial buildings (LEED-NC), LEED has gone through major update in 2003 and now several versions exist to serve different building types and function. The system got a major overhaul in 2009 where additional functionalities were added with the changes in points allocation and reweighing of some functions. In the latest system, the entire process is expected to be flexible to adapt to changing technology, account for regional differences and encourage innovation. Though primarily developed for US building and construction sector, over the years, LEED has gained world-wide popularity with the system being adopted in countries like Canada, UK, Brazil, China, India and the Mid-East.

Supported by Ministry of Land Infrastructure and Transport (MLIT), Japan GreenBuild Council(JaGBC)/Japan Sustainable Building Consortium (JSBC) along with subcommittees consisting of members from academia, industry and government have developed and launched CASBEE in 2004. Secretariat of CASBEE is administered by the Institute for Building Environment and Energy Conservation (IBEC). According to Prof. S.

Murakami, Chair of JSBC, “CASBEE creates incentives for building owners, designers and users to develop high quality sustainable buildings. The system meets both political requirements and market needs for achieving a sustainable society.” The latest version of CASBEE is released in 2008. The system has been increasingly adopted by industry in Japan and several regional governments have made it mandatory reporting of CASBEE ranking for new buildings.

3. COMPARISON BETWEEN LEED AND CASBEE

Table 1, 2 and 3 give the comparison between LEED and CASBEE. Please note that lists are non-exhaustive and the comparison is based on available information and technical manuals of the two systems. Major sources includes, CASBEE (2009), CASBEE NCe (2008), Fowler et al. (2006), LEED Manual (2009), Saunders (2008) and USGBC (2009).

Table 1: General Comparison: LEED vs. CASBEE

	LEED	CASBEE
Start year	1998	2001
Developer	USGBC in a consensus process with non-profit organizations, government agencies, architects, engineers, developers, builders, product manufacturers and other industry leaders	Joint industry / government / academic project. Support from MLIT, developed by JaGBC/JSBC (secretariat by IBEC) and subcommittees
Project registered	24,679 commercial projects, June 2009 (about 5 billion square feet)	Unknown
Project certified	3,111 commercial projects, June 2009 (floor space: 385 mil sq.ft.)	80 (as of August 14, 2009)
Member number & type	> 20,000 paying members, July 2009 Builders, Developers, Architecture firms, NGOs, Municipalities, Universities, Product manufacturers	Unknown, webpages (CASBEE & IBEC) do not provide information
Assessors	LEED Professional (LEED AP & GA) : 131,700 (as of June 30, 2009)	3,885 (as of October 2008)
Assessor countries	at >40 countries	Japan
International presence	Projects in 103 countries (25% of total floor space, 9% of projects)	Unknown
International adaptation (versatility)	LEED Canada, LEED India (LEED Brazil & LEED Italia in discussion phase)	Concept of CASBEE incorporated in GOBAS, the Green Building standard of Beijing Olympics (2005) and National Green Building Standard of China (2006)
Use in local governments	-Boston, Massachusettes and Washington DC (from 2012) requires LEED certifications for buildings > 50,000 sq.ft. -Babylon, NY: permits only to buildings >4,000 sq.ft. with a LEED checklist -Arlington, Virginia requires site plans applications with LEED score card and LEED assessors in project	15 local governments in Japan require mandatory submission of CASBEE assessment of their buildings (Total submissions 3,664 by 2008)

Table 1 continues to next page..

..Table 1 continued from previous page

Incentive programs using the system	-Chicago: Expedited permitting for LEED certified -San Francisco: Priority permitting for LEED Gold certified -Arlington, Virginia: Graded density bonuses for LEED certified -Seattle: Greater height to floor space area for certain LEED certified	Some cities provide incentives. -City of Osaka subsidizes residential buildings with a A-rank -City of Nagoya has graded subsidy for residential buildings based on CASBEE ranking -Financial sectors, such as banks, are offering better interest rates to high ranked CASBEE houses
Revisions, last update	When needed April 2009 (major update)	Periodic, September 2008
Alliance with other organizations	-BRE (UK), Green star (Australia) Objective: Develop common CO_2 metrics -Canada GBC, India GBC, GBC Italia, GBC Brazil; Objective: LEED adaptation -Clinton Climate Initiative Objective: Develop 16 large-scale urban projects in 10 countries	-SB Alliance: CSBT (France, initiator), BRE (UK), DGNB (Germany) Objective: R&D co-ordination and sharing, shared use, promotion
Visiting delegation, internship program	Visiting delegations comprising students, building professionals, government officials, and market analysts from China, Russia, Japan, the Nordics, UK and Australia.	Unknown
Communi-cation & Transparency	Financial statements online and open, tools and manuals available on purchase, assessment process known, appeals possible, organizational structure transparent, prompt e-mail enquiry service, Credit Interpretation Request (CIR) possible with fee	Tools and manuals available free, assessment process known, organizational structure somewhat known
Open Resources	-USGBC homepage: Research publications, project case studies, GB links, research fund proposals, general presentation, government resources, resources for K12 students, commercial real estate resources, LEED manuals(purchase) & CIRs (membership needed), links to chapter resources -GBCI: Credentialing resources, certification resources, data graphs	CASBEE homepage, certified project database
Webpage status	Up-to-date with links and resources Three main webpage (USGBC, GBCI, GreenBuild365), easy to navigate	Up-to-date with latest tools, Japanese page more recent and up-to-date
Promotion	USGBC Chapters, GreenBuild365, USGBC website	CASBEE webpage
Language	English	Japanese and English (partial)
Information channel	E-mail and USGBC chapters	E-mail & telephone
Known Cost premium & payback period	Cost-premium: Vary with studies --> minimal to non-existent to an average of 2% (0.66% for LEED-certified to 6.5% for LEED-Platinum); 3-6 years payback period for existing buildings	No known studies

Table 1 continues to next page..

..Table 1 continued from previous page

Growth rate	-Membership: Quadrupled since 2000 -Every business day, $464 mil registered with LEED -Compound annual growth rate: 86% (2002-2007)	-Assessors: 2700-->3885 (from Aug. to Oct. 2008) -Certified Buildings: 34-->80 (from Aug. 2008 to Aug. 2009) (>100% growth) -Mandatory submission by local govt.: 2479 --> 3664 (from March to year end 2008)
Growth forecast	-Overall green building market in USA to double to $96-140 billion	Unavailable
Google hits	6,210,000 on 11 August 2009	60,000 on 11 August 2009

3.1 General comparison

Looking at the general comparison in Table 1, it is evident that both systems have grown over the years due to the increasing demand of sustainable housing around the world. LEED is gaining tremendous popularity and growth when compared with CASBEE. Google popularity of LEED is more than 100 times of its peer. This is because while its main focus is on the domestic US market, USGBC is being increasingly adopted internationally for its transparent, market-based and internet-based approach. Over the years, it has evolved itself into three focus-based entities; Green Building Certification Institute (GBCI) to focus on certification and credentials, GreenBuild360 for education and outreach and USGBC for administration, strategy and system formulation. When compared with CASBEE, its accomplishment in advancing sustainability in the building sector also matches its popularity. With project in more than 100 countries, it has certified more than 3000 projects as of June 2009 compared to CASBEE’s 80, and with a huge pool registered project in the pipeline (>24,000). It has more assessors (about 121,000 presently) than probably assessors of all major GB assessment systems combined. LEED assessors comprise of not only engineers or architects, but also environmentalists, lawyers, students, product manufacturers, government officials, insurance agents etc, or simply anyone who is interested in advancing/proving their credentials in sustainability. Whereas, CASBEE has restricted their eligibility criteria for assessors examination to only first class Japanese architects. In case of CASBEE, local governments have been most active to adopt it under the nation’s Environment Preservation Act. CASBEE is now being adopted as a mandatory reporting standard by 15 local governments across Japan. However, reporting does not make certification mandatory here. In coming years, LEED may also see an upsurge as a mandatory system by local governments since a large number of USGBC’s more than 20,000 members are now local governments. In case of CASBEE, though the Beijing Olympic’s GoBAS system was based primarily on it, its international presence and activities have been limited compared to LEED.

3.2 Assessment System Comparison

LEED is a point based system with 4 ratings (Certified, Silver, Gold,

Table 2: Assessment System Comparison: LEED vs. CASBEE

	LEED	CASBEE
Credit elements	Sustainable Sites Water Efficiency Energy and Atmosphere Materials and Resources Indoor Environmental Quality Awareness and Education Location and Linkages Neighborhood Pattern and Design Green Infrastructure and Building Innovation in Design Regional Priority	Environmental Quality (Q) Q1: Indoor Environment Q2: Quality of Service Q3: Outdoor Site Environment Environmental Load (L) L1: Energy L2: Resources & Materials L3: Off-site environment ----------------------- Building Environmental Efficiency, BEE = Q/L
Versions	-LEED for New Construction (includes major renovation) -LEED for Existing Buildings -LEED for Commercial Interiors -LEED for Core and Shell -LEED for Homes -LEED for Neighborhood Development -LEED for Schools LEED for Retail	*Basic Tools:* -CASBEE for Pre-design -CASBEE for New Construction -CASBEE for Existing Building -CASBEE for Renovation *Extended Tools:* -CASBEE for temporary construction -CASBEE [local] (e.g. Nagoya) -CASBEE for Urban Development -CASBEE for Heat Island -CASBEE for Detached House -CASBEE Urban Design+Buildings
Sustainability issues addressed	Global warming mitigation, Resource efficiency, Biodiversity conservation, Pollution prevention, Community development, Contribution to regional economy & community, Equity	Global warming mitigation, Resource efficiency, Biodiversity conservation, Pollution prevention, Durability, Disaster risk reduction
Scoring system	- Point based with pre-requisites - Static set of equal-weight credits can be reweighted using a scenario tool and/or to address regional priority - better performance more points	-Eco-efficiency based BEE concept -complex weighted points -high Q & Low L, high BEE
Info gathering /paperwork	Design/project team or Assessor	Design/ project team
Assessment & certification body	-Assessor participates through design and construction process to achieve points and puts in the paperwork to GBCI for certification -GBCI certifies based on submitted evidence, random audits done	-Self certification -Third party verification is possible
Tools and Manuals	-Manual can be purchased online -Online checklists, scorecard and relevant document submission upon registration of project	-Manuals can be downloaded -Excel tools/scorecard can be downloaded
Language	English	-Tools in Japanese and English -Manual in Japanese, English, Korean and Chinese
Registration cost	$450 (members) - $600	$0
Certification cost	-$1,250-$22,500 (increase from 2010) -Additional fee for CIRs and appeals -Expedited review: additional $10,000	$3,570-4,500

Table 2 continues to next page..

..Table 2 continued from previous page

Tools and manuals cost	Project tools free with registration, manuals $175	Free
Result communication	100 points, additional 6 in Innovation in Design and 4 in Regional Priority - Certified : 40-49 - Silver : 50-59 - Gold : 60-79 - Platinum: > 80	Radar chart, histograms, numerical values and BEE C : BEE 0-0.49 B- : BEE 0.5-0.99 B+ : BEE 1.0-1.49 A : BEE 1.5-2.99 S : BEE 0-0.49
Result product	Award Letter, Certificate, Plaque	Certificate and published in webpage
Availability of implementation strategies	Strategies available in the manual, credit interpretation requests, project case studies	Strategies available in manual, project case studies
Education	Dedicated education wing, GreenBuild365. It organizes seminars, conferences and provides year-round green building related courses onsite and online. Resources for K-12 students available	CASBEE has been used in education in universities and private sector
R & D	$2 million for GB research grant	Unknown
Benchmarking	Yes	Yes
Checklist	Yes	Scorecard available
Type	Online	On-line Excel spreadsheet
At what stage	Design Review and Construction Review	Preliminary design, execution design and completion
Third party evaluation	Yes	Available
Scope for innovation	-Credits for innovation in design -Designs submitted under innovation in design credit is open for members and registered project -CIRs open to members and projects -R & D for innovative technologies	Flexible system that facilitates innovation
Assessment verification	-Mandatory commissioning prerequisites and enhanced commissioning points -Energy and water usage data to be submitted to USGBC annually -Existing building recertified in a two-year cycle	Building certified for three years
Result delivery potential (Various improvements)	-On average LEED buildings are 25-30% more efficient than non-LEED (Platinum and Gold: >45% efficient) -Studies available on improvements	Unavailable
Credit related design enquiry	CIR (paid enquiry), *leeduser.com* to navigate the latest rating system	Unknown

Platinum) based on total number of points achieved. It has a static set of credits with equal weights which can be re-weighted using a credit weighting tool with selectable scenarios. Total operational GHG emission for the chosen scenario can be calculated. CASBEE uses a complex calculation methodology to calculate an index called Building

Environmental Efficiency (BEE). BEE is based on the eco-efficiency concept by WBCSD and OECD. Weights, decided by questionnaire survey of building practitioners and researchers, are applied to each category and subcategories to derive environmental quality and performance and environmental loadings. However, unlike LEED, there is very little information on how the credits are actually assessed, other than the performance level required. In that sense, inconsistencies may occur and they may be interpreted in different ways. In CASBEE, credits can be earned for ease of renewal or earthquake resistance, not available in LEED, which are useful in an earthquake prone country like Japan. Also, credits such as humidity control or flexibility for storey height are not available in LEED. CASBEE also approximately calculates life cycle CO_2 from the building project. On the other hand, LEED has points, not seen in CASBEE, to encourage regional use of resources and to encourage compact city and mass transportation.

However, it would be difficult to compare the systems directly because of their difference in approach to calculate ratings. Especially, in case of CASBEE, effect/value of addressing individual issues or modifications in deign can not be worked out until the final BEE value is calculated. This also reduces the value of CASBEE as a design tool (Saunders, 2008). However, CASBEE's BEE approach can provide trade-off between environmental loading and quality of space provided. Also, since its metrics can be interpreted in different ways, there is more flexibility and scope for more innovative designs to be incorporated. This, on the other hand, provides loopholes for proving effectiveness of a inefficient design. Most important of all, while both system addresses the major issues of building environmental issues, as a system LEED provides a stronger basis for whole building design with clearly stated intent, requirement and strategies for each credit and explaining synergies with other credits to better pursue whole building design. The latest LEED V3 also provides points for integrating sustainability features with education program in case of school projects.

3.3 Assessor System Comparison

Assessors assess and/or help design the buildings to be certified under a GB system. At the same time, an assessor indirectly promotes and spreads the principles of the system he is accredited to assess. It is evident that, LEED is taking a more active role in spreading the green building movement among all stakeholders by taking a more open stance to its assessor certification program. Apart from engineers and architects, this has generated interests also among builders and developers to product manufacturers, lawyers, insurance providers etc., to serve and advance the green building market and movement effectively. Since building assessment systems are ideal actionable frameworks to pursue sustainability with a business case, understanding them also provides excellent education for a shift towards sustainability thinking. In other words, with too few sustainability education and certifications available, passing the assessor examination adds to one's sustainability credentials.

Table 3: Assessor System Comparison: LEED vs. CASBEE

	LEED	CASBEE
Assessor training	-Non-mandatory; available from USGBC, USGBC Chapters, third party training providers recognized by GreenBuild365 and other private providers (range from $99 USD online to > ~$1,500 USD)	-Mandatory from JSBC -Held at 9 major cities across Japan once in a year -In Japanese only, 10,000 yen
Criteria for Accredited Assessor	-Before June 2009: Pass exams only -From August 2009: Pass a two-part exams; GB experience and continuing education required (Those passing before June 2009 need proof by 2011)	Designated JSBC training + Japanese first class Architect license + pass exams
Certification agency	GBCI	IBEC and four other bodies.
Assessor Examination	-Held at all major cities of USA and the world, all continents, year round -Detailed FAQ at GBCI homepage -Student pricing, special requirements (handicaps etc.) available -2 parts, total 4 hours, computer-based 200 multiple choice questions -Pass score: 85%, Pass rate: ~ 25-30% -$100 application fee, $450 exams fee, online reservation, free certificate -Immediate result and name listing in GBCI webpage	-Held once in a year at 9 major cities around Japan -Information in Japanese in CASBEE homepage -40 multiple choice questions, 2 hours -Pass score: 77-80%, Pass rate :~70-90% -15,000 yen exam fee, 10,000 yen certification fee -Reserve by fax and money transfer -Result published in webpage, excel file of assessor list in IBEC webpage
Assessor continuing education	Credential Maintenance Program through GBCI and GreenBuild365	No such program
Assessor points	Project receives points for having active accredited assessors in project team	No points for having accredited assessor in the team

With a transparent, flexible and global assessor education and assessor examination system, LEED is effectively spreading its vision, principles and creating interests also in other sectors in pursuing sustainability with a business case. CASBEE accredited assessor system is only open to first class Japanese architects and having the examination in Japanese and only in Japan makes it exclusively a national system. Training for becoming a CASBEE assessor is exclusively provided by JSBC whereas for LEED, it has a dedicated training provider (GreenBuild365.com) which also organizes seminars, conferences and provides substantial amount of its training online to reach broader audience worldwide. Moreover, regional chapters of LEED and third party private providers are also allowed to provide training. To address the lack of experience and proper background in many LEED assessors, new criteria is introduced in LEED V3 with a two tier system with mandatory experience in GB projects along with continuing education (but not professional background).

4. COMPETITIVE ADVANTAGE

Building assessment systems are primarily non-profit initiatives with a goal to provide actionable framework to the building and construction industry to address sustainability issues such as elimination of building construction and operations' contribution to climate change and natural resource depletion and thereby serve as catalyst for active participation by the sector towards achieving sustainable cities and communities. While their primary goal is same and is of global interest, their acceptability within the sector depends heavily on their ability to show and prove the business case behind adoption of their proposed framework and their involvement with all stakeholders in the building sector and society as a whole. Large scale adoption through market transformation is the key to the advancement and survival of their vision. Since pursuing sustainability with an integrated whole building design approach increases the value of a property through decreased operating expenses, decreased environmental risks, increased reputation through increased environmental credentials, increased well-being such as productivity and health of occupants (Ries et al., 2009), these systems are increasingly becoming key marketing and profit-generation tools for the industry. And in a globalized world, owners and builders alike now prefer to adopt systems that have better reputation and are effective, transparent, innovative and are adopted by their peers or competitors. In that sense, in the business sphere, these systems are in competition with each other and the advancement and survival or their vision and mission depends on their competitiveness in the long run.

Primary factors for competitive advantage are innovation, reputation and relationships. There are not many studies to compare the performance of both LEED and CASBEE on a same building. Also, since two systems are designed mainly for climatic and other regional conditions of their respective country, comparing them directly would not give any conclusive result on which is better overall. However, there are more studies on LEED on their effectiveness in delivering results (with hard numbers) than CASBEE. In leadership and market transformation, both are at the forefront in their country of origin. However, LEED has gone beyond USA and developed a worldwide reputation and awareness about green buildings with projects in numerous countries. CASBEE is clearly the winner in Japan with Japanese corporations adopting it as the default standard. Also, it has been adopted by the local governments as a mandatory system. Without another assessment system available in Japanese language, probably there was also no alternative for these local governments. However, the system is much less transparent and less open compared to LEED. While LEED is taking a professional market-based approach everything from system development, marketing, outreach, education and networking, CASBEE is taking a rather voluntary and conventional approach in its expansion. In terms of cost of pursuing certification, CASBEE is much cheaper to pursue. Moreover, concept of CASBEE system has been able to shift from single buildings to regional development and sustainable city with its array of tools. However, in an international arena and from a business perspective, apart from environmental and other tangible benefits from pursuing an assessment system, LEED would clearly add more value to a project through its burgeoning reputation itself.

5. CONCLUSION

With increasing interest in sustainability, a green building movement is taking place around the world. Green building assessment systems have been instrumental in generating interests in the building and construction sector to pursue sustainability with a business case. We carried out a descriptive comparison of two major assessment systems, LEED and CASBEE. Due to their difference in methodological approach and target region for design considerations, it is difficult to compare the performance of the assessment systems directly. However, it terms of market transformation, green building advocacy, stakeholder involvement, transparency & communication and adoption, LEED is found to be in a leading position. In terms of adoption, both systems are leader in their respective origin country, however, adoption of CASBEE is relatively slower. Transparency and a strong strategy-driven market-based approach are found to be the keys to rapid adoption of LEED. These, along with its increasing partnership & outreach as well as reputation, are providing it with a competitive advantage over CASBEE in the international arena.

REFERENCES

Baruah, P.J., Sumi, A., and Endo, T., 2008. Green Building: Current Status and Prospects, In: *Proc. 7th International Symposium on New Technologies for Urban Safety of Mega Cities in Asia*, Beijing, Oct 21-22, 2008, pp 767-778.

CASBEE, 2009. *Comprehensive Assessment System for Built Environment Efficiency homepage,* http://www.ibec.or.jp/CASBEE/english/overviewE.htm (*accessed on 10 September, 2009).*

CASBEE NCe, 2008. *CASBEE for New Construction Technical Manual 2008 English Edition*, IBEC, 262 pp.

Fowler, K.M, and Rauch, E,M., 2006. *Sustainable buildings rating systems summary*, Pacific Northwest National Laboratory, 47 pp.

IPCC, 2007. *Climate Change 2007: Synthesis Report.* Intergovernmental Panel on Climate Change, 57 pp.

LEED Manual, 2009. *Green Building Design and Construction*, USGBC, 675 pp.

Nelson, A.J., 2007. *The Greening of U.S. Investment Real Estate-Market Fundamentals, Prospects and Opportunities*, RREEF Research, 47 pp.

Ries, R., Bilec, M.M., Gokhan, N.M., Needy, K.L., 2009. The Economic Benefits of Green Buildings: A Comprehensive Case Study, *The Engineering Economist,* 51(3), 259-295.

Saunders, T., 2008. *A discussion document comparing international environmental assessment methods for buildings*, UK-BRE, 46 pp.

UNEP-SBCI, 2006. *Sustainable Buildings & Construction Initiative, 2006 Information Note*, United Nations Development Program, 12 pp.

USGBC, 2009. *US Green Building Council homepage,* www.usgbc.org. (*accessed on 10 September, 2009).*

PARALLEL SESSION 2

IMPORTANCE OF OVERALL EVALUATION OF CIVIL STRUCTURES TO MAINTAIN SAFETY

TAKETO UOMOTO
Professor Emeritus, The University of Tokyo, Tokyo, Japan
Professor, Shibaura Institute of Technology, Tokyo, Japan
uomoto@sic.shibaura-it.ac.jp

ABSTRACT

Tremendous amount of structures have been built in recent years throughout the world. These structures are important properties to the people as far as they are used by the people. Looking at the situation now in our country, although the amount of the structures is tremendous, these structures are not always being maintained well by the public. Especially in Japan, due to natural hazards, such as earthquakes, typhoons, floods, etc., and the change of the economy and politics, it is difficult to maintain all the structures in convenient state. This paper explains how we have been looking at the problem and maintains the existing structures especially reinforced concrete structures. The technologies related to maintenance are also explained in the paper.

1. INTRODUCTION

Up till now in Japan, the economic growth was rapid in the period of 1960 ～1980. More than 100million cubic meters of concrete were used to construct the structures such as buildings, bridges, tunnels, dams, etc. to support the activities of Japanese people. As a result, these infrastructures rapidly reached 50 years in service, and due to deterioration of the structures, maintenance of these structures has become a major interest among the owners and the civil engineers.

On the other hands, population of Japan will reduce from now on because of fewer babies in a family approximately 1.2 children per one family. Although high technologies have been developed in recent years, it is sure that fewer engineers have to take care of the huge amount of structures from now on, which has never experienced in the past. Due to reduction in the economical growth, the budget for both construction and maintenance will be reduced in the future. The maintenance of existing structures must be done with the following conditions: 1) rapid increasing of the amount of existing structures reaching to the age of 50 years, 2) less amount of engineers to maintain the structures, 3) less amount of budget can be used to maintain the structures.

Although there are many hazards in each country, concrete structures are expected to be safe for long period of time. Main hazards for the structures in Japan are as follows:

1. Earthquake and volcanic action
2. Landslide and flood
3. Typhoons and strong wind
4. Fire and Thunder
5. Accidents
6. Terrorism

If the structure is deteriorated before the hazards, the structure may easily collapse andit is difficult to maintain the safety of the people. The Figure 1 shows an example of a collapsed pier during Hanshin Awaji Great Earthquake. As shown in the photo, the pier was deteriorated to large extent due to alkali aggregate reaction. Concrete is cracked severely and is just like a bundle of concrete blocks.

Figure 1: Collapsed reinforced concrete pier affected by alkali aggregate reaction

In order to keep the safety of urban area, it is important to study and investigate not only on hazards but also on durability aspects of existing structures. Even a small amount of concrete spalling may cause traffic accidents to large extent as we experienced in Sanyo-Shinkansen in 1999.

Considering these situations now, this paper explains what is happening now in Japan and how we are dealing with the problems through researches and engineering.

2. GENERAL MAINTENANCE METHODS BEING USED UP TILL NOW

The maintenance of concrete structures has been done mostly by the owners of the structures. In case of public structures, the ministries, etc. maintain the structure after the structures are completed. For the time being, the methods for the maintenance differ according to the owners of the structures. Although there are some differences, the main concept of the maintenance can be summarized as follows (Uomoto and Misra, 2001):

1. Periodic inspection and evaluation of deterioration degree
2. Detailed inspection and decision making
3. Repairing and strengthening of deteriorated structures

For periodic inspections, the inspectors inspect the structures visually, sometimes with the help of binoculars and hammers, once a year or once in several years according to the importance and time after the structure is completed. The inspectors are mostly trained engineers with experiences. The detailed inspection is done when the estimated degree of deterioration exceeds certain limit, or when some new phenomenon is found during the periodic inspection. The detailed inspection is done by visual inspections with the aid of non-destructive tests or taking core samples out from the inspected structure. The purpose of the inspection is to decide the cause of the deterioration and also to evaluate whether repair and/or strengthening is needed or not.

To repair or strengthen the existing structures, it is important to design and select sufficient methods and materials. The most popular repair method for corrosion of steel bars due to carbonation is to eliminate the carbonated concrete and replace it by new concrete and apply coatings with and without FRP sheets. But in case of steel corrosion due to chlorides from the surrounding environment, the highly chloride concentrated portion of concrete are taken out, anti-corrosive treatment is applied to the surface of the bar, and polymer cement mortar is generally used to repair the concrete before coating the concrete surface.

3. CASE STUDIES OF ACTUAL EXISTING STRUCTURES

In the cities, many underground tunnels exist in the urban area. When a new construction work is planned to build houses, facilities, etc., it is common to survey whether there are ny under ground structures exist or not at the point of the new construction site. If any tunnels exist, designer must check whether the structure may affect the tunnel or not before the construction occurs. But in some cases, the designer may not consider the affect well, and it may cause effects to the existing structures.

In this chapter, two examples encountered in actual existing tunnels are discussed. The first case is the effect of a dike of a river on the tunnel located underneath and the second case is the effect of earth fill on the tunnel underneath. In the first case, at the design stage of the dike, it was assumed that some effect may occur on the existing tunnel and reinforcement was applied to the existing tunnel. But the inspected results show that the effect was much larger than expected and due to the load cracking has occurred inside the tunnel lining. In the second case, the earth fill was only 1 to 2 meters in depth and nothing was done. Through these investigations, the importance of the behavior of the tunnels constructed in soft ground or reclaimed land was clarified.

3.1 Effect on concrete tunnel under river dikes (Case 1) [1,2]

3.1.1 Outline of the inspected tunnel

The figure 2 shows the relation between the tunnel being inspected and the dike above the tunnel. As shown in the figure, the tunnel is located about 10 to 20m below the dikes. The clay above and underneath the tunnel is soft compared to sand layer, and they may settlement after the construction of dikes above.

The diameter of the tunnel is 2590mm and non-reinforced concrete lining is applied as the secondary lining. In the normal section, steel segment with secondary lining is applied. In the reinforced section, reinforced concrete linings are applied inside the tunnel to increase the strength of the lining. . The thickness of the secondary lining is 246mm, and the third or reinforced lining is 160mm tin thickness.

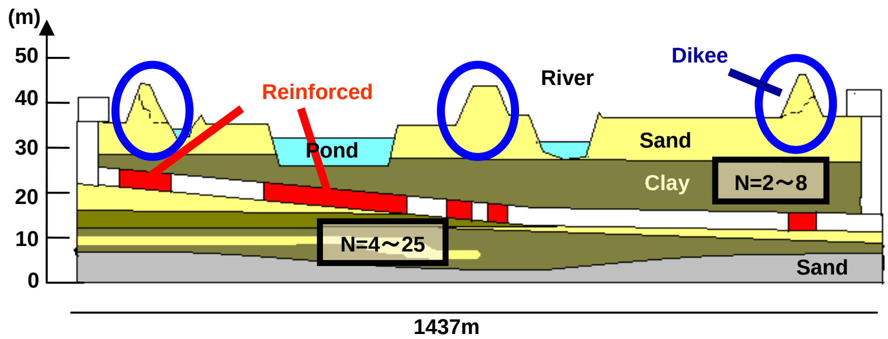

Figure 2: Location of a tunnel and dikes above the tunnel (Takeuchi and Suzuki 2007)

3.1.2 Inspected results of the tunnel

An example of the inspected result is shown in Figure 3. As shown in the figure the cracks are observed elsewhere and the distribution is large especially S10 to S11. Most of these cracks are vertical to the tunnel axis, indicating that the cracks may be made by force rather than deterioration such as corrosion or alkali aggregate reaction.

After the construction, the tunnel has been used for 30years and quite a large amount of settlement was observed. Every year, the height of the tunnel is measured. Figure 4 shows the height and settlement of the tunnel just after the construction and after 30 years. As shown in the figure, the largest settlement was observed in the span No. S 13, and another portion was in the span No. 69. On the contrary, a large rise was observed in the span No. 43. These figure shows that the tunnel has moved downwards in some places, but also some portion moved upwards after the construction.

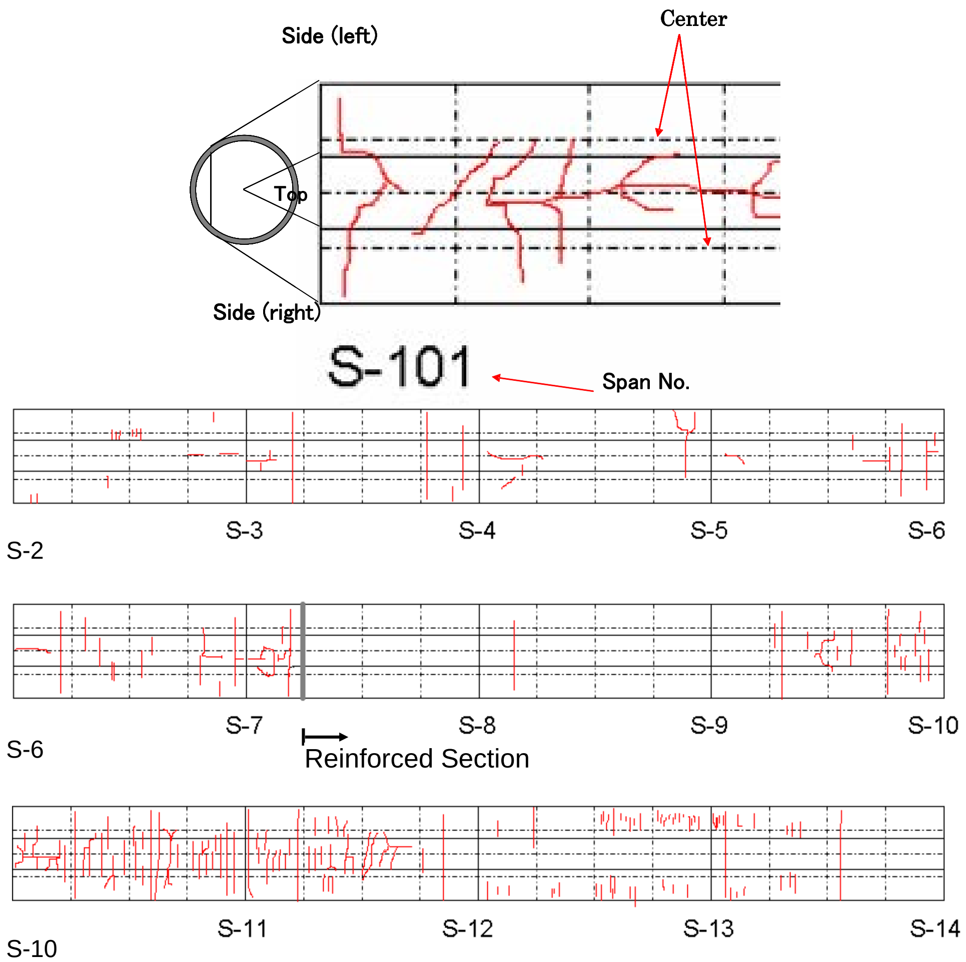

Figure 3: Crack distribution of the tunnel from Span S2 to S14 (Takeuchi and Suzuki 2007)

Comparing the measured height with the structures above, we can easily find that the tunnel just underneath the dikes has large amount of settlement and the tunnel below the pond has the rise as mentioned in the Figure 5.

These results indicate that the tunnel was affected by the structures constructed above the tunnel. When dikes are newly constructed, the tunnel sunk down with the movement of the ground and when the load above the tunnel reduces, the tunnel rise upward as in the case of the pond excavated after.

3.1.3 Numerical analysis

To check the movement of the tunnel, FEM analysis was performed. As shown in Figure 6, a large tensile stress occurs at the bottom of the tunnel when the Elastic modulus of the ground becomes low. On the contrary, the stress is negligible small when the Elastic modulus of the ground becomes high. These results indicate that this inspected tunnel has suffered a lot from the load above the tunnel after the tunnel is being constructed. As a result, the linings of the tunnel were cracked mostly by the movement of the tunnel due to newly constructed structures just above the tunnel.

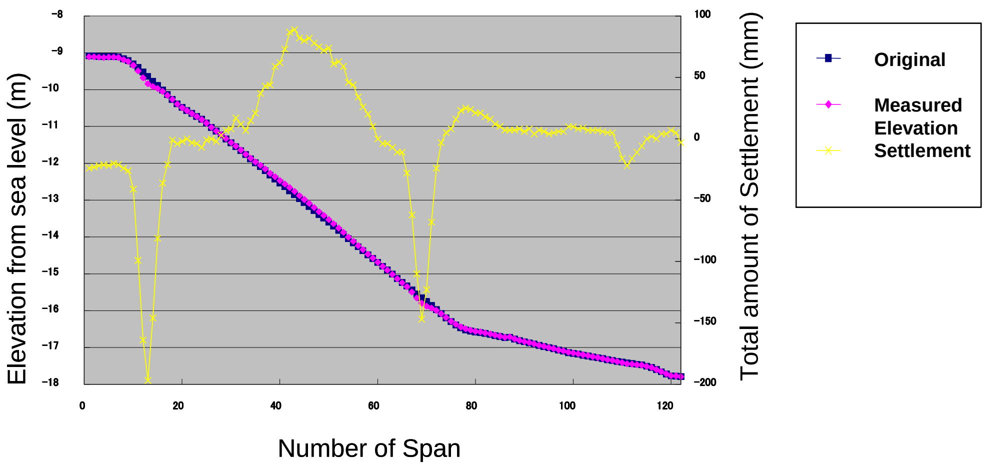

Figure 4: Level of the tunnel and the amount of settlement measured after 30 years (Takeuchi and Suzuki 2007)

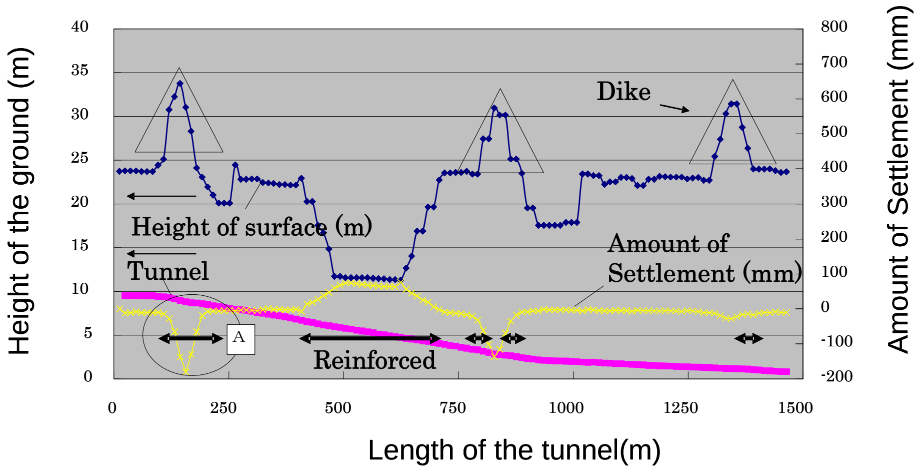

Figure 5: Comparison of the tunnel and the structures on the surface of the ground (Takeuchi and Suzuki 2007)

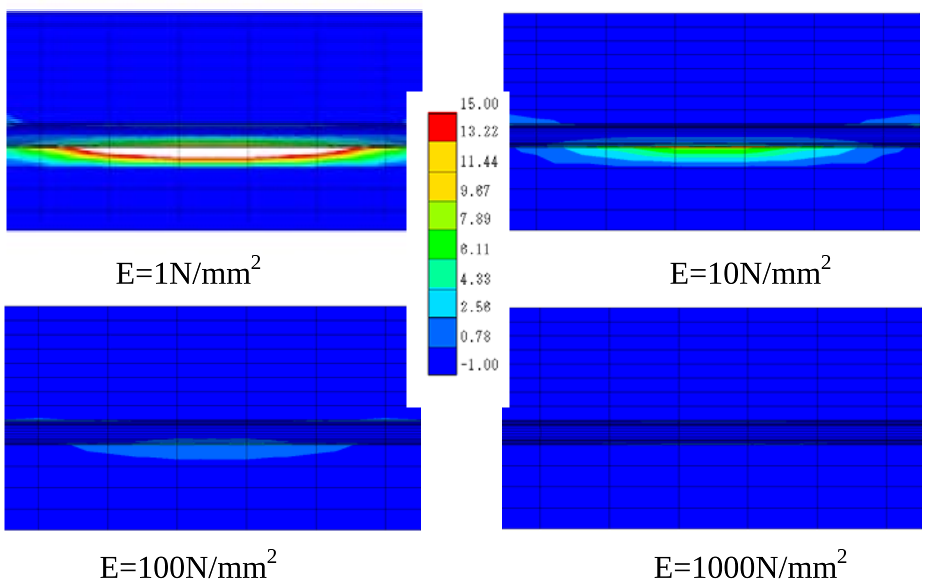

Figure 6: Tensile stress distribution of tunnel in a ground with different elastic modulus (Takeuchi and Suzuki 2007)

3.2 Effect on concrete tunnel in reclaimed land (Case2) [3]

3.2.1 Outline of the inspected tunnel

The figure 7 shows the relation between the tunnel being inspected and the earth fill above the tunnel. As shown in the figure, the tunnel is located about 3 to 10m below the ground at the time of construction and earth fill was applied about 2 to 1 meters after 13 years. The ground above and underneath the tunnel is soft with the N value of 1 to 20, and they may settle after the construction. The cross section of the tunnel is shown in figure 8. The height of the tunnel is 5.2m and the width is 3.5m. The thickness of the wall is 40cm with steel reinforcements.

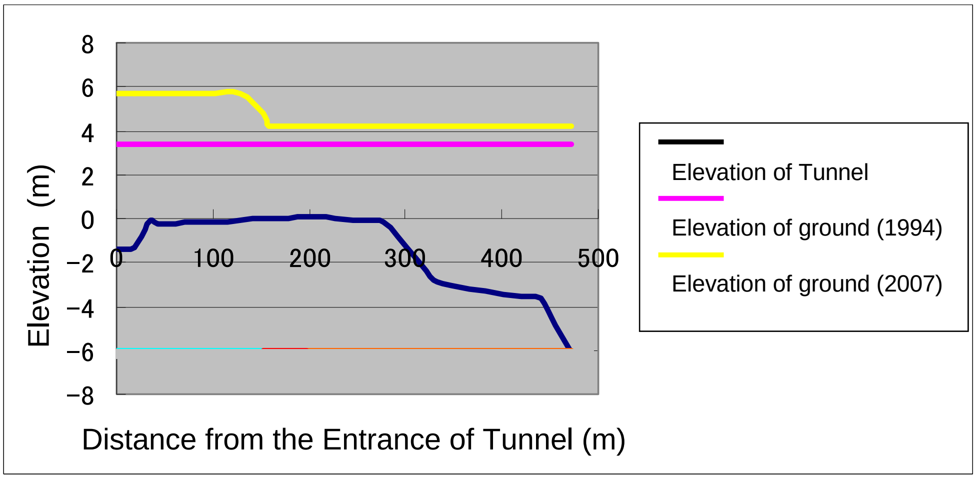

Figure 7: Elevation of the tunnel and ground surface (Kato 2008)

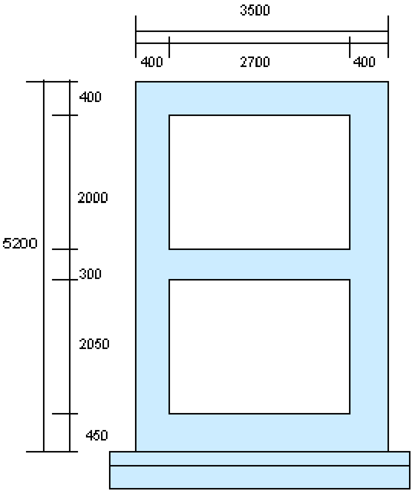

Figure 8: Cross section of the tunnel (unit:mm)

3.2.2 Inspected results

The arrangement of the steel reinforcements was measured by electro-magnetic method. Figure 9 shows an example of the bar arrangement. It coincides well with the designed drawings but the shear cracks were observed as shown in figure 10.

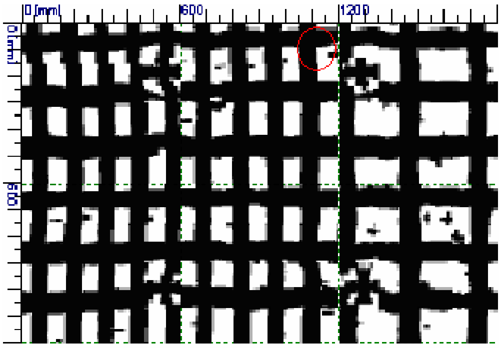

Figure 9: Measured steel bar Arrangement

Figure 10: Crack observed on the wall

The levels of tunnel are measured every year since 2004, and the total amount of settlement is calculated from the data. The result is shown in Figure 11. As shown in the figure, the level of the tunnel is almost constant except the portion between 40m to 180m from the entrance of the tunnel. The cause of the settlement may be caused by the earth fill load applied above the tunnel in 2005 after the construction of the tunnel.

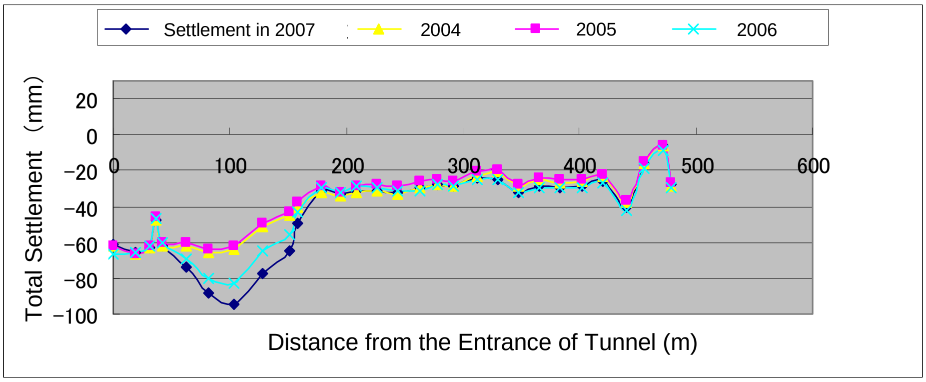

Figure 11: Total settlement of tunnel since 2004 (Kato 2008)

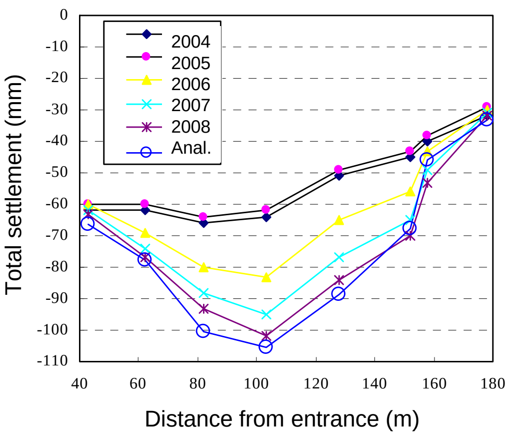

Figure 12: Analyzed settlement of Tunnel (Kato 2008)

3.2.3 Numerical analysis

To estimate the final settlement of the tunnel, 3-dimensional FEM analysis was performed. The entrance (distance: 40m) is composed of vertical shaft, and there is a pile foundation at the distance point of 180m. In the analysis, these two points are assumed as fixed points in the vertical direction. The elastic modulus of the soil was calculated from the measured N-value. The load on to the surface was estimated from the specific gravity of the earth fill.

The calculated settlement is shown in Figure 12. As shown in the figure, the calculated value coincide well with the measured settlement in the year 2008. From the result, it can be estimated that the settlement was caused by the earth fill mounted on the surface just above the tunnel. From these two case studies, it is important to know that the tunnels in soft foundation may be cracked due to settlement of the surrounding land. To check the cause, periodic overall measurement of level of the structure is a good method to estimate the cause of cracks.

4. PROBLEMS IN ACTUAL EXISTING STRUCTURES

When a civil engineer is asked by the owner to check the safety of an old existing structure, one of the largest problems is that there are neither drawings nor construction records of the structure available. No problem may occur in case of important facilities, which is maintained with great care. But in case of normal structures, the owners do not know the importance of these documents.

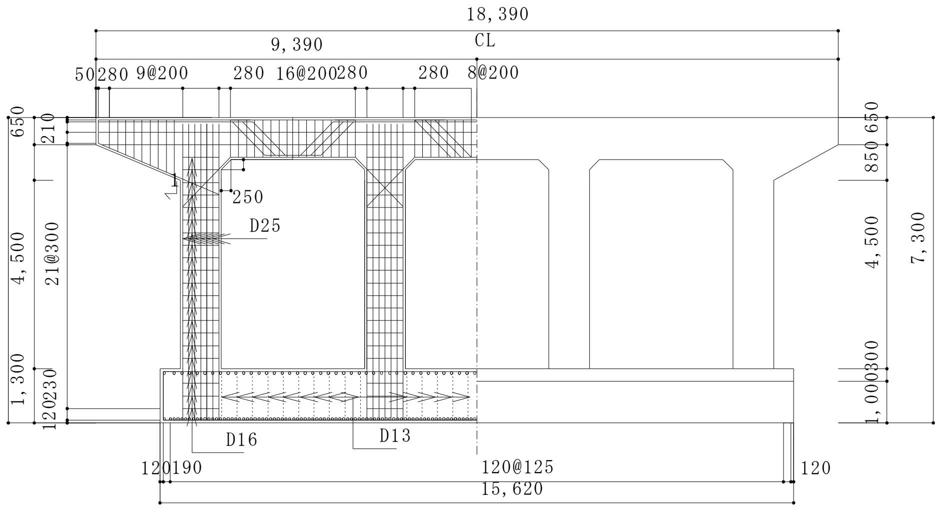

Figure 13: Re-designed reinforced concrete pier of a bridge (Okazaki ,2005)

To deal with the problem, NDI is not enough. Fortunately, our structures are not too old, and they are mostly designed and constructed by the method specified by JSCE, AIJ or other associations. Considering these, the only way is to re-design the structure again using the methodologies used at the time of construction. Figure 13 shows an example of re-designed bridge pier constructed about 35 years ago. From the figure, it is much easier for a civil engineer to check the safety of the structure under several hazards. It will become more important for the owners and engineers to keep these documents throughout the service life of a structure.

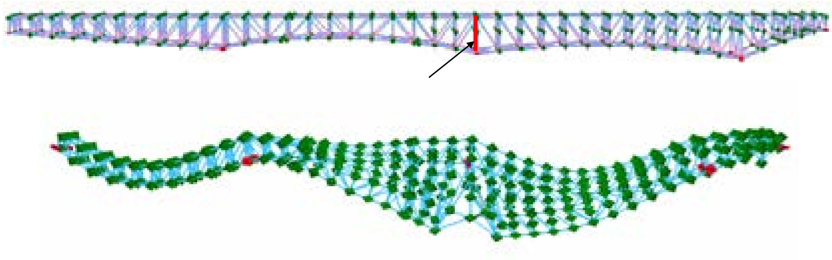

Figure 14: Estimation of the movement of a steel truss bridge when a member is deteriorated (Yasuzawa 2007)

When we have to monitor existing structures by NDT, important point is where and how to monitor. Because the amount of fee is limited, we can not monitor everything at all points. As mentioned in Chapter 3, it is important to keep the structure safe to the public. To do so, the engineers have to estimate where and how to monitor. The figure 14 shows how the steel bridge behaves if a member of the steel truss bridge is deteriorated. The calculation is done by 3 dimensional analysis, checking all the members what may happen if the member is deteriorated and can not support the load. As can be seen from the figure, the vertical member at the point of support is very important to maintain the bridge safe enough for the people to go across.

Knowing the evidence, we can monitor the bridge at this point. May be strain measurement is enough to check the safety of this bridge. Further, if we wish to monitor the structure as a whole, several points may be enough for the monitoring. We can reduce the cost to maintain and monitor the structure not to cause catastrophic failure.

5. CONCLUDING REMARKS

Engineering is not always complete, and further research works are needed. To sustain existing structures, durability of the structure is important. One good method is to construct durable structures, but for the existing structures maintenance is the only way to deal with the problem. Although concrete committee of JSCE has set up a good system for maintenance of existing concrete structures, there are still many things to be done: not only researches but also education to the students and engineers about durability and maintenance. I hope this paper may become a help to the concrete engineers of the world who are trying to design, construct and maintain concrete structures.

REFERENCES

Concrete Committee of JSCE, Standard Specifications for Concrete Structures-2007 “Design”. JSCE, Tokyo.
Concrete Committee of JSCE, Standard Specifications for Concrete Structures-2007 “Materials and Construction”. JSCE, Tokyo.
Concrete Committee of JSCE, Standard Specifications for Concrete Structures-2007 “Maintenance”. JSCE, Tokyo.
T. Uomoto and S. Misra,. Role of Engineers to Improve Quality of Concrete Structures. Proceedings of EASEC-8, Singapore, 2001.
S. Suzuki, K. Kinoshita and T. Uomoto: Fundamental study on crack distribution and settlement of Shield Tunnel Lining, JSCE General Meeting of Kanto-shibu, 2008
M. Takeuchi, Y.S hirane and T. Uomoto: Fundamental study on relation between crack and surface load on Tunnel Lining, JSCE General Meeting of Kanto-shibu, 2008
M. Kato and T. Uomoto: Fundamental study on causes of tunnel deterioration in urban area, JSCE General Meeting of Kanto-shibu, 2009
Okazaki, S., 2005. Development of monitoring system for RC bridge based on restoration design method. Thesis submitted to the University of Tokyo for Master of Engineering degree.
S. Yasuzawa and T. Uomoto: Estimation of dangerous points of an existing steel truss bridge, JSCE General Meeting of Kanto-shibu, 2008

NONLINEAR ANALYSIS OF SHEAR STRENGTHENING OF REINFORCE CONCRETE COLUMNS BY USING FIBER REINFORCE POLYMER

PRAGASIT JUNTANALIKIT
Sirindhorn International Institute of Technology,
Thammasat University, Pathumthani, Thailand
pj_bank2@hotmail.com
AMORN PIMANMAS
Sirindhorn International Institute of Technology,
Thammasat University, Pathumthani, Thailand
amorn@siit.tu.ac.th

ABSTRACT

Seismic assessment and retrofit of existing columns in buildings require accurate prediction of the available deformation capacity. In last decade, Fiber Reinforced Polymer (FRP) has been used widely to enhance strength and deformation capacity of deficient reinforce concrete (RC) column. This paper presents a study of a RC rectangular column strengthened by wrapping FRP sheet. An analytical model is proposed to represent potential plastic hinge regions of RC columns under cyclic loading by fiber-section spring model. The shear transfer mechanism of the specimen reinforced with FRP sheet was developed based on previous proposed model, represented by one nonlinear shear spring. The proposed analytical model is verified with the available cyclic test data of an earlier study on five columns with and without FRP. The study shows that conventional concrete column strengthened with FRP could be predicted with a Fiber-section element spring model which is capable of capturing essential features of the response such as strength degradation due to lap splice slippage. Furthermore, it is observed that, in estimating the response of existing deficient columns, parameters such as plastic hinge length, concrete strength and splice length are important sources of uncertainty. Good agreement was shown between the analytical models and the experimental results.

1. INTRODUCTION

The aim of the seismic design of reinforced concrete (RC) column is to avoid brittle failure modes. In terms of the strength, shear failure in column can be avoided by making shear failure capacity exceeding maximum flexural feasible capacity. For under-designed column with low shear strength, shear strengthening is required to increase the shear capacity. Externally bonded FRP for increasing shear resistance has been popular recently. The deformation capacity can also be enhanced because FRP confinement can delay concrete crushing.

There are vast experimental works on using FRP for retrofitting substandard columns. Experiments performed on the retrofitting substandard column with FRP lamina demonstrated the increase in strength and deformation capacity. The result also displays the great increase in energy dissipation of FRP-confined column, similar to those confined with internal steels. The external confinement of concrete using FRP is also effective in increasing the splice strength compared with the internal confinement provided by ordinary transverse steel.

It is possible to predict the behavior of RC column strengthened with FRP lamina using the concept of fiber-discretized nonlinear frame element together with the associated constitutive modeling of steel and concrete. The aim of this paper is to propose an analytical model that can be simulate gravity-designed reinforced concrete columns confined by FRP confinement under reversed cyclic loads. The backbone shear force-shear displacement is adopted from previous research. The general framework on nonlinear frame element is proposed and verification with available experimental data is presented

2. ANALYTICAL MODELING

The cantilever column fixed at base is modeled as a nonlinear frame element that is divided into two zones; the nonlinear zone that models the plastic hinge at the base and the elastic zone above the nonlinear zone (Matrin 2007). This model is extended to investigate the cyclic response of column confined by FRP.

2.1 Length of Plastic hinge

In a cantilever RC column, plastic hinge forms at the section of largest moment which is at the base of the column. The reinforcement yields in this zone and the concrete is loaded to nonlinear range. The length of plastic hinge is determined based on the work of Paulay and Priestley (1992) as

$$L_p = 0.08L + 0.022 d_b F_y \tag{1}$$

As mentioned, the entire column is divided to two zone; elastic and plastic zone. The plastic zone has the length determined from equation 1. The remaining length of column is therefore governed by a linear elastic response.

2.2 Elastic-frame element

The upper portion of the column is linearly elastic, thus it can be modeled by elastic frame element. The flexural and axial stiffness used in elastic frame element can be calculated according to the recommendations of ATC-40 (ATC,1997).

$$Effective\ Flexural\ Rigidity = 0.7 E_c I_g$$

$$Effective\ Axial\ Rigidity = 1.0 E_c I_g$$

2.3 Fiber discretization in the plastic zone

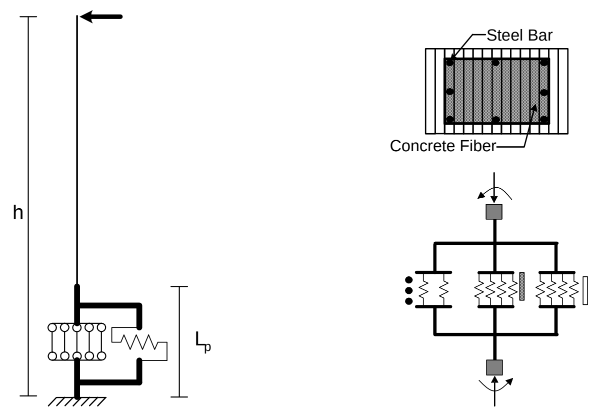

(a) RC column model *(b) Discrete fiber section*

Figure 1: Geometry of fiber-section element

The nonlinear plastic hinge zone is to model the nonlinear flexural and shear behaviors. The nonlinear flexural response can be modeled using the concept of fiber discretization in figure 1(a). In this concept, the cross section is divided into several fibers; each containing concrete, steel or both (Figure 1(b)). The fiber section adopts the assumption of "plane section remains plane". The concrete and steel fibers can be modeled with nonlinear springs. If the properties of steel and concrete spring are known, it is possible to analyze the response of the column. The constitutive models can be modified FRP confinement. As for shear behavior, a nonlinear shear spring is also attached at the plastic hinge. The following sections explain the nonlinear properties of concrete and steel under the external confinement of FRP.

2.4 Concrete spring

For the RC column section confined with transverse reinforcement, the concept of the effectively confined concrete area proposed by Mander et. al. (1989a) is used. The strength enhancement due to confinement is determined by stirrup spacing, strength of reinforcement and configuration of sectional dimension. The maximum axial stress of confined concrete and the corresponding strain can be computed as follows:

$$f'_{cc} = Kf'_{co} \tag{2}$$

$$\varepsilon_{cc} = \varepsilon_{co}\left[1 + 5\left(\frac{f'_{cc}}{f'_{co}} - 1\right)\right] \tag{3}$$

Consider confined concrete wrapped with FRP jacket. Lam and Teng (2003a) presented the maximum stress and maximum confinement pressure as follows:

$$f'_{ccu} = 3.3K_a f_l \tag{4}$$

$$f_l = \frac{2E_f n t_f \varepsilon_{fe}}{D} \tag{5}$$

$$\varepsilon_{ccu} = \varepsilon'_c\left[1.50 + 12K_b \frac{f_l}{f'_c}\left(\frac{\varepsilon_{fe}}{\varepsilon'_c}\right)\right] \tag{6}$$

The maximum compressive strain of the FRP confined concrete can be found using equation 6 where K_a and K_b are the effective factor accounting for the geometry of the section.

Roy and Sozen (1964) introduced the formula for computation the slop of descending line. The value of strain at one-half of peak concrete stress can be calculated as follows:

$$\varepsilon_{50} = \frac{3 + 0.29 f'_{co}}{145 f'_{co} - 1000} \tag{7}$$

2.5 Steel bar spring

The cyclic model of longitudinal reinforcement is assumed to be straight line to represent elastic condition followed by the horizontal line representing the yielding of reinforcing bar. The stiffness of reinforcement is computed as total area of reinforcement (ΣA_s) multiplied the elastic modulus of steel (E_s) and divided by plastic hinge length (L_p). The yield force can be obtained from multiplying the yield stress of reinforcement (F_y) with total area of reinforcement.

2.6 Lap splice spring

The stress in bar along the lap splice zone is assumed to be developed along the development length in the plastic hinge zone. Along the development length of the spliced bar, the yielding portion of reinforcement (L_y) and the elastic portion of reinforcement (L_e) can be computed by equation 8 and equation 9 respectively. The amount of slip is computed by integration of strain along required development length $(L_e + L_y)$ and is expressed by Equation 10.

$$L_e = \frac{f_e d_b}{4u_e} \tag{8}$$

$$L_y = \frac{(f_s - f_e)d_b}{4u_y} \tag{9}$$

$$\Delta_s = 0.5\left(L_e \varepsilon(f_e) + L_y\left[\varepsilon(f_e) + \varepsilon(f_s)\right]\right) \tag{10}$$

The bond stress-slip relationship is proposed by Alsiwat and Saatcioglu (1992), and Lowes et al. (2003). The average elastic bond stress (u_e) is determined by substituting value of development length (L_d) recommended by ACI318-05 into equation 8. For the average values of bond stress in yielding portion of reinforcement (u_y), the value of $0.4\sqrt{f_c'}$ as proposed by Harajli (2004) is assumed in this study.

2.7 Shear spring

The experimental and theoretical analysis was applied to develop a simple method for calculating the shear strength of FRP confined section. The modified shear model divides the shear capacity into three components. The first component represents the shear transfer mechanism of concrete denoted by V_c which depends on the magnitude of axial load, shear span to effective depth ratio and concrete cross-section. The second component is transverse reinforcement contribution, V_s.The third component is the shear force contribution of FRP, V_f .

$$V_n = V_c + V_s \tag{11}$$

$$V_{si} = V_c + V_n + V_f \tag{12}$$

In order to investigate of mechanism of shear behavior, shear resistance for RC column under monotonous increasing lateral deformation was studied by Halili Sezen (2008). The shear model was adopted for nonlinear shear-spring as shown figure 2. The critical points of the model are maximum shear strength, the onset of strength degradation and the loss of axial-load carrying capacity. The formula for the maximum shear strength (V_n) is given by equation 13.

$$V_n = k\frac{A_v f_{vy} d}{s} + k\left(\frac{0.5\sqrt{f_c'}}{a/d}\sqrt{1 + \frac{P}{0.5\sqrt{f_c'}}}\right)0.8A_g \tag{13}$$

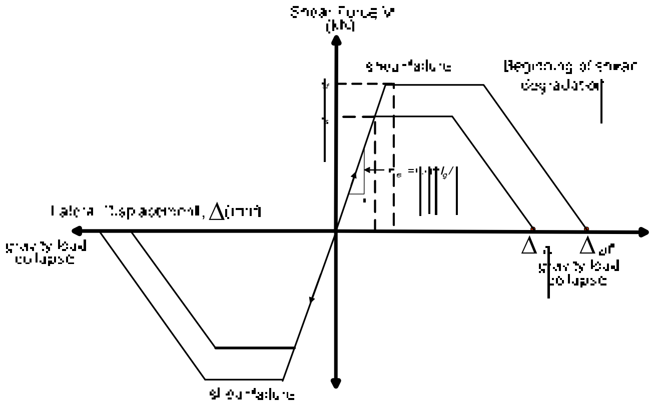

Figure 2: Proposed shear model

The factor k is defined to be 1.0 for the displacement ductility less than 2, 0.7 for displacement ductility exceed 6.0, and to vary linearly for intermediate displacement ductility. For the column that fail in shear, the average shear strain at the maximum shear force is influenced by many parameters such as, the axial load ratio, yield strength of reinforcement, and longitudinal steel ratio. The value of shear strain at the maximum shear force can be calculated from equation 14.

$$\gamma_u = \frac{f_{yl} \cdot \rho_l}{5000 \cdot \frac{a}{d} \cdot \sqrt{\frac{P}{A_g f_c'}}} - 0.0004 \tag{14}$$

The shear strength is assumed to be constant until the onset of strength degradation. The shear strain at the onset of strength degradation is calculated from equation 15.

$$\gamma_n = \left(4 - 12\frac{v_n}{f_c'}\right)\gamma_u \tag{15}$$

The last point on the shear envelope defining the axial load failure is also considered to completely the shear model. The deformation capacity at this point is derived from the shear friction model proposed by Elwood and Moehle (2005). The angle of the shear crack is assumed to be 65 degree.

$$\Delta_{ALF} = 0.04 \cdot \frac{1 + \tan^2\theta}{\tan\theta + P\left(\frac{s}{A_v f_{vy} d_c \tan\theta}\right)} \cdot L \tag{16}$$

Regarding the shear transfer mechanism of RC member, shear force resisted by the FRP is assumed to follow the truss mechanism, similar to truss mechanism carried by transverse reinforcement as shown in figure 3.

The shear contribution of FRP can be determined using equation 17. In the FRP-confined column, the shear strain of FRP is very small before diagonal shear crack occurs and increases very quickly after shear cracking. However, the strain of FRP does not reach the ultimate value at the maximum shear strength of the column, while the transverse steel was assumed to attain yielding.

Thus, in the shear model, the first straight line segment in the figure 2 can be divided into two-sub-stiffnesses: the first segment to represent the elastic shear stiffness of the RC column, and the second segment to represent the elastic shear stiffness after shear cracking. It is noted that the shear stiffness of strengthened depends on the tensile modulus, width of FRP reinforcement, and the thickness of the layer as shown in figure 4 (G. Promis (2008)). However, the last two points of the shear model of FRP confined column lacks supporting experimental evidence. As a result, the point at the onset of shear degradation and axial load failure are assumed to follow equation 15 and equation 16 for unconfined section.

$$V_f = \frac{A_{fv} f_{fe} (\sin\alpha + \cos\alpha) d_{fv}}{S_f} \tag{17}$$

$$A_{fv} = 2nt_f w_f \tag{18}$$

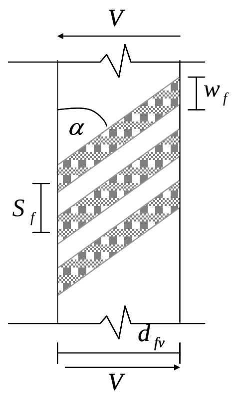

Figure 3: Shear transfer mechanism of FRP

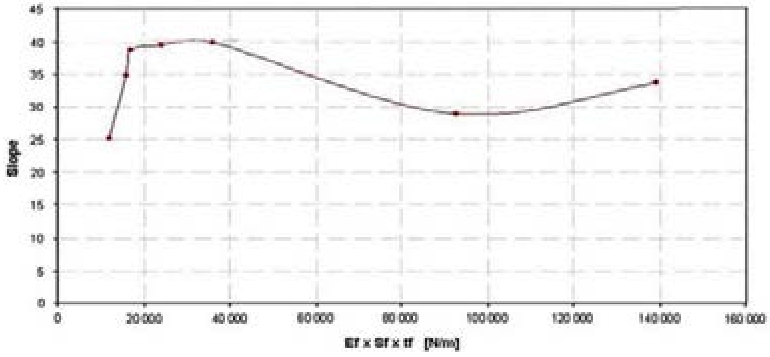

Figure 4: Influence of stiffness in relation to width of the band and slope

3. VERIFICATION OF REINFORCED COLUMNS WITH AND WITHOUT FRP CONFINEMENT

The results of two experimental programs conducted by Lieping Ye at. al. (2002), used for validation of the analytical model. The specimens were tested under a single curvature set-up and assigned reverse lateral displacement under constant axial load. One reference specimen and one CFRP-retrofitted specimen were analyzed using the developed models. In strengthened specimen (CS20-1-15), the length of CFRP confinement was covering the entire column length with partial wrapping. The column is modeled using a fiber-section method with each fiber being ten millimeter width. The columns section was 200mm x 200mm with round corner to avoid stress concentration in FRP sheets. Eight longitudinal reinforcing bars with diameter of 22 mm were assigned round the section perimeter. The transverse reinforcement hoops were 6 mm diameter with spacing of 200 mm for both specimens.

Table 1: Specimen's Parameter

Code of column	f'_c (MPa)	a/h	CFRP sheet	n
CS20-0-15	48.2	2.0	-	0.13
CS20-1-15	48.2	2.0	20x60	0.13

Table 2: Material Properties

Diameter (mm)	Area (mm^2)	Yield strength (MPa)	Tensile strength (MPa)	Elastic modules
22	380.1	381	571	2.0×10^5
6	28.3	345	492	2.1×10^5

The experimental parameters for both specimens are listed in table 1 and table 2. The tensile strength and elastic modules of CFRP were 3500 MPa and 2.35×10^5 respectively. The comparison of cyclic responses of both columns with the experimental results is presented in figure 5. It can be observed that significant strength degradation of unstrengthened column occurs after reaching the peak strength. For the FRP-retrofitted column, the peak shear strength is increased and the load degradation is delayed.

The model simulations of strength and deformation at maximum load are agreeable with experimental results. The slope of descending branch on the envelope curve also have good match between analytical and experimental results.

The developed model is also verified with the columns tested by Melanie Marcos-Regino (1999). Three column specimens were tested under cyclic lateral load. The specimens represent lightly transverse-reinforced RC column with the spacing of transverse steel of 300mm. The 1350 mm-tall and 300 mm-square cross-section columns were reinforced with 20 deformed D13 bars. The column height-to-diameter ratio was 3.7, indicating the shear failure mode in a single curvature condition. The compressive strength of concrete was 32.1 MPa, and the tensile strength of the longitudinal reinforcement and transverse reinforcement was 434 MPa and 346 MPa, respectively. One control specimen was compared with two CFRP-retrofitted specimens. The difference was the technique of strengthening with a layer thickness of 0.11 mm. One strengthened column (SP-2) was partially wrapped transverse to the column axis and the other specimen (SP-3) was diagonally wrapped from the base as shown in figure 6. Figure 7 shows the comparison between the model and experimental result. It is found that the response of analytical model agreed closely with the experimental results.

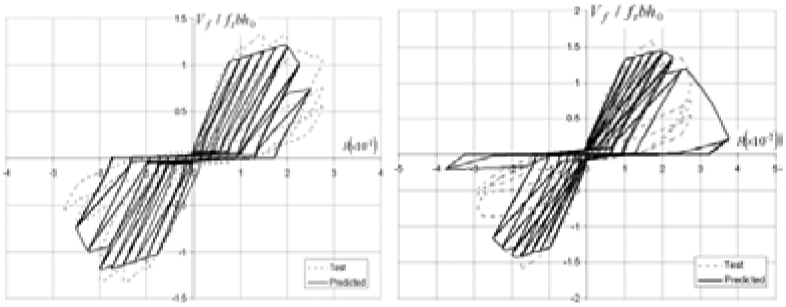

(a) CS20-0-15 *(b) CS20-1-15*

Figure 5: Comparison of test and predicted result

Table 3 Test Result

Specimen	Lateral Force		Failure Mode
	Experimental (kN)	Analysis (kN)	
CS20-0-15	147	150	Shear
CS20-1-15	177	179	Shear

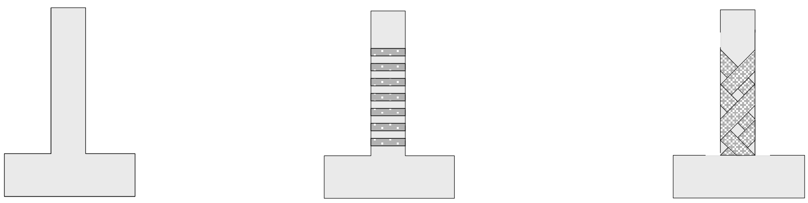

(a) SP-1 *(b) SP-2* *(c) SP-3*

Figure 6: Technique of strengthening CFRP

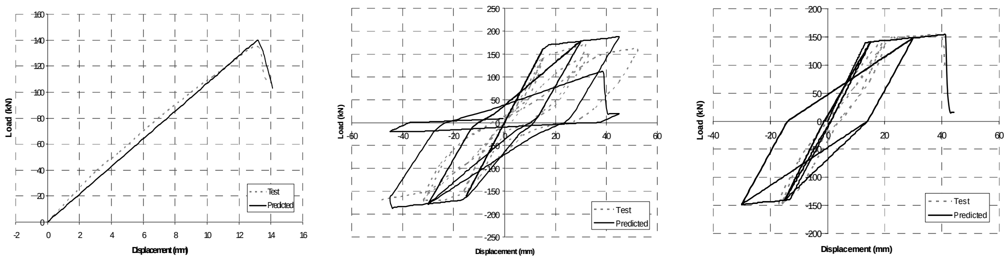

(a) SP-1 *(b) SP-2* *(c) SP-3*

Figure 7: Comparison of test and predicted result

4. CONCLUSIONS

This study was carried out to develop a model to analyze RC column confined by FRP under cyclic lateral displacement. The columns are those that are susceptible to shear failure. The analytical model is described to be based on the fiber-section technique. The nonlinear models for concrete and steel spring incorporating the effect of FRP confinement are described. The nonlinear shear model taking into account the effect of FRP confinement is also proposed based on the previous model developed for unconfined column. The developed models have been applied to analyze columns tested in the past. A good agreement is found for both experimental series. The nonlinear shear model should be enhanced especially for the point of strength degradation and the point of axial load failure for the section that is confined by FRP.

NOTATION

The following symbols are used in this paper:

A_v = area of transverse reinforcement (mm^2)
A_{fv} = area of FRP external reinforcement (mm^2)
ε_{co} = compressive strain of unconfined concrete (mm/mm)
ε'_c = maximum strain of unconfined concrete (mm/mm)
ε_{cc} =compressive strain of confined concrete (mm/mm)
ε_{fe} = effective strain level in FRP reinforcement attained at failure (mm/mm)
ε_{ccu} =compressive strain of FRP-confined (mm/mm)
f'_{co} =compressive strength of unconfined concrete (MPa)
f_l = maximum confining pressure (MPa)
f_e = maximum stress of reinforcement in elastic portion (MPa)
f_{fe} = effective stress in the FRP attained at section failure (MPa)
f_{vy} = yield strength of transverse reinforcement (MPa)
f_s = maximum stress of reinforcement in yielding portion (MPa)
f'_{cc} =compressive strength of confined concrete (MPa)
f'_{ccu} =compressive strength of FRP-confined (MPa)
K = effective confinement coefficient
L_y = development length required for yielded portion of reinforcement (mm)
L = length of column (mm)
L_e = elastic portion of reinforcement (mm)

L_p = plastic hinge length (mm)
u_e = average elastic bond stress (MPa)
u_y = average plastic bond stress (MPa)
d_b = diameter of longitudinal reinforcement (MPa)
F_y = yield strength of longitudinal reinforcement (MPa)
E_c = elastic modulus of concrete
E_s = elastic modulus of reinforcement
E_f = tensile modulus of elasticity of FRP
I_g = moment of inertia of the gross section
A_g = area of the gross section (mm^2)
s = spacing of transverse reinforcement (mm)
d = effective depth (mm)
d_{fv} = effective depth of FRP shear reinforcement (mm)
a = shear span (mm)
k = degarrding coefficient
P = axial force (N)
ρ_l = longitudinal steel ratio

REFFERENCE

Richard D. Lacobucci, Shamin A. Sheikh, and Oguzhan Bayrak, Retrofit of Square Concrete Columns with Carbon Fiber-Reinforced Polymer for Seismic Resistance, *ACI Structural Journal*, V.100, No.6, Nov-Dec 2003.

Mohamed H. Harajli and Ahmad A. Rteil, Effect of Confinement Using Fiber-Reinforced Polymer of Fiber-Reinforced Concrete on Seismic Performance of Gravity Load-Designed Columns, *ACI Structural Journal*, V.101, No.1, Jan-Feb 2004.

Muhammad S. Memon and Shamin A. Sheikh, Seismic Resistance of Square Concrete Columns Retrofitted with Glass Fiber-Reinforced Polymer, *ACI Structural Journal*, V.102, No.5, Sep-Oct 2005.

S. Matthys, H. Toutanji, K. Audenaert and L. Taerwe, Axial Load Behavior of Large-Scale Columns Confined with Fiber-Reinforced Polymer Composites, *ACI Structural Journal*, V.102, No.2, Mar-Apr 2005.

Kent A. Harries, James R. Ricles, Stephen Pessiki, and Richard Sause, Seismic Retrofit of Lap Splices in Nonductile Square Columns Using Carbon Fiber-Reinforced Jackets, *ACI Structural Journal*, V.103, No.6, Nov-Dec 2006.

Melanie Marcos-Regino (1999), Shear strength enhancement of reinforced concrete bridge piers by wrapping of fiber reinforced plastic sheet, *M Eng Thesis*, Saitama University, Japan.

ACI 440 American Concrete Institute committee 440, (2008) Guide for the design and construction of externally bonded FRP systems for strengthening

concrete structures. *American Concrete Institute committee 440*,Farmington Hills, Michigan.
G. Promis, E. Ferrier, P. Hamelin, Effect of external FRP retrofitting on reinforced concrete short columns for seismic strengthening, *Composite Structures 88 (2009)*, 367-379.

EXAMINATION CONCERNING THE ACCEPTANCE INSPECTION FOR QUALITY ASSURANCE OF STRUCTURAL CONCRETE

SHOTA MIZUKAMI
Department of Civil Engineering, Shibaura Institute of technology
m509091@sic.shibaura-it.ac.jp
TSUGIO NISHIMURA
Institute of Industrial Science, University of Tokyo
tsugio@iis.u-tokyo.ac.jp
YOSHITAKA KATO
ICUS, Institute of Industrial Science, University of Tokyo
katoyosh@iis.u-tokyo.ac.jp
FUTOSHI KATSUKI
Shibaura Institute of technology
katuki@sic.shibaura-it.ac.jp

ABSTRACT

The construction process greatly influences the quality of structural concrete, so it is necessary to improve the inspection method of the process. In particular, the acceptance inspection of the current state does not appropriately consider durability, so this research aims at the establishment of an appropriate concrete acceptance inspection for quality assurance considering durability, and examined stiffening behavior and flesh properties. As a result, it was found that the influence of environmental condition on compressive strength and air permeability is different, and it was clarified that it is difficult to use compressive strength as a representative parameter for durability. By changing the fineness modulus, sand-aggregate ratio, and unit water content in the tamping test, the segregation resistance was determined by calculation of flow coefficient, and the usefulness of the tamping test became clear. In the future, it will be necessary to relate this result with other viscous measurement technique.

1. INTRODUCTION

In recent years, the importance of quality control and inspection systems has increased due to the large amount of careless construction works done by low bids. Since the construction process greatly influences the quality of structural concrete, it has become necessary to introduce the execution process. To improve the inspection system, the influence on durability factors should be controlled and the results should be applied immediately.

Based on those current conditions, this research aims at the establishment of a quality inspection system for structural concrete. For the basic examination, fundamental tests were performed on the acceptance inspection of concrete. Compressive strength is one acceptance inspection criteria, and is used as a substitute index to evaluate durability. However, when the curing method is changed, resistance to mass transfer in cover concrete changes greatly, but this is difficult to confirm using only the compressive strength test, so the influence of curing method was measured and the air permeability of the concrete compared with the compressive strength. Next, testing of fresh property was conducted and the workability estimated by consistency and segregation resistance. Slump is highly influenced by the yield stress of the sample, so it is difficult to evaluate segregation resistance by slump test. Therefore, the tamping test and cylinder penetration test were conducted to evaluate the materials' segregation resistance and water content per unit volume.

2. EXPERIMENTAL OUTLINE

2.1 Air permeability test

Concrete mix proportions are shown in Table 1. Specimens were cast in summer (July), autumn (September), and winter (December) and cured outside to consider the influence of the seasonal climate conditions; these conditions in Otemachi, Tokyo, are shown in Table 2. Materials for mixing were prepared and stored at 20ºC for 24 hours before casting. The specimens were cylinders φ 100×200mm.

Table 1: Mix proportions (air permeability and compressive strength test)

Cement	W/C (%)	s/a (%)	Slag substitution rate(%)	Amount of unit(kg/m^3)						
				W	C	BS	S	G	AE	AE water reducing agent
OPC	40	41	−	179	448	−	667	986	C*0.01%	C*0.25%
	50	43	−	171	342	−	746	1015		
	60	45	−	171	285	−	804	1007		
BB	40	41	45	179	246	202	661	977	(C+BS)* 0.01%	(C+BS)* 0.25%
	50	43	45	171	188	154	742	1010		
	60	45	45	171	157	128	799	1002		

Table 2: Climate condition during curing period (OPC)

Average temperature : ℃			Precipitation in total : mm		
Summer	Autumn	Winter	Summer	Autumn	Winter
Average			Total		
28.5	22.2	9.1	168.5	247.0	39.5
Average humidity : %			daylight hours : h/day		
Summer	Autumn	Winter	Summer	Autumn	Winter
Average			Average		
70.0	69.8	48.3	5.5	3.3	7.1

Three curing methods were used, as shown in Figure 1, and the total curing period was 28 days for all three conditions. The period of wet curing was decided by the average temperature during the period, per the Japan standard specifications for concrete structures (JSCE, 2007). After curing, a 40mm section was cut from the center of the cylinder with a wet process cutter and spin-dried with a furnace dryer.

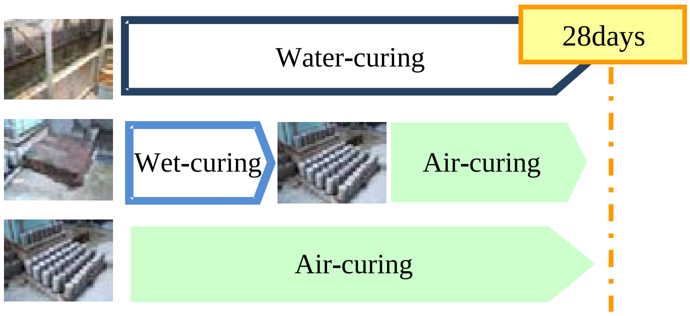

Figure 1: Curing method environmental conditions

These specimens were then fitted in a rubber cylinder and set up in a cell of the air permeability device (Fig. 2). Compressed air is injected into a cell, and once the air flow reaches steady state, the volume can be measured by the amount of water displaced, and the air permeability coefficient can be calculated by equation (1) from this value and the loading conditions (Ujiie and Nagataki, 1988).

$$K = \frac{2rLP_2Q}{A(P_1^2 - P_2^2)} \tag{1}$$

Where, K is coefficient of air permeability (m/s), P_1 is loading pressure (N/m^2), P_2 is atmospheric pressure (N/m^2), L is the thickness of the specimen (m), Q is quantity of air penetrating (m^3/s), A is surface area of specimen (m^2), r is unit volume mass of the air (=11.81(N/m^3)).

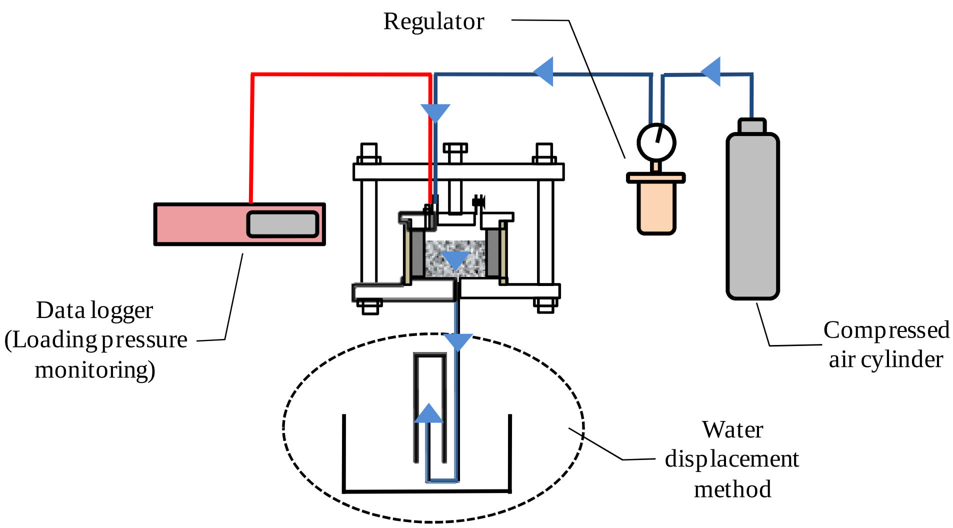

Figure 2: Schematic of air permeability test machine

Compressive strength test specimens were prepared under the same conditions as air permeability specimens in order to compare the effect of curing environment on air permeability and compressive strength. Results for are the average of three specimens.

2.2 Tamping test

The tamping test is a test method used to evaluate the segregation resistance and consistency of concrete (Ishii et al., 2008). Measurement items and methods are shown in Table 3 and Figure 3.

Table 3: Measurement items and methods for tamping test

Measurement item	Method
Slump flow	When slump cone is raised and slump flow is 250, 300, 350, 400, and 450mm, the following items are measured.
Slump	At the time of each slump flow value.
Upper circle	At the time of each slump flow value; circular presence and diameter are examined.
Number of tamping times	A wooden stick of mass 1.2kg is dropped from 50cm high sequentially on the four corners of the slump board. The necessary tongue Ping number of times to reach each slump flow is recorded.

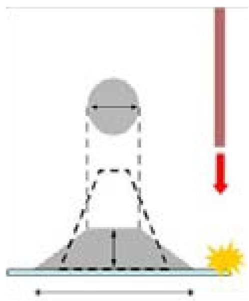

Figure 3: Schematic view of the tamping test

Mix proportions are shown in Table 4. Fineness modulus was selected as one experimental parameter to evaluate segregation resistance. As the fineness modulus becomes larger, segregation resistance increases but consistency decreases. Two sizes of coarse aggregate, "5-13mm" and "10-20mm", were used and three kinds of fineness modulus were set by changing their mixture ratio. Similarly, sand percentage (s/a) was used by "40%", "45%", and"50%" to understand its effect of viscosity. Finally, three mix proportions with varying water content per unit volume were also tested. The Ministry of Land, Infrastructure, Transport and Tourism in Japan (MLIT) specifies that water content per unit volume should fall within the range of ±15kg/m^3. Therefore, the water content was varied ±15kg/m^3 to test this effect.

Table 4: Mix proportions (for tamping test)

Change item	s/a (%)	Amount of unit(kg/m^3) W	C	S	G	G:5-13mm	G:10-20mm	AE	AE water reducing agent	Slump (cm)
Water content per unit volume	45	156	260	827	1046	504	504	C*0.01%	C*0.25%	8.5
	45	171	285	804	1007	504	504			10.0
	45	186	310	763	964	504	504			17.5
Fineness modulus	45	171	285	804	1007	806	201			11.5
	45	171	285	804	1007	504	504			10.0
	45	171	285	804	1007	201	806			9.0
Sand percentage	40	171	285	714	1099	504	504			9.5
	45	171	285	804	1007	504	504			8.5
	50	171	285	892	916	504	504			7.5

3. RESULTS AND DISCUSSION

3.1 Air permeability results

The results of the compressive strength and air permeability tests when expressed as the change in relation to water curing are shown on the Table 5 for all test cases. For both cement types, the compressive strength tends to decrease as water-cement ratio increases. In addition, the results decreased in order "water"→"wet+air "→"air". Air permeability tends to increase under the conditions given above. This shows that there is an inverse relationship between strength and air permeability. However, in comparison with the rate of change of compressive strength, the rate of change of air permeability is very high.

Table 5: Results of the compressive strength and air permeability tests

Kind of tests		Compressive strength			Coefficient of air permeability		
Water-cement ratio・Seasons	Cement	Water	Wet+Air	Air	Water	Wet+Air	Air
W/C=40%・Summer	OPC	1	0.92	0.80	1	2.60	2.80
W/C=50%・Summer		1	0.99	0.81	1	3.09	5.81
W/C=60%・Summer		1	0.98	0.77	1	1.75	6.85
W/C=40%・Autumn		1	0.95	0.95	1	1.73	1.46
W/C=50%・Autumn		1	1.01	0.94	1	2.21	1.92
W/C=60%・Autumn		1	1.04	0.93	1	1.48	2.28
W/C=40%・Winter		1	0.90	0.83	1	3.59	3.08
W/C=50%・Winter		1	0.88	0.82	1	4.19	4.21
W/C=60%・Winter		1	1.00	0.89	1	2.66	5.06
W/C=40%・Summer	BB	1	0.89	0.74	1	2.32	2.34
W/C=50%・Summer		1	0.87	0.68	1	1.74	2.76
W/C=60%・Summer		1	0.89	0.61	1	1.59	3.02
W/C=40%・Autumn		1	0.90	0.84	1	2.01	1.83
W/C=50%・Autumn		1	0.92	0.86	1	1.57	1.35
W/C=60%・Autumn		1	0.92	0.85	1	1.54	1.74
W/C=40%・Winter		1	0.76	0.72	1	3.56	2.47
W/C=50%・Winter		1	0.78	0.70	1	1.59	3.38
W/C=60%・Winter		1	0.73	0.65	1	1.47	4.81

A conceptual diagram of the general tendencies of the test results, when expressed as the change in relation to water curing, is shown in Figure 4. First, the "quantity of water" is considered because it is necessary for hydration of cement. Supply of water decreases in order of "water"→"wet+air"→"air", and it can be seen that the results follow this trend. Therefore, strength decreases according to decrease of water supply and air permeability increases. In the case of the lower water-cement ratio, the compressive strength showed a similar tendency, but air permeability did not change from "wet+air"→"air". Air permeability is generally related to the quantity, size, and network of voids whereas strength is related to the quantity of voids and degree of hydration. Therefore, the change in strength is an effective method to understand the degree of hydration, whereas the change in air permeability can be used to understand change in the void structure. Since the content of mixing water is low for low water cement ratio, longer wet curing is necessary to develop pore structure. However because the wet curing period is short, pore structure does not develop enough, and voids do not close, so after wet curing free water may easily evaporate. Furthermore, for air curing, the hydration reaction may be delayed.

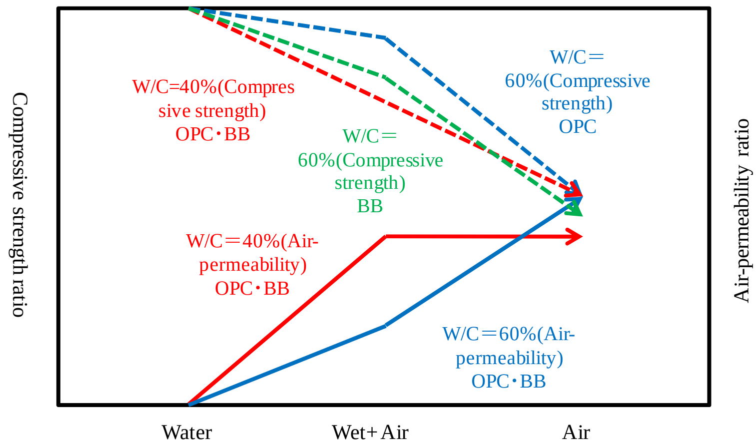

Figure 4: Conceptual diagram of the influence of curing condition on air permeability and compressive strength

The compressive strength and air permeability test results in case of lower water-cement ratio are considered as follows. Since the compressive strength decreased in order of "water"→" wet+air"→" air," less hydration occurred in air curing than in wet curing. However, hydration development under curing did not influence the results of the air permeability test. Although hydration occurred under wet curing, development of hydration product was not enough to reduce voids and decrease air permeability. Possibly, hydration occurred just enough to influence the air permeability by affecting the quantity of solid space (particles of cement and aggregate). Particularly in the case of lower water-cement ratio, there is little water available for hydration, so more non-hydrated cement is present than in the case of high water-cement ratio. Therefore, under the curing period set by the Japan Standard Specifications for Concrete Structures, it is believed that the curing was insufficient for air permeability because the degree of hydration did not increase enough. By that reasoning, the change in air permeability was confirmed in order of "water"→" wet+air". However, a change was not confirmed in order of "wet+air "→"air".

Furthermore, when considering the influence of climate condition in summer and winter, the results followed the above tendency because the quantity of supplied water decreased in order of "water"→"wet+air"→"air". On the other hand, in autumn the air permeability is around 50% for W/C=40%, and around 70% for W/C=60%. This rate of change is much lower than the other case (Fig. 5). In addition, compressive strength decreased 5%, and the rate of change of “wet+air” and ”air” was similar too, although air permeability did not change much for W/C=40%. When all the above points are considered, the change ratio of both results is much smaller than the case for lower water-cement ratio in particular. No change in compressive strength and air permeability was observed in the case of “wet+air”→”air”. It is possible that this was due to the high temperature and large volume of rainfall in autumn and the small difference in quantity of water supplied between the wet-curing and air curing conditions.

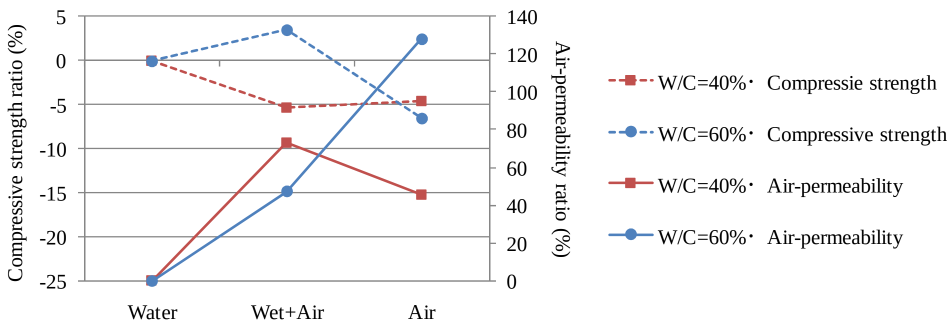

Figure 5: Relationship between air permeability ratio and compressive strength ratio (in autumn)

3.2 Result of tamping test

Result for slump flow and number of tamping times for variable fineness modulus of coarse aggregate are shown in Figure 6. The number of tamping times that is necessary to arrive at slump flow 450mm for fineness modulus 6.82 and 6.68 is more than 10 times less than that for 7.07. The measurement of the number of tamping times may evaluate consistency more easily than slump because the result of the slump test was 10±1.5cm. The upper circle of the sample could be confirmed until slump flow reached 300mm in the case of fineness modulus 7.07, but only until slump flow reached 250mm for fineness modulus 6.82, and unable to be confirmed from the measurement start for fineness modulus 6.68. The validity of this result was confirmed by the other research works, which also observed the change in upper circle due to fineness modulus.

The effect of sand percentage was similar to that of fineness modulus. Although initial slump was 8.5cm±1.0cm, the number of tamping times for sand percentage 50% was more than 10 times that for sand percentage 40% and 45% (Fig. 7). The upper circle of the sample could be confirmed until slump flow reached 300mm for sand percentage 50%, but only until slump flow reached 250mm for sand percentage 45%, and unable to be confirmed from the measurement start for sand percentage 40%.

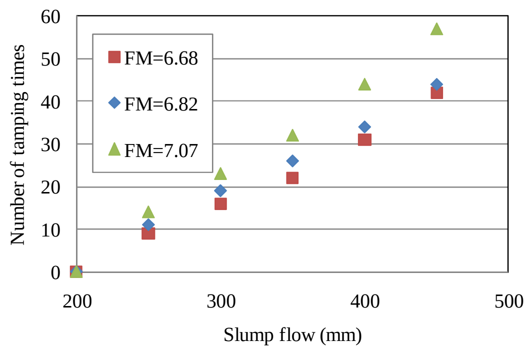

Figure 6: Relationship between number of tamping times and slump flow (fineness modulus)

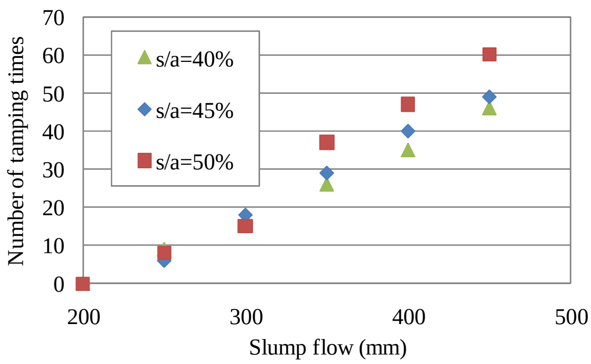

Figure 7: Relationship between number of tamping times and slump flow (sand percentage)

To evaluate this more clearly, the “flow coefficient” was defined as the slump flow divided by the slump. A high flow coefficient value expresses that the slump greatly increases with increasing slump flow, but a low flow coefficient value means that slump does not greatly increase with increasing slump flow. Therefore, the upper circle remained in some cases because the viscosity of the samples was high. For example, in the case of sand percentage 50%, the flow coefficient was generally lower than the other cases, but in the case of sand percentage 40%, the flow coefficient suddenly increased (Fig. 8), so the viscosity was low. In other words, since the segregation resistance was low, segregation occurred immediately and there was a possibility that the sample would collapse. To summarize, the flow coefficient could show the possibility of segregation resistance.

When water content per unit volume was changed, it was found that evaluation by slump test was sufficient due to the large negative relationship which was identified between the initial readings of slump and the numbers of tamping times necessary to reach slump flow of 450mm. The upper circle could be confirmed until slump flow of 450mm in the case of water content per unit volume 156kg/m^3. However, it could not be confirmed from the measurement start in the case of water content per unit volume 186 kg/m^3. As a result, it was concluded that the evaluation of segregation resistance by flow coefficient was difficult (Fig. 9).

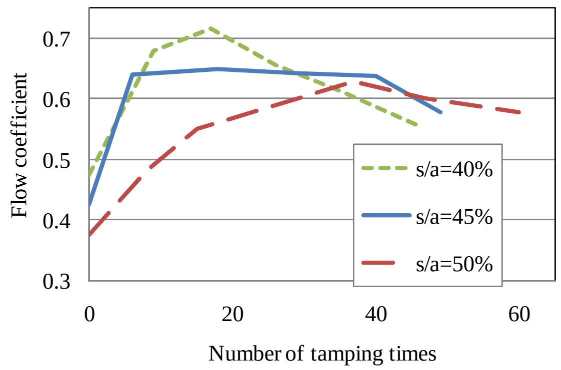

Figure 8: Relationship between flow coefficient and number of tamping times (sand percentage)

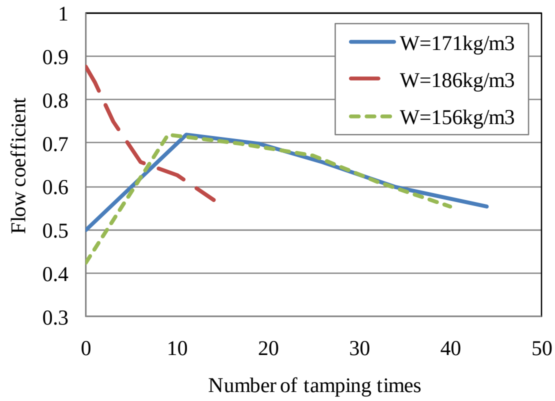

Figure 9: Relationship between flow coefficient and number of tamping times (water content per unit volume)

4. CONCLUSION

This study aimed to establish the acceptance inspection for securing the quality of structural concrete by conducting an experimental examination on the effect of the assessment methods for resistance to mass transfer and segregation resistance on durability. It was confirmed that the water-cement ratio and curing method had an influence on compressive strength and air permeability. Furthermore, it was found that in the actual environment, there was a large difference between mix proportions. In the future, curing over other time period should be carried out so that segregation resistance can be understood quantitatively under different environmental conditions. To evaluate segregation resistance, it is important that the presence of the upper circle on the sample is confirmed when the slump test is performed. Finally, it was shown that the transformation of the sample due to changes in segregation resistance might be estimated quantitatively. Previously established tests for evaluate viscosity should be conducted to more clearly understood these changes and to compare with the results in this paper.

REFERENCES

The authors would like to express their thanks to Mr. Michael W. Henry who generously assisted.

REFERENCES

JSCE, 2007. Japan Standard Specifications for Concrete Structures, pp. 122-124.

Ishii, Y., Uji, K., Ueno, A., 2008. A study on quantitiative evaluation of air permeability of concrete. Proceedings of the Japan Concrete Institute Vol.30 No.2, pp. 37-42. (in Japanese)

Ujiie, I., Nagataki, S., 1988. Simple method for evaluation of workability by tamping test. Journal of Materials, Concrete Structures and Pavements, JSCE, Japan. (in Japanese)

ESTIMATION OF SEISMIC CAPACITY OF KOREAN TYPICAL SCHOOL BUINDINGS UNDER DESIGN RESPONSE SPECTRUM

HO CHOI
Institute of Industrial Science, The University of Tokyo, Japan
choiho@iis.u-tokyo.ac.jp
YOSHIAKI NAKANO
Institute of Industrial Science, The University of Tokyo, Japan
iisnak@iis.u-tokyo.ac.jp

ABSTRACT

In the current seismic design provisions of Korea, school buildings are specified as evacuation shelter after an earthquake and are constantly requested the seismic design. However, there are no investigations on whether existing school buildings can play a role as evacuation shelter against future earthquakes.

In this study, the seismic capacity and the damage class of existing typical school buildings in Korea are therefore analytically estimated. For this purpose, a 4-story frame including unreinforced concrete block walls based on the standard design of Korean school buildings in the 1980s is selected as a model structure, and 6 artificial ground motions corresponding to Korean design response spectrum level are used to estimate the seismic capacity of the model structure.

All of the analysis results of first story for 6 artificial ground motions exceed the maximum strength and reach in the state of damage class III through V. This result means that existing typical school buildings in Korea do not escape at least moderate damage and then may not be able to play a role as evacuation shelter against the earthquakes of Korean design acceleration level.

1. INTRODUCTION

In Korea, countermeasures against earthquake disasters such as the seismic capacity evaluation and/or retrofit schemes of buildings have not been fully performed since Korea had not experienced many destructive earthquakes in the past. However, due to more than eight hundred earthquakes with slight/medium intensity in the off coastal and inland of Korea during the past 30 years as shown in Figures 1 and 2, and due to the recent great earthquake disasters in neighboring countries, such as the 1995 Hyogoken-

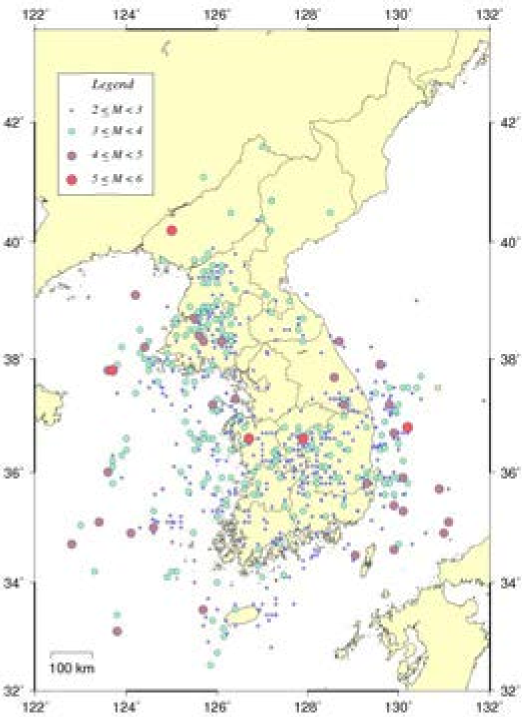

Figure 1: State of earthquake occurrence in Korea after 1978

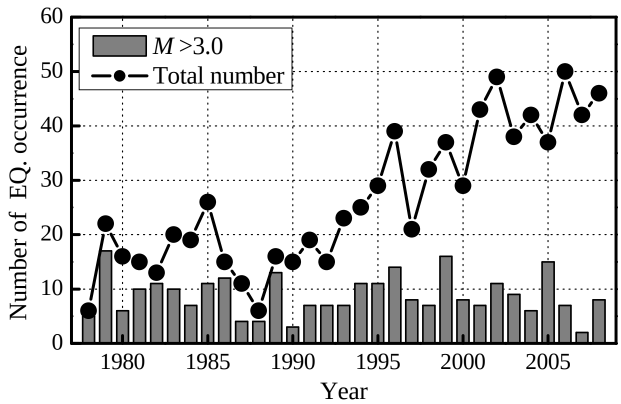

Figure 2: Frequency rate of earthquake occurrence

Nanbu Earthquake with more than 6,500 fatalities in Japan and the 1999 Chi-Chi Earthquake with more than 2,500 fatalities in Taiwan, the importance of the future earthquake preparedness measures in Korea is highly recognized.

Seismic design provisions for building structures in Korea first were introduced in 1988 and were revised in 2000 and 2005. Since the seismic design, however, was requested for the buildings more than 6 stories before 2005, school buildings which are mainly less than 5 stories have been excluded from the seismic design. In the current seismic design provisions of Korea, school buildings are specified for the first time as evacuation shelter after an earthquake and are constantly requested seismic design regardless of the number of stories. However, there are no investigations on whether existing school buildings can play a role as evacuation shelter against future earthquakes.

In this study, the seismic capacity and the damage class of existing typical school buildings in Korea are therefore analytically estimated under Korean design response spectrum level. For this purpose, a 4-story frame including unreinforced concrete block (CB) walls based on the standard design of Korean school buildings in the 1980s is selected as a model structure, and 6 artificial ground motions corresponding to Korean design response spectrum level are used to estimate the seismic capacity of the model structure.

2. OUTLINE OF MODEL STRUCTURE

Figure 3 shows a standard design of Korean school buildings in the 1980s (The Ministry of Construction and Transportation, 2002). In this study, the 4-story RC frame including CB walls as shown in this figure is analytically investigated as a model structure. Since seismic design provisions for building structures in Korea first were introduced in 1988 as mentioned above, the model structure studied herein is not designed to seismic loads. Therefore, they have (1) large spacing of hoops (300*mm*) and (2) 90 degree hook at both ends of hoops. The design strength of concrete is $21N/mm^2$, and the deformed bar SD40 (nominal yield strength: $395N/mm^2$) is used for longitudinal and shear reinforcement. The size of a CB unit is 390×190×190*mm*. It has three hollows inside and a half-sized hollow on both ends.

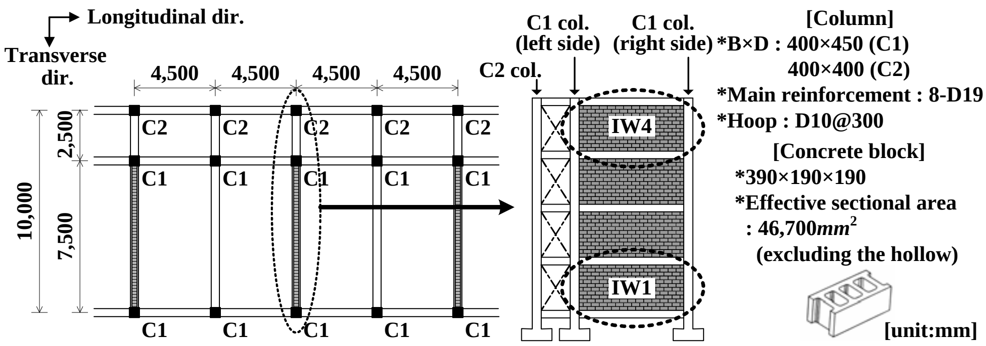

Figure 3: Standard design of Korean school buildings in the 1980s and model structure

3. SEISMIC CAPCITY AND DAMAGE CLASS OF EXISTING TYPICAL SCHOOL BUILDING IN KOREA

3.1 Hysteretic characteristics of model structure

In this section, shear strengths of each column and CB wall are calculated based on the test results previously performed, and the load-deformation curves of each story are determined with a simplified model.

3.1.1 *Outline of experiment*

In order to calculate the shear strengths of each column and CB wall of the model structure, the test results previously performed by authors are referred (Nakano and Choi, 2005). In the tests, 2 specimens representing a first or fourth story of 4-story RC school buildings are investigated as shown in Figure 3. They are an infilled wall type (IW1) assuming the first story and an infilled wall type 2 (IW4) assuming the fourth story. Material properties of C1 and C2 columns (see Figure 3) obtained the test results are shown in Table 1. Although the design strengths of concrete and reinforcement specified in the standard design of Korean school buildings in the 1980s are 21*N*/*mm*^{2} and 395*N*/*mm*^{2}, respectively, as mentioned in the previous chapter, those strengths exceed the design values. Figure 4 shows the relation between the lateral load and the drift angle of specimens IW1 and IW4. Assuming the discrepancy between the observed peak load of overall frame and the calculated shear strength of both columns is carried by the CB wall, the average shear stresses τ_B of CB wall to sectional area A including hollow (A=390×190*mm*) for both specimens are identically 0.4*N*/*mm*^{2} as plotted in Figure 4.

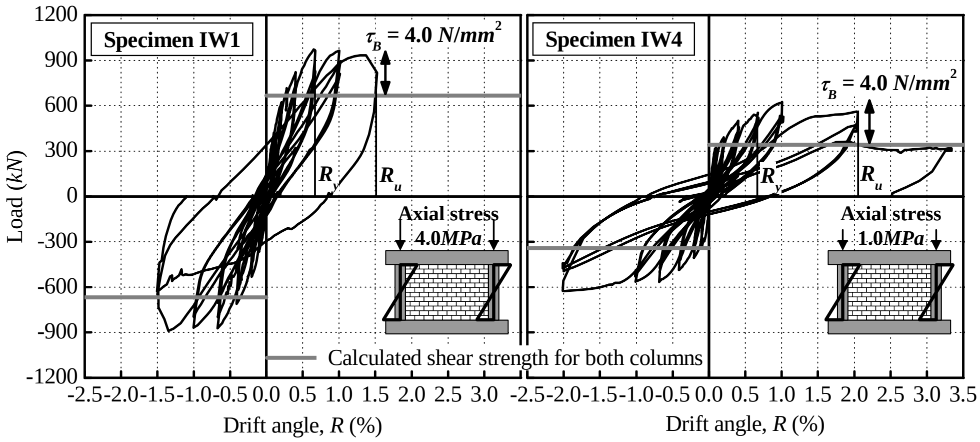

Figure 4: Load vs. drift angle of specimens IW1 and IW4

Table 1: Material properties of C1 and C2 columns

Col.	Column width b (mm)	Column depth D (mm)	Column height h_0 (mm)	Compressive strength of concrete F_c (N/mm^2)	Yield strength of longitudinal reinforcement σ_y (N/mm^2)	Yield strength of transverse shear reinforcement σ_{wy} (N/mm^2)
C1	400	450	2,800	26.2	432	404
C2	400	400				

3.1.2 ***Determination of hysteretic characteristics***

To simulate the inelastic behaviors of the model structure, the load-deformation curve is represented by a simplified hysteretic model with assumptions (1) through (3) described below.

(1) The Takeda model is employed for the basic hysteretic rule assuming (a) no hardening in post-yielding stiffness and (b) stiffness degradation factor α of 0.7 derived from the test results during unloading.

(2) Table 2 shows the shear strengths of each column and CB wall calculated using each value of Figure 4 and Table 1. The yield load Q_y is simply calculated as the sum of shear strengths of three columns and

one CB wall, and the average shear stress τ_B of the CB walls for each story are identically assumed 0.4N/mm^2 from test results. The yield drift angle R_y for each story is equally assumed 0.67%, and the load Q_{cr} and drift angel R_{cr} at cracking point are assumed $Q_y/3$ and $R_y/15$, respectively, based on test results.

(3) The ultimate ductility factors μ of specimens IW1 and IW4 defined by R_u/R_y, where the ultimate drift angle R_u is defined as the drift angle when the lateral load carrying capacity decreases to 80% of the peak load, are approximately 2.0 and 3.0 (see Figure 4). According to this result, the factors μ of first story through forth story are assumed 2.0, 2.5, 2.5 and 3.5, respectively.

Figures 5(a) through 5(d) shows the load-deformation relation of each story determined by assumptions above together with damage class determined by definition for RC members in the Guidelines for Post-Earthquake Damage Evaluation and Rehabilitation of RC Buildings in Japan (2001) shown in Figure 6.

3.2 Korean design response spectrum and artificial ground motion

In this section, design response spectrum provided Korean seismic design provisions is discussed, and artificial ground motions corresponding to design response spectrum are determined.

In the current seismic design provisions of Korea, general response spectrum with 5% of critical damping can be obtained by the design short-period spectral response acceleration parameter of S_{DS} and the design spectral response acceleration parameter at one second of S_{D1} as shown in equation (1) (Architectural Institute of Korea, 2005). Figure 7 shows spectral response acceleration determined by equation (1). The parameters S_{DS} and S_{D1} are determined respectively from Tables 3 and 4, based on the site class and the seismic zone as shown in Tables 5 and 6, respectively. In this study, site class, S_C, at seismic zone 1 is selected since the soil type of Korea mainly consists of soft rock.

$$\begin{aligned} S_a &= 0.6\frac{S_{DS}}{T_0}T + 0.4S_{DS} && \text{for } 0 \le T < T_0 \\ S_a &= S_{DS} && \text{for } T_0 \le 0 \le T_S \\ S_a &= \frac{S_{D1}}{T} && \text{for } T > T_S \end{aligned} \tag{1}$$

where, T_0 and T_S are given by the equations (2) and (3).

$$T_0 = 0.2\frac{S_{D1}}{S_{DS}} \tag{2}$$

$$T_S = \frac{S_{D1}}{S_{DS}} \tag{3}$$

Table 2: Shear strengths of each column and CB wall

Story	C1 column (right side)		C1 column (left side)		C2 column		CB wall
	Axial force N (kN)	**Shear strength Q_c (kN)**	**Axial force N (kN)**	**Shear strength Q_c (kN)**	**Axial force N (kN)**	**Shear strength Q_c (kN)**	**Shear strength Q_B (kN)**
4	165	109	221	116	55	84	521
3	331	131	441	144	110	91	
2	496	150	662	168	165	97	
1	662	168	882	190	221	103	

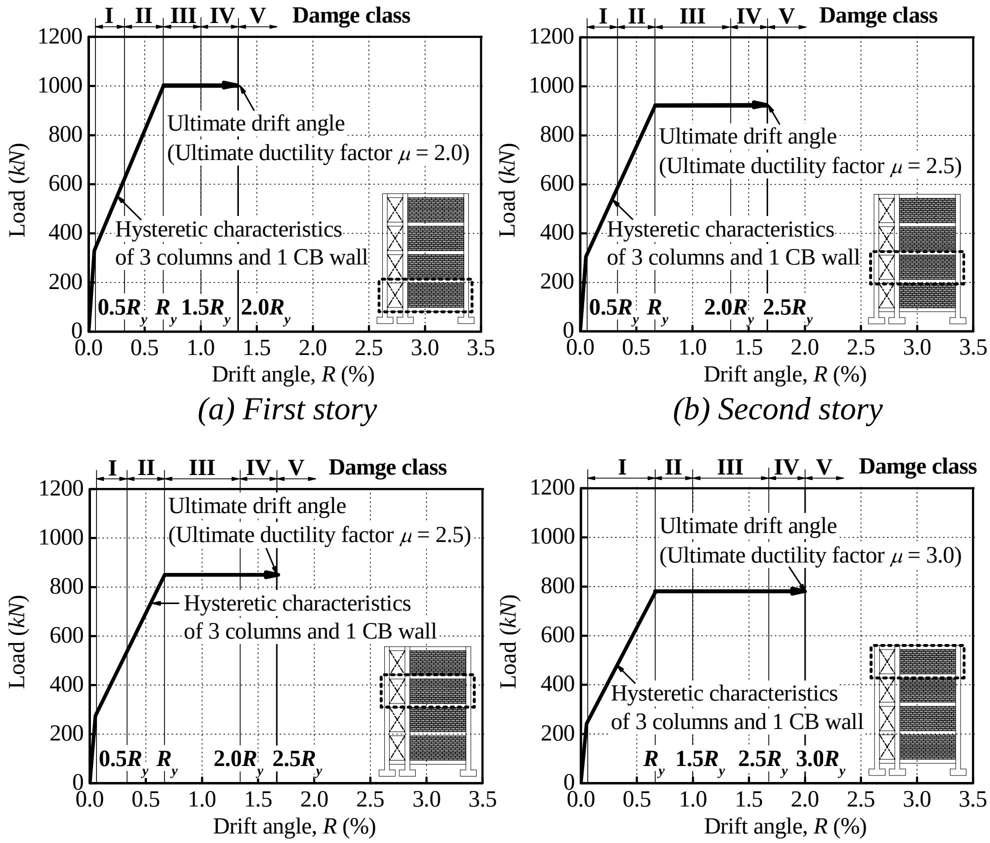

(a) First story *(b) Second story*

(c) Third story *(d) Fourth story*

Figure 5: Load-deformation relation of each story

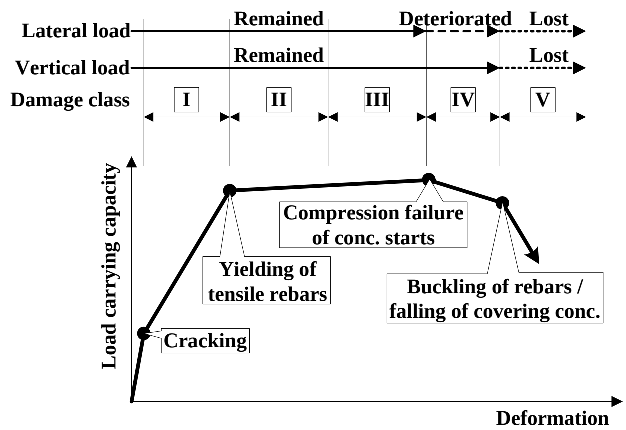

Figure 6: Schematic illustration of damage class (Ductile member)

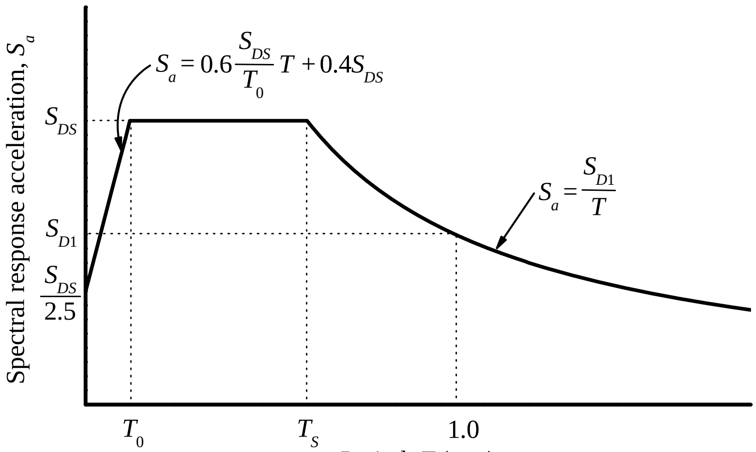

Figure 7: General response spectrum

Table3: Short-period spectral response acceleration parameter, S_{DS}

Site class	Seismic zone, *A*	
	1	**2**
S_A	$2.0M^{*1}A^{*2}$	1.8*MA*
S_B	2.5*MA*	2.5*MA*
S_C	3.0*MA*	3.0*MA*
S_D	3.6*MA*	4.0*MA*
S_E	5.0*MA*	6.0*MA*

Table4: Spectral response acceleration parameter at one second, S_{D1}

Site class	Seismic zone, *A*	
	1	**2**
S_A	0.8*MA*	0.7*MA*
S_B	1.0*MA*	1.0*MA*
S_C	1.6*MA*	1.6*MA*
S_D	2.3*MA*	2.3*MA*
S_E	3.4*MA*	3.4*MA*

*1 M =1.33 (M is a response acceleration parameter at 2%/50 year probability of exceedance (2,400 years of mean return period))
*2 A : Seismic zone factor (see Table 6)

Table 5: Site classes in Korea

Site class	Soil class	Shear wave velocity V_s (*m/s*)	Standard penetration test blow count *N* (/300*mm*)	Undrained shear strength S_u ($\times 10^{-3} N/mm^2$)
S_A	Hard rock	>1,500	-	-
S_B	Rock	760 - 1,500	-	-
S_C	Very dense soil, Soft rock	360 - 760	>50	>100
S_D	Stiff soil	180 - 360	15 - 50	50 - 100
S_E	Soft clay	<360	<15	<50

Table 6: Seismic zone factor corresponding to each zone

Seismic zone	Zone	Seismic zone factor *A*	Remarks
1	All of zone Except seismic zone 2	0.11	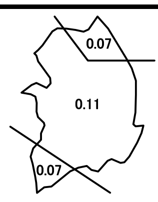
2	North Gangwon-do, South Jeolla-namdo, Jeju-do	0.07	

Since the earthquakes of maximum acceleration level specified in the current seismic design provisions of Korea have not been occurred, 6 artificial ground motions herein are used to estimate the seismic capacity of the model structure. The following 6 records are used to determine phase angles of ground motions: the NS component of El Centro 1940 record (ELC), NS component of Kobe 1995 record (KOB), EW component of Hachinohe 1968 record (HAC), NS component of Tohoku University 1978 record (TOH), NS component of Uljin 2004 record (ULJ) which has the highest maximum acceleration among the earthquake data measured by Korean meteorological office, and random excitation (RAN). Figure 8 shows 5 earthquake record data except random excitation, and Figure 9 shows the elastic acceleration response spectra of artificial ground motions with 5% of critical damping corresponding to the design response spectrum at seismic zone 1 and site class, S_C.

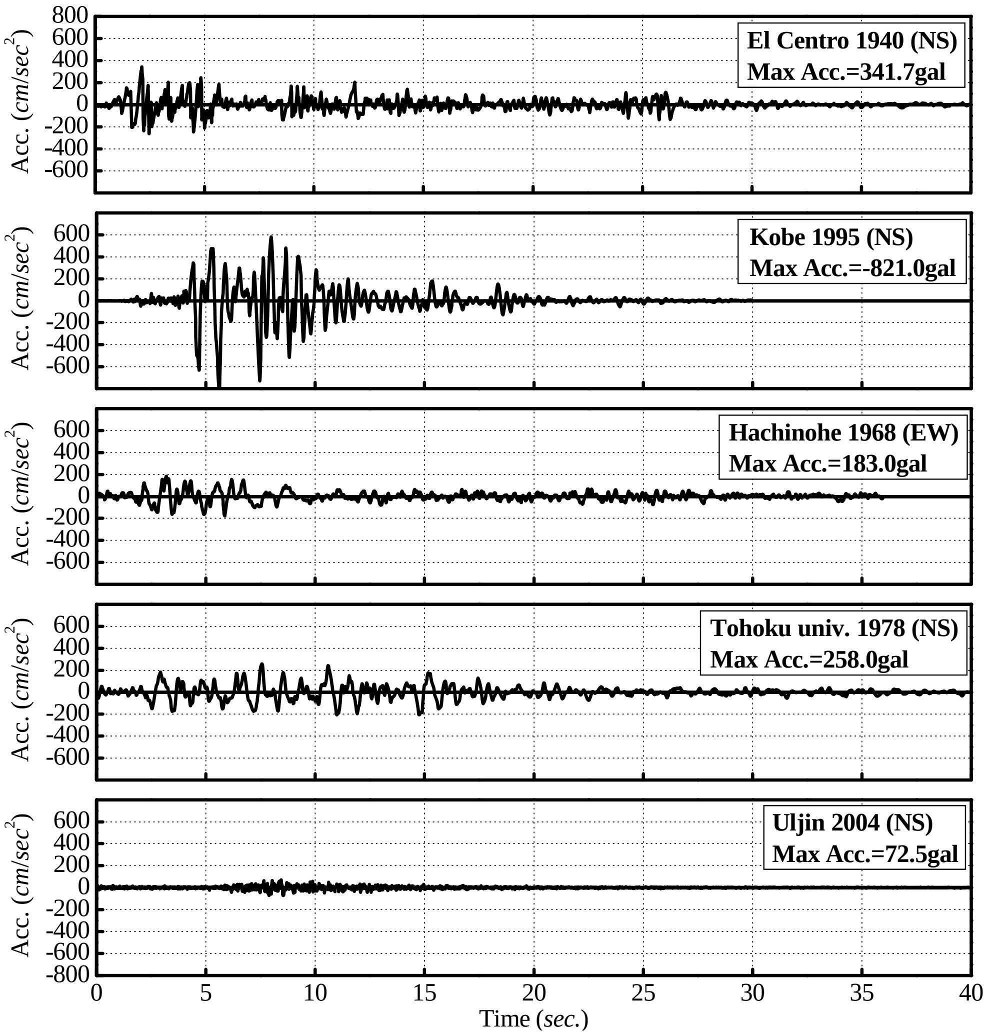

Figure 8: Earthquake record data

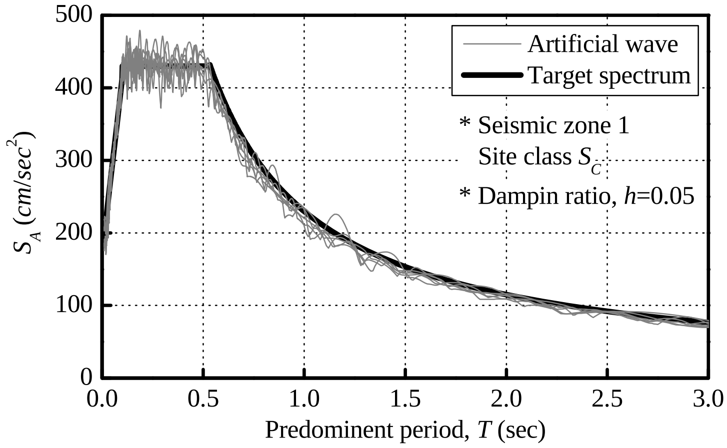

Figure 9: Elastic acceleration spectra of artificial ground motions

3.3 Seismic capacity and damage class of existing typical school building in Korea

In this section, the seismic capacity and the damage class of existing typical school buildings in Korea, which should be properly functional as evacuation shelter as well as structurally safe after an earthquake, are analytically investigated using the hysteretic characteristics and 6 artificial ground motions mentioned in previous sections.

Figure 10 shows the inelastic behaviors of first story, where the most serious damage is found, for 6 artificial ground motions together with the damage class. As shown in this figure, the behaviors and damage classes are slightly different due to phase angles of each ground motion. However, all of analysis results exceed the maximum strength and reach in the state of damage class III. The results due to KOB, HAC and RAN particularly exceed the ultimate drift angle of 1.35% and reach in the state of damage class V (i.e., collapse). For the RC frame without CB wall, more serious damages are expected since the lateral load carrying capacity is relatively small than that with CB wall. This result means that existing typical school buildings in Korea do not escape at least moderate damage and then may not be able to play a role as evacuation shelter against the earthquakes of Korean design acceleration level.

4. CONCLUSIONS

The seismic capacity and the damage class of Korean school buildings, which should play a role as refuge facilities after an earthquake, are analytically estimated under Korean design response spectrum level based on the test results. All of the analysis results of first story for 6 artificial ground motions exceed the maximum strength and reach in the state of damage class III through V. It is revealed that existing typical school buildings in Korea do not escape at least moderate damage and then may not be able to play a role as evacuation shelter against the earthquakes of Korean design acceleration level.

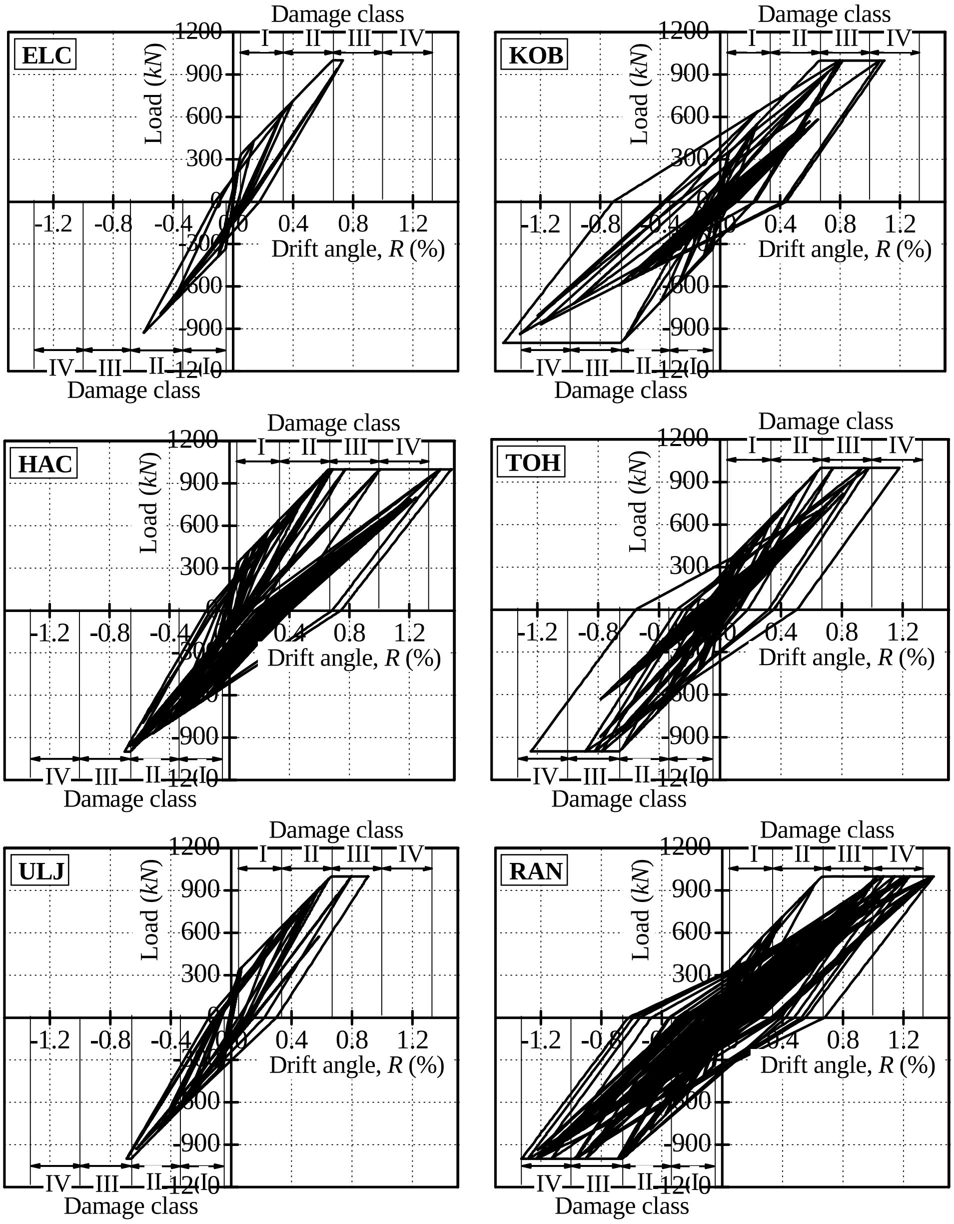

Figure 10: Inelastic behaviors and damage class of first story

REFERENCES

The Ministry of Construction and Transportation, 2002. A Study on the Seismic Evaluation and Retrofit Low-Rise Buildings in Korea. pp.113-155.

Nakano, Y. and Choi, H., 2005. Experimental Study on Seismic Behavior and Crack Pattern of Concrete Block Infilled RC Frames. *New Technologies for Urban Safety of Mega Cities in Asia (USMCA)*, ICUS/INCEDE Report 2, Singapore.

JBDPA (The Japan Building Disaster Prevention Association), 2001. Guidelines for Post-Earthquake Damage Evaluation and Rehabilitation.

AIK (Architectural Institute of Korea), 2005. Commentary on the Guideline for the 2005 Korea Building Seismic Code.

SHAKING TABLE TESTS OF TRADITIONAL TIMBER FRAMES INCLUDING KUMIMONO – MODELING OF HORIZONTAL RESISTANCE FORCE -

IUKO TSUWA
Graduate School of Engineering, the University of Tokyo, Japan
tsuwa@iis.u-tokyo.ac.jp
MIKIO KOSHIHARA
Institute of Industrial Science, the University of Tokyo, Japan
kos@iis.u-tokyo.ac.jp

ABSTRACT

This paper presents the results of the shaking table tests of traditional timber frames with mud wall and without it. The aim of this research is to clarify the vibration characteristics of the whole frames and structural elements which are column, Nuki, Kumimono, and mud wall, and to identify the difference of the behaviour about Kumimono in two types of specimens.

The results of the specimen with mud wall were compared with those of one without mud wall. The way to model stiffness of each element and both whole frames is discussed using the previous theory and experimental and material results. It is clarified that the relationship between load and displacement of a whole frame can be evaluated by adding the restoring force characteristics of each structural element. The restoring force characteristics of Kumimono have a very small effect on one of a frame because the stiffness of Kumimono is much higher than one of column and mud wall.

1. INTRODUCTION

Traditional timber structures have been built by empirical knowledge of carpenters. However recently the quantitative evaluation of their structural behaviours is needed in order to build new traditional timber structures or for restoration works of such structures. Therefore the quantitative evaluation of their structural behaviors is indispensable. In the buildings such as temples and shrines, column, mud wall, *Nuki* which is a tie beam extending from one pillar to another, and *Kumimono* which is a structural component between a column and roof, etc, are considered as structural elements. Each element has been researched and modeled experimentally and analytically. However it is not clear how each element contributes to the whole structural behavior. In this study, shaking table tests were performed with the two types of specimens. One specimen consisted of columns, *Nuki*, and *Kumimono*. Another one included mud wall with the other type. The aim of this research is to clarify the vibration characteristics of each element in a frame and the difference of the behavior about *Kumimono* in the two types of specimens.

2. OUTLINE OF EXPERIMENT

2.1 Test specimens

The specimens were the 2/3 scale model of a frame in the *Asuka* style of the five-storied timber pagoda as shown in Figure 1. The span between columns was an outside plane of structure in the first story of the pagoda as shown in Figure 1, in order to clarify the modeling method of the structures consisting of *Nuki*, columns. *Kumimono* modeled the parts of 2 pairs on the central two columns because *Kumimono* in corners is projecting at 45-degree angle in a flat and has complex forms and the aim of this study was to get basic data of each element. A cornerstone was put under each column. They were connected with a dowel. Tree species were yellow cedar.

Two types of specimens were used in the tests as shown in Figure 2. Specimen 1 consisted of columns, *Nuki*, and *Kumimono*. Specimen 2 was made by adding mud wall between the columns of the Specimen 1.

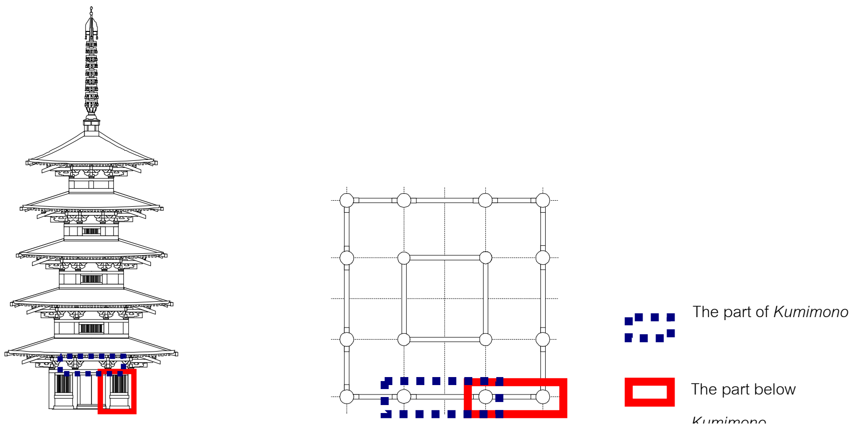

(a) Elevation (b) Plan

Figure 1: Subject plane of structure

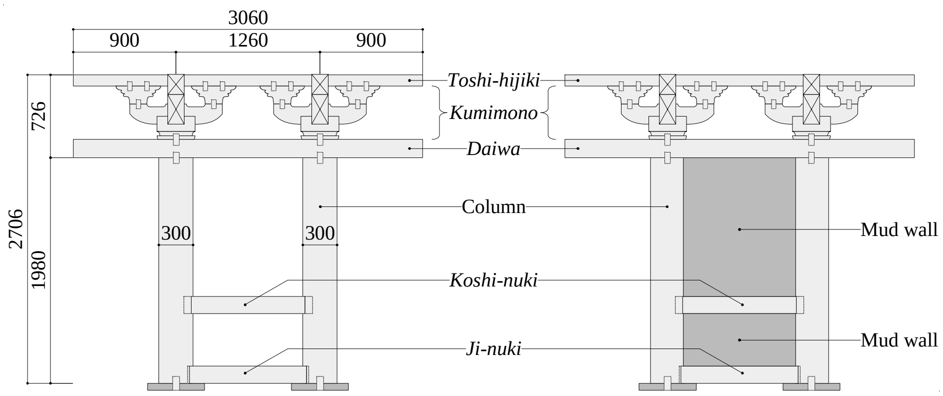

Figure 2:Specimens

2.2 Experimental method

The shaking table tests were carried out at the shaking table of Chiba Experiment Station of Institute of Industrial Science, the University of Tokyo. Horizontal unidirectional shaking was conducted. Figure 3 shows the experimental method. The vertical load of 39.9kN made of steel frames and lead was put on the specimen. A load cell to measure axial force and shear force was placed under each column. The acceleration, displacement and the strain of specimens were measured using about 75 devices.

BCJ-L2, the level 2 of a simulated wave provided from the building center of Japan, was used as a large input motion. In the tests of Specimen 1, the maximum input acceleration was increased by 10% from 10% (35.6 gal) to 100% (356 gal). In the tests of Specimen 2, one input with BCJ-L2 20% and two inputs with BCJ-L2 100% were carried out.

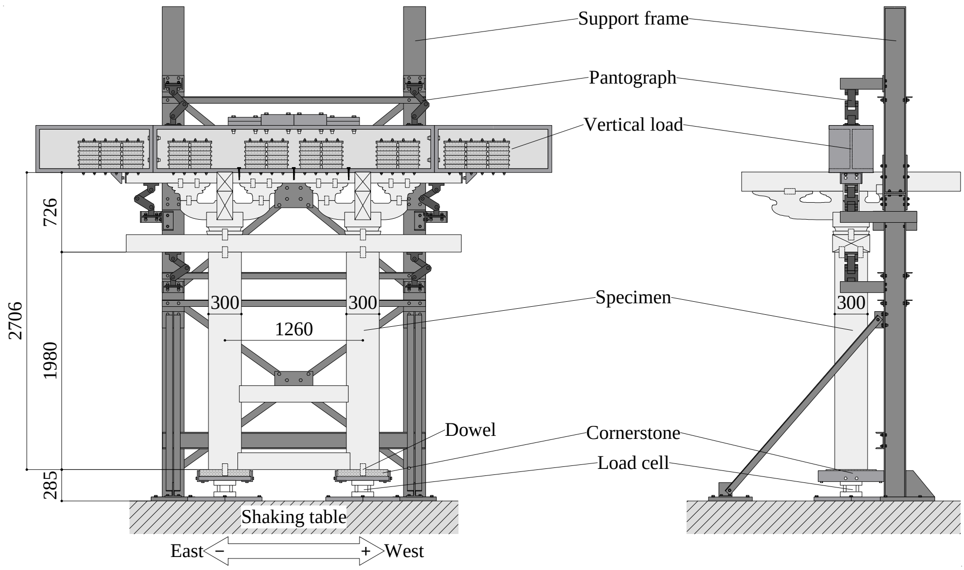

Figure 3: Experimental method

3. EXPERIMENTAL RESULTS

3.1 The relationship between load and displacement

Figure 4 shows the relationship between load and displacement from the inputs of BCJ-L2 20%, 40%, 80%, 100% to Specimen 1. Until the test of 20%, the relationship between load and displacement was linear. After the test of 30%, the relationship became nonlinear. The stiffness went down at the displacement of about 5mm. After the yield point, the hysteresis curve became swollen. The negative gradient appeared in the deformation from the maximum to the origin. The maximum shear force was 10.75kN at the test of BCJ-L2 80%. The maximum displacement was 180.2mm, 1/13rad deformation angle of a column, at the test of BCJ-L2 100%. After the experience of a large deformation, a load around an origin point was increased drastically

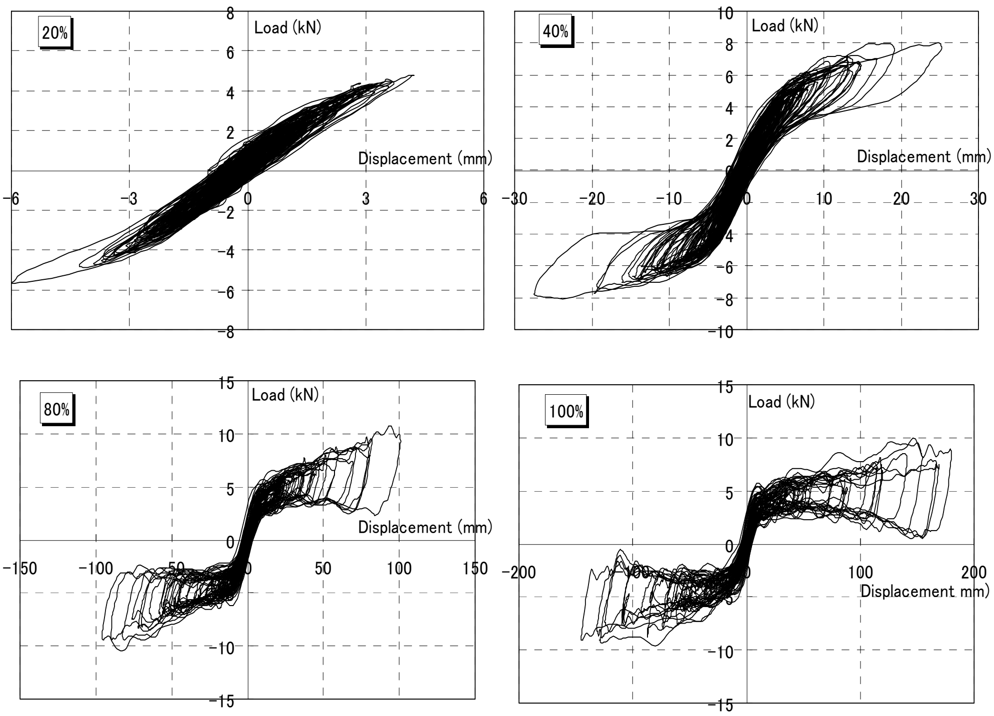

Figure 4: The relationship between load and displacement of Specimen1

Figure 5 shows the relationship between load and displacement for the inputs of BCJ-L2 20% and BCJ-L2 100% to Specimen 2. In the test of BCJ-L2 20%, the stiffness was higher than that in the test of 20% for Specimen 1. It was assumed to be due to the resistance of the mud wall.
In the first BCJ-100%, the load went up to about 12kN within 40mm displacement. It can be assumed to be due to the resistance force of the mud wall. After the collapse of the mud wall, the resistance force of the specimen dropped and a hysteresis curve changed to a gray line in Figure 5. Therefore, in the test of the second BCJ-100%, the load did not rise like the first one. At around 5kN load, the stiffness changed and a load increased gradually up to around 10kN.

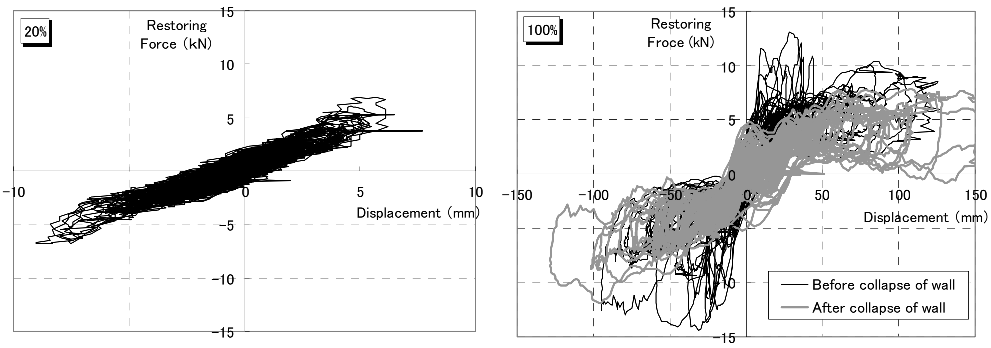

Figure 5: The relationship between load and displacement of Specimen2

Figure 6 shows the relationship between load and displacement for BCJ-L2 100% of Specimen 1 and Specimen 2. The characteristics of every hysteresis curve were almost same after the collapse of the mud wall. However the load of Specimen 2 in the range of less 50mm became higher than that of Specimen 1. It can be assumed to be due to the resistance force of mud wall.

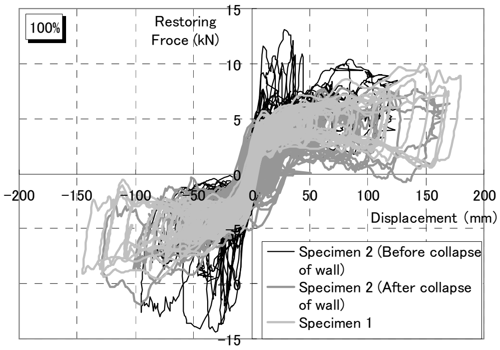

Figure 6: The comparison of the relationship between load and displacement

3.2 Deformation

Figure 7 shows the horizontal deformation of specimens in the range of the maximum amplitude from the test of BCJ L2 100%. Most of the displacement of Specimen 1 was the displacement from the inclination of columns. The line between *Daiwa* and *Toshi hijiki* was vertical almost all time. It means that the displacement of *Kumimono* was very minute. As for Specimen 2, the characteristic was almost same. However, at the maximum deformation, the line between *Daiwa* and Top inclined. It can be seen that the deformation of *Kumimono* increased slightly.

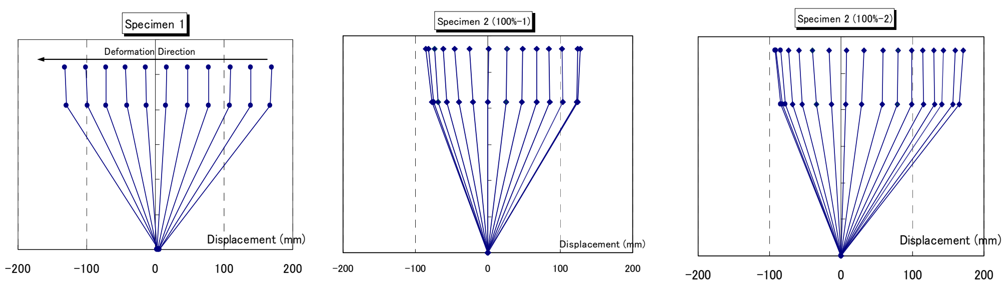

Figure 7: Behavior in 100% tests

3.3 The share force at the bottom of columns

Figure 8 shows the share force measured at the bottom of columns of Specimen 1. Each share force of right and left columns went up and down with the opposite stiffness. It is because the compressive force occurred at *Jinuki* and the force toward a direction spreading the width of columns happened when both columns leaned.

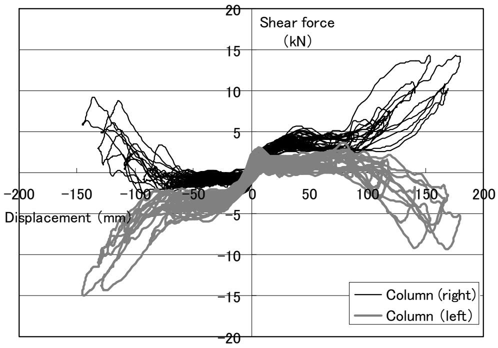

Figure 8: The Shear force at the bottom of columns

4. Modeling of each element

Whole frames including columns, compressive strains inclined to the grain at *Koshinuki and Jinuki*, *Kumimono*, and Mud wall were modeled as shown in Figure 9. The restoring force of each element was calculated by the measurement values from experiments or material experiment results. Each element model is as follows.

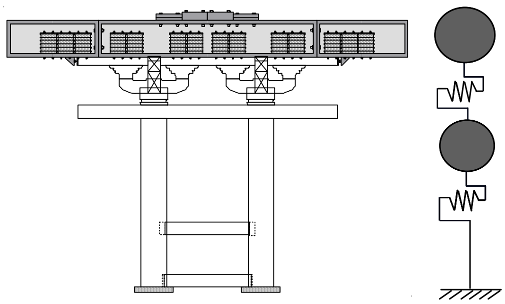

K_k :Spring of Kumimo

$K_{c}+K_n+K_j+K_w$
: Spring of Column, compressive strains inclined to
the grain at Koshinuki and Jinuki, and Mud wall

Figure 9: The model of a whole frame

4.1 Restoring force of Column

Restoring force of columns was calculated with reference to previous experiments and researches of Ban, 1942 and Kawai, 1992.

$$y=H_0\{1-\delta/b+0.99625e^{-7.5675\delta/b}-1.9963/(25\delta/b+1)\} \qquad (1)$$

y: Restoring force, δ : Horizontal displacement, b: Diameter of column,
H_0: = Pb/h Restoring force of rigid body, h: The length of column,

The factor b considered the rabbet like Figure 10. The maximum of restoring force was 80% of H_0. The horizontal displacement of this force was 0.088 times of a column width. Assuming that two columns were connected with a parallel spring, the stiffness of both columns can be added. In addition, it is assumed that deformation and vertical load of both columns were same.

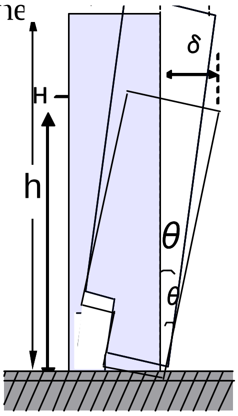

Figure 10: The model of a column

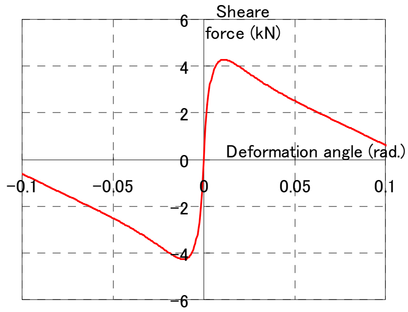

Figure 11: The restoring force of columns

4.2 Evaluation of *Koshinuki*

Perfect elastoplasticity hysteresis shown in Figure 11 and 12 was given by using *Merikomi* theory (Inayama, 1992) , the theory for calculating the theoretical stiffness of timber perpendicular to the grain, based on the hypothesis that compressive strains inclined to the grain were at place shown in Figure 12. On the other hand, bending moment of *Koshinuki* measured by strain gauges was given from experiment results. By the values and calculating deformation angle of the column-*Koshinuki* joint, rotational stiffness was calculated. Figure 13 and 14 show the rotational stiffness of the right column-*Koshinuki* joint in Specimen 1 and 2. In both specimens, experimental results from strain gauges were higher than theoretical ones. For this reason, hysteresis curves like heavy line in Figure 13 and 14 were modeled.

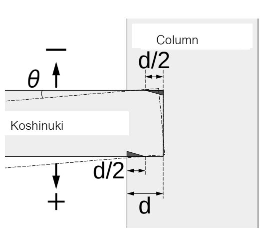

Figure 12: The place of compressive strains

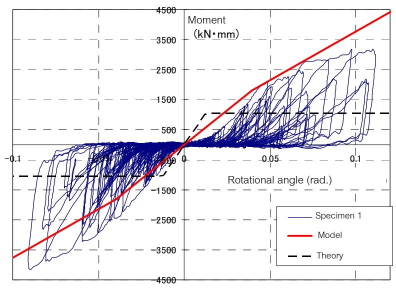

Figure 13: The restoring force of Koshinuki (Specimen 1)

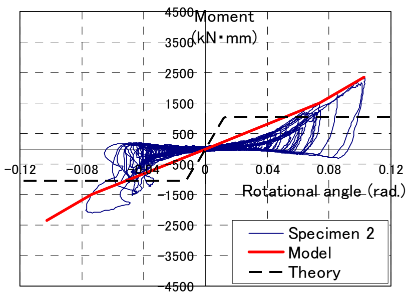

Figure14: The restoring force of Koshinuki (Specimen 2)

4.3 Evaluation of *Jinuki*

After experiments, compressive strains inclined to the grain occurred due to the joint of columns were observed on *Jinuki*. By calculating rotational stiffness assuming that compressive strains occurred at places shown in Figure 15, first stiffness became 146,000 kN・mm/rad., and yield resistance were 1,982 kN・mm. By using the theoretical values, the restoring force as shown in Figure 16 were given because no measurement values like Koshinuki were.

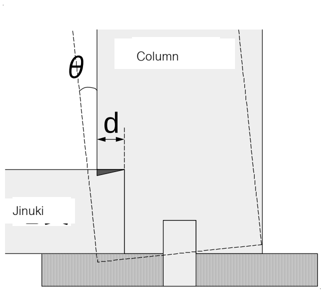

Figure 15:The place of compressive strains

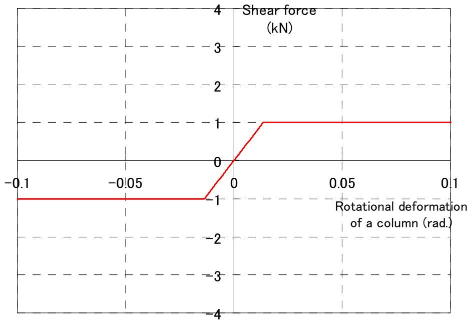

Figure 16: The restoring force of Jinuki

4.4 Restoring force of *Kumimono*

The horizontal displacement of Kumimono was calculated by subtracting one of Daiwa from one of top. The relationship between load and displacement of *Kumimono* was gained shown in Figure 17. Restoring force of *Kumimono* in Specimen 1 and 2 were evaluated like heavy lines in Figure 17.

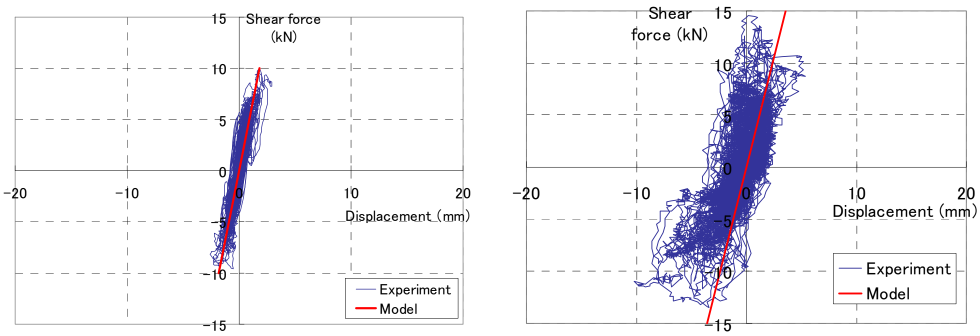

Figure 17: The restoring force of Kumimono

4.5 Restoring force of Mud wall

In order to figure the strength of mud wall out, material tests for mud wall were performed as shown in Figure 18. From the results, the hysteresis curve of mud wall was modeled like a heavy line shown in Figure 19.

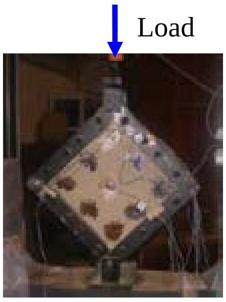

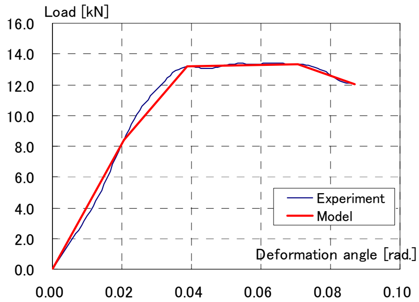

Figure 18: Material test

Figure 19: The restoring force of mud wall

5. Analysis Results and Discussions

The restoring force characteristics of Specimen 1 and 2 given by adding each hysteresis model shown above were compared with the load-deformation relationship given by experiments. Figure 20 shows the hysteresis curve given by adding downside elements of columnm, Nuki, and mud wall. Figure 21 shows the hysteresis curve given by adding a model shown in Figure 20 and *Kumimono*. It is assumed that no restoring force of compressive strains inclined to the grain occurred during unloading. It is clarified that experimental model corresponds to theoretical one. The restoring force can be calculated by adding each restoring force model of elements.

It can be seen that in the range of the first stiffness, the ratio of the restoring force of columns is the highest in Specimen 1. In the range of deformation more than 100mm, one of *Koshinuki* is high. On the other hand, the ratio of restoring force for mud wall is the highest in the Specimen 2. After collapse of mud wall, the restoring force of *Koshinuki* accounts for high percentage of the whole bearing force. The horizontal derfomation of Kumimono was very little in both specimens.

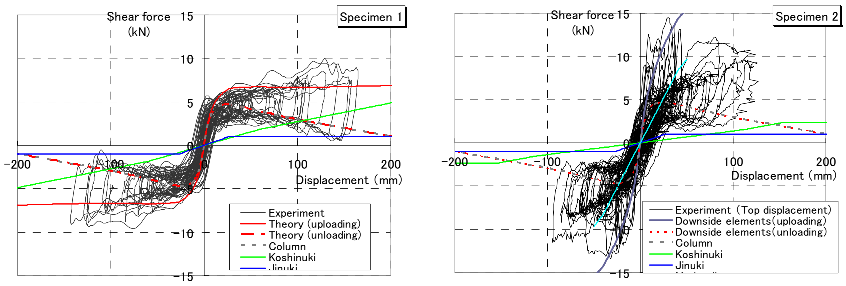

Figure 20: The comparison between experimental and theoretical results (Structural elements without Kumimono)

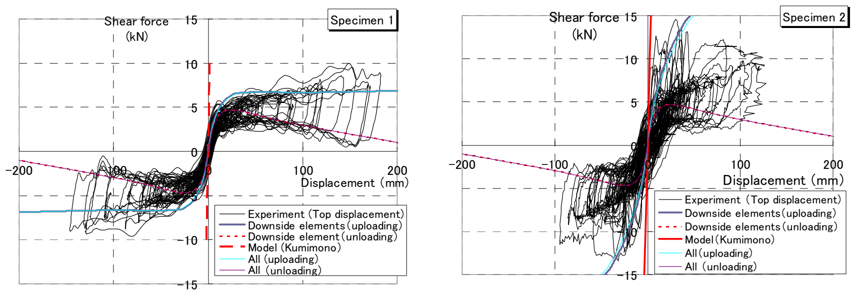

Figure 21: The comparison between experimental and theoretical results (Structural elements including Kumimono)

6. CONCLUSIONS

Shaking table tests were performed using a traditional timber frame consisted of columns having large diameter, *Kumimono*, *Nuki*. Specimens were with mud wall and without one. It is found that the restoring force characteristics of *Kumimono* in both specimens have a very small effect on one of a frame. It is because the stiffness of *Kumimono* is much higher than one of column, *Nuki* and mud wall making the weakest structural frames in traditional timber structures. It is clarified that the relationship between load and displacement of a whole frame can be evaluated by adding the restoring force characteristics of each structural element.

ACKNOWLEDGMENT

The specimens used in the tests were made by master carpenter Mr. Yasugoro Kaneko of Fudosyaji. The tests were performed with staff and students of Koshihara Laboratory, Yosuke Simawaki, Assistant, Mr. Hideo Otsuka, a Technical Staff, Dr. Kim Hye Won, Postdoctoral Fellow, Mr. Kei Kato, a Graduate Student, and Ms. Tomoka Takase, an Undergraduate Student of Isoda Laboratory at Shinshu University. The authors wish to express their sincere gratitude to all of people above for their generosity and help without which this experiment could not be accomplished.

REFERENCES

Ban, S., 1942. A study on the determination of the stability about main hall structures, Vol. 3: a mechanical study on the Japanese Traditional Frame, 1, the stability restoring force of a column. March, 252-258. (in Japanese).

Kawai, N., 1992. A study on the structural stability of traditional timber structures, The Building Center of Japan, March. (in Japanese).

Inayama, M., 1991. The theory of compression perpendicular to the grain in wood and its application, Dissertation of the University of Tokyo. (in Japanese).

Kato, K., Tsuwa, I., and Koshihara, M., 2008. Shaking table tests of traditional timber frames including *Kumimono* Part 1 Experimental outline and results, Annual Meeting Architectural Institute of Japan. C-1, Structures III, pp.43-44 (in Japanese).

Tsuwa, I., Kato, K., and Koshihara, M., 2008. Shaking table tests of traditional timber frames including *Kumimono* Part 1 Experimental outline and results, Annual Meeting Architectural Institute of Japan. C-1, Structures III, pp.45-46 (in Japanese).

RESIDUAL DISPLACEMENT PREDICTION OF R/C BUILDING STRUCTURES USING EARTHQUAKE RESPONSE SPECTRA

RISA KUWAHARA
Graduate Student, Graduate School of Eng., The University of Tokyo, Japan
kuwarisa@iis.u-tokyo.ac.jp
NORIYUKI TAKAHASHI
Institute of Industrial Science, The University of Tokyo, Japan
ntaka@iis.u-tokyo.ac.jp
HO CHOI
Institute of Industrial Science, The University of Tokyo, Japan
choiho@iis.u-tokyo.ac.jp
YOSHIAKI NAKANO
Institute of Industrial Science, The University of Tokyo, Japan
iisnak@iis.u-tokyo.ac.jp

ABSTRACT

Strong earthquake motions exceeding the current design standard level have been recorded during recent severe earthquakes in Japan. Collapsed reinforced concrete building structures are very few because the Japanese building code requires high performance for their seismic safety. Some of them, however, show moderate or severe damage, and the total cost for their repair often exceeds that of reconstruction. It is, therefore, important that the building design code ensure not only its seismic safety, but also its reparability performance. The residual displacement after earthquakes is one of the most important factors for predicting their reparability performance. In previous studies, most of researchers estimate the residual displacement of buildings based on non-linear earthquake response analyses.

In this paper, a simplified method is proposed to predict the residual displacement where it is approximated by the point where the line connecting two displacement peaks in positive and negative domains of load-deflection curves crosses the abscissa. Considerable prediction errors are found between predicted displacements in the proposed method and those directly obtained after non-linear response analyses. The accuracy of predicted residual displacement is, however, much improved when the 3rd displacement peak is taken into account in addition to the 1st and 2nd displacement peaks. The proposed method is further extended and applied to the conventional capacity spectrum method to predict peak displacements. It is revealed that the method can successfully predict the residual displacements and enhance the conventional capacity spectrum method.

1. INTRODUCTION

Most buildings, which satisfied the current design criteria, survived recent severe earthquakes in Japan, owing to the high requirement of the seismic performance to prevent building collapse and human casualties. Some building structures, however, showed damage to some extent after earthquakes and it cost much more than expected by building owners to have them repaired. They are concerned with not only direct but also indirect losses such as business downtime. Performance-based design therefore should include reparability and functionality of buildings after earthquakes.

To identify the reparability performance, an effective evaluation index is required. In recent studies especially for the precast concrete members, the residual displacement control is considered an effective method to assure the reparability performance. In this paper, the residual displacement after excitations is employed as an index to identify reparability performance of reinforced concrete structures. A simplified method is proposed to predict the residual displacement after excitations, and its accuracy is discussed through comparison with results of non-linear response analyses.

2. PREDICTION OF RESIDUAL DISPLACEMENT WITH PEAK RESPONSE DISPLACEMENTS

2.1 Definition of estimator *R* of residual displacement

Reinforced concrete structures are idealized with an SDOF system in this study as shown in Figure 1. Goto et al. (1970) estimate the residual displacement δ_r after excitations (point A) with the mean value of maximum response displacements in the positive and negative directions. Kitamura et al. (2009) concludes that the response after the maximum displacement particularly influences the residual displacement δ_r. In this study, the estimator R of residual displacement δ_r is defined for better predictions under rational assumptions in the following manner.

The 1st peak P_1 in a non-linear earthquake response analysis is defined as the maximum response point, which is supposed to be found in the positive domain hereafter, as shown in Figure 1. The 2nd peak P_2 is defined as the maximum response point in the opposite negative domain after P_1, and the 3rd peak P_3 is then defined as the 2nd maximum response point in the opposite positive domain after P_2. As shown below, subsequent peaks P are then defined in the analogous manner described above (Figure 2).

・P_{2i-1}: *i*-th max in the positive domain.
・P_{2i} : *i*-th max in the negative domain.

The estimator R_N of residual displacement δ_r is then defined as the point where a line connecting P_N and P_{N+1} crosses the abscissa as shown in Figure 1.

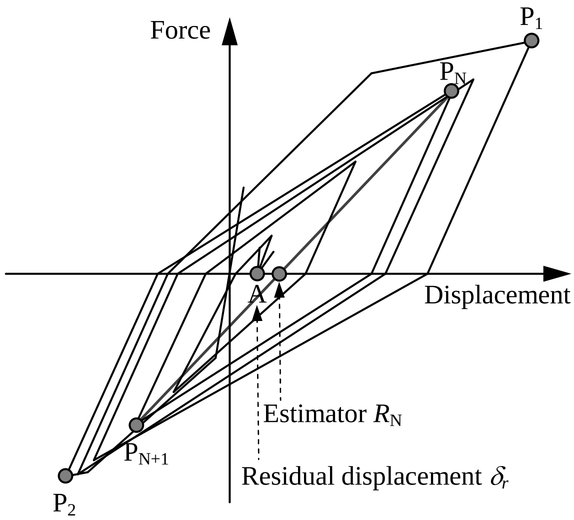

Figure 1: Definition of estimator R of residual displacement

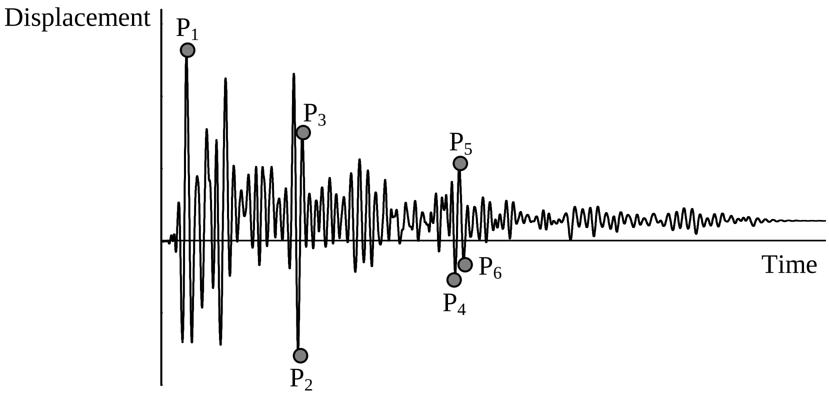

Figure 2: Definition of peaks

2.2 Modeling of building structure

The hysteretic rules for building structures are idealized with Takeda model (Takeda et al., 1970) in the nonlinear earthquake response analyses (Figure 3). The base shear coefficient and the natural period of the structures are 0.3 and 0.3(s), respectively, in all analyses. A viscous damping factor proportional to instantaneous stiffness is assumed to be 5% of the critical damping. The cracking strength is assumed 1/3 of yielding strength and the secant stiffness at yielding is assumed 30% of the elastic stiffness. The post-yielding stiffness is assumed 0.1% of the elastic stiffness. The hysteretic parameter α for unloading stiffness in Takeda model is 0.5. Three observed earthquake records are applied for excitation, which are El Centro NS 1940, Tohoku NS 1978, and JMA Kobe NS 1995. The accelerations are scaled so that the maximum ductility factor μ of the model should reach 1.0, 2.0 and 3.0, respectively. Note that the residual response, rather than the structural safety during large inelastic response, is the primary concern in this study, and the maximum ductility factor μ is therefore limited to 3.0 herein.

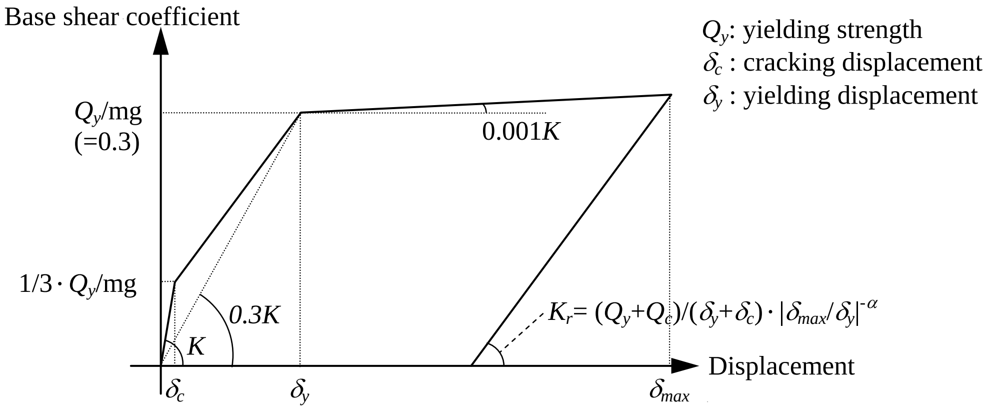

Figure 3: Hysteretic model

2.3 Results of analyses

Nine cases consisting of 3 parameters for input earthquake records and 3 target maximum ductility factors are investigated in this study, and the prediction error ε_R of estimator R_N defined in Equation (1) is examined in each case:

$$\varepsilon_R = \left(R_N - \delta_r\right)/2\delta_y \tag{1}$$

where, R_N is the N-th estimator of δ_r (N=1, 2, 3,…), δ_r is the residual displacement after non-linear response analysis, and δ_y is the yielding displacement of the model structure.

Figure 4 shows prediction errors ε_R with respect to N. In case of μ=1.0, the error ε_R is negligibly small regardless of the value of N in any earthquake since the values of R_N and δ_r are much smaller than δ_y. In cases of μ=2.0 and 3.0, the error is much larger and does not necessarily decrease with increase in the value of N. The results found in Figure 4 can be explained as fallows.

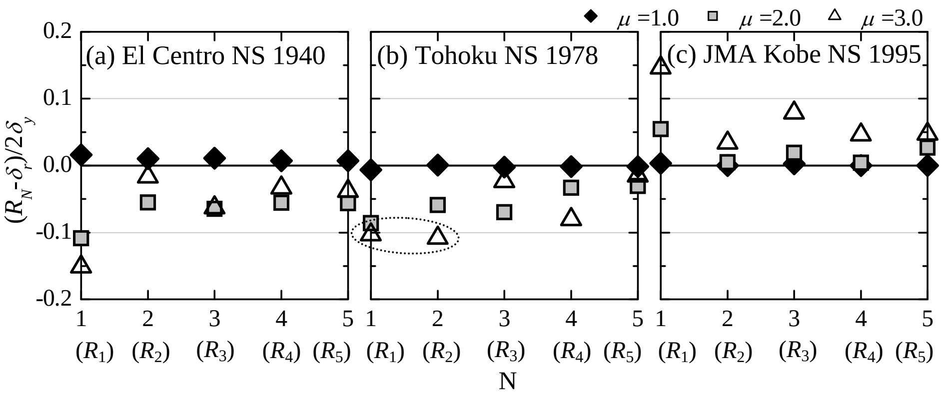

Figure 4: Prediction error ε_R

Supposing the 1st peak P_1 falls within the positive domain and bearing the definition of estimator R_N described in section 2.1 in mind, the values of

R_1 to R_5 satisfy the following relation: $R_2<R_1$, $R_2<R_3$, $R_4<R_3$, $R_4<R_5$ (cf. Figure 5). When δ_r is smaller than R_2 (Figure 5 left), R_2 (N=2) is always a better estimator of δ_r than R_1 (N=1) due to the relation of $\delta_r<R_2<R_1$. Thus the prediction is improved with increase in N. On the other hand, when δ_r is larger than R_1, R_1 (N=1) is a better estimator than R_2 (N=2) due to the relation of $R_2<R_1<\delta_r$. Thus the prediction is not improved with increase in N. The estimator R_N with larger value of N does not necessarily give a better estimator of δ_r under the values of N equal to around 5 or 6 as investigated in this study, and the accuracy depends on the relation between R_{N-1}, R_N and δ_r.

Figure 6 shows the ratio $\rho=|(R_2-\delta_r)/(R_1-\delta_r)|$ to identify a better estimator, where R_2 is a better estimator when $\rho<1.0$ and R_1 is a better estimator when $\rho\geq 1.0$. As can be found in the figure, a plot in case of Tohoku NS 1978 (μ=3) can be better predicted by R_1, and this is consistent with the result found in Figure 4 as enclosed by a dotted line where the prediction error of R_2 is larger than that of R_1.

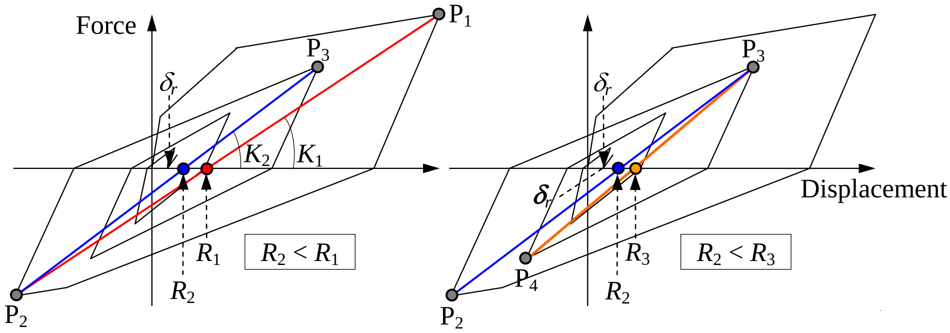

Figure 5: Relationship of R_1, R_2, R_3, and δ_r

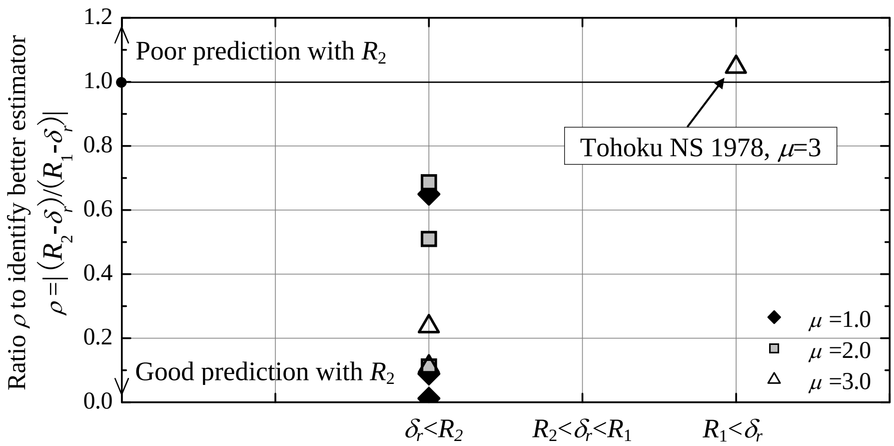

Figure 6: Relationship between ρ, R_1, R_2, and δ_r

2.4 Determination of estimator *R*

The simplest procedure to predict the residual displacement δ_r is to employ R_1 discussed above. There are, however, some cases where R_2 is a better estimator than R_1 as shown in Figures 4 and 6. To identify a better estimator between R_1 and R_2, the following procedure is discussed herein.

The difference between R_1 and R_2 is first examined. As can be found in Figure 6, the following tendency can be derived.

(1)When δ_r is larger than R_1, the ratio ρ is close to 1.0 and the difference between R_1 and R_2 is therefore small.

(2)When δ_r is smaller than R_1, the ratio ρ is generally much smaller than 1.0 and the difference between R_1 and R_2 is large.

To describe the closeness of R_1 and R_2 discussed above, an equivalent stiffness ratio K_1/K_2 is employed, where K_N signifies the equivalent stiffness connecting peak values P_N and P_{N+1} as shown in Figure 5. Additionally, a new parameter γ defined in Equation (2) is considered to express which of R_1 and R_2 is closer to δ_r. When δ_r is located just on the center of R_1 and R_2, γ is equal to 0.

$$\gamma = \left\{ \delta_r - \frac{(R_1 + R_2)}{2} \right\} \Big/ 2\delta_y \tag{2}$$

Figure 7 shows the relationship between γ and K_1/K_2. When K_1/K_2 is smaller than 1.0, γ tends to be negative, which means δ_r is closer to R_2. On the other hand, when K_1/K_2 is close to 1.0, γ tends to distribute around 0 or in the positive domain, and δ_r is therefore closer to R_1.

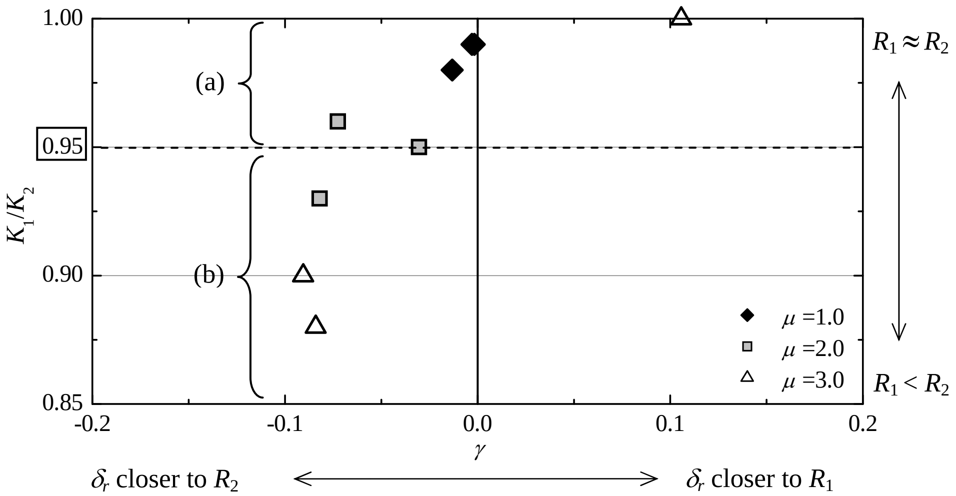

Figure 7: Relationship between γ and K_1/K_2

As stated earlier, R_1 can be the simplest estimator of δ_r. As can be found in Figure 7, however, R_2 can be a better estimator of δ_r in case of K_1/K_2 smaller than 0.95. Considering the results above, the following practical procedure to predict δ_r is proposed.

· $\delta_r = R_1$ when $K_1/K_2 \geq 0.95$ as shown (a) in Figure 7.

· $\delta_r = R_2$ when $K_1/K_2 < 0.95$ as shown (b) in Figure 7.

Figure 8 (1) shows results simply predicted by R_1 and Figure 8 (2) shows those obtained by the procedure above. As can be found in the figure, the prediction error is, as shown in Figure8 (2), significantly reduced after considering R_2 or the 3rd peak displacement and the proposed procedure can be an effective tool to predict the residual displacement δ_r.

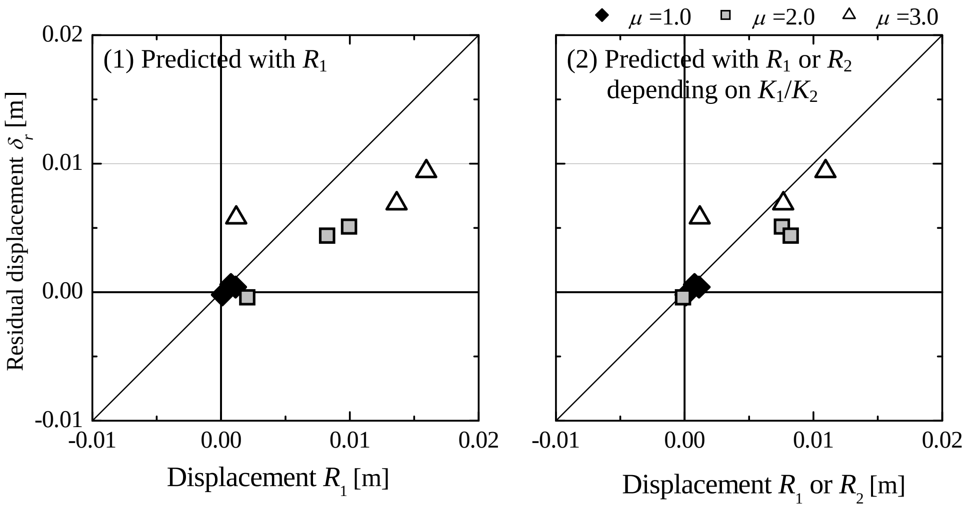

Figure 8: Relationship between δ_r, R_1 and R_2

3. PREDICTION OF RESIDUAL DISPLACEMENT USING EARTHQUAKE RESPONSE SPECTRA

In the previous section, a procedure to predict δ_r with R_1, R_2 and K_1/K_2 (or P_1, P_2 and P_3) are proposed. If the parameters above can be successfully predicted from the capacity spectrum method, the proposed procedure can be practically applicable in the structural design stage.

In the subsequent sections, a new approach to predict R_1 and R_2 from the capacity spectrum method is first proposed. It is then combined with the procedure described in section 2.4 and its applicability is discussed.

3.1 Prediction of peak responses with capacity spectrum method

A new approach to predict peak responses including those after the maximum using the capacity spectrum method is discussed. The procedure is shown in detail below. Note that the maximum response, i.e., the 1st peak response, is supposed to be found in the positive domain in this study.

[1]Firstly, the maximum displacement is predicted with the conventional capacity spectrum method in the positive domain using the structural capacity curve (i.e., backbone curve) and the demand spectrum (i.e., S_{A1}-S_{D1} curve) as shown point P_1* in Figure 9.

Setting i equal to 1 in Equations (3) and (4), the demand S_{A1}-S_{D1} curve is obtained by multiplying a reduction factor F_{h1} and the response spectrum with a 5% damping factor to consider the effect of hysteretic energy dissipation due to non-linear response. The equivalent damping factor

h_{eq1} in Equation (3) is evaluated by Equation (4), and the definitions of dissipated energy ΔW_1* and W_1* are illustrated in Figure 10. The factor α_1 in Equation (4) is set 0.8 to predict the 1st peak response considering the notification No.1457 by the Japanese Ministry of Construction, which is generally applied in Japan and Midorikawa et al. (2003):

$$F_{h_i} = \frac{1.5}{1+10\left(h_{eqi}+0.05\right)} \quad (3)$$

$$h_{eq_i} = \frac{1}{4\pi}\cdot\frac{\Delta W_i*}{W_i*}\times\alpha_i \quad (4)$$

where, ΔW_i* is the hysteretic energy dissipation in one cycle, W_i* is the equivalent potential energy, and α_i is a reduction factor to allow for non-stationary responses to predict P_i*.

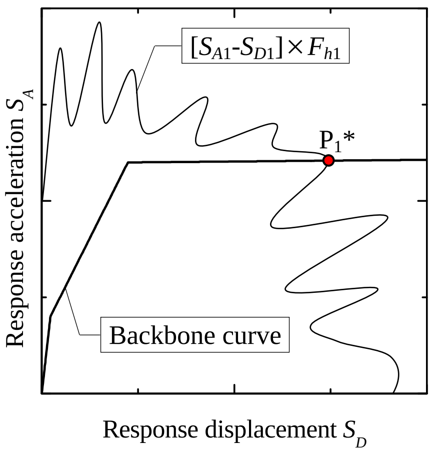

Figure 9: Prediction of P_1*

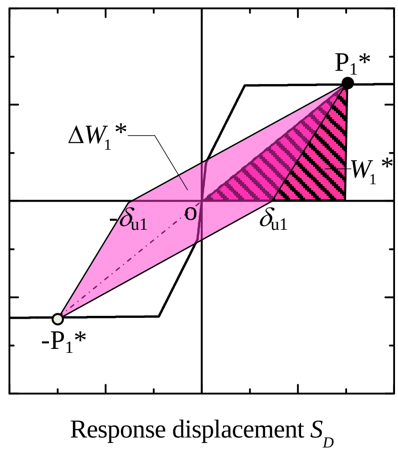

Figure10: Definition of ΔW_1* and W_1*

[2]Secondly, the 2nd peak is predicted in the negative domain using the concept analogous with the conventional capacity spectrum method as employed above.

The employed backbone curve to predict the 2nd peak P_2* is shown in Figure 11, where the reloading curve in the negative displacement domain after P_1* is used. Setting i equal to 2, the S_{A2}-S_{D2} curve is obtained from the spectrum of 2nd peak defined in section 2.1 and F_{h2} in Equations (3) and (4) where the factor α_2 is tentatively set 0.8 considering preliminary studies on the ratio of hysteretic energy dissipation to ΔW_2 during non-linear response analyses in chapter 2. The definitions of ΔW_2* and W_2* are shown in Figure 12 where the unloaded displacement in the negative domain $\delta_{u2}{}^{n}$ is assumed to follow the unloading rule of the Takeda model and the distance $|o'- \delta_{u2}{}^{p}|$ is equal to $|o'- \delta_{u2}{}^{n}|$ to represent a stationary response. During calculations, the 2nd peak P_2* is initially assumed $-P_1*$, and iterative calculations are performed until the predicted peak converges.

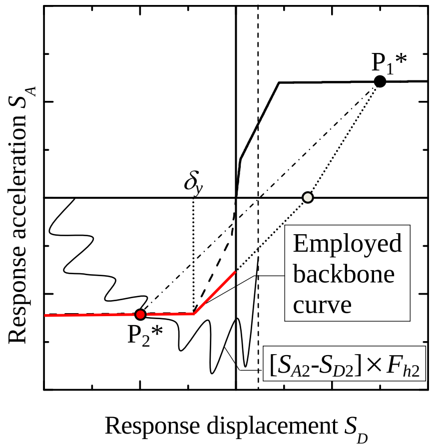

*Figure 11: Prediction of P_2**

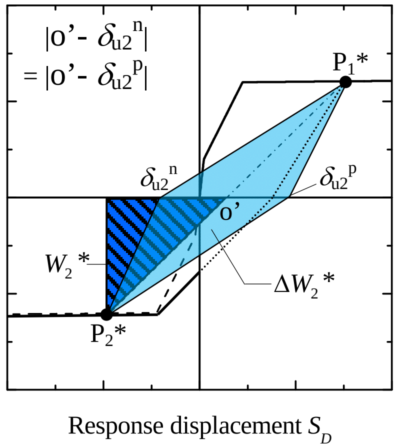

Figure12: Definition of ΔW_2 and W_2**

[3]The 3rd peak is evaluated in the positive domain in the analogous manner described earlier. The employed backbone curve to predict the 3rd peak P_3* is shown in Figure 13, where the reloading curve in the positive displacement domain after P_2* is used. Setting i equal to 3, the S_{A3}-S_{D3} curve is obtained from the spectrum of 3rd peak defined in section 2.1 and F_{h3} in Equations (3) and (4) where the factor α_3 is tentatively set 1.0 considering preliminary studies as is done for α_2. The definitions of ΔW_3* and W_3* are shown in Figure 14 where the unloaded displacement in the positive domain $\delta_{u3}{}^{p}$ is assumed to follow the hysteric rule and the distance $|o' - \delta_{u3}{}^{p}|$ is equal to $|o' - \delta_{u3}{}^{n}|$. During calculations, the 3rd peak P_3* is initially assumed P_1*, and iterative calculations are performed until converged.

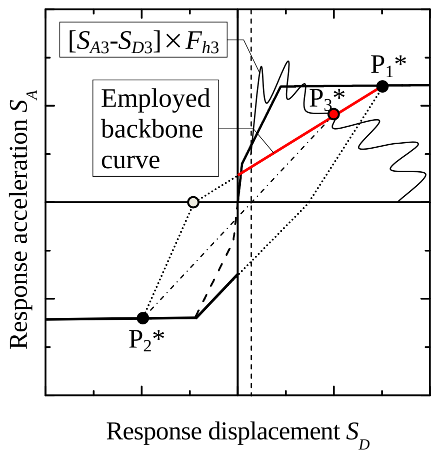

*Figure 13: Prediction of P_3**

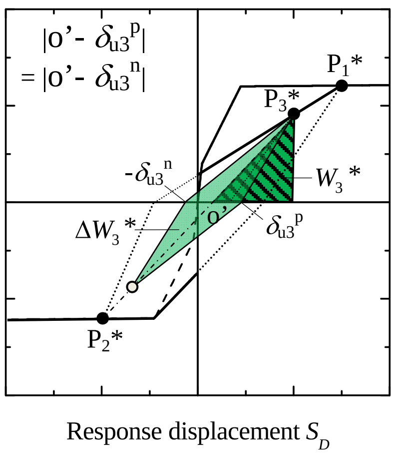

Figure14: Definition of ΔW_3 and W_3**

3.2 Residual displacement predicted through capacity spectrum concept

Peak responses P_1*, P_2* and P_3* are obtained as shown in section 3.1 and then the residual displacement δ_r can be predicted by either R_1* or R_2*, which is the point where a line connecting P_N* and P_{N+1}* crosses the abscissa.

Predicted results considering criteria shown in section 2.4 are compared with those obtained in the non-linear response analyses in Figure 15. As can be found in the figure, the predicted displacement using the capacity spectrum method compares well with those obtained from the non-linear response analyses and the proposed method can successfully predict the residual displacement.

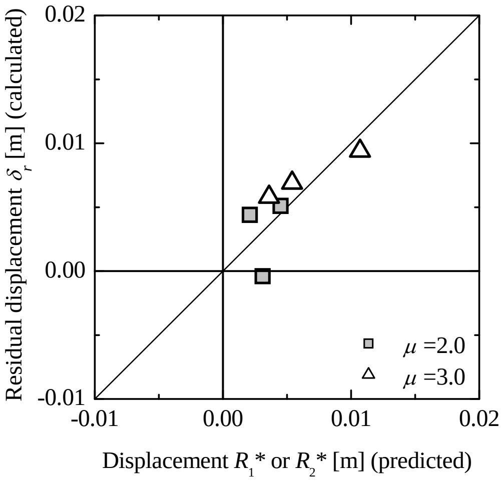

Figure 15: Relationship between δ_r, R_1, and R_2**

4. CONCLUSION

(1)A simplified method is proposed to predict the residual displacement where it is approximated by the point where the line connecting two displacement peaks in positive and negative domains of load-deflection curves crosses the abscissa. Its accuracy is much improved when the 3rd displacement peak is taken into account in addition to the 1st and 2nd displacement peaks.

(2)The proposed method above is further extended and applied to the conventional capacity spectrum method to predict peak displacements. It is revealed that the method can successfully predict the residual displacements and enhance the conventional capacity spectrum method.

REFERENCES

Goto, H. and Iemura, H., 1970. A study on the Plastic Deformation of Elasto-Plastic Structures in Strong Earthquakes. *Proceedings of Japan Society of Civil Engineers*, Vol. 184, pp.57-67 (in Japanese).

Kitamura, H., Nomura, A., Kawasaki, M., Dan, K. and Satou, T., 2009. A Proposal for Cumulative Damage Evaluation Method for Longevity Life Steel Buildings Considering Plural Strong Ground Motions. *Journal of Structural and Construction Engineering*, AIJ, Vol. 74, No. 642, pp. 1443-1452 (in Japanese).

Takeda, T., Sozen, M. A. and Nielsen, N. N., 1970. Reinforced concrete response to simulated earthquakes. *Journal of the Structural Division*, ASCE, Vol.96, No.ST 12, pp. 2557-2573.

Ministry of Construction, 2000. Notification No.1457 by the Japanese Ministry of Construction (in Japanese).

Midorikawa, M., Okawa, I., Iiba, M., and Teshigawara, M., 2003. Performance-Based Seismic Design Code for Building in Japan. *Earthquake Engineering and Engineering Seismology*, Vol. 4, No. 1, pp. 15-25.

PARALLEL SESSION 3

DHAKA CITY: HOT SPOT OR NOT?

MEHEDI AHMED ANSARY
MOHAMMAD SALAHUDDIN RIZVI
Department of Civil Engineering, BUET, Dhaka-1000, Bangladesh
ansary@ce.buet.ac.bd

ABSTRACT

Dhaka is prone to damaging and costly flooding, both from the rivers that bound it and from rainfall that generates runoff that is beyond the capacity of the drains. In less than 20 years, the city has faced three major floods, each causing huge damage and economic loss. Although the government has taken a number of measures to improve Dhaka's capacity to withstand floods, there is further opportunity. Dhaka is now the world's eighth largest city. The relationship between climate change and cities is complex. City-based activities contribute significant amounts of greenhouse gases (GHG) and, simultaneously, are often more vulnerable to the impacts of climate change. The most adverse impacts of climate change are likely to be in urban areas where people, resources, and infrastructure are concentrated. Dhaka is the capital of Bangladesh and epicenter of the current urbanization surges. The responsibility of responding to climate change impacts and consequences will fall on the city government and on its communities. There is a strong local commitment and organization is required to deal with behavior and technological change to reduce carbon emissions and the disasters that climate changes consequences and regional threat represent.

Climate change will require concerted actions by local government and their partners to manage a changing and more invasive environment. The need to promote changes in technologies, citizen participation and urban growth patterns are equally important parts of the behavior of the urban populations that contribute to global warming and create vulnerabilities to disasters. Mainstreaming these issues into policy and practice will lead to a holistic rather than sectoral engagement in climate change.

The objective of this study is to assess Dhaka city's human and built environment characteristics, potential impacts of climate change, and natural or other hazards. Beyond that, the assessment will also identify local government prerogatives and authorities that would allow it to take action in dealing with potential climate change impacts and natural hazards. The ultimate determination from the assessment is to identify the areas which are risky and more vulnerable. This knowledge is then applicable for defining priority actions that prevent (or "cool down") the city from becoming a "Hot Spot."

1. INTRODUCTION

Dhaka is situated between latitudes 23°42' and 23°54'N and longitudes 90°20' and 90°28'E. The city is bounded by the rivers Buriganga to the south, Turag to the west, Balu to the east, and Tongi Khal to the north. Figure 1 shows the location of Dhaka city. The city has three distinct seasons: winter (November-February), dry with temperatures ranging from 10° to 20°C; the pre-monsoon season (March-May), with some rain and hot temperature reaching up to 40°C; and the monsoon (June-October), which is very wet with temperatures around 30°C. Dhaka experiences about 2,000 mm of rain annually, of which about 80% falls during the monsoon.

Dhaka is one of the populous mega city in the world. The Statistical City Corporation Area of Dhaka has about 7.3 million people within 360 km^2 now. It will become fifth largest city by 2030 in terms of population. Over 40% of the population of Dhaka is poor, who live in slums and fringe areas and are extremely vulnerable to disaster and climate risks

Urbanization in Dhaka is restricted mostly to the north bank of the river Buriganga. The four-hundred-year history of Dhaka city can be divided into five different stages of development: Pre-Mughal period, Mughal period, British period, Pakistan period, and Bangladesh period.

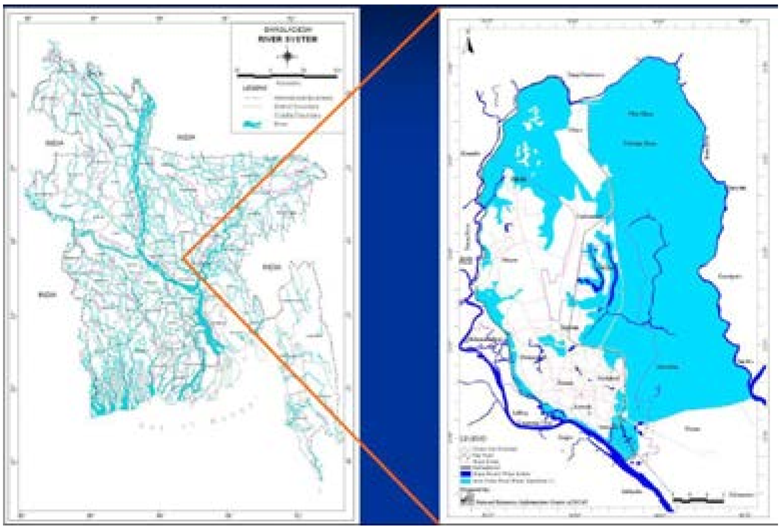

Figure 1: Location of Dhaka City

Rapid urbanization without considering the geological aspects has brought significant changes in the geo-environment of the city area. Water logging, pollution, changes in the hydrogeological system, localized land subsidence, and building collapse are the hazards associated with these changes in the geo-environment. Groundwater withdrawal has increased more than 90% over the last 30 years resulting in groundwater mining and lowering of the water level by 20 m. Water resources of the city are being polluted by the indiscriminate disposal of untreated industrial and municipal wastes in swamps and natural channels in and around the city.

In this study, Dhaka city's human and built environment characteristics have been assessed based on a recently published World Bank Primer (2008) on Reducing Vulnerabilities to Disasters. To assess the Dhaka city's characteristics, officials from Dhaka City Corporation, Department of Environment etc. have been interviewed.

2. OBJECTIVE OF THE PRIMER

The Primer is intended to be a tool and an applied knowledge resource for local governments and their stakeholders to address climate change impacts and disaster risk management issues in the city. It is not an exhaustive compilation of thought and practice to prove that climate change is a threat and does not present recipes for action. Rather it offers principles and examples of sound practice that a city can adapt to its particular context.

The primer offers illustrative examples of addressing disaster risk management and climate change as essential components of urban development and management. The primer reinforces the idea that sustainable development in urban areas must include disaster risk reduction and climate change actions to reduce vulnerabilities. Figure 2 illustrates the linkages between the disaster risk management, climate change, and development policy.

This primer initiates a learning process that can be carried forward by local government on the issues of climate change, and the critical relationship between current urban and financial trends with climate change, disaster risk management and sustainable development.

Figure 2: Integrating climate change and disaster risk management into development policies

The main objectives of this study are as follows:

a. assess the Dhaka city's human and built environment characteristics
b. potential impacts of climate change, and natural or other hazards

c. understand the different types of impacts of climate change and natural disasters
d. systematically organize their communities to take proactive actions in reducing vulnerabilities through mainstreaming resilience

3. HOT SPOT ASSESSMENT

3.1 Completing the City Typology and Risk Charaterization Matrix

After collecting adequate background material, it should complete the city Typology and Risk Characterization Matrix. Designed to give an overview of all important issues and activities that could affect the city, the city Typology and Risk Characterization Matrix is divided into 11 categories of attributes (A through K), in six main areas:

- City description (A-B)
- Governance and management (C-E)
- Built environment (F)
- Political and economic impacts (G-H)
- Natural hazards (I-J)
- Climate change impacts (K)

Category A identifies the geographic location of the city. This helps in identification of impacts of climate change and the likely natural hazards that are of concern of the city.
Category B indicates the size and characteristics of the city area and population. Resident population, floating population, density and growth rate are important indicators of the concentration of problems and their rate of increase over time.
Category C relates to governance structure and hazard management.
Category D establishes the responsibilities for disaster risk management and climate change management.
Category E focuses on the financial resources of the city.
Category F relates to the city’s built environment.
Category G relates to the political impact of a disaster affecting some cities.
Category H establishes the impact of disasters on the most relevant urban economic activities of the city.
Category I assesses the threat of natural hazards.
Category J relates to disaster response system and existence of a city’s emergency response plan.
Category K relates to climate change impact

3.2 Additional Testing for A Hot Spot

A clear link between climate change impacts and the city vulnerability assessment can be established by completing the figure, in which cities evaluate the consequences of specific climate factors such as temperature rise, precipitation change and sea level rise on the main sectors in the city.

A benchmark evaluation of risk can also be helpful in motivating the city to understand where the main gaps and difficulties are in preparing for disasters and natural hazards. To establish a benchmark evaluation on Disaster Preparedness and Response in specific sectors for specific natural hazards, the city officials and their Climate Change Team should assess the level of preparedness for each sectors such as industrial, service, financial, tourism and hospitality etc.

4. WHEN IS A CITY A HOT SPOT?

Being a Hot Spot implies that the city has a high level of vulnerability to climate change impacts (at least in some sectors, activities, and areas) and is at high risk of being adversely affected by natural disasters

Based on the completed City Typology and Risk Characterization Matrix and rating levels, the city government and climate change Team should determine their vulnerability assessment that leads to a Hot Spot categorization : the higher a city's vulnerability, the hotter the city is as a Hot (Figure 3).

Figure 3: The climate change Hot Spot spectrum

The greater the number of adverse conditions that are satisfied (ratings of High and Medium and Yes responses), the "hotter" the city's categorization is as a Hot Spot. The level of "hotness" can be used by the city to prioritize its activities and to motivate integration of development plans considering climate change impacts and disaster risk management. Figure 4 shows the links among consequences and sectors with potential impacts and climate change mitigation and adaption options.

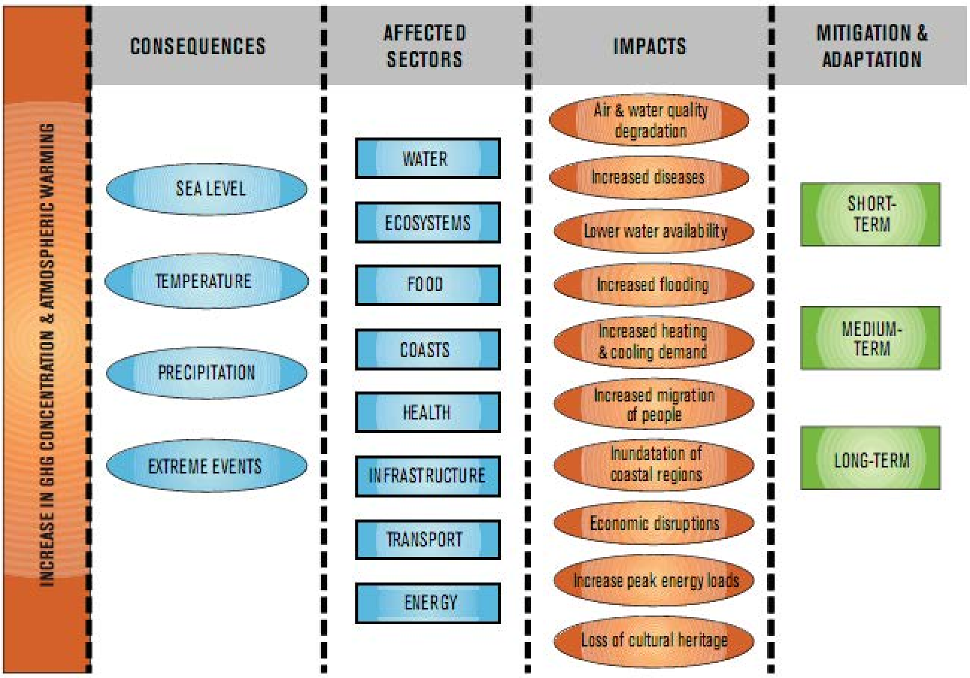

Figure 4: Linking consequences and sectors with potential impacts and climate change mitigation and adaption options

5. THE OUTCOME

According to primer the following outcome has been found for Dhaka city based on the guidelines recommended in the Primer. Figures 5 (a) to 5 (h) show the assessment results for the individual component.

A. City description	
1. City location	
a. In a coastal area? (Y or N)	N
b. On or near mountain area? (Y or N)	N
c. On inland plain? (Y or N)	N
d. On inland plateau? (Y or N)	N
e. Near or on a river(s)? (Y or N)	Y
f. Near earthquake fault lines? (Y or N)	N
B. Size characteristics of city	
1. Resident population (VH, H, M, or L)	H
VH = Greater than 10 million H = 2 million to 10 million M = 0.5 million to 2 million L = up to 0.5 million	
2. Population growth during last 10 years (H, M, or L)	M
H = Greater than 10% M = Between 2% to 10% L = Less than 2%	
3. Floating population (VH, H, M, or L)	H
VH = Greater than 30% of resident population H = Between 20%–30% of resident population M = Between 10%–20% of resident population L = Less than 10% of resident population	
4. Area in square kilometers (km^2)	360
5. Maximum population density (day or night) (H, M, or L)	H
H = Greater than 2,000 persons per km^2 M = Between 1,000 to 2000 persons per km^2 L = Less than 1,000 persons per km^2	

Figure 5(a): Typology and Risk Characterization Matrix: City description and size characteristics

C. Governance structure as related to disaster risk management	
1. Appointed head of government? (Y or N)	N
a. Term of assignment? (Years)	
2. Elected head of government? (Y or N)	Y
a. Term of elected officials? (Years)	5
3. Local government office structure: Does it have…	
a. Disaster risk management department? (Y or N)	N
b. Environment, sustainability or climate change department? (Y or N)	N
c. Are (a) and (b) in the same department? (Y or N)	N
4. Other government office structure (state, national): Does it have…	
a. Disaster risk management department? (Y or N)	Y
b. Environment, sustainability, or climate change department? (Y or N)	Y
c. Are (a) and (b) in the same department? (Y or N)	Y
D. City management on climate change and disaster risk management	
1. Responsibilities clearly specified? (Y or N)	N
2. Responsibility for climate change management established? (Y or N)	N
3. Responsibility for disaster risk management established? (Y or N)	N
4. Authority to contract for services? (Y or N)	N
E. Financial resources	
1. Total budget	Tk.1411.58 Cr
2. From local taxes and levies (% of total)	

Figure 5(b): Typology and Risk Characterization Matrix Governance structure, city management, and financial resources

F. Built environment	
1. Does the city have urban growth Master Plans? (Y or N)	Y
2. Does the city have urban development plans and land-use plans? (Y or N)	Y
a. Population in authorized development? (% of total)	
b. Population in informal colonies? (% of total)	40%
c. Population density of informal colonies? (H, M, or L)	
H = Population of informal colonies >20% of total	
M = Population of informal colonies <20% but >10% of total	
L = Population of informal colonies <10% of total	
d. Population in old tenements and historical development? (% of total or H, M, or L using ratings in 2c)	
3. Does the city have building codes? (Y or N)	Y
a. Level of compliance? (% compliant buildings)	10%
4. Observed vulnerability of buildings in past natural disasters (extent of disruption of building functionality)	
a. Informal buildings (H, M, or L)	H
H = Greater than 15% of informal buildings highly vulnerable	

Figure 5(c): Typology and Risk Characterization Matrix: Built environment

G. Political impact of disasters	
1. Is the city a national/provincial capital or where a large number of decision-makers live? (Y or N)	Y
2. Is impact of disaster in the city likely to influence political activity in areas far away from affected regions? (Y or N)	Y
H. Economic impact of disasters	
1. Is the city a major center of economic activity in regional or national context? (Y or N)	Y
2. Do the following sectors have major activity in the city?	
a. Industrial sector? (Y or N)	N
b. Services sector? (Y or N)	Y
c. Financial sector? (Y or N)	Y
d. Tourism and hospitality sectors? (Y or N)	Y

Figure 5(d): Typology and Risk Characterization Matrix Political and economic impacts

I. Threat of natural hazards	
1. Earthquake? (Y or N)	Y
2. Wind storm? (Y or N)	Y
3. River flood? (Y or N)	Y
4. Flash rainwater flood or extreme precipitation? (Y or N)	Y
5. Tsunami? (Y or N)	N
6. Drought? (Y or N)	N
7. Volcano? (Y or N)	N
8. Landslide? (Y or N)	N
9. Storm surge? (Y or N)	N
10. Extreme temperature? (Y or N)	Y
J. Disaster response system	
1. Does a disaster response system exist in the city? (Y or N)	Y
2. Is the response system comprehensive and equipped for all natural hazards specified? (Y or N)	N
3. Is the disaster response system regularly practiced? (Y or N)	N
4. Is the disaster response system regularly updated? (Y or N)	N

Figure 5(e): Typology and Risk Characterization Matrix Hazards and a disaster response system

K. Climate change impact	
d. Energy generation and distribution system? (Y or N)	Y
e. Health-care facilities? (Y or N)	Y
f. Land use? (Y or N)	Y
g. Transportation system ? (Y or N)	Y
h. Parks and recreation areas? (Y or N)	Y
k. Tourism? (Y or N)	Y
3. Is climate change assessment based on local studies instead of regional/global models? (Y or N)	Y
4. Does the city have a climate change strategy (maybe as a component of national policy)? (Y or N)	N
5. Does the city have climate change programs in place? (Y or N)	N
6. If Yes, do the climate change programs consider:	
a. Mitigation? (Y or N)	Y
b. Adaptation? (Y or N)	Y
c. Resilience? (Y or N)	Y

Figure 5(f): Typology and Risk Characterization Matrix Climate change impacts

Attribute matrix	Climate factor		
	Temperature rise	Precipitation change	Sea-level rise
Rate the level of vulnerability in each of the following areas. H= Very important consequences and priority for action M= Important and should be considered in city development plans L= Unimportant			
Built environment (H, M, or L)	H	H	L
Cultural and religious heritage (H, M, or L)	H	H	L
Local business, industry, and economy (H, M, or L)	H	H	L
Energy generation and distribution system (H, M, or L)	H	H	L
Health-care facilities (H, M, or L)	H	H	L
Land use (H, M, or L)	H	H	L
Transportation system (H, M, or L)	H	H	L
Parks and recreation areas (H, M, or L)	M	M	L
Social equity system (H, M, or L)	H	H	L
Water management (H, M, or L)	H	H	L
Tourism (H, M, or L)	H	H	L

Figure 5 (g): Vulnerability assessment for different consequences of climate change in urban areas

Attribute matrix	Disaster preparedness and response			
	Industrial sector	Service sector	Financial sector	Tourism and hospitality sector
Define the level of preparedness for each event for each sector. H = High level of preparedness and readiness to respond to disaster and hazard; M = Somewhat high level and the basic/key informants are present (i.e., a basic disaster management system is in place, but may not be comprehensive or consider specific hazards); L = Low (i.e., no disaster management system, no warning system, etc.)				
1. Earthquake (H, M, or L)	L	L	L	L
2. Wind storm (H, M, or L)	L	L	L	L
3. River flood (H, M, or L)	M	M	M	M
4. Flash rainwater flood or extreme precipitation (H, M, or L)	L	L	L	L
5. Tsunami (H, M, or L)	L	L	L	L
6. Drought (H, M, or L)	L	L	L	L
7. Volcano (H, M, or L)	L	L	L	L
8. Landslide (H, M, or L)	L	L	L	L
9. Storm surge (H, M, or L)	L	L	L	L
10. Extreme temperature (H, M, or L)	L	L	L	L

Figure 5 (h): Preparedness and response to different natural hazards in urban sectors

From the above data, it can be said that the vulnerability level of Dhaka city is **Medium** to **High** and preparedness and response level to different natural hazards is **Low**. So Dhaka can be termed as a “Hot Spot”.

7. RECOMMENDATION

To remove Dhaka from “Hot Spot” classification, following measures can be cosidered immediately:

a. City planning must incorporate climate issues
b. Decentralization and pro-poor development
c. Institutional integration at national, city government, inter agency and local levels
d. Promote adaptation by building resilience in human, social and natural systems with greater capacity, awareness and local action in the current and future climate contexts
e. Adaptation strategies are to be integrated into DRR, urban planning, poverty alleviation
f. Poor need greater resilience with new knowledge, engagement in adaptation action, resources and technology supports
g. Promotion of Adaptation and mitigation together (energy efficiency, solar energy and conservation of energy, water, social forestry on city embankments etc).

8. CONCLUSION

The Primer initiates a learning process for local governments. It looks at the issues of climate change, the potential consequences of climate change that can affect cities and the critical relationship between current urban development and local government financial trends with climate change, disaster risk management and sustainable development. The primer recommends a thorough city self assessment and a comprehensive information base as starting points. It provides sound practices, case studies and resources that a city can use as follow up to building its programmes for resilience.

Dhaka city is experiencing urbanization at an unexpected rate. The growth is far beyond the capacity of city governments to provide infrastructure and basic civic amenities. As a result, Dhaka city is becoming more vulnerable to the impacts of natural hazards including those due to potential impacts of climate change. The degree of impact from which the city has been suffering from climate change will depend on the actions and initiatives local governments take to build a resilient city. City officials need to understand the urban characteristics that make the city susceptible to disaster risk and climate change, such as determining if the city is a Hot Spot. The city needs to establish and manage a consolidated information base that can play a huge part in devising the most appropriate urban management strategies.

REFERENCES

Alam and Rabbani (2007). Vulnerabilities and responses to climate change for Dhaka, *Environment and Urbanization.* Vol. 19: 81-97.

Cities Alliance (2007). *Guide to City Development Strategies: Improving Urban Performance*, City Alliance, Washington DC.

Pelling, M. (2006). International Data on Disaster Risks, World Disaster Report, IFRC, Geneva.

Rahman, A. and DL Mallick (2006). *Climate Change Impacts on Cities of Developing Countries: A Case Study on Dhaka*.

Schipper, L., and M. Pelling (2006). Disaster Risk, Climate Change and International Development: Scope and Challenges to Integration, *Disasters* Vol. 30 (1): 19-38.

Van Aalst, M.K. (2006). The Impacts of Climate Change on the Risk of Natural Disasters, *Disasters,* Vol. 30(1): 5-18.

World Bank (2007). *East Asia Environmental Monitor: Adapting to Climate Change*, World Bank, Washington DC.

World Bank (2008). *Climate Resilient Cities: A Primer on Reducing Vulnerabilities to Disasters,* published by the World Bank, Washington, DC.

PROPOSAL FOR REVIEWING AND REVISION PROCESS OF DISASTER MANAGEMENT PLAN IN BANGLADESH -2007 CYCLONE SIDR AS A CASE STUDY-

[1]TAIKI KOU and [2]KIMIRO MEGURO

[1] Graduate Student, Department of Civil Engineering
The University of Tokyo, Japan
kou@risk-mg.iis.u-tokyo.ac.jp
[2] Director/Professor, International Center for Urban Safety Engineering
Institute of Industrial Science, The University of Tokyo, Japan

ABSTRACT

Natural disasters have been causing huge economic and human losses every year in Bangladesh. Well prepared disaster management plan is an essential element to mitigate damage and to implement disaster response operations successfully. Through the experience of several devastating flood and cyclone damages between 1980s and 90s, total disaster management plan was published and has contributed to decrease the damage. However, after 10 years of its implementation, several controversial points have been noted these days.

In this paper, the authors discuss future agenda of disaster management plan and actual situation in Bangladesh. Firstly, present situations of disaster management plan called "Standing Orders on Disaster (SOD)" and actual operations are discussed. The 2007 Cyclone Sidr is taken as a case study for actual situation analysis. Information on actual operations was collected by the authors and researchers in Bangladesh University of Engineering and Technology (BUET) through field surveys and briefing papers prepared at that time. Agendas such as absence of disaster management operations' total picture, description amount gap among actors, and obscurity of feasibilities are pointed out about the current disaster management plan. In addition, agendas such as not fully achieved situations due to the human/physical limitation, concentration of operation and scarcity of disaster management operation records are pointed out about the current disaster operations. Secondly, based on these agendas, an actually suited disaster management plan model and a precise disaster management reviewing model are discussed. To implement disaster management operations exhaustively at disaster response stage and to make clarify what can or cannot be done at disaster reviewing process, breakdown structure of disaster management plan is proposed. To evaluate each operation appropriately and to revise disaster management plan for more actually suited disaster management plan, disaster response operation information database is proposed. Finally, possible usages of these models are discussed. The authors believe these proposals will contribute to enhancing disaster management plan and increasing efficiency of disaster management operations.

1. INTRODUCTION

1.1 Background

Standing Orders on Disaster (SOD), which is equivalent to the basic plan to implement disaster management operations in Bangladesh, was published in 1997. The principal thinking behind the formulation resulted from the experiences of devastating flood and cyclone damages during the 1980s and 1990s. Before formulating SOD, each disaster management plan (such as flood or cyclone) rarely had uniformity in the plan. To improve such situation, total disaster management plan; SOD was formulated, which was adoptable even though the types of disasters are different. The Orders comprehensively describe total disaster management plan for each of the 38 actors, which are related to disaster management operations by each stage such as “Normal Times”, ”Alert Stage”, ”Warning Stage”, “Disaster Stage” and “Rehabilitation Stage”.

However, as it has passed more than 10 years since the Orders were put into effect, several controversial points have been noted,

- No description of total picture of disaster management operations
- Obscurity of coordination and linkage of operations / information with other agencies
- Planned operations are only listed, and a time axis is not considered.
- Not updated since the publication in 1997

These arguments increase the momentum towards upgrading the Orders into further practical steps these days.

1.2 Purpose of the study

Taking these controversial points into consideration, in this study, we aim to figure out future agenda of disaster management plan and actual situation. Next, we aim to propose appropriate countermeasures against these agendas and set proposal for upgrading disaster management plan.

Firstly, we have analyzed present situation of disaster management plan and actual situation in Bangladesh. Also, we have analyzed SOD and compared it to actual operations during and just after the 2007 Cyclone Sidr. Through the analysis of disaster management plan and actual disaster management operations, we have extracted several future agendas for each plan and actual situation.

Secondly, we have discussed an actually suited disaster management plan model and a precise disaster management reviewing model from a view point of efficient implementation of operations, sufficient accumulation of disaster management operation records at disaster stage and comprehensive reviewing of disaster management operations.

2. ANALYSIS OF PRESENT SITUATION

2.1 Methodology

2.1.1 Operation category analysis

Operation category analysis makes it possible to look overview of own disaster management operations in the total picture of disaster management, and this analysis makes it easier to point out insufficient descriptions in the SOD. These processes help the SOD to be more collectively exhaustive. In addition, this analysis makes it possible to figure out other actors implementing cognate disaster management operations.

As it is pointed out in the previous chapter as a controversial point, it is quite difficult whether the descriptions of disaster management operations in the SOD exhaustively provide necessary operations (***Figure 1*** left) since the absence of disaster management operation's total picture in the SOD, which is raised as a controversial point of SOD.

To check up this point, general category which can define total picture of disaster management operations universally is needed, which has empirically reviewed and revised to describe for actual suited disaster management plan. As one competent category which possibly defines general disaster management operations, we adopted category of Japanese Basic Disaster Prevention Plan as a reference, which has reviewed and revised along with Japanese disaster experiences for about half a century. (***Figure 1*** *right*) For operation category analysis, attribution data which are the components of category are tagged each description in the SOD (***Figure 2*** *left*). And choosing actors and operation category as two axes, each description in the SOD is plotted on the operation category field (***Figure 2*** *right*).

2.1.2 Three dimensional analysis

To visualize amount of disaster management operation descriptions in the SOD for each phase, we conducted three dimensional analysis.

In order to express and analyze disaster management operations described in the SOD along with more precise time line, we introduced relative time axis, which divided three stages into seven phases, which is from disaster foreseeing phase to assistance beginning phase (***Figure 3***).
To visualize the amount of disaster management operation descriptions for each phase, we added attribution data of relative time axis into each description in the SOD (***Figure 4*** *left*). Choosing actors, time axis and amounts of operations' description, each actor's amounts of operations relative to time is visualized (***Figure 4*** *right*).

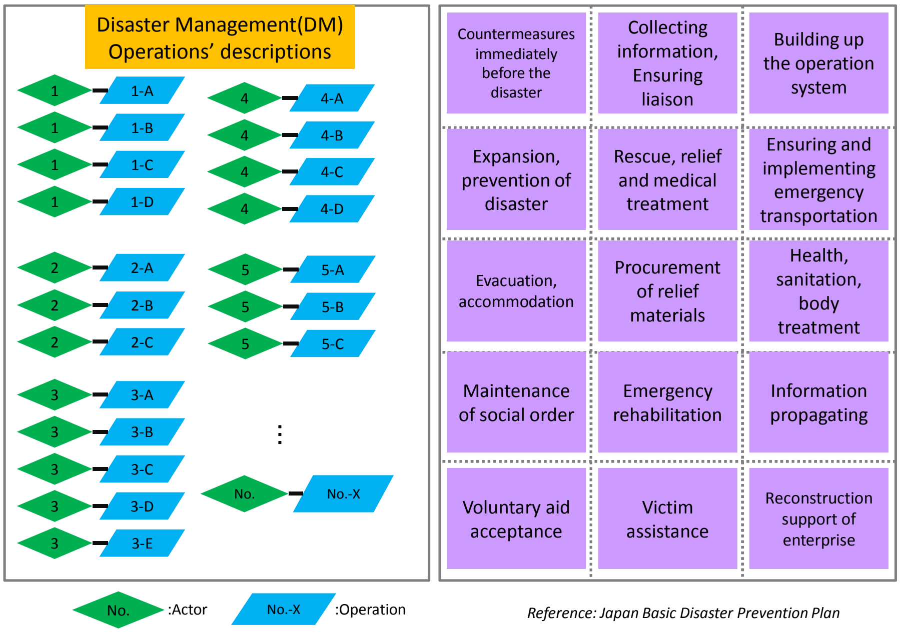

Figure 1: Overview of operation category analysis (1)

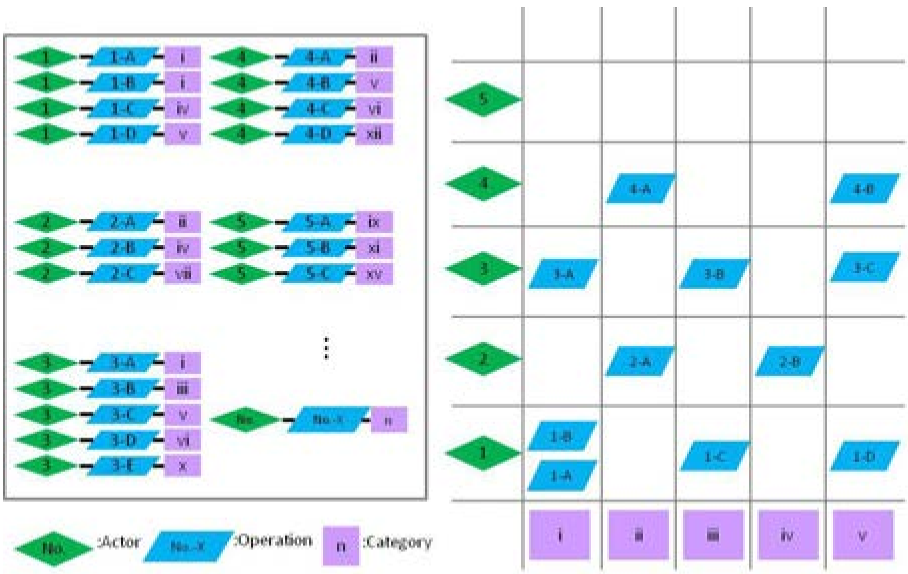

Figure 2: Overview of operation category analysis (2)

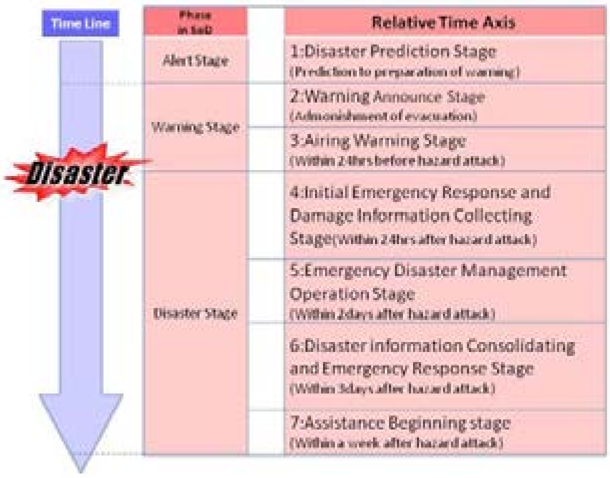

Figure 3: Overview of three dimensional analysis (1)

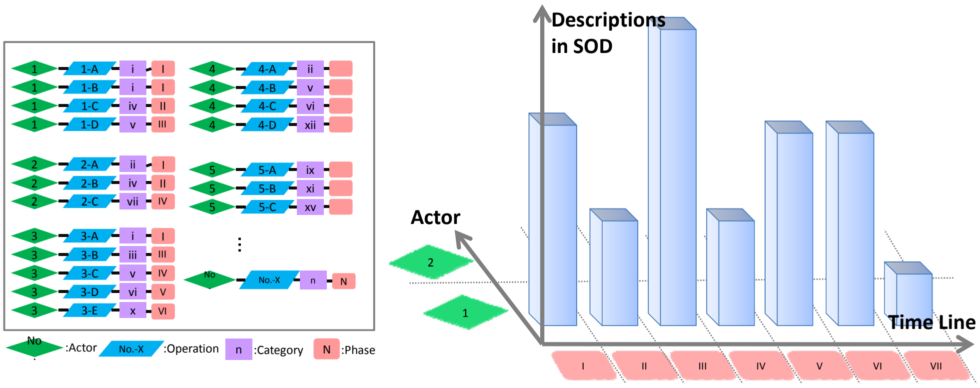

Figure 4: Overview of three dimensional analysis (2)

2.2 Analysis of present SOD

Using the operation category analysis, we analyze description amount gap among actors or components of the category in the SOD or operation feasibilities toward descriptions in the SOD (***Figure 5***).

From ***Figure 5***, it can be seen that, some plans of disaster management operations were fully described to implement comprehensive disaster management operations, such as Ministry of Home Affairs (MoHA), Ministry of Shipping (MoS), Ministry of Health and Family Welfare (MoH&FW), Ministry of Local Government (MoLG). During disaster stage, every actor faces the scarcity of both the artificial and the physical. It is quite important for each actor to describe not only disaster management operations related to its usual operations but also, disaster particular operations such as rescue, relief operations excepting the particular operations which require some authorities or abilities, such as the distribution of relief aid, rehabilitation of the infrastructure system or medical relief as a description of SOD.

However, the problem is that "Is it possible or not to implement the whole operations illustrated in the SOD during the disaster stage which faces the crucial scarcity"

If not, the SOD would be an all-round less effective plan. At the stage of comparison with actual disaster management operations, the SOD have to be checked against whether the SOD was formulated with taking consideration of that point.

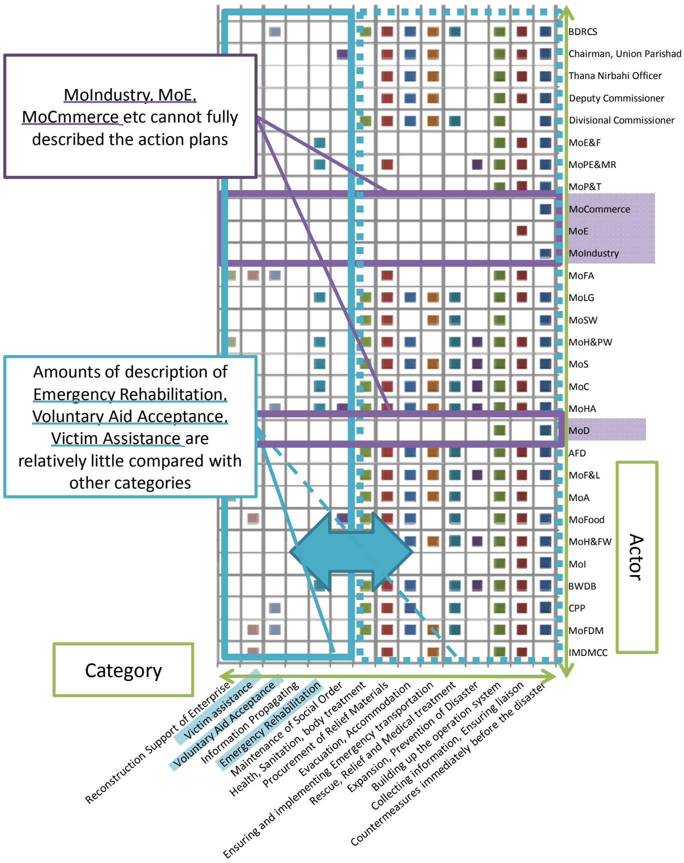

Figure 5: Clarification of disaster management operation field of each actor based on operation category analysis

2.3 Analysis of actual disaster management situation -2007 Cyclone Sidr as a case example-

2.3.1 Follow-up period

This study sets from 13th to 22nd November as a follow-up period of disaster management operations led by the government and public administration of Bangladesh for the following reasons:

Situation Report about Cyclone Sidr had been published on 13th November (15:30, 13th Nov, '07). After 22nd November, international coordination relief operations called "Cluster Approach" which both described actors and not described actors in SOD committed had started. This was triggered by the Disaster Emergency Response (DER) Meeting which government, donor, international organization and NGO participated in.

2.3.2 Limited information of disaster management operation

Before starting the analysis, there are some controversial points about disaster management operation records; partial and limited records of disaster management, no detailed description of time and date, amount of time required or head-count required. These ambiguous points were confirmed as possible by the field surveys conducted by the authors and BUET research members. The results of field surveys were reflected to this analysis as much as possible along with the operations defined in SOD.

However, to set an efficient feedback and update system of disaster management operation in place, it will be also required to amend how to record the disaster management data in the future.

2.3.3 Comparison of actual operations and planned operations by using operation category analysis

Figure 6 shows a comparison result of actual and planned operations by using operation category analysis (Left: planned, Right: actual). From the result of analysis and field survey, the following points can be indicated:

1) Disaster management operations were not or could not be implemented, nor was there a mechanism of information transmittance to the upper organization even though the operations were done
2) Disaster management operations were mainly done within normal time's operation fields of each organization
3) Only limited organizations were able to implement measures in the operation field while several organizations were supposed to implement the operation.

From the insight of field survey, the reason for point 1) and 2) could be divided into two aspects. One was a human resource problem, involving insufficient numbers of public officers or officer's affliction. The other was physical problem: insufficient number of motor boats to distribute the relief materials or shortage of budget to keep up a distribution operations.

Related to 2), it could be indicated that there was no room to enlarge the operation field to disaster-particular operation fields, such as rescue or relief operations for the problem of the scarcity of human or physical resource problem.

About 3), in 2007 Cyclone Sidr case, Armed Force Division (AFD) played a leading role of operations in the field just after the cyclone. Especially, long-range transportation of relief materials was almost totally implemented only by AFD.

Besides, the blank areas of the right figure, which means that planned operations were not done, were substituted by internal/international aid agencies, NGOs or NPOs.' relief operations. These situations could be realized by analyzing not only records but also field surveys.

2.3.4 Comparative analysis of planned and actual disaster management by three dimensional analysis

Figure 7 is a result of comparison of actual and planned operations (Left: planned, Right: actual). From the result of the analysis, not fully achieved situation of disaster management operations can be seen as same as the result of operation category analysis. In addition to that point, from this analysis, situation such that a small portion of central organizations were forced to implement more operations than the Order provisioned is observed. Such situation was can be seen at the central disaster management organizations such as Ministry of Food and Disaster Management (MoFDM) or Disaster Management Bureau (DMB). The reasons for the excess amount of operations, which were confirmed by the field survey, were the concentration of operations such as coordination operations with several donors and UN agencies or operation works at field emergency operation center (at Barisal).

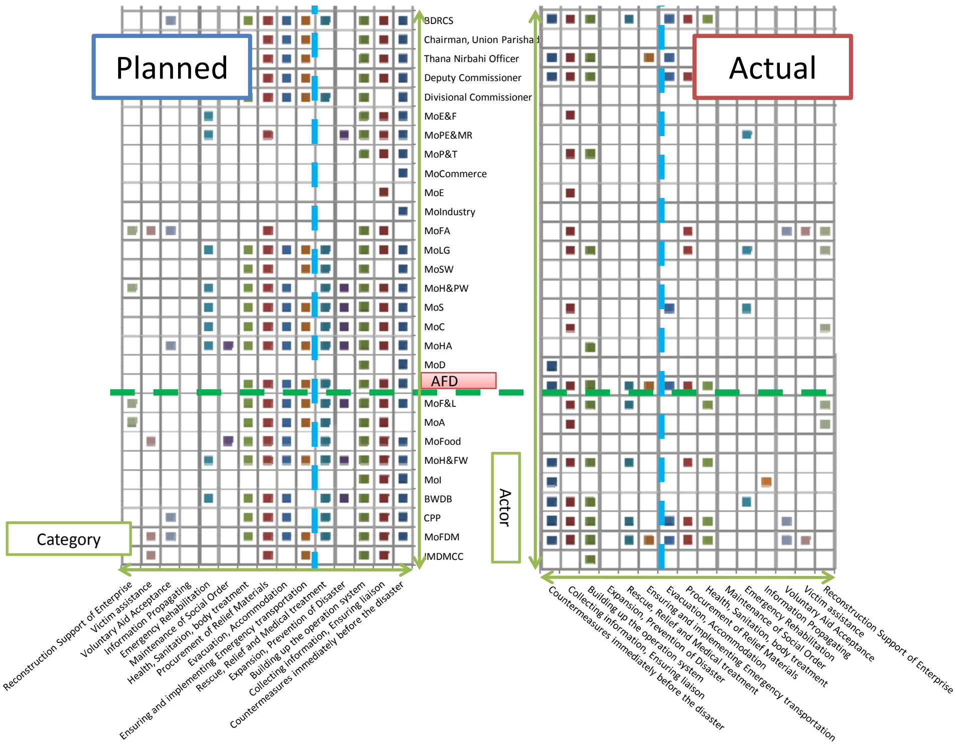

Figure 6: Reviewing process of disaster management operations by using operation category analysis

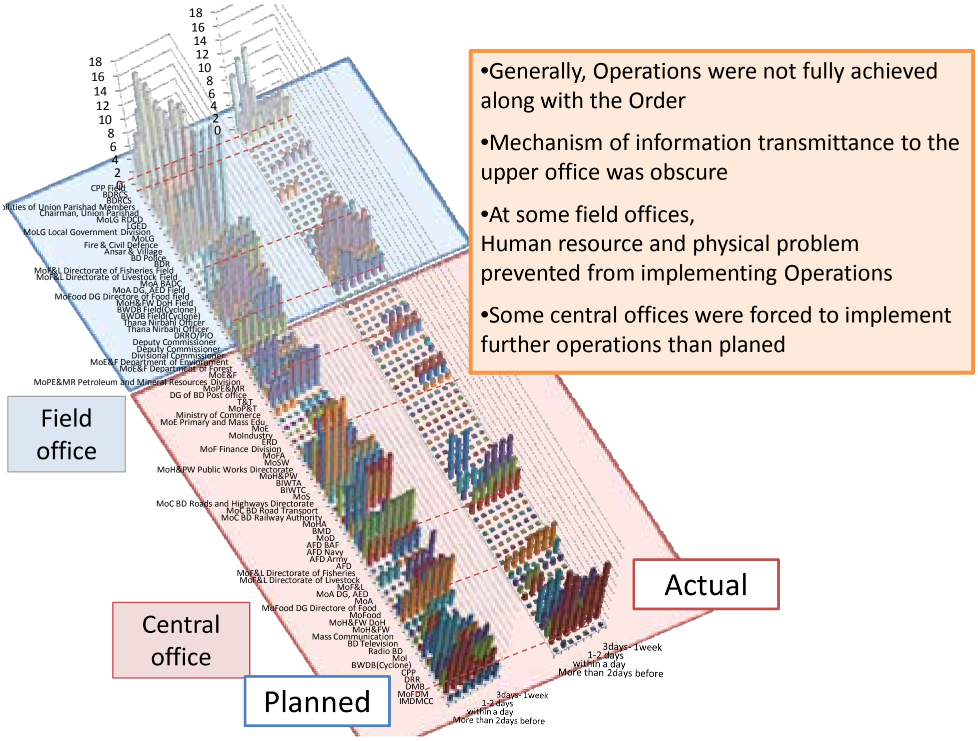

Figure 7: Comparative analysis of planned and actual disaster management by three dimensional analysis

As pointed out above, insufficient information transmittance mechanism to the upper organization can be observed through the above analyses. We would like to point out the reason for this insufficiency from two elements, damage information transmittance structure and damage fill-in form in Bangladesh, Form-D.

As an ideal situation, damage information transmittance to the central office would be done by two ways (***Figure 8*** *left*); one is Disaster Management Council route which is the main route of information transmittance by using Form-D, and the other is ministry route which supplement detail attribution information (such as where, who, when the damage information was gathered) which cannot be contained in Form-D.

However, at the actual situation in 2007 Cyclone Sidr, damage information gathering were done almost only by the main route; "Form-D route". And the function of supplement information transmittance route could not be observed through the field survey. Therefore, as referred in **Figure 8**, at the central control room level and even at the District DMC level, it was quite difficult to trace which actor did disaster damage survey and where at the field level. Such situations caused information transmittance obscurity and made it difficult to make decisions of relief operations contingent at the disaster management council.

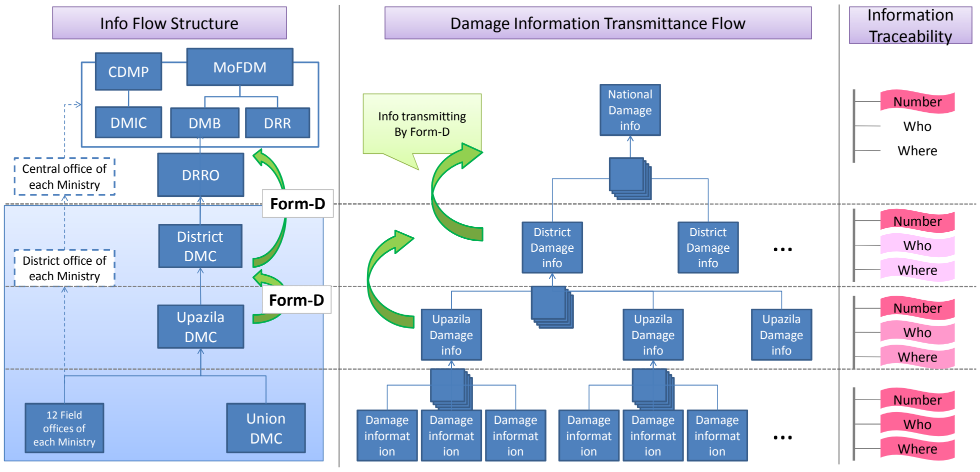

Figure 8: Information transmittance structure and information traceability

2.3.5 Future agenda of disaster management operations

Comparison of planned and actual operations by using category analysis and three dimensional analysis enables us to review and evaluate total picture of disaster management in Bangladesh, which had not been done sufficiently before.

At the present stage, as we have discussed above, such disaster management operations described in the SOD could not be fully achieved, it is necessary to set priorities on actual disaster management operations under the human, physical resource and time limitation.

In concrete terms, conducting the following validations enables us to review actual situation and renew the SOD into more actual suited orders:

- Figuring out whether each actor could conduct the disaster management operations along with the SOD or not, through looking around the whole situation of disaster management
- About the blank areas which can be seen in right side of ***Figure 6***, confirming the capacity of implementing disaster management operations of each actor planned in the Order
- If there is sufficient capacity, clarifying and ensuring the implementation framework of the SOD for upcoming disaster. If not, confirming which actor could substitute the operations, and re-allocating the operations
- Considering which is adoptable and efficient for the actual situation, coming to terms with the concentrated situation or seeking alternative solutions (Ex: concentration on AFD to transform the relief materials)

3. PROPOSAL FOR ACTUAL SUITED PLAN MODEL AND REVIWING MODEL

3.1 Discussion for present agenda for reviewing and revising disaster management plan

Based on disaster management operation records and data of field survey, we can look into the overview of disaster management operation and point out some action agendas for disaster management operations through the analyses toward 2007 Cyclone Sidr's situation. However, the quantity and quality of each disaster management operations or disaster management information have not been discussed yet because of the scarcity of disaster management records which can support to analyze from these points of view.

To objectively figure out the entirety of the disaster management situation, the more precise and structured record of disaster management operations and reviewing system has to be proposed. At the same time, for practical use of the disaster management plan at the disaster stage, also precise and easily understandable disaster management plan is required.

From these aspects, we would like to propose some solution countermeasures toward reviewing and revising process of disaster management plan.

3.2 Solution countermeasures

3.2.1 Breakdown structure of disaster management plan

For implementing efficient disaster management operation, disaster management plan should be not abstract but more concrete one. For this, it is quite necessary to establish more precisely broken down structure disaster management plan which helps both emergency operation center (EOC) and field officer to get into action.

Setting Operation category as a highest (most abstract) level, disaster management operations are broken down gradually into from large, medium to small operations, whose levels are similar to actions at field level (***Figure 9***). And the present descriptions' level in the SOD are not unified (some descriptions' level is equivalent to large operation and others' level is equivalent to medium operation). Establishment of unified and structured disaster management plan is one of future agenda of present SOD. Further, for sufficient disaster management record accumulation, disaster management operation records at disaster stage should be noted along with that breakdown structure with some attribution data which can record the quantity, quality or information flow of disaster management collectively (***Figure 10***).

For the record accumulation, disaster management operation information database should be established, in which several attribution data closely related to disaster management operations. Although they are contained such as time information data: start/end time of the operation; organization data: person who committed the operation, resources which are used for the operation; information flow: from whom information which make it possible to implement the operation were given, what information were generated through implementing the operation, and to whom the generated information were transmitted; quantity information (operation amount information): man-hour data, related operations data.

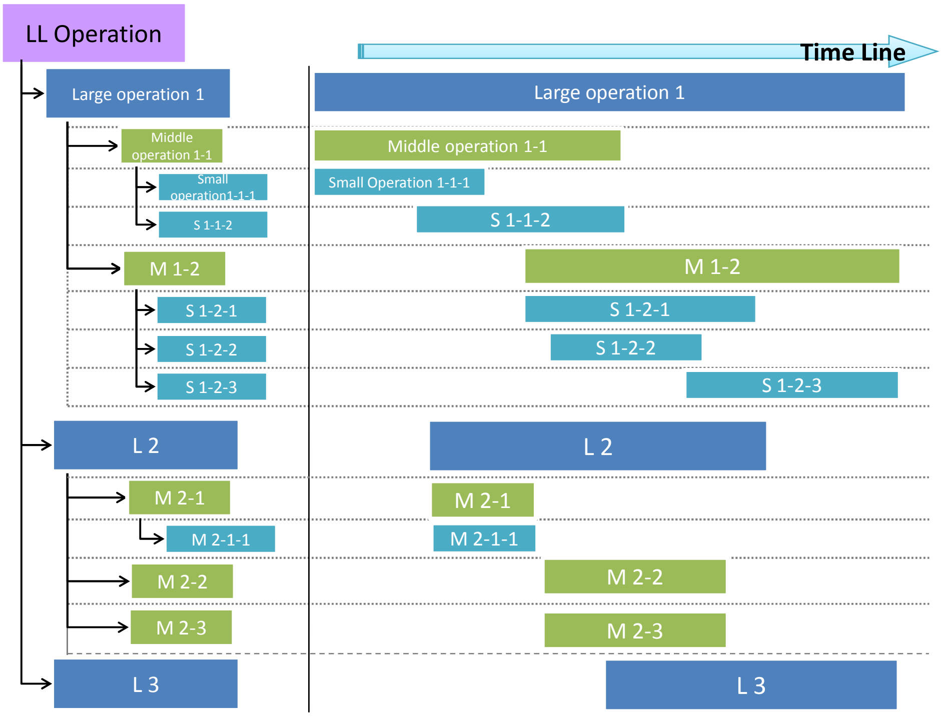

Figure 9: Breakdown structure of disaster management plan

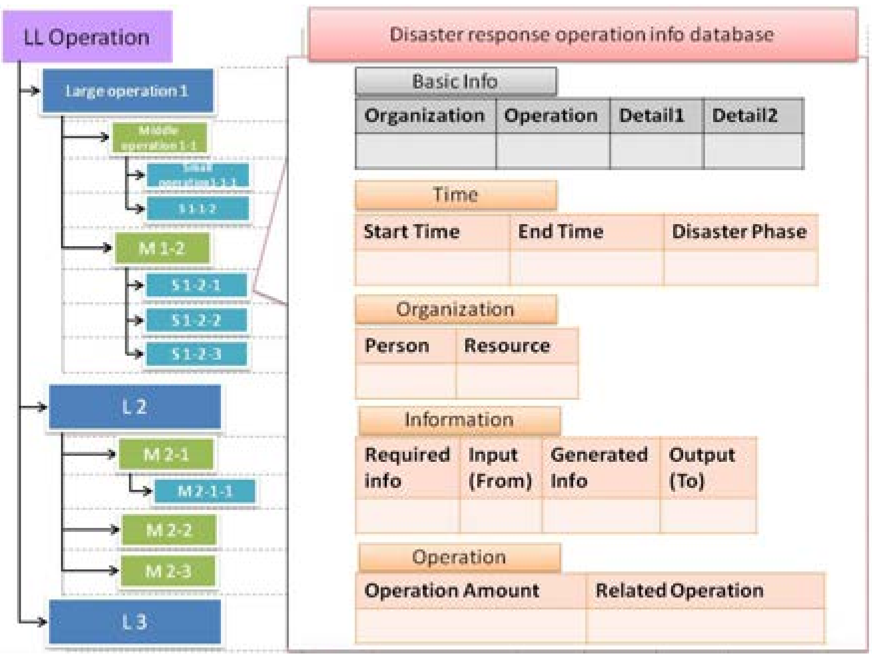

Figure 10: Disaster response operation information database

3.2.2 Organizational / inter-organizational information

Thus far, we have discussed the contents of operations implemented by each actor. However, it is quite necessary to clarify own organizational or inter-organizational information to effectively implement disaster management operations or to coordinate relief operations among actors.

According to Yamamoto (1981), organization can be expressed as a formation of four structures (***Figure 11***); resource structure, decision making structure, implementing structure and value evaluation structure. Especially focusing on disaster stage, efficiency of the organization is defined by the decision making structure and implementing structure. Further, these structures are regulated by the resource structure.

Resource structure can be expressed by the "Flow Stock". "Flow Stock" is expressed by human resource, which is mainly typified by its Organograms (person / Position / Decision making authority descriptions) and physical resource amount which is typified by its equipment and material retention list. This "Flow Stock" can make clear the organization's resources, which can be applied for disaster management operation.

Decision making structure and implementing structure can be expressed by diagram. The diagram can be divided into two elements; information flow diagram and operation flow diagram. Operation flow diagram makes clear the disaster operation flow, i.e. from whom the operation is taken over to whom the operation takes over, what operations will be triggered by the finish of the operation and with whom the operation has to be implemented. Information flow diagram makes clear the damage information flow or operation assignment flow; from whom the information should be acquired to implement own operation, what kind of information will be generated in own organization by implementing this operation, and to whom this generated information should be transmitted.

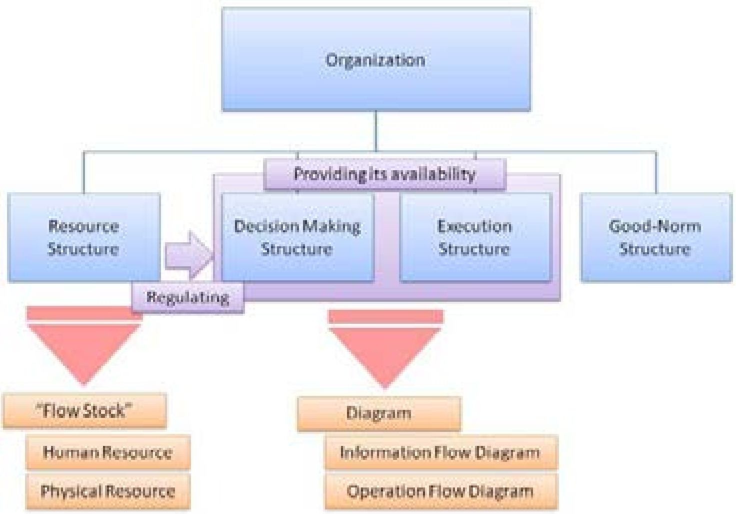

Figure 11: Organization Structure

Based on the above solution measures, following discussion would be possible about disaster management operation reviewing for updating the disaster management plan.

- Setting appropriate Countermeasures Toward Unfulfilled Operations

As illustrated above at the present situation, we have not had a discussion foundation of disaster management quality. Using the breakdown structure disaster management plan for reviewing process, extracting descriptions of operations and those details from disaster response operation information database, we would be able to discuss each operation's quality more precisely. In other words, we would be able to look into every element, which compose disaster management operation exhaustively and the critical reason that prevented from implementing the disaster management (***Figure 12***). This process would be informative to avoid searching abstract reasons and setting only abstract "all-round less effective" countermeasures for the unfulfilled operations.

- Argument of Operation Quantity and Quantity Equalization

By extracting "man-hour data" from disaster response operation information database, we would be able to discuss operation quantity of each operation and each actor objectively and quantitatively. Based on this operation quantity analysis, excess burden of operation or room for implementing operation would be discussed.

If the "man-hour data" of disaster response operation information database would be recorded in unified format, it would be able to discuss inter-organizational disaster quantities gap. For the actor whose operation quantity excesses own disaster management capacity, it would be able to discuss operation quantity equalization countermeasures, i.e. operation quantity share among disaster management actors toward to handle quantity imbalances (***Figure 13***).

- Clarifying Actual Operation / Information Flow

By extracting "start/end time of the operation" from disaster response operation information database, we would be able to visualize each disaster management operation in time axis as ***Figure 9*** shown in. On this foundation, we would be able to review disaster management by using Gantt chart. Further, sorting these operations along with time line, we would be able to acquire actual disaster management operation flow within the actor. Summing up each operation flow, we could get inter-organizational disaster management operation flow.

As illustrated in

Figure 15 *upper,* we could trace information which should be required, generated and transmitted along with operations' moving ahead.

Summing up such information in time line, we also could get information flow.

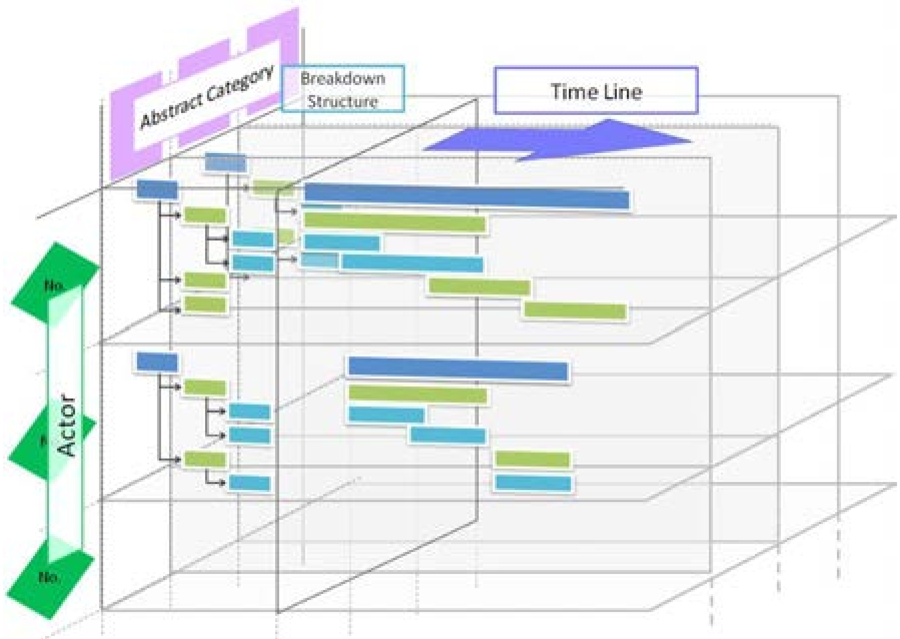

Figure 12: Concept of operation quality argument

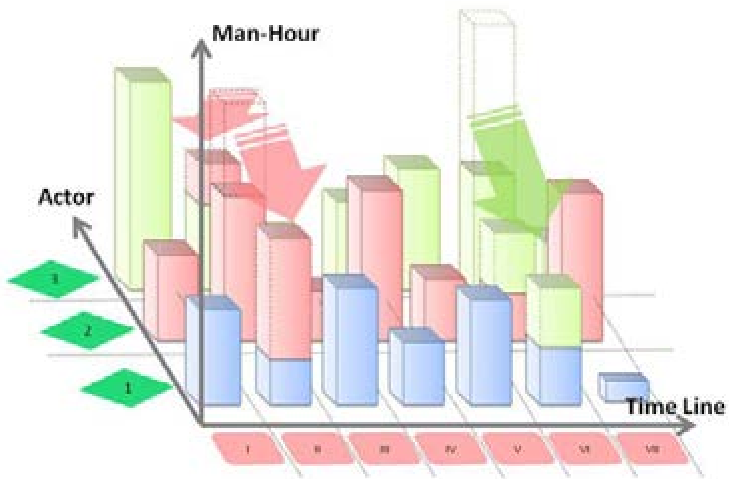

Figure 13: Operation quantity share argument

- Critical Path Clarification and Necessary Information Extracting for Efficient Disaster Management Operation

Based on the Gantt chart and actual operation flow, we could draw up PERT operation diagram, i.e. operation flow diagram in which each bottleneck for implementing operations is clarified (***Figure 14***). This diagram clarifies operations on the critical path, which has a possibility to delay whole disaster management operations. This analysis would help each actor to set countermeasures for these operations on the critical path in advance and contribute to improving the precision of planned operation flow.

Based on the information flow, by re-assembling disaster management operations from information flow, we could extract necessary information to implement disaster management operations along with passage of time. In other words, who would like to use this information at which phase of disaster stage would be figured out (

Figure 15 *lower*).This necessary information would be a benchmark for the operations.

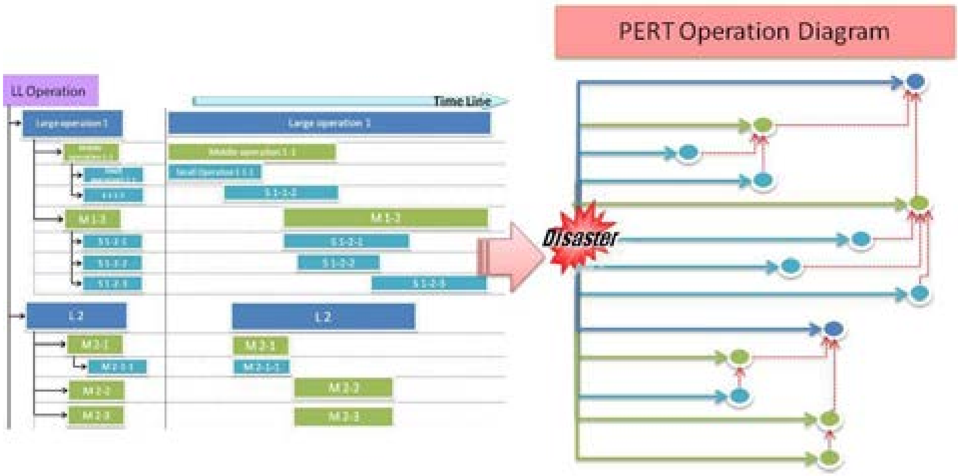

Figure 14: PERT operation diagram

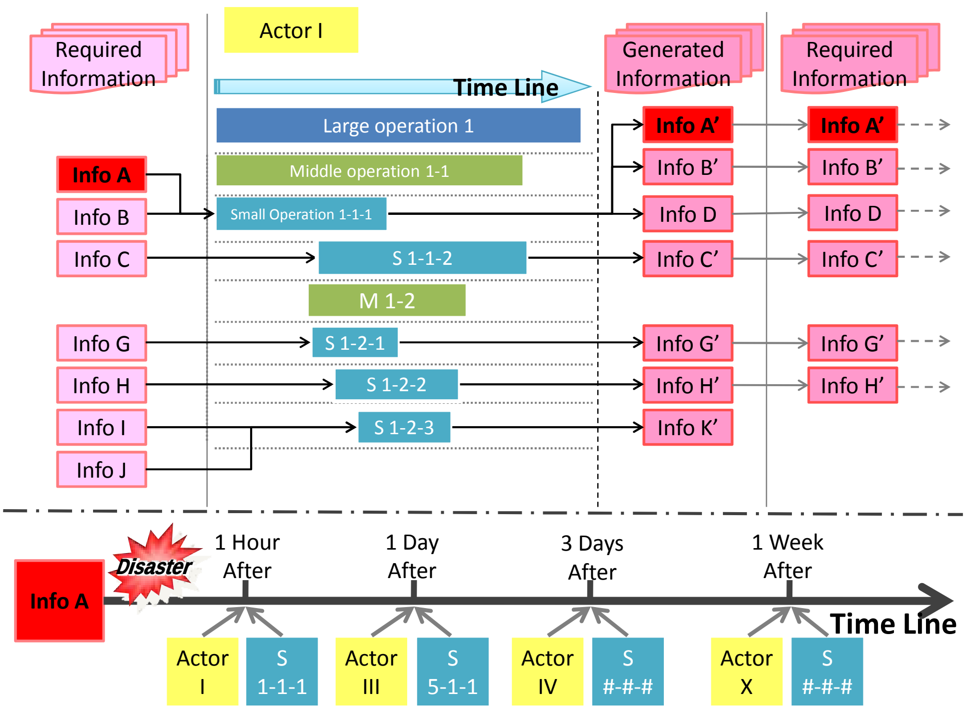

Figure 15: Extracting necessary information with passage of time for implementation of disaster management operation

4. CONCLUSIONS

We have looked into future agenda of disaster management plan and actual disaster management operations' situation. And we have proposed appropriate countermeasures against these agendas and set proposal for updating disaster management plan.

Firstly, about present disaster management operations' situation, it is necessary to set priorities on actual disaster management operations under the human, physical resource and time limitation. And it is also necessary to consider the efficiency validation of operation's concentrations.

Secondly, for efficient disaster management operation implementing, it is quite necessary to establish more precise and easily understandable disaster management plan. For such a plan, setting structurally broken down disaster management plan is required. And for efficient disaster management reviewing, foundation for disaster management operation records accumulation should be also established. It is hoped that if these proposals would be put into effect, disaster management plan and reviewing process of actual disaster management operation would be much more enhanced.

ACKNOWLEDGEMENT

The authors would like to express their sincere gratitude for all the support by Prof. Mehedi Ahmed Ansary and Researcher Afifa Imtiaz, Urban Safety Engineering Department, BUET for conducting the field surveys.

REFERENCES

Shinya KONDO, 2002. *Proposal of Supporting System to Prepare Disaster Manual for Improvement of Proper Disaster Countermeasures,* 20-53.

Yoshiki HIRUMA, Kimiro MEGURO, 2009. Study on Crisis Management of Organization and Disaster Information Management, *Building up Methodology of Disaster Management Operation,* 1-36.

Mehedi Ahmed Ansary, Rubel Das, Afifa Imtlaz, 2008. *Role of Logistics during Cyclone SIDR*, BNUS, BUET, USMCA 2008, 249-254.

Yasumasa YAMAMOTO, 1981. Social Scientific Approach for Disaster. *Disaster and Organization.* Hirotada Hirose, Japan.

World Bank, 2008. *Cyclone Sidr in Bangladesh,* World Bank Report, April, 2008.

Government of the People's Republic of Bangladesh, 1999. *Standing Orders on Disaster.* Ministry of Food and Disaster Management, Bangladesh.

DEVELOPMENT OF THE DISASTER INSTANCE MAP INCLUDING HISTORCIAL DISASTER INSTANCES DAMAGED BY NATUAL DISASTERS

SEONHWA, CHOI
National Institute Disaster Prevention, Republic of Korea
shchoi333@nema.go.kr

ABSTRACT

Numerous historical records about damage caused by diverse natural disasters and recoveries from those reinforce us to grow conscious of our safety and a sense of national disaster management. Although a service providing information on historical disaster instances in a country is an essential system among various information systems, there are no systems providing information on historical disaster instances from the time existing annals to the present in Korea. We present here a new system called "DiMap", which provides the information on historical disaster instances due to natural disasters since the era of the Three States and visualizes that on a map considering a location at which a disaster instance occurred for high usability and high comprehensive faculty by intuition. Through DiMap, we would like to provide not only the changes of disasters happening in a specific region by time-series but also damage information, the counter-plan of damage, the implication learned through a disaster, and documents about a disaster instance. In the future, enhancing the contents and user interface of DiMap by degrees, we will provide various information of a disaster totally.

1. INTRODUCTION

Numerous historical records about damage caused by diverse natural disasters and recoveries from those reinforce us to grow conscious of our safety and a sense of national disaster management and are put knowledge for preventing and preparing disasters to practical use as well by a person in charge of disaster management.

Although a service providing information on historical disaster instances in a country is an essential system among various information systems, there are no systems providing information on historical disaster instances from the era of the Three States to the present in Korea. In 2008, the database of the main disaster instances which are built by National Emergency Management Agency provide several disaster information such as a damage, a cause of a damage and photographs related to major disasters to a person in charge of disaster management. However, an amount of information provided by this system is too small and not various, and also user interface of this was not designed by a user-friendly method.

We present here a new system called “DiMap”, which provides the information on historical disaster instances due to natural disasters since the era of the Three States and visualizes that on a map considering a location at which a disaster instance occurred for high usability and high comprehensive faculty by intuition. By recycling the disaster instance database constructed previously, by integrating scattered data stored in a personal computer of a person in charge of disaster management, by collecting documents related to disasters such as a research report, a report of on-the-sport investigation, the disaster instance database of DiMap was made.

Through DiMap, we would like to provide not only the changes of disasters happening in a specific region by time-series but also damage information, the counter-plan of damage, the implication learned through a disaster, and documents about a disaster instance.

In the future, enhancing the contents and user interface of DiMap by degrees, we will provide the information on various types of disaster and as well disaster information enlarged by integrating and connecting with related disaster information systems. Also we will apply the technology of Semantic Discovery to DiMap, so that a user will be provided the user-specific data.

2. DEVELOPMENT OF DISASTER INSTANCE MAP

For successful development of DiMap, first of all, we made a prototype of DiMap as following steps:

a. Sampling data from documents on reporting disasters
b. Define an initial data structure and functions
c. Build a prototype of DiMap
d. Collect and analyze needs of user, feed back to c

By reflecting needs of user repeatedly, a prototype of DiMap was modified

2.1 A target user and contents of DiMap

2.1.1 *A target user of DiMap*

DiMap will provide information for a person in charge of disaster management, a researcher on disaster, and the public by degrees. At first, a person in charge of disaster management will be serviced, and a service for a researcher on disaster, and the public will be operated by way of showing an example.

2.1.2 *Contents of DiMap*

Contents of DiMap should be inclusive of data from the ancient Korea to the present. Since the composition of disaster records of the ancient Korea and those at present about disasters are too different to extract a common item, we defined contents separately. Table 1 shows the contents which DiMap services

Table 1: The contents of DiMap.

Times	**Contents**
Three States Goryeo Joseon	▪ the summary of a research report ▪ the original and translation of disaster historical records
20C and 21C	▪ damage information due to disasters ▪ the counter-plan of damage ▪ the implications learned through disasters ▪ the on-the-spot pictures before and after recovery ▪ documents about disaster instances ▪ article and report of broadcasting ▪ the disaster history of a specific region by time-series

DiMap includes disaster instances from the era of the Three States to 2008, and contains information of three types of natural disaster such as a heavy rain, an earthquake, and a drought. Additionally, information of seven types of natural disaster such as a typhoon, a strong wind, a tidal wave, a heavy snow, a steep slope, a lightning, and a forest fire are constructed by way of showing an example and are planned to expand more. In Figure 1, we present the plan for a service of DiMap by degrees.

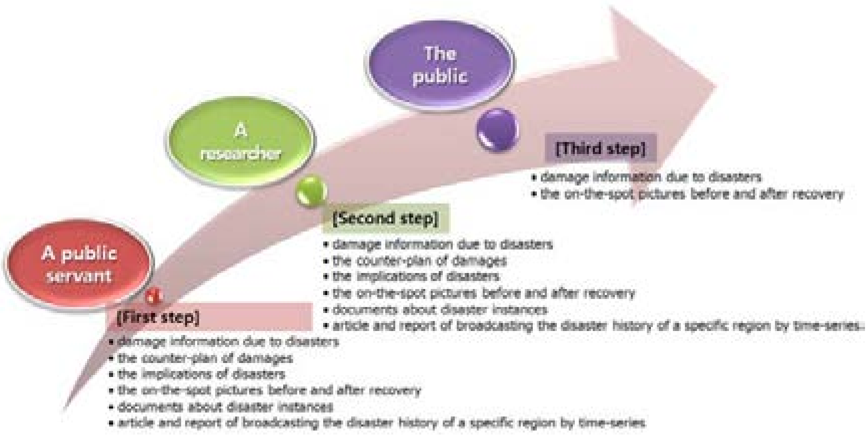

Figure 1: DiMap service by degrees

2.2 The functions of DiMap

For explaining the functions of DiMap, we above all describe user interface of DiMap divided by four parts (*Figure 2*): the menu part for statistical data about disaster instances, the information visualization part based on a map, the result list of searching, and the input part of conditions such as a type of disaster, a period, and a region for searching

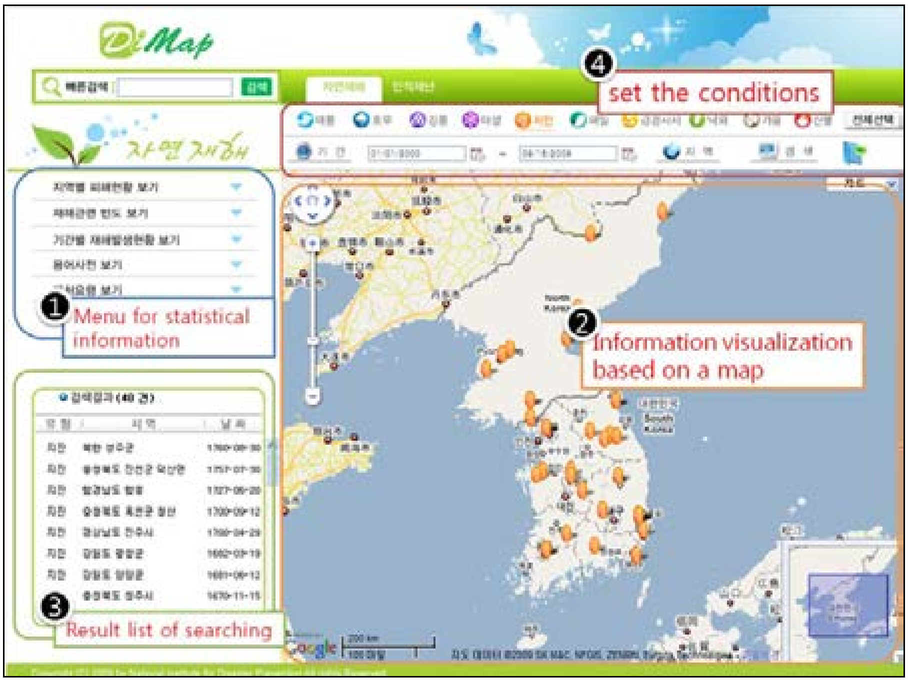

Figure 2: Four parts of UI of DiMap

2.2.1 *Statistical Information about disaster instances*

DiMap provides the amount of damage due to a disaster by a district with color-map, the trend of disasters which happen in a district using a graph.

2.2.2 *Visualization of information based on a map*

Information of disaster instances are visualized on a map considering a location at which a disaster instance happen for high usability and high comprehensive faculty by intuition. We developed DiMap using Open API functions offered by Google Map for building a base map.

If mouse is over a spot, the list of disaster instances happening in an adjacent area pops up (*Figure 3*) and we can select one of disaster instances.

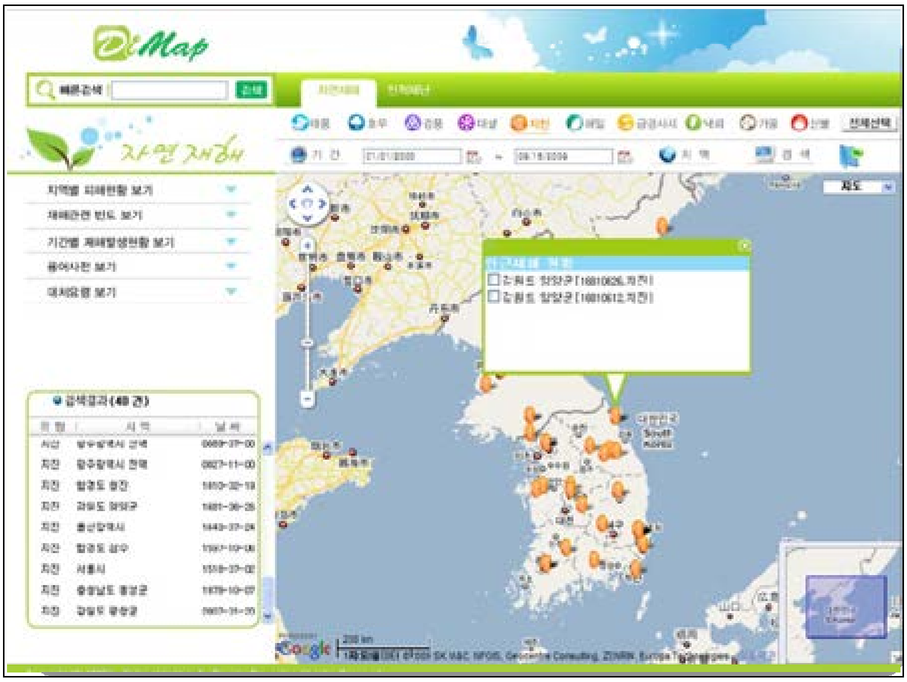

Figure 3: The list of disaster instance happening in an adjacent area

Also, concise information (*Figure 4*) and detail information (*Figure 5*) on a selected disaster instance can be given. Concise information shows damage information briefly and provides the on-the-spot pictures before and after recovery. These pictures are visualized on a location at which a disaster instance happened. If a small picture box is clicked, the enlarged picture before and after recovery appears. All functions for manipulating a map are provided.

Figure 4: Concise information: pictures before and after recovery

To gain more detail information about a disaster instance, click “show the detail” and then detail information on a selected disaster instance are given as *Figure 5*.

- damage information due to disasters
- the counter-plan of damage
- the implication learned through disasters
- the on-the-spot pictures before and after recovery
- documents about disaster instances
- article and report of broadcasting

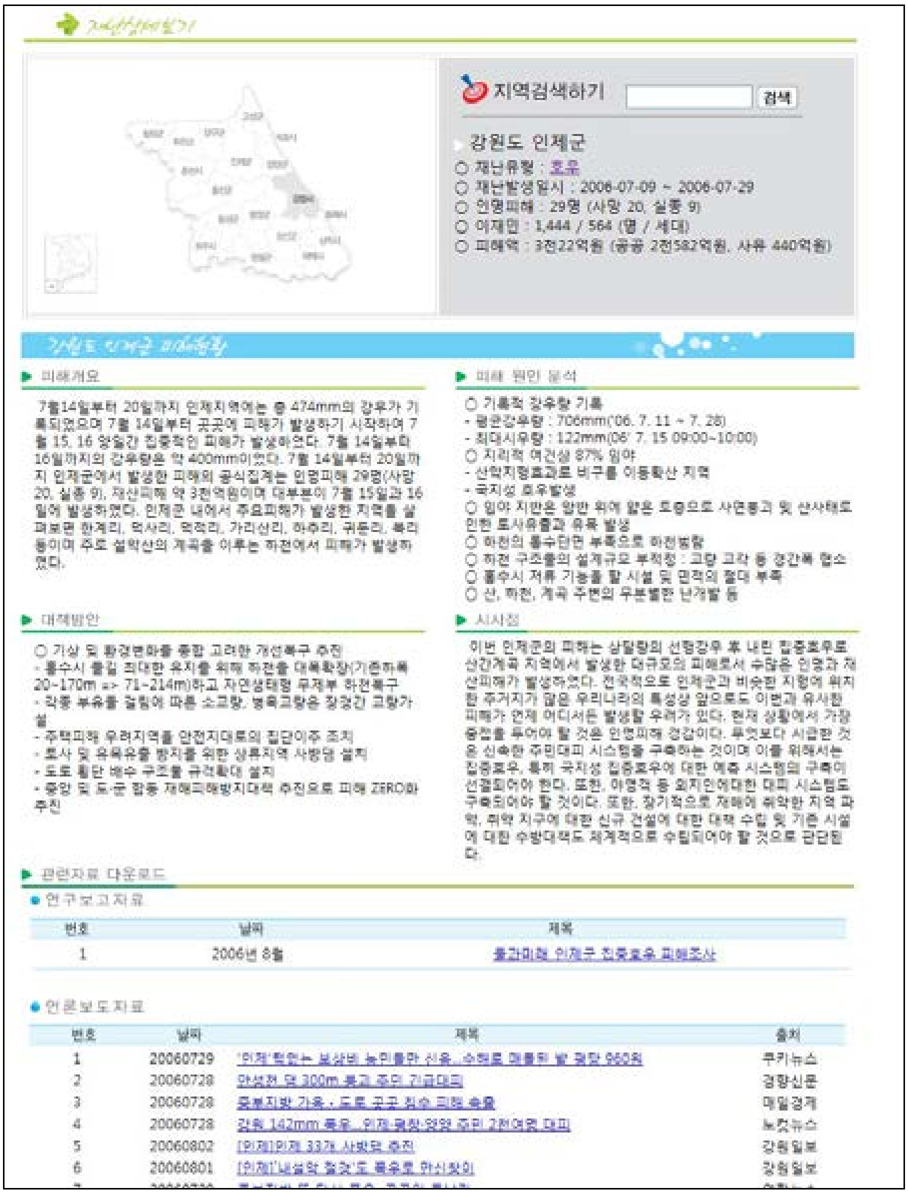

Figure 5: Detail information

Additionally, DiMap gives the disaster chronicle of a specific region. We can be given information on a specific area by time-series. For example, we can know how many disasters happen or which disasters happen in our place of residence.

3. CONCLUSION AND FUTURE WORKS

In this paper, we present a new system called “DiMap”, which provides the information on historical disaster instances due to natural disasters since the era of the Three States. DiMap visualizes information on a map considering a location at which a disaster instance happened for high usability and high comprehensive faculty by intuition.

Through DiMap, we would like to provide not only the disaster chronicle of a specific region by time-series but also damage information, the counter-plan of damages, the implications of disasters, and documents about disaster instances. First of all, DiMap services to an officer servant and then the service of DiMap plans to be expanded for a researcher and the public by degrees.

In the future, we will enhance the contents and user interface of DiMap by degrees. Through expanding information on a man-made disaster as well as information on natural disaster, we plan on providing various and abundant information. Disaster information enlarged by integrating and connecting with related disaster information systems will be included in DiMap.

Also we will apply the technology of Semantic Discovery to DiMap, so that a user will be provided the user-specific data.

REFERENCES

Choo, G.S., 1999. *Evaluation and Collective Arrangement of Historical Damaging Earthquakes for the Suggestion of New Korean Seismic Map*. The research report , NIDP, Korea.
The chronicle of Disaster Management, 2009. NEMA, Korea.
Dean Allemang, Jim Hendler, 2008. *Semantic Web for the working ontologist*. ELSEVIER.
Ramesh R. Rao, Jon Eisenberg, and Ted Schmitt, 2005. *Improving Disaster Management : The Role of IT in Mitigation, Preparedness, Response, and Recovery*, The National Academies Press.

THE CONCEPT OF U-SAFE CITY AND SERVICE MODELS IN DISASTER PREVENTION

Hyun Ju KIM, Hyeong Jun Im
National Institute for Disaster Prevention, Republic of Korea
hjkim5, imhjun@korea.kr

ABSTRACT

The rapid development of information technology has greatly effected on our life and urban paradigm. In this research, a u-Safe City and a u-Safe City service are proposed as a national disaster management system. Firstly, a u-Safe City is defined as a city which uses ubiquitous technology to minimize damages from disaster. The vision and goals of u-Safe City are derived from investigating the social change and urban paradigm for the development of information technology, the condition of disaster management within a ubiquitous society and the informative circumstances. Secondly, a u-Safe City service is defined as a set of ubiquitous activities to provide disaster information to support decision-making.

u-Safe City service models are classified into 5 detailed services of the monitoring service, the safe management service, the damage estimation service, the prediction and warning service, and the situation management service. Based on the definitions in this research, the u-Safe City concept will be applied to urban developments. This research closes by proposing the scheme of the systematic and long-term strategy development, the feasible plan for the promotion and the test-bed projects, and the policy directions for the u-Safe City promotion.

1 INTRODUCTION

1.1 Background and Purpose

Recently, the rapid advance of information technology has changed our life and the urban paradigm through integrating the ubiquitous information service with the urban space. Local governments have conducted the u-City developments and gradually modified to enhance the regional characteristics and to improve their growth potential.

The purpose of this research is to define the u-Safe City and the u-Safe City services for the application on the urban development. It is crucial to establish the integrated and interrelated u-Safe City service models among the central and local governments and related organizations for efficient emergency response and disaster prevention. However, there are constraints such as discontinuity between the new and the old systems, discordance between different disaster prevention systems of local governments. Therefore, it is urgent to develop the national guideline for disaster prevention in u-City.

1.2 Definition of u-City

Development of ubiquitous city Act, which is the fundamental law on u-City development in Korea, defines u-City as a city where u-City services are provided through u-City infrastructures to improve quality of life and to develop competitive power of city. The Act defines a u-City infrastructure as an infrastructure which is related to telecommunication or utilized to provide u-City services, such as RFID, uSN, W-CDMA, WiBro, DMB, etc. A u-City service is defined by the Act as a service which interactively collects and provides information of primal urban functions such as administrative, transport, welfare, environment, disaster prevention, etc.

2. CONCEPT OF u-SAFETY CITY

2.1 Definition of u-City

A u-Safe City is defined as a city uses ubiquitous technology to minimize damages from disaster. In terms of national safe management, u-Safe City is practical and strategic plan of "u-Safe Korea" which aims to guarantee safety from disaster in Korean peninsula in the manner of ubiquitous.

2.2 Vision of u-Safety City

The vision of a u-Safe City is "People-oriented Safe City". A u-Safe City is the model of a safe city where daily life is not interrupted by disaster, and guarantees continuity in urban function. Also, u-Safe city provides efficient disaster management services. In Korea, many cities experienced disasters which became serious due to the inconsiderate urban developments, and they caused a lot of casualties. A u-Safe City values individuals' life and safety in urban developments. The disaster prevention system with ubiquitous technology can provide rapid responses, and disaster information can be managed very efficiently.

Figure 1: Vision and Goal of u-Safe City

There are layers of elements to achieve the vision of the u-Safe city (Figure 2). Basically, there are u-City infrastructures like ubiquitous Sensor Networks (uSN), Radio-Frequency IDentification (RFID), etc. Based on u-City infrastructures, u-Safe City services organize another layer. They provide disaster prevention services to people and governments. Disaster prevention is not a task for a single city, but cities in the co-operational system. In many cases, even all national power and resources need to be assigned quickly and systematically, which can be done effectively by connections among u-Safe Cities.

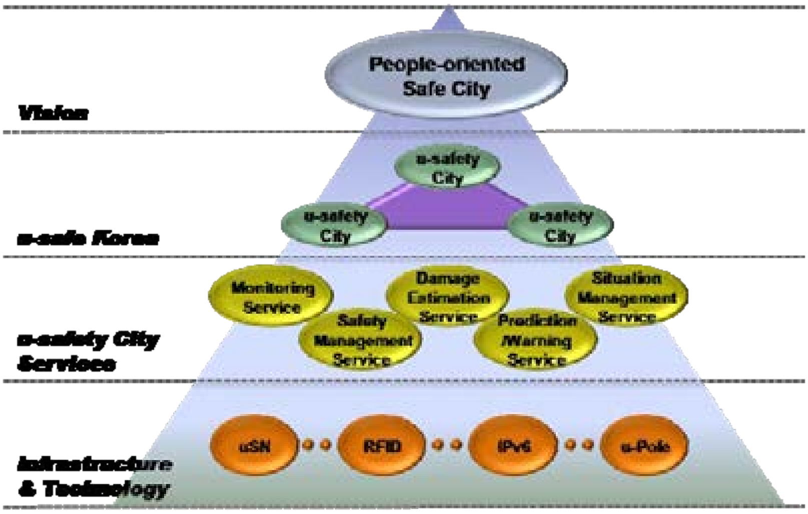

Figure 2: Target System of u-Safe City

3. u-SAFE CITY SERVICE

A u-City service can be defined as a set of ubiquitous activities to collect and process information, and provide a proper result for a certain purpose. In u-Safe City, a certain purpose is the disaster prevention, and the information is about disasters. Therefore, u-Safe City service can be defined as a set of ubiquitous activities to provide disaster information to support decision-making of disaster management system.

The model for u-Safe City services is classified into 5 detailed services. They are the monitoring service, the safety management service, the damage estimation service, the prediction and warning service, and the situation management service. Figure 3 shows the examples of service applications.

Figure 4 is a conceptual master plan of u-Safe City services. Emergency Operations Center (EOC) is the main body of u-Safe City services. EOC operates the monitoring service as well as the damage estimate service and the safety management service. When there is a symptom of disaster, EOC delivers warning messages to local government, the individuals in the vulnerable area and the relative organizations. EOC also delivers disaster information to support the situation management.

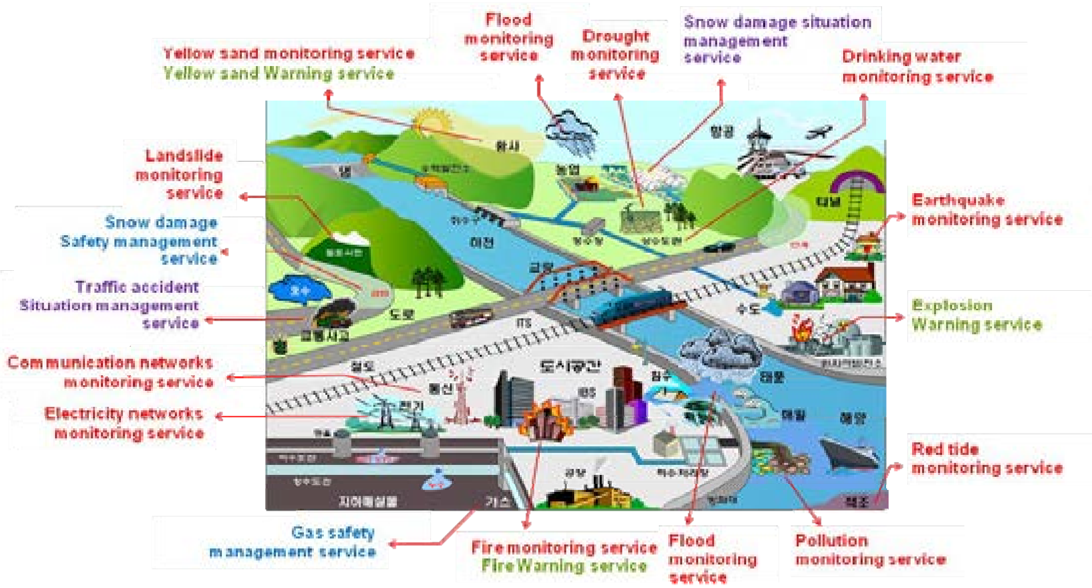

Figure 3: u-Safe City Services (NIDP, 2008)

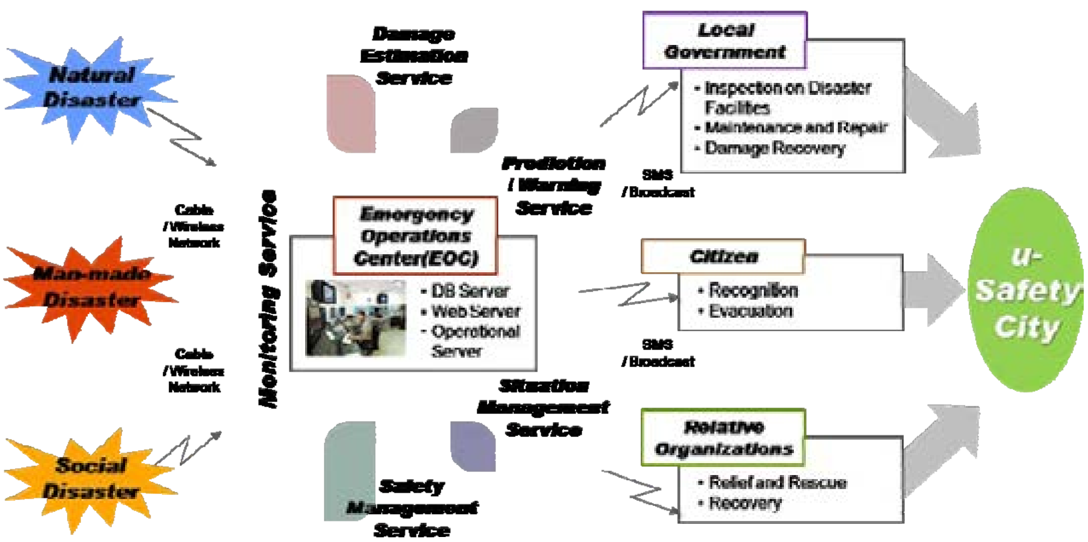

Figure 4: Concept of u-Safe City Service

Figure 5 shows an example of the u-Safe City flood mitigation service. First of all, there is a set of monitoring services on the spots. The sensors are installed on the riverside to monitor the flood control facilities. The sensors in the inner city collect information of the urban underground space and the low level area. Hydrological and meteorological information are also collected and directly sent to EOC by cable or wireless networks. EOC has data-base servers, web servers and operational servers. Information delivered to EOC are stored in the database servers and released to public by web servers. When EOC catches abnormal symptoms, EOC immediately responds and recovers remotely or manually. EOC also conducts the damage estimation based on the flood hazard map. Then, they develop preparation scheme such as flood response guidelines and co-operational system with the relative organizations. If flood outbreaks and is caught by sensors, the information will be sent to the EOC operators. The information also will be sent to the individuals on the low level area to help their evacuation on occasion. In case of road inundation, EOC directs vehicle bypassing by controlling the traffic signal or variable message sign (VMS). EOC Servers exchange real-time information with relative organizations and neighborhood cities for cooperation and their preparation. After flood, sensors collect the damage information to re-assign the vulnerable area and conduct recovery projects. Pre and post disaster information is collected in systematic and automatic manners, and reported to the central government for national aid.

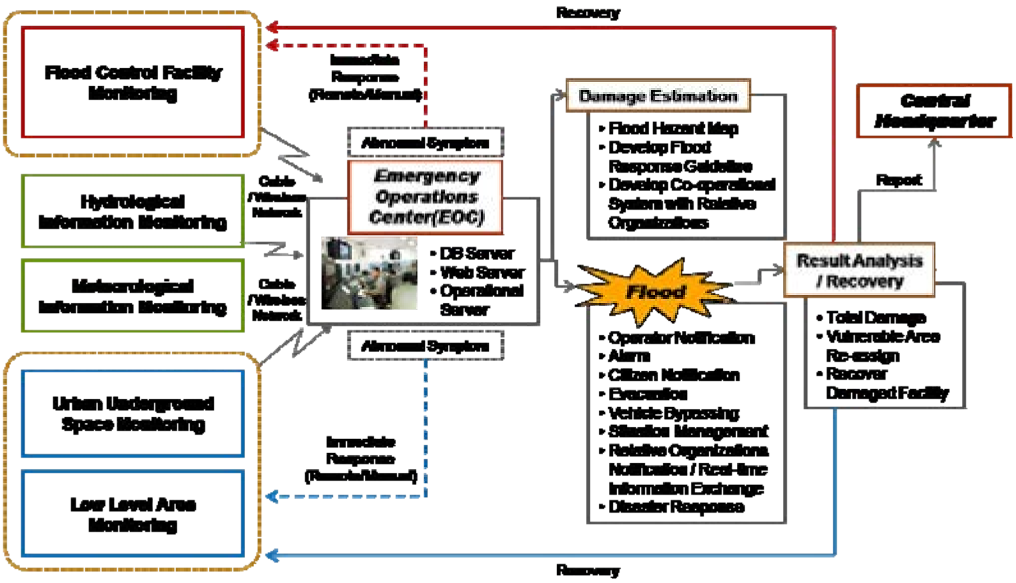

Figure 5: Concept of u-Safe City Flood Mitigation Services

Figure 6 shows an example of u-Safe City fire prevention service. There are three objects in the fire prevention service. They are the district office which operates EOC, the field manager, and the fire department. The sensors at the target site collect the site information of flame, movement, smoke, and temperature to send to EOC which operates DB server, WEB server, SMS server, and control server. The EOC processes information from the site and operates the services such as the damage estimation and the real-time surveillance. If there is a signal of fire at the target site, EOC makes a request of dispatch to the fire department

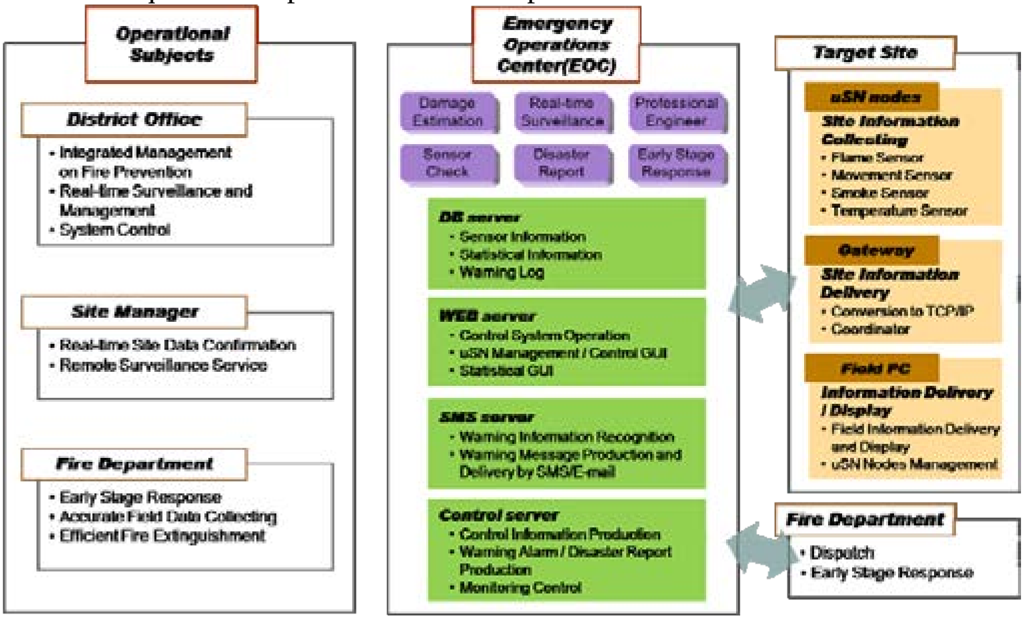

Figure 6: Concept of u-Safe City Fire Prevention Services

4. CONCLUSIONS

A u-Safe City is a city which uses ubiquitous technology to minimize damages from disaster. The goal and the vision of a u-Safe City satisfies the goals of the national ubiquitous projects such as the e-government project by Ministry of Public Administration and Security (MOPAS), the national safety management information project by NEMA and the u-Safe Korea project of NIDP. Complement and linkage with the projects above are necessary as well as comprehensive planning and strategic approach on disaster prevention system, while the platforms for u-Safe City system and EOC with ubiquitous technology are necessary for u-Safe City service operation.

Many local governments are interested in u-Safe City, on the other hand, they have distinct condition on u-City infrastructure, disaster characteristics, and disaster management system. Accordingly, it is important to promote u-Safe City projects on a certain type of disaster, and to gradually procure the requirements for u-Safe City and u-Safe City services.

There are 3 elements on u-Safe City promotion scheme. Firstly, Systematic and long-term strategy development is necessary for effective promotion and synergy effect. Further researches are recommended for the elaboration of u-Safe City services based on the demand analysis and the verification to allow for the trend of the information technology and the changes in the ubiquitous environments. Secondly, the feasible promotion plans as well as the test-bed projects based on the super ordinate development plan and the related projects are important. The model projects of governments are able to verify its adequacy and to be applied to the new urban developments. Finally, the policy direction needs to be formulated for investment and cooperation among governments, private companies, academy, and research institutes.

REFERENCES

Kang, Yejin, 2006, *A study on paradigm shifts of disaster management and the betterment of urban disaster management system*, Ajou Univ.

Busan, 2007a, *A report for the establishment of strategy regarding Busan u-Safe City model*

Busan, 2007b, *A study on u-Busan urban disaster prevention system*

Jeremy Morley, 2003, *MasterMap in Academia-Experiences at UCL*, University College London

Kim, Sang Bong, Cho, Woo Jin, 2007, A Study on the Development and Application of 3Dimensional Spatial Information of Virtual City Using Digital Photogrammetry, *Geodesy, Photogrammetry, and Cartography*, Korean Society of Surveying

Korea Institute of Construction & Transportation Technology Evaluation and Planning, 2006, *Construction of the 3D Virtual Land Information and Development of its Application*

Lee, Seong-Kil, Cho, Jung-Rak, Kim, Jung-Jae, 2008, *Ubiquitous city to lead u-City project*

Masahiko Murata, 2004, 3D-GIS Application for Urban Planning based on 3D City Model, *ESRI International User Conference 2004*

MIC, 2006, *u-Korea master plan to realize the first leading ubiquitous society*

NIA, 2005a, *The development history of information policy in Korea*

NIA, 2005b, *A study on the core applied technology and standardization*

NIDP, 2008a, *Introduction of principles for disaster prevention planning in u-City*

NIDP, 2008b, *Development of the standard model for ubiquitous disaster prevention City*

NIDP, 2008c, *A study on the construction for the u-Safe Korea system*

Park, Inhye. Jun Chulmin. Lee Jiyeong, 2008, *GIS-based Fire Evacuation Simulation using CA Model*, Geographic Information System Association of Korea

P. Frederiksen. J, Grum. L.T, Joergensen, 2006, Strategies for Updating a National 3-D Topographic Database and Related Geoinformation, National Survey and Cadastre, Seoul Development Institute, *A Study on development of Seoul Virtual City using 3D GIS*

Shin, Seong-Beom, 2006, *A comparative study on Korea and Japan for Ubiquitous IT strategy*, Tong-Myong Univ.

Shim, Jae-Kang, 2002, *A study on integrated emergency management and emergency information system - the seoul metropolitan emergency operation center*, Univ. of Seoul

URISA, 2006, 3D Geospatial, 2006 Workshop

METHOD FOR PROBABILISTIC DISASTER RISK EVALUATION USING RISK CURVE ANALYSIS

PARK, SOSOON
National Institute for Disaster Prevention,
sspark@korea71.kr

ABSTRACT

Recently, damage magnitude of disaster is sharply increasing but its occurrences and damage scales are so uncertain that it is hard to construct a reasonable response, mitigation plan and its infrastructures. Therefore, the needs for an advanced risk management technique based on a probabilistic and stochastic risk evaluation are increased. In this study, these evaluation methods were investigated and an advanced disaster risk evaluation method, which is based on the probabilistic or stochastic risk assessment theory and also on a quantitative evaluation technique by risk curve analysis, was suggested. With this method, each risks of human-induced disaster for recent 10 years were evaluated respectively and compared. Through the consilience of the traditional risk assessment methods and this method, a probabilistic risk estimation technique for the uncertainty of future disaster's damage could support for a reasonable decision making on disaster damage mitigation.

1. INTRODUCTION

Various disaster management policies were developed in Korea after NEMA was started 5 years ago. Disaster damage occurrence status for recent years was over-viewed and it is clear that the national disaster rate and its total damage were reduced in a large scale compared to those of human-induced disaster (National Institute for Disaster Prevention, 2008). Therefore, the safety and damage loss reducing technology for human-induced disaster mitigation was started to development recently. For the reasonable and effective disaster mitigation plan, disaster's damage risk must be evaluated clearly as like risky factor's distribution over around areas and their occurrence probabilities and severities also. If prediction for the future's risk is possible, it is so much the better for decision making. But it is very difficult to predict the future's risk .

Therefore, various quantitative disaster risk indexes of human-induced disaster, which is based on the risk-based analysis method dealing with statistics technique and probabilistic risk assessment using risk curve, was investigated in this research. From the results, some quantitative disaster risk evaluation functions are suggested, which is able to evaluate quantitatively disaster risk without concern of area neither dimension nor disaster's type. Through the results of this research, surveying the occurrence states of domestic human-induced disaster as quantitative disaster risk's change behavior and its characteristics could be possible. And the safety states of future risk level could be exactly estimated relatively in range of trustworthy if the system structure of the industry facilities and its distribution/infrastructures of nation/city/region were not changed in a large scale.

2. RISK MAP AND RISK CURVE

2.1 Definition of risk and risk map

According to the Kaplan and Garrick, risk $R(x)$ is the accident scenario with event series of disaster which was caused by troublesome event/factors and expanded to incident in a construction, local society or system of industry. From the definition of risk, a general concept figure of the observed data, which is the discrete probability of event and time series data during monitoring period, is called risk map. Risk map can be expressed by triple set of $T(i)$, $S(i)$ and $X(i)$. Statistical risk values of time series data in risk map is given by Equation 1.

$$\begin{aligned} &RiskMap =< S(i), p(i), x(i), t(i) > \\ &[x(i), t(1)] < [x(2), t(2)] < \cdots < [x(i), t(i)] < \cdots < [x(N_0), t(N_0)] \\ &i = 1,2,3,\cdots, N_0 \end{aligned} \tag{1}$$

Here, accidents caused during monitoring period T can be expressed as a disaster risk map shown at Figure 1. And an accident and its damage scale were resulted in accordance with its scenario gotten over a local system or area. Then, some scenario list can be elicited from the disaster risk map and these scenarios were sorted as a sequential list in inverse order of the damage magnitude from maximum to minimum. In Table 1, N_0 sets of accident's scenario $S(k)$, its each occurrence probability $P(i)$ and damage scale $X(k)$ were given, which is called scenario list. A scenario list of exceedance cumulated probability as like Table 1 can be made by calculating the exceedance cumulated probability for each threshold of damage scale. When a total count number of accident scenario causing disaster in a target system is N_0, accident scenario is $S(k)$, its each occurrence probability is $P(k)$ and threshold of damage scale for account is $X(k)$, a triplet set which was composed with these three factors is defined as the risk itself in a target system, which is shown in Equation 2.

$$\begin{aligned} &Risk =< S(k), p(k), X(k) >, \\ &X(1) = X_{Min} < \cdots < X(N_0 - 1) < X(N_0) = X_{Max}, k = 1,2,3,\cdots, N_0 \end{aligned} \tag{2}$$

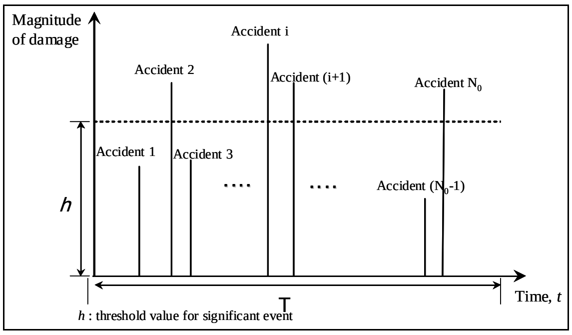

Figure 1: Disaster risk map for observation period T

Table 1 : Scenario list and exceedance cumulated probability

Scenario	Damage scale	Probability $P = F / N_0$	Exceedance cumulated probability, $P_{excd} = F_{excd} / N_0$
S_{N0}	$X(N_0) = X_{Max}$	P_{N0}	$P_{excd(N0)} = P_{(N0)}$
S_{N0-1}	$X(N_0 - 1)$	P_{N0-1}	$P_{excd(N0-1)} = P_{(N0-1)} + P_{excd(N0)}$
.	.	.	.
S_k	X_k	P_k	$P_{excd(k)} = P_k + P_{excd(k+1)}$
.	.	.	.
S_2	X_2	P_2	$P_{excd(2)} = P_{(2)} + P_{excd(3)}$
S_1	$X_1 = X_{Min}$	P_1	$P_{excd(1)} = P_{(1)} + P_{excd(2)}$

2.2 Statistic disaster analysis and the disaster risk curve function

If each value of damage scale X and its exceedance cumulated probability Y are plotted respectively, then a disaster risk curve during monitoring period T can be expressed as a stairs-type function with the discrete damage magnitude which was shown at Figure 2. From statistical risk value of time series data, risk map was represented in Equation 1 and Figure 1 in details. If the damage scale (probability variable, X) has continuous values, the disaster risk curve can be expressed as a curve with a continuous line. It can be called as a disaster damage characteristic curve as well. Here, let the probability variable of damage scale as X and let the cumulated frequency of each scenario's occurrence probabilities of that X exceeds h as $P(h)$. Then, X and $P(h)$ at the X can be represented as shown in Figure 2. CDF is a exceedance cumulative distribution function and the relationship between X and $P(h)$ is given as follow (equation 3):

$$F_{excd}(h_i) = CDF[X \geq h_i] \text{ or } P_{excd}(h_i) = \Pr[X \geq h_i], i = 1,2,3,\cdots, M \qquad (3)$$

If the discrete time series data of a finite number of accident occurrences are arranged as N_0 accidents from the Figure 1, then the relationship between X and $P(h)$ can be expressed in the followings (equation 4):

$$F_{excd}(h) = \int_h^{\infty} C(x)dx \propto h^{-Ds}, Ds > 1$$
$$\therefore P_{excd}(h) = F_{excd}(h)/N_0 = h^{-Ds}, Ds = Ds - 1 > 0 \qquad (4)$$

This type of distribution function is called Pareto type distribution that depends on Ds dimensional fractal distribution with self-similarity and only the inverse power law function satisfies the fractal distribution (Takayasu Hideki, 1991). And this distribution is the disaster risk curve if values $\log h$ are plotted at X-axis and $\log P(h)$ values at Y-axis. Disaster risk function of Equation 4 means that the relationship between damage magnitude and its exceedance cumulative probability can be evaluated by the dimensional fractal distribution with self-similarity.

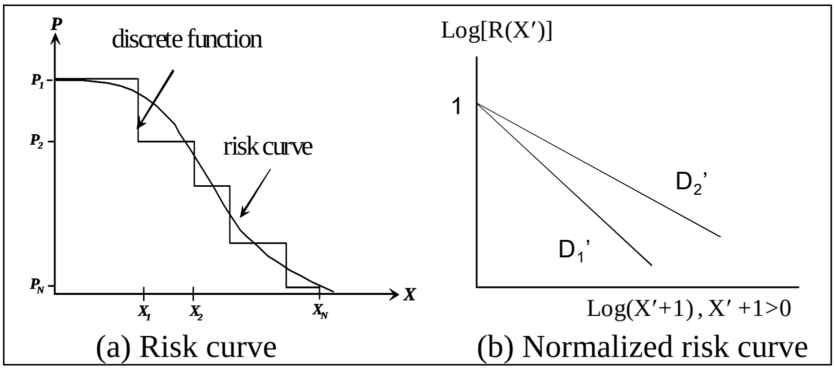

Figure 2: Concepts of stairs-type disaster risk function, risk curve and normalized risk curve

Here, if statistic disaster analysis was conducted within a same group having a fixed total count number of disaster, and if the probability variable X has continuous value, $P(h)$ is able to represent as an exceedance probability. That is expressed as an exceedance probability distribution function (PDF). Therefore, $F_{excd}(h)$ and $P_{excd}(h)$ are able to consider as an equivalent value.

In Figure 2, the risk curve plotting cannot be entirely described by a log-log linear relation even though the results in the range of high damage magnitude are well fitted. Thus, in order to represent the frequency-damage magnitude relation in a log-log linear type over the entire distribution region, a certain location parameter, say γ, was introduced. In other words, the time series data in Figure 1 can be considered to be on a base line γ. Then the data is rearranged under $h + \gamma (= h')$ in the damage magnitude range value instead of h which was used as threshold value in Figure 1. Then the function of damage magnitude and probability at that damage will be represented as follows (equation 5 and equation 6):

$$F_{excd}(h) \propto (h+r)^{-Ds'}, Ds' = Ds - 1 > 0 \tag{5}$$

$$F_{excd}(h)/N_0 = [(h/r)+1]^{-D'}, h \geq 0 \tag{6}$$

$$R(h) = F_{excd}(h)/N_0 = [(h/r)+1]^{-D'}, h \geq 0 \tag{7}$$

This equation can also be considered as a same kind of Pareto type Fractal distribution as represented in Equation 4. The location parameter γ is estimated by the least square method to the assumed regression risk curve. In selection of introducing γ, Equation 5 depends on the shape of the original risk curve. From these conclusions, a location parameter γ would be a meaningful parameter because it is not only a location parameter that approximates a linear function, but also has a specific value particular for the subject accident data group. As given in Figure 2, damage magnitudes due to those accidents depend on an inverse power law function of the Equation 5 in case of location parameter of γ was introduced.

Here, $R(h)$ is referred as "upper exceedance cumulated probability distribution function". The parameter of γ in Equation 6 and Equation 7 is a location parameter of Pareto type distribution function in a statistical meaning as mentioned also. Here, let introduce a new concepts of damage scale variable as $X' = h/\gamma$ then X' can be defined as a normalized damage scale variable which has no dimension. Hence, the exceedance probability distribution function $P_N(x)$ and the upper exceedance probability distribution function $R_N(x)$ of X' are given as follows:

$$P_N(x) = \Pr(X' < x) = 1 - (1+x)^{-D'} \tag{8}$$

$$R_N(x) = R_n(x) = \Pr(X' \geq x) = (1+x)^{-D'} \tag{9}$$

At the Equation 9, $R_N(x)$ is referred as a normalized risk curve. This normalized risk curve can be represented on a log-log scale plotted graph based on the relation between $R_N(x)$ and $1+x$ for overall x value as a linear straight curve as shown in Figure 2. As like this, the magnitude of damage in this risk curve can be scaled by the normalized unit of X' without concerning of damage's type or its unit. It is the reason why the various kinds of disasters can be expressed, evaluated and compared quantitatively each other even though disaster kind or their damage type is different.

3. SUGGESTION AND COMMENTARY OF QUANTITATIVE DISASTER RISK INDICATOR INDEX

From the disaster risk curve, various indicator indexes to evaluate the disaster risk and disaster risk parameter are introduced.

1) $|D|$ and $|D|^{-1}$

They are come from the slope value of tail part in the disaster risk curve, which is a territory where the reverse Pareto function (power law function) is formed. It can be expressed as $D = -\log F(x)/\log(x)$ and it's a kind of the dimensional fractal distribution with self-similarity.

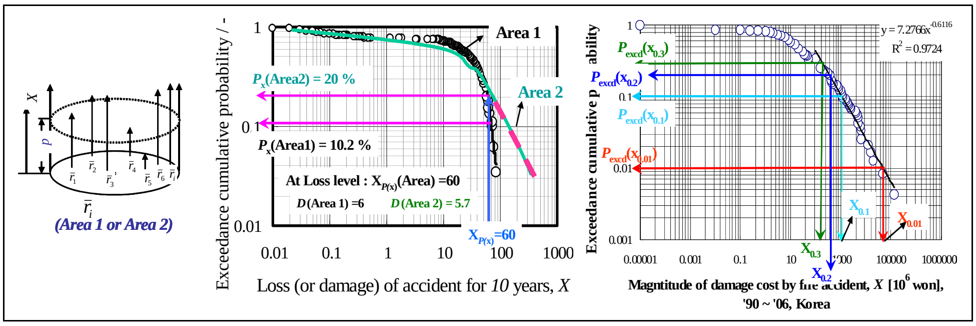

Figure 3: Concepts of local disaster risk analysis and comparison between two areas and deducting disaster risk monitoring parameters from risk curve

This parameter $|D|$ can be employed as a safety index which characterizing the relationship between the damage scale and its occurrence probability (frequency) in a certain system. This is a parameter that indicates the functional ability index or a safety yardstick of fail-safe organizations statistically. Here, $|D|^{-1}$ can be used as a disaster risk intensity factor because it represents the ratio of increased damage scale per unit accident or event, which can be understood from the function of $|D|$.

2) $< X_k >$ and $< X_{Nk} >$, $< X_{Max} >$ and $< X_{NMax} >$

They are the statistical damage magnitude and normalized damage magnitude at a focused occurrence probability range, which can be referred from Figure 3. Damage magnitude in evaluating disaster risk is an important index. The value of k is the exceedance occurrence probability with the threshold damage level to be monitored or controlled. These values can be set by the decision maker to manage the disaster risk in a range of acceptable risk level according to the status of the society's needs for safety. For example as like $< X_{0.03} >$, $< X_{0.1} >$, $< X_{0.2} >$ and $< X_{0.3} >$, which means a value of statistical damage magnitude at a monitoring risk level probability 3%, 10%, 20%, 30% respectively. Values of $< X_{Max} >$ and $< X_{NMax} >$ are also very important indexes. They are the magnitude of maximum damage, which can be used for maximum risk degree by disaster. And the scenario of the accident can be the worst scenario at the same type of disaster.

4. SUGGESTION OF QUANTITATIVE DISASTER RISK EVALUATION METHOD

4.1 Quantitative disaster risk function using risk curve analysis

As a disaster risk evaluation index, $|D|^{-1}$, $< X_k >$, $< X_{Nk} >$, $P(X_k)$, $P(X_N)$ could be useful. Using these indexes, disaster risk function can be represented in Equation 10. The meaning of these indexes are examined and explained before. If disaster risks among different kinds of disaster that happened within the same area and same periods are compared, the population characteristic of their group is same. Therefore, the regional disaster risk depends on just $Function[Xp(i), |D|, p(i)]$ and the comparison of various type of disaster is possible with only $Xp(i)/|D|$. Then the disaster risk function can be given as follow, which has the same form with local disaster risk evaluation function of a'Albe (Emergency Management Agency, 2008).

$$DisasterRisk \propto Function\{|D|^{-1}, < Xp(i) >, < p(i) >\} = \frac{< X_a > \times p(< X_a >)}{|D|}$$
$$MaximunDisasterRisk = \frac{X_{Max} \times p(X_{Max})}{|D|} \qquad (10)$$

4.2 Comparison of human-induced disaster's risk

It has been possible to quantitatively compare the degree of disaster risk according to each human-induced disaster through the using risk curve analysis method and disaster risk function of a'Albe, which utilizes the risk curves. Further, it has been possible to secure the objectivity and the efficiency for priority decision about disaster countermeasures.

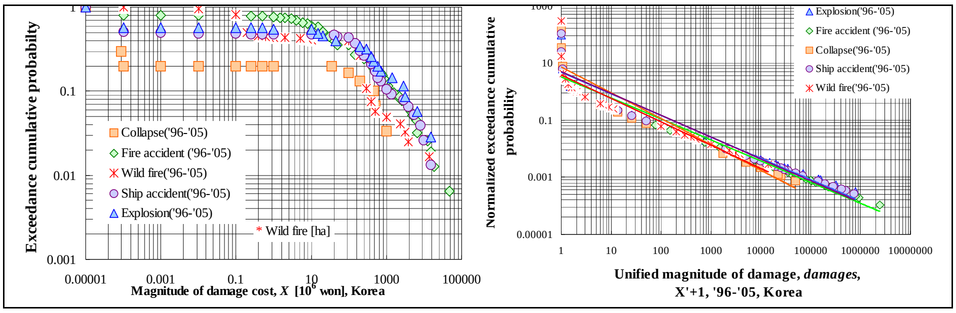

(a) Damage cost (b) The death

Figure 4: Risk curves and normalized ones of human-induced disasters

At 3% upper exceedance cumulated probability of damage cost, it was Explosion that showed the highest risk level with the highest risk intensity factor. And Explosion and Collapse at 10% and 20% showed the highest risk level with the highest risk intensity factor respectively. In details of 10% upper exceedance cumulated probability of damage cost, risk level of Explosion was the highest and Collapse showed the lowest risk level. Also, Explosion was 1.7 times of Collapse's risk, Ship accident was 1.4 times, and Fire accident was 1.2 times. In terms of fatality risk level, Ship accident showed the lowest level and Fire accident showed the highest risk level which was 11.4 times of Ship accident's risk. While Collapse was 2.4 times and Explosion was 1.2 times of it. In a same way, risks of each disaster were analyzed at 3% and 20% upper exceedance cumulated probability also. But the results of at the 10% upper exceedance cumulated probability were shown as representatives.

As like this, it is possible to utilize the damage magnitude regarding each exceeding cumulative probability as a disaster risk index. As another usage of disaster risk curve, if an accident "A" was happened and its damage magnitude was $X = 60$. Here, the risk curve was given of the area as Figure 3 (left), then it is possible to understand that the accident A's risk degree is in range of the worst upper 10% at Area 1 and the worst upper 20% at Area 2. From this, decision maker can rearrange the risk management policy and method depends on the areas.

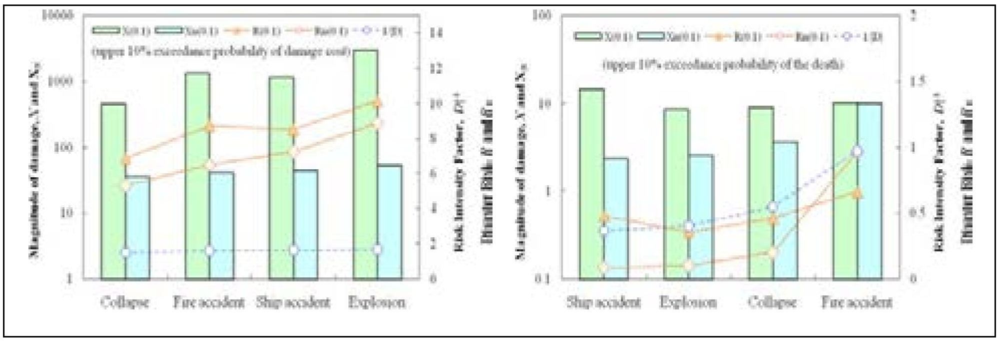

Figure 5: Quantitative disaster risks for the last 10 years

5. CONCLUSION

It is still difficult to apply existing techniques to the whole region of city or nationally with conventional risk assessment. However, this research was not aimed to examination of complicated physical characteristics of the accident, but aims to the simple and quantitative evaluation method of disaster risk including the statistical probability and damage scales. For that, lots of accidents and just simple emergency information as like damage magnitude, accident' area and date and disaster type that happed over a whole area were used. It is certain that it is possible to evaluate the disaster risk of whole regions easily and quantitatively from the results. Furthermore, the estimated results by risk curves showed that the magnitude of damage and risk directly depends on their probability. Therefore, it is easy for the decision maker to understand the total risk states (or safety state) due to disasters over a region of district or nation.

In fact, the quantitative disaster risk index and the disaster risk evaluation technique, utilizing disaster risk curve in this paper, has shown high level of confidence regarding large scale disaster. Also, it has been possible to quantitatively compare and analyze the observatory frequency according to disaster type/region/facility, regardless of damage types.

From these conclusion, disaster risk evaluation technique and related prognosis technique by risk curve method, which is trustworthy and quantitative, may be able to play an important role in producing information for an effective decision making in the field of emergency management in Korea.

REFERENCES

Hanayasu, S. and Sekine, K., 2003. *Statistical damage modeling and analysis of industrial accidents and its application to industrial safety problems*, Applications of Statistics and Probability in Civil Engineering, San Francisco, California, USA, July 6-9, pp.792 ~ pp.799.

Wackerly, D.D., Mendenhall, W. and Scheaffer, R.L., 1996. *Mathematical Statistics with Applications* (Fifth Edition), Duxbury.

National Emergency Management Agency, 2008. *Disaster and Safety Management LAW*, Homepage of Ministry of Legislation.

National Institute for Disaster Prevention, 2008. *The Major Outcomes of Disaster Prevention Researches in 2008*, pp.259 ~ pp.276

Hideki T., 1991. *Fractals in Physical Sciences*, Manchester University Press, New York, pp. 1 ~ pp. 58

PARALLEL SESSION 4

FAILURES AND SUCCESSES OF JAPAN'S EARTHQUAKE ENGINEERING

TSUNEO KATAYAMA
Professor, Tokyo Denki University, Japan
katayama@cck.dendai.ac.jp

ABSTRACT

People often say that Japan is one of the most advanced countries in the field of earthquake engineering. It may be true in a sense. But, because Japan is located in one of the most earthquake prone areas on earth, we also made so many failures in the past. We did learn from failures, but at the same time some of our successes were followed by different types of failures.

1. UNTIL THE KOBE EARTHQUAKE

1.1 Our Earlier Failures

Probably we made our first major failures near the end of the 19th century. In 1891, a disastrous earthquake took place in central Japan and in 1894 the Tokyo area was strongly shaken by a medium-sized earthquake. Japan was eagerly importing the western culture and science during this period, but the damage caused by these earthquakes showed that the simple import was inadequate and pointed to the importance of establishing some standards for earthquake resistant structures.

Although a written form of earthquake-resistant construction requirements was not made available immediately following those events, younger engineers in Japan adopted a commonsense engineering approach. The 1906 San Francisco earthquake gave impetus to the problem. It was proposed that earthquake-resistant structures could be built by assuming lateral force proportional to the structure's weight. A coefficient $k = a/G$ was to be laterally multiplied to the weight of a structure, where a is the acceleration assumed for design and G the acceleration of gravity.

1.2 The 1923 Kanto Earthquake

Damage to engineered buildings by the 1923 Kanto earthquake left both successes and failures. Although reinforced concrete buildings were considered to be the most earthquake resistant in those days, the earthquake revealed that some of them were very dangerous. The guiding principle was to keep the building deformation small. Stiff buildings generally fared well. It was reported that buildings designed along the principles of strong boxes

Figure 1: European-Style Structures Heavily Damaged (1891 M8.0 Nobi Earthquake)

were safe whereas those of skeleton framing with weak curtain walls invariably suffered great damage.

Shocked by the devastation by the earthquake, building engineers realized the need for an earthquake resistant building code. And k = 0.1 and 0.15 were specified for general structures and chimney-like structures, respectively. These numbers were based on the estimated acceleration of 0.1G in the up-town area of Tokyo.

1.3 From Conservative to Obsolete

These values of k's were incorporated into the revised 1924 Building Code together with the height limit of 31m. The experience of stiff building suffering less damage left a continued effect on the Japan's earthquake resistant design. The 1924 Building Code remained practically unchanged until the 1948 Fukui earthquake that claimed about 4,000 lives. A new Building Standard Law introduced in 1950 increased the design seismic coefficient from 0.1 to 0.2. The allowable stresses of building materials for short time seismic loading conditions were set at about twice the value allowed in the 1924 code.

Although nearly 10 earthquakes with almost or over 1,000 death tolls took place after the 1923 Kanto earthquake, urban areas were not seriously affected until the 1948 Fukui earthquakes. And hence, a rather conservative earthquake resistant design continued to be made together with the 31m height limit. In the 1950 Law, the effect of flexibility was taken into account by gradually increasing k value for the portions above a certain height of a building. Practicing engineers were disappointed, because design of tall buildings became even more difficult.

In the early '50's, studies were vigorously carried out on the effective dynamic k value, the probabilities of destructive earthquakes and the effects of sub-soil conditions. In 1955, the Building Standard Law Enforcement

Order was modified to reduce *k* by taking into account the seismicity of the district and subsoil conditions.

1.4 Height Limit Lifted

By reading papers published in the 50's and 60's, we could see how much study Japan's researchers and engineers performed in that period, especially on the dynamic effects of earthquakes.

In 1959, the first systematic research started to investigate the possibility of construction of a tall building in Japan. The 24-storied building was modeled by a shear building with 5 concentrated masses and the dynamic analysis was carried out by using an analog computer. This research was followed by several similar studies. General conclusions from these studies were that the 31m height limit could at least be partially lifted. The height limit of 31m was finally lifted in 1963, and the Japan's first 157m tall building was completed in 1968.

The 1963 revision of the Building Standard Law was such that, for the time being, the current Law at that time was to be used for a building with less than 45m in height. When the construction of a taller-than-45m building was proposed, a special examination board individually reviewed the soundness of the design. This approach was effective to encourage engineers with different ideas for the earthquake-resistant design of tall buildings.

1.5 Pitfalls under Our Eyes

Japan's earthquake engineering seemed to be making considerable advances. We had come to be able to build tall buildings in one of the most earthquake prone regions in the world.

During the 1968 Tokachi-Oki earthquake, however, a number of reinforced concrete buildings were badly damaged. They were mostly low-rise and earthquake-resistant designed. The most notable mode of damage was the explosive shear failure of short columns due to the lack of ductility. Lessons from this earthquake led to the 1971 revision of the Building Standard Law.

Many researchers and engineers, however, thought that the Japan's earthquake design code was obsolete because of the conservatism assumed in the past. A 5-year research and development project started in 1972 to update the then existing code by taking account of most advanced knowledge in the field. The outcome of the study resulted into the 1981 revision of the Building Standard Law and also incorporated in earthquake-resistant design regulations of several other structures. A number of new concepts were introduced. (1) Higher lateral seismic shear force in the upper part of a structure than that used in the previous codes, (2) Consideration of the effect of story deflection in the building, and (3) Two levels of design earthquake motion with the concept of ductility and ultimate strength.

While vigorous studies were being made to improve an obsolete code into a modern one, those buildings we thought had been conservatively designed were damaged again by the 1978 Miyagi-Ken-Oki earthquake.

2. THEN, THE KOBE EARTHQUAKE

2.1 Our Worst Failure in Recent Years

At 5:46 in the early morning of January 17, 1995, a magnitude 7.2 earthquake rocked the city of Kobe and its vicinity with a total population of almost 2 million. Since earthquake disaster mitigation programs had previously been directed toward the Tokyo area, both officials and citizens in the hardest hit region were largely unprepared. The nation was also appalled by the lack of leadership and absence of crisis management at the national level.

The 1995 Kobe earthquake revealed that we had made another and one of the biggest failures in recent years. Until then, we had been lucky that strong earthquakes did not take place near our urban areas for almost half a century. During the same period of time, Japan’s earthquake engineering technology made significant advancement. By simply combining these two apparently independent facts, we were beginning to wrongly believe that Japanese structures and cities had become strong enough to survive even severe earthquakes.

2.2 Self-Confidence Totally Shattered

The death toll reached about 5,500 in a fortnight, making it the worst earthquake since the 1923 Kanto earthquake. Within the five years following the earthquake, the death toll increased by another 900 due to the indirect causes. About 100,000 houses and buildings were totally destroyed, and more than 100 reported fires burned down about 7,000 houses killing some 560 people. The region's infrastructures were crippled, paralyzing business and financial operations. The direct and indirect damages were estimated at 37% of the total property in the stricken region, or 1.6% of GDP.

We realized how self-conceited we had been about the earthquake

Figure 2: Modern Bridges Collapsed in Kobe

safety of our structures and communities. Before the Kobe earthquake, we were beginning to place more emphasis on economic and social issues of earthquake disasters than on their technical and engineering aspects. But, hundreds of thousands of the traditional Japanese wooden houses were totally destroyed, and a number of non-ductile reinforced concrete bridges and buildings built according to the old codes were badly damaged. We were forced to accept the fact that strength of structures is still a crucial issue in Japan's earthquake risk mitigation.

3. AFTER THE KOBE EARTHQUAKE

3.1 Headquarters for Earthquake Research Promotion Established

The Kobe earthquake has greatly changed Japan's earthquake disaster mitigation policies. In July, 1995, half a year after the earthquake, the Special Measures Law on Earthquake Disaster Prevention was proposed by Parliament Members, and was immediately enacted. Based on this Law, the Headquarters for Earthquake Research Promotion was established in the Prime Minister's Office to conduct the basic and comprehensive research of seismology on a nationally integrated way. The Basic Disaster Prevention Plan, often referred to as the constitution for disaster mitigation issues, was revised in June 1997, expanding contents related to earthquake and tsunami disasters.

The Headquarters evaluates and disseminates information on the current seismic activities of Japan based on the in-depth analyses by experts. When a significant earthquake occurs, by collecting all available records, the Headquarters disseminates a unified opinion about the earthquake to the public through the media. Establishment of the Headquarters is one of the best legacies that the Kobe earthquake has left.

3.2 Construction of "E-Defense"

Before the Kobe earthquake, it was hard to imagine Japanese structures would fail in a similar way that some structures did in the other parts of the world. We had, however, to accept that structures still collapse and kill people, and that there are millions of old and/or weak houses, and also thousands of modern-looking but low-quality structures in large urbanized areas in Japan. Assessment of the earthquake strength of existing structures and of the effects of their strengthening was mandatory. Unless these weaker structures are properly strengthened, the tragedy of Kobe will happen again.

Limited damage has to be tolerated when structures are subjected to an extremely strong earthquake, otherwise the construction cost will become unacceptably high. New design and effective strengthening methods must be based on the understanding of the reliable characteristics of structural failures. Full-scale collapse tests were thought necessary to eliminate scaling effects inherently involved in scale-model tests. A large-sized 3-dimensional shaking table "E-Defense" was constructed for this purpose. The table size is 20m×15m, and the maximum testing weight is 1,200 ton-f roughly corresponding to the weight of a real-sized 6-storied reinforced concrete building with a floor area of 20m x 15m.

In the collapse tests of traditional Japanese wooden houses, two identical wooden houses were placed on the shaking table side by side. Then one of them was strengthened, and both were subjected to one of the strongest 3-D shaking recorded during the Kobe earthquake. The non-strengthened house collapsed within some 10 seconds, while strengthened one survived the strong 3-D shaking in spite of substantial damage. The tests were televised and made much stronger impact to the people about the significance of structural strengthening than any of the previous efforts made by municipal governments. Since then, "E-Defense" has been used for collapse or failure tests of, among others, reinforced concrete buildings, steel frames, reinforced concrete bridge piers, multi-storied wooden buildings, components of nuclear power reactors.

3.3 K-NET, Hi-net, and F-net

The national program of monitoring earthquakes started in August 1997. This program consists of establishment of seismometer and GPS station networks, and active fault surveys. Today, there are about 3,500 seismometers at around 1,800 locations covering Japan, about 2/3 of which are maintained by the National Research Institute for Earth Science and Disaster Prevention (NIED).

K-NET is a network of about 1,000 digital strong-motion seismometers installed on the free field at an average station-to-station distance of about 25km. The seismometer has a maximum measurable acceleration of 2,000 cm/s^2. Hi-net system utilizes about 800 velocity-type seismometers to obtain precise ground motions. Seismometers are encased in anti-pressure vessel and placed with an average spacing of 15 to 20km. They are located at the bottom of a bore hole of 100m or deeper to eliminate noises caused by human activities. Two strong-motion acceleration-type seismometers are installed at each of the Hi-net stations, one at the bottom of the bore hole and the other on the free field. F-net is a network of about 70 broadband seismometers with a natural period of 300s. The records from F-net are used for researches of earthquake source mechanisms and the structure of the earth's interiors.

Records from the networks are freely obtained through the Internet within the shortest possible time. In the case of the Niigataken Chu-etsu Oki earthquake of July 16, 2007, which may be known for its damage to a nuclear power station, 390 records were obtained by K-NET alone.

3.4 Earthquake Early Warning (EEW)

In an attempt to best utilize the records from the dense seismometer array, a 5-year research program started in 2003 on the real-time estimation and warning of earthquake motions. Two major organizations in this program were JMA (the Japan Meteorological Agency) and NIED. The purpose of the researches was to develop a system of real-time determination of seismic parameters, and transmission of the seismic intensity and the expected arrival time at a site of interest, within several seconds after the earthquake occurrence but before the arrival of ground shaking.

The NIED's system is able to determine the epicenter within a few seconds when P-waves are detected at 2 stations, by also utilizing the information that records have not reached the other near-by stations.

Presently data are collected from the JMA's tsunami and earthquake detection network consisting of 200 strong motion seismometers and the NIED's Hi-net consisting of about 800 velocity-type seismometers. All the data are sent to and analyzed by JMA in real-time, and the results disseminated from JMA. The system went into full operation on October 1, 2007.

JMA issues two kinds of EEW: One for the general public, and the other for the special users. The EEW for the general public is transmitted through TV, radio, and mobile phones. The special advanced users will directly receive the successively renewed information from JMA and use it in their most effective way. Schools, hospitals, or plants may be able to find their best applications:

I do believe in the great potentiality of EEW, but at the same time, I understand the general dissatisfaction about EEW regarding the very short lead time and accuracies. In spite of the present shortcomings, there still are a number of fields where the EEW can be practically and effectively used for earthquake disaster mitigation.

4. NATURE DISLIKES US?

I still vividly remember the scenes in the hard-hit area in Kobe after almost 15 years. I was at a loss, because, very foolishly, I was beginning to think our structures had become strong enough to resist a most powerful earthquake like the one that devastated Tokyo and Yokohama in 1923. I could not imagine our bridges collapsing so badly. Even at that time, our building codes were reasonably well composed, we built structures with good materials and workmanship, and we thought we knew the significance of preparedness. Then, why did such a disaster take place?

The ground motion was much stronger than those previously recorded in Japan. But, it should have been expected. Because seismometers had been only sparsely located before the Kobe earthquake, we could only rarely record very strong ground motions. Structures designed according to the contemporary standards were found earthquake resistant. But, we had not paid enough attention to a large number of low-quality structures. Wooden houses had been built according to old building codes, many reinforced concrete structures had been designed taking insufficient notice of ductility, and hundreds of bridges had been constructed before we learned the lessons of the 1971 San Fernando earthquake or even those of the 1964 Niigata earthquake.

But, I do not think the root of our failures was simply scientific or technical. To get to the heart of the issue, we have to consider the circumstances surrounding the society, and the subsequent attitudes of earthquake experts. During the 70's and 80's, Japan's economy was "bubbling." "Make it faster" was a slogan of the time. After having successfully constructed the Shin-Kansen bullet train, expressways, and numerous tall buildings, we had become too much confident of what we had been doing.

Excellence accompanies arrogance. We had become arrogant and self-conceited in spite of our ignorance, and we did not try to clearly tell people what we knew as well as what we did not know. When people began to think earthquake prediction would soon become practical, scientists failed to tell people what they do under the name of earthquake prediction were simply basic studies of earthquakes. In fact, practical prediction was still very far. Engineers also mislead people. It was true we could build earthquake resistant wooden houses. But when it was wrongly interpreted wooden houses were generally strong against earthquakes, we did not rectify the difference.

The problem of earthquake disaster mitigation in Japan, especially in large cities, is huge and heavy. Urban areas are full of potentially hazardous structures. Practical earthquake prediction is difficult to make, we have millions of low-quality houses in densely built-up areas, many of them are inflammable, and the number of houses retrofitted after the Kobe earthquake is appallingly small.

Always only after a big disaster, we realize that the nature is not always kind to us, that we are so small and powerless in front of it, and that we know so little about it. I would like to emphasize that experts should try to more seriously learn the laws of nature. We should not forget that our ignorance and arrogance often magnified disasters in the past.

TRAP DOOR TESTS FOR EVALUATION OF STRESS DISTRIBUTION AROUND A BURIED STRUCTURE

HIROAKI EBIZUKA
Graduate Student
Department of Civil Engineering, The University of Tokyo, Japan
ebizuka@iis.u-tokyo.ac.jp
REIKO KUWANO
International Centre for Urban Safety Engineering,
Institute of Industrial Science, The University of Tokyo, Japan
kuwano@iis.u-tokyo.ac.jp

ABSTRACT

A trap door test apparatus is developed to evaluate the change in earth pressures acting on a buried structure in an embankment due to differential settlements. Base of a soil chamber consists of five separated blocks, any combination of those can move downward, in order to simulate the uneven settlement. Small load cells were placed on the base blocks to measure the load distribution. Change in stress and deformation within the model ground are tried to be captured also by the technique of shear wave velocity tomography using a series of bimorph piezo-ceramic elements.

1. INTRODUCTION

Earth pressures acting on underground structures are highly dependent on the interaction between ground and structure. Increase in the vertical earth pressures acting on a buried structure in high embankment should be, therefore, considered, depending on the size and depth of structure and type of foundation, since differential settlements are often expected in such conditions, as schematically shown in Figure 1. However, in practice, the increment of vertical earth pressures on underground structures is estimated in the empirical manner, mainly based on the information of past earth pressure measurements in the limited number of sites (see for example General guidelines for road earthworks, 1999). In such estimation, the degree of settlement and/or mechanical properties of backfill materials are not always taken into account.

Kuwano et al. (2007) investigated the effects of differential settlements on earth pressures acting on a buried structure in sandy soil by a series of trap door tests (see Figure 2). It was found that the size, shape and burial depth of a buried structure and mechanical properties of backfill soil are governing factors for the increment of vertical earth pressure at the top of the structure, while the construction/settlement history showed only minor effects. It was also reported that even a simple calculation, where the friction forces generated between the soil mass above the structure and surrounding soil are taken into account, can offer reasonable estimation for the increment of earth pressure. However, due to the limited performance of earth pressure transducers used in the experiment, details of the earth pressure distribution were not clearly understood.

A sophisticated trap door apparatus is newly developed in this research, in order to improve the previous study. Shear wave velocity tomography technique is also attempted in the soil chamber for the evaluation of stress and strain condition within the model ground.

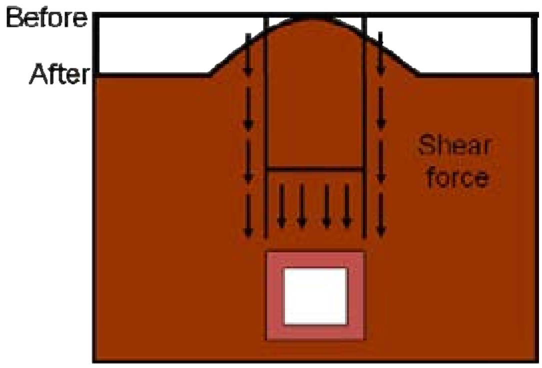

Figure 1: Increment of the earth pressure due to the uneven settlement.

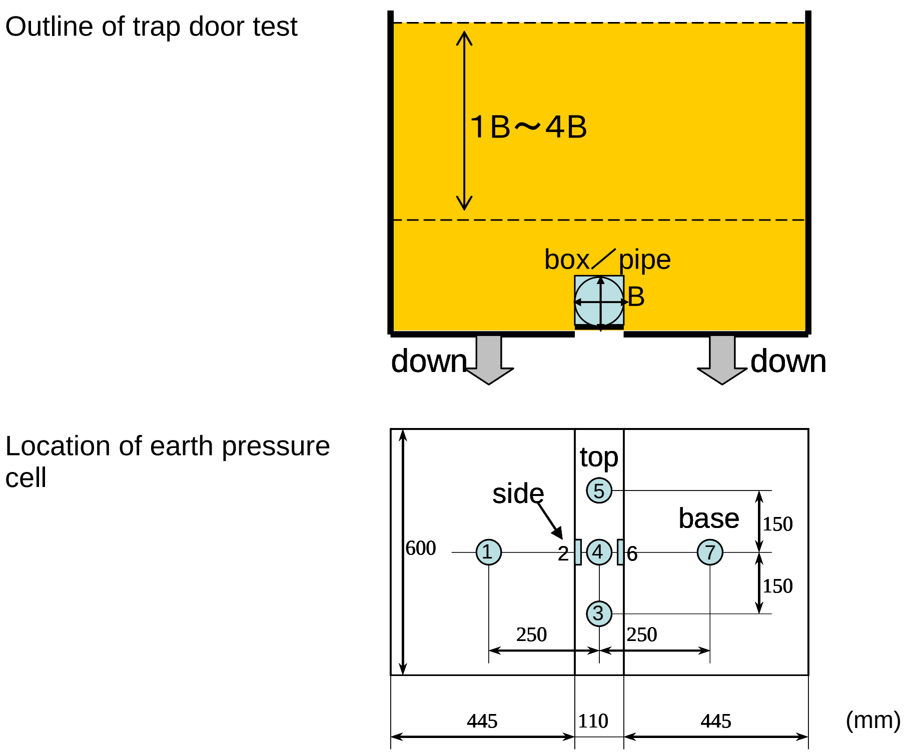

Figure 2: A soil chamber having separated moving base platens and location of earth pressure transducers (Kuwano et al.2007).

2. A TRAP DOOR APPARATUS

2.1 Soil chamber

A soil chamber for trap door testing is constructed, the inside of which is shown in Figure 3. It can accommodate model ground of 700mm wide, 294mm long and 555mm high. The base of the chamber consists of five separated movable blocks whose size is 99.8mm wide, 293.6mm long and 105mm high, and fixed parts in both sides, in order to create uneven settlement in the model ground, as schematically shown in Figure 4.

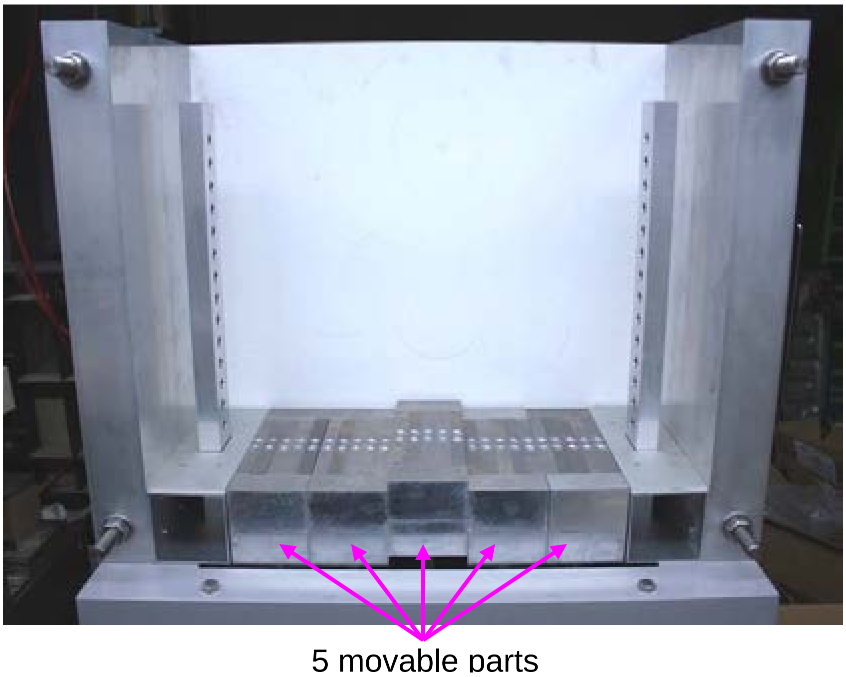

Figure 3: Inside of the soil chamber

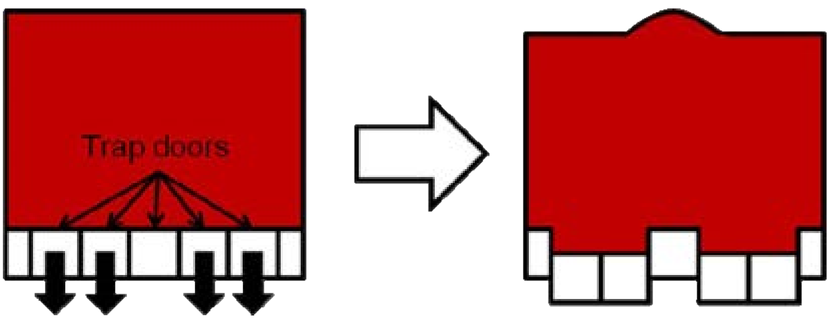

Figure 4: Reproducing an uneven settlement in model ground

Each base block is equipped with five two-way load cells to measure the load distribution on the base, as shown in Figure 5. A load cell is attached with a plate of 19.8×199.6mm. Its loading capacity is 0.3kN for both normal and shear forces.

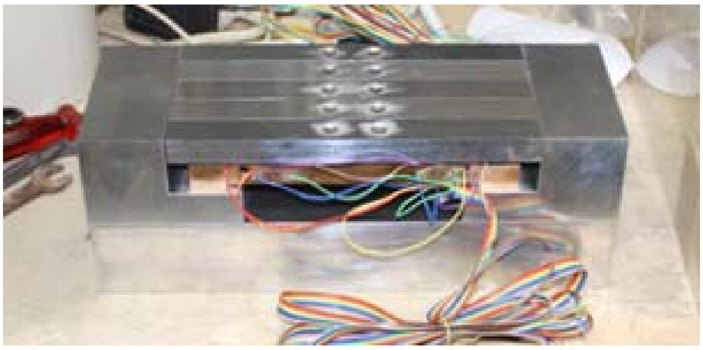

a) Base block

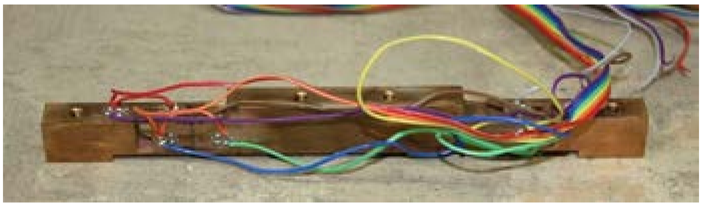

b) Load cell

Figure 5: Movable base block with small load cells

2.2 Movable base

Figures 6 and 7 present the device for the control of base blocks. Descent or ascent of the lower shaft controlled by a motor is transmitted to the upper shaft only when the upper clamp is tightened, so that any combination of blocks can be chosen to move or stay. Overall shape of the apparatus is shown in Figure 8.

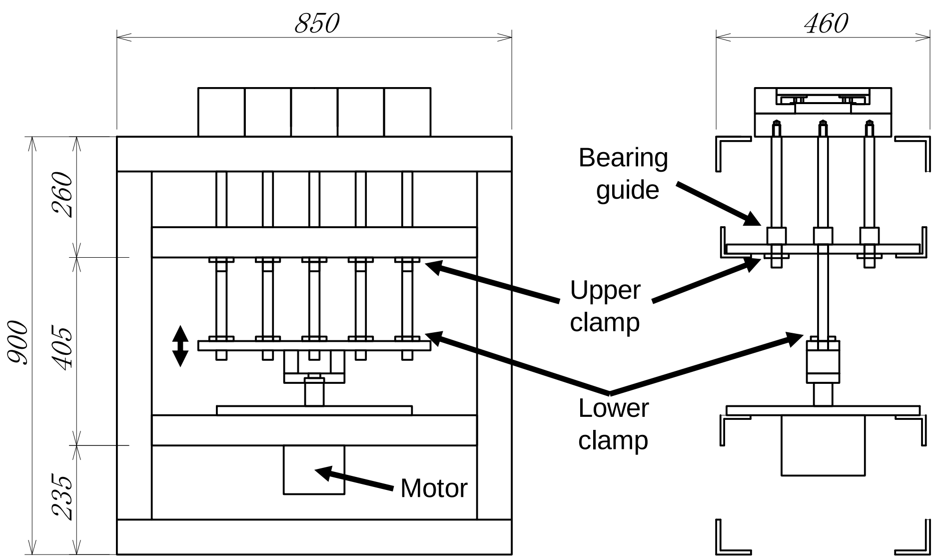

Figure6: Device for controlling movement of base block

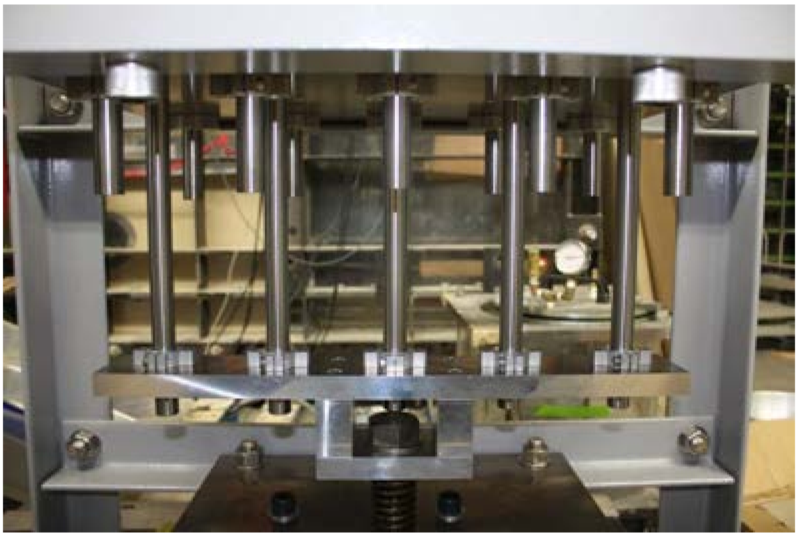

Figure7: Upper shafts and clamps

Figure8: Overall shape of the trap door apparatus

2.3 Tomography of shear wave velocity in the model ground

Tomography of shear wave velocity measurement is attempted in the model ground. Bimorph piezo-electric ceramic elements, so called bender elements, are used for transmitter and receiver of shear wave. Forty-six elements are used in total. Twenty-eight elements are placed in both sides of the model ground. Nine elements are located at the bottom and surface, as shown in Figures 9.

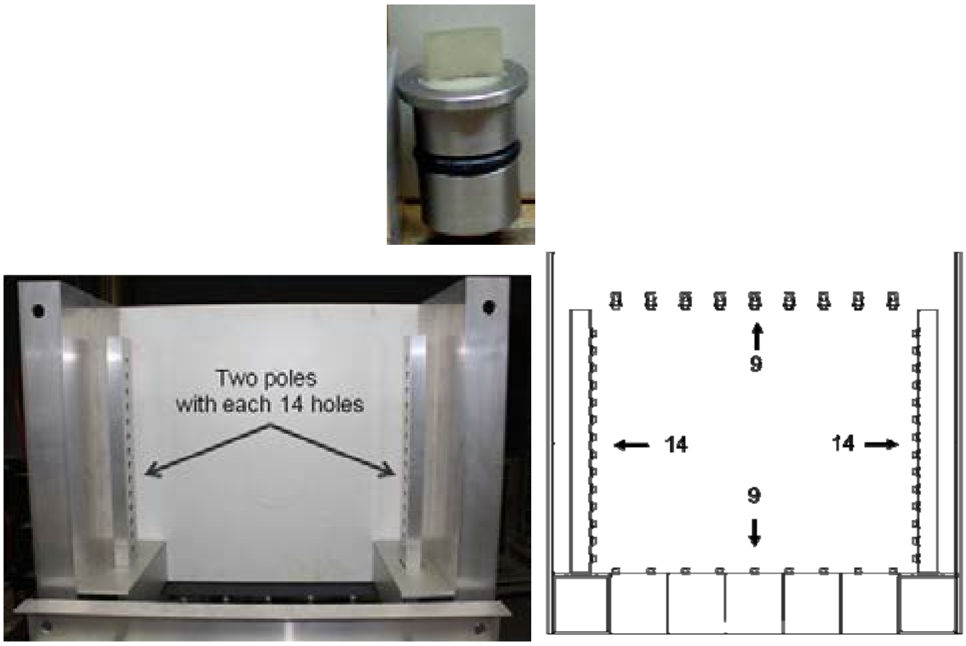

Figure 9: Bender element and its arrangement

Magnitude of shear wave velocity in soil generally reflects its small strain stiffness, which is mainly dependent on current state of density and stress. Technically speaking, then, the distribution of shear wave velocity may give some important information on the stress condition in the ground. Further study is now underway.

3. SUMMARY

A sophisticated trap door apparatus is newly developed in this study, in order to investigate effects of differential settlements on earth pressures acting on a buried structure. Shear wave velocity tomography technique is attempted for the evaluation of stress states within the model ground.

REFERENCES

General guidelines for road earthworks - culvert work -, 1999. Japan road association, ISBN 978-4889504101, Maruzen Print Co. Ltd. (in Japanese).

Kuwano, R., Horii, T. and Kohashi, H., 2007, Increment of Earth Pressure Acting on a Buried Box Structure due to Differential Settlements, *New Frontiers in Chinese and Japanese Geotechniques, Proceedings of the Third Sino-Japan Geotechnical Symposium*, 2007, 309-314.

FAILURE MECHANISM AND SEISMIC CAPACITY OF RC FRAMES WITH URM WALL CONSIDERING BEAM DEFORMATION

KIWOONG JIN
kwjin@iis.u-tokyo.ac.jp
Graduate Student, Graduate School of Eng., The University of Tokyo, Japan
HO CHOI
Institute of Industrial Science, The University of Tokyo, Japan
choiho@iis.u-tokyo.ac.jp
NORIYUKI TAKAHASHI
Institute of Industrial Science, The University of Tokyo, Japan
ntaka@iis.u-tokyo.ac.jp
YOSHIAKI NAKANO
Institute of Industrial Science, The University of Tokyo, Japan
iisnak@iis.u-tokyo.ac.jp

ABSTRACT

The objective of this study is to evaluate in- and out-of-plane seismic capacity of unreinforced masonry (URM) walls built in reinforced concrete (RC) frames. For this purpose, RC frames with unreinforced concrete block (CB) wall for typical school buildings in Korea are experimentally investigated to evaluate their failure mechanisms and seismic capacity. One-fourth scale, one-bay specimens having different boundary condition of CB walls due to beam deformation, which is considered one of important factors affecting their out-of-plane failure, are designed, and in-plane tests under cyclic loadings are carried out as a first step herein. In this paper, the failure mechanism and the load bearing capacity of overall frames due to beam deformation are discussed.

1. INTRODUCTION

In some earthquake-prone regions of Asia, Europe, and Latin America, serious earthquake damage is commonly found resulting from catastrophic building collapse. Such damaged buildings often have unreinforced masonry (URM) walls, which are considered non-structural elements in structural performance even though URM walls may interact with boundary frames as has been often found in the past damaging earthquakes.

In the past few years, the authors have conducted cyclic loading tests of full-scale reinforced concrete (RC) frames with unreinforced concrete block (CB) walls to investigate their structural characteristics including residual seismic capacity (Nakano et al., 2005). The specimens had rigid beams above and below the CB wall, as was generally employed in other experimental researches. However, experimental studies related to the effects of boundary condition of CB walls on their out-of-plane failure due to beam deformation, as well as the following strength degradation of the frame, are necessary to fully understand their seismic capacity. For this purpose, 1/4-scale, one-bay specimens having different boundary condition of CB walls due to beam deformation, which is considered one of important factors affecting their out-of-plane failure, are designed, and in-plane tests under cyclic loadings are carried out as a first step herein.

2. OUTLINE OF EXPERIMENT

2.1 Prototype building and experimental parameters

The test specimens are designed according to the standard design of Korean school buildings (referred to as "prototype building" shown in Figure 1) in the 1980's (The Ministry of Construction and Transportation, 2002), which is the same as the full-scale test previously investigated (Nakano et al., 2005). In this study, 4 specimens having different levels of axial load (first and fourth story) and different boundary conditions of beam (rigid and flexural beam) are tested under cyclic loading. Among these specimens, test results of the 2 specimens with different boundary conditions of beam under the axial load assuming a first story are discussed in this paper.

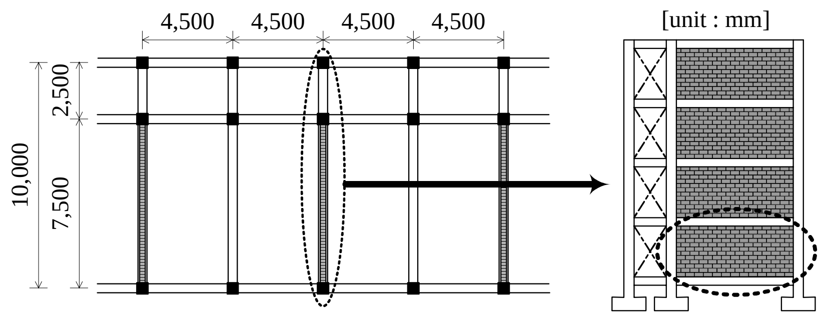

Figure 1: Standard design of Korean school buildings in the 1980's

2.2 Design of small-scale specimen

Figure 2 shows the two types of specimens. They are an infilled wall type with rigid beam (IFRB) and with flexural beam (IFFB), respectively. The design details and methods for each member are briefly described as follows.

2.2.1 *Columns and beams*

The size of column section is 1/4 of that of prototype building. The axial stress in columns, the ratio of longitudinal reinforcement, and that of shear reinforcement are almost same as the prototype building. As shown in Figure 2, the upper beam of specimen IFRB is designed to remain elastic even after the columns and CB wall fail. On the other hand, specimen IFFB

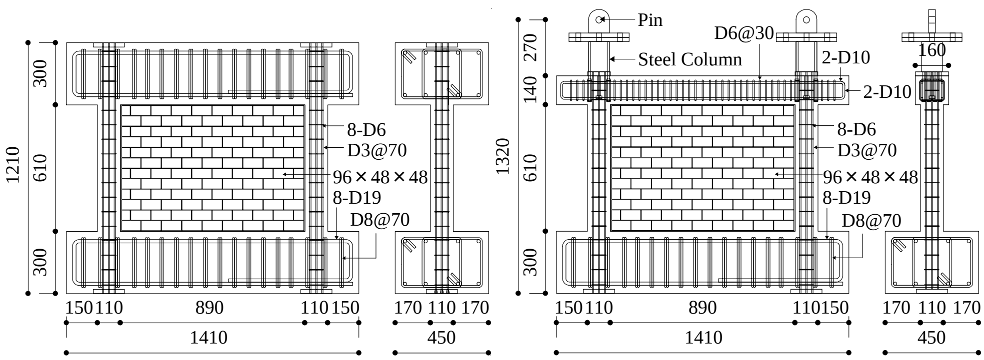

(a) *Specimen IFRB* (b) *Specimen IFFB*

Figure 2: Details of specimens (unit:mm)

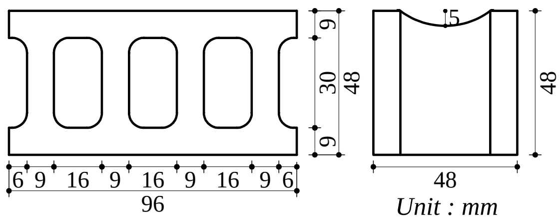

Figure 3: Details of small scale CB unit


Photo 1: Small scale CB unit

is designed to have steel columns above the upper beam to simulate the moment distribution of the prototype building (typical 4-story building) shown in Figure 1. The upper beam with a rectangular section is designed to fail in flexure, where the shear-to-flexural strength ratio (Q_{SU} / Q_{MU}) and the maximum deflection level within elastic range are both similar to those of the prototype building.

2.2.2 *Concrete Block units*

The concrete block unit is 1/4 of that of the full-scale unit. Three layered CB prism specimens are tested, where the cement-to-sand ratio is adjusted so that the strength and stiffness should be close to those of the full-scale. It has three hollows inside and a half-sized hollow on both ends as shown in Figure 3 and Photo 1.

2.3 Material test

Tables 1 through 3 show the material test results, where the values represent the average of 3 samples in each test. Although the design strength of concrete specified in the standard design of Korean school buildings in the 1980's is 21 *MPa*, the compressive strength of test pieces exceeds the design value as shown in Table 1. The yield strength of reinforcement shows higher values by 5 to 20% than the nominal strength. The compressive strength and Young's modulus from the 3 layered CB prism tests are around 90% and 50% of the full-scale CB prism, respectively. Although the Young's modulus of CB prism is not reproduced, it is found through previous investigations according to the Equations (1) and (2) (FEMA 306, 1998) that the reduction of Young's modulus does not have much effect on the shear strength V_c of CB wall, and those 1/4-scale CB units are therefore applied to the test specimens.

Table 1: Mechanical properties of concrete (Average)

Compressive strength	Elastic modulus	Split tensile strength
30*MPa*	2.1×10^4*MPa*	2.8*MPa*

Table 2: Mechanical properties of reinforcement

Bar	Use / Member	Yield strength (*MPa*)	Tensile strength (*MPa*)	Young's modulus (*MPa*)
D3 (SD390)	Hoop / Column	420	495	1.90×10^5
D6 (SD345)	Main bar / Column	365	525	2.09×10^5
D6 (SD785)	Stirrup / Flexural beam	890	1,150	2.01×10^5
D10 (SD785)	Top main bar / Flexural beam	960	1,080	1.95×10^5
D10 (SD295)	Bottom main bar / Flexural beam	360	520	2.05×10^5

Table 3: Mechanical properties of concrete block and joint mortar

Concrete block		Joint mortar
Block prism*		
Compressive strength	Young's modulus	Compressive strength
6.5 (7.3)*MPa*	1.0 (2.0)$\times10^4$*MPa*	21.6 (20.8)*MPa*

* 3 layered specimen, ( ) : Material test results of full-scale CB unit

$$V_c = W_{eq} \cdot t \cdot f_m \cdot \cos\theta \tag{1}$$

$$W_{eq} = 0.175 \cdot \left(\frac{4 \cdot E_c \cdot I_c \cdot h_m}{E_m \cdot t \cdot \sin 2\theta \cdot h^4} \right)^{0.1} \cdot l_d \tag{2}$$

where V_c is the shear force carried by the equivalent diagonal strut of CB wall, W_{eq} is the equivalent strut width, t is the thickness of CB wall, f_m is the 50% of prism strength, θ is the angle of CB wall height to length, E_c is the Young's modulus of concrete, I_c is the moment of inertia of column, h_m is the height of CB wall, E_m is the Young's modulus of CB prism, h is the column height, and l_d is the diagonal length of CB wall, respectively. The joint mortar has the cement-to-sand ratio of 1:3.5, which is generally used in Korea and the same with the full-scale specimen (Nakano et al., 2005).

2.4 Loading plan

The loading system of specimen IFFB is shown in Figure 4. For the other specimen IFRB, a steel beam is placed between the loading beam and rigid upper beam to have the same loading point with specimen IFFB. Cyclic lateral loads are applied to each specimen through the loading beam tightly fastened to the specimen.

Figure 5 shows the loading history, where a peak drift angle (R) is defined as "lateral deformation (δ) / column height (h_0=610*mm*)". As shown in the figure, peak drift angles of 0.1, 0.2, 0.4, 0.67, 1.0, and 2.0% are planned and 2.5 cycles for each peak drift are imposed to eliminate one-sided progressive failure (unsymmetric failure pattern in positive or negative loadings). It should also be noted that 0.4% loading is imposed after 1.0% to

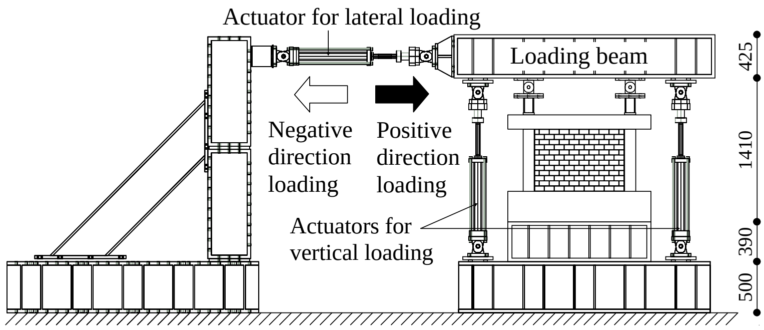

Figure 4: Test setup of specimen IFFB (Unit:mm)

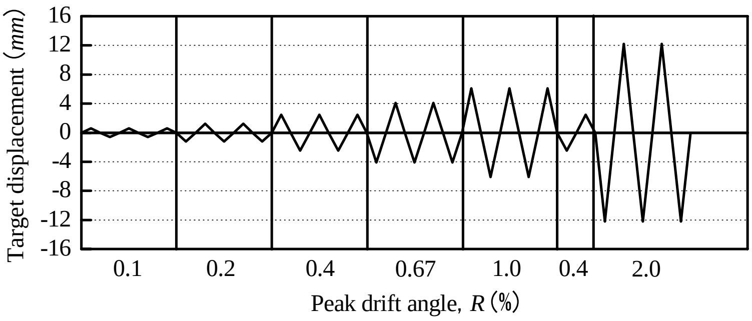

Figure 5: Loading history

investigate the effect of small amplitude loading (i.e., aftershocks) after large deformation. A constant axial load of 96*kN* is applied to each specimen.

2.5 Measurement plan

The measurement system of specimen IFFB is shown in Figure 6. The relative lateral displacement between upper and lower beams, the vertical displacement of each column, and the diagonal deformation of frame are measured. To measure the curvature distribution in columns, displacement transducers (LVDTs) are attached on both sides of each column at an interval of 150*mm*. Strains of longitudinal and shear reinforcement in columns of both specimens and in the upper beam of specimen IFFB are measured.

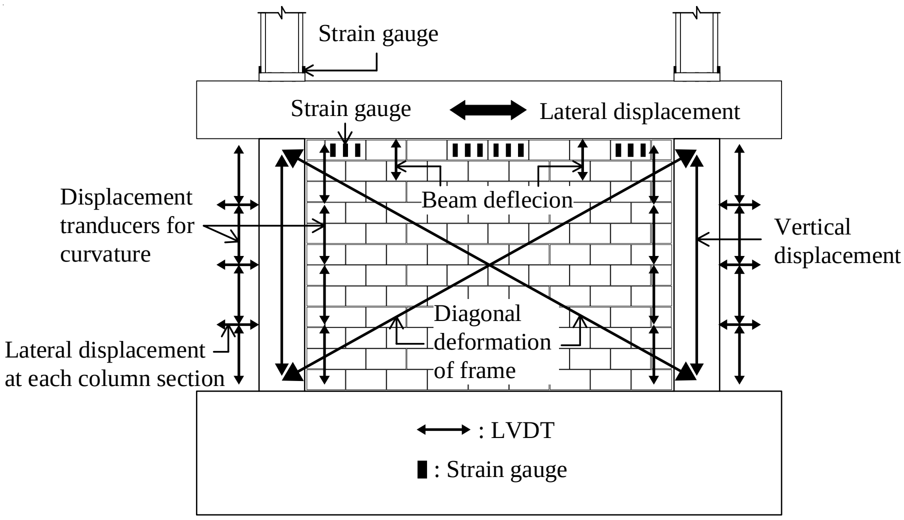

Figure 6: Measurement system (Specimen IFFB)

3. TEST RESULTS

3.1 Failure patterns

Figure 7 shows the crack patterns of both specimens at their maximum strength. The failure patterns observed in each specimen are as follows.

3.1.1 *Specimen IFRB*

Specimen IFRB has flexural cracks in RC columns and vertical and horizontal cracks in joint mortar between CB units at the first cycle with peak drift angle of +0.1%. During +0.2% loading, stair-stepped cracks in the CB wall due to diagonal strut are observed, and some cracks in joint mortar extend diagonally into CB units. Clear shear cracks at the top of tensile column and the bottom of compression column are observed at the peak drift angle of +0.4%. The crack running through the entire bed joint (horizontal joint) under the middle row of the CB wall induces slippage at the joint during -0.67% loading. Since the shear cracks at the column base of compression side rapidly open with increase in the drift angle up to -1.8%, the test is terminated during the first cycle of -1.0% loading.

3.1.2 *Specimen IFFB*

The specimen IFFB shows a failure pattern totally different from that of specimen IFRB. At the first cycle with peak drift angle of +0.1%, flexural cracks develop in columns and beam, and diagonal cracks into CB units are observed in the top row of the CB wall. Since the beam deformation causes large compressive force into the CB units at the compression corner of the wall underneath the beam, resulting in their diagonal cracks and crushing, the area of bed joint under the top row of the wall reduces and eventually the joint becomes relatively weaker than other rows. As a result, cracks causing slippage at the joint successively occur fully under the top row. It is, therefore, considered that severe damage in CB units and the following slippage at the joint caused by beam deformation imply the higher possibility of out-of-plan failure due to orthogonal excitations even in a small drift ratio. During +0.2% loading, the remaining part of CB wall under the top row acts as a diagonal strut developing stair-stepped cracks in the wall. Clear shear cracks develop in columns and beam at the peak drift angle of +0.4%. Between the peak drift angles of 0.67% and 2.0%, the damage in the beam is concentrated on its critical sections. Since the cracks at the critical sections are abruptly widened and the strains of longitudinal reinforcement in the beam significantly increase, the test is terminated at the drift angle of +3.0%.

3.2 Relation between lateral strength and drift angle

3.2.1 *Specimen IFRB*

As shown in Figure 8(a), the maximum strength of 48.6kN is recorded at the drift angle of +0.67% after the longitudinal reinforcement in columns yield at around +0.60%, and no remarkable strength deterioration is found until the drift angle of +1.0%. Shear cracks at the bottom of compression column rapidly open at the drift angle of -1.0%, resulting in sudden deterioration of the lateral load carrying capacity as shown in Figure 8(a). This specimen finally fails in shear after flexural yielding in columns.

3.2.2 *Specimen IFFB*

As shown in Figure 8(b), the yielding drift angle of the longitudinal reinforcement in the upper beam is about -0.67%, and the maximum strength of 39.8*kN* is recorded at the drift angle of +1.8% after the longitudinal reinforcement in columns yield at around +1.3%. No remarkable strength deterioration is observed until the drift angle of +3.0%.

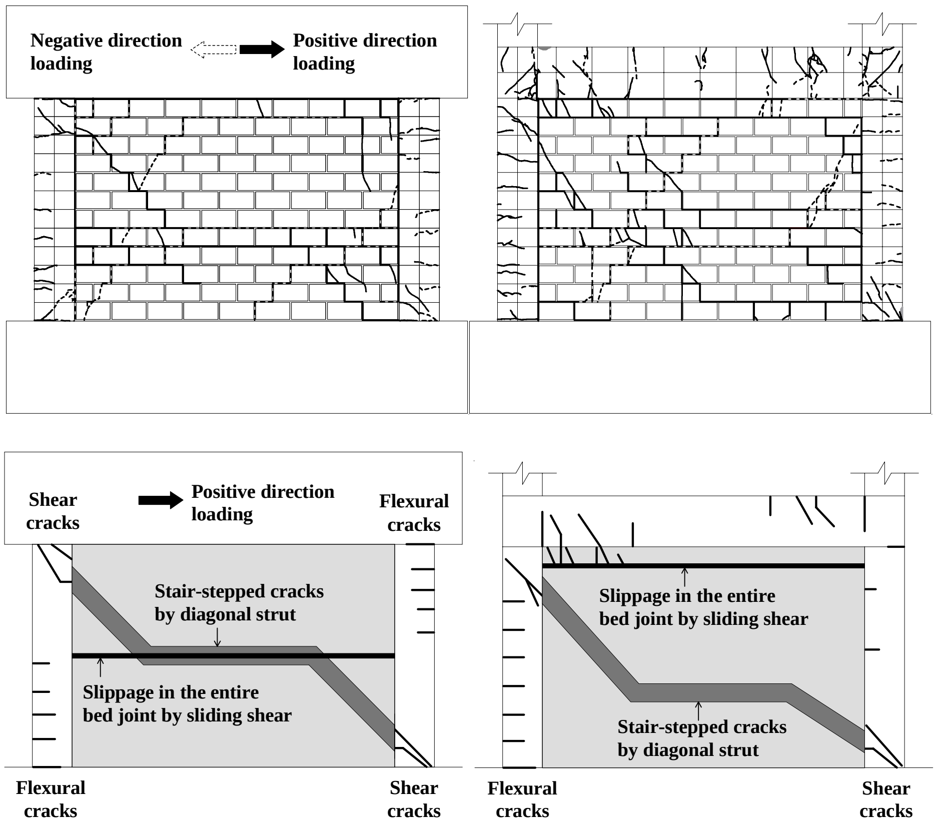

(*a*) *Specimen IFRB* (+0.67%) (*b*) *Specimen IFFB* (+2.0%)

Figure 7: Crack patterns at maximum strength

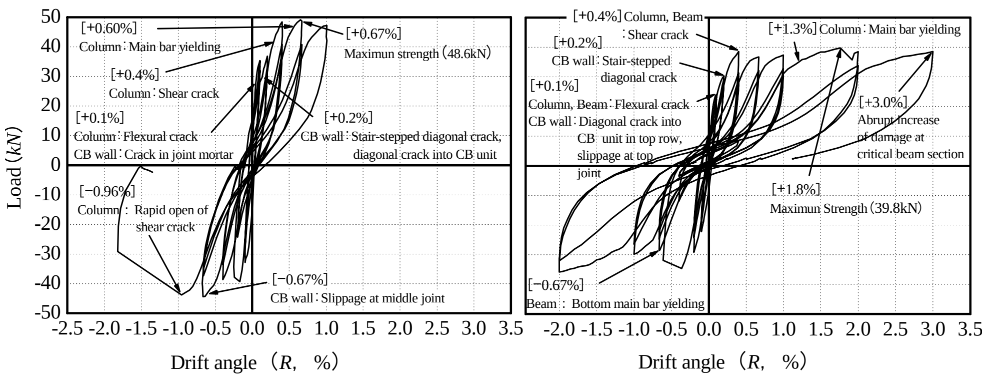

(*a*) *Specimen IFRB* (*b*) *Specimen IFFB*

Figure 8: Lateral strength and drift angle relation

4. MAXIMUM STRENGTH OF OVERALL FRAME

4.1 Maximum strength evaluation based on column moment distribution

4.1.1 *Specimen IFRB*

Figure 9(a) shows the curvature distribution and yield hinge zones in both columns, where measured strains of main bars exceed the yield strain. They are formed over a distance of column depth *D* (110*mm*) at both ends in each column, and their bending moment distribution assumed from the hinge formation is also shown in the figure. The flexural strength Q_{MU} (23.6*kN*) of each column is evaluated by $2M_U$ / 3.5*D*, where the ultimate bending moment M_U of columns is calculated based on the plane-section assumption setting the ultimate strain ε_{CU} at the compression fiber of concrete equal to 0.003 with an equivalent rectangular stress block coefficient 0.85. The overall lateral strength *P* derived from the assumptions above agrees well with the recorded capacity as shown in Figure 10 (a).

4.1.2 *Specimen IFFB*

The curvature distribution and yield hinge zones in both columns are shown in Figure 9(b). They are formed over the height of 4.0*D* at the bottom of tensile column and 1.0*D* at the bottom of compression column, respectively. The bending moment distribution assumed from the yield hinge formation is also shown in the figure. The bending moments at the beam-column joints are determined to meet the moment equilibrium, where the beam end at the top of

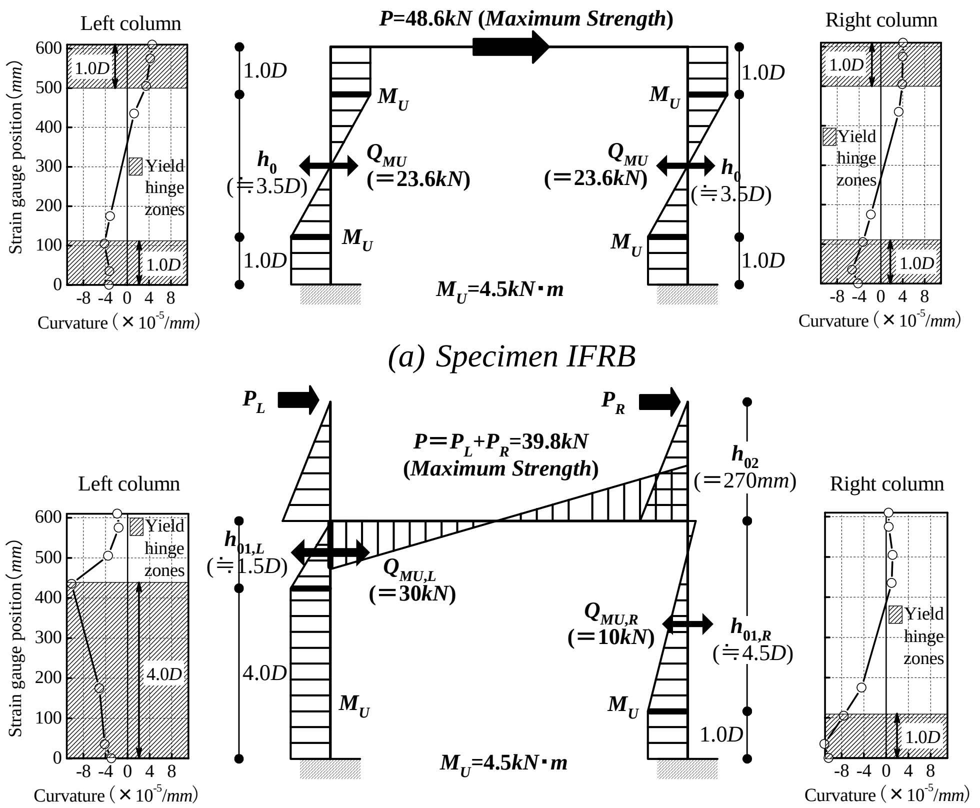

(a) Specimen IFRB

(b) Specimen IFFB

Figure 9: Curvature of columns and moment distribution at maximum strength

tensile column is assumed yielded while the moments at the bottom of upper steel columns and at the column top in compression side are derived from observed strains, which remain elastic throughout loadings. The ultimate bending moment of the beam end is calculated based on the same assumption with that of the column of specimen IFRB, where the tensile axial load (-10.5*kN*) acting in the beam is considered. The flexural strength Q_{MU} in each column is then calculated considering the rest span length (1.5*D* in the tensile column and 4.5*D* in the compression column) above yield hinge zones as shown in Figure 9(b). The overall lateral strength *P* considering the column hinge zones agrees well with the recorded capacity as shown in Figure 10(b).

4.2 Maximum strength estimation by practical method

In the previous section, the overall lateral strengths of RC frames with CB wall are evaluated according to the observed moment (or curvature) distribution in columns. In the design stage, however, the moment distribution discussed earlier based on the curvature profile is not given and the lateral strength can not be predicted as is done in this study. A simplified strength

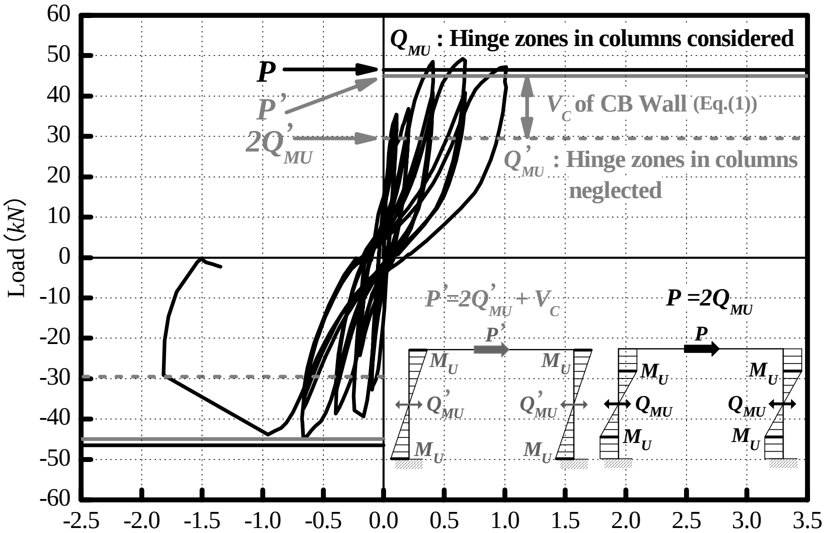

(a) Specimen IFRB

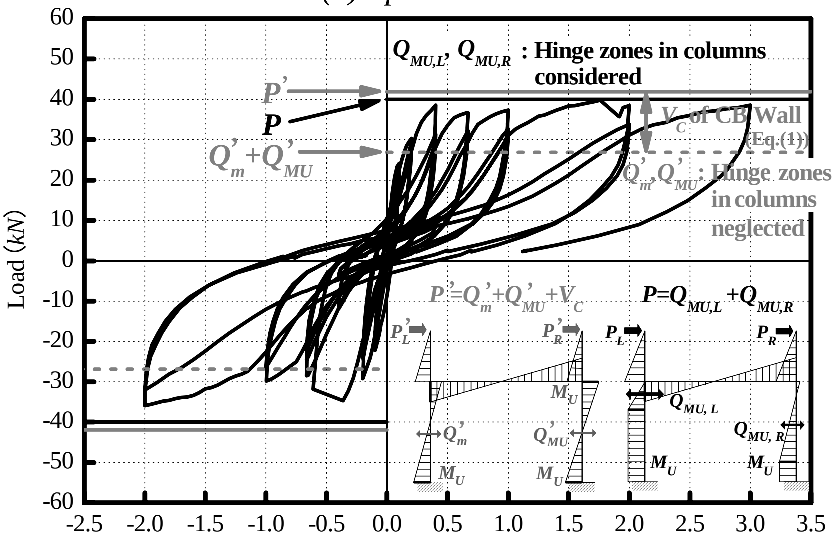

(*b*) *Specimen IFFB*

Figure 10: Maximum strength of overall frame

evaluation of the specimens is, therefore, made based on the FEMA 306 (1998), where the strength is calculated from column moments neglecting hinge zones resulting from the presence of CB wall.

In the simplified evaluation, the ultimate strength of the bare frame is first calculated, and the shear force V_C contributed by CB wall is then added to the strength above to obtain the overall strength. For specimen IFRB, as shown in Figure 10(a), yield hinges are assumed at both column ends, and the column strength Q'_{MU} is computed by $2M_U$ / 610*mm* (column height), where M_U is defined in subsection 4.1.1. For specimen IFFB, as shown in Figure 10(b), the column strength Q'_{MU} in compression side is obtained by the same assumption with that of specimen IFRB, while the yield hinge is assumed both at the beam end and at the column bottom to obtain the strength Q'_m in tensile side. The ultimate bending moment at beam end, where the tensile axial load (-2.3*kN*) acting in the beam is not taken into account for the practical estimation because of its negligible effect on the beam strength and accordingly column strength, is distributed to the top of tensile column in accordance with the elastic moment distribution ratio at its top and the bottom of steel column. The shear force V_C (15*kN* for both specimens) of CB wall carried by the equivalent diagonal strut is computed by Equation (1) (FEMA 306, 1998). The sum of shear forces of the bare frames and CB walls, plotted in Figure 10, shows good agreement with the recorded maximum strength of overall frames in both specimens.

5. CONCLUSIONS

Seismic performance of RC frames with unreinforced CB wall for standard Korean school buildings were experimentally investigated under cyclic loadings. The major findings can be summarized as follows.

(1) Because of beam deformation above CB wall and resulting different yield hinge zones, the moment distribution in columns and load bearing capacity of specimen IFFB are totally different from those of specimen IFRB. It should also be noted that severe damage in CB units and slippage at the joint is developed in the early stage of loading due to beam deformation in specimen IFFB, and it implies the higher possibility of out-of-plan failure even in a small drift ratio when the beam is not fully rigid.
(2) The maximum strength evaluated by the moment distribution along columns considering hinge zones agrees well with the load bearing capacity recorded in both specimens.
(3) A simplified method consisting of the bare frame strength neglecting hinge zones and the contribution of CB wall computed based on FEMA 306 (1998) can successfully predict the load bearing capacity of overall frame.

REFERENCES

The Ministry of Construction and Transportation, 2002. A Study on the Seismic Evaluation and Retrofit of Low-Rise RC Buildings in Korea (in Korean).
Nakano, Y. and Choi, H., 2005. Experimental Study on Seismic Behavior and Crack Pattern of Concrete Block Infilled RC Frames. *New Technologies for Urban Safety of Mega Cities in Asia (USMCA),* ICUS/INCEDE Report 2, Singapore.
FEMA 306, 1998. *Evaluation of Earthquake Damaged Concrete and Masonry Wall Buildings*. Applied Technology Council (ATC-43 Project).

A CASE STUDY OF GROUND CAVE-IN CAUSED BY SUBSURFACE EROSION IN LARGE SCALE FILL GROUND

REIKO KUWANO
International Centre for Urban Safety Engineering,
Institute of Industrial Science, The University of Tokyo, Japan
kuwano@iis.u-tokyo.ac.jp
YUKIHIRO KOHATA
Department of Civil Engineering and Architecture
Muroran Institute of Technology, Japan
kohata@news3.ce.muroran-it.ac.jp

ABSTRACT

Ground cave-in is usually initiated by the formation of cavity within the ground due to soil loss. When the location of the cavity is deep in the ground, the detection of the cavity is not easy. Then it is possible that the hidden cavity expands for a long time to eventually cause sudden large-scale collapse.

A case of large scale ground collapse in the old fill ground was studied and described in this paper. The underground cavity appeared to be caused by subsurface erosion deep in the ground and to expand/extend upward till it was ended by the catastrophic ground failure. It highlighted the importance of proper drainage work in a large scale land fill.

1. INTRODUCTION

A sudden collapse of the ground occurred in the 8th fairway at the Le Petaw golf course in Hokkaido on April 2, 2009, when a woman golfer unfortunately stepped on it. She fell into a hidden hole formed underneath the ground and by the time a rescue team arrived she had passed away.

The hole was 5m deep and 7m wide at the bottom. Although the golf course was daily checked by maintenance staff, they could not get any sign of the hidden hole even in the morning of the accident. The ground collapse seemed to have happened all of sudden, as the victim's son who walked just a couple of meters behind her saw her suddenly disappearing into the ground.

A detailed investigation took place by Hokkaido prefectural police, assisted by the authors. This paper reports findings in the investigation, based on which the mechanism of the hidden cavity formation is discussed.

2. OUTLINE OF THE COLLAPSE

2.1 Topography and ground condition

The golf course was originally built more than 15 years ago in hilly land, by filling a valley with local soil. The ground consists of mud rock covered with silty volcanic ash. The thickness of the land fill seems to be 10 to 15 meters. The surface layer of about 0.5m was added fertile soil for the growth of lawn. It is a gentle slope in the 8^{th} fairway and there used to be a stream along the east-west direction at the location of the collapse. Although the exact locations are not identified, drain pipes should be installed underground to carry away the subterranean water while preventing soil from seeping out. There are several artificial ponds around the fairway for water hazards in the course, as shown in Figure 1. When the accident occurred, the ground water level was considered to be higher than usual, as it was the thawing season.

Figure.1 Photo at the location of collapse (after Asahi Newspaper 090417)

2.2 Underground cavity

The hidden hole had a flask shape with a 1 m wide opening at the ground surface (see Figure 2), and was 5m deep and 7m wide at the bottom. There was an about 0.6m deep shallow water pool in the east side of the hole, and the water flew to the west direction. Noticeable erosion was found in both west and east sides at the bottom as schematically shown in Figure 3.

The volume of the soil for the cavity is about $75m^3$. One of the questions is that where such amount of soil went. There is a water reservoir in the down stream of the 8^{th} fairway as shown in Figure 4, where large amount of soil sediment was found. It may be the possible destination of the soil flown from the cavity.

Figure.2 Opening at the ground surface (from Hokkaido Newspaper)

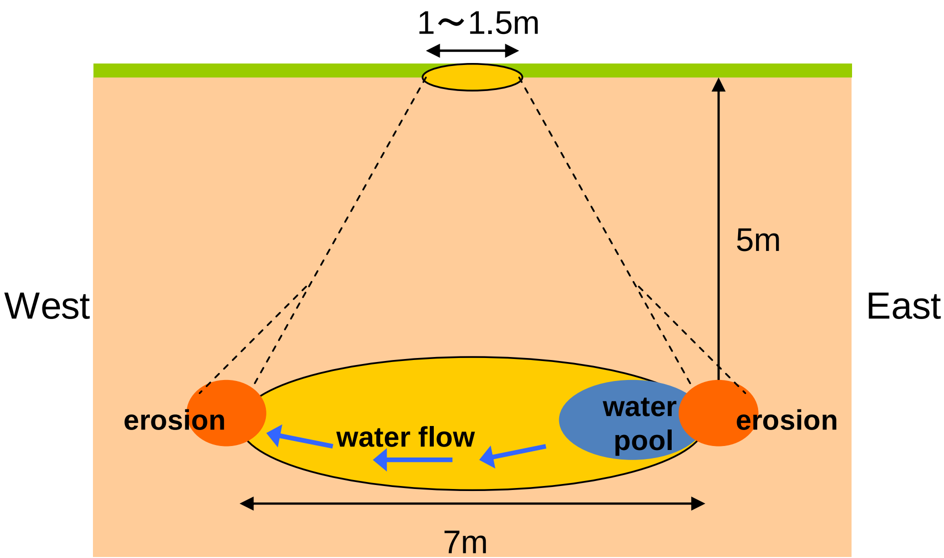

Figure.3 Schematic of the underground cavity

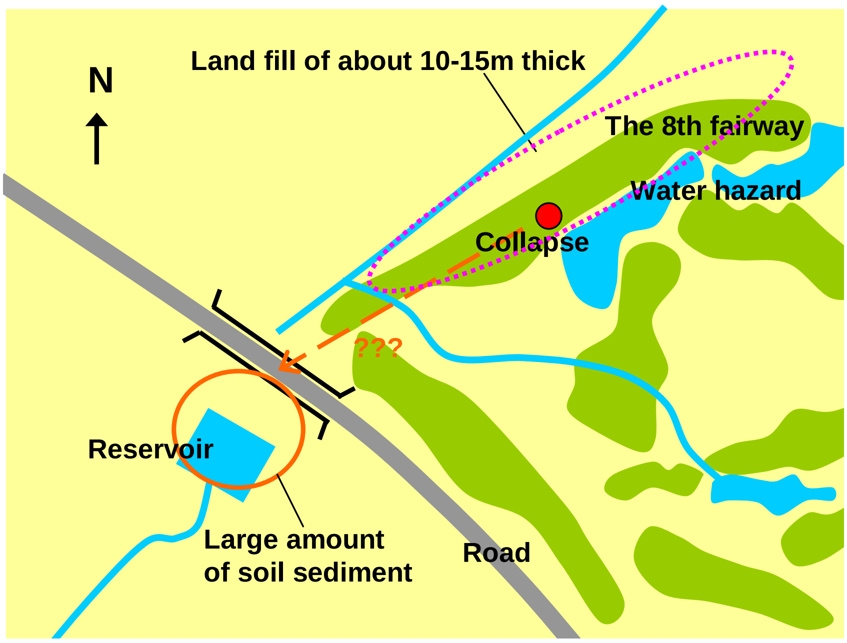

Figure.4 Possible destination of the lost soil

3. INVESTIGATION BY EXCAVATION

A large scale excavation was carried out around the hole to understand how and why such a huge underground cavity was created. Soil sample was taken from three locations to characterize their physical properties.

3.1 Soil pipe discovered beside the hole

Figure 5 is a photo of excavation. Excavated soil was mixture of volcanic clay, silt, sand, and relatively small gravel, as shown in Figure 6. Roots of plants were also included, which indicates the excavated strata was filled soil.

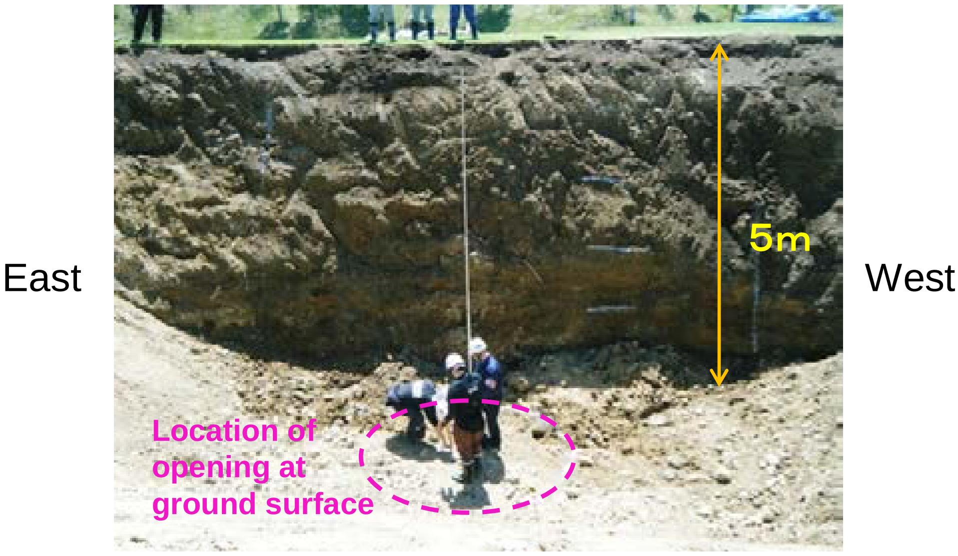

Figure.5 Excavation around the hole

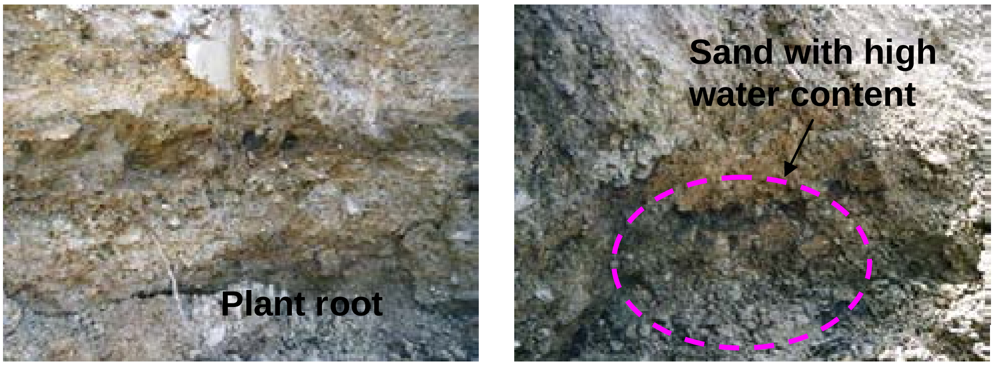

Figure.6 Soil in the excavated wall (GL-approx.6m)

At the depth of 8m from the ground surface, there was the boundary between original stiff ground and filled soil, where a lateral ground cavity of about 2m wide was discovered in about 20m west from the center of the hole, as shown in Figure 7. The sound of water flow was clearly heard in the cavity. The length of the cavity was at least 6m, but could not be confirmed as the further excavation was not conducted. It seemed to be a path through which soil with water was transported out of the hole.

Figure.7 Natural soil pipe due to the internal erosion

3.2 Search for the destination of the water flow in the soil pipe

Water colored by fluorescent paint was poured into the cavity to search for the destination of the water flow in the soil pipe. After 20 minutes, the colored water started flowing out at the reservoir, 700m down from the cavity. It can be considered that a soil pipe is formed in the ground between the collapsed location and the reservoir (see Figure 4).

3.3 Location of the water inflow

In the excavation on the east side, the point where the water flew into the hole was found at about 10m away from the center (Figure 8).

Figure.8 Water inflow at the east side of the hole

4. ESTIMATION OF UNDERGROUND CAVITY FORMATION

Comparison between old and current map of the location revealed that the ground collapse occurred at the land fill exactly on the old stream, as shown in Figure 9. The locations of the water inflow and outflow were identified at east and west side of the hole respectively.

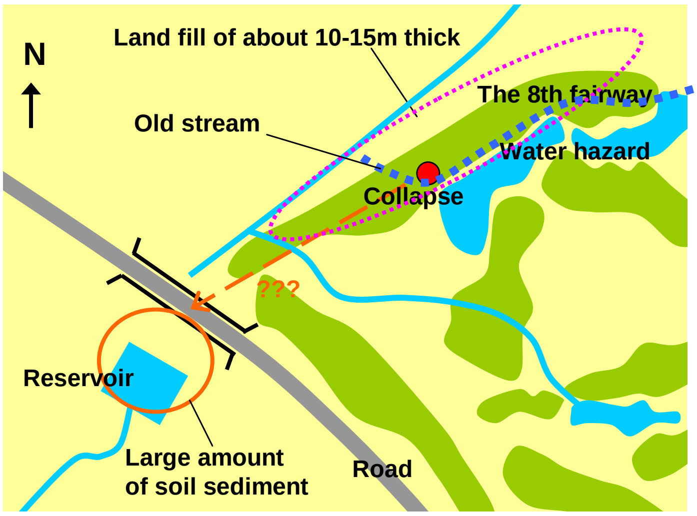

Figure.9 Location of the old stream

Ground appeared to be internally eroded by the natural water path formed at the old stream. It is like a natural drainage pipe, so that it is called soil pipe. As the erosion of the soil at the location of the collapse seemed to be accelerated for some reason, a distinctive ground cavity was created. The hidden cavity grew silently, possibly due to the change of ground water level and eventually caused ground collapse. Such a process is schematically shown in Figure 10. However, the state and the condition of the installed drainage pipes are not yet examined. Further investigation is required in this aspect.

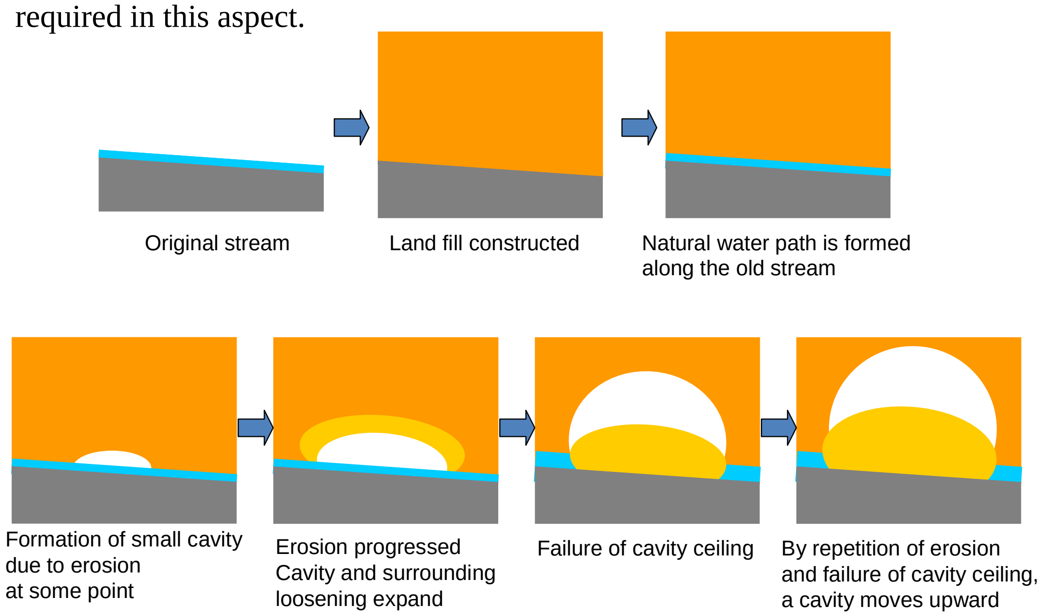

Figure.10 Formation of underground cavity

Kuwano et al. (2006), Sato & Kuwano (2008), Kuwano & Sato (2009) investigated the mechanism of ground cavity and surrounding loosening due to the failure of sewer pipes. It was found that the state of water infiltration and soil properties are the governing factors for the growth of the ground cavity and loosening, while the failure of pipe is a trigger of the phenomenon. Based on the research, the followings are considered to be key issues for explaining the formation of large underground cavity in this case.

(1) Soil properties

The soil was permeable, subjected to the erosion relatively easily. Fines can be first flown away with water, which created ground loosening around the cavity.

(2) Ground water

There was a subsurface water path which can transport soil out of the hole with water. There is also seasonal change in ground water level, which may accelerate the cavity growth as the saturation of soil at the ceiling helps failure and expansion of the cavity.

(3) Soil loss

Direct trigger of the formation of natural water path may be a defect of drainage pipe. But the state and the current condition of the pipes have not yet examined.

5. SUMMARY

A case of large scale ground collapse in the old fill ground was investigated and described in this paper. The underground cavity appeared to be caused by subsurface erosion deep in the ground and to expand upward till it was eventually caused the catastrophic failure. It should be noted again the importance of proper drainage work in land fill construction.

REFERENCES

Kuwano, R., Horii, T., Kohashi, H. and Yamauchi, K., 2006, Defects of Sewer Pipes Causing Cave-in's in the Road, *Proc. 5th International symposium on new technologies for urban safety of mega cities in Asia,* USMCA, Phuket, November 2006.

Sato, M. and Kuwano, R., 2008, Experimental Study on the Evaluation of Loose Ground Surrounding a Cavity in Soil, *Proc. 7th International symposium on new technologies for urban safety of mega cities in Asia*, USMCA, Beijing, October 2008, 751-758.

Kuwano,R. and Sato,M., 2009, Basic study for prevention of ground cave-in, *Seisan Kenkyu, Bimonthly Journal of Institute of Industrial Science*, The University of Tokyo, Vol.61, No.4, 57-61 (in Japanese).

SEISMIC FRAGILITY FUNCTION FOR UNREINFORCED MASONRY BUILDINGS IN KOREA

Jung-Han LEE, Hye-Won KIM, Byung-Cheol PARK and Waon-Ho YI
Structural Safety Research Team,
National Institute for Disaster Prevention, Korea
ljhunk@nema.go.kr

ABSTRACT

The objectives of this research are to evaluate the seismic fragility curve and function for "Slight", "Moderate", "Extensive", "Complete" structural damage states of URM buildings including the major parameters such as the interstory drift at threshold of damage state and spectral displacement in HAZUS and to develop the seismic fragility function of the existing unreinforced masonry buildings in Korea. To develop the seismic fragility function of the existing URM buildings in Korea, capacity spectrum analysis of the URM building using the Midas GEN Ver.741 is surveyed. From the capacity spectrum analysis results, spectral displacements for 4 kinds of damage state adopting the suitable drift ratio of damage state in Korea are suggested, and the seismic fragility function for existing URM building in Korea is developed.

1. INTRODUCTION

In worldwide, huge casualty and economic losses are steadily occurred with collapsing of the unreinforced masonry buildings due to the earthquakes. The crustal activity does not affect directly to the Korea different from the Japan, China and there is no experience of destructive earthquakes in the past. Also, countermeasures against earthquake disasters such as the damage estimate and disaster reduction measures have not been fully performed. However, with more than eight hundred earthquakes with medium intensity that centered on off-coastal and inland areas of Korea during the past 31 years, and due to the great earthquakes which occurred recently in neighboring countries, such as the 1995 Hyogoken-Nambu Earthquake with more than 6,500 fatalities in Japan, the 1999 Chi-Chi Earthquake with more than 2,500 fatalities in Taiwan, and the 2008 Sichuan Earthquake with more than 69,000 fatalities in China, the importance of the future earthquake preparedness measures is highly recognized in Korea. In many countries, most of the residential buildings are constructed with unreinforced masonry. More than 46 percent of buildings in Korea are constructed using unreinforced masonry. Unreinforced masonry buildings have advantages of reducing the construction time and are easy to construct. However, unreinforced masonry buildings have limited strength against lateral forces.

Moreover, most of low rise buildings have not adopted seismic designs, and for that reason, critical damage can be expected with an earthquake.
Therefore the preparedness of the damage estimate and disaster reduction measures for the unreinforced masonry buildings which accounted for the majority of residential buildings is needed for the future earthquakes.

2. PREVIOUS RESEARCH

From the previous research(Yi, W.H., et. al; 2006), a survey on 98 URM buildings in Seoul is executed by dividing URM buildings into single-family housing, multi-family housing, and neighborhood facilities. Thereby it identifies the distribution of floor number and height; gross floor area; wall length; wall quantity and ratio; and opening ratio. Based on the result of the survey, for a modular planning, data about wall and opening length is extracted from the investigation by types, area-scales, and room configurations, and proposed are 2 types of a standard drawing for each type and a design standard for future URM buildings. Because the construction accuracy of URM buildings is very low and does not meet the current standard, to improve their seismic performance, a large scale of repair-reinforcement would be necessary. Previous research including the shaking table tests surveyed by Kim, J.K., (1999) and Kwan, K.H., (2001) are investigated to evaluate the damage status, drift ratio and the other vibration characteristics for the unreinforced masonry buildings. From the shaking table tests results, damage status and drift ratio at damage are quite different from the HAZUS. And, to evaluate the main variables such as the response modification factor and the period equation for the seismic design and seismic capacity evaluation of the unreinforced masonry buildings, previous research and codes are investigated. From the investigated results, 1.5 of response modification factor and $0.049Hn^{(3/4)}$ of period equation suggested from the KBC-2005 are more appropriate to use.

3. DEVELOPMENT OF SEISMIC FRAGILITY FUNCTION FOR URM BUILDINGS

3.1 Fragility Curve by Using HAZUS Classification

In HAZUS, 36 model building types that are used by the methodology are defined. These model building types are based on the classification system of FEMA 178, NEHRP Handbook for the Seismic Evaluation of Existing Buildings [FEMA, 1992]. And 4 kinds of damage state such as “Slight”, “Moderate”, “Extensive” and “Complete” are defined in each structural type. From the mean value of spectral displacement at which the building reaches the threshold of damage state and the standard deviation of the natural logarithm of spectral displacement for the damage state, seismic fragility curve.

$$S_d = \bar{S}_{d,ds} \cdot \varepsilon_{ds} \quad (1)$$

Where, $S_{d.ds}$: Median value of spectral displacement of damage state, ds
ε_{ds} : Lognormal random variable with unit median value and logarithmic standard deviation,

The conditional probability of being in, or exceeding, a particular damage state, d_s, given the spectral displacement, S_d, (or other PESH parameter) is defined by the function:

$$P\left[ds \middle| S_d\right] = \Phi\left[\frac{1}{\beta_{ds}} \ln\left(\frac{S_d}{\bar{S}_{d,ds}}\right)\right] \quad (2)$$

Where, $\bar{S}_{d,ds}$: Median value of spectral displacement at which the building reaches the threshold of damage state,
β_{ds} : Standard deviation of the natural logarithm of spectral displacement for damage state,
Φ : Standard normal cumulative distribution function

It is considered that the material nonlinear by a wide use structural analysis program. It can be evaluated the capacity spectrum curve for URM buildings by the capacity spectrum analysis in this chapter. It is estimated that the drift ratios of damage states and spectral displacement for buildings by the capacity spectrum results. It is also estimated that the medium values and seismic fragility curve by using the spectral displacement. It is developed that the suitable seismic fragility curve for URM and estimated the adequacy of seismic fragility curve computing solution in Korea by comparison and analysis of HAZUS and derived one.

Table 1: Parameter of Fragility Curve in Pre-Seismic Code of Analytic Example

Type	Interstory Drift at Threshold of Damage State				Spectral Displacement, inches (cm)							
	Slight	Moderate	Extensive	Complete	Slight		Moderate		Extensive		Complete	
					Median	Beta	Median	Beta	Median	Beta	Median	Beta
URML	0.0024 (1/417)	0.0048 (1/208)	0.0120 (1/83)	0.0280 (1/36)	0.32 (0.81)	1.15	0.65 (1.65)	1.19	1.62 (4.11)	1.20	3.78 (9.60)	1.18

3.2 Seismic Fragility Curve by Using CSM

3.2.1. Verification of Analyzed Program

In this research, the application is verified through comparison and analysis of practiced experimental results and analytical them of URM by midas GEN Ver.741. Analytical results are also compared with the experimental results of 10 unreinforced masonry walls practiced by W. H. Yi (2003, 2006) to verify the midas program. Representative comparison specimens are totally 10 unreinforced masonry walls. The list of specimens and experimental results are shown in Table 2, and 3.

Table 2: Specimen List

Label	Size (h×l)	Aspect Ratio (h/l)	Wythe (t)	Axial Stress (MPa)	Opening (h×l)
270W-1F	2.7m×2.7m	1.00	1.0B(190mm)	0.086	-
270W-2F	2.7m×2.7m	1.00	1.0B(190mm)	0.250	-
270W-2F-0.5B	2.7m×2.7m	1.00	0.5B(90mm)	0.250	-
270W-2F-W	2.7m×2.7m	1.00	1.0B(190mm)	0.250	window (1.2×1.5m)
270W-2F-D	2.7m×2.7m	1.00	1.0B(190mm)	0.250	door (2.15×1.0m)
120W-2F	2.7m×1.2m	2.25	1.0B(190mm)	0.250	-
180W-2F	2.7m×1.8m	1.50	1.0B(190mm)	0.250	-
360W-2F	2.7m×3.6m	0.75	1.0B(190mm)	0.250	-
400W-2F	2.7m×4.0m	0.68	1.0B(190mm)	0.250	-
540W-2F	2.7m×5.4m	0.50	1.0B(190mm)	0.250	-

Table 3: Maximum Load of Experimental and Analytical Results of Specimens

Specimen	Variables	Maximum Load (kN)		
		Analytical Results	Experimental Results	Ratio of Exp. and Ana.
270W-1F	Vertical Load	84.14	81.43	1.03
270W-2F	Prototype	136.12	134.36	1.01
270W-2F-0.5B	Wythe	103.75	106.44	0.97
270W-2F-W	Opening (w/wo)	49.72	50.88	0.98
270W-2F-D		73.65	57.78	1.27
120W-2F	Aspect Ratio	35.89	35.08	1.02
180W-2F		63.43	59.73	1.06
360W-2F		195.84	179.16	1.09
400W-2F		192.90	199.07	0.97
540W-2F		277.53	268.75	1.03

It is applied the pushover analysis of URM walls by midas GEN Ver.741. URM walls are modeling by nonlinear beam elements, and it is applied that axis stress and material properties of URM walls equal with values of specimens. The hinge property of pushover determined ratios of ductility and yield through trial and error method from the experimental results values. The type of buildings is existing buildings and the prism press strength applies 6.18 MPa that is result value of material experiment. In case of the value of shear strength for URM, it is determined 0.14 MPa from results of existing material experiment and URM walls experiment through trial and error method.

3.2.2 Seismic Fragility Curve

To develop the seismic fragility curve, it is selected an analysis piece of URM buildings in order to deduce a seismic fragility curve of them in domestic and then achieve the pushover analysis. From the results of pushover, it calculates the average spectral displacement of each damage conditions. Each damage conditions is called "Slight", "Moderate", "Extensive", and "Complete" which is presented by HAZUS. It calculates the average spectral displacement through the application of story drift ratios of HAZUS and Korea Infrastructure Safety and Technology Corporation (KISTC). From the computed average spectral displacement and standard deviation, the seismic fragility curve is deduced. It is required the definition of spectral average displacement and standard deviation through basic story drift ratios as damage conditions by deducing the seismic fragility curve. In internal URM buildings, it is hardly applied the HAZUS to internal situation because it is different from structural systems and construction materials of U. S. URM buildings. So it is proper an application to employ KISTC guaranteed. It would be compared with the results of story drift ratios by two kinds of damage states were shown in Table 4. Fig. 1~3 show the spectral displacement from pushover analysis.

Table 4: Story Drift Ratios of Each Damage Conditions

	Slight	Moderate	Extensive	Complete
HAZUS	0.0024(1/417)	0.0048(1/208)	0.0120(1/83))	0.0280(1/36)
Standard of Domestic	0.0020(1/500)	0.0040(1/250)	0.0067(1/150)	0.0100(1/100)

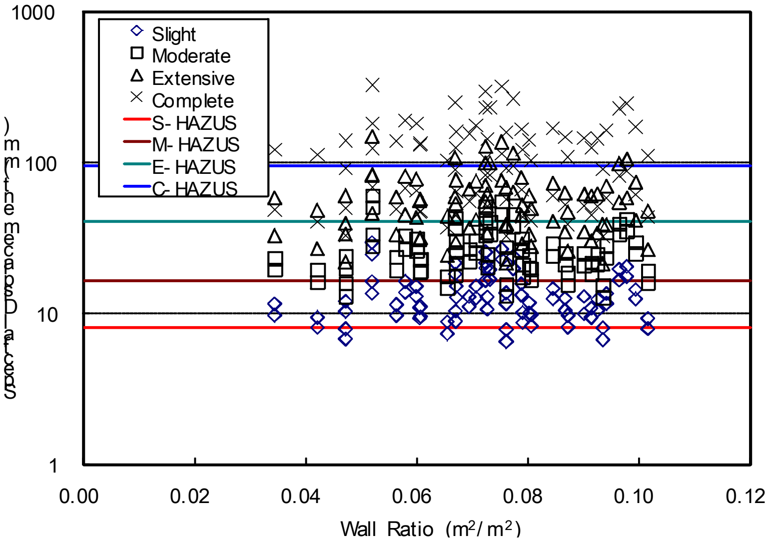

Figure 1: Entire Spectral Displacements during Damage States

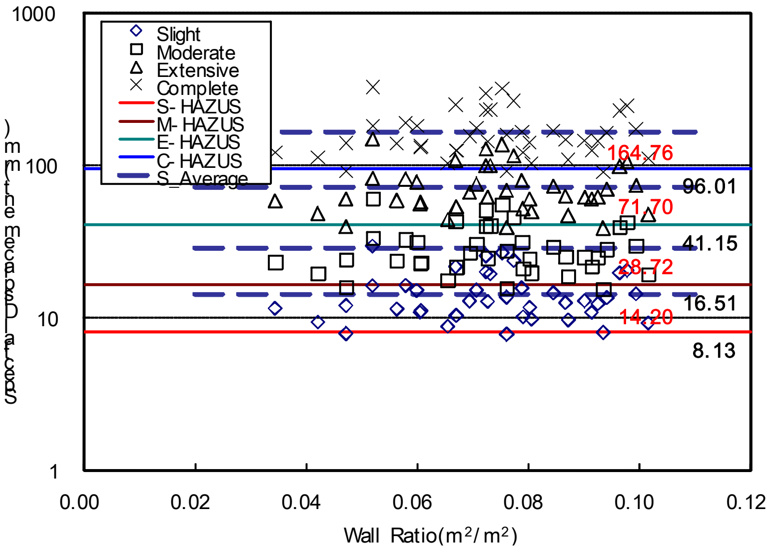

Figure 2: Spectral Displacements with HAZUS Story Drift Ratios

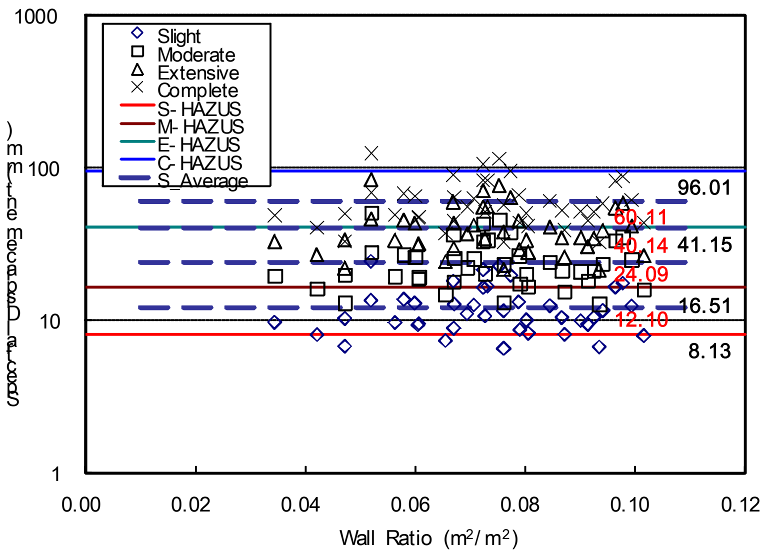

Figure 3: Spectral Displacements with Korea Story Drift Ratios

3.2.3 Proposal of Seismic Fragility Function

It is determined to underestimate the spectral displacement as application of HAZUS story drift ratios. Therefore it is proper to apply the standard of Korea Infrastructure Safety and Technology Corporation (KISTC). Spectral displacement is also shown in Table 5 and seismic fragility curves of each damage states are also shown in Fig. 4.

According to these results, Table 6 shows the story drift ratios and average spectral displacement for each damage states of seismic fragility function in internal URM buildings. Seismic fragility curve for each parameter of URM buildings in Korea is as follows as Fig. 5.

Table 5: Spectral Displacement of Each Damage State

		Sm	Mm	Em	Cm
HAZUS	Sd (mm)	8.13	16.51	41.15	96.01
Applied Story Drift Ratio for HAZUS	SdH (mm)	14.20	28.72	71.70	164.76
	SdH/Sd	1.747	1.740	1.742	1.716
	Drift Ratio	0.0024 (1/417)	0.0048 (1/208)	0.0120 (1/83))	0.0280 (1/36)
Applied Story Drift Ratio for Domestic State Estimation Grade	SdK (mm)	12.10	24.09	40.14	60.11
	SdK/Sd	1.488	1.459	0.976	0.626
	Drift Ratio	0.0020 (1/500)	0.0040 (1/250)	0.0067 (1/150)	0.0100 (1/100)

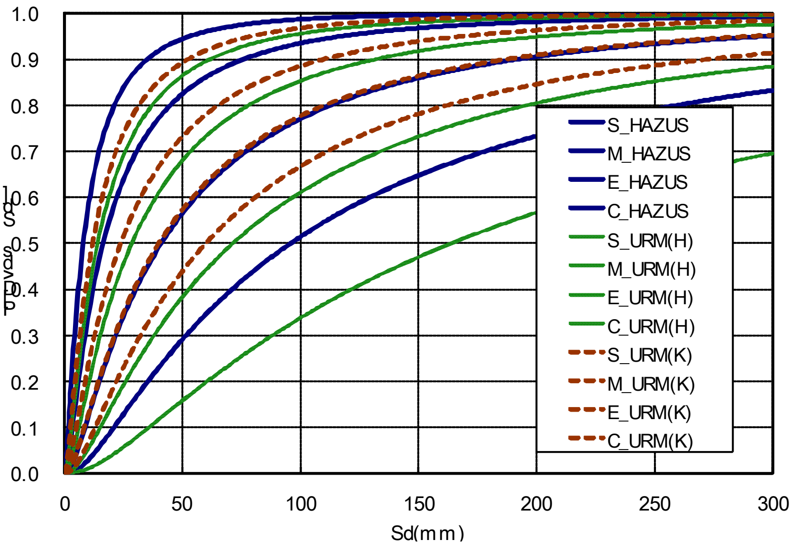

Figure 4: Entire Comparison of Seismic Fragility Curve

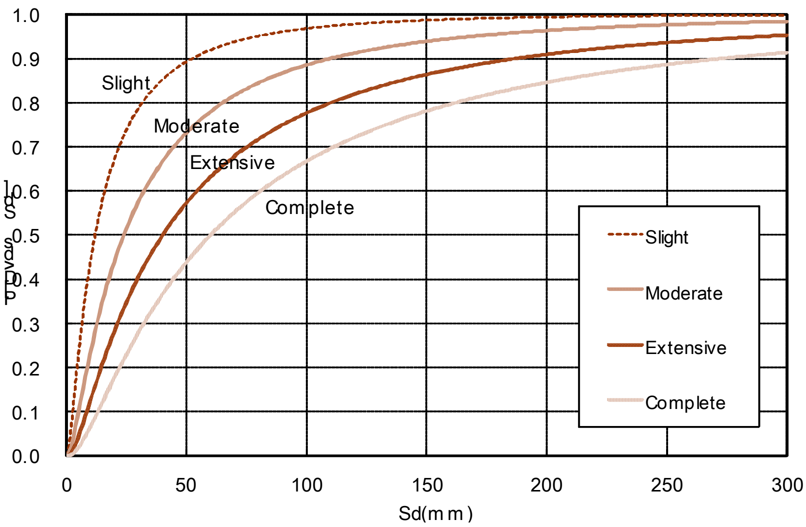

Figure 5: Seismic Fragility Curve for URM in Korea

Table 6: Spectral Displacement and Drift Ratio for URM in Korea

	Sm	Mm	Em	Cm
Sd (mm)	12.10	24.09	40.14	60.11
Drift Ratio	0.0020(1/500)	0.0040(1/250)	0.0067(1/150)	0.0100(1/100)

4. CONCLUSION

From the capacity spectrum analysis results, spectral displacements for 4 kinds of damage state adopting the suitable drift ratio of damage state in Korea are suggested, and the seismic fragility function for existing URM building in Korea is developed.

1) Suitable drift ratio for "Slight", "Moderate", "Extensive" and "Complete" damage state of URM buildings in Korea is suggested.
2) From the capacity spectrum analysis results, spectral displacements for 4 kinds of damage state adopting the suitable drift ratio of damage state in Korea are proposed.
3) The seismic fragility function for existing URM building in Korea is developed.

REFERENCE

Architectural Institute of Korea, *Korean Building Code*, 2005. pp. 337-394.
FEMA, 1999. HAZUS99 Technical Manual.
MIDASIT, 2008. MIDAS GEN Ver.741
MIDAS SDS Ver.340
MIDAS GEN Analysis Reference.
NEMA, 2008. Earthquake Disaster Management System.
Kim, J.K., Kim N.H., Ryu, H., Chae, Y.B., 1999. *Seismic Response of Unreinforced Masonry Residuntial Building*, Proceedings of EESK Conference, Vol.3 No. 2, pp. 383-387.
Kwon, K.H., 2001. *Development of retrofitting method of unreinforced masonry structures*, University of Seoul, pp. 263.
Guido M. and Gian M. C., 1997. *In-Plane Seismic Response of Brick Masonry Walls*, Earthquake Engineering and Structural Dynamics, Vol. 26, pp. 1091-1112.
Yi, W.H., et al., 2006. *A study on a method of the improving the seismic performance of unreinforced masonry structures and realizing high-rise buildings with using masonry finishing*, Construction & Transportation R&D Report, pp. 216.

PARALLEL SESSION 5

INUNDATION PREVENTION AT THE UNDERGROUND SPACE IN KOREA

[1]GYEWOON CHOI, SEONGJOON BYEON
[1]Department of Civil and Environmental Engineering
University of Incheon, Incheon, Korea
gyewoon@incheon.ac.kr

ABSTRACT

In Korea, localized heavy rainfall frequently happens especially in summer recently owing to the global abnormal climate. The phenomenon of subsurface infiltration capacity reduction and direct runoff increase is owing to the economic development plan for industrialization and urbanization in the late 1960s. There is an increase tendency of flood damage scale and the typhoon Rusa (2002) and Maemi (2003) have cost about 10,400 billion KRW to recover. This study discusses how to prevent underground inundation which directly linked with surface inundation and is critical especially in urbanized area with a scope of damage diagnoses, mitigation strategies and improvement plans. Almost all underground structures have an inundation protection swell installed at the entrance. However, if a flood depth is higher than the height of swell, inundation of underground space is easily happened and hardly recovered because of lower elevation than surface. Therefore, the most important component for prediction and action to mitigate damage is a flood depth at the flooded area if it is higher than the protection swell and it can be predicted through flood depth analysis activities such as researching past actual conditions of flood, mapping flood risk and river & coastal flood simulations. Although natural flood risk map should be drawn up in natural disaster countermeasure, the propulsion is still adapting because of insufficient consist of standard system and inhabitant resistance. To protect people from inundation damage at underground facilities, administrators should consider for infrastructure safety management practices for user and measure for clearway as soon as possible in the expected inundation areas, when underground facilities were planned and improve the regulations for buildings. As shown above statements, inundation damage in underground is quite serious and complicated due to low elevation, several inlets and hard to be drained. Therefore prevention systems are needed to be developed so that flood area and depth can be predicted and such as National Flood Risk Map and related regulations should be improved in flood frequently occurring areas to reduce inundation damages.

Keywords: *Underground, Inundation damage reduction, Flood risk map*

1. INTRODUCTION

In Korea, localized heavy rainfall frequently happened recently owing to the global abnormal climate. The phenomenon of subsurface infiltration capacity reduction and direct runoff increase is owing to the economic development plan for industrialization and urbanization in the late 1960s. There is an increase tendency of flood damage scale. The Rusa typhoon of 2002 and Maemi typhoon of 2003 have cost about 10,400 billion KRW. Although the loss of lives and property increased during the flood, the inundation precautions are still insufficient. To prevent inundation, the causes of inundation were analyzed in the underground and presented the developmental tendency in this presentation.

The National Emergency Management Agency (NEMA) under the Ministry of Government Administration and Home Affairs (MOGAHA) manages overall measures to counter natural disasters in Korea. From June 1, 2004 the Disaster and Safety Management Basic Law is enacted designating disaster management competent organizations based on the disaster definition, identifying the Central Safety Management Committee, establishing rapid information dissemination system, and enhancing disaster-related research functions. Disaster Impact Assessment (DIA) system aims at fundamentally eliminating potential causes of disasters inherent in various development projects in advance and ultimately protecting the life and property of the people. This program is one good example for implementing sustainable development. The disaster impact assessment system is implemented when the area of targeted development is not less than 300,000 m2. With respect to small- and medium-sized development projects (150,000 m2 to less than 300,000 m2 in size), each city and province has introduced a local disaster impact assessment system. To protect lives and property in downstream areas from the impact of large-scale development, facilitating disaster prevention facilities such as retention reservoir in the development area, the DIA has been introduced since 1996 and the coverage of DIA has been expanded in 2001. Currently, DIA is applicable to 24 categories in 6 fields such as urban development, industrial area development, touring attraction development, and mountain area development.

For feasibility investigation of landslide monitoring and warning system, analysis of landslide susceptibility using GIS technology is introduced. Application of GIS technology and determination of affecting factors are most important aspect of hazard mapping and assessment. Gangneung City in Gangwon Province has landslide hazard mapping. Same techniques will be applied to other areas in the near future. Flood hazard mapping is currently under developing by the Korea Water Resources Corporation. Korea identified 537 sites most susceptible to inundation, collapse, and isolation by typhoons and floods, and labeled them as Disaster Prone Areas. These areas are classified and managed by type, grade, managing entity, size, etc. A total of $1.1 billion will be invested for wide-ranging improvements for seven years from 1998 to 2004. Under this plan, $496 million has been invested to improve 488 disaster prone areas from 1998 to 2002. Automated high-quality alert facilities, automatic voice response service regarding the status of disasters and IT system for disaster prevention are in operation. 182 disaster vulnerable areas, which include river, mountainous valley, etc., have been selected. In stormy weather, the people in this area are not allowed to enter and warned to take shelters to reduce the casualties.

To reduce the loss of life, property damage, and economic hardship caused by natural disasters, the Korean government put in practice several actions. For large scale construction sites, such as subways, golf courses, dams, and residential development sites, Disaster Preparedness Plans are arranged and maintained, in which assigning multiple government officials to monitor large-scale construction sites and setting construction priority. Plans for repairing disaster prevention facilities including retaining walls, embankments, and reservoirs are established and inspection and repairs for the facilities are to be completed before the rainy season. Equipment and facilities for emergency countermeasures have been secured according to the need averaged over the last ten years and local conditions. For proactive disaster prevention activities and emergency recovery during severe natural disasters, the Special Fund has been allocated in 16 cities and 232 districts since 1997. Small rivers in Korea are vulnerable to overflow. Thus, the first step of the improvement for vulnerable small rivers is to refurbish from 2000 to 2009 at the cost of about $3.9 billion. Since 2002, small river sites totaling 800km were refurbished at the cost of $32 million, and $11 million is being invested to 278km in 2002. The Korean government prepares various disaster prevention plans such as basic and action plans. Basic disaster prevention plan, which is a long-term plan against disasters including disaster prevention systems and relevant countermeasures, is formulated every five years. The sixth basic disaster prevention plan is currently in effect since 2002. In accordance with basic disaster prevention plans, specific action plans are formulated and implemented on a yearly basis by the government.

2. FLOOD DAMAGE SCENARIOS

Recent urban floods such as Seoul flood in Korea in 2001 and 2006 induced inundation into underground spaces such as basements, underground malls and subways. Underground spaces are located in the deepest areas of the city, therefore they are very likely to be damaged by floods, and it is very important to examine inundation flow behavior in underground space from the hydraulic and disaster preventive aspects. Regarding these engineering problems, the possibility of evacuation from underground space in inundation and necessity of suitable evacuation system are discussed. In this study both of domestic (5) and overseas (3) severe inundation damage cases were reviewed and summarized by comparative studies. Major cause of these damages found that swell height mitigation is more important to protect inflow to the subway from the overland flow.

2.1 Domestic Flood Damage Scenarios

Underground passage and underground roadway Serious flood damage caused owing to the uninstalled bump or installed in the low-position at the entrance of underpass and underground roadway (Fig.1a). A subway and a railway Damage occurred owing to the insufficient draining pump, overflowing nearby river and unsuitable drainage inlet design (Fig.1b).

Figure 1a: Domestic Inundation Damage Case (1)

Figure 1b: Domestic Inundation Damage Case (2)

Underground Shopping Center Serious damages occurred owing to the insufficient path, unreliable electric equipments, and improper partitions and so on. If inundation occurs the damages become much more serious. Because population density high in this location (Fig.2.a). Underground house Damages occur almost every year, especially in the coastal regions where damages are much worse. Because back water occurred in drain system due to simultaneous high tide and heavy rainfall (Fig.2.b).

Figure 2.a: Domestic Inundation Damage Case (3)

Figure 2.b: Domestic Inundation Damage Case (4)

Underground Multistory building It is very difficult to recover the damages such as in the department stores and large apartments(Fig.2.c).

Figure 2.c: Domestic Inundation Damage Case (5)

2.2 Overseas Flood Damage Scenarios

In Czech Republic, 2002 subway effected by severe flood damage lack of drainage inlet, uninstalled bump or installed in the low position at the entrance of underpass (Fig.3). In England in 2000 and in Mexico in 2007 residential buildings were damaged due to overland flood flow (Fig. 4). In 2007 in England and USA railway was collapsed by flooded water (Fig.5).

Figure 3: Oversea Inundation Damage Case (1)

Figure 4: Oversea Inundation Damage Case (2)

Figure 5: Oversea Inundation Damage Case (2)

3.

3.1 Underground Inundation Damage Diagnosis

Damages by increasing inflow water occur due to the bump of underground entrance which is lower than flood depth. In the case of insufficient drain system or by poor maintenance and management, inundation damages are more serious because water stayed for a long time in the underground facilities. If water is drained through the underground drainage without proper size of water collection tank, serious damages occur due to decreasing pump efficiency and backwater effect. In the underground installation, the damage is more serious, when the facilities which are broadcasting system, light, ventilating holes and so on are insufficient for shelter.

Inundation damages by stopping drain facilities due to disconnecting from electric source causing leakage circuit and blackout, etc. in the underground facilities. Flooded water can inflow through the lighting windows and ventilating holes because they linked on outside and installed on low position. The damage occurs due to ground water inflow through the wall, roof, and bottom while differential settlement exists on underpass and underground roadway. Damages which can be overcome occur due to ignorance of citizen such as insensibility of safety and negligent education. Prospective flood depth can be decided with flood depth analysis such as researching past actual conditions of flood, flood risk map, river flood simulation and coastal flood simulation. Decision making tools depends on (i) Improving D/B related underground facilities for analysis of actual condition of past flood, (ii) Compositing national flood risk map and suggesting the prospected flood depth and (iii) Standardizing the flood modeling such as river flood simulation, tsunami flood simulation, and regional system development accounts these strategies to diagnosis the underground damage inundation. .

Figure 6: Standardization of various data system related with disaster prevention and improving related D/B to decide underground inundation depth

3.2 Development of National Flood Inundation Risk Map

Although natural flood risk map should be drawn up in natural disaster countermeasures, the propulsion is still unfinished because of insufficient consist of standard system and inhabitant resistance. Analyzing levee overflow, compositing flood map (ex. Han River) required (i) collecting data and site investigation, (ii) flood scenarios, (iii) numerical map production, DEM, hydraulic and hydrologic analysis, (iv) GIS mapping with flood depth and inundation area. Compositing numerical flood risk mapping project guidelines were established by Korean Water Resources Engineering in 1999 and updated in 2001-2002. Inundation prediction, catchments modeling and DEM shown in Fig. 7.a. National flood inundation risk map shown in Fig 7.b by DEM, mesh & 2D drainage basins coupling model in Fig.7.c.

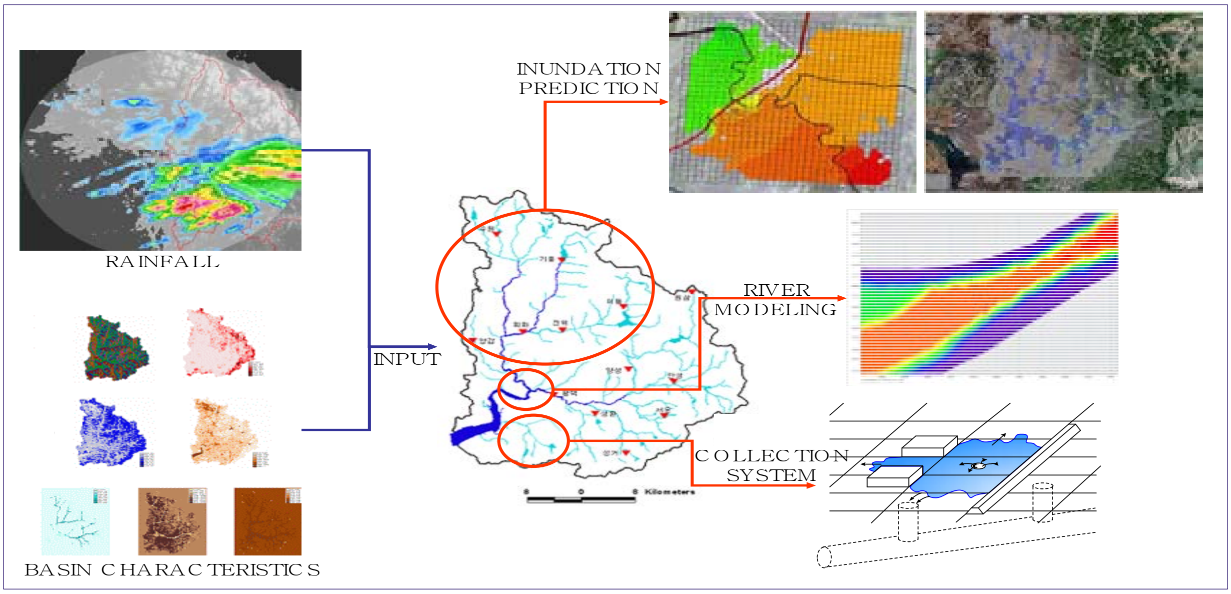

Figure 7.a: Starting the developing project for flood inundation risk map

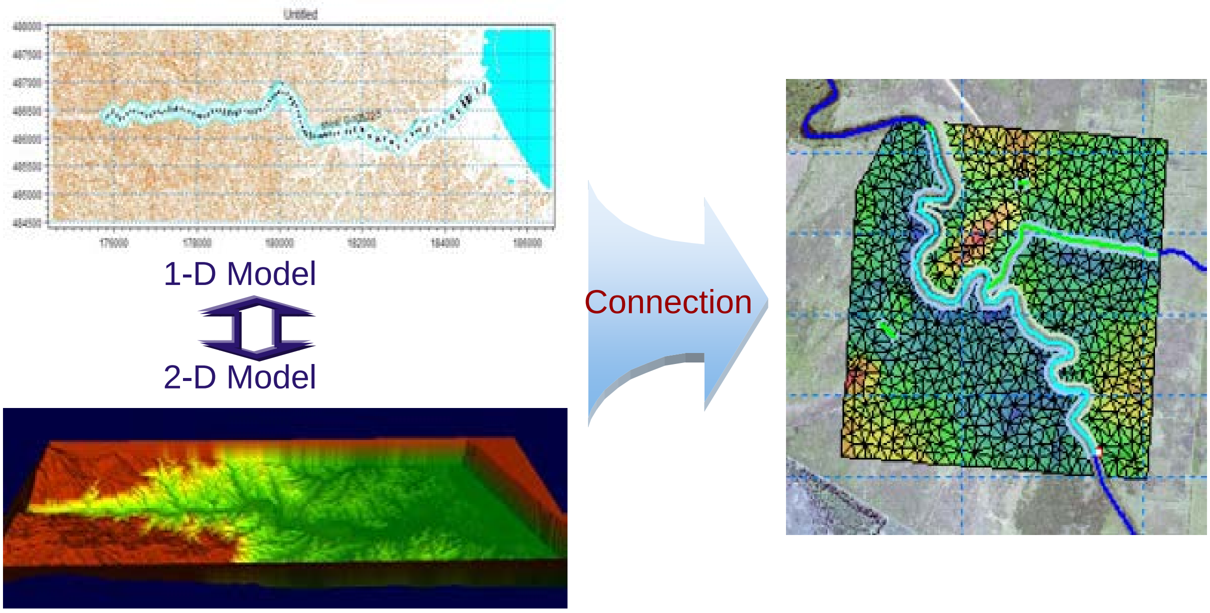

Figure 7.b: Development of National Flood Inundation Risk Map and connection of 1-D and 2-D Model

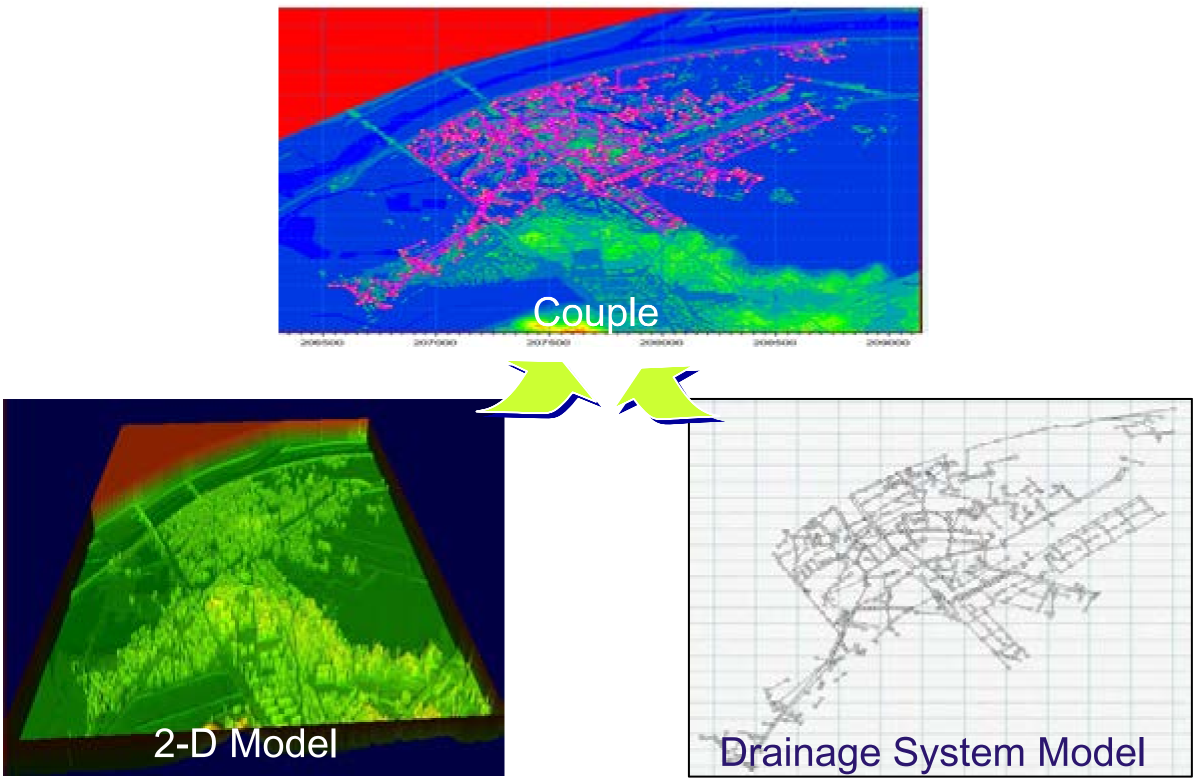

Figure 7.c: Development of National Flood Inundation Risk Map and connection of Drainage Catchments and 2-D Model

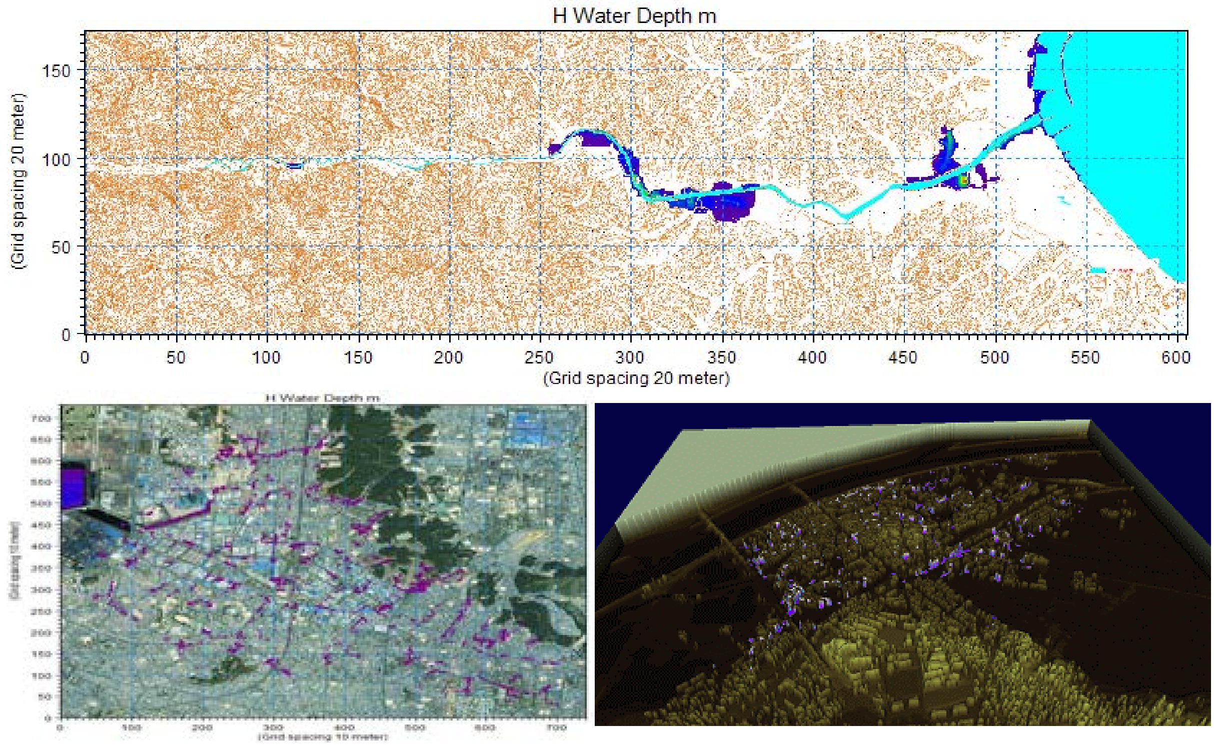

Figure 8.a Development of Hazardous Area mapping

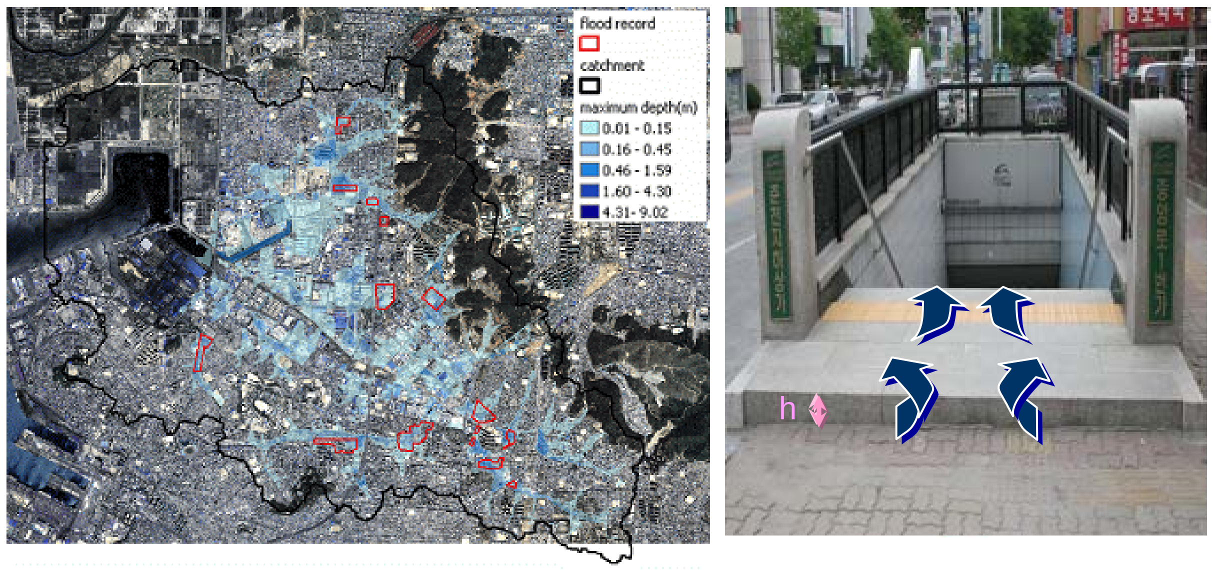

Figure 8.b: Development of Flood Depth and Risk mapping

4. THE ESTABLISHMENT OF MEASURES FOR INUNDATION PREVENTION AND REGULATION

In the expected inundation areas, when underground facilities were planned, administrators should consider for safety for user and measure for clearway as soon as possible. The measure for preventing inundation was executed step-by- step. The first stage accounts (i) the inundation prevention of underground and the measure for delaying inundation time, (ii) the number of users for underground and ensures the expected inundation time by safe shelter and (iii) to confirm securing the safety of shelter. Second stage accounts (i) forewarned of inundation dangerousness and execution instruction, (ii) accurately, rapidly collecting and transmitting flood information, (iii) the training to prevent the damage from inundation in the underground space, (iv) to present the plan of a taking shelter from the underground space and (v) presenting the measure for reducing inundation damage.

Building construction law must be followed i.e. the sheltering space of building, supplies restriction, regulation of underground, disaster management area and regulation amendment for elevator. According to Housing construction regulation amendment about construction industry approval, safety management plan and education (i) regulation of city planning and underground (ii) the standard of decision about underpass and overpass road, the standard of installation about the structure of square and public areas. Design standard of electric facilities required the improvement of substation facilities, electric wires of underground and management standard. Design standard of apartment house required the improvement of electric devices, installation of IT and security management standard facilities. Standards for more detailed information that can be used for installing and operating underground facilities than the existing state should be provided in order to prevent the damage.

5. CONCLUSION

About 40,000 buildings are damaged owing to localized heavy rainfall every year. The loss of property has reached 1,200 billion KRW over the past decade in Korea. Inundation damage in underground is more serious than surface due to low elevation, several inlets and hard to be drained. Prevention systems are needed to be developed so that flood area and depth can be predicted such as National Flood Risk Map. Related regulations should be improved in flood frequently occurring areas to reduce inundation damages. Several realistic case studies recommend that these advanced measures should be account significantly to reduce the flood damages. This development strategy must be functional for disaster preventing aspects.

REFERENCES

Choi, G. W, Lee, H. S, Lee, S. Y, 2007, *Urban Inundation Analysis using the Integrated Model of MOUSE and MIKE21*, Journal of Korean Society of Hazard Mitigation Vol. 7 No. 4, KOSHAM

Choi, G. W, Choi, J. Y, Li, J. W, 2003, *Reduction Rate of the Total Runoff Volume though Installing a Rainfall Storage Tank in the Sub-Surface*, Journal of Korea Water Resources Association Vol. 36 No. 3, KWRA

Choi, G. W, Lee, H. S, Ahn, S. J, 1994, *Simulation of Moving Strom in a Watershed using Distributed Models*, Volume5, Korean Association of Hydrological Sciences, pp 1-16

Ishigaki, T., Toda, K. and Inoue, K., *Hydraulic model tests of inundation in urban area with underground space*, Proc. of XXX IAHR Congress, Theme B, pp.487-493, 2003.
Ministry of Public Administration and Security, 2004, *The Research on Scheme to Prevent Inundation at The Underground Space*, MOPAS, Korea.
Smith, G.P. and Carr, R.S., 2004, *Linked 2D Overland and 1D Pipe System Modelling for Urban Flooding*. Conference Proceedings, NZWWA Stormwater Conference, Rotorua, New Zealand.
Toda, K., Kuriyama, K., Oyagi, R. and Inoue, K., 2004, *Inundation analysis of complicated underground space*, Journal of Hydroscience and Hydraulic Engineering, Vol.22, No.2, JSCE, pp.47-58.

EXPERIMENTAL STUDY OF MASONRY WALLETTE MADE OF SHAPELESS STONES RETROFITTED BY PP-BAND MESH

[1]KOTARO SAKURAI, [2]NAVARATNARAJAH SATHIPARAN and [3]KIMIRO MEGURO

[1]Graduate Student, Department of Civil Engineering,
The University of Tokyo, Japan
sakurai@risk-mg.iis.u-tokyo.ac.jp
[2]JSPS Post Doctoral Fellow, Institute of Industrial Science,
The University of Tokyo, Japan
sakthi@risk-mg.iis.u-tokyo.ac.jp
[3]Director/Professor, ICUS, Institute of Industrial Science,
The University of Tokyo, Japan
meguro@iis.u-tokyo.ac.jp

ABSTRACT

Unreinforced masonry structure is one of the most popularly used constructions in the world, especially in developing countries. It is also unfortunately, the most vulnerable to the earthquake and its damage has caused many human casualties. Therefore, from global viewpoint, retrofitting of low earthquake-resistant masonry structures is essential to reduce the casualties significantly from earthquake disaster.

In developing countries, retrofitting method should be technically feasible and economically affordable, the retrofitting material, accessible, and the workmanship, locally available. Considering these points, PP-band (polypropylene bands, which is worldwide available and cheap material, commonly used for packing) retrofitting technique has been developed and many different aspects have been studied using brick and adobe masonry structures by Meguro Laboratory, Institute of Industrial Science, The University of Tokyo.

In this research, we conducted a series of experiments to verify the suitability of PP-band retrofitting for masonry structures made of shapeless stones. Material tests were conducted to understand the basic parameters of stone masonry, i.e. shear, tension and compression strength. After the material tests, diagonal compression test and out-of-plane test were carried out using masonry wallette made of shapeless stones with and without retrofitting. From both test results, it was clear that PP-band retrofitting improved drastically the overall stability and ductility of stone masonry structures made of shapeless stones.

INTRODUCTION

Masonry structure, constructed by piling burned bricks or unburned, just sun-dried bricks called adobes, stones or concrete blocks, is one of the most popularly used constructions in the world, but also most vulnerable to the earthquakes. Because distribution of the masonry structures overlap with high seismology area, it has caused many human casualties during earthquake. Therefore in global viewpoint, retrofitting of low earthquake-resistant masonry structures is very important to save people from earthquake disaster. Considering these points, a new retrofitting technique for masonry has been developed and proposed based on the use of polypropylene band (PP-band) meshes by Meguro laboratory. This PP-band retrofitting technique prevents masonry structures from collapsing by giving the stabilization.

Up to now PP-band retrofitting study mainly focus on houses build by regularly shaped bricks and adobes. But the masonry has many different kinds of construction and the effect of PP-band is not confirmed for all kinds of masonry. Especially in the mountainous region in developing countries, stone masonry is constructed using shapeless or shaped stones as constructing material. But stone masonry house, particularly shapeless stone masonry house is the most vulnerable during earthquake (Table 1). Therefore further test of stone masonry wallettes should be carried out.

Table 1: vulnerability table (European Macroseismic Scale, 1998)

Type of structure		Vulnerability Class					
		A	B	C	D	E	F
MASONRY	Rubble stone, field stone	O					
	Adobe (earth brick)	O—	—|				
	Simple stone	|···	O				
	Massive stone		|—	O···	···|		
	Unreinforced, with manufactured stone units	|···	O	···|			
	Unreinforced, with RC floors		|—	O···	···|		
	Reinforced or confined			|···	O	—|	
REINFORCED CONCRETE	Frame without earthquake-resistant design (ERD)	|···	···—	O	—|		
	Frame with moderate level of ERD		|···	···—	O	—|	
	Frame with high level of ERD			|···	···—	O	—|
	Walls without ERD		|···	O	—|		
	Walls with moderate level of ERD			|···	O	—|	
	Walls with high level of ERD				|···	O	—|
STEEL	Steel structures			|···	···—	O	—|
WOOD	Timber structures		|···	···—	O	—|	
O	: Most likely vulnerability class						
—	: Probable range						
······	: Less probable range, exceptional cases						

2. MATERIAL TEST

2.1 Test setup

Figure 1 shows the specimens used for shear, tension and compression tests to obtain the mechanical properties of the masonry. Shapeless stones whose size range from 60mm to 80mm were used for specimens. A mortar mix of cement: lime: sand = 1: 5: 14 and cement/water ratio = 0.20 in weight was used. To make the specimens close to real stone masonry structures made of shapeless stones in developing countries, gravel were put between the shapeless stones. The number of shapeless stones used for specimen was 3, 2 and 5 for shear, tension and compression tests specimen, respectively. Five identical specimens were constructed for each test. Specimens were tested 28 days after construction under displacement control condition and the loading rate was 0.1mm/min.

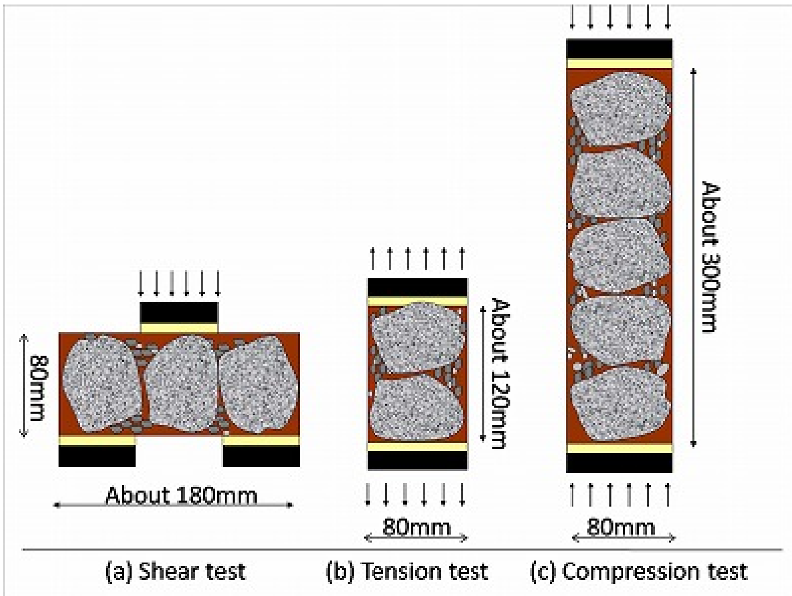

Figure 1: The structure of the specimens for material test

2.2 Result of material tests

Due to different failure mechanism, major failure patterns of masonry can be divided into 3 types.

a) Failure occurred within the mortar.

b) Failure occurred along the interface between mortar and stone surface.

c) Failure occurred within the brick or stone.

Only in case of special combination of very strong mortar and very weak brick or stone, type c) failure can be observed.

From the shear test's results, it is found that the failure pattern of masonry made of shapeless stones is type b) that is the separation along interface between stone surface and mortar because interface strength is less than that of mortar. Figure 2 shows the average strength of each test, i.e. shear, tension and compression tests. Figure 3 shows the failure pattern of stone masonry made of shapeless stones.

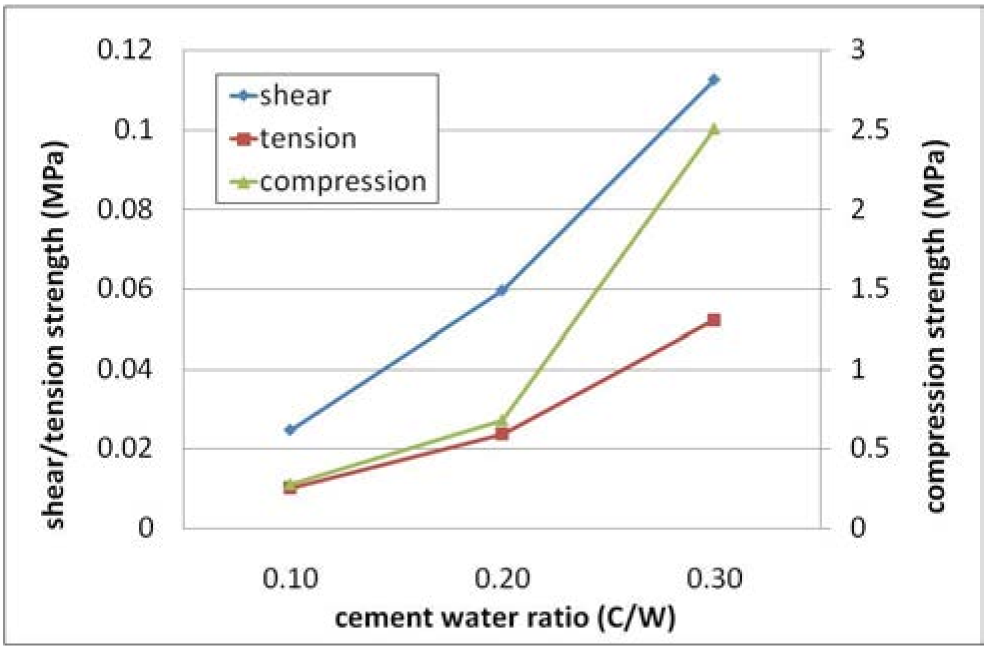

Figure 2: Mechanical properties from material tests

Figure 3: Separation along stone-mortar interface

3. DAIAGONAL SHEAR TEST

3.1 Outline of the diagonal compression test

To verify the suitability of PP-band retrofitting technique for stone masonry, ¼ scaled model diagonal shear test was conducted. The wallette dimension was $300 \times 300 \times 150mm^3$ and it was composed of 5 x 3 stones, and 2 stones in the direction of depth as seen in Figure 4. Because the size and shape of stones were variable, there is approximately 10mm variation in the height of the specimens. Considering the result of material tests, we used a mortar with the mixture ratio of cement : lime : sand = 1 : 7.3 : 18.7 in weight for diagonal shear test to make the specimens close to real masonry structures made of shapeless stones in developing countries. Cement/water ratio adopted was 0.15.

In this experimental program, masonry wallettes made of shapeless stones with and without retrofitting were prepared. In addition, specimens with 10mm surface finishing were prepared. Three identical wallettes were constructed for each test. Specimens were tested 28 days after construction, under displacement control loading condition. The loading rate was 0.5mm/min up to the first 10mm of diagonal deformation, and then it was increased to 2mm/min up to 50mm and 5mm/min up to 100mm of diagonal deformation.

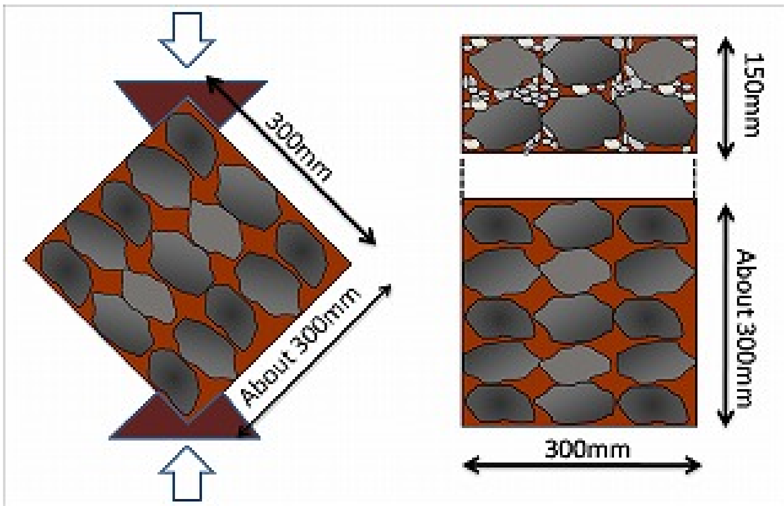

Figure 4: Specimen for diagonal shear test

3.2 Result of the experiment

Figure 5 shows the diagonal shear stress variation with strain for the non-retrofitted and retrofitted specimens. In the non-retrofitted case, there was no residual strength after first crack occurred and the specimens split into two pieces at strain equal to 1.1%. In the retrofitted case, although the initial crack was followed by a sharp drop, at least 64% of the peak stress remained. Subsequent drop were associated with new cracks such as the one observed at the strain of 2.5%. After this, the stress was regained by readjusting and packing by PP-band mesh. The stress equal to 72% and 81% of the initial peak stress was remained at the strain equal to 10% and 20% respectively. The residual peak stress of the specimen was 99% of initial peak stress. Specimen didn’t break at the strain equal to 24%, which indicate that; retrofitted specimen was at least 21 times more ductile than non-retrofitted one.

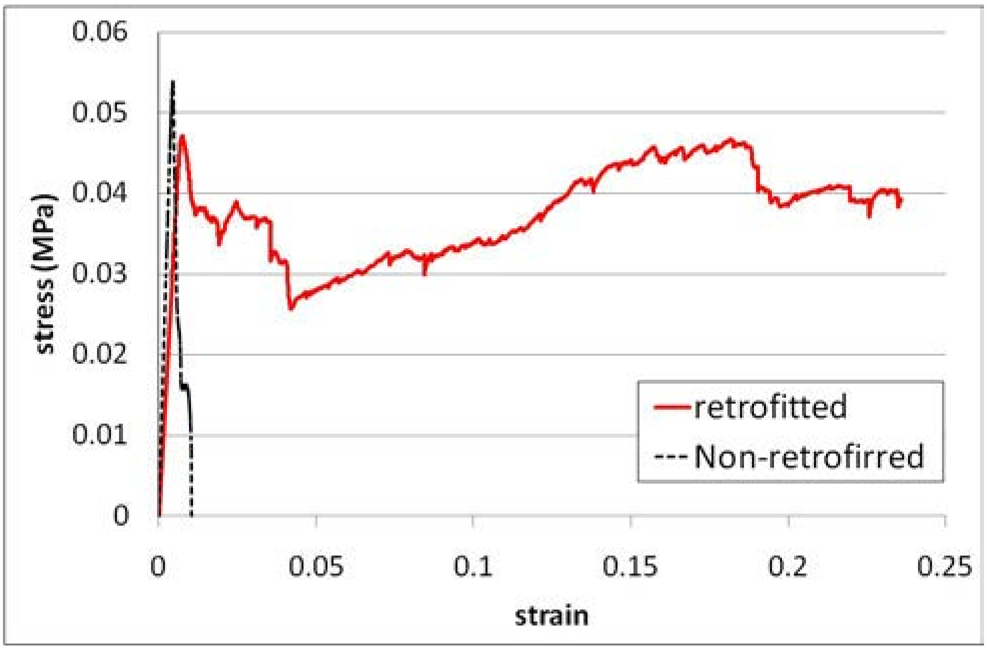

Figure 5: Stress vs. strain for stone masonry wallette with and without retrofitting by PP-band mesh

Figure 6 shows the non-retrofitted and retrofitted specimens at the end of test, which corresponded to strain equal to 1.1% and 24% respectively. As strain became larger, due to very low mortar strength, PP-band was penetrated to the specimens. Therefore, increase of strength was not observed with strain. However, for specimens used for 1/4 scaled experiment, scaled PP-band which width was approximately 6mm was used and it was increased penetration-rate. But in case of full scale, 15mm PP-bands will be use, penetration of PP-band mesh to the masonry houses will be reduced relatively. Therefore additional increase of strength will be expected, when retrofitting the real scale masonry structures by PP-band meshes.

Figure 6: Failure pattern of stone masonry wallette (Left: without retrofitting, Right: with retrofitting)

Figure 7 shows the diagonal shear stress variation with strain for retrofitted and retrofitted specimen with surface finishing. In this case, surface finishing on specimens applied by mortar mix with the width of 10mm was used. In case of retrofitted specimen without surface finishing, 64% of the peak stress was remained after first crack. On the other hand, retrofitted specimen with surface finishing, 77% of the peak stress was remained after first crack. By overlaying mortar onto PP-band mesh, surface finishing fill the gap between PP-band mesh and masonry wallette and the residual strength was higher than the specimens without surface finishing. It was found that surface finishing makes beneficial effect in residual strength for masonry made of shapeless stones as well as for adobe and brick.

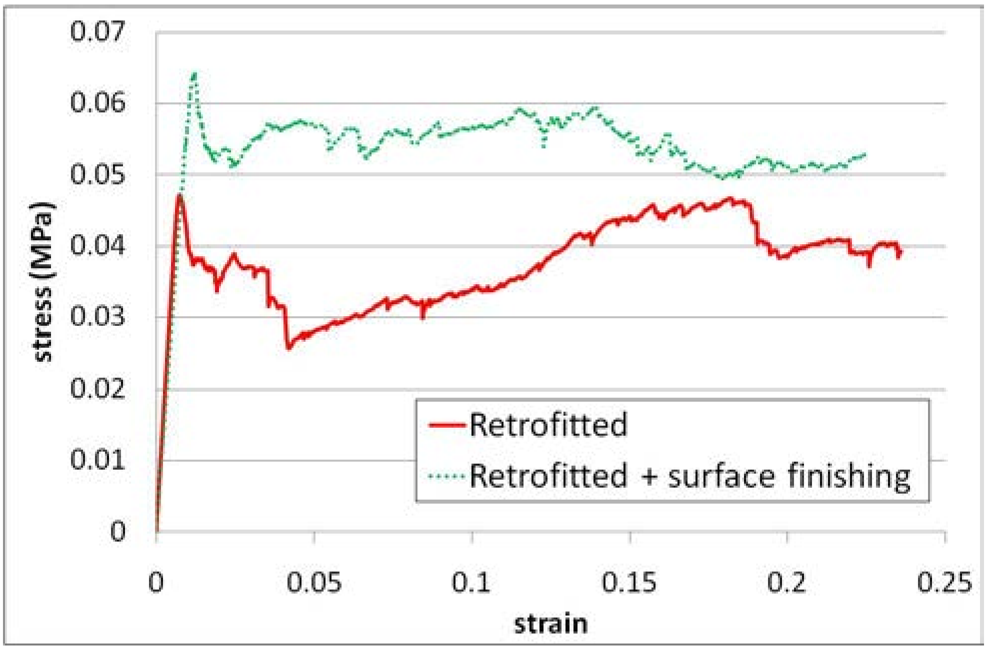

Figure 7: Stress vs. strain for retrofitted stone masonry wallette with and without surface finishing

4. OUT-OF-PLANE TEST

4.1 Outline of the out-of-plane test

Out-of-plane test was carried out to investigate the effectiveness of PP-band mesh in walls exhibiting arching action. Wallette used was 1/4 scaled model and its dimension was $480 \times 240 \times 150mm^3$ and it was composed 4 x 5 stones, and 2 stones in the direction of depth as seen in Figure 8. Because the size and shape of stones were variable, there is the approximately 10mm variation in the height of the specimens. Considering the result of material tests, we used a mortar with mixture ratio of cement : lime : sand =1 : 4 : 11.2 in weight for out-of-plane test to make the specimens close to real masonry structures made of shapeless stones in developing countries. And also, not to give damage to the specimen before test, the cement/water ratio used was 0.25.

Masonry wallettes made of shapeless stones with and without retrofitting were prepared and three identical wallettes were constructed for each test. Specimens were tested 28 days after construction under displacement control loading condition. The wallettes were simply supported with a 440mm span and steel rods were used to support the wallette at the two ends. The masonry wallettes were tested under a line load which was applied by a 20mm diameter steel rod at the wallette mid span. The loading rate was 0.5mm/min for the first 6mm of vertical deformation, and then it was increased to 2mm/min up to 65mm vertical deformation.

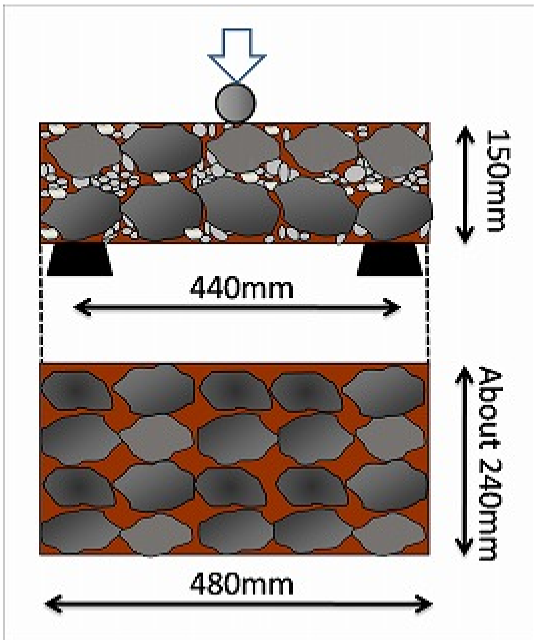

Figure 8: Specimen for out-of-plane test

4.2 Result of the experiment

Figure 9 shows the out-of-plane load variation with net vertical deformation for the non-retrofitted and retrofitted specimens at the mid span. In the non-retrofitted case, the initial strength was 1.34 KN and the specimens split into two pieces at the mid span deformation equal to 1.4mm. While in the retrofitted case, although the initial crack was followed by a sharp drop, at least 33% of the peak strength remained. After this, the strength was regained progressively due to the PP-band mesh effects. The strength equal to 225% and 433% of the initial peak strength was observed at the mid span deformation equal to 20mm and 40mm, respectively. The residual peak strength of the specimen was 439% of initial peak strength. Specimen didn’t break at the mid span deformation equal to 62mm, which indicates that; retrofitted specimen was at least 45 times more ductile than non-retrofitted one.

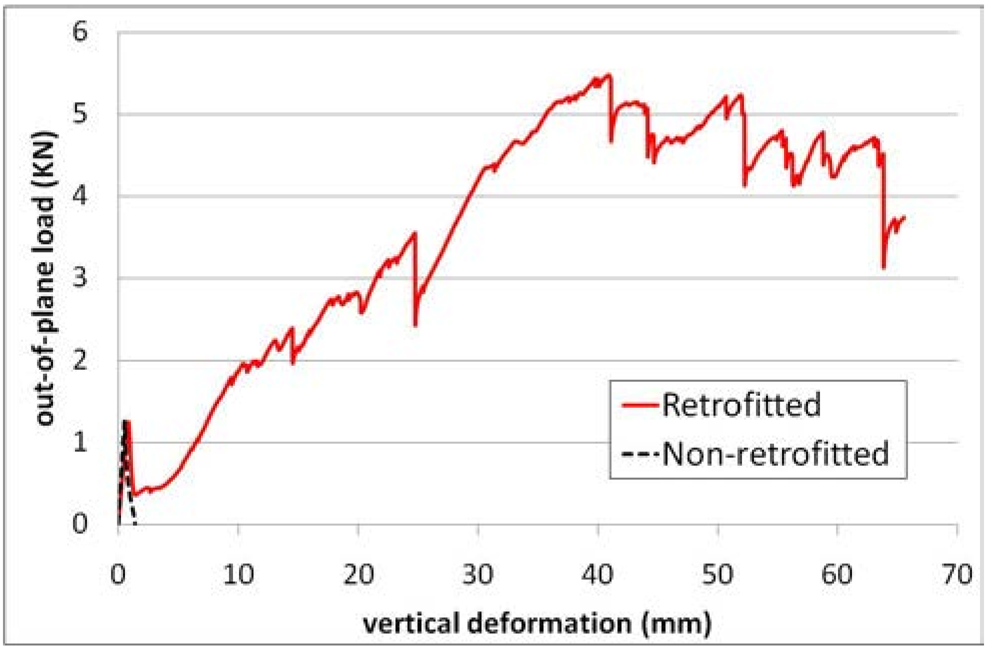

Figure 9: Out-of-plane load variation vs. vertical deformation

Figure 10 shows the non-retrofitted and retrofitted specimens at the end of test, which corresponded to deformation equal to 1.4mm and 62mm, respectively. In out-of-plane test, the improvement of final strength became much bigger than that of diagonal compression test. The cement/water ratio of the specimens used for the diagonal shear test was 0.15, but in case of out-of-plane test, the cement/water ratio equal to 0.25 was used. Because strength of mortar is high enough, PP-band didn't penetrate to the specimens and the drastic improvement of residual strength was observed.

Figure 10: Failure pattern of stone masonry wallette
(Left: without retrofitting, Right: with retrofitting)

5. CONCLUSIONS

This paper mainly discusses the result of a series of diagonal compression tests and out-of-plane tests that were carried out using both non-retrofitted and retrofitted wallettes by PP-band meshes.

5.1 Summary of diagonal compression test

1. Masonry wallette without PP-band mesh lost the entire load bearing capacity after crack appeared.
2. Masonry wallette with PP-band mesh retrofitting lost some of load bearing capacity immediately after the crack-initiation, but 64% of the peak stress was remained. With the effects of the PP-band meshes, it could regain the load bearing capacity, and its strength and deformability improved. According to the experimental result, 1.3 times higher peak stress and at least 21 times larger ductility were observed.
3. By overlaying mortar onto PP-band mesh retrofitted masonry wallette, 77% of the peak stress was remained after first crack. It was relatively higher than that of the specimens without surface finishing.

5.2 Summary of out-of-plane test

1. In case of out-of-plane tests, the mesh effect was not observed before the wall cracking. After cracking, the mesh presence positively influenced the wallette behavior. Also in case of retrofitted wallette, 33% of the peak strength was remained after first crack occurred, and then strength was regained and improved.
2. The retrofitted wallettes achieved 2.9 times higher strength and 45 times larger deformation than those of the non-retrofitted ones.

Considering the overall performance of the specimens, we can conclude that PP-band mesh retrofit method can effectively increase the seismic capacity of masonry wall made of shapeless stones, too. Based on the fact, we can expect that with PP-band mesh retrofit method, seismic capacity of weak stone masonry houses made of shapeless stones can also be improved very much.

REFERENCES

Paola MAYORCA and Kimiro MEGURO, 2004. *Proposal of an Efficient Technique for Retrofitting Unreinforced Masonry Dwellings*. Proceedings of 13th World Conference on Earthquake Engineering, Vancouver B.C., Canada, Paper No.2431.

Navaratnarajah SATHIPARAN, Paola MAYORCA, Kourosh Nasrollahzadeh NESHELI, Ramesh GURAGAIN and Kimiro MEGURO, 2005. *Experimental Study on In-plane and Out-of-plane Behavior of Masonry Wallettes Retrofitted by PP-band Meshes*, SEISAN-KENKYU **57**, pp.530~533.

Marjana LUTMAN. *STONE MASONRY CONSTRUCTION* (www.world-housing.net), as retrieved on April 1st , 2009.

Navaratnarajah SATHIPARAN, 2005. *Experimental Study of Retrofit of Masonry Buildings by PP-band Mesh*, M.Eng. Dessertation, The University of Tokyo, Japan.

SHEAR STRENGTHENING OF REINFORCED CONCRETE BEAMS USING FERROCEMENT

PRAGASIT JUNTANALIKIT
Sirindhorn International Institute of Technology,
Thammasat University, Pathumthani, Thailand
pj_bank2@hotmail.com
PANUWAT JOYKLAD
Sirindhorn International Institute of Technology,
Thammasat University, Pathumthani, Thailand
joy.civil@gmail.com
AMORN PIMANMAS
Sirindhorn International Institute of Technology,
Thammasat University, Pathumthani, Thailand
amorn@siit.tu.ac.th

ABSTRACT

The methods for strengthening rectangular reinforced concrete beams using ferrocement attached onto the surface of the beams are described in this paper. The study is based on an experimental program carried out on 5 beams designed to fail in shear mode. One of them is control specimen and the others are strengthened by various ferrocement techniques. In these techniques, two centimeter thick ferrocement jacket is used together with additional external web reinforcement. The difference among each specimen is the installation method, shape of ferrocement jacket, spacing of additional external web reinforcements and surface roughness between original beam and ferrocement cover. Results from tests, such as ultimate strength, ductility and cracking pattern, of strengthened specimens are compared with control specimen. Load-deflection responses are obtained up to failure or reach the capacity limit of measuring devices, and the performance of the various proposed methods are compared with conventional ACI procedure. The effect of various parameters, such as shape of ferrocement cover, spacing and configuration of external web reinforcements and surface roughness are considered. Results show that the proposed strengthening method provides better ductility, ultimate strength and mode of failure. Therefore, it is found that the proposed shear strengthening method is very effective and strongly confirms that ferrocement is a viable alternative material for strengthening reinforced concrete structure.

1. INTRODUCTION

The market for maintenance and repairing existing structures has been enormous in the past years, due to the deterioration and/or the requirements on the existing structures to carry more loads. Of the various retrofitting techniques available, steel plate bonding is one of the most effective and convenient methods of strengthening. Ferroceemnt jacketing is found to be one such attractive technique due to its properties such as good tensile strength, light weight, overall economy and water tightness. The skeleton steel combined with ferrocement cover is one of several suitable choices for use in developing country. Ferrocement is a type of thin composite material made of cement mortar reinforced with uniformly distributed layers of continuous, relatively small diameter, wire meshes and skeleton steels. Originally, ferrocement materials were used only in housing applications. However, during the last two decades, the applications of ferrocement in the field of repair and strengthening have been developed rapidly. Ferrocement construction requires conventional technology and offers better performance even when handled by less experienced workers.

Many experimental studies have been conducted in recent years to increase flexural capacity. Paramasivam et al. reported the test of six simply-supported inverted T-beams under static and cyclic loads applied at mid-span. The results show that the beams were substantially strengthened and stiffened with the provision of additional stirrups and wire meshes in the thickened sections encasing the beams' web and the tension face.

Rafeeqi et al. tested five reinforced concrete beams designed to fail in brittle shear-compression. The strengthened beams showed a marked improvement in performances at service load, greatly improved ductility at ultimate load with either a ductile shear failure or seemingly a transition from shear to the flexural mode of failure.

However, the research on using ferrocement to increase shear capacity has been limited. In this paper, the authors apply the combined use of external skeleton steel and ferrrocement cover for shear strengthening of reinforced concrete beam. The proposed method focuses on strength and ductility. The simple calculations recommended by ACI code are also compared with tested results in order to guide the designers.

2. EXPERIMENTAL PROGRAM

The simply supported reinforced concrete beams with four-point bending was tested in this study. Five identical beams were strengthened by different techniques using external skeleton bars and ferrocement cover. The cross section was 200 mm wide and 300 high. The total length was 2400 mm and the effective span was 2200 mm. The beams were designed to fail in shear failure. The nominal moment capacity to nominal shear capacity ratio,

$M_n/(aV_n)$, and shear span-to-effective dept ratio, a/d, was greater than 1.2 and less than 3.0, respectively. The details of material properties and test set up are explained in the next section

2.1 Material Properties

The beams reinforced with four bars of 20 mm diameter in tension and two bars of 12 mm diameter in compression were cast using the same batch of ready mix concrete. The transverse reinforcements consisted of RB6 bars spaced at 125 mm center to center. The tested yield and tensile strength of reinforcements were given in Table 1.

Table 1: Mechanical property of rebar

Diameter (mm.)	Grade	Yield strength (MPa)	Tensile strength (MPa)
20	SD30	347.13	454.81
12	SD40	479.19	605.90
9	SR24	341.20	471.24
6	SR24	406.61	511.85

Hexagonal wire mesh was used for ferrocement. The mortar mix is made of 1:1.8 cement sand mortar and w/c ratio 0.40 by weight. The average cylindrical compressive strength of concrete was given in Table 2.

Table 2: Mechanical property of concrete

Specimens	f'_c (MPa)	f'_m (MPa)
CON	20.40	-
S200	23.05	48.74
S200SR	23.64	48.75
S200CL	23.54	48.75
U200	23.54	48.35

The average 50 mm x 50 mm x 50 mm cube strength of mortar was 49 MPa. The average tensile force of mortar was found to be 4.71 kN by direct tensile test using 20 mm x 100 mm specimen as shown in Figure 1.

Figure 1: Direct Tensile Test of pure mortar and ferrocement specimen

2.2 Strengthening techniques

Out of the five beams, one was used as control beams (CON). The S200 specimen was strengthened by ferrocement attached onto the both side surfaces of the beam. Before the 20 mm thick ferrocement panels were plastered onto beam, the beam was predrilled by an augur on both sides. The spacing of the holes was 200 mm which was the spacing of additional external web reinforcements (Table 3). Next, the prefabricated skeleton steel, made from RB6 with 2 layers of wire meshes, was attached onto beam faces. Then, RB9 reinforcing bars that had been bent in C-shape were inserted into holes and fixed with beam via chemical epoxy as shown in Fig. 2.

Table 3: Description of specimens

Specimens	Spacing of Main additional rebars (mm.)	Special Detail
CON	-	-
S200	200	-
S200SR	200	Surface roughening
S200CL	200	extra clip reinforcements
U200	200	-

(a) C-shaped reinforcement (external web reinforcement) *(b) Plastering* *(c) Finishing the surface*

Figure 2: Construction procedure for specimen S200.

Specimens S00SR and S200CL had the same properties as S200 with some modifications. For S200SR, the surface of the original beam was roughened by chisel to increase the bonding with ferrocement covers (Fig. 3 (a)).

To reduce the cost of drilling hole and epoxy and save the construction time and labor, specimen S200CL, with 200 mm c/c spacing of C-shaped reinforcements, was also provided with additional C-clip steels spaced at 200 mm. It should be noted that the C-clip steels were not inserted into the drilled hole. In effect, the spacing of external reinforcements in S200CL was 100 mm c/c (Fig. 3 (b)). For specimen U200, the beam was covered with ferrocement panel on the side face as well as the bottom face (U-shape). The RB9 external web reinforcements were bent in U-shape as shown in Fig. 4(a). The spacing of these reinforcements was 200 mm.

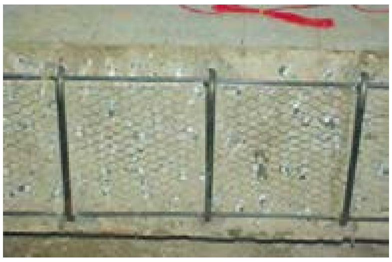

(a) Increase the surface roughness for S200SR

(b) Extra C-clip steel for S200CL

Figure 3: Construction Techniques for specimens S200SR and S200CL

(a) U-shape external web reinforcements

(b) Installing U-shape bars and skeleton steel

(c) Plastering mortar at the bottom face

(d) Finishing the surface

Figure 4: Construction Techniques of specimen U200

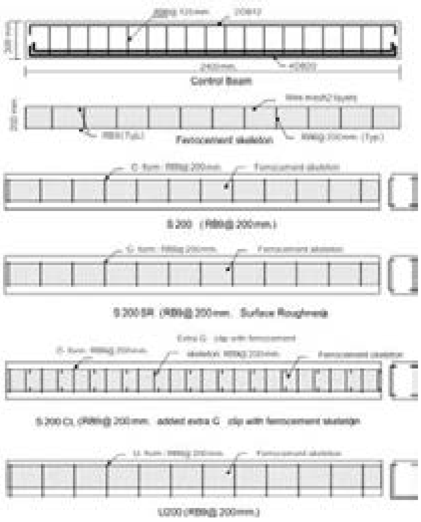

Figure 5: Details of specimens

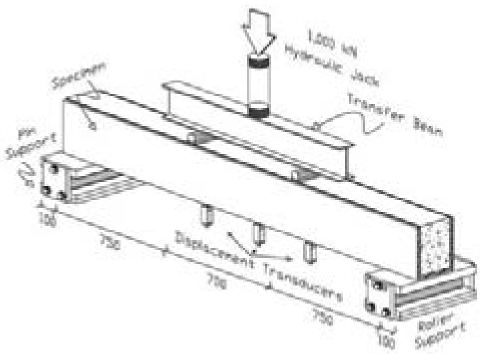

Figure 6: Test Setup and loading

Figure 5 shows details of the five beams together with specimen designation. It shall be noted that ferrocement cover was not patched for the full depth of the beam, but the clear distance of 10 mm offset from the loading face of beam was provided to prevent any non-uniform contact between load and the ferrocement cover. Table 4 shows the calculated shear and flexural capacity and the failure mode of the beams.

2.3 Testing Arrangement

All five beams were tested using hydraulic jack mounted vertically over the test beams. Two concentrated loads were applied at 700 mm spacing (see Figure 6) in a four-point bending layout. The specimens were tested using a strong steel frame. The specimens are supported by roller and pin support on each end. In the first stage, before reinforcements reached the yield strength, specimens were tested under load control with monotonically incremental load of 10 kN for each load step.

After reinforcements reached the yield strength, specimens were tested under displacement control with monotonically incremental displacement of one mm for each step. The deflection of the beam was measured using displacement transducers placed at mid span and at the location of distributed load. The strain gauges were attached to the main reinforcing bars, transverse reinforcing bars and additional external transverse reinforcing bars.

3. RESULTS AND DISCUSSION

Figure 7 shows the load versus deflection behaviour at the mid span of the tested beams. The experimental results are summarized in Table 5, as well as the failure patterns shown in Figure 8. It is observed that the control specimen that was designed to fail in shear reached the maximum load when a large single shear crack developed. The other specimens demonstrated dramatic improvement in shear capacity.

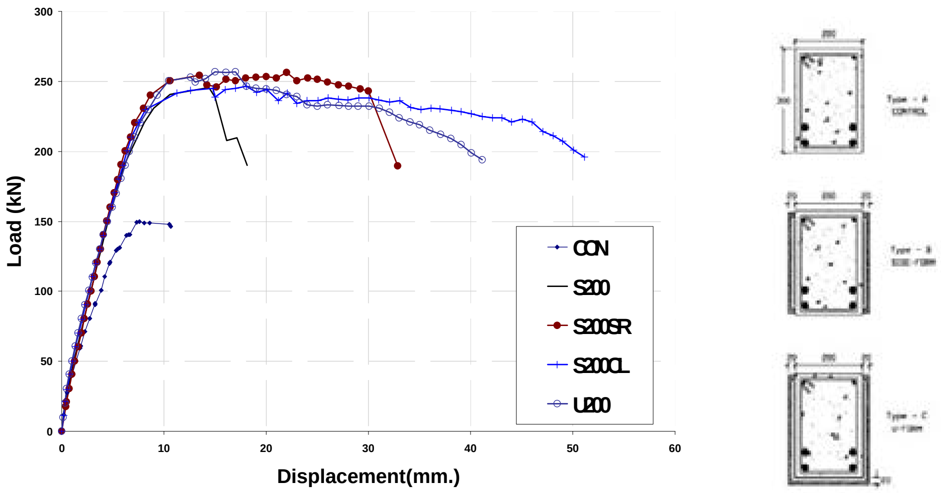

Figure 7: Load-displacement curve for all test specimens

Table 4: Specimen sectional force properties

Code	M_n (kN-m)	V_n (kN)	$M_n/(aV_n)$	P_p predict (kN)	Failure (Predict)
CON	89.28	86.73	1.37	173.46	Shear
S200	94.93	147.34	0.85	253.14	Flexure
S200SR	94.93	147.83	0.85	253.14	Flexure
S200CL	94.93	182.95	0.69	253.14	Flexure
U200	95.54	149.60	0.85	254.77	Flexure

Table 5: Result of experiments

Code	P_t Tested (kN)	P_p/P_t	Ductilit ratio	Failure (Tested)
CON	147.40	1.17	1.39	Shear
S200	239.20	1.05	1.71	Shear
S200SR	249.40	1.01	1.64	Flexure/shear
S200CL	241.95	1.04	2.83	Flexure
U200	254.75	1.00	2.60	Flexure

The mode of failure in most specimens changed from shear to flexure. Only specimen S200 failed in combined shear and flexure. Nevertheless, all specimens show significant increase in load capacity. U200 shows the same level of strength enhancement as S200, but the failure of U200 is flexural failure which is different from shear failure of S200. As shown in Table 4, the ductility ratio of U200 is 2.60, which is higher than specimen S200. Consequently, the U-shaped ferrocement has certain benefits compared with side ferrocement.

In order to increase bonding between surfaces of two materials, the roughness between original beam and ferrocement cover was increased by roughening the surface of the original beam. The effect of surface roughness can be evaluated by comparing the result of S200 and S200SR. The maximum load capacity is almost the same for both specimens but the ductility of S200SR is larger.

To prevent the shear failure in S200, specimen S200CL was provided with extra clip reinforcements attached on the surface of the beam. It is noted that the extra clip reinforcements are not fixed into the holes. As a result, there is no extra cost of drilling hole and adhesive. As shown, the specimen shows better performance as compared with S200 and S200SR. The failure mode is flexural failure with large ductility.

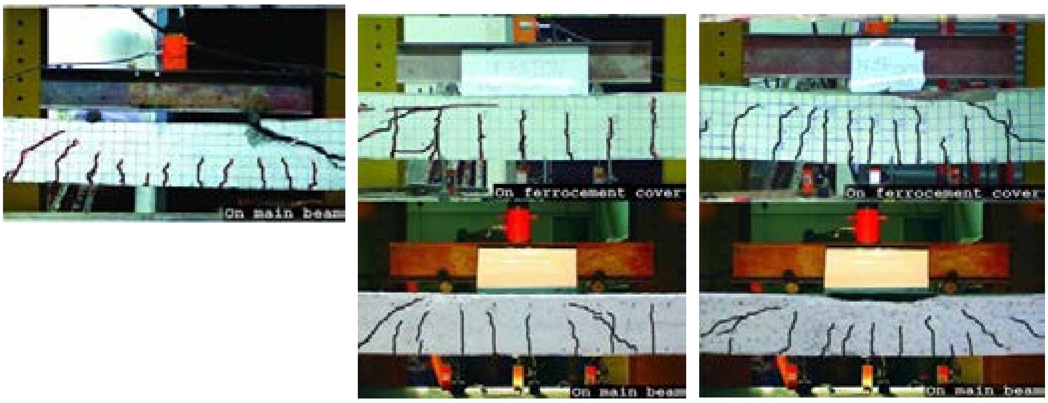

(a) CON (b) S200 (c) S200SR

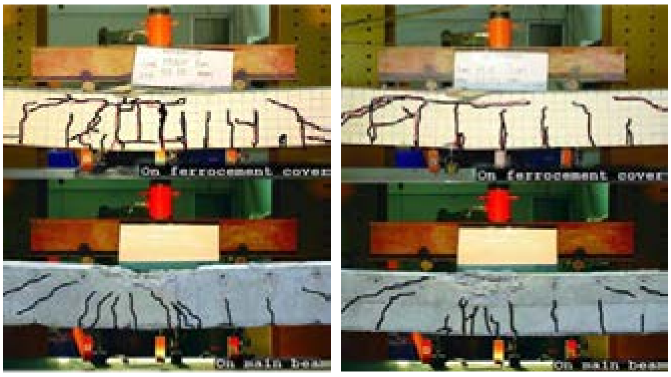

(d) S200CL (e) U200

Figure 8: Crack pattern at failure of specimens

4. PREDICTION OF CAPACITY USING ACI CODE

In order to predict the capacity of strengthened beams, the general procedure of ACI318 had been adopted and modified to analyze beams with ferrocement cover.

4.1 Ultimate Moment Capacity

The theoretical ultimate moment capacity of the composite beam sections was calculated by means of the conventional reinforced concrete theory. The compressive force contributed by concrete was calculated based on simplified stress block proposed in ACI318. The influence of ferrocement in the compression zone was omitted. The tensile forces of the section were contributed by tension steels and ferrocement tensile force. In this case, ferrocement tensile force was previously obtained via tensile test of ferrocement panels. The compression forces acting on the section can be expressed as,

$$C = 0.85 f_c' ab + \sum A_{sc} f_y \tag{1}$$

The total tensile forces in the tension zone can be expressed as,

$$T = \sum A_{st} f_y + T_f \tag{2}$$

where
f_c' = compressive strength of concrete, (MPa)
f_y = tensile strength of steels, (MPa)
T_f = tensile force of ferrocement, (N)
A_{st} = tension steel area, (mm.^{2})
a = depth of compressive stress block, (mm.)
b = section breadth, (mm.)

Based on equilibrium of forces on the section, the depth of compressive zone can be determined. The moment capacity can then be computed as the product between either tension or compression force and moment arm. Figure 9 shows the equilibrium of forces on the composite beam section.

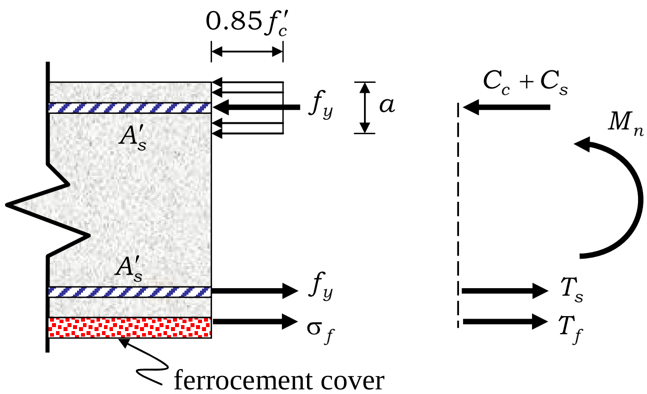

Figure 9: Stresses and forces on the section

4.2 Shear Strength

The shear strength of concrete section was evaluated using ACI318 simplified equation.

$$V_c = (1/6)\sqrt{f_c'}bd \tag{3}$$

The shear strength contributed from mortar was ignored. Additional, shear strength contributed by internal and external web reinforcements were computed by conventional formula.

$$V_s = \frac{A_v f_y d}{s} \tag{4}$$

where
d = effective depth, (mm.)
s = spacing of web reinforcements, (mm.)

The comparison of failure load using ACI procedure is shown in Table 4 and Table 5. A good agreement is obtained except specimen “con” in which the ACI code seems to give higher load compared with the test result.

5. PRACTICAL APPLICATION OF THE METHOD

Based on the results of the testing program, the proposed method has been applied in real building. The 20 year old three-story residential house was strengthened in shear by ferrocement cover with additional web reinforcements. The side cover method was applied to the edge beam while the U-cover method was applied to the intermediate beams. The contractor’s opinion was that this strengthening method offered lots of advantages in terms of fast time construction, low budget, low labor demand and easy constructability. Figure 10 shows the real application in the field.

(a) Side-cover was applied for edge beams

(b) Finishing the surface

(c) U-cover was applied for intermediate beams

(d) Finishing the surface

Figure 10: React application in the field

6. CONCLUSIONS

Based upon the test results of the experimental, five reinforced concrete beams were tested under monotonic loading. The main parameters are the shape of ferrocement cover, surface roughness and extra clip reinforcement. From these experiments, the following conclusions can be drawn.

- The failure of strengthening beam is developed by flexural crack in compressive zone.
- The capacity of strengthened specimens increased approximately 70% compared to the control specimen.
- After strengthening, all of beam showed large deflection at ultimate load.
- Using special C-clip bars can save the construction times, prevent shear failure and gain more ductility.
- The surface roughness can increase ductility.
- The specimen with U ferrocement cover has higher load carrying capacity, preventing shear failure, and larger ductility compared with specimens strengthened by side cover ferrocement.
- The conventional ACI method can be adopted for strengthening design purposes.

7. ACKNOWLEDGEMENTS

The authors are very grateful to Thailand Research Fund (TRF) for providing the research fund RSA S280034 to carry out the research.

REFERENCES

P. Joyklad, T. Pheeraphan, and P. Nimityongskul, Development of Ferrocement Panel to Resist Blast Load, *The 10th National Convention on Civil Engineering, Chonburi*, May 2-4, 2005.

A. W. Anwar, P. Nimityongskul, R. P. Pama and Robler-Austriaco, Method of Rehabilitation of Structural Beam Elements Using Ferrocement, *Journal of Ferrocement*, Vol. 21(3), 1991.

K. C. G. Ong, P. Paramasivam and C. T. E. Lim, Flexural Strengthening of Reinforced Concrete Beam Using Ferrocement Laminates, *Journal of Ferrocement*, Vol. 22(4), 1992.

M. Z. Jamin and M. A. Alam, Flexural Strengthening of Reinforced Concrete Beams Using Ferrocement Laminate with Skeleton Bars, *Journal of Applied Sciences Research*, Vol. 2(9), 2006.

H. F. Ezzat, B. I. S. Yousry and S. K. Yasser, Repairing Reinforced Concrete Beams by Ferrocement, *Journal of Ferrocement*, Vol. 27(1), 1997.

P. Paramasivam, C. T. E. Lim and K. C. G. Ong, "Strengthening of RC Beams with Ferrocement Laminates", Cement and Concrete Composites, Vol. 20, 1998.

S. F. A. Rafeeqi, S. H. Lodi and Z. R. Wadalawala, Behavior of Reinforced Concrete Beams Strengthening in Shear, *7th International Symposium on Ferrocement and Thin Reinforced Concrete Composites, National University of Singapore,* June 27-29, 2001.

ACI318-99, *Building Code requirements for structural concrete and complementary*. American Concrete Institute, Farmington Hills, Michigan, 1999.

A STUDY ON SEISMIC REPAIR COST OF R/C BUILDING STRUCTURES USING A GEOMETRICAL DAMAGE ESTIMATION MODEL OF R/C MEMBERS

NORIYUKI TAKAHASHI
Institute of Industrial Science, The University of Tokyo, Japan
ntaka@iis.u-tokyo.ac.jp
YOSHIAKI NAKANO
Institute of Industrial Science, The University of Tokyo, Japan
iisnak@iis.u-tokyo.ac.jp

ABSTRACT

To evaluate visible damage of reinforced concrete (R/C) members such as crack width and length, cyclic load tests of one third scaled R/C members were carried out. Based on the tests, a geometrical damage estimation model is proposed to quantify each crack width and corresponding length. The model consists primarily of a geometrical condition for the relationship between the sum of crack widths and drift ratio and a probabilistic model between crack widths and lengths.

Applying the proposed model to seismic response analyses of R/C building structures modeled as fish-bone shaped frames, the damage and repairing process, as well as life cycle economic loss were simulated. Life cycle economic loss was defined here as the repairing cost for maintenance of the functionality of a building through its life length. As a result, it is implied that the case of main damages on beams will suffer more life cycle economic losses than the case of main damages on columns because of the extent of damaged area and the construction cost of falsework.

1. INTORODUCTION

Loss estimation of a building due to earthquake events in its life length is important to facilitate the decision making of the building owner to choose the reasonable seismic performance. In this paper, life cycle economic loss defined as the repairing cost of a building structure through its life length was simulated using a new damage estimation model which is partially based on cyclic load tests of one third scaled R/C members.

2. EXPERIMENTAL PROGRAM

2.1 Test specimens, setup and instrumentation

Two R/C beam specimens proportioned to approximately 1/3 of full scale were tested under cyclic loading. The design parameters and corresponding values are given in Table 1. The dimension for the test specimens and test setup are shown in Figure 1. To obtain the propagation of crack width and length corresponding to attained and present drift ratio, the cyclic displacement pattern shown in Figure 2 was operated. Crack widths were measured at the points shown in Figure 3 by crack gauges. Crack lengths were measured by image processing of sketched and scanned cracking pattern.

Table 1: Description of Test Specimens

Specimen	Concrete Strength (N/mm^2)	Rebar - Tensile reinforcement ratio to the section	Yield strength of rebar (N/mm^2)	Lateral reinforcement - Lateral reinforcement ratio to the section	Yield strength of lateral reinforcement (N/mm^2)	Failure mode
F-1	30	8-D13 - 0.0121	295	D4@60 - 0.0022	295	Flexure
S-1	18		785		295	Shear

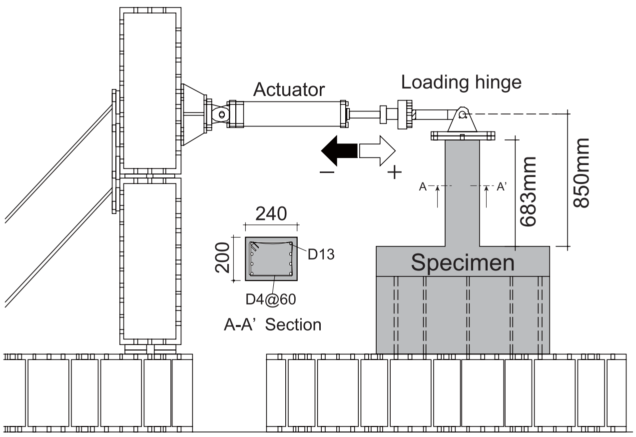

Figure 1: Dimension of Beam Specimen and Test Setup

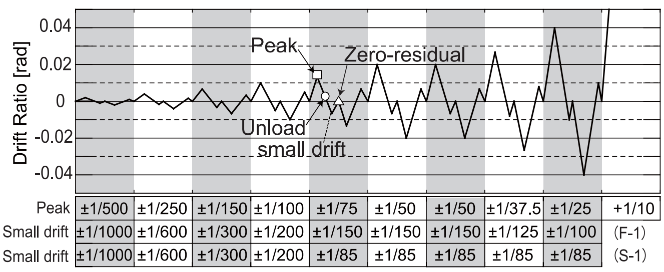

Figure 2. Cyclic Displacement Pattern

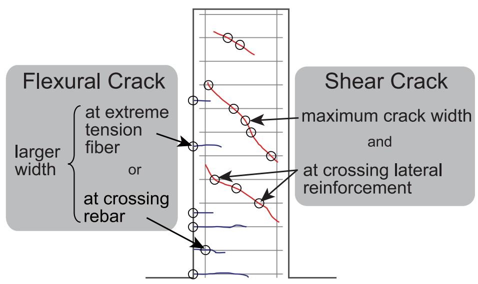

Figure 3: Crack Measurement Point

2.2 Test results

Figure 4 shows the shear force versus drift response for each specimen and the cracking pattern at 4.0% drift. Measured maximum and average crack widths are shown in Figure 5. Measured crack lengths are shown in Figure 6. Crack width and length of specimen S-1 increased rather than specimen F-1 in large drift.

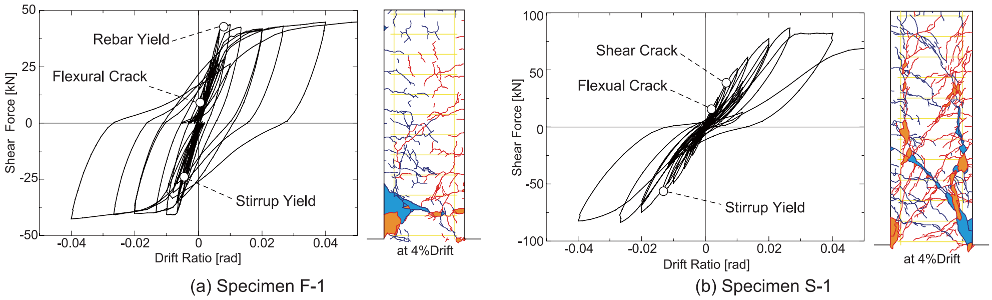

Figure 4: Shear Force versus Drift Ratio Response, and Cracking Pattern

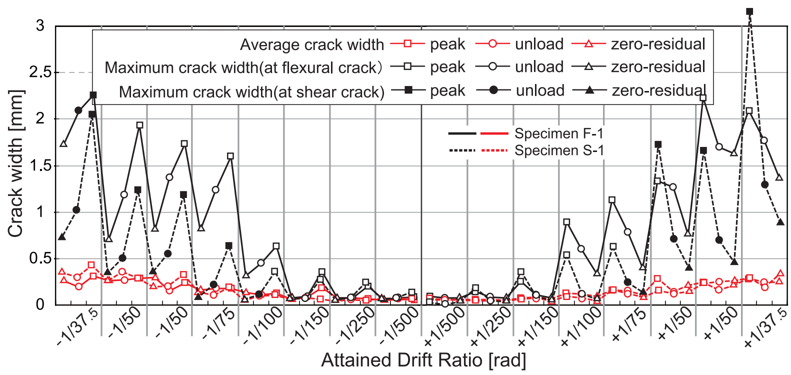

Figure 5: Crack Width for Attained Drift Ratio

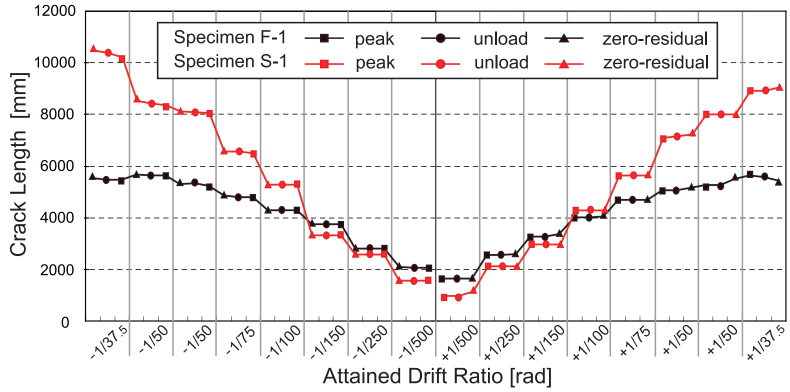

Figure 6: Crack Length for Attained Drift Ratio

3. GEOMETRICAL DAMAGE ESTIMATION

3.1 Geometrical damage estimation model

Architectural Institute of Japan (AIJ, 2004) proposed geometrical macro model of relation between crack width and drift ratio shown in Figure 7. In this paper, this relation is expressed as

$$R = R_f + R_s = \frac{\sum w_f}{D - x_n} + \frac{2\sum w_s \cdot \cos\theta}{L} \tag{1}$$

where, R_f: flexural drift ratio, R_s: Shear drift ratio, w_f: flexural crack width, w_s: shear crack width, D: depth, x_n: distance from extreme compression fiber to neutral axis, and L: clear span, respectively. CEB-FIP (1978) proposed crack spacing shown in Figure 8. Crack length at stabilized crack pattern due to Figure 8 is expressed as

$$l_{av,f} = \frac{\zeta \cdot L \cdot (D - x_n)}{S_{av}} \tag{2a}$$

$$l_{av,s} = \frac{D}{\sin\theta}\left(\frac{D\cos\theta + L\sin\theta}{S_{av}} - 2q\right) + \frac{q \cdot (q+1) \cdot S_{av}}{\sin\theta\cos\theta} \tag{2b}$$

where, $l_{av,f}$: stabilized flexural crack length, $l_{av,s}$: stabilized shear crack length, S_{av}: crack spacing, θ: crack angle, and q: quotient of $D\cos\theta$ / S_{av}, respectively.

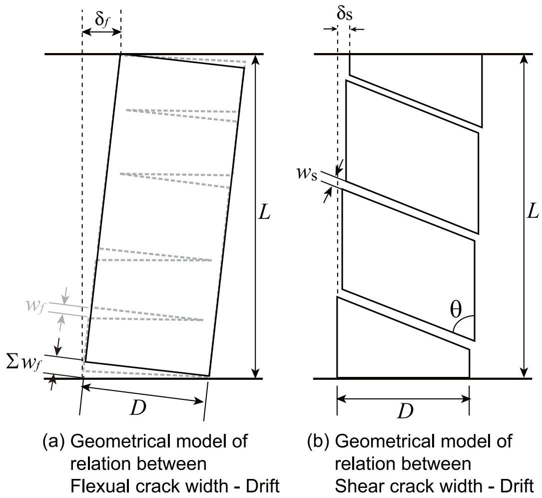

Figure 7: Geometrical Model between Crack Width and Drift

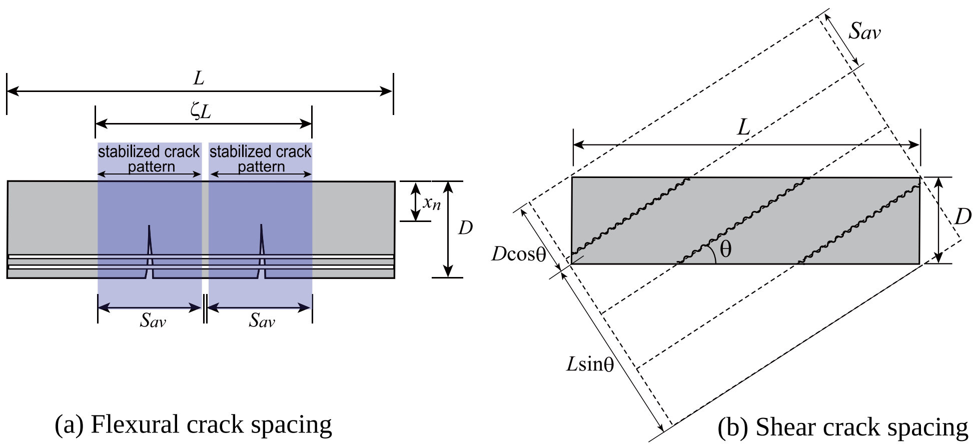

Figure 8: Crack Spacing

Estimation results of crack width of specimen F-1 and S-1 due to this geometrical model are shown in Figure 9 and 10, respectively. The estimated crack width of specimen F-1 can approximately simulate the experimental result. On the contrary, that of specimen S-1 can approximately simulate the experimental result only at the unloaded drift, and it overestimates at the peak drift and underestimates at the zero-residual drift. It implies that the geometrical model shown in Figure 7 matches up with the unloaded drift condition. In the after-mentioned study on life cycle economic loss estimation, the residual drift after excitation is supposed to be similar to the unloaded drift, and it is assumed that the crack width can be calculated from the residual drift after excitation with the geometrical model.

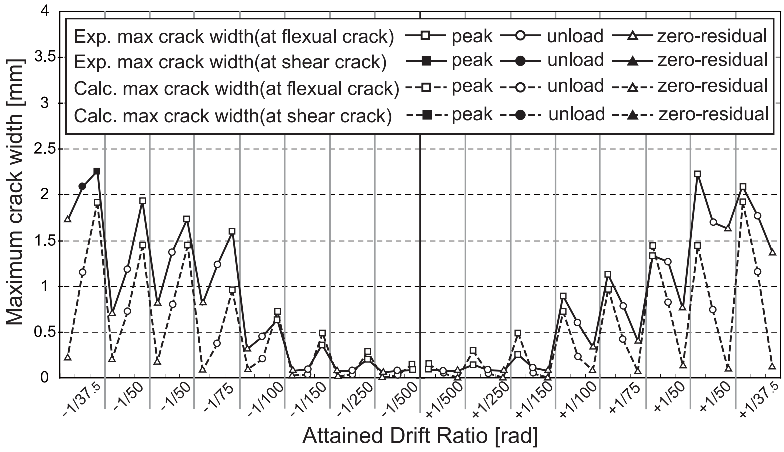

Figure 9: Crack Width Estimation of Specimen F-1

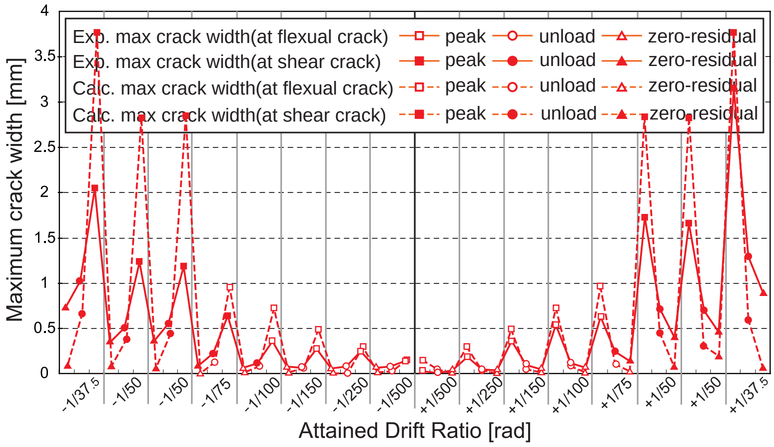

Figure 10: Crack Width Estimation of Specimen S-1

Estimation results of crack length of specimen F-1 and S-1 due to the geometrical model are shown in Figure 11. The estimated crack length represents essentially the length at stabilized crack pattern, thus the propagation of crack length can not be expressed. Based on Figure 11, a new crack length propagation model is proposed in Figure 12. In Figure 12, β means the ratio of flexural drift to total drift. In the after-mentioned study on life cycle economic loss estimation, it is assumed that the clack length can be calculated from the attained maximum drift with the geometrical model.

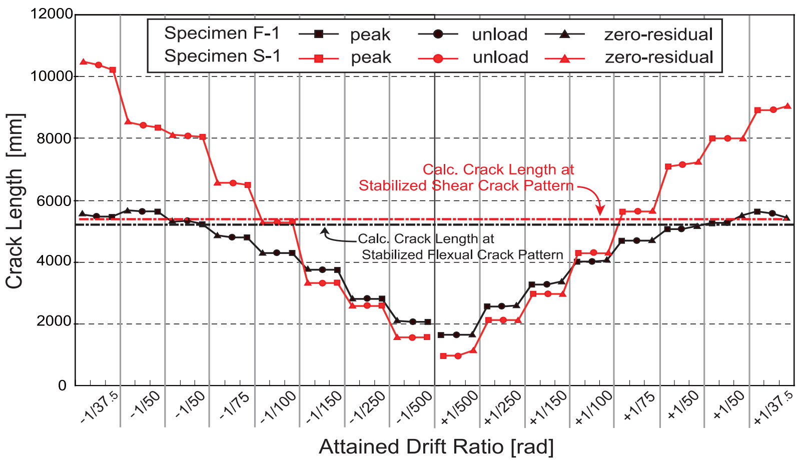

Figure 11: Crack Length Estimation

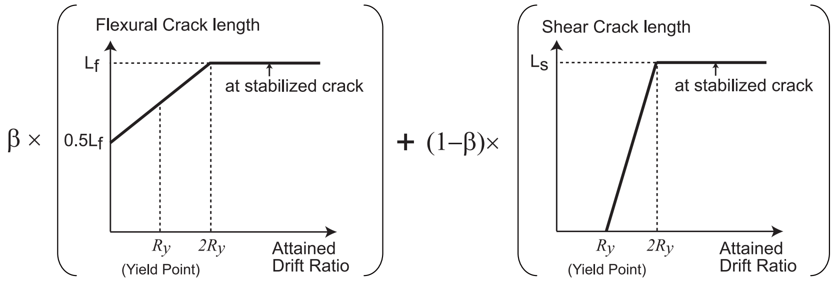

Figure 12: Crack Length Propagation Model

Additionally, the spalling propagation model based on previous research (Takahashi, 2005) shown in Figure 13 is proposed, though it depends not on the geometrical model but on the empirical model. It is formulated as

$$SR = \alpha_{sp} \times (IDR_{max} - R_0) \tag{3}$$

where, SR: spalling ratio [m^2/m^2], α_{sp}: constant value (= 3.67), R_0: initial spalling drift ratio (= 0.01), and IDR_{max}: attained maximum drift ratio.

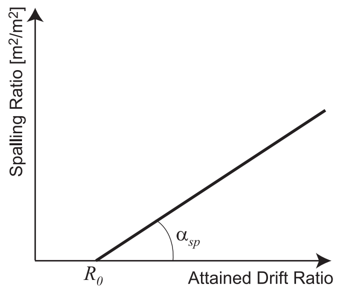

Figure 13: Spalling Propagation Model

3.2 Probabilistic model between crack width and length

A new probabilistic model between crack widths and lengths is also introduced. Crack length distribution to crack width is represented as log-normal distribution in this proposed model. Figure 14 shows the crack length distribution histogram at the drift of +0.01 rad. Comparing the calculated results with experimental results, the crack length distribution of both specimen can be simulated by log-normal distribution with standard deviation σ = 3.0. As concern with the standard deviation, the different values, σ = 0.22~1.49, were proposed by other researchers (Takimoto et al., 2004 and Igarashi et al., 2009). It means that the standard deviation of crack length distribution is unstable. In the after-mentioned study on life cycle economic loss estimation, the standard deviation is assumed to be 1.1.

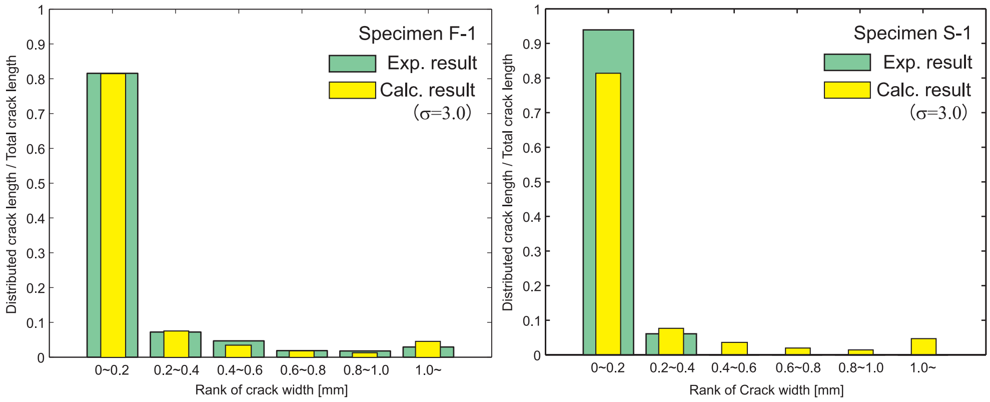

Figure 14: Crack Length Distribution to Crack Width (at +0.01 rad.)

4. LIFE CYCLE COST ESTIMATION

4.1 Input ground motion

To estimate the lifecycle economic loss, the scenario of earthquake events through lifecycle is necessary, then peak velocities of ground motion on engineering bedrock are firstly calculated based on the seismic hazard curve proposed by National research Institute for Earth science and Disaster prevention (NIED, 2005). Secondly, a series of peak velocities on the medium soil through lifecycle is created such that they fit the probabilistic distribution using the plotting position equation. Plotting position equation is represented by

$$F(x) = \frac{i - \alpha}{N + 1 - 2\alpha} \tag{4}$$

where, N: total number of years in record, i: rank in descending order (i.e. from highest to lowest), x: value of i_{th} data, $F(x)$: exceedance probability and α: constant value. α is calculated as Equation 5 to define the probability of exceedance for the largest earthquake as $P(i)$% in lifecycle years,

$$\alpha = \frac{(N+1)\ln(1-P(i))+iT}{2\ln(1-P(i))+T} \tag{5}$$

where, $P(i)$: i_{th} data's probability of exceedance in T years. The sequence of earthquake is rearranged in a random order. This series of peak velocity is used as a target to modify an input base accelerogram. Figure 15 shows the seismic hazard curve in Tokyo proposed by NIED (NIED, 2005). Figure 16 shows the example of lifecycle peak ground velocities on the medium soil in Tokyo in the case of 50 years life length and 10% in 50 years as the probability of exceedance for the largest earthquake.

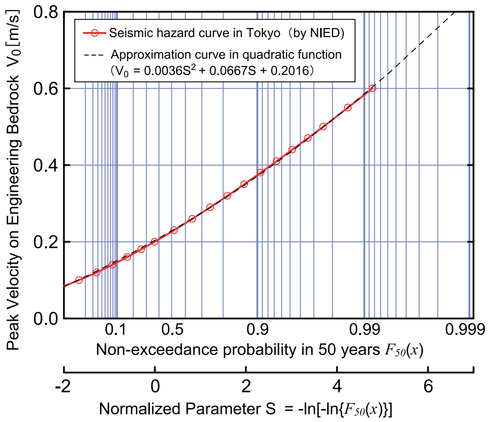

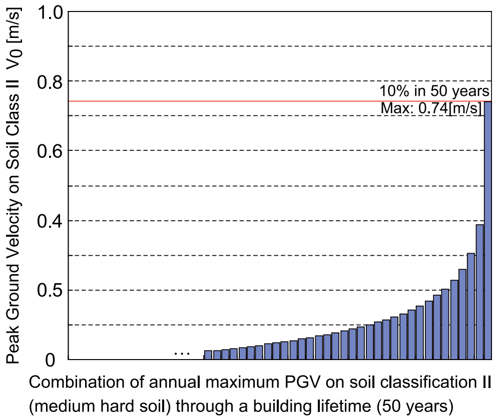

Figure 15: Hazard Curve in Tokyo *Figure 16: Example of Life Cycle PGV*

4.2 Structural model

Two fishbone-shaped frames shown in Figure 17 are studied for estimating the life cycle repair cost. One is strong-column and weak-beam frame with beam rebar strength σ_s=390kN. Another is weak-column and strong-beam frame with beam rebar strength σ_s=490kN. Takeda hysteresis model (Takeda et al. 1970) is used for each member modeled as one-component model. Viscous damping factors proportional to instantaneous stiffness are assumed to be 3%. The cracking strength is assumed to be one third of yielding strength, the secant stiffness at yielding point is assumed to be 30% of the linearly elastic stiffness, and the third stiffness after yielding is assumed to be 1% of the linearly elastic stiffness for each member.

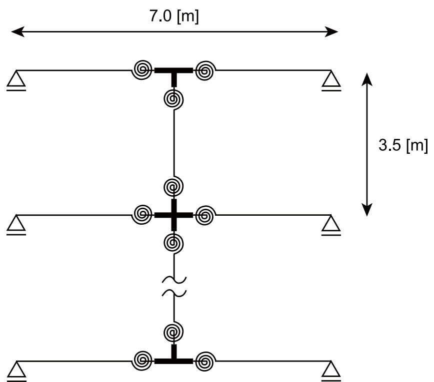

Common Variable:
Mass : 1.2 tonf/m^2
Column : 700×700 (Fc32, 8-D32/ σ_s=390kN)
Beam : 400×800 (Fc24, 8-D25/ σ_s=*)
Footing : 600×1800 (Fc32, 12-D32 / σ_s=390kN)

*Analytical Parameter:
(a) Strong-column and weak-beam type
Beam rebar strength: σ_s=390kN
(b) Weak-column and strong-beam type
Beam rebar strength: σ_s=490kN

Figure 17: Structural Model

4.3 Calculation results of life cycle economic loss

Providing the maximum drift ratio is larger than yielding drift (assumed to be 1/120 rad. in this study), structures are repaired according to the scenario described in Table 2. If the maximum displacement is smaller than yielding drift, structures are left unrepaired with damage such as a stiffness degradation. Estimated life cycle economic losses of two structures defined as the repairing cost of structures through their life length are shown in Figure 18. Life cycle economic loss due to repairing the cracks are higher in the strong-column and weak-beam structure than the weak-column and strong beam strucutre, but life cycle economic loss due to repairing the spalling are higher in the weak-column and strong beam strucutre than the strong-column and weak-beam structure.

Repairing cost of spalling depends on the maximun interstory drift ratio through the life length. As shown in Figure 19, the maximum interstory drift ratio, which come out at the 2nd floor, is larger in the the weak-column and strong beam strucutre than the strong-column and weak-beam structure. On the contrary, repairing cost of cracking depends not on the maximun drift ratio but on the extent of cracking area. The strong-column and weak-beam structure shows the smaller maximum drift ratio at the 2nd floor, but its drift ratio at the other floor is larger than that of the weak-column and strong beam strucutre. This extent of cracking area affects the repairing cost of cracking. Life cycle economic loss due to falsework is larger in the case of the exterior frame or the strong-column and weak-beam structure because of the extent of damaged area.

Table 2: Repairing Scenario

<table>
<tr><th>Condition</th><th colspan="2">Repair method</th><th>Unit price</th></tr>
<tr><td>Crack width < 0.2mm</td><td colspan="2">Sealing</td><td>$9.1 /m</td></tr>
<tr><td>Crack width < 1.0mm</td><td colspan="2">Epoxy injection</td><td>$66.0 /m</td></tr>
<tr><td>Crack width ≥ 1.0mm</td><td colspan="2">U-cut sealing / Cement grout</td><td>$125.4 /m</td></tr>
<tr><td>Spalling ratio < 0.05</td><td colspan="2">Patching resin mortar</td><td>$270.0 /m²</td></tr>
<tr><td>Spalling ratio ≥ 0.05</td><td colspan="2">Jacketing / Replacement</td><td>$542.3 /m²</td></tr>
<tr><td>at Interior Column</td><td colspan="2">No falsework</td><td rowspan="4">$20.0 /m²</td></tr>
<tr><td>at Interior Beam</td><td rowspan="3">False-work hight</td><td>Half floor hight</td></tr>
<tr><td>at Exterior Column</td><td>Damaged floor level</td></tr>
<tr><td>at Exterior Beam</td><td>Damaged floor level
+ half floor hight</td></tr>
</table>

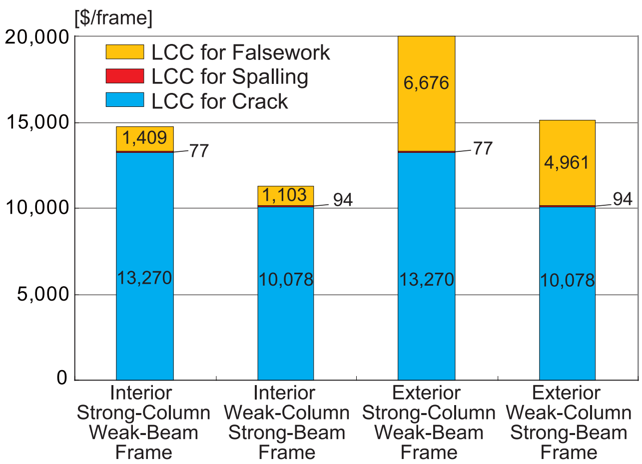

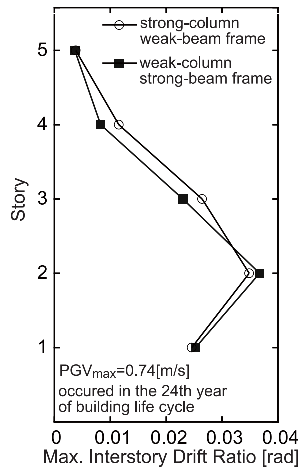

Figure 18: Calculated Life Cycle Economic Loss *Figure 19: Maximum IDR*

5. CONCLUDING REMARKS

Life cycle economic loss defined as the repairing cost of a building structure through its life length was simulated using a new damage estimation model which is partially based on cyclic load tests of one third scaled R/C members. It is concluded that strong-column and weak-beam system will suffer more life cycle economic loss than weak-column and strong-beam system because of the extent of cracking area and the construction cost of falsework.

REFERENCES

AIJ, 2004. *Guidelines for Performance Evaluation of Earthquake Resistant Reinforced Concrete Buildings (Draft)*. (in Japanese)

CEB-FIP, 1978. *Model Code for Concrete Structures*

Igarashi, S., 2009. Development of Analytical Model for Reparability Evaluation of RC Columns Based on Damage (Part 1 – Part 3), Summaries of Technical Papers of Annual Meeting of Architectural Institute of Japan, Vol.C-2, 513-518. (in Japanese)

NIED, 2005. Japan Seismic Hazard Information Station (J-SHIS), http://www.j-shis.bosai.go.jp/j-shis/

Takahashi, N. et al., 2005. Repair Cost Function in Seismic Reparability Assessment for R/C Structures, Proc. of Japan Concrete Institute, Vol.27, No.2, 1543-1548. (in Japanese)

Takahashi, N. et al., 2006. Life Cycle Input Ground Motion Intensities for the Seismic Loss Estimation of the Building through its Lifetime, Proc. of 12th Japan Earthquake Engineering Symposium, 422-425. (in Japanese)

Takimoto, K. et al., 2004. Study on Evaluation of Damage of RC Beams using Crack Data, Journal of the Japan Society of Civil Engineers, No.760/V-63, 135-145. (in Japanese)

Takeda, T. et al., 1970. Reinforced concrete response to simulated earthquakes, Journal of Structural Division, ASCE, 96:ST12, 2557-2573

EXPERIMENTAL STUDY ON PP-BAND MESH SEISMIC RETROFITTING FOR LOW EARTHQUAKE RESISTANT ARCH SHAPED ROOF MASONRY HOUSES

NAVARATNARAJAH SATHIPARAN
Post Doctoral Fellow, The University of Tokyo, Japan
sakthi@risk-mg.iis.u-tokyo.ac.jp
PAOLA MAYORCA
Project Research Associate, ICUS, Institute of Industrial Science,
The University of Tokyo, Japan
paola@iis.u-tokyo.ac.jp
KIMIRO MEGURO
Director/ Professor, ICUS, Institute of Industrial Science,
The University of Tokyo, Japan
meguro@iis.u-tokyo.ac.jp

ABSTRACT

Unreinforced masonry structure is one of the most popularly used constructions. It is also unfortunately the most vulnerable to the earthquakes. It would collapse within a few seconds during earthquake movement, and does become a major cause of human fatalities. Therefore, retrofitting of low earthquake-resistant masonry structures is the key issue for earthquake disaster mitigation to reduce the casualties significantly. When we propose the retrofitting in developing countries, retrofitting method should respond to the structural demand on strength and deformability as well as to availability of material with low cost including manufacturing and delivery, practicability of construction method and durability in each region. Considering these issues, a technically feasible and economically affordable PP-band (polypropylene bands, which is commonly utilized for packing) retrofitting technique has been developed and many different aspects have been studied by Meguro Laboratory, Institute of Industrial Science, The University of Tokyo.

Unreinforced masonry structures with masonry arch shaped roofs are generally characterized by weak, brittle materials, weak element connections and excessive weight. The main points of weakness of the traditional masonry arch roofs that contributed to poor seismic response can be inability of the roof to act as a diaphragm and heavy weight of the roof. But ability of PP-band mesh kept the structure integral during the shaking will help to overcome this issues. Therefore, to evaluate the beneficial effects of the PP-band mesh retrofitting method, shaking table tests were carried out on arch shaped roof masonry structure with and without retrofitting.

From tests' results, a scaled model with PP-band mesh retrofitting is able to withstand larger and more repeatable shaking than that without PP band retrofitting, which all verified to reconfirm high earthquake resistant performance. Therefore proposed method can be one of the optimum solutions for promoting safer building construction in developing countries and can contribute earthquake disaster reduction in future.

1. INTRODUCTION

Unreinforced masonry structures with masonry arch roofs are generally characterized by weak, brittle materials, weak element connections and excessive weight. The main points of weakness of the traditional masonry arch roofs that contributed to poor seismic response can be summarized as follows:

- Inability of the roof to act as a diaphragm: Masonry arch roofs are incapable of diaphragm action. This is due to their curved geometries, the load-carrying mechanisms and the weak and brittle materials. The load-carrying mechanism of these types of roofs is primarily in compression. The non-homogeneous masonry of the roofs is unable to carry tensile or flexural loads. As a result, they are not capable of restraining the top of their supporting walls during ground shaking, nor are they capable of transferring excessive horizontal inertia forces. Furthermore, they induce a pre-earthquake static horizontal force at the top of the walls as they transfer their compressive load to the walls. In the shared load-bearing walls, the thrust from the two adjoining arches cancel each other out. However, in end arches this force causes an unbalanced outward thrust on the wall.
- Heavy weight of the roof: Perhaps the most important seismic weakness of the masonry arch is their excessive weight. The masonry arch roofs are, by nature heavy, as a minimum roof thickness is required to enable the successful transfer of the gravity load in an arch action.

2. EXPERIMENTAL PROGRAM

2.1 Description of the specimens

For shaking table experiment, three models were built in the reduced scale of 1:4 using the unburnt brick as masonry units and cement lime and sand (1:2.8:8.5) mixture as mortar with cement/water ratio of 0.33. Attention was paid to make the models as true replica of adobe masonry buildings in developing countries in terms of masonry strength even though the construction materials used were those available in Japan.

Buildings dimensions were 933mmx933mmx720mm box shape with 380 mm height arch shape roof as shown in Figure 1. Wall thickness is

50mm. The sizes of door and window in opposite walls were 243x485mm^2 and 325x245mm^2 respectively.

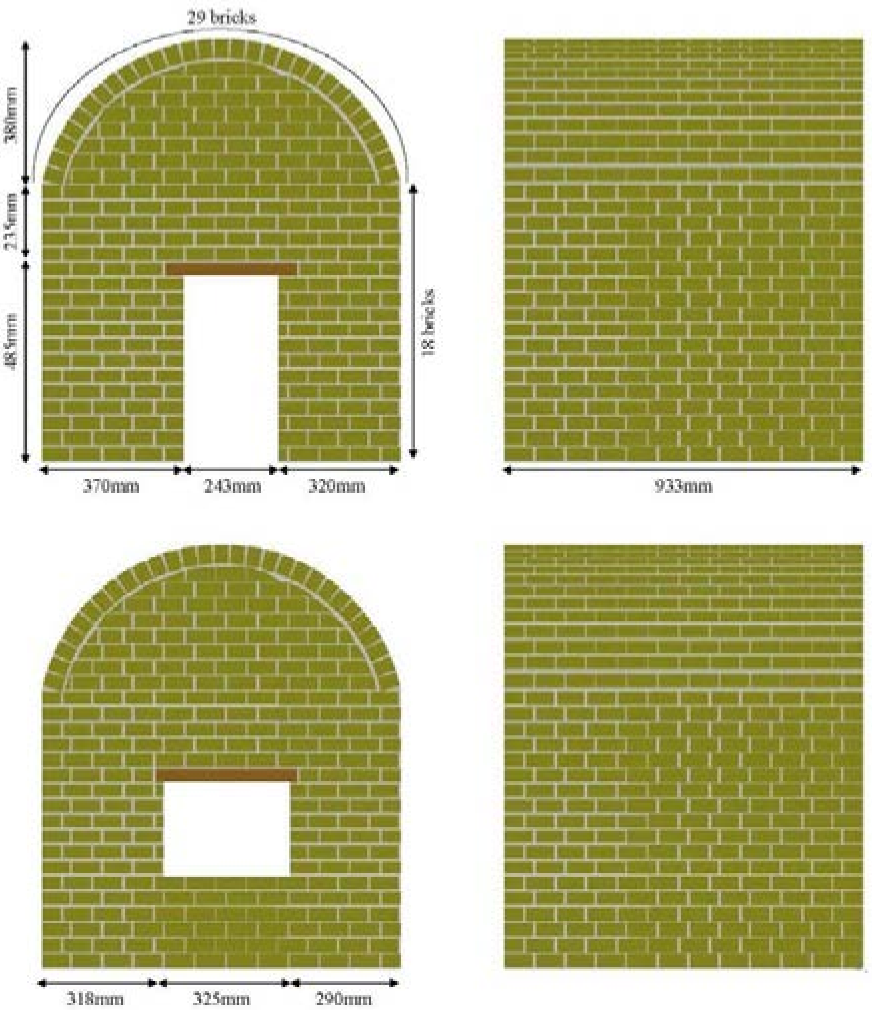

Figure 1: Model dimension (mm)

Table 1 shows the shaking table testing programs. The specimens were named according to the following convention: **B-R-P-S** in which;

B is Brick type used for construction of the model
A: unburned brick;
R is Roof type - **AR**: arch roof
P is Retrofitted condition
NR: non-retrofitted
RE: retrofitted;
S is Condition of tie bar
TB: with tie bar (10 mm bar with 160x160mm^2 timber plate at end)
TX: without tie bar

Table 1: Summary of shaking table test

Case No.	Specimen Name	PP-band Retrofitting	Tie bar
1	A-AR-NR-TB	X	O
2	A-AR-RE-TX	O	X
3	A-AR-RE-TB	O	O

Totally two out three models were retrofitted with PP-band mesh after construction. The cross-section of the band used was $6x0.24mm^2$ and the mesh pitch was 40mm. The mechanical properties of masonry in terms of compressive, shear and bond strength were given in Table 2.

Table 2: Mechanical properties of masonry specimens (in MPa)

Specimen	Diagonal shear strength	Compression strength	Shear strength	Bond Strength
A-AR-NR-TB	0.042	4.36	0.0055	0.0050
A-AR-RE-TX	0.052	4.44	0.0052	0.0055
A-AR-RE-TB	0.048	4.28	0.0062	0.0046

2.2 Construction and retrofitting procedure

All specimens have two part; box shape house and arch roof. Box shape house consisted of 18 rows of 44 bricks in each layer except openings and arch roof consisted of 29 rows of 11½ bricks in each layer. Box shape house construction process takes place in two days, first 11 rows in first day and remaining rows construct in following day. Arch roof construction procedure take place after 7 days from initial construction of box shape house. Remaining two side walls constructed take place 7 days after arch roof construction.

In case of retrofitted specimen initially boxed shaped was constructed and retrofitted. Then arch framework place above box house model and PP-band mesh cover that arch frame. Arch roof construction procedure take place after 7 days from initial construction of box shape house. After 4 days of curing arch framework was removed. PP-band mesh come from inside the arch roof and box house model were welded by ultrasonic welding machine. Remaining two side walls constructed 7 days after arch roof construction. And finally PP-band mesh come from outside the arch roof and outside box house model were welded and retrofitted by wire connectors. Construction and retrofitted procedure of house model was shown in Figure 2.

2.3 Input motion

Simple easy-to-use sinusoidal motions of frequencies ranging from 2Hz to 35 Hz and amplitudes ranging from 0.05g to 1.4g were applied to obtain the dynamic response of both retrofitted and non-retrofitted structures. This simple input motion was applied because of its adequacy for later use in the numerical modeling. Figure 3 shows the typical shape of the applied sinusoidal wave.

Loading was started with a sweep motion of amplitude 0.05g with all frequencies of 2Hz to 35Hz for identifying the dynamic properties of the models. The numbers in Table 2 indicate the run numbers. General trend of loading was from high frequency to low frequency and from lower amplitude to higher amplitude. Higher frequencies motions were skipped towards the end of the runs.

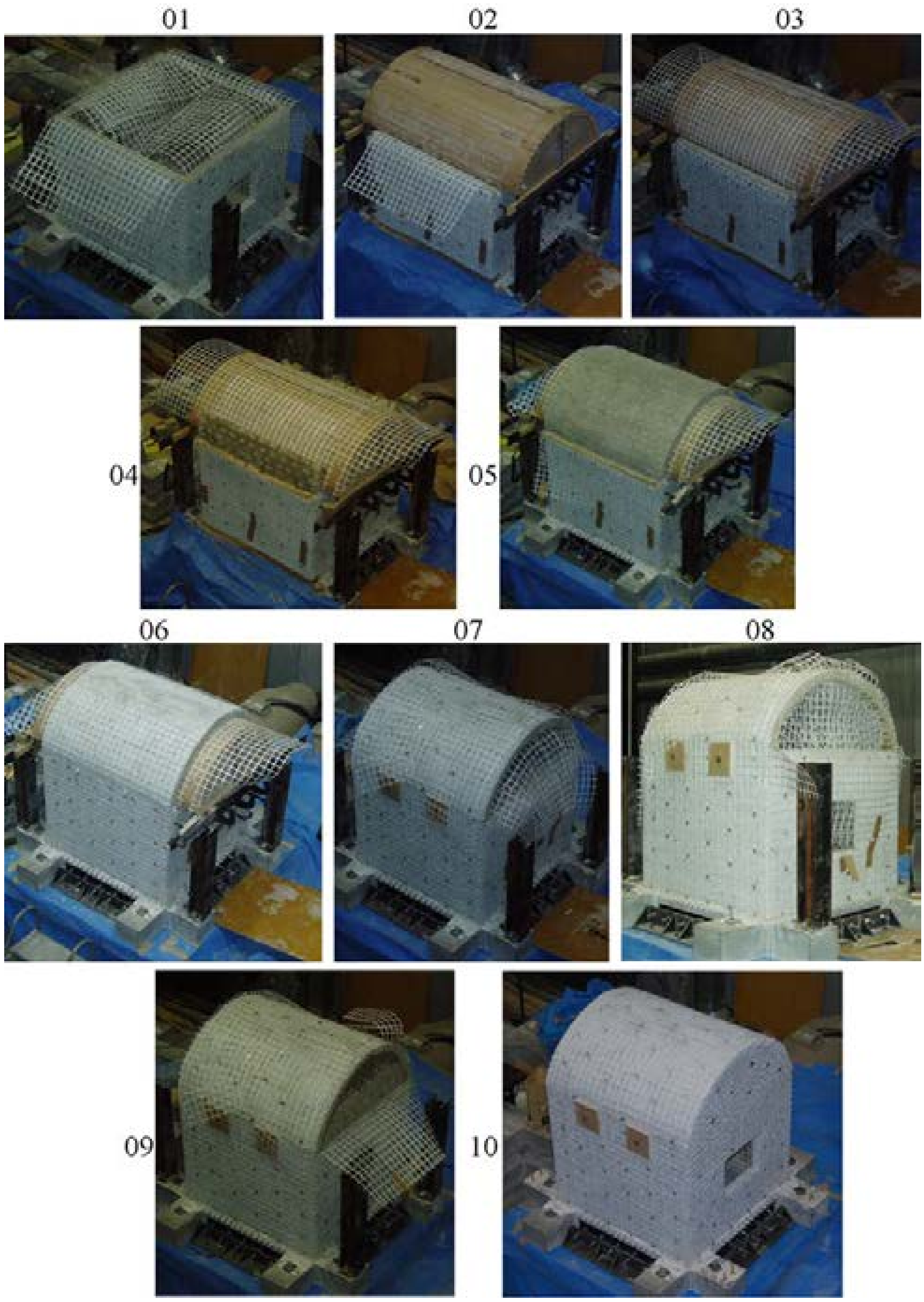

Figure 2: Retrofitting Procedure

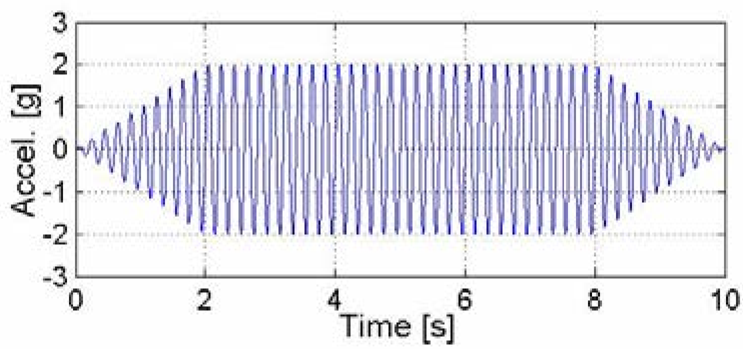

Figure 3: Typical Shape of Input Sinusoidal Motion

Table 2: Loading Sequence

Amplitude	Frequency							
	2Hz	5Hz	10Hz	15Hz	20Hz	25Hz	30Hz	35Hz
1.4g		50						
1.2g	54	49						
1.0g		48						
0.8g	53	47	43	40	37	34	31	28
0.6g	52	45	42	39	36	33	30	27
0.4g	51	44	41	38	35	32	29	26
0.2g	46	25	24	23	22	21	20	19
0.1g	18	17	16	15	14	13	12	11
0.05g	10	09	08	07	06	05	04	03
sweep	01,02							

3. CRACK PATTERN AND ENERGY DISSIPATION MECHANISM

For specimen A-AR-NR-TB up to run 21, no major crack was observed in this model. Major cracks were observed closer to openings from run 22. After that, cracks widened with each successive run. At run 30, cracks appear three corner of the window opening and propagate towards the corner of the wall. Also crack observed left half circle of the east wall-arch interaction and this crack propagate full circle of east wall-arch interaction with successive runs. At run 36, wall-arch interaction in both east and west wall was totally cracked. Even it totally cracked, presence of tie bar, arch roof prevented from splitting outward. Also large amount cracks were observed in roof part. Particularly, long horizontal crack at initial roof part of walls in direction shaking was observed. At run 39, top part of the east wall (part, above the window opening) was totally separated from the specimen and it was fallen from specimen. At run 41, top part of the west wall (above the door opening) was totally separated from the specimen and it’s fallen from specimen. As a result arch part only supported by two walls, which are in the direction of shaking and due to walls subjected to out-of-plane load; arch part was bursts outwards in shaking direction. This finally led to the structure collapse at run 42.

For retrofitted specimen A-AR-RE-TX up to Run 21, no major crack was observed in this model. Major cracks were observed closer to openings from Run 22. After that, cracks widened with each successive run. At run 33, wall-arch interaction in both east and west wall was totally cracked. Long horizontal cracks were observed in top of the arch roof. Also large amount cracks were observed in roof part. Particularly, long horizontal crack at initial roof part of walls in direction shaking was observed. At run 45, although at the end of this run almost most of the mortar joints were cracked, the specimen did not lose stability. Although PP-band mesh kept the structure integral during the shaking, it allowed the sliding of the bricks along these cracks to some extent. At the final stage of the test, run 54, with 50mm base displacement, 33 times more than the input displacement applied in run 42 and 7 times more velocity, virtually all the brick joints were cracked and the building had substantial permanent deformations. However, building did not loose the overall integrity as well as stability and collapse was prevented in such a high intensity of shaking. Another important point to mention that this retrofitted model has sustained 12 more runs with higher input energy before this run.

In smaller input motions in case of retrofitted specimen A-AR-RE-TB, amount of crack relatively fewer than that case of specimen A-AR-RE-TB. But in higher input motion, in both models, there are not much difference observed in dynamic performance. Like specimen A-AR-RE-TX, run 54 was the last run for specimen A-AR-RE-TB.

4. FAILURE BEHAVIOR AND PERFORMANCE EVALUATION

The performances of the models were assessed based on the damage level of the buildings at different levels of shaking. Performances were evaluated in reference to five levels of performances: light structural damage, moderate structural damage, heavy structural damage, partially collapse and collapse.

Table 3: Damage categories

Category	Damage extension
D0: No damage	No damage to structure
D1: Light structural damage	Hair line cracks in very few walls. The structure resistance capacity has not been reduce noticeably.
D2: Moderate structural damage	Small cracks in masonry walls, falling of plaster block. The structure resistance capacity is partially reduced.
D3: Heavy structural damage	Large and deep cracks in masonry walls. Some bricks are fall down. Failure in connection between two walls.
D4: Partially collapse	Serious failure of walls. Partial structural failure of roofs. The building is in dangerous condition
D5: Collapse	Total or near collapse

The Japan Meteorological Agency seismic intensity scale (JMA) is a measure used in Japan to indicate the strength of earthquakes. The JMA scale was colored according to the following convention:

Index	JMA ~4	JMA 5-	JMA 5+	JMA 6-	JMA 6+	JMA 7

4.1 Performance evaluation based on JMA scale

Table 4 shows the performances of non retrofitted model A-AR-NR-TB with different JMA intensities. Partial collapse of the non-retrofitted building was occurred at the 39th run at intensity JMA~4 and total collapse at the 42nd run at intensity JMA~4. But it should be noted that the model was already cracked in different loadings as discussed in previous section.

Table 4: Performance of A-AR-NR-TB model

Acceleration (g)	Frequency (Hz)							
	2	5	10	15	20	25	30	35
1.4								
1.2								
1.0								
0.8				D4	D3	D2	D2	D2
0.6			D5	D4	D3	D2	D2	D1
0.4			D4	D3	D2	D2	D2	D1
0.2		D1	D1	D1	D1	D0	D0	D0
0.1	D1	D1	D1	D1	D1	D0	D0	D0
0.05	D0	D0	D0	D0	D0	D0	D0	D0

Table 5 shows the performances of non retrofitted model A-AR-RE-TX with different JMA intensities. The A-AR-RE-TX performed at heavy structural damage at 42nd run at which A-AR-NR-TB was collapsed. Heavy structural damage level of performance was maintained until 52nd run. Test was stopped after the 54th run due to limitation of the shaking table capacity. It should be noted again that this model survived 13 more shakings in which many runs were with higher intensities than A-AR-NR-TB was collapsed before reaching to the final stage at the 54th run.

Table 5: Performance of A-AR-RE-TX model

Acceleration (g)	Frequency (Hz)							
	2	5	10	15	20	25	30	35
1.4		D3						
1.2		D3						
1.0		D3						
0.8	D4,D4	D3	D3	D3	D3	D2	D2	D2
0.6	D3	D3	D3	D3	D2	D2	D2	D2
0.4	D3	D3	D3	D3	D2	D2	D2	D2
0.2	D3	D2	D1	D1	D1	D0	D0	D0
0.1	D0	D0	D0	D0	D0	D0	D0	D0
0.05	D0	D0	D0	D0	D0	D0	D0	D0

Table 6 shows the performances of retrofitted model A-AR-RE-TB with different JMA intensities. The A-AR-RE-TB performed at moderate structural damage at 42nd run at which A-AR-NR-TB was collapsed. In the same run specimen A-AR-RE-TX was performed at heavy structural damage level. In the 47th run, another JMA 5+ intensity shaking, the A-AR-RE-TB got the heavy structural damage level, which is crushing, extensive cracking, and damage around openings. Test was stopped after the 54th run due to limitation of the shaking table capacity. It should be noted again that this model survived 13 more shakings in which many runs were with higher intensities than A-AR-NR-TB was collapsed before reaching to the final stage at the 54th run.

Table 6: *Performance of A-AR-RE-TB model*

Acceleration (g)	Frequency (Hz)							
	2	5	10	15	20	25	30	35
1.4		D3						
1.2		D3						
1.0		D3						
0.8	D3,D3	D3	D2	D2	D2	D2	D1	D1
0.6	D3	D2	D2	D2	D2	D2	D1	D1
0.4	D3	D2	D2	D2	D2	D2	D1	D1
0.2	D2	D1	D1	D1	D1	D0	D0	D0
0.1	D0	D0	D0	D0	D0	D0	D0	D0
0.05	D0	D0	D0	D0	D0	D0	D0	D0

4.2 Performance evaluation based on Arias intensity scale

The Arias intensity was initially defined (Arias, 1970) as

$$I_a = \frac{\pi}{2g}\int_0^t a^2(t)dt \tag{1}$$

and was called scalar intensity. It is directly quantifiable through the acceleration record a*(t)*, integrating it over the total duration of the earthquake. The arias intensity is claimed to be measure of the total seismic energy absorbed by the ground.

Figure 4 shows the performance level of each specimen against dynamic motion. Figure 5 shows the specimen capacity against dynamic motion for each specimen. From results, it's clearly show that; retrofitted model damage level performance at least 5 times better than that of non-retrofitted model.

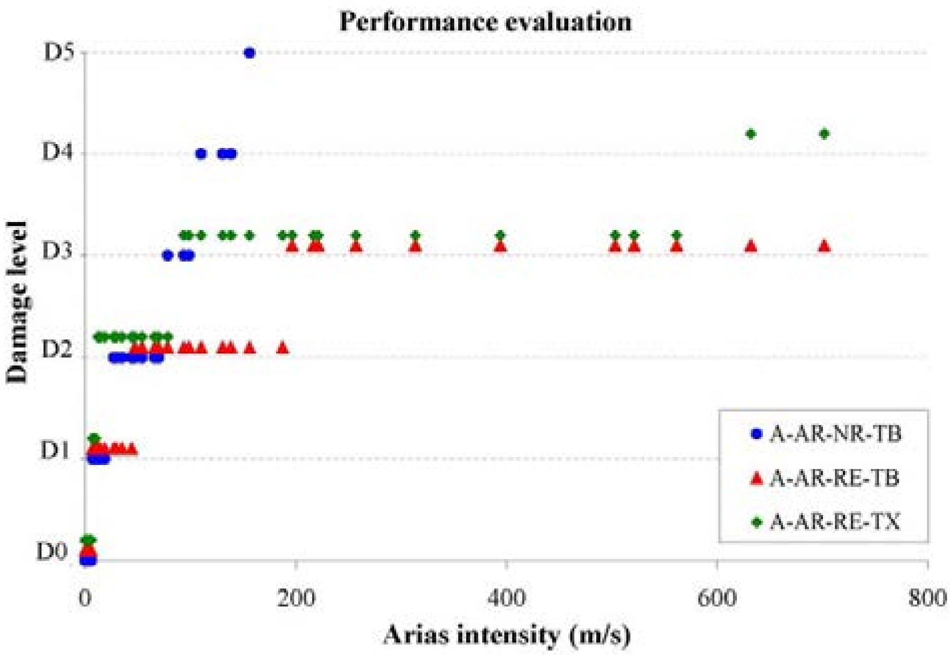

Figure 4: Performance evaluation based on arias intensity

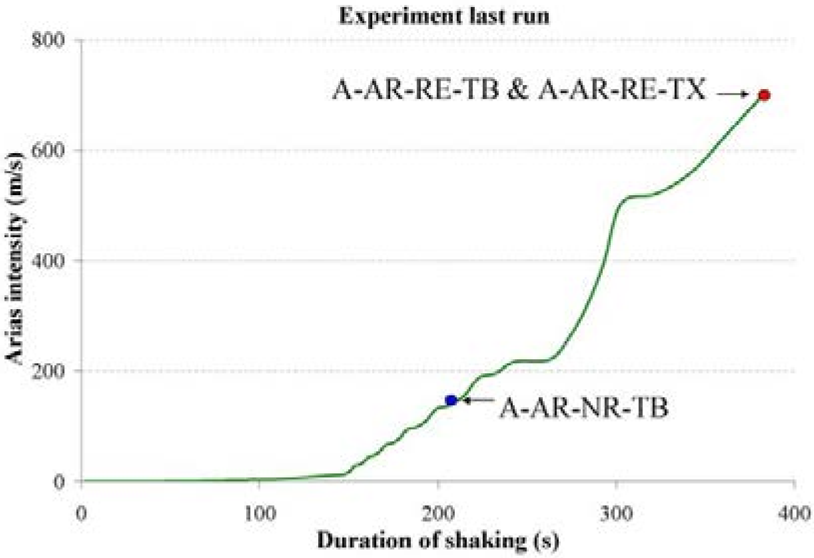

Figure 5: Specimen capacity against shaking

5. CONCLUSION

This paper introduced the shaking table test program on arch shaped roof masonry houses. Form test result showed that;

- For specimen A-AR-NR-TB, after run 36; due to presence of tie bar, even wall-arch interaction in both east and west wall was totally cracked; arch roof prevented from splitting outward. It totally failed at run 42.
- AR-RE-TX & A-AR-RE-TB were withstands base displacements 50 times larger and velocities 10 times higher than the A-AR-NR-TB. It should be noted again that these models survived 13 more shakings in which many runs were with higher intensities than A-AR-NR-TB was collapsed before reaching to the final stage at the 54th run.
-

Considering overall performance of the both specimens, PP-band can effectively increase the seismic capacity of masonry houses and therefore reduce the number of casualties in the coming earthquakes.

REFERENCE

Mahmoud R. Maheria. *Performance of Building Roofs in the 2003 Bam, Iran Earthquake*, Earthquake Spectra, Volume 21, No. S1, pages S411–S424, December 2005

T.Fujieda, P.Mayorca, N.Sathiparan and K.Meguro, *Experimental Study on the Behavior of PP-band Mesh Retrofitted Masonry Houses using Miniature Models*, Bulletin of Earthquake Resistant Structure Research Centre, March 2008, No.41, 67-72

Pilot Studies for Knowledge Assistance for Verification and Promotion on a New Seismic Retrofitting method for existing masonry Houses by Polypropylene Band Mesh (The Islamic Republic of IRAN), Final Report, JBIC, ICUS, OYO International Corporation, July 2007.

REPLACEABLE SLAB OF OPEN-TYPE PIERS AS NEW COST-EFFECTIVE TECHNOLOGY

Yuichiro KAWABATA, Mitsuyasu IWANAMI, Ema KATO
Structural Mechanics Division
Port and Airport Research Institute, Japan
kawabata-y@pari.go.jp, iwanami@pari.go.jp, katoh-e@pari.go.jp
Hiroshi YOKOTA
Research Group of Sustainable Infrastructure System
Hokkaido University, Japan
yokota@eng.hokudai.ac.jp
Masahiko FURUICHI
Director for Special Research
Port and Airport Research Institute, Japan
furuichi-m2dd@pari.go.jp

ABSTRACT

The authors proposed an idea of "replaceable" slab for open-type piers as an appropriate maintenance solution of port structures without interrupting the facility services. The replaceable slab is a precast RC member, placed on RC beams with rubber shoes. It is recommended to utilize precast members in constructing superstructure of open-type piers in order to reduce construction costs and construction period and to obtain higher quality of RC members. When severe deterioration occurs in the slab during the service period, the slab can be repaired by removing on land, or replaced by a new intact slab so as to maximize net present value (NPV) of the facility.

This paper presents the structural performance and the cost-effectiveness of the replaceable slab of open-type piers. Joint details were investigated to realize the replaceable slab of open-type piers through loading tests on models of precast RC slab connected to beams by the proposed joint. Based on the test results, the replaceable joint system was proposed by comparing structural performance and fracture behavior of the replaceable slab with those of the conventional RC slab. One trial calculation revealed that the replaceable slab was cost-effective compared to the conventional RC slab in case of development of large-scale container terminal.

1. INTRODUCTION

Reinforced concrete (RC) members consisting of superstructure of open-type piers are exposed to very severe conditions, resulting in early deterioration of concrete structures due to chloride attack. In such conditions, corrosion of reinforcing steel bars progresses rapidly, because protective coatings are inadequate around the bars, and structural performance of RC members degrades as the cross-section of reinforcing bars reduces. For such deteriorated RC superstructures, appropriate maintenance should be required from the viewpoints of durability and safety of the piers. In Japan, a lot of piers need repair works only a few decades after completion of construction because durability of RC in design had not been considered appropriately. In repairing superstructure of the piers, it is necessary to set up temporary scaffolds under the superstructure. Since working time is strictly limited due to interference of tidal actions and waves, and working conditions are considerably poor due to narrow clearance under the superstructure and high humidity, the repair works to deteriorated RC superstructure of the piers are costly, causing an increase in life-cycle costs of the piers and beneficial loss due to restricting cargo handling operations.

The authors proposed an idea of “replaceable” slab for open-type piers (see Fig. 1) as an appropriate maintenance solution of port structures without interrupting the facility services. The replaceable slab is a precast RC member, placed on RC beams with rubber shoes. It is effective to utilize precast members in constructing superstructure of open-type piers in order to reduce construction costs and construction period and to obtain higher quality of RC members. Normally, after placing the precast slab on the beams, the slab is rigidly connected to the beams by splicing projecting rebars from RC members and casting concrete between them. Fig. 2 shows one of the typical methods to connect concrete members in superstructure of the piers. The structural behavior of the superstructure constructed by the connection method such as Fig. 3 are similar to those of the conventional superstructure in which beams and slabs are simultaneously constructed in-situ.

On the other hand, the replaceable slab is connected temporarily by the replaceable joint system to the beams so that the slab can be removed easily during the service period. Hence, when severe deterioration is detected in the slab at periodical inspections during services, the slab can be repaired on land after removing, or replaced by a new intact slab. As a result, it enables us to omit repair works on temporary scaffolds under the slab, resulting in reduction of maintenance costs of the piers without interrupting cargo handling operations.

In this study, joint details were investigated to realize the replaceable slab of open-type piers through loading tests on models of precast RC slab connected to beams by the proposed replaceable joint. In the tests, a variety of joint types and structural details were examined to determine appropriate joints for the replaceable slab. Based on the test results, the replaceable joint system was proposed by comparing structural performance and fracture behavior of the replaceable slab with that of the conventional RC slab. Structural design method of the replaceable slab was examined as well in terms of supporting condition and span length.

In addition, cost-effectiveness of replaceable slab was investigated using Net Present Value (NPV) analysis. NPV of the replaceable slab was compared with that of the conventional RC slab in a large-scale container terminal as a case study.

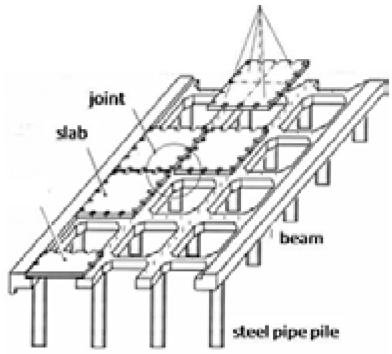

Fig. 1 Replaceable slab

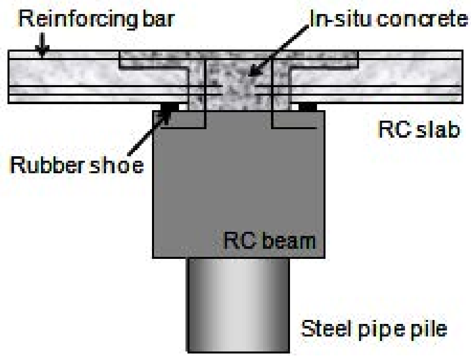

Fig. 2 Typical connection method

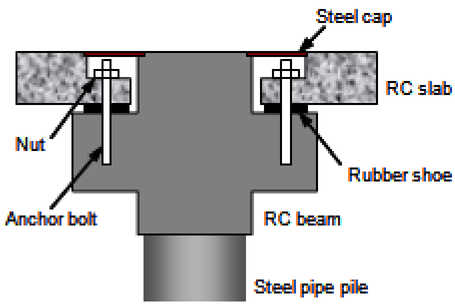

(a) Type A

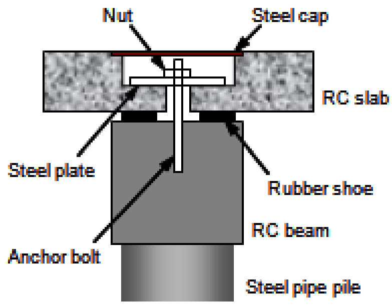

(b) Type B

Fig. 3 Replaceable joint

2. REPLACEABLE JOINT FOR PRECAST RC SLAB

To realize the idea of replaceable slab of open-type piers, two types of joint structures were proposed as shown in Fig. 3. In Type A, a precast RC slab is connected by using anchor bolts projecting from a supporting beam. The slab is placed on rubber shoes on the beam with the anchor bolts through holes in the edges of the slab, and then the nuts are tightened to fix the slab. The nuts will be loosened, when removing the slab.

In Type B, the slab is connected by using a steel plate, which is fixed by an anchor bolt projecting from the beam. The edges of the two adjacent slabs are held down simultaneously. Compared with Type A, the number of anchor bolts can be reduced, as shown in Fig. 3. However, since the height of the beam is smaller, it is necessary to arrange more reinforcing bars or to enlarge the width of the beam in order to keep flexural rigidity of the beam. There is no need to make holes in the slab for anchor bolts as in case of Type A.

Paying attention to the degree of connection between the slab and the beam by these types of joints, the connection is not completely rigid. Compared with simply supported members, they are connected more or less by the anchor bolts or the steel plate. The degree of connection is dependent on details of the joint, degree of tightening the nuts, type and size of rubber shoes, position of the rubber shoes, and so on. It is essential to structural design of the slab to investigate their effects on structural performance of the connection part.

For the purpose of establishing a design method of the replaceable slab for open-type piers, structural performance and fracture behavior of the slab connected to beams by the proposed joints should be made clear through the experimental program.

3. STRUCTURAL PERFORMANCE OF REPLACEABLE SLAB

3.1 Experimental Outline

3.1.1 Experimental Set-up

In the experimental program, loading tests on models of precast RC slab connected to beams by the joint of Type A or Type B were conducted as shown in Fig. 4. Concrete blocks modeling beams were anchored by PC bars to a load bearing floor, and then a precast RC slab was placed on the rubber shoes on the blocks. To connect the slab to the block, anchor bolts and steel plates were used in case of Type A and Type B, respectively, as illustrated in Fig. 4. The span of the slab was 3000mm, and the cross section of the slab was 1000mm by 300mm. The total length of the slab was changed depending on the type of joint used.

The width and the height of rubber shoes were 150mm and 23mm, respectively. The hardness of rubber material used was 61 degrees, which was commonly used as shoes for bridges in Japan. The PC bars used as anchor bolts were of SBPR930/1080, and the diameter was 32mm. The steel plate used for connection by Type B was of SS400, and the size was 750mm by 500mm by 20mm. In the models used in this experiment, two anchor blots were used for connection in each edge of the slab. The distance of two anchor bolts was 500mm.

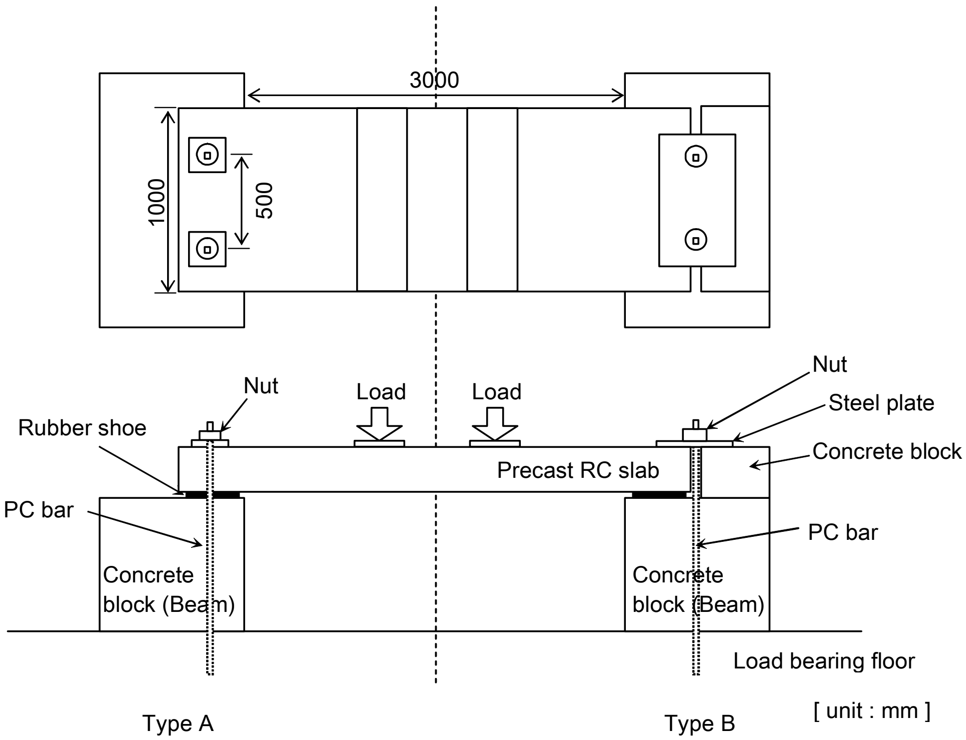

Fig. 4 Experimental set-up

Table 1 Test cases

Model	Connection	Size of slab (m)	Strain of PC bars (μ)	Overlapped length (m)	Remarks
R	rigid	-	-	-	Rigid connection (Conventional)
S	-	4.4x1.0x0.3	-	0.7	Simply supported
A1	Type A	4.0x1.0x0.3	200	0.5	
A2	Type A	4.0x1.0x0.3	600	0.5	
B1	Type B	3.4x1.0x0.3	200	0.2	
B2	Type B	4.4x1.0x0.3	200	0.7	

3.1.2 Test Cases

The test cases are indicated in Table 1. For comparison, models of conventional slab which was constructed together with beams (Model R) and of simply supported slab (Model S) were prepared. Two models were tested for each type of joint. Model A1 and Model B1 were fundamental cases. In Model A2, initially introduced strain of PC bars used as anchor bolts was increased up to 600μ in order to examine how the degree of tightening the nuts affected the test results. In Model B2, the overlapped length of slab over beam was enlarged up to 0.7m. Comparing Model B1 and Model B2, influence of the position of rubber shoes on the test results was evaluated.

3.1.3 Material Properties and Bar Arrangement

The water to cement ratio of concrete used in the slab was 0.57, and the compressive strength and Young's modulus of concrete cylinders at the loading tests was 33.1N/mm^2 and 31.6kN/mm^2, respectively. Two types of deformed bars were used as reinforcing bars of the slab. Yield strength and tensile strength of the bars were 371N/mm^2 and 597N/mm^2 for the bars of 13mm in diameter (D13), 404N/mm^2 and 567N/mm^2 for those of 16mm in diameter (D16), respectively.

In considering actual arrangement of reinforcing bars in superstructure of open-type piers [3], bar arrangement of the precast RC slab was determined as follows: in the lower layer, D13 and D16 were placed with the interval of 200mm. In the upper layer of reinforcing bars, the edge part of the slab had the same bar arrangement as the lower layer in order to resist negative moment occurring near the supporting points. In the center part of the slab, D16 was placed with the interval of 200mm in the upper layer. The cover thickness was 73.5mm for both layers of reinforcing bars.

According to the results of calculation based on the beam-bending theory, the first cracking load, the first yielding load and the ultimate load of simply supported slab (Model S) were 49kN, 155kN, and 184kN, respectively.

3.1.4 Loading Test

The vertical loads were applied to the slab by using a hydraulic jack mounted to a steel loading frame. The distance of two loading points was

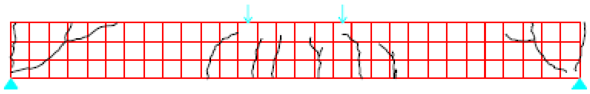

(a) Model R

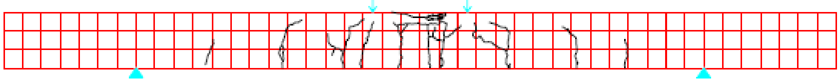

(b) Model S

(c) Model A1

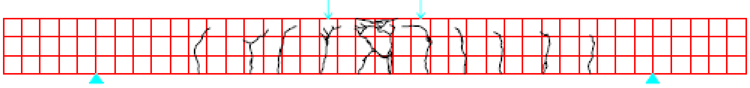

(d) Model A2

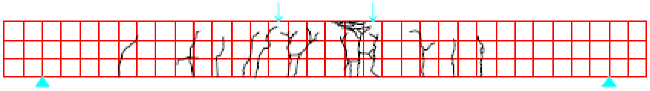

(e) Model B1

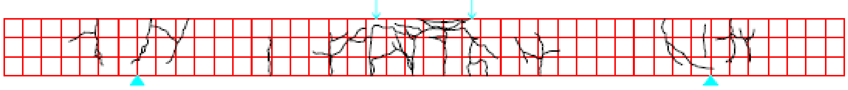

(f) Model B2

Fig.5 Crack pattern

500mm. The loads were increased monotonically up to the ultimate failure of the slab.

During loading, applied loads, deflections of the slab, strains of reinforcing bars and concrete, strains of PC bars, and displacements and strains of steel plates were measured by a data logger.

3.2 Results and Discussions

3.2.1 Crack Pattern and Fracture Process

Fig. 5 shows crack patterns observed in a side surface of slabs after the loading tests. As shown in Fig. 5, Model R failed in shear after flexural cracks occurred on the top surface near the connection part of the slab and the beam due to negative moment. It was because bending capacity of the slab was high since the shear span was short due to rigid connection of the slab and the beam. On the other hand, Model S showed typical flexural failure, in which compressive fiber of concrete was crushed after yielding of tensile reinforcing bars.

In the both slabs connected by Type A joint, typical flexural failure was observed. The crack patterns were similar to that of Model S. From this, in case of slabs connected by Type A joint, the slab seemed to behave like a simply supported member. Besides, the degree of tightening the nuts, that is, strain of PC bars had little influence on crack pattern and fracture process of the slab within the limit of this experiment.

As for the slab connected by Type B joint, when the overlapped length was 0.2m (Model B1), the slab failed in bending, and the crack pattern was similar to that of the simply supported case (Model S) and the slabs with Type A joint (Model A1 and Model A2). On the other hand,

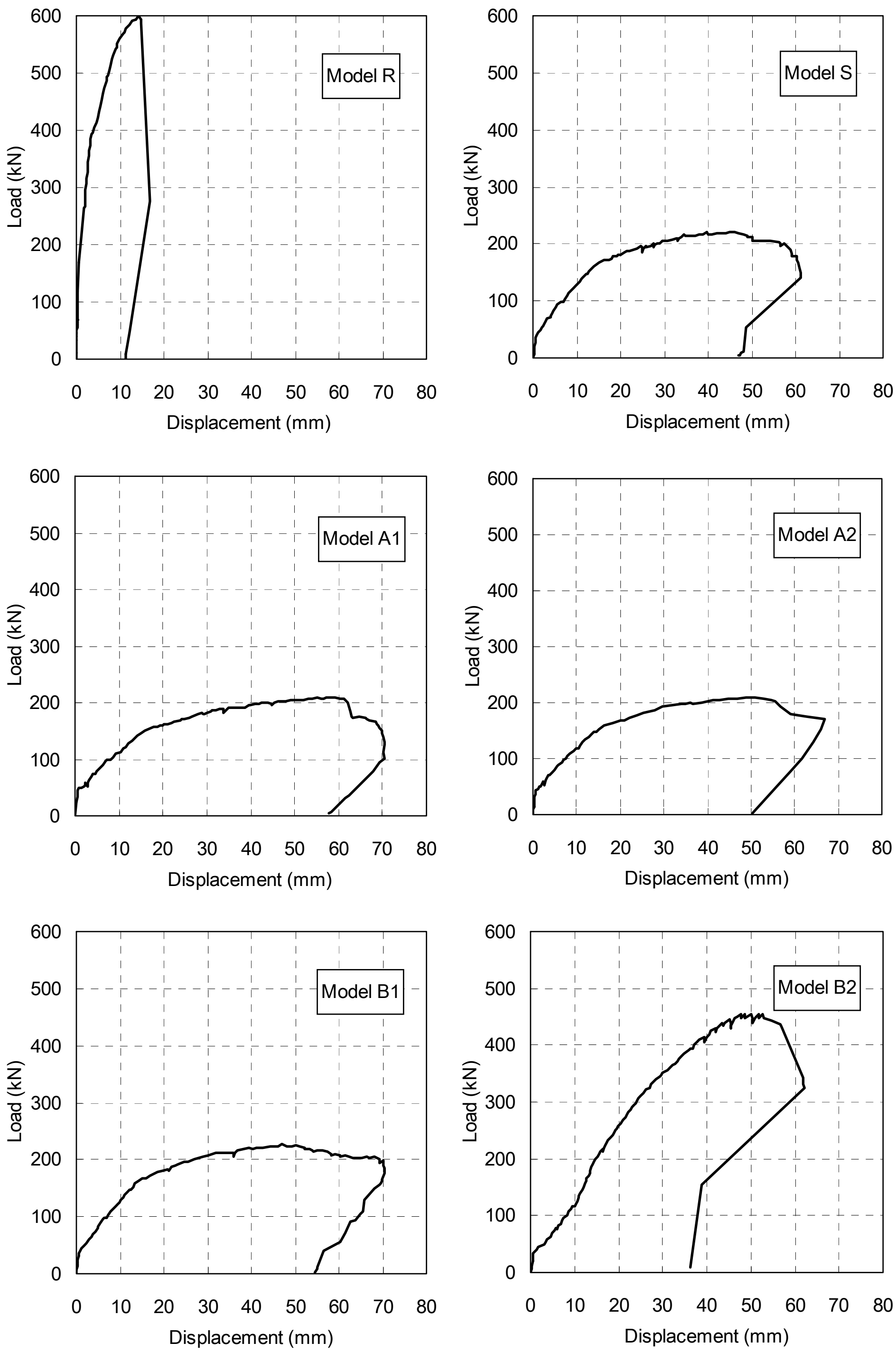

Fig. 6 Load-displacement curve

when the overlapped length was 0.7m (Model B2), flexural cracks occurred near the supporting points on the top surface as well as the bottom surface near the midspan. It was because negative moment was induced near the supporting points since the distance between the supporting points and the PC bars fixing the steel plate was long.

3.2.2 Load-Displacement Curve

Fig. 6 shows load-displacement curves obtained from the loading tests.

Table 2 Load bearing capacity of slab

Case	Cracking load (kN)	Yielding load (kN)	Maximum load (kN)
R	119	394	600
S	40	161	220
A1	40	151	209
A2	40	219	454
B1	40	162	226
B2	42	143	210
Cal	49	155	184

In the figure, the displacement is the measured deflection at the midspan of the slab subtracting the average vertical displacements at the supporting points.

Table 2 summarizes load bearing capacities of the slabs obtained from the loading tests together with the calculated ones of simply supported slab, which was explained in 3.1.3.

In Model R where the slab failed in shear, since the shear span was short due to rigid connection, flexural rigidity and load bearing capacity of the slab was considerably large compared with other test cases. The maximum load was three times larger than that of the simply supported case (Model S).

The load-displacement curves of Model A1 and Model A2 were similar to that of the simply supported slab (Model S). Therefore, load bearing capacities of these slabs were almost the same as that of Model S, regardless of strain of PC bars (the degree of tightening the nuts). It means that structural performance of slabs connected to beams by Type A joint can be evaluated by assuming to be a simply supported beam whose span length is the distance between the two rubber shoes.

On the other hand, in case of slabs connected by Type B joint, when the overlapped length was 0.2m (Model B1), the load-displacement curve was similar to that of the simply supported case (Model S), and the load bearing capacity was almost the same as that of Model S, similarly to the slabs connected by Type A joint. However, when the overlapped length was 0.7m (Model B2), the load-displacement curve was quite different from that of Model B1. Also, the maximum load was much larger than that of Model B1 although there were little difference in cracking load and yielding load between Model B1 and Model B2. The reason for this difference can be explained as follows: Before yielding of reinforcing bars, deformation of the slab was so small that negative moment was not induced near the supporting points. Consequently, structural behavior of the slab were similar to those of the simply supported case so that cracking load and yielding load were almost the same as experimental and calculated ones of the simply supported case. However, after yielding of reinforcing bars, deformation of the slab became so large that fixing by steel plates started to get remarkable, causing negative moment near the supporting points. As a result, the apparent shear span became short like Model R, and therefore flexural rigidity and load bearing capacity increased. The maximum load of Model B2 was double of that of Model B1 where the overlapped length was shorter.

It was found that the slab connected to beams by Type B joint with larger overlapped length had greater load bearing capacity. However, flexural cracks occurred on the top surface due to negative moment, causing less durability of concrete members. Also, structural design of such slabs was more difficult to establish than that of simply supported members. It was considered that the overlapped length of slab over beam in case of Type B joint should be as short as possible, such as 0.2m.

4. COST-EFFECTIVENESS OF REPLACEABLE SLAB OF OPEN-TYPE PIER

4.1 Target structure

NPVs of a 15meter-deep berth at Island City Container Terminal, Port of Hakata in Fukuoka Prefecture, Japan, were calculated for several scenarios as a case study of a large-scale container terminal. The berth was constructed with jacket-type piers, of which total area was 5,250m^2. Expected container throughput capacity of the berth was 230 thousand TEU/year.

4. 2 NPV analysis

In case of port facility, large-scale repair works inevitably interrupt cargo handling operations resulting in a considerable decrease of annual benefit of the facility. When assessing maintenance scenarios of the port facility, its social benefits are to be taken into account as well as life-cycle cost (LCC). Therefore, Net Present Value (NPV) was adopted as one of the solution of cost-benefit analysis in this study.

The berth was assumed as open-type piers of which area and container throughput capacity are the same as Island City Container Terminal for simplified calculation. Social discount rate was assumed 4.0%. LCC and beneficial loss caused by large-scale repair works for the superstructure were calculated according to the several maintenance scenarios (Table 3). Construction and maintenance costs were determined according to the previous research (Kodama et al., 2001).

Table 3 Maintenance scenario

Scenario	Type of slab	Beam	Slab	Beneficial loss
C-P1	Conventional slab	surface coating at initial and every 15 yrs.		None
C-C1		Cross-sectional repair at 30 yrs.		1/3 of cargo handling for 2 yrs.
C-C2		Cross-sectional repair at 30 yrs.	Renewal at 30 yrs.	1/2 of cargo handling for 2 yrs.
R-C1	Replaceable slab	Cross-sectional repair at 30 yrs.	Replace at 30 yrs.	None

Table 4 Results of NPV analysis (unit: billion yen)

Scenario	Type of slab	LCC	TB	NPV

C-P1	Conventional slab	32.1	106.1	74.0
C-C1		31.3	105.0	73.7
C-C2		32.8	104.5	71.6
R-C1	Replaceable slab	31.2	106.1	74.9

Expected total benefit was 106.1 billion yen (Ministry of Land, Infrastructure and Transport, 2006). Therefore, TBs were calculated with subtraction of beneficial losses from expected total benefits. NPVs were calculated with subtraction of LCCs from TBs.

4.3 LCM scenarios

Maintenance scenarios were assumed in service of 50 years (Table 3). The basic strategy of C-P1 was based on preventive maintenance while that of other cases was based on corrective maintenance. In R-C1 of which slab was replaceable, however, the facility could be maintained without restricting cargo handling operations. The beneficial losses of C-C1 and C-C2 were determined empirically.

4. 4 Results and Discussion

Comparison of replaceable slab with conventional slab due to the results of NPV analysis revealed that R-C1 was the most cost-effective maintenance scenario. Replaceable slab could reduce LCC without restricting cargo handling operations, even if its strategy was based on corrective maintenance. Therefore, “replaceable” slab would be evaluated as a cost-effective technology because it enables the facility well maintained with optimum NPV of the project among the options.

5. CONCLUSIONS

From the experimental results of the loading tests on models of the replaceable slab, it was concluded that the proposed replaceable joints, Type A and Type B, may be used as the joint system for the replaceable slab of open-type piers. The overlapped length of slab over beam in Type B joint should be determined appropriately since its influence on structural behavior of slabs was not negligible.

NPV analysis revealed that replaceable slab was a cost-effective technology because it enables the facility well maintained with optimum NPV of the project.

REFERENCES

Kodama, S., Tanabe, T., Yokota, H., Hamada, H., Iwanami, M. and Hibi, T.. 2001, Development of maintenance management system for existing open-piled piers, *Technical note of the PHRI* (in Japanese)

Ministry of Land, Infrastructure and Transport, 2006, http://www.mlit.go.jp/tec/hyouka/public/jghks/karute/img/05111189001/05111189001_2.pdf (in Japanese)

DESIGN OF CRACK SELF-HEALING ON CONCRETE STRUCTURES

TAE-HO AHN
Institute of Industrial Science, The University of Tokyo, Japan
than@iis.u-tokyo.ac.jp
TOSHIHARU KISHI
Institute of Industrial Science, The University of Tokyo, Japan
kishi@iis.u-tokyo.ac.jp

ABSTRACT

This study aims to develop and apply self-healing concrete as a new method for crack control and enhanced service life in concrete structure. This concept is one of the maintenance-free methods which, apart from saving direct costs for maintenance and repair, reduces the indirect costs – a saving generally welcomed by contractors. In this research, the self-healing phenomenon of autogenous healing concrete using geo-materials for practical industrial application was investigated. Moreover, a self-healing concrete was fabricated by ready-mixed car in a ready-mixed concrete factory, then used for the construction of artificial water-retaining structures and actual tunnel structures.

1. INTRODUCTION

The serviceability limit of concrete structures is primarily governed by the extent of damage. Cracks, one of various types of damage, play an important role in the serviceability limit. However, if it were possible to know the reason for differing behavior of concrete structures exposed to largely similar conditions, we might have the key for designing high-durability structures with low or negligible maintenance and repair costs. Furthermore, the serviceability limit of concrete structures by cracking might be overcome by crack control methodologies; the enhanced service life of concrete structures would reduce the demand for crack maintenance and repair. In particular, the utilization of self-healing technologies has high potential as a new repair method for cracked concrete under the water leakage of underground civil infrastructure such as tunnels, as shown in Figure 1.

Recently, K. Van Breugel reported that the market survey for self-healing cement-based materials as follows (K. V. Breugel , 2007). First, in case of the USA, the cost for reconstruction of bridges has been estimated between $20 and $200 billion. The average annual maintenance cost for bridges in that country is estimated at $5.2 billion. Comprehensive life cycle analyses indicate that indirect costs due to traffic jams and associated loss of productivity are more than 10 times the direct cost of maintenance and repair. For the United Kingdom, repair and maintenance accounts for almost 45% of the UK's activity in the construction and building industry. In case of Netherlands, one third of the annual budget for large civil engineering works is spent on inspection, monitoring, maintenance, upgrade, and repair. In case of Japan, East Japan Railway Company reported that maintenance and repair cost of railway bridges and tunnels is estimated at $10 billion (T.H. Ahn and T. Kishi, 2007).

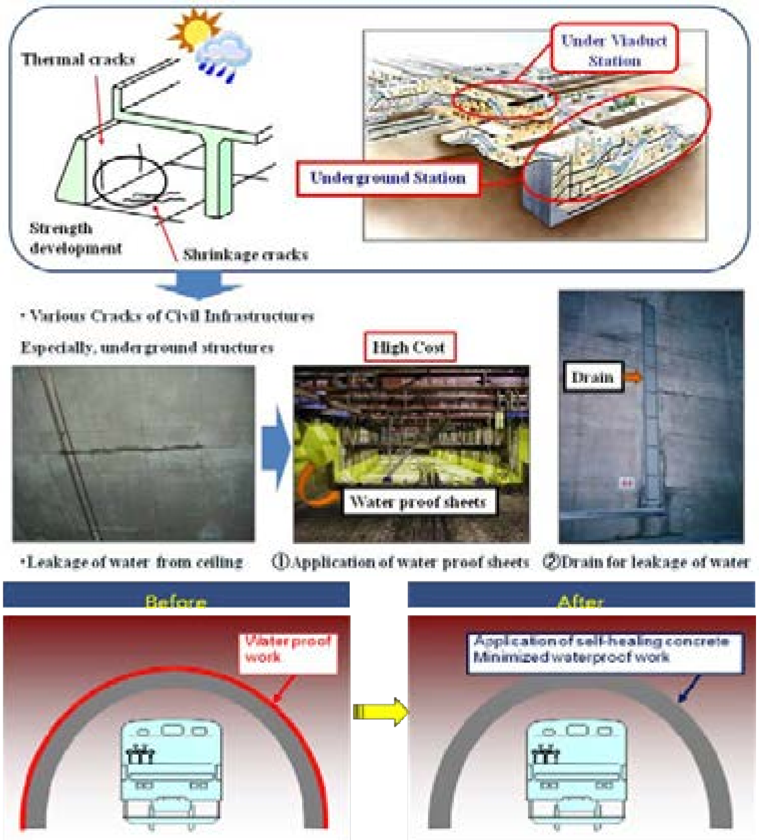

Figure 1: Application concept of self-healing concrete for the water leakage of underground civil infrastructures as tunnels

The performance of structures with elapse of time is often reported with graphs like that shown in Figure 2. In general, for high durability and normal designs, increasing the volume of cracks in a structure increases the repair costs as shown Figure 2(b). However, when considering the self-healing design, if a crack occurs, it will be healed autogenously after minor damage, as shown Figure 2 (c) and (d). This concept is one of the maintenance-free methods which, apart from saving direct costs for maintenance and repair, reduces the indirect costs – a saving generally welcomed by contractors. Furthermore, general construction philosophy has begun to change from [Design and Construction concept: constructor responsibilities for maintenance and repair of structures are limited] to [Design, Construction and Maintenance concept: constructor has responsibilities including the maintenance, monitoring and repair for life cycle of structures] as shown Figure 2. This trend shows that it is necessary for both the industrial and research fields to develop concrete including self-healing crack concepts in the near future.

The aim of this study is to develop autogenous healing concrete using various mineral admixtures for practical industrial application. Especially, it was investigated based on consideration with self-healing performance of materials and cost effectiveness as shown Figure 2(d), in order to apply self-healing concrete as a new method for crack control and enhanced service life in concrete structures.

This study focused on two primary issues: (1) experimental and analytical design of cementitious materials with self-healing capabilities, (2) development of a self-healing concrete using new cementitious materials at normal water/binder ratio [over W/B=0.45] (T.H. Ahn and T. Kishi, 2008).

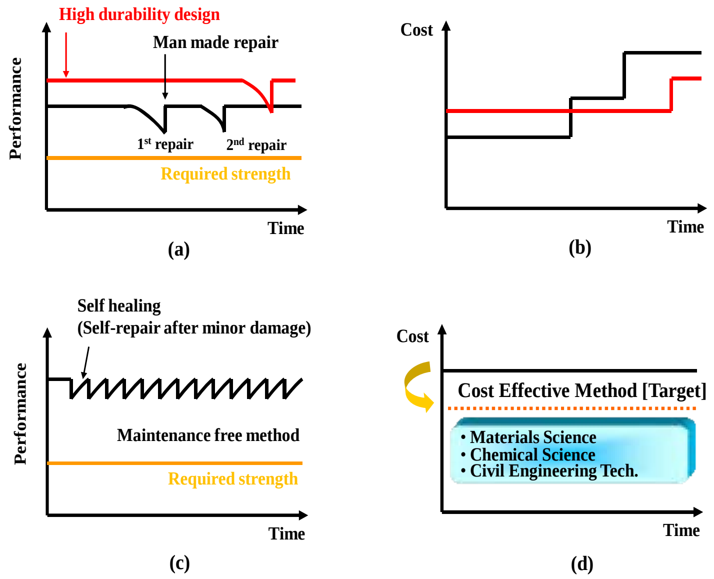

Figure 2: (a), (b): Performance (a) and costs (b) over time for normal structures (black line) and high durability design structures (red line). (c), (d): Performance (c) and cost (d) over time of the structure made with self-healing concrete. (K. V. Breugel , 2007)

2. TEST PROGRAMS

2.1 Materials

(1) Cement

Type I Japan Portland cement was used in all cementitious composite and concrete mixtures.

(2) Mineral admixtures & Chemical agents

In order to compare the self-healing capability of cementitious composite with various compositions, mineral admixtures such as expansive agent, geo-materials and chemical agents were used. These materials were prepared based on self-healing performance as reported in the previous researches (T.H. Ahn, 2008), (T.H. Ahn and T. Kishi, 2008). The expansive agent, two geo-materials (A, B) and chemical agent used were commercial products produced in Japan. Geo-material A was used for this investigation; It has an SiO_2 content of 71.3% and an Al_2O_3 content of 15.4%. It shows the XRD pattern of geo-material, which reveals that it is mainly SiO_2 and sodium aluminum silicate hydroxide [$Na_{0.6}Al_{4.70}Si_{7.32}O_{20}(OH)_4$]. It also contains montmorillonite, feldspar, and quartz, and its swelling is mainly caused by the swelling of montmorillonite, which is a swelling clay mineral. This type of geo-material swells 15-18 times its dry size when wetted by water. Polycarboxylate-based superplasticizer was also used in order to fabricate specimens.

2.2 Specimens

Table 1 shows the mix proportions of cementitious composite materials in this research. All cementitious composite pastes in this research were made at a constant water/cement ratio of 0.45. 200grams of cement were used to make the cementitious paste. All the prepared cementitious composite pastes were mixed manually for 5 minutes at ambient temperature. The slump test was then conducted on a small volume of paste using the mini-slump cone. The dosage of each superplasticizer was set in the range of 0.8 – 2.50% in order to obtain the initial target flow. Paste flow was measured at 30 minute intervals up to 90 minutes from mixing.

Table 1 Mix-proportions of cementitious composite materials based on the self-healing design

Sample	OPC	Expansive agent	Geo-Materials (A ,B type)	Chemical additives
I	90%	O	O	
II	90%	O	O	O

2.3 Estimation method of cementitious composites for crack healing

Cementitious composite pastes cylinders 5Φ x 10 cm in size were prepared following the mini-slump test. They were cured for 120 days and then artificially cracked in order to clarify the self-healing process. Crack width was controlled between 0.1 and 0.3 mm in consideration of the maximum tolerable crack widths according to construction codes. After cracking, the specimens were again water cured for 200 days.

2.4 Verification of self-healing capability on fabricated self-healing concrete

All cementitious composite materials with self-healing capability [called pre-mixed products] in this research were manufactured in the laboratory. Table 2 and Table 3 show the mixing proportions of concretes;

Table 2 Mixing proportion of concrete

Binder (B) (kg/m^3)	OPC (93%)	344.1
	Pre-mixed Products (7%)	25.9
Water/Binder (kg/m^3)	W (W/B= 47.3%)	175
Sand (kg/m^3)	S	809
Gravel (kg/m^3)	G	920
Superplasticizer (% B by weight)	SP (1.15~1.35%)	4.26~4.99

a W/B ratio of 47.3% and a S/A ratio of 46.6% were applied to all concretes. Slump flow of concrete was measured at the initial point and after 30 and 60 minutes. Self-healing concrete 10Φ x 20 cm cylinders were prepared after conducting the concrete slump test. They were cured for 1 month and then artificially cracked in order to clarify the self-healing process. Crack width was controlled between 0.1 mm and 0.3 mm according to the maximum allowable crack widths dictated by construction code. The specimens were then water cured for another 1 month after cracking.

Table 3 Mix-proportions of Binder

Sample	Binder	
	OPC	Mineral admixtures
Plain Concrete	100%	0%
Expansive Concrete	90%	10%
Self-healing Concrete	93%	7%

3. RESULTS AND DISCUSSION

3.1 Self-healing capability of cementitious composite materials

(1) Effects of geo-materials on the self-healing

In order to develop cementitious composite materials with self-healing capability compared to normal cement without self-healing capability at the normal W/C ratio, sample I [OPC + Expansive agent + Geo-materials] was investigated considering expansion and swelling terms.

Figure 3 shows the healing process of the cracked three-component system under water supply. In this case, the crack with an initial width of 0.2 mm was almost healed after 28 days. Rehydration products between cracks were clearly observed after 14 days, and the cracks self-healed perfectly even though there were small cracks between the rehydration products after 200 days, as shown in Figure 3 (f). Figure 4 shows the entire self-healed shape of the cracked specimen by top, side, bottom and cross-section. It was composed of different phases between the original and self-healing zone. Therefore, microscopy and SEM with EDS-detector were carried out to investigate the morphology, shape, and size of re-hydration products and to clarify re-crystallization.

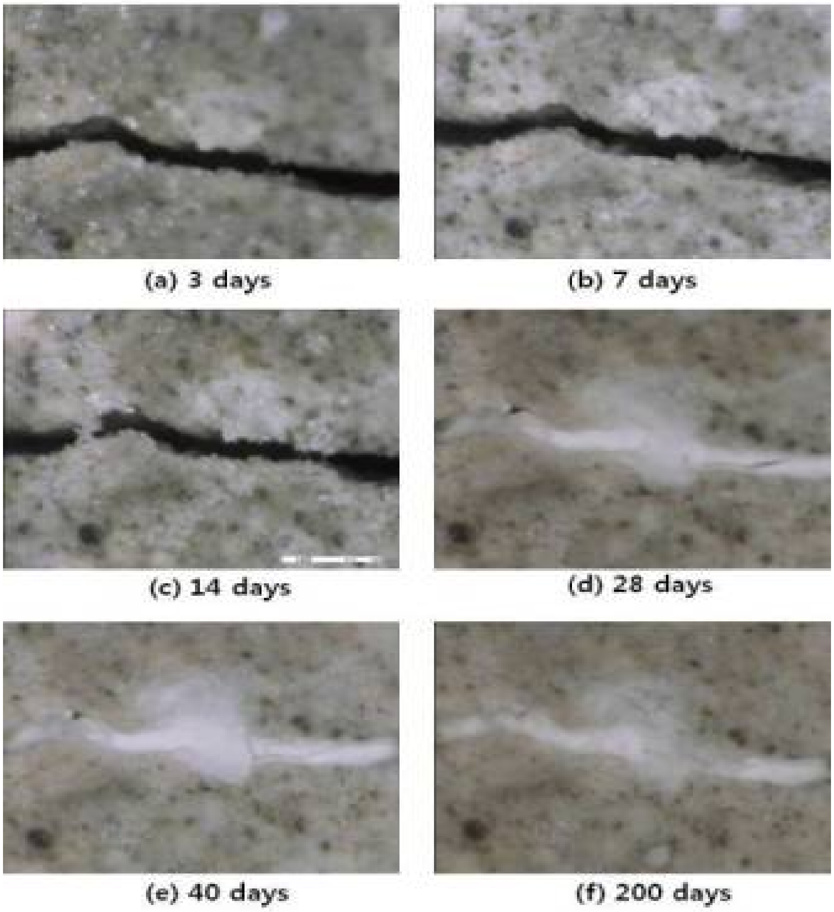

Figure 3: Process of Self-healing on the sample I pastes at normal water/binder ratio of 0.45 (the three-component system)

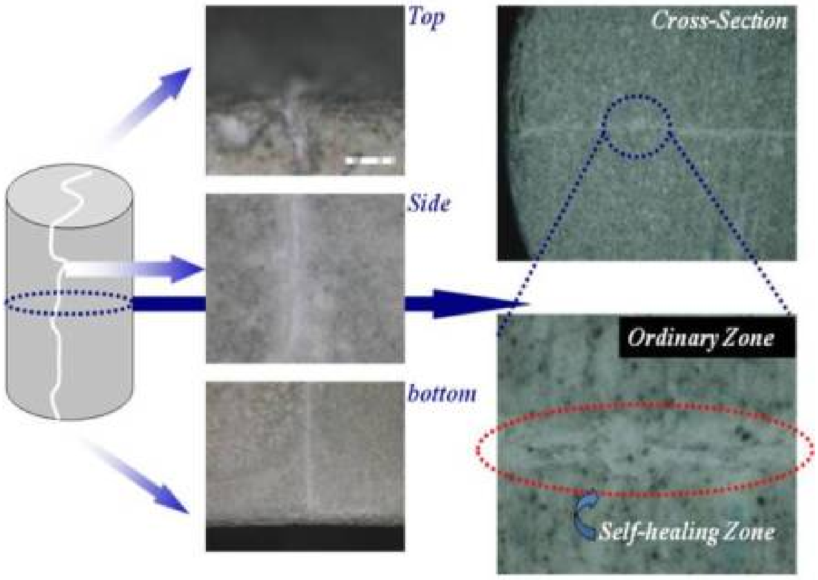

Figure 4: Self-healed shape of cracked pastes according to regions such as top, side, bottom and cross-section [in case of Sample I]

Figure 5 shows the re-hydration products on the surface of the specimen between the original and self-healing zones in case of sample I. Figure 5 (b) shows the X-ray map and spectra taken from rehydration products. It was found that the re-hydration products were mainly composed of high alumina silicate materials as shown in the X-ray mapping results. The self-healing zone was composed of modified gehelite phases (CASH) with high alumina ions compared to original zone. This self-healing phenomenon seems to be related to the crystallization by aluminosilicate with calcium ion. This seems effective for sealing against water leakages. From these results, it was concluded that application of geo-materials are desirable for the application of self-healing concrete. However, self-healing velocity for rapid water proof effect of water leakage needs to be improved in order to apply for underground civil infrastructures. Therefore, sample II has been tested in order to improve this. These results are reported and discussed in the following section.

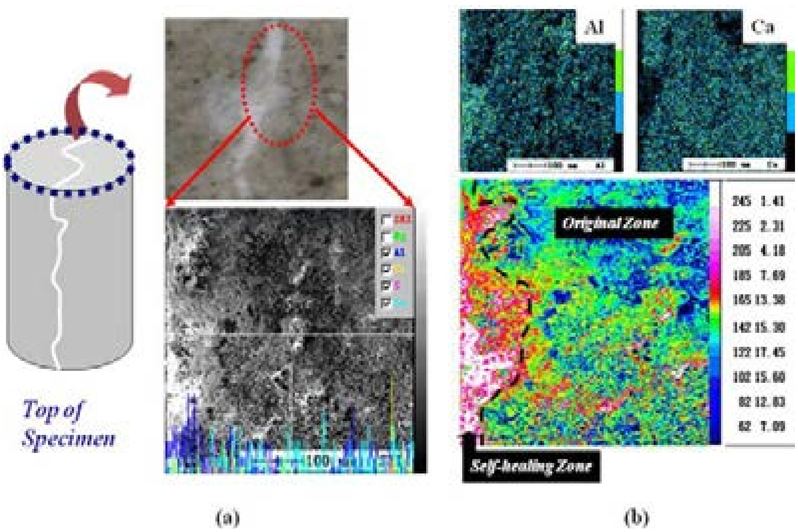

Figure 5: Self-healing phenomenon of crack by crystallization of aluminosilicate phases on the cementitious pastes incorporating expansive agent and Geo-materials [Surface Analysis of specimen]

(2) Effects of chemical additives on the self-healing (Upgrade design)

The objective of upgrade design was to consider the chemical stability as well as the improvement of self-healing velocity for the cementitious composite materials. Figure 6 shows the process of self-healing of sample II under water supply. In this case, the crack was healed after re-curing for 3 days, as shown in Figure 6 (b). It was found that this design had greater chemical stability compared to other results

Chemical additives significantly affected the formation of re-hydration products with high chemical stability as compared to the previous design. Furthermore, it didn’t show loss of re-crystallization products compare to previous results after re-curing 3 days as shown in Figure 6 (c).

These rehydration products were mainly composed of fibrous phases from chemical additives and calcite as shown in Figure 7. This indicates that these fibrous phases, which were formed from chemical additives, play an important role in crack bridging between cracks. From these results, it was concluded that various composite upgrade designs are desirable for the application of self-healing concrete. Premix cementitious composite materials based on these results were prepared for concrete mixing in order to give self-healing capability. These results are reported and discussed simply in the following section.

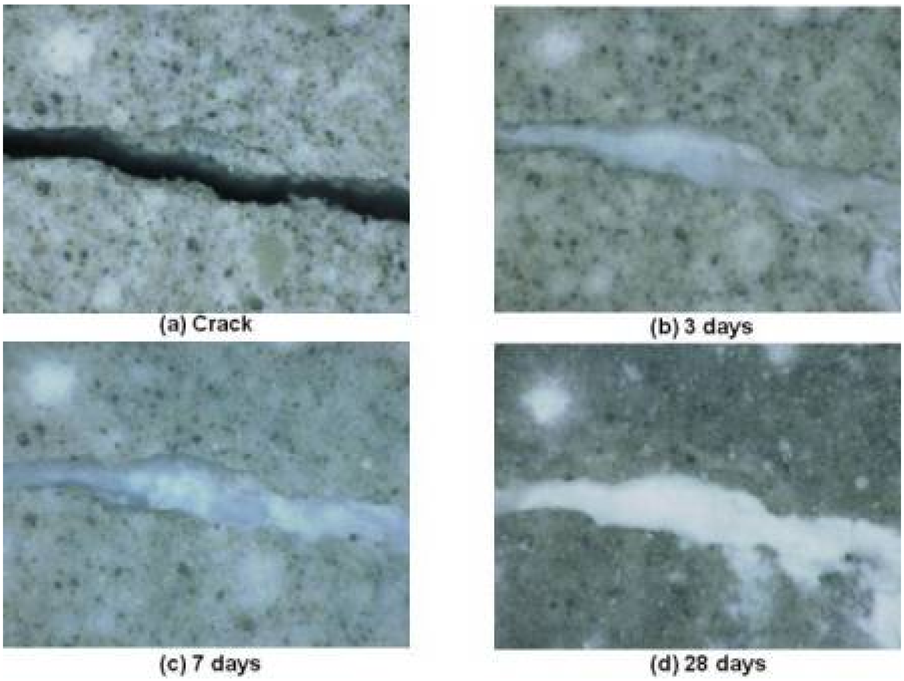

Figure 6: Self-healing process of sample II [Upgrade design, Water/Binder ratio of 0.45]

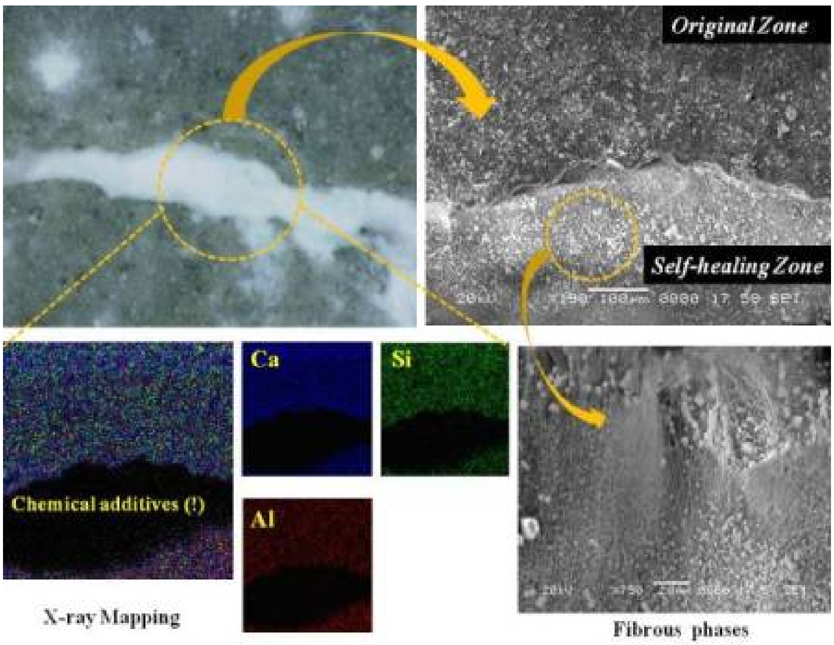

Figure 7: X-ray mapping results of fabricated fibrous phases and C-A-S-H phases [Sample II, Water/Binder ratio of 0.45]

3.2 Physical properties of self-healing concrete

Cement-based materials like concrete and mortar are quasi-brittle materials. These materials show a softening behavior when tested in uni-axial tension. In order to quantify the early age behavior of self-healing concrete as compared to those of conventional and expansive concrete, a temperature-stress testing machine (TSTM) test was conducted. Three types of concrete – plain concrete, expansive concrete (EC) and self-healing concrete (SHC)–were prepared for TSTM test and their experimental results are presented in Figure 8. Under the same semi-adiabatic temperature condition, the temperature evolution of the expansive concrete is slightly higher than normal concrete, and that of self-healing concrete is slightly lower than normal concrete. The first phenomenon was due to the replacement of cement by expansive agent, which has a higher hydration activity, thus the hydration heat on the first day elevated slightly. The second phenomenon was caused by the cement amount, which is 10% less in self healing concrete.

It is well known that expansive concrete can induce extra expansion to compensate for shrinkage. The test results showed this tendency. After 20 hours, the compressive stress of the expansive concrete was 0.8MPa higher than that of normal concrete, whose was 1 MPa. After temperature of specimens returned to room temperature, the tensile stress of expansive concrete was slightly lower than that of normal concrete. This is because the extra expansion of expansive agent becomes stagnant after one day due to the lack of water and the developing stiffness of surrounding hydrated matrix. The restrained stress evolution of self healing concrete is between these two concrete, the maximum compressive stress was 1.4MPa, and the final tensile stress was 1.6MPa. Even though the premix added in the self-healing concrete was composed of many composites, its restraint stress development is similar to that of the expansive concrete. When comparing the Young's modulus, it can be seen that there is not large difference among these types of binders. Based on the above, it could be concluded that the cracking sensitivity of self-healing concrete is similar to expansive concrete and has a better cracking resistance than normal concrete. Furthermore, in case of compressive strength, it can be seen that SHC exhibits similar compressive strength to Plain as shown in Figure 9. This means that self-healing concrete also passed the minimum field requirement for compressive strength (red line).

For estimating the durability of concrete structures, it is necessary to understand the permeation of water into concrete. Water permeability of self-healing concrete is one of several important concrete properties for the prevention of water leakage from water-retaining or underground structures. In order to measure the permeability of concrete, this research adopted an output method which enables the measurement of the permeation directly by observing the reliability and starting point of hydraulic divergence of permeation in concrete(T.H. Ahn, 2008). Table 4 shows the water permeability test results of self-healing concrete. Generally, the function of water permeability coefficient is as follows.

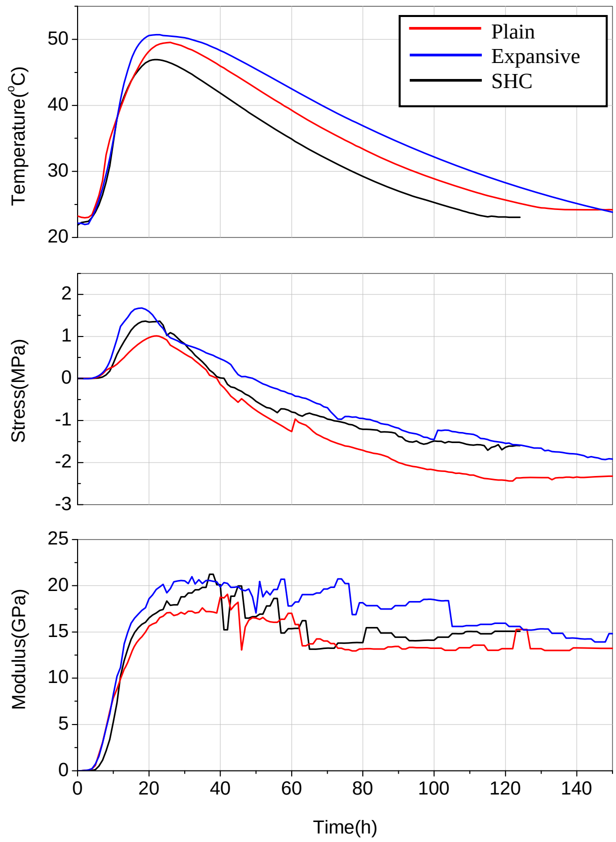

Figure 8: TSTM results of various concrete

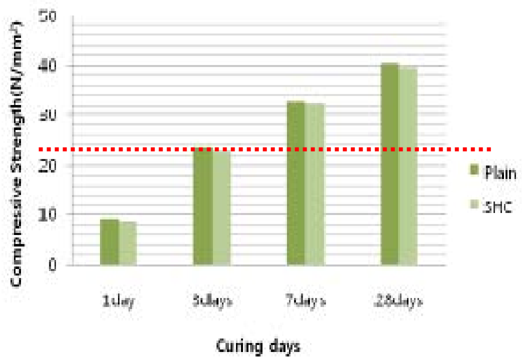

Figure 9: Compressive strength of self-healing concrete

$$\boldsymbol{k = q / i} \qquad (1)$$

Where
K : water permeability coefficient (m/sec),
q: water flow /unit time and volume (m^3/m^2/sec),
i : hydraulic gradient

Table 4 Comparison water permeability between conventional concrete and self-healing concrete

Sample	Time (s)	V (cm/s)	K (m/s)
Plain	60	0.000294	5.35E-05
SHC	1800	8.69E-06	1.65E-06

Water pressure was 2.0 MPa (=2 x 10^6 N/m^2) in this research. Each specimen was cured for 28 days, and then immersed in water again for 2 days in order to estimate the water permeability. The result showed that water permeability coefficient of self-healing concrete was significantly lower than that of conventional concrete. This indicates that self-healing cementitious composite could be used as a mineral admixture for the sealing of water leakage.

3.3 Self-healing capability of self-healing concrete

In case of self-healing concrete, the crack was significantly self-healed up to 28 days re-curing. Figure 10 shows the healing process of cracked self-healing concretes made at the same mixing condition as the conventional concrete. A 0.15 millimeter crack was self-healed after 3 days re-curing, as shown Figure 10 (b). After re-curing for 7 days, the crack width decreased from 0.22 millimeters to 0.16 millimeters. Furthermore, it was almost completely self-healed at 33 days as shown in Figure 10 (d).

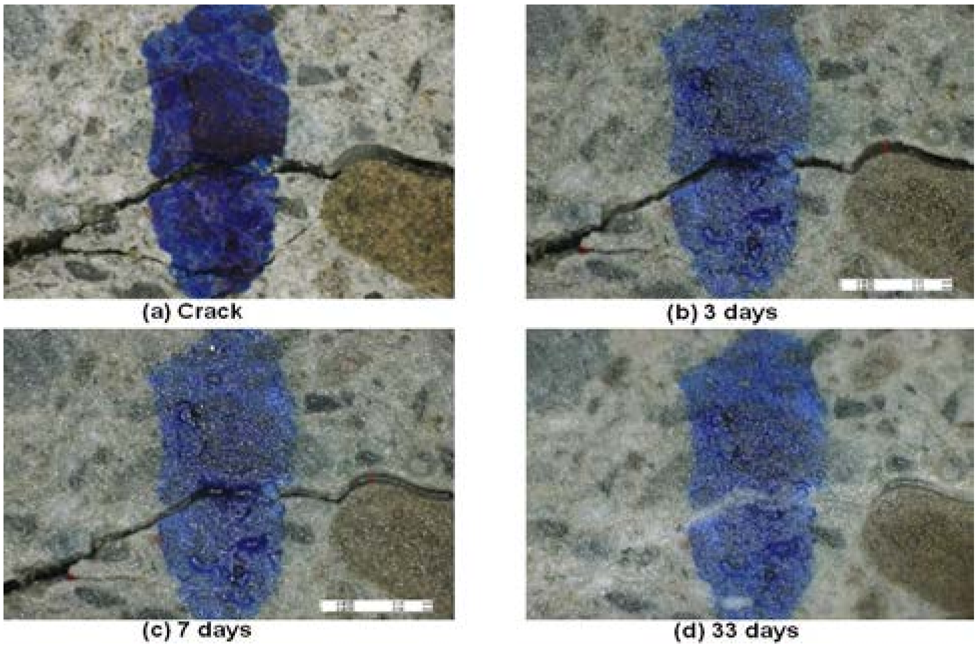

Figure 10: Process of self-healing on self-healing concrete at water/binder ratio of 0.47

This recovery appeared to include self-healing phenomenon such as the swelling effect, expansion effect and re-crystallization as mentioned above. However, in general, it should be considered that cracked aggregate didn't heal by itself. Self-healing at the initial stage occurred in the cementitious paste area between cracks as shown in Figure 11, resulting in the healing between the cementitious paste and surface of aggregate. However, this type of crack did not perfectly self-heal at the same time as shown in Figure 11. Some re-crystallization structure from the cementitious paste was deposited on the aggregate surface or in the crack between aggregates as shown in Figure 12. Therefore, this indicates that cracks of these types will take more time for self-healing.

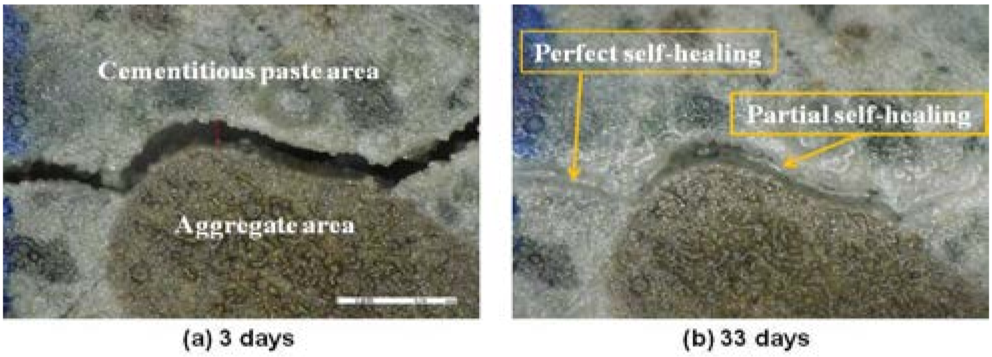

Figure 11: Process of self-healing on self-healing concrete at water/binder ratio of 0.47

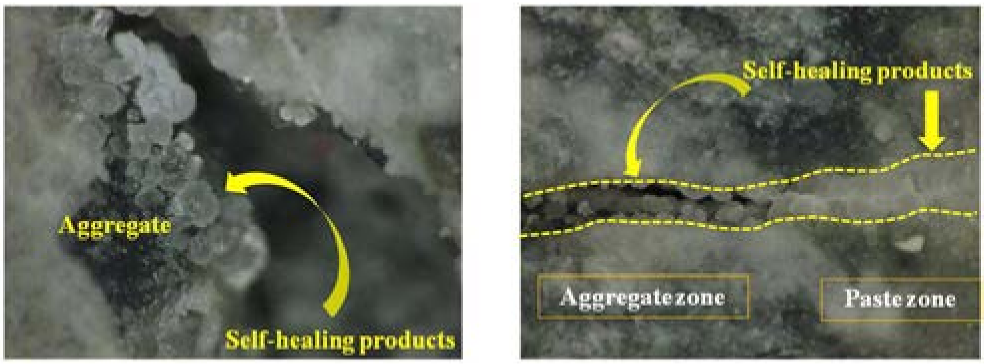

Figure 12: Self-healing images on crack between aggregate zone and aggregate zone of self-healing concrete

4. CONCLUSIONS

In this study, the self-healing properties of concrete using various mineral admixtures were investigated.

(1) Self-healing capability was significantly affected by aluminosilicate materials and various modified calcium composite materials.

(2) The essential properties such as expansion, swelling and re-crystallization for self-healing design were analyzed and discussed.

REFERENCES

K. V. Breugel, 2007. Is there a market for self-healing cement-based materials?, Proceedings of the 1st International Conference on Self-Healing Materials, 18-20 April

T.H. Ahn, T. Kishi, 2007. 1st International conference on self-healing materials, Con ference Review, Magazine of Korea Concrete Institute (KCI), Vol 14(4), pp.82-85.

T.H. Ahn, 2008. Development of self-healing concrete incorporating geo-materials : A study on its mechanism and behavior in cracked concrete, *Ph.D. dissertation*, Department of Civil Engineering, University of Tokyo, Japan.

T.H. Ahn, T. Kishi, 2008. The effect of geo-materials on the autogenous healing behavior of cracked concrete, Proceeding of 2nd ICCRRR2008, Cape town, South Africa.

EXPERIMENTAL EXAMINATION ON THE REPAIR EFFECT OF EMERGENCY RAPID RETROFITTING METHOD TST-FiSH

MASAMITSU SUZUKI
Department of Architecture and Civil Engineering,
Shibaura Institute of Technology, Japan
m-suzuki@iis.u-tokyo.ac.jp
RYOTA KASAKURA
Tokyu Construction, Japan
kasakura.ryouta@tokyu-cnst.co.jp
MASANORI ITO
Tokyu Construction, Japan
itou.AI9184@tokyu-cnst.co.jp
YOSHITAKA KATO
ICUS, IIS, University of Tokyo, Japan
katoyosh@iis.u-tokyo.ac.jp

ABSTRACT

After disasters such as earthquakes, it is necessary to quickly repair damage in order to ensure safety and speed recovery efforts. However, conventional methods require large-scale operations and the repair effect may be delayed. Therefore, the authors proposed an emergency rapid retrofitting method utilizing fiber sheets containing hydraulic resin (TST-FiSH) for the repair of reinforced concretes structure. The goals of this new method are to provide higher safety, speed, and ease of application compared to conventional methods. The basic properties were evaluated by adhesion test, the repair effect was investigated by beam specimen, and the structural performance was confirmed by column specimen. As a result, in comparison with conventional fiber sheet wrapping method, it was confirmed that TST-FiSH can provide the same repair effect and with only one-tenth of the application time. This paper reports these experiment results and the applicability of emergency rapid retrofitting method TST-FiSH.

1. INTRODUCTION

In Japan, the importance of seismic reinforcement in concrete structures was realized after the Hanshin/Awaji great earthquake disaster of 1995. Seismic reinforcement improves ductility primarily by avoiding the brittle “shear fracture" which occurs in column members. Main transportation and emergency transportation roads in the Tokyo metropolitan area are mostly reinforced by this method; however, there are still many structures which may suffer serious damage due to the scale of the earthquake. In addition, new structures cannot avoid damage, as they are designed to permit some damage during a large-scale earthquake. When structures are damaged by natural disasters, they require emergency retrofitting to ensure safety and functionality. Conventional methods, however, cannot adequately cope with subsequent aftershocks, and large-scale repair works are time consuming. From a concept inspired by medical plaster casts, a new repair method utilizing fiber sheets containing hydraulic resin (TST-FiSH) was developed to address this problem. This method can repair reinforced-concrete structures through the hardening effect of hydraulic resin when sprayed with water, and can provide higher safety, speed, and ease of application compared to conventional methods (Figure 1).

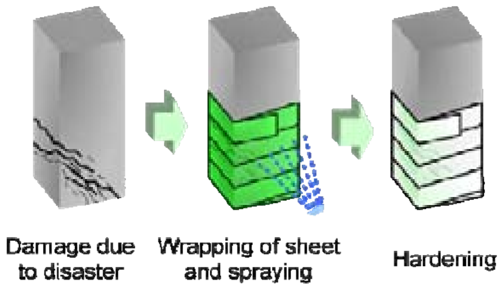

Figure 1: Summary of conceptual method

When the repair effect of sheets using polyurethane resin and glass fiber sheets was examined experimentally it was found that the stress capacity recovered to the same level or higher than before damage, indicating that practical application is possible (Suzuki et al., 2008). However, several questions remain: first, how much damage can be repaired by the emergency rapid retrofitting method, and second, what is the behavior of different fiber sheets, such as carbon, aramid, or vinylon. This research examined the potential application of the hydraulic resin using various types of fiber sheets, and the repair effect was confirmed by experimental testing of damaged and repaired beam and column members.

2. EXPERIMENTAL PROCEDURE

2.1 Materials

2.1.1 *Hydraulic polyurethane resin*

The hydraulic polyurethane resin used in this study is a single liquid-hardening resin which reacts and begins hardening after contact with water and in the presence of carbon dioxide. The resin was diluted with glycol ether solvent because the pure resin was difficult to handle due to high viscosity. Resin density 66% was chosen based on experimental results.

2.1.2 *Fiber Sheet*

The physical properties of the fiber sheets used in the experiments are shown in Table 1. The carbon fiber sheets are 2-directional and high strength; aramid fiber sheets are 1-directional; and vinylon fiber sheets are 2-directional. The physical properties in Table 1 are published values.

Table 1: Physical properties of fiber sheets

Fiber sheet	Weight (g/m^2)	Tensile strength (N/mm^2)	Young modulus (N/mm^2)	Fracture strain (%)
Carbon	300	3400	2.45×10^5	1.5
Aramid	280	2060	1.18×10^5	1.8
Vinylon	285	2000	4.30×10^4	4.8

2. 2 Beam member loading test

The repair effect of TST-FiSH test was tested on beam specimens under two-point loading. From the test results of the adhesion test (conducted in a separate investigation), TST-FiSH using three kinds of fiber sheets (carbon, aramid, and vinylon) with resin density 66% test cases were selected. Specimen dimensions are shown in Figure 2, specimen specifications and test cases are shown in Table 2, and material properties are shown in Table 3. First, the beam was damaged in shear under primary loading, then repaired by wrapping TST-FiSH in a single-layer in the shear span with a 150mm overlap on top of the beam. Secondary loading was conducted after 6 days curing. Loading was applied one-directionally with gradual but steady increase. Cracks were observed visually, and load, vertical displacement, axial reinforcement strain and shear reinforcement strain were measured.

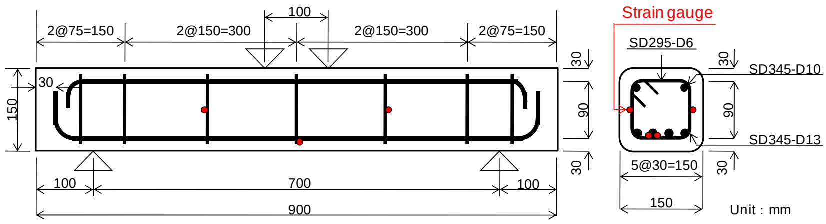

Figure 2: Beam specimen dimensions

Table 2: Specimen specifications and test cases for beam member loading test

Specimen No.	Equivalent height d (mm)	Span a (mm)	a/d	Axial direction rebar: Material	Axial direction rebar: steel ratio (%)	Shear reinforcement: Material	Shear reinforcement: Steel ratio (%)	Damage degree	Fiber sheet	Resin
1	120	300	2.5	SD345 D13	2.8	SD295A D6	0.094	Nothing	-	-
2								Low	Carbon	Hydraulic Polyurethane
3									Vinylon	
4									Aramid	
5								High	Carbon	
6									Vinylon	
7									Aramid	
8									Carbon	Epoxy

Table 3: Material properties for beam member loading test

	Compressive strength (N/mm^2)		Young modulus (N/mm^2)
Concrete	27.8		2.30×10^4
Steel	Yield stress (N/mm^2)	Tensile strength (N/mm^2)	Young modulus (N/mm^2)
Axial direction rebar SD345 D13	374	566	1.80×10^5
Shear reinforcement SD345 D6	310	462	1.69×10^5

Two levels of damage were applied to the specimens, following the Japan Road Association specification (JRA, 2007). For low damage degree, the load was removed when shear reinforcement reached the initial yield strain of 1830μ (see Figure 4). This value was determined by the occurrence of diagonal cracking when the residual crack width W<0.5mm. For high damage degree, specimens were unloaded at 80% of the maximum load, and the residual crack width was 0.5mm≦W<2mm.

2.3 Column member loading test

The repair effect and shear capacity of TST-FiSH selected by the results of the beam member tests were tested by cyclic lateral loading on a column member without axial force. The member was fixed at the base with the top of the member free. Specimen dimensions are shown in Figure 3, specimen specifications and test cases are shown in Table 4, and material properties are shown in Table 5. Specimen size and bar arrangement were decided based on a previous study (Katsuki et al., 1997).

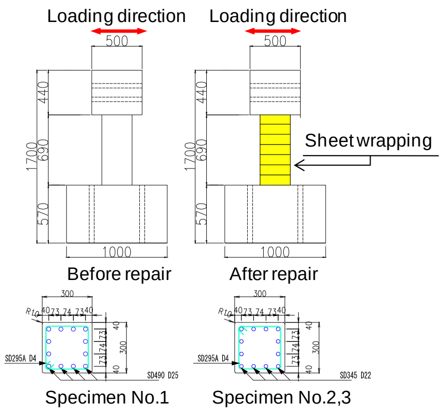

Figure 3: Column specimen dimensions

Table 4: Specimen specifications and test cases for column member loading test

Specimen No.	Fracture mode	Equivalent height d (mm)	Span a (mm)	a/d	Axial direction rebar		Shear reinforcement		Damage degree	Fiber sheet	Resin
					Material	steel ratio (%)	Material	Steel ratio (%)			
1	Shear	260	910	3.5	SD490 D25	7.8	SD295A D4	0.072	Nothing	Aramid	Hydraulic Polyurethane
2	flexural				SD345 D22	6.0			High		Epoxy
3											Hydraulic Polyurethane

Table 5: Material properties for column member loading test

	Compressive strength (N/mm²)		Young modulus (N/mm²)
Concrete	29.4		2.58×10^4
Steel	Yield stress (N/mm²)	Tensile strength (N/mm²)	Young modulus (N/mm²)
Axial direction rebar SD345 D22	374	443	1.97×10^5
Axial direction rebar SD490 D25	543	710	1.86×10^5
Shear reinforcement SD295A D4	320	488	1.84×10^5

In order to calculate the shear capacity carried by TST-FiSH, specimen No.1 was repaired without primary loading damage. Specimen No. 2 and 3 compared the conventional epoxy method and the TST-FiSH to understand the repair effect after damage. Shear damage by residual crack width (high damage degree 0.5mm≦W＜2mm) was given to the specimen by primary loading, and secondary loading was conducted after 100mm-wide aramid fiber sheets were wrapped around the shear span with 0mm displacement. The aramid fiber sheet was overlapped 200mm for each specimen. Loading was displacement-controlled by member angle, and member angle was increased sequentially (1/1000, 1/500, 1/250, 1/100, 1.5/100, 2/100, 3/100 …) until failure. After yield of axial reinforcement, three additional loading cycles were applied for each member angle. Cracking was observed by visual inspection, and load, vertical displacement, axial reinforcement strain, shear reinforcement strain and aramid fiber sheet strain were measured.

3. EXPERIMENTAL RESULT AND CONSIDERATION

3.1 Beam member loading test

The calculated maximum stress capacity, experimental value, and fracture mode for beam specimens are shown in Table 6. The shear capacity was calculated by Equation (2) and Equation (3) (JSCE, 2000).

$$V_{fyd} = V_{cd} + V_{sd} + V_{fd} \quad (2)$$

Where, V_{fyd} is the shear capacity of member, V_{cd} is the shear capacity carried by concrete, V_{sd} is the shear capacity carried by shear reinforcement, V_{fd} is the shear capacity carried by fiber sheet.

$$V_{fd} = K \cdot [A_f \cdot f_{fud} (\sin \alpha_f + \cos \alpha_f) / s_f] \cdot z \quad (3)$$

Where, K is the shear reinforcement efficiency of the fiber sheet, A_f is the total cross section of the fiber sheet in section s_f, s_f is the disposed interval of the fiber sheet, f_{fud} is the design tensile strength of the fiber sheet, α_f is the angle of fiber sheets with respect to member axis, z is distance from the resultant force of the compressive stress to the centroid of tensile steel.

Table 6: Fracture mode and maximum load for beam specimens

Specimen No.	Primary loading					Second loading		Fractual mode
	Calculate value		Experimental value	Residual crack width (mm)	Damage degree	Calculate value	Experimental value	
	Shear capacity (kN)	Flexural capacity (kN)	Load (kN)			Shear capacity (kN)	Flexural capacity (kN)	
1	84.5	114.6	120.1	-	-	-	-	Shear
2			126.7	0.15	Low	205.4	153.1	flexural
3			105.6	0.20		151.1	141.5	Shear
4			110.0	0.25		174.2	162.5	flexural
5			125.0	0.60	High	205.4	167.1	flexural
6			114.1	1.10		151.1	125.0	Shear
7			136.1	0.60		174.2	161.4	flexural
8			120.0	0.60		205.4	165.9	flexural

The load-displacement relationship for specimen No.1 is shown in Figure 4. In this case, the load was 64.5kN when diagonal cracking occurred, loading continued to increase after yielding of shear reinforcement, and the maximum load was 120.1kN. The fracture mode was shear fracture after yielding of the shear reinforcement.

3.1.1 *Resinous influence*

Load-displacement results of specimen No. 5 and 8 with different resin and damage degree are shown in Figure 5. Carbon fiber sheets with epoxy and hydraulic polyurethane and high damage degree were used. Both cases underwent flexural fracture, and the load increased slowly after yielding of axial reinforcement until the test was finished at displacement 15mm due to crushing of the concrete at the upper edge.

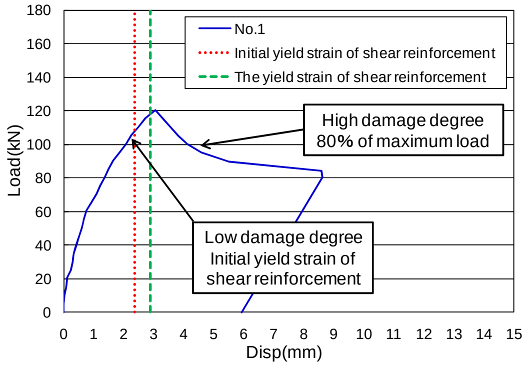

Figure 4: Load-displacement (specimen No.1)

In comparison, load increase behavior after secondary loading began was slightly different, which may indicate that the resinous hardness has an influence on the stiffness of the repaired specimen. The repair effect (maximum load after repair / maximum load before repair) was calculated from the maximum loads given in Table 8; for specimen No.5 (TST-FiSH) it was 1.34 and for specimen No.8 (conventional method) it was 1.38. This result showed both had a similar repair effect in this experimental condition.

3.1.2 *Influence of the damage degree*

The load-displacement results for specimen No. 2 and 5 are shown in Figure 5. The resin used was hydraulic polyurethane with different damage degree and repaired by carbon TST-FiSH. The displacement at the start of the second loading was different due to primary loading, but both underwent flexural fracture, and the load increased slowly after yield of axial reinforcement until the test ended at displacement 15mm due to crushing of the concrete at the upper edge. It was seen that the damage degree did not have an influence on the repair effect, as found in previous studies.

3.1.3 *Influence of fiber sheet type*

The load-displacement result for specimen No. 7 is shown in Figure 5. In this case, high damage degree was repaired by aramid TST-FiSH. The behavior of aramid TST-FiSH was similar to carbon TST-FiSH (Figure 8); it underwent flexural fracture, and the load increased slowly after yield of axial reinforcement until the test ended at displacement 15mm due to crushing of the concrete at the upper edge.

The load-displacement result of specimen No. 6 is shown in Figure 5. In this case, high damage degree was repaired by vinylon TST-FiSH. Shear fracture was observed, and the load decreased slowly after maximum load until the test ended at displacement 11mm due to failure of the vinylon fiber. For the vinylon TST-FiSH, the Young's modulus of the sheet itself (Table 1) is roughly the same as concrete and lower than the other sheets, so it was assumed that the repair effect was less because the sheet followed the transformation of specimen and broke after diagonal cracking occurred. However, the repair effect (maximum load after repair / maximum load before repair) calculated from maximum load shown in Table 6 exceeded 1.0, indicating that there was a recovery effect.

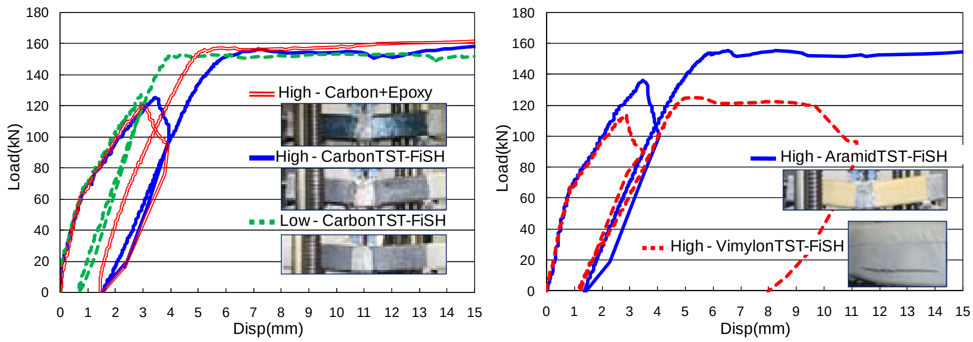

Figure 5: Load-displacement behavior of specimens with different resin and damage degree (left) and differ fiber sheet types (right)

3.1.4 *Comparison of construction time*

The application time for the conventional method (specimen No.8) and TST-FiSH were calculated, and it was found that the conventional method required around 5 hours, whereas TST-FiSH could be finished in only 30 minutes – roughly one-tenth the time. This confirmed that TST-FiSH is an effective method for rapid retrofitting after structural damage.

3.1.5 *Summary*

Summarizing the previous experimental results, it was found that the hydraulic polyurethane resin of resin density 66% could provide the same repair effect as epoxy resin in one-tenth of the application time. For the following column member loading test, the aramid fiber sheet was selected based upon consideration of its application characteristics.

3.2 Column member loading test

The calculated maximum stress capacity, experimental value, and fracture mode for column specimens are shown in Table 7. The calculation values were calculated by Equations (2) and (3), similar to beam members.

Table 7: Fracture mode and maximum load for column specimens

Specimen No	Primary loading							Second loading					Fractual mode
	Calculate value				Experimental value	Residual crack width (mm)	Damage degree	Calculate value				Experimental value	
	Shear capacity (kN)			Flexural capacity (kN)	Load (kN)			Shear capacity (kN)				Flexural capacity (kN)	
	V_c	V_s	V_d					V_c	V_s	V_f	V_d		
1	-	-	-	331.0	-	-	-	113.1	15.6	130.2	258.9	292.1 (-273.0)	Shear
2	110.3	15.6	125.9	163.0	166.7 (-150.1)	0.5	High	-	15.6	130.2	145.8	229.9 (-221.5)	flexural
3	110.3	15.6	125.9	163.0	172.8 (-160.1)	0.5	High	-	15.6	130.2	145.8	218.6 (-210.5)	flexural

3.2.1 *Shear capacity carried by TST-FiSH*

The load-displacement curve for specimen No.1 with aramid TST-FiSH is shown in Figure 6, with the load at the time of yielding of the outer-most axial reinforcement shown as a dashed line. Specimen No.1 shear reinforcement yielded between 1.5/100 and 1/250 member angle, maximum load occurred at 3/100 and -2/100, and the fracture mode was shear compression failure and destruction of web concrete. Loading was continued only on the positive side after load decreased, and the aramid fiber sheet broke when the load suddenly decreased after exceeding 9/100.

Load-strain curve for specimen No.1 with aramid fiber sheet is shown in Figure 6. The strain meter was installed on the side of the column, 325mm above the base, and the strain meter for shear reinforcement was also installed in the same position. Up to the load of 120kN, strain was approximately equal for both shear reinforcement and aramid fiber sheet; however, at 161kN the shear reinforcement yielded. After that, strain of aramid fiber sheet increased continuously, indicating that the aramid fiber sheet was carrying the shear force after the shear reinforcement yielded. The strain value at the maximum load was around $12{,}200\times10^{-6}$, which was 71% of the failure strain found in previous study (Nakajima et al., 1997). The failure mode in this experiment was shear compression failure; the shear capacity carried by the fiber sheet was calculated by truss theory to be 152.6kN in the plus side and 133.5kN in the minus side. Since these values exceed the calculated shear capacity (Table 7 V_f = 130.2kN) and shear reinforcement efficiency, it was concluded that this method provides a safe estimate of the shear capacity. In addition, this result demonstrates that the shear capacity can be evaluated by the sum of the individual shear capacity contributions, verifying the past research work (JSCE, 2000).

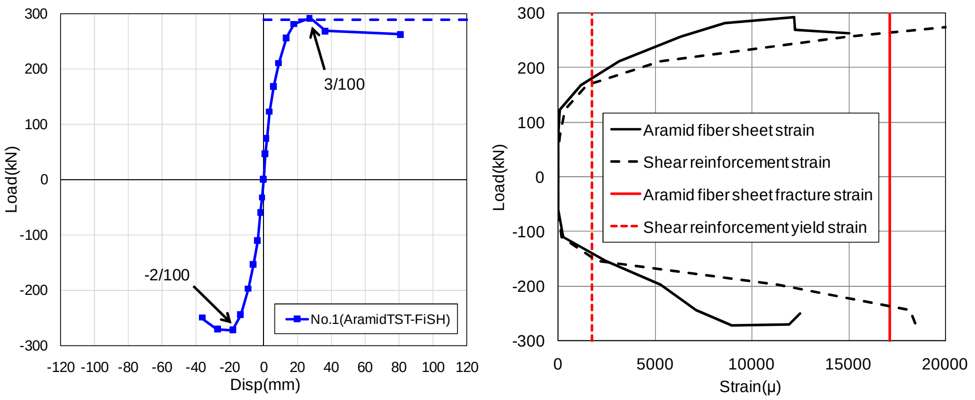

Figure 6: Load-displacement curve (left) and load-strain curve for specimen No. 1

3.2.2 *Verification of the repair effect*

The load-displacement curves for primary loading of specimens No.2 and 3 are shown in Figure 7. For primary loading, both specimen No.2 and 3 showed the same load-displacement behavior, with diagonal cracks at member angle 1/250, and yielding of shear reinforcement at member angle 1/200. Loading ended when it was judged that high damage degree conditions were satisfied per 2.2, and the residual crack width was measured as 0.5mm after ending member angle 1/100. The strain of axial reinforcement in specimens No.2 and 3 was just before yielding.

The failure conditions after secondary loading are shown in Figure 8, the load-displacement curves of the second loading for both specimens are shown in Figure 7, and the loads at yielding of the outer-most axial reinforcement for both specimens are shown as dashed lines in Figure 7.

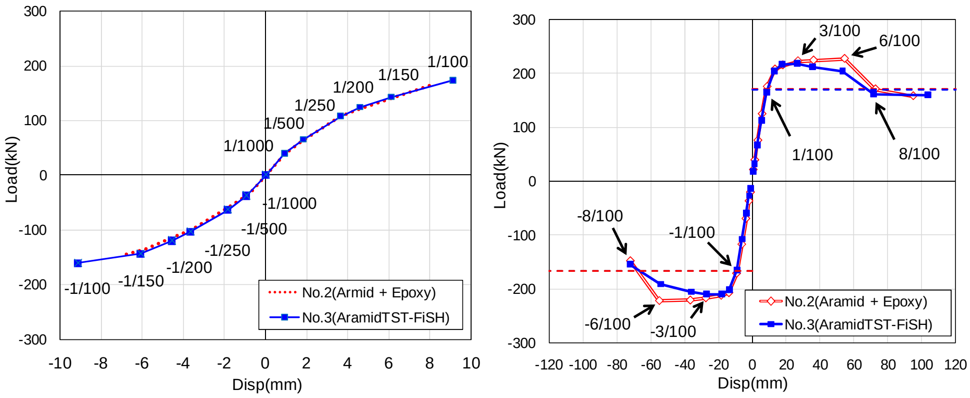

Figure 7: Load-displacement curve for primary (left) and second loading (right)

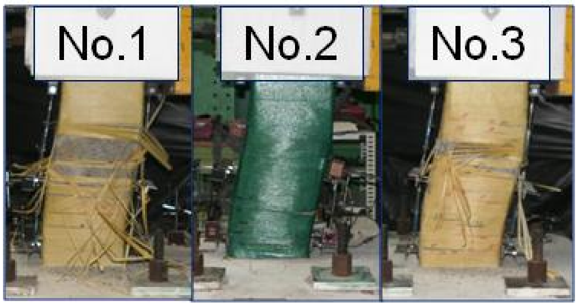

Figure 8: The failure conditions after secondary loading

The stress capacity of specimen No.2 with epoxy resin and aramid decreased at member angle ±8/100, and after yielding of the axial reinforcement displacement occurred along the diagonal crack surface which was formed during primary loading. The failure condition (Figure 8) was predominantly due to shear deformation caused by the diagonal cracks from the primary loading. The fracture mode was likely flexural failure because the characteristics of shear failure, such as load increase after yielding of axial reinforcement, breaking of fiber sheet, or destruction of web concrete (as seen in specimen No.1) were not observed. Loading continued only on the plus side and after member angle 10/100 the aramid fiber sheet broke when the failure load was reached. Specimen No.3 repaired with aramid TST-FiSH suffered greater displacement along the diagonal crack surface formed during primary loading after yielding of axial reinforcement. The load began to decrease slowly from ±4/100, until it became less than the yield load at member angle ±8/100. The failure mode appeared to be flexural failure, the same as specimen No.2, due to the influence of the diagonal cracks from the primary loading. The repair effect of TST-FiSH for column member with shear damage was confirmed to be the same as that of the conventional method. Loading continued only on the plus side, and after member angle 10/100 the aramid fiber sheet broke when the failure load was reached.

When comparing the load-displacement curves for specimens No. 2 and 3, although there is a slight difference in the maximum stress capacity and the rate of stress decrease, since the failure load is similar it is assumed that same design stress capacity can be used for both methods. It’s possible that this small difference in behavior is due to the constraint effect of the materials, particularly the epoxy and the hydraulic polyurethane resins.

4. CONCLUSION

This research examined the potential application of the hydraulic resin using various types of fiber sheets, and the repair effect was confirmed by experimental testing of damaged and repaired beam and column members, in order to clarify the performance and potential of TST-FiSH. TST-FiSH could be applied much faster than the conventional method using epoxy resin. The materials selected for TST-FiSH were hydraulic polyurethane resin of density 66% and fiber sheet of weight around 300g/m², with finishing conducted just after water spraying. The shear capacity of RC members repaired by TST-FiSH could be evaluated as the sum of the individual shear capacities. Although a small difference in behavior due to the constraint effect of the concrete was observed and attributed to the physical properties of the resins, it was concluded that for medium damage degree TST-FiSH can provide a repair effect similar to that of the conventional method with epoxy resin.

ACKNOWLEDGMENT

This research was supported by a financial grant from the Japanese Ministry of Land, Infrastructure, Transport, and Tourism (MILT) for the research and development of construction technology. The authors would also like to thank MC Industries, Co., Ltd., Tokyu Construction Co., Ltd., and Mr. Michael W. Henry for their support.

REFERENCES

Japan Society of Civil Engineers., 2000. Concrete library 101. *The repair and reinforcement guidelines of concrete structure using fiber sheet*, JSCE, Japan. (in Japanese)

Japan Road Association., 2007. *Road earthquake disaster measures manual volume earthquake disaster restoration*. JRA, Japan. (in Japanese)

Nakajima, N., Nakai, Y., Watanebe, T., Matsumoto, N., 1997. Shear behavior of railway viaducts columns strengthened with aramid fiber reinforced sheet, *Proceedings of the Japan Concrete Institute*, Vol. 19, No.2, pp.255-260. (in Japanese)

Katsuki, F., Nakai, Y., Watanabe, T., Moriyama, T., 1997, Experimental study on deformation capacity of railway viaducts columns using aramid fiber sheets, *Proceedings of the Japan Concrete Institute*, Vol. 19, No.2, pp.1569-1574. (in Japanese)

Suzuki, M., Suzuki, R., Ito, M., Kato, Y., 2008. Development of emergency retrofitting method using fiber sheet containing hydraulic resin, *Proceedings of the Japan Society of Civil Engineers*, Vol. 63, pp. 645-646. (in Japanese)

PARALLEL SESSION 6

INFORMATION MANAGEMENT FOR DISASTER REDUCTION

[1]KIMIRO MEGURO and [2]SHINYA KONDO

[1]International Center for Urban Safety Engineering
Institute of Industrial Science, The University of Tokyo, Japan
meguro@iis.u-tokyo.ac.jp
[2]The Great Hanshin-Awaji Earthquake Memorial
Disaster Reduction and Human Renovation Institute, Kobe, Japan

ABSTRACT

Quality and quantity of disaster can be discussed by the relations between characteristics of hazard as an input, such as magnitude, location of hypocenter, fault mechanism, etc. in case of earthquake and characteristics of the affected region as a system, such as soil condition, infrastructure and housing condition, politics, economy, religions, education, history, culture, etc. The regional characteristics can be divided into two groups, one is on natural environment and the other is on social environment. Also, since activities of people and society are strongly reflected by time, time related factors, such as season, day of the week, and event occurrence time, etc. should be considered as a part of the system. Disaster can be considered as an output of the above mentioned input-system mechanism.

While there are seven countermeasures for disaster reduction, namely, "mitigation", "preparedness", "prediction and early warning", "damage assessment", "emergency disaster response", "recovery", and "reconstruction". For implementation of all seven measures, "information and communication" is a key and information management plays essential role for "information and communication".

The ideal disaster management measures are to be conducted by properly balancing these seven measures considering hazard characteristics and regional characteristics of the target area. In this paper, the authors sort out important issues on information management and propose their solutions for total disaster management to minimize negative impact due to hazards.

1. INTRODUCTION

For total disaster management, there are seven countermeasures. Figure 1 shows these seven measures, namely, "mitigation", "preparedness", "prediction and early warning", "damage assessment", "emergency disaster response", "recovery", and "reconstruction". For implementation of all seven measures, "information and communication" is a key and information management plays essential role for "Information and communication". The ideal disaster management measures can be conducted by properly balancing these seven measures considering both the hazard characteristics and regional characteristics of the target area.

In this paper, the authors point out important issues on information management and propose their solutions for total disaster management to minimize negative impact due to hazards.

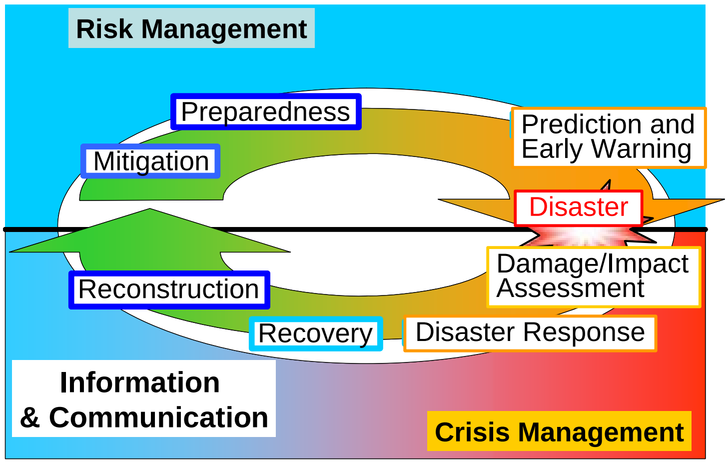

Figure 1: Elements of disaster countermeasures and total disaster management system

2. CONSTRUCTION OF DATABASE

After a hazard attack, survey on information required by the affected people and/or people who should take care of affected ones is often carried out through questionnaire survey and interview survey. Figures 2 and 3 show some examples of these survey results, however, they are not enough for proper actions. As Figure 4 shows, it is important that from before a hazard attack to just after, and to recovery and reconstruction stages, and from national level to prefecture, city and town, and to citizens' levels, all activities by all divisions and information needed for those activities are analyzed. In this chapter, the method for analysis and database prepared based on the result of analysis will be introduced.

2.1 Information on Disaster Response Activities for Analysis

In Japan, we had an earthquake with the magnitude of 6.8 called the 2004 Mid Niigata Prefecture Earthquake in the central part of Niigata Prefecture on October 23, 2004. The death toll and injured due to this earthquake was 68 and 4,805, respectively. The total number of heavily and partially damaged houses and buildings was approximately 16,000. The records of disaster response activities by the Niigata Prefectural Government during this earthquake disaster were used for analysis. The records summarized by the Niigata Prefectural Government employees contain time series actions of each section with actors and their start and finish times.

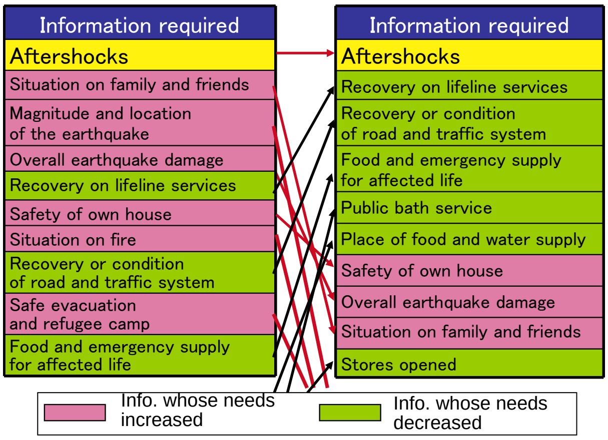

Figure 2: Changes of needs of information after the 1995 Kobe earthquake

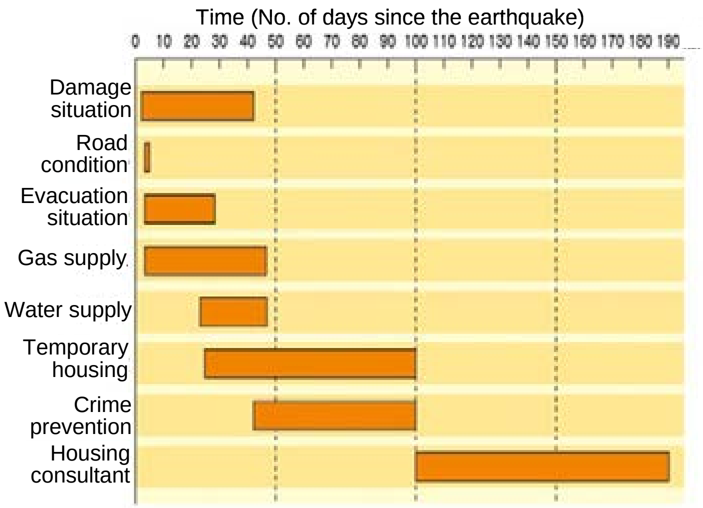

Figure 3: Changes of information that Niigata Prefecture government has been disseminating through Web after the 2004 Mid Niigata Prefecture Earthquake

2.2 Activities and Required Information

In order to provide appropriate responses to the various tasks at appropriate times, organizations do not respond to any single situation, but instead they take an overview of the entire situation. Kondo and Meguro [1] have proposed an environment for provision of appropriate responses (see Figure 5). People should improve their temporal and spatial grasp of the environment and what will happen after the disaster (imagination), as well as sort out potential problems (analysis), design and develop countermeasures (design & development), implement disaster drills (implementation), and assess each element (assessment).

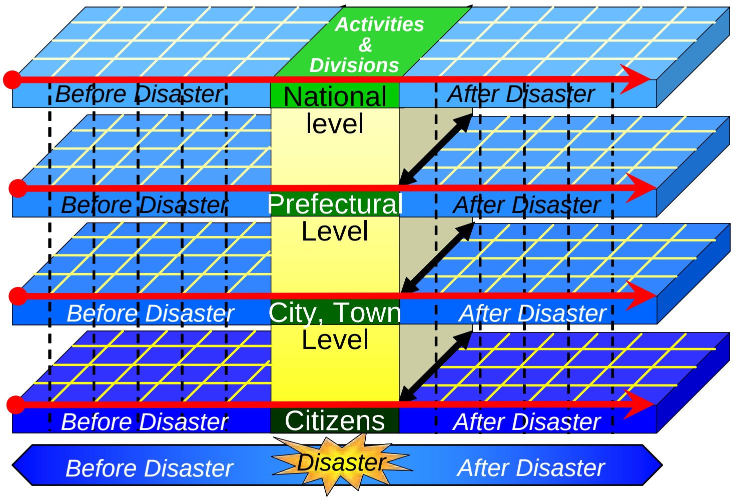

Figure 4: Disaster Information Image of Disaster Information Database

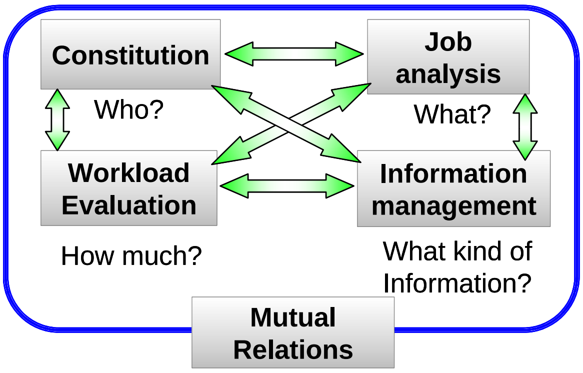

Figure 5: Environment for provision of appropriate responses [1]

Figure 6 shows a series of activities as time goes that need information (A) and (B). Also, actor organization/division and required accuracy on the information are shown in the figure. In order to prepare this figure using real data, we should make clear the relations between information and activity. However, there is no person who can trace activities from the viewpoint of information required for each activity. Therefore in the study, we picked up all works from large scale and broke down these works up to concrete actions by interview survey from all divisions related disaster response as shown in Figure 7 (a). After getting all concrete actions, we asked the people at each division and could get information and accuracy required for each action, and its provider division. About required accuracy of the information, there are three factors; quantity, location, and time. Accuracy on these three factors becomes quite different with actor division/organization, time, and action. When we can prepare all relations among action, required information, and its accuracy and provider, we finally can trace all activities from the viewpoint of each required information as shown in Figure 7 (b). Adopting this approach, we can make disaster information matrix and when we make disaster information plat form using this concept, each division of all levels from national to city and town levels can get necessary information in favorite time with required resolution. Therefore, with this plat form system, people belonging to local governments don't have to report damage situation to the higher level governments. With the following chapters, we will explain this approach using real data.

2.3 Database Specifications

It is necessary to organize the input items for disaster response analysis from the five viewpoints. There were 12 attributes in this study as shown in Figure 8: responsible organizations, services provided, actions taken, terms of measurement, start and finish times of events, workloads, necessary information, division(s) to access information, output information, division(s) of information destinations, and related actions. If some records lacked certain attributes, details from the 2004 Mid-Niigata Prefecture Earthquake were supplied through interviews with Niigata Prefectural Government employees and reference materials [3 – 6] of this earthquake.

For sorting out potential problems, people should analyze the current disaster from five viewpoints, i.e. "Constitution", "Job analysis", "Workload evaluation", "Information management", and "Mutual relations." "Constitution" means defining each group's role, depending on how the situation unfolds after the hazard attack. "Job analysis" means comparing needs in the disaster area with what the organization should do. "Workload evaluation" means estimating the quantity of work to be done for effective use of limited resources (i.e., people, goods, capital, and information). "Information management" means not only obtaining, controlling, communicating, sharing, and using information to do work, but managing cooperation with outside organizations. "Mutual relations" means analyzing disaster response activities from the multiple viewpoints described previously.

If the organization considers countermeasures based on these analyses, each person's actions will be linked so that things will be organized in a timely fashion with spatial efficiency. However, most existing reports lack analysis from these five viewpoints. In a previous paper, the authors proposed "A New Style Disaster Information Database," which was a system for multilateral analysis and assessment of a database consisting of newspaper articles, reconnaissance reports, compilations of lessons [2], and a new method for disaster response assessment using a disaster information database constructed based on current available systems, such as fax machines [1]. This system and method together form an environment that provides information to all people for the development of their mental images of the situation after disaster struck. However, they do not have the five viewpoints to analyze the organization's disaster response. In this study, the authors propose an environment to improve disaster management of the organization in a disaster-free period. Specifically, the records of disaster response activities in past disasters were analyzed from five viewpoints (constitution, job analysis, workload evaluation, information management, and mutual relations), issues for improvement in disaster management of the organization were sorted out, and the contents and structure of improvements were identified.

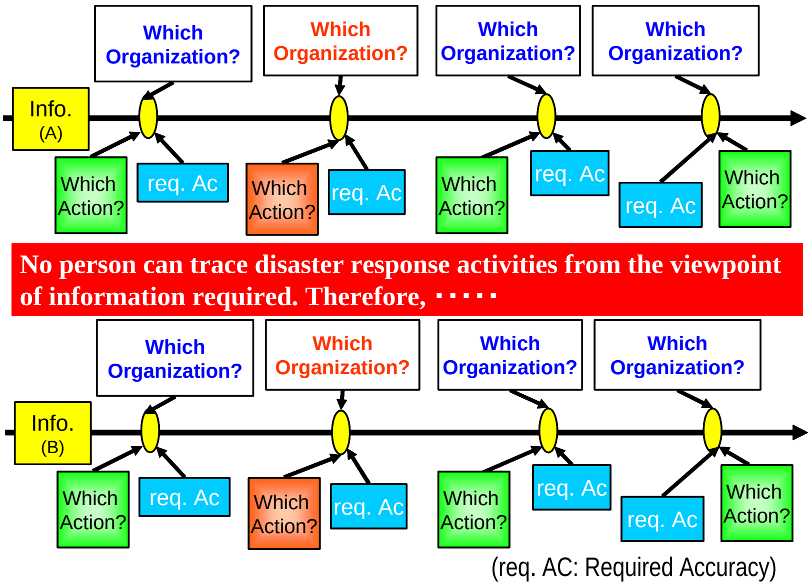

Figure 6: Activities are traced from the viewpoint of each information required for the activity

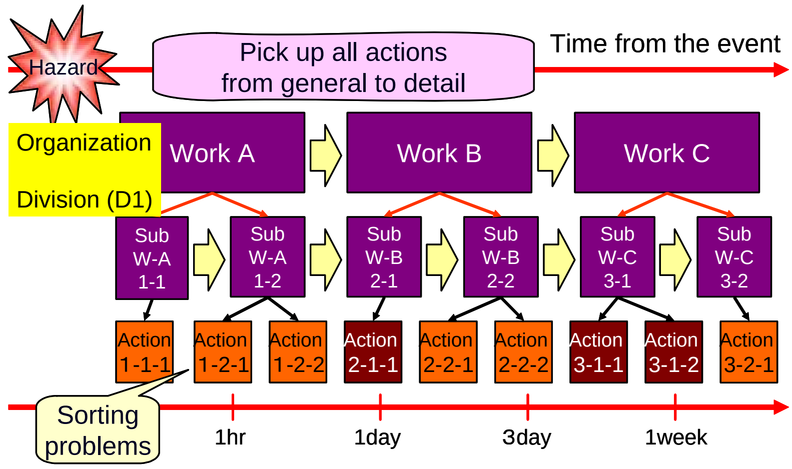

(a) Break down of works

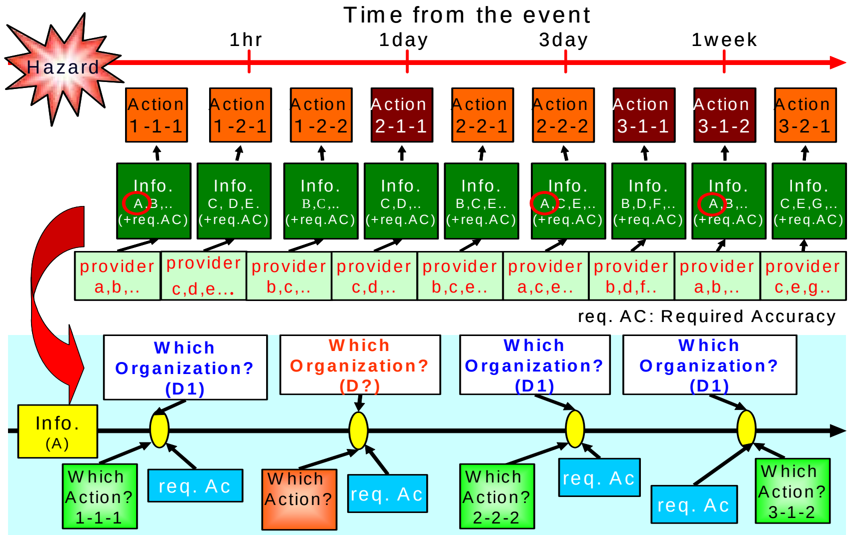

(b) Activity traceability by required information

Figure 7: Method for trace of activities from the viewpoint of each information required for the activity

In this research, the records of the Niigata Prefectural Government's disaster response activities during the 2004 Mid-Niigata Prefecture Earthquake were collected and used for analysis from five viewpoints. The validity of the analysis from the five viewpoints was verified, and lessons of the organization's disaster response were summarized.

ID	Responsible organization(s)	Service
1	Civil Engineering, Building and Housing	Construction of temporary housing

ID	Action
1	Research construction site for temporary housing

ID	Term(s) of measures	Time to start	Time to finish	Workloads
1	Emergency	100 (hours)	180 (hours)	10 (division x day)

ID	Input information	Division(s) to access information	Output information	Division(s) for information destination
1	No. of households with refugee	Life and environment division	Candidate site for temporary housing	General affairs division, Administrative promotion office

ID	Related action
1	Budget for temporary house construction

Figure 8: Specifics of the database

3. ANALYSIS OF THE ORGANIZATION'S DISASTER RESPONSE BASED ON THE DATABASE

In this section, the organization's disaster response is analyzed using the database. In this study, "Analysis" is defined as "breaking combined operations down into their constituent parts and sorting those constituents and their characteristics." The current state of disaster response can be understood from an analysis of all operations, but problems are not sorted out quickly. Analysts (the authors and staff who responded to the disaster in this study) determine the constituents and characteristics of the disaster response and discuss its validity from the results of analysis. In addition, problems emerged as gaps between an ideal situation and the actual situation.

3.1 Constitution

After the 2004 Mid-Niigata Prefecture Earthquake struck, 17 departments were established under the Niigata Prefectural Emergency

Operation Center (EOC). EOC meetings were held as needed. Some groups, which consisted of several departments, reported on the situation at the time.

Table 1 shows the evolution of the structure. Many groups were established in the EOC meetings: five groups in the first step (October 27, 2004), two groups in the second step (October 31, 2004), and one group in the third step (November 13, 2004). The reason for this was the need to provide careful service. In the fourth step (December 24, 2004), all groups except five were disbanded.

Table 1: Evolution of the Niigata Prefectural EOC structure

	Local plan for disaster prevention	First	Second	Third	Numbers (Max)	4th
Date		2004/10/27	2004/10/31	2004/11/5		2004/12/24
Structure	Headquaters commission	Headquaters commission	Headquaters commission	Headquaters commission	8	Headquaters commission
	General affairs	General affairs	General affairs	General affairs	5	General affairs
	Countermeasure	Countermeasure	Countermeasure	Countermeasure	15	Countermeasure
	Bulletin	Bulletin	Bulletin	Bulletin	5	Bulletin
		Ministry on-site support team	Ministry on-site support team	Ministry on-site support team	40	Dissolution
	Liaison to ministry	Liaison to ministry	Liaison to ministry	Liaison to ministry		Dissolution
		Control of SDF	Control of SDF	Control of SDF	60	Dissolution
	Liaison to SDF	Liaison to SDF	Liaison to SDF	Liaison to SDF	15	Dissolution
	Liaison to disaster prevension agency	Liaison to disaster prevension agency	Liaison to disaster prevension agency	Liaison to disaster prevension agency	10	Dissolution
	Lifeline	Lifeline	Lifeline	Lifeline	8	Dissolution
		Rescue	Rescue	Rescue	16	Dissolution
		Information on evacuation center	Information on evacuation center	Information on evacuation center	5	Dissolution
		Supply of food	Supply of food	Supply of food	18	Dissolution
			Livingware	Relief goods and logistics	50	Relief goods and logistics
			Liaison to Governers	Liaison to Governers	10	Dissolution
					265	

SDF: Self Defense Force

In other words, the Niigata Prefecture EOC meetings decided on countermeasures that could be implemented from soon after disaster struck to two months after the Mid-Niigata Prefecture Earthquake. Thus, changes in the organization’s structure proportional to changes in the disaster-affected community were made.

3.2 Job Analysis

Job analysis means the breaking down and refining of work to lead planning operations to action. The first level was the EOC’s work as listed in regional disaster prevention plan. The second level was the division’s work listed in the regional disaster prevention plan. The third level was intermediate tasks between the second and fourth levels. The fourth level was concrete action. For the Civil Engineering Bureau Building and Housing division, the first level was “Housing” and the second level, “Construction and provision of temporary housing” consists of the third level: “Procuring of site,” “Budget,” “Manufacturers,” “Dwellers,” and “Orders,” as shown in Figure 9. In addition, the fourth level, “Procuring,” consisted of “Households of refugees,” “Damage to construction sites,” and “Number of collapsed houses.”

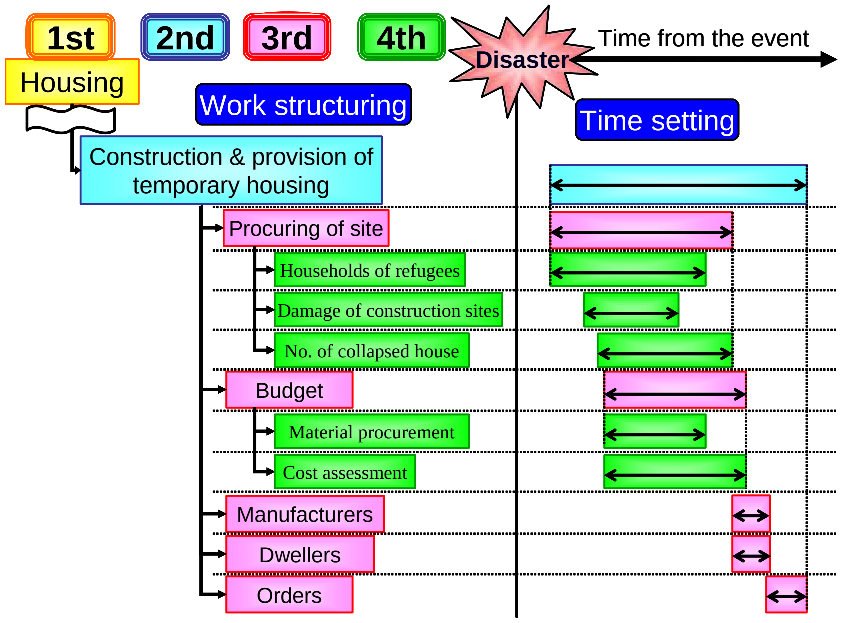

Figure 9: Job analysis (Civil engineering bureau, housing construction)

3.3 Workload Evaluation

In this section, each type of work to be done was quantified. This was done by compiling the duration of first level works, with eight hours equaling one unit per day. Figure 10 shows the prefectural staff's workload at each first level. "Setting and management EOC" was the largest category of work in terms of quantity. "Public establishment" and "Agriculture, Forestry and Fisheries" are the second and third-largest categories of work in terms of quantity, respectively. The features of the 2004 Mid Niigata Prefecture Earthquake were collapsed houses, blocked roads, isolated settlements, and floods due to landslides. Local structures – rice terraces and carp ponds – were damaged in Yamakoshi village. Rice terraces fell under the category of "Public Establishments," carp ponds under the category of "Agriculture, Forestry and Fisheries." The amount of work to be done by each division was analyzed for clarification of the division's workload. Table 2 is an analysis of the responsibility of the Living Environment Bureau. The main work of this bureau was the following: A) Setting and management EOC, C) Debris and human waste, and I) Volunteers. These work categories were listed on the local disaster prevention plan. This bureau also worked with other bureaus' main work categories, such as J) Relief money and K) Commerce and industry. This analysis included each bureau's work, both its main work and complementary work. The work categories listed in the local disaster prevention plan and carried out in real situations were compared and analyzed. Figure 11 is an analysis of the Civil Engineering Bureau's work, where the x-axis is the organization responsible, the y-axis is time from the event, and the z axis is the number of work categories, with the local disaster prevention plan on the left and the real situation on the right. The plan did not have a concept of a timeline; therefore, related records were used in setting the times. This analysis showed concrete actions taken in the implementation of the plan, as well as unplanned work. Table 3 is an analysis of unplanned work. Local government staff should not only know the tasks listed on the plan, but also recognize "Routine work," "Conclusion of agreements," "Assistance to other divisions," "Publication and notices," and "Demands and requests."

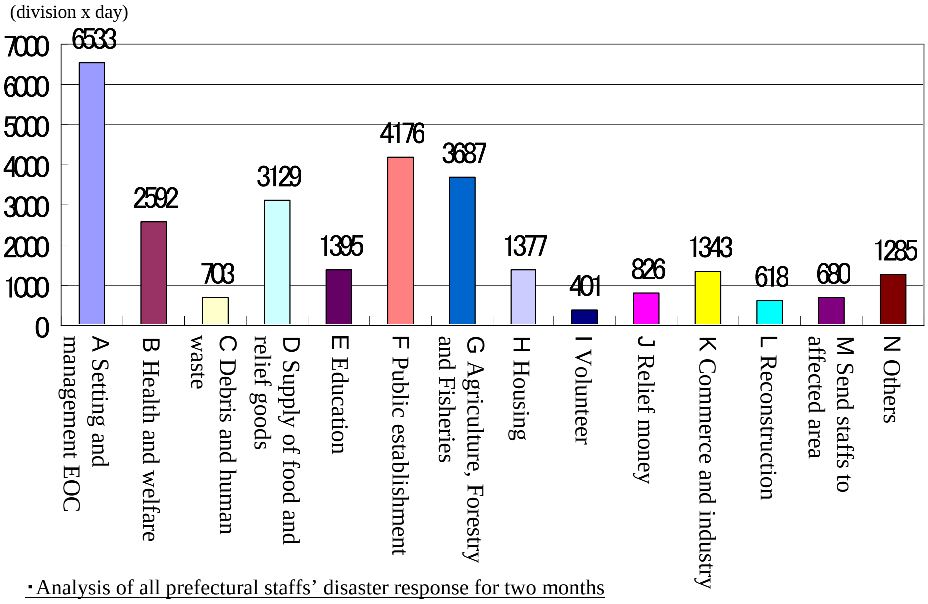

・Analysis of all prefectural staffs' disaster response for two months

Figure 10: Prefectural staff's workload for each first-level task

Table 2: Analysis of the responsibility for each division of the Life and Environment Bureau

	A	B	C	D	E	F	G	H	I	J	K	L	M	N
Crisis management	52	0	0	47	0	0	0	0	0	0	0	0	0	0
Environmental plan	125	1	64	1	0	0	7	0	13	1	0	0	5	20
Environmental measures	124	5	75	2	0	0	0	0	9	0	0	0	0	0
Life	81	0	0	5	0	0	0	0	265	0	8	0	0	0
Nuclear safety measures	142	0	0	0	0	0	0	0	0	0	0	0	0	139
Fire difense	676	0	25	4	0	0	0	0	0	0	0	0	4	133
Promotion of gender equality	4	0	0	2	0	0	0	0	11	0	0	0	0	53
Debris measures	0	0	523	0	0	0	0	0	0	0	0	0	0	0
Cultural administration	18	2	0	0	0	4	0	0	29	0	0	0	0	0
Total	1222	8	687	61	0	4	7	0	327	1	8	0	9	345

・Analysis of all prefectural staffs' disaster response for two months (division * day)

3.4 Information Management

Disaster response, from information managed at the time, has been analyzed as follows. The work analyzed in Section 3.2 was "set-related" information. Information and work did not always have a one-to-one relationship. Figure 12 shows the result of associating related information with structured second-level work, such as "the Construction and provision of temporary housing." Related information was separated into input and output as seen in Figure 13. Based on these processes, information-related disaster response was arranged on a timeline.

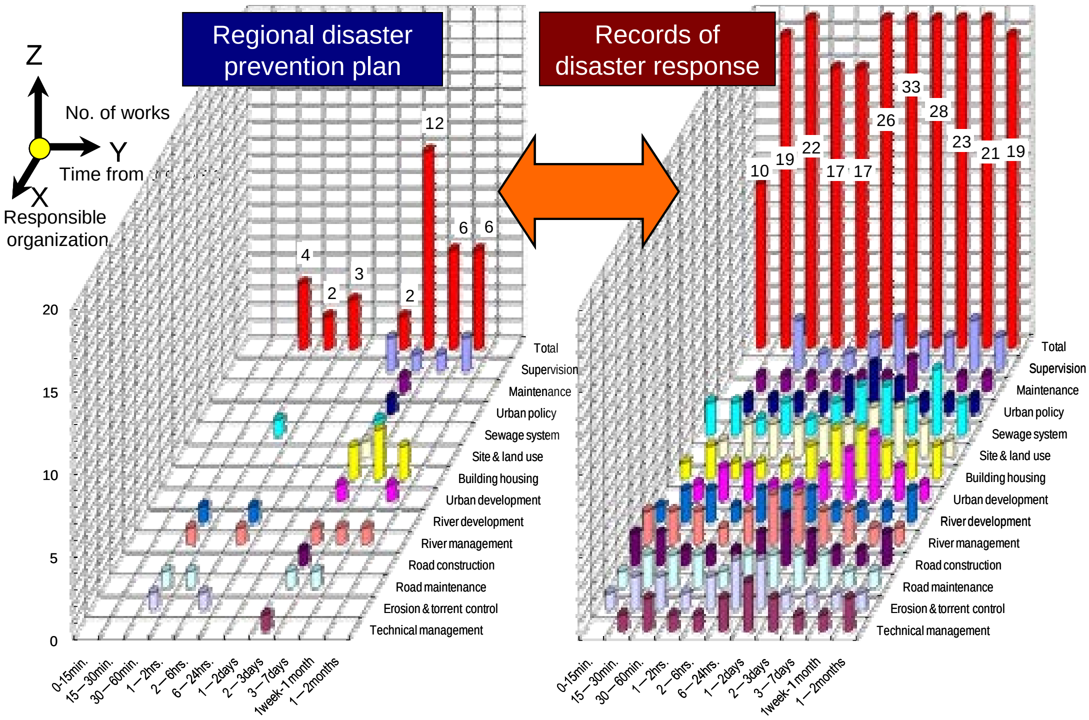

Figure 11: Analysis of Civil Engineering Bureau's work

Table 2: Unplanned work categories

2nd level
Carrying in and out relief supplies

Classification	Action
Disaster response	Carry in relief supplies at Niigata Airport
	Prepare rice ball at parking
Routine work	Provide house map to related divisions
Conclusion of agreements	Conclude collaboration agreement with prefectural land development corporation
Assistance to other divisions	Assistance to Nagaoka branch office
	Assistance to empty room information center
Publication and notices	Notify regional agency of case example of site acquisition in the 1995 Kobe earthquake disaster through written statements
	Notify regional agency of site acquisition at disaster area through a written statement
Demand and requests	Go off to MLIT to demand special national taxation measures for site acquisition
	Request site office outside disaster area to assistance site acquisition
	Support to respond to the media (Prime Minister inspection)

With the introduction of this process into the entire organization, information regarding each division's needs was arranged on the timeline (see the upper part of Figure 14). Which section needs information and which section provides information were focused on and arranged on a timeline. The lower part of Figure 14 shows an example of focus on "Refuge information."

In this study, the above method of analysis was called "information traceability." "Information traceability job analysis" focuses on "Refuge information" and "Road damage information." "Information traceability job analysis" was an analysis of providers, users, and times for information use, arranged in a table. Work related to taking refuge was not routine work and was work related to various bureaus. Road damage information was used by various work categories.

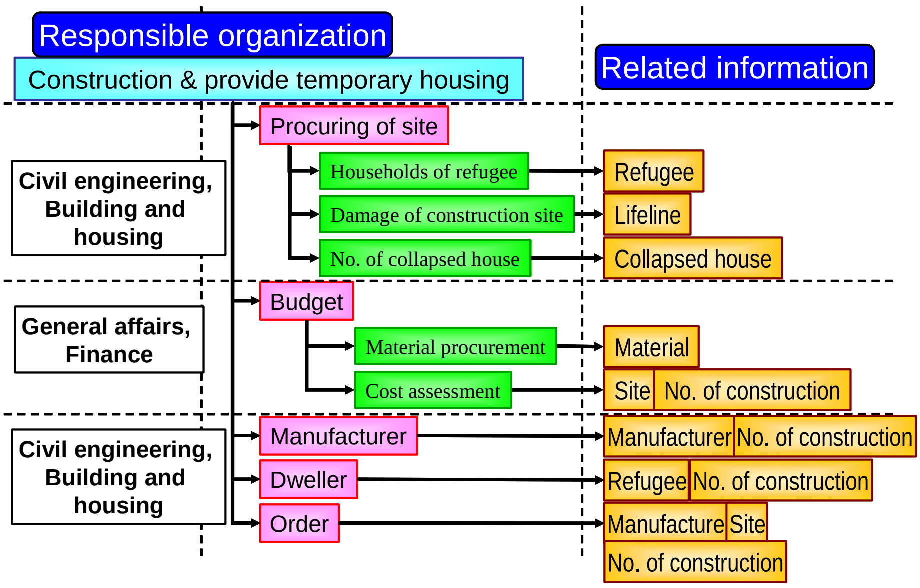

Figure 12: Result of associating related information with structured second-level work

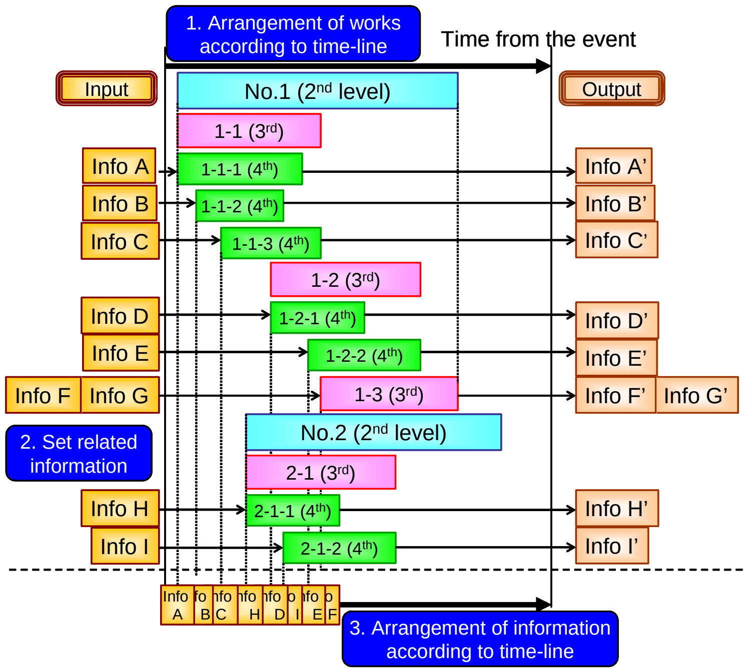

Figure 13: Arrangement of information by division

Figure 15 shows example of "job analysis from information management." The upper table is "Refuge information." and he lower one is "Road damage information." We have focused on 12 hours after the earthquake struck; refuge information is only used for damage surveys on shelters. Road damage information was used for early works, such as damage surveying and traffic regulating, setting up detours for transporting relief supplies, and surveying isolated settlements when making surveys on earthquake victims. Such work was needed for the working out of prefectural policy. Therefore, it was necessary to improve the sharing of road damage information. Figure 16 shows the arrangement of work and the division responsible using refuge information from the timeline. Various divisions provide service to refugees. Based on this figure, the relationships among divisions, which were not listed in the local disaster prevention plan, were shown.

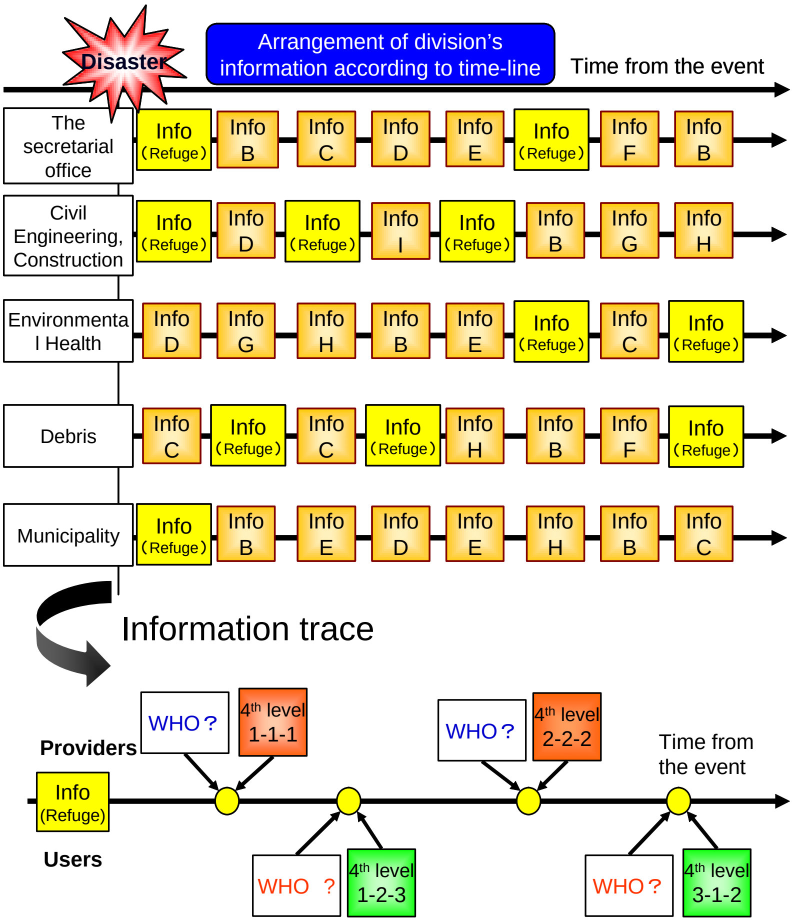

Figure 14: Information traceability

Figure 17 is an analysis of the effect of information sharing. It was apparent from the "information traceability job analysis" that different divisions collected the same information at different times. It was assumed that the information system would have shared refugee information with the Niigata Prefectural Emergency Operation Center. The effort of collecting information had therefore been decreased. By collecting information early, logistic support, such as the provision of heaters and medicine and the promotion of same via the media, could be done earlier. In other words, information sharing was not for the good of disaster response organizations, but for the good of the victims.

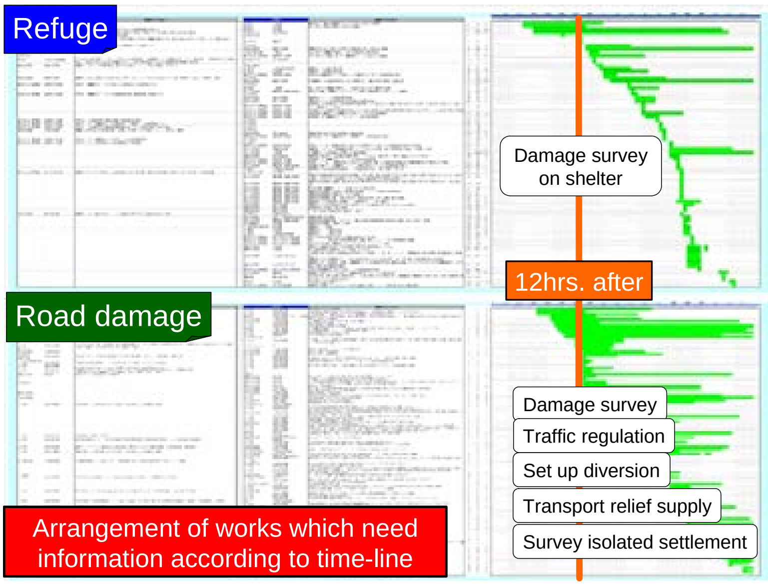

Figure 15: Job analysis from information management

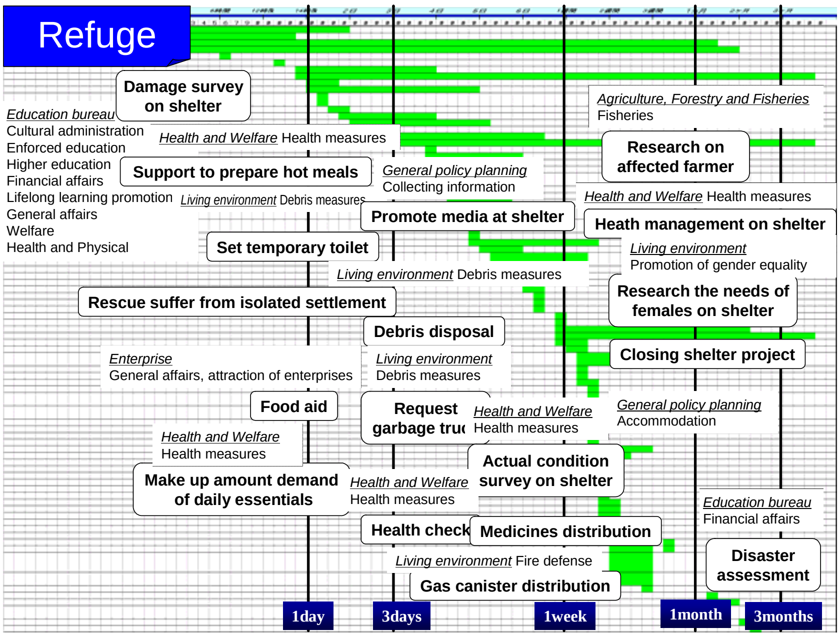

Figure 16: Information traceability job analysis

3.5 Mutual Relations

In this section, the relationship between information providers and receivers was arranged with focus on types of information. Figure 18 shows an example focus on refuge area information. The left side references the division providing and reporting information. The upper portion references the divisions needing and receiving information. In this study, this figure was defined as an input-output information matrix. From Figure 18, divisions of the Education Bureau provided information to General Affairs. This division edited information and provided it to the national government. Figure 19 shows input-output information matrix- related road damage information. The Civil Engineering Bureau's Road Management Division received this information not only from the Road Construction Division but also from related outside organizations, such as municipalities and the MLIT Regional Development Bureau. This division edited and controlled information and provided it to the prefectural EOC, the city and national governments.

In light of the above results, it was possible to improve the environment-related outside organizations and central division for information management with arrangement of divisions providing or receiving types of information. It was necessary to construct relationships with related organizations and to learn information management.

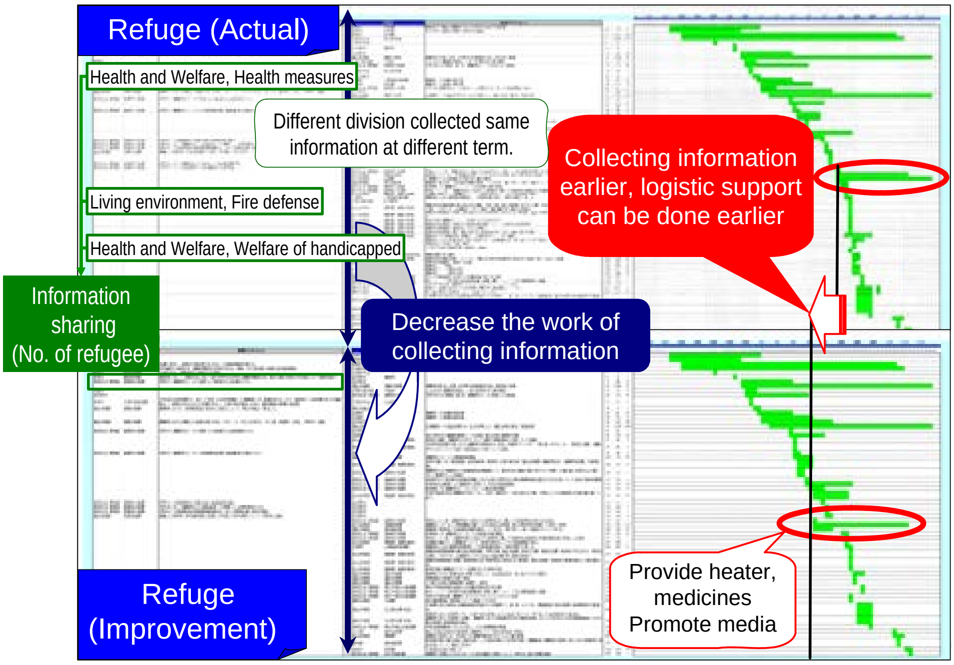

Figure 17: Effect of information sharing

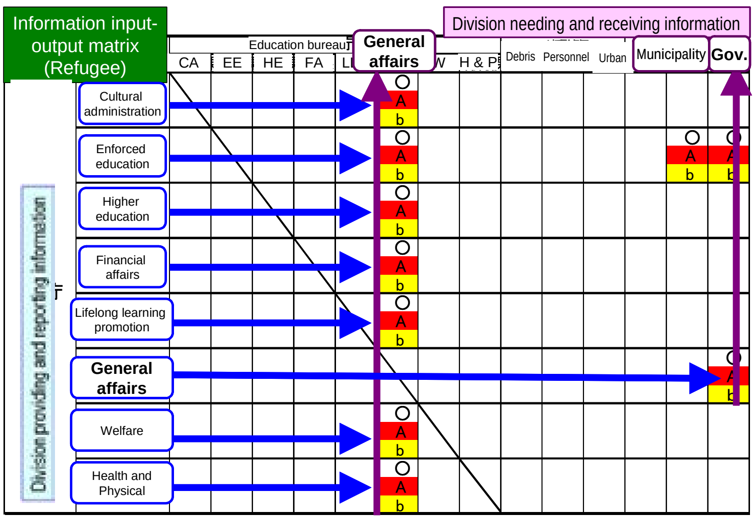

Figure 18: Input-output information matrix (refugees)

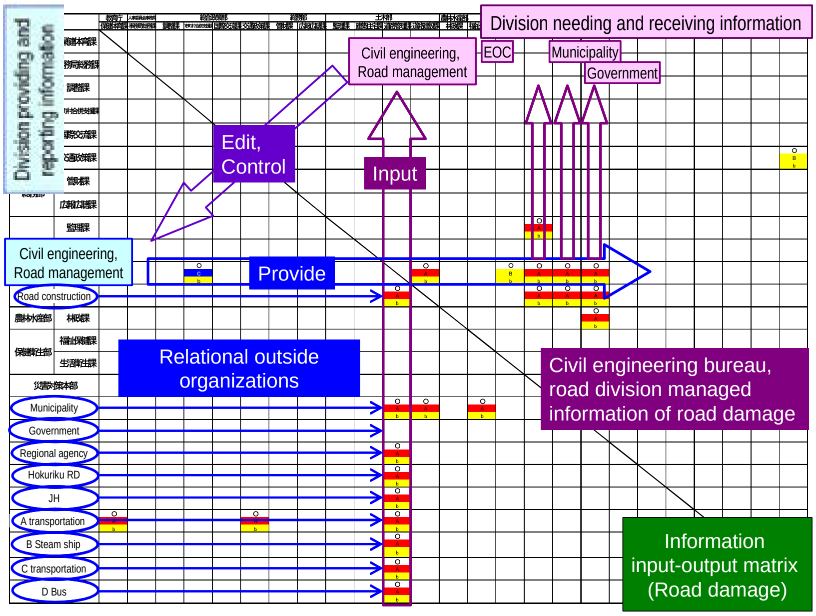

Figure 19: Input-output information matrix (Road damage)

4. CONCLUSIONS

In this study, for implementation of proper disaster management, we have mainly done two issues related disaster information management. One is a proposal of a new approach to make clear the relationship among activities for disaster reduction in different time phases, actor organizations/divisions, required information, its accuracy and providers in order to make efficient disaster information matrix. Adopting this concept, we have proposed disaster information plat form. With this system, damage data collection and report systems become efficient and quite different from conventional one as shown in Figure 20. As Figure 21 shows, when disaster related organizations had this system, efficient information sharing could be done and disaster response activities might be smoother and more efficient.

The other is that we have proposed an environment to improve disaster management of organizations in a disaster-free period. To do so, the records of the Niigata Prefectural Government disaster response activities during the 2004 Mid-Niigata Prefecture Earthquake disaster were analyzed from five points of view (constitution, job analysis, workload evaluation, information management, and mutual relations). Results are shown below.

- From the viewpoint of constitution, changes in the Niigata Prefectural Emergency Operation Center's structure proportional to changes in the disaster-affected community were cleared.
- From the viewpoint of job analysis, the work divisions listed in the regional disaster prevention plan were broken down and refined for putting planning operations into action. This analysis enabled inexperienced people to get a grasp of the time required to carry out the works.

- The workload of each type of work was quantified. The amounts are calculated by compiling the duration of first level work, with eight hours equaling one workday. This analysis included both the main work and complementary work of each bureau.
- The works categorized in the local disaster prevention plan and carried out in real situations were compared and analyzed. This analysis showed concrete actions to be taken to in the implementation of the plan, and also shows unplanned work.
- From the viewpoint of information management, which section needs information and which section provides information were focused on and arranged on a timeline.
- This analysis showed that the relationships between divisions, which are not listed in the local disaster prevention plan, was shown, and the effect of information sharing was not for the good of disaster response organizations but for the good of the victims.
- From viewpoint of mutual relations, the relationships between information providers and receivers were arranged in a matrix with the focus on information input-output.
- From this matrix, it could be understood that it is possible to improve the environment-related outside organizations and central division of information management with arrangement of divisions providing or receiving types of information. It was necessary to construct relationships between related organizations and to learn information management.

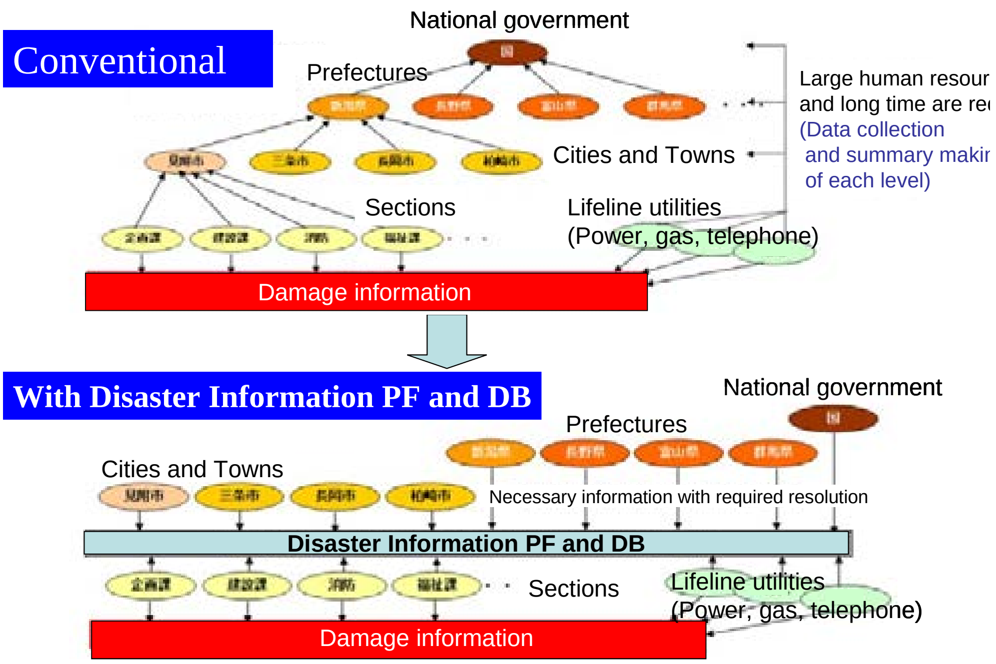

Figure 20: Changes of damage data collection and report among disaster related organizations with and without disaster information plat form

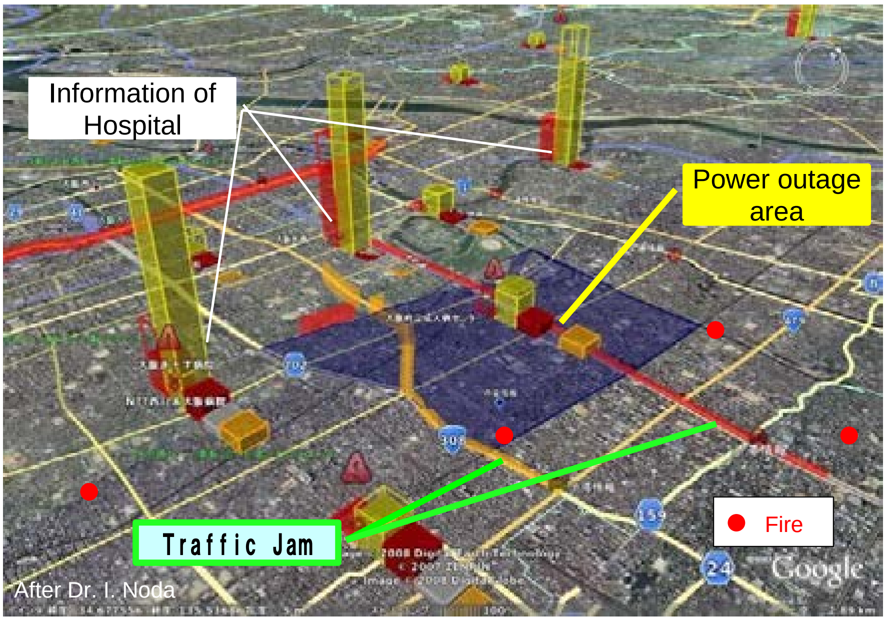

(after Dr. I. Noda)

Figure 21: Disaster information sharing using disaster information plat form

REFERENCES

[1] S. Kondo and K. Meguro: *Development of a New Method for Disaster Response Assessment Using Disaster Information Obtained by Current System*, JSCE Journal of Earthquake Engineering, Vol.28, 2005.

[2] S. Kondo and K. Meguro: *Development of New Style Disaster Information Database for Implementation of Efficient Disaster Countermeasures*, Journal of Social Safety Science, No.4, pp. 261-266, 2002.

[3] Niigata Prefecture: *The local disaster prevention plan –Earthquake measures–*, 2004.

[4] Niigata Prefecture: *Information about the Mid-Niigata Prefecture Earthquake in 2004*, http://www.pref.niigata.jp/content/jishin/jishin1.html

[5] Fire and Disaster Management Agency: *The Mid-Niigata Prefecture Earthquake in 2004*, http://www.fdma.go.jp/concern/index.html

[6] Disaster Reduction and Human Renovation Institution: *Studies on the Niigata Chuetsu Earthquake Disasters of 2004*, 2005.

DEVELOPMENT OF LIFE CYCLE MANAGEMENT SYSTEM FOR OPEN-TYPE WHARF

EMA KATO and MITSUYASU IWANAMI
Port and Airport Research Institute, Japan
katoh-e@pari.go.jp

HIROSHI YOKOTA
Hokkaido University, Japan

ABSTRACT

The authors have proposed the strategic maintenance method for port facilities based on the life-cycle management (LCM) concept. In this paper, the fundamental concept of the computer-based program to formulate the maintenance plan for an open-type wharf based on the LCM system was discussed. The proposed program was composed of 4 main components in the LCM system: inspection, assessment and prediction of performance, and implementation of appropriate intervention. The program should be improved by accumulating further inspection data and experiments; however, the authors expect that rational and effective maintenance would be realized by the results of this research and subsequently the life-cycle cost reduction and performance maximization could be attained.

1. INTRODUCTION

Port and harbor facilities generally face severe environmental conditions compared to other infrastructure. They often tend to suffer performance degradation during their service period due to various reasons including materials deterioration and damage of structural components. Therefore, the facilities need to be maintained systematically and appropriately so as to prevent them from failing the performance requirements during their service period. According to the Ministerial Ordinances on the Technical Standards for Port and Harbour Facilities revised on April 2007, the basic principles of facility maintenance and maintenance procedures (method, content, timing, frequency and procedure of inspection, assessment, prediction and countermeasure/intervention) should be stipulated in advance in a maintenance plan that conforms to series of basic maintenance procedures in order to ensure effective maintenance. As reference work for preparing maintenance plans, the Guidebook for Preparation of Port and Harbor Facility Maintenance Plan (Ports and Harbours Bureau, 2007) and Manual on Maintenance and Rehabilitation of Port and Harbor Facilities (Port and Airport Research Institute, 2007) were published.

The authors have proposed the strategic maintenance method for port facilities based on the life-cycle management (LCM) concept. The overall concept of the LCM, its individual philosophies and perspectives have been distributed through publishing the guidebook, the manual, etc. The individual components and methodologies in the LCM system, regarding inspection, assessment, prediction, and planning of countermeasures and their timings, have been established by the authors' previous research (eg. Yokota et al., 2008 and Kato et al., 2009). In this paper, the fundamental concept of the computer-based program to formulate the maintenance plan for an open-type wharf based on the LCM system was discussed. The computer-based program was developed to distribute the concept of LCM system to port managers and engineers. The program was composed by uniting the individual components developed by the authors, such as performance assessment and performance prediction based on the inspection, and countermeasures planning based on inspection and prediction.

2. OVERALL CONCEPT OF LIFE-CYCLE MANAGEMENT SYSTEM

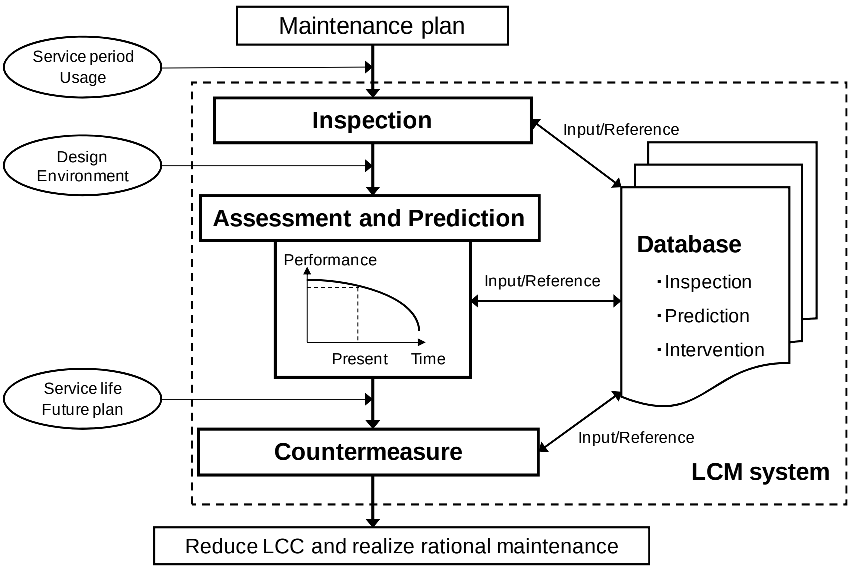

Figure 1: Procedure of life-cycle management.

Maintenance of port and harbor facilities is conducted according to procedures that include accurate inspection of deformation (that is, damage or deterioration) of structures, components or parts by timely and appropriate method, comprehensive evaluation of the results of inspections, and implementation of necessary countermeasures. In the implementation of these maintenance procedures, the following concept of LCM, as shown in Figure 1, represents an effective approach to rational and efficient maintenance. The LCM system is composed of the following 4 main components: 1) Inspection of present condition according to standardized criteria, 2) Evaluation of residual performance, 3) Prediction of future performance degradation based on the result of inspections and comprehensive evaluation considering the plans for future usage of facilities, the remaining service period and life-cycle cost, and 4) Implementation of appropriate countermeasures based on the results of the comprehensive evaluation.

3. MAINTENANCE LEVEL AND MAINTENANCE LIMIT

3.1 Maintenance level

Table 1 lists the three kinds of maintenance levels indicating basic concepts of how the performance will be guaranteed beyond the required performance limit and the maintenance limit. Selection of the maintenance level as the basic maintenance policy is necessary when designing and formulating a maintenance plan of the facility. The performance of each component should satisfy their performance requirements during their service life according to the selected maintenance level. It is ideal to select Level 1 for all the components of a facility. However, considering the severity of marine environmental conditions on the maintenance work, it may not always be practical from the viewpoint of life-cycle cost. Therefore, it becomes necessary to select the appropriately maintenance level of each component. It can be concluded that the maintenance level is the most important concept to achieve the strategic maintenance based on the LCM concept.

Table 1: Definition of maintenance level.

Level	Definition
Level 1	When predicting deterioration or deformation of components in the design stage and the maintenance planning, no performance degradation is expected. It is ensured that deterioration and deformation affecting their performance are minor during the design service period (that is, the performance is always kept above the maintenance limit).
Level 2	When predicting deterioration or deformation of components in the design stage and the maintenance programming, the performance degradation is controlled. Minor countermeasures are repeatedly applied to keep the performance above the maintenance limit.
Level 3	When predicting deterioration or deformation of components in the design stage and the maintenance programming, the performance degradation is expected. Major countermeasures may be applied once or twice for performance recovery. Application of preventive countermeasures is expected to be difficult or uneconomical.

In an open-type wharf conforming to the Ministerial Ordinances on the Technical Standards for Port and Harbour Facilities, the maintenance level of RC decks, steel pipe piles and corrosion protection treatments are set as Level 1, 2 or 3, Level 1, and Level 1, 2 or 3, respectively. The reason why the steel pipe pile is set as Level 1 is depending on the difficulty of its implementation of inspection and countermeasures against corrosion. Once corrosion of steel pipe pile occurs, its structural performance, which is directly related to the serviceability and safety of the entire structure, becomes decreasing thereupon. Therefore, from the viewpoint of the safety of structures and cost for countermeasures, applying the corrosion protection treatment before corrosion occurring is considered to be appropriate.

3.2 Definition of maintenance limit

In the maintenance work based on the LCM concept, the performance of each component in a facility shall be kept above the maintenance limit and/or the performance limit according to the selected maintenance level. However, definitions of each limit and performance degradation curves have been shown in conceptual and non-quantitative image (eg. Ports and Harbours Bureau, 2007) to date.

Concerning the state of performance degradation of components, there are a lot of research and inspection results of materials deterioration. In addition to those, the trend of structural performance degradations of reinforced concrete member and steel member has gradually been clarified by recent ardent research. However, detailed inspections with advanced expertise are generally required to evaluate the performance degradations quantitatively. Therefore, at present, a visually inspected deterioration or deformation in a component is judged as the deterioration grade in standardized criteria. Then, the deterioration grade is generally considered to be an index of performance degradation of the component.

Table 2: Basic policy of judgment of deterioration grades.

Grade	Basic policy
d	Performance of component is seriously degraded.
c	Performance of component is degraded.
b	Performance of component is slightly degraded.
a	Performance of component is not degraded.

In this study, the deterioration grades, Grade *d* to *a*, according to the general grading criteria in the Manual on Maintenance and Rehabilitation of Port and Harbor Facilities were considered as an index of performance degradation of components (Port and Airport Research Institute, 2007). Table 2 lists the basic policy of judgment of each deterioration grade. In the Manual, the grading criteria for each part and component of the structure are proposed by focusing on the visible deterioration and deformation, which affects the performance of the component.

Aiming at making the theoretical relation between the visible deterioration and the actual performance of component, the deterioration grades and load carrying capacities of concrete members extracted from the existing RC decks of open-type wharves were investigated (Kato et al., 2008). To compare the load carrying capacities of tested members with various structural details, the load carrying capacities were normalized by corresponding calculated results based on the beam theory by using designed values of material properties, shape and dimensions of the members, and so on. Figure 2 shows the relationship between the deterioration grades and load carrying capacities of concrete members. In tested members judged as Grades *c*, *b* and *a*, there were large variations in the load-carrying capacity. There existed the cases of which maximum load ratios are smaller than 1.0 in Grades *c*, *b*, and *a*. From the safety evaluation point of view, when deterioration grade was judged as Grades *c*, *b* and *a*, in other words, symptom of deterioration appeared on the surface of concrete members, the load carrying capacity might become smaller than the design expectations.

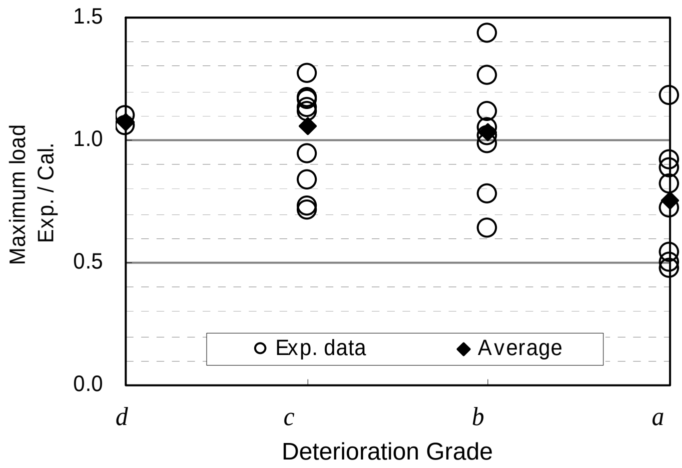

Figure 2: Structural capacity vs. deterioration grade.

According to the definition of maintenance level listed in Table 1, it is necessary to ensure that the deterioration affecting the performance of a component is minor during the designed service period in Level 1. Based on the consequence of the relationship between the deterioration grades and structural performance shown in Figure 2, it was considered to become the important constraint that the deterioration grade of the component of which maintenance level was selected as Level 1 should be kept Grade *d* throughout its service period without any countermeasures.

The structural performance of components is strongly related to the serviceability and the safety of a facility. In fact, the limitation of the performance requirements, such as serviceability and the safety, of a component was considerably depended on its importance of structural severity and the importance of a facility. However, considering the structural performances of tested members and the rapid progress of steel bar corrosion in concrete members judged as Grade *a*, it was considered to become the important constraint that the deterioration grade of the component of which maintenance level was selected as Level 3, at which major countermeasure was scheduled to be applied before loss in required performances, should be kept above Grade *b* during its service period.

For the components of which maintenance level was selected as Level 2, countermeasures as the preventive maintenance are required to keep the performance above the required performance limit. Considering the constraints for Levels 1 and 3 in addition to the above condition, the important constraint of the component for Level 2 was considered to be kept the performance above Grade *b* or Grade *c*. Whether the maintenance limit was Grade *b* or Grade *c* should depend on the importance of the components and the easiness of its countermeasure.

In this study, the maintenance limit of performance of a component for each selected maintenance level was defined as shown in Figure 3. This definition was applied to all the components in open-type wharf in the developed computer-based program. Because these limits were proposed based on the test results of structural performance degradation of concrete members, it is not considered appropriate to apply these limits to other types of members than concrete members such as steel pipe piles, corrosion protective treatments and so on. Definition of the maintenance and required performance limits of each component should be improved by accumulating further inspection data and experiments.

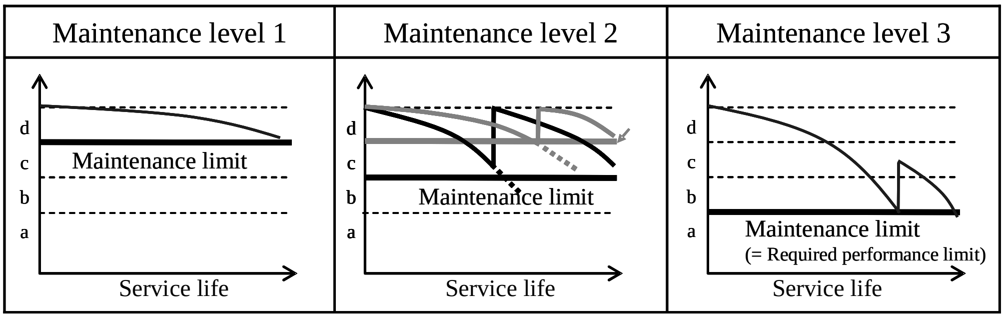

Figure 3: Definition of maintenance limit for each maintenance level.

4. SUMMARY OF THE COMPUTER-BASED PROGRAM TO FORMULATE A MAINTENANCE PLAN

Figure 4 shows the flow of the computer-based program to formulate a maintenance plan. The program is composed of 4 main components in the LCM system shown in Figure 1.

Program users can formulate the comprehensive maintenance plan with considering the life-cycle cost and the remaining service life of the target facility. Maintenance levels of each component shown in Figure 3 are set at the first stage of the program. The maintenance plan formulations of each component are automatically controlled for each selected maintenance level in the programs. In addition to those, the items and timings of the inspection for each component during their service life can be planned in the program. Because the open-type wharf was located in the severe environmental conditions affected by wave, splash, tidal changes and so on, the implementation of inspections generally requires the special techniques, such as shipboard inspections, inspections by divers, inspections from platforms etc. Therefore, the cost related to the inspections was considered to have an influence on the life-cycle cost of the open-type wharf compared with that of the land structures.

In this study, two kinds of programs, for newly designed open-type wharves and for existing ones, were developed, while the bases of overall system were the same. For newly constructed open-type wharves, the application of the performance based design and the formulation of the maintenance plan consequently bring the ensured prevention of performance degradation during the service period. However, for existing ones, only implementation of the maintenance plan based on the result of inspections can supplement non-ensured performances of structures in the design stage.

In the program for existing open-type wharves, the deterioration prediction using the result of inspection was available. Moreover, the probabilistic prediction considering the dispersion of the deterioration grades in the actual conditions can be carried out based on the Markov chain model (Yokota et al., 2006). The example of the maintenance plan for an existing open-type wharf formulated by the developed computer-based program was described in the following chapter.

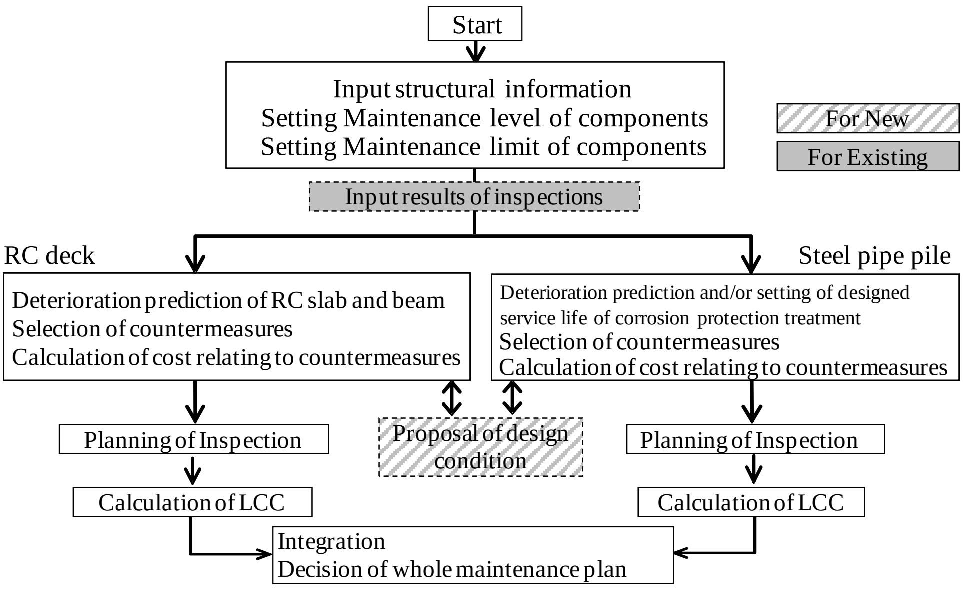

Figure 4: Flow of the computer-based program to formulate a maintenance plan.

5. EXAMPLE OF MAINTENANCE PLAN

The target structure shown in Figure 5 was an open-type wharf which had been in service since 1983. Its designed service period was 50 years. In 1995, the cathodic protection was applied to the parts of steel pipe piles in the submerged zone. The maintenance levels and the maintenance limits of decks and the corrosion protection treatments were set at Level 2 and Grade *b*. The maintenance level of steel pipe pile was set at Level 1. Table 3 lists the deterioration grades of each component judged by visual inspection carried out in 2008. Because almost all of mortar lining for corrosion protection and RC beams already became Grade *b*, the target structure was considered to require the application of countermeasures as soon as possible. However, measured protective potential of steel pipe piles at the submerged zone were below -800 mV vs. Ag/AgCl electrode; therefore, the cathodic protection system was still effective.

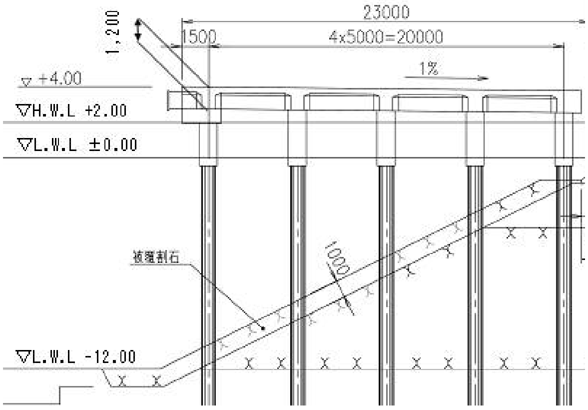

Figure 5: Cross-sectional view of target structure.

Table 3: Deterioration grades of each component.

Component		Deterioration grades and its ratio			
		d	*c*	*b*	*a*
RC deck	Slab	0.0 m^2 0.0 %	253.2 m^2 66.4 %	108.6 m^2 28.5 %	19.6 m^2 5.1 %
	Beam	18.9 m^2 5.1 %	76.0 m^2 20.6 %	205.9 m^2 55.7 %	68.9 m^2 18.6 %
Steel pipe pile (at tidal zone)	Mortar lining	0 pile 0.0 %	5 piles 20.8 %	15 piles 62.5 %	4 piles 16.7 %

Comparing the repair costs for the RC deck and the mortar lining, the cathodic protection to RC deck and the petrolatum lining to the parts of piles in the tidal zone were recommended to apply as the countermeasures considering the remaining service life of the target structure. In addition to this, because the cathodic protection system at the submerged zone was predicted to be effective until 2014 according to the prediction result of the consumption amount of galvanic anodes, the galvanic anode of which designed service duration was 20 years was scheduled to re-install to all piles in 2014.

Table 4 lists the items and timing of inspections. Visual and detailed inspections were scheduled to carry out every 3 years and 10 years respectively. The shipboard inspections and inspections implemented by divers were classified as the detailed inspection items. The amounts and the number of parts of the inspections were decided according to the Guidebook for Preparation of Port and Harbor Facility Maintenance Programs (Port and Harbours Bureau, 2007).

Considering the schedules and each cost of the countermeasures and inspections, the LCC in the remaining service life of the target structure was calculated as shown in Figure 6.

Table 4: Items and amounts of inspections.

Component	Inspection item	Visual inspection	Detailed inspection
RC deck	Visual inspection	100 %*	100 %*
	Detailed visual inspection	No	20 %*
	Measurement of chloride ion concentration in concrete	No	5 samples
	NDT for estimating cover depth	No	5 points
	NDT for corrosion of steel bar	No	5 points
	Survey (position and level)	Yes	No
Steel pipe piles at the tidal zone	Visual inspection	100 %*	No
	Detailed visual inspection	No	50 %*
Steel pipe piles at the submerged zone	Detailed visual inspection	No	100 %*
	Measurement of protective potential	20 points	20 points
	Measurement of consumption amount of galvanic anode	No	3 points
	Measurement of galvanic anode current	No	1 point

* Ratio to the total surface area of components (%)

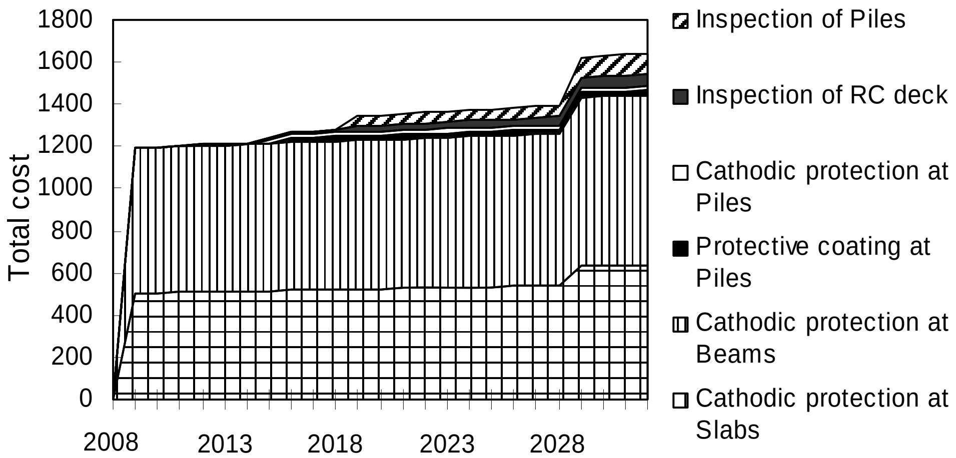

Figure 6: LCC of the target structure.

6. CONCLUDING REMARKS

In this paper, the fundamental concept of the computer-based program to formulate a maintenance plan for an open-type wharf was discussed. Some of evaluation and prediction methods in the proposed program, such as the definition of the maintenance limit and required limit of each component, should be improved by accumulating further inspection data and experiments. However, the authors expect that rational and effective maintenance would be realized by the results of this research and subsequently the life-cycle cost reduction and performance maximization could be attained. The part of this present research has been financially supported by the JSPS Grant-in-Aid for Scientific Research (B) No. 20360195.

REFERENCES

Kato, E., Yokota, H., Iwanami, M., Akira, Y. and Kawabata, Y., 2008. Simplified assessment for structural performance of deteriorated RC deck. *Proceedings of 2nd International Workshop on Life Cycle Management of Coastal Concrete Structures*, Hangzhou, China, pp.75-80.

Kato, E., Iwanami, M. and Yokota, H., 2009. Development of Life Cycle Management System for Open-type Wharf, *Report of the Port and Airport Research Institute*, Vol. 48, No.2, pp.3-35.

Port and Airport Research Institute, 2007. *Manual on maintenance and rehabilitation of port and harbour facilities*, Coastal Development Institute of Technology. (in Japanese)

Port and Harbours Bureau, 2007. *The Guidebook for Preparation of Port and Harbor Facility Maintenance Plan,* Service Centre of Port Engeering.(in Japanese)

Yokota, H., Komure, K. and Takahashi, H., 2006. Lifecycle Management of Concrete Deck by Markov Model, *Lifetime Engineering of Civil Infrastructure*, pp.137-149.

Yokota, H., Iwanami, M., Yamaji, T. and Kato, E., 2008. Life-Cycle Management of Concrete Structures in Coastal Areas. *Proceedings of 2nd International Workshop on Life Cycle Management of Coastal Concrete Structures*, Hangzhou, China, pp.53-58.

URBAN DISASTER AND EMERGENCY EXERCISE IN REAL TIME 3D SOCIAL VIRTUAL ENVIRONMENTS

ALI ASGARY
Emergency Management, School of Administrative Studies, Faculty of Liberal Arts and Professional Studies, York University, Canada
asgary@yorku.ca

ABSTRACT

This review-case study paper introduces real time 3D social virtual environment and their educational and practical applications in urban disaster and emergency exercises. Second life (http://secondlife.com/) is one of the most popular 3D virtual world platforms in use today, with an emphasis on social interaction. Conducting real world large urban disaster exercises are very costly. Real time 3D social virtual environments provide virtual environment in which disaster simulations and exercises could be integrated with social interactions and communications which are essential elements for a successful exercise This paper describe some urban disaster and emergency simulation and exercise cases from Second Life, including the first International Virtual Swine Flue Exercise conducted in the York University Virtual Emergency Operations Centre in Second Life in May 2009 (supported by the International Association of emergency Managers-IAEM). The goal is to show how real time 3D virtual environments could be used for disaster simulations and exercises that need stakeholders' social interactions. The potentials applications of Second Life in urban disaster simulation and exercise are then discussed, as well as some issues and challenges related to the use of virtual worlds.

1. INTRODUCTION

Simulations and exercises facilitate improved disaster and emergency management. They improve emergency planning, coordination and communication and have many other educational and training benefits such as the development of a shared or common language and enabling similar thinking regarding the nature of the emergency (Galley et al., 2004). Simulations and exercises provide a common understanding of the ensuing issues and their prioritization, identification of available resources and their deployment, and the articulation of a system to communicate with organizations in an effort to produce a coordinated response. Increased knowledge of the risks and impacts of a threat through simulation and exercise improves awareness of the need for effective planning and the need and usefulness of training. Such knowledge also provides a realistic appraisal of the problems related to an event, allowing responders to act in an informed manner rather than without prior ideas and thoughts.

Furthermore, the use of simulation and exercise as a means of establishing realistic expectations serves to reduce emergency managers' stresses (Boin et al., 2004). This rationale argues for the importance of providing realistic training through the use of simulations and exercises. Using disaster simulations in an active engagement, realistic frameworks and shared learning is one way of incorporating all of the education components and aid disaster and emergency managers in dealing with disaster events (Taraban, Box, Myers, Pollard & Bowen, 2007; Bluestone, 2007; Hake, 1998; Micheal, 2006). While simulations cannot quite replay actual crises, they are the closest form of exposure many participants might have to a disaster prior to an actual event, thereby providing an opportunity to learn and practice in a calm, controlled environment.

Computer base simulations are becoming an important element of disaster simulation and exercise planning (Smith, Dowell & Ortega-Lafuente, 1999). Conventional computer-based simulations allow participants to interact in a dynamic disaster domain model through the use of video, audio and/or computer graphics. Complex systems allow interaction with multiple users within the scenario enabling the process of coordination. Today a new component has been added to the computer based simulation; that of the real time virtual on line environments. This is a relatively new and emerging learning environment. This paper explains how on line virtual environments such as second life can be used in disaster simulation and emergency exercises. The remaining parts of re organized as follow: Section 2 provides some backgrounds on disaster simulations and the virtual world. Section three discusses the use of Second Life virtual environment in disaster simulations and emergency exercise. Section four reviews the use of Second Life by the author at York University. Section five concludes the paper

2. DISASTER SIMULATIONS AND EMERGENCY EXERCISES AND THE VIRTUAL WORLD

2.1. Types of Disaster Simulations and Emergency Exercises

Disaster simulations and emergency exercises are common tools used throughout the world to evaluate and improve responses during an event and they range in type, scope and the number of players involved. All simulations and exercises share the common goal of identifying areas requiring improvement, thereby necessitating an evaluation of the simulation or exercise (Green et al., 2003).

Disaster simulations and emergency exercises are developed to allow individuals to experience uncertain and unknown conditions and provide an opportunity for organizations to work collectively during stressful and varied contexts. The benefits of exercises and lessons learned are variable (Lonka & Wybo, 2005). Several gains can be realized through the use of emergency simulations, including allowing participants to increase their familiarity and test all aspects of emergency management which otherwise can only be experienced through in vivo exposure (Boin et al., 2004).

Exercises are invaluable in providing information regarding emergency management related to a specific incident (Lonka & Wybo, 2005). Simulations provide an easy method to obtain lessons learned, identification of issues and an opportunity for multi-agency communications. Often participants are unaware of the politics involved in crisis decision-making; therefore simulations give participants insight into how and why some strategies are employed and why some are not, and present participants with a greater understanding of the process and its limitations (Hermann, 1997). While real emergencies do not allow for failure, an exercise does and it provides an opportunity to try again. In addition, systematic and spontaneous feedback following the simulation is important to allow participants an opportunity to evaluate their own behavior, the rationale for decisions made and identify problems specific to their organization especially when used for training, teaching and planning purposes (Kleiboer, 1997). Successful exercises depend on two main variables: similarity to real circumstances and motivation of the players (Lonka and Wybo, 2005).

Simulations are tools for learning and a variety of types are utilized. Traditional approaches include “table-top” discussion based exercises, drills, functional and full scale exercises. Table-top exercises provide disaster managers an occasion to practice the activation of the response plan in a controlled, low stress environment and are often based on policy issues with a focus on processes (Canton, 2007; Coppola, 2007). Rather than having participants perform their functions, a detailed discussion occurs and problems and weakness are identified and dealt with. Table-top exercises are effective because they eliminate stress and time limitations often found during an event. Discussions also identify poor planning assumptions and provide a platform to clarify misunderstandings. These exercises are versatile in terms of length and cost. According to Smith et al. (1999) the learning takes place through the experience of discussion. While discussion based exercises lack the realism of other exercise types, they offer several instructive strengths including face to face discussion, exposure to each others’ technical language, priorities, interpretations, organizational needs, favored resolutions and assumptions (Smith et al., 1999).

Drills are supervised, controlled exercises during which a single emergency operation is tested. Drills are often cost effective, require less planning time and focus largely on one issue. Functional exercises test disaster manager capabilities by simulating an event that requires a response. This exercise type tests a variety of related activities that collectively accomplish an overall response (Canton, 2007; Coppola, 2007). Functional exercises add the element of time, therefore introducing stress into the scenario. Participants must respond to the request as opposed to discussion only, adding to the realism of the exercise. Functional exercises require a moderate amount of resources and several months of planning. Full-scale exercises are complex, scenario based, and attempt to simulate a real disaster, using actors and props. These exercises test all aspects of a plan for functionality, accuracy and effectiveness. This type of simulation requires many resources including the participation of all functional roles as outlined in the emergency operations plan, the activation of multiple response levels and tests the functionality of the plan. The exercise occurs in real time utilizing all procedures and equipment required in a real event.

Disadvantages of this type of exercise are the vast cost and planning time required. This method is the best for testing jurisdictional emergency management capacity.

2.2. Disaster Simulations and Exercises in the Virtual World of Second Life

Multi-user virtual environments offer several benefits including providing a more leisurely approach to learning, interacting with digital objects, representing themselves through an avatar, communicating with other participants while engaging in collaborative learning activities and taking part in modeling and mentoring experiences similar to those in real world contexts.

Training in the virtual environment can be more cost effective and realistic in ways that staged disasters cannot. For example, in the simulated environment, if first responders fail to put on their safety vest or reflective jacket when approaching the scene of an accident, their avatar may be hit by a car a negative reinforcement that could not occur in a real-life training exercise (Raths, 2008). Virtual disaster simulations provides emergency responders from all disciplines the opportunity to train together in real time for the purpose of learning the latest best practices in incident scene safety, coordination, and quick clearance of emergency events (The Center for Advanced Transportation Technology, 2008).

Second Life (SL) is a free online virtual world imagined and created by its residents (www.secondlife.com). It is a “digital world filled with people, entertainment, experiences and opportunity”. It was publicly released in 2003 by Linden Labs based out of California (Linden Research Inc., 2009). Within SL environments, participants can share slides, audio and video, engaging in discussions, presentations, group projects, and explorations. Second Life is currently one of the largest virtual worlds operating (Williams & Hudson, 2008). At any time there may be over 65,000 users logged in and exploring different aspects of the world. Once in-world, users are able to do a variety of everyday things such as strolling through the park, shopping at the mall or going for a drive down the coast (Linden Research Inc., 2009). Second life is a completely user-generated content, is relatively easy-to-use and build in which users own the intellectual property for their creations.

Virtual disaster simulations and exercises in places like Second Life have attracted many people because they are cost- and time-effective (Wyld, 2009). Since its opening public and private organizations, colleges and universities and independent researchers and developers have used second life for various disaster and emergency simulations and exercises. One of the reasons that SL can be used for emergency training and exercises is that it allows “for rich sensory immersive experiences, authentic contexts and activities for experiential learning, simulation and role-play (Kay, Educational uses of second life, 2009). These are the key ingredients for a successful emergency simulation and exercise. Further, SL notes that the opportunities for collaboration and co-operation are possible in virtual worlds like SL but are not as easily experienced using other platforms. Using SL, disaster and emergency trainers and educators can radically expand the problems that participants are able to address. This increase happens in two areas. The first is with problems that are infeasible to experience due to a lack of resources and second is with problems that are impossible to experience because of the limits of the physical world (Mason, 2007).

Second life has been used as a platform for disaster and emergency related training and education by universities, research institutes, public and government agencies and the private sector. At the University of Maryland's Center for Advanced Transportation Technology, researchers have been developing a virtual-world training exercise encompassing many different traffic scenarios, from minor accidents to major incidents for use by emergency responders in the I-95 Corridor Coalition. These simulations can now include hundreds of participants playing out their real-world response functions in the virtual environment (Lynch, 2008). US government organizations such as National Oceanic and Atmospheric Administration (NOAA), CDS, and DHS have created their own site in second life and provide various hazard and emergency management education and training. Usefulness of virtual environments such as second life has attracted private companies as well. SRA International Inc. is a technology provider with presence on Second Life. It provides services to organizations in the national security, government, health care and public health markets by designing, developing and integrating systems which, among other things, help facilitate efficient responses to disasters.

3. YORK UNIVERSITY'S VIRTUAL EMERGENCY MANAGEMENT LAB IN SECOND LIFE

At York University in Toronto, Canada, Ali Asgary (the Author), uses Second Life for distance education, research and professional exercises. Because of the dynamic nature of the subject matter, moving from a print-based to a 3D environment offers a more realistic visual sense of the temporal spatial dimensions of a disaster scene, which distinguishes it from the usual discussion-based simulations that occur in class. It would be prohibitatively expensive and logistically too complex to arrange real-life disaster simulations especially for university courses, so the SL environment provides an opportunity for students normally outside the scope of what can be taught in a structured learning environment. By utilizing the real-time audio function, students, who are assigned roles for the exercise such as mayor, fire chief, paramedic, etc., are able to coordinate their activities to manage the different aspects of a given disaster from their multiple perspectives by talking to each other in real time. The disaster simulation is set in the York University Virtual Disaster and Emergency (DEM) Lab in Second Life on a private island. The lab includes a Virtual Emergency Operations Centre (VEOC), a Media and Training Room, and a Virtual Disaster and Emergency Management Exhibition Hall, not yet completed, in which emergency management-related technology products will be showcased and tested. It is this virtual scenario that is used for the live table-top exercises.

3.1 The Trillium Emergency Exercises

Two table top emergency management exercises have been conducted by students taking an emergency management course at York University. The first exercise was conducted by students who took the course in summer 2008 as an internet course and the second exercise was conducted by students who took the course in campus during Winter 2009. While the first exercise was very much a virtual table top exercise without any simulation of the disaster scene, the second exercise involved some simulations of the actual disaster event. The emergency scenario was adopted from a real world emergency exercise developed by the Emergency Management Ontario as a community training tool. Both exercises took place in the fictional industrial town of Trillium, a mid-sized region with a population of approximately 250,000 to 300,000 inhabitants located in United County. During the summer and in the middle of the business week at approximately 8:37AM, a single explosion occurs at the Trillium Chemical Factory that is preceded by a series of secondary blasts that result in numerous deaths and injuries.

Students played a different role as a member of the Emergency Operations Centre (EOC), such as the mayor, community emergency management coordinator, fire chief, police chief and medical officer of health etc. In the winter in-campus emergency management course, students were offered three distinct options for the final term project. One of these options was a virtual emergency table top exercise that was to be orchestrated online in the Second Life virtual environment. In the eyes of the students affiliated with this project, this option proved to be one of the scarcest opportunities to be granted at the undergraduate level. After all, the sheer thought of utilizing innovative virtual technology to replicate actions, meetings, and exercises stemming from an emergency scenario were likely to be the closest interactive experience to a real life emergency.

Figure 1: A scene from the virtual disaster and emergency management exercise conducted by on line students in Second Life in July 2008

The virtual tabletop exercises were conducted fully online. In order for the virtual tabletop exercise to be implemented as smoothly as possible at various transition points, the exercise team had devoted much time in revising the script, organizing joint meetings after class and online, and further rehearsing several times prior to the actual presentation. The final exercise script was made in compliance with the scene that we intended to create, as well as the feedback from members after each rehearsal. Apart from each character's line, a detailed description of character placements for each scene was included in the script to ensure that each member would know exactly where to be at which scene. A majority of the meetings conducted were held online in Second Life in order to accommodate individual schedules and to help familiarize all members with the Second Life environment.

All students who participated in these exercises provided their feedbacks and evaluations of the exercise. Distance learning tends to be impersonal, but the Second Life online environment provided an opportunity for creative collaboration and real-time interaction between students that would have otherwise never met. The students seemed to enjoy and learned very much from the virtual experience. They found it very interesting, engaging and fun and a very creative approach as to simulating a table-top exercise. Students in distance education course found it interesting to be able to hear everyone's voice and communicate with them through Second Life. Students believed that Second Life has the capability of incorporating a class-like atmosphere in an online course, one that is less monotonous and allows for more interactions.

Students believed that the scenario provided a very useful learning tool for students fresh to the field of disaster and emergency management. And they highly recommended this type of project for future introductory courses to disaster and emergency management. The Second Life exercise put in perspective how serious and fatal a real disaster can be. This exercise was useful in learning how a community must work as a team and utilize all available resources to overcome such a catastrophic event. Through this project and practice, students learned the process of emergency response vividly and gained a better understanding of the whole scenario. It helped them understand the duties of an emergency response team. They also learned that effective communication in emergency management is important. As for Second Life, they mentioned that it is a good way to do some table-top exercises in emergency management.

Many students highlighted that it was very interesting for them to conduct a group project through Second Life and were able to act out scenes that appear in real life. The learning experience of this virtual exercise helped a lot in terms of understanding the importance of working together during the planning process of an emergency and that such processes cannot be done by one person. Overall, this exercise was useful as it allowed those that are interested in the emergency management field to have a glimpse and some sort of "hands-on" experience with the possible happenings each role would have to encounter.

Some of the students mentioned that the Second Life experience was unlike any other they had encountered at York University. To engage in distance learning of this caliber and still listen and contribute in real time as if we were in a classroom is something unheard of in Internet-assisted learning. The program gave us (the group members) the flexibility to sit at home and plug into group meetings and take part in voice-to-voice discussions over our headsets. The Second Life table top presented the standard operations of an Emergency Operations Centre while adding a heavy visual component in the design of the aptly named 'York DEM Island'. According to the participant this option should be available for students taking part in ADMS 3700 for years to come".

According to the team members the Second Life program is a great way of learning emergency management procedures and guidelines as well as providing distant assistance. In terms of usefulness this exercise does benefit students greatly in learning and applying the knowledge of in class information to a disaster scenario. The table top exercise in Second Life is an excellent tool to expose students to the process of responding to an emergency. According to the students this second life virtual exercise was a success despite a few technical problems. The concept of the Second Life program for emergency management exercises is very useful; however the program itself still has many technical problems to be improved. Although students ventured into the concept of Second Life with no prior knowledge in both the fundamentals of emergency management and in virtual technology software, they came out with a cohesive, well-executed disaster scenario. Technical issues aside, the online table top provided students with a real grasp on the operation procedures which take place within an EOC. The usefulness of this specific format is highlighted in its ability to allow for flexible meeting times and let students think outside of the classroom. For most of the students this was the first time that they were using Second Life. It was an engaging and fun experience for students and they learned a lot from the project on how emergency situations are actually handled and what happens behind the scenes from the moment an emergency is detected until the end.

Figure 2: Students participated in the Trillium table top exercise in Second Life in May 2009

3.2. The First International Virtual Emergency Exercise

The first international virtual emergency exercise was held in the York University Virtual Emergency Management Lab in Second Life on May 5 and May 7, 2009. This event was organized by the Emergency Management Program at York University, Toronto, Canada, in collaboration with the International Association of Emergency Managers (IAEM). More than 50 participants and observers, mostly the IAEM members who received the call for participants through the IAEM discussion list, were from the USA, Canada, United Kingdom, Spain, Turkey, Australia and the Netherlands. They came together in real time and participated in these exercises. The exercise scenario was an H1N1 Influenza (swine flu) pandemic developed based on a Rand Corporation pandemic exercise impacting a hypothetical city between April to July 2009 (www.rand.org/pubs/technical_reports/TR319/). This scenario was chosen mainly because of the ongoing worldwide concerns regarding the swine flu. The exercise goals were: 1) to examine the usefulness, challenges and issues of using the Second Life virtual environment as a platform for conducting emergency exercises from emergency professionals' perspectives. 2) To understand and exercise the key preparedness and response elements of a swine flu emergency (surveillance and epidemiology; command, control and communications; risk communication; surge capacity; disease prevention and control) at a typical local government setting.

As with a real world emergency exercise, these virtual tabletop exercises were held in the York University virtual EOC conference room (snapshots of the May 5 exercise are temporarily available at www.yorku.ca/cst/zDEMmovies-temp/). These exercises simulated what would happen in a face-to-face tabletop exercise. Considering that many participants were first-time Second Life users but still were able to actively participate in the virtual exercise shows that the learning curve is not a major issue when it comes to using Second Life for such virtual exercises. Participants must have the basic required hardware (a recent computer with a good graphic card and a headset) and software (Second Life browser available free after registering at www.secondlife.com).

Figure 3: The first International Emergency Management Exercise in Second Life conducted on May 2009

At the end of each exercise, a polling station was used to evaluate the exercise. Overall participants' responses to the survey questions showed that these virtual exercises were successful in achieving their initial goals. Respondents found the exercise to be "very impressive, fun and interesting," "very useful" and a "good and new experience". Some of the participants were impressed with how the conversation developed over the course of the exercise and with the visualization and simulation capacities of the virtual world for conducting various emergency management exercises. Most participants mentioned that virtual environments such as this seem to be a viable distributed environment for tabletop exercises, especially when it is difficult or costly to bring people together in one physical place.

4. CONCLUSION

Overall, using Second Life virtual environment seems to be a feasible and an excellent learning experience for disaster and emergency simulation and exercises. Through experimentation and learning how to use SL, the simulation and exercise team members can see potentials for virtual simulations. It is a safe learning environment and a cost effective way of exercising emergency plans once the scenario is set up. As with other complex software systems, the full benefit of SL can only be realized with informed and expert manipulation. The end product of the simulation could be used for exercise purposes as described in the research literature. The benefits of using SL are greater than the drawbacks. The uses of Second Life in the practice of emergency management should be further explored, with expert guidance.

The Second Life emergency table top exercise has proven to be an innovative solution to the standardized exercises currently undertaken. The ability to create life like avatars and base functions in a virtual Emergency Operations Centre adds depth and a new level of realism that simply can not be replicated within the confines of a conference or class room. The concept itself of bridging virtual technology with emergency management concepts allows the user(s) to interact, listen, and showcase their knowledge in the operations cycle of a disaster.

ACKNOWLEDGEMENT

The author would like to thank the York university students and IAEM members who participated in these exercises and provided their feedbacks and learning experiences. This work could not be accomplished without their interest, enthusiasm and support.

REFERENCES

Alexander, D., 2000. Scenario methodology for teaching prinicples of emergency management. *Disaster Prevention and Management* 9, 89 - 97.

Bluestone, C., 2007. Infusing active learning into the research methods unit. *College Teaching , 55*, 91 - 95.

Boin, A., Kofman-Bos, C., & Overdijk, W., 2004. Crisis simulations:exploring tomorrow's vulnerabilities and threats. *Simulation and Gaming 35*, 378 - 393.

Canton, L., 2007. *Emergency management concepts and strategies for effective programs.* John Wiley & Sons, New Jersey.

Coppola, D., 2007. *Introduction to international disaster management.* Elsevier, New York:.

Galley, I., Leonard, G., Johnston, D., Balm, R., & Paton, D., 2004. The Ruspehu lahar emergency response plan development process: An analysis. *The Australasian Journal of Disaster and Trauma Studies* 1.

Green, G., Modi, S., Lunney, K., & Thomas, T., 2003. Generic evaluation methods for disaster drills in developing countries. *Annals of Emergency Medicine* 41, 689 - 699.

Hake, R., 1998. Interactive-engagement versus traditional methods: A six-thousand-student survey of mechanics test data for introductory physics courses. *American Journal of Physics* 66, 64 - 74.

Hargis, J. P., 2008. *A second life for distance learning.* Retrieved May 25, 2009, from Turkish Online Journal of Distance Learning: http://tojde.anadolu.edu.tr/tojde30/index.htm

Hermann, M., 1997. In conclusion: the multiple pay-offs of crisis simulations. *Journal of Contingencies and Crisis Management* 4, 241 - 243.

Kay, J., 2009. *Educational uses of second life*. Retrieved May 29, 2009, from Second Life in Education: http://sleducation.wikispaces.com/educationaluses

Kleiboer, M., 1997. Simulation methodology for crisis management support. *Journal of Contingencies and Crisis Management* 4, 198 - 206.

Kolb, D., 1984. *Experiential learning: experience as a source of learning and development.* Prentice Hall, Englewood Cliffs.

Linden Research Inc., 2009. *What is second life?* Retrieved May 25, 2009, from Second Life: http://secondlife.com/whatis/

Lonka, H., & Wybo, J., 2005. Sharing of experiences: a method to improve usefulness of emergency exercises. *International Journal of Emergency Management* 2, 189 - 202.

Mason, H., 2007. Experiential education in second life. *Second Life Education Workshop 2007* (pp. 14 - 18). Chicago: www.simteach.com.

Micheal, J., 2006. Where's the evidence that active learning works? *Advances in Physiology Education* 30, 159 - 167.

Mitchell, J., 1997. Can hazard risk be communicated through a virtual experience? *Disasters* 21, 258 - 266.

Smith, W., Dowell, J., & Ortega-Lafuente, M., 1999. Designing paper disastersw: an authoring environment for developing training exercises in intergrated emergency management. *Cognition, TEchnology & Work* , 119 - 131.

Taraban, R., Box, C., Myers, R., Pollard, R., & Bowen, C., 2007. Effects of active-learning experiences on achievement, attitudes and behaviours in high school biology. *Journal of Research in Science Teaching* 44, 960 - 979.

Williams, A., & Hudson, M., 2008. Reflections in wonderland. *SCONUL focus* 43, 19 - 21.

Wyld, D., 2009. Government in 3D: How Public Leaders Can Draw on Virtual Worlds', IBM.

QUANTITATIVE EVALUATION OF ESCAPE SAFETY CONSIDERING EXTENSION OF ESCAPE TIME BY ESCAPE DISTANCE AND ESCAPE BARRIER

GUNSIK JEONG and YOUNGCHULL AHN
Pusan National University, Geumjeong-gu, Busan 609-735, Korea
gunsik72@hanmail.net

ABSTRACT

Escape distance and escape barrier are main elements for the quantitative evaluation of escape safety and they have been analyzed and proved by theoretically for their generalization and adaptation using a simple and a real plane model in previous studies. However, we should consider that there are many complex barriers in the escaping route, and the actual conditions must be considered in the study of escape safety. So the quantitative analysis on the effects of each barrier and escape conditions to the escape safety is necessary.

In this study, the quantified function which can predict various escape barriers in the escaping route is derived by theoretical analysis of escape barriers and conditions. The derived function is substituted for the evaluation tool, which is suggested in the previous study for the evaluation of escape safety, and evaluated with the simultaneous consideration of the escape conditions and the barriers. The results can be simulated in a hospital that has complex escape routes and various barriers, then it is anticipated more exact and actual escape analysis model can be acquired.

1. INTRODUCTION

Expansion of urban area and overpopulation cause large, complex and high rise buildings, however, it is more difficult to build a plan for preventing disasters such as a fire, an earthquake, a storm, a flood and a terror. So more tight regulations than the building law and the Fire Services Act are needed. Researches about the improvement of safety of a city and a building have been performed in the various field and also there are many fruitful results. But the results are not sufficient and there needs more improvements.
If we can recognize quantitatively the degree of hindrance of the leaved things and establishments in the escaping way which can reduce effective width of the way, and obstacles such as doors and stairs, then it can be considered during the design process and contribute to plan of urban and architectural design. Also it can affect custom of users and administrators to develop safety and performance of disaster prevention.

In this study, obstacles which are located on the evacuation way are investigated and analyzed according to the evacuation conditions such as power of locomotion and moving pattern, And a function which can quantify the degradation of evacuation safety due to the obstacles is derived. Also the validity of the function is verified by comparing with the previous works.

2. PREVIOUS WORKS AND THEORIES

2.1 Previous works

There are several researches about the evaluation method of evacuation safety. Choi, Jae-Pil(2006) suggested an evaluation model for special space using a concept of evacuation expenses by visibility graph analysis, and analyzed with a case of actual building. Oh Jung Woo(2007) suggested a network model of indoor area using a network theory and studied possibility of automatic search of evacuation path. Kim, Jong-Hun(2007) researched evacuation of multiplex cinema using a fire simulation and evacuation simulation based on the CO concentration and evacuation time.

Berlin evaluated escape potential, Mikio TAKAGI(1991) suggested exponential constants for network analysis and adapted to the analysis of underground passage, Yoshitsugu AOKI(2001) suggested modification of value of weight of network using neural network, Shigeyuki OKADA(2003) adapted a concept of degree of risk to network analysis, and Kouji SHIDA(2002) considered behavior ability of a people to the evaluation of evacuation safety.

2.2 A model for change of reliability due to the escape distance and obstacles

2.2.1 *Evacuation safety and reliability*

A "reliability" is used as an index of evacuation safety and it is defined as "a probability which can insure the safe evacuation way from the initial evacuation place to the final safe place in disaster circumstances." However, the reliability has a meaning of relative comparison because the results are not reflected any experimental or simulated analysis. That is, it can not be believed that the safety is double when the reliability is double. However, if we establish a database based on the actual in the near future.

2.2.2 *Reliability of a link and a network*

Fig. 1 shows an example of network graph for the connection from evacuation starting node S to finishing node G, G1 and G2.

The passing through probability of each connection is represented as "link reliability", and "network reliability" represents combined reliability which is considered from all the link reliability.

The network reliability in a network model can be calculated,
In case of series connection (Fig. 1 (a))

$$R_{ij} = r_i \times r_j \quad (1)$$

In case of parallel connection (Fig. 1 (b))

$$R_{ij} = 1-(1-r_i)(1-r_j) \quad (2)$$

R_{ij} : Combined reliability(network reliability) between link i and j.
r_i : Reliability of link i.
r_j : Reliability of link j.

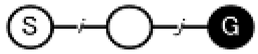

(a)Series connection between link i and j

(b)Parallel connection between link i and j

Figure 1: Network graph for the connection of node S and G(G1,G2)

2.2.3 *Model for escape safety according to the escape distance*

The previous model for the evaluation of evacuation safety using network analysis method has some weak points. Adjustments(addition or subtraction) of nodes which can not affect the size and type of network graph shows different network reliability. And if the connection type of network graph is same regardless of the size, the reliability shows always constant.

To modify these problems, the reliability, which is different from the length, is assumed that it is changed exponentially and Gunsik, JEONG(2007, 2008) is suggested Equation (3).

$$r(d) = {r_0}^{d/d_0} \quad (3)$$

$r(d)$: Reliability of a link at the distance of d.

r_0 : Reliability of a base link at the distance of d_0.

d_0 : The distance of a base link.

2.2.4 *Model for escape safety according to the obstacles*

The evaluation model which has a consideration of escape distance was very useful to solve many problems which can not be solved using previous model.

However, there needs to consider more actual escape conditions to the calculation of network reliability. So Gunsik, JEONG(2007, 2008) suggested a new model which adopted escape obstacles to the calculation of network reliability and proved the adequateness and the generality using a simple network model. The change of reliability of a link, which implies a change of escape safety, according to the escape obstacles and distance on the escape way is suggested as a Eq. (4)

$$r(d) = r_0^{d/d_0} \prod h_k \qquad (4)$$

$r(d)$: Reliability of a link according to the distance "d".

h_k : Passing through reliability of k_{th} door on the escape way.

Eq.(4) implies that the reduced reliability of a link due to the passing through a door is the same condition of increased escape distance in case of no obstacles on the escape way.

3. QUANTIFICATION OF EFFECTS BY THE ESCAPE OBSTACLES

3.1 Classification and characteristics of escape obstacles

This investigation is based on the case of a hospital which has publicity and much kinds of handicapped pedestrians in the view of escape.

There are 5 types of obstacles of difference of floor elevation, inclination, width of corridor, door and crowd. Table 1 shows the detail characteristics of the 5 types of obstacles.

① Difference of floor elevation may occur overturning and increase the escape time.

② Over 4°of inclination of a floor can increase the escape time.

③ Change of a effective width of a corridor increase of crowd density and it can increase the escape time and the overturning.

④ The open ration of a door can change the safety of evacuation and also increase the time.

Table 1: Classification and characteristics of escape obstacles

Type	Characteristics
difference of floor elevation	It can cause overturning and affect decrease of escape velocity. A wheelchair and a movable bed may not pass through due to the elevation. In case of step, there may be an overturning and a misstep. If it is modeled to evaluate escape safety, it can cause a bottleneck effect by decrease of effective width of corridor.
inclination	If the inclination of floor is larger than 4° there occur variation of pedestrian speed in general case and more larger variation of pedestrian speed using a wheelchair. Especially, in a long upward slope evacuation is sometimes impossible, and in a downward slope the increased speed cause an overturning or a collision.
width of corridor	Decrease of effective width of a corridor is closely related with crowd density. The winding escape way decrease escape time and leaved things act as critical obstacles not to allow smooth evacuation.
door	The door open ratio becomes effective width regardless of the corridor width. According to the type of door, the opening time is determined and makes stagnation to the evacuation stream. In case of the door frame is installed protruded, it makes overturning of peoples and difficult to pass through using a wheelchair. Generally, when the protrusion exceeds 2 cm, the pass through rate of people decreases in emergency. Sometimes, the effective width of an emergency gate is too

	small to pass through a wheelchair or a movable bed.
crowd	The persons can be obstacles each other in the crowded situation and heavy crowd density make increase the escape time and the overturning.

⑤ The persons can be obstacles each other in the crowded situation and heavy crowd density make increase the escape time and the overturning.

Moreover, intensity of illumination on the escape way, heat and toxic gases during fire, psychological instability, vibration during earthquake, and snowfall can affect escape conditions, but they are out of limit of this research and can be discussed in the next research.

Fig. 2 shows the relationship of mobility of occupants and escape types. The occupants are classified a group with ability and a group with disability. Generally, normal peoples with abilities can escape with his own ability, but peoples with disabilities need extra considerations when they escape.

In Fig. 2, when a people with abilities is drunk, he is lacking of mobility and power of judgement so classified as a people with disabilities using a dotted line.

The types of escape are free walk, crutch, wheelchair, movable bed and so on, and the left side shows large capability for self supporting escape.

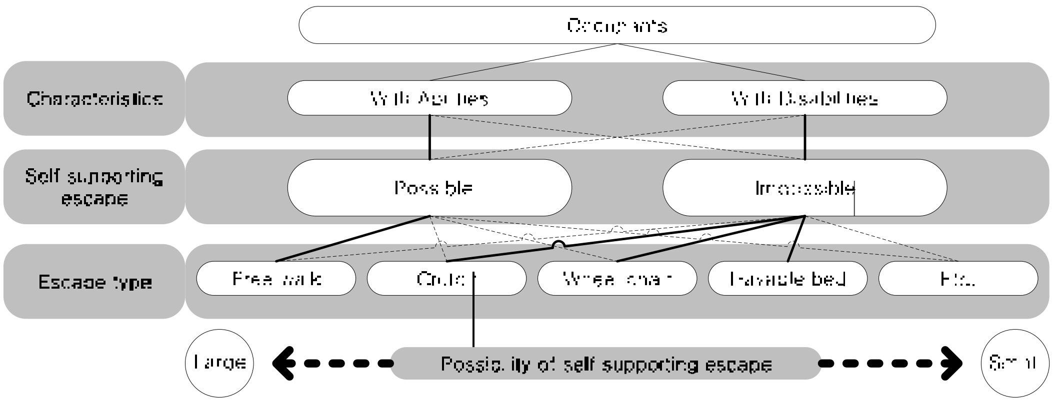

Figure 2 : Classification of various escape types

3.2 Quantification of effects by the escape obstacles

The degree of effects by the escape obstacles are defined as "Degree of Hindrance (DOH)" in this study.

When we consider if we pass through an obstacle of door, the reliability of pass through is determined by the DOH of the door.

That is, the DOH shows the degradation ratio of reliability. $O_b = 1$ menas impossible to pass through the escape way due to the obstacles and $O_b = 0$ means no obstacles on the escape way. Let the minimum escape time is T_s at the escape distance of D_s without any obstacles on the way, and T_e at the same distance but with obstacles such as stairs, then the extended escape time T_d due to the obstacles is

$$T_d = T_e - T_s \qquad (5)$$

If the escape velocity is the same, the moving distance during the extended time is

$$D_d = T_d \times V_0 \qquad (6)$$

Therefore, the extended escape time is expressed as elongation of escape distance $D_s + D_d$ and Eq.(7).

$$(D_s + D_d) = V_0 \times T_e \qquad (7)$$

Fig. 3 shows escape distance with and without obstacle such as stairs and the obstacle is converted as elongated escape distance.

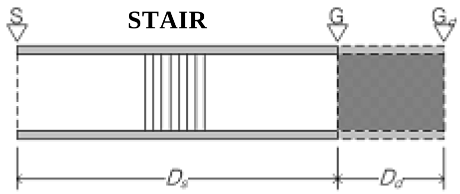

The stairs are converted into an elongated escape distance, so total escape distance will be Ds+Dd.

Figure 3: Elongated escape distance by escape obstacles.

Using the Eq.(3), the calculation of reliability in case of no obstacles that is the escape distance of D_s is Eq. (8) and in case of obstacles that is the escape distance of $D_s + D_d$ is Eq. (9).

$$r(D_s) = r_0^{D_s / d_0} \qquad (8)$$

$$r(D_s + D_d) = r_0^{(D_s + D_d)/d_0} \qquad (9)$$

And the DOH can be expressed like Eq. (10).

$$O_b = 1 - \frac{r(D_s + D_d)}{r(D_s)} \qquad (10)$$

3.3 Investigation of adaptation using simple network model

In this study, the evaluation of evacuation safety is performed more precisely and synthetically by analyzing various obstacles on the escape way, even though the previous works used a single value of DOH.

Fig. 4 shows a comparison between the previous and the newly designed network model. Simply, an escape distance and an existence and nonexistence of obstacle are used in the previous model but information about the types of obstacles are included in the new model.

In the new network model in the Fig. 4, the length of all the links are the same and only consider the shortest path from the node "S" to the node

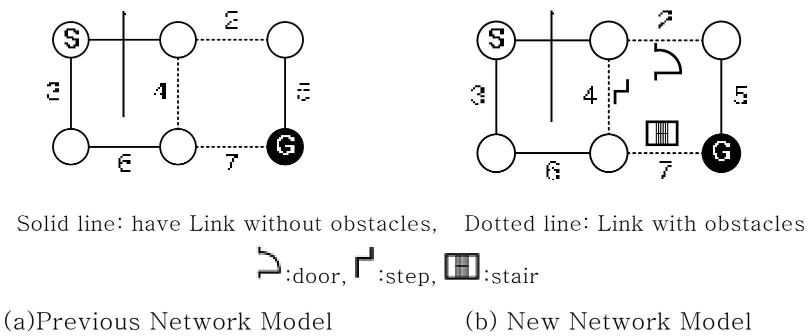

Figure 4: Comparison of the previous and the new network model

Table 2 : Matrix of shortest path

Link number	1	2	3	4	5	6	7
Path1	1	1	0	0	1	0	0
Path2	1	0	0	1	0	0	1
Path3	0	0	1	0	0	1	1

Table 3 : Values of reliabilities according to the escape types and obstacles

	Free walk	Assistance	Crutch	Wheelchair	Movable Bed	Aged person
step	1.0	0.9	0.9	0.6	0.6	0.9
stair	0.8	0.7	0.6	0.0	0.0	0.7
door	0.8	0.7	0.7	0.7	0.7	0.7

"G". Table 2 shows a matrix to find the shortest path.

The link 2, 4, and 7 represent a door, a step, and stairs, respectively, and DOH of each obstacles are shown in Table 3.

The reliability of a link without any obstacles is 0.9 and the reliabilities of a link with obstacles are 0.9 product each values in the Table 3. Assume that the escapes of a wheelchair and a movable bed through stairs are impossible. So the case of path 2 and 3 are excluded.

Fig. 5 shows the calculation results of network reliability. The previous network model can not show the difference of escape types, however new model shows various changes of network reliability.

The escapes using a wheelchair and a movable bed are disadvantageous than free walk and it is generally accepted in the actual situation.

This results shows deep consideration should be required in the design of hospital and social welfare facilities and it can be used for judgments of an evacuation plan.

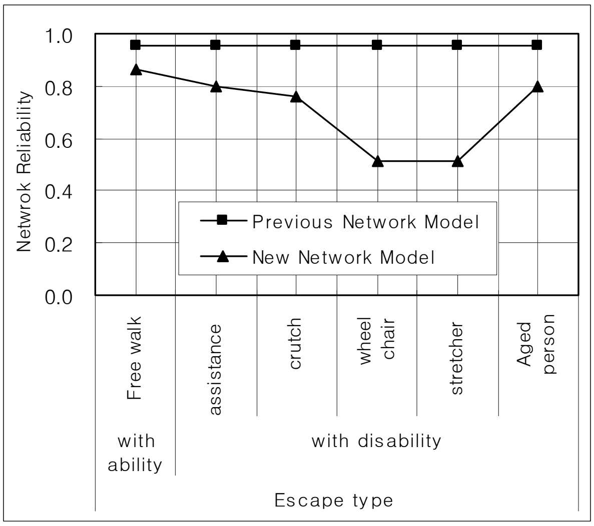

Figure 5 : Change in the escape form and network reliability

4. ANALYSIS USING AN ACTUAL PLAN

4.1 Calculation of network reliability

Fig. 6 shows an actual floor plan of a hospital and it consists of 52 nodes and 54 links. Each wards are set as evacuation starting nodes and a special evacuation stairway and a outdoor evacuation stairway are set as finishing nodes. The floor plan in Fig. 6 is slightly changed for the several reasons in the actual building.

Nurse rooms, storehouses, a locker room, and lavatories are excluded in the evacuation starting nodes, and two stairways inside the building also excluded in the finishing nodes.

The neonate room and the intensive care unit are expanded to the corridor in different from the floor plan, so the link 28 and the link 34 can not be used as an evacuation way.

The door on the link 39 is closed all the time from the site investigation, so it is treated as an impossible way to pass through in this study.

It is impossible to move from ward to balcony but consider the path to balcony and the path from balcony to evacuation stairway, because the neonates can not escape without assistances. Also compared the results to the case of evacuation using indoor paths.

Put the distance of a base link(d_0) 60 m, and reliability(r_0) 0.6, and the reliabilities are 0.8 for free walk, and 0.7 for wheelchair.

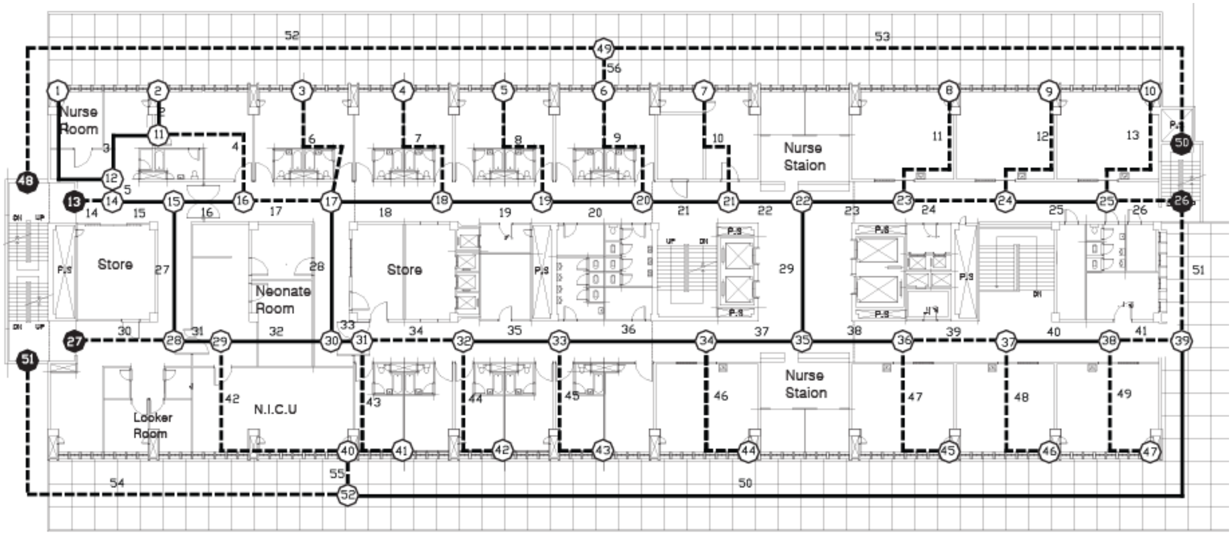

Figure 6 : Network model using an actual floor plan.

Table 4 represents the reliabilities of the network according to the escape types and compared the original floor plan to the modified actual building as a reduction ratio.

Table 4 : Comparison of the network reliability between the original floor plan and the actual building

		START NODE																	
		Node 1	Node 2	Node 3	Node 4	Node 5	Node 6	Node 7	Node 8	Node 9	Node 10	Node 40	Node 41	Node 42	Node 43	Node 44	Node 45	Node 46	Node 47
STANDARD		0.910	0.968	0.909	0.903	0.899	0.899	0.910	0.905	0.903	0.910	0.870	0.910	0.901	0.897	0.899	0.904	0.906	0.911
(A) Floor Plan	WHEEL CHAIR	0.290	0.295	0.168	0.164	0.130	0.119	0.131	0.184	0.251	0.359	0.273	0.170	0.124	0.114	0.126	0.181	0.182	0.359
	FREE WALKING	0.436	0.485	0.325	0.334	0.295	0.282	0.296	0.347	0.397	0.484	0.421	0.341	0.283	0.271	0.285	0.341	0.342	0.483
(B) Actual Building	WHEEL CHAIR	0.289	0.293	0.159	0.114	0.089	0.081	0.088	0.147	0.233	0.351	0.265	0.126	0.017	0.025	0.039	0.043	0.043	0.350
	FREE WALKING	0.433	0.477	0.297	0.244	0.214	0.202	0.208	0.267	0.355	0.464	0.398	0.246	0.056	0.073	0.099	0.118	0.119	0.457
Reduction Ratio (A:B)	WHEEL CHAIR	0.2%	0.8%	5.6%	30.9%	31.2%	32.0%	32.9%	20.1%	7.1%	2.1%	2.8%	26.0%	86.6%	77.9%	69.0%	76.1%	76.1%	2.5%
	FREE WALKING	0.6%	1.5%	8.7%	26.9%	27.5%	28.5%	29.7%	23.0%	10.6%	4.1%	5.6%	27.7%	80.4%	72.9%	65.1%	65.3%	65.3%	5.5%

The escape safety from node 42 to 46 decreased remarkably than other nodes, it because the link 34 and the link 28 are excluded from the evacuation way due to the expansion of the neonate room and the intensive care unit.

Table 5 shows the comparison of the network reliability with and without consideration of balcony escape at the node 6 and the node 40.

It shows considerably increased reliability and safety in both cases, and the evacuation plan using a balcony is very effective and useful especially to the peoples with disabilities.

5. CONCLUSIONS

The development of quantitative evaluation tool for actual escape safety is performed by the analysis of various escape obstacles and types and it is evaluated using an actual floor plan of hospital.

Main achievements of this research are like belows.

① Classification and analysis of escape obstacles by the investigation of design drawings and previous works.
② Investigation of human characteristics related evacuation and escape type according to the mobility.
③ Derivation of a function to convert the delay of escape time due to obstacles to the elongated escape distance.
④ Development of actual evaluation tool for escape safety by the combination of the previous model and the derived function.

The escape way of short and no obstacles is always best in the previous network analysis, however this research proved that it may be changed according to the escape type and obstacles even it is shortest way. For more accurate analysis, analytical and experimental investigations are needed simultaneously, and it will be performed in the future.

A remodeling or a change of floor plan are necessary because all the changes can not predict at the initial design stage, but it should be very careful if it has bad influences to the basic function of building, especially in the view of safe evacuation.

It is anticipated to be used to design a hospital, and social welfare facilities where are aimed to accommodate peoples with disabilities and to be designed evacuation plan using a balcony.

REFERENCES

Choi, Jae-Pil Kim, Min-Seok Choi, Hyun-Chull. 2006. Development of Evacuation Cost Analysis Method Based on Euclidean Distance with Visual Depth, *J. Archit. plan., AIK*. No. 22, 115-112

Oh Jung Woo, Kim Kyung Hwan, Lee Yoon Sun, Kim Byeong Su, Kim Whoi Yul, Kim Jae Jun. 2007. Network Model for Managing Interior Space in Real-Time, *STPAM of AKJCEM. KICEM*, pp.840-843

Kim, Jong-Hun Joo, Sung-Yong Lee, Jurng-Jae. 2007. An Evaluation on Evacuation Safety in Multiplex Cinema based on Fire & Evacuation Simulation, Vol.1, No.1, *KIAEBS* pp.7-13

Gunsik JEONG and Hidemasa YOSHIMURA. 2007. Quantiative Estimation of Escape Safety in Buildings Considering Eecrease of Reliability According to Escape Distance, *J.Archit. Plann., AIJ*, No. 616, 71-76

Gunsik JEONG and Hidemasa YOSHIMURA. 2008. Quantitative Evaluation of Escape Safety in Buildings Considerirng Decrease of Reliability by Escape Barrier, *J.Archit. Plann., AIJ*, No. 625, 551-557,

Mikio TAKAGI, Hirokuni TANIGUCHI and Jong-seok KIM. 1991. Basic Study of Indexes of Grapbs and Networks and Analysis of Street Structures of Underground Towns by Applying Them, *J.Archit. Plann., Environ. Engng, AIJ*, No. 422, 37-44

Yoshitsugu AOKI, Haruyuki FUJII and Yoshiro KINOSHITA. 2001. A Modeling of Expert-Judgement on Fire Safety Evaluation, *J.Archit. Plann., Environ. Eng, AIJ*, No. 546, 149-154

Shigeyuki OKADA and Nobuhiro KURDA. 2003. Study on The Evaluation of Seismic Casualty Risk Potential in Dwellings, *J. Struct. Constr. Eng., AIJ*, No. 563, 83-89

Hiroki MURAI, Kouji SHIDA, Takeshi YATOGO and Kan MOMURA. 2002. Study on The Refuge and Safety in The Fire at Nursing Home and Health Care Facilities, *J.Archit. Plann., Environ. Eng, AIJ*, No. 551, 181-187

Hidemasa YOSHIMURA. 1987. On Measuring Escap Ability from A Maze, *J.Archit. Plann., Environ. Engng*, AIJ, No. 375, 49-56

Hidemasa YOSHIMURA. 1989. A Metrical Evaluation of The Arrangement of Fire Escapes by Goal Programming, *J.Archit. Plann., Environ. Engng, AIJ*, No. 403, 9-20

Hidemasa YOSHIMURA. 1992. An Evaluation Method of Escape Safety of Building Plans Based on Weights of Safety Indexes Estimated AHP Analysis, *J.Archit. Plann., Environ. Engng, AIJ*, No. 437, 87-96

19.N.B.Berlin. 1980. A Modeling Procedure for Analyzing the Effect of Design on Emergency Escape Potential. PB80-204738

PROPOSAL OF AN EVACUATION NAVIGATING SYSTEM IN CASE OF NATURAL DISASTER

AYAKO FUKUSHIMA[1], BYONG-PYO JEONG[2], ATSUYUKI IDA[3], SHIN'ICHI TSUCHIYA[4], YUJI HASEMI[5]

[1]Graduate student, Waseda Univ., Japan

[2]National Institute of Information and Communications Technology, Japan

[3]Visiting Research Associate, Research Institute for Science and Engineering, Waseda Univ. M. Eng., Japan

[4]Visiting Researcher, Research Institute for Science and Engineering, Waseda Univ., PhD, Japan

[5]Prof, Department of Architecture, Waseda Univ., Dr.Eng., Japan

[1]a_fukushima@akane.waseda.jp

[2] jeong@nict.go.jp

[3]ida@kurenai.waseda.jp

[4]tsuchiya@afri.jp

[5]hasemi@waseda.jp

ABSTRACT

Japan is well known as a country being hit by strong earthquakes that may make numerous victims and collapse. After a heavy earthquake, information networks and infrastructure could be disconnected for several days. In the case of those disconnections, every victim, even the person who have no difficulty in evacuating, are capable to become vulnerable people because they could not make any decisions due to lack of information.

Especially, people that are not able to acquire and utilize information such as Foreigners with less Japanese communication skill and less experiences of earthquakes will be placed in disadvantaged situations. Therefore, Navigating Evacuation System (HINAVI; HInan(=Evacuation) NAVIgation system) is proposed as an information providing system with interface to make evacuating activity easier and safer.

The system is composed of several functions as follows; Evacuation guidance, SOS-maps function, Family Safety Confirmation, Citizens Information Application function, Translation and Risk Forecasting function.

This paper mainly deals with the evacuation guidance and SOS-maps function to rescue activities of the buried alive person. GPS (Global Positioning System) and GIS (Geographic Information System) are applied to these functions. Technical problems that need to be resolved are also discussed.

1. INTRODUCTION

As a typical damage of great disaster, telephone disconnection and traffic damage are expected. Under that circumstance, information requisite for evacuation would be unacquirable even for a person with normal functional capacity. And then, their evacuation will delay and might be caught in dangers.
In addition, the number of foreigners visiting Japan for the purpose of business and sightseeing has increased in recent years. Because of their inexperience in earthquake, there is a higher possibility that they will delay in evacuating.
Caused by diversification of traffic networks and lifestyles, even Japanese has high risks that they will be hit by disaster in unusual situation such as in a new place, transport facilities and so on. Those situations may cause their less level judgment and great confusion.
On the other hand, from a viewpoint of rescuing a large indefinite number, the difficulty of determination of the extent of the damage will make proper placement of rescue crews difficult.
Therefore, it is imperative that victims make judgments and actions themselves, and that rescue crews determine the extent of the damage correctly.

In this paper, we will aim disaster mitigation focusing on the role of information that will assume in case of disaster. We will study how information should be provided for people that are not able to acquire and utilize information, and propose HINAVI system.

2. BASIC CONCEPT of HINAVI

There are very few information providing systems that combine scattered information depending on individual attribute and location, though various information needed for evacuation and rescue after disaster (Fukushima et al, 2008). From viewpoint of disaster victim, it is needed to make a reasonable selection among massive amount of information spread out for public and to make some decision and action. However, proper decision-making is not facile for anybody, and difficulty for the disadvantaged is expected.
Therefore, we advance structure of information providing system (HINAVI; HInan(=Evacuation) NAVIgation system) that helps efficient information accession and evacuation behaviors. These information and data are supposed to be exchanged via portable devices (e.g. Mobile phone).
An example of evacuation activities of a HINAVI user is figured in Figure 1. HINAVI is activated and starts help user in town A evacuate just after earthquake has happened. Around the same time, situation of damage and usage of temporary evacuation area (B park), aid station for injured (C hospital) and evacuation center(D elementary school) are aggregated and reflected to evacuation routes. In the result, the route to Park B, which is the most accessible park from town A, is displayed and the user walk to Park B based on the guidance. Based on the information that the user has received

minor injuries, the user stops at C hospital for treatment on the way to refuge center, D elementary school.
If the user is visited by earthquake near the high-risk coast of tsunami disaster, HINAVI issues a tsunami warning and urges quicker evacuating. In the case of the user turned into unconscious under collapse, rescue crew that got the report rushes to the site, transports him to C hospital that can accept patients. In Addition, the system enables users inform their conditions to the families far away during evacuation life.

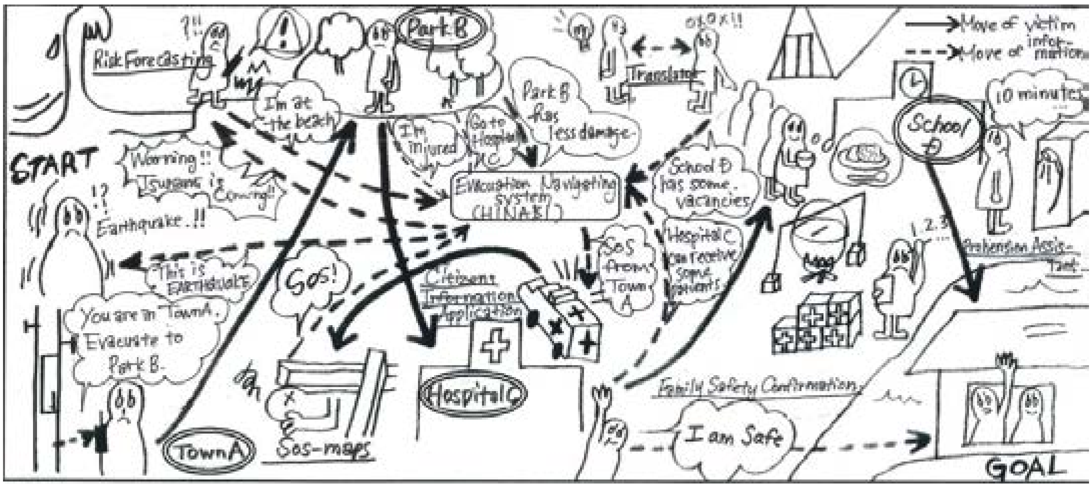

Figure 1: An example of evacuation activities of a HINAVI user

In this system, information that transacted in the case of emergency is classified into Inputs and Outputs. Inputs from victims to providers (The organizations retaining information) come to "Components that affect filtering of providing information" and Outputs from provider to victims are "Necessary information" as figured in Figure 2.

Existing model	**HINAVI model**
Provider Large amount of information Victim	Provider Inputs=individual attribute, condition Proper Outputs Victim
Users are forced to make a choice from a great deal of information sent from provider.	Provider outputs the information proper to users based on individual attribute and situation.(via personal device)

Figure 2: Models of information transaction (comparing existing model and HINAVI model)

Inputs are divided into "Advance registration inputs" such as age, sex, and "Post-Disaster inputs" are grasped after earthquake happened such as the collapses and the injuries. Table 1 shows correspondences between Inputs and Outputs. Corresponding Advance registration inputs are figured as O, and Post-Disaster inputs are described with implements and contents.

Post-Disaster inputs can be divided into “Inputs rely on self-diagnosis” and “Inputs remotely-monitored”.

#1 Inputs rely on self-diagnosis are as follows; Physical status (injuries, fatigue), Report of the fires and collapses happened in one’s neighborhood.

#2 Inputs remotely-monitored are as follows; Damage of the area undesignated a temporary refuge area for application as a refuge, Congestion condition of refuge centers.

According to inputs combined individual attribute and environmental condition, personal directions and information will be output (Table 2). It is necessary to construct the system that allows “facile and proper transmission” from victims to provider and “quick and precise provision of information” from provider to the victims.

Table 1: Correspondences between components affect filtering of providing information (Inputs) and Information provided by HINAVI (Outputs)

			OUTPUTS					
			Earthquake fundamental information	Evacuation direction	Evacuation area	Surrounding danger information	Water supplement & Toilet	Evacuation Center information
INPUTS	Advance registration	Earthquake experience	O					
		Language	O	O	O	O	O	O
		Sex					O	
		Age					O	O
		Health condition		O	O		O	O
		Location		O	O	O	O	
		Home address						O
	Post-Disaster	Remotely-monitored		Sensor-acquired info. of bldg.	Sensor-acquired info. of candidate site	Sensor-acquired info. of bldg. and roads	Damage of the toilet and channel	Congestion of evacuation center
		Rely on self-diagnosis		Detailed location		Visual observation	Physical status	

Table 2: Name and content of information provided by HINAVI (Outputs)

Style	Content	Example
Earthquake fundamental information	Information about earthquake for inexperienced victims	This shaking is "Earthquake". Calm down and evacuate to wide space with alerting to fires and collapses.
Evacuation direction	Information about appropriate actions	Use the stairs to ground floor noting overhead
Evacuation area	Information about a large space to avoid from spread of fire. Location and route.	Your nearest evacuation area is **park. It takes 5 minutes by foot.
Surrounding danger information	Information about surrounding danger (fires, collapses)	The road is cordoned off in 100 meters.
Water supplement & Toilet	Information about water supplement and toilet during evacuation	Turn to the right and take a rest in convenience store.
Evacuation Center information	Information about the life in evacuation center. Location and route.	Your evacuation center is OO elementary school.

3. FUNCTIONS INCLUDED IN HINAVI

3-1 The function of evacuation route guidance

Key function of HINAVI is route guidance. The rough flow of usage in the case of earthquake is as follows (Figure 3);

(1) The users enter their information about attribute such as sex, age and so on in advance. (Advance registration inputs)

(2) After earthquake happens, entries of injuries condition by users and of damages such as collapses and fires by remote sensors are aggregated. (Post-Disaster inputs)

(3) As guiding them depending on the situation, this system assists their safe and comfortable evacuation.

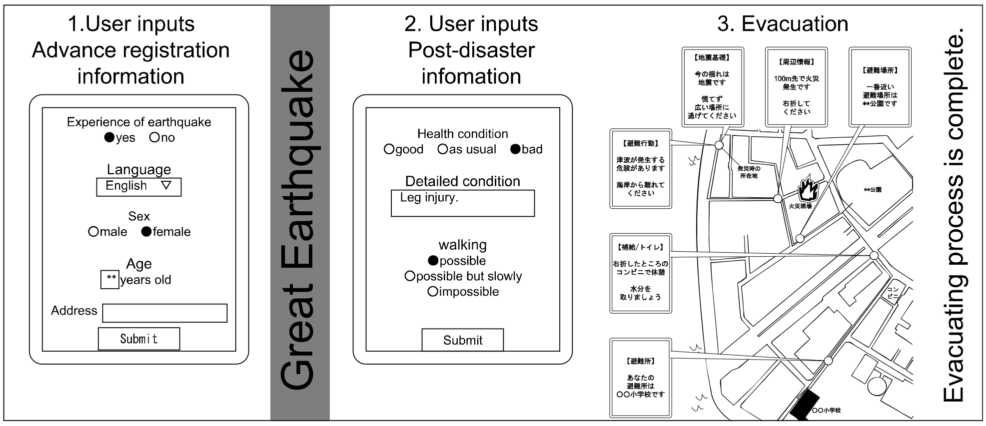

Figure 3: Flow of HINAVI usage (from a viewpoint of user)

Just after earthquake, “Earthquake fundamental information” and “Evacuation direction” will support their start of safe evacuation. During evacuation by walk, the user is navigated according to ”Evacuating Area Information”, “Evacuating Center information” about his own evacuate areas or centers. As necessary, HINAVI informs the user an alternative path when they approach dangerous area in order to avoid secondary disaster (Surrounding danger information). “Water Supplement & Toilet” will make their evacuation safer. (Figure 4)

It is necessary that the system possesses some functions for efficient evacuation route guidance depending upon the situation.

(1) Risk forecasting
This function is to determine and present degree of risk of the present location mainly by “Post-Disaster inputs”. The user with no experience of earthquake will be urged to evacuate, as a result keeps himself in safety.

(2) Citizen Information application

This function is to aggregate the information of fires and collapses gathered by users evacuating, and to use that information as indications of rescue and fire fighting.
(3) Translation
This function aims to maintain minimum communication skill even though all of the communication facilities are interrupted and real-time information is deprived.
(4) Prehension assistant
This function complements information for prehension and action when information is inadequate for user.
As it gives the users explanation about vocabulary (such as “Temporary evacuate aria”) and systems (such as life in evacuate center), it will supply lack of knowledge and encourage appropriate behaviors.

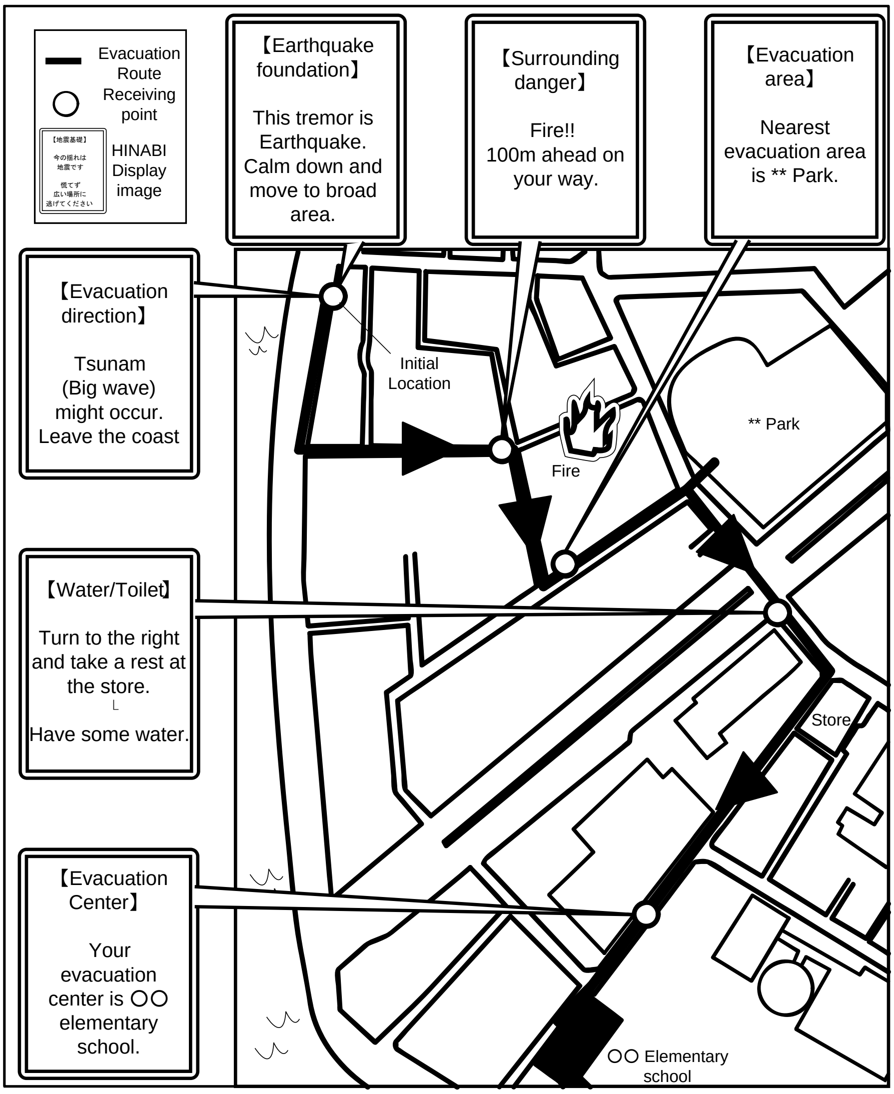

Figure 4: Image of route guidance

(5) Family Safety confirmation

This function assists the relatives confirm the safety of user. As the past has already shown, for foreigners struck by earthquake in Japan were forced to contact their family through embassy or international phone call. Those actions are often hampered by communication troubles or long-distance movement to embassy location. Therefore, this function is proposed to realize communication among family members through portable device.

The application of these functions in parallel with route guiding might realize proper information provision to individuals.

3-2 SOS-maps function

SOS-maps function is to make rescue easier with prehension of location and condition of victims when disconnection for a given length of time or impossibility of evacuation by one's own ability are occurred. This is essential function required right after great earthquake under chaos and life-threatening condition. In the Great Hanshin-Awaji Earthquake, 1995, 150,000 people had been buried alive and 35,000 of that had been unable to evacuate on one's own (Yamamura, 1995). Since amount of collapses happen over large areas, the strong cooperation among neighborhood residents and public rescue crews is necessary. This can be achieved by collection and sharing information about victims waiting for recues. However, it is difficult to collect information about damage under disaster situation, and there are few interagency information sharing systems. Figure.5 is showing outline of SOS-map function (SOS-map function includes identification of location by GPS and visually-adjustment and display by GIS.) and immediate rescue structure with information unification.

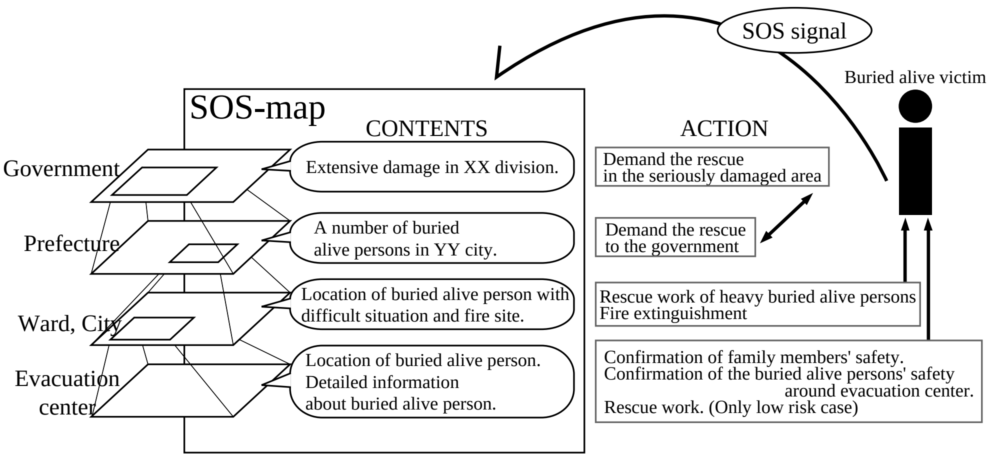

Figure 5: Survey of SOS-map function (Contents and action of relevant organizations)

Some efficient functions for relief of victims and readily feasible with existing technologies are as follows:

1. Determination of location of buried alive person with the mobile phone equipped with a GPS location service

By comparing the coordinate of user before and after earthquake, their movement is determined. It determines the user is a buried alive person or not based on displacement of user's device and location before hit by earthquake. (Table 3)

Table 3: Guideline for determination of buried alive person by location information

Location before the quake	Indoors or Outside	Indoors				Outside				Unclear (Disconnection)
	Calculated collapse ratio	high	high	low	low	high	high	low	low	
Move of the user after the quake		moved	stayed	moved	stayed	moved	stayed	moved	stayed	
Determination		-	Buried alive	-	-	-	Buried alive	-	-	Buried alive

2. Display of SOS-maps of buried alive persons with GIS
Figure.6 shows an example of SOS-map composed of location information (mentioned at 1.) and post-disaster inputs.

Since the category and the scope of required information differ according to organization, it is necessary to draw a map corresponds well to each organizations' needs and to share it widely. Organizations, such as fire companies and neighborhood residents, refer to SOS-map and cooperate in rescue activities.

Figure 6: Contents about buried alive victim displayed on SOS-map

3-2-1 *Future tasks of SOS-maps function*

When the victim is in underground area or communication knocked out area, it is difficult to determine locations of buried alive persons because of difficulty of accession of location. Expansion of range of communication with GPS relay-antenna, Wi-Fi and RFID technology is needed. Further to technical issues, role-sharing arrangement and upgrading of telecommunication networks are demanded to achieve the cooperation among some organizations such as refuge centers, fire department and so on.

4. CONCLUSION

We discussed about the information provision responding to individual condition, and we proposed HINAVI in this study.
The entire system includes technical problems as follows;
(1) Securing the availability of the base station.
In the past heavy earthquake, large amount of communications traffic concentrated to the local basement and caused the congestions. It is also necessary that the base station facilities will be enhanced earthquake safety or dispersed. Adoption of other network technologies (such as peer-to-peer network) needs to be explored.
(2) Securing the power supply of the cellular phone terminals.
It is difficult to supply power to the personal cell phone terminals ,though early restoration of power supply is expected. Because under such circumstance, continuity of medical activity or operation of refuge will be given priority over individual usage.
In the case of past earthquake, probability of survival of rescuees had reduced 3 days later (Iokibe, 1996). Therefore, as considering SOS-map function usage, the devices should work as long as 3 days when it is normally charged.

REFERENCES

Fukushima, A., Tsuchiya, S., Ida, A., and Hasemi, Y., 2008, *Proposal of a Navigating Evacuation System in Case of Natural Disaster for Foreigners*, Summaries of technical papers of annual meeting AIJ 2008, A-2, pp.11-12 (in Japanese)
Yamamura, T., 1995, *Self-disaster prevention organizations (Their missions and activities)*, Bousai System Kenkyu-jo. (in Japanese)
Iokibe, M., 1996, *Risk Management-Response taken by Government*, Hanshin-Awaji Daishinsai-shi , Asahi Shimbun Japan, p.347. (in Japanese)

INFLUENCE OF THERMAL CONDITION ON THE WIND ENVIRONMENT EVALUATION FOR BUILDING DESIGN

HONG HUANG[1], RYOZO OOKA[2], HOM B. RIJAL[2],
TAKEAKI KATSUKI[2] and BYOUNGCHULL OH[2]
[1]Center for Public Safety Research,
Tsinghua University, Beijing, 100084, P.R. China
hhong@tsinghua.edu.cn
[2] Institute of Industrial Science, The University of Tokyo,
4-6-1 Komaba, Meguro-ku, Tokyo, Japan
{ooka,rijal,wtakeaki,ohbc}@iis.u-tokyo.ac.jp

ABSTRACT

Computational Fluid Dynamics (CFD) simulation has become a powerful tool for wind environment evaluation for building design. In this study, the wind environment in an existing urban block is investigated under isothermal and non-isothermal conditions in summer daytime (15:00) using CFD simulation. The wind velocity under non-isothermal conditions is considerably higher than isothermal conditions. This is probably a realistic prediction considering the actual thermal environment in the urban block. It is concluded that consideration of non-isothermal conditions is required in numerical simulations for wind environment evaluations of urban blocks and building design. The linear regression equation is proposed to predict a realistic wind velocity for the urban block.

1. INTRODUCTION

The wind environment evaluation for new building design is usually carried out experimentally in wind tunnels. However, following the development of Computational Fluid Dynamics (CFD) simulation technology in recent years, CFD has become a powerful tool for wind environment evaluation. When a wind environment is evaluated by numerical simulation, isothermal conditions are often used (Hu et al, 2005) by assuming a large wind velocity compared with the atmospheric stability and instability effect (Bulk Richardson number is small). Huang et al (2008) carried out a CFD analysis on traffic-induced air pollutant dispersion under non-isothermal condition in a complex urban area. However, there has been little research on wind environment evaluation for building design in actual urban blocks under non-isothermal conditions. Therefore, this research focuses on an actual urban block, and the wind environment was evaluated by CFD simulation under both isothermal and non-isothermal conditions. The investigated area is located in a very dense urban area with mid-rise and high-rise buildings that include offices, commercial and residential buildings, which is shown in Figure 1.

2. METHOD DESCRIPTION

In this research, the coupled simulation of radiation and convection was used (Huang et al, 2005 and Yoshida et al, 2000). At first, the radiation calculation was performed, and this result is used for the CFD simulation. Three-dimensional city model data (Remote Airborne Mapping Systems-E (RAMS-E), Kokusai Kogyo Co., Ltd.) measured by an aircraft equipped with a laser scanner are used. In this data, the heights of buildings and the terrestrial surface are precisely measured by a laser scanner from the aircraft. The three-dimensional city model data is first read by CAD software, and then converted into Initial Graphics Exchange Specification (IGES) file format. After this, the IGES file is read by the computational grid-making software (Gridgen, VINAS Co., Ltd.). An unstructured computational mesh is constructed which is an effective means of conducting a CFD simulation in a complex urban block. RADX software was used for the radiation calculation (Ooka et al, 2006) and the commercial CFD code StarCD was used for the convection calculation.

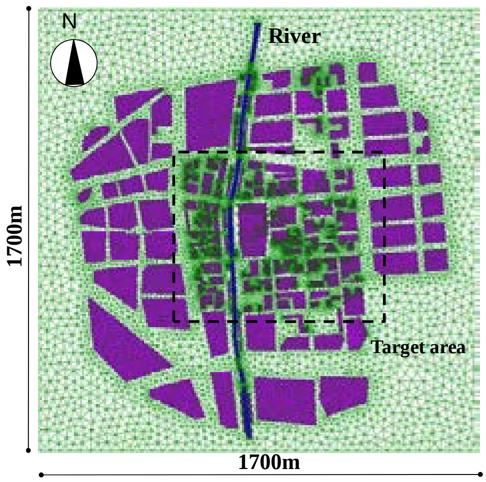

Figure 1: The simulated urban block, with the main 'target area' indicated within the dotted line

The date and meteorological conditions are shown in Table 1. The analysis date is 23rd July and the investigated time is 15:00 which is a fine summer's day. The wind velocity was 1 m/s at 18 m above ground level. The prevailing wind is southerly at the simulated time. The air temperature is 31.6°C at the same height.

The radiation calculation conditions are shown in Table 2. The Discrete Transfer Method (DTM) is used in the radiation simulation. All the buildings have concrete walls with 0.22 m thick. The radiation calculation was conducted in an unsteady condition, and the pre-calculation time is 15 hours. The surface temperature, which was obtained from the radiation calculation, is used as a boundary condition in the CFD simulation.

The CFD calculation conditions are shown in Table 3. The vertical wind profile of the inlet followed the 1/4 power law. The turbulent model is a standard k-ε model. Discretization is based on the Finite Volume Method (FVM) and the algorithm is the SIMPLE method. A first-order upwind scheme was used as the differencing scheme. The side boundary is no slip, while the sky boundary is free slip. The generalized logarithmic law with the parameter E=9 was applied to buildings and the ground surface as smooth walls. The dimension of the computational domain is 1,700 m (x) × 1,700 m (y) × 600 m (z) with a mesh size of 810,642. In order to investigate the effect of the temperature, the CFD simulation was performed under both isothermal and non-isothermal conditions.

Table 1: Meteorological conditions

Day and time	23 July (15:00)
Wind direction	Southerly
Wind velocity	1 m/s (18.0 m above ground level)
Air temperature	31.6°C
Latitude	35.18°N
Longitude	136.90°E

Table 2: Boundary conditions for the radiation calculation

Building	Wall	Concrete
	Solar reflectivity	0.1
	Solar transmittance	0
	Thickness	0.22 m
	Conductivity	1.64 W/(mK)
	Indoor convection heat transfer coefficient	4.64 W/(m^{2}K)
	Indoor air temperature	26°C
	Long wavelength emissivity	0.9
Ground	Ground	Asphalt
	Solar reflectance	0.1
	Long wavelength emissivity	0.9
	Underground temperature	26°C (0.5 m below ground level)
River	Surface temperature	28°C

Table 3: Conditions of the CFD calculation (Huang et al, 2005)

Turbulent model	Standard *k*-ε model (inclusion of buoyancy effect)
Discretization	Finite volume method
Algorithm	SIMPLE method
Differencing scheme	First-order upwind scheme
Side	No slip
Sky	Free slip
Wall	Generalized logarithmic law
Inlet (Power law)	$U = U_0(Z/Z_0)^{0.25}$, Z_0=18.0 m, U_0=1.0 m/s Z_0: Representative height (meteorological station) (m) U_0: Wind velocity at Z_0 (m/s) Z: Height from the ground level (m) U: Wind velocity at Z (m/s)
Turbulent kinetic energy (*k*)	k=1.5$(IU)^2$, I=0.1 I: Turbulent intensity

Turbulent kinetic energy dissipation rate (ε)	$\varepsilon=C_\mu k^{1.5}/l$, $C_\mu=0.09$
Turbulence length scale (l)	$l=4(C_\mu k)^{0.5}Z_0^{0.25}Z^{0.75}/U_0$

3. RESULTS AND DISCUSSION

3.1 Surface temperature distribution

The distribution of the surface temperature, which was obtained from the radiation calculation at 15:00, is shown in Figure 2. Due to the influence of solar radiation, the variation in surface temperature of the buildings or ground is high in the shaded and non-shaded areas. The sun is in the southwest direction at 15:00 and thus the surface temperature of the south- and west-facing walls is higher than the north- and east-facing walls. The surface temperature of the roof rises to 56°C due to the effect of direct solar radiation. The surface temperature is about 50°C on the south- and west-facing walls, and about 40°C in the north- and east-facing walls. The surface temperature of the ground is about 50°C in areas exposed to the sun, and about 40°C in shaded areas. These surface temperatures are used as the boundary conditions under non-isothermal conditions.

3.2 Air temperature distribution under non-isothermal condition

The horizontal air temperature distribution at 1.5 m above ground level is shown in Figure 3. The mean and standard deviation are shown in Table 4. The air temperature is high around the area where the surface temperature is also high. Due to the effect of the river, the air temperature near the river is about 0.5K lower than the urban areas. Due to poor ventilation, heat is likely to accumulate in the densest spaces (alleys, narrow spaces) and thus the air temperature is highest in such areas. Conversely, the ventilation is good in open spaces (wide streets, open land) and thus the air temperature is comparatively lower there.

The vertical temperature distribution across the A-A' section is shown in Figure 4. The mean and standard deviation are shown in Table 4. The vertical temperature distribution decreases as the height increases. This result shows that an unstable layer is formed near ground level. The vertical temperature distribution of the whole calculated area is shown in Figure 5. The Bulk Richardson number is about -14.4 when the maximum building height of the calculated area is taken as the representative length, which shows an unstable condition. There are many buildings up to 50 m above ground level, and thus the temperature gradient is small. The number of buildings decreased above that height and thus the temperature gradient is large.

3.3 Relationship between the air temperature and wind velocity under non-isothermal conditions

The correlation coefficient of the air temperature and wind velocity is shown in Table 4. The correlation coefficient is relatively high (0.50 ~

0.65) in the lower parts of the urban area (0.5 ~ 75 m). The coefficient decreases significantly above that height. The results showed that the

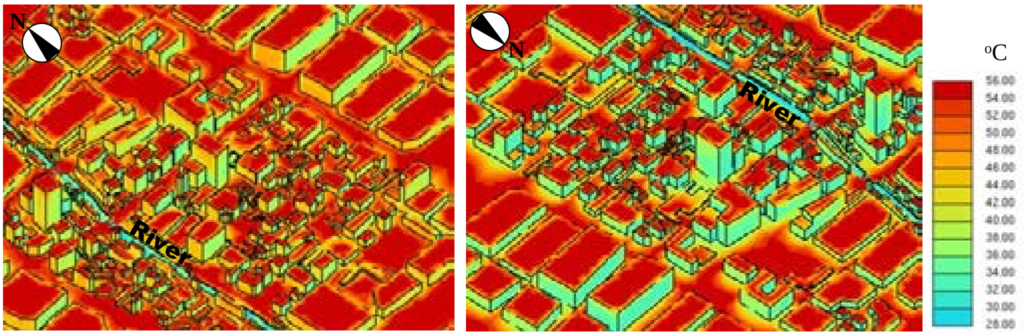

(a) South- and west-facing walls *(b) North- and east-facing walls*

Figure 2: Distribution of the surface temperature in the 'target area'

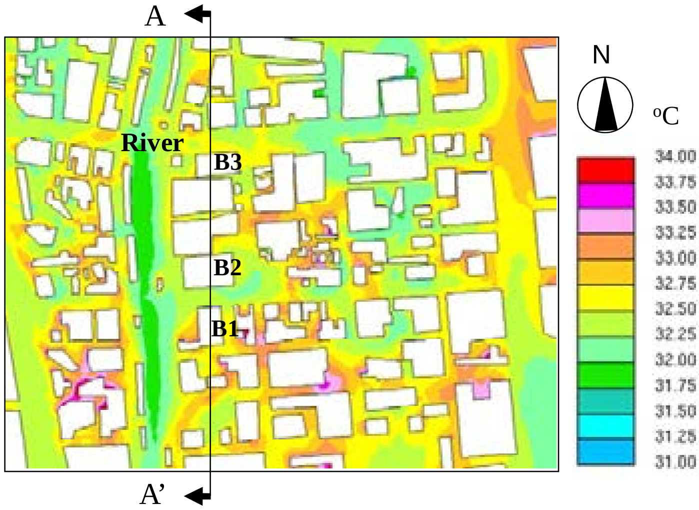

Figure 3: Horizontal air temperature distribution at 1.5 m above ground level across the 'target area'
B1, B2 and B3 indicate the buildings which appear in the cross-section.

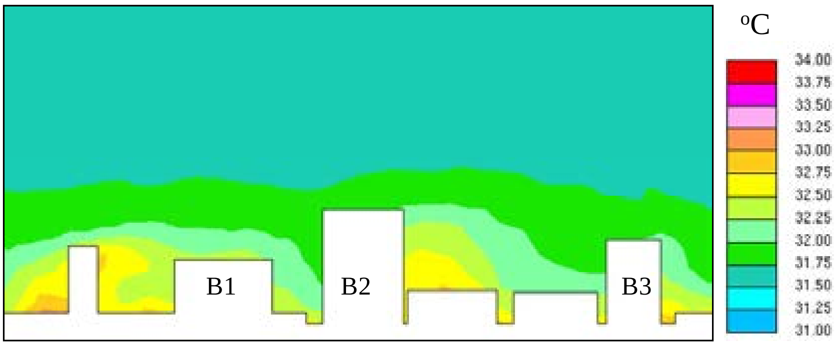

Figure 4: Vertical air temperature distribution at A-A' section

----

Bulk Richardson number (R_b) is calculated using the following equation and parameters.

$$R_b = \frac{gZ}{(T+273.15)} \times \frac{T_a - T_s}{U^2}$$

g: Acceleration due to gravity (9.8 m/s^2), *Z*: Calculated height (100 m), *T*: Mean temperature (38.3°C),
T_a: Air temperature at *Z* (31.6°C), T_s: Surface temperature (45°C), *U*: Wind velocity at *Z* (1.71 m/s)

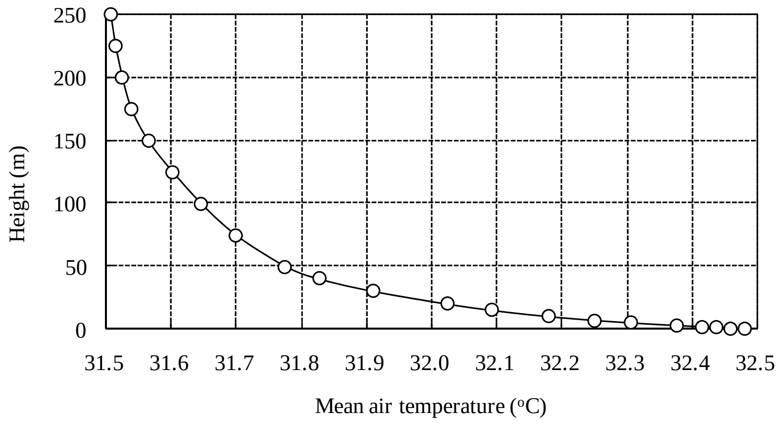

Figure 5: Vertical air temperature distribution of the whole calculated area (The figure is derived from the mean value shown in Table 4)

Table 4: Mean, standard deviation (SD) and correlation coefficient of the air temperature and wind velocity across the entire calculated area

Height (m)	Number of meshes [a]	Air temperature T_o (°C)		Wind velocity (m/s)				Correlation coefficient (r)			
				Non-isothermal V		Isothermal V_i		T_o:V		V:V_i	
		Mean	SD	Mean	SD	Mean	SD	r[b]	p	r	p
0.5	11,362	32.5	0.4	0.88	0.48	0.41	0.33	-0.54	<0.001	0.65	<0.001
1	11,362	32.5	0.4	0.88	0.48	0.41	0.33	-0.54	<0.001	0.64	<0.001
1.5	11,362	32.4	0.4	0.88	0.48	0.41	0.33	-0.54	<0.001	0.64	<0.001
2	11,362	32.4	0.4	0.89	0.47	0.42	0.33	-0.54	<0.001	0.64	<0.001
3	11,362	32.4	0.4	0.90	0.47	0.42	0.33	-0.52	<0.001	0.64	<0.001
5	11,362	32.3	0.4	0.92	0.46	0.43	0.32	-0.51	<0.001	0.63	<0.001
7	11,362	32.3	0.3	0.95	0.46	0.44	0.33	-0.50	<0.001	0.62	<0.001
10	11,362	32.2	0.3	0.99	0.45	0.46	0.33	-0.50	<0.001	0.61	<0.001
15	11,362	32.1	0.3	1.06	0.45	0.51	0.33	-0.54	<0.001	0.58	<0.001
20	11,362	32.0	0.3	1.14	0.44	0.58	0.32	-0.59	<0.001	0.54	<0.001
30	11,362	31.9	0.3	1.32	0.42	0.76	0.28	-0.65	<0.001	0.45	<0.001
40	11,362	31.8	0.3	1.47	0.38	0.94	0.25	-0.65	<0.001	0.38	<0.001
50	11,362	31.8	0.3	1.55	0.34	1.09	0.22	-0.62	<0.001	0.34	<0.001
75	11,362	31.7	0.2	1.66	0.27	1.35	0.16	-0.50	<0.001	0.35	<0.001
100	11,362	31.6	0.2	1.71	0.23	1.53	0.11	-0.37	<0.001	0.38	<0.001
125	11,362	31.6	0.2	1.77	0.19	1.66	0.05	-0.23	<0.001	0.34	<0.001
150	11,362	31.6	0.1	1.81	0.15	1.76	0.03	-0.03	<0.001	0.28	<0.001
175	11,362	31.5	0.1	1.85	0.12	1.83	0.03	0.08	<0.001	0.31	<0.001
200	11,362	31.5	0.1	1.88	0.10	1.89	0.03	0.07	<0.001	0.32	<0.001
225	11,362	31.5	0.1	1.92	0.07	1.95	0.03	0.00	0.916	0.31	<0.001
250	11,362	31.5	0.1	1.95	0.06	1.99	0.03	-0.11	<0.001	0.24	<0.001
All	238,602	32.0	0.3	1.35	0.33	1.01	0.21	-0.79	<0.001	0.82	<0.001

[a] The number of meshes is equal at each height because all values are extracted using the mesh at ground level. Thus, the values are interpolated in the upper parts of the urban area where the same mesh does not exist.
[b] Even though some of the correlation coefficients are quite small or zero, they are included in the overall model because this provides a higher correlation coefficient.
p: Significant level

correlation coefficient is different with and without buildings present, since these affect the air temperature and wind velocity. The correlation between the air temperature and wind velocity of the whole calculated area is illustrated in Figure 6. The linear equation, which is obtained from the regression analysis, is shown in Equation 1.

T_o=-0.662V+32.9 (n=238,602, r=-0.79, p<0.001) (1)

where, To is the air temperature, V is the wind velocity under non-isothermal condition, n is the number of meshes, r is the correlation coefficient, and p is the significant level of the correlation coefficient or the regression coefficient. The correlation coefficient is high (r=–0.79) and the equation is statistically highly significant (p<0.001). This means that the air temperature is high when the wind velocity is low, and the air temperature is low when the wind velocity is high. Due to the low wind velocity, the air temperature is high in the lower part of the urban area.

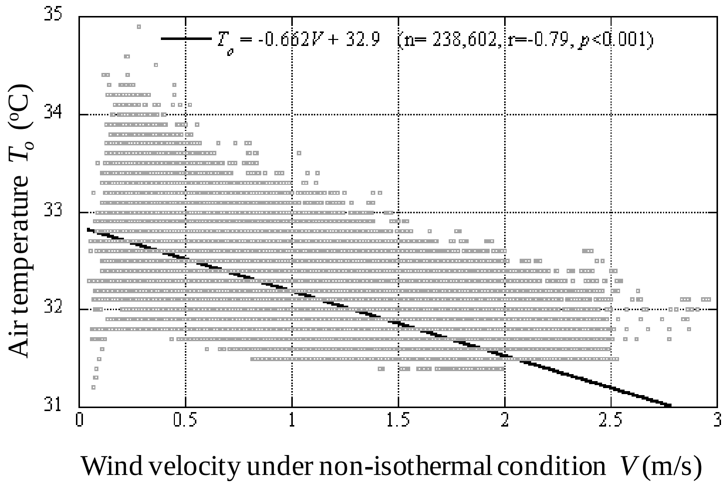

Figure 6: Relationship between air temperature and wind velocity across the whole calculated area
(The figure is derived from all data shown in Table 4)

3.4 Wind velocity under isothermal and non-isothermal conditions

The distribution of the wind velocity vector at 1.5 m above ground level under isothermal and non-isothermal conditions is shown in Figure 7 and the differences of the wind velocity scalar are shown in Figure 8. Mean value and standard deviation are shown in Table 4. The wind velocity in the open areas is high, but is low in dense areas. The variation in wind velocity under isothermal and non-isothermal conditions is high, and in most areas, the wind velocity under non-isothermal conditions is higher than isothermal conditions (Figure 8). As indicated by dotted circles in Figure 7, the wind flows from the urban areas back to the river under isothermal conditions, whereas under non-isothermal conditions, such flow is reversed. The results showed that the cool air generated by the river flows into the urban areas due to the southerly wind under non-isothermal conditions.

The vertical distribution of the wind velocity vector under isothermal and non-isothermal conditions is shown in Figure 9. The wind velocity under non-isothermal conditions is high, and a strong vertex is found in the leeward side of the buildings due to the temperature gradient. In order to compare wind velocity under isothermal and non-isothermal conditions across the entire calculated area, the vertical distribution of the wind velocity is shown in Figure 10. For reference, the wind velocity as calculated by the power law (Table 3) is also shown.

(a) Isothermal conditions *(b) Non-isothermal conditions*

Figure 7: Horizontal distribution of the wind velocity vector 1.5 m above ground level across the 'target area'

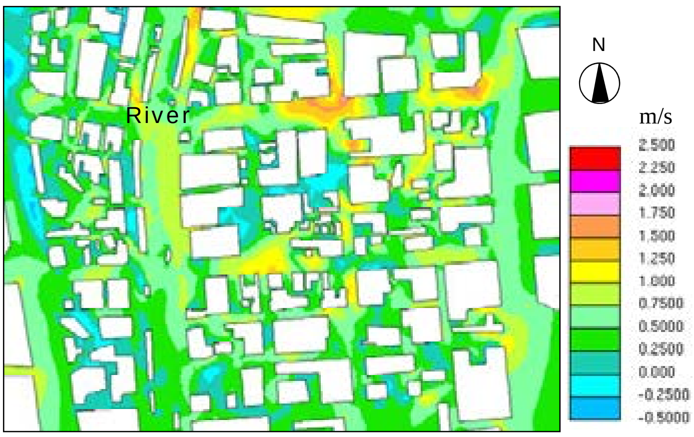

Figure 8: Horizontal wind velocity differences under non-isothermal and isothermal conditions 1.5 m above ground level across the 'target area'

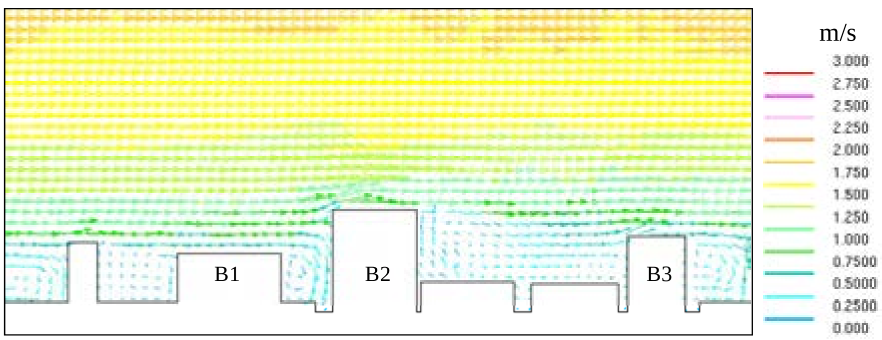

(a) Isothermal condition (B-B' section of Figure 7)

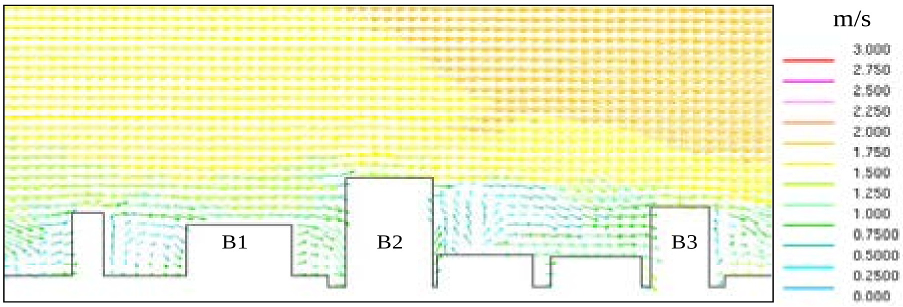

(b) Non-isothermal condition (C-C' section of Figure 7)

Figure 9: Vertical distribution of the wind velocity vector across the 'target area'

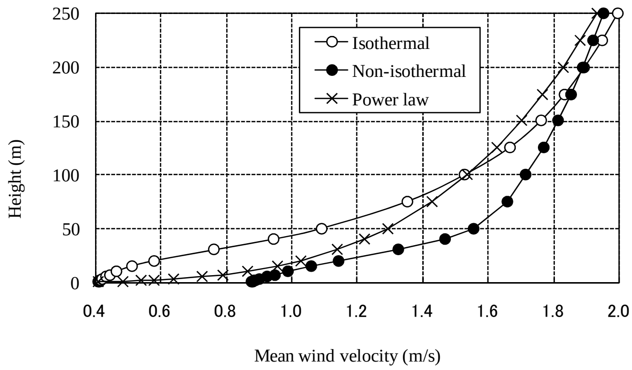

Figure 10: Vertical distribution of wind velocity across the entire calculated area (The figure is derived from the mean value shown in Table 4)

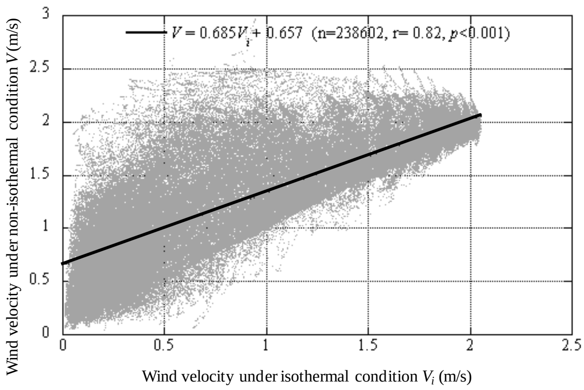

Figure 11: Relationship between wind velocity under isothermal and non-isothermal conditions across the entire calculated area (The figure is derived from all data shown in Table 4)

The wind velocity across the urban area increases with height. However, standard deviation of the wind velocity is small as the height increases. The reason could be that the wind velocity is stable in the upper regions of urban areas due to the decrease in the number of buildings. In the lower part of the urban block, the wind velocity under isothermal conditions is smaller than the wind velocity as per the power law. One reason could be that the wind velocity might decrease due to obstruction by the buildings. On the other hand, the wind velocity under non-isothermal conditions is higher than the wind velocity as per the power law. The reason could be that the wind is stimulated by the buoyancy effect. The difference in wind distribution under isothermal and non-isothermal conditions starts to decrease from about 100 m above ground level. This is because there are few buildings above that height and the buoyancy effect is also small.

The correlation coefficient of the wind velocity under isothermal and non-isothermal conditions is shown in Table 4. The correlation coefficient is relatively high (0.54 ~ 0.65) in the lower parts of the urban area (0.5 ~ 20 m), but decreases above that height. The correlation between wind velocities under isothermal and non-isothermal conditions is illustrated in Figure 11. The linear equation, which is obtained from the regression analysis, is shown as Equation 2.

$$V=0.685V_i+0.657 \quad (n=238{,}602,\ r=0.82,\ p<0.001) \qquad (2)$$

where, V is the wind velocity under non-isothermal conditions, Vi is the wind velocity under isothermal conditions, n is the number of meshes, r is the correlation coefficient, and p is the significant level of correlation coefficient or regression coefficient. The correlation coefficient is high (r=0.82) and the equation is statistically highly significant (p<0.001). If we know the wind velocity under isothermal conditions from a similar model or the calculation conditions of this research, the wind velocity under non-isothermal condition can be predicted using Equation 2.

As we explained above, it is confirmed that significant differences exist in wind velocities under isothermal and non-isothermal conditions. The wind velocity under non-isothermal conditions can be considered more realistic because it considers the actual thermal environment of the urban block. Thus, if the Bulk Richardson number is large, it is desirable to perform a CFD simulation under non-isothermal conditions to evaluate the wind environment. However, further research may be required using parametric studies or wind tunnel experiments for fully acceptable conclusions.

4. CONCLUSION

In order to evaluate the wind environment of an actual urban block, numerical simulations of the thermal and wind environments were conducted, and the following results were obtained for the differences under isothermal and non-isothermal conditions.

1. The wind velocity under non-isothermal conditions is higher than under isothermal conditions. The wind velocity under non-isothermal conditions is more realistic considering the actual thermal environment of the urban block. Thus, if the Bulk Richardson number is large, a CFD simulation is required under non-isothermal conditions to evaluate the wind environment for building design.

2. By using the proposed equation, the wind velocity under non-isothermal conditions can be predicted from the wind velocity under isothermal conditions.

3. The air temperature around the river is 0.5K lower than the urban area. It was confirmed that the cool air flows from the river into the urban areas.

4. The heat is likely to diffuse in open spaces (wide streets, open land) and thus air temperatures are comparatively lower in such spaces. Conversely, the heat is likely to accumulate in the densest areas (alleys, narrow spaces) and thus the air temperature is highest in such areas. These phenomena are also confirmed by the high correlation between air temperature and wind velocity.

REFERENCES

Hu, C. and Wang, F., 2005. Using a CFD approach for the study of street-level winds in a built-up area, *Building and Environment* 40, 617-631.

Huang, H., Ooka, R. and Kato, S., 2005. Urban thermal environment measurements and numerical simulation for an actual complex urban area covering a large district heating and cooling system in summer, *Atmospheric Environment* 39, 34, 6362-6375.

Huang, H., Ooka, R., Chen, H., Kato, S., 2008. CFD analysis on traffic-induced air pollutant dispersion under non-isothermal condition in a complex urban area in winter, *Journal of Wind Engineering and Industrial Aerodynamics*, 96, 1774-1788.

Ooka, R., Chen, H., Huang, H. and Nakashima, M., 2006, Study on impact factor index of buildings on outdoor thermal environment using coupled simulation of convection, radiation and conduction, *Proceedings of 19th National Symposium on Wind Engineering* 91-96.

Yoshida, S., Murakami, S. Mochida, A., Ooka, R. Tominaga, Y. and Kim, S., 2000. Influence of green area ratio on outdoor thermal environment with coupled simulation of convection, radiation and moisture transport, *J. Archit. Plann. Environ. Eng., AIJ*, 529, 77-84.

EMERGENCY MANAGEMENT IN KOREA: JUST STARTED, BUT RAPIDLY EVOLVING[1]

Kyoo-Man HA
Senior Researcher (Ph.D. & CEM), the National Institute for Disaster Prevention, Korea
kyooha@nema.go.kr

ABSTRACT

The purpose of this paper is to examine emergency management in Korea, with the ultimate goal of contributing to its development. Thus, the paper will carefully study three major factors in the area of Korean emergency management, namely: 1) vulnerability, 2) organization, and 3) challenges and opportunities. In conclusion, it has been observed that Korea has begun to manage its emergency comprehensively, after experiencing various dreadful emergencies. No single factor has characterized the feature of this dynamic emergency management in Korea. Rather, diverse factors play their own roles in formulating the complexity of its emergency management.

1. INTRODUCTION

The fact that Korea is the "Land of the morning calm" is no longer true, owing to the various emergency situations that have occurred in recent years. When the Sampoong department store collapsed in 1995 and when a fire accident took place at Daegu subway train in 2003 and killed many people, the majority of Koreans thought that these incidents were a disgrace, or even a shame on Korea. As a result, Korea has begun to comprehensively manage its emergency situations at the national level. Therefore, it is interesting to review how Korea has dealt with emergency management.

The purpose of this paper is to examine emergency management in Korea, with the ultimate goal of contributing to its development. Thus, the paper will carefully study three major factors in the area of Korean emergency management, such as 1) vulnerability, 2) organization, and 3) challenges and opportunities. These three factors are prerequisite to study one national emergency management system.

2. VULNERABILITY IN KOREA

[1] This paper has been posted on the website of U.S. Emergency Management Institute's Comparative Emergency Management Book Project since May 2009. Related URL is followings: http://training.fema.gov/EMIWeb/edu/CompEmMgmtBookProject.asp

Vulnerability means many things to different people. Some may think vulnerability to be a certain negative aspect in a specific hazard or emergency situation, while others consider it to be a broad problem in the field of emergency management. In this study, vulnerability indicates something that is extremely susceptible or being exposed to an attack or possible damage in the whole field of emergency management. Like any society, Korea has many negative aspects in emergency management with respect to the series of emergency situations that occur throughout the year. Among those negative aspects, one of the most vulnerable aspects is related to the national culture.

Many Koreans are now willing to talk more seriously about the consequences of emergencies than about the preconditions of disasters or the preparedness level before the outbreak of these events. For example, in the case of Daegu subway fire in 2003, very few people opted for safety of the subway in Korea before this accident. Despite the fact that there were many problems with regard to the subway, such as non-availability of platform screen (or platform edge) door, lack of appropriate firefighting equipment, use of non-fireproof material in the subway cabin, etc., most people did not pay much attention to the safety of subway train and subway station in particular, before the accident.

However, many began to seriously criticize the government's failed policy and pointed out the importance of safety in subway for a limited period of time after the Daegu subway fire that resulted in the death of 192 people and injured many others (National Emergency Management Agency of Korea 2009). Accordingly, the government tried to solve the related problems, but it has not made significant progress yet. As the government did not attempt to replace all non-fireproof materials in the subway train owing to its high cost, there may be a possibility of fire accidents in the future. In short, many Koreans have already forgotten the consequences of this emergency.

Similarly, Korea has emphasized the significance of the recovery phase more than that of the other three phases, namely the prevention and mitigation phase, the preparedness phase, and the response phase in the emergency management process. Theoretically, each phase should be given equal or at least similar importance in modern emergency management process, considering that each phase has its own value for the ultimate purpose of emergency management. Therefore, all the four phases require equal efforts in emergency management process. However, through public or private affairs, it has been revealed that the Korean society has invested emergency personnel, funds, and other resources primarily for the recovery phase (Ha & Ahn 2008-1).

For example, the National Emergency Management Agency (NEMA) of Korea, which is a single comprehensive agency on emergency management field, had four sub-headquarters, namely the prevention and mitigation headquarters, the preparedness headquarters, the response headquarters, and the recovery headquarters under its authorities. The NEMA intends to emphasize the importance of each phase in its policy process, but currently it provides more support to the recovery phase than the other three phases.

There are many reasons to explain why the Koreans have considered the result of emergency without equal emphasis to emergency preparedness. For instance, Korea has nationally emphasized the importance of recovery more profoundly than the other phases. One of the important reasons is related to the communications revolution in the Korean society. As a result of the development of many cutting-edge information channels in Korea, such as high-definition TV, Internet, and mobile phones, breaking news can spread very quickly. In other words, because of expanded information, people have an increased tendency to consider what has just happened such as the outbreak of emergency, but they forget what happened before the event, such as the poor level of emergency preparedness.

Besides the communication revolution, another reason for vulnerability is that for a long time, many Koreans used to consider emergency as a sort of destiny. As controlling emergency was beyond the ability of humans, many Koreans believed in the supremacy of hazards for several years. For instance, Koreans used to treat flood with typhoon as an annual activity, rather than trying to figure out how to prepare for it. Thus, this kind of emergency awareness under a unique environment has partially encouraged the Koreans to seriously discuss the results of emergency.

3. ORGANIZATION OF EMERGENCY MANAGEMENT

In the field of Korean emergency management, public organization has historically dominated the relationship with the private organization. A popular thought has been that emergency management is a sort of public goods. Also, the unitary government system has been developed that consists of three-level governments, such as the central government (similar to the U.S. federal-level government), the province and the metropolitan government (similar to the U.S. state-level government), and the local government. When compared with the federal government system, lower-level governments in Korea have had less autonomy.

The central government established the National Emergency Management Agency (NEMA) of Korea in June 2004 to start comprehensive emergency management, though it was not completed. In viewpoint of comprehensiveness, the NEMA has not been substantially successful. Before the establishment of NEMA, several institutions used to manage their own special emergency area. Now, the NEMA, under the Ministry of Public Administration and Security (MOPAS), has substantially focused on managing both firefighting and civil engineering. The MOPAS recently tried to setup its own policy area by giving more emphasis to the function of policy decision than the NEMA.

Lower-level governments, such as the provincial government, the metropolitan government, and the local government, have set up their own "Section of Emergency Management" in each institution, to primarily handle flood with typhoon. Also, fire stations are located in each local community to handle fire accidents. Furthermore, police stations in each community play a major role in taking care of terrorism in Korea more than other emergencies.

An increasing number of business corporations are setting up their own business continuity plans (BCP) since the establishment of NEMA in 2004. In particular, the export-oriented corporations have expanded their BCP activity because they may find it difficult to work on international affairs without implementing their own BCP, according to the agreement with World Trade Organization. The governments have also tried to help them to establish BCP by passing a related act, which is the “Act on Government’s Helping Business Corporations to Voluntarily Set Up their BCP.” However, small- and medium-sized corporations have worked for BCP, mainly by setting up their computer backup systems.

Voluntarism without being paid has not historically been a popular activity in Korea, although its activity has recently increased. However, the virtue of cooperation has been very popular by giving and taking diverse forms of assistance during emergency. To elaborate, cooperation entails a reciprocal exchange of service. However, when a person helps another, he or she assumes that they will return the favor at a later time in Korea (Ha & Ahn, 2008).

There are not many professional voluntary organizations in Korea. Instead, community-based organizations (CBOs) have played diverse roles in emergency management, which include the Young Men Group, the Married Women Group, etc. To boost voluntary activity, the NEMA, as a government institution, has participated in voluntary organizations as their members, which include the Korean Disaster Safety Network (KDSN) and the Citizen Corps Active in Disaster (CCAD).

Residents and their community have to deal with emergencies more directly than anyone else. Since the establishment of NEMA, many residents have increased their awareness of disasters and emergency management, although there is still room for improvement. When an emergency receives national attention via mass media or Internet, awareness among residents and their community dramatically increases. However, a majority of the residents have not attempted to set up their own written emergency operation plan (EOP), though some have done it verbally (Ha & Ahn 2009).

4. CHALLENGES AND OPPORTUNITIES

Korea faces numerous challenges in emergency management. For instance, serious challenges include the national culture of giving importance to the consequences of emergencies, lack of emergency awareness, unpopularity of voluntary activity, and so on. In this section, one of the biggest challenges in Korea is examined.

The Korean government has mainly focused on managing both firefighting and civil engineering, though they have officially claimed that the government policy has made or will make efforts to manage all kinds of emergency. For example, civil engineering is related to flood from typhoons. As a result, government policy has been substantially oriented towards those two disasters, without any significant emphasis on other types of emergencies. To make matters worse, two categories of emergency personnel have been major players in the field—firefighters and civil engineers. Some critics state that these two categories might dominate the field of emergency management without incorporating other professionals.

As floods from typhoons hit the Korean peninsula annually, it is no wonder that the nation has focused on civil engineering. Similarly, as fire accidents have dramatically increased in the society, it is needless to say that firefighting is heavily emphasized. However, neither firefighting nor civil engineering can accomplish its own purpose without the help from other specialties, such as medical science, psychology, sociology, public administration, law, military science, meteorology, other engineering, etc. Emergencies including fire, flood, and typhoon, are very complicated in nature or have multiple facets, and hence, they should be comprehensively managed. In short, Korea may face much more difficulties in accomplishing the goal of emergency management in the near future, as long as it focuses on two kinds of emergencies only.

There are many opportunities in Korea, depending on the individual's viewpoint. One of the most appealing opportunities is that Korea has started to practice the modern concept of emergency management at the government level, and even nationally. For example, Korea has initiated emergency management at the central government level via four scientific steps that include prevention and mitigation, preparedness, response, and recovery. In Korea, a popular belief is that human beings would have their own destiny. Hence, people accepted emergencies in their lives, rather than daring to challenge them. Without doing anything significant, Koreans used to stay at home and then just wait for the moment of being hit by natural disaster or other emergencies.

However, many terrible emergencies, such as typhoons, floods, and subway-train fires, took place in Korea at the beginning of the twenty-first century, and numerous innocent people became victims. The angry public strongly asked their government to take significant action to curb those emergencies. As a result, the governments established the National Emergency Management Agency (NEMA) of Korea in June 2004. This is a single comprehensive agency, which began to take charge of emergency management in Korea. Further, the governments passed "the Basic Act on Emergency and Safety Management," incorporating a number of previous laws and regulations. At the same time, the governments are willing to accept the principles of modern emergency management by allowing stakeholders to study about it in advanced countries, such as the U.S., Japan, and Australia.

Although the field of emergency management has been surrounded by many difficult challenges, the fact that Korea has already started to utilize the modern emergency management system is a very positive signal to the nation. It would be almost difficult to exactly predict the future of emergency management. However, based on the modern concept of emergency management, Korea is predicted to make every effort to solve serious problems in this field.

5. CONCLUSIONS

This paper has reviewed the emergency management system in Korea using three key factors. In short, it has been observed that Korea has begun to manage its emergency comprehensively, after experiencing various dreadful emergencies. No single factor has characterized the feature of this dynamic emergency management in Korea. Rather, diverse factors play their own roles in formulating the complexity of its emergency management.

Based on the results of this research, many in the international community as well as in Korea are expected to have a better understanding about the process of Korean emergency management. The result of this research, including both positive and negative aspects of Korea, is assumed to contribute to the development of emergency management in other nations. Furthermore, the results of this research are expected to increase the interest of many international scholars in comparing their ways of emergency management with those of Korea.

REFERENCES

Ha, Kyoo-Man. 2009. Emergency Management in Korea: Just Started, but Rapidly Evolving. *Comparative Emergency Management Book Project*. Available at
http://training.fema.gov/EMIWeb/edu/CompEmMgmtBookProject.asp
Accessed on August 1, 2009.

Ha, Kyoo-Man & Ahn, Ji-Young. 2008-1. Developing voluntary agencies in emergency management: The United States and Korea. *Journal of Emergency Management*. 6(4): 39-50.

Ha, Kyoo-Man & Ahn, Ji-Young. 2008-2. "National emergency management systems: The United States and Korea." *Journal of Emergency Management* 6(2): 31-44.

Ha, Kyoo-Man & Ahn, Ji-Young. 2009. Local emergency management systems in the U.S. and Korea. Unpublished Manuscript.

Ministry of Public Administration and Security. 1995. *Past 30 Year History on Emergency: 1963-1993* (written in Korean). Seoul.

Ministry of Public Administration and Security. 2002. *Past 6 Year History on Emergency* (written in Korean). Seoul.

National Emergency Management Agency of Korea. 2007. *Annual Report on Emergency in 2007* (written in Korean). Seoul.

National Emergency Management Agency of Korea. 2009. NEMA Website. Available at http://eng.nema.go.kr/ (Search date: February 20, 2009).

CRITICAL REVIEW OF THE STANDING ORDERS ON DISASTER MANAGEMENT, BANGLADESH

MEHEDI AHMED ANSARY and RIPON HORE
Department of Civil Engineering, BUET, Bangladesh
ansary@ce.buet.ac.bd

ABSTRACT

The Standing Orders (SoD) on Disaster Management on Bangladesh have been prepared with the objective of making the concerned persons understand their duties and responsibilities regarding disaster management at all levels. All Ministries, Divisions/Departments and Agencies shall prepare their own Action Plans in respect of their responsibilities under the Standing Orders for efficient implementation. According to the SoD, the National Disaster Management Council (NDMC) and Inter-Ministerial Disaster Management Coordination Committee (IMDMCC) will ensure coordination of disaster related activities at the National level. The Disaster Management Bureau will render all assistance to them by facilitating the process. The Ministries, Divisions/Departments and Agencies will organize proper training of their officers and staff employed at District, Thana, Union and village levels according to their own Action plans so that they can help in rescue, evacuation and relief work at different stages of disaster. The different activities of different organizations are described at different Phase namely, Normal Phase, Alert and Warning Phase, Disaster Phase and Recovery Phase.

Although SoD is there, the disaster preparedness and management operations of the country lacks in activity and long term plans during normal times as well as the implementation of the action plans taken after recovery of a disaster. This is the basic reason behind the huge damages and losses of properties as well as significant number of the death toll caused by Disasters. In some cases, overlapping of the different activities among the different organizations created a huge problem. On the other hand, the SoD is not properly followed by the different organizations. The SoD lacks structural solution/mitigation which is sometimes required in the pre-disaster as well as post-disaster cases. The coordination between the international and national agencies is not clearly defined in the SoD. The SoD itself needs modification and clarifications of the roles of personnel and organizations. This paper tries to summarize different salient features of the SoD and prescribe modifications which will improve the disaster management system in Bangladesh.

1. INTRODUCTION

Bangladesh is the largest delta in the world situated at the northern fringe of the tropics. The country is the worst victim of natural disasters through the prevailing weather systems during pre- and post- monsoon, causing at times huge loss of lives and damage to properties, and also the sufferings and displacement of affected population. Natural and human induced hazards such as floods, cyclones, droughts, storm surges, tornadoes, earthquakes, riverbank erosion, fire, infrastructure collapse, the high arsenic contents of ground water, water logging, water and soil salinity, epidemic and various forms of pollution are frequent occurrences. Over the years, Bangladesh has developed a system of disaster management. But in the system the focus of disaster management has been relief and rehabilitation.

The standing orders on disaster outlines the disaster management arrangements in Bangladesh and describes the detailed roles and responsibilities of committees, Ministries, Departments and other Organizations involved in disaster risk reduction and emergency response management and establishes the necessary actions required in implementing Bangladesh’s Disaster Management Model.

A Bangladesh Network Office for Urban Safety (BNUS) team has visited the cyclone SIDR affected areas from May 4 to 11, 2008. They have met different professionals from Government and NGO sectors and some affected population and compiled a report on cyclone SIDR. In this paper, the activities of the different organizations according to the SoD have been analyzed with respect to Draft-Sidr Report (CDMP, 2008) and BNUS Report. Aslo the activities of the different organizations of two worst affected districts Patuakhali and Barguna due to cyclone SIDR have been analyzed.

2. ORGANIZATIONS INVOLVED

The different organizations involved during cyclone SIDR as reported by CDMP (2008) is listed below:

- Meteorological Department
- Public Health Engineering Directorate (DPHE)
- Local Government Engineering Department (LGED
- Bangladesh Water Development Board (BWDB)
- Bangladesh Inland Water Transport Authority (BIWTA)
- Ministry of Education (MOE)
- Ministry of Fisheries and Livestock (MOFL)
- Directorate of Fisheries
- Ministry of Environment and Forestry (MOEF)

The different organizations whose activities are analyzed by BNUS team are as follows:

- Armed Forces Division (AFD)

- Deputy Commissioner (DC)
- District Relief and Rehabilitation Officers (DRRO)
- Field Office of Executive Engineer of BWDB
- Upazila Nirbahi Officer (UNO)
- Field level CPD Officials
- Bangladesh Red Crescent Society Officials
- Field Office of Executive Engineer of LGED

3. FEATURES OF THE EXISTING SOD

The existing SoD has Normal Phase, Alert and Warning Phase, Disaster Phase and Recovery Phase. A short definition of the phases are provided below:

Normal Phase (Normal Time):
A period when there is no immediate threat but long-term actions are required in anticipation of the impact, at some unknown time in the future, of known hazards.

Alert and Warning Phase:
The period from the issuing of an alert or public warning of an imminent disaster threat to its actual impact, or the passage of the threat and the lifting of the warning. The period during which pre-impact precautionary, or disaster containment measures are taken.

Disaster Phase:
The period during which direct impact of a natural calamity is felt. Disaster phase is long in case of slow on-set disasters (draughts, normal monsoon flood) and short in case of rapid on-set disasters (flash flood, cyclone, earthquake, fire, industrial accident, landslide etc).

Recovery Phase:
The period, following the emergency phase, during which actions are to be taken to enable victims to resume normal lives and means of livelihood, and to restore infrastructure, services and the economy in a manner appropriate to long-term needs and defined development objectives.

The existing SoD is divided in to following parts:
Part 1: introduction, part 2: national policy and coordination, part 3: local level coordination, part 4: roles and responsibilities, part 5: other matters. Also in the SoD, Overlapping of the different activities among the different organizations can be observed; No structural solution is provided; The SoD Mainly focusing on the post disaster stages.

4. ACTIVITIES OF THE DIFFERENT ORGANIZATION DURING SIDR

Different organizations obey the SoD rules mainly during Disaster and Rehabilitation Stages. Armed Forces Division (AFD) of Bangladesh played a significant role in SIDR Management. AFD involved its own workforce and logistics in damage assessment and relief and rehabilitation activities. They immediately launched a massive search and rescue operation and also assisted in the burial of dead bodies and removal of debris and dead livestock. AFD were not only maintained the standing order for disaster management (SoD) but also provided some additional services. The activities of the LGED are not clearly defined in the SoD. During SIDR, LGED assisted AFD. “Ensure effective training and orientation of the volunteers, formed for cyclone preparedness programmer drawn through CPP and other agencies”, “Arrange tree plantation at shelter places for protection against the severity of tidal bore due to flood and cyclone and arrange proper maintenance of ponds, village roads, embankments and sluice gates”, these are the activities of the Deputy Commissioner (DC) who are incharge of the districts. In reality, no such activities are performed (BNUS, 2008; CDMP, 2008). The activities are maintained by the respective authorities such as BDRCS, few local NGOs, LGED, and WDB etc. The activities between of Cyclone Preparedness Program (CPP) and Bangladesh Red Crescent Society (BDRCS) are sometimes overlapped. The number of different activities followed by different organization during SIDR is shown in Figure 1. Figure 2 shows their activities according to SoD.

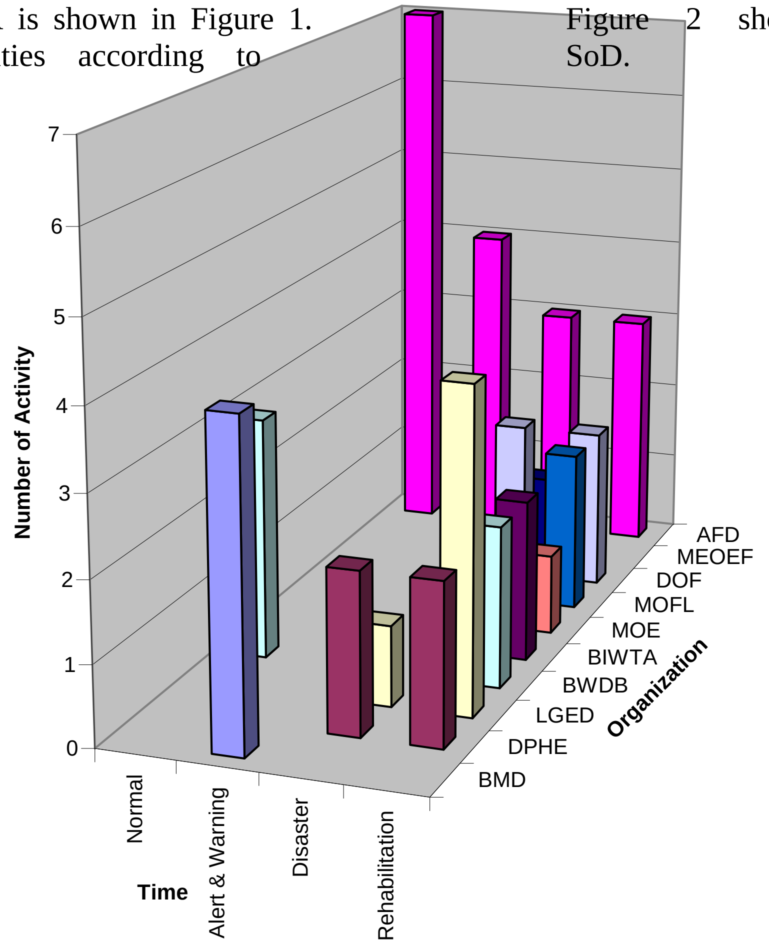

Figure 1: Activity Checklist for different organizations during SIDR

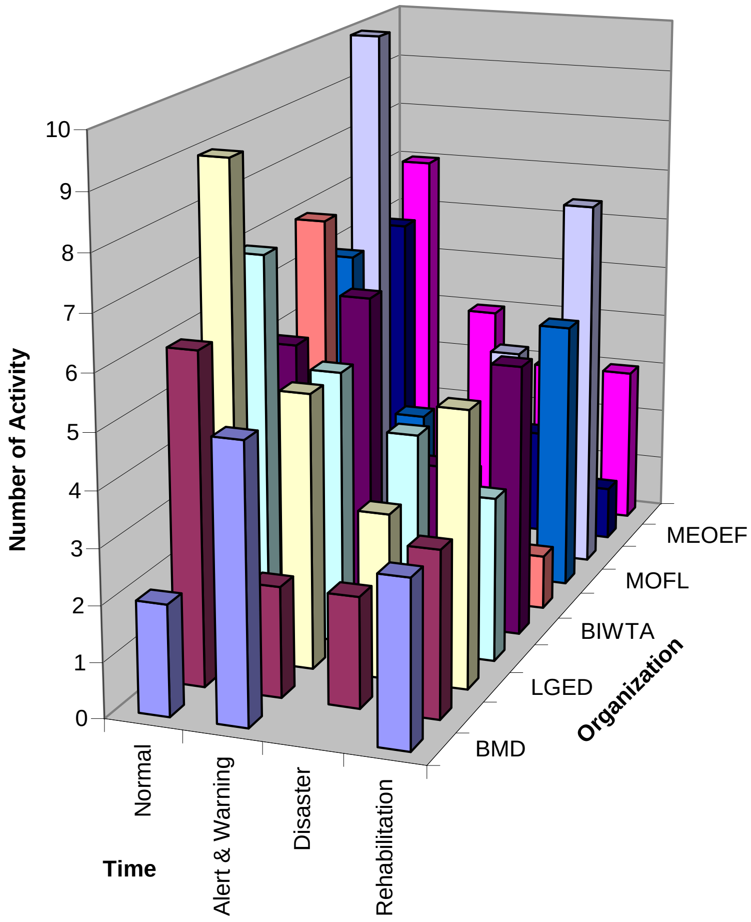

Figure 2: Activity checklist for different organizations according to SoD

Figures 3 and 4 show activity checklist of different field level offices during SIDR and in SoD, respectively.

5. PROPOSED MODIFICATIONS IN THE EXISTING SOD

The Disaster Stage of the Meteorological Department is not mentioned in SoD. The SoD needs some modification and mention the role of the Bangladesh Meteorological Department (BMD) during the disaster stage clearly. The roles of BMD during the disaster stage in SoD may be as follows:

- Continuously monitoring the weather condition and supply information through Fax/telephone/teleprinter to the Ministry of Food and Disaster Management (MOFDM) and other concerned organizations.
- Monitoring the position of the cyclone, speed, direction and supply information through Fax/telephone/teleprinter to the Ministry of Food and Disaster Management (MOFDM) and other concerned organizations.

During normal time, the awareness about the SoD needs to be created among the administration level and the related personnel. The structural solutions for different disasters need to be included within SoD and actions to be carried out by the relevant organizations should be mentioned.

An advisory committee must be established under the Ministry of Food and Disaster Management (MOFDM) to monitor the different stages of SoD and provide advice for the Minister of MOFDM for immediate actions just after a disaster takes place. Local contingency plans must be prepared by national level and field level organizations to cope during a disaster event.

Research center must be built with skill persons and a continuous research needs to be carried out for better management and engineering solution of disaster problems. The coordination between the different foreign and local organization during the post disaster situation must be defined in the SoD. A time frame may be established to activate the different activities.

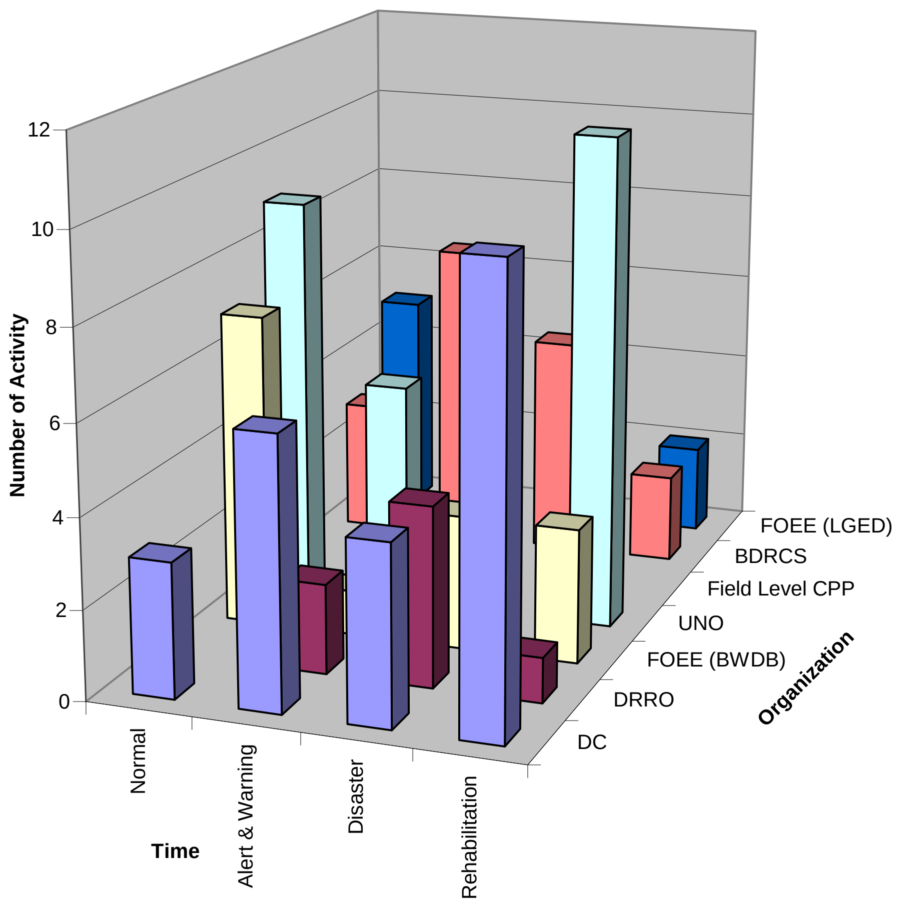

Figure 3: Activity checklist for different field level organizations during SIDR

6. CONCLUSIONS

Bangladesh has got a well organized network for cyclone early warning system and preparedness at all stages which contributed significantly in reducing human causalities due to several recent cyclones Still the disaster preparedness and management operations of the country lacks in activity and long term plans during normal times as well as the implementation of the action plans taken after recovery from a disaster. This is the basic reason behind the huge damages and losses of properties as well as significant number of the death caused by a disaster in Bangladesh. The existing SoD also needs some modification and clarifications of the roles of personnel and organizations as mentioned in the paper. The authors hope that the Government of Bangladesh need to take necessary steps to overcome this situation. With proper planning pre-disaster and post disaster situation can be better managed.

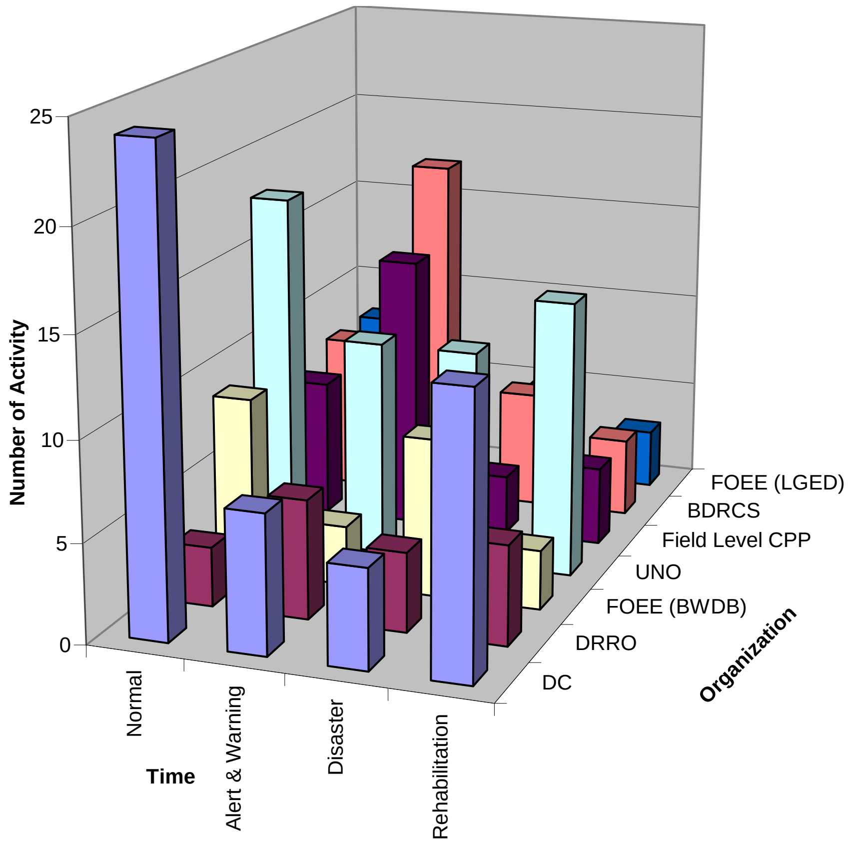

Figure 4: Activity checklist for different field level organizations according to SoD

REFERENCES:

BNUS (2008). *Report on Cyclone SIDR*, BUET, Dhaka.

CDMP (2008). *DRAFT Report on Cyclone SIDR in Bangladesh, Damage, Loss and Needs Assessment for Disaster Recovery and Reconstruction.*

Government of People's Republic of Bangladesh (1999). *Standing Order on Disasters.*

World Bank Report (2008). *Cyclone SIDR in Bangladesh*, April, 2008.

PARALLEL SESSION 7

SEISMIC PERFORMANCE OF REINFORCED CONCRETE STRUCTURES

HIROSHI SHIMA
Kochi University of Technology, Japan
shima.hiroshi@kochi-tech.ac.jp

ABSTRACT

Reinforced concrete is ductile when design and construction is properly so that it should be suitable for mega cities not only without earthquake but also with frequent earthquakes. Seismic design code in Japan has been revised sometimes based on experiences of past earthquake damages. Performance-based seismic design code for civil structures in Japan was published in 1996 just after 1995 Hyogo-ken Nanbu Earthquake. Seismic performance required to reinforced concrete structures for civil structures and method for verification of the performance of structures are described in this paper.

1. INTRODUCTION

One of causes of disaster in mega cities in Asia is earthquake. Concrete structures have been damaged by large scale earthquakes. The number of concrete structures in a mega city is going to increase with the degree of development. Normally, reinforced concrete is ductile if it is designed and constructed properly. The reinforced concrete should be suitable structure system for the mega cities in Asia especially with frequent earthquakes.

Japan is one of countries which are subjected to large scale earthquakes frequently. Design code for the reinforced concrete structures in Japan was

Photo 1: A seismic damage at Kobe City in 1995

published firstly in 1933. Calculation method for seismic design was proposed in this code. The number of the concrete structures in Japan increases with economic growth since that time. However, not a few concrete structures have been damaged by every large scale earthquakes. Seismic design code has been revised sometimes based on these experiences.

Hyogo-ken Nanbu Earthquake in 1995 was the most disastrous earthquake at a mega city on record that had ever been experienced after the reinforced concrete structures came popular in Japan as shown in Photo 1. The seismic design code was revised to performance-based design method with the experience of this earthquake. In this paper, the seismic performance required to reinforced concrete structures for civil structures and the verification method for the seismic performance are described.

2. SEISMIC DESIGN CODES FOR CONCRETE STRUCTURES IN JAPAN

Several specifications or guidelines of seismic design for concrete structures have been issued from different organizations in Japan, such as Japan Society of Civil Engineers (JSCE) for civil structures, Architectural Institute of Japan (AIJ) for buildings and Japan Road Association.

Codes of seismic design for reinforced concrete structures are going to change to be performance-based type. For example, JSCE published a code for seismic design in Standard Specification for Concrete Structures after one year of Hyogo-ken Nanbu Earthquake in 1995. This part of seismic design prescribed how to verify the seismic performances in advance of the other parts of the specifications. The latest seismic design method is described in Chapter 11 ‘Seismic Performance Verification’ in “Standard Specifications for Concrete Structures-2007, Design” (JSCE, 2007) .

3. CONCEPT OF DESIGN METHOD

Definition of terms “Design” and “Verification”, especially definition of “Design” is not always clear. “Verification” is the step in which checks that a given structure satisfies the required performance to the structure or not. “Design” in narrow sense means to create or set up type of structure, shape and dimensions, materials, details of cross section and so on for the previous step of the verification. “Design” in wide sense is a total system to decide structure from type to details including the step of verification.

The concept of the performance-based design method is to decide the performance required to the structure and verify that the given structure satisfies the required performance. However, in most cases, the required performance is conceptual so that the technique to verify the required performance directly has not been developed yet. For example, JSCE Standard Specifications define the seismic performance as follows.

> In general, seismic performance level of a structure may be classified into the following three levels.
> (i) Seismic Performance 1 : Function of the structure during an earthquake is maintained, and the structure is functional and usable without any repair after the earthquake.
> (ii) Seismic Performance 2 : Function of the structure can be restored within a short period after an earthquake and no strengthening is required.
> (iii) Seismic Performance 3 : There is no overall collapse of the structural system due to an earthquake.

However, it is impossible to verify above performances numerically under present condition. In order to make verification, designers prescribe the limit state which can guarantee these performances and replace the performance verification with the examination of limit state as shown in Figure 1. At the examination of limit state, the index which represents the state is selected and limit value according to the required performance is given. Namely, seismic performance verification of a structure is carried out by confirming that calculated response value (S_d) under assumed earthquake ground motion does not exceed limit value (R_d) using specified safety factors γ as given in Eqs.(1) to (3).

$$\gamma_i S_d / R_d \leq 1.0 \tag{1}$$

$$S_d = \gamma_a S \tag{2}$$

$$R_d = R / \gamma_b \tag{3}$$

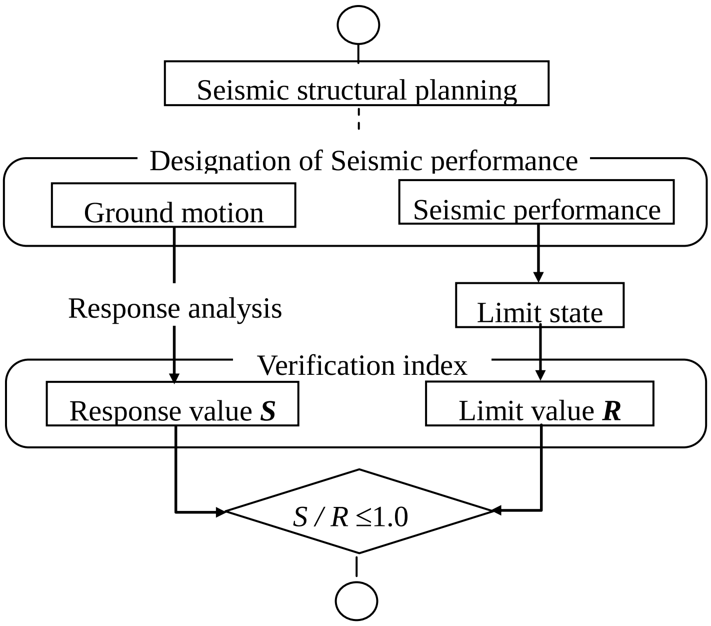

Figure 1: Flow of seismic performance verification

4. DESIGNATION OF SEISMIC PERFORMANCE

Seismic forces which are supposed to act to a structure in its service lifetime vary from small to big. Therefore, the seismic design of structures should be done to have designated seismic performance against to supposed earthquake ground motions. For example, the requirement is such that “a structure does not need any treatment after medium scale earthquake which occurs sometimes and is not destroyed by large scale earthquake which occurs with low probability”. When a structure is designed only to not be destroyed by large scale earthquake, the required performance for no damage to medium scale earthquake has possibility to be satisfied. However, this fact is not generally truth. In general, the seismic performance should be designated to some various scales of earthquake ground motion.

Concerning on the earthquake ground motion supposed in design work, JSCE Specification suggests the following two levels of earthquake ground motion.

> In general, two kinds of design earthquake ground motions – Level 1 and Level 2 as given below, may be considered.
> (i) Level 1 Design Earthquake Ground Motion: earthquake ground motion that is likely to occur a few times within the lifetime of a structure.
> (ii) Level 2 Design Earthquake Ground Motion: very strong earthquake ground motion that has only a rare probability of occurrence within the lifetime of a structure.

Seismic performance required to a structure is necessary to be designated with corresponding to level and return period of earthquake ground motion. In JSCE Specification, the relationship between the assumed ground motion and required seismic performance is described as follows.

> In general, the following verification may be carried out.
> (i) The structure satisfies Performance 1 against Level 1 Earthquake Ground Motion.
> (ii) The structure satisfies Performance 2 or 3 against Level 2 Earthquake Ground Motion.

5. DESIGNATION OF LIMIT STATE AND LIMIT VALUE

In case of verification on seismic performance of structures, it is necessary to decide the limit state from which the seismic performance comes to be unsatisfied correspondingly with each designated seismic performance. The seismic performance is, in general, designated as a performance to the structure. The limit state corresponding to the performance of structure should be designated also as a limit state of the structure. However, the relationship between the damage of structure level and damage of member level is mostly not clear. On the other hand, the verification techniques for the limit state of member level have been advanced. Therefore, it is general that the limit state is designated to the member or element composing structure.

A way of approaching the limit values corresponding to each seismic performance in JSCE are described below.

5.1 Seismic Performance 1

Concerning on the performance "Function of the structure during an earthquake is maintained", when it is necessary that safety of moving vehicles should be examined, the maximum response displacement should be defined as the limit value.

The performance "The structure is functional and usable without any repair after the earthquake" can be satisfied unless re-bars yield. Therefore, yield displacement of a member can be decided as the limit value of Seismic Performance 1 on the assumption that members do not fail in shear. Before yielding of re-bars, stress of concrete does not reach the compressive strength. However, when reinforcement ratio is large, it may be necessary that the compressive strength is defined as the limit value.

5.2 Seismic Performance 2

The performance "Function of the structure can be restored within a short period after an earthquake and no strengthening is required" can not be satisfied if members fail in shear or torsion. Therefore, shear and torsional capacity of a member become to the limit value.

On the other hand, when members do not fail in shear or torsion, it becomes a problem that how to represent the degree of damage corresponding to the performance "Function of the structure can be restored within a short period after an earthquake and no strengthening is required". Load-displacement relationship of a member is closely related with the degree of damage as shown in Figure 2 (Watanabe et.al., 2001). For example, it was found that buckling of longitudinal bars associated with spalling of concrete cover causes drop of flexural capacity in flexural failure type column. From these information, the performance "Function of the structure can be restored within a short period after an earthquake and no strengthening is required" when members do not fail in shear or torsion can be confirmed by checking the maximum response displacement of the member. JSCE Specification defines the ultimate displacement as one of the limit values for Seismic Performance 2.

In some structures, there may happen troubles in reusing them, when the residual displacement becomes remarkably large. In those cases, the residual displacement may be defined as the limit value which is determined considering time and cost necessary for restoration and expected residual functions.

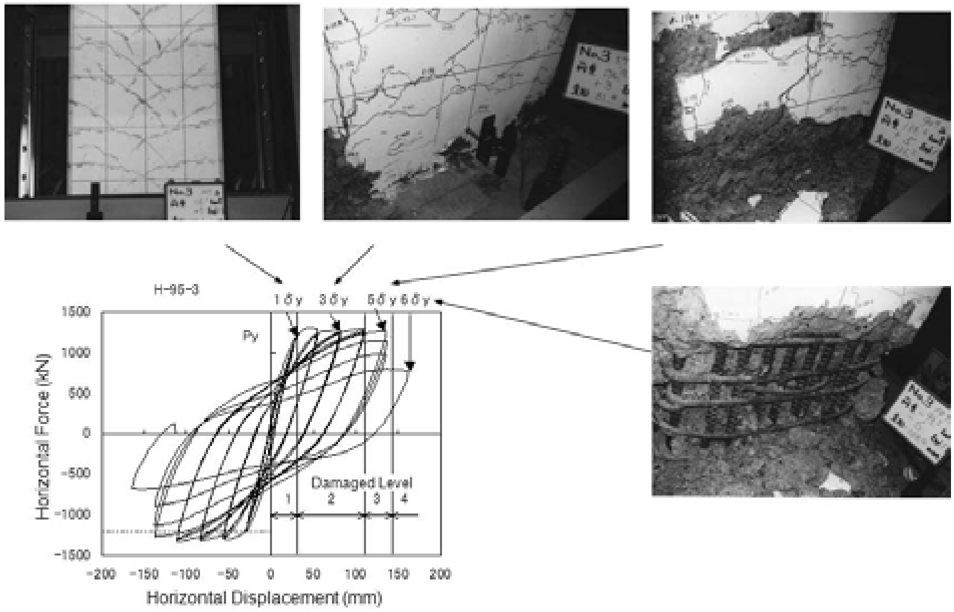

Figure 2: Relationship between load-displacement curve and damage level of a column (Watanabe et.al.,2001)

5.3 Seismic Performance 3

The technology to verify the performance “There is no overall collapse of the structural system due to an earthquake” is developing. In general, this performance is satisfied when vertical members do not crush in vertical direction. This kind of collapse can be normally prevented when the member is sufficiently safe against shear failure. However, in the case of high axial force, column collapses due to reversed loading after longitudinal bars yield even if shear failure does not occur. It is found that downward displacement of a column increases with repetition of loading from Figure 3.

In some cases, however, displacement of the whole structure becomes excessive, and additional bending moment as well as longitudinal displacement of member increase due to self-weight. These sometime may lead to self-collapse. Therefore, it should be necessary to confirm using the response analysis of structures during earthquake that the structure does not reach to the condition of self-collapse due to self-weight.

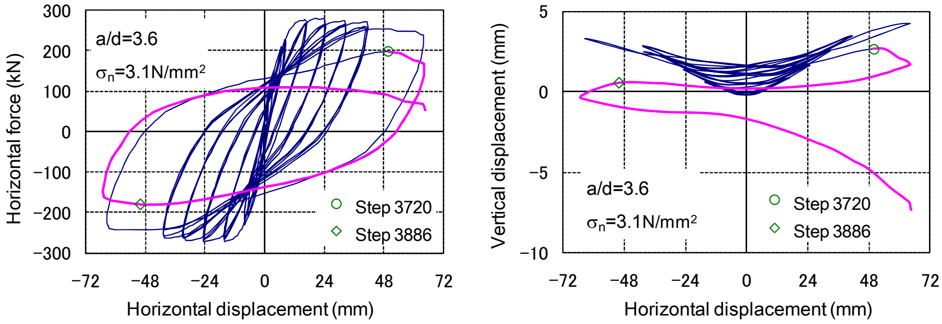

Figure 3: Horizontal force and vertical displacement under reversed cyclic loading of column (B400×D400, H=1350mm, N=500kN)

6. CALCULATION OF RESPONSE VALUE

The response value caused by assumed earthquake motion is calculated correspondingly with the limit value.

6.1 Analytical method

There are several analytical methods to calculate the response value. Typical examples are static analysis, quasi-dynamic analysis such as response spectrum method and time history response analysis. Recently, the numerical simulation technique has been developed notably and reliability of analytical results has also been improved sufficiently through comparisons with several kinds of experimental results. The time history response analysis is the most rational to analyze overall structure system including surrounding ground. JSCE Specification describes that the response should be estimated by carrying out the time history response analysis for the estimation of response values.

6.2 Representation of ground motion

Representation method of ground motion is different with analytical method. A design seismic coefficient is used in the static analysis and an elastic or nonlinear response spectrum is used in the quasi-dynamic analysis.

It is necessary to represent earthquake ground motion as a waveform in time history in order to execute the time history response analysis. The waveform of ground motion can be represented in terms of displacement, velocity and acceleration. The acceleration waveform is generally used because of convenience in equation of motion. A sample of acceleration waveform given in JSCE Specification is shown in Figure 4.

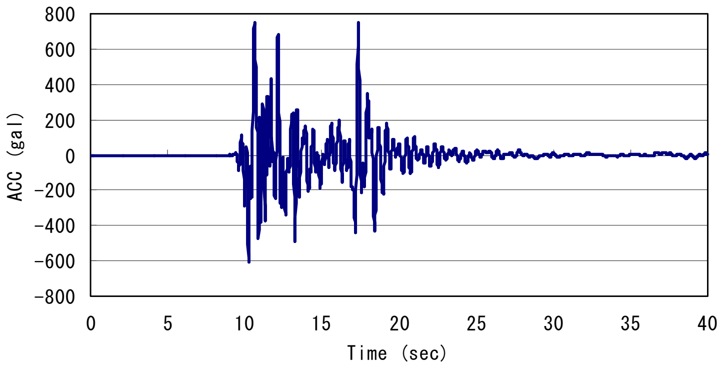

Figure 4: An example of acceleration waveform given in JSCE Specification

6.3 Modeling of structure system and input point of earthquake motion

The seismic force which acts to a structure is affected by the properties of subsurface ground at the location of the structure. Also, there is an effect of interaction between structure and surrounding ground on the seismic response of structure. The combinations of types of structure and surrounding ground are infinite. A whole structural system including foundation or surrounding ground should be analyzed in order to estimate the effects of subsurface ground and its interaction properly. JSCE Specification describes as follows.

(2) For the whole structure system, a coupled analysis considering the structure and the ground together shall be carried out. However, if dynamic interaction between the structure and the ground can be neglected or it can be appropriately modeled, the structure may be analyzed independently.

An example of structure and ground in coupled analysis is shown in Figure 5. Standard method to analyze the structure and the ground independently is shown in Figure 6. The usual underground structure constructed in the subsurface ground is hard to cause the relative vibration against the ground. The structure follows the displacement and deformation of circumference ground during an earthquake, and the influence of inertia force caused by the mass of structure is small. When the oscillation mode of the ground coincides with that of the structure, it can be used that the deformation of the ground during the earthquake is obtained firstly and the result is acted statically on the structure as forced displacement. This method is called as response displacement method.

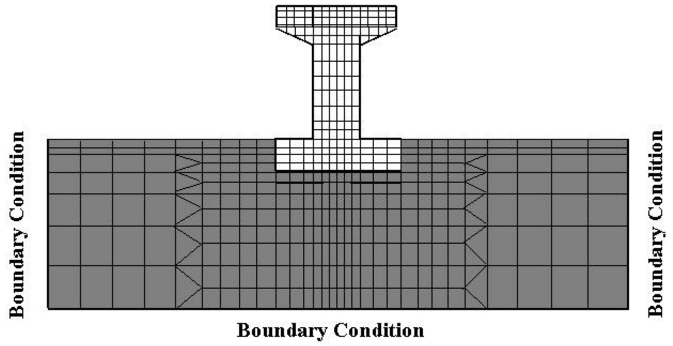

Figure 5: Example of structure and ground in coupled analysis

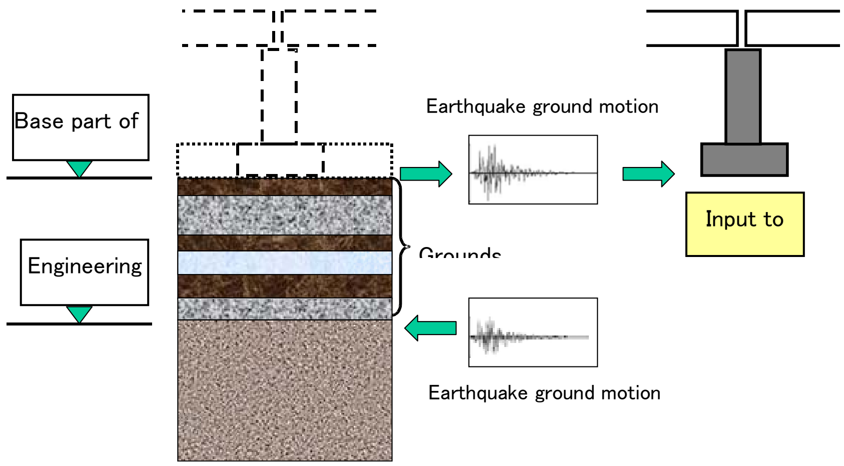

Figure 6: Method to analyze a structure independent of the ground

6.4 Modeling of structures

In order to analyze the structural response, it is necessary to represent structure by an appropriate structural model. As structure is composed of members connected in three dimensions, strictly speaking, it may be modeled in three dimensions. Two-dimensional modeling of structure, however, may be applied in case that only response in two-dimensional plane is enough to be considered according to the characteristics of structural response.

In modeling of structure, it is general to use two types of models: one is finite element model and another is beam element model. The beam element model represents column and beam by one line as shown in Figure 7. Applicable range is limited and quality of modeling affects to the accuracy of analytical results. The finite element model represents constituent members such as column, beam, wall and so on, as an assembly of small elements as shown in Figure 8. This model can be applicable to the arbitrary shape of structures and members.

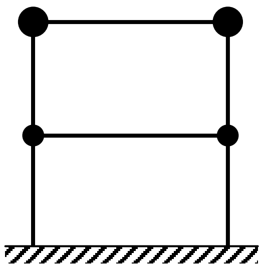

Figure 7: Beam element model

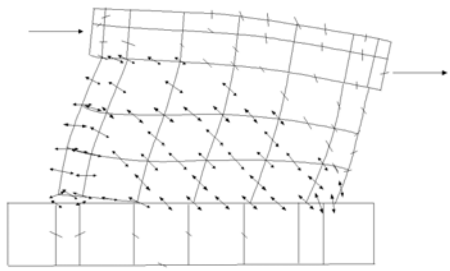

Figure 8: Finite element model

JSCE Specification defines the modeling of structures as follows.

(3) Structures should be modeled as 3-D or 2-D assembly of members.
(4) Structures should be analyzed using finite element or beam element models.

6.5 Modeling of materials

Even in any structural modeling, it is necessary to model material properties so that the structural properties can be reproduced. Stress-strain relationship of constitutive materials is used in the finite element model and moment-angle relationship at end of member is used in the beam element model. These material models should be able to take nonlinear behavior under reversed cyclic loading into account. In JSCE Specification describes the details of analytical models of structure by finite elements as shown in Figure 9, by lumped mass and beam element, and analytical models of ground as shown in Figure 10.

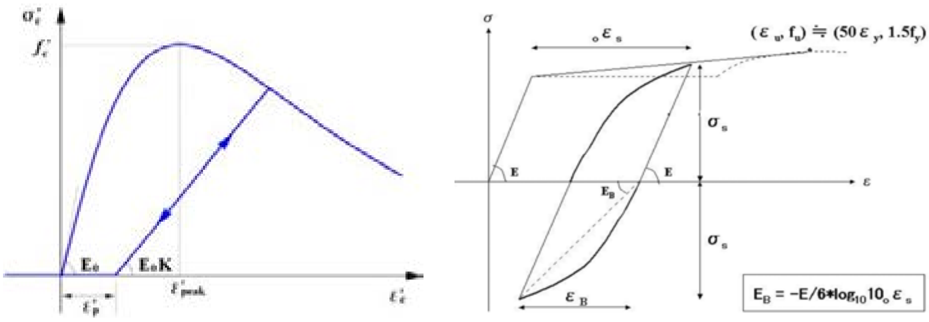

(a) Concrete (b) Reinforcing bar

Figure 9: Hysteresis model of materials

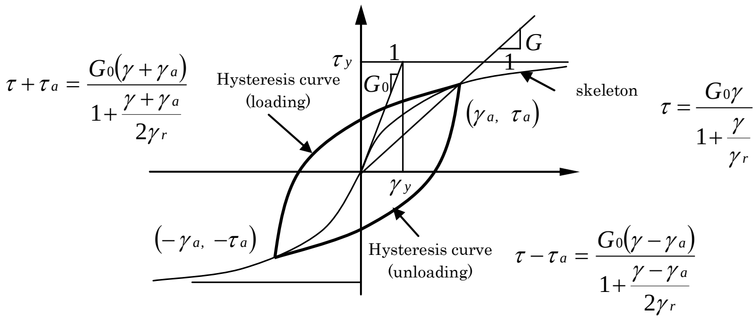

Figure 10: Dynamic shear stress-strain curve of soil

7. CONCLUSIONS

It is clear that reinforced concrete structure is indispensable to mega cities. The reinforced concrete structures should maintain their functions during and after an earthquake. The performance-based design method must be suitable for facilities with a great wide variety of performance requirements in mega cities. The technology for the performance-based seismic design is developing. It is believed that progress of the technology to simulate the response of reinforced concrete structures against to an earthquake will contribute to the urban safety of mega cities in Asia.

REFERENCES

JSCE, 2007. *Standard Specifications for Concrete Structures-2007 'Design'*, Japan Society of Civil Engineers

Watanabe, T. et.al., 2001. Evaluation method of deformation capacity related to damage conditions for reinforced concrete members, *Journal of materials, concrete structures and pavement*, Japan Society of Civil Engineers, No.683/V-52, pp.31-45, 2001.8

MODELING OF RC COLUMN WITH LAP SPLICES STRENGTHENED BY FIBER REINFORCED POLYMER

DAM XUAN THAI
Sirindorn International Institute of Technology, Thammasat University, Thailand
AMORN PIMANMAS
Sirindorn International Institute of Technology, Thammasat University, Thailand

ABSTRACT

This paper presents a two-dimensional (2D) nonlinear analytical model for analyzing reinforced concrete (RC) column with short lap splice strengthened by fiber reinforced polymer (FPR) under seismic force. The model was developed based on previous proposed nonlinear model, and applied to simulate experiment studies on RC column with lap splice strengthened by FRP sheets or prefabricated plates for verification. The model is applicable to both rectangular and circular section, and to both full and partial wrapping. The model is divided into an elastic frame and an assembly of nonlinear springs to represent the elastic portion and the plastic hinge, respectively. The effectiveness of FRP wrapping for strengthening lap splice is taken into account by modifying properties of nonlinear springs. Finally, the model was incorporated into Ruaumoko2D (Carr 1998) software for analyzing RC column strengthened by FRP wrapping around lap splice zone.

1. INTRODUCTION

The critical non-seismic reinforcement details of sub-standard columns which violate modern seismic design theory were identified. These include short lap splices of column reinforcement located immediately above floor levels or lap splice with starter bars from footing, widely spaced column ties, inadequate hoop reinforcement in potential plastic hinge regions and joint. Lap splice length designed for gravity only was normally shorter than that required in current seismic design standards, thereby possibly aggravating seismic performance of structure. The transfer of forces across the interface between steel and concrete through bond plays a major role on the behavior of reinforced concrete members. Cracking, deflections, structural strength, energy absorption and dissipation capacities under seismic loading are all related directly or indirectly to bond.

Several methods, such as external jacketing by steel plate, composite materials, or steel fiber concrete, were used to strengthen lap splice capacity. Some experiments and analytical models were conducted to assess the effect of strengthening lap splice on seismic resistance of column, and also to assess the effectiveness of each strengthening method on lap splice capacity improvement.

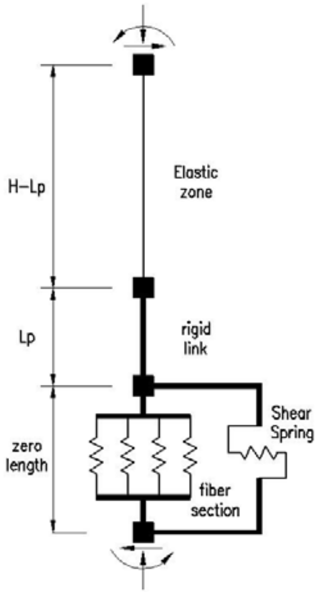

Figure 1: RC column model, Matrin (2007)

Fiber reinforced polymer (FRP) composites have found increasingly wide applications in civil engineering due to their high strength-to-weight ratio and high corrosion resistance. One important application of FRP-composites is as a confining material for concrete in the retrofit of existing reinforced concrete (RC) columns. As a result of FRP confinement, the compressive strength and the ultimate strain of concrete can be greatly enhanced. The bond stress between reinforced bar and concrete is also increased.

Lowes et al. (2003) formulated a versatile two-dimensional macro-model that represents a reinforced concrete beam-column joint. In their model, the bond slip and shear deformation responses of joints were considered as separate springs. The zero-length bond-slip springs were representatives of the force transferring ability between flexural reinforcement and the surrounding concrete while the zero-length shear springs represented the ability of shear transferring at the interface between frame members and the joint.

Matrin (2007) developed a reinforced concrete column two-dimension model (Figure 1) to simulate behavior of reinforced concrete column without jacketing, subjected to seismic excitation. Basically, a single-curvature column model consists of two major parts; the first part is an elastic frame of $H - L_p$ length, which represents the elastic behavior of column. The second part consists of a zero-length fiber section which is an assembly of nonlinear springs to represent the concrete and reinforcement nonlinear behavior. The second part is connected to the first part by a rigid link of L_p length.

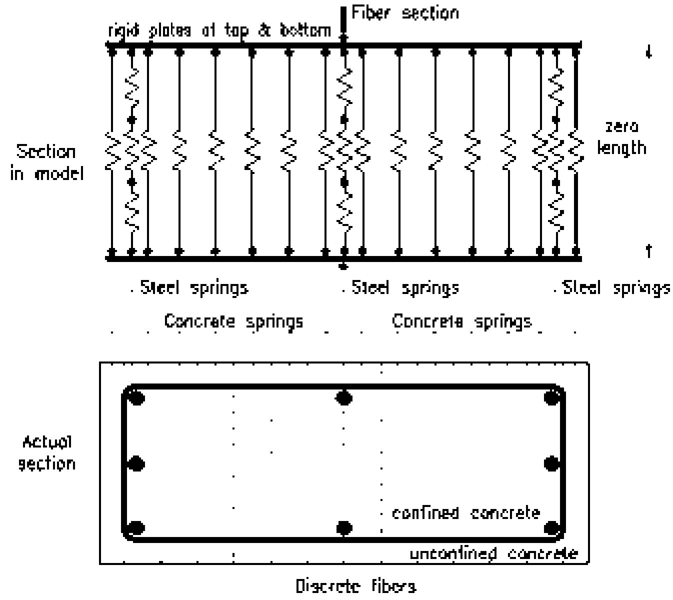

Figure 2: Discrete fiber section, Matrin (2007)

The fiber section was divided into a number of discrete fibers (Figure 2). Each fiber will be modeled as concrete spring or steel spring, whose characteristics can be calculated from the section of fiber and material properties. The concrete springs are classified into two types, confined concrete and unconfined concrete. The steel springs represent the reinforcement in each fiber (Figure 3). The steel spring normally consisting of three sub springs, i.e. steel bar sub-spring, lap splice spring, and bond-slip spring connected in series from top of fiber. Shear behavior of column can be simulated by a separate nonlinear shear spring.

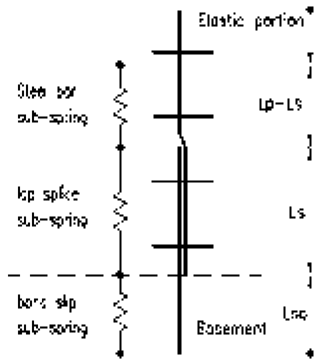

Figure 3: Model a reinforced bar by 3 sub-springs

Ruaumoko2D is a well known platform for modeling reinforced concrete structure, especially with capacity of degradation simulation and a huge database of hysteresis model embedded in the program. Martin (2007) used Ruaumoko2D to simulate cyclic behavior of several reinforced concrete members, and found that the comparison between analytical model and experimental result were closed. In this paper, the authors employed Ruaumoko2D to simulate reinforced concrete column externally confined by FRP sheet around the lap splice region. The nonlinear model of lap splice spring model with FRP confinement is incorporated into Ruaumoko2D. The suitability of the nonlinear model is extensively verified via several experiments conducted in the past.

2. NUMERICAL MODELING PARAMETERS

Various nonlinear parameters for modeling RC column strengthened by FRP confinement are described here. Particular attention is paid to the nonlinear properties of lap splice spring with and without FRP wrapping.

2.1 Length of plastic hinge region

The length of plastic hinge (L_p) is an essential parameter, which separates a column into 2 parts, i.e., elastic (frame) and plastic (fiber section) part. Priestley and Seible (1991) suggested the following plastic hinge length formulas for analyzing inelastic flexural behaviors of reinforced concrete columns with and without FRP jacketing:

Without FRP jacketing $\quad L_p = 0.08H + 0.022 d_b f_y \quad$ (1)

With FRP jacketing $\quad L_p = g + 0.044 d_b f_y \quad$ (2)

where g is a gap at the bottom of the jacket; d_b and f_y are diameter and yield strength of reinforced bar, respectively.
Xiao and Ma (1997) proposed an approach, in which the plastic hinge length was assumed variable corresponding to the steel stress of the extreme tensile bar f_s. The expressions (3) and (4) take the same format of (1) and (2) but use variable steel stress f_s, instead of the yield strength f_y.

Without FRP jacketing $\quad L_p = 0.08H + 0.022 d_b f_s \quad$ (3)

With FRP jacketing $\quad L_p = g + 0.044 d_b f_s \quad$ (4)

2.2 Elastic frame element

Elastic-frame element is used to simulate flexural and axial stiffness in the elastic part (top portion of the cantilever column). As recommended by ATC-40 (1996), the effective flexural rigidity is set to $0.7E_cI_g$; the effective axial rigidity is set to $1.0E_cA_g$; the effective shear stiffness is set to. Elastic modulus of concrete E_c is set to $15200\sqrt{f'_c}\,(ksc)$ as recommended by ACI318 (2005). In which, f'_c is compressive strength of unconfined concrete; A_g and H are gross area of section and the height of column, respectively.

2.3 Nonlinear Shear spring

Nonlinear shear spring is used to capture shear mechanism (deformation and stress) of column. Effective shear stiffness is set to $\frac{0.4E_c A_g}{L_p}$ as adopted from ATC-40 (1996)

Shear strength of column with and without FRP wrapping can be calculated by equation (5) (Ye et al. (2002)).

$$V_u = V_n + V_f \tag{5}$$

In which V_n is shear strength of column without FRP wrapping obtained by equation (6), (Sezen (2002)). V_f is additional shear strength provided by FRP sheets given by (7)-(9) ,Ye et al. (2002).

$$V_n = k\left[\frac{6\sqrt{f_c'}}{a/d}\sqrt{1+\frac{P}{6\sqrt{f_c'}A_g}}0.8A_g + \frac{A_{st}f_{yt}d}{s}\right] \tag{6}$$

$$V_f = v\lambda_f f_t b d \tag{7}$$

$$v = \frac{1.639\left(0.403 \blacksquare 1.053\frac{P}{A_g f_c'} + 0.176\frac{a}{\blacksquare}\right)}{\sqrt{\lambda_f} + 1.207} \tag{8}$$

$$\lambda_f = \frac{2t_f b_f}{b s_f}\frac{f_f}{f_t} \tag{9}$$

$$\frac{\Delta_r}{H} = \frac{4}{100}\frac{1+(\tan\theta)^2}{\tan\theta + P\left(\frac{s}{A_{st}f_{yt}d\tan\theta}\right)} \tag{10}$$

Lateral displacement (10) of gravity load collapse Δ_r is proposed by Moehle et al. (2000). A monotonic curve that governs the behavior of shear spring is shown in Figure 4, in which V_r is lateral force corresponding to state of gravity load collapse and assumed equal to $0.1V_u$.

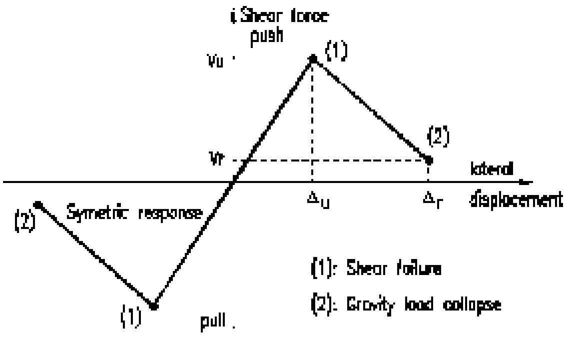

Figure 4: Monotonic curve for nonlinear shear spring

2.4 Concrete spring

The peak compressive force of concrete spring F_c (11) depends on area of concrete in a fiber A_c and confined compressive strength of concrete $f_{cc}^{'}$ which can be obtained from unconfined compressive strength $f_c^{'}$ by multiplying with confinement factor K shown in Eq. (12).

$$F_c = f_{cc}^{'} A_c \tag{11}$$

$$f_{cc}^{'} = K f_c^{'} \tag{12}$$

Calculation of confinement factor K follows a uniaxial stress-strain model (13); (14) for confined concrete with either FRP or transverse reinforcement as proposed by Harajli et al. (2006). The model is applicable to various conditions of cross section (rectangular and circular), wrapping method (partial and full), thickness and number of FRP sheets, types of steel stirrups (spiral and tie).

$$f_{cc}^{'} = f_c^{'} + k_1 \left(f_{lf} + f_{ls} \frac{A_{ce}}{A_g} \right) \tag{13}$$

$$\varepsilon_{CC} = \varepsilon_0 \left(1 + k_2 \left(\frac{f_{CC}}{f_C^{'}} - 1 \right) \right) \tag{14}$$

$$\varepsilon_{c0} = \frac{3 + 0.002 f_c^{'}}{f_c^{'} \blacksquare 1000} \quad (psi) \tag{15}$$

The degradation of concrete spring is determined by a point of remaining 50% peak stress with corresponding strain (15) (Roy and Sozen (1965)). A monotonic curve that governs the behavior of concrete spring (confined or unconfined) is shown in Figure 5.

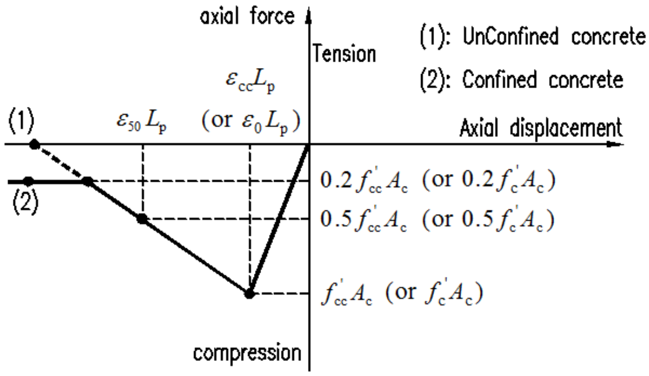

Figure 5: Monotonic curve for concrete spring

2.5 Bond slip sub-spring

A bi-linear bond-stress model proposed by Sezen and Moehle (2003) is adopted. The anchored bar length was generally divided into two parts, elastic L_e and plastic L_y zone with constant bond stresses u_e and u_y, respectively. The length of elastic zone is given as $L_e = \frac{f_s d_b}{4u_e}$, while the length of plastic zone L_y is set equal to $\frac{(f_s - f_y) d_b}{4u_y}$ (if $f_s > f_y$). When the stress acting on steel bar f_s is less than yield strength f_y, the plastic zone disappears, the anchorage behavior is purely elastic.

Plastic bond stress u_y depends on the state of stress in the anchorage zone. For tension and compression zone, $u_y = 0.4\sqrt{f_c'}$ (Shima et al. (1987)) and $u_y = 3.6\sqrt{f_c'}$ (Lowes et al. (2003)), respectively. Elastic bond stress can be approximately estimated by $u_e = \frac{f_y d_b}{4L_e}$, in which the required length L_e is recommended by ACI318 (2005) for tension (16) and compression (17) zone.

$$L_e = \frac{f_y}{1.1\sqrt{f_c'}} \frac{\psi_t \psi_e \psi_s \lambda}{\left(\frac{c_b + K_{tr}}{d_b}\right)} d_b \qquad (16)$$

$$L_e = \max\left(\frac{0.24 f_y}{\sqrt{f_c'}} d_b; 0.043 f_y d_b\right) \qquad (17)$$

The critical force at bond failure can be obtained by trial procedure, in which the stress of bar will be increased until the satisfaction of $L_e + L_y = L_{sa}$. Fig 6 shows two types of bond failures, before and after bar yielding depending on the anchorage length L_{sa}. The bond-slip can be computed as $\Delta_s = 0.5\left(L_e\varepsilon_e + L_y\left(\varepsilon_e + \varepsilon_s\right)\right)$.

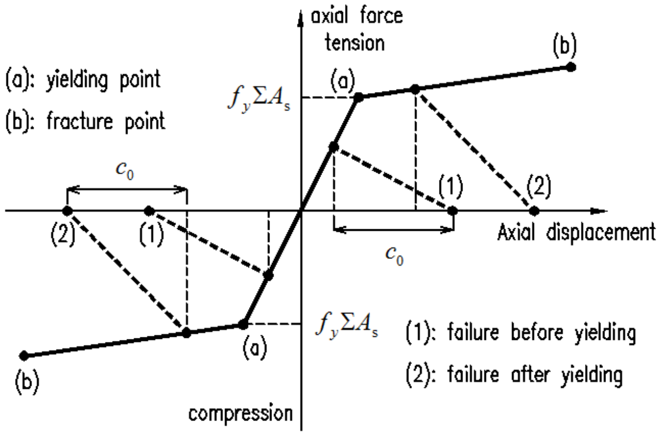

Fig 6: Monotonic curve governs bond and lap splice spring

<u>Steel bar sub-spring</u>

This spring represents the behavior of steel reinforcement in zone of plastic hinge L_p. The yield force of the spring is $f_y\Sigma A_s$. The elastic and plastic stiffness of spring are equal to $\dfrac{E_s(\Sigma A_s)}{L_p}$ and $E_p(\Sigma A_s)L_p$, respectively.

<u>Lap splice sub-spring</u>

In case of RC column without confinement, the behavior of lap splice spring follows the same concept as bond-slip spring. The calculation follows section 0, in which the lap splice length L_s is used instead of anchorage length L_{sa}.

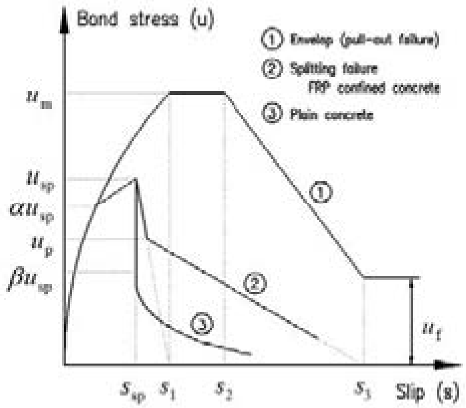

Fig 7: bond stress–slip model by Harajli (2009)

Since FRP wrapping around lap splice zone provides additional lateral stress, thereby increasing the bond stress. Harajli (2009) proposed a bond-slip model (Fig 7) for lap splice strengthened by FRP, the peak value of bond stress and corresponding slip s_{sp} at bond splitting failure are given in equations (18) and (19), respectively.

$$u_{sp} = 0.75\sqrt{f_c'}\left(\frac{c + 56\frac{E_f \alpha_f n_f t_f}{K_s n_s}}{d_b}\right)^{2/3} \leq u_m \qquad (18)$$

$$s_{sp} = s_1 e^{3.3\ln\left(\frac{u_{sp}}{u_m}\right)} + s_o \ln\left(\frac{u_m}{u_{sp}}\right) \qquad (19)$$

In which u_m is the maximum bond stress at pullout mode of bond failure given as $u_m = 2.57\sqrt{f_c'}$. Factor α_f represents the method of wrapping, with fully wrap $\alpha_f = 1$ and partially wrap α_f taken as expression (20), in which N_f is number of FRP strips with equal width b_f.

$$\alpha_f = \frac{N_f b_f}{L_s} \qquad (20)$$

As observed from eq.(18), bond strength is dependent on compressive strength of unconfined concrete f_c', and a ratio $\frac{c}{d_b}$ (ratio of concrete cover depth to diameter of bar). Bond strength is also enhanced by increasing the number of FRP sheets or thickness of sheet. The effect of wrapping method on bond strength is accounted for by factor α_f, in which full wrapping provides greater bond strength than partial wrapping.

Built-in Hysteretic Rules in Ruaumoko2D

All nonlinear springs described above are incorporated as back bone curve in Ruaumoko 2D. The model parameters are calculated from the actual geometrical sections and material properties. The built-in degradation model and hysteresis rules were combined with the above-mentioned envelope to provide the complete cyclic spring models. In the present study, the modified Takeda Degrading Stiffness hysteresis is used for steel spring, the Bi-linear with Slackness hysteresis is used for concrete spring and the SINA Degrading Stiffness hysteresis is applied to shear spring.

Selected experimental program

Xiao and Ma (1997) conducted an experimental study on seismic retrofit of reinforced concrete circular columns with poor lap-splice detail using prefabricated composite jacketing. In the study, three half scale model circular columns were tested. One column C1-A was tested under condition of "as built" and the other two columns C2-RT4 and C3-RT5 were tested after being strengthened with 4 and 5 FRP layers. All columns were 2.44m tall and 0.61m diameter. Longitudinal reinforcements were 20 deformed #6 bars ($d_b = 19.1$ mm, 2% reinforcement ratio, grade 60) with lap splice length of 0.38m ($20d_b$) at the base. Round #2 hoops ($\phi 6.4$ mm) spaced at 127mm intervals were used as transverse reinforcement. Concrete strength was 44.8 MPa (28 days cylinder specimen). Composite jacketing layer was 3.2mm thick prefabricated unidirectional glass fiber sheets. The elastic modulus and ultimate strength in the circumferential direction are 48300

MPa and 552 MPa, respectively. The sheets were attached to the column via two part epoxy.

The axial load applied to the column is 712 kN $\left(\frac{P}{A_g f_c'} - 5\%\right)$. An analytical model was built to simulate these columns. Core concrete section (inside stirrup perimeter) was symmetrically divided into 42 discrete fibers of 1.30cm width. Thus, 42 springs with various properties were used to model confined concrete fiber and 11 steel springs were used to model all reinforcing bars. Cover unconfined section (outside stirrup perimeter) was symmetrically divided into 42 discrete fibers of 1.30cm width and 6 fibers of 1.50cm width. Thus a total of 48 springs with various properties were used to represent unconfined concrete. One spring was used to model column shear behavior and one elastic element to represent elastic behavior zone of column.

Harajli and Dagher (2008) conducted an experimental investigation on the use of external fiber reinforced polymer (FRP) confinement for bond strengthening of spliced reinforcement in rectangular reinforced concrete columns and the consequent effect on the seismic response. Nine 0.4m deep x 0.2 m wide x 1.5m high columns were divided into 3 series based on steel diameter used; 14mm diameter series named C14FP1, C14FP2 and C14E; 16mm diameter series named C16FP1, C16FP2 and C16E; and 20mm diameter series named C20FP1, C20FP2 and C20E. In each specimen label, suffixes “FP1” and “FP2” meant the number of FRP sheets, and suffix “E” means column with no lap splice of reinforcing bars. Each specimen consists of 8 reinforcing bars with lap splice length of $30d_b$. The ratio of concrete cover to bar diameter $\frac{c}{d_b}$ is 1.4, 2.1 and 1.0 for series C14, C16 and C20 respectively. Transverse steels were 8mm diameter spaced at 200mm throughout the height of the strengthened column, while in unconfined “E” column, stirrup was 8 mm diameter spaced at 50mm within 500mm from the base and spaced at 100mm within the remaining height. Yield strength of bars f_y in series C14, C16 and C20 were 550MPa, 528MPa and 617MPa respectively. Compressive strength of concrete f_c' varied from 32MPa to 40MPa. The FRP sheets were 0.13mm thick; with elastic modulus of 230000MPa and tensile fracture strain of 1.5%. An analytical model was built to simulate these specimens. Core section (inside stirrup perimeter) was symmetrically divided into 42 discrete fibers of 0.857cm width, thus 42 springs were used to model confined concrete fiber and 3 (or 4 in series C16) steel spring combinations were used to model all reinforced bars. Cover unconfined concrete part (outside stirrup perimeter) was symmetrically divided into 42 discrete fibers of 0.857cm width and 6 fibers of 0.667cm width, thus 48 springs were used to represent unconfined concrete. One spring was used to model column shear behavior and one elastic element to represent elastic behavior zone of column. The behavior of analytical model was compared with corresponding experimental result shown in the next section.

Verification of the nonlinear modeling

Series C14 tested by Harajli and Dagher (2008)

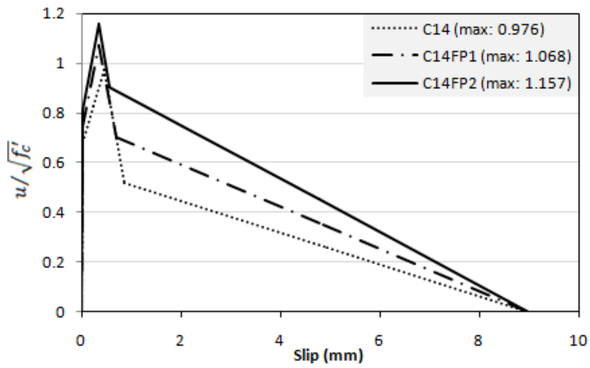

Fig 8: Bond stress–slip in C14 series

Fig 8 presents the backbone relation between bond slip and ratio of bond stress (u) to unconfined concrete compressive strength (f'_c) as explained in section 0. This backbone relation is combined with the built-in hysteresis rules to obtain the complete cyclic bond-slip model. According to the model, ratios $u/\sqrt{f'_c}$ reach maximum values of 0.976, 1.068 and 1.157 in specimens C14, C14FP1 with one FRP layer and C14FP2 with two FRP layers, respectively.

Table 1 shows the comparison between experimental and analytical results of series C14. The maximum experimental lateral force of columns C14, C14FP1 and C14FP2 was 81.2, 87.2 and 92.2 kN respectively while the analysis was 82.0, 92.3 and 97.2 kN respectively. The differences are only 1%, 6% and 5% respectively. It is found that in both analytical and experimental results, the lateral force increased with the increasing number of FRP sheets.

Table 1: Series C14 results

Specimen	Lateral force – kN			Type of lap splice failure
	Exper.	Analysis	Differ.	
C14	81.2	82.0	1.01	Before yielding of bar
C14FP1	87.2	92.3	1.06	Before yielding of bar
C14FP2	92.2	97.2	1.05	After yielding of bar
		Average	1.04	
		S.D	0.03	

Fig 9b and Fig 10b show analytical response of series C14, which demonstrates the performance of FRP wrapping to confine lap splice of RC column. Fig 9a and Fig 10a show corresponding experimental results. It is noted that the analytical results agreed well with experimental ones.

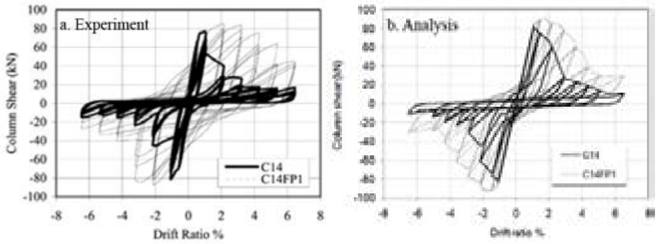

Fig 9: Response of columns C14 and C14FP1

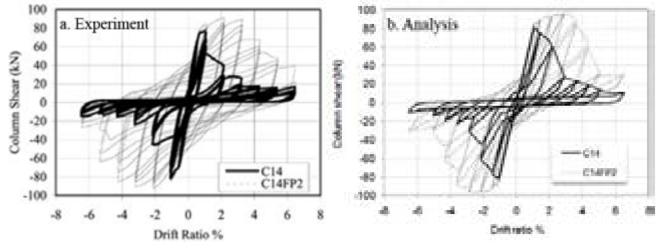

Fig 10: Response of columns C14 and C14FP2

<u>Series C16 tested by Harajli and Dagher (2008)</u>

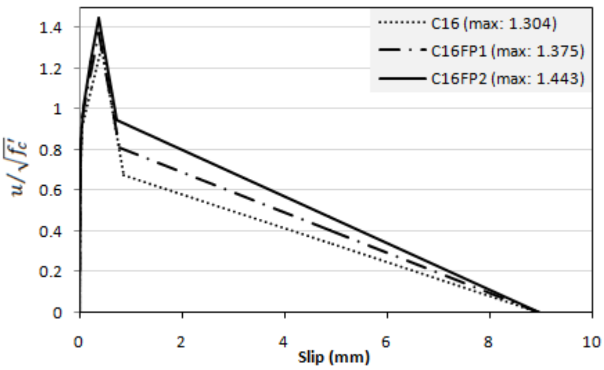

Fig 11: Bond stress–slip in C16 series

Fig 11 presents the backbone relation between normalized bond stress versus slip obtained from the model. The ratios $u/\sqrt{f'_c}$ reach maximum values of 1.304, 1.375 and 1.443 in specimens C16, C16FP1 with one FRP layer and C16FP2 with two FRP layers, respectively.

Table 2: Series C16 results

Specimen	Lateral force			Type of lap splice failure
	Exper.	Analysis	Differ.	
C16	107.4	97.9	0.91	After yielding of bar
C16FP1	112.5	108.0	0.96	After yielding of bar
C16FP2	107.4	109.0	1.01	After yielding of bar
		Average	0.96	
		S.D	0.05	

Table 2 shows the comparison between experimental and analytical results of series C16. The maximum experimental lateral force of columns C16, C16FP1 and C16FP2 was 107.4, 112.5 and 107.4kN while the analysis gave the values of 97.9, 108.0 and 109.0 kN respectively. The differences between results are 9%, 4% and 1% respectively. It is found that in the analysis results, the lateral force increased with increasing number of FRP sheets, while the experiment gave strange results with column C16FP2 wrapped by two FRP layers has the lateral strength equal to un-strengthened column C16 and less than the strength of column C16FP1 with one FRP layer.

Fig 12b and Fig 13b show analytical response of series C16, which represents the enhancement of the lateral capacity and the ductility provided by FRP confinement around lap splice zone. Fig 12a and Fig 13a show corresponding experimental results. It is found that the analytical results agreed closely with experimental ones.

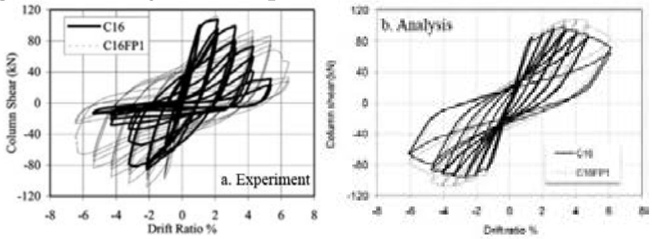

Fig 12: Response of columns C16 and C16FP1

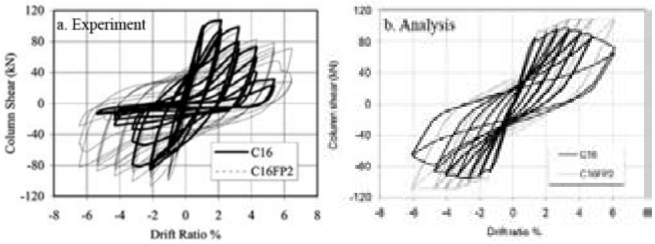

Fig 13: Response of columns C16 and C16FP2

<u>Series C20 tested by Harajli and Dagher (2008)</u>

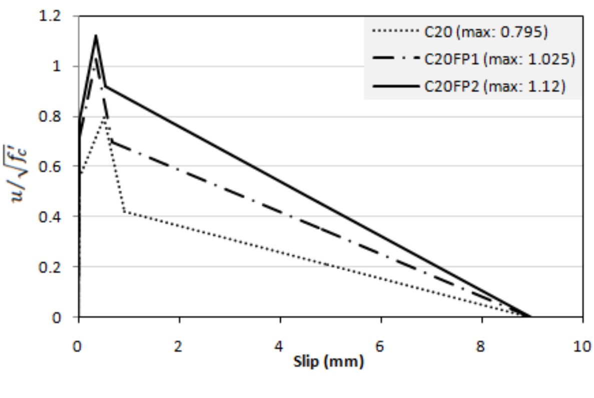

Fig 14: Bond stress–slip in C20 series

Fig 14 presents the backbone relation between normalized bond stress versus slip as obtained from the model. The ratios $u/\sqrt{f_c}$ reach maximum values of 0.795, 1.025 and 1.120 in specimens C20, C20FP1 with one FRP layer and C20FP2 with two FRP layers, respectively.

Table 3 shows the comparison between experimental and analytical results of series C20. The maximum experimental lateral force of columns C20, C20FP1 and C20FP2 was 91, 126 and 141.8 kN while the analysis gave the values of 83.9, 130 and 135 kN respectively. The differences are 8%, 3%

and 5% respectively. It is found that in both analytical and experimental results, the lateral force increased with increasing number of FRP sheets.

Table 3: Series C20 results

Specimen	Lateral force			Type of lap splice failure
	Exper.	Analysis	Differ.	
C20	91	83.9	0.92	Before yielding of bar
C20FP1	126	130.0	1.03	Before yielding of bar
C20FP2	141.8	135.0	0.95	Before yielding of bar
		Average	0.97	
		S.D	0.06	

Fig 15b and Fig 16b show analytical response of series C20, which demonstrate the increase of the lateral capacity and the ductility provided by FRP wrapping around lap splice zone. Fig 15a and Fig 16a show corresponding experimental results. As shown, the analytical results agreed well with experimental ones.

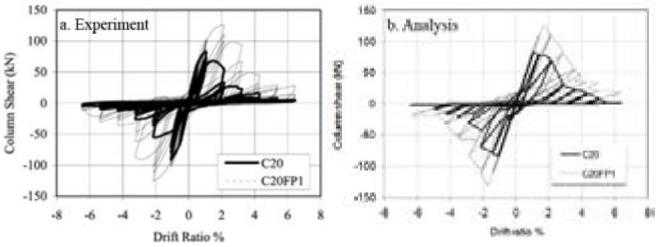

Fig 15: Response of columns C20 and C20FP1

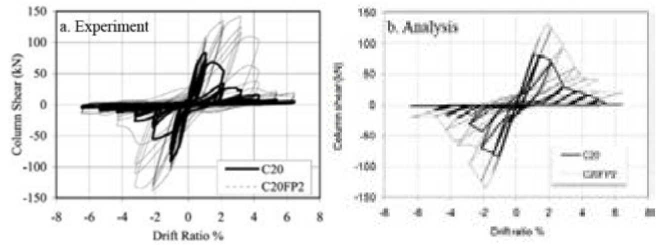

Fig 16: Response of columns C20 and C20FP2

Circular RC columns tested by Xiao and Ma (1997)

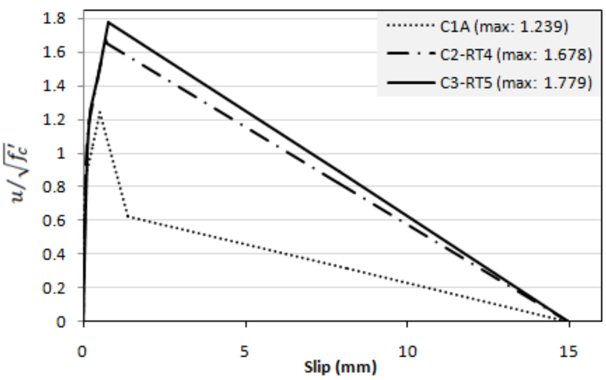

Fig 17: Bond stress–slip in Xiao and Ma (1997) columns

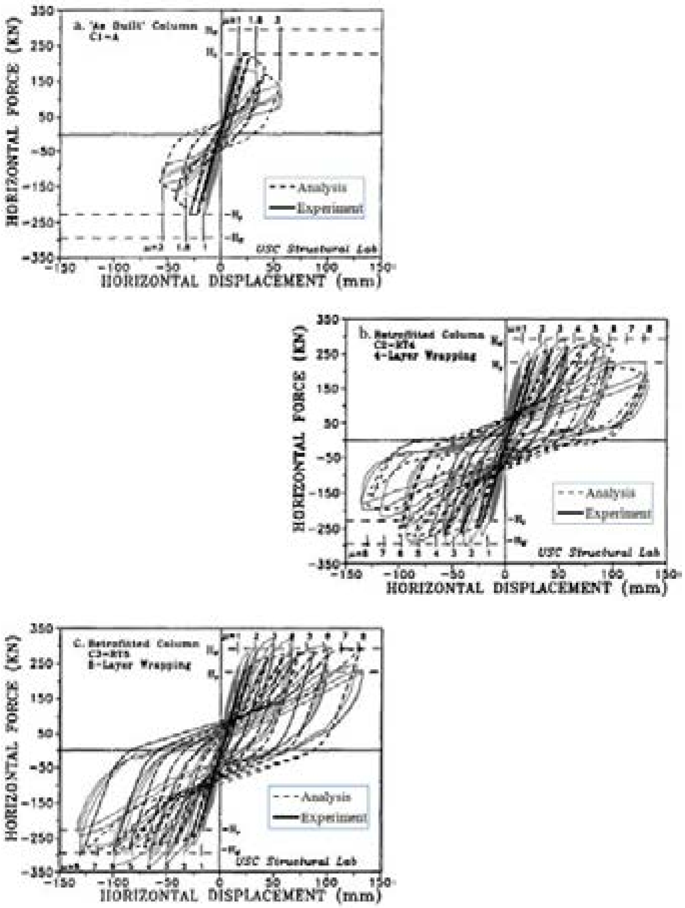

Fig 18: Response of columns C1-A; C2-RT4 and C3-RT5

Fig 17 presents the backbone relation between normalized bond stress versus slip as obtained from the model. The ratios $u/\sqrt{f'_c}$ reach maximum values of 1.239, 1.678 and 1.779 in specimens C1A, C2-RT4 with four FRP prefabricated plates and C3-RT5 with five FRP prefabricated plates, respectively. Table 4 shows the comparison between experimental and analytical results of Xiao's columns. The maximum experimental lateral force of columns C1-A, C2-RT4 and C3-RT5 was 231, 290 and 330 kN while analysis gave the values of 228, 276 and 289 kN respectively. The differences between results are 1%, 5% and 10% respectively. It is found that in both analytical and experimental result, the lateral force increased with increasing number of FRP prefabricated plates.

Table 4: Xiao's columns results

Specimen	Lateral force			Type of lap splice failure
	Exper.	Analysis	Differ.	
C1-A	231	228.0	0.99	Before yielding of bar
C2-RT4	290	276.0	0.95	After yielding of bar
C3-RT5	330	298.0	0.90	After yielding of bar
		Average	0.95	
		S.D	0.04	

Fig 18a, b, c show both analytical and experimental responses of columns C1-A, C2-RT4 and C3-RT5. As seen, the lateral capacity and the ductility of column strengthened by FRP wrapping around lap splice zone of RC column were increased. It is noted that the actual columns tested in Xiao and Ma (1997) experiment was wrapped by FRP prefabricated plates not only around the lap splice zone, but also around the middle and top parts of column.

Conclusion

The nonlinear analytical model was constructed to simulate the cyclic response of RC columns strengthened by FRP confinement around lap splice zone. The model consisted of one elastic frame element and an assembly of nonlinear springs, to simulate the elastic zone of RC column as well as the plastic hinge region. The effect of FRP confinement around lap splice zone is taken into account by applying confined bond-slip model of spliced bars. Through the increase of FRP layers, the splice strength and ductility is enhanced.
The comparison between model predictions and experimental results shows a good agreement. The discrepancy is within the range of 10%. The analysis results can be used to predict the responses of column with lap splice confined by FRP jacketing. The model is found to be widely applicable. It can be used to predict both rectangular and circular cross section.

Acknowledgement
The author would like to express his appreciate to the Asian Development Bank (ADB), Japanese Government for granting the scholarship for his study at SIIT. The authors are also grateful to Thailand Research Fund to provide the research grant RSA 5280034.

Nomenclature

The following symbols are used in this paper:

a	Shear span of column
A_g	Gross area of section
A_c	Area of concrete in a fiber
A_{cc}	Area of concrete core
A_s $\left(\Sigma A_s\right)$	Area of reinforcement (total in fiber)
A_{st}	Area of transverse reinforcement
b	Section width
b_f	Width of a FRP strip
c_b	Smaller of (1) distance from center of bar to the nearest concrete surface and (2) one-half center-to-center spacing of bars.
d	Effective depth of column section
d_b	Diameter of reinforced bar
E_c	Modulus of elasticity of concrete
E_f	Modulus of elasticity of transverse FRP
E_p	Modulus of plasticity of reinforcement
E_s	Modulus of elasticity of reinforcement

F_c	Yield force of concrete spring element
f_c'	Compressive strength of unconfined concrete
f_{cc}'	Compressive strength of confined concrete
f_f	Tensile strength
$f_{lf}; f_{ls}$	The lateral passive confining pressure
f_s	Stress of longitudinal reinforcement
f_t	Tensile strength of concrete
f_y	Yield stress of longitudinal reinforcement
F_y	Yield force of spring element
f_{yt}	Yield stress of transverse reinforcement
g	Gap provided at the bottom of the jacket
[redacted]	Section depth
H	Height of column
I_g	Moment of inertia of the gross section
k	Shear degrading coefficient
K	confined strength ratio
$k_1; k_2$	Confinement effectiveness coefficient
k_{tr}	Transverse reinforcement index
L_e	Length of elastic zone in bond model
L_p	Length of plastic hinge zone
L_s	Length lap spliced zone
L_{sa}	Length anchorage bar zone
L_y	Length of plastic zone in bond model
n_f	Number of transverse FRP layers
N_f	Number of partial FRP strips
n_s	Number of lap splices in tension
P	Axial load applied on column
s_0	Local slip factor
s_1	Local slip at peak pullout mode failure
s	Spacing between transverse hoops or spirals
s_f	Distance of FRP strips
s_{sp}	Local slip at peak bond strength
t_f	Thickness of one FRP layer
u_e	Average elastic bond stress
u_m	Maximum bond stress at pullout mode
u_{sp}	Local splitting bond stress
u_y	Average plastic bond stress
v	Shear strengthening coefficient of FRP
V_n	Shear strength of column without FRP
V_r	Remain shear strength at collapse
V_u	Shear strength of column with FRP

▮	Lateral displacement at V_r
▮	Bond slip of reinforcement
▮	Lateral displacement at shear strength V_u
α_f	Factor of partial wrapping
ε_{50}	Concrete strain at stress of 50% of peak stress
ε_{cc}	Concrete strain for confined concrete
ε_{co}	Concrete strain at the intersection point between the 1st and 2nd stage of the stress–strain curve
ε_e	Elastic strain
ε_o	Strain at max stress of unconfined concrete
ε_s	Strain of reinforcement
θ	Critical crack angle at shear failure
ψ_e	Coating factor
ψ_s	Reinforcement size factor
ψ_t	Reinforcement location factor
λ	Lightweight aggregate concrete factor
λ_f	Parameter of ratio of FRP amount to concrete

Reference

ACI318 (2005). "ACI 318-05, Building Code Requirements for Structural Concrete and Commentary." *American Concrete Institute* ACI Committee 318, 2005, 430 pp.

ATC-40 (1996). Seismic evaluation and retrofit of concrete buildings (vol 1), *Applied Technology Council*.

Carr, A. J. (1998). Ruaumoko - Program for inelastic dynamic analysis, Christchurch: Department of Civil Engineering, University of Canterbury.

Harajli, M. H. (2009). "Bond strengthening of lap spliced reinforcement using external FRP jackets: An effective technique for seismic retrofit of rectangular or circular RC columns." *Construction and Building Materials* 23(3): 1265-1278.

Harajli, M. H. and F. Dagher (2008). "Seismic Strengthening of Bond-Critical Regions in Rectangular Reinforced Concrete Columns Using Fiber-

Reinforced Polymer Wraps." *ACI Structural Journal* Volume: 105 Issue: 1 Pages: 68-77.

Harajli, M. H., E. Hantouche, et al. (2006). "Stress-Strain Model for Fiber-Reinforced Polymer Jacketed Concrete Columns." *ACI Structural Journal* Volume: 103 Issue: 5 Pages: 672-682.

Lowes, L. N., N. Mitra, et al. (2003). "A Beam-Column Joint Model for Simulating the Earthquake Response of Reinforced Concrete Frames." *Pacific Earthquake Engineering Research Center* PEER 2003/10.

Matrin, S. (2007). "Nonlinear modeling of gravity load designed reinforced concrete buildings for seimic performance evaluation." Msc degree *Civil Engineering Department. Asian Institute of Technology*. Bangkok, Thailand.

Moehle, J. P., K. J. Elwood, et al. (2000). "The Second U.S.-Japan Workshop on Performance-Based Earthquake Engineering Methodology for Reinforced Concrete Building Structures " *Pacific Earthquake Engineering Research Center* PEER 2000/10.

Priestley, M. J. N. and F. Seible (1991). "Seismic Assessment and Retrofit of Bridges." *University of California, San Diego* SSRP 91/03 pp. 84-149.

Roy, H. E. H. and M. A. Sozen (1965). "Ductility of Concrete." *American Concrete Institute* Volume: 12 Pages: 213-235 Date: January 1, 1965.

Sezen, H. (2002). "Seismic Behavior and Modeling of Reinforced Concrete Building Columns." Ph.D. Thesis. *University of California, Berkeley*.

Sezen, H. and J. p. Moehle (2003). "Bond-slip behavior of reinforced concrete members." *fib - Symposium (CEB-FIP); Concrete Structures in Seismic Regions* 6-9 May 2003. Athens, Greece.

Shima, H., L. L. Chou, et al. (1987). "Bond Characteristics in Post-Yield Range of Deformed Bars." *Concrete Library of JSCE* 10: 113-124.

Xiao, Y. and R. Ma (1997). "Seismic Retrofit of RC Circular Columns Using Prefabricated Composite Jacketing." *Journal of Structural Engineering* 123(10): 1357-1364.

Ye, L., Q. Yue, et al. (2002). "Shear Strength of Reinforced Concrete Columns Strengthened with Carbon-Fiber-Reinforced Plastic Sheet." *Journal of Structural Engineering* 128(12): 1527-1534.

AN EXPERIMENTAL STUDY FOR THE QUALITY EVALUATION OF COVER CONCRETE

KENJI HAYAKAWA
Tokyu Construction Co. Ltd., Tokyo, Japan
hayakawa.kenji@tokyu-cnst.co.jp
YOSHITAKA KATO
ICUS, Institute of Industrial Science, The University of Tokyo, Japan
katoyosh@iis.u-tokyo.ac.jp

ABSTRACT

The quality of cover concrete, which is affected by the execution conditions of works such as consolidation and curing, strongly influences the durability of concrete structures. Currently, the quality of the structural concrete is confirmed by examining the fresh properties and compressive strength of a test specimen. However, these examinations do not evaluate the durability of the structural concrete directly, and the influence of the execution condition of work is uncertain.

The purpose of this study is to evaluate the influence of the execution condition of works on the cover concrete quality for ensuring the durability of structure concretes. This experiment investigated the air permeability index, percentage of voids, and carbonation depth in test and full size specimens under variable execution condition of works and variable slump and cement type of the concrete materials. Air permeability test of the concrete surface was carried out by the Torrent method for non-destructive test which can be utilized in the field.

As a result, the air permeability examination can evaluate the quality of cover concrete by the difference of curing days. In this case, variation of air permeability index for full size specimen is larger than that of small size specimen. This can be attributed to the fresh concrete properties such as bleeding of concrete, consolidation times, and compaction by the self-weight. Finally, concrete using Portland blast-furnace slag cement is more easily affected by curing condition and execution of work than that using ordinary Portland cement.

1. INTRODUCTION

Durability of concrete structures depends on the mass transfer resistance of cover concrete, which is a primary factor in deterioration due to chloride ion and carbon dioxide, oxygen, water. Therefore, the quality of the cover concrete is very important for ensuring the concrete structures' durability. The quality of cover concrete is influenced by factors other than the water-cement ratio, especially the execution conditions of works such as the consolidation and curing method, and the relative influence is different for constructive quality of fresh concrete such as workability and consistency.

Currently, the quality of structural concrete is confirmed by examination of the fresh condition, such as slump, and the compressive strength of test pieces. However, these examinations do not evaluate the durability of the structural concrete directly, and the influence of execution condition of work is uncertain. If the evaluation of quality of cover concrete, such as permeability, could be conducted directly on the structures, it would be very effective for ensuring durability. Therefore, this study utilized nondestructive testing methods which can examine air-permeability on the structures. The purpose of this study is to evaluate the influence of the execution condition of works on the quality of cover concrete for ensuring structural concrete durability. This experiment investigated air permeability index, percentage of voids, carbonation depth in test and full size specimens under variable execution condition of works and testing pieces. Also, the influence of construction works and conditions was evaluated by comparing full size specimens to test pieces.

2. TEST PROCEDURE

2.1 Materials

Mix proportions are given in Table 1. In this study, ready mixed concretes which satisfy JIS A 5308 were used. Three types of concrete with different slump and cement types were investigated. Ordinary Portland cement and Portland blast-furnace slag cement were both used, and the water-cement ratio of these mix proportions was set at 55.1 and 57.0%. The slump for water unit weight of 180 kg/m^3 was 18.0 cm, whereas the slump for water unit weight of 159 kg/m^3 was 8.0 cm.

Table 1 Concrete mix proportions

No.	Concrete Type	Air (%)	W/C (%)	s/a (%)	Unit Weight(kg/m^3)				
					W	C	S	G	Ad.
1	24-8-20N	4.5	57.0	46.6	159	279	858	1002	2.79
2	24-18-20N	4.5	57.0	49.3	180	316	866	906	3.16
3	24-8-20BB	4.5	55.1	46.1	159	289	840	1002	2.89

※1 :Strength-slump-Maximum Aggregate Size（Cement type）

※2: AE water reducing agent

2.2 Specimens and conditions

Figure 1 illustrates the full size specimen dimensions and reinforcing steel bar arrangement. The dimension of specimens similar to the original structure is 1.0×1.0×1.0m (Series 1) with no reinforcement, and 0.9×0.9×1.2m (Series 2) with reinforced (both form sides) and non-reinforced cases in order to investigate the influence of reinforcing steel bar on cover concrete quality. The side surface was also investigated for some specimens.

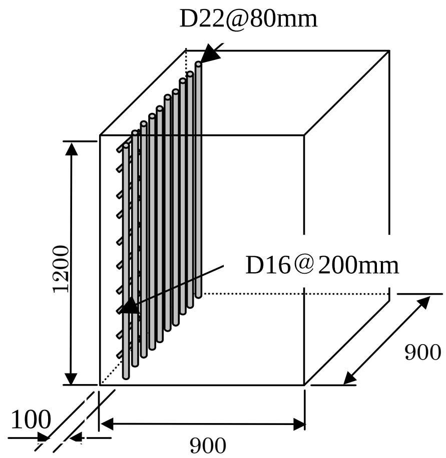

Figure 1 Full size specimen dimensions and rebar arrangement

Table 2 shows the construction works and specimen conditions. Concrete was cast using a concrete pump-piston and consolidated with a high-frequency vibrator of ϕ 50 mm. Vibration time is 15 seconds for standard construction works, and was determined from experience and compressive strength. In addition to the standard time, 45 seconds vibration case was also investigated to examine the most suitable vibration time for concrete quality of fresh condition. The curing conditions were varied by the removal time of forms and moist curing after form removal. After curing specimens were exposed to a warm outdoor environment unaffected by chloride ions.

Table2 Construction works and specimen condition

	Execution condition and Parameter
Series1	Non-reinforced (Concrete mix 1)
Casting	June (concrete temperature 28ºC)
Casting speed	5 m/h (Continually)
Curing times	4 days, 7 days, 28 days (removed form)
Series2	Reinforced and non-reinforced (Concrete mix 1-3)
Casting	March (concrete temperature 13 to 17ºC)
Casting speed	2 to 3 m/h
Vibration times	15 seconds, 45 seconds
Curing times	1 day, 5 days (removed form) 9 days, 28 days (moisture after removing at 5 days)

3.3 Test items and methods

Table 3 shows the test items and methods. The fresh condition was examined by slump, air content, concrete temperature, and bleeding tests, which are performed for the acceptable inspection of ready mixed concrete.

In order to investigate the fundamental characteristics of the concrete mixes, compressive strength (φ10×20 cm), air permeability at the concrete surface (15×15×15 cm), and accelerated carbonation (φ10×20cm) tests were performed on test pieces. These pieces were exposed to 20ºC and 60% RH after water curing until 28 days. Air permeability was tested by the non-destructive Torrent method which can also be used in the field (Torrent, 1992). This method uses a two-chamber cell, with an inner and outer chamber, based on the guard-ring principle. Since the air permeability is generally influenced by the water content at the concrete surface (Ujike, 1988), the water content ratio at the concrete surface was measured by capacitance measurement method, and air permeability was tested during dry periods.

Testing of the full size specimens examined air permeability and moisture ratio at the concrete surface. Carbonation depth was measured for one specimen by taking drilled cores. These results were compared to test piece results, which were not influenced by construction works and conditions.

Table 3 Tests items and method

Tests items	Test method
Tests on fresh condition	Slump, Air, Temperature JIS A 1123: Bleeding of concrete
Air permeability	Torrent method (Torrent, 1992)
Compressive strength	JIS A 1107, 1108
Moisture ratio	Capacitance measurement method
Air space ratio	ASTM C 642
Carbonation depth	JIS A 1151: Method for measuring depth JIS A 1152: Accelerated test 20ºC, 60% RH, CO_2 5%

3. TEST RESULTS AND DISCUSSION

3.1 Fresh condition concrete quality

Table 4 shows the test results for fresh conditions. These concrete mixes satisfied the standard values specified by JIS A 5308. The bleeding content and ratio of 24-18-20N and 24-8-20BB is larger than that of 24-8-20N.

Table 4 Fresh conditions test results

Concrete Type	Slump (cm)	Air (%)	Concrete Temp. (ºC)	Temp. (ºC)	Bleeding Content (cm^3/cm^2)	Bleeding Ratio (%)
24-8-20N	6.5	4.9	17.1	11.9	0.074	1.85
24-18-20N	16.0	5.3	16.0	9.1	0.148	3.58
24-8-20BB	10.0	3.1	13.4	8.2	0.128	3.04

3.2 Test pieces fundamental characteristics

Table 5 shows the compressive strength at 28 days, surface air permeability, and air space ratio at 100 days in dry conditions, and accelerated carbonation depth at 28 days. The compressive strengths used for inspection of the ready mixed concrete were 29.7 to 34.1 N/mm^2, larger than the nominal strength of 24 N/mm^2, and had little difference between concrete mixes. However, the difference between the direct durability indices – the coefficient of air permeability at 100 days and accelerated carbonated depth at 28 days – was greater than the difference in compressive strength.

Table 5 Test results for fundamental quality of concrete

	Compressive Strength (N/mm^2)	Coef. of Air-permeability (10^{-16}m^2)	Air space Ratio (%)	Carbonated Depth (Accelerated curing：28 days) (mm)
24-8-20-N	33.9	0.207 (0.16)	9.0	9.8
24-18-20-N	29.7	0.402 (0.36)	10.3	12.0
24-8-20-BB	34.1	0.114 (0.14)	7.0	13.9

( )：Coefficient of variation

Figure 2 shows the relationship between age of concrete test pieces and coefficient of air permeability and moisture ratio. The coefficient of air permeability was below 0.1×10^{-16}m^2 at 35 days (7 days exposed in dry condition) and increased gradually. The moisture ratio at 35 days was about 7 to 7.5%, and decreased gradually to about 5 to 5.5% over the drying period. Air permeability showed the influence of water content in concrete, primarily because air permeability increased as moisture content decreased over the drying period. It is therefore important to note the influence of water content on air-permeability when examining in the field.

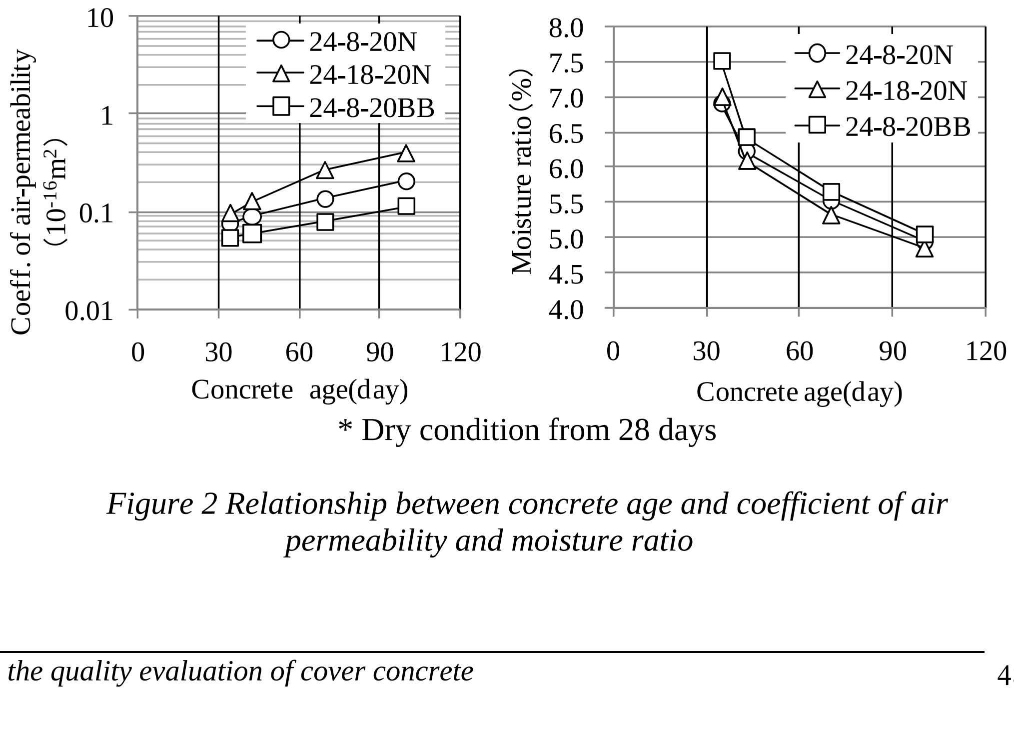

Figure 2 Relationship between concrete age and coefficient of air permeability and moisture ratio

When comparing concrete types, the coefficient of air permeability for 24-18-20N is higher than 24-8-20N with the same water-cement ratio due to the unit water content. 24-8-20BB using blast-furnace slag cement is lower than 24-8-20N with the same water-cement ratio in the case of normal curing at 28 days in 20ºC water, but the carbonated depth for blast-furnace slag cement was larger than for ordinary Portland cement due to the difference in alkali quantity.

3.3 Influence of construction works and condition

Figure 3 shows the effect of curing time on the coefficient of air permeability at the concrete surface. Upper, middle, and lower areas are plotted as well as the average of the three values. The coefficient of air permeability decreased with curing time, and some correlation between the coefficient of air permeability and carbonation depth could also be seen in Figure 3. These results shown that it is possible to determine the extent of curing by the coefficient of air permeability at the concrete surface.

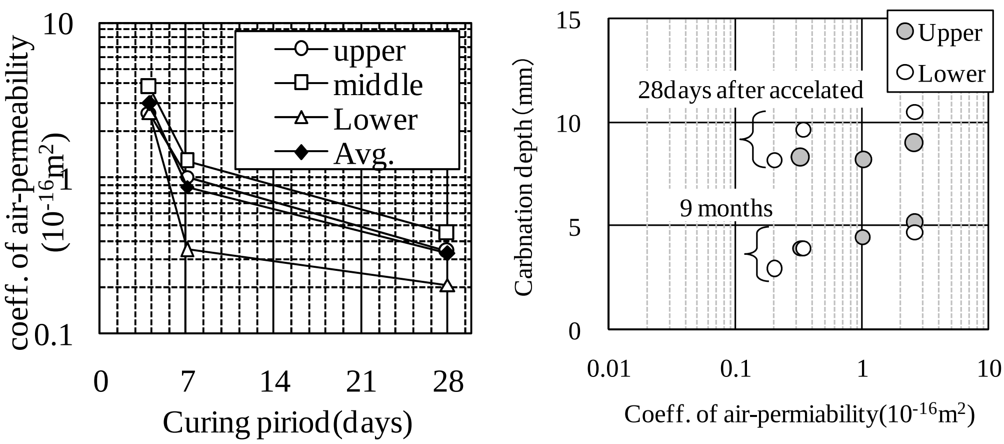

Figure 3 Test results of coefficient of air permeability and carbonation depth (Series 1, 24-8-20N)

Figure 4 shows the coefficient of air permeability results and their related coefficient of variation for various construction works and conditions. In this case, the form was removed at 5 days. Comparing reinforced and non-reinforced results, it can be seen that for reinforced specimens the air permeability in all areas of the specimens are fairly similar, whereas for non-reinforced specimens measurements in the upper area tended to be larger than the middle and lower areas. This is because the concrete is affect by consolidation due to self-weight and bleeding. This effect wasn’t seen in the case of reinforced concrete because the reinforcing steel-bar affected the self-load of the cover concrete.

For vibration time, vibrating for 45 seconds resulted in lower air permeability and lower coefficient of variation than the 15 seconds standard vibration time used in real construction works. The fact that coefficient of air permeability at the concrete surface and the coefficient of variation decreased for long vibration times suggests that the vibration time appropriate for permeability is different than that appropriate for compressive strength for the concretes used in this study.

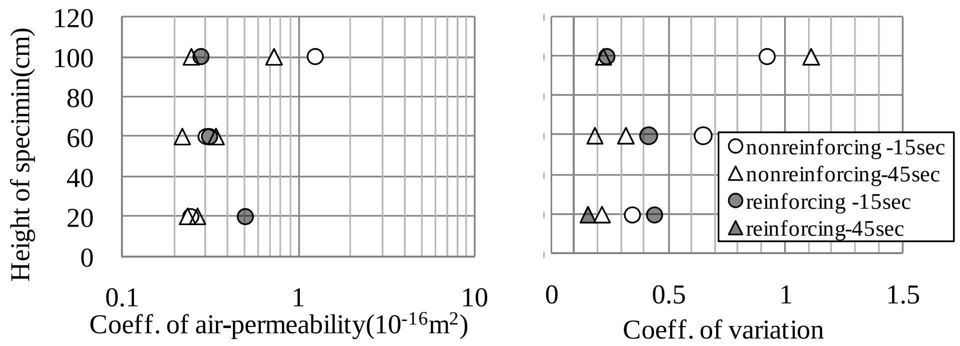

Figure 4 Influence of reinforcement and vibration time for consolidation (Removed form at 5 days, 24-8-20N ordinary Portland cement, tested at 91 days)

Figure 5 shows the influence of reinforcement and concrete slump. The coefficient of air permeability and variation for 18cm slump are larger than those of 8cm slump. One reasons for this result is that the air permeability of concrete itself is largely influenced by the unit water content. It is also possible that the coefficient of variation for 18cm slump increased due to excess vibration. However, it should be noted that segregation such as aggregate settling and bleeding due to vibration occur for concretes with high slump which are consolidated by excess vibration.

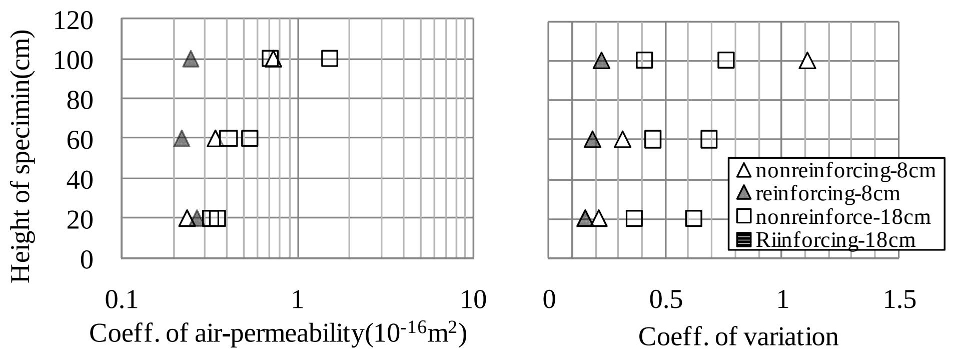

Figure 5 Influence of reinforcement and concrete slump (Removed form at 5 days, ordinary Portland cement, test at 91 days)

Figure 6 shows the influence of reinforcement and curing period. When comparing different cement types, the air permeability of concrete using blast-furnace slag cement and removed at 5 days was generally higher than that of concrete using ordinary Portland cement. There was little effect observed due to extended curing time in the case of removal at 12 days.

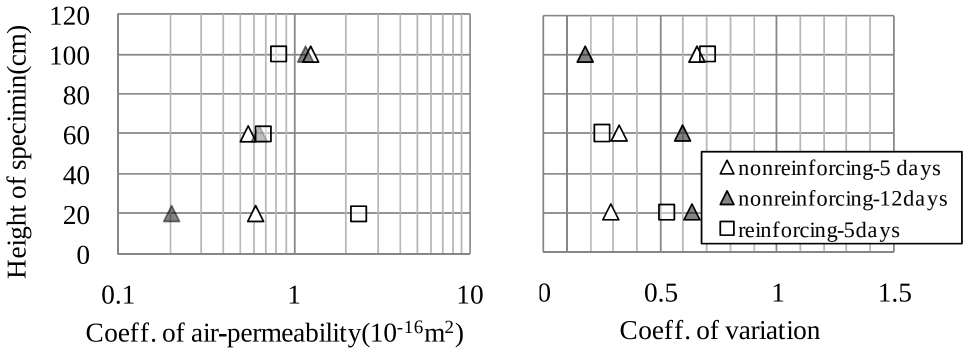

Figure 6 Influence of reinforcement and curing period
(Removed form at 5 days, 24-8-20BB blast furnace-slag cement, tested at 91 days)

The test results presented in Figures 4 through 6 were measured at 91 days, and the moisture ratios at the concrete surface at the measurement time were 4.4% to 5.8% (Figure 7). However, as was shown in Figure 2, the coefficient of air permeability is affected by the moisture ratio. Therefore, for comparing the full size specimens to the test piece, the average of test pieces results measured at 70 and 100 days is used because they have similar moisture ratio and concrete age.

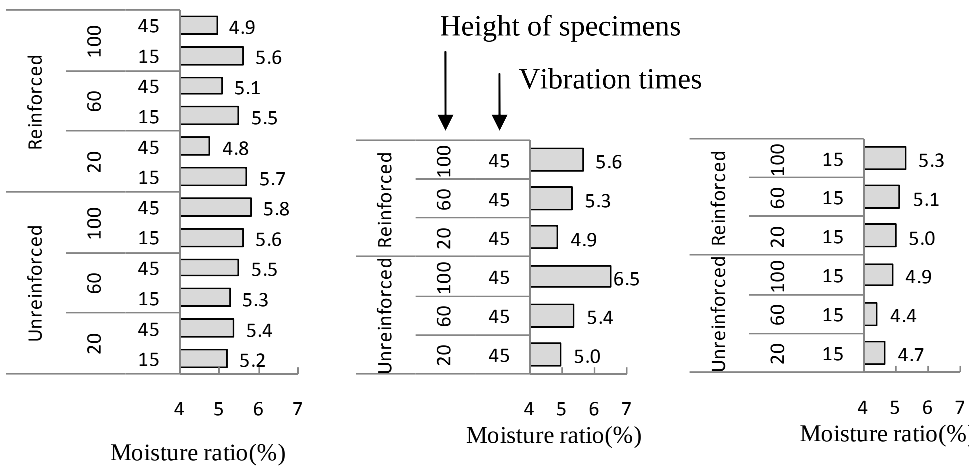

Figure 7 Moisture ratio of full size specimens

Figure 8 shows the ratio of the coefficient of air permeability affected by construction works and condition. The air permeability ratio of 24-8-20N and 24-18-20N with ordinary Portland cement was near 2, particularly for the 45 seconds vibration cases, but a few test results for the upper area were largely influenced by bleeding and low consolidation due to self weight. These test results were measured in the condition where forms were removed at 5 days. The coefficient of air permeability decreases as curing period increases, as shown in Figure 9, so the air permeability ratio will be smaller than the 5-day curing case if the curing period is extended.

On the other hand, the air permeability ratio of Portland blast-furnace slag cement is larger than the case for ordinary Portland cement. These tendencies are different from the results of test pieces for standard curing, suggesting that the influence of curing and bleeding is strong in the field.

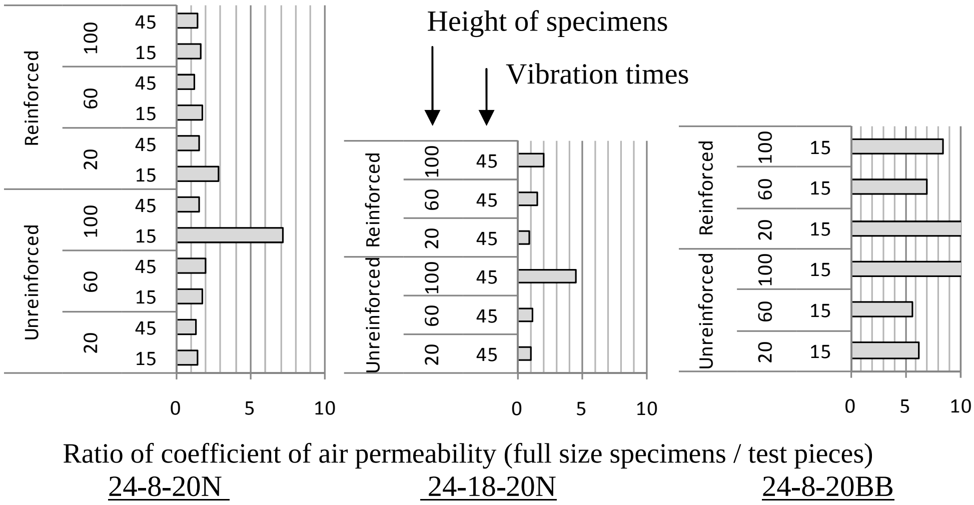

Figure 8 Ratio of coefficient of air permeability affected by construction works and conditions

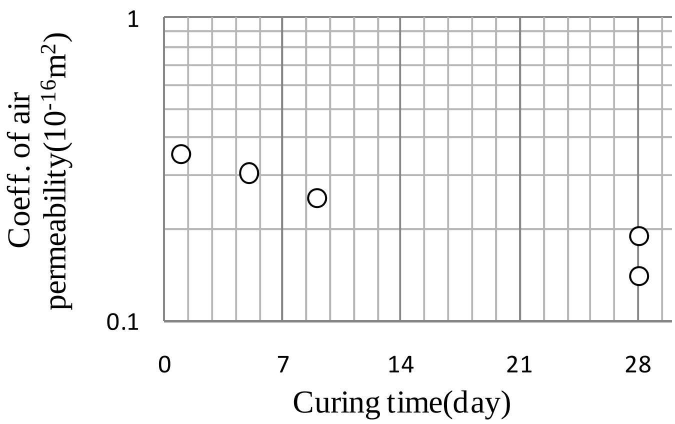

Figure 9 Relationship between concrete age and coefficient of air permeability (24-8-20N, vibration time 15 seconds, non-reinforced)

4. CONCLUSION

This study carried out an experimental investigation to evaluate the influence of the execution condition of works on the quality of cover concrete for ensuring the durability of structure concretes. The conclusions of this study are as follows:

1) The air permeability examination used this study may be able to evaluate the quality of cover concrete by the difference in curing time.

2) Air permeability index for full size specimens is larger than that of small size specimens (test pieces). This is due to the fresh concrete properties such as bleeding, consolidation time, and compaction by self-weight.
3) For concrete with 8cm slump, the air permeability index tended to decrease for of vibration times longer than the standard method. This result suggests that the vibration time appropriate for permeability is different than that appropriate for compressive strength.
4) The concrete which used Portland blast-furnace slag cement was more easily affected by the curing conditions and execution of work than concrete used ordinary Portland cement.

ACKNOWLEDGEMENT
The authors would like to express their thanks to Mr. Michael W. Henry of Katoyosh Laboratory, University of Tokyo who generously assisted.

REFERENCES

Torrent, R.J., 1992. A two-chamber vacuum cell for measuring the coefficient of permeability to air the concrete cover on site. *Materials and Structures*, Vol. 25, pp.358-365.
Isao UJIKE and Shigeyoshi NAGATAKI, 1988. A study on the quantitative evaluation of air permeability of concrete. Journals of the Japan Society of Civil Engineers, Vol.396/V-9, pp.79-87

THE SECULAR CHANGE OF TIMBER BRIDGE, "KINTAI-KYO"

Mikio KOSHIHARA
Institute of Industrial Science, the University of Tokyo,
4-6-1 Komaba, Meguro-ku, Tokyo 153-8505, Japan
kos@iis.u-tokyo.ac.jp

ABSTRACT

The timber bridge, "KINTAI-Kyo", is located in Iwakuni City, Yamaguchi Prefecture, JAPAN. It was built in 1673 and rebuilt several times until 2001 for washed away or its deterioration.
In 2001 "KINTAI-Kyo" was rebuilt as same shape in 1953. It is marked by the beauty of its five arches. The bridge length is 193m, every arch length is about 35m, its rise is about 5m and the wide is 5m. This bridge was made by some structural elements, KYOROKU(timber beam), KURA-GI(timber bracing), TASUKE-GI(timber parts), TAGA(iron hoop), KASUGAI(iron cramp), DABO(timber shear connector), etc.

After rebuilt in 2002, the shape of bridge, temperature and humidity are measured. The following results were provided by these measurements.
In the first year, the deformation at the center of bridge move 2cm downward for gaps between the structural elements. And there is a seasonal change of the deformation at the center of the bridge. At the center of bridge it moves upward in summer and downward in winter. The range of seasonal change is about 2cm. These changes are influences by temperature and humidity. In 2005 the irregular change of shape was observed in the autumn because no.1 bridge was washed away by the typhoon. These measurements have a possibility of safety diagnosis for timber bridge.

1. INTRODUCTION

Figure.1 shows an elevation of "KINTAI-KYO" bridge. The bridge consists of five timber ones and is supported on each stone pillar. The bridge is 193.3m long and 5m wide. Three bridges of the middle part, from No.2 to No.4, are 35.1m long and the rise is about 5m.

It was constructed first in 1673 of Edo era by a feudal lord of the time, Hiroyoshi Kikkawa, to meet the transportation problems which the people faced every time when the Nishiki River flooded. The structural idea of the bridge is said to have come from a story of a Chinese priest of the Ming Dynasty who settled in Japan about the arch-type stone bridges of China.

Unfortunately, the entire bridge was washed away by a flood in May, 1674. But it was reconstructed in October, 1674. After that the bridges were often repaired and reconstructed partially. Figure.2 shows the history of repair and reconstruction of the bridge. Each bridge was repaired about every 12–15 years and reconstructed about every 20 years. The bridge we can see today was constructed in 1953, because the entire bridge was washed away by a flood due to a typhoon in 1950, and a replica of the original bridge was reconstructed after the Edo design. This bridge has long life of about 50 years with replacement of the floorboards in 1967. The entire bridge was reconstructed from 2001 to 2004.

"KINTAI-KYO" bridge is composed of a lot of members. The main structure is KYOROKU (girder). The KYOROKU is composed of KETA (beam), KURAGI, TASUKEGI, HEIKINGI and ATOZUME. They are connected with DABO (dowels), KASUGAI (cramps), nails and MAKIGANE (hoops), as shown in Fig.2.

There are past researches about the secular changes of "KINTAI-KYO". The properties of vibration are measured and static loading tests were conducted by Waseda university[1]-[3] from 1953 with the interval of 5 years.

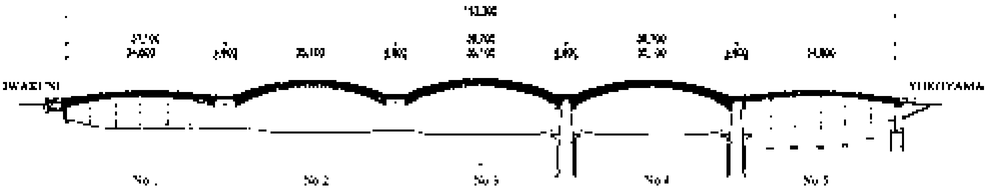

Figure 1: Elevation of "KINTAI-KYO" bridge

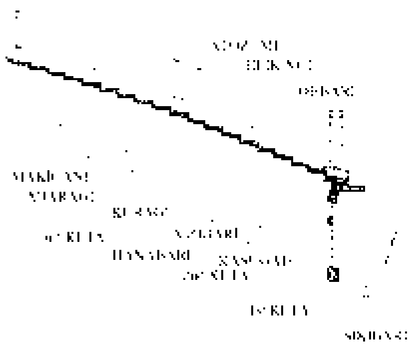

Figure 2: Detail of "KINTAI-KYO" bridge

Photo 1: "KINTAI-KYO" bridge

2. MEASUREMENT METHOD

2.1 Measurement Plan

The bridge shape and factors of change are being measured from 2003. In this year the no.4 and no.5 bridges were completed and just one year was passed from the no.3 bridge was completed. The no.2 and no.1 bridges were reconstructed in 2004 and there are the no.2 bridge passed about 50 years in 2001.

2.2 Shape

The shapes of the middle three bridges (no.2, no.3 and no.4) are being measured with theodolite. 13 targets were measured on every one side of bridge and 26 targets were measured on every bridge. Target points are the rivets bottom of the balustrades(*Photo.2*).

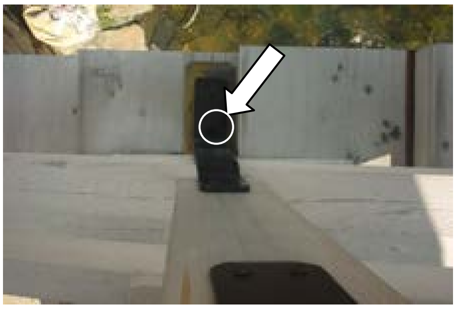

Photo 2: Target point of measurement

Measurements were started on March 14, 2003. In the first month the shape was measured with the interval of one week and in next two months it was measured with the interval of two weeks. After three month it was measured with the interval of one month and it was measured every 3 month from August 1, 2005.

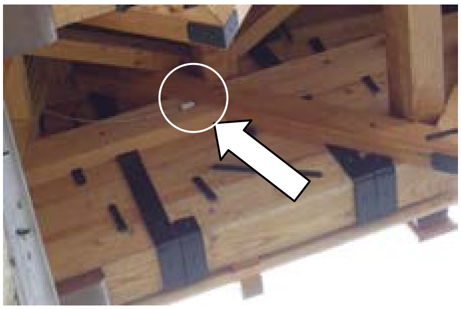

Photo 3: Thermo recorder

2.3 Temperature and humidity

Temperature and humidity influence the water content and the strain of wood. Especially wooden bridge is located in hard environment, above the river. Temperature and humidity under the bridge are being measured with thermo recorder(TandD's TR72S) every one hour(*Photo.3*).

2.4. Live load

The bridge is loaded by crossing persons and this load influences the deformation of the bridge. The number of sold tickets to cross the bridge was counted as the number of persons crossing bridge.

3. RESULTS

3.1 Secular change of the bridge shape

Figure.3 shows the deformation of the center of bridge. The horizontal axis shows how many days passed from the completion of each bridge. In the first year, from 0 to 365 days, the deformation of center of all bridges went down about 2 cm. But the deformation of no.2 was a little small. It is because this no.2 bridge has completed lastly and there is no construction after completion. After the first year they go up in summer and go down in winter. The width of change is about 1.5cm. The deformation of each point of no.4 bridge in the summer (Aug. 1, 2006) and in the winter (Feb. 1, 2007) are shown in Figure.4. The maximum deformation of bridge is at the point of a third part of bridge.

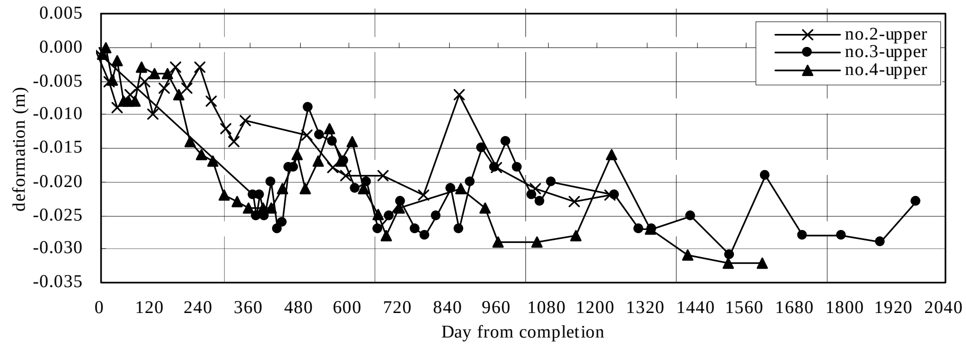

Figure 3: Deformation of the center of bridge (Upper part of a river)

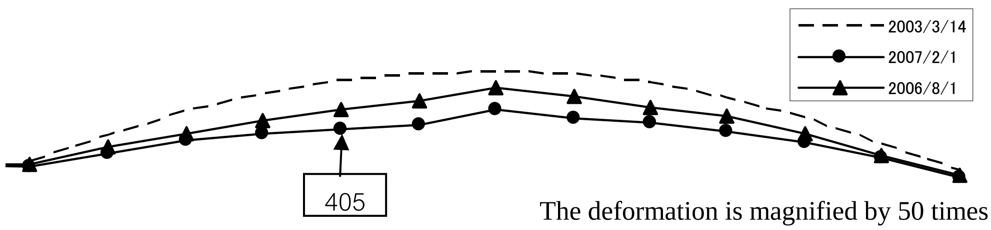

Figure 4: The deformation of no.4 bridge (Upper part of a river)

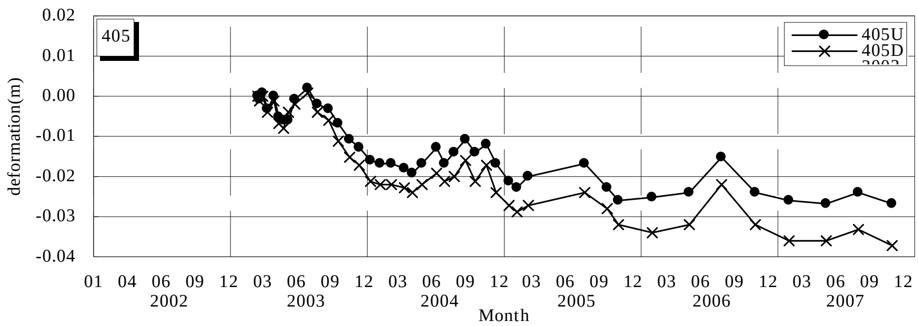

Figure 5: The deference between the upper part and the lower part of the river in bridge

The deference of the deformation between at the upper part and lower part of the river in bridge is shown in Figure.5. This figure shows the deformation at the point 405 shown in Figure.4. The deformation at the upper part of the river in bridge is larger than at the lower part of the river and its difference grows larger. The deference is about 1cm in 500cm width.

3.2 Factors of change

3.2.1 *Temperature and humidity*

Temperature and humidity were measured by thermo recorder every one hour. The results are shown in Figure 6 and Figure 7. Both temperature and humidity value are 7-day average before measuring the shape of bridges. The horizontal axis shows how many days from every January 1.

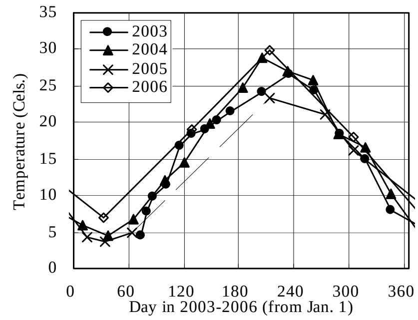

Figure 6: Change of temperature

Temperature changes cyclically. The highest temperature, about 30 degrees Celsius, was recorded in August and the lowest temperature, about 5 degrees Celsius, was recorded in February. Considering the change of relative humidity, it is high because this bridge is located above the river. Especially it is over 90% in every night and in every morning. But the change in the year is not cyclically and it is different from every year.

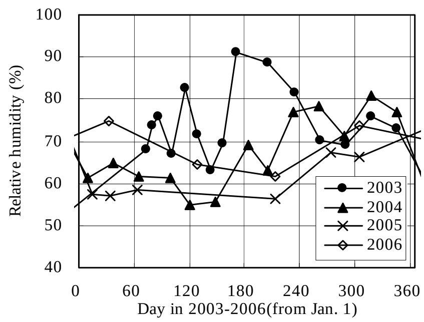

Figure 7: Change of relative humidity

3.2.2 *Live load*

The number of sold tickets to cross the bridge was counted. This ticket is round-trip ticket, so the number of crossing the bridge is twice as this number. The number of sold tickets in month is shown in Figure 8. About 80-240 thousand persons cross the bridge every month. There are two peaks and over 100 thousand persons cross the bridge in April and November. In April they enjoy the cherry blossom on the bank of river and in November they enjoy autumn leaves. There is small peak in August and this reason is summer vacation. There are two off-peak in July and December. In June and July is the rainy season in Japan and in December it is cold in Iwakuni-city.

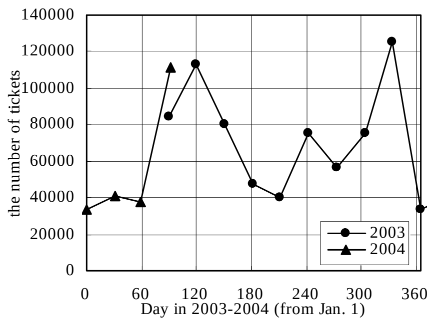

Figure 8: The number of persons crossing the bridge

These numbers are reference value and maybe lower limit because there were the crossing persons who did not buy the tickets.

3.2.3 *Gap of connectors*

"KINTAI-KYO" bridge is mainly composed of beams and these beams are connected to the other beam with dowels. These dowels are deformed by the shear force between beams. This deformation influences the shape of the bridges. By the field experiments in 2003[4]-[5] it is cleared

Photo 4: Deformation of dowel

Photo 5: The damage of no.1 bridge after Typhoon

that the vertical deformation of the center of bridge is 14.3mm if the gap between beams is 0.28mm and that deformation is 27.39mm if the gap is 0.67mm. By the survey of elements when the bridge was taken to pieces, the dowels were deformed about 2-4mm as shown Photo 4.

3.2.4 *Typhoon*

On September 6, 2005, the column of the no.1 bridge was washed away by a flood. The damage of no.1 bridge after typhoon 14 is shown in Photo 5.

4. DISCUSSION

4.1 The degree of influence to secular change

Timber bridge, "KINTAI-KYO" is changing its shape secularly and cyclically. Considering the cause of secular change of wooden bridge, there is many factors described in 3.2. In this chapter the degree of influence is considered.

4.2 Temperature and humidity

Temperature and humidity influence to the moisture contents of wooden members. Figure 8 shows the relation between the deformation of center of bridge and the moisture content. The moisture content of wooden member is calculated according to the theory of Hawley, Keywerth, Kollmann et.al.

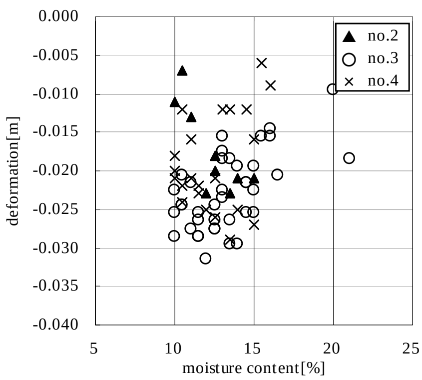

Figure 8: Relationship between moisture content and deformation

In the no.3 and no.4 bridge the correlation between the deformation and moisture content, but in the no.2 bridge there is no correlation. In this figure the moisture content is changing from 10% to 15%. If the moisture content of wooden member is change from 10% to 15%, the change of length parallel to grain is about 0.15% and length perpendicular to grain is about 1.5%. Supposing to the “KINTAI-KYO” is a 5m depth beam, the total shrinkage of beam depth is about 75mm. This deformation is larger than observed deformation. In the arch construction the deformation of the center moved upper if the length of the element is longer for the change of the moisture content of wooden elements. This is the reason for the seasonal change.

Figure 9 shows the deformation of the center of bridge. The “KINTAI-KYO”, especially the no.1 bridge, suffered terrible damage in the typhoon on September 6, 2005. In 2005 the irregular change of shape was observed from September to March, because no.1 bridge was washed away by the typhoon. These measurements have a possibility of safety diagnosis for timber bridge.

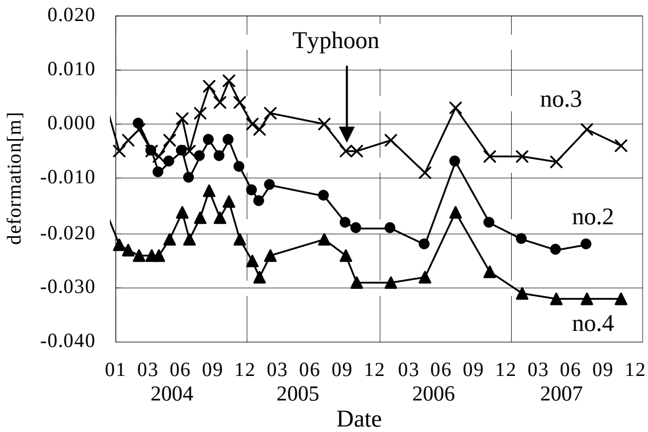

Figure 9: Deformation of the center of bridge and the Date

5. CONCLUSION

After rebuilt in 2002, the shape of bridge, temperature and humidity are measured. The following results were provided by these measurements.
In the first year, the deformation at the center of bridge move 2cm downward for gaps between the structural elements. And there is a seasonal change of the deformation at the center of the bridge. At the center of bridge it moves upward in summer and downward in winter. The range of seasonal change is about 2cm. These changes are influences by temperature and humidity. In 2005 the irregular change of shape was observed in the autumn because no.1 bridge was washed away by the typhoon. These measurements have a possibility of safety diagnosis for timber bridge.

ACKNOWLEDGEMENTS
The authors graciously acknowledge the financial support of the project granted from Iwakuni-city, Yamaguchi prefecture.

REFERENCES

[1] Takeshi SHINAGAWA: Report about reconstruction of “KINTAI-KYO”, Iwakuni-city, 1955
[2] Kusuo AOKI: Report about static and dynamic tests of “KINTAI-KYO”, 1953
[3] Research Center, Science Faculty, Waseda: Report about the Load Test of “KINTAI-KYO”,1998
[4] Mikio KOSHIHARA et al.: A study about “KINTAI-KYO” in Iwakuni Part 1-3, Summaries of technical papers of Annual Meeting Architectural Institute of Japan. C-1, pp.277-283, 2002
[5] Mikio KOSHIHARA et al.: A study about “KINTAI-KYO” in Iwakuni Part 4-6, Summaries of technical papers of Annual Meeting Architectural Institute of Japan. C-1, pp.469-474, 2003

THE SAFETY ASSESSMENT TO URBAN CITY OF COASTAL AREA BY WAVE-STRUCTURE INTERACTION

JINHONG KIM
Dept. of Civil Engineering, Chung-Ang University, Korea
Jinhkim@cau.ac.kr
SUNGDUK KIM
Dept. of Civil and Environment Engineering, Cheong-Ju University, Korea
Sungduk@cju.ac.kr

ABSTRACT

The present study is to estimate the wave height at the front face of breakwater, when the dredging is performed in the distant offshore from outer breakwater. The wave field of the problem is considered to be 2D plane and the configuration of the dredging region is designated by single horizontal long-rectangular type. The numerical simulation is performed by using the Green function based on the BIEM (Boundary Integral Element Method). The results of the present numerical simulations are illustrated by applying the normal incidence. It is shown that the ratios of wave height reduction at the front face of breakwater are approximately 20% by the effect of dredging on the sea bed. This study can effectively be utilized for safety assessment to various breakwater systems in front of urban city near the coastal area.

1. INTRODUCTION

To protect urban city of coastal area, many kinds of breakwaters have been installed and extended. Nevertheless, the disaster has attacked to the coastal region. This study is to investigate the reduction effect of wave height by dredging using the depth-discontinuity for the safe of coastal urban city behind the breakwater. The early studies on the interaction of incident waves with a dredge region has been investigated by Newman(1965), Hilay(1969), Lee and Ayer(1981), Miles(1982), Kirby and Dalrymple(1983). In all these researches, dredge region was assumed to be infinitely long and the problem was restricted to the horizontal and vertical coordinates.

Later, Williams(1990) and McDougal et al.(1996) presented the numerical model for involving two horizontal plane in case of single or multiple pits. 3D(three dimensional) model, which is based on the Airy wave theory, was investigated by Williams and Vazquez(1990) to analyze wave diffraction through a single trench. However, all of these studies in above, attentions were restrict to interaction for one or two aspects, which were occurred over pit(or trench) with discontinuity water depth.

The present study is about interaction of wave, which is propagated over pit with discontinuity water depth, and investigates this wave affecting the font face of breakwater and vicinity of coastal city. The wave interaction is connected to three boundary problems, which are interaction of discontinuity water depth and pit, discontinuity water depth within pit and breakwater, and pit and breakwater. The problem is considered in a two dimensional plane, and the configuration of dredging region on sea bed is a single-long rectangular type. The numerical simulation is performed by using the solution of the boundary integral equation based on the Green function.

In order to verify the present numerical model, comparison is made with the results of absolute and approximation solution presented by Koji and Mutsuo(1976) for regular wave diffraction at the front face of refracted breakwater without pit. The decreasing effects of diffracted wave field in vicinity of breakwater by dredging place with discontinuity water depth were investigated. The present study can provide information to design dredge line of the outer breakwater, and can effectively be utilized for safety assessment to various breakwater systems in front of urban city near the coastal area.

2. THEORETICAL DEVELOPMENT

The geometry of the problem is presented in figure 1 and figure 2. The boundary regions express S_1 (dredging boundary) and S_2 (breakwater boundary, respectively. Figure 2 is configuration of trench and division of region at the CD line in figure 1. AA line in figure 1 represents the points of wave diffraction investigated by present numerical model.

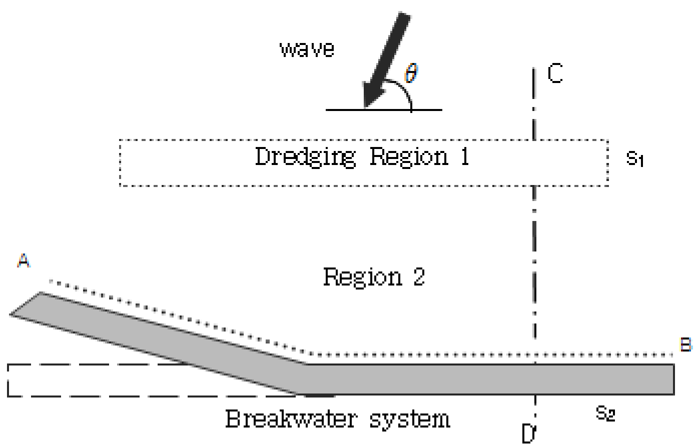

Figure 1: Layout of dredging region and breakwater systems.

The fluid region is taken to be inviscid and incompressible, and the flow irrotational, then it will be assumed that the fluid motion may be described in terms of a velocity potential $\phi(x,y,z,t)=\Phi(x,y,z)e^{-i\omega t}$. This potential must satisfy Laplace's equation, $\nabla^2\Phi=0$. It is subject to the usual boundary conditions on the free surface and seabed, and the solution of velocity potential can be given flowing forms.

$$\Phi_1(x,y,z)=\frac{ga}{\sigma}f_1(x,y)\frac{\cosh[k_1(z+d)]}{\cosh(k_1 d)} \quad ; \text{ Region 1} \tag{1}$$

$$\Phi_2(x,y,z)=\frac{ga}{\sigma}f_2(x,y)\frac{\cosh[k_2(z+h)]}{\cosh(k_2 h)} ; \text{ Region 2} \tag{2}$$

where, a is incident wave amplitude, d is water depth within dredging region, h is water depth of fluid region(vicinity of breakwater), f_j (j =1, 2) is wave function, subscript 1 represents dredging region, subscript 2 represents region without dredging region, and the wave numbers k_j (j =1, 2) are defined by

$$\omega^2 = gk_1\tanh(k_1 d) \qquad ; \text{Region 1} \tag{3}$$

$$\omega^2 = gk_2\tanh(k_2 h) \qquad ; \text{Region 2} \tag{4}$$

where ω is angular frequency and g is the gravitational acceleration.

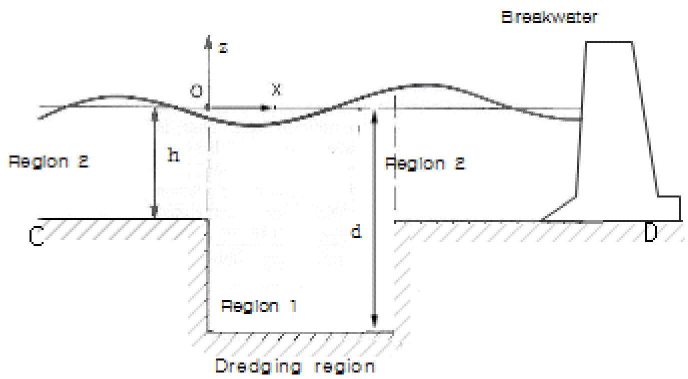

Figure 2: Definition sketch of dredging region and boundary surfaces.

The wave function can be described as following form.

$$f(x,y)_j = f_{i_j}(x,y)+f_{r_j}(x,y)+f_s(x,y) \qquad j=1,2 \tag{5}$$

$$f_{i_j}(x,y)=-ie^{ik_j(x\cos\theta+y\sin\theta)} \qquad j=1,2 \tag{6}$$

$$f_{r_j}(x,y)=-ie^{ik_j(x\cos\theta-y\sin\theta)} \qquad j=1,2 \tag{7}$$

where f_i is incident wave function, f_r reflective wave function, and f_s is scattered wave function. $f_s(x,y)$ should be satisfied by Helmholtz equation.

$$\frac{\partial^2 f_s}{\partial x^2} + \frac{\partial^2 f_s}{\partial y^2} + k_j^{\,2} f_s = 0 \qquad j = 1, 2 \tag{8}$$

Continuity of mass flux and pressure across the fluid interface between the interior dredging region (S_1) and vicinity of breakwater region (S_2) requires the following conditions be satisfied there:

$$d\frac{\partial f_1}{\partial n} = h\frac{\partial f_2}{\partial n} \qquad j = 1, 2 \qquad \text{on } S_1 \tag{9}$$

$$\Phi_1 = \Phi_2 \qquad \text{on } S_1 \tag{10}$$

The boundary condition of vicinity of breakwater region without dredging region are described as,

$$\frac{\partial f_2}{\partial n} = 0, \quad \frac{\partial f_s}{\partial n} = -\left(\frac{\partial f_{i_2}}{\partial n} + \frac{\partial f_{r_2}}{\partial n}\right) \qquad \text{on } S_2 \tag{11}$$

The boundary condition each regions can be taken as eqn. (12) and (13) through $\partial f_1 / \partial n = 0$, $\partial f_2 / \partial n = 0$ and eqn. (9), respectively.

$$\frac{\partial f_s}{\partial n} = -\frac{h}{d}\left(\frac{\partial f_{i_1}}{\partial n}\right) \qquad \text{on } S_1 \tag{12}$$

$$\frac{\partial f_s}{\partial n} = -\frac{h}{d}\left(\frac{\partial f_{i_2}}{\partial n} + \frac{\partial f_{r_2}}{\partial n}\right) \qquad \text{on } S_2 \tag{13}$$

Finally, the scattered component of the fluid potential in the S_3 is subject to a radiation or far-field boundary condition at large radial distances r, which may be written as

$$\lim_{r\to\infty} \sqrt{r}\left(\frac{\partial f_s}{\partial r} - ik_j f_s\right) = 0 \qquad j = 1, 2 \tag{14}$$

Applying Green's second identity to $f_s(x, y)$ and extending to full regions ($S_1 + S_2 + S_3$), boundary integral equations can be yielded as without dredging region (eqn. (15)) and with dredging region (eqn. (16)), respectively.

$$f_s(x, y) = -\frac{1}{2}\int_{S_2+S_3}\left[f_s(\xi,\eta)\cdot\frac{\partial}{\partial n}\left(-\frac{1}{2} iH_0^{(1)}(k_2 R)\right) - \left(-\frac{1}{2} iH_0^{(1)}(k_2 R)\right)\cdot\frac{\partial}{\partial n} f_s(\xi,\eta)\right] \tag{15}$$

$$f_s(x, y) = -\frac{1}{2}\int_{S_1+S_2+S_3}\left[f_s(\xi,\eta)\cdot\frac{\partial}{\partial n}\left(-\frac{1}{2} iH_0^{(1)}(k_j R)\right)\right.$$

$$-\left(-\frac{1}{2}iH_0^{(1)}(k_jR)\right)\cdot\frac{\partial}{\partial n}f_s(\xi,\eta)\Bigg] \qquad j=1,2 \qquad (16)$$

where, (ξ,η) is the coordinate of point on the boundary(S_1, S_2) and (x,y) is the coordinate of arbitrary point in the Region 1 and 2, n is the normal direction to S, $H_0^{(1)}$ is the Hankel function of the first kind of order zero, and $R^2=(x-\xi)^2+(y-\eta)^2$. The scattered wave has no effect on the imaginary boundary line (S_3) and then $f_s(x,y)=0$ on S_3 . Applying boundary condition to eqn. (15) and (16) and considering reflection coefficient K_r, eqn. (15) and (16) become

$$f_s(x,y)=-\frac{1}{2}\int_{S_2}\left[f_s(\xi,\eta)\cdot\frac{\partial}{\partial n}\left(-\frac{1}{2}iH_0^{(1)}(k_2R)\right)\right.$$
$$\left.+K_r\left(-\frac{1}{2}iH_0^{(1)}(k_2R)\right)\cdot\left(\frac{\partial f_{i_2}}{\partial n}+\frac{\partial f_{r_2}}{\partial n}\right)\right]ds \qquad (17)$$

$$f_s(x,y)=-\frac{1}{2}\int_{S_1}\left[f_s(\xi,\eta)\cdot\frac{\partial}{\partial n}\left(-\frac{1}{2}iH_0^{(1)}(k_1R)\right)+\frac{h}{d}\left(-\frac{1}{2}iH_0^{(1)}(k_1R)\right)\cdot\left(\frac{\partial f_{i_1}}{\partial n}\right)\right]ds$$
$$-\frac{1}{2}\int_{S_2}\left[f_s(\xi,\eta)\cdot\frac{\partial}{\partial n}\left(-\frac{1}{2}iH_0^{(1)}(k_2R)\right)+K_r\left(-\frac{1}{2}iH_0^{(1)}(k_2R)\right)\cdot\frac{h}{d}\cdot\left(\frac{\partial f_{i_2}}{\partial n}+\frac{\partial f_{r_2}}{\partial n}\right)\right]ds \qquad (18)$$

Approaching the coordinate of arbitrary point (x,y) to the coordinate of point (ξ,η) on the boundary(S_1, S_2), the following integral equation can be written as,

$$f_s(x,y)=-\int_{S_2}\left[f_s(\xi,\eta)\cdot\frac{\partial}{\partial n}\left(-\frac{1}{2}iH_0^{(1)}(k_2R)\right)\right.$$
$$\left.+K_r\left(-\frac{1}{2}iH_0^{(1)}(k_2R)\right)\cdot\left(\frac{\partial f_{i_2}}{\partial n}+\frac{\partial f_{r_2}}{\partial n}\right)\right]ds \qquad (19)$$

$$f_s(x,y)=-\int_{S_1}\left[f_s(\xi,\eta)\cdot\frac{\partial}{\partial n}\left(-\frac{1}{2}iH_0^{(1)}(k_1R)\right)+\frac{h}{d}\left(-\frac{1}{2}iH_0^{(1)}(k_1R)\right)\cdot\left(\frac{\partial f_{i_1}}{\partial n}\right)\right]ds$$
$$-\int_{S_2}\left[f_s(\xi,\eta)\cdot\frac{\partial}{\partial n}\left(-\frac{1}{2}iH_0^{(1)}(k_2R)\right)+K_r\left(-\frac{1}{2}iH_0^{(1)}(k_2R)\right)\cdot\frac{h}{d}\cdot\left(\frac{\partial f_{i_2}}{\partial n}+\frac{\partial f_{r_2}}{\partial n}\right)\right]ds \qquad (20)$$

A diffraction coefficient of regular wave, K_d is defined as

$$K_d=\left|f_s(x,y)\right| \qquad (21)$$

3. NUMERICAL RESULTS AND ANALYSIS

3.1 Validation of the numerical model.

A computer program has been developed to implement the above theory for regular wave diffraction vicinity of breakwater by dredging on the sea bed. The present numerical results have been investigated the reduction of wave height at the front face of refracted breakwater by comparing the absolute- and approximate solutions presented by Koji and Mutsuo(1976). The present numerical model can be studied wave height distributions at the vicinity of breakwater with dredging or without dredging, respectively. The conditions of calculation and configuration of refracted breakwater in regular waves by Koji and Mutsuo(1976) are defined as incident wave angle $\theta = 45^\circ$, angle of refracted breakwater $\beta = 135^\circ$, reflection coefficient $K_r = 0.8$, and length of breakwater =2*L*, respectively.

Figure 3 shows a comparison of the results at the AB line(Fig. 1) for the diffraction coefficient of regular waves at the front face of refracted breakwater obtained by the present numerical model and those of Koji and Mutsuo(1976).

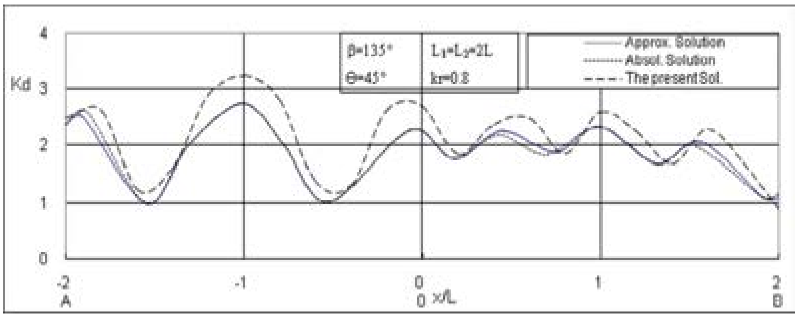

Figure 3: Comparision of wave diffractions of present study with those of approximate and absolute solutions.

In a comparison from Figure 3, it is noticed that the diffraction coefficient at the front face of refracted breakwater by present numerical model is little bit higher than results of Koji and Mutsuo(1976), because they performed at the infinite refracted breakwater. So, present numerical model have been performed at the finite refracted breakwater considering phase difference and wave scattering by interaction between incident waves and reflect wave, this study is more accurate than previously results.

3.2 Numerical examples

Numerical examples are presented to investigate the influences by dredging at the front face of refracted and straight breakwaters.

In this study, the condition of calculations are water depth in the vicinity of breakwater $h = 7m$, water depth within dredging region $d = 14m$, and incident wave angle $\theta = 90^\circ$ for regular wave, respectively. Figure 4 presents the results for the diffraction coefficient obtained by the present numerical model with and without dredging at the front face of refracted and straight breakwater, respectively.

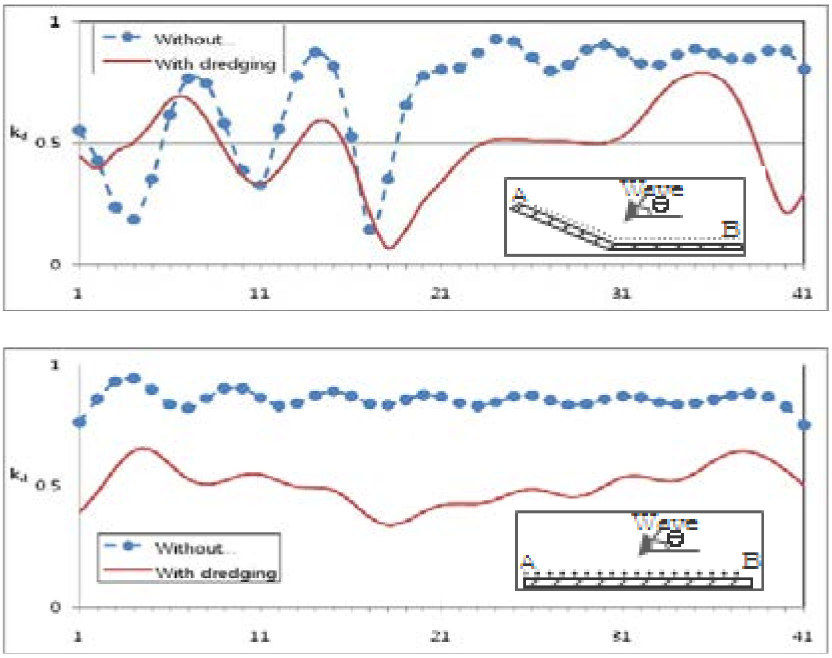

Figure 4: Wave height distributions at the front face of breakwater systems with or without dredging.

For the case of refracted breakwater with a dredging at the offshore sea bed as shown in Figure 4, the reduction of the relative wave height can be observed right side of breakwater from refracted point. This reduction is 15.4% less than the numerical results for the case without dredging. For the case of straight breakwater with a dredging, wave height is reduced all line of breakwater. This reduction is 20.4% less than results without dredging.

Figure 5 presents the contours of the wave height near the breakwater due to regular diffraction wave with two case of breakwater. From the results a dredging pit may provide an excellent mean to protect from wave attack. It can be seen that wave energy is weak by discontinuity water depth (dredging) and coastal city behind breakwater can be saved during stormy season.

4. CONCLUSIONS

The present study is to estimate the decreasing effects of diffracted wave fields around breakwater, for the case of dredging is performed at offshore sea bed. This study is about to the compositive interaction for the three problems; dredging boundaries, depth discontinuity of dredging, and breakwater boundaries. The boundary conditions are established for those problems and applied to the boundary integral equation.

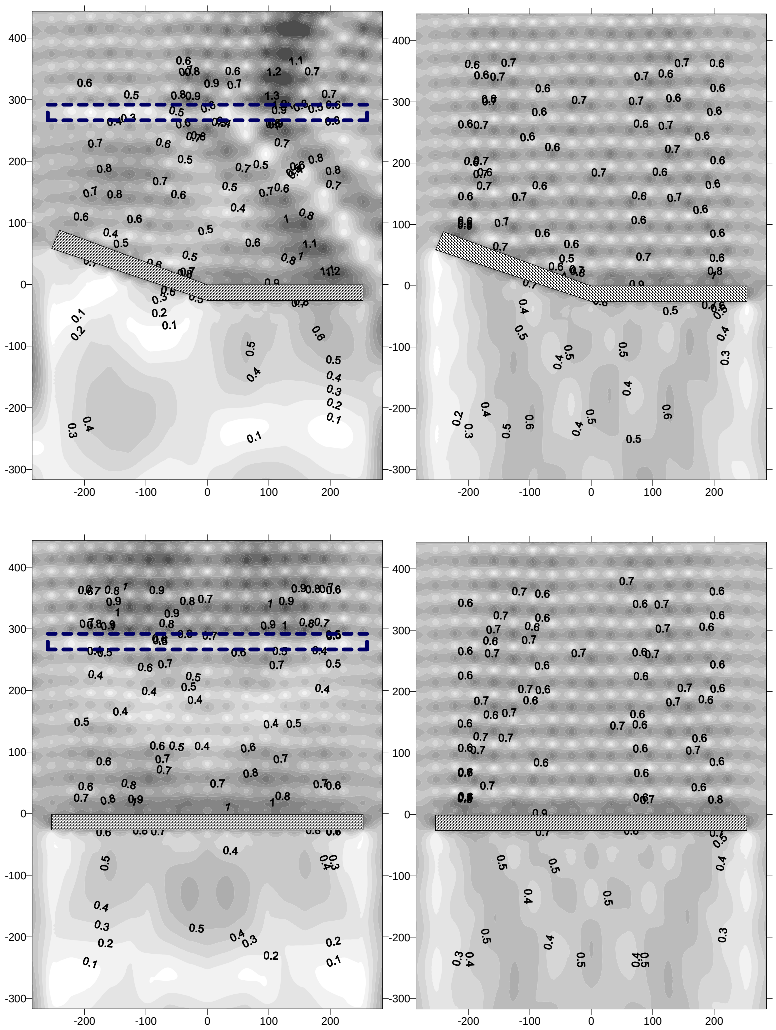

Figure 5: Contour plots of diffraction coefficients at the breakwater systems with or without dredging.

Results for the incident wave conditions have been presented to illustrate the wave height distribution of the wave field of breakwater by dredging. A dredging pit may protect from severe wave attack and it can be contributed for the safety of coastal city by sever wave environment such as storm surge.

It is noticed that the results from the present numerical model accurately provides the diffracted wave height of vicinity of breakwater systems, when dredging is performed at the offshore sea bed, and so may be extended to apply with confidence in harbor planning and design applications.

REFERENCES

Brown, A., 1997. *How to format references*. Unpublished report, NIWA, Christchurch, New Zealand.

Davoren, A., and Mosley, M. P., 1986. Observations of bedload movement, bar development and sediment supply in the braided Ohau River. *Earth Surface Processes & Landforms* 11, 643-652.

Mosley, M. P., 1979. Sediment sources in the Harper-Avoca Catchment. *Forest Research Technical Paper* 68, New Zealand Forest Service, Wellington.
Mosley, M. P., 1997. Motu River. In Jayawardena, A. W., Takeuchi, K., and Machbub, B. (editors), *Catalogue of Rivers for Southeast Asia and the Pacific*, Vol 2, UNESCO-IHP Regional Steering Committee, Jakarta, 226-235.
Schumm, S. A., Mosley, M. P., and Weaver, W. E., 1987. *Experimental geomorphology: the study of small landforms.* John Wiley, New York.

Hilaly, N., 1969. Water waves over a rectangular channel though a reef. *Journal of Waterways and Harbor Division, ASCE*, 95(1):77-94.
Kirby, J.T. and Dalrymple, R.A., 1983. Propagation of obliquely incident water waves over a trench. *Journal of Fluid Mechanics*, 133, 47-63.
Koji, K. and Mutsuo, O. 1976. A study of wave height distribution along a breakwater with a corner. *Report of the Port & Harbor Research Institute*, 15(2), 55-88.
Lee, J.J. and Ayer, R.M., 1981. Wave propagation over a rectangular trench. *Journal of Fluid Mechanics*, 110, 335-347.
McDougal, W.G., Williams, A.N. and Furukawa, K., 1996. Multiple-pit breakwaters. *Journal of Waterway, Port, Coastal and Ocean Engineering, ASCE*, 122(1), 27-33.
Miles, J.W., 1982. On surface wave diffraction by a trench. *Journal of Fluid Mechanics*,115, 315-25.
Newman, J.N., 1965. Propagation of water waves over an infinite step. *Journal of Fluid Mechanics*, 23, 399-415.
Williams, A.N., 1990. Diffraction of long waves by rectangular pit. *Journal of Waterway, Port, Coastal and Ocean Engineering, ASCE*, 116(4), 459-469.
Williams, A.N. and Vazquez, J.H., 1991. Wave interaction with a rectangular pit. *Journal of Offshore Mechanics and Arctic Engineering*, 113, 193-198.

PARALLEL SESSION 8

ANALYZING IMPACTS OF SEA LEVEL RISE ON COASTAL CITIES WITH FOCUS ON FLOODS AND SALINITY FLUX

MD. JABED ABDUL NASER BHUIYAN AND DUSHMANTA DUTTA
Monash University, Churchill, VIC 3842, Australia
Dushmanta.Dutta@sci.monash.edu.au

ABSTRACT

Coastal zones are particularly vulnerable to climate variability and change. In the last century, sea level rose on average 10-12cm per decade and in much higher rates in some coasts due to land subsidence. The 4th IPCC report highlights the increased vulnerability of the coastal urban areas around the world due to sea level rise in 21st Century. Key concerns due to sea level rise include flooding and salinity and its implications for water resources. Rising sea level increases the salinity of both surface water and ground water through salt water intrusion.

It is important to determine the impacts of sea level rise on flooding and salinity to devise suitable adaptation and mitigation measures to reduce impacts of floods and salinity intrusion in coastal cities. The paper presents the outcomes of a study conducted in the coastal area of Gorai river basin in the south west Bangladesh for developing a comprehensive understanding of the possible effects of sea level rise with the aid of hydrodynamic modelling. A newly developed salinity flux model was integrated with an existing hydrodynamic model to simulate floods and salinity in the complex waterways in the coastal zone of Gorai river basin. The model was applied under a range of future scenarios and the results indicate both spatial variability of risk and changes in flood and salinity characteristics between now and under sea level rise scenarios.

1. INTRODUCTION

Coastal and shallow marine regions are among the most productive systems in the world (Mann, 1988; Glantz, 1992). The Intergovernmental Panel on Climate Change (IPCC) in its fourth assessment report presents some observational evidences of climate change in the coastal region. Some of the evidences are increased ocean temperatures, changes in precipitation amounts and corresponding upstream river discharge, rising sea level, increased flooding and inundation etc.

Flood magnitudes and frequencies will very likely increase in most regions — mainly as a result of increased precipitation intensity and variability —

and increasing temperatures are expected to intensify the climate's hydrologic cycle and melt snowpacks more rapidly (IPCC, 2007). Flooding can affect water quality, as large volumes of water can transport contaminants into water bodies and also increase transport through overloaded storm and wastewater systems. The lives of human beings and aquatic life are greatly dependant on the availability of fresh water and sea level rise can change the availability and distribution of fresh water. The water quality is a current problem in the coastal zone which is expected to be exacerbated by climate change and sea level rise. Sea level rise may also affect freshwater quality by increasing the salinity of coastal rivers and bays and causing saltwater intrusion, movement of saline water into fresh ground water resources in coastal regions resulting in decreasing water quality (Bashar and Hossain, 2006). Sea level rise may cause saline intrusion into the land and larger or more frequent storm surges may impact salinity in coastal zone. It would be more acute in the dry season, especially when freshwater flowing from rivers has diminished. Salinity intrusion due to reduction of freshwater flow from upstream, salinisation of groundwater and fluctuation of soil salinity are major factors and concerns. In Bangladesh the causes behind water quality deterioration in coastal areas are: climate change and sea level rise, decrease of upstream flow due to the Farakka Barrage in India, expansion of shrimp farms and Coastal Embankment Project, implemented during the 1960s. Coasts will be exposed to increasing risk, including coastal erosion due to sea level rise. The impact is exacerbated by increasing human-induced pressures (Nicholls *et al*., 2007).

The impacts of salinity are: more land will be salinity-affected and the intensity of the salinity effect will be increased, decreased productivity of agricultural land, increased food insecurity as naturally growing species disappear, serious scarcity of safe drinking water, loss of biodiversity, e.g. decrease in tree species and freshwater fish and socioeconomic problems, generally women are more vulnerable. There is clear evidence of increased saline intrusion in the coastal zones. For example in Bangladesh, in the coastal city of Khulna the main power station uses fresh water to cool its boilers by sending a barge upstream to get fresh water. Over the last one decade the barge has had to go further and further upstream to get suitable fresh water for the purpose (NAPA, 2005). Increased salinity intrusion due to sea level rise poses a great threat to the Sundarban forest. The Sundarban has already been affected due to reduced freshwater flowing through the Ganges river system over the last few decades particularly during the dry season. This has led to a definite inward intrusion of the salinity front causing various species of plants and animals to be adversely affected. Increased salt water intrusion is considered as one of the causes of top dying of Sundari trees.

Computer based mathematical model is now a well recognized tool for simulating these complex problems. Mathematical modeling has been carried out for more than three decades (Dutta, 1999). Growing needs of mathematical model made to improve its quality and technique. Traditional lumped conceptual type models cannot rightfully be claimed to be scientifically sound (Klemes, 1988). The study aims to develop a comprehensive understanding of the sea level rise impact on coastal water quality with the aid of mathematical model. The objective of the study is to develop a salinity flux model and integrate with an existing hydrodynamic model. Then the integrated model is used to assess the impact of sea level rise on flooding and salinity in the coastal zone.

2. STUDY AREA AND SALINITY INTRUSION

2.1 Location and Geophysical Environment

The model was applied to simulate flood event and salinity intrusion in the Gorai river basin located on the South West region of Bangladesh. Salinity intrusion is a major concern in this area as the rivers are tidal and sea salinity intrusion in these rivers is a major issue. The study area comprises an area of 32,280 sq. km between latitude 21˚30' N to 24˚00' N and longitude 88˚50' E to 90˚10' E. The annual average rainfall is 1,700 mm/year (ADB, 2005). The area is bounded by Ganges River in the north, tributaries from Meghna River in the east, international boundary in the west and the Bay of Bengal in the south (Fig. 1). The topography of the region is rather flat, and gently sloping towards the Bay of Bengal. Most of the area is protected with polders against river flooding. The downstream part of the area is covered with Sundarban forest.

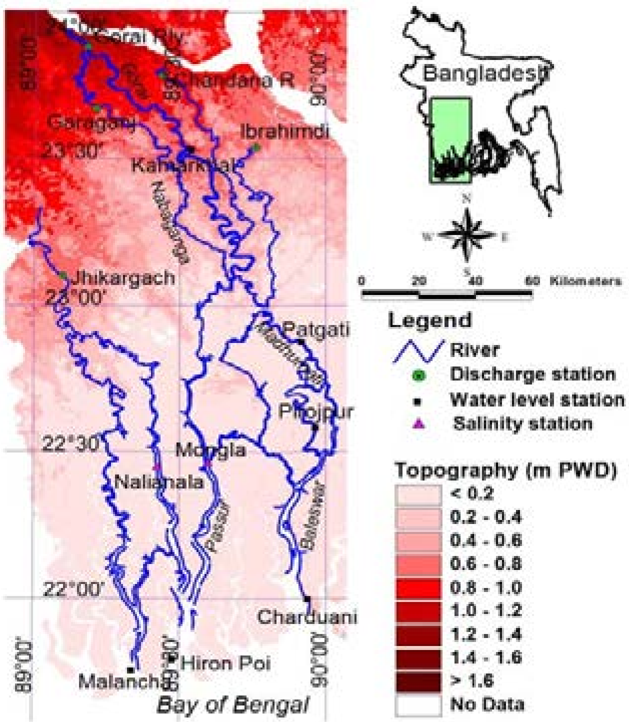

Figure 1: South western part of Bangladesh

2.2 Coastal flooding and Salinity Intrusion

The coastal zone is particularly vulnerable to flooding due to its low-lying lands and very poor defenses against flooding. Salinity intrusion in the river system downstream of the study area has been an issue. The Gorai-Madhumati River, a Ganges tributary, reduces its flow during the dry season. Due to the reduced flow of these rivers during the dry season, salinity intrudes into the river systems.

3. METHOD OF SIMULATION

3.1 Hydrodynamic Model

The hydrodynamic (HD) model was originally developed at the Public Work Research Institute (PWRI) of Japan (Yoshimoto *et al.*, 1992). The model has two major components: a one dimensional river flow component and a two dimensional floodplain component. The main characteristic of the model is the coupling between the river and floodplain components and dynamic flow exchange through the links. The flow exchange between the river and floodplain may occur for various scenarios such as levee failure or overtopping, flow through structures such as pump or sluice gate, etc. Points and extent of flood levee failure is governed by the water level in the river and the height of levee through the use of unsteady flow calculation in the river. The model uses the one dimensional unsteady dynamic wave form of St Venant's equation for river flow simulation and two dimensional unsteady equations for floodplain flow. These equations are derived using explicit solution scheme from the continuity and momentum equations (Dutta *et al.*, 2007). The river nodes and floodplain grids are linked through suitable conceptual equations representing different conditions of flow exchange.

3.2 Development of River Salinity Transport Model

A salinity transport model has been developed as part of this study to investigate transport processes within the entrance of a coastal lagoon through estimating the advection dispersion coefficients and integrated with the existing hydrodynamic model. Both the models work in FORTRAN environment.

The transport and dispersion of solute in the longitudinal case involves a mathematical representation in the form of the following single dimensional, partial differential equation (Fischer *et al*., 1979; Orlob, 1983; Henderson Sellars *et al*., 1990; Young and Wallis, 1992), usually known by Fickian Diffusion Equation or Advection Dispersion Equation (ADE),

$$\frac{\partial x(s,t)}{\partial t} + U\frac{\partial x(s,t)}{\partial s} = D\frac{\partial^2 x(s,t)}{\partial s^2} \quad (1)$$

where, $x(s,t)$ is the concentration of the solute at spatial location s and time t; U is the cross-sectional average longitudinal velocity; and D is the longitudinal dispersion coefficient.

The distance-time (x-t) planes for formulating explicit finite difference schemes of advection dispersion equation is shown in figure 2.

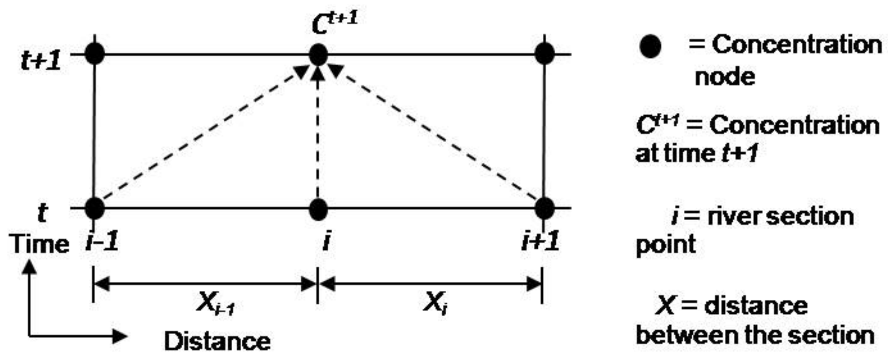

Figure 2: Distance-time plane used in the solution scheme of salinity model

In this equation, water is considered to be completely mixed over the cross-sections and the dispersive transport is proportional to the concentration gradient

3.3 Model Setup and Calibration

The model setup includes the calibration and verification. The total number of square grid is 129,120 with 500 m resolution. The existing polder heights have been added with the topography to represent the river bank protection. For river network, the Gorai river and its tributaries are considered. Daily discharges at Gorai Railway Bridge and Garaganj stations are used as upstream boundary and three hourly water level data at Charduani, Hironpoint and downstream point of Malancha are used as downstream boundary. Daily rainfalls at 24 gauging stations are used as internal runoff. No lateral overland flow is considered. The river network data included cross-sections at every 500 m interval between Gorai Railway Bridge and Bay of Bengal. Roughness coefficients for rivers and surface were estimated on the basis of the land use types (Dutta *et al*., 2009).

For the salinity model, freshwater salinity is considered as the upstream boundary (0.5 ppt). Observed salinity at Katka (Betmar Gang River), Hironpoint (Nilkamal River) and Dobaki South (Arpangasia River) have been used as downstream boundary. All the necessary data for HD and salinity model have been collected from the Institute of Water Modelling (IWM).

The hydrodynamic model has been calibrated and verified for two events of the year 2002. The calibrated parameter is manning's roughness in the river. Calibration and verification was performed using the water level data at some selected stations. Dry period flow during the month of April and May in the year 2002 has been used for calibration. The roughness coefficients were adjusted by trial and error. The coefficients were found to be within 0.015-0.035. Figure 3 shows the comparisons of simulated water level at Kamarkhali and Patgati with the observed data where the water levels are measured based on the datum of the Public Works Department (PWD). The PWD datum is 0.46 m lower than the mean sea level (Tingsanchali and Karim 2005).

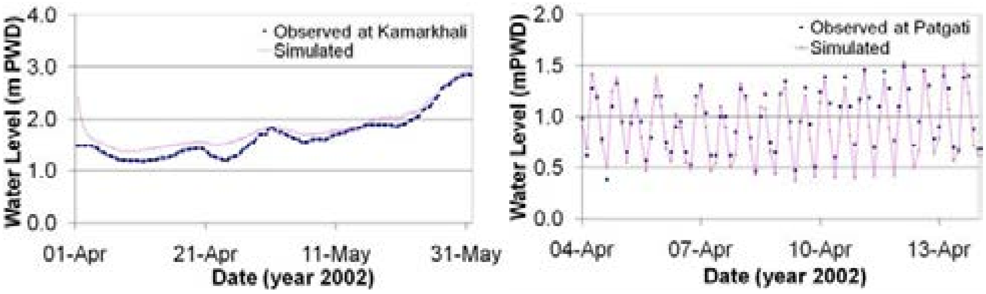

Figure 3: Water level comparisons at Kamarkhali and Patgati in calibration

For verification of the model parameter, wet season flow during the month of July and August has been considered in the year 2002. Figure 4 shows the comparisons of water level at Kamarkhali and Patgati.

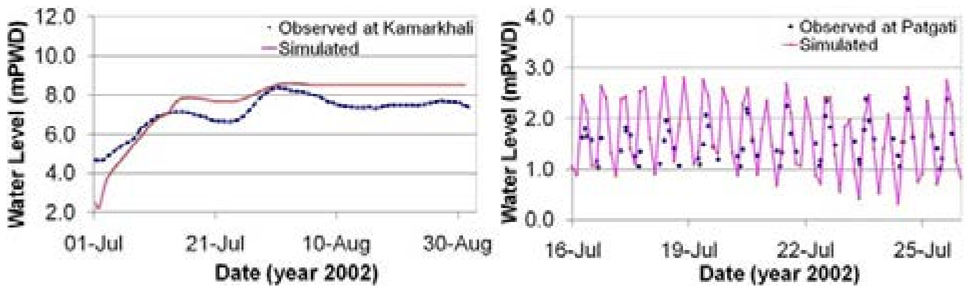

Figure 4: Water level comparisons at Kamarkhali and Patgati in verification

The model performance was determined based on mean and coefficient of determination (R^2). The computed mean value at Patgati and Pirojpur were found to be almost the same as the observed mean values, with a variation of +6% and +9% respectively. The R^2 values between the observed and computed hydrograph of water level were found to vary within 0.81 to 0.91, while this value should be 1 for perfect agreement. The scatter plots of observed and simulated water level at Kamarkhali and Patgati stations have been shown in the figure 5.

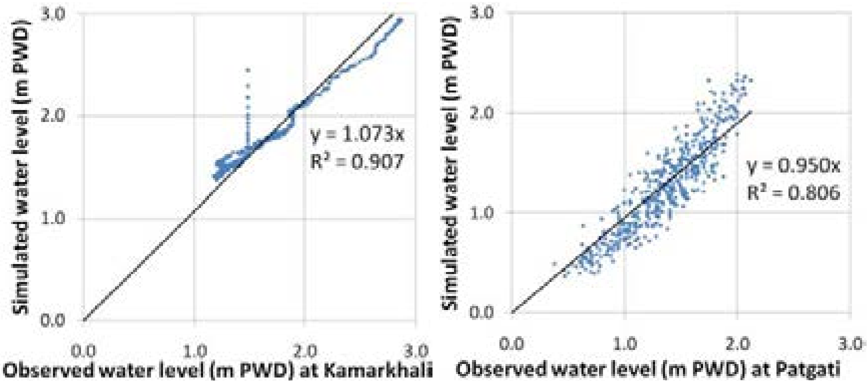

Figure 5: Scatter plots of observed and simulated water level at Kamarkhali and Patgati

The summarized results from the statistical analysis of water level data are shown in Table 1.

Table 1: Summarized results of water level data analysis

Station Name	**Mean water level (meter above PWD datum)**		**Coefficient of determination (R^2)**
	Computed	**Observed**	
Kamarkhali	1.83	1.68	0.91
Patgati	1.27	1.35	0.81

The salinity model has been calibrated by systematically adjusting values of selected system parameter to achieve an acceptable match between measured salinity and salinity with corresponding values predicted by the one dimensional advection dispersion model (Gates *et al*,. 2002). The calibration parameter is the dispersion coefficient in the river which was adjusted by trial and error. Figure 6 shows the comparison of observed and simulated salinity at Mongla station where the unit is parts per thousand (ppt).

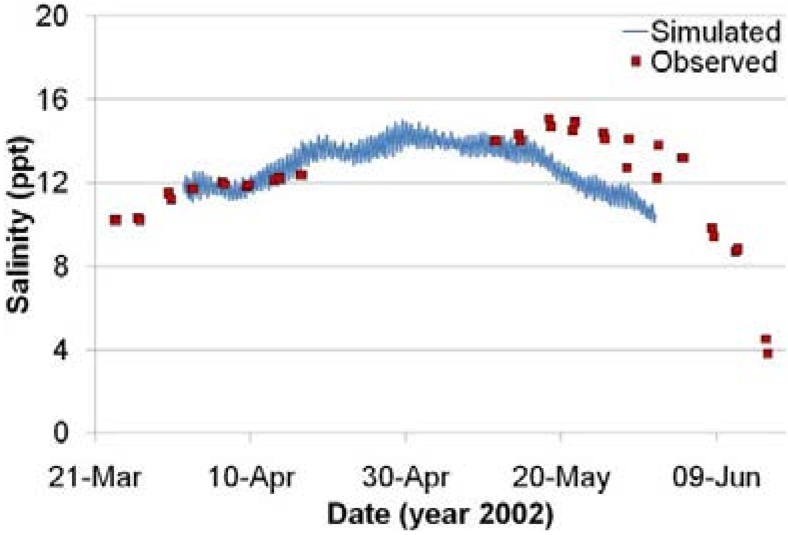

Figure 6: Salinity comparison at Mongla in calibration

4. IMPACT ANALYSIS

4.1 Flooding Extent

To analyze the effects of sea level rising, the sea level is raised by 59 cm in the hydrodynamic model to simulate flood at the end of 21st century. The depth of flooding in each grid was calculated by subtracting land elevation from the computed flood level. This methodology is similar to that described in the Manual of Economic and Social Commission for Asia and the Pacific (ESCAP, 1991). The flooded area was classified into four hazard categories based on three critical depths, 0.6, 1.0 and 3.5 m. Similar type of classification has been used in Tingsanchali & Karim (2005). The basis of selecting critical depths is briefly described herein. In general, plinth level above the ground is 0.6 m in school buildings, community centers and public buildings. In case of flood depths of more than 1.0 m, there is a possibility of death, and huge damage to agricultural production is expected. The minimum height of sills for shelters and also for one-storey buildings is usually 3.5 m. Typical flood maps without and with 59 cm SLR has been shown in Fig. 7. The flooded areas under different depth categories have also been summarized in table 2.

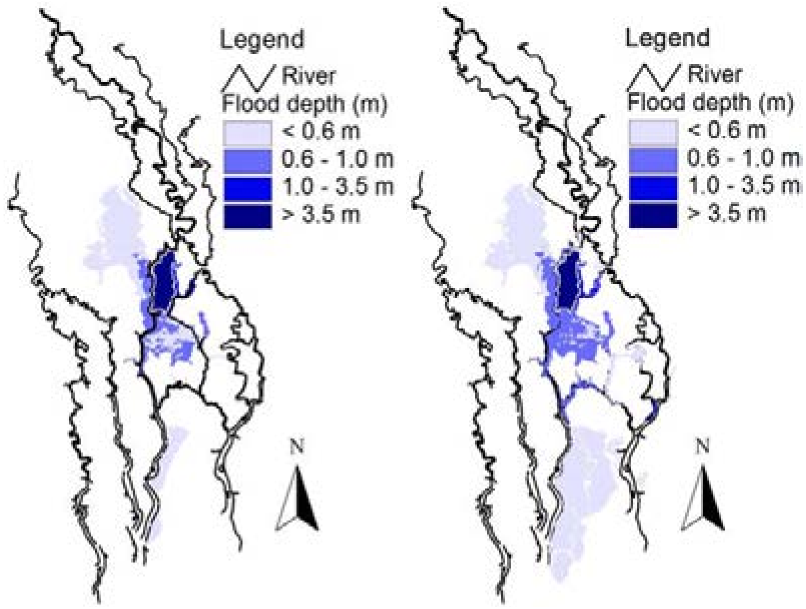

Figure 7: Simulated flood extent map without and with 59 cm SLR

Table 2: Computed flooded area under different depth category

Depth Category	Depth of flooding (m)	Flooded area (sq. km)		
		Present condition	**With 59 cm SLR**	**Increase (%)**
1	< 0.6	1146	1817	59
2	0.6 - 1.0	386	582.5	51
3	1.0 - 3.5	36	46.5	29
4	> 3.5	160.5	161	0.3

4.2 Salinity Increase

Due to sea level rise, the changes in maximum salinity at different stations have been shown in the following table (Table 3).

Table 3: Changes in maximum salinity due to 59 cm SLR

Name of Station	**Present condition (ppt)**	**With 59 cm SLR (ppt)**	**Salinity Increase (ppt)**
Mongla	14.9	15.7	0.8
Nalianala	16.3	17.0	0.7

The intrusion of salinity in the Passur river for 5 ppt and 10 ppt concentration has been simulated from the salinity model which has been summarized in the following table (Table 4);

Table 4: Salinity intrusion length in Passur river

Salinity front line (ppt)	**Salinity intrusion length (km)**
5	25.2
10	7.1

5. CONCLUSION

The sea level rise impact on coastal flooding and salinity increase has been estimated with an integrated hydrodynamic and salinity model. The study analyzed the impact in terms of flooding depth and extension, changes in salinity concentration and salinity intrusion. The results shows if Sea level is rised by 59 cm, the flooding depth below 0.6 m will be increased by more than 50% and 5 ppt salinity front will move about 25 km upstream. Such detailed impact assessment can be effectively used by planners and decision makers for adaptation to climate change in the highly vulnerable coastal areas of Gorai river basin. The model can be applied in other study area to quantify the changes in salinity due to climate change and salinity intrusion through the river.

REFERENCES

ADB, 2005. *Southwest Area Integrated Water Resources Planning and Management Project in Bangladesh*, Asian Development Bank.

Bashar, K. E. & Hossain, M. A., 2006. *Impact of Sea Level Rise on Salinity of Coastal Area of Bangladesh*. 9th International River Symposium. Brisbane, Australia.

Dutta, D. & Nakayama, K. 2009. *Effects of Spatial Grid Resolution on River Flow and Surface Inundation Simulation by Physically Based Distributed Modelling Approach*. Hydrological Processes, 23, 534-545.

Dutta, D., Alam, J., Umeda, K., Hayashi, M. & Hironaka, S., 2007. *A two-dimensional hydrodynamic model for flood inundation simulation: a case* *study in the lower Mekong river basin*. Hydrological Processes 21: 1223-1237.

Dutta, D., 1999. *Distributed modeling of flood inundation and damage estimation*. University of Tokyo. Doctor of Engineering: 168.

ESCAP, 1991. *Manual and Guidelines for Comprehensive Flood Loss Prevention and Management*. Bangkok, Economic and Social Commission for Asia and the Pacific.

Fisher, P., Abrahart, R. J. & Herbinger, W., 1997. *The sensitivity of two distributed non-point source pollution models to the spatial arrangement of the landscape*. Hydrological Processes 11: 241-252.

Gates, T. K., ASCE, M., Burkhalter, J. P., ASCE, M., Labadie, J. W., ASCE, M., Valliant, J. C. & Broner, I., 2002. *Monitoring and Modeling Flow and Salt Transport in a Salinity-Threatened Irrigated Valley*. Journal of Irrigation and Drainage Engineering, 128, 87-99.

Glantz, M.H., 1992. *Climate Variability, Climate Change, and Fisheries*. Cambridge University Press, New York, 450 pp.

Henderson-Sellars, B., Young, P. C., and Ribeiro da Costa, J., 1990. *Water quality models: rivers and reservoirs*, in Proc. 1988 Int. Symp. on Water Quality Modelling of Agricultural Non-Point Sources; US Agriculture Dept, Agricultural Research Service; 1990; Publication No. ARS-81, 381-420.

IPCC, 2007. *Climate Change Impacts, Adaptation and Vulnerability*. Fourth assessment report of the Intergovernmental Panel on Climate Change.

Klemes, V., 1988. *A Hydrological Perspective*. Journal of Hydrology, 100, 3-28.

Mann, K.H., 1988. *Production and use of detritus in various freshwater, estuarine and coastal marine ecosystems*. Limnology and Oceanography 33, 910-930.

NAPA (Bangladesh), 2005. *Formulation of Bangladesh Program of Action for Adaptation to Climate Change Project*.

Nicholls, R. J., Wong, P. P., Burkett, V. R., Codignotto, J. O., Hay, J. E., McLean, R. F., Ragoonaden, S. & Woodroffe, C. D., 2007. *Coastal systems and low-lying areas. Climate change 2007: Impacts, Adaptation and Vulnerability. Contribution of Working Group II to the Fourth Assessment Report of the Intergovernmental Panel on Climate Change*, M. L. Parry, O. F. Canziani, J. P. Palutikof, P. J. van der Linden and C. E. Hanson, Eds., Cambridge University Press, Cambridge, UK, 315-356.

Orlob, G. T. (ed.), 1983. *Mathematical Modelling of Water Quality: Streams, Lakes and Reservoirs*. J. Wiley, Chichester.

Tingsanchali, T. and M. F. Karim, 2005. *Flood Hazard and Risk Analysis in the Southwest Region of Bangladesh*. Hydrological Processes 19(10): 2055-2069.

Yoshimoto, T., Fueda, T., Ikeda, Y. & Kawakami, T., 1992. *Flood Simulation of Two Dimensional Unsteady Flood Model*. Technical Memorandum of Public Work Research Institute (PWRI). Japan, T. M. of PWRI No. 3105, ISSN 0386-5878, Public Works Research Institute.

Young, P.C., and Wallis, S.G., 1992. *Solute transport and dispersion in channels*, forthcoming in: K.J. Beven and M.J. Kirby (eds), Channel Networks, J. Wiley, Chichester.

INTEGRATED PLAN FOR FLOOD DISASTER MANAGEMENT BY CLIMATE CHANGES

KEEOH SHIM, BYUNGTAE YOO and KYUNGHO PARK
National Institute for Disaster Prevention, NEMA, Rep. of Korea
shimko, procsys, kh302@nema.go.kr

ABSTRACT

This research examined and presented the research tasks to be promoted in an effort to prevent disasters centered on the current work of the National Emergency Management Agency (NEMA) in terms of storm and flood damage so that damage due to natural disaster caused by climate change can be minimized. To explore the areas from the research aspect related to policy, this research presented the research tasks that can prevent or minimize damage caused by climate change as part of presenting NEMA's comprehensive plan pertaining to climate change by maintaining and developing the work promoted by NEMA based on the causes of and countermeasures for recent damage caused by natural disaster.

To determine the status of damage of such major facilities, this research collected and analyzed various damage survey reports, research reports and journal articles discussing the status, and cause analyses and countermeasures against damage caused by large-scale storm and flood-related disasters. Based on the collected data, this research classified and analyzed damages, causes, and countermeasures related to each of the facilities damaged by natural disaster. This research selected and presented 48 research tasks on climate change to be promoted by work in relation to NEMA's major work concerning storm and flood damage.

1. INTRODUCTION

As the average of global temperature continuously rises, climate change due to global warming causes unforeseeable and extreme meteorological changes such as heavy rainfall, typhoon, drought, and lightning. All these disasters are caused by the disruption of the water circulation system on earth by melting iceberg in the polar regions.

As the sea level rises due to the melting iceberg or swelling seawater caused by the rising_temperature, the rising level of seawater stood at 0.20cm/year in 2000, compared to 0.07cm/year in 1990 in the East Sea. In the West Sea, the rising level of sea level was also 0.20cm/year in 2000, compared to 0.14cm/year in 1990. On the other hand, in the South Sea, the rising rate of sea level stood at 0.34cm/year in 2000, compared to 0.32cm/year in 1990.

In other words, the average of the rising level of seawater was observed to increase in 2000, compared to 1990.

To explore the areas from the research aspect related to policy, this research presented the research tasks that can prevent or minimize damage caused by climate change as part of presenting NEMA's comprehensive plan pertaining to climate change by maintaining and developing the work promoted by NEMA based on the causes and countermeasures for recent damage caused by natural disasters.

To determine the status of damage of such major facilities, this research collected and analyzed various damage survey reports, research reports and journal articles discussing the status, and cause analyses and countermeasures against damage caused by large-scale storm and flood-related disasters. Based on the collected data, this research classified and analyzed damages, causes, and countermeasures related to each of the facilities damaged by natural disaster.

This research examined and presented the research tasks to be promoted in an effort to prevent disasters centered on the current work of the National Emergency Management Agency (NEMA) in terms of storm and flood damage so that damage due to natural disaster caused by climate change can be minimized.

2. VULNERABILITY ANALYSIS OF DISASTER CONTROL FACILITIES

As the population increases, bridges are built to cross rivers, and tunnels are constructed to address the inconvenience of climbing mountains. Note, however, that damages to those facilities built for man's convenience are on the rise each year as typhoon and heavy rainfall become stronger due to climate change. To minimize damages caused by natural disasters, presenting disaster prevention measures for coping with climate change as well as identifying the status and causes of damage are essential.

2.1 Amount of Damage to Facilities

This research used data from annual disaster reports according to facilities such as river, road, and farmland from 1977 to 2006 to minimize damages caused by disaster. In consolidating data, the amount of damage was categorized into the average damage amount for the last 10, 20, and 30 years.

Korea's damage amount according to facilities is ranked as follows: rivers/streams, roads, irrigation, farmland, erosion control work, military facilities, buildings, water channel, harbors, railways, ships, and schools.

2.2 Damage Status and Countermeasures according to Facilities

2.2.1 River/Stream Facilities

Korean peninsula is surrounded by the sea except the northern side; hence its oceanic climate. Therefore, damages caused by torrential rain are actually concentrated in summer, due mainly to the impacts of heavy rainfall and typhoon during summertime. Damages to rivers caused by torrential rain and typhoon cause various types of damages to the rivers. As such, damage cause analysis and countermeasures for preventing the recurrence of the damages were presented. We gathered storm and flood damage reports related to climate change as examined and analyzed by various on-site disaster reports.

2.2.2 Road Facilities

Damages caused by torrential rain and typhoon give rise to various types of damages to road facilities. In this context, damage cause analysis and countermeasures to prevent the recurrence of damage were presented in relation to road facilities including bridges. In this research, parts related to road facilities damage in various on-site disaster reports and journal articles dealing with storm and flood damage are extracted and consolidated.

2.2.3 Irrigation Facilities

Irrigation facilities in annual disaster reports referred to those related to farmland, such as reservoir. Interest in irrigation facilities related to farmland is huge, since farmers' attachment to land is strong considering the fact that Korea developed as an agricultural country. Damages to irrigation facilities caused by torrential rain and typhoon as a result of climate change cause various types of damages to irrigation facilities. Thus, damage cause analysis and countermeasures for preventing the recurrence of the damages that were presented. In this research, parts dealing with disaster caused by climate change in various on-site disaster reports dealing with irrigation facilities were extracted and arranged.

2.2.4 Farmland

Koreans' interest in farmland is huge, since farmers' attachment to land is strong, considering the fact that Korea developed as an agricultural country. Damages to farmland caused by torrential rain and typhoon as a result of climate changes, cause various types of damages to farmland. Thus, damage cause analysis and countermeasures for preventing the recurrence of the damages were presented. By examining and analyzing various on-site disaster reports dealing with farmland, this research extracted and consolidated parts dealing with disaster caused by climate change.

2.2.5 Erosion Control Work

As the strength of heavy rainfall and typhoon increases due mainly to climate change, damage to erosion control work caused by heavy rainfall and typhoon, comes in various forms. Thus, damage cause analysis and countermeasures for preventing the recurrence of the damages were presented. By examining and analyzing various on-site disaster reports dealing with erosion control work, this research extracted and consolidated parts dealing with disaster caused by climate change.

3. COMPREHENSIVE PLAN ACCORDING TO MEASURES FOR PREVENTING DAMAGES

For the tasks in the relevant research field, the work carried out by NEMA was identified and classified according to the criterion of relevance to the work. Toward this end, this research presented the details of the major work on storm and flood damage as performed by NEMA.

3.1 Presentation of Major Work Area

Measures for addressing the presented storm and flood damage based on the damage status and cause analysis in the reports and published manuscripts were selected as research area. The areas of major work carried out by NEMA based on storm and flood damage including the Natural Disaster Countermeasure Act are presented below.

- Rainwater runoff reduction facilities
- Consultation on pre-disaster impact review
- Natural disaster risk zone
- Comprehensive plan for reducing storm and flood damage
- Establishment and operation of flood control criteria for facilities
- Establishment and operation of flood control criteria for underground space
- Establishment of storm resistance design criteria
- Insurance for storm and flood damage

3.2 Presentation of Comprehensive Plan by Area

In presenting the comprehensive plan for countering storm and flood damage, this research classified related research tasks drawn from damage countermeasures by work area based on the areas of major work carried out and presented by NEMA.

3.2.1 Rainwater Runoff Reduction Facilities

○ Development of rainwater runoff reduction facilities: new rainwater runoff reduction facilities need to be developed through continuous research.

○ Development of runoff amount reduction criteria by basin : To reduce the peak runoff amount in relation to increasing runoff due mainly to climate change, the runoff amount may be reduced by causing rainwater to infiltrate underground during rain. There is a need to introduce the criteria for rainwater runoff reduction by basin and apply such as a pilot project by setting the runoff amount by basin to be reduced during rain.

○ Development of criteria for the establishment of rainwater runoff reduction facilities : The developed rainwater runoff reduction facilities are generally burdensome from an economic point of view; hence the need for the installation of rainwater runoff reduction facilities based on certain criteria when undertaking a development project. When a subject project installs facilities meeting the installation criteria, the development of various incentives and evaluation criteria based on which runoff reduction capability can be evaluated is considered necessary. In developing the installation criteria, the introduction of the charge system against projects generating a runoff amount beyond the appropriate amount is a worthwhile research area.

3.2.2 Consultation System for Pre-Disaster Impact Review

○ Disaster reduction area considering the development project's characteristics: Research tasks are promoted as follows to achieve the goal of implementing the system by analyzing the characteristics of the subject projects for consultation on pre-disaster impact.

3.2.3 Natural Disaster Risk Zone Control

○ Natural disaster risk zone criteria: Various risks can be managed by improving the type categorization of natural disaster risk zones into 6 through the amendment of the Enforcement Ordinance of the Natural Disaster Countermeasure Act. In designating natural disaster risk zones, there is a need for the central government to use the budget impartially through objective and common decision criteria.

○ Perceived area of natural disaster risk zone : Gradual improvement is promoted by categorizing natural disaster risk zones into 6 types. Note, however, that damage should be prevented by arousing consciousness on those zones through the education and promotion of local residents' perception of those zones to avoid damages.

○ Extension of natural disaster risk zone types : Natural disaster risk zones come in 6 types, but there is a need to expand the existing 6 types due to the diversification of disaster types as a result of the recent climate change; hence the need for the expansion of the selection of disaster types.

3.2.4 Comprehensive Plan for Reducing Storm and Flood Damage

○ Flood disaster : Disaster risk evaluation is needed, since the rainfall phase differs as a result of climate change. Determining the flood disaster risk requires evaluating the risk of areas adjacent to rivers and determining the inundation risk on the densely populated low land area.

○ Slope collapse : The need to suggest countermeasures against a region with landslide risk is raised by assessing the landslide risk stemming from rainfall concentration and vegetation change of mountains and forests due to climate change. Toward this end, there is a need to analyze areas with landslide risk associated with climate change using GIS and forecast those areas with landslide risk based on the analysis results.

○ Earth and sand runoff : The earth and sand runoff amount increases as the torrential rain's frequency rises as a result of climate change. The runoff earth and sand are deposited on the river bed, reducing water flow capability, which in turn may cause flood damage owing to insufficient water flow capability in case of flood.

○ Damage due to wind : Although climate change may reduce the frequency of typhoon, the size of typhoon increases; thus possibly causing huge casualties and property damage. Such damage is believed to be attributable to the increase in the maximum instantaneous speed of the wind.

3.2.5 Establishment and Operation of Flood Control Criteria for Facilities

○ Maintenance of design criteria for river and stream facilities : Uniformly deciding the design frequency of river facilities is not advisable; the impacts of urbanization within the basin and the importance of the river need to be considered; ditto for the evaluation of the impact of disaster risk associated with climate change. In this context, systematic supplementation and maintenance should be carried out by conducting continuous research in relation to the design frequency of river facilities.

○ Reinforcement of sewerage facilities-related criteria : The frequency of the planned rainfall amount exclusion plan of the sewerage facilities criteria should be upgraded considering the recent precipitation trend. This is because the existing design criteria may not be able to cope with the recent torrential rain or typhoon.

○ Maintenance and supplementation of agricultural production infrastructure (reservoir, etc.) : A reservoir among the agricultural production infrastructure is an effective means of securing the water amount; over 30,000 facilities including small reservoirs are built in Korea. The maintenance and supplementation of reservoir facilities are truly necessary to make them function smoothly.

3.2.6 Establishment and Operation for Underground Space

○ Introduction of flood control criteria for underground space : There is a need to decide continually whether the flood control criteria for underground space are appropriate through the investigation and examination of inundation risk of underground facilities by categorizing those structures where inundation damages often occur due to urbanized area flood and by estimating the areas to be surveyed for inundation by structure; examining the criteria for the design and inundation measures of advanced countries and introducing them to Korea are also essential.

○ System to cope with the inundation of underground space : When subways, underground malls, underground driveways, and common underground openings are flooded, an information system-based system should be established to cope with such inundation. Such system should be able to identify situation information in real time and determine the predicted inundation scale promptly. Ultimately, a comprehensive disaster prevention system for underground space needs to be built to disseminate situation information quickly, secure safer evacuation access, and minimize casualties.

○ Evacuation system in case of underground space inundation : Considering the underground space features, there can be restrictions in evacuation owing to the obstacles in the course of evacuation. Moreover, since there are few temporarily safe places before evacuating to a ground-level area in the case of flooding, large-scale casualties may occur due to sudden flood or inundation; hence the need for the establishment of an evacuation system for underground space and periodic education/training of local residents to reduce casualties.

3.2.7 Establishment of Storm Resistance Design Criteria

○ Correction of basic wind velocity and evaluation method development : Although the value of the basic average wind velocity has been determined in Korea, disasters are not appropriately forecast due to the lack of related criteria for various facilities. The reasonable evaluation and adjustment of the basic wind velocity require the establishment of wind velocity DB and evaluation technology on the wind environment.

○ Reinforcement of design criteria to cope with abnormal wind damage : Although there may be numerous types of national infrastructure facilities for considering wind load, the load calculation criteria applied to various facilities are not unified. As a result, different criteria are applied. Storm resistance design can be optimized by applying unified criteria to various facilities and by securing safety beyond a certain level at the national level. The technical level should be improved through complementation between technical levels.

3.2.8 Insurance for Storm and Flood Damage

○ Expansion of the relevant products and enhancement of efficiency of damage assessment : The operating system should be decentralized and adjusted to expand the insured items and to avoid the duplication of insurance products. For the efficient management of insurance for storm and flood damage, an integrated management system for damage appraisal and sales should be prepared. A system for rate calculation should also be established through close monitoring.

○ Establishment of an agency exclusively in charge of insurance : For the systematic operation and management of the dispersed insurance system for storm and flood damage, an agency exclusively in charge of insurance is necessary through work adjustment with the relevant institutions. In relation to the introduction of a national reinsurance fund, reviewing the establishment of the abovementioned integrated agency is essential since the insurance market for storm and flood damage is not big enough to introduce each governmental ministry's national re-insurance fund.

4. CONCLUSIONS

Climate on earth has changed alongside the development of civilization. Thus, the average damage of the various facilities caused by heavy rainfall, typhoon, and drought is increasing. As such, now is the time to make sincere efforts to minimize damages. Although people have made such efforts a long time ago, voices clamoring for the restoration of damaged facilities have mostly died down every time they clashed with economic logic.

Many research tasks in various areas as presented in this research are expected to be helpful to the work development of NEMA in connection with financial source acquisition for future research. The final results in this report are presented below.

First, whereas Korea used to be passive in coping with climate change, now, it is actively coping with it by establishing the Countermeasure Planning Organization Against Climate Change affiliated with the Prime

Minister's Office after Myung-Bak Lee was elected President of Korea. When the relevant government ministries' basic plans on climate change are confirmed, various plans related fields are considered to be activated.

Second, judging from foreign cases of coping with climate change, a large-scale budget seems to be injected considering the size of related facilities. All these are part of advanced judgment, and misunderstanding with regard to excessive design and plan is believed to be avoided later.

Third, this research selected and presented 48 research tasks on climate change to be promoted by work in relation to NEMA's major work concerning storm and flood damage.

The tasks to be promoted according to NEMA's work as presented in this report should be improved through periodic changes based on the research progress or priorities.

REFERENCES

Back, S.K., J.H., Ryu and S.B., Ryoo, 2002, Analysis of the CO2 Doubling Experiment using METRI AGCM, PART 1: The Characteristics of Regional and Seasonal Climate Responses. J. Korean Meteor. Soc. 38(5), 465-477

Bae, D.H., and J.H. Oh, 1998, A Fundamental Study on the Snowmelt Effects for Long-Term Runoff Analysis, Journal of Korea Water Resources Association, 31(6), 833-844

Jung, H.S., Lim, G.H., and J.H. Oh, 2001, Interpretation of the transient variations in the time series of precipitation amounts in Seoul, Korea. Part I : Diurnal Variation. Journal of Climate 14(13), 2989-3004.

MOCT, 2001, Water Vision 2020. Document of Ministry of Construction and Transportation, Seoul, Korea, 5-11 (in Korean).

HYDRAULIC EFFECTS ON VEGETATION IMPACT BY FLOOD FLOW IN URBAN STREAMS

JINHONG KIM
Department of Civil Engineering, Chung-Ang University, Korea
jinhkim@cau.ac.kr

ABSTRACT

Hydraulic effects on the vegetation impact by the flood flow and the habitation status of the vegetation behavior by the flood flow of the aquatic plants were investigated in this paper.

The results showed that most of the aquatic plants except for Salix gracilistyla were bent and destroyed by the high tractive force of the flood flow, but the scrubs and the floating trashes enabled to make higher the dynamic pressure of the flow and they destroyed even the Salix gracilistyla. Vegetation behavior was classified into 4 stages of stable, recovered, damaged and swept away. Criteria between recovered and damaged status were determined by the bending angle of the aquatic plants. Vegetation whose bending angle is lower than 30~50 degree is recovered, but the vegetation whose bending angle is higher than 30~50 degree is damaged and is not recovered. Phragmites japonica and Salix gracilistyla were stronger than the other aquatic plants against the flood flow

1. INTRODUCTION

Seasonal changes of the vegetation area in the urban streams follow the repeated cycle of the contraction and the expansion, which is originated by destruction by flood flow and by the restoration of vegetative behavior, respectively. Transport of bed sediments during flood resulted in the deposition of the vegetated area. During flood seasons, the vegetation may be destroyed by the high tractive force of the flood flow, and be buried and damaged by the transportation of the riverbed sediments. Thus, the vegetation behavior is strongly affected by the hydraulic parameters such as flow velocity, turbulence and flow depth. Flow characteristics and the riverbed sediments affect the vegetation impacts.

Vegetation in the river is affected by flow structure, but inversely affects flow structure. It reduces the flow conveyance, increases the flow resistances and raises the water level. Thus, the vegetation and flow structure has mutually reciprocal relationships.

This paper presents the hydraulic effects on the vegetation impacts against the flood flow in the urban streams. Vegetation impacts by flood flow were investigated at Anseong-cheon, Seongbuk-cheon and Tan-cheon, and its behavior against flood flow was analyzed.

2. VEGETATION IMPACTS BY FLOOD FLOW

Vegetation impacts by the flood flow were investigated in the urban streams. For this purpose, Anseong-cheon, Seongbuk-cheon and Tan-cheon were chosen and the habitation status of the vegetation by the flood flow of the aquatic plants was investigated. Flow parameters such as flow velocity and flow depth also measured. Measurements of the flow features during flood times are very difficult and dangerous. Thus, the flow velocity is usually measured at the bridge using floats. In this study, the flow velocity and the flow depth were measured using current meter and staff within the vegetated area in case their values are not so high, but they were measured at the bridge near vegetated area in case their values are so high. Flow velocity was measured using the floats, and flow depth was measured using the traces of the water levels.

Figure 1: Measurement of flow velocity and flow depth

Vegetation status at Seongbuk-cheon after flood is shown in figure 2. All the aquatic plants except for *Salix gracilistyla* were bent and destroyed by the high tractive force of the flood flow. This phenomenon was also shown at Anseong-cheon and Tan-cheon. Large flood occurred at Anseong-cheon in July 5th, 2007 and most of the aquatic plants were destroyed shown in figure 3. In case of Tan-cheon, large flood occurred in August 13th, 2008 and most of the aquatic plants were destroyed shown in figure 4. Scrubs and floating trashes enabled to make higher the dynamic pressure of the flow, and even the *Salix gracilistyla* was destroyed.

Figure 2: Vegetation status at Seongbuk-cheon after flood

Figure 3: Vegetation status at Anseong-cheon after flood

Figure 4: Vegetation status at Tan-cheon after flood

3. VEGETATION BEHAVIOR AGAINST FLOOD FLOW

Vegetation behavior against flood flow is usually divided into four stages such as stable, recovered, damaged and swept away shown in figure 5.

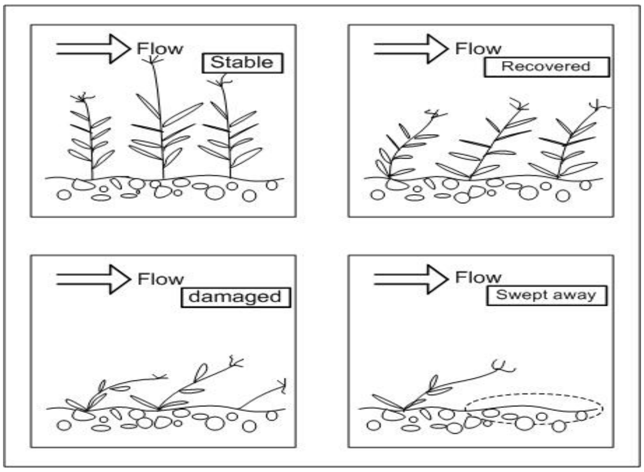

Figure 5: Four stages of vegetation behavior against flood flow

In figure 5, ‘stable’ means the vegetation is not affected against the flood flow and thus stable. ‘Recovered’ means the vegetation is affected by the tractive force of the flood flow, but is easily recovered its features. ‘Damaged’ means the vegetation is affected seriously by the tractive force of the flood flow and is not recovered its features even if the flood disappeared and is finished. ‘Swept away’ means some or all the parts of the vegetated area are swept away to downstream part by the high flood flow.

Field study showed that the division criterion between ‘recovered’ and ‘damaged’ of the vegetation was about 30~50 degree of the bending angle of the aquatic plants. Vegetation whose bending angle is lower than 30~50 degree is recovered, but the vegetation whose bending angle is higher than 30~50 degree is damaged and is not recovered.

This criterion may be a little different by the species of the aquatic plants. Bending angle of *Phragmites japonica* and *Salix gracilistyla* will be larger than that of *Phragmites communis, Miscanthus sacchariflorus* and *Persicaria blumei.* They must be further studied through more data of the field study.

Examples of the four stages of the vegetation behavior are shown in figure 6.

(a) Stable

(b) Recovered

(c) Damaged

(d) Swept away

Figure 6: Examples of four stages of vegetation behavior

According to the above criterion, vegetation behaviors of some aquatic plants were analyzed as below.

3.1 Vegetation behavior of *Phragmites japonica*

Vegetation behavior of *Phragmites japonica* against flow velocity and flow depth is shown in figure 7. Here, V(m/s) is flow velocity and H(m) is flow depth.

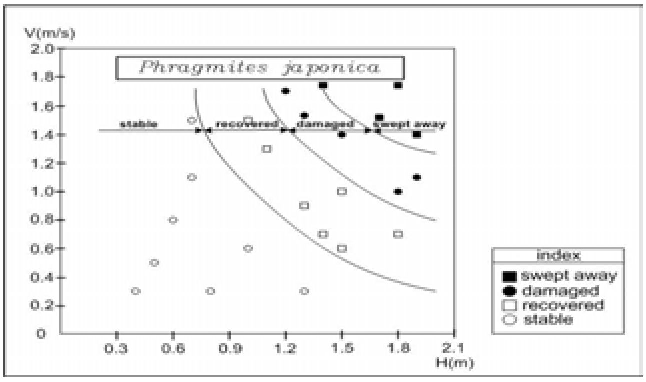

Figure 7: Vegetation behavior of Phragmites japonica

- Stable stage ; V <1.4(m/s), H <1.3(m)
- Recovered stage ; 0.6(m/s) < V <1.6(m/s), 1.0(m)< H <1.8(m)
- Damaged stage ; 1.0(m/s) < V <1.8(m/s), 1.2(m)< H <2.0(m)
- Swept away stage ; V >1.4(m/s), H >1.4(m)

Phragmites japonica was inhabited in the hydraulic condition of high velocity and low flow depth, thus inhabited in the relatively high Froude number. This shows that it was inhabited in the upstream reaches of the stream.

3.2 Vegetation behavior of *Phragmites communis*

Vegetation behavior of *Phragmites communis* against flow velocity and flow depth is shown in figure 8.

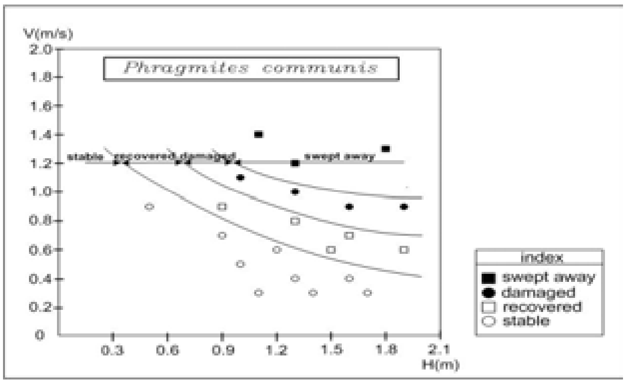

Figure 8: Vegetation behavior of Phragmites communis

- Stable stage ; V <0.9(m/s), H <1.7(m)
- Recovered stage ; 0.6(m/s) < V <0.9(m/s), 0.9(m)< H <1.9(m)
- Damaged stage ; 1.0(m/s) < V <1.1(m/s), 1.0(m)< H <2.0(m)
- Swept away stage ; V >1.2(m/s), H >1.1(m)

Phragmites communis was inhabited in the hydraulic condition of low velocity and high flow depth, thus inhabited in the relatively low Froude number compared with *Phragmites japonica*. This shows that it was inhabited in the downstream reaches of the stream.

3.3 Vegetation behavior of *Miscanthus sacchariflorus*

Vegetation behavior of *Miscanthus sacchariflorus* against the flow velocity and the flow depth is shown in figure 9.

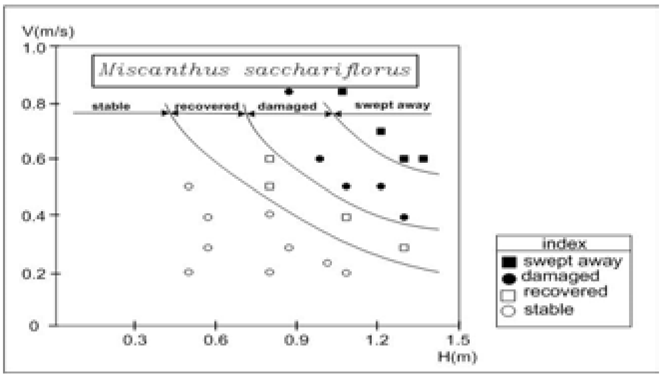

Figure 9: Vegetation behavior of Miscanthus sacchariflorus

- Stable stage ; V <0.5(m/s), H <1.1(m)
- Recovered stage ; 0.3(m/s) < V <0.6(m/s), 0.8(m)< H <1.3(m)
- Damaged stage ; 0.4(m/s) < V <0.9(m/s), 0.9(m)< H <1.3(m)
- Swept away stage ; V >0.6(m/s), H >1.0(m)

3.4 Vegetation behavior of *Persicaria blumei*

Vegetation behavior of *Persicaria blumei* against the flow velocity and the flow depth is shown in figure 10.

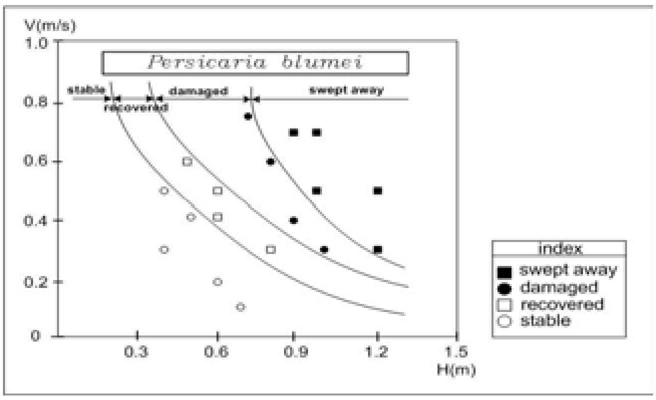

Figure 10: Vegetation behavior of Persicaria blumei

- Stable stage ; V <0.5(m/s), H <0.7(m)
- Recovered stage ; 0.3(m/s) < V <0.6(m/s), 0.4(m)< H <0.8(m)
- Damaged stage ; 0.3(m/s) < V <0.8(m/s), 0.7(m)< H <1.0(m)
- Swept away stage ; V >0.3(m/s), H >0.9(m)

Persicaria blumei was found in the relatively wide range of flow velocity and flow depth, which shows that it was inhabited in the middle and downstream reaches of the streams.

3.5 Vegetation behavior of *Persicaria thunbergii*

Vegetation behavior of *Persicaria thunbergii* against flow velocity and flow depth is shown in figure 11.

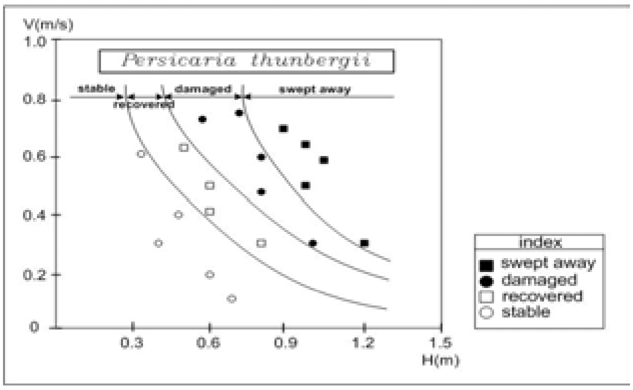

Figure 11: Vegetation behavior of Persicaria thunbergii

- Stable stage ; V <0.6(m/s), H <0.7(m)
- Recovered stage ; 0.3(m/s) < V <0.6(m/s), 0.5(m)< H <0.8(m)
- Damaged stage ; 0.3(m/s) < V <0.7(m/s), 0.6(m)< H <1.0(m)
- Swept away stage ; V >0.5(m/s), H >0.9(m)

Criterion on the vegetation behavior of *Persicaria blumei* was not clear as shown in figure 10, which implies that it may be effected by the flow turbulence rather than flow velocity and flow depth. This must also be further studied after collecting more data through the field study.

4. CONCLUSIONS

Hydraulic effects on the vegetation impact by the flood flow and the habitation status of the vegetation behavior by the flood flow of the aquatic plants were investigated. Most of the aquatic plants except for *Salix gracilistyla* were bent and destroyed by the high tractive force of the flood flow, but the scrubs and the floating trashes enabled to make higher the dynamic pressure of the flow and they destroyed even the *Salix gracilistyla.*

Vegetation behavior was classified into 4 stages of stable, recovered, damaged and swept away. Criteria between recovered and damaged status were determined by the bending angle of the aquatic plants. Vegetation whose bending angle is lower than 30~50 degree is recovered, but the vegetation whose bending angle is higher than 30~50 degree is damaged and is not recovered.

Phragmites japonica was inhabited in the hydraulic condition of high velocity and low flow depth, thus inhabited in the relatively high Froude number. This shows that it was inhabited in the upstream reaches of the stream. *Phragmites communis* was inhabited in the hydraulic condition of low velocity and high flow depth, thus inhabited in the relatively low Froude number compared with *Phragmites japonica*. This shows that it was inhabited in the downstream reaches of the stream. *Persicaria blumei* was found in the relatively wide range of flow velocity and flow depth, which shows that it was inhabited in the middle and downstream reaches of the streams. Criterion on the vegetation behavior of *Persicaria blumei* was not clear, which implies that it may be effected by the flow turbulence rather than flow velocity and flow depth. This must be further studied after collecting so much field data.

Criterion of the vegetation behavior suggested in this study may be a little different by the species of the aquatic plants. Bending angle of *Phragmites japonica* and *Salix gracilistyla* will be larger than that of *Phragmites communis, Miscanthus sacchariflorus* and *Persicaria blumei.* They must also be further studied after collecting more data through the field study.

ACKNOWLEDGEMENT

This work was supported by the Korea Science and Engineering Foundation (KOSEF) grant funded by the Korea government MOST (No. R01200700020 44202007).

REFERENCES

Nagata, A., Yanani S., and Nagasaka Y., 2006. Differences in up and downstream inhabitant opinions responding to the alteration of watershed environment. *Ecology and Civil Engineering*, Vol. 9, No. 1, 73-84.

Ministry of Environment, 2007. Survey and Evaluation of Aquatic Ecosystem Health in the Nakdong River, *National Institute of Environmental Research*, Seoul.

National Rivers Authority, 1992. River Corridors Survey-Methods and Procedures, London.

Park, Y.-S., T.-S. Chon, I.-S. Kwak and S. Lek, 2004. Hierarchical community classification and assessment of aquatic ecosystems using artificial neural networks. *Science of the Total Environment* **327**, 15-122.

EFFECT OF CLIMATE CHANGE IN BANGLADESH AND DAMAGES DUE TO TWO RECENT CYCLONES

MEHEDI AHMED ANSARY
Department of Civil Engineering, BUET, Bangladesh
ansary@ce.buet.ac.bd
MD. SAIDUR RAHMAN
Research Engineer, BNUS, BUET, Bangladesh

ABSTRACT

Climate change, which is predicted by the scientist of the world, is the most unanimous topic in the 20th century due to the assessment of some global climatic variables. Scientific study has found that global mean daily temperature has increased with a rate of 0.74±0.18°c per 100 years as well as sea level is rising 3mm per year. Due to climate change, distribution, frequency and intensity of weather related hazards has increased, increased precipitation is causing more flooding, and sea level rise is increasing storm surge height.

Bangladesh is the practical example of a severely affected nation due to tropical cyclone, flood, drought, landslides, and salinity intrusion as well as other disasters due to climate change. High population density, high level of poverty, its landscape, geographical position and climate variability has made it vulnerable to natural disaster. The climate change scenarios in Bangladesh are analyzed through the frequently occurring natural disasters like cyclones. On the 15th November 2007, the cyclone SIDR formed in the central Bay of Bengal, and quickly strengthened to reach peak sustained winds speed of 223 km/hr. Estimated total damage and losses caused by SIDR was $17 billion, and 3400 people were killed.

The cyclone AILA hit the coastal area of Bangladesh especially Khulna and Satkhira districts, caused 200 death and 50,000 homeless. Coastal polders constructed in 1960, were damaged by the tidal surge. According to BWDB, cyclone AILA damaged 32.4 km embankments completely while 178.84 km partially, where cost for maintenance and reconstruction of these embankments will be $7.75 million.

Moreover, for repairing and reconstruction of Sluice gate/regulator, protective work, closure and other hydraulic structures will require another $4.3 million. Mud houses and shrimp production were also damaged by storm surge.

1. INTRODUCTION

On 15th November 2007, the cyclone Sidr formed in the central Bay of Bengal, and quickly strengthened to reach peak sustained wind speed of 223 km/hr. A total of 650,000 people evacuated to emergency shelter. About 3,363 were blamed on the storm and 1,001 people were missing and 55,282 sustained physical injury. Maximum death was 1292 at Barguna. Estimated total damage and losses caused by the cyclone was $1.7 billion. The effects of Cyclone SIDR are equivalent to 2.8% of Bangladesh's GDP.

The recently occurred cyclone Aila (May, 2009), which hit Khulna and Satkhira districts, caused 190 death, 50,000 homeless, 500 fishermen missing and 3000 dysentery affected people. Coastal polders, which were constructed at early 1960s, had been damaged by the tidal surge. According to BWDB, cyclone Aila damaged 32.4 km embankments completely while 178.8 km are partially damaged where cost for maintenance and reconstruction of these embankments will be $7.75 million. Moreover, for repairing and reconstruction of Sluice gate/regulator, protective work, closure and other hydraulic structures will require $4.3 million. According to LGED, cyclone Aila damaged 153.86 km embankments in Satkhira district and the estimated cost of repair/rehabilitation maintenance will be $2.41million. Mud houses and shrimp production have been damaged by the storm surge.

2. CLIMATE CHANGE SCENARIOS

2.1 Worldwide climate change scenarios

Climate change and related global concerns are the most important agenda in the 21th centuries because of climate variability in all over the world. The atmospheric scientists and environmentalist have confirmed the worldwide climate change by increasing the frequencies of natural disaster. The Intergovernmental Panel on Climate Change (IPCC) predicts that global temperatures will rise between 1.8 ℃ and 4.0 ℃ by the last decade of the 21st century. The impacts of global warming on the climate, however, will vary in different regions of the world.

The IPCC also forecasts that global warming will result in sea level rises of between 0.18 and 0.79 metres, which could increase coastal flooding and saline intrusion into aquifer and rivers across a wide belt in the south of the country, although most of the area is protected by polders. Rainfall is predicted to become both higher and more erratic, and the frequency and intensity of droughts are likely to increase, especially in the drier northern and western parts of the country.

2.2 Climate change scenarios in Bangladesh

Bangladesh is likely to be among the countries that are the worst affected by climate change. Tropical cyclones, storm surges, flood, drought and river erosion are likely to become more frequent and severe in the coming years. So, it is very important to combat against natural disaster for our future existence in Bangladesh. Losses due to natural disaster can be mitigated by policy making and planning. Proper assessment and action plan is a key point to tackle disaster. UNDP has identified Bangladesh to be the most vulnerable country in the world to tropical cyclones and the sixth most vulnerable country to floods (UNDP, 2004). Bangladesh is susceptible to floods, tropical cyclones, storm surges, and droughts. The regions of the country affected by these different hazards are shown in Figure 1.

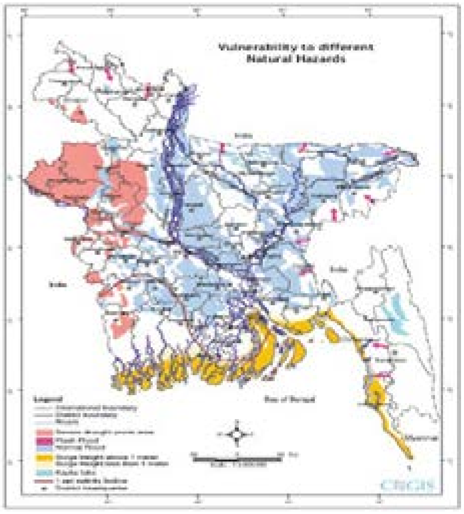

Figure 1: Vulnerability to different natural hazards in Bangladesh (Source: CEGIS, Dhaka)

Most of Bangladesh lies in the delta of three of the largest rivers in the world – the Brahmaputra, the Ganges and the Meghna. These rivers have a combined peak discharge in the flood season of 180,000 m^3/sec. (the second highest in the world, after the Amazon) and carry about two billion tones of sediment each year. The topography of the country is mostly low and flat. Two-thirds of the country is less than 5 metres above sea level and is susceptible to river and rainwater flooding and, in lower lying coastal areas, to tidal flooding during storms (MoEF, 2009).

In the last 25 years, Bangladesh has experienced six severe floods. In 2007, two successive and damaging floods inundated the country in the same season. During high floods, river bank erosion is common. It can result in the loss of thousands of hectares of agricultural land and scores of villages, and displace many thousands of people from their homes. Flash floods can also be a problem in the more hilly north-eastern and south-eastern regions of the country.

One quarter of the country is inundated due to flooding. The people living in these areas have adapted by building their houses on raised mounds and adjusting their farming systems. In the past, people here grew low-yielding deepwater rice during the monsoon season. Now they mostly cultivate high-yielding rice crops, often using irrigation. Once in every 4 to 5 years, however, there is a severe flood that may cover over 60% of the country and cause loss of life and substantial damage to infrastructure, housing, agriculture and livelihoods. During severe floods, it is the poorest and most vulnerable who suffer most because their houses are often in more exposed locations.

Droughts in Bangladesh are seasonal and can devastate crops, causing hardship to poor agricultural laborers and others who cannot find work. In these areas, unemployment leading to seasonal hunger (“Monga”) is often a problem; especially in the months leading up to the November-December rice harvest. If the crop totally fails because of drought, the situation for poor people can become critical. Droughts most commonly affect the northwestern region, which generally has lower rainfall than the rest of the country.

A severe tropical cyclone hits Bangladesh, on average, every 3 years. These storms generally form in the months just before and after the monsoon and intensify as they move north over the warm waters of the Bay of Bengal. The wind speed of the most catastrophic cyclone in Bangladesh ranges between 150 kph to 225 kph and can result in storm surges up to eight metres high, resulting in extensive damage to houses and high loss of life to humans and livestock in coastal communities.

The tropical cyclones in 1970 and 1991 are estimated to have killed 500,000 and 140,000 people, respectively. The storm surges are higher in Bangladesh than in neighbouring countries because the Bay of Bengal narrows towards the north, where Bangladesh is located. In recent years, general cyclonic activity in the Bay of Bengal has become more frequent (Figure 2), causing rougher seas that can make it difficult for fishermen and small craft to put to sea. The climate change in Bangladesh may be estimated from the rainfall data analysis. The climate change scenarios are identified by tropical cyclone like the recently occurring the super cyclone ‘Sidr ‘in 2007 and the cyclone’ Aila’ in 2009.

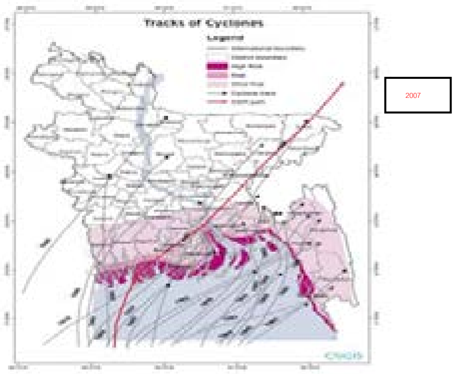

Figure 2: Tropical cyclone at different time and Path in Bangladesh (Source: CEGIS, Dhaka).

3. THE IMPACT OF THE SUPER CYCLONE SIDR IN 2007

The Super cyclone ‘Sidr’ hit at 9 p.m. on 14 November 2007 about 670 km south of Mongla port. In Barisal coast the catastrophic of the cyclone Sidr was observed on 15 November at 21:00 hour’s local time during ebb tide. Wind speeds reached up to 240 km per hour affecting 15 districts with 15 others partly affected. The tract of the Super cyclone is shown in Figure 2. More than 8.9 million people in 1,950 unions of 200 Upazilas under 30 districts were affected by Cyclone SIDR. Official reports indicated a total of 3,406 Bangladesh nationals perished during this event with 1,001 missing and 55,282 sustained physical and psychological injuries as a result of the disaster. Total damage is estimated to be 1.7 billion US Dollars. Total 3,319 people died in 12 affected districts, which is 97% of the total death reported as of 21 January 2008. Highest death toll was reported in Barguna district (1,335) followed by Bagerhat (810), Patuakhali (457) and Pirojpur (400). The MoFDM Official report indicates that 1.75 million families were affected in 12 districts, which is also 84% of the total affected families in 30 districts. Over 564,967 houses are fully damaged and 957,110 houses are partially damaged. Bagerhat suffered the most in terms of fully damaged housing (118,899 houses, 22%), followed by Barguna (95,412), Jhalakathi (69685), Pirojpur (63,896) and Patuakhali (53,291).

A comprehensive analysis undertaken by a team of Bangladesh Government and international experts, using state of the art assessment methodologies, estimated the total damage and losses caused by the cyclone to be BDT 115.6 billion (equivalent to US$ 1.7 billion). The effects of Cyclone SIDR are equivalent to 2.8% of Bangladesh’s GDP. The damage and losses were notably concentrated in the private sector, rather than in the public sector. This has significant implications in the strategy that must be adopted for recovery and reconstruction.

Damage and losses were concentrated on the housing sector ($0.83 billion), productive sectors ($0.48 billion), and on public sector infrastructure ($0.25 billion). Most affected sectors were, in decreasing order, housing, agriculture, transport, water control structures, education and industry.

Some photographs of the cyclone Sidr affected areas in Bangladesh are shown in Figure 3.

(a) Erosion of soil *(b) Uprooted trees*

(c) Fracturing of soil *(d) Road damage*

(e) Death of animals *(f) Flooding*

Figure 3: Some pictures collected from Sidr affected areas in Bangladesh.

4. THE IMPACT OF THE CYCLONE AILA IN 2009

On 25th May 2009, the cyclone Aila passed through 14 districts in the coastal area of Bangladesh. The Aila affected 14 districts were Satkhira, Khulna, Bagerhat, Barisal, Bhola, Pirojpur, Patuakhali, Borguna, Jhalokathi, Chittagong, Cox's Bazar, Laxipur, Feni, and Noakhali (Figures 4 and 5).

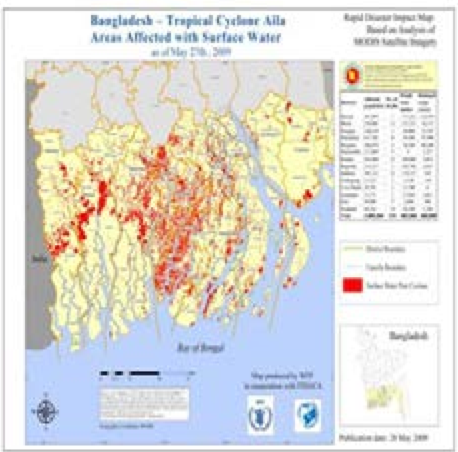

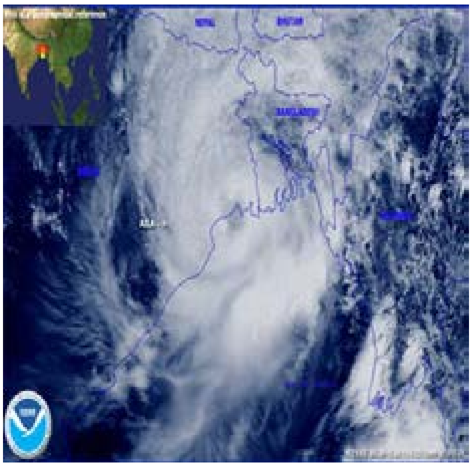

Figure 4: Tropical cyclone Aila (Map courtesy: NOAA)

Figure 5: Tropical cyclone Aila Areas affected with surface water (After MoFDM, 2009).

Loss of life, damages to houses, livestock, crops, educational institutions, roads and embankments have been reported from 529 unions of 64 upazillas of14 districts. Official sources admitted about 190 deaths and more than 50,000 homeless people. Table 1 presents summary of damage due to 2009 cyclone Aila. Total or partial destruction of about 6,12,594 thatched houses, 3,19,930 hector harvestable paddies, large number shrimp Gher, 1,47,628 livestock and poultry. At least 7108 people were injured by the storm and about 48,26,630 people were affected. Figures 6 to 9 show danage statistics in different Aila affected districts and upazillas.

Mud houses and shrimp production have been damaged by storm surge. In Nizum dwip, 20,000 people are homeless, 58,950 animals are killed and 50,000 deer have been missed. Severity of damages in different districts is shown in Figure 5. Storm surge of 3m impacted western region of Bangladesh, submerging numerous villages. More than 4,00,000 people were reportedly isolated by severe flooding in coastal regions of Bangladesh. Numerous villages were either completely submerged in flood water. In Patuakhali, a dam broke and submerged five villages. Numerous homes were destroyed by the subsequent flooding and tens of thousands of people were left stranded in the village.

Table 1: Summarized information on damage and loss due to the cyclone Aila (after MoFDM, 2009).

Sl. No.	Item	Quantity (No./km)
1	Affected District	14
2	Most affected district	11
3	Affected Upazillas	64
4	Affected Union	529
	a. Fully affected	195
	b. Partially affected	334
5	Damaged Households	612584
	a. Fully Damaged	242882
	b. Partially Damaged	369702
6	Affected Family	862570
7	Affected People	4826630
8	Crops damaged(ha)	319930
	a. Fully damaged(ha)	67840
	b. Partially Damaged (ha)	252090
9	No. of death	190
10	Injured persons	7103
11	Missing persons	0
12	Dead livestock &poultry	147628
13	Damaged educational Institution	2497
	a. Fully damaged	357
	b. Partially damaged	2769
14	Damaged roads (km)	6427
	a. Fully damaged (km)	1319
	b. Partially damaged(km)	5108
15	Damaged Bridged/Culvert (No.)	157
16	Damaged embankment (km)	1732.75
17	People took Shelter	52955

5. THE EFFECT OF THE CYCLONE AILA ON THE INFRA-STRUCTURES

Coastal polders, which are constructed at the time of 1960, have been damaged by the tidal surge. In Satkhira districts cyclone Aila damaged 10 km embankments completely and 120 km partially, where cost for maintenance and reconstruction of these embankments is $3.8 million.

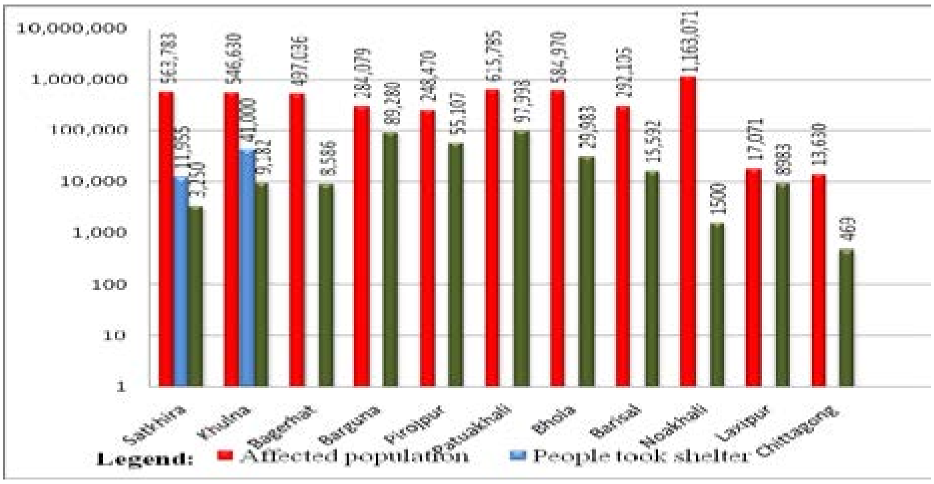

Figure 6: Aila affected Districts in Bangladesh (After MoFDM, 2009)

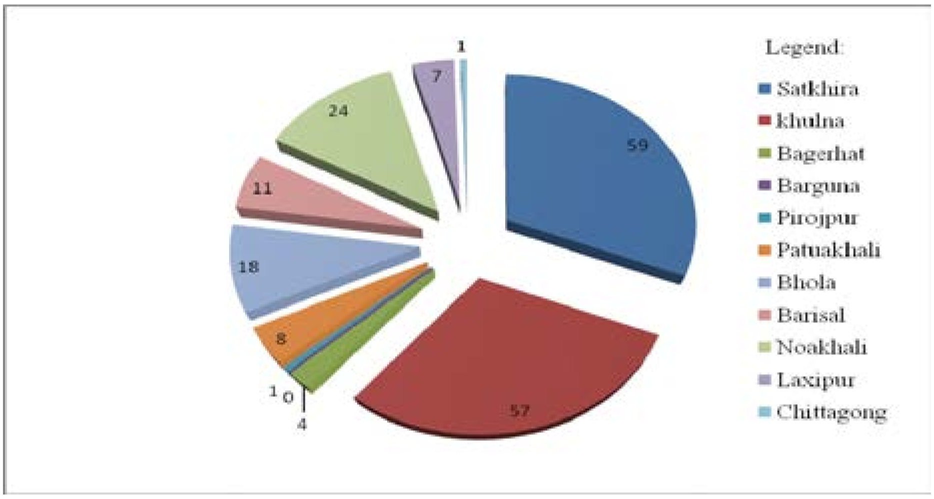

Figure 7: Total death in the Aila affected districts (After MOFDM, 2009)

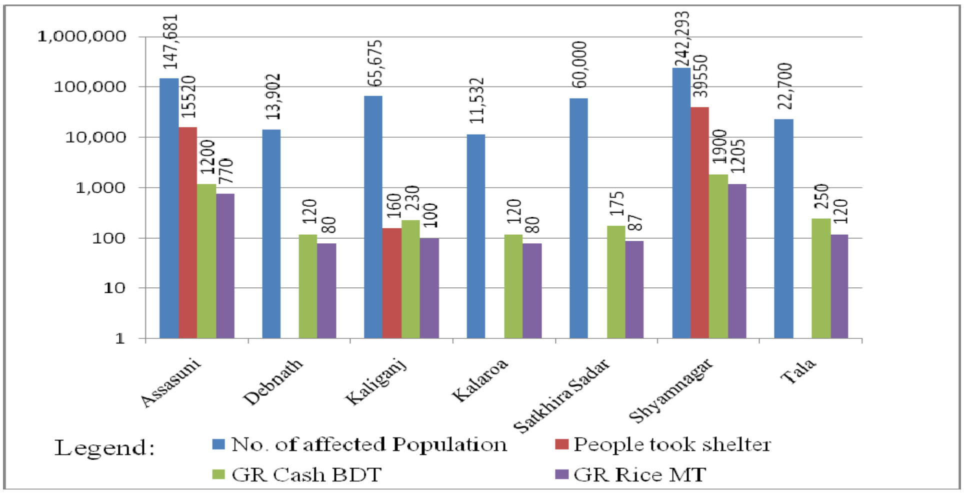

Figure 8: Aila affected upazillas in Satkhira District (After MoFDM, 2009)

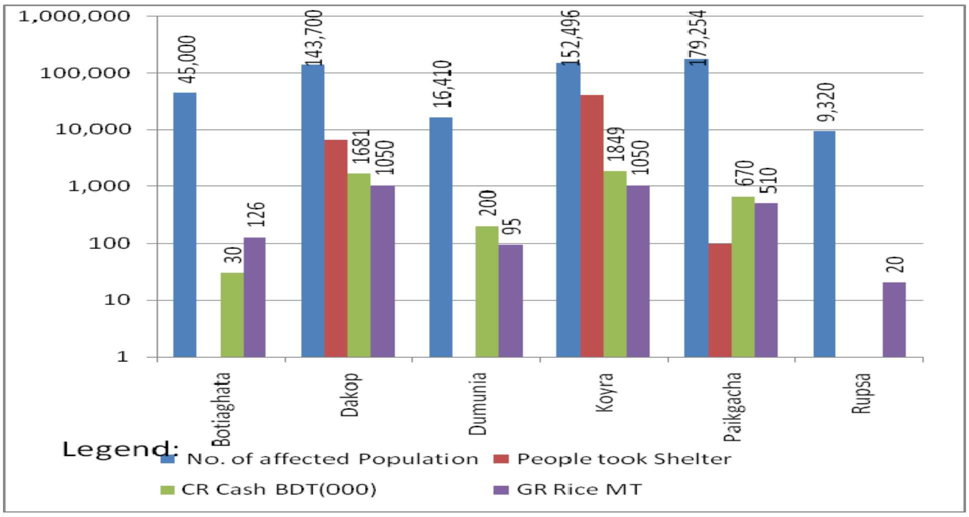

Figure 9: Aila affected upazillas in Khulna District (After MoFDM, 2009)

In Khulna district, 32.4 km were damaged completely and 178.84 km partially $7.75million is required for maintenance and reconstruction (after BWDB, see Table 2).

Table 2: Summary of damaged Infrastructure under BWDB, Upazilla-Shyamnagar, Assasuni and Koyra due to Cyclone "Aila" on dated-25/05/2009 (after BWDB, 2009)

Type of damaged component	**Actual damaged Quantity**		**Estimated cost to repair/Rehabilitation (Taka in lac) [1 USD=TK 69]**
	km	No.	
Embankment	211.24	-	5425.00 [$7.86 Million]
Sluice/Regulator	-	20	1010.00 [$1.45 Million]
Protective work	1.53	-	1040.00 [$1.51 Million]
Closure/etc.	-	24	970.00 [$1.41 Million]
Total cost			8445.00 [$12.23 Million]

Table 3: Summary of damaged Infrastructure under LGED, Upazilla-Shyamnagar and Assasuni due to Cyclone "Aila" on dated-25/05/2009

Type of damaged component	**Actual damaged Quantity**			**Estimated cost to repair/ Rehabilitation maintenance (TK. in lac) [1 USD=TK 69]**
	km	m	No	
Paved Road	63.49	--	--	675.00 [$978,261]
HBB road	54.15	--	--	373.00 [$540,580]
BFS road	18.75	--	--	76.00 [$110,145]
Soling road	18.33	--	--	67.00 [$97,101]
Culvert	--	2	--	6.00 [$8,696]

Growth Centre	--	--	1	21.00 [$30,435]
UP/Complex Bhaban	--	--	3	114.00 [$1,65,217]
Cyclone Shelter	--	--		120.00 [$1,73,913]
Residential Bhaban	--	--	6	18.00 [$26,087]
GC & Bazar			1	24.00 [$34,783]
UTDC Bhaban			1	100.00 [$1,44,928]
Total	154.72	2.00	12.00	1594.00 [$23,10,145]

Moreover, for repairing and reconstruction of Sluice gate/regulator, protective work, closure and other hydraulic structures require $6.96 million (after BWDB, 2009).

Cyclone Aila damaged 154.72 km embankments in Shyamnagar and Assasuni upazillas in Satkhira District of which maintenance and repairing cost is $2.68 million. Moreover, estimated cost for repairing and maintenance of Culvert, Bazar, Union Parishad Bhaban, Cyclone Shelter, Growth center and Residential Bhaban is $0.5million (after LGED, See Table 3).

6. PROBLEMS AFTER AILA

Most of the people living in the southern part of Bangladesh have seen the devastating and destructive scenarios of cyclone SIDR. But in Cyclone Aila, damage has been increased due to the breaching of the coastal polders. The authority has to face difficult situation to tackle the effect of Aila.

- The polders of coastal belt in Bangladesh have been damaged due to the attack of storm surge. As a result, many villages have been inundated.
- Agricultural lands have been severely affected by the intrusion of saline water.
- Most of the coastal areas were under water. As a result, people could not communicate each other due to flooding.
- Due to breaching of embankments the relief works have been hampered.

Some photographs of Embankment damage from the coastal areas in Bangladesh after the cyclone Aila are shown in Figure 10.

(a) (b)

(c) (d)

Figure 10: Damage of embankment due to the Cyclone Aila in Satkhira district by the side of the Kapatakha River

7. ACTION PLAN FOR UPCOMING CLIMATE CHANGE

In 2005, the GoB has developed the National Adaptation Programme of Action (NAPA) after extensive consultations with communities across the country, professional groups; and other members of civil society. The process has been taken forward, including through the adaptation of the Bangladesh Climate change Strategy and action plan (BCCSAP) in 2008, which is the main basis of Bangladesh's efforts to combat climate change over the next ten years. The following action Plans have been taken to combat the upcoming Climate change:

- Repair and maintenance of existing flood embankments
- Repair and maintenance of existing cyclone shelters
- Repair and maintenance of existing coastal polders
- Adaptation against floods
- Adaptation against future cyclones and storm-surges
- Planning, design and construction of river training works

To mitigate the problem after disaster following suggestion are provided (BCCSAP, 2008).

- Survey of the condition of coastal polders and preparation of GIS maps with present coverage of areas protected by these polders.
- Repair, reconstruction and maintenance of existing coastal polder based on future projected sea level rises and storm surges.
- Reconstruction and repair of polders/embankments to design height and section

Specific recommendations due to cyclone Aila:

- Quantify and periodically update the assessment of risk.
- Implement more effective mechanisms for coordination and operation.
- Upgrade engineering design procedures and practice to place greater emphasis on safety.
- Engage independent experts in high level reviews of all critical life-safety structures, including cyclone and flood protection system.

- Correct the system's deficiencies by establishing mechanisms to incorporate changing information, making the embankment survivable if overtopped, strengthening the affected embankment.

Bangladesh is a disaster prone country. Right way construction of embankment is required to take shelter and combat intrusion of saline water. Coordination is mandatory for managing pre and post disaster situation. Government has taken action plan about the constructing the embankment. Without constructing the embankment it is not possible to implement proper disaster management.

8. CONCLUSIONS

Although Bangladesh is not responsible for the top most country of GHG emission, some effective steps have been taken under the Kyoto Protocol. To fight against climate change as well as tropical Cyclone, the following considerations might be implemented. For cyclone resistant infrastructure strengthening, foundation improvement, raising the plinths level for storm surge, cyclone shelter construction considering facilities for women and engineered constructed house should be erected. The coastal polders, which are fully and partially damaged, may be repaired and reconstructed by appropriate design. The minor scour on the crown and the backside of the embankment may be repaired. Design of embankment should be inspected to reduce the risk of saline water intrusion by over passing the storm surge. The properties of soil sample collected from embankment and borrow pit should be tested accurately to apply soil improvement techniques. During the time of construction, the compaction of the soil should be applied on the basis of soil test data.

REFERENCES

BNUS (2007). Post Disaster Survey Sidr, Bangladesh Network office for urban safety, Bangladesh University of Engineering and Technology (BUET), Dhaka, Bangladesh.

BWDB (2009). Preliminary Assessment of Bangladesh Water Development Board Infrastructure in Coastal Area of Bangladesh, Bangladesh Water Development Board, July, 2009.

ITHACA (2009). Bangladesh-Tropical Cyclone Aila. Areas affected with surface water as of May 27th, 2009, Information Technology for Humanitarian Assistance, Co-operation and Action. Website: www.ithaca.polito.it/maps.php.

LGED (2009). List of Affected/Damaged Infrastructure by Recent Cyclone Aila on 25-05-2009, Local Government and Engineering Division, July, 2009.

MoEF (2005). National Adaptation Programme of Action (NAPA). Ministry of Environment and Forests, Government of the People's Republic of Bangladesh, Dhaka, Bangladesh.

MoEF (2008). Bangladesh Climate Change strategy and Action Plan 2008. Ministry of Environment and Forests, government of the People's Republic of Bangladesh, Dhaka, Bangladesh.

MoFDM (2009). Tropical cyclone Aila areas Affected with Surface Water, Ministry of Food and Disaster Management, Dhaka, Bangladesh June, 2009.

NOAA (2009). Tropical cyclone Aila, Website: www. reliefweb. Int /rw/ fullMaps_Sa.nsf/luFullMap.
UNDP (2004). A challenge for Development, A Global Report on Reducing Disaster Risk. Website: www. undp. org/cpr/ we_do/integrating risk. shtml).

COMPUTATIONAL ASSESSMENT OF WINDSTORM HAZARD IN URBAN CANYON

SUNGSU LEE[1], HAKSUN KIM[1],
GULGI CHOI[1] and KWANGHYUN NAM[2]
School of Civil Engg., Chungbuk National University,
Seongbong-ro, Cheongju Chungbuk 361-763, Korea
{joshua,haksun}@cbnu.ac.kr, gulgi-c@nate.com
[2]Cubersolution co. ltd., Cheongju, Republic of Korea
khnam@ cuber.co.kr

ABSTRACT

During windstorm period, urban area suffers from not only physical damages on the frame and the envelopes of structures, but fierce wind along the urban canyon. Strong wind inside a building complex often threats livability by generating windborne debris or heavily fluctuating flow. This paper presents a computational study of windstorm hazard inside an urban canyon. A large-eddy simulation (LES) is utilized to compute the unsteady and turbulent wind flow with Smagorinsky subgrid scale model. A log-law-based wall model was employed on all the solid surfaces including the ground and the surface of buildings to replace the no-slip condition. The shape of buildings was implemented on the Cartesian grid system by an immersed boundary method. Key flow quantities for the windstorm hazard assessment such as mean and RMS values of wind speed along the corridors are presented. In addition, characteristics of the velocity field at some selected locations vital to safety of human beings are also reported.

1. INTRODUCTION

Recent interest in eco-friendly environment has raised needs for analysis of wind field in urban area. In spite of numerous studies on computational methods for wind flow around bluff bodies, the wind around building complex has posed high difficulty in computations, most of which have been done by experiments. This paper presents a large eddy simulation of wind flow around a building complex using the immersed boundary method (IBM). The complicated geometry of the building complex does not pose any computational issues since IBM (Kim et al, 2001) allows for usage of Cartesian grids with forcing terms in the governing equations.

2. FORMULATION

2.1 Governing Equations

Based on the immersed boundary method and the mass forcing for continuity by Kim et al. (2001), the governing equations for incompressible fluid flow using IBM and LES are as follows;

$$\frac{\partial \overline{u}_j}{\partial x_j} - q = 0 \qquad \text{and} \quad \frac{\partial \overline{u}_i}{\partial t} + \frac{\partial \overline{u}_i \overline{u}_j}{\partial t} = -\frac{\partial p}{\partial x_i} - \frac{\partial \tau_{ij}}{\partial x_i} + \frac{1}{\mathrm{Re}} \frac{\partial^2 \overline{u}_i}{\partial x_i \partial x_j} + f_i \tag{1}$$

where x_i and $\overline{u}_i$ denote Cartesian coordinate and velocity component, respectively. p represents pressure, q and f_i denote mass source and momentum forcing, respectively. τ_{ij} is the Reynolds stress to be modeled. Re is Reynolds number based on reference length, h and inflow velocity U .

This study employs the Smagorinsky model based on the eddy viscosity.

$$\tau_{ij} = -2\nu_{SGS} \overline{S}_{ij} \, . \tag{2}$$

where $_{SGS}$ is the eddy viscosity for LES which has the form of

$$\nu_{SGS} = (C_S \Delta)^2 \sqrt{2 \overline{S}_{ij} \overline{S}_{ij}} \quad \text{and} \quad \overline{S}_{ij} = \frac{1}{2}\left(\frac{\partial \overline{u}_i}{\partial x_j} + \frac{\partial \overline{u}_j}{\partial x_i} \right) \tag{3}$$

The governing equations are discretized by a finite-volume method which has the second-order accuracy in space. The time integration is carried out by a fractional step method in which convection terms are integrated by a 3rd order Runge-Kutta method and diffusion terms are by Crank-Nicolson scheme.

$$\frac{\hat{u}_i^k - u_i^{k-1}}{\Delta t} = (\alpha_k + \beta_k) L\left(u_i^{k-1}\right) + \beta_k L\left(\hat{u}_i^k - u_i^{k-1}\right) - \gamma_k N\left(u_i^{k-1}\right) - \zeta_k N\left(u_i^{k-2}\right) - (\alpha_k + \beta_k) \frac{\partial p^{k-1}}{\partial x_i} + f_i \tag{4}$$

$$\frac{u_i^k - \hat{u}_i^k}{\Delta t} = -\frac{\partial \phi^k}{\partial x_i} \tag{5}$$

where L and N denote diffusion and convection operators, respectively, and the coefficients used in Eq. (4) are in Ref. [1].

In order to evaluate the momentum forcing f_i in Eq. (4), approximation of Eq. (1) is made by using a 3rd order Runge-Kutta method for convection term and a forward Euler method for diffusion terms;

$$\frac{U_i^k - u_i^{k-1}}{\Delta t} = (\alpha_k + \beta_k) L\left(u_i^{k-1}\right) - \gamma_k N\left(u_i^{k-1}\right) - \zeta_k N\left(u_i^{k-2}\right) - (\alpha_k + \beta_k) \frac{\partial p^{k-1}}{\partial x_i} + f_i \tag{5}$$

where U_i^k is the velocity inside the body, to be determined by the interpolation scheme described above. Rearranging Eq. (5) leads to the momentum forcing f_i which is used in Eq. (4).

2.2 Immersed Boundary Method

The forcing of mass and momentum depends on the relative location of the body boundary to the Cartesian grid line. Figures 1(a) and (b) illustrates the determination strategy for momentum forcing. When a velocity node in staggered grid line is immersed in the body, bilinear interpolations are implemented for A in Fig. 1(a) using adjacent velocity nodes in fluid domain or linear interpolations for B and C in Fig. 1(b). In addition, mass imbalance due to the fictitious flow inside the body is adjusted by introducing mass forcing, as shown in Fig. 2.

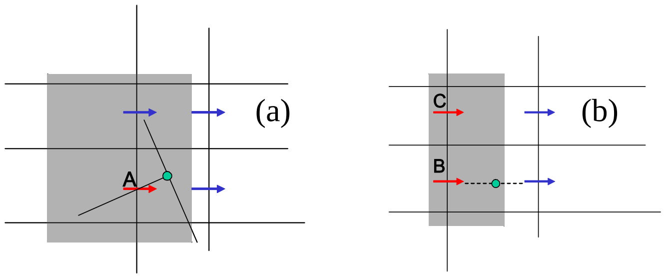

Figure1: Momentum Forcing

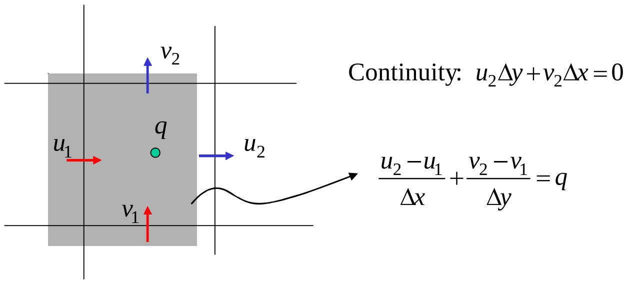

Figure 2: Mass Forcing

3. COMPUTATIONAL RESULTS

The building complex modeled in this study was a multi-block configuration using 9 of the Wind Engineering Research Field Laboratory building (WERFL) at Texas Tech University (TTU) shown in Figure 3. Scaled geometry was used with 1:50 to compare the present results with experimental data (Chang & Meroney, 2003). The domain, shown in Figure 4, is 10m, 1.2m and 4m in x,y and z direction, respectively, along which 320x52x192 grid is used.

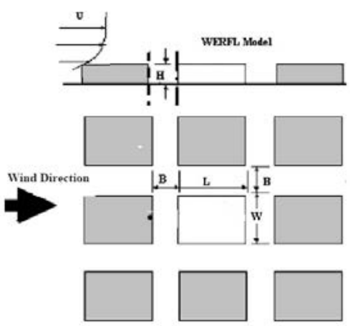

Figure 3: Model Configuration

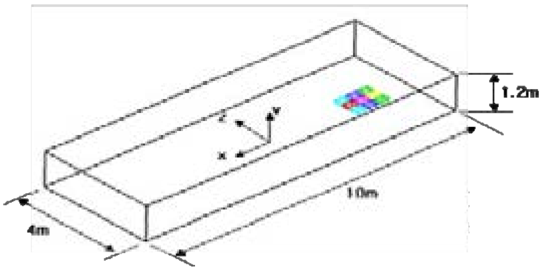

Figure 4: Computational Domain

Figure 5 compares experimental sketch [2] with the computed time-averaged velocity vectors. The recirculating flow field in the urban canyon is well reproduced and the acceleration right outside the canyon is clearly demonstrated.

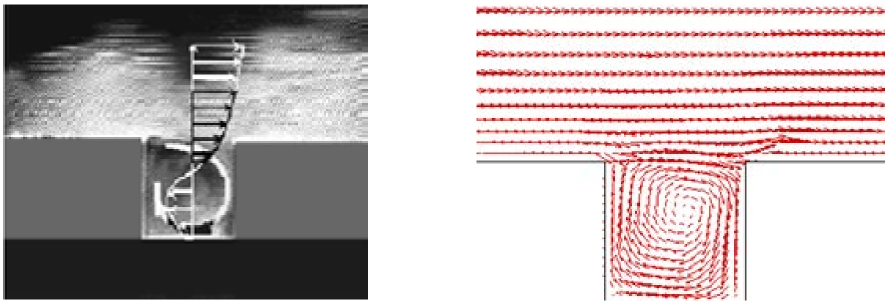

Figure 5: Experimental (Chang & Meroney, 2003) and Computed Flow Field inside Urban Canyon

Figure 6 shows instantaneous wind pressure and velocity on the pedestrian level, identifying hazardous region inside the urban canyon.

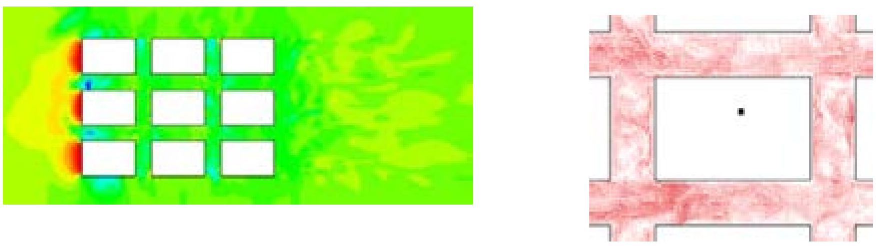

Figure 6: Instantaneous Wind Pressure and Velocity on Pedestrian Level

4. CONCLUDING REMARKS

A practical method to simulate the wind flow around a building complex has long been pursued in the wind engineering community. Hindered by computational capacity and/or numerical difficulties, wind flow around a building complex has been studied mostly by experiments.

This study presents a computational method for wind flow around a building complex. LES is employed to simulate the wind flow of high Re with wall function. Conflicts between complicated geometry and grid are resolved by using IBM. A complex of 9 buildings is modeled and wind flow is simulated. The present method shows that wind flow around the complex can be well predicted and it can be used on practical purposes.

ACKNOWLEDGMENTS

This work was supported by the grant from Natural Hazard Mitigation Research Group funded by National Emergency Management Agency, South Korea

REFERENCES

[1] J. Kim, D. Kim and H. Choi (2001), An Immersed-Boundary Finite-Volume Method for Simulations of flow in Complex Geometries, *J. Comp. Ph*ys., Vol. 171, pp. 132-150.

[2] C.H. Chang and R.N. Meroney (2003), Concentration and flow distributions in urban street canyons: wind tunnel and computational data, *J. Wind Engrg. & Ind. Aerodyn*., Vol. 91, pp.1141-1154.

PARALLEL SESSION 9

DEVELOPMENT OF THE WEB-BASED TOTAL SATETY MANAGEMENT SYSTEM

GEONHO HONG
Professor, Dept. of Architectural Engineering, Hoseo University, Korea
honggh@hoseo.edu
CHEEKYEONG KIM
Professor, Dept. of Architectural Engineering, Sunmoon University, Korea
ckkim@sunmoon.ac.kr
HEEKYU KIM
Senior Researcher, National Institute for Disaster Prevention, Korea
pietrokim@nema.go.kr

ABSTRACT

Safety of the public facilities is one of the most important factors to guarantee the citizens' living and government responsibility. The purpose of this study is to design and develop the web-based total safety management system (TSMS) for the specific control buildings and facilities in Korea. This system supports the all safety management works from safety inspection plan to execution and making reports of the facilities by officials and experts in special field. To increase the efficiency and serviceability of the system, link plan to the existing national safety management system in Korea was also investigated and suggested. Standards of the inspection work flow and checklist were developed for the computerization of the safety management works and reliability of the inspection results. This system consists of several user types. User type is classified by their affairs; supervisor, safety management officer, expert in special field and central government officer. This system will provide the information data to prevent the disaster, and help the establishment of safety management policy.

1. INTRODUCTION

Safety of facilities is the most primarily problem in order to guarantee a stable life and properties of citizens in modern society. Change of domestic industrial structure caused advancement and concentration of city scale, and various kinds of facilities increase the safety accidents and disaster on the scale and frequency.

Government make a rule to carry out safe management by the each responsibility agency such as central and local government, disaster prevention agency and manager of the facilities. Each specialty such as fire, structure, gas, electric and elevator carry out the safety inspection works by themselves, but it is true that integrated evaluation of the safety on the facilities is insufficient.

Also, structural safety and maintenance of the specific facilities divided by group 1 and group 2 is on the line by the specific law on the safety control of the facilities established in 1995. But the other facilities are not under the safety check and control.

To make efficient and scientific safety control and management of the specific control facilities assigned by the government, it is needed to improve the classification of facilities suitable to the computational system, and to construct web-based safety management information system based on standard safety check items and database.

The purpose of this paper is to demonstrate the web-based total safety management system (TSMS). This is based on the "Guide of the assignment and control on the specific control facilities" established in 2007 by the National Emergency Management Agency to prevent the disaster of the facilities.

2. ANALYSIS OF THE SAFETY MANAGEMENT WORKS

2.1 Overview on the safety management system in foreign countries

Safety management of the social facilities is a matter of concern in all of the countries. Safety management computational systems are usually developed and used in the field of social facilities such as bridge, tunnel and so on in foreign countries, but they do not check directly by government offices in the case of personal and public buildings. Most countries control the safety of personal and public buildings by the insurance system because of the lack of budget and usable officers. They focus to the speedy action after disaster than disaster prevention in the fields of private and public buildings. But the integrated safety management information system is required to achieve the prevention of the man-made disaster and being advanced country.

2.2 Facility classification in Korea

Legal structure on the safety management of the facilities divided into 2 categories. One is group 1 and group 2 facilities by the specific law on the safety control of the facilities established in 1995. And the other is specific control facilities by the basic law for the disaster prevention and safety management. Usually, group 1 and group 2 facilities consist of large scale facilities, and specific control facilities are middle and small scale or special use. Specific control facilities have large number up to 2 times compared with group 1 or group 2 facilities. Efficient safety control of the specific control facilities is more important because safety consciousness of the facility manager and budget of the safety inspection is insufficient.

2.3 Requirement analysis of the total safety management system

The system requirements for the web-based total safety management system according to laws and field practice are described in this section. First of all, "The Code for Assignment and Management of Specified Management Facilities" provide that an integrated database should be built and operated in order to share the disaster information and the result of inspection performed periodically or occasionally can be saved in this system. Currently, NDMS (National Disaster Management System in Korea) is a good system from the point of manager's view but the field worker may feel uncomfortable because there is a big gap between the system and field practice.

These problems prohibit the field workers to use this system and the amount of data cannot reach to an enough one.

Therefore, total safety management system should be not separated from the field practice and supports one stop service to field workers. In addition, sharing of the safety management information can be done through NDMS and the data connection between our system and NDMS is essential. To do this, we should cooperate with the developer of NDMS to integrate and connect these two kinds of database.

Considering the large amount of work of the officers of regional government, the final system should save the overburdened work. Therefore the system serves their work to select, make plan, inform, make a creditable check list of safety management, write reports and input to the national disaster management system. It means that this system should be a one stop service system for the officers of regional government.

The system requirements summarized from the interview with the officers of regional government are as follows;

a) The NDMS is a very complex system and inconvenient to the end user. TSMS need to be simpler than NDMS and easy to use.
b) The information which is managed in NDMS is composed of only text format database. It is very difficult to keep the information consistency throughout continuous inspection in this structure.
c) TSMS should reduce the amount of work of the officers in regional government. To do this, an integrated system which serve making plan of inspection and writing reports and input work to NDMS should be developed.
d) The number of specific control facilities is too big for an officer to manage. Therefore, TSMS is needed to manage the facilities efficiently.

e) It is one of time-consuming works to write various kinds of reports before and after safety inspection. In the new system, a standard format should be designed in order to reduce the amount of work for making reports and plans.
f) Most of the officers in regional government are not expert in architectural engineering. The system can make them feel convenient in inspection work by providing the safety management guideline and check list.

2.4 Connection of the existing safety management system in Korea

The domestic information system which relates with the facility safety management such as the facility management system (FMS) which is in the process of operating from the KISTEC (Korea Infrastructure Safety and Technology Corporation), and National Disaster Management System (NDMS) which is operated by National Emergency Management Agency were analyzed. However, these systems don't have much in common with the web-based safety management system being developed in this paper. Therefore we decided that our system have a role of giving the major information to NDMS in order to help the decision related to the safety management policy of government.

The main contents of the special law for facility safety management are to manage the maintenance plan/result, facility expenses and inspection diagnosis. The main contents of the special law are focused on 1 and 2 type facilities. It is general the safety manager submits within 3 months in order to report inspection and diagnosis result etc.

Ministry of Land, Transportation and Maritime operates the information system “Seumter”. It is made to store architectural plan and report at the permission of the new building. This system provides the basic design information of the building. So it could be usefully used at the time of safety management of the facility. Use of this system started from 2008 April to be enforced, so until currently the burden of data is not many drawing and it is in difficulties. Nevertheless, the drawings of buildings built after 2008 April are gathered and our system can use them for the safety management.

NDMS is a nation-wide system to prevent the natural and man-made disasters and supports making the policies about disasters and performing the safety management. However NDMS deals with the natural disasters such as storms, earthquakes and man-made ones and the input format to the system is text-based. Therefore, it is difficult to search and make summary even though the retrieve functions are very excellent. NDMS has powerful functions for searching and summary and the safety management result should be input to the system every November. So the connection between NDMS and TSMS is significant to increase the efficiency and usefulness of the two systems. The data connection diagram between the existing systems and TSMS is given in Figure 1.

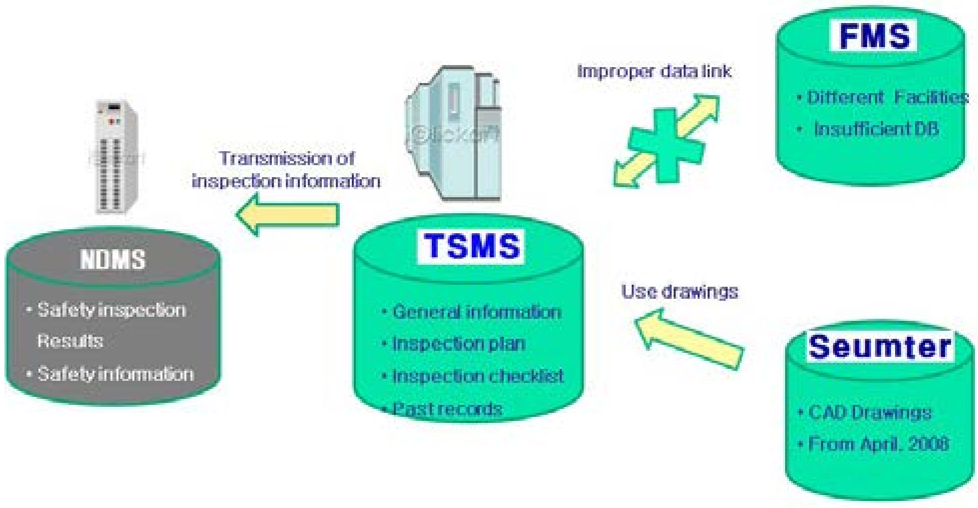

Figure 1: Data connection flow

3. Development of TSMS

3.1 System operation scenario

An integrated database is developed to manage efficiently the safety management information and disaster data. In addition, TSMS is designed to send the inspection results to NDMS.

As shown in figure 2 about operation scenario, the system manage the specific control facilities and the database is managed for each facility. The main users of this system are the officers of regional government. The system development environment is composed of 3-tier, which are DB tier, Business tier, and UI tier. The facility safety management database is the DB tier, and TSMS server is the business tier which performs various kinds of works actually related to the professional work. The followings summaries each process.

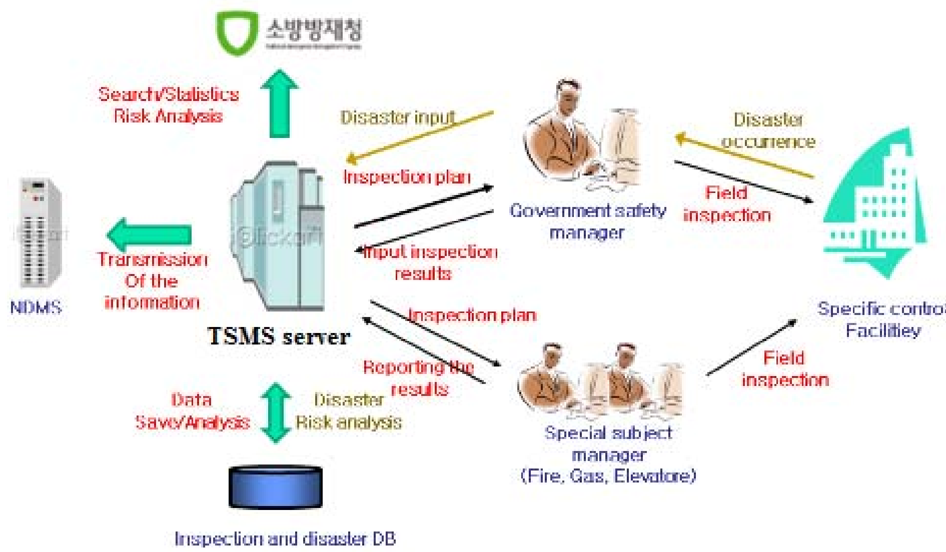

Figure 2: Operation scenario of TSMS

a) **Inspection Period and Items:** Facility safety management server which is operated based the related law should inform inspection period and contents according to the predefined period to the inspectors and facility managers. This notification is the starting point of new inspection.
b) **Site Inspection:** The safety managers and each field managers visit and inspect the facilities using predefined checking list. The checking list needs to be designed in order to make reasonable evaluation grade. So it was made based on the deep discussion by field experts.
c) **Input of Inspection Result through WEB:** The inspection result is input to the TSMS server through WEB by the safety managers and field managers. This information is saved into the facility safety management database automatically, and used in order to build the maintenance strategy and statistical work.
d) **Analysis of Inspection Result and Decision about Follow-up Work:** The follow-up decision was made using analysis algorithm based on the input information. This analysis algorithm is another research topic in the following research project. This decision-making algorithm is one of the cores in the final system to be used practically and widely.
e) **Notification of Inspection Result:** Based on the analysis of site inspection results, the inspection result is informed to the facility safety managers and field managers, and facility owner. When some follow-up works are needed to keep the safety of the facilities, the contents of follow-up works and due date are informed to them.
f) **Follow-up Work on Demand:** When the inspection results include some follow-up works, the result of follow-up works should be input to the system after doing them. The facilities which need follow-up works are separated and managed and an UI is implemented to review the treatment.
g) **Total Safety Management:** It is an integrated work to do the process of inspection period notification, site inspection, input of inspection results, safety evaluation and follow-up works. In addition, periodical inspection result can be managed in the format of physical report when they are required.
h) **Reporting:** TSMS server provides some function by which the status of safety management is analyzed. It also has an algorithm to provide the information required by NDMS.
i) **Management by Special Field Expert:** The special fields such as gas, electronics, fire-resistance, and elevators have an independent server operated by specialized experts or organizations. It may reduce the efficiency of the system if the information should be input to TSMS because it makes some additional works to the existing work process. This means that the best way under the current process is gather the summarized information such as the final results and follow-up works.
j) **Management of Disaster Information:** The man-made disaster information database has a role that it links the disaster information with safety management information and analyzes the characteristics of the disaster occurrence according the type of facility and the magnitude of the damage and build the response strategy. To do this, the contents of the magnitude of damage, the response, the status of rebuild, and etc are input to the system and the system provide various kinds of search function from several points of view in order to be used to analyze the characteristics of each disaster.

3.2 Construction of system database

The level of user's grade is divided into 4 levels according to the assigned works. The chief safety manager, the safety manager, and each field managers are some of them. The goal is focused to the efficiency of the officers of the regional government because they are the end user of the system and they actually do the safety management work.

The starting point of the development of safety management system is the design of safety information database. The detailed schema of the safety information database is shown in Figure 3. The database is organized around the building object because all information should be gathered and managed for each building. The database includes information related to the facility information, safety manager information, results of inspection work. The database for man-made disaster is also designed around each building same as the safety information database.

The followings are the contents of man-made disaster database.

- Building Collapse and Damage on Structural Members
- Fire and Explosion
- Disasters on Facilities such as Elevators
- Electronics, Gas Disasters

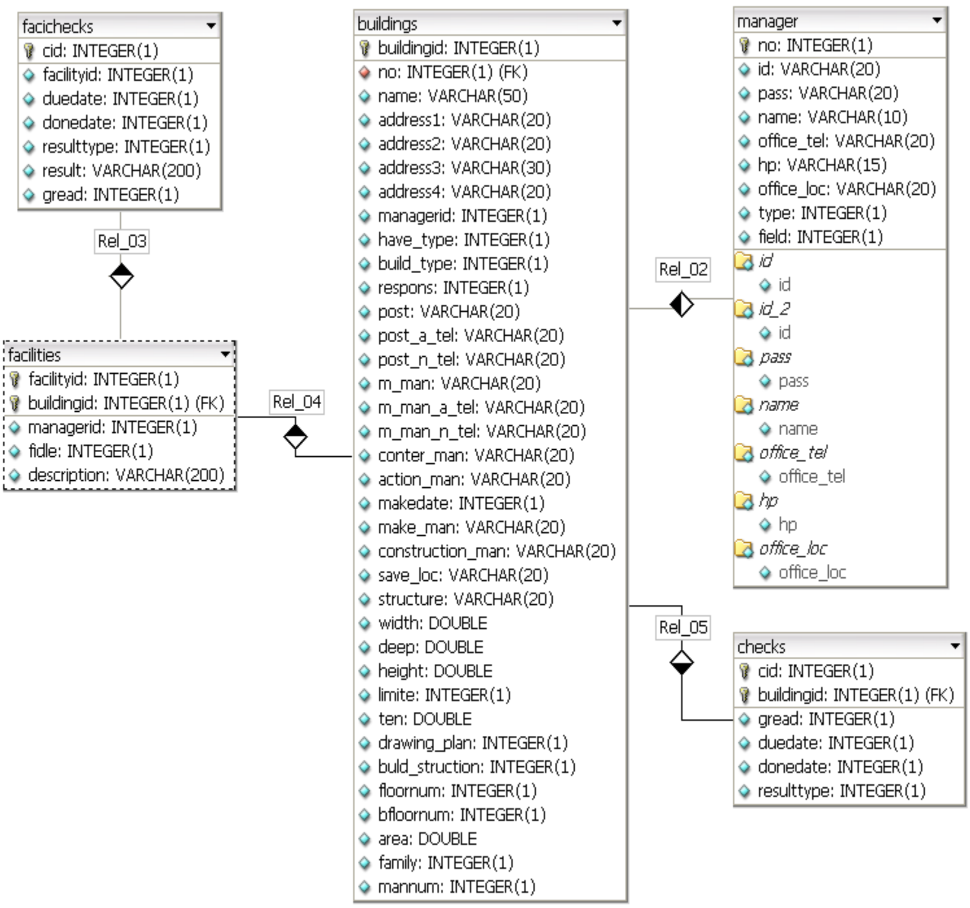

Figure 3: Design of safety management information database

The Figure 4 shows the database schema for man-made disaster information. The cause of disaster, the magnitude of disaster and etc are expressed by predefined digital code, and they can be categorized and summarized.

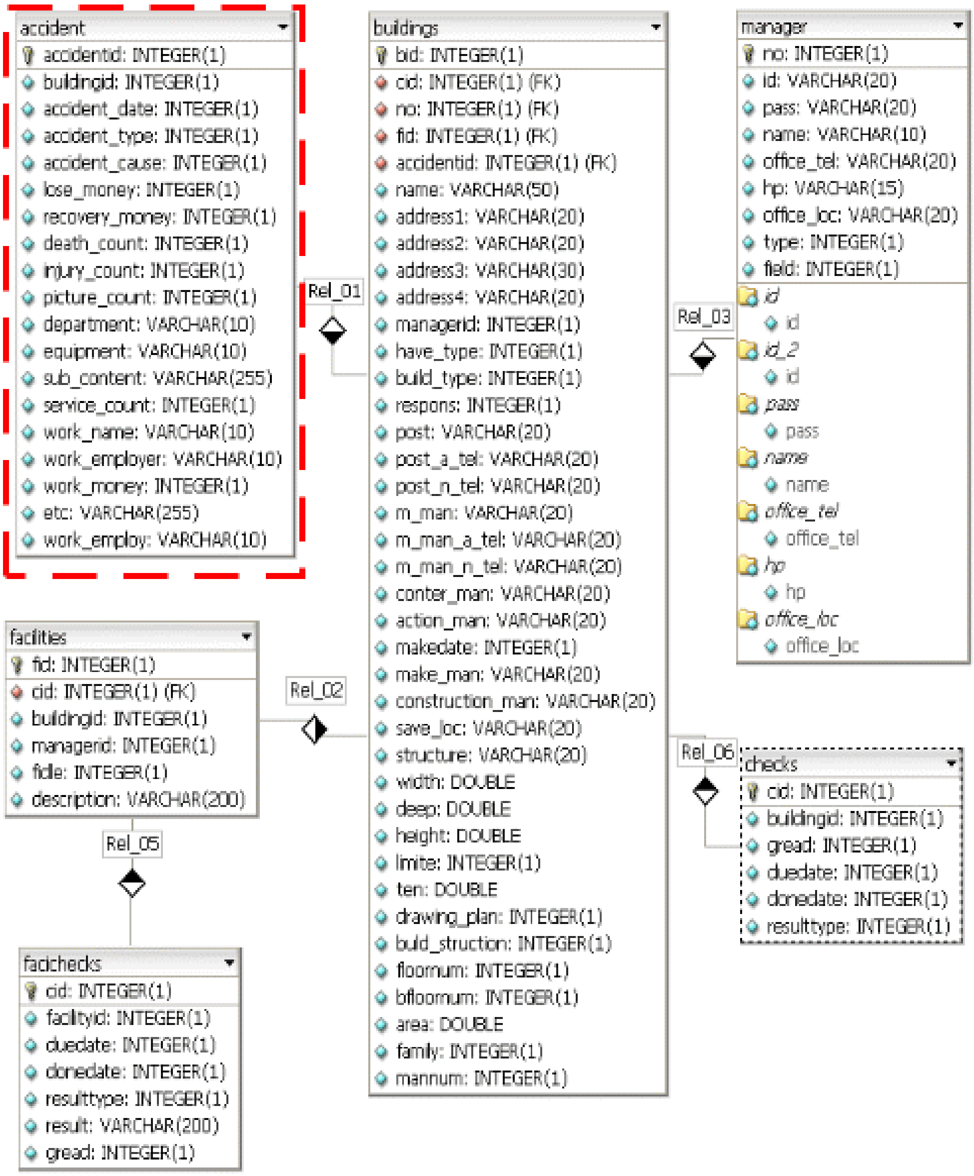

Figure 4: Database schema for the man-made disaster

3.3 Construction of TSMS

TSMS is constructed based on the system requirements and operation scenario. Figure 5 and 6 shows the system operation screen at the web. Working screen is composed of 3 categories. Top of the screen represent the system title, and left of the screen is composed of main working menu according to the system user group. Right of the screen is main working space on the working menu.

Figure 5 represent the facility list and function of search. Main working screen is constructed on the tab-based menu. Figure 6 represent the making of safety inspection check list. Check list can be hard print or mail to the parties concerned.

Figure 5: Example of TSMS display (Facility list)

Figure 6: Example of TSMS display (Check list)

4. CONCLUSION

Safety of the public facility is one of the important responsibilities of the government. Construction and application of the computational system is the most efficient method to increase the overall efficiency of safety management works. In this paper, analysis of the safety management works was performed and organizes the work flow. And construction of system database and web-based computational system for safety management works is introduced.

REFERENCES

NIDP, 2008. *Design of the On-line Safety Management System for the Specific Control Buildings and Facilities*. NIDP Research Report, Korea

NIDP, 2008. *The Construction Plan of the Integrated Safety Management System for Specific Control Buildings and Facilities*. NIDP Research Report, Korea

NIDP, 2007. *Development of the Web-based Safety Management Information System for the Facilities*. NIDP Research Report, Korea

Hjork, B. C., 1994. RATAS Project – Developing an Infrastructure for Computer-Integrated Construction, *Journal of Computing in Civil Engineering*, Vol.8, No.4

Howrd, H. C., 1992. Primitive-Composite Approach for Structural Data Modeling, *Journal of Computing in Civil Engineering*, Vol.6, No.1

Sause, R., 1990. A Design Process Model for Computer Integrated Structural Engineering, *Engineering with Computers*, Vol. 6

CURRENT DEVELOPMENT OF AN INTEGRATED STEEP-SLOPE MANAGEMENT SYSTEM FOR URBAN DISASTER RISK REDUCTION IN KOREA

DUGKEUN PARK, JEONGRIM OH,
YOUNG-KARB SONG and MIN-SEOK LEE
National Institute for Disaster Prevention (NIDP),
National Emergency Management Agency (NEMA), Korea
drpark, jeongrim, sonyjin2002, sky2ms@korea.kr

ABSTRACT

Large scaled Landslide disasters in steep slopes in urban areas are increasing due to climate change, showing uncertainties in occurrence. In Korea most of the steep-slope disasters are induced by typhoons and torrential rains in the Summer time, causing many casualties, property damages, and recovery costs.

To mitigate these disasters and ensure citizens' safety, the National Emergency Management Agency (NEMA) has established the "Steep-slope Disaster Prevention Act" in 2008 focusing on the efficient and effective steep-slope maintenance and management. One of the measures for steep-slope disasters is to enforce early warning and evacuation practice to minimize human casualties. NEMA is trying to establish an integrated system not only for an early warning system based on the empirical correlations between rainfall characteristics and steep-slope disaster occurrences, but also for an database for previous steep-slope disaster events, classification schemes, and field-survey methodologies for steep-slope disasters.

This paper reviews the characteristics of steep-slope disasters in Korea and proposes steep-slope maintenance and management system in general which can be adapted effectively in Korea.

1. INTRODUCTION

The risks of steep-slope related disasters are increasing due to urbanization and increased rainfall intensity by climate change in Korea. Most of the steep-slope related disasters are concentrated in the summer period when most of torrential rains and typhoons have major impacts in urban areas.

The natural disaster characteristics have been changing in Korea. The characteristics can be simply described as, compared to the previous decades, that the impact of natural disasters is much severer in urban areas in Korea over the last ten years and most of the killer disasters are related to the steep-slope disasters.

It is agreeable that preventing the occurrence of steep-slope disasters is one of the hard tasks in disaster management simply due to technical constraints and budget limitations. However, it may be possible to reduce the impact by steep-slope disasters when new technologies, policies, awareness are developed, implemented, and built.

To tackle problems regarding steep-slope disasters comprehensively, the Korean government established the "Steep-slope Disaster Prevention Act" and has enacted since July 28, 2008 covering inspection and maintenance procedures, monitoring requirements, early warning and evacuation practices, etc. Also, the National Institute for Disaster Prevention (NIDP) has been performing research projects on landslide early warning systems considering rainfall characteristics in both urban and rural areas for appropriate preparedness and response to steep-slope disasters.

2. STATUS OF STEEP-SLOPE DISASTERS IN KOREA

Over the last ten years human casualties by various natural disasters in Korea are reported every year and the number of deaths by steep-slope related disasters is also reported continuously (NDMS, 2008; Park et al., 2008a; Park et al., 2008b; Park et al., 2007a; Park et al., 2007b). Serious cased can be found during the typhoon events, i.e., Typhoon Rusa in 2002 and Typhoon Maemi in 2003.

According to the statistics over the past ten years from 1999 to 2008, it is found that the number of deaths by various natural disasters is 805 and, among them, 217 deaths are due to steep-slope related disasters indicating that about 27% of human deaths by natural disasters is attributed to slope-stability related geological disasters in Korea. Table 1 shows the number of deaths by natural disasters, steep-slope disasters, and their relative ratios in Korea (NIDP, 2008).

3. STEEP-SLOPE DISASTER MANAGEMENT SYSTEM IN KOREA

To mitigate steep-slope disasters several agencies and organizations are performing related researches and routine maintenance tasks for mountainous areas, cut-slopes along national roads, natural terrains, and slopes in urban areas.

Table 1: Death by natural and steep-slope related disasters in Korea over the past ten years

Year	by Natural Disaster	by Slope-stability related Disaster	Ratio (%)
Total	805	217	27.0
Average	80.5	21.7	
1999	89	32	36.0
2000	49	12	24.5

2001	82	9	11.0
2002	270	79	29.3
2003	148	37	25.0
2004	14	3	21.4
2005	52	11	21.2
2006	62	22	35.5
2007	23	4	17.4
2008	16	8	50.0

The Korea Institute of Construction Technology and the Korea Expressway Corporation perform stability analysis and maintenance of cut slopes in national roads based on the specific research requests from R&D donor agencies, and stability analysis and maintenance of cut slopes in national highways, respectively.

On the other hand, the Korea Institute of Geoscience and Mineral Resources and the Korea Forest Research Institute carry out researches on landslides and cut slopes based on the specific research requests from R&D donor agencies, and landslides in mountainous areas for forest protection and recovery, respectively. Table 2 shows main research functions of different agencies in Korea regarding slope-stability related tasks.

Table 2: Research areas in various institutions in Korea

Institution	**Main Function**
National Institute for Disaster Prevention	- Researches on geological disasters including landslides and slope disasters in national level for disaster management aspects
Korea Institute of Geoscience and Mineral Resources	- Researches on landslides and cut slopes based on the specific research requests from R&D donor agencies
Korea Institute of Construction Technology	- Stability analysis and maintenance of cut slopes in national roads based on the specific research requests from R&D donor agencies
Korea Forest Research Institute	- Landslides in mountainous areas for forest protection and recovery
Korea Expressway Corporation	- Stability analysis and maintenance of cut slopes in national highways

Most of the agencies in Korea have their own slope management systems with a sort of early warning systems based on the measurement of physical properties and parameters generated by ground movement and geotechnical monitoring. Each system has pros and cons.

However, main disadvantage of the existing early warning systems in the view of disaster management practice for the residents arises from that the leading time for evacuation and preparedness is not assured. Also, installations and operations of various monitoring equipments are sometimes limited due to the cost covering vast of potentially-hazardous slopes and areas.

Therefore, it is necessary to develop a low-cost, highly-efficient, and practical early warning system for scattered and uncertain areas with disaster-prone steep slopes. Especially, NIDP is trying to establish an early warning system reflecting rainfall characteristics in local and urban areas.

4. STUDIES ON EARLY WARNING AND EVACUATION SYSTEM FOR STEEP-SLOPE DISASTERS

Based on the "Steep-slope Disaster Prevention Act" an early warning system, data management system, and five-year research project for steep-slope disasters have been proposed.

As shown in Figure 1, the research project is composed of three tiers such as fundamental technology development, establishment of early warning system, and operation of pilot systems and test beds. Main objectives of the project are to analyze the factors affecting landslide occurrence, to review the applicability of GIS, to propose the relationship between rainfall characteristics and slope failures, to set up warning and critical boundaries for feasible early warnings, to develop evacuation scenarios and response system, to operate pilot system in the test beds, and produce manuals and documents for local officials and residents.

The outcomes of the integrated steep-slope management system for urban disaster risk reduction will include practical and tangible landslide early warning system considering geological, landslide-occurrence, and socio-geographical characteristics in Korea. When the project produces successful outcomes, it is expected to be used for real-time disaster management in steep-slope disaster-prone areas saving people’s lives and reducing property damages.

5. CONCLUSIONS

Korea is suffering from disaster impacts by geological and meteorological hazards such as torrential rain, typhoon, drought, heavy snow, and steep-slope failure. The disaster impacts are worsened in urban areas due to the increased vulnerability and exposure to climate change. The seriousness of steep-slope disasters is especially increased in residential areas partly due to the reckless and concentrated development.

To tackle the increased localized incidents by steep-slope failures, an integrated steep-slope management system for urban disaster risk reduction

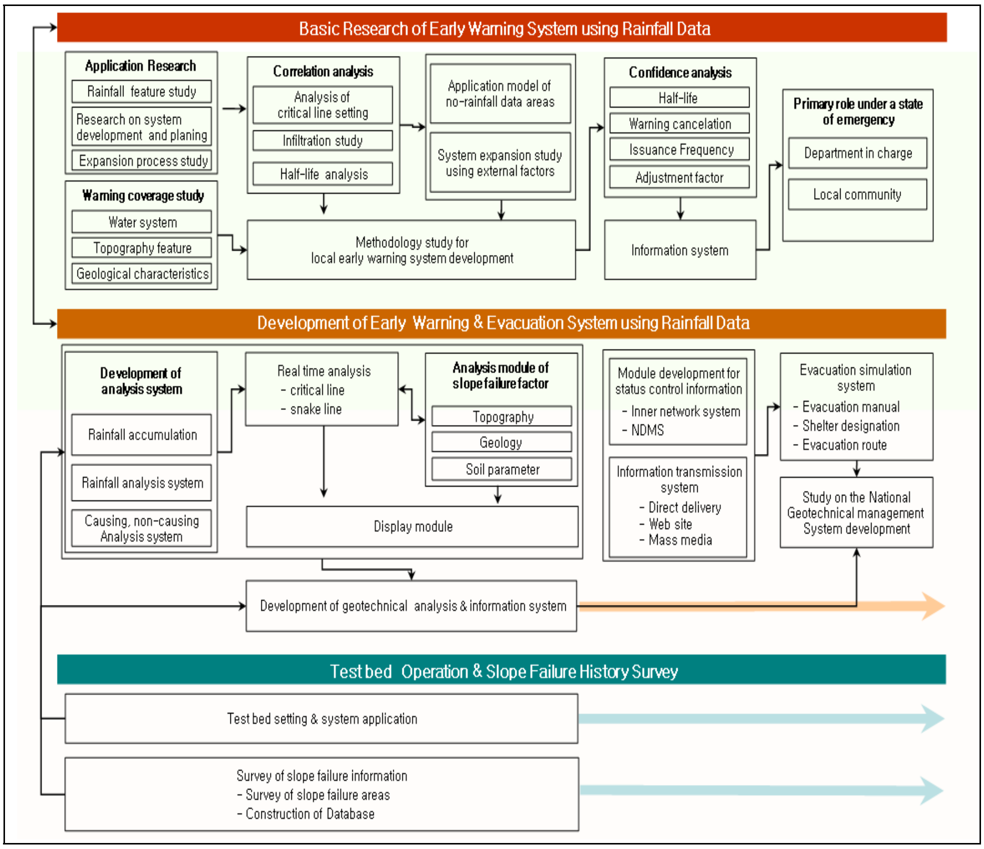

Figure 1: Technical road map of the integrated steep-slope management

has been proposed focusing on early warning systems based on the relationship between landslide occurrence and rainfall characteristics. Six test beds are under operation for the system refinement. Three test beds are located in mountainous areas and other three test beds are in hilly areas. By 2010 three additional test beds will be installed in coastal areas so that rainfall characteristics in three different regions can be analyzed.

In the future accumulated data and technologies will be shared with international initiatives such as the International Consortium on Landslides and also shared with less developed countries through technology transfer and expert exchange.

REFERENCES

NIDP, 2008, Study on the Steep-slope Early Warning and Evacuation System using Rainfall Data (I), the National Institute for Disaster Prevention, the National Emergency Management Agency, Research Report (in Korean).

NDMS, 2008, The National Disaster Management System, Nation-wide Disaster Information Compilation and Database System operated by the National Emergency Management Agency (in Korean).

Park D, Oh J, Park J, and Chae B (2007a), Slope-stability Related Disasters and Regulatory Countermeasures in the Republic of Korea, Proc. the Int. Symp. on Landslide Risk Analysis and Sustainable Disaster Management (IPL 2007), January 21-24, UN Univ., Tokyo, pp. 19-23.

Park D, Oh J, Park J (2007b), An Application Method for Landslide Early Warning in Wangsan Myeon Area using Rainfall Data, Proc. Korean Geotechnical Society Spring Conf., March 23-24, Korea Univ., Seoul, pp. 1,112-1,118.

Park D, Oh J, Son Y, Park J, Lee M (2008a), Steep-slope management system in Korea, The 2nd East Asia Landslides Symposium, Seoul, Korea, May 22-23, pp. 7-11.

Park D, Oh J, Son Y, Lee M (2008b), Preliminary Approach for a Nation-wide Regional Landslide Early Warning System in South Korea, The First World Landslide Forum, November 18-21, UN Univ., Tokyo, pp. 469-472.

PROPOSAL OF EFFICIENT ROAD SPACE UTILIZATION IN URBAN ARTERIAL STREET

SHINJI TANAKA and MOTOMUNE KATAOKA
ICUS, IIS, The University of Tokyo, JAPAN
stanaka@iis.u-tokyo.ac.jp

ABSTRACT

In urban arterial streets, traffic congestion happens frequently but available space for countermeasures is normally limited. Therefore, an efficient utilization of the limited road space is very important.

In this study, a road section which has a lot of congestion is picked up and the cause of the congestion is identified. Then, a countermeasure which reallocates the road space in order to increase the traffic capacity was proposed. This is to create right-turn bay at the intersection and on-street parking space in the middle of the link by shifting the through traffic lanes so that right-turn vehicles and on-street parking vehicles do not block the through traffic flow.

The effect of the proposed countermeasure was examined by a mathematical analysis and a driving simulator experiment. From the mathematical analysis, it was revealed that the capacity for through traffic would be increased by 27 %, which was enough improvement to alleviate the congestion. Through the driving simulator analysis, it was checked whether drivers have difficulties in driving or not by the proposed geometrical alignment. The result showed that there are no serious risks in their driving behavior.

1. INTRODUCTION

There are still a lot of traffic congestions in urban streets. It deteriorates the utility and the reliability of the transportation network a lot. If we have enough budget and space, we can solve it by expanding the road or constructing a new highway. However, available land is usually very limited in urban area therefore it is very important to make use of the existing available space to extract the maximum utility.

The fundamental reason why congestion happens is the traffic demand is larger than the capacity of the road facility. In other words, when the configuration of the road facility does not match the actual demand, the congestion occurs. Therefore we have to make sure whether the configuration of the facility is appropriate or not considering the current traffic situation. And if it does not suit the situation, we need to modify it. Otherwise, it produces a lot of congestion and it means a large waste of resources. In this study, a road section where a lot of congestion happens is picked up and a countermeasure to alleviate it is proposed with some evaluation of the effect.

2. STUDY AREA

2.1 Current situation

The study area is located in the center of Kochi city in Japan, whose population is approximately 340 thousand. The target is the main street of the city, running east-west through the center. It has 3 lanes for each direction, and tram track in the middle. In the morning and evening peak period, 1 lane out of 3 is used for the exclusive bus lane. The street carries more than 35,000 vehicles per day. As it is the center of the city, there are a lot of on-street parking vehicles although it is not allowed in this section. As a result, this street is ranked as the most seriously congested section in Shikoku Region as shown in Figure 1.

Figure 1: Traffic congestion loss by section in Shikoku, Japan

2.2 Causes of congestion

To consider the cause of this traffic congestion, let's look at the detector data of this section. Figure 2 shows the traffic volume data on each lane in the evening peak counted by traffic detectors. Here, traffic volume of 3 lanes is shown, where "left" means the shoulder side lane and "right" means the median side lane. From these figures, we can understand that the lane usage is unbalanced very much, that is, the center (2nd) lane always carries larger traffic volume whereas the left (1st) and the right (3rd) lanes have less traffic in both directions. It means that the road space is used inefficiently.

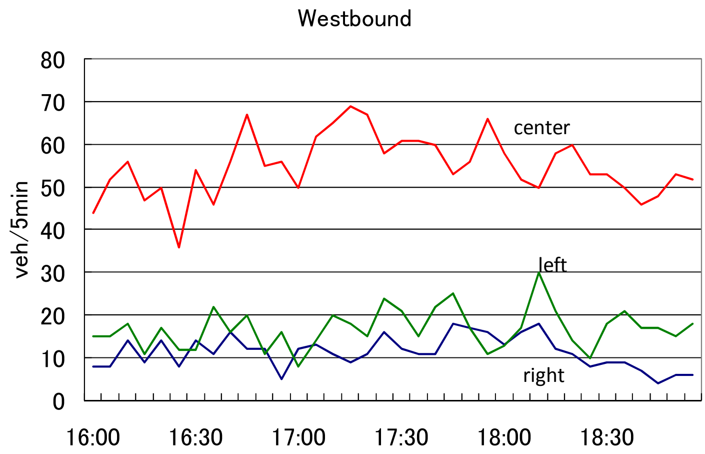

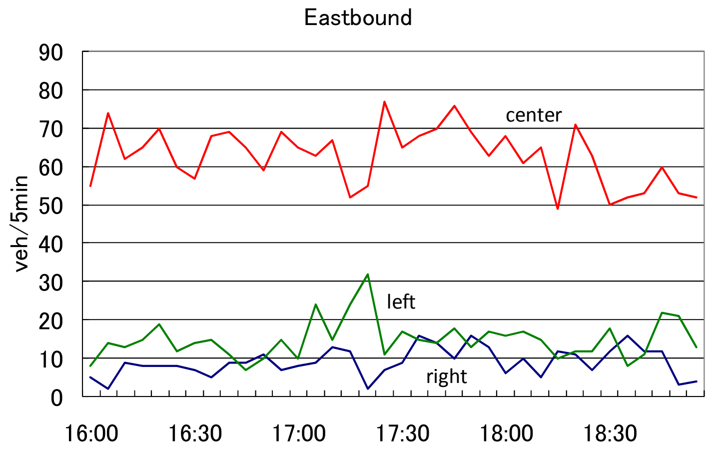

Figure 2: Traffic volume by lane

The reason why this phenomenon happens is illustrated in Figure 3. On the left (1st) lane, there are often illegal on-street parking vehicles because this area has a lot of business and commercial activities. On the other hand, the right (3rd) lane is a mixed use of through and right-turn traffic, therefore sometimes right-turn vehicles stop and wait for the oncoming traffic in front of the tram track, and block following through traffic. As a result, through traffic vehicles tend to concentrate on the center (2nd) lane and form a queue even though the other lanes are not crowded yet. This is the mechanism how the traffic congestion happens in this section.

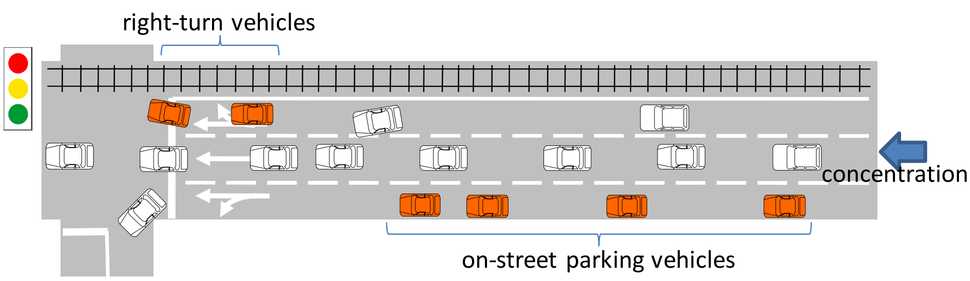

Figure 3: Typical phenomena during congestion

3. PROPOSAL OF COUNTERMEASURE

3.1 General idea

In the current situation, the road space is not fully utilized because the left (1st) lane and the right (3rd) lane only carry much less traffic as shown in Figure 2. Therefore we should utilize this space as much as possible. In other words, the unused road space should be reallocated so as to suit the traffic demand.

3.2 Geometric design

Figure 4 shows the proposed geometric design of the countermeasure. Here, 2 lanes out of 3 are assured for through traffic although the total width of the street remains the same as the current geometry. They are shifted to the left at the approach of the intersection so that right-turn vehicles can stop at the right-turn bay. Also, they are shifted to the right in the middle of the link so that an on-street parking space is created. In this design, the road space is efficiently used for through traffic, right-turn and on-street parking vehicles as shown in the figure. Through traffic vehicles can use 2 lanes without major obstacles like right-turn vehicles or on-street parking vehicles, so this design should have significant improvement of the situation.

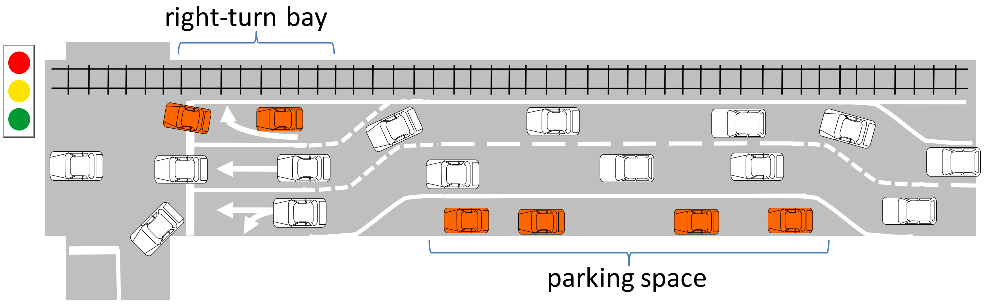

Figure 4: Geometric design of the proposed countermeasure

4. EFFECTIVENESS ANALYSIS

4.1 Mathematical analysis

To evaluate the effect of this proposal, we estimated the amount of the improvement by a mathematical analysis first. Specifically, as the through traffic is congested in the current situation, the capacity improvement of the through traffic is analyzed according to the guideline “Plan and Design of Grade Intersection”.

4.1.1 *Prerequisite*

In the current condition, there are very few through traffic vehicles running on the left (1st) lane because there are almost always on-street parking vehicles there. Therefore we presume that the through traffic use the center (2nd) and the right (3rd) lane in the current condition, and use the left (1st) and the center (2nd) lane in the proposed condition.

4.1.2 *Possible through traffic capacity on each lane*

Next the possible capacity for through traffic is calculated on each lane. Here, we employ the standard value of the saturation flow rate of through traffic (*SFR*) as *2,000* [veh/green hr].

(a) Center (2nd) lane

The capacity for the center (2nd) lane C_2 is the simplest, that is,

$$C_2 = SFR \cdot \frac{G}{C} = 2000 \cdot \frac{G}{C} \; [veh/h] \tag{1}$$

where, C: cycle length [sec], G: effective green length [sec]

(b) Right (3rd) lane

For the capacity of the right (3rd) lane, we need to calculate the conversion factor of right-turn to through traffic (E_{RT}). First, the capacity of exclusive right-turn lane C_R is,

$$C_R = 1800 \cdot f \cdot \frac{SG - qC}{S - q} \cdot \frac{1}{C} + K \cdot \frac{3600}{C} \; [veh/h] \tag{2}$$

where, S: saturation flow rate of opposite traffic [veh/h], q: opposite traffic flow [veh/h], f: probability of right-turn gap during opposite traffic q ($f=0$ under $q>1{,}000$), K: number of right-turn vehicles which can stop inside the intersection [veh/cycle] (approx. 3 [veh/cycle]).

The conversion factor of right-turn to through traffic (E_{RT}) is calculated by dividing (1) by (2), that is,

$$E_{RT} = \frac{2000\frac{G}{C}}{1800 f \cdot \frac{SG - qC}{C(S - q)} + 3600\frac{K}{C}} = \frac{1.1}{f \cdot \frac{SG - qC}{G(S - q)} + \frac{2K}{G}} \tag{3}$$

Then, the correction factor of the saturation flow rate for the mixed lane of right-turn and through traffic α_{RT} is,

$$\alpha_{RT} = \frac{100}{(100 - R) + E_{RT} \cdot R} \tag{4}$$

where, R: right-turn vehicles ratio

Therefore the capacity for the right (3rd) lane C_3 is,

$$C_3 = SFR \cdot \frac{G}{C} \cdot \alpha_{RT} = 2000 \cdot \frac{G}{C} \cdot \alpha_{RT} \; [veh/h] \tag{5}$$

(c) Left (1st) lane

Similarly for the capacity of the left (1st) lane, we need to calculate the conversion factor of left-turn to through traffic (E_{LT}). First, the capacity of exclusive left-turn lane C_L is,

$$C_L = 1800 \cdot \frac{(1-f_P)G_P - (G-G_P)}{C} \ [veh/h] \tag{6}$$

where, G_P: pedestrian green length [sec], f_P: reduction ratio of left-turn throughput by pedestrians (0.15 - 0.50)

The conversion factor of left-turn to through traffic (E_{LT}) is calculated by dividing (1) by (6), that is,

$$E_{LT} = \frac{2000\dfrac{G}{C}}{\dfrac{1800\{(1-f_P)G_P + (G-G_P)\}}{C}} = \frac{1.1G}{(1-f_P)G_P + (G-G_P)} \tag{7}$$

Then, the correction factor of the saturation flow rate for the mixed lane of left-turn and through traffic α_{LT} is,

$$\alpha_{RT} = \frac{100}{(100-L) + E_{LT} \cdot R} \tag{8}$$

where, L: left-turn vehicles ratio

Therefore the capacity for the left (1st) lane C_1 is,

$$C_1 = SFR \cdot \frac{G}{C} \cdot \alpha_{LT} = 2000 \cdot \frac{G}{C} \cdot \alpha_{LT} \ [veh/h] \tag{9}$$

4.1.3 *Estimation of the effect*

Using the possible traffic capacity on each lane derived as above, the effect of the proposed design is estimated. Table 1 shows the values used in this estimation.

Table 1: Parameter values for the estimation

Parameter		**Value**
SFR	Saturation flow rate of through traffic	2,000 [veh/green hr]
R	Right-turn vehicle ratio	10 [%]
L	Left-turn vehicle ratio	10 [%]
C	Cycle length	120 [sec]
G	Effective green length	60 [sec]
G_P	Pedestrian green length	55 [sec]
f	Probability of right-turn gap	0
f_P	Reduction ratio of left-turn by pedestrian	0.5

From Eq. (1),

$$C_2 = 2000 \cdot \frac{60}{120} = 1000[veh/h] \tag{10}$$

From Eq. (3) and (4),

$$E_{RT} = \frac{1.1}{\frac{2\times 3}{60}} = 11 \tag{11}$$

$$\alpha_{RT} = \frac{100}{(100-10)+11\cdot 10} = 0.5 \tag{12}$$

Then, from Eq. (5),

$$C_3 = 2000 \cdot \frac{60}{120} \cdot 0.5 = 500\ [veh/h] \tag{13}$$

From Eq. (7) and (8),

$$E_{LT} = \frac{1.1\times 60}{(1-0.5)\cdot 55 + (60-55)} = 2.03 \tag{14}$$

$$\alpha_{RT} = \frac{100}{(100-10)+2.03\cdot 10} = 0.91 \tag{15}$$

Then, from Eq. (9),

$$C_1 = 2000 \cdot \frac{60}{120} \cdot 0.91 = 907[veh/h] \tag{16}$$

Finally, the through traffic capacity of the current situation and the proposed one are,

Current: $C_2+C_3=1,500\ [veh/h)$ (17)

Proposed: $C_1+C_2=1,907\ [veh/h]$ (18)

From this result, the through traffic capacity is increased by 27%, that is enough value compared with the excess demand of the normal traffic congestion. Therefore we can expect to solve the congestion by this proposed geometric design.

4.2 Driving behavior analysis

Even though the proposed design has a significant advantage in congestion alleviation, it is difficult to apply it if we cannot confirm the driving safety. Especially, as the proposed design includes a lateral shift of the lanes in the middle of the link, it is essential to examine whether this shift makes a negative impact on the safety or not. To evaluate this, we conducted a driving simulator experiment.

4.2.1 *Settings*

Figure 5 shows the appearance of the driving simulator used in this analysis. The features of this driving simulator are 6-axis motion platform, turn table, 360 degrees screen and so on. It can record various indices of driving behavior, such as speed, acceleration / deceleration, steering angle etc. And it can also record driver’s behavior by video cameras.

Figure 5: Appearance of the driving simulator

2 scenarios were prepared for the experiment, which are the current geometric design and the proposed one. Each testee drove on the course 4 times per scenario, following some practice runs. The testees were interviewed after their driving about their subjective evaluation. Table 2 shows the attributes of the testees.

Table 2: Attributes of the testees [num, (%)]

Age	25 or less	26 - 64	65 or more	
	5(38.5)	7(53.8)	1(7.7)	
Sex	Male		Female	
	11(84.6)		2(15.4)	
Driving history	~ 1 year	~ 5 year	~ 10 year	More
	0(0.0)	3(23.1)	2(15.4)	8(61.5)
Driving frequency	4 or more /week	1 - 3 /week	1 - 3 /month	Less
	1(7.7)	3(23.1)	2(15.4)	7(53.8)
Know the location?	Yes		No	
	2(15.4)		11(84.6)	

4.2.2 *Results*

4 checkpoints were examined from the recorded data, that is, whether brake was used or not at the lateral shift, how much the maximum value of lateral acceleration was, whether the value of lateral acceleration was different from the existing section, and whether sharp steering maneuver was found or not. The results are shown in Table 3.

Table 3: Experiment result [num, (%)]

Use of brake	Yes	1(7.7)
	No	12(92.3)
Max lateral acceleration [G]	0.2 ~ 0.35	1(7.7)
	0.15 ~ 0.2	2(15.4)

	~ 0.15	10(76.9)
Comparison with the existing section	More	2(15.4)
	Same	5(38.5)
	Less	6(46.2)
Sharp steering maneuver	No	13(100.0)

As for the brake use, only 1 testee used it. However the deceleration rate was not so hard (0.12 [G]) and the testee answered that he used a brake not because of the lateral shift but the difference of the driving feeling from the actual vehicle.

Previous studies indicate that the lateral acceleration value more than 0.15 [G] may influence some patients on an ambulance and the value of 0.22 [G] is used to detect potential risks in expressway. The maximum value of lateral acceleration in this experiment showed less than 0.15 [G] in most of the cases, but more than 0.2 [G] in 1 case. This testee also answered that it was difficult to maneuver the steering of the simulator but not difficult about the alignment, so it seems a matter of the experiment equipment.

As for the comparison of the lateral acceleration with the existing section, larger acceleration was observed in 2 cases. However, their absolute values were not dangerous level in either case.

Finally, there were no sharp steering maneuvers found in all 13 testees' runs.

5. CONCLUSIONS

This study insisted on the importance to utilize road space efficiently in urban area to alleviate traffic congestion. And taking an example of an arterial street in Kochi city, road space reallocation to alleviate congestion was proposed. This proposal does not require extra land, so it is relatively feasible measure than a large scale renovation in urban area. The effect of the proposal was evaluated by a mathematical analysis and a driving behavior analysis from a viewpoint of efficiency and safety, respectively. The result showed that enough capacity improvement was expected for through traffic to solve the congestion and no serious behaviors leading to risks were found in the experiment. We believe this kind of fine and careful management of infrastructure is very important to keep the traffic network working and to establish sustainable urban environment.

REFERENCES

Kamimura, A., Kataoka, M., Tanaka, S., Kumagai, Y., Kuwahara, M., and Nasu, S., 2007. Proposal of new road manner of operation and untie a traffic jam project, *Proceedings of the 35th Conference of Infrastructure Planning, Spring Meeting*, JSCE, CD-ROM (in Japanese).

Kataoka, M., Tanaka, S., Kumagai, Y., and Kuwahara, M., 2008. Proposal of ease traffic jam measures by dynamic lane, *Proceedings of the 37th Conference of Infrastructure Planning, Spring Meeting*, JSCE, CD-ROM (in Japanese).

Kataoka, M., Kumagai, Y., Nakagawa, T., Yamaguchi, D., Tanaka, S., Suda, Y., and Kuwahara, M., 2009. Safety verifications of countermeasures to alleviate traffic congestion on Route 32 using driving simulator, *Proceedings of the 40th Conference of Infrastructure Planning, Autumn Meeting*, JSCE, CD-ROM (in Japanese).

STUDY ON THE COASTAL DISASTER PREVENTION SYSTEM USING EVACUATION MODEL

SUNGJIN HONG
Senior Research, National Institute for Disaster Prevention, NEMA, Korea
hongsj@nema.go.kr
TAEKJO KOH
National Institute for Disaster Prevention, NEMA, Korea
HYOUNGSEONG PARK
National Institute for Disaster Prevention, NEMA, Korea

ABSTRACT

The objective of this research is to investigate the evacuation system of coastal inundation area and to support a decision by effective selection of shelter and routes by using evacuation model. In this report, numerical models for evacuation such as network model, potential model and multi-agent system model are reported. And its applicability of them is also discussed. The result shows that the potential model has advantage for representing individual behaviors with particles. The disaster management for reduction of coastal inundation damages is tested in numerical model. The numerical experiments are carried out in the Woryeong-dong, Masan for analyzing evacuation routes and shelter. Furthermore, a questionnaire is designed to determine escape route selection, parameters and initial conditions of the evacuations. The questionnaire survey is performed for analyzing the resident's knowledge about coastal inundation.

1. INTRODUCTION

Coastal disasters have become one of the most important issues in every coastal country. In Korea, coastal related disasters such as storm surge, sea level rise and extreme weather have placed many coastal regions in danger of being exposed or damaged during subsequent storms and gradual shoreline retreat. A storm surge is an onshore gush of water associated with a low pressure weather system, typically in typhoon season. However, it is very difficult to predict storm surge height, tsunami height and inundation due to the irregularity of the course and intensity of a typhoon, tsunami and so on. Therefore, it is necessary that adequate evacuation system is prepared in accordance with formalities.

A well-designed system for evacuations warning issues is essentially necessary to reduce human loss and damages. A lack of tools of an evacuation system has such problem as long time simulation time. The objective of the present study is to develop the effective evacuation system by survey and numerical experiments. Detailed contents are as follows: (i) Firstly, questionnaire is designed to be distributed at the time of the drill, which provided us information to determine route selection, parameters and initial conditions of the evacuations. Various parameters like as regional knowledge, altitude, road information, road signs, following process, and functions on the route to be major factors in the route selection are determined to analyze the evacuation system. Consequently, moving speed and earlier starting of evacuation are important parameters to minimize total morality and missing rate. Using selected parameters, field survey is carried out to clarify various factors that influence selection of evacuation routes for making a synthetic judgment model. (ii) Secondly, numerical experiments using the potential model are applied to analyzing the evacuation situation in study area. It is possible that the potential model shown in Figure 1 presents individual behavior of evacuees as particles. Recently, various studies using the potential model have been carried out in the field of coastal prevention.

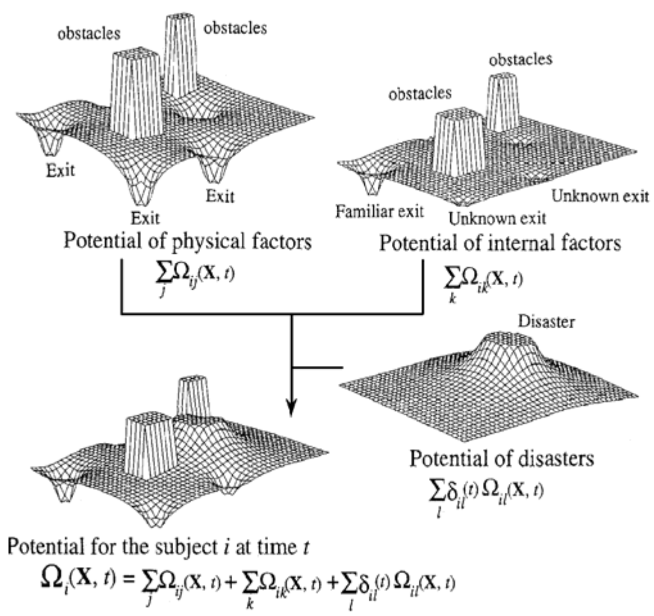

Figure 1: Method of risk potential

2. COUNTERMEASURES FOR DISASTER PREVENTION

It is necessary that establishment of evacuation building is established for preparing emergency situation in coastal inundation area as shown Figures 2 and 3. In Korea, however, building owner is reluctant to be selected for evacuation building because of the lack of public relations and management problems. Consequently, it is try to find the solutions to the problems that are costs of management and damage according to selection for evacuation building. It is required that solid buildings are positively appointed evacuation shelters through its many incentive programs. Also, it is desirable that evacuation building is selected with consideration of a collision between building and ship, flotage by storm surge or tsunami and so on.

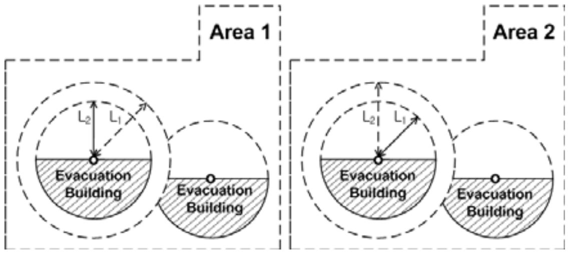

Figure 2: Selection method of evacuation region within the limits

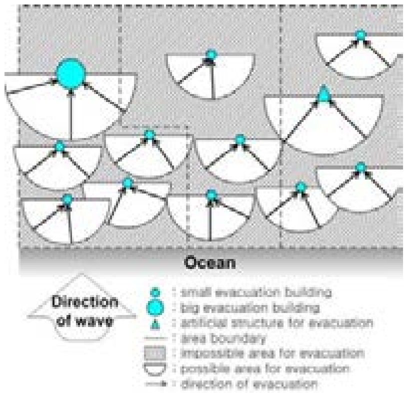

Figure 3: Concepts of evacuation building

In the choice of evacuation routes, it is important that routes near to seek rather than the short distance are selected. If evacuation route goes across through a residential street, tourists and foreigner cannot look for shelter so readily. Though evacuation building is completely not guarantee the safety of evacuees, it is applied to safety against coastal disaster for the nonce. Therefore, it is necessary that a standard of the utilization and management for evacuation building is established in process of previous structured and unstructured prevention measures.

Though structural surge prevention measures such as construction of breakwater, installation of shelter, and maintenance of tidal observation instrument are progressing, it is not enough for perfect prevention of coastal disaster for surge. Because of occurring of damages which are different from past are expected due to possibility of unexpected big surge, change of land utilization on the coast area, development of tourist and ocean leisure industry.

Even though prevent of property loss is important, more important factor is protection of people's life. To avoid huge casualty, disaster warning and evacuation advisory, and fast forwarding to local residents is needed in adequate time. But this process is hardly executed. Also, if residents don't want to evacuate after they listen evacuation advisory also could be a problem. Possible reasons of such behavior could be uncleanness of advisory, unable to judgment because of no specific standard, no research about natural phenomena and dike which are factors of disaster. Also, residents don't know how to be acting, cannot recognize the danger of them. In particular, the recent characteristics of the problem are about the evacuating of elderly, infants. To minimize the damage in the expected coastal disaster area, the evacuation system for residents, installation of shelter in safe area, set routes for rapid evacuation, set coastal inundation area are need to be established for evacuation system for quick and safe evacuation of residents.

In this research, analysis of resident' cognition on coastal inundation from survey of a study area is performed. With this result, disaster prevention measures for safe evacuation will be researched. Evacuation model represents the delivery type of disaster information, social phenomena (about evacuation system), and physical phenomena (tsunami arrived in the coastal area). Also, it is possible that the model calculates the feasibility of positioning shelter, the effective evacuation route and required time by the numerical simulation based on actual tsunami damage data.

3. APPLICATION OF EVACUATION MODEL

It is difficult that real training for evacuation is carried out in the field of disaster prevention against earthquake, fire, flood, inundation and so on. That is why numerical experiment is applied for analyzing the presumption of damage scale and assessment of prevention plan. In previous studies, small-scale numerical experiments were carried out. However, recently large-scale numerical models are developed for simulating the behavior of human. Essentially, it is prepared that evacuation system against storm surge, tsunami in coastal area is established for risk reduction of human loss. In interest of prevention, proper evacuation routes must be selected through analyzing the behavior of human.

In this chapter, we explain the evacuation numerical models like as network model, potential model and multi-agent system model and its applicability is also discussed.

3.1 Evacuation model

Evacuation models are applied to investigate the disaster prevention measures against earthquake, tsunami, storm surge, flood and so on. They are divided by (i) application region, (ii) constitution of evacuees and (iii) determination method of their behavior.

Because it is possible that the potential model represents individual behavior of evacuee as particles, various studies have been carried out recently on the potential model in the field of coastal prevention.

As shown Figure 4, the potential model has the advantage of representing behaviors of individuals by particles. The potential model is a kind of physical model that represents the behavior according as assumption of specified law for individuals in a group. It is possible that the potential model establishes a proper potential energy about geographical features of evacuation routes, personal features of evacuation and disaster situations in various evacuation simulations. Also, the potential model can represent the bottleneck situation of evacuees by setup of numerical parameters.

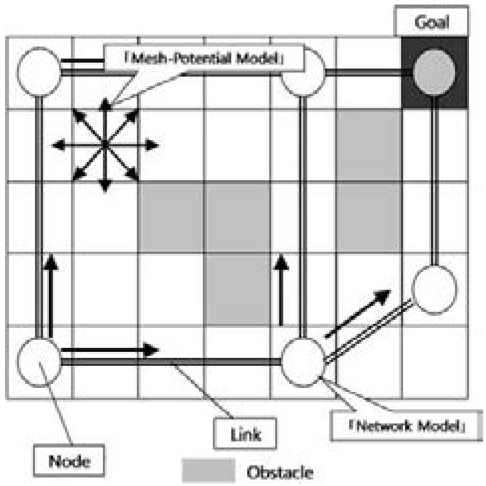

Figure 4: Explanation of the potential model and network model

3.2 Theory of potential model

The potential model is consisted of grid system by dx × dy. Each grid represents risk potential for evacuation situation in coastal inundation area. The distribution of potential is defined as follows:

$$\Omega_N(X,t) = \sum_j \Omega_{Nj}(X,t) + \sum_k \Omega_{Nk}(X,t) + \sum_l \delta_{Nl}(t)\Omega_{Nl}(X,t) \qquad (1)$$

$\Omega_N(X,t)$: distribution of potential applied to evacuee N

$\sum_j \Omega_{Nj}(X,t)$: distribution of common potential applied to every evacuees

$\sum_k \Omega_{Nk}(X,t)$: distribution of potential for personal features applied to evacuee N

$\sum_l \delta_{Nl}(t)\Omega_{Nl}(X,t)$: distribution of potential for disaster cause applied to evacuee N

In order to reach the destination, each evacuee selects the shortest course which represents the lowest potential from between numerical grids. Therefore, the potential model represents simply a disaster situation like as personal feature, topographical conditions and so on. Furthermore, it is possible to analyze the characteristic of individual behavior in a group.

4. RESULTS AND ANALYSIS

The numerical experiments are carried out for analyzing the characteristics of evacuation routes and shelter in Woryeong-dong, Masan. According to the report (Masan, 2004), typhoon 'MAEMI' caused extensive damage in this area. In detail, about 85 people died (with 25 others reported missing) in the storm and 250,000 people were forced to evacuate. The prevention measures of disaster are required for evacuation system because this area is not only strengthened an intensity of typhoon but also expanded a risk of inundation by storm surge.

Four areas are assigned the shelters for coastal inundation as follows: Hae-An elementary school, Seo-Masan middle school, the office of Woryeong-dong and Shin-Masan hospital. In numerical experiments, two area (Hae-An elementary school and Seo-Masan middle school) are selected from among them for numerical simulation following as Figure 5. Furthermore it is assumed that the wave is propagated from the east to the west.

Figure 6 shows evacuation situation at each time series. Evacuee calculates the shortest route to the shelter and they make a detour when they meet obstacles. Result shows that 90% of residents evacuate in 25 minutes. But preparing time for evacuation is almost takes 30 minutes, so actual evacuation time takes about 55 minutes. The result is quite different from 'Emergency 30 minutes plan' of government. It means because of preparing time to evacuate takes a lot of time, quick evacuation order can't guarantee the safety of resident. To solve this problem, continuous education about area of coastal inundation, location of shelter, evacuation route is required. To calculate the actual required time and find the ideal location of shelter, verification and modification of the plan are required by real evacuation simulator or numerical simulation. And more public relations of the plan such as a PR brochure or a guidebook is needed.

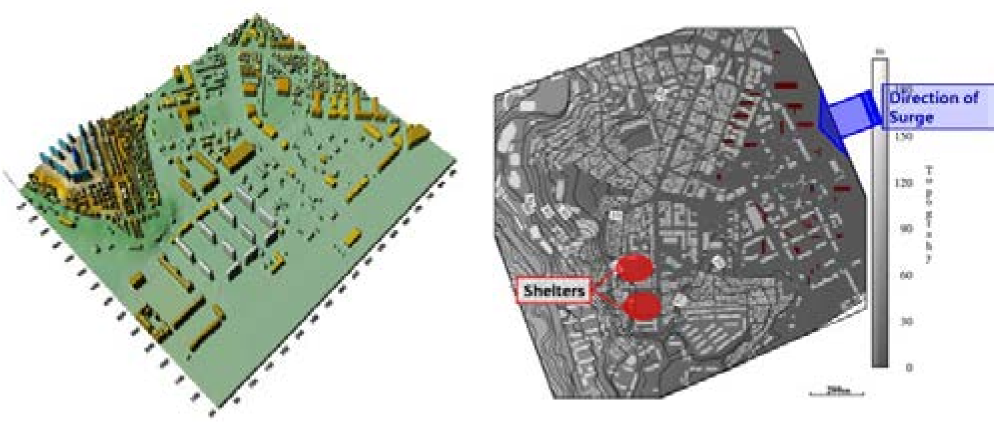

(a) Topography for study area *(b) Wave direction, locations of shelter and evacuees*

Figure 5: Information for numerical simulations in Woryeong-dong, Masan

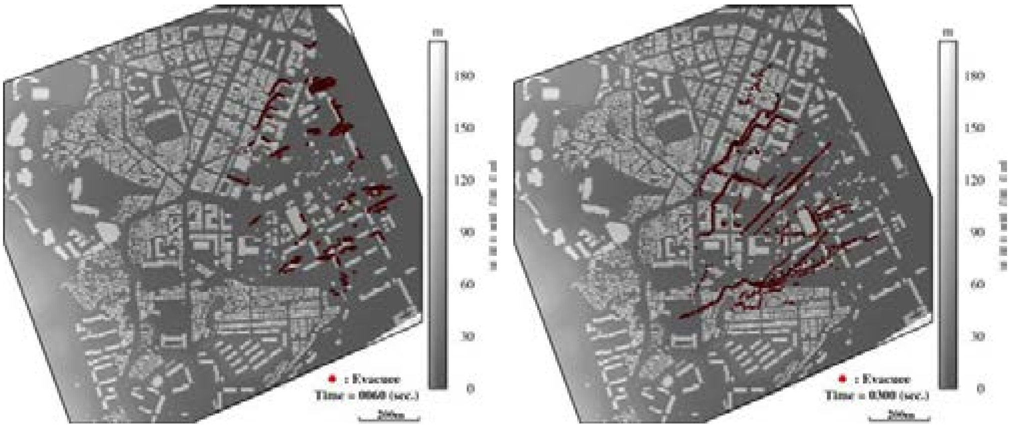

(a) After 1 minute *(b) After 5 minutes*

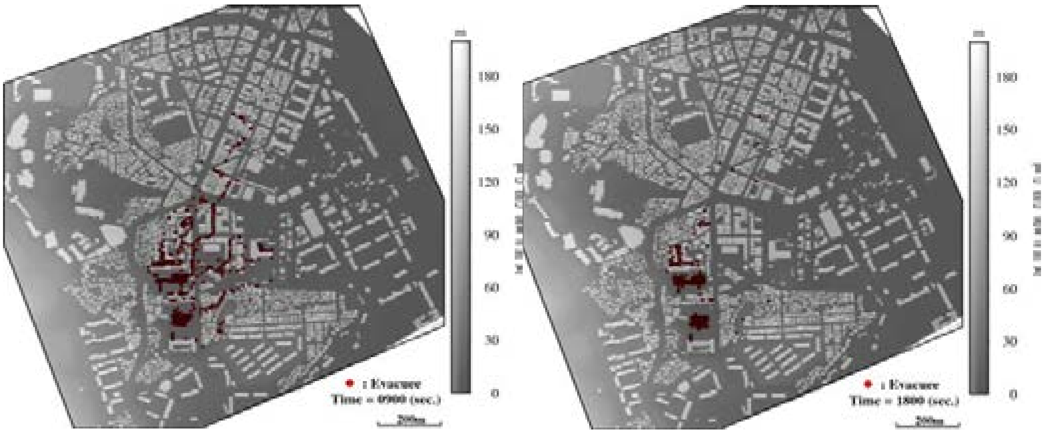

(c) After 15 minutes *(d) After 30 minutes*

Figure 6: Locations of evacuees at each time by numerical experiments

5. CONCLUSIONS

Quick evacuation is important to reduce casualties by inundation. Quick and exact transmissions of surge monitoring and adequate evacuation system are required. For these we developed system to support decision making to find effect escape routes and the results obtained from this research are following as: (i) Shelter building is need to be install in predicted coastal disaster area; (ii) Easy accessibility is more important than the shortest route to the shelter; (iii) Active promotion and education plan are need to improve cognition about inundation through a survey; and (iv) Provide a direction to improve the 'Plan for evacuation in 30 minutes' and the 'Guidelines for coastal disaster map'. Evacuation model need to improve for decision support system or disaster management system as follows: (i) Residents consider only short route and risk potential when they evacuate. accordingly, they used to use narrow route so that congestion of evacuation route is occur; (ii) Technique to install a fence is required to prevent congestion of evacuation route; and (iii) Numerical model which has not only evacuation simulation but also coastal inundation is required.

REFERENCES

Fararo, T. J., 1981. Based Network and Social Structure Theorems, *Social Networks*, 3, 137-159.

Ichimura, T., M. Hori, K. Terada, and Yamakawa T., 2002. On intergrated earthquake simulator prototype : Combination of numerical simulation and geographical information, *J. Strcu. Mech. Earthquake Eng.*, JSCE.

Imamura, F., 1996. Review of Tsunami Simulation with a Finite Difference Method, Long-Wave Run-up Models, World Scientific, *River Edge*, NJ, 43-87.

Koshimura, S., H. O. Mofjeld and Moore A., 2002. Modeling the 1100bp poletsunami in Puget Sound, Washington, *Geophysical Research Letters*, 29(20), 91-94.

Masan, 2004. *Analysis of Typhoon 'MAEMI' and Coastal Disaster Prevention*, Research Report, KSCE, 241p.

Okazaki, S., 1979. *A Study of Simulation Model for Pedestrian Movement on Architectural Space, Part 1 : Pedestrian Movement by the Application of Magnetic Models*, Transaction of Architectural Institute of Japan, 111p.

Okazaki, S., 1979. *A Study of Simulation Model for Pedestrian Movement on Architectural Space, Part 3 : Along the Shortest Path, Taking Fire, congestion and Unrecognized Space into Account*, Transaction of Architectural Institute of Japan, 137p.

Okazaki, S. and Matsushita, S., 1993. A Study of Simulation Model for Pedestrian Movement with Evacuation and Queuing, *Proceeding of the International Conference on Engineering for Crowd Safety*, 271-280.

Yang, F., T. Ichimura and Hori M., 2002. Earthquake simulation in virtual metropolis using strong motion simulator and geographic information system, *Journal of Applied Mechanics*, JSCE, 5, 527-534.

INTRODUCTION OF DISASTER IMAGINATION WORKSHOP INTO RISK-MANAGEMENT TRAINING FOR NURSERY SCHOOL LEADERS

[1]MARIKO ABE, [2]KIMIRO MEGURO, and [3]MARI YOKOYA

[1]Department of Civil Engineering, The University of Tokyo, Japan
abe@risk-mg.iis.u-tokyo.ac.jp
[2] International Center for Urban Safety Engineering,
Institute of Industrial Science, The University of Tokyo, Japan
[3]Institute of Industrial Science, The University of Tokyo, Japan

ABSTRACT

Japan is expected to face several big earthquakes in the near future. There are two important points for nursery school people to protect small children from such big earthquakes. First, each member of a nursery school should improve the disaster imagination. Second, members should share their image and experiences with each other. Therefore, we designed and conducted a Disaster Imagination Work Shop (DI-WS) at a nursery school (Abe and Meguro, 2005).

In this paper, to expand the field of DI-WS application to other risks and let it popular, we attempted to introduce DI-WS into general risk management training for nursery school leaders. However, since Japan is an earthquake disaster prone country and leaders are strongly interested in earthquake disaster, as the first step of the approach, we picked up earthquake disaster as an example from all risks that we should consider. We have designed a training program composed of two workshops. The first half is Problem Sharing Work Shop (PS-WS) concerning all risk issues, and the latter half is DI-WS based on PS-WS. Then, we carried out this program and examined the possibility of expanding DI-WS approach. Finally, based on the result, we listed up problems for expanding this approach and proposed a DI-WS support system.

1. INTRODUCTION

Japan is expected to face several big earthquakes in the near future. There are two important points for nursery school people to protect small children from such big earthquakes. First, each member of nursery school should improve the disaster imagination. Second, members should share their images and experiences with each other.

Therefore, we have designed and conducted a Disaster Imagination Work Shop (DI-WS) at a nursery school (Abe and Meguro, 2005). In this WS, the participants first decide the conditions such as season, day of the week, occurrence time, weather, and seismic intensity, etc. Then, they start imaging the situation around them as time goes since the hazard attack, and make a story in which they are central figure (Figure 1). In addition, they write down the questions and problems on the memo pads. After writing, they line up their story seats on the table and read each story, comparing along time passage. Sometimes the images of each member are different. Through this practice, WS members can imagine their possible disaster situation and share their images, questions and problems.

To expand the field of DI-WS application to other risks and let it popular, we attempted to introduce DI-WS into general risk management training for nursery school leaders. However, since Japan is an earthquake disaster prone country and leaders are strongly interested in earthquake disaster, as the first step of the approach, we picked up earthquake disaster as an example from all risks that we should consider. We have designed a training program composed of two workshops. The first half is Problem Sharing Work Shop (PS-WS) concerning all risk issues, and the latter half is DI-WS based on PS-WS. Then, we carried out this program and examined the possibility of expanding DI-WS approach. Finally, based on the result, we listed up problems for expanding this approach and proposed a DI-WS support system.

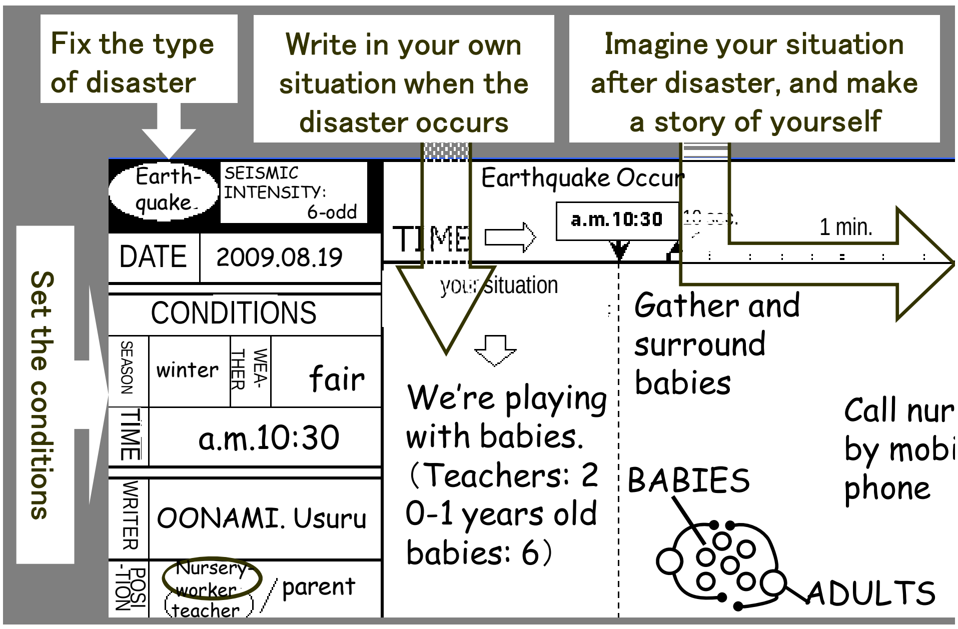

Figure 1: Disaster imagination tool

2. DESIGN OF RISK MANAGEMENT TRAINING FOR NURSERY SCHOOL LEADERS

In this chapter, we will introduce the situation of the risk-management of nursery schools today in Japan and the risk management training for nursery school leaders, and explain about the flow of design of the training program.

2.1 Risk management training for nursery school leaders

National guideline for nursery school, which was revised in 2008, clearly describes that a nursery school director should take responsibility in matters of safety of children at his/her nursery school. Recently, risk management training for nursery school leaders, such as director and chiefs who help director, are being held. These trainings are executed by the social welfare corporation or the municipality. Medical Doctors, lawyers, risk consultants, NPOs and others related to children’s safety give lectures in the training. The lecturer is decided by direct nomination or competition, etc. Training takes several hours to several days. However, support system for feedback for participants after going back to their nursery school, or the succession of the previous year's training data for next year is not enough yet.

2.2 Design of the training program

In order to introduce DI-WS into the training for the directors and the chiefs who are leaders of nursery schools, we designed training program that include DI-WS, and applied it for the competition of the 2009 risk-management training sponsored by the Tokyo Municipality Training Institute. The competition was nominated tender, and Ms. Yokoya, one of the authors, her NPO was also nominated. The number of participants expected was about 60, and the time of the training planned was 6 hours.

In this study, in order to expand the field of DI-WS application to other risks and let it popular, we tried to introduce DI-WS into general risk-management training for nursery school leaders. However, since Japan is an earthquake disaster prone country and leaders are strongly interested in earthquake disaster, as the first step of the approach, we picked up earthquake disaster as an example from all risks that we should consider. We have designed a training program composed of two workshops. The first half is Problem Sharing Work Shop (PS-WS) concerning all risk issues, and the latter half is DI-WS based on PS-WS.

We divided approximately 60 participants into 9 groups composed of 6-7 members. Emcee, facilitation and recording were done by 6 staffs (2 NPO members and 4 postgraduate students). To share information smoothly among participants, basic information of all nursery schools must be understood first. Therefore, we prepared some basic information seats to fill in the number of staffs and children, construction year of school buildings, indoor map, outdoor map, playground map, and map around the nursery school (route to the park, feature around and so on).

In PS-WS, each participant writes past accidents, shivering events, uneasiness, questions and problems freely on the cards. Then, they arrange the cards on a large paper, discussing in each group. Finally, presenter of each group explains about their discussion result, sharing information as a whole. We designed the cards in order to arrange the data easily after the training.

In DI-WS, we set 5 conditions - weather, seismic intensity, season, earthquake occurrence time and a day of the week, which may change the situation and the correspondence after the earthquake. The disaster imagination can be widely shared in a limited time by imaging different conditions in each group and sharing them with all participants. However, extreme different conditions may cause confusion when they compare their situations. So, in this program, we set a common condition for weather and seismic intensity as "fine and JMA intensity of 6+" among all groups, and different conditions for season, earthquake occurrence time and a day of the week.

3. RESULTS OF THE PROGRAM

The program we designed received high valuation and was adopted by the Tokyo Municipality Training Institute, and we carried out the program in August, 2009 (Figure 2, 3). This chapter describes the result of this training program.

Figure 2: participants and staffs

Figure 3: PS-WS (left) and DI-WS (right)

PS-WS (Problem Sharing Work Shop)

When a big earthquake occurs, can nursery school teachers really move and protect the children?

DI-WS (Disaster Imagination Work Shop)

30min later	Is my house OK? Do fires occur? How about the neighborhood of my house?
5min later	I should go to nursery school, but are families all right?
20min later	Can I bring my mobile phone? Can I contact with my husband?
1hour later	Usually it takes 7 minutes by walk to the nursery school, but can I pass the road?
2hours later	Is the building of the nursery school all right? Isn't there any child who has been injured?
others	I wasn't worried about the toilet and the meal.

Figure 4: Example of problems going detail

Table 1 Setting condition and content of the presentation of each group

group	season	day of the week	occur-ing time	Situation when the earthquake occurs	Contents(Extracts)
1	summer	weekday	8:00	going to work	・How to contact with the parents?
2	summer	weekday	10:00	Taking care of children	・The tasks changes according to the standpoint. The director and the chief should think about the whole matters, and the other teachers should take care of children's mental aspect.
3	winter	weekday	10:00	Taking care of children	・Can we serve warm meals? ・Because it is cold, small children cannot refuge in clothes alone .
4	summer	weekday	12:00	Eating lunch /brushing teeth /children taking a nap	・Tableware may be scattered ・I'm worried about the heat under hot weather.
5	summer	weekday	14:00	children taking a nap, adults taking a break	・Can I understand the whole situation at once? Some of the staffs are taking a rest.
6	summer	weekday	16:00	Taking care of children(inside and outside)	・Check the injured children.
7	winter	weekday	16:00	Taking care of children	・There is fear of a fire because we use the stoves.
8	summer	weekday	18:00	shifts to the overtime childcare	・Correspondence is difficult because of the time zone shifting to night. ・How can we respond by few people?
9	summer	holiday	16:00	Few people are taking care of children /at home\	・How can we respond by few people? ・If parents' offices are far, pick-up might be next day.

In PS-WS, participants wrote 304 cards (accident: 102, shivering event: 119, uneasiness/questions/problems: 83). The risk described in the cards varied in topics such as earthquake, accident, suspicious person invasion, allergies, and bees. The number of cards collected concerning earthquake was 21 in PS-WS and 77 in DI-WS. When we compared PS-WS and DI-WS, problems written in DI-WS were more concrete and detailed than those of PS-WS (Figure 4). In presentation time in DI-WS, presenters explained peculiar contents due to the conditions of his/her group to understand the difference of the situation by different condition (Table 1). We will arrange the cards and the stories, and analyze the contents according to the type of danger or various characteristics of parties and so on, and apply to design of the support system (proposed in chapter 4).

The 38 questionnaires of participants' impressions were broken down into 3 categories – 22 were positive such as "I felt that the training under the various conditions are necessary", 11 were negative such as "Time was limited", and 5 were both. Most of negative answers concerned about the time scheduling. In the training, the discussion time exceeded 25min-40min than that of what we had expected. Therefore, we had to shorten the time of lecture and presentation (Figure 5). We will redesign the time schedule of the training based on this result.

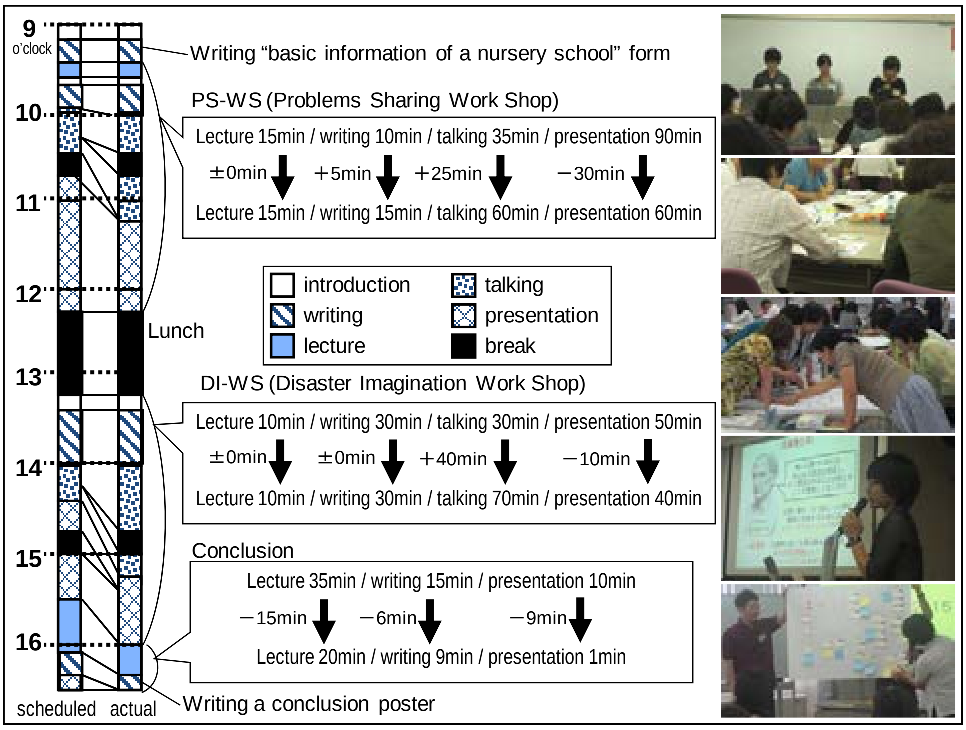

Figure 5: program (scheduled/actual)

In the questionnaires, we found some motivation such as "I want to download the writing form of DI-WS". Moreover, few days after the training, we got a mail from a participant that "we want to do DI-WS in our nursery school", and two nursery schools will do DI-WS in next October, 2009. It shows possibility that DI-WS in the training for the leaders of nursery schools may lead to the DI-WS in nursery schools.

Based on the situation explained above, we could conclude that there is the high possibility of expanding field of DI-WS approach by introducing DI-WS into risk management training for nursery school leaders.

4. PROPOSAL OF THE DI-WS SUPPORT SYSTEM BASED ON THE RESULT OF THE TRAINING

For establishing a new DI-WS system in risk management training for nursery school leaders, it is necessary to build the WS support system. First of all, it is necessary to improve contents and time schedule of current DI-WS and prepare the DI-WS training set by which a nursery school members can carry out WS based on each characteristics by themselves smoothly. Moreover, to answer the participant's question in WS, the lecturer should know the knowledge such as the life patterns of the nursery school members, besides the knowledge on disaster mitigation. Therefore, a support system to get information and hints listed below is necessary.

- Various information which helps carrying out DI-WS
- Hints for solving questions and problems arisen from DI-WS

The system will be designed based on the data obtained from the DI-WS. For updating the system, we will add the lessons learned from past disaster and accidents, and knowledge and comments by specialists, data from the future WSs. In the future, we will deal with the other risks besides the earthquake disaster, and make the support system for nursery schools by which nursery schools can manage their total risks improving their risk imagination.

5. CONCLUSIONS

In this paper, we attempted to introduce a Disaster Imagination Work Shop (DI-WS) into risk management training for nursery school leaders. As the first step of the research, we picked up earthquake disaster as an example from all risks that we should consider. We have designed a training program composed of two workshops. The first half is Problem Sharing Work Shop (PS-WS) concerning all risk issues, and the latter half is DI-WS based on PS-WS. Then, we carried out this program and examined the possibility of expanding DI-WS approach. Finally, based on this result, we listed up problems for expanding this approach and proposed a DI-WS support system. In the future, we will collect more data for the support system by conducting WSs and hearing surveys.

REFERENCES

Abe, M., and Meguro, K., 2005. A proposal of disaster imagination Work Shop (Meguro-maki WS) for improving total disaster reduction ability of nursery schools and others, *SEISAN-KENKYU –Report of the Insititute of Industrial Science, the University of Tokyo* - 57, pp.538-542 (In Japanese)

Abe, M., and Meguro, K., 2007. A study for improving total disaster reduction ability of nursery schools and kinder gartens, *2007 New Technologies for Urban Safety of Mega Cities in Asia*, pp.521-528.

Application of Analytic Network Process to Design Emergency Capability Assessment Index System

SHEN SHIFEI，CHU YANYAN，DU LIGANG，QIAO LIFENG, YANG RUI
Center of Public safety Research, Tsinghua University, Beijing, China
chuyan@mail.tsinghua.edu.cn

ABSTRACT

In order to develop emergency capability assessment objectively and impartially, emergency capability assessment index system should be established comprehensively. Emergency capability assessment elements are summarized based on the analysis of Chinese emergency response law. Emergency capability assessment index system network model is established using the analytic network process method and index weight are calculated according to the importance of all indexes, by mean of which, independence relation of elements in the different group is embodied. In order to verify the objectivity of ANP method, study on emergency capability assessment index system of a city in north china has been developed and the global weight result shows the priority of every element.

1. INTRODUCTION

As SARS crisis in 2003, Indonesia tsunami in 2004, Paris mass riots in France in 2005, London blast in England in 2006, natural disasters, man-made disasters, public health emergency, social security and other incidents occur frequently and pose a serious threat to life, property, social order and economic development. Governments are making efforts to improve emergency management capabilities to reduce consequence caused by various incidents.

ECA can help making emergency management system more solid, flexible and efficient. It also provides a reliable basis for emergency capability development. Considering the characteristics of incidents, such as diversity, complexity, abruptness and unexpectedness, etc, it is difficult to make an objective and impartial emergency capability assessment. As the key to reflect the level of assessment object, it is important to establish a comprehensive emergency capability assessment index system.

At present, emergency capacity assessments have been developed in some countries. The U.S. state and local governments develop emergency management response preparation capability assessment. Japanese local public organizations develop disaster prevention capacity and crisis management capability assessment. Those assessment projects adopt Delphi method, Set-value Iteration method, Analytic Hierarchy Process (AHP) and other methods. As AHP method, weight determination is only considered dominant role of the upper elements on the lower elements and suppose that element in the same level is independent with each other. In fact, emergency capacity assessment elements are mutually affected.

In this paper, analytic network process method（ANP）is used to establish emergency capability assessment index system, in which not only impact by lower elements on upper elements but also relation of elements in the different group can be represented by the assessment index weight.

2. Emergency Capability Assessment Elements

Emergency capacity assessment index system development is a systematic project and need to analysis and quantify various emergency functions. Emergency capacity assessment index system should involve many elements such as law, medical, communications, logistics and equipment, etc. "Emergency response law" is a complete description of the incidents emergency elements and emergency functions and it is Chinese most authoritative legal basis for emergency management. Through analysis of all clauses in the emergency response law can be establish a more comprehensive emergency capability assessment index system.

Be consistent with the ‘Law of the People's Republic of China on Emergency Response’, our ECA index system consists of three levels. Each level contains a number of elements such as laws and regulations, risk analysis, hazard prevention and mitigation, emergency organizational, emergency plan, etc. The first level is the emergency capability of assessment object. The second level is the four-stage emergency management process. The third level is emergency capabilities involved in the stages. ECA index system not only represents the emergency management process, but also covers all aspects of emergency management.

(1) Emergency Prevention and Preparedness Capability

Emergency prevention and preparedness is the basis of emergency management. It lies in six aspects: laws and regulations, emergency plan, emergency resource, risk analysis, emergency education and exercise, emergency team.

(2) Monitoring and Prediction Capability

Monitoring and prediction capability is the precondition for emergency preparedness and response. It lies in three aspects: incidents prediction, emergency information report and emergency information monitoring.

(3) Emergency Response and Rescue Capability

Emergency response and rescue capability is the key part of emergency management. It can prevent incidents spreading and derivative events developing and lies in four aspects: emergency response, emergency command, emergency organization, emergency information publishing.

(4) Recovery and Restoration Capability

Recovery and restoration means recovery production, work and social order as soon as possible. It lies in four aspects: emergency disposal, recovery and restoration, incident assessment and investigation, reward and punishment. All elements of emergency capability assessment index system are list in Tab. 1.

Tab.1 Emergency Capability Assessment Index System Elements

Evaluation object	Element Group	Element
Emergency Capability	Prevention and Emergency Preparedness Capability	laws and regulations emergency plan emergency resource risk analysis emergency education and exercise emergency team
	Monitoring and Prediction Capability	emergency monitoring emergency information report incidents prediction
	Emergency Response and Rescue Capability	emergency response emergency command emergency organization information publishing
	Recovery and Restoration Capability	emergency disposal recovery and restoration incident assessment and investigation reward and punishment

2. Emergency Capability Assessment Index System

The ANP developed by Thomas L. Saaty (1996) of University of Pittsburgh, is a theory of measurement generally applied to the dominance of influence among several alternatives with respect to an attribute or a criterion. It can be used as a risk evaluation model. It has the advantage of utilizing qualitative, as well as quantitative. The ANP allows us to quantify important factors, considers whether a factor influences another or is influenced by another, that is to say, dependence and feedback. So, ANP was chosen to research the effect of all elements in emergency capability assessment index system.

Using ANP method , emergency capability assessment index system elements are sorted into two layers. The first layer is emergency management capability. The second part is network layer. Each element means one aspect of emergency management. There are totally four element groups, C_1, C_2, C_3, C_4 , which are emergency prevention and preparedness capability, monitoring and prediction capability, emergency response and rescue capability, recovery and restoration capability and seventeen elements, $e_{i1}, e_{i2}, \cdots, e_{in_i}$. Every element plays a different part in the emergency response and management, which means every element has a different weigh in the index system. Emergency capability assessment index system is shown as Fig.1.

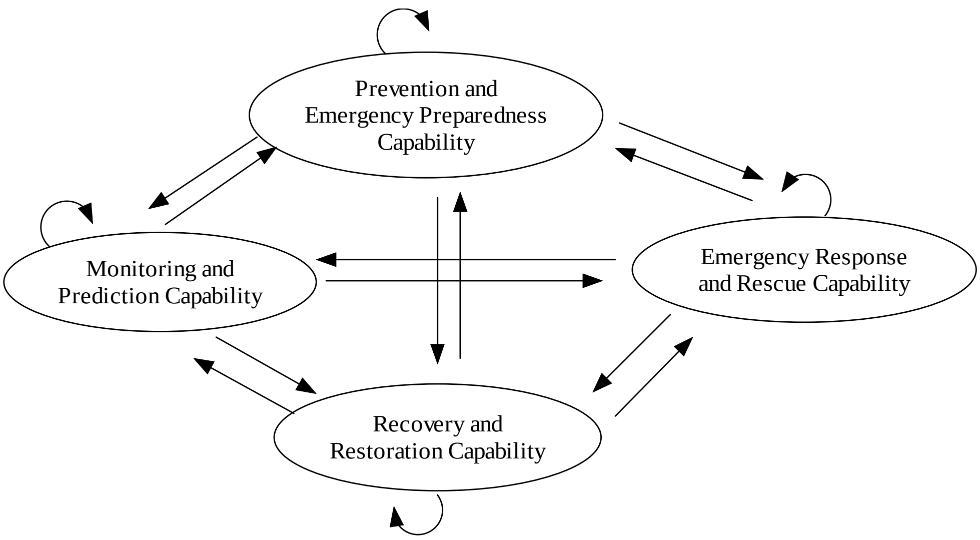

Fig. 1 Management Capability Assessment Index system

Since there are too many uncertain factors, it is very difficult to get the element weight directly. Element weight will be calculated as follow calculation program.

(1) Element e_{jl} in group C_j is used as the criteria. Judgment matrix can be established according to comparison between two elements in group C_i .

(2)Vector $(w_{i1}^{jl}, w_{i2}^{jl}, \cdots, w_{in_i}^{jl})^T$ is got through calculating characterize root of judgment matrix. Similarly, vector is calculated using other elements in group C_j . Then, W_{ij} can be constructed, shown as equal (1).

$$W_{ij} = \begin{bmatrix} w_{i1}^{j1} & w_{i1}^{j2} & \cdots & w_{i1}^{jn_j} \\ w_{i2}^{j1} & w_{i2}^{j2} & \cdots & w_{i2}^{jn_j} \\ \vdots & \vdots & \vdots & \vdots \\ w_{in_i}^{jn_j} & w_{in_i}^{jn_j} & \cdots & w_{in_i}^{jn_j} \end{bmatrix} \quad (1)$$

Column vectors of W_{ij} representation impact by elements in group C_i on elements in group C_j. If there is no connection between elements in group C_j and elements in group C_i, W_{ij} will be 0.

(3) Super matrix W is got through synthesis of all W_{ij}, shown as equal (2).

$$W = \begin{bmatrix} w_{11} & w_{12} & \cdots & w_{1N} \\ w_{21} & w_{22} & \cdots & w_{2N} \\ \vdots & \vdots & \vdots & \vdots \\ w_{N1} & w_{N2} & \cdots & w_{NN} \end{bmatrix} \qquad (2)$$

Super matrix W is anti-negative matrix. W_{ij} is a sub-block of super matrix W and it is column normalization.

(4) Get weighted matrix A. Comparing between two different groups, judgment matrix is established as follow.

C_j	C_1	C_2	…	C_N
C_1	c_{11}	c_{12}	…	c_{1N}
C_2	c_{11}	c_{12}	…	c_{1N}
…	…	…	…	…
C_N	c_{11}	c_{12}	…	c_{1N}

Through calculating characteristic vector, weight matrix A is got as equal (3)

$$A = \begin{bmatrix} a_{11} & \cdots & a_{1N} \\ \vdots & & \vdots \\ a_{N1} & \cdots & a_{NN} \end{bmatrix} \qquad (3)$$

(5) Weighted super matrix W is got through weighting super matrix W_{ij} as equal (4).

$$W = a_{ij}\mathrm{W}_{ij}, \qquad i = 1,\cdots,i\,;\; j = 1,\cdots,j \qquad (4)$$

(6)In a weighted super matrix W, w_{ij} is one step dominance, which means influence of element e_{il} to element e_{jl}. Two step dominance can be got using equal (5)

$$W^2 = \sum_{k=1}^{n} w_{ik} w_{kj} \qquad (5)$$

If $W^{\infty} = \lim_{t\to\infty} W^t$ can be got, j column vector of W^{∞} means limiting sort vector, which is relative element e_{jl}.

4 Application of Emergency Capability and Results Analysis

Our method has been applied to the emergency capability assessement of a mega-city in north China to demonstrate the application of ANP. The emergency capabilities assessment index weight is calculated to analyze relationship of assessment elements.

4.1 Judgment Matrix Establishment

Various indexes have different influence on emergency capability. According to 1~9 scale rule, judgment matrix can be established to calculate their weights. Emergency capacity assessment index judgment matrix determination process is shown as Fig.2.

Fig.2 comparison between two factors

4.2 Element Weight Determination Using SuperDecisions Software

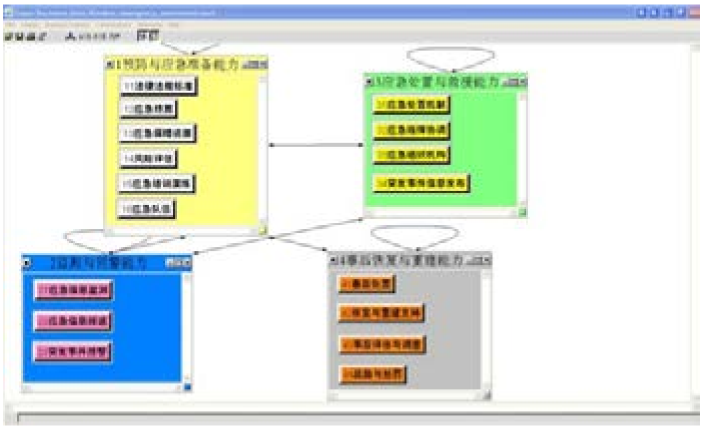

Fig. 3 construct network model

Emergency capability assessment index weight calculation is complete by Super Decisions. First, emergency capability assessment index system network model is established using Super Decisions software, as Fig.3.

Global super matrix is calculated using Super Decisions software after judgment matrixes are input into network model. According to ANP, global super matrixes should be weighted. Comparison matrixes between different two groups are calculated as weighted matrixes. Then, weighted super matrixes are got through multiplying non-weighted matrix and weighted matrix. Finally, stability calculation can transform the weighted super matrixes to the limiting super matrix, which means index global weight, shown as Tab. 2.

The global weights embody interdependence relation of assessment indexes. Priorities are calculated based on comparison of two indexes not only in same group but also in different groups. From Tab.2, it is shown that index "emergency response" has maximum priorities in assessment index system.

Tab.2 Global Weight Result

Element		Priorities
laws and regulations		0.22175
emergency plan		0.19330
emergency resource		0.07892
risk analysis		0.06787
emergency education and exercise		0.26363
emergency team		0.17454
emergency monitoring		0.13342
emergency information report		0.65729
incidents prediction		0.20929
emergency response		0.46680
emergency command		0.18810
emergency organization		0.19176
emergency information publishing		0.15333
emergency disposal		0.47004
recovery and restoration		0.29203
incident assessment and investigation		0.19826
reward and punishment		0.03967

5 Conclusion

Since the indexes of emergency capability assessment system are closely related to each other, index weight cannot be obtained by simple comparison. The application of ANP method to setup a emergency capability assessment index system shows that by using ANP method, the global weighted index can be achieved, which is determined not only by relationship between the same group but also by all the elements in different groups.

ACKNOWLEDGEMENT

This research is supported by National Science and Technology Program (Grant No. 2006BAK04A08) and National Nature Science Foundation of China (Grant No. 70973063).

REFERENCES

2006. *Chinese Incident Emergency plan*
2007. *Chinese Emergency Response law*
Federal Emergency Management Agency, 1997. *State Capability Assessment for Readiness*. A Report to the United States Senate Committee on Appropriations
ZHENG Shuang-zhong; DENG Yun-feng, 2006. Capability assessment system for urban emergency incident readiness and its application. *Journal of Liaoning Technical University*, 12：943~946
Saaty, T.L. and Vargas, L.G, 2000. *Models, Method, Concepts and Application of the analytic Hierarchy Process.* Boston: Kluwer Academic Publishers
Saaty, T.L, 1980. *The Analytic Hierarchy Process.* New York: McGraw Hill. 1~20
Michael K. Lindell, Carla S. Prater and Ronald W.Perry, 2007. *Introductin to Emergency Management.* New York: John Wiley & Sons, Inc,. 386~415
Florida Emergency Preparedness Association. Local Capability Self-assessment and Accreditation Tool, 2001
Huang Dianjian, Wu Zongzhi, Cai Sijing, Jiang Zhonghan, 2004. *Comprehensive Assessment of Emergency Management Capacity to Urban Major Accidents.* Proceedings of 2004 International Symposium on Safety Science and Technology, Shanghai, Beijing: Science Press.
WANG Liang fen, 2001. The Theory and Algorithm of Analytic Network Process, *Systems Engineering-theory & Practic* : 3, 44-50

EMERGENCY RELIEF DELIVERY WITH DEMAND CONFLICT COORDINATION AND GOAL SOFTENING

ZHANG JING, SHEN SHIFEI, YANG RUI
Department of Engineering Physics, Center for Public Safety Research,
Tsinghua University, China
jing-zhang05@mails.tsinghua.edu.cn

Abstract

Large scale disasters usually lead to great damage of multiple regions and cause the sharp increase of relief consumption. When the relief supply could not meet the needs of multiple regions at the same time, there is the demand conflict for the limited relief among regions involved. Emergency decision maker should take into account the response time, the cost and the delivery fairness to develop appropriate relief delivery plans. Because it is usually difficult to achieve simultaneously the optimization of multiple objectives of decision making under disaster cases, the goal of emergency decision making is needed to be soften from seeking the optimal solution to looking for acceptable solutions. This paper presents the relief delivery model with demand conflict coordination and goal softening to make the efficient delivery for a multi-regional, multi-factor and multi-criteria emergency resource allocation. The integrated model is developed based on demand model, delivery model and assessment model with comprehensive analysis of affecting factors.

Keywords: *emergency resource allocation; relief delivery; demand conflict; goal softening in emergency; cross-regional coordination*

1. INTRODUCTION

Large scale disasters, including natural disaster and man-made catastrophe, usually involve multiple regions and lead to great damage and lots of fatalities. The Indian Ocean earthquake and tsunami involved 12 countries and more than 200 thousand of death. The technical disaster in the northeast of China, the double benzene plant explosion on November 13, 2005, released hundreds tons of benzene pollutants into the Songhua River and caused large-scale disruption of water supply. The urgency inherent of disasters and multiple regions involved make the emergency relief be consumed very fast so brings lots of challenge for decision making. When the relief supply could not meet the demands of multiple regions at the same time, the demand conflict for the limited relief exists among multiple regions. Governments should not only consider the response time and the cost to develop the relief delivery plans, but also balance the fairness of delivery among multiple regions involved to make the right decision. However, it is usually difficult to achieve simultaneously the optimization of multiple objectives of decision making.

As one of key issues of emergency decision making with complexity, there is an increasing research in emergency resource allocation and relief delivery. Fiedrich et al. (2000) investigate the modelling of emergency resource allocation for earthquake disasters. Fiorucci et al. (2004) develop a dynamic model of allocation to achieve real time control of forest fires. Chang et al. (2007) research the flood emergency logistics preparation problem under uncertainty. Willis (2007) investigates the emergency resource allocation for terrorism events. Lodree and Taskin (2009) develop a model wind speed information updates for hurricane response. The models with mathematical programming, such as integer programming and goal programming have general applications in resource allocation (Wei and Ozdamar, 2007), like for first response organization deployment (Taylor et al., 1985; Basu and Ghosh, 1997; Sharma et al., 2007).

Although recent literature investigated many important and interesting issues in emergency relief delivery, there are challenging problems existing in real emergency response. The challenges includes: 1) The investigation on demand model. The models of demand estimation should be developed with comprehensive consideration of affecting factors. 2) The dynamic network of supply and demand of emergency relief. With the development of disasters, the regions involved, the storage of relief supply, the risk of transportation and the amount of demand probably change so the dynamic models need to be studied. 3) The coordination of demand conflict. The decisions should be made not only aiming at the optimization of total time or cost, but also taking into account the restriction of supply and demand among each regions and the distribution fairness under demand conflict. 4) The goal softening in emergency decision making. It is usually difficult to achieve the optimal solutions in the face of the urgency and complexity of disaster condition. The goal softening is a soft approach for solving complicated optimization models. Lau and Ho (1997) explain the goal softening concept in ordinal optimization. The basic idea of goal softening is to look for a good enough solution instead of an optimal solution. The goal softening in emergency decision making is an approach to soften the goals of emergency plan and response to the acceptable solutions under disaster cases.

2. THE FRAMEWORK

2.1 Comprehensive analysis of affecting factors

The relief delivery network is composed of regions involved, relief warehouse, transfer areas and routes. The risk of these elements is affected by various factors so change continuous with the development of disaster. To achieve the real time demand analysis of emergency relief, it is necessary to investigate the static states of the relief delivery network such as the variety of relief and the amount of storage, and development of the relief delivery network such as the availableness of relief and the destruction of routes.

2.2 Identification of relief demand conflict

As a common issue in emergency resource allocation, the demand conflict exists in two dimensions: the supply shortage of scarce resource caused by the sharp increase of consumption and the relief priority of regions involved. The analysis of the severity of disaster and the real affection of each region is needed. The standard of demand satisfaction should be conformed according to requirement of decision maker to define what a good enough solution is. The priority of regions should be evaluated and ranked comprehensively to establish an appropriate method for coordinating relief conflict.

2.3 Softening and assessment of objectives

Considering the extreme condition of disasters, the acceptable solutions instead of optimal solutions are looked for to soften the goals of emergency decision making. The trade-off of multiple objectives should be made, including to minimize emergency response time, to mitigate the risk during transportation, to distribute fairly, to minimize cost and waste, to balance the kinds of relief and so on. It is difficult to optimize all the objectives of decision making so it is important to develop the utility function of goal softening and corresponding assessment approach.

The analyse procedure of emergency relief delivery is shown in figure 1.

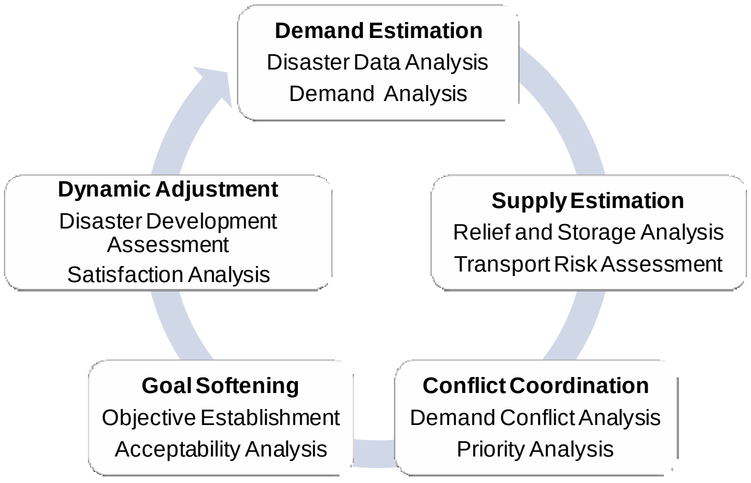

Figure 1: The analyse procedure of emergency relief delivery

3. THE MODELS

3.1 Multi-regional demand model

It is needed to integrate the static and dynamic factors impacting supply and demand to establish demand model. The static factors we focus on in this paper include:

- Affected area related factors

  Regional geographic feature, regional population distribution, regional critical infrastructure, the distribution of key target for protection, etc.
- Relevant factors of relief supply

  Relief type, functions, storage sites, storage quantity, etc.
- Transport pathway related factors

  Road conditions, traffic conditions, vehicles type, etc.
- Relief object related factors

  Basic requirements, the minimum requirements, special needs, etc.

The dynamic factors include:

- Factors that affect the risk of the affected region

  Development of events, the possibility of secondary disasters, etc.
- Factors that affect supply

  relief availability, substitutability, etc.
- Factors that affect the risk of transport pathways

  Road damage, road repair efficiency, transportation alternatives, protection states of power, etc.
- Completeness of information

Judgement and filter of pseudo-demand and repeated demand, etc.

- Relief object factors

  Historic satisfaction degree of demand, expectations of demand satisfaction, satisfaction in reality, etc.

3.2 Delivery model under demand conflict

Firstly it is necessary to determine the intensity of disaster and the areas impacted. With the analysis of the probability of destruction of warehouses and network, the risk analysis for availability of relief and transport will be made to establish the mode of relief delivery model under demand conflict game. In the dynamic game with incomplete information, the relief needs of regions are considered as strategies, based on different coordination mechanisms. The existence of multiple equilibria allows obtain multiple feasible plans at the same time to support emergency decision more comprehensively.

The analysis of possibility and severity of demand conflict should be combined with the regional priority and the relief need satisfaction investigated in demand model. A classification approach is used to coordinate regional conflict. For relief that can be partitioned in quantity, such as food, drinking water, quilts, tents, etc., the equity in distribution of should be regarded as these supplies are related to daily life closely. For relief that could not be partitioned, such as large equipment for rescue and co-workers required, it is needed to determine the priority of regions with severity of damage and availability of transport to minimize the disaster losses and achieve the rescue effectiveness.

3.3 Dynamic assessment model

The determination of multiple objectives should be combined with the practical needs of emergency decision-making for the multi-regional, multi-factor deployment problem. The trade-off for the allocation fairness, the time and the cost of response is made to establish a rational utility function and assessment method of acceptable solutions. The dynamic adjustment of deployment is carried out by communicating with actual decision-making needs of emergency manager and development of disasters.

The architecture of the integrated model is shown in figure 2.

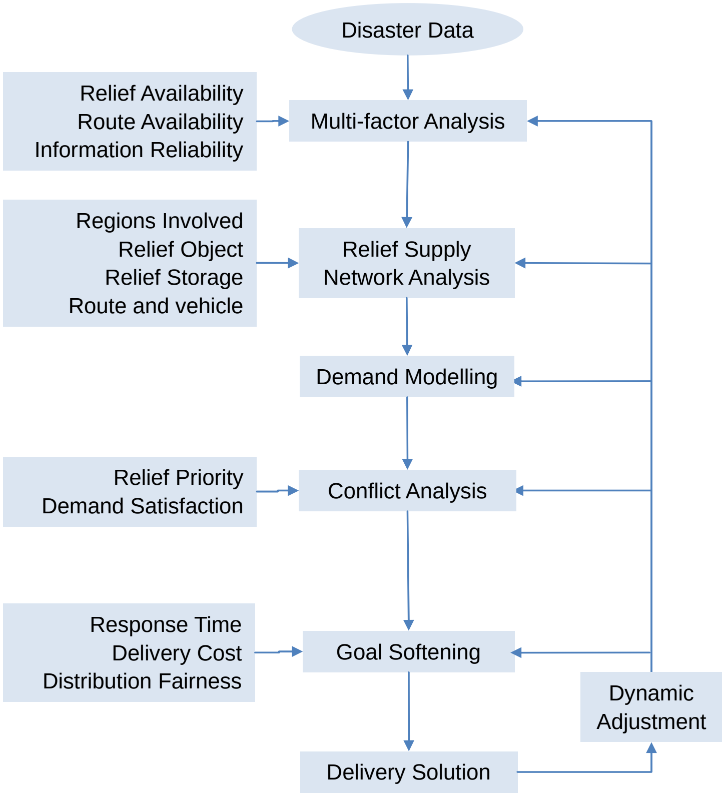

Figure 2: The integrated model architecture

4. CONCLUSIONS

The urgency and complexity of disasters make the efficient delivery of emergency relief a challenge in emergency decision making. There are usually multiple regions to be involved in large scale disasters and the sharp increase of consumption of relief may lead to regional demand conflict. This paper presents the framework for multi-regional, multi-factor and multi-criteria relief delivery modeling of emergency resource allocation. In the future, simulations incorporated with GIS data will provide a reality environment for analyzing and assessment the emergency relief delivery.

ACKNOWLEDGEMENT

This research is supported by National Nature Science Foundation of China (Grant No. 70973063) and National Science and Technology Program (Grant No. 2006BAK04A08).

REFERENCE

Basu, M. and Ghosh, D., 1997. Nonlinear goal programming model for the deployment of metropolitan police patrol units. *Opsearch* 34(1): 27-42.

Chang, M. S., Tseng, Y. L. and Chen, J. W., 2007. A scenario planning approach for the flood emergency logistics preparation problem under uncertainty. *Transportation Research Part E: Logistics and Transportation Review* 43(6), 737-754.

Fiedrich, F., Gehbauer, F. and Rickers, U., 2000. Optimized resource allocation for emergency response after earthquake disasters. *Safety Science* 35, 41-57.

Fiorucci, P., Gaetani, F. and Minciardi, R., 2004. Dynamic models for real time control of forest fires. Proceedings of the 15th International Workshop on Database and Expert Systems Applications.

Lau, T. W. E. and Ho, Y. C., 1997. Universal Alignment Probabilities and Subset Selection for Ordinal Optimization. *Journal of Optimization Theory and Applications* 93(3), 455-489.

Lodree, E. J. and Taskin, S., 2009. Supply chain planning for hurricane response with wind speed information updates. *Computers and Operations Research* 36(1), 2-15.

Sharma, D. K., Ghosh, D. and Gaur, A., 2007. Lexicographic goal programming model for police patrol cars deployment in metropolitan cities. *International journal of information and management sciences* 18(2), 173-188.

Taylor, B. W., Moore, L. J., Clayton, E. R., et al., 1985. An integer nonlinear goal programming model for the deployment of state highway patrol units. *Management Science* 31(11), 1335-1347.

Wei, Y. and Ozdamar, L., 2007. A dynamic logistics coordination model for evacuation and support in disaster response activities. *European Journal of Operational Research* 179, 1177-1193.

Willis, H. H., 2007. Guiding Resource Allocations Based on Terrorism Risk. *Risk Analysis* 27(3), 597-606.

PARALLEL SESSION 10

REGIONAL FLOOD RISK MANAGEMENT IN KOREA

[1]BYUNG HA SEOH, [2]BYUNG SIK KIM and [3]DAE WON JANG

[1]Department of Civil and Environmental Engineering,
INHA University, Incheon, Korea
seohydro@inha.ac.kr
[2]Water Research Division,
Korea Institute of Construction Technology, Korea
hydrokbs@kict.re.kr
[3]Department of Civil and Environmental Engineering,
INHA University, Incheon, Korea
hydrojdw@naver.com

1. INTRODUCTION

Although many regions in South Korea became urbanized through the growth-centered urbanization in the 70s to 80s, there were many regions that were developed randomly without necessary verifications on various parts. In recent, new cities and urban districts are being developed centering on quality of life from growth through the planning on various environmental aspects such as education, society and economy, but the existing cities and old urban districts are deteriorating thereby causing regional imbalance.

Such imbalance is not limited to just visible things such as road system or social infrastructure but applied to natural disasters such as landslide. The blow figure shows the aspect of flood damages that are occurring recently. As shown in the figure, personal casualties and flood area are decreasing but property damages are rapidly increasing. Such rapid increase of damages results from the population concentration and industrial foundation and properties concentration according to urbanization and industrialization.

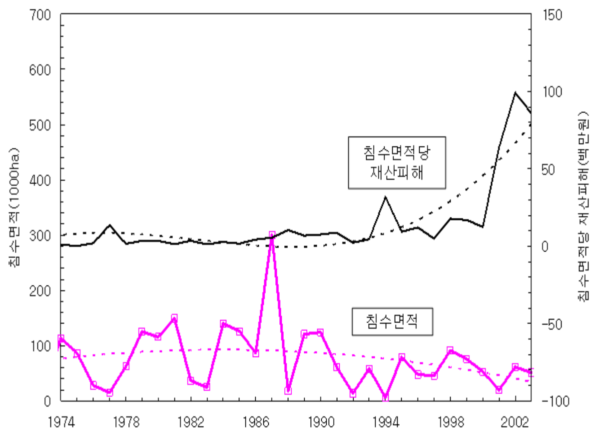

Figure 1: Flood damage trend of Korea

Also, it is because the existing facilities for preventing natural disasters are not fully functioning at the increase of the degree of intensity of localized torrential downpours and typhoons resulting from the abnormal weather phenomenons that are occurring frequently in recent. For such reason, appropriate response measure strategies must be established to improve comprehensive disaster prevention function in cities. Namely, there is a need for methodological study and to provide practical services that can be utilized in preventing, preparing for and responding to natural disasters based on quantitative evaluation of the natural disaster prevention capability of the existing cities from the aspect of disaster risk management.

From such perspective, this study overall reviewed the effects of climate change on flood damage and, especially, it forecasted the effects of flood risk management in cities. Lastly, it mentioned adaptive policy plans to respond to abnormal flood from the climate change in future.

2. CHANGES FROM CLIMATE CHANGE

2.1 The Present Condition of Disaster Occurrences in Korea

In Korea, the trend is that the frequency of severe weather such as typhoon is increasing from the temperature increase since the late 1980s and the frequency of torrential rain disaster occurrence in summer season is increasing from in the annual average of 5.3 times (1940~1970) to 8.8 times (1980~1999). Especially, damages from localized torrential downpour continuously occurred between 1998 to 1999, and, in Ganghwa and Paju regions, the downpour amount equivalent to 70% of the annual precipitation amount in 3 to 4 days caused damages such as flooding of farmland and production facilities and sweeping away social overhead capital. After 2000, the economic damages from weather disaster such typhoon rapidly increased, and the damages from the typhoon 'Lusa' in 2002 and 'Maemi' in 2003 were respectively 5,469.6 billion won (124 deaths, 60 missing and 88,625 victims) and 4,781 billion won (117 deaths, 13 missing and 10,975 victims). Although it is difficult to state that such localized torrential downpours and floods occur strictly from the climate change, it is true that the characteristic of extreme situation of precipitation in the Korean peninsula is changing from the climate change. According to the announcement by Korea Meteorological Administration, the temperature of our country has increased 1.5℃ during the 20th century and the number of rainy day decreased 14% while the precipitation amount increased 7% during the past 20 years and the frequency of torrential downpour of over 80mm increased. Such change of extreme precipitation characteristics can cause changes in human lives and ecosystem and, especially, it will have effects on flood frequency and size.

2.2 Change of Paradigm from Climate Change

In general, the risk of water related disasters can be expressed by multiplying the three elements of 'hazard' that displays the probability of disaster occurrence, 'exposure' of economic properties or human lives that are located within disaster risk region and 'vulnerability' that signifies the lack of protection ability.

Figure 2: Flood Risk Management

Thus far, the main purpose of water management has been the maintenance of living and production foundation and it basically controlled water supply through water resource development. For floods, it basically planned, designed, managed and operated flood control facilities through which planned flood amount can be accommodated and controlled by setting it using reproduction probability as the basic index. However, such response alone can no longer satisfy every demand of the era that includes future climate change and preservation of environment and ecosystem. Also, there is a need to prevent future problems from surfacing or preventing them from expanding in their degree of risk by introducing risk management techniques related to excess flood and reviewing planning method or facility capacities.

As mentioned earlier, very large amounts of precipitation are frequently occurring and floods in excess of planned frequency are frequently occurring and, even though the flood area and personal casualties are decreasing from the river and water system maintenance project that has been continually implemented, our living spaces are nearing closer and closer to river for production and living and the geographical change from urbanization is increasing the amount of flood damage per unit area by increasing the vulnerability to flood risk.

This signifies that the current flood defense measure has reached its limitation, and it reveals the need for a new flood control measure to respond to the recent phenomenons such as unexpected flood and abnormal floods since the flood control through dam and levee for the past 30 to 40 years can only assure the basic flood control safety. There is a need to convert the paradigm established by flood defense measure from the concept of surface of drained area to line concept of river into region or district unit flood control measure. This signifies the need to convert the current flood control measure being implemented centering on flood control facility of levee into potential damage region around river centered flood control measure. The need for regional measures in potential damage regions is being raised that can consider the characteristics of the region in terms of its weather, geography and socio-economic since there are limitations with the construction of river centered levee in the diversification of flood control measure.

3. THE LIMITATIONS AND PROBLEMS OF THE EXISTING FLOOD DEFENSE MEASURES

3.1 Unplanned River Maintenance According to Rapid Progress of Urbanization

In our country, the urbanization has been rapidly progressing through its economic growth. In the case of Seoul, it also changed from water permeable surface such as undercurrent, forest with high permeation function and paddies and dry fields to impermeable paved region that hardly has any undercurrent or permeation ability at the development from population concentration. The possibility of flood damage risk increased from the occurrence of the development of relatively inexpensive river surrounding region without the review of flood control during the process of housing development, industrial complex development or commercial facilities development.

Especially, in the case of regional grade 2 rivers, they are not being well maintained compared to national rivers. The rivers with established river maintenance basic plan is only about 45% thereby the irrigation of river and its flood control measure have not been properly established. Therefore, flood damages are repeatedly occurring from the insufficient maintenance of river width and levee section and budget is being wasted as the flood damage recovery is being implemented centering on restoration to the original state instead of improvement restoration. Also, the current circumstance is that the connectivity of the entire area drained is insufficient from the dispersed implementation of various flood control projects such as dam, levee, water supply pump facility and debris barrier according to authorities and projects and the damage risk is being added from the river maintenance focusing on structures such as levees.

3.2 Lack of Disaster Prevention Facilities and Standardized River Management Focusing on Flood Control

The general disaster prevention facilities that can be commonly seen in our country are the facilities that control flood amount to prevent internal flood by discharging water when external water level is lower than internal water level according to the difference between the two by holding a part of influx amount gathered in the low land around river during floods. However, flood control is being implemented only through the combined form of minor house modification and pump facility in most of urban regions since assuring appropriate areas of undercurrent land is difficult from the increase of land price from the development.

Also, the standardized occurrence of the installation of concrete shore protection and development of river terrace land in the maintenance of river without considering the characteristics of the river is not only deteriorating the surrounding environment of the river and utilization level of the residents but also adding the risk of flood. Therefore, there is a need to develop and manage rivers according their characteristics.

3.3 Levee Focused Flood Defense Policy

The flood control policy of our country thus far can be simply summarized as the attempt to stop flood through levees. This resulted from the intent to solve the problem of flood within rivers by building levees at rivers to maximize the land usage according to economic development since the usable area is lacking in our country. However, it is causing the side effect of increasing the possibility of flood occurrence through the concentration of population and properties at the downstream from the repetition of the enlargement construction of levees to prevent flood damages resulting from the expansion of urbanization around river and the enlargement of peak flood amount from excessive construction of levee at the upper stream from the continuous river levees from the upper stream to down stream. However, as mentioned earlier, the personal casualties decreased in spite of the flood control policy that has been continually implemented for the past 30 years based on such foundation, but the error of the existing flood control policy can be pointed out from the fact that the amount of flood damage is increasing exponentially. Namely, levee centered flood control policy has fundamental limitations. As shown in Figure 3, when a flood occurs in a natural condition, A community becomes flooded as well as B community, but, in the case of constructing levees in A community to stop flood (defended condition), B community can potentially receive damages from even bigger flood even though A community might be safe from it from the undercurrent of the flood in A community.

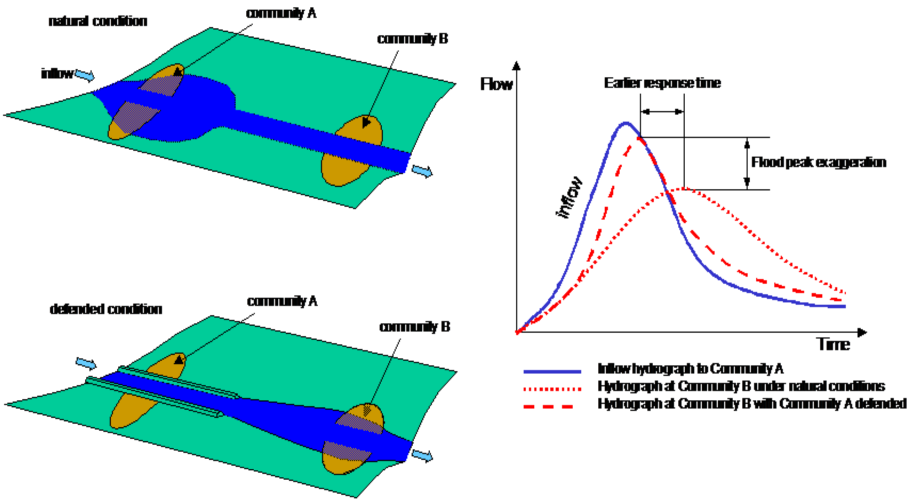

Figure 3: Showing the outline of the risk of flooding

Although the current flood control measure is occurring centering on administrative district, the problem is occurring of increasing flood damage from the lack of selective defense from flood damage in the administrative district centered flood control measure. Therefore, discussions among the regions within river areas must occur to effectively stop flood according to the characteristics of river.

Although the levee centered flood prevention policy is being perceived as an efficient option in the aspect of cost, the flood prevention measures besides levees can be more effective when considering the environmental and economical aspects. Therefore, there is a need to share the burden of flood in the entire river regions by developing flood prevention policy besides levees to stop such ill practice. Namely, there is a need to develop unique and own flood measure that is suitable to the characteristics of the region such as undercurrent land, riverside undercurrent land, flood control land, and flood control channel. Also, there is a need to divide the flood burden by reducing impermeable region in cities and assuring flood undercurrent spaces such as playing field, park, small scale undercurrent land.

4. THE EFFECTS OF CLIMATE CHANGE ON FLOOD CONTROL

The increase of precipitation amount and intensity from climate change has enormous effects on flood structure such as dam. Since enormous damages can be caused to the lower stream areas of a dam when it breaks, probable maximum precipitation needs to be considered when designing a dam. In general, the probable maximum precipitation increases about 10% when the temperature increases by 1℃. To presume that the temperature increases by 1℃～2℃ from the climate change, it is fully possible that the probable maximum precipitation increases more than 10%.

Since the climate change changes the extreme floodgate phase that is the most important variable in designing flood control facilities, the fact that the flood control technicians that plan and design flood control related infrastructure need to consider climate change is becoming a reality. Also, the gradual change effect of floodgate process from climate change is expected to change the size and frequency of peak flood amount during the design period of flood control related infrastructure. The potential change of future precipitation intensity will change the service level of flood control related infrastructure and will require the change of design methodology used in the planning of flood control related structure design.

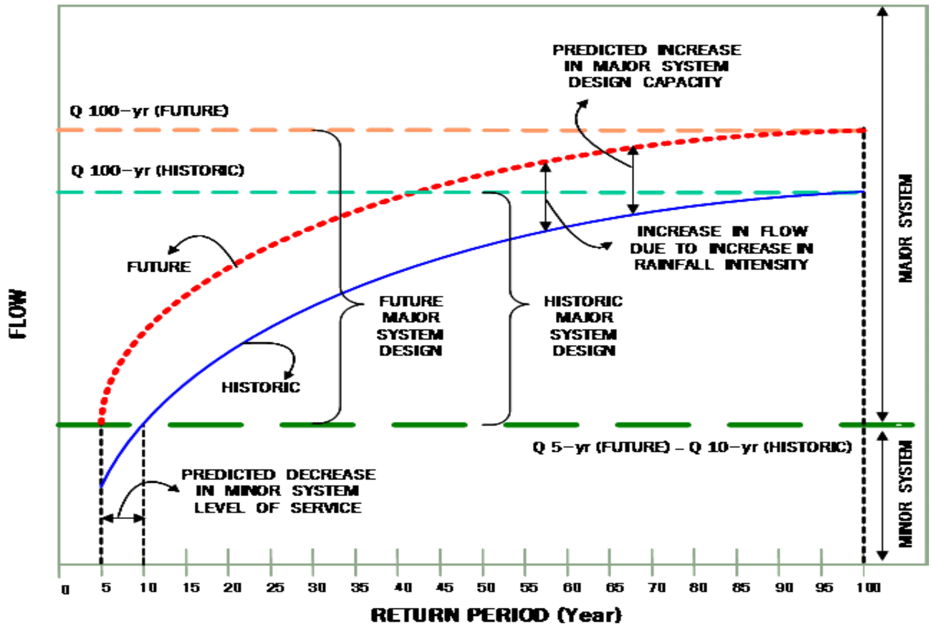

Figure 4: Change of design frequency curve according to climate change

Picture 4 is a conceptual display of design frequency curve change of flood control structure according to climate change, and the blue solid line is design frequency curve using only the past information and the red dotted line shows the design frequency curve of future. As it can be seen from the figure, the 10 year frequency design flood amount of the past will decrease in future to 5 year frequency design flood amount and, in the case of 100 year frequency design flood amount, it is showing the increase from the past in the future and it can be found that the difficult of flood control could increase from the reduction in the flood defense ability of the existing flood control structure, namely, the reduction in flood control safety level.

5. THE OUTLOOK ON THE EFFECTS OF CLIMATE CHANGE ON FLOOD DISASTER AND CONTROL IN THE KOREAN PENINSULA

In this part, the outlook on the effects of climate change that has been continually mentioned earlier on the occurrence of extreme precipitation in the Korean peninsula. As the result of illustrating the tendency of climate change by calculating the differences according to index of the present future to consider the change in climate change, it was confirmed that the propensity according to season and reason displayed clearly. According to the climate characteristics of Korea, precipitation has been concentrating in the summer season and the precipitation from typhoon during the late August to September is continuing. Considering such seasonal characteristics, the summer season (June～August) and fall season (September～November) were compared for the limit index related to precipitation in this part. Figure 5-(a), (b) and (c) are respectively the critical point of localized torrential downpour the displayed the degree that corresponds to 90% from the day in which precipitation occurred, maximum precipitation amount for 5 consecutive days that signifies precipitation when torrential downpour continued for over 5 days and limit index result of the future compared to the present for precipitation intensity.

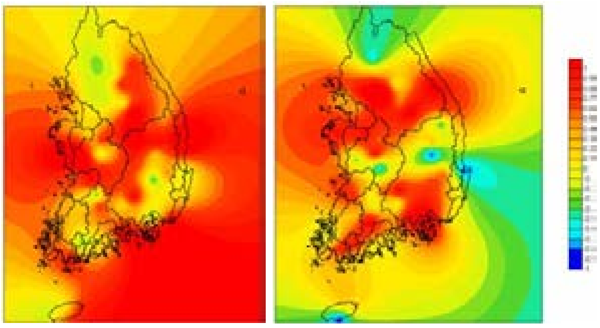

summer season (6~8) fall season (9~11)

Figure 5-(a)

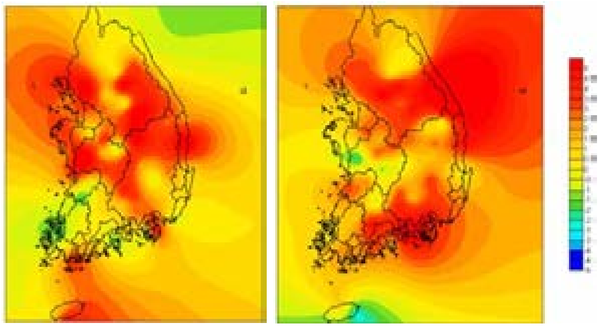

summer season (6~8) fall season (9~11)

Figure 5-(b)

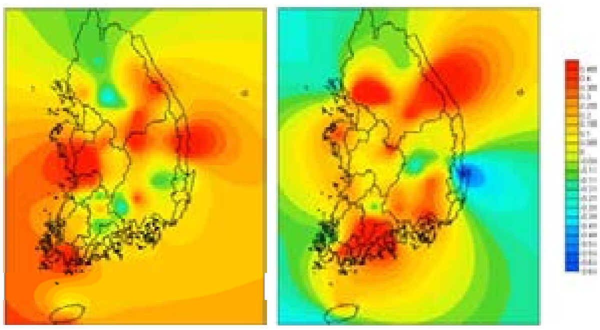

summer season (6~8) fall season (9~11)

Figure5-(c)

As also mentioned in the previous paragraph, the frequency of localized torrential downpour in the Korean peninsula is increasing from the climate change and, accordingly, design precipitation is changing. As the result of comparing the space distribution of the precipitation of the past (until 2000) according to the reproduction period for the calculated design precipitation degree (2001-2090) that took into account the climate change by implementing frequency change analysis according to major points based on A2 scenario, it was revealed that design precipitation increased in most of the regions.

Also, it was forecasted that the flood risk will increase from the lowering of the frequency to in the average of 50 years for the current 100 year frequency design precipitation within the next 100 years. Figure 6 is a spatial display of the lowering of frequency in the 2031s to 2060s according to climate change for the 100 year frequency design precipitation.

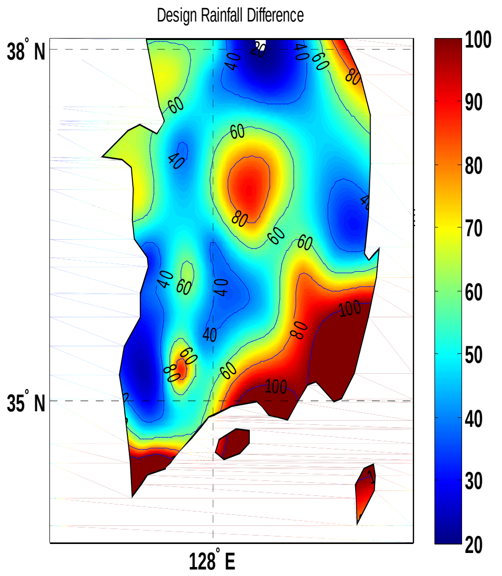

Figure 6: Reduce spatial distribution of the design frequency at 100 year frequency

6. THE OUTLOOK ON THE EFFECTS OF CLIMATE CHANGE ON FLOOD DISASTER AND CONTROL IN THE KOREAN PENINSULA

6.1 Improvement of the Calculation Method of Design Precipitation that Considered Climate Change

As analyzed earlier, it was confirmed that the extreme precipitation characteristics in the Korean peninsula is changing from climate change and climate change of the future can increase the design frequency and size. As the effort to maximize the benefit of adaptation to the climate change and minimize the negative effects of climate change, it can be said that adapting to the effects of climate change on flood control structure is the stopping the increasing flood risk and maintaining the services of the facilities. The common method that is still being used in design has the premise of the fact that the future circumstance can be fully reflected from the climate information of the past alone since climate does not change and the normality of the mean and distribution of climate information no changing according to time. However, it can be said that such design method with the presupposition of the existing normality is the cause of the destruction of many flood control structures and deviating from the design scope. Therefore, as mentioned earlier, we can no longer insist on the design flood amount calculating method based on the past records. The plan through which the effects of the climate change of the future that is partially being realized and displaying needs to be urgently researched and developed and efforts should be made to use it in actual work.

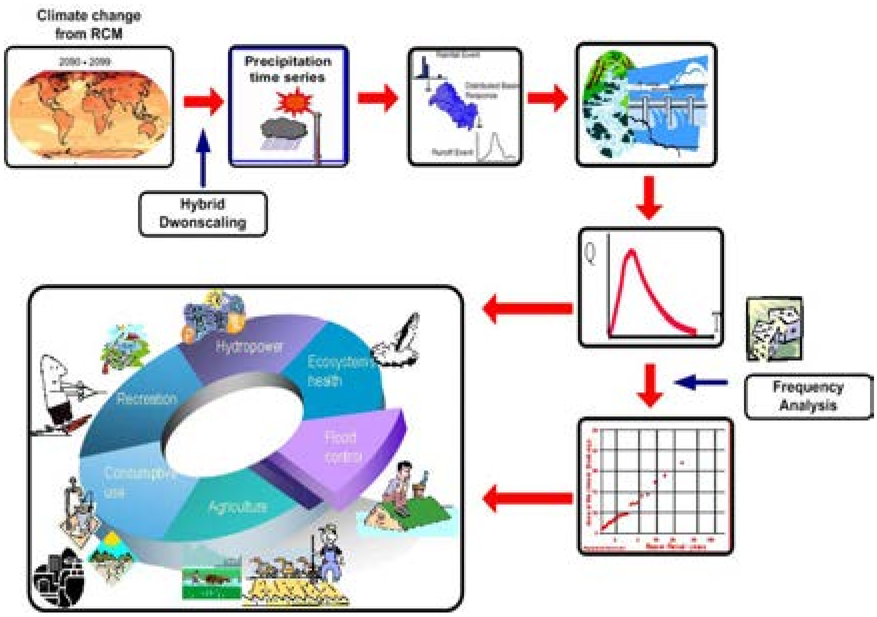

Figure 7: Considering climate change, water planning and design to improve

6.2 Establishment of Custom-tailored Flood Defense Response Strategy that Considered Regional Characteristics in Response to Abnormal Flood

To perfectly protect from flood is impossible from not only technical aspect but also economical and environmental aspect. Setting design standards for protection is deception as well as trickery. Such standards contradict every principle of controlling flood. It is because it is impossible to generally estimate the power of extreme flood since the fluctuation from climate change is significant.

Whether or not to set up defense plan to protect from large-scale flood is also a dilemma. Its is because bigger damages can occur from the occurrence of more extreme flood by reducing the damages from floods that occur everytime. A prime example is the 'Great Flood of New Orleans' in the U.S. that occurred in 2005 through which the limitation of flood control ability of levees was recognized and the danger of the potential damage that can be brought forth from the collapse of levee was shown. Ultimately, the potential risk of flood will gradually increase at river from the continuous stacking up of levees even though the perception might be that risk at the river is decreasing from the levees that are continuously stacked up. In the places like Europe, including Germany, and Japan, the task of constructing the flood control measure of a new concept has been persistently implemented upon recognizing the risk of such levees. Therefore, the possibility of failure at the occurrence of the flood that surpasses in its size than the design standard needs to be presumed and its management needs to be considered. Therefore, the recognition that every flood problem can't be fundamentally solved only through the existing river channel centered flood control measure is needed to respond to the external force that is increasing from the climate change and, accordingly, the introduction of a new "Room for the water" concept is needed through which the increased flood amount from the increased precipitation from regional development or climate change is shared, and river area centered three dimension flood defense control concept of line+surface+space, namely, integrated flood management (IFM) from the river levee centered linear flood defense is needed.

6.3 Multi-layered Flood Response Policy Establishment

In consideration of the increase of precipitation in the future, there is a need to significantly increase design peak flood amount if the current flood control safety level is to be maintained. However, it is extremely difficult to construct the facilities through which the increased flood amount is controlled due to various conditions of limitation such as budget, human resource and surrounding environment in which structures are installed, therefore, the limitation of the simple structural measure for flood measure from climate change is clear. Also, a very long time is required to complete the construction of structure in general. Therefore, the flood response measure the considered the climate change of the future needs to be multi-layered. Namely, to satisfy the target flood amount, the traditional 'flood response policy that assures safety in the level of river' that used to depend on river improvement and flood control structure installation and 'flood response policy that assures the safety in the level of area' need to be established to respond to the possibility of excessive flood, namely, excess flood.

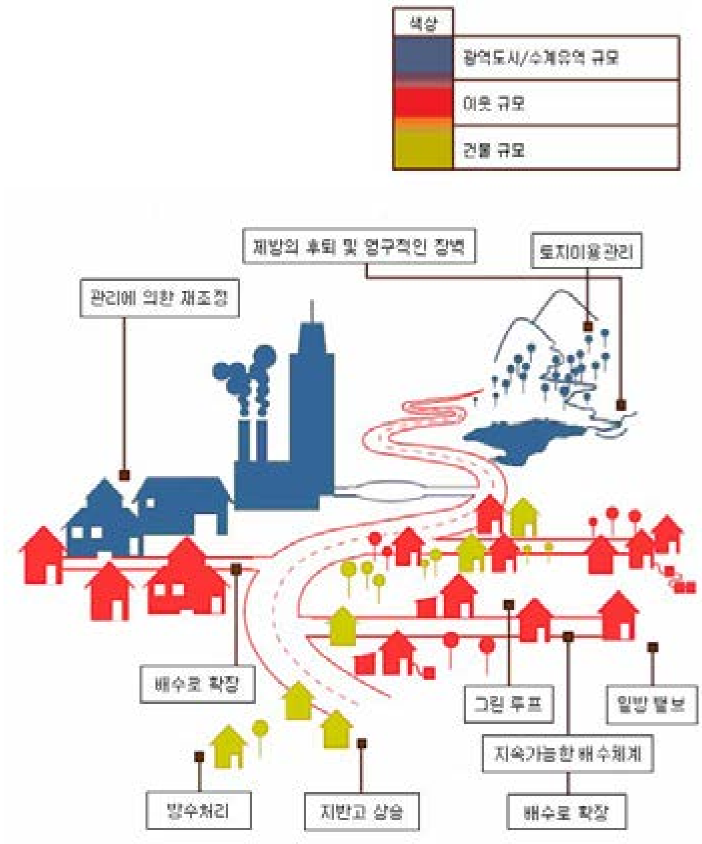

Figure 8: Multi-layered Flood Response Policy Establishment

As the strategy for responding to abnormal flood, the strategy of appropriate mitigation, adaptation and risks management non-structural through non-structural approach is needed, along with structural analysis. To establish such strategy, the areas that are vulnerable to flood need to be identified and investments should be made for them first of all when establishing flood defense measure. Accordingly, there is a need to evaluate on whether or not the social infrastructures related to flood such as already installed levees, dam and river bridge possess design defense ability in response to abnormal flood that is caused from climate change.

7. SUMMARY AND CLOSING

Korea Meteorological Administration has decided to not forecast rainy spell that announces the start and end of rainy spell from this year. The reason is from the fact that the precipitation patter in the summer season has changed to the form of much rain before and after rainy spell at the acceleration of the global warming. However, considering the concentration of 2/3 of the summer season precipitation from June to September and trend of guerilla style localized torrential downpour frequently occurring regardless of the announcement of the rainy spell forecast, it can be said that the war against abnormal flood has just begun. Therefore, it can be said that our society is now at the point of trying to accept a new paradigm for flood control.

However, the flood control measure of our country has not been able to deviate much from the existing frame. As mentioned earlier, the main problems of the existing flood control policy can be summarized into the standardized flood control measure from levee, uniform defense through areas, administrative district centered river management and post-recovery centered investment. To respond to the external force that is increasing from the climate change, there is a need for the perception that every flood problem can't be fundamentally solved only through the existing river channel centered flood control measure and diversification of flood control measure is need. Accordingly, the introduction of a new "Room for the water" that shares the increased flood amount from the increase precipitation from regional development or climate change is needed and river area centered three dimension flood defense control concept of line+surface+space from the river levee centered linear flood defense is needed.

REFERENCE

Communities and Local Government (2006). Planning Policy Statement: Planning and Climate Change –- Supplement to PPS1. Consultation

Gill, S., Handley, J., Ennos, R., and Pauleit,S. (2007). Adapting Cities for Climate Change: the Role of the Green Infrastructure. Built Environment, 33(1): 115–-133.

IPCC. (2001). "*Climate Change 2001; Impacts, Adaptations, And Vulnerability. Contribution of Working Group II to the Third Assessment Report of the Intergovernmental Panel on Climate Change."*, Cambridge, UK and New York, NY, USA.

Kim, Byung Sik, Kim, Bo Kyung, Kyung, Min Soo, Kim, Hung Soo(2008), Impact Assessment of Climate Change on Extreme Rainfall and I-D-F Analysis, Journal of Korea Water Resources Association, Vol 41, Issue 4, April 2008. Pp. 379-394

Servat, E., et. al., 1999: De differents aspects de la variablilite de la pluviometrie en Afrique del'Ouest et Centrale non Sahelienne. Rev. Sci. Eau, 363-387

A COMPARATIVE STUDY OF URBAN VULNERABILITY BETWEEN DHAKA AND TOKYO

MD. FAIZ SHAH
Doctoral Student, Department of Risk Engineering, Graduate School of Systems and Information Engineering, University of Tsukuba, Japan
mdfaizshah@yahoo.com

OSAMU MURAO
Associate Professor, Department of Risk Engineering, Graduate School of Systems and Information Engineering, University of Tsukuba, Japan
murao@risk.tsukuba.ac.jp

ABSTRACT

The objective of this study is to make a comparative study of urban vulnerability between Dhaka and Tokyo by visual comparison with google earth and main data analysis. Dhaka and Tokyo are two important megacities in Asia characterized by big population, high density, rapid urbanization, and increasing risk of big disasters like earthquakes. Both are vulnerable to earthquake and had big earthquakes in the past which has come to the time of recurrence. But in terms of mitigation there is a big difference between the two megacities. The possibility of recurrence of big earthquakes in Tokyo like Tokai, Tonankai, Nankai and Tokyo Inland earthquake is 70% in 30 years time. Learning from the big loss of the great Kanto earthquake of 1923, Tokyo is promoting 'safe city' by improving the urban infrastructure like reconstruction of vulnerable houses, road networks and evacuation places. On the contrary, the rapid urbanization process of Dhaka did not concentrate much on to the risk of earthquake. The primary reason is that, after the Great Indian Earthquake of 1897, there was no big earthquake occurred in and around Dhaka. As per the shaking intensity data, the future earthquake estimation says that the same earthquake will recur in the same area. This necessitates good level of earthquake knowledge of the local people and earthquake resistant infrastructure, urban planning, evacuation places, road networks to mitigate earthquake loss. But this type of practice is absent to a great extend, and, which makes the people's lives at risk in consideration of any upcoming earthquake. Based on the circumstance and using the visual comparison, main data analysis, and some specific criteria, it is found that the urban vulnerability is higher in Dhaka than that of Tokyo.

1. INTRODUCTION

1.1 Background and Purpose:

Dhaka and Tokyo are two megacities in Asia with a high population and density. Both cities are prone to natural disasters, which pose threat to urbanization. In the past, earthquake hit two cities and caused severe damages. For example, the Great Indian earthquake of 8.7 affected Dhaka in 1897 and caused extensive damage to masonry structures (Al-Hussaini, 2003). Recently Bilham and England (2001) cited that this earthquake will recur and affect Dhaka at anytime. Another big event, the Bengal earthquake of 7.0 generated near Dhaka and caused much destruction in 1885. This earthquake with its possible epicenter near Dhaka is of great concern for a megacity like Dhaka. The earthquake damage and consequent casualty risk of Dhaka is very high for its high population and large percentage of unplanned buildings and structures. The earthquake risk index (EDRI) for Dhaka stands top among the 20 high risk cities in the world (Khan, 2005), mainly due to its inherent vulnerability of building infrastructure (lacking earthquake resistant features), high population density, and poor emergency response and recovery capacity (Al-Hussaini, 2003). On the other hand, Tokyo had devastating earthquake in the past like the great Kanto Earthquake in 1923, and has anticipation of big earthquakes like the Tokai, Tonankai, Nankai and Tokyo Inland Earthquake in the next few decades (Cabinet office, 2007). These are also of great concern for Tokyo as the damage and casualty risk is very high. However, Tokyo has taken several countermeasures to mitigate this earthquake's impact. The urbanization of two cities has inherent links with disaster vulnerability. This paper checked the urban vulnerability status of two cities based on their urban characteristics, disaster profile, and preparedness.

1.2 Data Used:

Two city's outline data have been used at the beginning to show the city characteristics. Then in the comparison section 3.1, population data of two cities have been used. For both cities, population is one of the main reasons for rapid urbanization. Section 3.2 showed the general disaster management outline of two countries. We found a similarity in disaster management framework of them. Both have same organizational framework. But there is a big difference in role distribution. Then we outlined the main comparison part of this study. We have shown the progress in disaster management laws and systems in two countries, which in most cases came out as an outcome measures for big disasters. Section 3.3 showed the disaster management strength and capacity of two countries, which reflects on the normal disaster mitigation activities. Section 3.4 showed the recurring earthquakes in Bangladesh and Japan, the probable vulnerable region, and section 3.5 discussed the preparedness and mitigation measures for them. Section 3.6 outlined the budget of disaster management in two countries. Finally, in section 3.7, we used Google Earth for some fixed point analysis and comparison. We chosen 3 important areas of the cities based on population, building density, road networks and open spaces.

2. CITY OUTLINES

Table-1: Basic data of Dhaka and Tokyo

Dhaka (BBS, 2009)	**Tokyo** (TMG, 2009)
Area	**Area**
Metropolitan Area 1500 sq. km.	Metropolitan Area 2187. km.
City Corporation Area 360 sq. km.	23 Special Ward Area 621 sq. km.
Population	**Population**
Metropolitan Area 10.9 million	Metropolitan Area 12.79 million
City Corporation Area 8.0 million	23 Special Ward Area 8.65 million
Growth rate 3%	Growth rate 0.9% (as of 2008, TMG)
Population Density	**Population Density**
Metropolitan Area 71/ha	Metropolitan Area 584/ha
City Corporation Area 222/ha	23 Special Ward Area 139/ha
Ward 23, City 0, Town 0, Village 0	Wards 23, City 26, Town 5, Village 8

Main data of two cities is shown in Table-1. Dhaka is the capital and main city of Bangladesh, locating in the central southeastern region of the flat deltaic plain of the transboundary rivers Ganges, Brahamputra and Meghna. The city is surrounded by rivers like the Buriganga in the south, Turag in the west, Tongi canal in the north and Balu in the east. Thus Dhaka is vulnerable to flooding and for geological location; Dhaka is also prone to earthquake. Tokyo is also the capital and main city of Japan, located in the mouth of 3 large rivers like Sumida, Ara and Edo. Therefore, Tokyo is also vulnerable to flooding. However, Tokyo has the vulnerability to typhoon and earthquakes and is characterized by large amount of assets, economic value and a highly developed network of infrastructure.

3. COMPARSION

3.1 Urban Population Trend in Dhaka and Tokyo:

Table-2: Populaiton trend and growth rate in Dhaka and Tokyo (United Nations, 2008), (TMG, 2009)

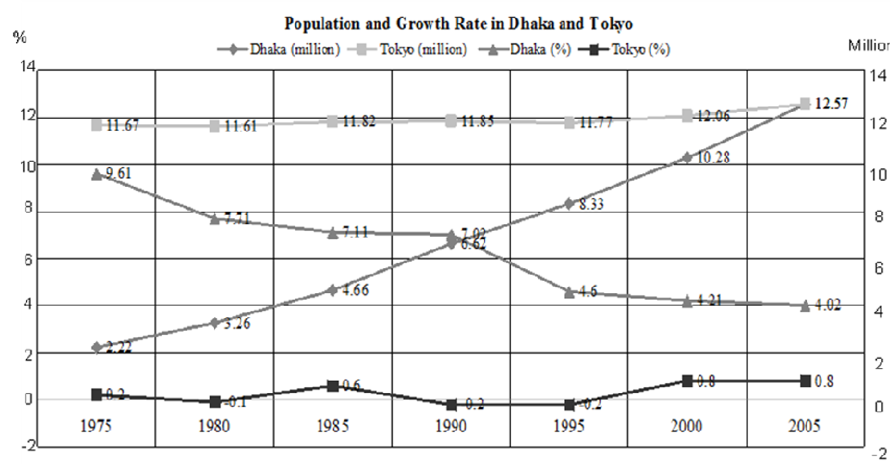

Population trend and growth rate in both cities is shown in Table-2. Dhaka is the fastest growing megacity in the world. It had 1.77 million population in 1974, which reached to 10 million in 2000. The growth rate during 1975-2000 was 6.71% (United Nations, 2008). If the high growth rate continues, it will grow at 3.34% in 2000-2015 and reach 17.0 million in 2015. It is not that for high industrial development of Dhaka. However, the city is characterized by poverty, risk of natural hazards, social vulnerability, shortage of housing, evacuation places and sites, road networks, poor infrastructure and insufficient urban management. Dhaka's increasing population can be subject to high risk in disasters.

Tokyo's growth rate in 1975-2000 was 0.18% (TMG, 2009), which reached to 12.89 million in 2008 at 0.9%. Since the end of Second World War, population concentrated to Tokyo at a high rate (Kumagai and Nojima, 1999). From the 1960s, Japanese rapid economic growth and urbanization expanded in Tokyo until 1980s. More than a quarter of a million people flowed to Tokyo every year and buildings mushroomed everywhere (Kumagai and Nojima, 1999). So the increasing number of population impacted on urbanization and a mixed construction process of buildings were found. Tokyo Metropolitan Government (TMG) has designated 95% of Tokyo ward area as special districts for fire suppression and reduction. The objective is to retard fire and permit evacuation in wake of an earthquake rather. Though there is shortage of open space for evacuation, 149 evacuation sites have been officially designated. TMG is supporting community with local government to reconstruct the old areas, so that people can be survived in big disasters.

3.2 Outline of Disaster Management System in Bangladesh and Japan

Table-3 discussed the disaster management system in Bangladesh and Japan. Both countries have disaster management structure with some similarity and dissimilarity. Bangladesh has four layer structures. The first layer is the national level, where there are three bodies. These bodies have the only role of policy formulation and implementation. The second layer is the executive layer, where districts and city corporation stands for policy implementation. The next layer is also a smaller executive layer, which is also responsible for policy implementation. The final layer is the smallest administrative layer, which should have a lot of responsibilities including plan formulation and execution in the local level. Japanese first layer is also the national layer. This layer has the specific role to follow up the implementation of Basic Disaster Management Plan. The second layer is similar to Bangladesh, the executive layer, which supposes to formulate and promote implementation of local disaster management plan. The next level is also similar to Bangladesh and plays same role as formulate and promote local disaster management plan. The last layer is residents' layer, which is the strengthening part of the structure. In every layer, Tokyo has only one body. But Bangladesh has more than one body. Bangladesh has only policy and plan formulation activities. But Japan has specific designation of action like policy formulation, implementation, following the law and resolutions.

Table-3: Disaster Management System in Bangladesh and Japan

Bangladesh (DMB, 2009)		**Japan** (CAO, 2009)	
System	***Roles***	***System***	***Roles***
National Level ①National Disaster Management Council ②Inter-Ministerial Disaster Management Coordination Committee ③National Disaster Management Advisory Committee	①Formulate policy, guidelines ②Implementation and coordination ③Advisory roles	National Level Central Disaster Management Council	Formulation and promoting implementation of the Basic Disaster Management Plan
District Level ①District Disaster Management Committee ②City Corporation Disaster Management Committee (DMC)	Formulate and implement local disaster management plan (DMP)	Prefecture Level Prefectural Disaster Management Council	Formulation and promoting implementation of Local DMP
Upazila Level Upazila/Thana Disaster Management Committee	Formulate and implement local DMP	Municipal Level Municipal Disaster Management Council	Formulation and promoting implementation of Local DMP
Union Level Union/Municipal DMC	Formulate and implement local DMP	Residents Level	

3.3 Progress in Disaster Management Laws and Systems:

Both countries have developed disaster management system and they have been experiencing a lot of natural disasters every year. The frequency and nature of destruction caused two countries to think about disaster management guidelines, acts, plans and systems well ahead. The following Table-4 has been made with the major disaster events of two countries and the acts and systems developed after that disaster event. The table has been separated into 3 time phases. In the first phase, Bangladesh had 6 big disasters but there was no progress in disaster management acts and systems. Japan had 5 big disaster events out of which 3 was earthquakes. Japan enacted 8 disaster management acts and 3 plans and systems based on the experience of those disasters. In the second phase, Bangladesh had 17 disasters with 2 earthquakes. One of the biggest floods in Bangladesh happened during this time in 1988. Bangladesh considered flood as number one hazard and cyclone as number two. So to manage them efficiently, Bangladesh first time formulated the standing order on flood in 1984 and standing order on cyclone in 1985. These were basically set code of conduct, explained how different organs of government will act during an impending situation. On the other hand, Japan faced 2 big disaster events, a volcanic eruption and an earthquake during this time. The geological society of Japan had declared a report on the possibility of anticipated Tokai earthquake and Japan had taken 4 acts and 1 plan and system on disaster management in this period. In the third phase, Bangladesh experienced 27 disasters. Among them, 14 were floods, 8 cyclones, 1 tornado, 3 earthquakes and 1 landslide. The devastating cyclone of 1991 happened during this time. Bangladesh enacted the national building code in 1993 and standing order on disaster in 1997. Japan faced 6 disasters during this time. Among them, 2 were big earthquakes like Hanshin-Awaji and Chuetsu earthquake. Based on the experience of Hanshin-Awaji earthquake, Japan enacted 7 acts, 8 other acts, and other 13 disaster management plans and systems. After every big disaster, Japan enacted several acts, laws or policies to reduce the casualty in the next disasters. So a lot of safeguards were applied in Japanese disaster management system. However, Bangladesh had many devastating disasters, but there were no safeguards enacted.

Table-4: Progress in Disaster Management Laws and Systems in 2 countries

Time	**Bangladesh** (DMB, 2009)			**Japan** (Cabinet Office, 2007)		
	Events	Disaster Management Acts	Disaster Management Plans and Systems	**Events**	Disaster Management Acts	Disaster Management Plans and Systems
1940-1960s	**1950** Earthquake **1951** Tornado **1961** Tornado **1964** Tornado **1969** Tornado **1969** Tornado			**1946** Nankai earthquake **1948** Fukui earthquake **1959** Typhoon Ise-wan **1961** Heavy snowfalls **1964** Niigata earthquake	**1947** Disaster relief act **1949** Flood control act **1950** Building standard law **1960** Soil conservation and flood control act **1961** Disaster countermeasures basic act **1962** Act on severe disasters **1962** Act on snowfall **1966** Act on earthquake insurance	**1961** Designation of disaster reduction day **1962** Establishment of central disaster management council **1963** Basic disaster management plan
1970-1980s	**1970** Cyclone **1972** Tornado **1973** Tornado **1977** Tornado **1989** Tornado **1984** Tornado **1985** Cyclone **1986** Flood **1986** Cyclone **1987** Flood **1988** Flood **1988** Cyclone **1988** Earthquake **1989** Tornado **1989** Flood **1989** Cyclone **1989** Earthquake		**1984** Standing order on flood **1985** Standing order on cyclone	**1973** Mt. Sakurajima eruption **1976** Report about the possibility of Tokai earthquake **1978** Miyagi ken-oki earthquake	**1973** Act on volcanoes **1978** Act on large-scale earthquakes **1980** Act on earthquake countermeasures **1981** Amendment of building standard law	**1979** Tokai earthquake countermeasures basic plan
1990-2000s	**1990** Flood **1990** Cyclone **1991** Flood **1991** Cyclone **1993** Flood **1994** Flood **1994** Cyclone **1995** Flood **1995** Cyclone **1996** Flood **1996** Tornado **1996** Cyclone **1997** Flood **1997** Cyclone **1997** Earthquake **1998** Flood **1999** Flood **1999** Earthquake **2000** Flood **2002** Flood **2003** Flood **2003** Earthquake **2004** Flood **2007** Landslide **2007** Flood **2007** Cyclone **2009** Cyclone		**1993** Bangladesh national building code **1997** Standing order on disaster (replaced 1984 Standing order on flood and 1985 Standing order on cyclone)	**1995** Great Hanshin-Awaji Earthquake **1999** Torrential rains **1999** JCO Nuclear accident **2000** Torrential rains **2004** Chuetsu earthquake **2005** Typhoons and torrential rains	**1995** Act on earthquake countermeasures **1995** Act on retrofit buildings **1995** Amendment of disaster countermeasures basic act **1995** Amendment of act on large-scale earthquakes **1996** Act on rights and profits of the victims **1997** Act on disaster resilience **1998** Act on livelihood recovery **1999** Act on nuclear disasters **2000** Act on sediment disaster **2002** Act on Tonankai and Nankai earthquake **2003** Urban river inundation act **2004** Act on trench type earthquake **2005** Amendment of retrofit of buildings **2005** Amendment of flood act **2005** Amendment of sediment disaster	**1995** Amendment of basic disaster plan **1995** Designation of volunteer day **2001** Establishment of cabinet office **2003** Policy framework for Tokai earthquake **2003** Policy framework for Tonankai and Nankai earthquake **2004** Tonankai and Nankai earthquake basic plan **2005** Tokai earthquake strategy **2005** Tonankai and Nankai earthquake strategy **2005** Policy framework for Tokyo inland earthquakes **2006** Policy framework for trench-type earthquakes **2006** Countermeasures basic plan for trench-type earthquakes **2006** Tokyo inland earthquake strategy **2006** Basic framework for nationwide movement for disaster reduction

3.4 Possible recurring earthquake in Bangladesh and Japan*:*

Figure-1 shows the recurring and anticipated earthquakes in two countries. Bangladesh anticipates 1885 Bengal and 1897 Great Indian Earthquake for recurrence. Roger Bilham and Philip England (2001) opined that the great Indian earthquake with maximum M ≥ 8 may constitute a significant seismic threat to nearby densely populated regions of Bangladesh and to the very large city of Dhaka. Khan's (2005) investigation suggested the return period of Bengal earthquake by 2015 having return period character of 130 years. On the other hand, Japan anticipates 5 earthquakes like Tokai, Tonankai, Nankai, Trench type and Tokyo Inland earthquakes. Among them, 4 may directly affect Tokyo.

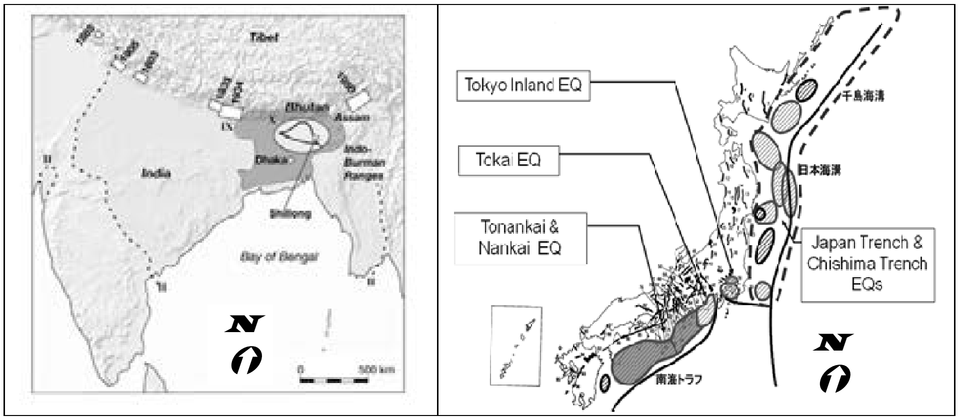

Figure-1: The Great Indian Earthquake 1897's recurring area (Bilham and England, 2001). Source region where large-scale earthquakes are anticipated in Japan (TMG, 2008)

3.5 *Preparedness for recurring earthquakes in Bangladesh and Japan:*

In the recent past, Bangladesh did not have any big earthquake. Thus, Bangladesh is generally complacent about the earthquake risk. Bangladesh has no notable program for earthquake preparedness, but has some primary awareness program and Disaster Preparedness Plan formulation activities with local government. The Comprehensive Disaster Management Program (CDMP) unit of Ministry of Food and Disaster Management is implementing programs like seismic risk assessment, awareness and training. Japan has estimated human causality and economic loss in anticipated earthquakes. Based on that, Japan is promoting program with local government and community to reduce the loss and casualty. Table-5 showed the preparedness for recurring earthquake in Japan.

Table-5: Preparedness for recurring earthquakes in Japan (CAO, 2007)

Estimation	Tokai Earthquake	Tonanki and Nankai Earthquake
Death Toll	9200 -> reduce to 4500	17800 -> reduce to 9100
House Destroy (increase the ratio of retrofitted houses 75% [2003] to 90% [2015]	260000	360000
Economic Loss (billion yen)	37 trillion yen -> reduce 19 trillion yen	57 trillion yen -> reduce to 31 trillion yen
Every municipality at risk expected to develop hazard maps by 2015		

3.6 *Disaster management related budget in Bangladesh and Japan:*

Bangladesh has no specific budget for disaster management. In practice, Bangladesh allocates emergency disaster response money from development budget. But development agencies in Bangladesh have their own budget for disaster preparedness and mitigation. Japan has specific budget for disaster management. As per the Disaster Countermeasures Basic Act 1961, both central and local government in Japan must have the budgetary arrangement for disaster management. The average budget for disaster management in Japan from 1995 to 2004 was approximately 4.5 trillion yen, which has the following breakdown (CAO, 2007) in Figure-2.

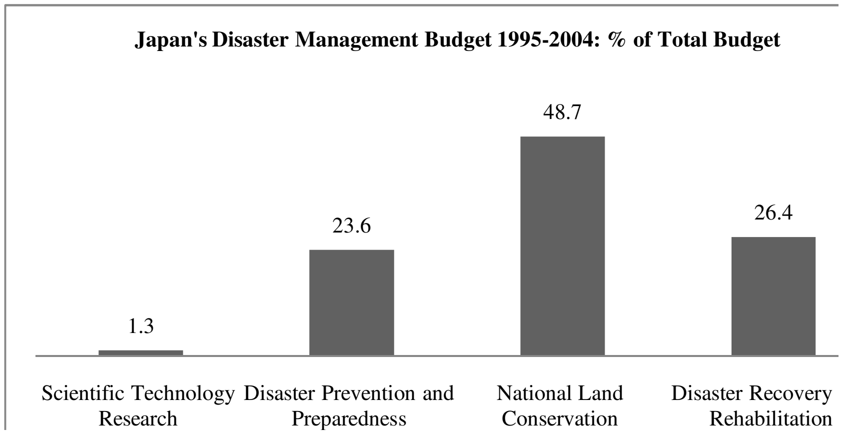

Figure-2: Disaster Management Budget Trend in Japan (CAO, 2007)

3.7 *Fixed point analysis and comparison using Google Earth*:

In this section, Figure-3, we used Google Earth to choose 1 km² area of 3 important parts of Dhaka city for the comparative analysis with Tokyo. The selected parts represent other parts of Dhaka. They are Bakshi Bazar, oldest business and residential part; Motijheel, main commercial part and Baridhara, the newer residential and diplomatic part. We considered road shapes, building density and open spaces. Areas in Tokyo we chosen were based on same criteria. They are Higashi Ikebukoro, old residential part, Asakusa, commercial place and Higashi Ginza, the biggest business place.

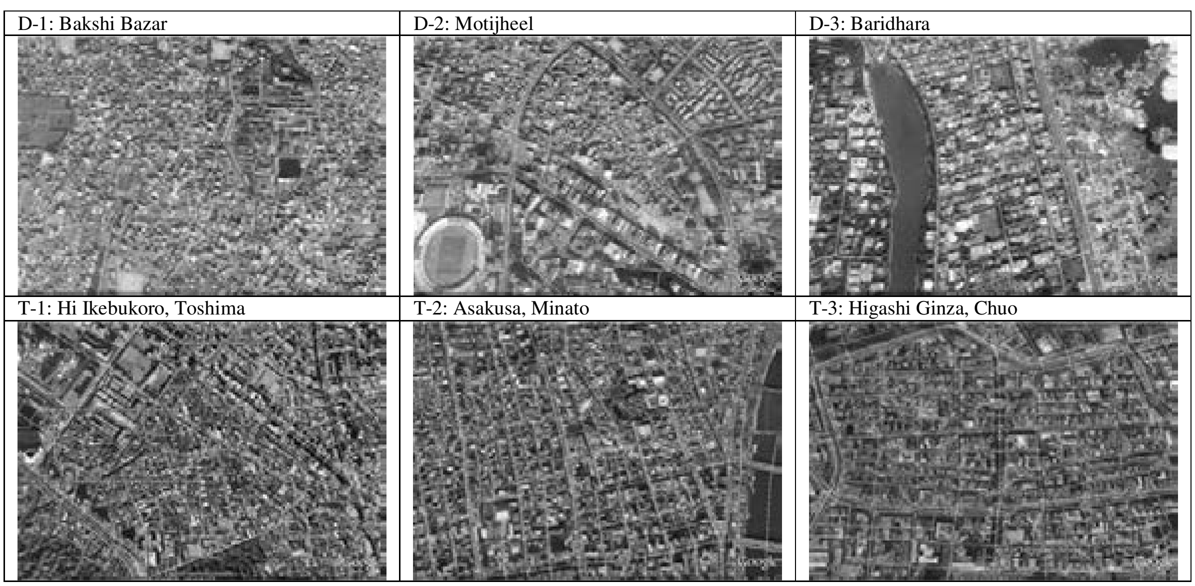

Figure-3: Fix point analysis of Dhaka and Tokyo using Google Earth

D-1: **Bakshi Bazar** in Dhaka: This area is characterized by disorder of construction of buildings and road networks. Roads are not straight and parallel. Some roads are dead-end. Buildings are congested and blocks are disorganized. Buildings are not high and have typical construction. A good number of wooden houses are there. No space between buildings and roads are narrow. Some scattered open spaces are seen, which seems insufficient for the area. T-1: **Higashi Ikebukoro** in Tokyo: This area is also characterized by disorder of construction of buildings and road networks. This area is densely crowded. Blocks are disorganized. Some roads are parallel and buildings are constructed on the road. Some dead end roads are also seen. Buildings are not much high and a good number of wooden houses are there. Space between houses is very narrow. Not much open space is visible. D-2: **Motijheel** in Dhaka: This area has disordered characteristics. The residential and commercial buildings do not have enough space between them. Few roads are straight and parallel. Some small roads have dead end. Houses are very dense looked. Residential buildings congested and blocks are disorganized. A lot of wooden houses are there. Some scattered open spaces are seen. It also looks insufficient for this area. T-2: **Asakusa** in Tokyo: This area is comparatively organized. Roads are straight and parallel. Buildings are constructed in blocks. A lot of buildings are constructed in each block. Blocks are rectangular. Both small and high buildings are visible. The space between buildings is narrow. Wooden houses are also seen. Some scattered open spaces are there. Road-networks looked very organized. D-3: **Baridhara** in Dhaka: This part looks organized than the other discussed two parts of Dhaka. Roads are parallel but buildings are congested in blocks. Small and narrow space between buildings is seen. The area has Lake in one side and congested area in other. Several open spaces are seen. But they seem insufficient for the area. T-3: **Higashi Ginza** in Tokyo: This area is organized. Roads are parallel. Buildings are in blocks. Many high commercial buildings are seen. Not much empty space between buildings is seen. Several open spaces are seen.

4. ANALYZE AND DISCUSSION

Table-6: Vulnerability comparison between Dhaka and Tokyo

	Dhaka			Tokyo		
	D-1	D-2	D-3	T-1	T-2	T-3
Road Shape						
Shape	disorganized	disorganized	organized	disorganized	organized	organized
blocks						
	disorganized	disorganized	organized	disorganized	rectangular	organized
building density						
Building density/ha	100	70	48	108	66	40
Space between building	no	no	narrow	no	small	small
Open spaces						
Type	empty space, playground	empty space, playground	playground, empty space	small parks	small parks, playground	parks, playground
Number/skm	2	2	5	2	4	5

As per the analysis, D-1 is most vulnerable to disaster like earthquake. Most of the buildings are old and had typical construction. They may not take the extra load of earthquake. If a building collapse, it has the possibility to fall on the nearby one. A good number of burnable wooden houses are there. They may cause big fire. Narrow road networks may obstacle for rescue and fire fighting work. There is a scarcity of open space too. So rescue, fire prevention and evacuation will be difficult here. The D-2 can be explained as same as D-1. Two big stadiums are nearby, which can be used for evacuation. The D-3 is comparatively in better position. But if the buildings collapsed, the question of open space will be important for this area. For Tokyo, T-1 area can be explained same as D-1. But this area is changing with the support of the local government. So the open space is increasing, buildings are restructuring to withstand with earthquake risks. The T-2 is also improving like increasing open space and changing the road shapes. The T-3 area is in the best position among the six points. It has wide road networks, several parks and playgrounds as open space. Comparing with other discussed data and criteria like population, disaster management laws and systems, big earthquake in the past, possible recurrence and disaster management budget, Dhaka is more vulnerable to urban disaster than Tokyo.

5. CONCLUSION

Based on the main data and fixed point analysis, Dhaka's urban vulnerability is evident. Though Tokyo is still vulnerable, but Tokyo promotes mitigation activities in an organized manner. So the vulnerability range is changing as per the estimated preparedness of the TMG. Thus cities like Dhaka can follow Tokyo's practice to reduce their urban vulnerability.

REFERENCES

Al-Hussaini, T.M., 2003. Critical Elements for Earthquake Disaster in Dhaka City, paper presented at *USMCA 2003 Symposium on New Technology for Urban Safety of Mega Cities in Asia*, Tokyo, Japan.

Bilham, R., and England, P., 2001. Plateau 'pop-up' in the great 1897 Assam earthquake, *Nature*, 410, 806-809.

Cabinet Office (CAO), Government of Japan, 2007. *Disaster Management in Japan*.

Khan, A.A., and Hossain, M.S., 2005. Recurrence of 1885 Bengal Earthquake and hazard vulnerability status of Dhaka metropolitan city, Bangladesh. *Oriental Geographer*, v.49(2), p. 205-216.

Kumagai, Yoshio, and Nojima, Yoshiteru, 1999. Urbanization and Disaster Mitigation in Tokyo, *Crucibles of Hazard: Mega-cities and Disasters in Transition*, Tokyo.

Sarkar, M.M.H., and Ferdousi, S., 2004. Assessment for role of GIS Based Natural Disaster Database in Environmental Management and Planning activity in Bangladesh, *Environmental Informatics Archives, Volume 2*, 855-836

United Nations, 1999. *World Urbanization Prospects: The 1999 Revision.* New York: United Nations.

United Nations, 2008. *World Urbanization Prospects: The 2007 Revision.* New York: United Nations.

Bangladesh Bureau of Statistics (BBS), 2009. At http://www.bbs.gov.bd/ checked on July 9, 2009.

Disaster Management Bureau (DMB), 2009. At http://www.dmb.gov.bd/ checked on June 26, 2009.

Tokyo Metropolitan Government (TMG), 2009. At http://www.metro.tokyo.jp/ENGLISH/ Checked on June 20. 2009.

A STUDY ON THE EFFICIENT EARLY-WARNING METHOD USING COMPLEX EVENT PROCESSING (CEP) TECHNIQUES

Kim, Hyung Woo
KT R&D Laboratory, Republic of Korea
hyungwoo@kt.com,
Kim, Goo Soo
KT R&D Laboratory, Republic of Korea
goosoo@kt.com
Chang, Sung Bong
KT R&D Laboratory, Republic of Korea
sbchang@kt.com

ABSTRACT

In recent years, there is a remarkable progress in ICTs (Information and Communication Technologies), and then many attempts to apply ICTs to other industries are being made. In the field of disaster managements, ICTs such as RFID (Radio Frequency IDentification) and USN (Ubiquitous Sensor Network) are used to provide safe environments. Actually, various types of early warning systems using USN are now being widely used to monitor natural disasters such as floods, landslides and earthquakes, and also to detect human-caused disasters such as fires, explosions and collapses. These early warning systems issue alarms rapidly when a disaster is detected or an event exceeds prescribed threshold value, and furthermore deliver alarm messages to disaster managers and citizens. In general, these systems consist of a number of various sensors measuring real-time stream data, which requires an efficient and rapid data processing technique. In this paper, an event-driven architecture (EDA) is presented to collect event effectively and to provide an alert rapidly. Additionally, a complex event processing (CEP) technique is introduced to process complex data from various sensors and to provide prompt and reasonable decision supports when many disasters happen simultaneously. A basic concept of CEP technique is presented and the advantages of the technique in disaster management are discussed briefly. An example of flood early alarm system using CEP is presented. It is found that the CEP based on the EDA will provide an efficient early warning method when disaster happens.

1. INTRODUCTION

With a rapid development of ICT (Information and Communication Technology), USN (Ubiquitous Sensor Network) is widely applied to disaster monitoring systems. Natural disasters such as floods, landslides, and earthquakes, and human-caused disasters such as fire, explosion, and collapse are monitored by these sensor networks. The disaster monitoring systems should collect accurate information from sensors, and provide rapid response for emergency management. In addition, it is necessary for the system to share information relevant to disaster with various organizations such as police, hospital, a fire brigade and military. Current disaster monitoring systems, however, use their own systems purchased from different vendors. The vendors follow their own proprietary and closed communication protocols, and thus it costs great money for enabling a communication channel between applications from two different vendors. Therefore, a new architecture is required for seamless integration between various applications in disaster management. There is also a need for implementation of an open standard for information interoperability.

Additionally, the current disaster monitoring system has a data bus that is closed and proprietary. This makes it very difficult to plug in third party applications. Moreover, for the communication between disaster authorities, the data format is proprietary. The feature of existing architecture is that the data bus carries only the data. Each application needs to come down to the data level, process the data and act upon the data. The architecture is largely data oriented rather than event oriented. Events make more sense than raw data on systems with a high demand for situational awareness and real time monitoring (Medhekar, 2008).

To solve these problems, an event-oriented architecture is introduced. The architecture is basically based on the web-service eventing technology which makes it possible to communicate with heterogeneous systems. In addition, a complex event processing method is introduced for real-time disaster monitoring.

2. DISASTER MANAGEMENT

2.1 Basic requirements

Generally, it is recommended that the disaster monitoring system should be designed to respond rapidly and implemented by reliable, stable and proven technology not to give a false alarm. It is also operated in real-time manner and designed to issue alert without delay. In addition to these requirements, disaster monitoring systems should have interoperability. Interoperability has several levels: organization, application, information and technical level operability. Organizational interoperability is ensured by a standard inter organization protocol, which expresses the way in which organizations have to communicate and share data. Application interoperability can be achieved by enforcing an inter application protocol. Information interoperability is ensured by complying with a standard information model. Finally, technical interoperability is achieved by using standard device level protocols. (Medhekar, 2008).

Early warning system for disaster management is especially characterized by distribution of unit systems comprising of sensor networks and distribution spread over a large geographical area. Disaster information gathered by unit systems should be shared between organizations. Therefore, coordination between these systems is required and achieved by interoperability.

3. EDA (Event-Driven Architecture)

3.1 Introduction

3.1.1 What is event?

An event is defined as something notable that happens inside or outside a system. Its occurrence may denote a problem, an impending problem, an opportunity, a threshold, or a deviation. Events are transmitted as event messages, each of which has an event header and an event body. Event header normally contains meta-data to be used for quick reference, such as event specification ID, event type, event name, event timestamp, event occurrence number, and event creator. Event body contains the full and detailed description of what has actually happened (Medhekar, 2008).

3.1.2 Event processing methods

Recently, various technologies that support event-driven architecture have been applied to disaster monitoring. Event processing methods are categorized as (1) simple event processing; (2) stream event processing and (3) complex event processing. In simple event processing, a notable event happens, initiating downstream actions. It is commonly used to drive the real-time flow of work, removing lag time and cost from the system. In stream event processing, both ordinary and notable events happen. Ordinary events are first checked for notability and then streamed to the information subscribers. Such kind of event processing is normally used to drive the real-time flow of information in and around the system. Complex event processing (CEP) deals with evaluating a confluence of events and then taking action. CEP is commonly used to detect and respond to business anomalies, threats, and opportunities (Michelson, 2006).

3.2 SOA (Service-Oriented Architecture)

3.2.1 What is SOA?

SOA is defined as an architecture that is made up of components and interconnections that stress interoperability and location transparency. SOA provides an approach for building systems that deliver application functionality as services to the end user applications or other services. SOA contains components, services and processes. A service is a grouping of components and these services are joined together by the processes to form a business process. This concept basically has three components: service provider, service broker, service requester. Three operations are publish, find and bind (Joshi, 2005).

SOA facilitates integration of heterogeneous systems and increases the reuse possibilities of programs. Rather than building or possessing every program component, developers are able to assemble the best services available on the internet according to their needs. In addition, real openness of systems will be achieved with SOA since the components are not limited to units of functionality or platforms developed by certain vendors. These components and operations bound together with SOA collaborations, which is based on publish-find-bind paradigm. According to this pattern, a service provider gives a description of the service it wants to publish to the service registry. This description includes a description of the interface at which the service instance is available. A service consumer performs a dynamic service location by querying the service registry for a service that matches its criteria. If the queried service exists, the registry provides the consumer with the interface contract and the endpoint address for the service (Joshi, 2005).

3.2.2 Web service

A web service is defined as an interface that describes a collection of operations that are network accessible through standardized XML messaging. It covers all the details necessary to interact with the service, including message format, transport protocols and location. The interface hides the implementation details of the service, allowing it to be used independently of the hardware or software platform on which it is implemented and also independently of the programming language in which it is written. This allows and encourages web services-based applications to be loosely coupled. The web service architecture is based upon publish-find-bind paradigm defined by SOA pattern (Joshi, 2005).

3.3 EDA (Event-Driven Architecture)

3.3.1 What is EDA?

In an event-driven architecture, a notable thing happens inside or outside one’s business, which disseminates immediately to all interested parties (human or system components). The interested parties evaluate the event, and optionally take action. The event-driven action may include the invocation of a service, the triggering of a business process, and/or further information publication (Brenda, 2006).

An event-driven architecture is extremely loosely coupled, and highly distributed. The source knows only how and when to create the event and has no knowledge about the event’s subsequent processing, or the interested parties. Hence, it is difficult to trace an event through a dynamic multipath event network. Event-driven architectures are best used for asynchronous flows of information (Medhekar, 2008).

3.3.2 EDA vs. SOA

SOA and EDA have many things in common, because they both are ways of combining multiple software modules into large distributed applications. However, they differ in the way they organize the relationships among the modules, and this makes them appropriate for different purposes. SOA uses directed, generally bidirectional, request/response communication, whereas EDA uses unidirectional messaging to communicate among two or more, largely independent peer procedures (Schulte, 2003).

EDA is more efficient than SOA if there are multiple destinations for the same data, because the source sends the event only once, whereas an SOA client would have to make successive calls to achieve the same wide distribution. Comparisons between SOA and EDA are shown in Table 1.

Table 1: Comparisons between SOA and EDA.

SOA	**EDA**
Has one-to-one connections	Supports many-to many connections
Has flow routing that is directed by the client (sender)	Has a flow of control that is determined by the recipient based on the message itself
Employs a linear path of execution through a hierarchy of modules	Supports dynamic, parallel, asynchronous flows through a network of modules
Is closed to new, unforeseen input once a flow is started	Can react to new, external input that may arrive at unpredictable times

3.3.3 Communication model

In an early-warning system, an efficient communication pattern is necessary between the data sources and the alerting services. Pull data model doesn't support proactive dispatching of data as in the case required in emergency warning situations, where data must be dispatched when certain event occurs. On the other hand, a push model overcomes the synchronous request/response pattern between the client and service by allowing asynchronous data dissemination. Push model corresponds to an event-based system, with which the components communicate over the asynchronous exchange of events (Joshi, 2005).

4. CEP (Complex Event Processing)

4.1 Introduction

4.1.1 What is CEP?

CEP is a processing methodology which can be used to detect patterns of events and infer new meanings. Key considerations for applications contains: (1) high throughput applications that process large volumes of messages (between 1,000 to 100k messages per second); (2) low latency applications that react in real-time to conditions that occur (from a few milliseconds to a few seconds); and (3) complex computation applications that detect patterns among events, filter events, aggregate time or length windows of events, join event streams, trigger based on absence of events, etc (EsperTech, 2009).

CEP is used for detection and processing of a confluence of events. CEP is extremely useful in applications which need to process and analyze large numbers of real-time events. CEP thus has a huge application in the highly dynamic systems, with frequently flowing, high volumes of real time data. Disaster monitoring is one such area (Medhekar, 2008).

4.1.2 Advantages over conventional approach

It takes time to store information in a database. Even if an in memory database is used, latency due to disk I/O cannot be avoided. Event processing is based on the push model, when as soon as events are pushed into the channel, they get processed. Data, however, needs to be processed by pulling it out of the database – making it less real time (Medhekar, 2008).

CEP allows applications to store queries and run the data through, instead of storing the data and running queries against stored data. Response from CEP is real-time when conditions occur that match queries. The execution model is thus continuous rather than only when a query is submitted (EsperTech, 2009).

4.2 Design patterns

There are basic CEP design patterns which may be thought of as building blocks that can be combined to create complete applications. They are filtering, in-memory caching, aggregation, database lookups, database writes, correlation and event pattern matching.

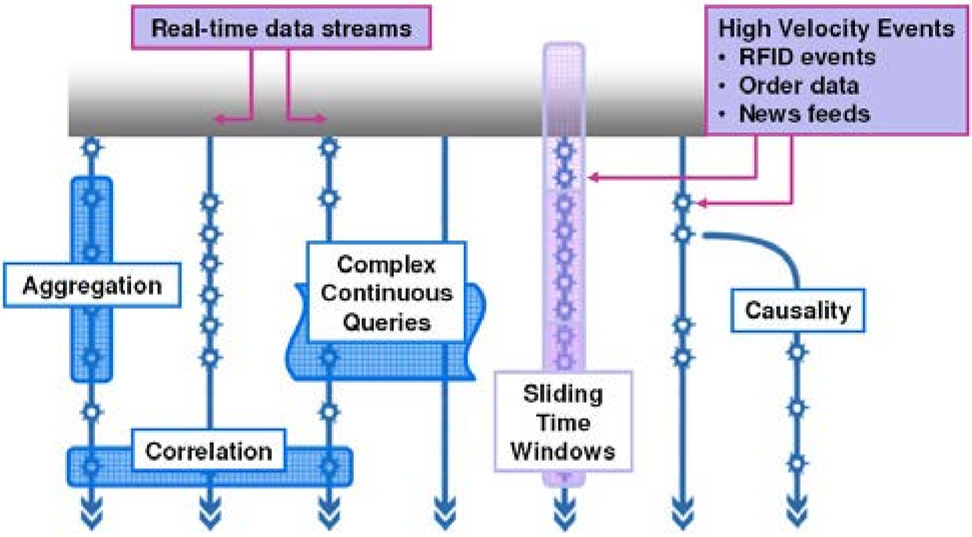

Figure 1: Complex Event Processing Functions [source: BEA]

Filtering involves filtering of events based on the event attributes and in-memory caching involves caching and accessing of streaming events and database data in the memory. Aggregation over windows involves computation of statistical metrics over various kinds of moving windows. It does not merely keep events in memory, but uses the stored values to compute various statistics. It has different types based on the characteristics such as kind of aggregators (sums, counts, min, max, standard deviation) and kinds of windows (time-based, count-based, moving). Correlation facilitates joining of multiple event streams. Most advanced applications must look at and correlate events across multiple streams. Event pattern matching facilitates complex, time-based matching of events across multiple event streams. It can be used to detect a number of relationships among events. Typical design patterns are presented in Figure 1 (Medhekar, 2008).

5. FLOOD EARLY WARNING SYSTEM

5.1 Rule based event processing

5.1.1 Flood forecasting

In this paper, flood early warning system for urban storm water is presented using CEP. Flood warning process has four stages such as detection, forecasting, warning and response stages. In the detection stage, real-time data is monitored and a flood event is generated. Forecasting stage uses the data to predict water level as well as the time of occurrence of flood event. Warning stage utilizes the information derived from the detection and forecasting stages and issue a warning to disaster authorities. Finally, response to the flood warning includes flood damage control measures such as flood control reservoir and evacuation of people (Joshi, 2005).

Up to now, a number of flood forecasting models are developed around the world, and they are mainly on the basis of hydrologic observations such as gauged rainfall and flows. Among the flood forecasting systems, there is a basic system that is typically based on exceedance of certain threshold value of hydrological parameter. In this case, a warning is triggered when one or more parameters are exceeded. This enables technical as well as non-technical decision makers to better understand the flood (Joshi, 2005).

5.1.2 Rules for flood forecasting

A rule based approach can be used to forecast flood and dispatch alert notifications. It is based on threshold value exceedance and can be applied to examples as follows:

- Rule 1: if river gauge level exceeds threshold value of 5 m in certain reach of the river, send alert message;
- Rule 2: if the river rise velocity exceeds threshold value of 0.5 m per 10 minutes, send alert message;
- Rule 3: if the moving average of river gauge levels for 30 minutes interval exceeds 5 m, send alert message;
- Rule 4: if sum of river gauge levels installed at the river basin exceeds threshold value of 20 m, send alert message;
- Rule 5: if cumulated rainfall depth in certain area exceeds 100 mm in 24 hours, send alert message.

Moreover, another rule is set by combining these rules. The threshold value for river level varies at different location of observations along the river reach. River gauge level is also influenced by rainfall depth. Therefore the minimum and maximum threshold values of the observation parameter such as river gauge level are to be predefined (Joshi, 2005).

5.2 Implementation

5.2.1 Architecture

When events from multiple sources are fed into the engine, CEP analyzes them based on current rules and upon detection, alerts are sent out as messages and actions are triggered. In our flood early warning system, Esper is used as a CEP engine because it is an open source and easy to use (EsperTech 2009). Figure 2 shows the architecture of flood early warning system which has been implemented.

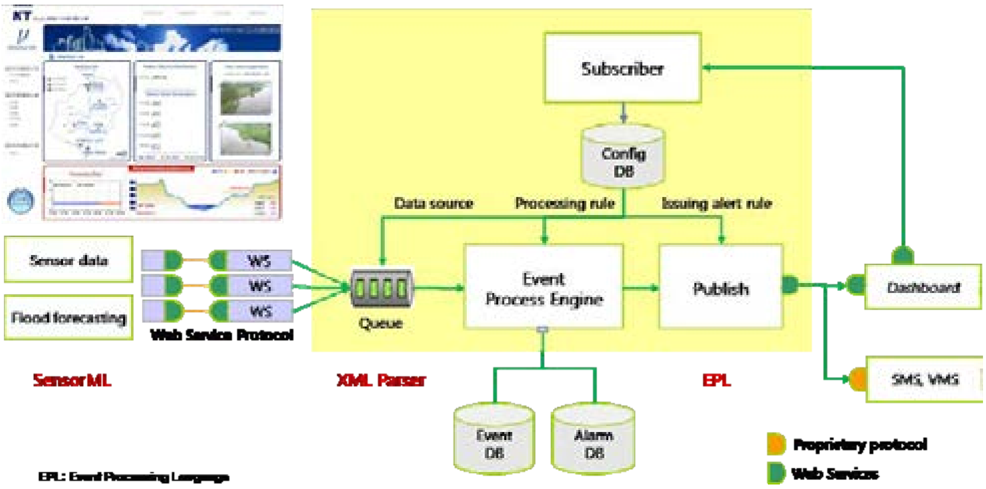

Figure 2: Architecture of flood early warning system

Data gathered by rainfall gauge and river gauge are sent to gateway via web service protocol. The gateway communicates with sensor nodes by means of communication module, and analyzes and answers the packets sent from sensor nodes. The detected data and detecting time from sensor nodes are fed into CEP engine where data are processed according to the predefined rules and alert messages are generated. Raw events are generated as standard formats and published and subscription data is registered so that subscriber can select them. The subscription time and data type can be also selected. Then, the subscription data is delivered to subscriber via event sinks such as SMS (Short Message Service) and VMS (Variable Message Sign).

5.2.2 Main features

We have developed flood early warning system using EDA-CEP. Since the system is based on the web service architecture, interoperability is assured, which means that information sharing between organizations is possible. Event sources are uploaded to a platform which can publish, subscribe and process them. End users then access the platform to search and fetch valuable information and value-added applications. Figure 3 shows a flood monitoring screen displaying real-time rainfall depth, water level and CCTV images. Assets such as monitoring stations can be easily added to this screen dashboard by mouse drag and drop. The rules for flood forecasting are easily input through this screen, and they are transformed to an EPL (Event Processing Language) for complex event processing. Events that exceed predefined threshold value are dispatched to the subscriber without delay via SMS and VMS.

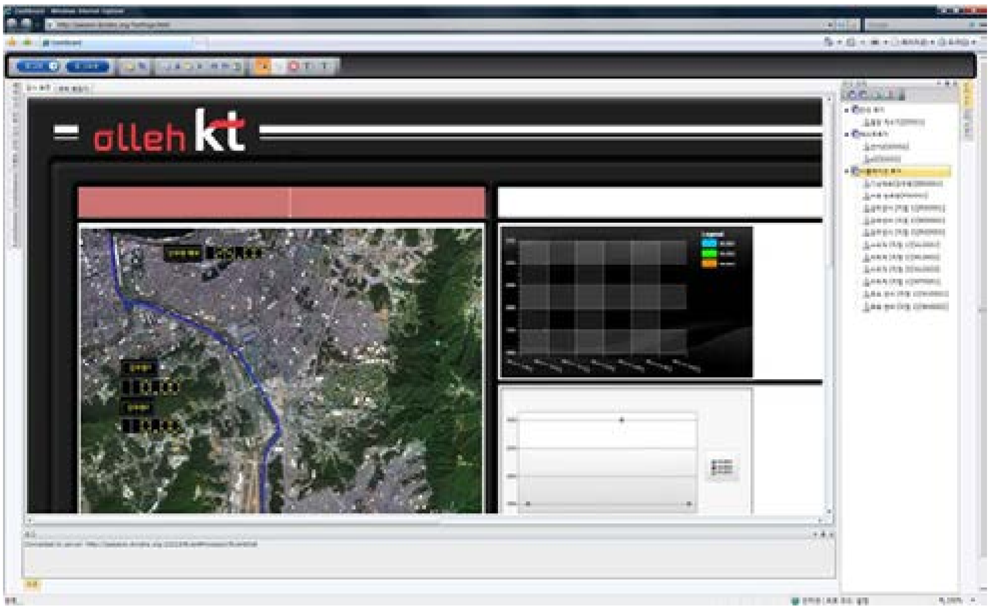

Figure 3: Dashboard of flood early warning system

6. CONCLUSIONS

We have described architectures for disaster management and introduced event processing methods. It is expected that the EDA is a suitable architecture for disaster management which requires organization and information interoperability. It is also expected that the CEP would be more relevant than a traditional data processing system in the field of disaster management. Thus, CEP based on EDA will be widely applied to flood early warning system. The system implemented in this paper is now being tested at the small urban river basin, and will be verified in the future.

REFERENCES

BEA, *Event Driven SOA.*

Brenda M. Michelson, 2006. *Event-Driven Architecture Overview*. Patricia Seybold Group.

EsperTech. 2009. *Esper Reference Documentation*.

Joshi, A. 2005. *Active Web Alert Service for Rule Based Alerting in Sensor Web – An Event Based Approach*. Thesis for the degree in Master of Science in Geoinformatics.

Medhekar, A. 2008. *Event-driven architecture for Indian Power Systems*. Dual Degree Project Report (Stage III), Department of Computer Science and Engineering, Indian Institute of Technology, Bombay, Mumbai.

Schulte, R. 2003. *Event-Driven Applications: Definitions and Taxonomy*. Gartner, Research Note.

Schulte, R. and Natis, Y. 2003. *Event-Driven Architecture Complements*

SOA. Gartner, Research Note.
US Army Corps of Engineers. 1993. *Application of Rainfall-Runoff Simulation for Flood Forecasting*.

A SURVEY ON RESIDENTS' RESPONSE TO EARTHQUAKE EARLY WARNING AT THE 2008 IWATE-MIYAGI INLAND EARTHQUAKE IN JAPAN

Miho OHARA
Interfaculty Initiative in Information Studies,
The University of Tokyo, Japan
ohara@iis.u-tokyo.ac.jp
Yasuhito JIBIKI
Interfaculty Initiative in Information Studies,
The University of Tokyo, Japan
Naoya SEKIYA
Toyo University, Japan
Tetustaro SUMI
Interfaculty Initiative in Information Studies,
The University of Tokyo, Japan
Kimiro MEGURO
ICUS, Institute of Industrial Science, The University of Tokyo, Japan
meguro@iis.u-tokyo.ac.jp
Atsushi TANAKA
Interfaculty Initiative in Information Studies,
The University of Tokyo, Japan

ABSTRACT

Japan Meteorological Agency (JMA) started the service of earthquake early warning (EEW) to the public since October 1, 2007. When the 2008 Iwate-Miyagi Inland Earthquake occurred on July 14, 2008, EEW information was provided to the regions whose intensities of shaking were expected to be more than JMA 4. The warning was widely broadcasted by TV, radio, mobile phones and loudspeakers. Unfortunately, the warning could not be transmitted before the arrival of strong tremors in areas that were close to the focus of the earthquake. However, in several cities outside those areas, the leading time between the warning and the arrival of strong tremors was around 10-15 seconds and residents could do some response to the warning. It was the first earthquake since October, 2007 that EEW could be successfully broadcasted before the arrival of strong tremors.

In Shonai Town, Yamagata Prefecture, EEW information was broadcasted at the 2008 Iwate-Miyagi Inland Earthquake by loudspeakers using J-Alert system that transmits information by satellite. In this research, a questionnaire survey was conducted to understand residents' response to the warning. 800 questionnaire sheets were distributed in the town and 591 answers were obtained. Just after hearing the warning, most of the respondents tried to get earthquake information by TV or radio. Very few residents tried to protect their bodies or protect their children and elder family members. The result of the survey revealed that residents'

understanding on proper response to EEW was insufficient and it is necessary to enhance residents' capacity to take proper action when they got the warning.

1. INTRODUCTION

Japan Meteorological Agency (JMA) started the service of earthquake early warning (EEW) to the public since October 1, 2007. This is a new system that quickly analyses seismic wave data observed by seismographs near the epicenter and provides prompt alerts before strong tremors (S-waves) arrive. It aims at mitigating earthquake-related damage by allowing countermeasures such as enabling people to quickly protect themselves in various environments such as houses, offices and factories. A warning is widely broadcasted by TV, radio, mobile phones and loudspeakers.

J-Alert is another warning system in Japan launched in February 2007. It is a satellite based system that allows authorities to quickly broadcast alerts to local media and to residents directly via system of loudspeakers. Figure 1 shows the process that EEW information is transmitted by J-Alert system. After the nearest seismometer observed P wave, the seismic wave data was analyzed and the focus, magnitude and intensities are estimated. After JMA announce EEW, the Fire and Disaster Management Agency (FDMA) sent EEW to local government by satellite. In the local governments, loudspeaker system automatically boots and starts to broadcast EEW to the residents. The FDMA operates J-Alert system for the purpose of protecting citizens. Alerts include not only natural disasters like tsunamis and earthquakes but also military threats such as missiles and terrorist attacks. According to the newsletter of the FDMA, 43 prefectures in total 47 prefectures and 150 local governments in total 1781 adopted J-Alert system as of January 9, 2009. These numbers will increase in the future as the FDMA is strongly promoting adoption of J-Alert system.

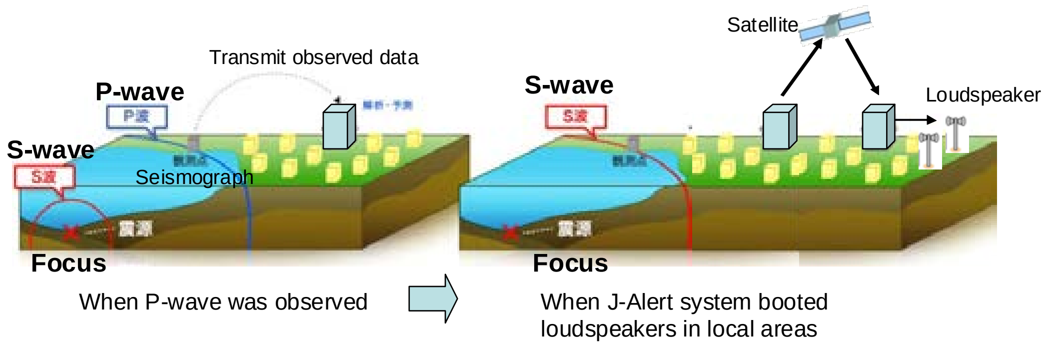

Figure 1: Process that EEW information is transmitted by J-Alert system

In Japan, the Iwate-Miyagi Inland Earthquake occurred in the south of the inland of Iwate Prefecture at 8:43 JST on Saturday morning, June 14, 2008. The JMA magnitude was estimated at Mj 7.2 and maximum JMA intensity was measured as "6 Lower" on the JMA intensity scale. According to the report by the FDMA, 17 people died, 426 people injured and 30 houses were totally damaged. Just after the earthquake, EEW was provided to the regions whose intensities of shaking were expected to be more than JMA 4. Figure 2 is a map published by the JMA showing the epicenter of the earthquake and the lead time before the arrival of strong tremors. Yellow parts in figure 2 show the areas that EEW is broadcasted. Unfortunately, the warning could not be provided before strong tremors in the areas that were close to the focus of the earthquake. However, in several cities outside those areas, the lead time between the warning and the arrival of strong tremors was around 10-25 seconds and residents could do some response to the warning. It was the first earthquake since October, 2007 that could be successfully broadcasted before the arrival of strong tremors. The warning was widely broadcasted by TV, radio, mobile phones. In addition, the warning was broadcasted to residents via loudspeakers using J-Alert system in the regions whose intensities were expected to be more than JMA 5 upper. This was the first broadcasting of EEW using J-Alert system although the regions were limited to be 2 cities and 1 town.

Shonai town, Yamagata prefecture was one of the regions where EEW was broadcasted by loudspeakers using J-Alert system. The location was illustrated in figure 2. In this research, a questionnaire survey was conducted in Shonai Town in order to understand residents' response to the warning. Authors think that residents' experience of receiving EEW by all the communication ways including loudspeakers by J-Alert system in Shonai town was very precious for discussing better use of EEW information.

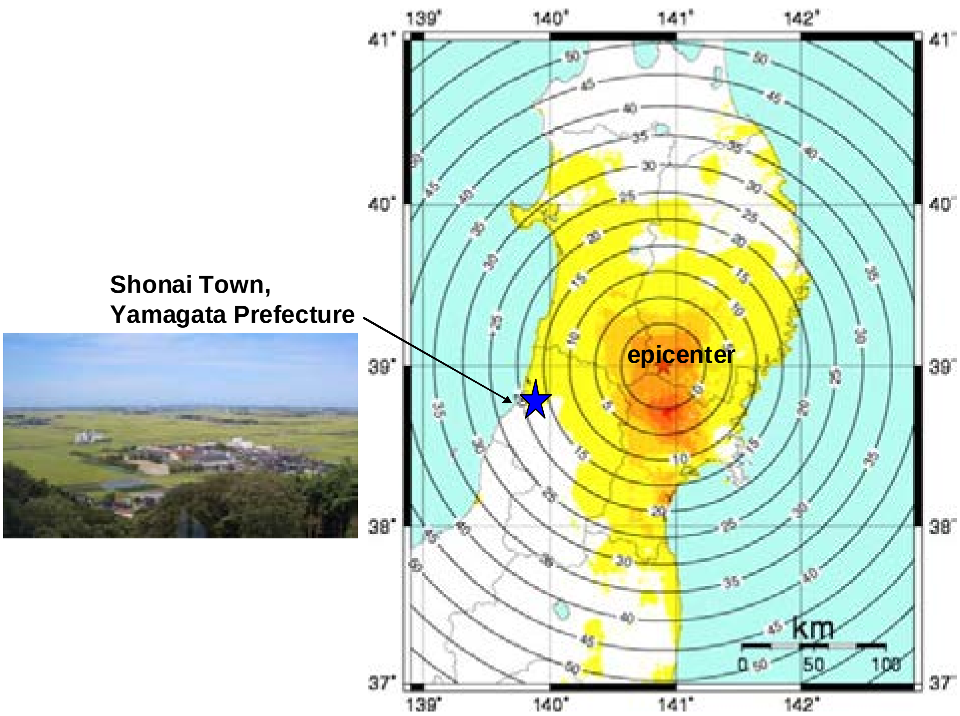

Figure 2: Epicenter and lead time between EEW and the arrival of strong tremors at the Iwate-Miyagi Inland Earthquake

2. PROCESS OF BROADCASTING OF EEW IN SHONAI TOWN

Shonai Town is a small town with 24,073 populations in 249.26 squire kilometers. Shonai Town adopted J-Alert system in April 2008. After 2 months, the Iwate-Miyagi Inland Earthquake occurred. Before April, the town office explained the start of J-Alert system to town leaders and announced it in the town news magazine in March.

Process of broadcasting of EEW using J-Alert system was shown in Table 1. The table includes the process after two earthquakes: the Iwate-Miyagi Inland Earthquake at 8:43 JST on June 14 and another earthquake offshore Iwate prefecture at 0:26 on July 24. At the Iwate-Miyagi Inland Earthquake, EEW was broadcasted to the public 10 seconds after the earthquake occurrence at the focus. After 1 seconds of this, J-Alert system in Shonai Town office received an alert of shaking with intensity 4 from the FDMA by satellite. However, J-Alert system didn't boot because the criterion of booting the system was set to be intensity 5 lower. At 28 seconds after the earthquake occurrence, expected intensity increased to intensity 5 lower and J-Alert booted. Finally, loudspeakers in Shonai Town started to announce EEW at 41 seconds after the earthquake occurrence, as preparation of broadcasting currently required 12 seconds.

Figure 2 shows the timing of broadcasting EEW at the Iwate-Miyagi Inland Earthquake. The periods of chime sound (8 seconds) and the warning saying "This is Big Earthquake, this is Big Earthquake" (6 seconds) were illustrated on the seismic waves recorded by the nearest seismograph of Kyoshin-Net (seismograph network by the National Research Institute for Earth Science and Disaster Prevension (NIED)). According to the Figure1, S- wave arrived at Shonai Town between the boot of J-Alert System and the start of EEW broadcasting by loudspeakers. Warning by J-Alert failed to broadcast before the arrival of S-wave although EEW was successfully broadcasted to the public on TV and Radios.

Based on the lessons from the Iwate-Miyagi Inland Earthquake in June, the criterion of booting J-Alert system was lowered to intensity 4 that is same as EEW broadcasting for the public. At the earthquake on July 24, J-Alert System in Shonai Town office received an alert from the FDMA by satellite 10 seconds after the earthquake occurrence at the focus. Loudspeakers in Shonai Town successfully started to announce EEW before the arrival of S-Wave at 23 seconds after the earthquake occurrence. This was the first broadcasting of EEW by J-Alert before strong tremor since J-Alert launched in Japan. In this case, the change of criterion for broadcasting to intensity 4 led to early information propagation. In order to increase possibility of successful warnings before strong tremors in the future, improvement of both EEW system and J-Alert system are necessary. Especially, cut down of the boot-time, increase of number of local governments that adopted J-Alert system are essential.

Table 1: Process of broadcasting of EEW at two earthquakes

	June 14			July 24		
	Time	Elapsed time(s)	Elapsed time(s) after P-wave in Shonai	Time	Elapsed time(s)	Elapsed time(s) after P-wave in Shonai
Earthquake occurrence at the focus	8:43:45			0:26:35		
EEW broadcasting to the puelic	8:43:55	10		0:26:56	21	5
Arrival of P wave at Shonai Town	8:44:04	19	0	0:26:51	16	0
Alert of intensity 4 from FDMA	8:43:56	11		0:26:45	10	
Alert of intensity 5 lower from FDMA	8:44:13	28	9			
Boot of J-Alert system	8:44:14	29	10	0:26:48	13	
Start of broadcasting EEW by loudspeakers	8:44:26	41	22	0:26:58	23	7

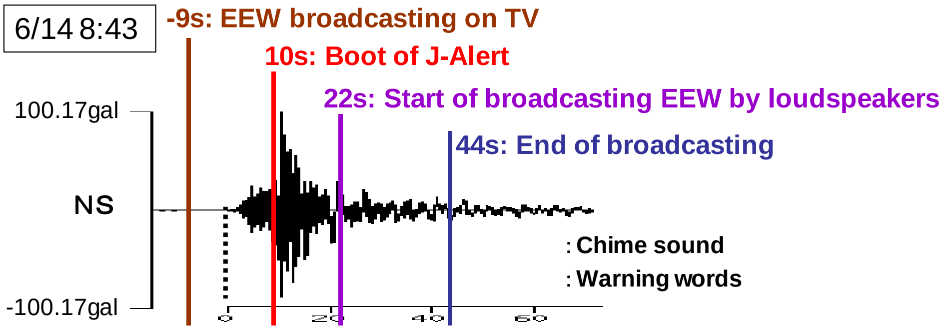

Figure 3: Timing of broadcasting EEW at the earthquake on June 14

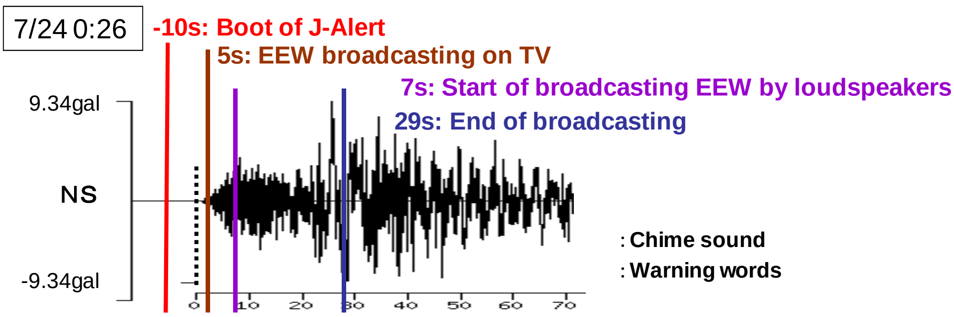

Figure 4: Timing of broadcasting EEW at the earthquake on July 24

3. OUTLINE OF QUESTIONNAIRE SURVEY

In order to understand residents' responses to the warning, a questionnaire survey for residents was conducted in Shonai Town thanks to the cooperation with Shonai Town office. 800 questionnaire sheets were distributed in the town and 591 answers were obtained in October 2008.

3.1 Characteristics of Respondents

Among 591 respondents, 57.2% of the respondents are male and 42.8% are female. Ratio of respondents' age is shown in figure 5. Half of the respondents are more than 60 years old. 79.9%, 16.3% and 1.8% of the respondents live in two-story single-family timber houses, one-story single-family timber houses and timber apartments. 13.7% of the respondents have elder family member who cannot walk by themselves. 7.8% of the respondents have infants and 23.6% have children kindergartens or elementary school.

Figure 6 shows the respondents who experienced past disasters such as the 1964 Niigata Earthquake, the 1983 Nihonkai-Chubu Earthquake. Regarding respondents' anxieties for disasters, anxiety for earthquakes is the highest among heavy rains, floods, landslides and strong winds. About 70% of the respondents have strong anxiety and 25% have little anxiety for earthquakes.

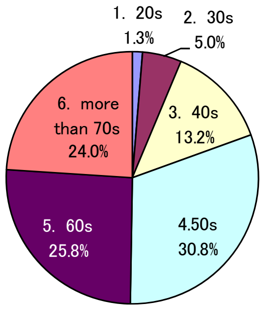

Figure 5: Ratio of respondents' age

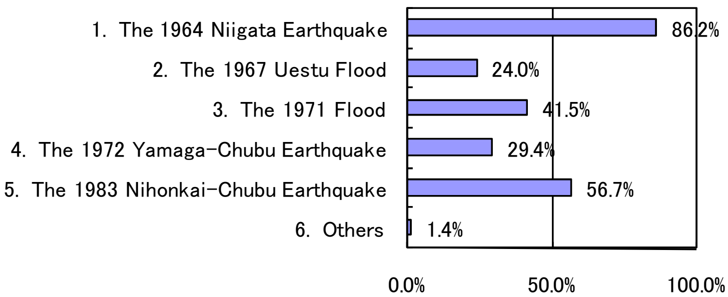

Figure 6: Ratio of respondents who experienced past disasters

3.2 Respondents' Knowledge on EEW

Next, respondents' knowledge on EEW and its broadcasting ways were asked. Figure 7 shows the ratio of their knowledge on EEW before both earthquakes. 48.7% knew both the name of EEW and the meaning that it forecast a strong tremor just before its arrival. However, 33.4% knew only the name of EEW and 17.9% knew neither its name nor its meaning. When the Iwate-Miyagi Inland Earthquake occurred in June 2008, almost 7 months had passed since its service for the public started. The low percentage of the respondents who fully understood the meaning of EEW before the earthquakes suggests the necessity for increasing peoples' knowledge on EEW.

Figure 8 shows the ratio of their knowledge on broadcasting ways of EEW before both earthquakes. 27.3% knew the broadcasting by both TV and loudspeakers. 43.1% knew the broadcasting only by TV, and 12.9%

knew only by loudspeakers. The ratio of the respondents who knew the broadcasting of EEW by loudspeakers was less than half. The reason for this might be J-Alert System was installed in Shonai Town just 2 months before the earthquake in June. The government of Shonai Town should pay continuous effort for raising residents' understanding of the broadcasting ways of EEW.

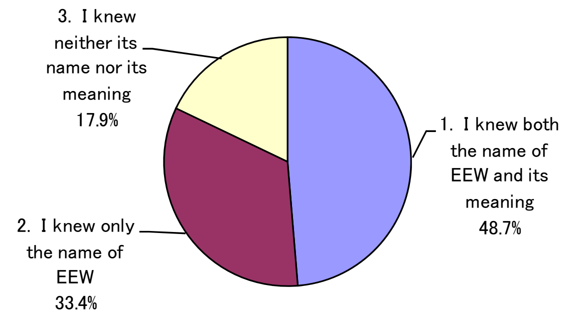

Figure 7: Respondents' knowledge on EEW before earthquakes

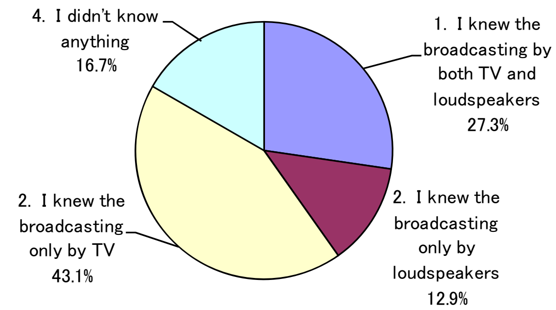

Figure 8: Respondents' knowledge on broadcasting ways of EEW before earthquakes

4. RESIDENTS' HEARING OF EARTHQUAKE EARLY WARNING

Here, residents' activities when the EEW was broadcasted were asked. Figure 9 shows where they were at two earthquakes. When the Iwate-Miyagi Inland Earthquake occurred in the Saturday morning, 65% of the respondents were at home. At that time, 30% of the respondents were watching TV and 40% were working at the office or at home. When another earthquake occurred in the midnight in July, 79% were staying at home and that was higher than in June. At that time, 63% of the respondents were sleeping and 16% were watching TV. Only 9% were working at the office or at home.

Table 2 and 3 show how residents heard EEW at the both earthquakes. At the earthquake in June, 63.9% heard EEW broadcasted by loudspeakers. Compared with the 31.2% who watched EEW on TV, the number of respondents who heard EEW by loudspeakers was larger. It suggests that loudspeakers can effectively convey EEW information to a lot of people although TV can alert only if its power is on. At the earthquake in

July, the percentage of the residents who heard by loudspeakers were larger as it was in the midnight. Figure 10 shows how clearly residents heard EEW at the both earthquakes. At the earthquake in June, 30% heard both chime sound and warning saying "Big Earthquake". 11% heard only warning saying "Big Earthquake". 22% could not catch the word although they heard some sound from loudspeakers. 23% didn't hear anything and 14% didn't remember. At the earthquake in July, the ratio of the residents who didn't remember was larger than in June as more people were sleeping in the midnight.

Figure 11 shows the relation between their hearing of EEW and their activities at the earthquake in June. Among the 164 respondents who heard both chime sound and the warning words, 86.6% heard them at home. On the other hand, among the 116 respondents who didn't hear anything, 39% were at home, 23% were in their office or school and 18% were driving a car or a motorbike. It shows that EEW is sometimes difficult to catch when people are in the middle of working inside the buildings or driving.

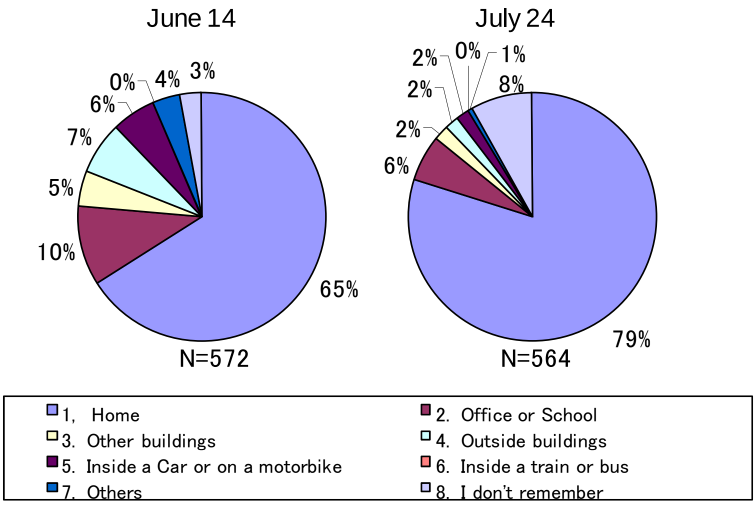

Figure 9: Ratio of where respondents were at two earthquakes

Table 2: Ratio of how residents heard EEW on June 14

		I watched on TV		
		Yes	No	Sum
I heard by loudspeakers	Yes	128	212	340
		24.1%	39.8%	63.9%
	No	38	154	192
		7.1%	28.9%	36.1%
	Sum	166	366	532
		31.2%	68.8%	100%

Table 3: Ratio of how residents heard EEW on July 24

		I watched on TV		
		Yes	No	Sum
I heard by loudspeakers	Yes	56	216	272
		10.5%	40.6%	51.1%
	No	33	229	262
		6.2%	43.0%	49.2%
	Sum	89	445	532
		16.7%	83.6%	100%

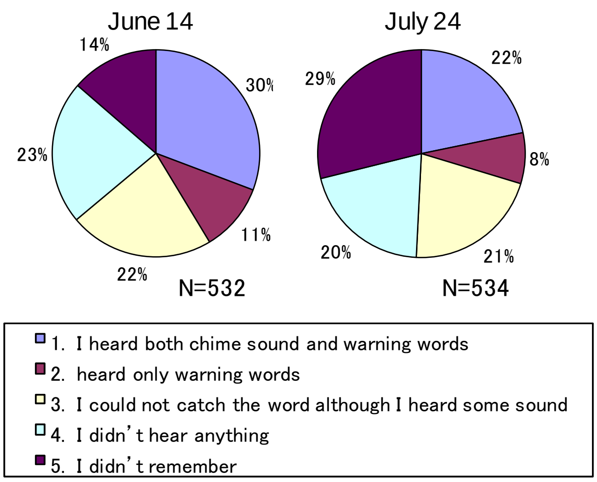

Figure 10: Ratio of how clearly residents heard EEW

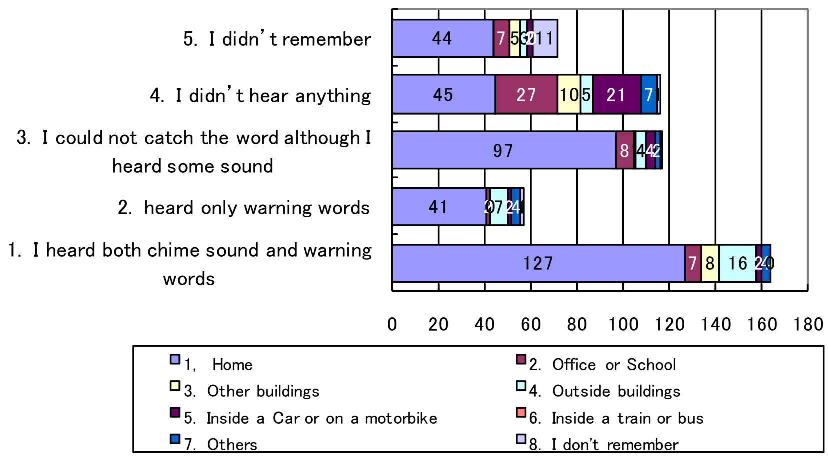

Figure 11: Relation between respondents' hearing of EEW and their activities at the earthquake in June

4. RESIDENTS' RESPONSE TO EARTHQUAKE EARLY WARNING

4.1 Response to Earthquake Early Warning at the earthquake in July

Then, residents' response to the EEW was asked. Here, we focused on the response to the EEW in July because the EEW in June failed in broadcasting before the arrival of strong tremors as shown in Figure 3.

Figure 12 shows what respondents did just after hearing EEW. Blue parts correspond to the 157 respondents who heard chime sound or the warning words. Red parts correspond to the 214 respondents who could not catch the words although they heard some sound from loudspeakers and who didn't hear anything. Most of the respondents tried to get earthquake information by TV or radio nevertheless they heard EEW or not. About 40% waited and about 25% informed their children or people near them of EEW. Aim of the EEW service is to enable people to quickly protect themselves before the arrival of strong tremors. However, very few residents tried to protect their bodies, protect their children and elder family members. It shows that their understanding of the meaning of EEW and their capacities to take appropriate response were insufficient.

Between two types of respondents, the difference of their respond was verified by the chi-square method. Asterisk marks * in the figure 12 shows that the responses were different with statistical significance as a result of chi-square test. In case that the respondents heard EEW, the percentages of the action such as “tried to get earthquake information by TV or radio”, “didn’t remember”, “opened the door or window.” and “went outside home or the building” increased compared with the case that the respondents didn’t heard EEW. It is thought that these responses were promoted by the hearing of EEW. However, the responses such as “opened the door or window.” and “went outside home or the building” sometimes cause the possibilities of secondary casualties. Instead of these responses, actions such as “protect their bodies” or “inform children or people near them of EEW” should be promoted by the hearing of EEW. From these results, it is said that education of public people on appropriate response to EEW is necessary.

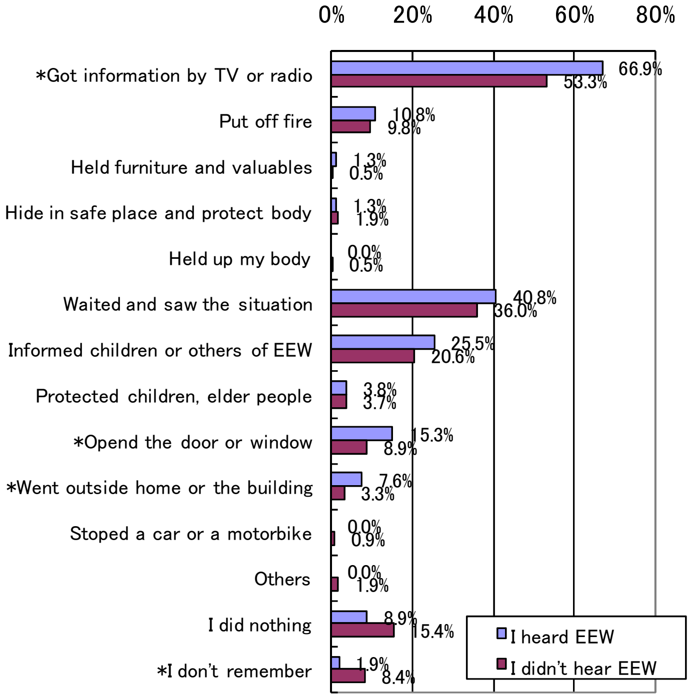

Figure 12: Ratio of responses after hearing EEW

4.2 Response to future Earthquake Early Warning

Finally, they were asked about what they would do if another earthquake same as the Iwate-Miyagi inland earthquake occur and they get EEW 10-20 seconds before the arrival of strong tremors. Figure 13 shows their answers. 79% of the respondents answered that they would put off fire. It was higher than that of the answer “I will get earthquake information by TV or radio”. It is understood that the response putting off fire was few as the earthquake in July occurred in the midnight. Now in Japan, gas system usually has automatic shut-down system in case of an earthquake. Considering the safety of people as the first priority, it is not necessary to put off fire just after an earthquake because these actions might cause secondary casualties. High percentage of putting off fire means people's misunderstandings of the current gas system. The percentage of the answer "I will hide in safe place and protect my body" was 47% and fourth largest. Compared with its low percentage in figure 12, it is said that people understood the necessity of protecting their bodies although they could not really respond as they thought.

In order to understand the difference of the answers by sex, ages, experience of past earthquakes, their anxiety for earthquakes and existence of their family members who need help in case of an earthquake, chi-square tests were carried out. Table 4 shows the p-value of chi-square test in each case. Pink, orange and yellow parts were verified to be statistically-significant with the probability of 5%, 1% and 0%, respectively. The Answer "I will put off fire" increased in case that they experienced past earthquakes. Their past earthquake experience might cause misunderstanding although recent gas system is not necessary to put off due to the automatic shut-down system. The answer "I will hide in the safe place and protect my body" increased as they were young. The Answer "I will inform children or people near me of earthquake occurrence" increased in case of female or respondents who have anxiety for earthquakes. It decreased in case of they were more than 70 years old. The Answer "I will protect children, elder and sick people" increased if they have infants, small children and elder family members who cannot walk by themselves. The answer "I will open a door or window" increased in case of female respondents. Any difference was observed for the answer "I will hold furniture or valuables in order to prevent falling down", "I will hold up my body by catching something", "I will stop a car or motorbike". It is said that potential trends of responding EEW are different according to their characteristics.

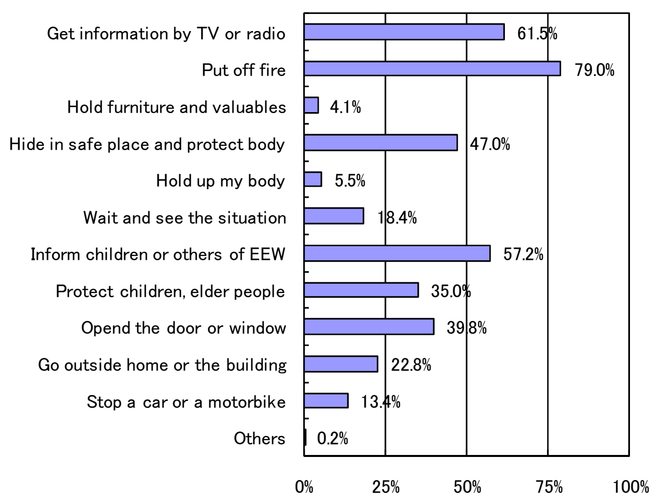

Figure 13: Response to future EEW

Table 3: Ratio of how residents heard EEW on July 24

Table 4: Ratio of how residents heard EEW on July 24

Resoinse to future EEW	Sex	Age	Experience of past disasters	Anxiety for earthquakes	Existence of their family members who need help
Get information by TV or radio	.933	.003		.378	.173
Put off fire	.418	.103	.000	.315	.023
Hold furniture and valuables	.220	.464	.846	.780	.813
Hide in safe place and protect body	.023	.000	.005	.006	.001
Hold up my body	.663	.063	.377	.223	.082
Wait and see the situation	.013	.440	.116	.410	.416
Inform children or others of EEW	.000	.000	.028	.001	.008
Protect children, elder people	.355	.002	.094	.281	.000
Opend the door or window	.000	.695	.021	.385	.050
Go outside home or the building	.112	.567	.534	.287	.433
Stop a car or a motorbike	.222	.178	.660	.620	.897

5. CONCLUSIONS

The 2008 Iwate-Miyagi Inland Earthquake was the first earthquake since October, 2007 that EEW could be broadcasted before the arrival of strong tremors. Shonai town, Yamagata prefecture was one of the regions where EEW was broadcasted by loudspeakers using J-Alert system. In this research, a questionnaire survey was conducted in Shonai Town in order to understand residents' response to the warning. 800 questionnaire sheets were distributed in the town and 591 answers were obtained in October 2008.

Regarding residents' knowledge on EEW, only 48.7% knew both the name of EEW and the meaning. The ratio of the respondents who knew the broadcasting of EEW by loudspeakers was less than half. These low percentages suggest the necessity of popularization of EEW knowledge among residents. At the earthquake in June, 63.9% heard EEW broadcasted by loudspeakers. Among the respondents who didn't hear anything, 39% were at home, 23% were in their office or school and 18% were driving a car or a motorbike. EEW is sometimes difficult to catch when people are in the middle of working inside the buildings or driving.

When we focus on the response to EEW in July, most of the respondents tried to get earthquake information by TV or radio. Very few residents tried to protect their bodies, protect their children and elder family members. It shows that their understanding of the meaning of EEW and their capacities to take appropriate response were insufficient. On the other hand, when the response to future EEW was asked, 79% of the respondents answered that they would put off fire. Its percentage increased in case that they experienced past earthquakes. High percentage of putting off fire means people's misunderstandings of the current gas system because it is not necessary to put off fire thanks to the automatic shut-down system.

From the chi-square tests on future response by respondents characteristics, several deference were statistically verified according to their sex, ages, experience of past earthquakes, their anxiety for earthquakes and existence of their family members who need help in case of an earthquake. In order to enable people to take proper actions to future EEW, education on what the proper actions are at various situations should be provided considering the potential trends of their responses observed in this survey.

In the future study, authors continue questionnaire survey for other EEW examples and accumulate the data regarding human behaviors to EEW. Based on these results, education material for increasing people's capacity to respond EEW will be developed in the future.

REFERENCES

The Fire and Disaster Management Agency, 2009.3. Newsletter of the Fire and Disaster Management, Japan.

The Fire and Disaster Management Agency, 2009.7. Report on the damage due to the 2008 Iwate-Miyagi Inland Earthquake, 78th edition, Japan.

The Japan Meteorological Agency: A list of Past Earthquake Early Warning, Website: http://www.seisvol.kishou.go.jp/eq/EEW/kaisetsu/joho/joho.html

Kyoshin-Net, the National Research Institute for Earth Science and Disaster Prevension(NIED), Website: http://www.k-net.bosai.go.jp/

SEISMIC MICROZONATION OF COX'S BAZAR MUNICIPAL AREA

A. B. AFIFA IMTIAZ[1] and MEHEDI AHMED ANSARY[2]
Dept. of Civil Engineering, BUET, Bangladesh
[1]afifaimt@gmail.com, [2]ansary@ce.buet.ac.bd

ABSTRACT

Cox's Bazar lies in the Southeastern part of Bangladesh, beside the Bay of Bengal. The area, having been a great tourist resort, has experienced a rapid urbanization in the last few decades including various establishments, construction of significant number of buildings and other structures in an unregulated manner and without seismic design considerations. Landslide and related casualties have also become very common in the hilly areas of the locality. In order to assess seismic vulnerability based on ground susceptibility and adopt mitigation strategies for urban areas, seismic microzonation is considered to be the first step. This study deals with the microzonation of the Cox's Bazar Municipal Area using geographic information system (GIS) where reflection of ground shaking and the site attributes of soil amplification, liquefaction and landslide are the salient features. The probable earthquake hazard and expected ground motion for this area were assessed using probabilistic approach. The liquefaction potential was estimated from Standard Penetration Test (SPT) following the methods suggested by Seed and Idriss combined with Japanese Code of Bridge Design. SHAKE analysis was performed for estimation of 1D site amplification. Slope stability analyses were performed for samples from the hilly regions of the area using the program XSTABL. The results obtained for site amplification, liquefaction and landslide potential were exported in GIS environment and presented as microzonation maps.

The findings of the study show that the rock level Peak Ground Acceleration (PGA) of the area is 0.18g for a 7.5 magnitude earthquake having a return period of 200 years. The surface PGA could be as high as 0.41g for an average 2.3 times amplification factor. Due to ground shaking amplified by 2, 2.5 and 3 times, respectively 47%, 42% and 11% of the municipal area can be affected. 87% of the study area is highly susceptible to liquefaction. Approximately 8% of the municipality consists of hilly region whose 97% is very unsafe regarding natural slope stability.

1. INTRODUCTION

Bangladesh, being located close to the boundary of two seismically active plates: the Indian plate in the West and the Eurasian plate in the East and North, is always under a potential threat of earthquake. In the seismic zoning map of Bangladesh, provided in BNBC (Bangladesh National Building Code, 1993), Cox's Bazar is shown under Zone II with design peak ground acceleration (PGA) value of 0.15g (Z=0.15). This level of acceleration may be considered as equivalent to a seismic intensity between VII and VIII. Historical information reveals that earthquakes of magnitude between 6 and 7 have occurred around the area in the past. The frequent earthquakes in and around the country, particularly Chittagong and Cox’s Bazar regions, also point toward the potential of such intensity earthquakes, even much higher and the consequences can be catastrophic to this area.

It is well known, and widely accepted amongst the earthquake engineering community, that the effects of surface geology on seismic motion exist and can be large. Nearly all recent destructive earthquakes have brought additional evidence of the dramatic importance of site effects. Accounting for such "site effects" in seismic regulations, land use planning or design of critical facilities thus has become one goal of earthquake hazard reduction programs. Local soil effects can amplify the ground motion and thus lead to intensity greater than the projected ones in certain areas causing more damage. Liquefaction phenomena can affect buildings, bridges, buried pipelines, lifelines and other constructed facilities in many different ways. Landslide has become very common in the hilly areas of Southeastern Bangladesh. Every year especially in the rainy season landslides take place in both natural and man-induced slopes. The loss of lives and properties due to landslide events in Cox’s Bazar is also very significant. Seismic hazard due to local site effects such as soil amplification, liquefaction, and landslide can be estimated by combining the available soil parameter data with the current hazard status of the region. Moreover, for accomplishing comprehensive regional hazard assessment, geographic information system (GIS) provides a perfect environment. Therefore this study deals with the microzonation of Cox’s Bazar Municipal Area using geographic information system based on ground shaking and the site attributes of soil amplification, liquefaction and landslide as the salient features.

2. COX’S BAZAR MUNICIPAL: THE STUDY AREA

2.1 Overview

Cox's Bazar is the only sea resort; a fishing port and a district headquarter of Bangladesh. It is known for its wide sandy beach which is claimed to be the world's longest natural sandy sea beach. It is located along the Bay of Bengal in Southeastern Bangladesh and 150 km South of Chittagong. Cox's Bazar municipality covers an area of 6.85 sq km with 27 mahallas and 9 wards and is bounded by Bakkhali River on the North and East, Bay of Bengal in the West, and Jhilwanja Union in the South. Population of the area is 51,918 (BBS, 2007). As one of the most beautiful and famous tourist spots of Bangladesh, the major source of economy of Cox's Bazar is tourism. Millions of foreigners and Bangladeshi natives visit this coastal town every year. Therefore, a number of hotel, guest house, and motel are built in this locality.

An important issue in developing a seismic microzonation map is the selection of an appropriate geographical reference, or geo-code, which will generally be driven by the availability of input data regarding soil conditions. Recently Cox's Bazar municipality has been expanded and the administrative map has not been finalized yet. For this study the proposed map as of January 2009, was collected from Municipal Office where total area is divided in to 9 wards. The map is shown in Figure 1. The existing municipal map was scanned and was converted into digital map.

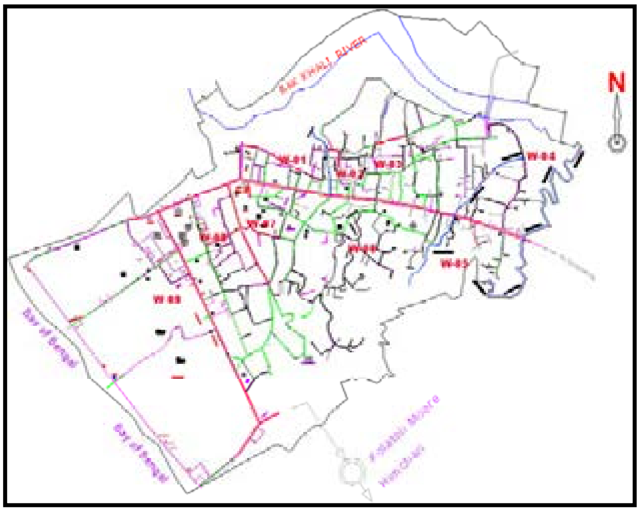

Figure 1: Boundary Map of Cox's Bazar Municipal area

2.2 Geology

The landmass of the district of Cox's Bazar includes two distinct geological settings namely Tertiary folded belt and coastal deposits. The tertiary folded belt extends North-South as part of the Indo-Burmese mobile belt, which is characterized by long narrow folds (Alam et al 1990). Cox's Bazar area lies within the Eastern flank of Inani Anticline, trending towards NNW-SSW, whose Western Flank is eroded. Figure 2 shows the Surface Geology of Cox's Bazar Municipal area after Alam et al (1990).

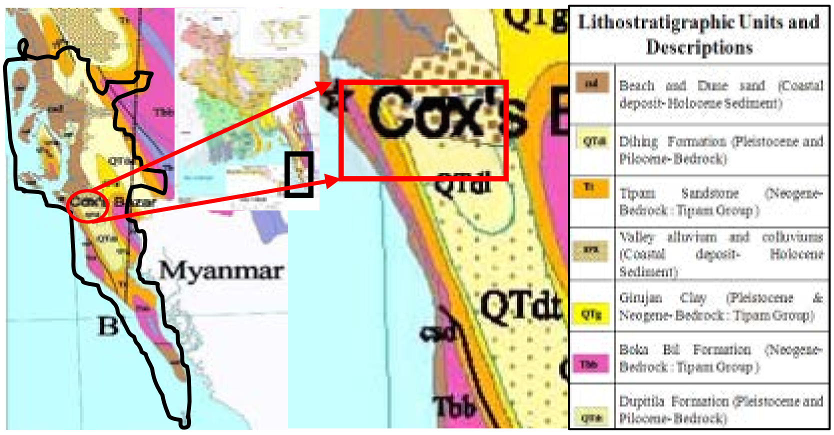

Figure 2: Location and Surface Geology of Cox's Bazar Municipal Area (after Alam et al, 1990)

Six Lithostratigraphic units were observed forming the surface geology of the area, from the Geological Map of Bangladesh. The Figure reveals that the area is predominantly composed of Valley Alluvium and Colluvium and Dihing Formation of Pliocene-Pleistocene age. Rocks of the Pliestocene, Pliocene and Neogene ages are also exposed in the area which is mostly composed of sandstone and claystone. To the West-most of the municipal boundary, the strand of Coastal Deposit, Beach and Dune Sand lies. This formation uncomfortably overlies Late Tertiary formations. To the East of Beach and Sandstone, there lie narrow zones of Boka Bil Formation and Tipam Sandstone of Neogene age. The South Eastern part of the town has basically Dihing Formation Bedrock. Dupi Tila Formation of Pleistocene and Pilocene age lies to the south of Dihing Formation which might have a slight influence in the surface geology of the area.

2.3 Seismicity

The seismic hazard is typically determined using a combination of seismological, morphological, geological and geotechnical investigations, combined with the history of earthquake in the region. Figure 3 shows the distribution of faults and lineaments capable of producing damaging earthquakes in and around Bangladesh. Here two major fault systems, Chittagong Fault system and Sitakunda Teknaf Fault system are observed to lie around the Cox's Bazar area.

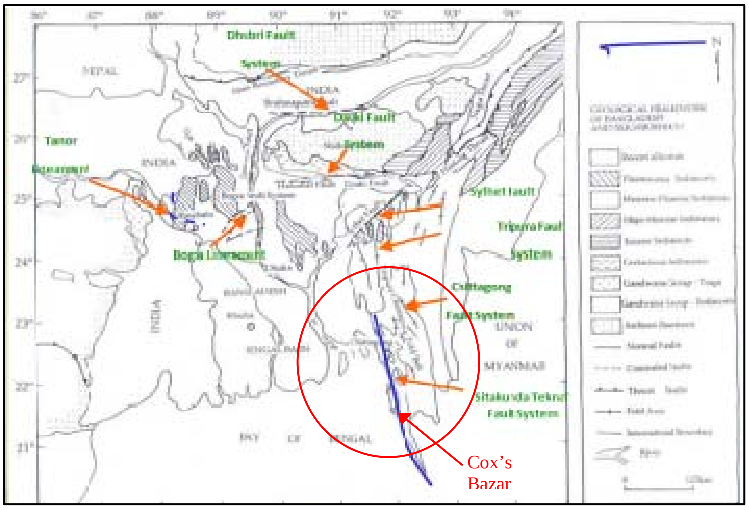

Figure 3: Seismo–tectonic lineaments and faults
(after Ali and Choudhury, 1992;Whitney, 2004, CDMP-UNDP, 2009)

Historical data for seismic activity affecting Cox's Bazar and surrounding area shows that the area has undergone frequently through earthquakes of magnitude ranging from 5 to 6 in Richter scale. Epicenters of these earthquakes with reference to the 250 km radius of the municipality area reveal that the earthquake with the highest magnitude (6.5 in Richter scale) occurred in this region in 1955. Again, considering 450 Km radius around the study area, it is observed that the highest magnitude earthquakes experienced occurred in 1664, 1858, 1912 with magnitudes 7.8, 7.66, 7.9 consecutively (after Ansary, 2009). Fig 4 shows that earthquakes having magnitude higher than 5, are recurring in almost every decade in this region.

Again the frequency of earthquakes with magnitude varied from 4 to 5 has increased markedly over the last four decades.

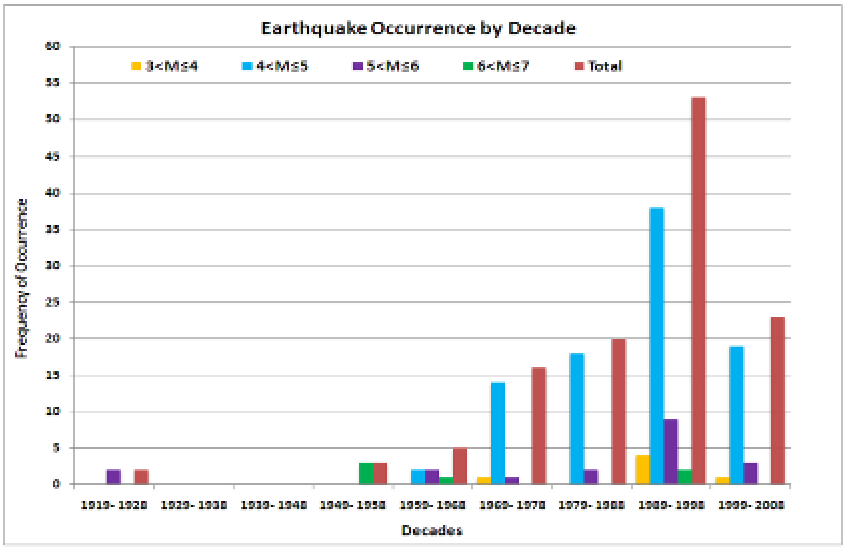

Figure 4: Earthquake Occurrences in and around Cox’s Bazar (1919-2008) (after Ansary, 2009)

3. SEISMIC MICROZONATION

Seismic microzonation can be defined as the subdivision of a region into zones that have relatively similar exposure to various earthquake related effects. It is the mapping of seismic hazard at local scales to incorporate the effects of local soil conditions. In general terms, it is the process for estimating the response of soil layers under earthquake excitations and thus the variation of earthquake characteristics on the ground surface. Seismic microzonation is the initial phase of earthquake risk mitigation and the final output contains recommendations suitable for application by local administrators, urban planners and engineers. A Seismic microzonation study consists of four stages: (1) estimation of the regional seismic hazard that is asessment of the expected input motion, (2) determination of the local geological and geotechnical site conditions (3) assessment of the probable ground response and ground motion parameters on the ground surface (4) finally, preparation of microzonation maps.

4. DATA COLLECTION

4.1 Geotechnical Data

A total of 26 borehole SPT data were used to study site amplification as well as soil liquefaction potential characteristics of municipality area. Among them, twelve subsoil investigations up to a depth of 15 metres were carried out under the current study. The borings were drilled vertically using the wash boring technique and equipment capable of pushing tube samplers by hydraulic pressure. SPT was carried out in each boring at nominal 1.5 m intervals and the N-values, i.e., number of blows count for each standard penetration was counted. The other fourteen boreholes’ SPT data up to a depth of 30 metres were collected from a research project on Cox's Bazar District, carried out under the Department of Civil Engineering, BUET in 2007-2008 (Dhar et. al., 2008). Figure 5 shows borehole locations of primary (current study) and secondary (previous study) source points of borehole SPT data. All the boring data include SPT N- values measured at 1.5 m interval. To obtain soil parameters such as grain size (soil type and D_{50}) grain size analyses of the SPT samples of different depth were performed in the laboratory.

4.2 Landslide Estimation Data

Hill ranges and hillock mainly appear to the Northern part of the Cox's Bazar municipal area. Baillarpara, Ghonarpara, Baiddorghona, Pahartali, Light House Para, Bus Terminal, Saikat Para, Kolatoli areas of the municipality are mainly consisted of these hillocks. These hills range from 15 meters to 40 meters in height. Hilly regions of this area were surveyed and location, height, slope and other relevant data were collected. The slopes of the hills range from 45 degree to almost 90 degrees. Most of the hill ranges contain some eroded slopes with almost vertical positioning. Dense population, houses and even multistoried buildings were observed on these eroded slopes and at their vicinity. Eleven disturbed samples from different locations of the area were collected for laboratory investigations including specific gravity test, grain size analysis, Atterberg's limits, standard compaction test and direct shear test. Figure 5 shows the locations of the sampling points from the hills.

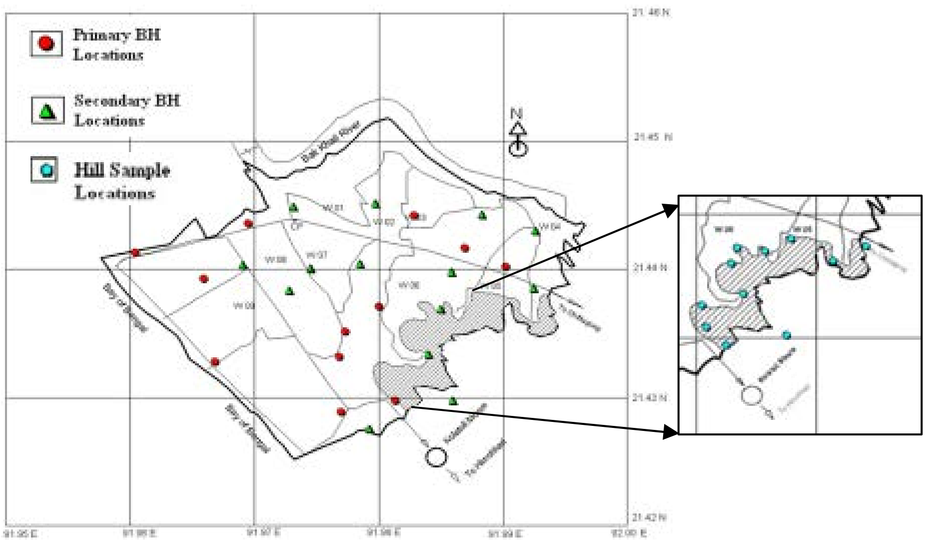

Figure 5: Cox's Bazar Municipal Map Showing Soil Sampling Locations

5. ASSESSMENT OF SEISMIC HAZARD

Seismic hazard analysis involves the quantitative estimation of ground shaking hazards at a particular area. A critical part of seismic hazard analysis is the determination of Peak Ground Acceleration (PGA) for an area/site. Numerous methods for earthquake hazard assessment in a given site are available today. In this study, point source is used as Earthquake Source Model. The seismicity of each of the modelled sources is first determined from past data available. The recurrence relationship relating the size of the past events in terms of Magnitude (M) and Peak Ground Acceleration (PGA) is derived. The seismicity model used in Molas and Yamazaki (1994) is usually taken as

$$\log(\nu) = a + b*M \tag{1}$$
$$\log(\nu) = a + b*\log(y) \tag{2}$$

where M is the earthquake magnitude, y is the peak ground acceleration, ν is occurrence rate per year and a and b are regression constants. T (=l/ν) is the return period in years.

Evaluation of seismic parameter was carried out using the seismic data over an area having a 250 km radius around Cox's Bazar Municipal (Figure 6). The historical earthquakes around the study area and their magnitude, epicentral distance, focal depth and intensity are considered to estimate PGA (%g).

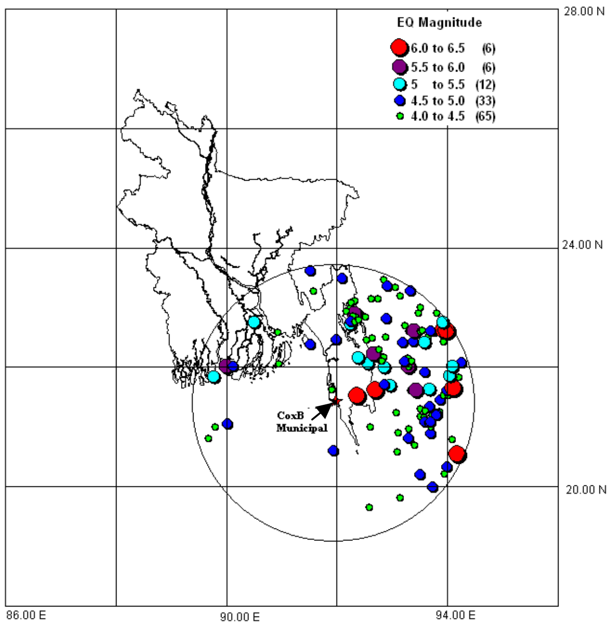

Figure 6: Historical Earthquakes around Cox's Bazar Municipal

Since no PGA based attenuation law was developed yet for Bangladesh, the methodology used in few previous studies (Sabri 2001, Sharfuddin 2001) was followed to select the most suitable attenuation law for predicting rock motions. McGuire (1978) equation for rock, which was observed to follow the PGA trend of most large earthquakes in and around Bangladesh, was thus selected for this study. The equation is:

$$PGA = 0.0306\, e^{0.89M}\ r^{-1.17} \tag{3}$$

Where, M is earthquake magnitude and r is hypocentral distance.

Seismic parameter b was evaluated from G-R relationship (Gutenberg and Richter, 1944), a method utilizing extreme, instrumented and complete catalogs. Figure 7 and 8 show the regression curves fitting for Cox's Bazar Municipal. The hazards in terms of the rock level PGA values and probable earthquake magnitude corresponding to return periods of 200 years are quantified from Equations (1) and (2) as, 0.18g and 8.26 consecutively. Since the largest Magnitude earthquake around the 350-450 km radius of the study area is 7.9 and around 250 km radius is 6.5, a cut-off Magnitude of 7.5 earthquake was considered as the expected one in 200 years.

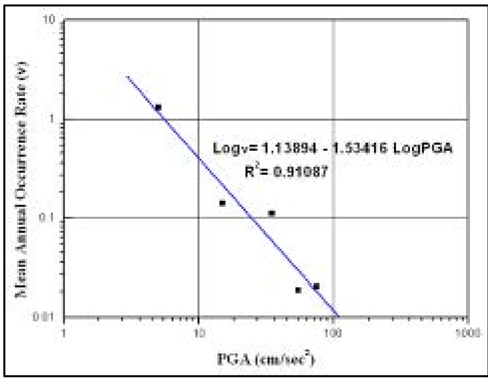

Figure 7: PGA versus Mean Occurrence Rate for the study area

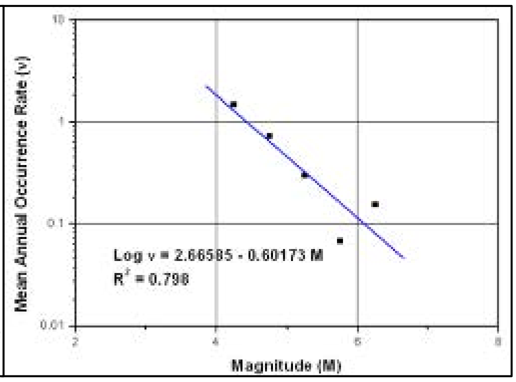

Figure 8: Magnitude versus Mean Occurrence Rate for the study area

6. ESTIMATION OF GROUND SUSCEPTIBILITY

6.1 Analysis of Site Amplification

It is well known that the surface ground motion of earthquakes is heavily influenced by the subsurface ground condition, especially in areas covered by thick sediments. Thus evaluation of the difference in subsurface amplification for each site is important to know the distribution of earthquake motion across the study area. For site amplification analysis, shear wave velocity for 26 borehole data up to a maximum depth of 30m were calculated by using equation of Tamura and Yamazaki (2002) presented in Equation (4). The engineering bedrock was assumed to be the layer at which the shear wave velocity (Vs) exceeds 400 m/s, which exist almost 30 m deep from the surface of the study area. The calculations show that the shear wave velocities at bedrock level vary from 400 m/s to 500 m/s.

$$Vs = 105\ N^{0.187}\ D^{0.179} \qquad (4)$$

Where Vs = Shear Wave Velocity (m/s); N = Corrected SPT blow count and D = Depth (m).

One dimensional wave propagation program SHAKE (Schanabel et. al., 1972) was employed to estimate the vibration characteristics at different points. An estimation of the fundamental frequency and the maximum value of the amplification were obtained at each site from plot of transfer functions. Typical graphical representation of frequency versus amplitude is shown in Figure 9.

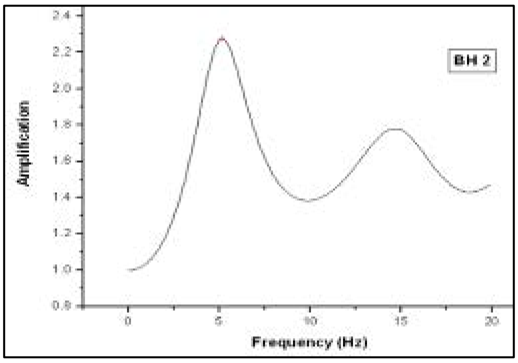

Figure 9: A sample plot of transfer function for the study area

6.2 Analysis of Liquefaction Potential

Evaluating the maximum amplification values for different locations, average amplification factor for the study area was estimated as 2.3. Thus the maximum ground surface acceleration was estimated as 0.41g by multiplying the PGA at bedrock level (0.18 g) with amplification factor. Particle diameter data for a particular depth of soil was obtained from grain size distribution curves. A simple method suggested by Seed and Idriss (1971) was used here to evaluate the Liquefaction Resistance Factor, F_L which can also be termed as Factor of Safety and defined as a ratio of Cyclic Resistance Ratio (CRR) to Cyclic Stress Ratio (CSR). Liquefaction is assumed to occur at that depth if F_L is less than 1.0. Here, CRR is the in-situ capacity of soil to resist liquefaction for earthquake of magnitude 7.5 and CSR is the earthquake load induced by a seismic motion. CRR is determined based on corrected SPT (Seed et al. 1983). The severity of foundation damage caused by soil liquefaction depends to a great extent on the severity of liquefaction, which cannot be evaluated solely by the F_L. In order to take care of this effect, the Japanese Bridge Code (Japanese Road Association, 1991) recommended a modification to the procedure suggested by Seed et. al., (1971). Following this procedure, the liquefaction resistance factor for the top 20m depth of soil, expressed as liquefaction potential index (I_L) (Iwasaki et al., 1982), for the 26 sites were calculated. The area was divided into different zones based on the range of the values I_L suggested by Iwasaki et. al., (1982). From the analysis no liquefaction potential index value was found in the range of 'moderate' zone. Therefore study area was characterized into three zones namely, high, low probability of liquefaction zones and non-liquified zones.

6.3 Analysis of Landslide Potential

XSTABL, a fully integrated slope stability analysis program was used for stability analysis in this study. XSTABL performs two dimensional limit equilibrium analysis to evaluate the Factor of Safety (FS) for a layered slope using the simplified Bishop Method. The strength parameters of the slope and foundation materials required for the analyses were obtained from consolidated undrained direct shear tests performed on soil samples. The minimum values of undrained cohesion (c_u) and undrained angle of internal friction (ϕ_u) were used in the slope stability analyses. The location of the water table in all the slope sections was assumed to be well below the toe of the slopes. The height of the slopes were considered as 30 m (100 ft) which was observed from field survey as the average height of the hills of Cox's Bazar. Generally the slopes were found to be 60° to 80°. Considering human activities and ongoing hill cutting activities the average slope of the hills were assumed to be 70° on an average. From the analyses it was observed that only single data contained the representative value of 'satisfactory' (FS=1.44) and the rest were 'unsafe' (FS<1). Thus the landslide potential was categorized as 'high' and 'low' for FS being greater than or equal to 1.2 and less than 1.2 consecutively. Figure 10 shows two hill locations studied for landslide potential.

(a) (b)

Figure 10: (a) Ghonerpara Hill, FS = 0.31; (b) Lighthouse Hill, FS= 0.69

7. GENERATION OF MICROZONATION MAPS

The computed results from the analyses were exported to a GIS environment and were plotted using spatial interpolation among the borehole locations and converting the vectorial point features into continuous raster map through grid generation. The developed microzonation maps are shown as Figure 11 to Figure 14.

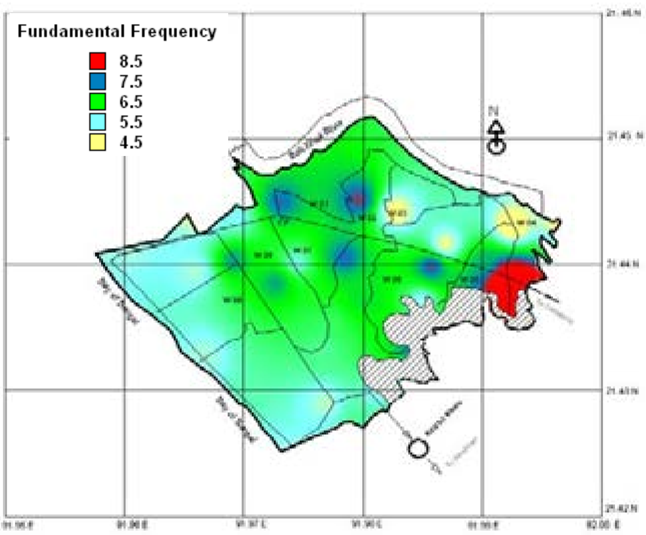

Figure 11: Microzonation map based on fundamental frequencies

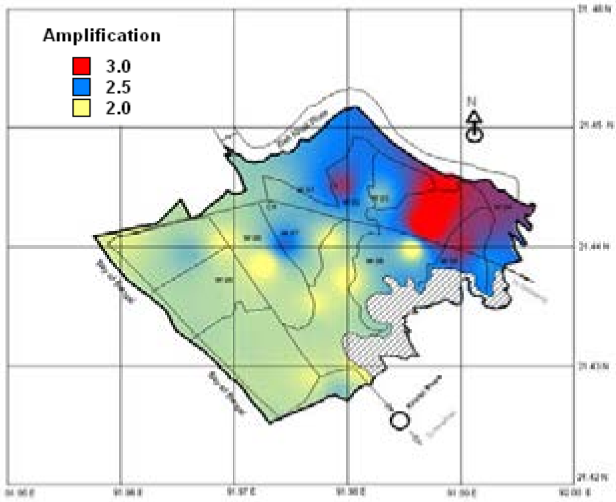

Figure 12: Microzonation map based on amplification

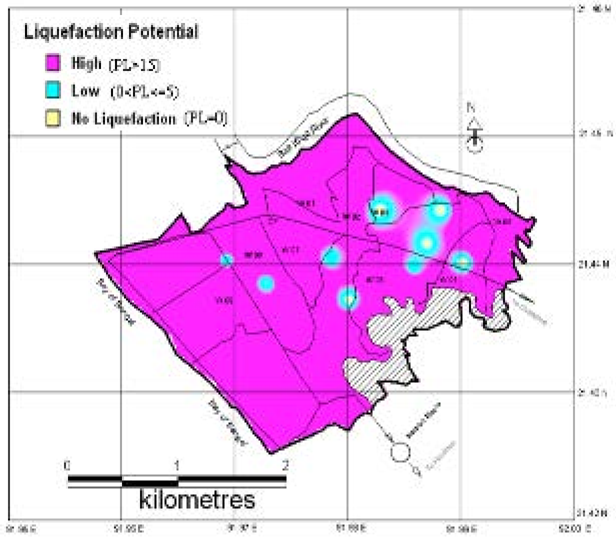

Figure 13: Microzonation map based on liquefaction potential

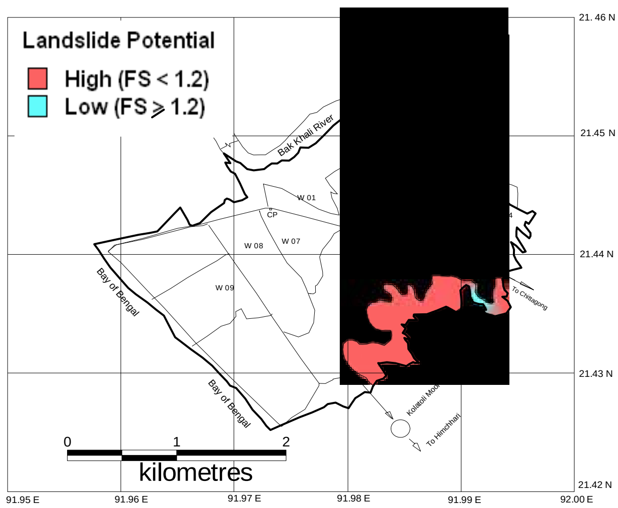

Figure 14: Microzonation map based on landslide potential

8. SEISMIC HAZARD INTEGRATION

The most important endeavor of this study is the estimation of seismic hazards linked with the local site attributes of soil amplification, liquefaction, and landslide and then integrating them in such a manner so that a reflection of probable actual disaster consequences can be represented. Since every analysis region is different; the quantification of the secondary site effects and the weighting scheme for combining the various seismic hazards is considered to be heuristic, based on judgment and expert opinion about the influence of local site conditions in the region and the accuracy of the available geologic and geotechnical information. The seismic intensity is basically a subjective one, based on the human sensations or damage during an earthquake. It is assumed that the final combined seismic hazard would be quantified in terms of Modified Mercalli Intensity (MMI).

First the regional distribution of ground shaking hazard (MMI_{GS}) considering 2.0, 2.5 and 3.0 times amplification of the surface PGA was calculated. The equation used here to convert PGA to intensity is developed by Trifunac and Brady (1975) and is given by equation (5). The MMI scale is subjective and assigned as integer values, therefore the MMI_{GS} values are rounded to the nearest 0.5.

$$\log PGA = 0.014+0.3 * I \tag{5}$$

where, I = Intensity of Earthquake

The heuristic rules were used to quantify the seismic hazards due to liquefaction and landslide. The rules for combining the various hazards were adopted based on expert opinion (after Stephanie and Kiremidjian, 1994). The final combined hazard (MMI_F) was computed as a weighted sum of the combination of various hazards. Figure 15 shows the regional distribution of combined hazards. Figure 16 shows the variation of Intensity (MMI_F) as a result of the combined effect of the hazards.

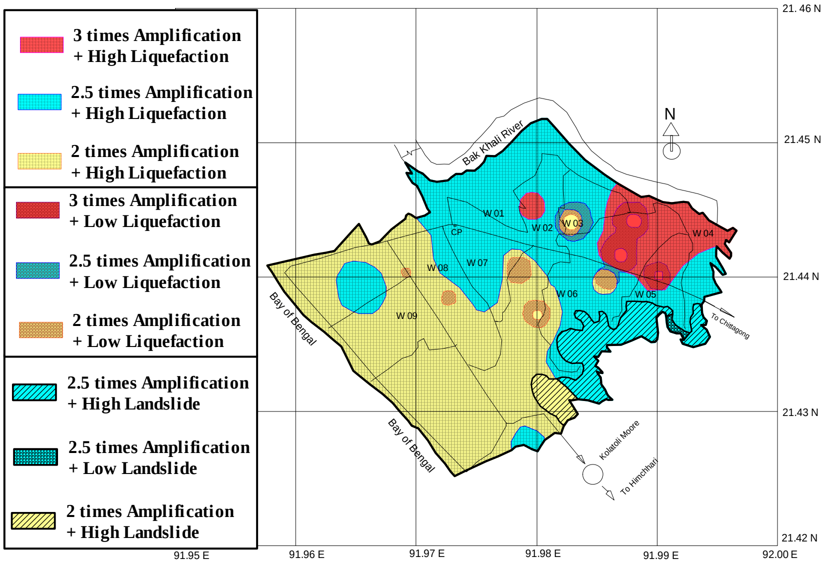

Figure 15: Map showing the zonation of the possible hazard combinations

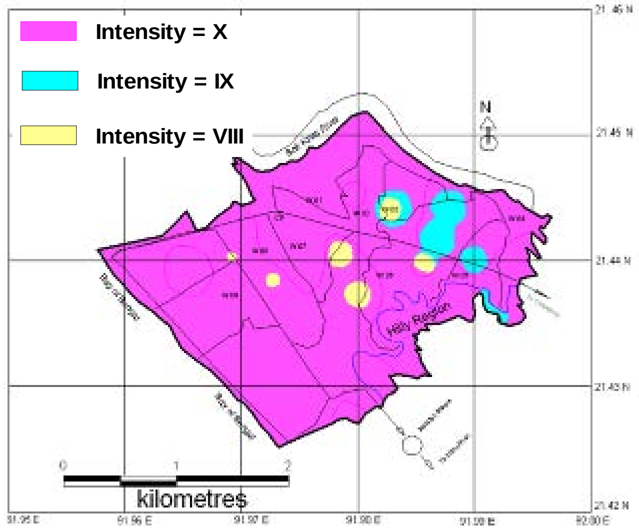

Figure 16: Map showing the regional distribution of combined seismic hazard (MMI_F)

9. CONCLUSIONS

From the developed microzonation maps, it can be observed that the Southeastern end of ward no. 5 will experience the highest frequencies. Ward no. 4 consisting of East Tekpara, Rumaliarchhara and Tarabaniachhara might be affected by 3 times site amplification. Liquefaction analysis for the study area reflects that it is susceptible to very high liquefaction potential. From the borehole investigations and grain size distributions, it was observed that the soil up to 20 meter depth is mostly sandy having D_{50} ranging from 0.12 mm to 0.22 mm. It was observed that the sandy silts with trace clay, layer of silt and sand, silty sand having greater particle diameters and low to medium SPT N-values showed higher liquefaction potentials. According to the study, the landslide potential of this area is very high. Approximately 8.13% area under the municipality is hilly. The hills located in Ghonerpara, Boiddorghona, Pahartoli and Boillarpara are found to be very unstable. The combined hazard analysis shows that if the area experiences both ground shaking and liquefaction during a scenario earthquake having a magnitude of 7.5, the area can be severely affected and the intensity due to the combined effect of the hazards can be as high as X in MMI scale. The town will be highly endangered (44% area is affected) if high liquefaction associates with amplification factor as low as 2 times. On the other hand if 2.5 to 3 times site amplification occurs, still there is a high risk (MMI = IX) even in case of low liquefaction occurrence. The hilly region is highly susceptible to slope instability, moreover, 77% of the hilly region is on the risk of experiencing very high intensity (MMI = X), if 2.5 times amplification of ground shaking occurs.

The developed maps can act as a guide for the authorities at the national and regional levels in land use management, revision and enforcement of appropriate building codes and formulation of plans for mitigating measures against earthquake risk affecting the region considered.

REFERENCES

Alam M.K., Hasan A.K.M. and Khan M.R., (1990). *Geological Map of Bangladesh*. *Geological Survey of Bangladesh, Govt. of the People's Republic of Bangladesh*

Ali, M.H. and J.R. Choudhury (1992). Tectonics and earthquake occurrence in Bangladesh. *36th Annual Convention of IEB,* Dhaka, January 1992.

Ansary, M.A. (2009). *Earthquake Database of Bangladesh.* Unpublished Report. Department of Civil Engineering, BUET, Dhaka, Bangladesh

BBS (2007). Census results by municipality. *Bangladesh Bureau of Statistics*. Available at www.bbs.gov.bd/dataindex/census/municip.pdf (accessed on 22.6.09)

BNBC (1993). Bangladesh National Building Code, *HBRI-BSTI.*

CDMP-UNDP (2009). Ongoing Research Work. *CDMP-UNDP Fault Map Delineation for Bangladesh, 2009.*

Dhar, A.S., Ansary, M.A., Imtiaz, A.B.A., and Saha, R., (2008). *Earthquake Vulnerability Assessment of Cox's Bazar District*. Report to United Nations Office for Project Services (UNOPS). Department of Civil Engineering, Bangladesh University of Engineering and Technology (BUET)

Gutenburg, B. and Richter, C. F. (1954). *Seismicity of the earth and associated phenomena.* 2nd Edition, Princeton, Princeton University press*.*

Japanese Road Association (1991). *Specifications for Highway Bridges*, Part V. Earthquake Resistant Design.

Iwasaki, T., Tokida, K., Tatsuoka, F. Watanabe, S., Yasuda, S. and Sato, H. (1982). Microzonation for soil liquefaction Potential using Simplified Methods. *3rd International Microzonation Conference, Proceedings, 1319-1329.*

McGuire, R. (1978). Seismic ground motion parameters relations. *Journal of Geotechnical Division, ASCE, Volume 104, pp.461 – 490.*

Molas, G. L. and F. Yamazaki (1994), Sesimic macrozonation of the Phillipines based on sesimic hazard analysis. *Journal of Structural Mechanics and Earthquake Engineering, JSCE, 489 (I-27), 59-69.*

Sabri, S. A., (2001). *Earthquake intensity-attenuation relationship for Bangladesh and its surrounding region.* M.Engg. Thesis, BUET, Dhaka,Bangladesh

Schnabel, P.B., J. Lysmer and H.B. Seed (1972). SHAKE: a computer program for earthquake response analysis of horizontally layered sites. *Report no. EERC 72-12.* Earthquake Engineering Research Center, Berkeley, California, 1972

Seed, H.B. and Idriss, I.M. (1971). Simplified Procedure for Evaluating Soil Liquefaction Potential. *Journal of the Soil Mechanics and Foundations Division, ASCE, 97(SM9), 1249-1273.*

Seed, H. B., I. M. Idriss and I. Arango (1983). Evaluation of liquefaction potential using field performance data. *Journal of Geotechnical Engineering, Volume 109, No. 3, pp. 458-482.*

Sharfuddin, M. (2001). *Earthquake Hazard Analysis for Bangladesh.* M.Sc. Engg. Thesis, Bangladesh University of Engineering and Technology (BUET), Dhaka.

Stephanie, A. K., and Kiremidjian, A. S. (1994). *Regional Seismic Hazard and Risk Analysis through Geographic Information System.*

Tamura, I. and F. Yamazaki (2002). Estimation of S-wave velocity based on geological survey data for K-NET and Yokohama seismometer network. *Journal of Structural Mechanics and Earthquake Engineering*, No. 696, Vol. I-58, 237-248 (in Japanese)

Trifunac, M. D. and A. G. Brady (1975). A study of the duration of strong earthquake ground motions. *Bulletin of Seismological Society of America, Volume 65, pp. b581-626.*

Whitney, J. (2004). *GSB-USGS Workshop, November 13-16, Dhaka.*

DEVELOPMENT OF WINDRISK®; A TOOL FOR REGIONAL WINDSTORM RISK ASSESSMENT

SUNGSU LEE[1], HEE-JUNG HAM[2], DONGHYUN LEE[3], YOUNGKYU LEE[3], JASUP KOO[3] and JINA JEONG[3]
[1]School of Civil Engg., Chungbuk National University, 410 Seongbong-ro, Cheongju Chungbuk 361-763, Korea
joshua@cbnu.ac.kr
[2]Division of Architecture, Kangwon National University, Chuncheon 442-749, Kanwon-do, Korea
heejham@kangwon.ac.kr
[3]Cubersolution co. ltd., Cheongju, Korea
{dhlee,yglee,koojs613,koojs613}@cuber.co.kr

ABSTRACT

This paper presents the development of a computational tool for regional windstorm risk assessment, WindRisk®. Three representative components form the tool, which are wind hazard, fragility and exposure. The wind hazards are specified by three types; the long-term, the typhoon and the user-defined winds. The long-term wind hazards corresponding to 30, 50, 100, and 200 year return periods are developed by extreme value analysis and typhoon simulations over all Korean regions. The typhoon winds are simulated by the empirical wind field model with data of the central pressures, the expecting track, and the radii of maximum winds. The WindRisk® also reflects the effects of surface roughness surroundings using the land cover map and topographic effects using the digital elevation model (DEM). Fragility curves to wind-vulnerable properties such as panel building structures, greenhouses and sheds are also incorporated into the program. The WindRisk® is applicable to the planning of budget to annual damage recovery cost and to estimate the damage by typhoons.

1. INTRODUCTION

With continuing development and construction of industrial facilities, loss and damage are widely spread and increasing due to natural disasters. For instance, more than 10 billion USD are lost in two events during typhoon RUSA (2002) and MAEMI (2003) in Korea [1]. Typhoons cause social losses such as casualties and victims as well as economic losses. The loss is further expanded when the national efforts and the humane commitment in recovery. Various efforts have been carried out to mitigate the damages and the loss, among which is to assess and estimate the probable loss in prior to the events of natural disasters. This paper describes one of the efforts, in which a computational tool, WindRisk® has been developed to assess damages and losses due to windstorms.

2. GENERAL PROCEDURE OF DEVELOPMENT

Three representative components form the tool, which are wind hazard, fragility and exposure. Figure 1 depicts the general procedure in WindRisk®.

The tool, first assess the wind hazard in the region of interest, which estimates the probable wind speed. Once the extreme or the probable wind speed is determined, the regional risk can be assessed using database for the exposures and corresponding vulnerability.

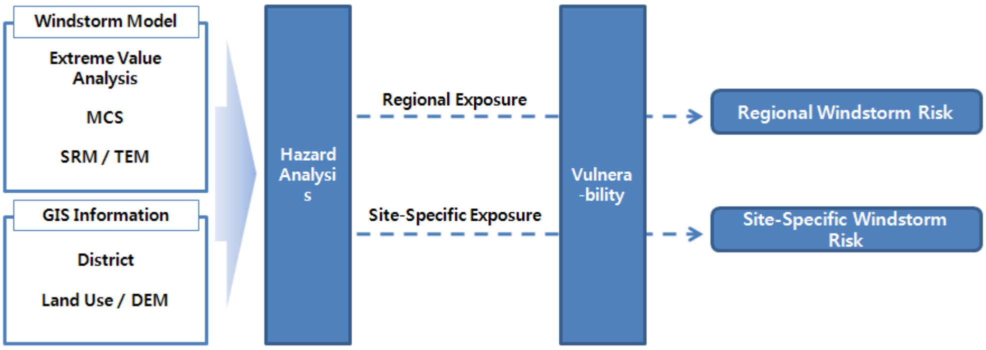

Figure 1: General Procedure in WindRisk

3. WIND HAZARD ANALYSIS

The wind hazards are specified by three types; the long-term, the typhoon and the user-defined winds. The long-term wind hazards corresponding to 30, 50, 100, and 200 year return periods are developed by extreme value analysis and typhoon simulations over all Korean regions. The typhoon winds are simulated by the empirical wind field model with data of the central pressures, the expecting track, and the radii of maximum winds . The wind field model is based on the study of Batts et al (1980) and the corrections made by Lee et al [3,4], which determine the maximum gradient wind, while the wind speed near the ground is estimated using the model developed by NOAA [5]. Figure 2 shows the simulated wind speed over Korean peninsula during typhoon MAEMI (2003).

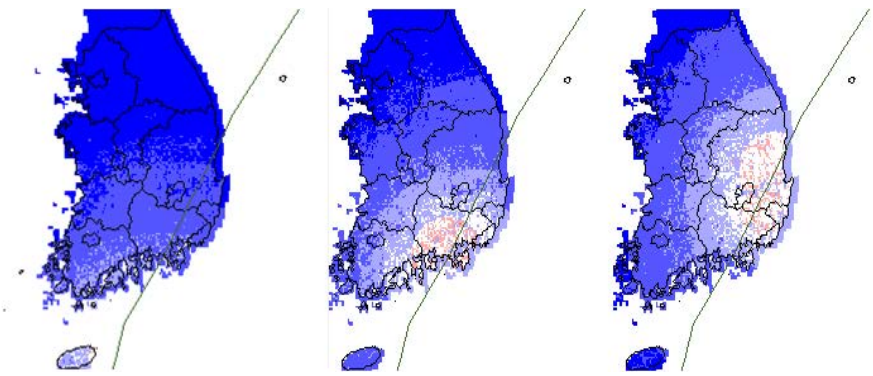

Figure 2: Simulated Wind Speed during Typhoon MAEMI (2003)

3.1 Surface Roughness and Topography

Even if the extreme wind speed over the region of interest is estimated, it considers only meteorological parameters not the local factors affecting the wind speed near ground. The essential factors profiling the wind near the ground are surface roughness and topography. Since wind, in general, slows down in the region of rough surface such as forest and urban area, GIS information of land use is utilized to account for the effects of surface roughness on the wind speed. In this paper, SRM (Surface Roughness Model) is developed based on the studies of Bietry et al (1978) and Buchene-Marullaz (1976). Upwind region is defined as the region up to 1000m in the direction of wind-coming according to KBC (2005) and AS/NZS (2005).

Another important aspect of wind speed near ground is that the wind tends to speed up when it approaches the crest of ridges or mountains due to the mass conservation in fluid dynamics. In this paper, TEM (Topographical Effects Model) is developed based on KBC (2005) and uses DEM (Digital Elevation Model).

Figure 3 illustrates SRM and TEM over Korean peninsula assuming that the wind blows from north.

3.2 Regional Wind Hazard

With GIS information of land use and DEM, the extreme wind speed can be converted into the local wind near the ground, which represents for the local wind hazard. In the program, WindRisk®, GIS engine is incorporated into the analysis to allow for convenient analysis. Figure 4 depicts the example of the wind hazard analysis in a small region.

4. EXPOSURES AND VULNERABILITY

Next steps to assess the windstorm risk are to gather information of exposures, i.e., inventory of assets in probable danger and to determine the vulnerability of the assets to the hazard using fragility curves. The exposures can be categorized into regional data or site-specific data, both of which can be handled using GIS. Fragility curves to wind-vulnerable properties such as panel building structures, greenhouses and sheds are also incorporated into the program. WindRisk® utilizes the results of Lee et al (2007, 2009) to determine the failure probability in strong wind. Figure 5 exemplifies a fragility curve corresponding to a greenhouse in strong wind.

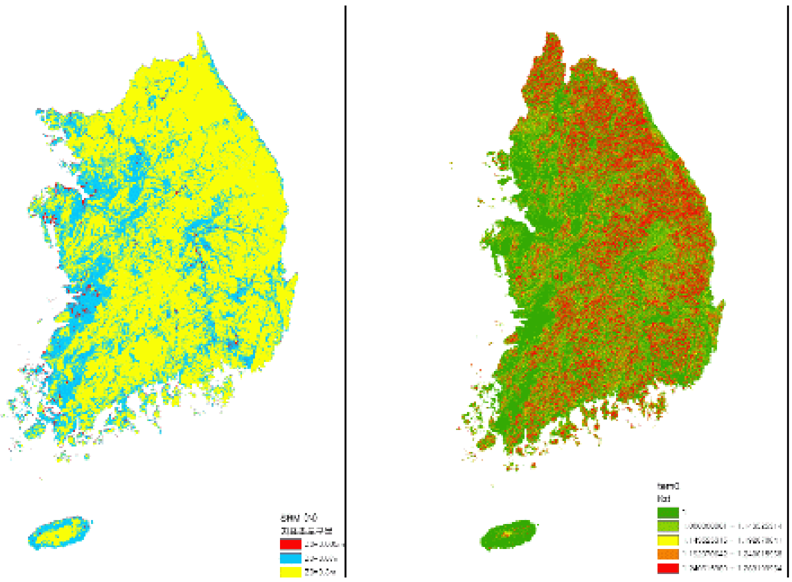

Figure 3: SRM (left) and TEM (right) in North Wind

Figure 4: GIS based Regional Wind Hazard Analysis

5. ASSESSMENT OF WINDSTROM RISK

In the developed tool, all the information is processed through GIS engine with analysis module. Since the risk is defined as the probability of failure of regional assets or a site-specific asset, combination of wind hazard and vulnerability applied to the assets of interest yields the amount or the probability of loss.

Figure 6 shows an example of windstorm risk map for a type of greenhouse which is known to its vulnerability to wind.

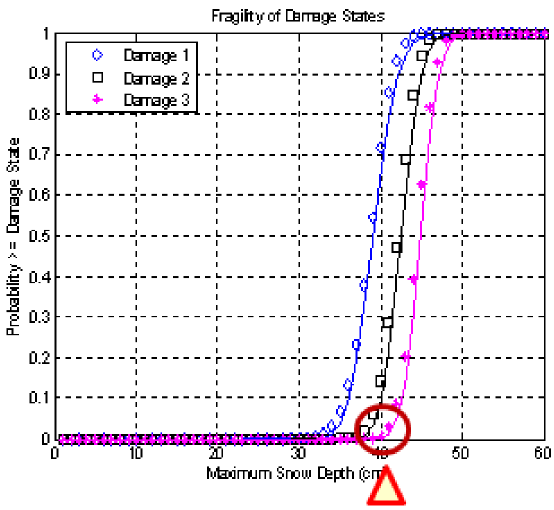

Figure 5: Fragility Curve of Greenhouse in Strong Wind

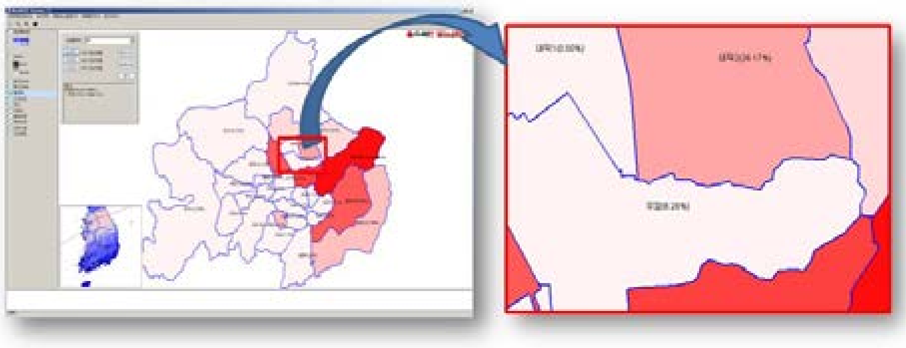

Figure 6: Failure Probability of a Greenhouse in Windstorm

6. CONCLUDING REMARKS

This paper presents development of a GIS-based computational tool to assess the regional windstorm risk. Using meteorological data and simulation method, the extreme wind speed over a region of interest is estimated as the hazard which is applied to the exposures of assets. Using structural vulnerability, the results are the probability of failure which corresponds to the windstorm risk. . The WindRisk® is applicable to the planning of budget to annual damage recovery cost and to estimate the damage by typhoons.

REFERENCES

[1] NEMA, Annual Reports for Disasters in Korea, 1991-2007.
[2] Batts, M.E., M.R. Cordes, C.R. Russell, J.R. Shaver, and E. Simiu, 1980, Hurricane Windspeeds in The United States, *National Bureau of Standards Report Number BSS-124*, U.S. Dept. of Commerce, Washington, DC.

[3] YK Lee, S Lee and HS Kim, 2007, Expectation of Extreme Wind Speed due to Typhoo, Proc. of WEIK, pp. 20 ~ 26.
[3] YK Lee, S Lee and CW Park, 2007, Analysis on Radii of Maximum Sustained Winds of Typhoons around Korean Peninsula, J. WEIK, Vol.11, No.2, pp. 203 ~ 210.
[4] NOAA, 1972, Revised Standard Project Hurricane Criteria for the Atlantic and Gulf Coasts of the United States, *Memorandum HUR7-120*, U.S. Dept. of Commerce.
[5] J Bietry, C Sacre and E Simiu, 1978, Mean Wind Profiles and Changes of Terrain Roughness, *J. Struct. Div.*, ASCE, 104, 1585-1593.
[6] P Duchene-Marullaz, 1976, Full-Scale Measurements of Atmospheric Turbulence in a Suburban Area, *Proceedings of the Fourth International Conference on Wind Effects on Buildings and Other Structures*, London, Cambridge Univ. Press. Cambridge, pp. 23-31.
[7] Architectural Institute of Korea, "Korean Building Code", 2005.
[8] J Holmes and A King, 2005, A Guide to AS/NZS 1170.2:2002, Wind Action, Warren Publishing
[9] S Lee et al, 2007, Development of Windstorm Vulnerability Functions of Industrial Buildings, NIDP.
[10] S Lee et al, 2010, Development of Risk Assessment Technique for Strong Wind and Heavy Snowfall, NEMA.

Development of an Intelligent Smoke Control Procedure using HVAC Operation and Door Control Strategy in a Building Fire

CHU YANYAN, ZHANG HUI
Center of Public safety Research, Tsinghua University, Beijing, China
chuyan@mail.tsinghua.edu.cn

ABSTRACT

In a high-rise building fire, sprinkler is the first defense and smoke exhausted system is the major equipment to control and reduce smoke. Traditional smoke control procedure does not utilize the HVAC system and door control strategy. A modified smoke control procedure is proposed in this paper using several closed systems to integrate door controllers, HVAC controllers and smoke exhaust fan controllers based on real-time sensor readings and video on occupants' location and fire propagation. The new procedure is capable of slowing down the smoke propagation and provides favor conditions for occupants' evacuation. In this paper, a zone model is used to study the smoke propagation under different modified control procedures. Simulation results show that door controllers and HVAC controllers can be utilized to manage the smoke movement and increase the safety of occupants.

1. INTRODUCTION

In a building fire, smoke is often the leading cause of fatalities. Smoke can travel a long distance from the fire room. In traditional smoke control procedure, ventilation vents are usually closed to prevent fresh air from entering fire room and sprinklers and smoke exhaust fan are usually turned on. It is an open system that sprinklers, ventilation vents, smoke fan and other controllers could be operated in accordance with a predetermined program. Much research has been performed focusing on how to control smoke propagation in a building fire using different equipments and facilities. Ventilation and extraction system drive the longitudinal motion of the fire-induced smoke and to extract it efficiently in zones near the fire source. Air curtain could be utilized for confinement of fire-induced smoke transportation along channels. Fire simulation results on the underground shopping mall show that the location of mechanical exhaust vents and mechanical exhaust rate can significantly impact the smoke extraction. Smoke control strategy with feedback utilizing all kinds of controllers may prevent smoke propagation more effectively.

Since the evacuation of occupants is extremely difficult, it is important to utilize all means to slow down the smoke propagation and supply fresh air to the place with occupants. Based on real-time occupants' information and other sensor readings such as temperature and smoke concentration, a modified smoke control procedure is developed to assist evacuation and to improve building safety performance limit. The new procedure utilizes door controller, ventilation vents, smoke exhaust fans and sprinklers according to sensor readings. The system can adjust control precepts, which can delay smoke propagation, save time and improve air quality for occupants' evacuation from the fire building. A zone model is used to study the smoke propagation with modified smoke control procedure. Simulation results are performed to study the smoke height, carbon monoxide concentration and carbon dioxide concentration at the fire room and corridors. Results show the effectiveness of the modified smoke control procedure for smoke propagation.

2. DEVELOPMENT OF CONTROL STRATEGY

2.1 Problem Setup

Air flow in the building can be moved by various equipments such as air condition units, VAV box, smoke exhaust fan, etc. In traditional smoke control procedure, fresh air valves in the fire floor are usually closed to prevent fresh air from entering fire room and air valves in fire neighbor floor are opened to supply air and assist evacuation. Back air valves in three floors are closed to prevent smoke propagation through pipes. Once a fire is detected in building, equipments in the fire floor, fire neighbor floors and refuge areas are switched to the fire mode. This strategy makes no effort on controlling smoke movement except for using smoke exhaust system, which in many times is insufficient to pump the smoke out the building in a high-rise building fire. Also no occupant information is utilized. In the modern building, videos are widely used for security purpose. With video and other sensors, occupants' location can be in-situ monitored during fire. It is therefore reasonable to direct the smoke into the empty rooms when smoke exhaust system is insufficient. Together with door control and HVAC operations, air environment of occupants may be improved so that safety of occupants may be improved.

A numerical model is developed in this paper to study the feasibility of utilizing modified smoke control procedure to enhance the safety performance limit of the building. A typical high-rise building floor consists of an office zone and a core. Elevators, equipment rooms and evacuation staircase lie in the core. The office zone is usually divided into several rooms by the walls based on tenements requirement. Every office zone has at least an exit to corridor. A typical layout is shown in Fig. 1. Building area of the fire zone is set to be 2700 m^2. Area of the office zone is about 2000 m^2 and area of the central core is 700 m^2. Building height of the fire zone is about 4 m and clear height is 2.7 m. Locations of the doors are also presented in Fig. 1. Smoke extraction vents and VAV ventilators of HVAC lie in office zone homogeneously. A fire is set at the right top room. We will study the effect of modified control system on the smoke propagation and discuss the control strategy.

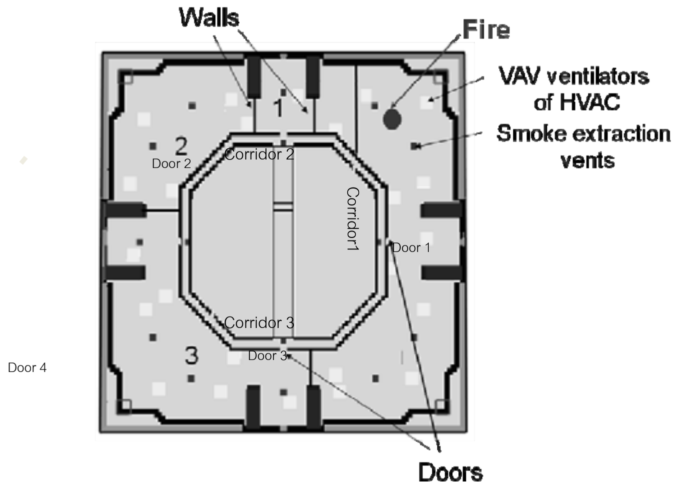

Fig. 1 Schematic of Fire Scenario used in the Simulation

2.2 Mathematics Model

In the zone model finite space is usually separated into two control volumes or zones. It is assumed that all relative parameters of each control volume/zone are consistent. Mass exchange between each interval is mainly caused by smoke plume and flesh air. Radiation loss is also included in energy besides the energy transmission by mass exchange. Differential equations for conservation of mass equations and persistence of energy equations are solved. Equations of the zone model are shown as follows:

$$\frac{dm_u}{dt} = \sum_i \dot{m}_{\mathrm{i,u}} \tag{3}$$

$$\frac{dm_{\mathrm{l}}}{dt} = \sum_i \dot{m}_{\mathrm{i,l}} \tag{4}$$

$$\frac{d}{dt}(c_{\mathrm{p}}\dot{m}_u T_u) = V_{\mathrm{u}}\frac{dp_{\mathrm{u}}}{dt} + c_{\mathrm{p}} w_{\mathrm{e}} B\rho T_{\mathrm{u}} - \dot{Q}_{\mathrm{u}} \tag{5}$$

$$\frac{d}{dt}(c_{\mathrm{p}}\dot{m}_{\mathrm{l}} T_{\mathrm{l}}) = V_{\mathrm{l}}\frac{dp_{\mathrm{l}}}{dt} + c_{\mathrm{p}} w_{\mathrm{e}} B\rho T_{\mathrm{l}} - \dot{Q}_{\mathrm{l}} \tag{6}$$

$$P = R\rho_{\mathrm{i}} T_{\mathrm{i}} \tag{7}$$

$$V = V_{\mathrm{l}} + V_{\mathrm{u}} \tag{8}$$

where subscripts ‘u’ and ‘l’ represent up and down volumes/zones, respectively; V is dimension of the control volume; unknown variables include m_u 、 m_l 、 V_u 、 V_l 、 T_u 、 T_l 、 p_u 、 p_l and $m_u = Z_u A\rho_u$, $m_l = Z_l A\rho_l$, $V_u = Z_u A$, $V_l = Z_l A$; H is height of finite space $H = Z_l + Z_u$.

3. DESIGN OF FIRE SCENARIOS

3.1 Development of Modified Smoke Control Procedure

The modified smoke control procedure is shown in Fig.2. The key issue here is that the occupants' location should be able to detect in real time by sensors such as video, RFID, wireless systems. Door controllers can operate the doors such as closing the doors of the fire room after everyone in the room has been evaluated. In this way, smoke can be contained in the fire room and its propagation can be slowed down. We need to check the fire room conditions continuously and we may open the doors of the fire room to release heat so that the flashover conditions in the fire room can be built up. It means that human intervention to the control system is needed. The HVAC controllers can supply fresh air to assist evacuation and can be turned off if there is no person in the area. The saved power can be redirected to the needed place. Smoke exhaust fan controllers could also be controlled to maximize the capability of smoke exhaust in the needed areas. The modified smoke control procedure can adjust control strategies of doors, smoke exhaust and HVAC based on real-time information of sensors and videos. In this paper, we will discuss the benefit obtained from such control procedure.

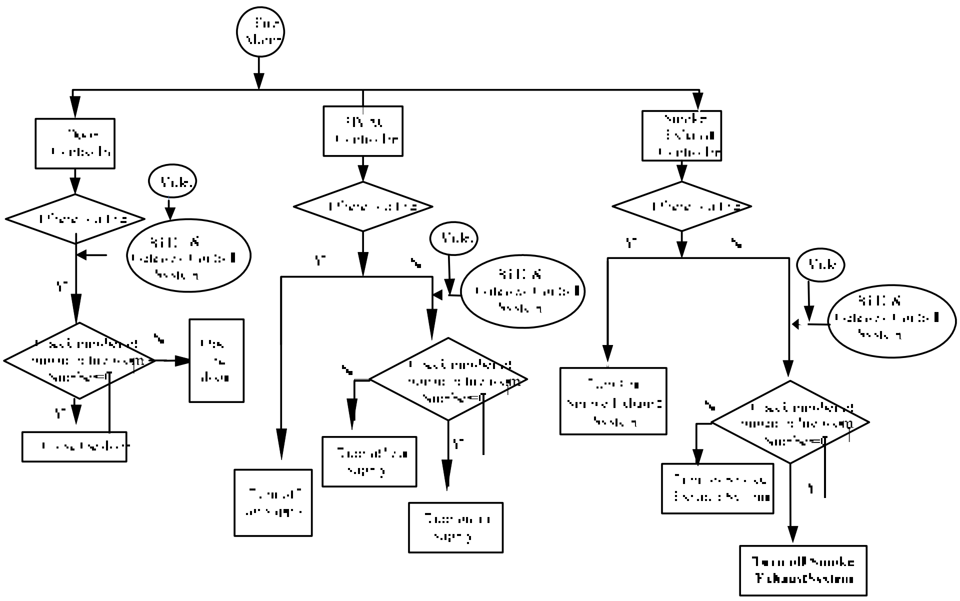

Fig. 2 Modified Smoke Control Procedure

3.2 Simulation Fire Scenarios Design

To study modified smoke control procedure, different fire scenarios are setup. Fire location is shown in Fig. 1. Fire source is considered as propane gas combustor and lies in the right top with the area of about 4 m^2. The sprinklers are functional. The maximum fire power is set to be 10MW and fire develops to the maximum fire power at 300s.

4. Simulation Results

CFAST from NIST is selected to study the smoke control parameters. Smoke propagation will be simulated with door controller and without door controller, with HVAC and without HVAC and with traditional smoke control procedure and with modified smoke control procedure.

4.1 Simulation with Door Controller and without Door Controller

In this case, door of fire room (door1 in Fig.1) will be closed when no person is detected in the room to prevent smoke propagation in corridors through door 1, as shown in Fig. 1. Evacuation time is assumed 200s. Door 1 is closed when no person is detected in fire room. Door 2 and 3 (rooms without fire) are always open. Smoke exhaust vents are always open. HVAC vents are always closed.

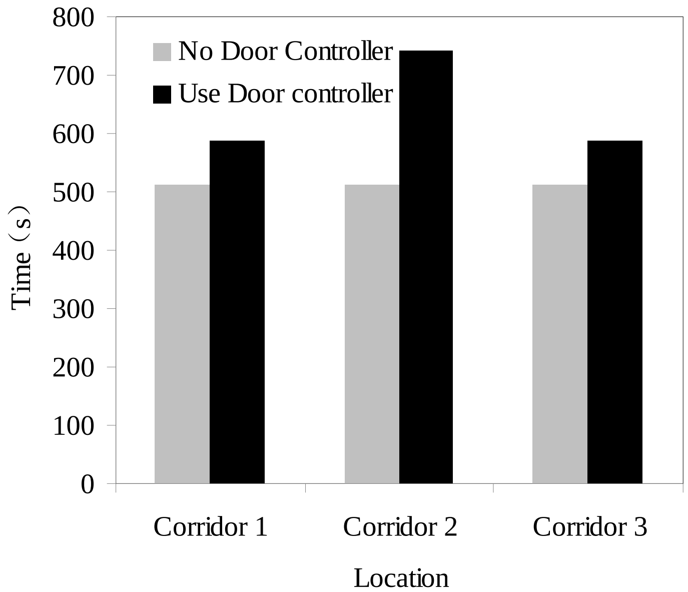

Fig.3 Time of Smoke Height reach to 1.8m comparison

Time for smoke height reaching 1.8m in corridor1 with door controller and without door controller is shown as Fig 3. It is proved that closing door of fire room can prevent smoke propagation in corridors through door 1. 8.8%~40% time is increased to help people evacuation. In corridors smoke height can be delayed effectively.

4.2 Simulation with HVAC and without HVAC

In this case, HVAC in rooms without fire will be turned on to prevent smoke moves down and assist evacuation of occupants. HVAC vents in room 2 and room 3 (rooms without fire) are always opened. Smoke exhaust vents are always open. Door 1 (room with fire) remains open. Doors 2 and 3 are always open.

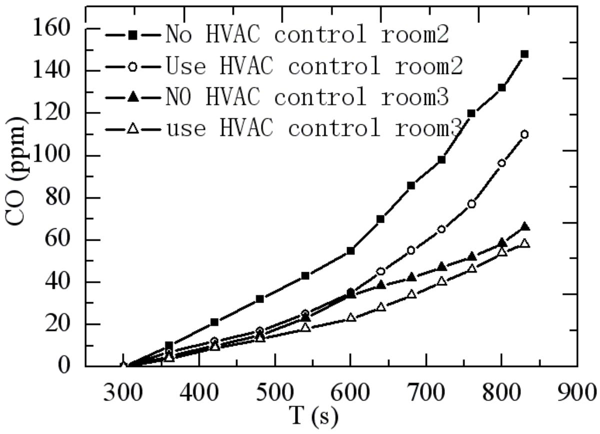

Fig. 4 Concentrations of Carbon Monoxide

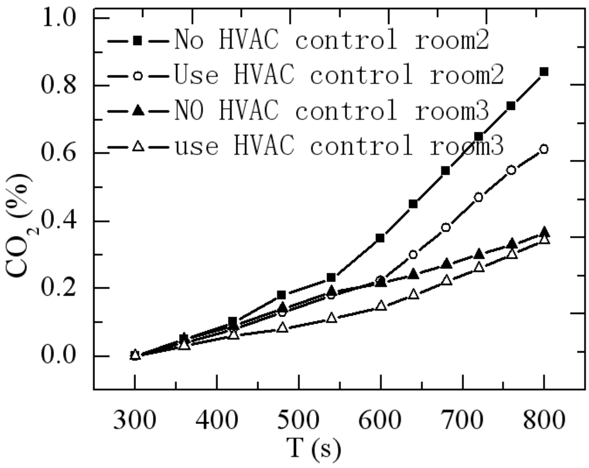

Fig.5 Concentrations of Carbon Dioxide

HVAC system in room 2 and room 3 are turned on and toxic and harmful gas concentration in rooms can be reduced by the fresh air. Carbon monoxide concentration curve is shown in Fig.4 and carbon dioxide concentration curve is shown in Fig.5. It is evident that concentration of upper layer carbon monoxide and carbon dioxide is reduced to about 30 % by fresh air.

4.3 Simulation with Tradition and Modified Smoke Control Procedures

In this case fire scenarios are designed according to modified smoke control system. It is assumed that time needed for evacuation from fire room, room 2 and room 3 are 200s, 150s, 200s, respectively. Door controller in fire room is turned on and door 1(room with fire) is closed after 200s.HVAC vents in room 2 and room 3 (rooms without fire) are opened during evacuation and closed after 150s and 200s. Smoke exhaust vents are always open.

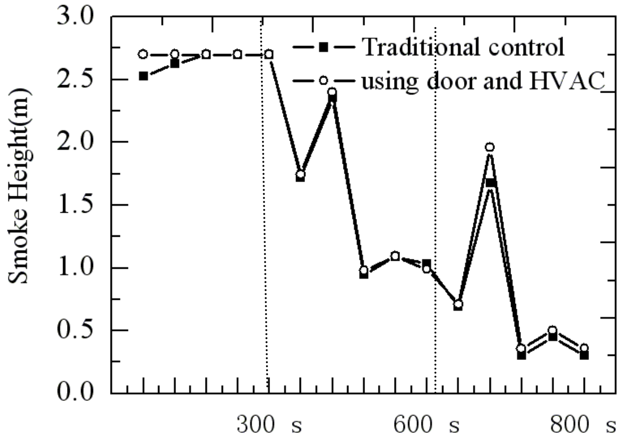

Fig.6 Smoke Height in rooms and corridors at 300s, 600s, 800s

Smoke height in rooms and corridors at 300s, 600s, and 800s are shown in Fig.6. It is clear that door controller of fire room can prevent smoke propagation through fire room door and HVAC can improve air condition in the rooms without fire. In rooms smoke height has almost no change in modified strategy comparing with traditional control strategy and in corridors smoke descends more slowly using door and HVAC operation. It is shown that smoke height is reduced by about 2% and in corridors smoke height delay rate is about 10% from Fig.6.

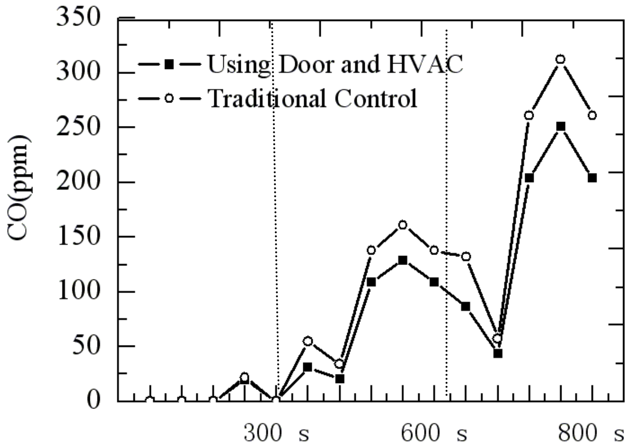

Fig.7Carbon Monoxide Concentrations in rooms and corridors at 300s, 600s, 800s

Concentrations of upper layer carbon monoxide and carbon dioxide are shown in Fig.7 and Fig.8. Concentrations of toxic gas in corridors and rooms can be reduced and air condition can be improved for human evacuation. It is shown that in concentration of upper layer carbon monoxide and carbon dioxide is reduced to 30%~40% and in corridors concentration of upper layer carbon monoxide and carbon dioxide is reduced to 20% from Fig.7and Fig.8.

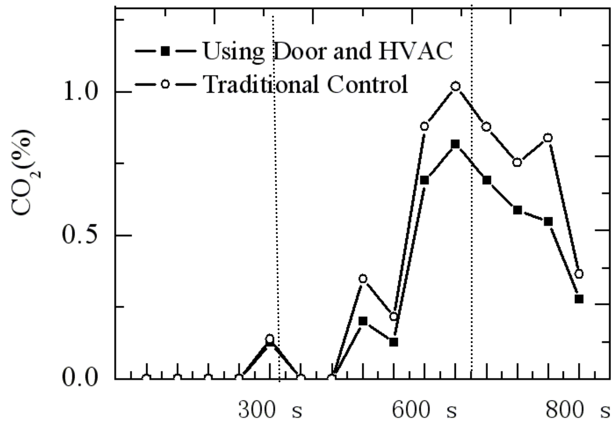

Fig.8 Carbon Dioxide Concentrations in rooms and corridors at 300 s, 600 s, 800 s

5. CONCLUSIONS

The intelligent smoke control procedure using HVAC operation and door control strategy can slow down smoke propagation in rooms and corridors by combined action of door controller and HVAC controller using sensor readings.

(1) With only door controller, closing door of fire room can prevent smoke propagation in corridors through door 1. 8.8%~40% time is increased to help people evacuation.

(2) With only door controller, concentration of upper layer carbon monoxide and carbon dioxide is reduced to 30 % rate by fresh air. And 10% time for toxic gas reach to safety limits can be improved.

(3) The intelligent smoke control procedure can prevent smoke propagation through door 1 and in corridors smoke height delay rate is about 10%.

(4) The intelligent smoke control procedure can reduce concentration of carbon monoxide and carbon dioxide in rooms by about 30-40% and it in corridors is reduced by about 10%.

ACKNOWLEDGEMENT

This research is supported by National Nature Science Foundation of China (Grant No. 70833003).

REFERENCES

W.Z. Black, George W and Woodruff , 2008. Smoke movement in elevator shafts during a high-rise structural fire, *Fire Safety Journal*,3, 1~15

Olivier Vauquelin, 2007. Experimental simulations of fire-induced smoke control in tunnels using an ‘‘air–helium reduced scale model’’: Principle, limitations, results and future, *Tunnelling and Underground Space Technology*,23,171~178

L.H. H, J.W. Zhou, R. Huo, W. Peng and H.B, 2007. Wang, Confinement of fire-induced smoke and carbon monoxide transportation by air curtain in channels, 12, 327~334

Yuan Shusheng and Zhang Jian, 2007. Large eddy simulations of fire smoke flow and control in an underground shopping mall, *Journal of University of Science and Technology of China*, 37, 61-69

Jong-Yoon Kim and Sung-Wook Yoon, 2006. A study on the smoke control characteristic of the longitudinally ventilated tunnel fire using PIV , *Tunnelling and Underground Space Technology*, 21, 302

Dong-Ho Rie, Myung-Whan Hwang and Seong-Jung Kim, 2006. A study of optimal vent mode for the smoke control of subway station fire, T*unnelling and Underground Space Technology,* 21, 300-301

Su M D, 1990. Algebraic modeling of large eddy simulation and its application, *Science in China (Series A)* , 33, 185～195

McGrattan K B, 2001.Computational fluid dynamics and fire modelling , *National Institute of Standards and Technology* , 21, l～50

Woodburn PJ and Britter RE, 1996. CFD simulation of a tunnel - Part 1. *Fire Safety*, 26, 35-62

Woodburn PJ and Britter RE, 1996. CFD simulation of a tunnel - Part 2. *Fire Safety*, 26, 63-90

XU Liang, ZHAN G Heping , YANG Yun , et al, 2004.Preparatory study on fire design in performance-based design. *Fire Science and Technology*, 23, 129~132.

J.Liu and X.Y.Lu, 2002. Application of Large Eddy Simulation to Smoke Movement, *Fire Safety Science*, 2, 5～15

McGrattan K and Forney G, 2004.Fire Dynamics Simulator (Version 4), *Technical Reference Guide [R]*. *NIST Special Publication,* 2, 10~18.

D.Madrzykowski and W.D. Walton ,2007.Cook County Administration Building Fir 69 West Washington, Chicago, Illinois, October 17, 2003: Heat Release Rate Experiments and FDS Simulations, *NIST Special Publication SP-1021*,7

Z. Dong Chen and David Yung, 2005.Numerical Study of Two Air Intake Strategies for a New Fire Laboratory, *Fire Protection Engineering*, 17, 27~41

PARALLEL SESSION 11

EVALUATION ON PERFORMANCE DEGRADATION OF DETERIORATED CIVIL INFRASTRUCTURE

HIROSHI YOKOTA
Graduate School of Engineering, Hokkaido University, Japan
yokota@eng.hokudai.ac.jp

YOSHITAKA KATO, REIKO KUWANO, TAKAHIRO ENDO
International Center for Urban Safety Engineering
IIS, The University of Tokyo, Japan

EMA KATO
Geotechnical and Structural Engineering Department
Port and Airport Research Institute, Japan

ABSTRACT

To realize the performance-based maintenance for civil infrastructure, it is necessary to evaluate structural performance by applying various measuring techniques. At present, however, established techniques are unfortunately not available that can collect accurate and quantified information how the structural performance is degraded. In particular, a comprehensive evaluation of an entire structure from the ground to the superstructure is rather difficult.

The ICUS, International Center for Urban Safety Engineering, of the Tokyo University set up Research Committee 62 in April 2008 to address the challenge of performance evaluation of an entire structure from structure to ground. This paper introduces the activity of this research committee and presents the outlines of the outputs during the first year. The first year of our activity focused on the review of current available measuring techniques for concrete or earth structures. Also the committee started to seek the future advancement of each technique as well as the merger of several techniques to make it possible to apply for a ground-concrete structure.

1. INTRODUCTION

Civil infrastructure has been built with several kinds of structural types and materials including concrete, earth materials, steel, plastics, etc. Those structures are well designed at first to have sufficient performance beyond the requirements. During the design service life, the initially provided performance will be lost gradually due to aging (material deterioration), obsolete functions, change in use, etc. To keep structural performance over the requirements, performance-based maintenance has to be introduced. To quantify structural performance that the structure possesses at the time of assessment, measurement techniques including NDT (non-destructive testing) have been applied, but most of them are limited to use only for quantifying physical response to corresponding structural performance. In particular, overall structural performance from the ground to the superstructure is very difficult to quantify by using current NDT techniques available in the market.

To meet this situation, the ICUS (International Center for Urban Safety Engineering) of the IIS (Institute of Industrial Science) in The University of Tokyo set up the research committee “Evaluation Technology of Degraded Performance of Civil Infrastructure due to Aging” which started its activity in April 2008. This research committee consists of two working groups: WG1-performance evaluation of structures and WG2-performance evaluation of ground and earth structures. This paper presents the interim report of the activity of this research committee during the first half of its activity.

2. PERFORMANCE EVALUATION

The time-dependent change in structural performance can be understood as shown in Figure 1. A civil structure is designed according to relevant design standards and specifications to have adequate safety and serviceability. However, the safety of structure is not fully simulated its degradation due to external actions including environmental action. To realize performance-based maintenance, structural performance should be quantified accurately at any time during the service life of structure. The WG1 has investigated the methodology to quantify the structural performance possessed and required taking into account material deterioration.

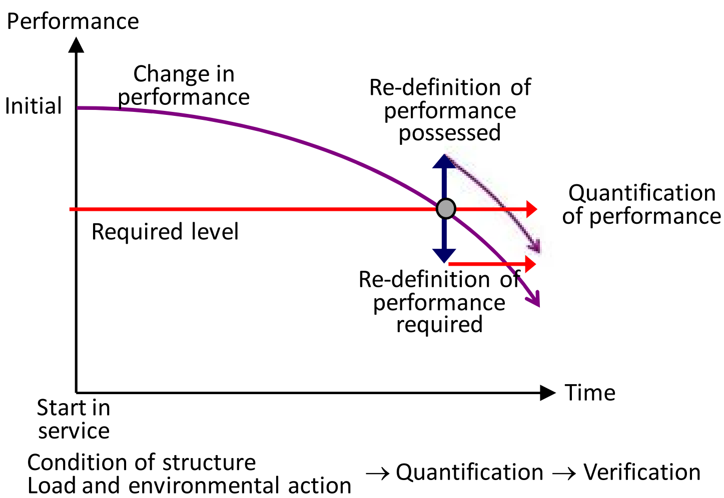

Figure 1: Concept of performance evaluation.

2.1 Scope

The WG1 has focused on the following targets for performance evaluation:

(a) Cause of deterioration: Time-dependent deterioration caused by environmental action such as chloride-induced deterioration, carbonation, etc. Change in external load over time such as hydro pressure, earth pressure, etc. excluding seismic action.

(b) Structural performance: Serviceability (deflection, stress, etc.) and safety (load-carrying capacity, deflection, etc.)

(c) Structural type: Concrete structures buried under the ground

2.2 Index for Performance Evaluation

Example analyses have been carried out to quantify performance degradation of the ground and earth structures by referring to published papers and reports. The references lists can be obtained from the ICUS Report, 2009.

2.2.1 *Water channel subjected to impulsive railway loads*

Damages of a reinforced concrete duct subjected to impulsive railway loads and water flows have been investigated by vibration property under irregular vibration and AE measurement. The damaged area that can be visibly observed showed a decrease in natural frequency compared to that of the sound area. There have been some correlations between AE property and vibration property. Therefore, the AE property may become an index for performance quantification.

2.2.2 *RC sewage pipe*

Chemical deterioration due to hydrogen sulfide was focused on for a reinforced concrete sewage pipe. Exposure tests of epoxy covered specimens in a sewage pipe have been carried out to measure the penetration depth of sulfur ion into epoxy coating layer and change in weight of the specimen. The applicability of the square-root *t* (*t*: exposure time) method was discussed.

2.2.3 *Irrigation canal pipe*

Time-dependent change in organic soil layer was discussed. Water leakage from the pipe has often been observed in the area where the thickness of the organic soil layer was changed. Long term settlement of the layer might have caused differential settlement of the pipe resulting in discontinuity of the joints, which resulted in the loss in serviceability (function) of the structure.

2.2.4 *Steel base plate of oil tank*

Corrosion of steel base plate of oil tank degrades the safety and causes oil leakage. The relationship between corrosion risk and AE activity has been verified by field measurements. It was concluded that AE detects peeling of corrosion products and minute cracks of steel.

2.2.5 *Cave and loosen part behind quay wall and sea walls*

Hydro pressure variation due to wave action and damage of joints and protective sheet produce sucking of backfilling materials, resulting in cave and cave-in of the ground behind the structure. The specific electrical resistance of the ground was measured by the frequency domain electro-magnetic induction (FDEM) technique. Subsurface properties and features were able to be deduced by FDEM. Using the relationship between relative density of the ground and specific electrical resistance, loosened part can be detected.

2.2.6 *Deterioration of concrete*

The following quantified indices may be applicable for performance evaluation of concrete structures themselves:

(a) Carbonation: carbonation depth, cross-sectional loss of embedded steel reinforcement due to corrosion, and width of corrosion crack

(b) Chloride-induced deterioration: chloride ion concentration, cross-sectional loss of embedded steel reinforcement, and width of corrosion crack

(c) Frost damage: frost damage depth and cross-sectional loss of embedded steel reinforcement

(d) Chemical deterioration: penetration depth of deterioration factor, carbonation depth, cross-sectional loss of embedded steel reinforcement

(e) Alkali-silicate reaction: remaining expansion and crack property

(f) Fatigue failure: crack density, deflection, cumulative damage, and cracks in steel

(g) Abrasion: abrasion depth and abrasion rate

2.3 Prediction of Performance Degradation

Technologies for evaluation of present structural performance and its future prediction can be categorized by the following methods:

(a) Direct evaluation

a-1) Grading system based on inspections

a-2) Performance degradation curves based on inspection results

a-3) Comprehensive evaluation including deterioration causes and interventions based on inspection results

a-4) Monitoring and analysis

(b) Long term exposure tests in natural environment

(c) Laboratory tests

(d) Numerical simulation

For actual concrete structures, the grading method (a-1) or the performance degradation curve based on the inspected grades (a-2) have often used as a practical approach. The other approaches have not reached the practically applicable stages.

2.4 Future Prospect

The results of inspections are utilized for the grading system and the degradation curves. This approach is reasonable for practical maintenance work, but some deficiencies in accuracy and in reflecting deterioration mechanism.

For detailed evaluation of performance, it is efficient that currently available design methods are applied including the determination of partial safety factors. For the evaluation, it is important to link the deterioration index and the input parameters for structural design with high accuracy. For taking the deterioration mechanism approach, the process from external factor to internal factor to performance degradation should be made clear and standard investigation method should be provided.

3. PERFORMANCE QUANTIFICATION TECHNIQUE

3.1 Scope

When picking up a bridge, the interaction between the main structure and the ground locates in its foundation. There are several kinds of foundation types such as spread footing and pile foundation, and all of which are very difficult to inspect directly. Moreover, abutment and pier are sometimes located in waterfront or in a river, in which they are exposed to very severe environments. Consequently, deterioration often occurs due to chloride ion, alkali-silicate reaction, frost attack, etc. In the pier of bridge, sliding due to scouring and deformation due to excessive earth pressure may occur, which are different types of deterioration from those in the main structure of bridge.

3.2 Investigation Technique

Investigation techniques for underground structures and earth structures are collected. Since underground structures are not visible directly, techniques to measure the position, length, etc. are focused on. For earth structures, techniques to investigate soil properties are mentioned.

For underground structures:

(a) Borehole radar- spacing of piles and conditions of underground structures (pile and foundation)

(b) Underground radar search- buried objects, cave, and loosened area

(c) Color imaging sonar- scouring

(d) Magnetic logging- searching metal

For the ground:

Velocity logging- physical properties of ground

3.3 Damage detection in structure

To detect damages of underground structures, the following techniques are available:

(a) Integrity test- cracks and defects in pile and length of pile

(b) Borehole camera- discontinuity and/or cracked areas in the hole

(c) Convergence meter- displacement

(d) Total station- shape and geometry

(d) Impulsive elastic wave- inner defects
(e) GPS- 3-D position

The most reliable method for detecting damages in a pile foundation is the visual inspection but it limited to the pile head area only. In some cases for buried parts of pile, the integrity test has been applied for damage detection, while minor damages may not be found. Borehole camera has also been applied as directly detective method, but quantified evaluation such as crack width is difficult.

The effectiveness of AE technique has been confirmed for damage detection of pile through laboratory and field tests. As NDT, elastic stress waves are trying to apply, where change in propagation property at the discontinuity points is utilized. This method is possible to detect minute cracks.

3.4 Monitoring

For continuous monitoring, the following are available:
(a) Optical fiber sensor
(b) Conductive paint

Monitoring has been sometime applied for damage and deformation detection in a pile foundation, in which sensors are pre-set. An optical fiber sensor is currently most popular for this purpose including SOFO type, OTDR type, B-OTDR type and their combinations. Instead of optical fiber, carbon fiber, as a trial, has been installed to measure strain and crack initiation. Other newly invented sensors are available. Besides them, piezoelectric device, permeable device with porous materials, current-carrying capsule, etc. have been in the process of practical realization for monitoring purposes.

4. INTEGRATION OF STRUCTURE AND GROUND

Performance degradation of concrete retaining walls and sea walls that are greatly affected by performance of the ground has been discussed from the concrete structures points of view.

4.1 Example Analysis

Reinforced concrete L-shaped retaining wall fell down due to excessive seismic action. Another example is collapse of a gravity type retaining wall due to erosion. These two examples have been fully investigated by means of structural analysis and numerical simulations.

4.2 Fault tree

The failure mechanism of a retaining wall and a sea wall is very complex due to the interaction of various elements including ground and structural components. Using a fault tree analysis is extremely useful as a way to understand possible failure mechanisms.

A sea wall and a revetment are typical structures with the principal function of preventing overtopping and flooding due to storm surges and waves. An overview of the common modes of failure of sea walls and revetments has been analyzed as a fault tree (JSCE, 2000). The failure modes of sea walls and revetments include the following:

(1) Sea bed scours and toe erosion in front of the structures caused by wave action

(2) Subsequent undermining of rubble foundation and piping of core material; dislodging of slab elements and displacement of crests and rear-side armor due to wave action; and subsequent wash out of core materials.

(3) Damage to parapets due to wave action; subsequent collapse of crests of sea walls.

Deterioration of seawalls and revetments progresses as follows:

(1) Occurrence of small cracks and chipping in elements of the structure due to environmental action.

(2) In case of soft seabed soils, the weight of the structure causes settlement due to progressive consolidation; subsequent opening of structure joints due to differential settlement and piping of fine materials from structure.

4.3 Performance degradation

Analysis of examples show that damages occurring in a retaining wall and a sea wall may be caused by the following performance degradation of the ground: excavation, embankment, uncertainty of soil properties, weathering, excessive seismic action, insufficient drainage, residual water level rise, and chemical deterioration. Those are not fully quantified the extent of performance degradation, but affect the overall performance of structure. When some of those occur, countermeasures are taken particularly for the ground. Therefore, maintenance work focusing on the interaction between concrete and the ground should be required for these types of structure. For this purpose, periodic inspection and monitoring are of use for early detection of deformation.

5. PERFORMANCE EVALUATION OF EARTH STRUCTURES

For understanding the performance degradation of earth structures, example analyses have been made in the first half year. The following examples have been collected:

(a) Failure and settlement of embankment, hollowing inside embankment, and cave in of sand beach

(b) Settlement of natural ground and reclaimed land

(c) Scouring of pier foundation

(d) Cave in of road and settlement of slope shoulder

(e) Failure of slope

(f) Deformation of tunnel, collapse of water supplying tunnel

(g) Water leakage from tunnel lining

(h) Carbonation of concrete foundation in acid ground and alkali silicate reaction

(i) Leaching of calcium ion from the cement stabilized ground

The change in performance may be detected as the following indices:

(a) Hollowing and cave in of seawall, embankment: distribution of infiltration contour, washout of fine soil particles

(b) Stability of structure: crack in structure, strength reduction

(c) Cave in of road: outflow of soil into damaged part, hollowing, extent of loosened part, and increase in void ratio

(d) Scouring of foundation: outflow of soil

(e) Failure of ground, slope, retaining structure: deformation of ground

(f) Collapse of tunnel: weathering and erosion

6. CONCLUDING REMARKS

Following the first year activity, the committee will be focusing on much detailed analysis for performance evaluation of the structure-ground system. During this, field measurements including monitoring will be applied to discuss the availability and accuracy. The members of the committee meeting are grateful for further supports by practical engineers.

The authors would like to extend their appreciation to all the research committee members for their activities.

REFERENCES

International Center for Urban Safety Engineering, 2009. Interim Report, Research Committee on Evaluation Technology of Degraded Performance of Civil Infrastructure due to Aging. *ICUS Committee Report 2009-001*, in Japanese.

Japan Society of Civil Engineers, 2000. Design Manual for Coastal Facilities, Maruzen.

REPORT OF NON DESTRUCTIVE TESTING FOR AN AIRPORT RUNWAY AND BRIDGE ASPFALT PAVEMENT BY USING INFRARED CAMERA

NOBORU SATO
Sankyo Co. Ltd, Tokyo, Japan
nsato@sankyo-net.co.jp

ABSTRACT

Asphalting is essential to an infrastructure as a freeway and airport runway. However, life cycle of asphalting is different from a concrete structure. It’s short, and degradation and damage of pavement materials. Detaching and dead water phenomenon arise at asphalt on the bridge, and blistering occurs at airport runway. This time, We report on damage of asphalting on a bridge and the detection method of "blistering" which occurs at airport runway.

1. Detection which damage of asphalting on bridge

Damages of asphalting on bridge are as follows.

① Crack
② Rut
③ Detaching between Surface layer and basis layer
④ Dead water under the asphalting

A rut investigation with a laser and a crack investigation with a video camera were main method for conventional maintenance of bridge asphalting. Core sampling is being performed in local way and asphalt is being checked adherently These were investigation of point and line, and case with plane-like investigation detaching and information on dead water is very few.

On the other hand, it's possible to be in creating an image of distribution of temperature in the pavement surface and presume damage inside the pavement by infrared thermography.

We show an example of a pavement investigation of steel box girder bridge

Detaching between the Surface layer and the basis layer was presumed by the temperature of the pavement surface. And then, dead water was presumed from the low surface temperature. After the part detected by infrared image was cut, inter layer peeling and the dead water under the pavement were found.

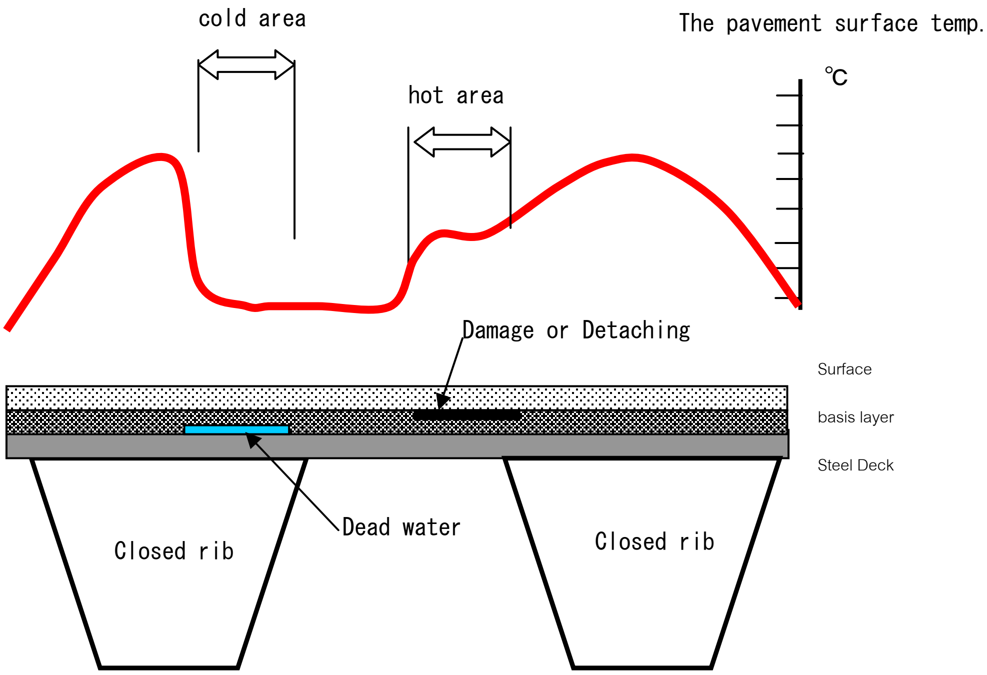

Figure 1: The Section of the bridge and the pavement surface temperature

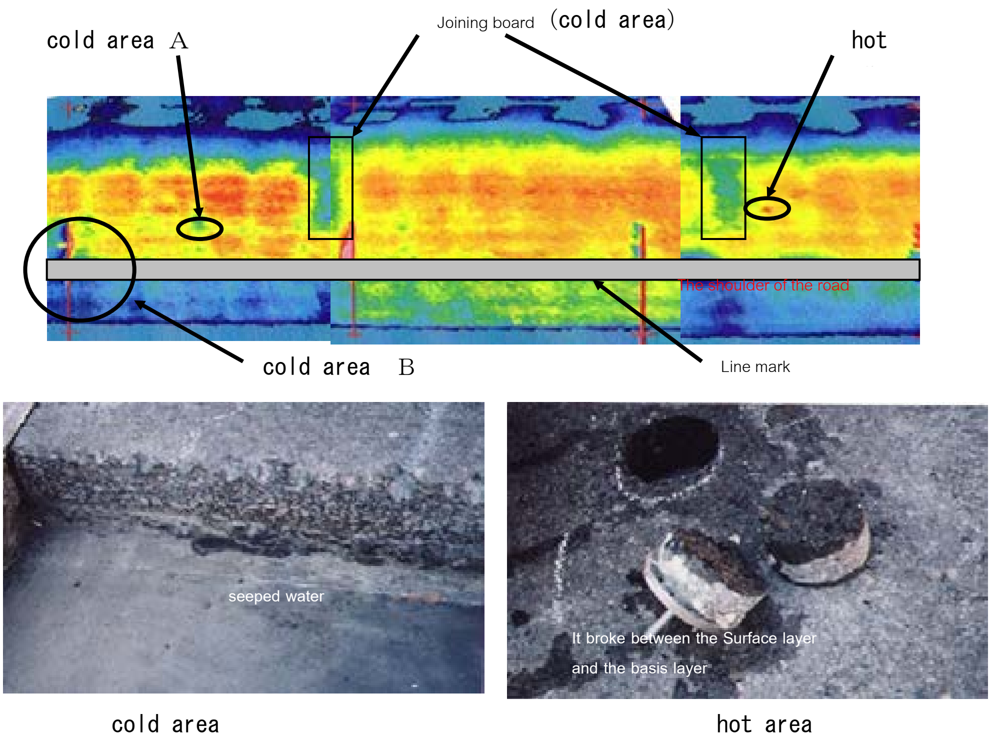

Figure 2: As a result of the distructive test.

2. DETECTION WHICH DAMAGE OF ASPHALTING ON THE RUNWAY.

On July 2, 2000, asphalting coiled around a tire at the time of a plane landing in one of airport in Japan. And then, asphalting came off and scattered. Therefore it caused a delay in the service of the plane.

The cause of the accident are high temperature in summer, and blistering that produced sealing up on the surface layer dense water of the asphalting inside. Such blistering phenomenon occurs at a runway in all over the world.

Many engineers find blistering with a hammer in the midnight now.

However, a correct test result is not provided. Because to be tired from work of the midnight when paving do not be smooth in the airport runway.

And then, it's very difficult to record the location of detected blistering correctly in the vast runway. We suggested infrared thermography that method which test result was full of objectivity and could record a correct position.

Tapping sound check by a hammer

Grooving on the pavement

2.1 Measurement principle

The infrared thermography method can find blistering from temperature distribution of the pavement surface.

Asphalting is heated up by sunshine in the daytime, and the heat move in the ground deeply.

In the night , and the temperature fall, heat in the pavement surface also falls. But the heat which heated up in the daytime, in the ground, it depends deeply and is being transmitted to the asphalt surface. But for an air layer of blistering to interrupt spread of heat from the ground, the part blistering generates becomes cold.

The above explains the part of blistering generates has low asphalting surface temperature and a good part indicates high temperature. But, the picture is reversed by daytime measurement.

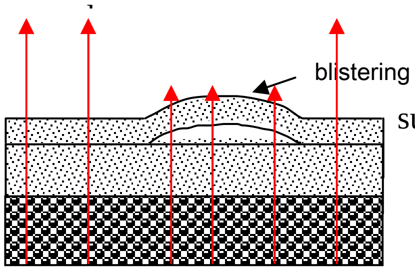

Figure 3: .Surface temperature in the night

Show a section of the runway asphalt pavement in figure 4.

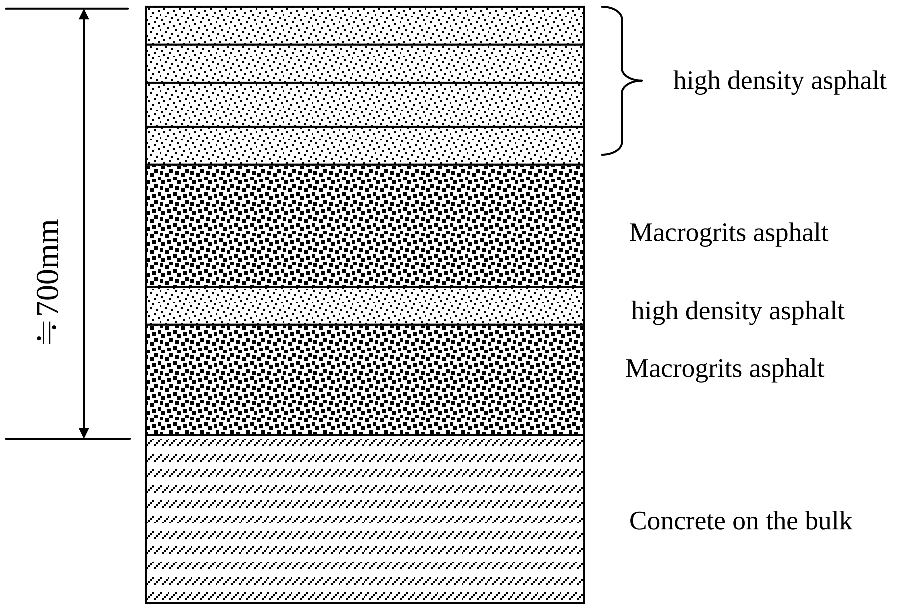

Figure 4: Runway section （the number of asphalt layers）

2.2 Method for measurement

At first, marking in square of 10m on the runway to grasp positioning information of the taken picture

An infrared camera is set in the high location of the vehicle for high lift work, and a picture is being recorded while running.After analyzing the respective pictures, a picture is connected and a picture in the whole runway is made. The part which indicated low temperature on the picture is blistering on above

Figure-5 shows the measurement situation with using the maintenance vehicle.

Figure-6 shows picture of blistering detected by an infrared camera. These results shows that blistering appears clearly at low temperature

We get such data at many runways, therefore blistering of about 10 cm in depth is detected as a result of core sampling.

There are few record of an investigation by infrared camera, but we expect that the investigation spreads at runways more.

Figure 5: The measurement situation

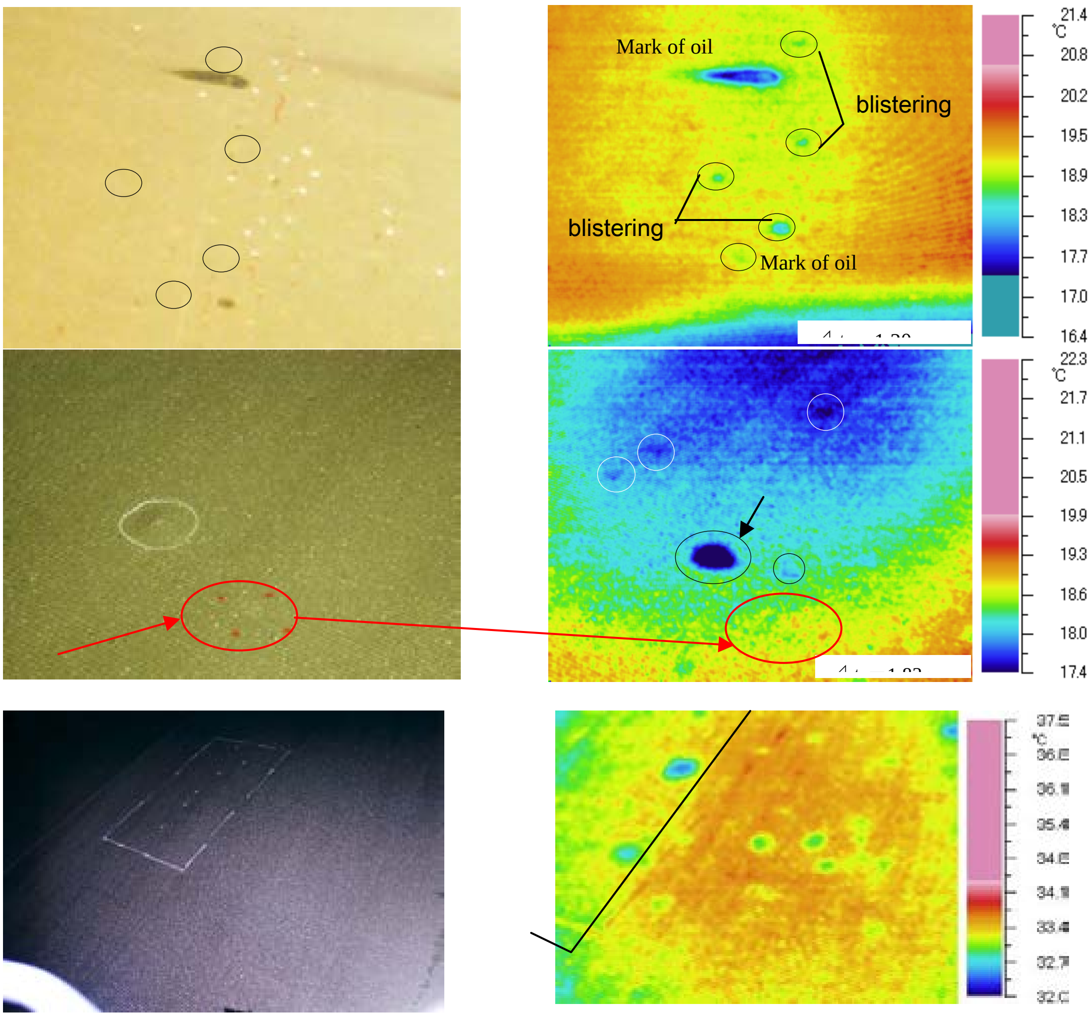

Figure 6: picture of blistering detected by an infrared camera

RECOVERY MECHANISM OF FIRE-DAMAGED HIGH-STRENGTH MORTAR

YOSHITAKA KATO
ICUS, Institute of Industrial Science, The University of Tokyo
katoyosh@iis.u-tokyo.ac.jp
MICHAEL HENRY
Department of Civil Engineering, The University of Tokyo
mwhenry@iis.u-tokyo.ac.jp
MASAMITSU SUZUKI
Department of Architecture and Civil Engineering,
Shibaura Institute of Technology
m-suzuki@iis.u-tokyo.ac.jp

ABSTRACT

The performance of concrete deteriorates when exposed to fire, but may be recovered by re-curing the concrete in water. A repair method for fire-damaged concrete which utilizes re-curing could reduce waste generation and resource consumption by restoring the performance of the damaged material. However, the capability and mechanisms for such a repair method are not clear. Experiments were conducted to resolve the recovery mechanism under by examining both the physical and chemical perspectives. It was found that durability characteristics could be fully recovered but strength could only recover to 80% of pre-fire levels. Mechanical deterioration was due to the occurrence of surface cracks and the coarsening of the pore structure, which were caused by thermal decomposition, and recovery was due to pore structure growth and crack self-healing. The growth observed in the pore structure could be attributed to the re-hydration and increase of hydration products which were dehydrated during heating. However, the re-hydrated pore structure is believed to be weaker than the original structure, thus resulting in lower strength even after re-curing.

1. INTRODUCTION

Concrete exposed to high temperatures undergoes a reduction in performance, such as decreased load-carrying capacity and durability. In order to restore these properties repairs should be conducted, which typically involve the removal of damaged areas and the casting of a patching material (Tovey, 1986). Unfortunately, the removal operations require intense labor and produce waste which must be disposed of. Past research has found that re-curing fire-damaged concrete in water can restore strength and durability (Crook & Murray, 1970; Sarshar & Khoury, 1993; Poon et al., 2001). A repair method which utilizes re-curing could potentially replace or reduce the extent of labor-intensive operations, saving energy and labor costs and reducing waste generation and resource consumption.

For re-curing to be realized as a repair method, the re-curing mechanism and capability should be understood. In a previous research by the authors on high-strength mortar damaged by fire, loss and recovery of strength and durability were attributed to changes in porosity and cracking caused by different cooling and re-curing conditions (Kato et al., 2008). However, the scope of the previous research did not include a chemical analysis component. This paper builds upon that previous research by considering the loss and recovery of strength and durability in terms of the changes in chemical composition, and combines the chemical changes with the observed changes in porosity and cracking to propose a recovery mechanism for fire-damaged high-strength cement mortar.

2. EXPERIMENTAL PROGRAM

2.1 Materials and specimens

High-strength cement mortar was prepared from water (W), Type 1 Portland cement (C), Fujigawa river sand (S), and air-entraining (AE) and super plasticizer (SP) admixtures, with a target 28-day compressive strength of 100 MPa. Complete mix proportions are given in Table 1. After mixing, cylinder specimens (5Ø×10cm) were cast and cured in the molds for 24 hours, then removed and placed in water curing at 20ºC for 13 days before being moved to air curing at 20ºC and 60% relative humidity (RH).

Table 1: Cement mortar mix proportions.

(by mass)		(kg/m^3)			(%C by mass)	
W/C	**S/C**	**W**	**C**	**S**	**AE**	**SP**
0.3	1.8	230	767	1380	0.4	1.5

2.2 Fire exposure

Fire exposure was conducted 28 days from casting using an electric furnace. As this furnace does not have a control mechanism for the rate of heat increase, the furnace was preheated to the target temperature before beginning specimen exposure. Based upon a trial series of tests, the exposure condition was set at 550ºC for 2 hours.

2.3 Re-curing regimes

After removal from heating, specimens were placed in one of three re-curing regimes, as shown in Table 2. These re-curing regimes consisted of a cooling period and re-curing period, where the cooling period refers to the first hour after removal, and the re-curing period is the period from cooling until testing. Environmental conditions were 20ºC and 60% RH for “air” exposure and 20ºC and total water submersion for “water” exposure.

Table 2: Re-curing regimes.

Regime	Cooling period Removal – 1 hour	Re-curing period 1 hour – 28 days
Air	Air	Air
Water	Water	Water
Air-water	Air	Water

2.4 Strength and durability tests

Compressive strength was measured under the unstressed residual condition. Three cylinders were tested at each data point and the average values are reported.

For air permeability, cement mortar cylinders were dried at 40ºC and checked by monitoring the weight change, and then air permeability specimens were cut 4 centimeters from the top of the cylinder. The specimens were then set into an air permeability test machine and the volume of flowing air was measured under steady state conditions. Two cylinders were tested at each data point and the average values are reported.

Compressive strength and air permeability tests were conducted before heating, 1 hour after heating (air and water cooling), and after 3 and 28 days (air, water, and air-water re-curing).

The accelerated carbonation test began after 28 days of re-curing (air, water, and air-water). Test conditions were 20ºC±2ºC, 60%±5% RH, and 5%±0.2% CO_2 concentration, and the carbonation depth was measured at 1, 4, and 8 weeks after 4 weeks of re-curing. Results are given in terms of the carbonation rate for specimens which were not exposed to fire, as well as for specimens in the three re-curing regimes.

2.5 Micro- and macrostructure observation

The cement paste microstructure was characterized utilizing mercury intrusion porosimetry (MIP). MIP specimens, approximately 5 mm in size, were taken from compressive strength cylinders after testing. These specimens were submerged in acetone to stop the hydration reaction and then dried using a D-dry vacuum pump. Testing for MIP specimens was conducted at the same time points and under the same exposure conditions as the compressive and air permeability tests.

In order to measure the macrostructure changes, the cracking pattern and crack recovery under different re-curing conditions was observed using an epoxy injection procedure (Iwaki et al. 2004). After re-curing, a fluorescent epoxy was injected via vacuum pressure. This process can inject epoxy into cracks as small as 6 micrometers, and the hardening of the epoxy helps to prevent secondary defects from forming. After epoxy injection, cylinders were cut in section 4 centimeters from the top, placed under ultraviolet (black) light, and the dispersion of the epoxy was recorded by photograph. Only air (7 days) and water re-cured (1 hour and 7 days) specimens were observed.

2.6 Chemical analyses

Three chemical compounds were investigated; calcium hydroxide ($Ca(OH)_2$), calcium oxide or lime (CaO), and calcium carbonate ($CaCO_3$). The two primary cement hydration products are C-S-H and $Ca(OH)_2$, but it is difficult to measure C-S-H so this research focused on $Ca(OH)_2$. CaO is produced by the thermal decomposition of $Ca(OH)_2$, and $CaCO_3$ is produced by the carbonation of CaO and $Ca(OH)_2$. Samples for chemical tests were taken 10 millimeters from the surface in the upper half of cylinder specimens, and fine aggregates were removed to produce cement powder.

The crystalline structure was observed using X-ray diffraction (XRD). Experiments were conducted using CuKα testing conditions with a range of $2\theta = 5 - 60^{o}$, 0.02 step scan, and scanning speed of 0.5^{o} per minute. The diffraction profile was acquired using JADE (Rigaku), and qualitative analysis of the diffraction profile was conducted by PDF (ICDD) and targeted the diffraction peaks of $CA(OH)_2$, $CaCO_3$, and CaO. Results are given in terms of the peak number ratio, which describes the change in the crystalline structure relative to the initial condition.

Evaluation of the hydration progress was conducted using thermo-gravimetric and differential thermal analysis (TG-DTA). A heating speed of 10ºC per minute and a maximum temperature of 1000ºC in a nitrogen gas atmosphere were set as the measurement conditions. Two properties were calculated: the amount of chemically-bound water, which was measured by the ignition loss between 105ºC and 1000ºC, and the amount of $Ca(OH)_2$, which was calculated by the mass change which occurred around 450ºC.

3. PREVIOUS RESULTS

In previous research works by the authors, the recovery of strength (Henry et al., 2008) and durability (Kato et al., 2008) were investigated under different re-curing conditions. These results are briefly introduced and summarized in the following section.

3.1 Compressive strength

Compressive strength results and the relative change in strength due to loss and recovery are given in Figure 1. Specimens which were cooled in the air before water re-curing had the highest final compressive strength, followed by water and air specimens. Although the air-water specimens had the least strength loss, they also recovered less strength than water specimens, which underwent the largest strength loss but also the largest strength recovery. Air specimens lost more strength than air-water specimens, but recovered the least strength. From these results, it was concluded that reducing the initial strength loss was more important than increased strength recovery for achieving higher final compressive strength.

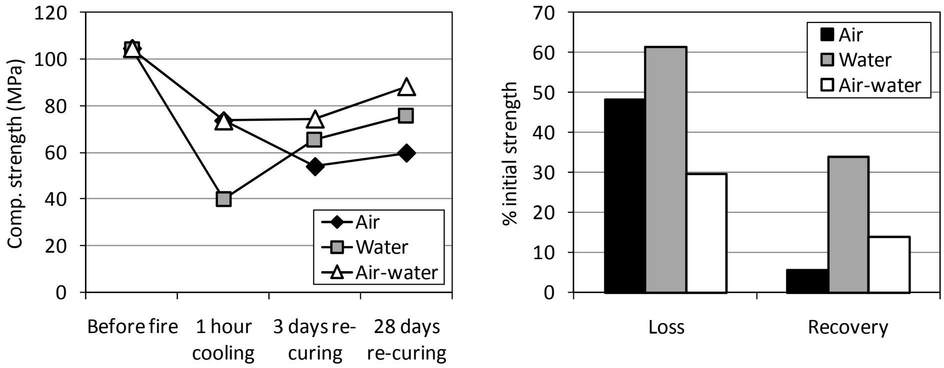

Figure 1 Compressive strength results (left) and loss/recovery (right)

3.2 Durability indicators

Durability was evaluated using two indicators, the air permeability coefficient and the carbonation rate, and the results are shown in Figure 2. It can be seen that the re-curing period – from 1 hour to 28 days – had the largest effect on the air permeability coefficient. During that period, the air permeability of air specimens increased slightly and that of water and air-water specimens greatly decreased. However, the initial cooling period affected the observed trend, as specimens first cooled in water had steady but constant recovery, whereas specimens first cooled in air recovered more quickly during the 1 hour to 3 day period with a slight increase over the following period. The effect of water re-curing on carbonation was also clearly seen, as only specimens re-cured in the air underwent carbonation. The performance of specimens re-cured in the water was similar to that of specimens not exposed to fire.

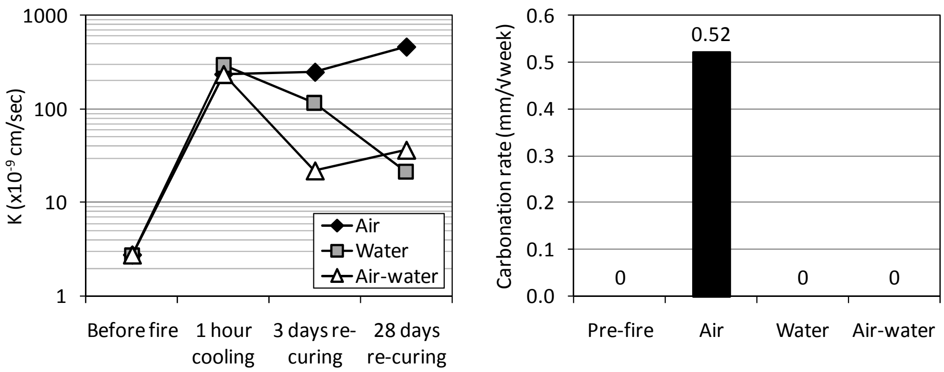

Figure 2 Air permeability results (left) and carbonation rate (right)

3.3 Micro- and macro-structure

The porosity results are given in Figure 3. Similar to the air permeability results, the largest effect can be seen during the re-curing period from 1 hour to 28 days. Also similar to the air permeability results, air specimens underwent little recovery, whereas the water and air-water specimens recovered to levels similar to that prior to fire exposure. The recovery behavior of water and air-water specimens followed the same trend, with water specimens recovering slightly more by 28 days.

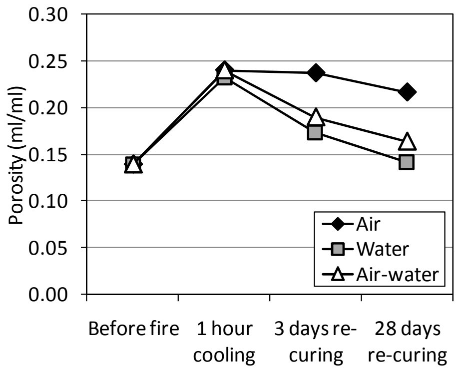

Figure 3 Porosity results

Figure 4 shows specimen sections after epoxy injection under exposure to black light. White areas show where the epoxy penetrated into cracks; dark areas are un-cracked. The specimen in the left image was immediately submerged in water after heat exposure; here, radial micro-cracks formed due to thermal shock. However, by 7 days these cracks had healed under water exposure, as seen in the middle image. Air specimens formed large surface cracks after 1 day of air re-curing, and these cracks did not self-heal in the air re-curing condition, as shown in the right image.

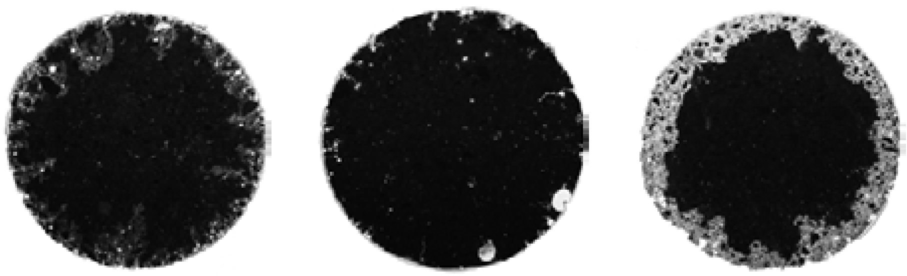

Figure 4 Cracking pattern after 1 hour water cooling (left), 7 days water re-curing (middle), and 7 days air re-curing (right)

3.4 Summary of previous results

From the previous results, it was concluded that the strength behavior was affected both by changes in porosity and the formation of macro- and micro-cracks. The occurrence of cracking was used to explain the difference in trends between the compressive strength and porosity. Re-curing by air led to the formation of macro-cracks due to differential thermal shrinkage, reducing strength. Water submersion, while causing a large reduction in strength due to thermal shock, also increased the strength recovery behavior due to water absorption. As a result, micro-cracks formed due to quenching were mostly healed within 7 days of water re-curing, and porosity recovered to pre-fire levels. Specimens cooled in the air before water submersion absorbed less water due to the lower specimen temperature at submersion, thus reducing recovery. Decrease in air permeability under water and air-water re-curing conditions can be attributed to crack healing and porosity recovery, whereas an increase in air permeability for air specimens was caused by significant cracking and an increase in porosity. Carbonation resistance was increased in water and air-water specimens by the decrease in porosity and the crack healing.

Although durability and porosity recovered to pre-fire levels after water and air-water re-curing and crack self-healing was observed, pre-fire compressive strength was not achieved. In order to explain this disparity, an investigation on the changes in the chemical composition under variable re-curing conditions was conducted.

4. CHEMICAL ANALYSIS RESULTS

4.1 XRD

XRD results are shown in Figure 5. For these results, only the air and air-water conditions are used in order to focus on the changes which occurred from 1 hour to 28 days. It can be seen that fire exposure causes an increase in the peak ratio of CaO and a decrease in the peak ratio for $Ca(OH)_2$. This is due to the thermal deterioration of $Ca(OH)_2$ into CaO. For air re-curing, the peak ratio for CaO decreases while that of $CaCO_3$ increases; this can be attributed to the carbonation reaction of CaO with CO_2, which produces $CaCO_3$. In the case of air-water conditions, however, the crystalline structure appeared to return to conditions similar to that before heating after only 3 days of water re-curing.

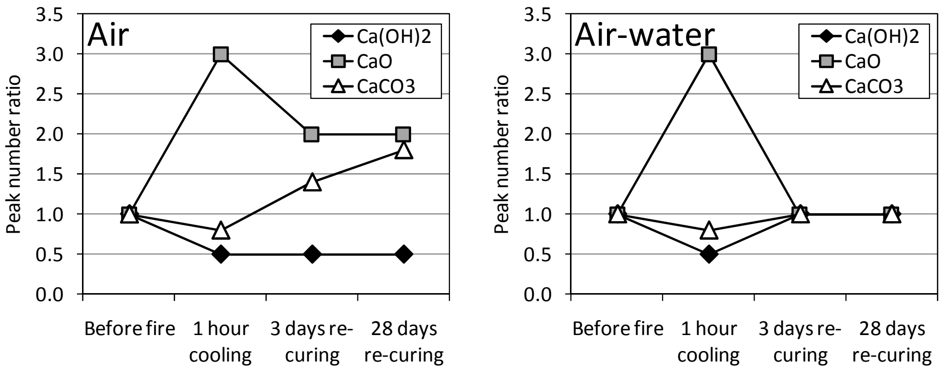

Figure 5 Peak number ratio for air (left) and air-water (right) conditions

4.2 TG-DTA

TG-DTA results for chemically-bound water and $Ca(OH)_2$ are shown in Figure 6. After 28 days, air-water re-curing specimens have more chemically-bound water than before fire exposure. This is due to the rehydration of CaO into $Ca(OH)_2$, as well as the hydration of unhydrated cement particules. In the air re-curing condition, the amount of chemically-bound water also increased, indicating that hydration was occurring even under low water supply conditions. The rehydration of CaO into $Ca(OH)_2$ is again seen in the increase in the amount of $Ca(OH)_2$ between 1 hour and 28 days. However, in air re-curing conditions the amount of $Ca(OH)_2$ decreases after a slight increase, indicating that the $Ca(OH)_2$ may be consumed in carbonation reaction with CO_2, implying that the increase in chemically-bound water is due to the rehydration of C-S-H gel.

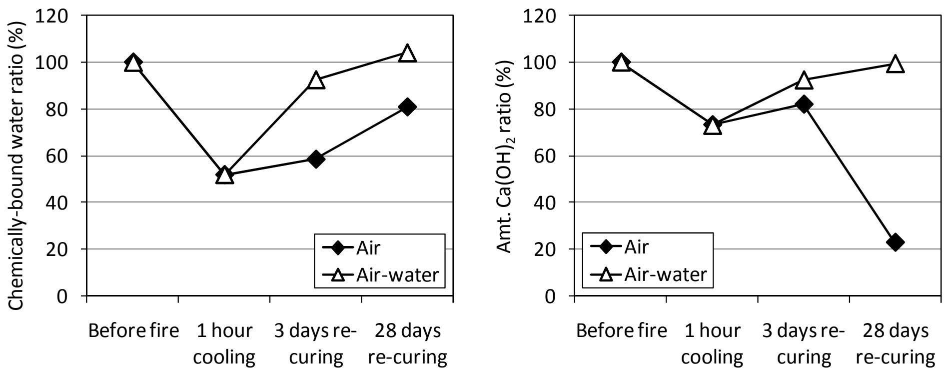

Figure 6 TG-DTA results for combined water (left) and $Ca(OH)_2$ (right)

5. PROPOSED RECOVERY MECHANISM

In the chemical analyses, it was found that water re-curing of the air-water specimens resulted in the development of a crystalline structure similar to that prior to fire exposure, and that the amounts of chemically-bound water and $Ca(OH)_2$, one of the primary hydration products, were also similar to volumes observed prior to fire exposure. Therefore, it still remains unclear why compressive strength did not recover to pre-fire levels, even though the porosity of this series was similar to that prior to fire exposure at 28 days and crack healing was observed under water re-curing conditions.

Since the results of the conducted chemical analyses cannot explain the lack of compressive strength recovery, it is proposed that this is caused by the weakness of the healed cracks and the rehydrated cement pore structure. Although the healing of cracks was both visually observed and supported by the increase in durability under water re-curing conditions, no mechanical testing of the healed crack interface was conducted. It is possible that there exist weaknesses or flaws in the newly-healed crack interface that cannot be detected by visual observation, but still produce improvement in durability. One reason may be imperfect cracking healing in this area; another reason may be that the crystalline growth in the healed crack is of a different or weaker composition than normal cement paste.

The recovery of durability, through reduction of air permeability and carbonation rate, can be clearly explained by the chemical analysis results. The crystalline structure, after water re-curing, returned to a form similar to that prior to heating, and the amount of hydration products was also similar to pre-fire amounts. In addition, the observed porosity and crack recovery also support the reduction of air permeability under water re-curing conditions. Furthermore, water re-curing reduced the amount of CaO available for carbonation by reacting with water to form hydration product, resulting in high carbonation resistance. In contrast, during air re-curing CaO reacted with atmospheric CO_2, increasing the crystalline growth of $CaCO_3$ and resulting in a much-higher carbonation rate. Finally, although porosity was slightly reduced due to carbonation and minor hydration from atmospheric H_2O, air permeability increased due to surface cracking.

6. CONCLUSION

The research conducted in this paper was intended to continue previous research works by the authors by combining a chemical analysis component with the previous mechanical evaluations and visual observations, with the goal of explaining the recovery mechanism of fire-damaged high-strength mortar. From the previous research works, it was unclear why compressive strength did not fully recover under water re-curing, even when porosity recovery and crack healing were observed.

After conducting chemical analyses and integrating those results with the previous observations, it was proposed that the strength of the healed cracks and the rehydrated pore structure is weaker than that prior to heating, resulting in strength reduction even when crystalline structure, amount of hydration product, and porosity are found to recover to pre-fire levels and crack healing is observed. While water re-curing could not fully recover compressive strength, durability characteristics such as air permeability and carbonation rate were recovered to pre-fire levels. The recovery of durability was primarily due to the crack self-healing and the rehydration reaction, which reduced porosity and the availability of CaO for carbonation. Since past research works have noted that concrete structures which were exposed to fire often undergo severe damage due to carbonation, the potential of water re-curing to reduce this damage is clear.

The purpose of any repair method for fire-damaged concrete is to restore three performance requirements: load-carrying capacity, durability, and fire-resistance. These research works have addressed the potential of water re-curing as a repair method by focusing on the first two requirements, considering the case of high-strength mortar. However, the results may be dependent on many of the experimental factors involved, such as mix proportions, fire exposure variables, specimen size, and so forth. While a mechanism has been proposed for the recovery of strength and durability, based on the selected experiment conditions, it will be necessary for future research works to consider, to what extent, other conditions may have on the explanation of the recovery mechanism and the potential for water re-curing as a repair method.

REFERENCES

Crook, D.N. and Murray, M.J., 1970. Regain of strength and firing of concrete. *Magazine of Concrete Research*, 22(72), 149-154.

Henry, M., Ahn, T.H., Kato, Y., and Kishi, T., 2008. Development of a damage-recovery relationship based on variable re-curing of fire-damaged high-strength mortar. *Proceedings of the First International Symposium on Life-Cycle Civil Engineering*, Varenna, Italy, 165-170.

Iwaki, K., Kato, J., Hirama, A., and Shiotani, T., 2004. Micro-structural evaluation of concrete damaged by acid attack using optical microscopy. *Proceedings of the Japan Concrete Institute*, 26(1), 999-1004. (in Japanese)

Kato, Y., Henry, M., and Suzuki, M., 2008. Evaluation of re-curing for the recovery of fire-damaged high-strength mortar. *Proceedings of the International Conference on Durability of Concrete Structures*, Hangzhou, China, 1310-1316.

Poon, C.S., Azhar, S., Anson, M., and Wong, Y.L., 2001. Strength and durability recovery of fire-damaged concrete after post-fire-curing. *Cement and Concrete Research*, 31, 1307-1318.

Sarshar, R. And Khoury, G.A., 1993. Material and environmental factors influencing the compressive strength of unsealed cement paste and concrete at high temperatures. *Magazine of Concrete Research*, 45(162), 51-61.

Tovey, A.K., 1986. Assessment and repair of fire-damaged concrete structures – an update. *ACI Special Publication 92: Evaluation and Repair of Fire Damage to Concrete*, 47-62.

EXPERIMENTAL STUDY OF ULTRA HIGH STRENGTH CONCRETE AND REACTIVE POWDER CONCRETE STRUCTURES UNDER BLAST LOADING

NA-HYUN YI[1], SUNG-HWAN PARK[1],
JANG-HO JAY KIM[1], KEUN JOO BYUN[1] and JONG -KWON CHOI[2]
[1]Yonsei University, 262 Seongsanno,
Seodaemun-gu, Seoul 120-749, Korea
{wwitch1, realpsh, jjhkim, byun}@yonsei.ac.kr
[2]Hyundai Institute of Construction Technology, Mabuk-Ri,
Kuseong-Myun,Yongin City Kyungki-Do, 449-710, Korea
tunes1022@hdec.co.kr

ABSTRACT

Generally, concrete is known to have a relatively high blast resistance compared to other construction materials. However, normal strength concrete structures require higher strength to improve their resistance against impact and blast loads. Therefore, a new material such as Ultra High Strength Concrete (UHSC) and Reactive Powder Concrete (RPC) with high-energy absorption capacity and high resistance to damage is needed for blast resistance design. In this study, the blast tests of UHSC and RPC slabs with 1000×1000×150 mm specimens were carried out to investigate their blast behavior. The applied blast load was generated by the detonation of 35lbs ANFO explosive charge at 1.5m standoff distance. From these tests, it became clear that UHSC and RPC have better blast explosions resistance compared to normal strength concrete. Based on this experiment test results, design procedure of the RC structure is recommended.

1. INTRODUCTION

In recent years, there have been numerous explosion-related accidents due to military and terrorist activities. Such incidents caused not only damages to structures but also human casualties. Especially, in metropolitan areas which are exposed to terror attack, these severe loading related accidents can cause great human causalities, economical losses, and public infrastructure destructions, and civilian structure collapses. To protect structures and save human lives against explosion accidents, better understanding of the explosion effect on structures is needed. In an explosion, the blast load is applied to structures as an impulsive load of extremely short duration with very high pressure and heat.

Generally, concrete is known to have a relatively high blast resistance compared to other construction materials. However, normal strength concrete structures require higher strength to improve their resistance against impact and blast loads. Therefore, a new material with high-energy absorption capacity and high resistance to damage is a better material for blast resistance design. Recently, Ultra High Strength Concrete (UHSC) and Reactive Powder Concrete (RPC) have been actively developed to significantly improve concrete strength. UHSC and RPC can improve concrete strength, reduce member size and self-weight, and improve workability. Commonly, UHSC and RPC produce compressive strength greater than 150MPa and sometime up to 180~200MPa. High strength concrete are used to improve earthquake resistance as well as constructions of high-rises and long span bridges. Also, UHSC and RPC can be implemented to blast resistance design of infrastructure against terror or impact (ASCE, 1999; Baker, 1973).

The Korean building code has been modified in year 2009 where any high-rises located in the city of Seoul with the height of over 50 above ground floors or 200m, the terror resistant design has to be incorporated. This code regulation reflects the keen public interest on blast resistance and protective design concepts. However, since UHSC or RPC has been recently developed, their blast resistant capacities have never been studied. In order to properly and efficiently incorporate UHSC and RPC into protective design scheme, an in-depth research on blast resistance behavior on UHSC and RPC is urgently needed at this time (Kim, 2009; Zineddin et al., 2007).
Therefore, in this study, the blast tests are performed to investigate the behavior of UHSC and RPC slabs subjected to blast load. Blast wave characteristics including incident and reflected pressures as well as maximum and residual displacements and strains in steel and concrete surface are measured. Also, blast damages and failure modes were recorded for each specimen. From these tests, UHSC and RPC are shown to effectively resist blast explosions compared to normal strength concrete. Based on these test results, the blast design procedure will be suggested.

2. LITERATURE LEVIEW

2.1 Characteristic of blast load

An explosion is a very fast chemical reaction producing transient air pressure waves called blast waves. For a free-air burst, the blast wave will travel away from the source as a spherical wave front as shown in Figure 1(a). The peak overpressure and the duration of the overpressure vary with distance from the explosives. The magnitude of these parameters also depends on the explosive materials from which the explosive compound is made. Usually the size of the explosive compound is given in terms of a TNT weight. Explosive behavior depends on a number of factors: ambient temperature, ambient pressure, explosive composition, explosive material properties, and the nature of the ignition source type. Additional factors include type, energy, and duration of the events as well as geometry of surroundings (i.e., confined or unconfined). When a condensed high explosive is initiated, explosion reaction generates several additional characteristics such as blast wave of very high pressure, fragmentation from the explosive case or structural elements, hot gas with a pressure from 100 up to 300 kilobar, and a temperature of about 3,000～4,000℃. The main blast effect is impulsive pressure loading from the blast wave as shown in Figure 1(b) (Baker, 1973; Mays and Smith, 1995).

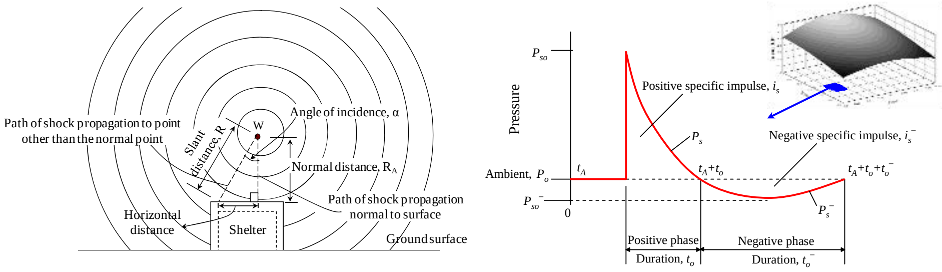

(a) Spherical free air blast *(b) Pressure-time history*

Figure 1: Spherical free air blast (TM5-1300, 1990; Kim et al, 2007)

After a short time, the overpressure behind the shock front drops rapidly and becomes smaller than that of the surrounding atmosphere as shown in Figure 1(b). This pressure domain is known as the negative phase. The front of the blast wave weakens as it progresses outward and its velocity drops toward the velocity of sound in the undisturbed atmosphere. The characteristics of a blast wave resulting from an explosion depend mainly on the physical properties of the source and the medium through which blast waves propagate. To create reference blast experiments, some controlled explosions have been conducted under ideal conditions. To relate other explosions with non-ideal conditions to the reference explosions, blast scaling laws can be employed. The most widely used approach to blast wave scaling is that formulated by Hopkinson, which is commonly described as the cube-root scaling law. The scaled distance, Z, is defined using the Hopkinson-Cranz's cube root law as (ASCE, 1999):

$$Z = R / E^{1/3} \text{ or } Z = R / W^{1/3} \tag{1}$$

where, Z is scaling distance; R is stand-off distance from the target structure; E is total explosive thermal amount of energy; W is charge weight of equivalent TNT amount. The scaling distance is used for evaluation of blast wave characteristics.

2.2 Research trends

Concrete is generally known to have a relatively high blast resistance capacity compared to other construction materials. However, concrete structures, which were not designed to have blast protective capacity, require retrofitting during their service life to improve their resistance against blast loads. Retrofitting method of attaching extra structural members or supports to increase the blast resistance is inefficient in the perspective of additional construction cost and eliminating useable space. Also, since this method does not greatly improve the overall structural resistance against blast load, a more feasible method of retrofitting to improve blast resistance would be to use Ultra High Strength Concrete (UHSC) or Reactive Powder Concrete (RPC). UHSC and RPC would also be very effective in new constructions since they can be used for concrete materials in reinforced concrete members.

In fact, beams and plates constructed using high strength concrete (HSC) showed better impact resistance capacity than ones made using normal strength concrete (NSC) in past researches. However, due to social and governmental constraints, this type of comparison study has not been carried over to blast resistance capacity study, resulting in insufficient database of HSC's role as blast resisting material (Kim, 2009).

Recently, several researchers have pursued static and impact capacity studies on fiber reinforced concrete members under time-dependent loading conditions. The reference study has shown that the impact and blast loaded UHSC or RPC study results are non-existing and blast loaded HSC study results are scarcely existing at best (Habel et al, 2008).

3. BLAST TEST DETAILS

In this paper, the failure behaviors of reinforced UHSC and RPC slabs under blast loading are studied. The tests were performed as 2 step process of preliminary and main tests at Agency for Defense Development of Korea's testing sight. In the preliminary test stage, TNT 35lbs was used as blast load on control specimens (NSC specimen). After the trial tests, ANFO 35lbs was selected as the blast explosive charge to be used for the main test stage.

3.1 Blasting test setup

In this study, in order to eliminate the 3-D effect, RC slab specimens are placed at a same level as ground surface (Razaqpur et al., 2007). A steel frame is constructed and buried in the ground as shown in Figure 2(a). For preventing the supporting frame distortion during blast loading, the stiffeners with 250mm spacing are installed on wall surface of supporting frame. Rubber pads of the same width and length as the steel angle legs were placed between the angles and test specimen to ensure uniform support conditions. The explosive used for the test was spherical ANFO, which was held by wooden horizontal bar. Figure 2(b) shows the test specimen setup with the 35lbs ANFO (28.7lbs TNT) explosive charge. The 1.5m standoff from specimens to explosive middle point is consistently maintained.

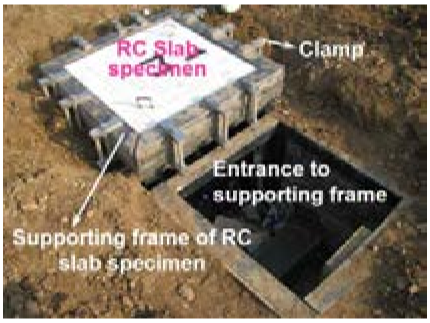

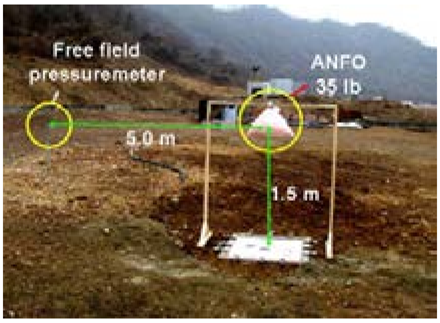

(a) Buried supporting frame (b) Explosive charge and specimen

Figure 2: Overview blast setup

3.2 Specimen Manufacturing and Details

For the relative and absolute comparisons between the specimens casted with UHSC, RCP, and NSC RC slabs with the dimensions of 1,000×1,000×150mm and D10 (71.33mm^2) mesh type reinforcements with 82mm spacing are used. The steel ratio of the reinforced NSC and UHSC specimens is same as the 2 volume % of short steel fibers used in RPC specimen. The mix proportions for NSC, UHSC, and RPC are tabulated in Table 2, 3, and 4, respectively. The 100×200mm cylindrical specimens are prepared for compressive and tensile strength tests performed at Hyundai Institute of Construction Technology. The number of specimens tested for NSC, UHSC, and RPC are 2, 4, and 4 specimens, respectively. The average compressive strength of NSC, UHSC, and RPC are 25.6, 202.0, and 203.0 MPa, respectively. The compressive strengths with a deviation over 15% are eliminated from consideration. The tensile strength of RPC is approximately 2.3 times greater (21.4MPa) than NSC (2.2MPa) and UHSC, (9.21MPa), respectively, due to the addition of 2 vol.% of short steel fibers in RPC.

Table 2: Mix proportion of normal strength concrete (NSC)

Max. Size of Coarse Aggregate (mm)	Target Strength (MPa)	Slump (mm)	W/B (%)	S/a (%)	Water (kg)	Binder (kg)		FA (kg)		CA (kg)	AE (kg)
						Cement	Fly-ash	S1	S2		
25	24	100	49.8	47.7	163	294	33	616	264	957	2.45

Table 3: Mix proportion range of ultra high strength concrete (UHSC)

W/B (%)	S/a (%)	Water (kg)	Binder (kg)	FA (kg)	CA (kg)	AE (%)
< 20	< 39.1	< 140	< 1300	< 450	< 700	1~3

Table 4: Mix proportion range of Reactive Powder Concrete (RPC)

W/B (%)	Cement (kg)	Water (kg)	Silica Fume (%)	FA (kg)	Filler (2.2~200 μm)	Admixture (%)	Steel Fiber (%)
< 20	< 800	> 200	10~30	800~1000	200kg ~	1~3	2

3.3 Measurement outline

The free field incident pressure was measured at 5m from the center of the test slab specimens where reflected pressure on concrete specimen was measure at the center of the top surface of the specimen and 230mm from the center. (e.g., 1/3 point of specimen diagonal length). To measure strain, 6mm strain gauges are attached on reinforcing steel at tensile region and 30mm strain gauges are attached on concrete top and bottom surfaces as shown Figure 3. In case of retrofitted specimen, FRP strain gauges are attached instead of concrete strain gauges on bottom surface. Also, LVDTs on the specimen center are used to measure the maximum and residual displacements.

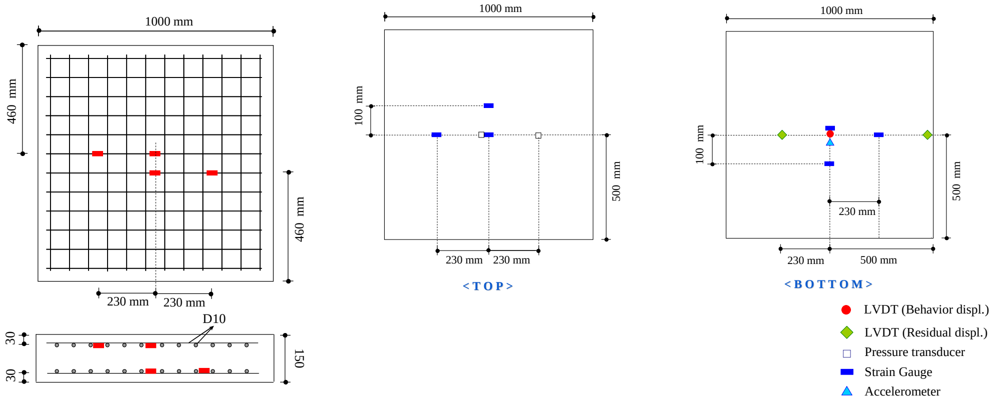

(a) *Steel strain gauge* (b) *Gauges on concrete surface*

Figure 3: Location of measuring sensor

4. BLAST TEST RESULTS

UHSC and RPC RC slabs are blast loaded to analyze their resistance performance. In the preliminary testing stage, NSC RC slab was tested to estimate the blast cracking behavior and the required explosive charge weight for the main tests.

4.1 Blasting tests

When ANFO 35lbs was used as the explosive charge, extreme wave of high pressure, temperature, noise, and energy dispersed out radially. The photos in Figure 4 are ANFO 35lbs detonation photos. Since ANFO detonation produces debrisless explosion, giving a more of pure pressure type of explosion loading, ANFO explosive charge is used for the main tests.

Figure 4: Explosive scene by ANFO 35lbs

4.2 Measured blast results

Due to the exploded metal debris of TNT steel container impacting and damaging the pressure gauge installed in the center–top surface of the specimen, the compressive blast pressure data was not obtained in the preliminary stage. The measured free field and reflected pressures of ANFO 35lbs are shown in Figure 5. And the other data are tabulated in Table 6.

The measured data are inconsistent due to the variations in experimental and environmental conditions (i.e., charge shape, charge angle, wind velocity, humidity, etc.). However, the obtained blast pressure data seem to agree well with ConWEP data.

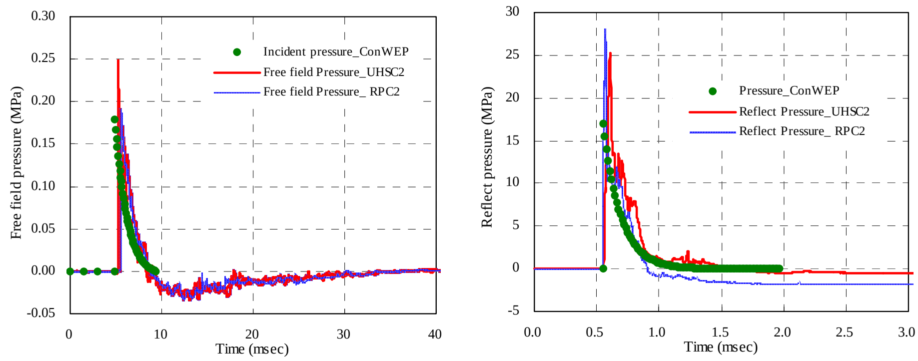

(a) Free field pressure *(b) Reflect pressure*

Figure 5: Measured pressure on specimens (ANFO 35lbs)

The incidental and residual deflections are measured from the blast test. Both deflection results of maximum and residual measurements are tabulated in Table 6. In the preliminary tests using TNT 35lbs, the maximum measured deflection at the center of the specimen was beyond 25mm measurement capacity of the LVDT. The specimen center deflection-time histories for NSC-TNT 35lbs, which exceeded LVDT measuring capacity, and NSC-ANFO 35lbs are shown in Figure 6. As shown in Table 6, the maximum and residual deflections from ANFO 35lbs for NSC, UHSC, and RPC are 18.57mm and 5.79mm, 12.83mm and 3..86mm, and 11.91mm and 4.31mm, respectively. As shown in Table 6, the bottom center concrete strains were over 16,000με for NSC, UHSC, and RPC specimens. However, when the strain measurements and displacements for NSC, UHSC, and RPC specimens are compared, RPC data at the specimen center tend to be less than those of NSC and UHSC specimens. This result is probably due to the short steel fiber reinforcing in RPC specimen where the fibers restrained crack opening by crack bridging and controlling effect.

Table 6: Test results

SPECIMEN		NSC1_2	NSC2	UHSC1	UHSC2	RPC1	RPC2
Charge		TNT 35lb	ANFO 35lb	ANFO 35lb	ANFO 35lb	ANFO 35lb	ANFO 35lb
Environ-ment	Temp.	11	5	8	NR	-9	NR
	Humid (%)	31	up 51	56	NR	39	NR
Reflect Pressure	Center (MPa)	NR	3079.64	NR	2454.1	NR	3189.9
	Impulse (MPa-msec)	NR	NR	NR	561.7	NR	409.9
	230mm (MPa)	NR	3854.4	NR	2720.7	3280.9	3205.3
	Impulse (MPa-msec)	NR	473.5	NR	437.6	294.4	477.75
Free Field Pressure	Peak overpressure	30.06	23.40	36.15	27.63	23.14	27.74
	Impulse (MPa-msec)	49.25	33.3	27.66	33.4	33.25	30.42
Max. displacement (mm)		over 25	18.565	10.517	15.14	10.73	13.09
Average of max displ.(mm)		18.565		12.829		11.910	
Residual displacement (mm)		12.260	5.790	1.860	5.86	3.202	5.41
Average of residual displ.(mm)		9.025		3.860		4.306	
Strain	Steel up	16012	5964	2796	2832	-	-
	Steel bottom	15998	28113	6711	7553.6	-	-
	Concrete up	NR	11848	4502	12821	11198	24214
	Concrete bottom	16007	NR	NR	NR	NR	4903

* NR : Not Record * NSC : Normal strength concrete(control specimen)
* UHSC : Ultra High Strength Concrete * RPC : Reactive Powder Concrete * - : Non-attached gauge

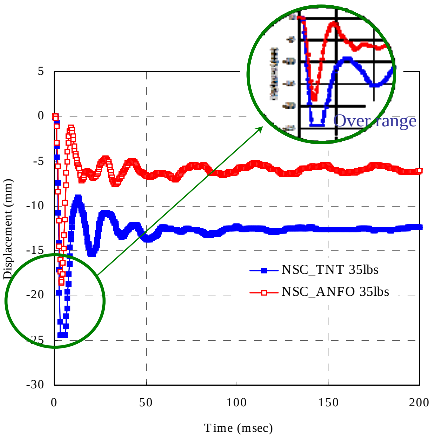

Figure 6: Displacement behavior of concrete specimen (NSC) center point under blast loading

4.3 Tested Specimen Examination

When the testing is completed and the safety is insured for the inspectors, the surface examination of the specimen was performed. Figure 7(a), 7(b), and 7(c) are the schematic drawings of NSC, UHSC, and RPC slab bottom surface crack distributions after ANFO 35lbs blasting, respectively. The NSC specimens had a well dispersed turtle back type crack pattern. The crack lines followed the cone prism type of plastic yield line from the center to the 4 corners, indicating a 2D membrane plastic failure mode. However, UHSC specimen's crack pattern showed mostly macro-cracks concentrated near or on the yield lines. The RPC specimens showed predominantly one directional, center bisecting type, macro-cracks. Since RPC specimen is made using cement mortar with short fibers, it tended to be brittle but the crack bridging effect of short fibers resisted crack propagation where the macro-cracks form only in the direction perpendicular to the principle tensile strain direction as shown in Figure 7(c).

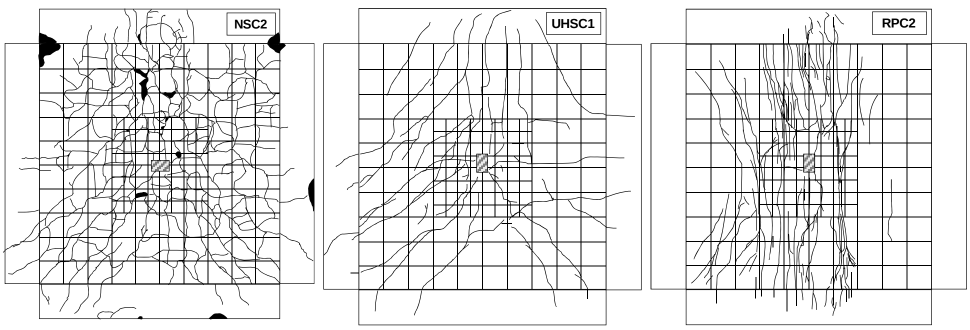

(a) NSC *(b) UHSC* *(c) RPC*

Figure 7: The crack pattern of blasted specimens (bottom side)

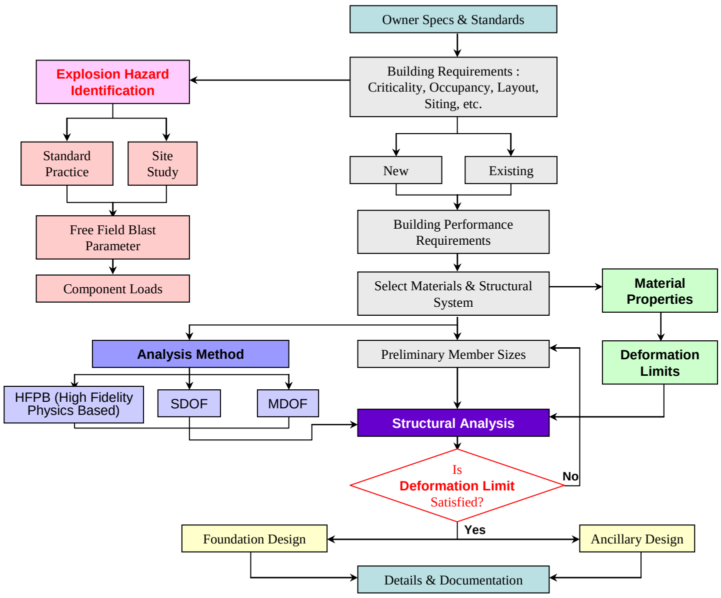

Figure 8: Blast design and analysis process

4.4 Blast design and analysis process

Based on the blast tests for NSC, UHSC, and RPC in this study, the blast design and analysis process are suggested. Most improtantly the building and owner requirements are needed for determination of blast resistance capacity of a targeted structure. To evaluate the building requirements, the blast loading on each component and resistance capacity can be derived from test results or research reports. If materials and structural system are selected, determination of deformation limit using analysis method such as HFPB (High Fidelity Physics Based) and SDOF, MDOF, etc. is selected for the blast analysis. The details of design will be accompanied with satisfaction of the deformation limit based on the analysis results.

5. CONCLUSION

From this study, Ultra High Strength Concrete (UHSC) and Reactive Powder Concrete (RPC) RC slabs' response induced by explosive of blast wave pressure are evaluated to understand the blast resistance capacity blast resisting repair materials and retrofitted structure. The reflected blast pressure and impulse values calculated using the ConWEP were in reasonable agreement with the experimental data. The performance comparison of UHSC and RPC specimens to NSC control specimens subjected to blast loads of ANFO 35 lbs has shown the high blast resistance capacity of about 30.9~35.9% increase with respect to average maximum displacement. An average of residual displacements was smaller than normal strength concrete specimen's residual displacement, even though there was no consistent trend due to variations in environmental conditions. Therefore, to evaluate the damage under blast load, failure mode must be considered. From the test results, the failure patterns of both UHSC and RPC indicate that they are much more resistant to blast loading and have higher blast resistance capacity than NSC.

ACKNOWLEDGMENTS

The research was supported the financial support provided Hyundai Engineering and Construction Co., Ltd and KOGAS from Ministry of Land, Transport and Maritime Affairs (Design standard of extremely large storage tank and optimum analysis technique).

REFERENCES

ASCE, 1999. *Structural Design for Physical Security: State of the Practice Report*. Task Committee on Physical Security, American Society of Civil Engineers, New York.

Baker, W.E., 1973. *Explosions in Air*. Wilfred Baker Engineering, San Antonio.

Harbel, K., and Gauvreau, P., 2008. Response of Ultra-High Performance Fiber Reinforced Concrete (UHPFRC) to Impact and Static Loading. *Cement and Concrete Composites*, Vol.30, 938-946.

Kim, H.J., Nam, J.W., Kim, S.B., Kim, J.H.J., and Byun, K.J., 2007. Analytical Evaluations of the Retrofit Performances of Concrete Wall Structures Subjected to Blast Load, *Journal of the Korea Concrete Institute*, Vol.19, No.2, 241-250.

Kim, J.H.J., 2009. *Experimental Evaluation for the Blast Resistance Capacity of Concrete Structure using Ultra High Strength Concrete*. Report of Hyundai Institute of Construction Technology.

Mays, G.C., and Smith, P.D., 1995. *Blast effect on Buildings: Design of Buildings to Optimize Resistance to Blast Loading*. Thomas Telford.

Razaqpur, A.G., Tolba, A., and Contestabile, E., 2007. Blast Loading Response of Reinforced Concrete Panels Reinforced with Externally Bonded GFRP Laminates. *Composite Part B : engineering*, Vol. 38, 535-546.

TM5-1300/AFR 88-2/NAVFAC P-39, 1990. *Structures to Resist the Effects of Accidental Explosions*. Joint Departments of the Army, Air Force and Navy Washington, DC.

Zineddin, M., and Krauthammer, T., 2007. Dynamic Response and Behavior of Reinforced Concrete Slabs under Impact Loading. *International Journal of Impact Engineering*, Vol. 34, 1517-1534.

OPTICAL SENSOR AND NEURAL NETWORKS FOR REAL-TIME MONITORING AND ESTIMATION OF HAZARDOUS GAS RELEASE RATE

WON SO, JAMIN KOO[1], DONGIL SHIN[2],
KYOSHIK PARK[3] and EN SUP YOON[1]
[1]School of Chemical & Biological Engineering, Seoul National University,
Seoul 151-744, Korea
[2]Dept. of Chemical Engineering, Myoungji University,
Yongin, Gyeonggi-do 449-718, Korea
[3]Institute of Gas Safety R&D, Korea Gas Safety Corp.,
Siheung-shi, Gyeonggi-do, Korea
sowon3036@pslab.snu.ac.kr

ABSTRACT

In this research, we propose a new method for estimation of the release rate using the concentration data obtained from the sensor network. We used optical sensor of the fence concept that has already been set surrounding the area where hazardous gas releases can occur. From real-time monitored data, we detected and analyzed releases of hazardous materials and their concentrations. Based on the results, the release rate is estimated using the neural network. This model consists of 14 input variables and one output. Case studies with chlorine and ammonia will be given to illustrate the implementation process. The proposed technique can provide precise estimates of release rates that can improve the accuracy and availability of information necessary for the success of the emergency information delivery system.

1. INTRODUCTION

Economic development and ever-increasing adoption of technology for everyday life have unavoidably introduced many dangerous facilities inside and nearby city. Accidental discharges of dangerous gases, either flammable or toxic, more likely to occur during manufacture, storage or transport could be considered as one of those cases. A feeling of insecurity for residents living nearby dangerous facilities increased, but response technologies are not accepted to be adequate [1, 2]. Many studies on real-time monitoring are progressing. The research of monitoring system based on sensor-network is practical to be applied in the field. However, existing methods are not easy to predict the release rate of toxic material using sensor-network. Thus, this research proposes a methodology for estimating release rate of toxic gases. This paper focuses on releases of material which are highly toxic gases produced and used in large quantities around the world. For example, chlorine, a highly toxic gas that is widely used for water disinfection, is produced and used in bottles of several dozens of kilograms all over the world [1].

In this research, we use an optical sensor network that has already been set up and operational surrounding an area where hazardous gas releases can happen. From real-time monitored data, we detect and analyze harmful materials releases and their concentrations. Based on the results, the rate of release is estimated using the neural network. This model consists of 14 input variables (sensor data, material properties, process information and meteorological conditions) and one output (release rate). Case studies with chlorine and ammonia will be given to illustrate the implementation process. The proposed technique can provide estimates of release rates that can improve the accuracy and availability of information key to the success of emergency information delivery system.

2. BACKGROUND

The availability of various dispersion models, artificial neural networks, and sensory equipments allowed the development of the monitoring technique proposed here. Thus, conceptual and practical description of each will be given throughout the rest of this section.

2.1 Dispersion models

There are three types of dispersion models that vary in complexity and application domains: three-dimensional, SLAB, and Gaussian. Three-dimensional models solve conservation of mass, momentum and energy equations and are especially effective in modeling the dispersion of clouds in complex geometry with obstacles. SLAB models are particularly useful with heavy gas dispersion. Gaussian models assume the distribution of dispersed molecules with standard deviations dependent on the atmospheric conditions and distance from the source [1].

In the context where the proposed technique is to be applied, geometrics of areas of interests may be complex but can be of a wide variety. Furthermore, hazardous gases whose release the technique attempts to monitor may be light or heavy. As a result, Gaussian model is selected as the dispersion model and the commercially available software PHAST is used in training the neural networks.

2.2 Neural networks

Neural networks are composed of simple elements operating in parallel. These elements are inspired by biological nervous systems. As in nature, the network function is determined largely by the connections between elements. One can train a neural network to perform a particular function by adjusting the values of the connections (weights) between elements. In general neural networks are adjusted, or trained, so that a particular input leads to a specific target output. The network is adjusted based on a comparison of the output and the target iteratively until the network output matches the target. Typically a large number of input/target pairs are needed to train a network. Neural networks have been trained to perform complex functions in various fields, including pattern recognition, identification visions and control systems [9].

2.3 Sensory Equipments

Different types of sensors are now available that can detect and measure concentrations of gaseous molecules in the perimeter. Among them, optical sensors appear attractive for their low cost, applicability and high sensitivity [11]. These sensors use the changes of optical absorption spectrum in reaction with molecules for detecting the target concentration. The ones used in the proposed technique rely on 4 submits for measuring the concentration: light-emitter, optical receiver, spectrum analyzer and concentration computing machine (fig. 2).

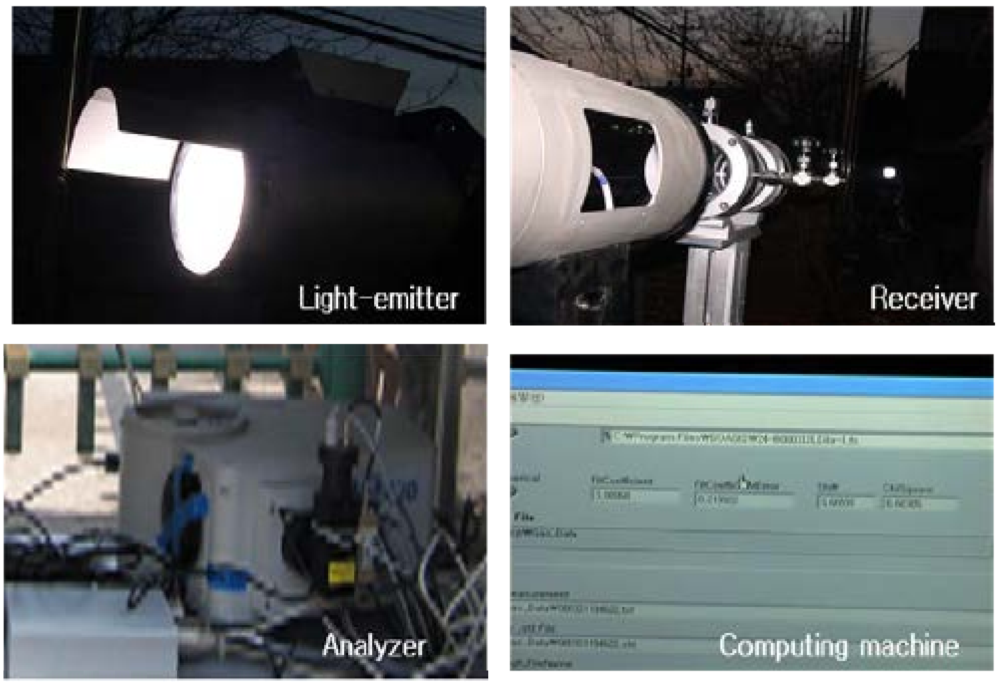

Figure 1: composing parts of the singular sensor network

3. METHODOLOGY

The combination of optical sensor network, back-propagation neural networks and the Gaussian dispersion model can build an effective, real-time monitoring system for storage vessels containing hazardous materials

3.1 Allocation of optical sensors

Optical sensors should be located in the way that the chances coverable area misses detection/measuring of releases is minimized, hopefully almost zero. With the optical sensors described in section 2.3, a single sensor forms a coverable area that extends cylindrically between the surface of the light emitter and receiver, as denoted by c_i. Meanwhile, the storage vessels containing hazardous materials-target for monitoring-forms an arbitrary three dimensional region *H* within which optical sensors attempt to detect/measure releases. Assuming that optical sensors detect and measure releases with a probability of 1 if the released molecules pass through the coverable area, the optimum allocation of n sensors is possible with respect to chances of detection/measuring and costs of sensors as in the following.

$$\min z_1 = \beta * \left(\int_H p(x,y,z)dV - \sum_{i=1}^{n} \int_{c_i} p(x,y,z)dV\right) + n * \alpha \qquad (1)$$

where p(x,y,z) is the probability that the released molecules pass the Cartesian point (x,y,z) within H, β is the cost per unit area for not being able to detect/measure releases, and α is the cost for a single optical sensor used.

Clearly, the specific allocation depends on the placement and shape of storage vessels containing hazardous materials, as well as the costs of sensors and missed releases. However, it is not easy, in fact cumbersome and case-specific to identify p(x,y,z) and β; if these are known, then the problem becomes a mathematical programming for which numerous solutions are available [12]. In a test experiment, a square H with 4 sensors placed at 1m above the ground that from a square-like fence around H has been tested for detection of releases.

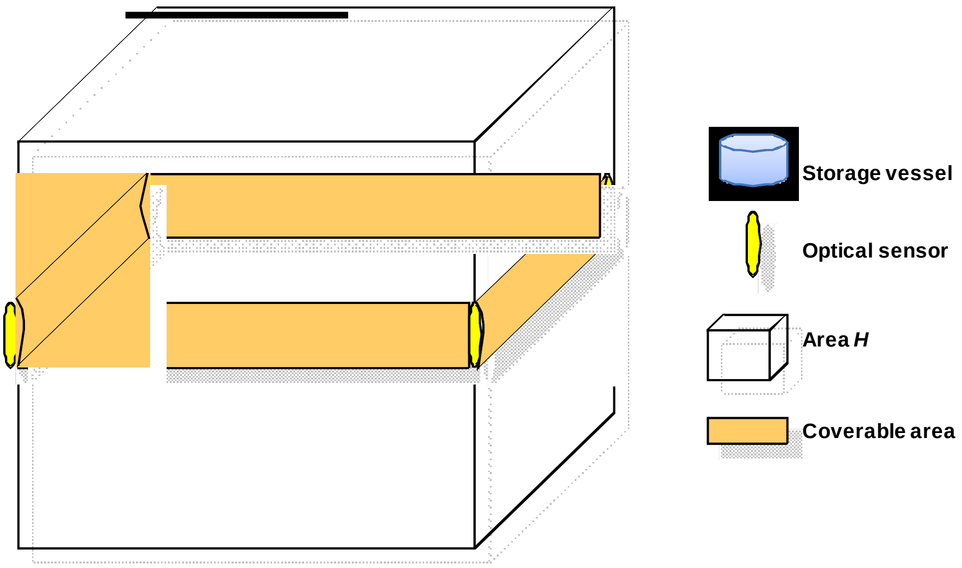

Figure 2: test experiment with 4 sensors covering a square H

3.2 Training the neural network

With the installation of optical sensors in the manner described in Section 3.1, the remaining issue is how to train the neural network. Since the proposed technique is designed to estimate the hazardous gas release rate, this becomes the target output layer in the neural network. The input layer consists of the selected input data from table 1. Then, the back-propagation algorithm is applied to calculate the weights between the input layer and the hidden layer of 20 units, and between the hidden layer and the output layer, under the MATLAB software package.

Table 1: Parametric sensitivities of input variables

Data	Release rate		Dispersion	
	Light gas	Heavy gas	Light gas	Heavy gas
Distance from source	0.0000 [a]	0.0000	-	-
Concentration	0.0000	0.0000	-	-
Wind velocity	0.0000	0.0000	649	375
Atmospheric stability	0.0000	0.0000	220	88
Temperature	0.0000	0.0000	67	21
Relative humidity	0.0000	0.0000	14	3
Storage pressure	0.0444	0.0623	118	46
Storage temperature	0.0024	0.0029	13	10
Storage quantity	0.0000 [c]	0.0000	3	5
Molecular weight	0.0443	0.0443	105	105
Density	0.0298	0.0674	157	251
Boiling point	0.0000	0.0000	0	0
Melting point	0.0000	0.0000	0	0
Vapor pressure	0.0000	0.0000	0	0

[a] The respective variable has no influence on the release rate.
[b] The concentration is the output variable in terms of which the dispersion parametric sensitivities have been calculated. Thus the obvious result, unitary sensitivity, has been recorded.
[c] The exact calculation result was not zero, but a number less than 0.0000 when rounded up.

There have been a limited number of release accidents in the past. So, a total of 1600 data generated from PHAST have been used for calculating the aforementioned parametric sensitivities. This is a size large enough to give R greater than 0.900 when a single kind of hazardous molecule is to be monitored; the specific value shows slight variance for different types of hazardous materials (Table 2). When more than one hazardous material is monitored, R remains acceptable while MSE increases like in Table 2. In this study, release rates of four different chemicals were estimated separately first, and then they were added to see how MSE changes (Fig. 3). As shown in the graphs, deviations from actual release rates do not increase substantially when the number of materials does not exceed 4. Indeed, MSE manages to be less than 0.1, which is still acceptable under the general view [15].

Table 2: Changes in R and MSE of the trained neural network

	1 (Cl_2)	1 (NH_3)	1 (SO_2)	1 (C_6H_6)	2	3	4
R	0.999	0.971	0.981	0.941	0.996	0.985	0.992
MSE	0.0225	0.0316	0.0399	0.0722	0.0734	0.0906	0.0988

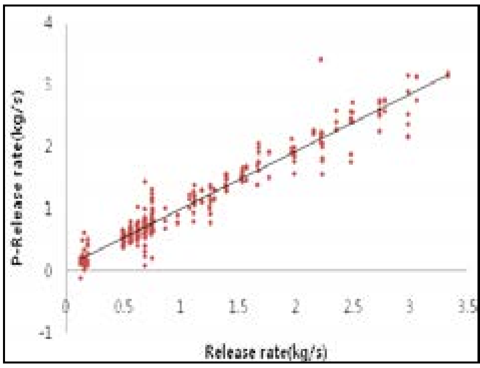

(a) 1 material

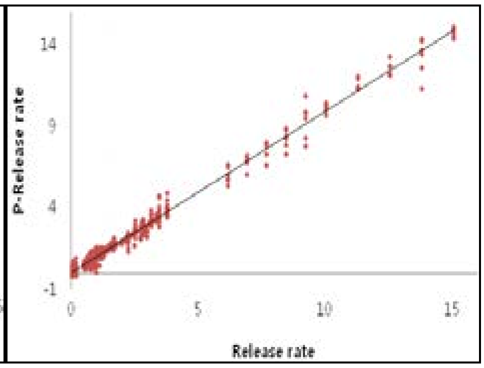

(b) 2 materials

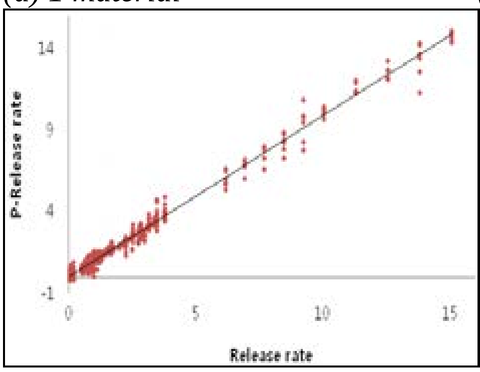

(c) 3 materials

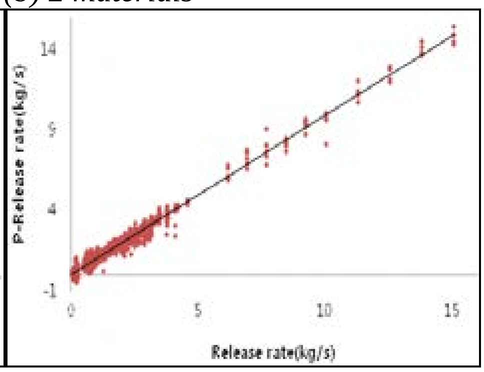

(d) 4 materials

Figure 3: Fitness analysis in the estimation of the release rate

4. CASE STUDY AND DISCUSSION

The proposed technique has been tested by an experiment conducted in a heat treatment factory located in southern East of Incheon City on March, 2008. An optical sensor was installed 100 meters away from the storage vessel containing ammonia; meteorological conditions were taken from the Korean Meteorological Administration Office. Ammonia was deliberately released from the vessel, and its concentrations dispersed at 100m away (where the sensor was installed) were measured throughout 3 weeks. The measurement data are presented in Fig. 4.

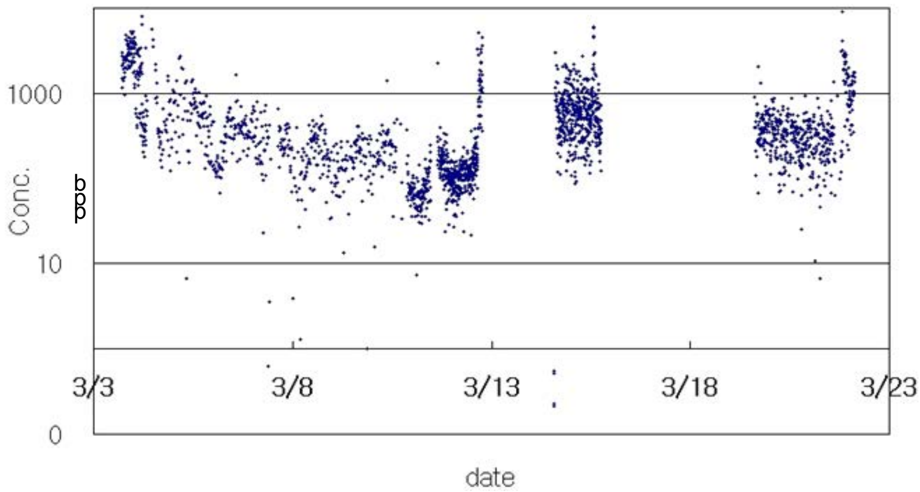

Figure 4: Ammonia concentration measured during a test experiment

As one may notice, measured concentrations deviate around 1,000ppb, or 1 ppm while the ERPG1 (Emergency Response Planning Guideline) of ammonia is 25ppm. In other words, the experiment was unable to validate the technique in a scale comparable to realistically threatening scenarios; therefore, a series of virtual scenarios (Table 3) is tested for reviewing the reliability and validity of the proposed technique. Specifically, the estimation of release rates by the proposed technique is compared against ones generated by commercially available software like TRACE. Phosgene and nitrogen oxide have also been included in the comparison so as to ensure the applicability of the proposed technique with materials other than the four mentioned in the previous section.

Table 3: Virtual release scenarios

	NH_3	Cl_2	$COCl_2$	NO_2
Distance from source	100 m	200 m	40 m	500 m
Concentration	2,500 ppm	1,000 ppm	200 ppm	100 ppm
Wind velocity	3.0m/s	1.5m/s	4.0m/s	2.0 m/s
Atmospheric stability	D	F	C	B
Temperature	7℃	20℃	30℃	10℃
Relative humidity	0.7	0.5	0.3	0.8
Storage pressure	1.0 bar	14.7 bar	2.0 bar	2.0 bar
Storage temperature	-20℃	25℃	20℃	10℃
Storage quantity	1,000 kg	2000 kg	100 kg	500 kg

Each scenario has been modeled with input variables of different magnitudes so that their collective range covers most of the accidents reported in Korea [14]. While the proposed technique directly estimates the release rate with the given input variables, it takes a trial and error approach for the commercially available software. The results are presented in Table 4.

Table 4: Comparison of release rates against by PHAST & TRACE

	NH_3	Cl_2	$COCl_2$	NO_2
Proposed Method	0.5727 kg/s	0.4849 kg/s	0.0764 kg/s	21.8927 kg/s
PHAST	0.6124 kg/s	0.4538 kg/s	0.1011 kg/s	21.9242 kg/s
TRACE	1.3015 kg/s	0.5887 kg/s	0.0416 kg/s	20.5200 kg/s

As illustrated in table 4, the proposed technique estimates the release rate within acceptable differences except for ammonia. The proposed technique estimates a value within 10% from that by PHAST, but the difference is more than 50% when compare to the result by TRACE. This is mainly due to the fact that the proposed technique is based on the Gaussian dispersion model like PHAST while TRACE is based on the slab model which is appropriate for heavy gases [1]; however, ammonia is a typical light gas. This tendency can be observed even when the target material is not a light gas like chlorine. The proposed technique gives values closer to that of PHAST for sharing the same dispersion model.

5. CONCLUSION

An efficient, real-time monitoring technique is proposed that can estimate the hazardous gas release rate by using optical sensor and neural networks. The comparison against widely used commercial software like TRACE and PHAST illustrate that the proposed technique can estimate release rates within acceptable differences; the proposed technique does so with a far less number of input variables in a shorter period of time-within seconds. Consequently, it offers advantages against the traditional monitoring systems in which release rates are, in the first places, assumed rather than estimated. The accurate, spontaneous measurement of release rates is crucial for taking immediate responses in the outbreak of release accidents. The proposed technique can be used to estimate this value, thereby contributing to the building of a more effective information delivery system. Additional validation of the technique with more materials will ensure its applicability in broader situations.

Nomenclature

C_{100} concentration (ppm) of dispersed molecules at 100 m away from the source

c_i area that extends cylindrically between the surface of the light emitter and receiver

d_i input data of type i

H arbitrary three dimensional region within which optical sensors detect/measure release

$p(x,y,z)$ probability that the released molecules pass the Cartesian point (x,y,z) within H

Q_m release rate in kg/s

s_1 parametric sensitivity of an input variable with respect to release rate

s_2 parametric sensitivity of an input variable with respect to dispersed concentration

α cost for a single optical sensor used

β cost per unit area for not being able to detect/measure releases

REFERENCES

[1] A. Dandrieux, J. P. Dimbour, G. Dusserre, 2006, *Are dispersion models suitable for simulating small gaseous chlorine releases*, J. Loss Prevention 19, 683-689.

[2] M. Abbaspour, N. Mansouri, 2005, *City hazardous gas monitoring network*, J. Loss Prevention 18, 481-487.

[3] R. K. Chohan, 1989, *Safety and fault detection in process control systems and sensors*, Fire Safety J. 14, 167-177.

[4] R. W. Lee, J. J. Kulesz, 2008, *A risk-based sensor placement methodology*, J. Hazard. Mater. 158, 417-429.

[5] S. Guo, R. Yang, H. Zhang, W. Weng, W. Fan, 2009, *Source identification for unsteady atmospheric dispersion of hazardous materials using Markov Chain Monte Carlo method*, Int. J. Heat and Mass Transf. 52, 3955-3962.

[6] S. T. Chung, K. I. Kim, 2009, *Case studies of chemical incidents and emergency information service in Korea*, J. Loss Prevention 22, 361-366.

[7] S. Alhajraf, L. Al-Awadhi, S. Al-Fadala, A. Al-Khubaizi, A. R. Khan, S. Baby, 2005, *Real-time response system for the prediction of the atmospheric transport of hazardous materials*, J. Loss Prevention 18, 520-525.

[8] H. Havens, M. E. Luther, S. D. Meyers, 2009, *A coastal prediction system as an event response tool: Particle tracking simulation of an anhydrous ammonia spill in Tampa Bay*, Mar. Pollut. Bull. 12

[9] A. T. C. Goh, 1995, *Back-propagation neural networks for modeling complex systems*, Artificial Intelligence in Engineering 9, 143-151.

[10] A. Arranz, S. Bordel, S. Villaverde, J. M. Zamarreno, B. Guieysse, R. Munoz, 2008, *Modeling photosynthetically oxygenated biodegradation processes using artificial neural networks*, J. Hazard. Mater. 155, 51-57.

[11] C. Massie, G. Stewart, G. McGregor, J. R. Gilchrist, 2006, *Design of a portable optical sensor for methane gas detection*, Sens. Actuators, B 113 , 830-836.

[12] A. D. Belegundu, T. R. Chandrupatla, 1999, *Optimization concepts and applications in engineering*, Prentice-Hall, New Jersey
[13] D. A. Crowl, J. F. Louvar, 2002, *Chemical Process Safety Fundamentals with Applications*, Prentice Hall, New Jersey
[14] J. Koo, S. Kim, H. Kim, E. S. Yoon, 2009, *A systematic approach towards accident analysis and prevention*, Korean J. Chem. Eng. 26, 262-269.
[15] B. Pradhan, S. Lee, 2007, *Utilization of optical remote sensing data and GIS tools for regional landslide hazard analysis using an artificial neural network model*, Earth Sci. Frontiers 14, 143–152.

EARLY EMERGENCY SYSTEMS BASED ON 3DGIS FOR DISASTER PREVENTION SAFETY-CITY

YOUNG-JIN PARK
National Institute for Disaster Prevention,
National Emergency Management Agency, Korea
yjpark@nema.go.kr

ABSTRACT

The rapid development of the information technology has passed over the implementation of the virtual reality. Virtual Reality has been applied to many fields: military, design, manufactory, information management, business, construction, disaster management, etc.. It is realizing information services that are form of the globalization, based on the Internet. In addition, the effort to apply IT to public administration for public services has been made. The remarkable development of computer hardware has overcome the limit of the information distribution and emerged for practical use in various fields such as public institution, underground facilities management, tourism industry development etc.

Geographic information system data and products have become a powerful resource, which is being utilized at all levels within our society. However, the practical use of Virtual Reality with Three-Dimensional GIS on disaster management by Korea National Emergency Management Agency is very much low.

This studies focus on how to use 3-Dimensional GIS for the purpose of fire disaster prevention. This paper presents an integrated Early Response Emergency System that uses 3D-GIS as the model source, CAD as the model generating tools, ArcGIS as analysis platform tools. This paper also discussed, through understanding of the limitations of 2-Dimensional GIS, the establishment of basis for fire prevention technology development and its utilization among those ubiquitous city paradigms, which have become so much issues these days.

1. INTRODUCTION

The most representative instances of the services are environmental geographic information system of the Ministry of Environment, aerial photography information system of National Institute of Science, satellite image search system of the Ministry of Land, Transport and Maritime

Affairs, geographic information system of Nuclear emergency management geographic information system, national park interview service, the service system of touring the national parks, etc.

As an Internet powerful country, we have 12.2 Fiber/LAN Internet service subscribers per 100 people as of the end of June, 2008, the first 1 place in ranking among the OECD 30 member countries, Japan, the second place with 10.2, Sweden, the third place with 6.0. However, comparing with the Internet subscription and access, its development seems to be restricted due to the limited kinds of contents and the higher dependency of software. Investment must be presciently made to develop the software of our own engine with dynamic ideas and more various kinds of contents through the cooperation between the private, Government, and academic sector.

Outside of the country, the United States, United Kingdom, Japan etc. have already built the 3 dimensional spatial information systems, and speedily lead an information age by providing the users with real sense of spatial information via web-base Internet. The diversified spatial information items are also freely applied to the spatial information industry field creatively.

As for the overseas countries, a private sector has firstly developed the terrain spatial information, which spreads to the open space on line from the restricted off-line place. In terms of the proposals and publicity activities to the national institution and the government and public offices, they are making a global standard in an industry information field both by ensuring a distribution network and creating benefits through the network linked by and between the private, Government, and academic sector.

This study, reviews will be made on the application importance and plan about the emergency management field, using GIS, especially complementing its business and analytical function which have not been embodied in the two-dimensional GIS, and an introduction will be made about the application instance of 3 dimensional GIS to copy with the social demand and expectation for multidimensional spatial information.

Especially, a research will be made on the application plan of 3 dimensional GIS, both by making a foundation for the technical development of emergency management information to embody the u-Safety City in line with this research and through an illustrative review over its application plan. Emergency management system can be briefly defined as the application of the GIS in the parts of the National land, City emergency management, etc. This means the application state or system, where the previous disaster information is processed in a database based on the GIS, and the GIS is usefully made use of both in a emergency management plan and daily works of management.

2 ROLES AND FUNCITON TO UPGRADE NATIONAL DISASTER MANAGEMENT

It is necessary to approach the disasters more from software side in order to prepare a scientific and systematic disaster plan, respond swiftly to the disasters, effectively rehabilitate the disasters. In this connection, we need to make a reasonable means to forecast the risk, extent, and size of the damage, not to mention the hardware emergency management policy like the installation of existing emergency management facilities. In order to achieve this, the following role and function are necessary in connection with the u-Safe Korea, which is being planned by the National Emergency Management Agency.

An integrated emergency management information DB is necessary to build in order to manage the national disasters. In order to build a country strong against disasters as well as to minimize at least the damages from the disasters, it is necessary to more actively carry out the project to build spatial information data related to disasters for each field according to the 6th general planning of emergency management. It is also necessary to build a database of spatial information for each type of disaster as per the place where it happens. Moreover, It is necessary to build a practical DB both through systematic data classification and checking the applicability on the basis of research result of terrain, geological features, soil, ground and floodgate.

An integrated disaster management system needs to be built with the precondition of liaison between related authorities and business alliance system. The e-government project, which was sought by the old Ministry of Government Affairs and Home Affairs, is clearly stated as building a general service of national security management based on the e-government road-map thirty one(31) tasks. To seek this, liaison and cooperation is definitely required by and between the related authorities.

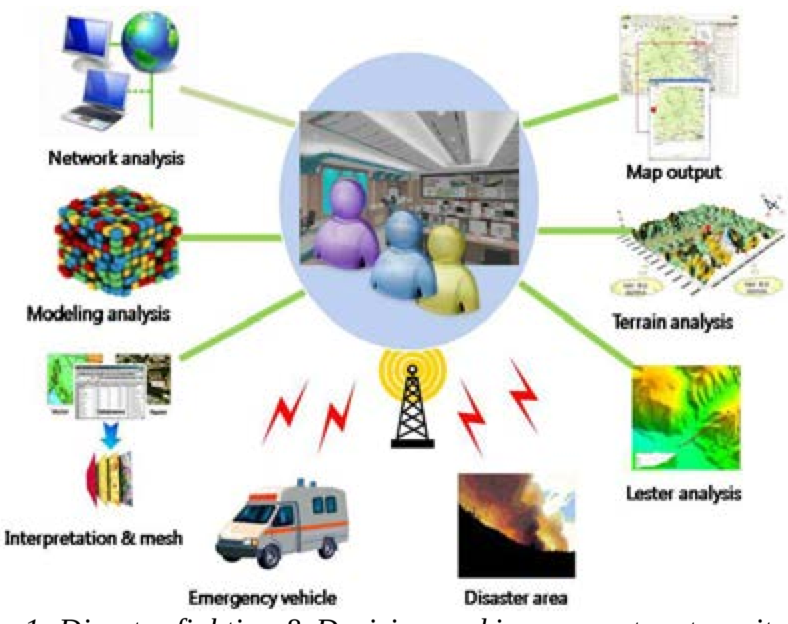

Figure 1: Disaster fighting & Decision-making support system situation propagation system of a local autonomous entity

It is necessary to solve the problems of technical disaster management which fights the variety of disasters and enhance the capability to confront the disasters through active use and application of high technology in emergency management field by upgrading the disaster fighting function and role, which have introduced GIS new technology.

2.1 Task for the application of multidimensional information

Emergency support navigator development for special purpose vehicles is proposed that a emergency management information navigator be developed for the exclusive use by special purpose vehicles, for which both of the spatial information where the information either of the facility in the disaster place, or of the place subject to disaster, or the danger facilities(city gas, drainage, hydrant, etc.) in the surrounding area are specified in detail, and of the detailed theme mapping is provided, where the detailed floor plan, spatial bird's-eye view, evacuation route, expected movement line, etc. are specified for the building of a certain facility which is highly subject to disasters.

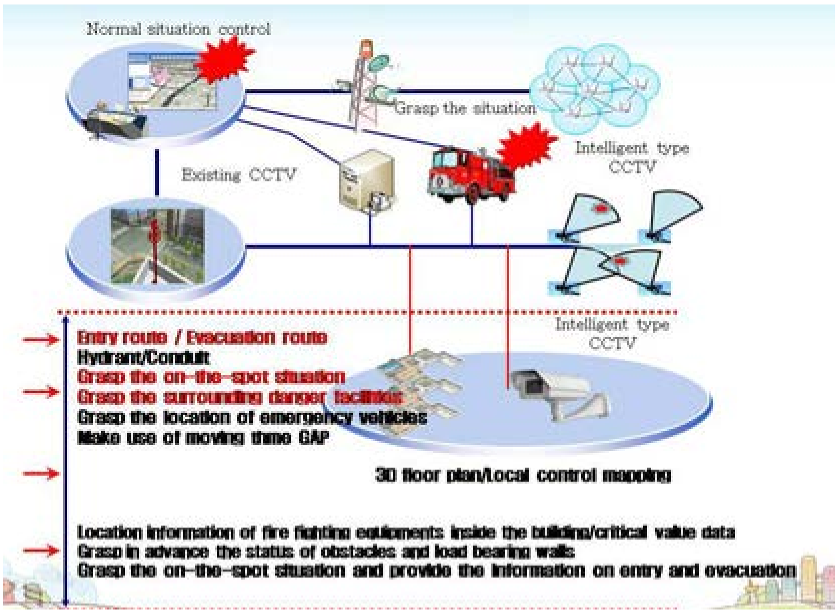

Figure 2: Development figurative of Navigator for special purpose vehicle

The joint application system of the national disaster management now being built and updated by the National Emergency Management Agency can be called a disaster situation manifestation system, which statistically manifests the real time disaster information collected from the nationwide disaster management system installed in Seoul and 16 cities and provinces all over the country. In order to perform this task, a test bed area was selected where it is easy both to collect the data for three dimensional modeling like numerical value mapping, aerial photos, fire protection data information, etc. and to design and build a prototype for the target area.

2.2 Regional range and prototype of testbed

The test-bed was implemented New City of Dongtan in Hwaseong city known as a sample of u-City was considered as second test bed area. However, the whole area of Bansong-dong in New City of Dongtan was selected as a target area of prototype designing, considering the difficulties with information safety in providing the data like aerial image photos and satellite photos, which are necessary in building a prototype. The test bed will be built in the whole area of Bansong-dong 17 in the city of Hwaseong, and the multiplex facility of Shinyoung Plaza building with 9 floors was selected as target building.

In this research, a prototype was built in connection with the prototype system demonstratively developed for the situation control, the research result of the “Standard Model Development of u-safe City” which had been sought by the National Emergency Management Agency in the year of 2007.

The implementation of the testbed monitors the condition of counter-fire facilities and structures and provides the person in charge with 24 hour/365 day real-time remote monitoring. If problems arise, alarm is automatically issued via 3D Web GIS based mobile systems so that the problem can be taken care of anywhere, anytime.

Especially, a prototype was built for the on-the-spot situation action to increase the adequacy of the application of fire monitoring service done in the previous research, on-the-spot action, and perception capability of disaster situation. Besides this, a domain was built for the fires happening in connection with human disaster, and "Disaster Situation Monitoring Service" was built for the purpose of on-the-spot action and handling the post-disaster problems.

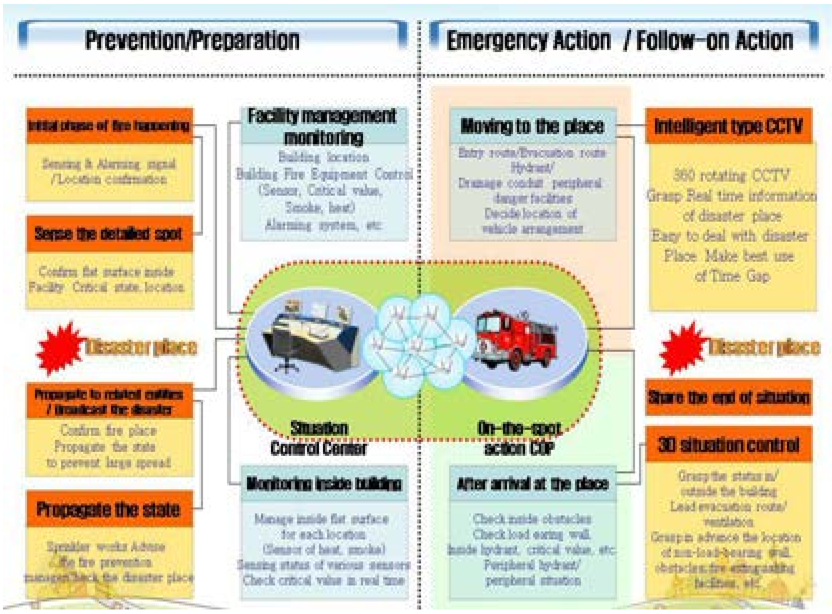

Figure 3: Situation monitoring service scenario assumption

3 ESTABLISHMENT OF PROTOTYPE STABLISHMENT OF SCENARIO FOR ON- THE-SPOT ACTION

This prototype scenario covers the on-the-spot situation management and disaster action for the "Disaster Situation Monitoring Prototype" out of the safety management services for the facilities subject to disaster and calamity (Standard Model Development of u-safe City, National Emergency Management Agency, 2007), the basic services of u-safe City.

The disaster control center of local autonomous entity or the control center of the fire fighting jurisdiction authorities is assumed as an integrated control center of the system, with a decision making support system which exchanges the information, in dualistic way, with a vehicle for moving to the disaster place (fire engine, emergency vehicle, special purpose vehicle, etc.).

The prototype in this research was designed so that a navigation can be used for a special purpose vehicle (fire engine, emergency vehicle, special vehicle, etc.) moving to a disaster place immediately after receiving such an order, assuming the disaster control center of local autonomous entity or the control center of the fire fighting jurisdiction authorities as the integrated control center of the system. In addition to this, the scenario was prepared with a purpose to build an unidirectional disaster fighting monitoring system, which is grafted on to the real time action against the disaster place by making use of the intelligent type CCTV, which is receiving an attention recently for the purpose of information safety, crime prevention and security

1) Arrangement function of emergency fighting vehicle

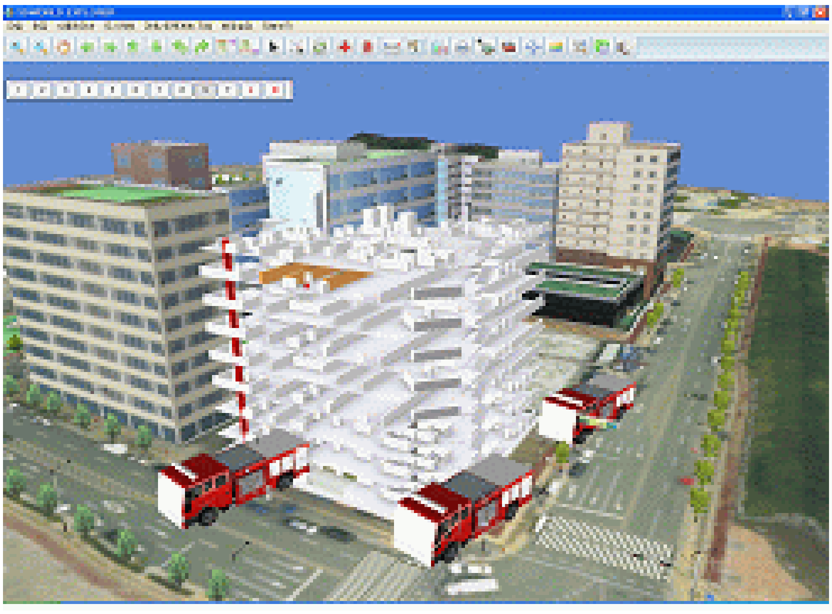

Figure 4 : Arrangement function of emergency fighting vehicle

○ Center:
- Constant support for emergency task of the group responsible for on-the-spot action
- Arrangement of fire fighting vehicles & Entry simulation to extinguish fire

○ Vehicle:
- Before moving·While moving
(Possible to simultaneously control with the Control Center)
- Proper arrangement of emergency vehicles & Entry route simulation
- Recognize overall emergency action by projecting the spatial floor plan of the entire building
- Discuss on fire extinguishing & disaster fighting while the group in charge are moving to the place

2) Location of hydrant inside Building

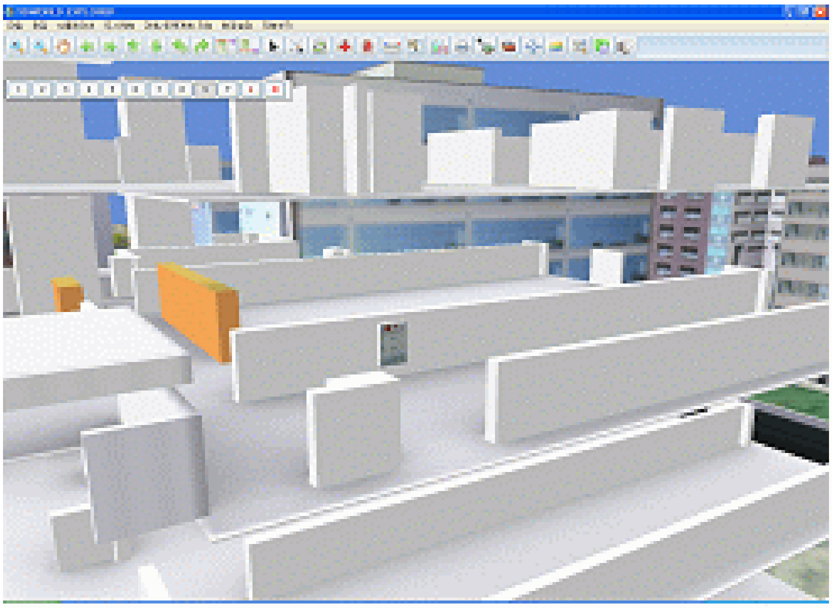

Figure 5: Location of hydrant inside Building

○ Center:
- Constant control of the flat surface inside the building in 3 dimensions
- Check the location and usability of Fire Extinguisher inside the building

○ Vehicle:
- Before moving·While moving
(Possible to simultaneously control with the Control Center)
- Check fire ignition point & available fire fighting equipments on the linked floor
- Discuss on fire extinguishing & disaster fighting while the group in charge are moving to the place

4 CONCLUSIONS

This prototype system was built for the test bed, and a 3 dimensional database was also built with the 3 dimensional transformation tool by making use of the existing 2 dimensional data. For the testbed, a prototype was built by making use of a [*Monitoring system of emergency area situation action system*]. For each situation by a scenario built, an explanation for each system and a detailed description for application plan were made. Especially, the system was test-run for the fire-fighting public servants now attending the University of Seoul to look into the application possibility and problems of this prototype system, obtaining an application plan of the research result and its improvement plan.

The improvement plan and application result of the developed prototype system are arranged as follows.

- *The system can be jointly used by the situation control center and the area office unilaterally or bilaterally.*
- *The upgraded situation control system can be more actively used.*
- *It is expected that the system will be more widely used considering its on-the-spot action capability and detailed information.*

It is the important point for the future system application both to increase the on- the-spot action capability by making use of the intelligent type CCTV and to develop the contents which provide the area situation realistically (considering the fact that the disaster situation system presently being used in each government ministry was upgraded, and both of the digital and real picture camera are actively used to take a picture of a disaster area situation). The system will provide the information which enables the users to expand the width of decision making.

As the present monitoring system has a variety of problems both technically and financially, like the enormousness of size, high cost, restricted provision of information, etc., it is important to provide each user with the information by adjusting its quantity by differently adjusting the equipment size and its application as per the location and time in consideration of the situation control center, emergency vehicle, on-the-spot action, etc.

For the recent skyscrapers, complex buildings, etc., fire prevention plan has been prepared to a certain degree. However, as for the old facilities etc., they are easily subject to disasters because of their building floor plan etc.

It is necessary to preferentially develop a system for the places which are easily subject to disasters, including the area between a city and farm village, general small-scale fire fighting targets, hot old housing district, etc.

ACKNOWLEDGMENTS

The authors would like to acknowledge Dr Sung Ho, Kim from the University of Seoul, and Technical Manager of Sung Heon, Jung from EGIS CO., LTD for their valuable contributions to this work.

REFERENCES

Kim, Sang Bong., Cho, Woo Jin, *A Study on the Development and Application of 3Dimensional Spatial Information of Virtual City Using Digital Photogrammetry*, Korean Society of Surveying, Geodesy, Photogrammetry, and Cartography, 2007.

Park, Inhye., Jun, Chulmin., Lee, Jiyeong, *Geographic Information System Association of Korea, GIS-based Fire Evacuation Simulation using CA Model*, 2008.7

Korea Institute of Construction & Transportation Technology Evaluation and Planning, *Construction of the 3D Virtual Land Information and Development of its Application*, 2006.8.19

Seoul Development Institute, *A Study on development of Seoul Virtual City using 3D GIS*, 2006

Jeremy Morley, 2003, *MasterMap in Academia-Experiences at UCL(University College London)*

P. Frederiksen. J, Grum. L.T, Joergensen, *STRATEGIES FOR UPDATING A NATIONAL 3D TOPOGRAPHIC DATABASE AND RELATED GEOINFORMATION*, National Survey and CadastreJ

Masahiko Murata, *3D-GIS Application for Urban Planning based on 3D City Model*, ESRI International User Conference 2004

IMPACT RESISTANCE OF REINFORCED CONCRETE WALL OF BREAKWATER CAISSON

[1]TAKU. MATSUBAYASHI, M. IWANAMI and [2]HIROSHI YOKOTA
[1]Port and Airport Research Institute, Japan,
(matsubayashi, iwanami)@pari.go.jp
[2]Hokkaido University, Japan, yokota@eng.hokudai.ac.jp

ABSTRACT

This paper describes experimental investigations on mechanical behavior of reinforced concrete (RC) walls under repeated impact loads, which are often observed in concrete caissons for breakwaters. In the experiment, mechanical behavior of one-way RC slabs under repeated impact loads was examined by conducting falling-weight impact loading tests. In the tests, two kinds of repeated impact loads were applied: repeated impact loads of which velocities were increased gradually from 1.0m/s to 6.0m/s, and repeated impact loads with constant velocity of 3.0m/s. The reinforcement ratio was changed to investigate the influence on the impact behavior of the slabs. As the results, it was found that the failure mode of all the test slabs was punching shear failure after yield of tensile reinforcement. Also, it was made clear that the number of repetition of impact loading until the ultimate failure was increased and that the maximum deflection of the slab was decreased, in case of RC slabs with higher reinforcement ratio. It was because increase in reinforcement ratio caused improved flexural rigidity and punching shear capacity. Accordingly, it was concluded that impact resistance of one-way RC slabs could be improved by increasing reinforcement ratio, showing the possibility of concrete caissons with higher resistance against impulsive wave forces or impact forces due to collision of concrete blocks.

1. INTRODUCTION

Figure 1 shows the typical structure of caisson-type breakwater in Japan. Filling materials such as sand are filled inside the reinforced concrete caisson to get sufficient weight. Moreover, there are concrete blocks in front of the caisson to reduce the wave forces. It is reported that huge impulsive wave forces or impact forces due to settlement of concrete blocks are acting

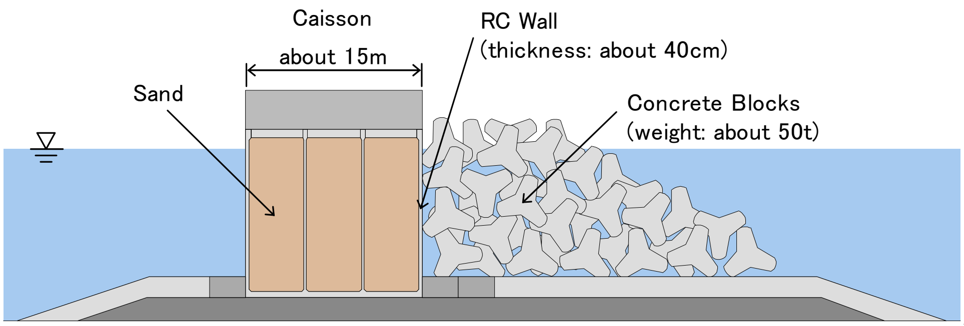

Figure 1: Typical structure of caisson-type breakwater

Photograph 1: The hole of the caisson-wall

repeatedly on such concrete structures, resulting in ultimate failure of concrete members (Hirayama, et al., 2005). Photograph 1 shows the hole of the caisson-wall which occurred by the impulsive wave forces. When the wall gets a hole, the sand inside the caisson is flown out, reducing the weight of caisson. It is serious because the stability of the caisson decreases.

In the present design of such concrete structures (Port and Harbor Association of Japan, 2007), impulsive wave forces, that have large variations with regard to time and space, are converted to equivalent distributed static loads in order to compare with the load carrying capacity of the structures in static conditions. Therefore, it is one of the problems that scatters of impulsive wave forces and dynamic behavior of concrete structures are not taken into account. A lot of studies on reinforced concrete (RC) members subjected to impact loading have been carried out (Kishi, et al., 2002, Chen, et al., 2009, Saatci, et al., 2009). However, the impact resistant design method considering such phenomena appropriately has not been completed.

In addition, it is necessary to examine countermeasures to improve structural performance of concrete members against repeated impact loads, which is applicable to breakwater caissons. However, there are few studies dealing with mechanical behavior of RC members subjected to repeated impact loading. In static conditions, the load carrying capacity of RC structures is improved by increasing reinforcement ratio. Similarly, it is expected that impact resistance of concrete members may be improved by increasing reinforcement ratio. Therefore, in this study, to investigate the influence of reinforcement ratio on impact resistance of caisson-type breakwaters, mechanical behavior of one-way RC slabs with different reinforcement ratios under repeated impact loads was examined by conducting falling-weight impact loading tests.

2. EXPERIMENTAL OUTLINE

2.1 Test slab

Two kinds of RC slabs were prepared: normal RC slabs (A-series) and RC slabs with higher reinforcement ratio (B-series). The reinforcement ratio of A-series is designed to be almost the same as the wall of concrete caissons. The tensile reinforcement ratio of B-series is about twice as much as that of A-series. The sizes of both series of slab are 1500mm in width, 160mm in thickness, and 2300mm in length, as shown in Figure 2. The slabs were tested under simply supported conditions with a shear span of 1000mm, leaving a 150mm overhang at each end. The thickness and span of the slabs are about 2/5 of the typical prototype of the wall of concrete caissons for breakwaters.

2.2 Material properties and calculated mechanical capacity of RC slab

Concrete and reinforcement used in the slabs have been widely applied in Japan. Table 1 lists concrete properties obtained from compressive tests on cylinders at the time of impact loading tests. Table 2 lists the yield stress of reinforcement from tensile tests. Table 3 presents static capacities of RC slabs which are calculated according to “Standard Specifications for Concrete Structures,” published by Japan Society of Civil Engineers (2007).

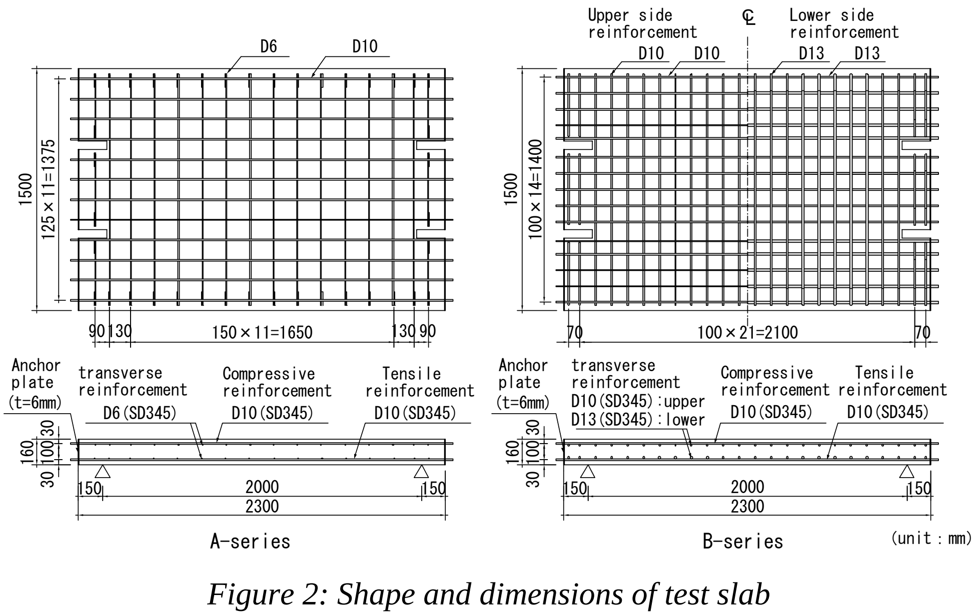

Figure 2: Shape and dimensions of test slab

Table 1: Concrete properties

Slab series	Designation	Compressive strength (N/mm^2)	Young's modulus (kN/mm^2)
A	A-1	40.8	30.2
	A-2	44.3	30.4
B	B-1	40.8	30.2
	B-2	44.3	30.4

Table 2: Yield stress of reinforcement

Steel bar	Yield stress (N/mm^2)
D6	365
D10	384
D13	380

Table 3: Calculated static capacities of RC slabs

Slab series	Designation	Flexural capacity (kN)	Punching shear capacity (kN)
A	A-1	95.1	175.2
	A-2	96.5	175.2
B	B-1	182.7	253.6
	B-2	184.6	253.6

2.3 Impact loading test

Table 4 summarises the test cases. In the tests, two kinds of repeated impact loads were applied: repeated impact loads of which velocities were increased gradually from 1.0m/s to 6.0m/s (Loading Method I), and repeated impact loads with constant velocity of 3.0m/s (Loading Method II). These impact velocities were determined in consideration of velocities of impulsive wave forces measured in actual breakwaters (Arikawa, et al., 2005). For the repeated impact loading tests, an impact loading testing machine was used, as shown in Photograph 2. A steel weight is lifted to the predetermined height by a small crane, and the weight free-falls by releasing a hook. The weight is dropped onto the center of the top surface of the slab. The mass of the weight is 400kg, and the impact face of the weight has a spherical shape with a diameter of 565mm. Figure 3 shows the shape of the steel weight. To prevent the slab from bouncing out, the slab is held with steel beams at the two supporting points. To reduce scatters of impact response, caused by local damage of the top surface of the slab, a rubber sheet of 10mm in thickness is placed at the impact position of the slab.

Table 4: Test cases

Slab series	Designation	Loading method	Impact velocity V (m/s)
A	A-1	I	1,2,3,4,5,6
	A-2	II	3
B	B-1	I	1,2,3,4,5,6
	B-2	II	3

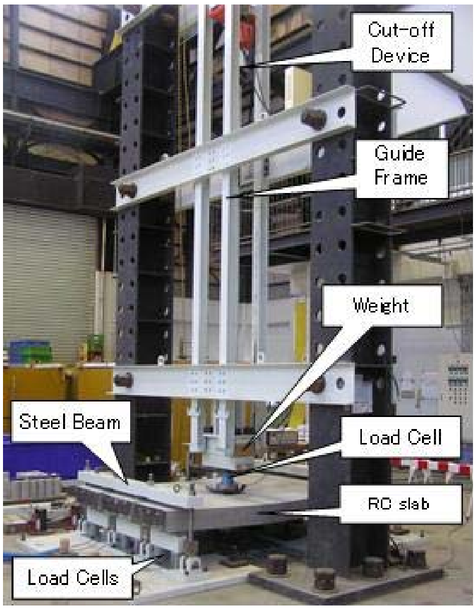

Photograph 2: Impact loading testing machine

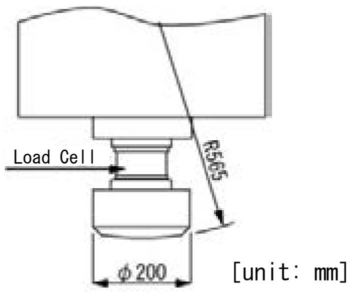

Figure 3: Shape of steel weight

The ultimate state of the slab was defined as clear formation of punching shear cracks in the slab. The impact loads were applied repeatedly until the ultimate state.

The impact force developed between the weight and the slab was measured using a load cell mounted to the weight. The reaction forces at supporting points were measured using load cells set at the supporting devices. The midspan displacement of the slab was measured using a laser-type displacement sensor. Also, cracks of the slab were observed periodically during the tests.

3. EXPERIMENTAL RESULTS

3.1 Results of impact test by Loading Method I

All the test slabs showed the punching shear failure after yield of tensile reinforcement. Figure 4 shows the relationships between impact velocity and displacement of the slab measured at the center of the bottom surface. The maximum displacement of A-1 increased from 1.5mm to 63.1mm when the impact velocity increased from 1.0m/s to 6.0m/s. Similarly, the maximum displacement of B-1 increased from 0.3mm to 44.0mm. It was found that the maximum displacement and residual displacement of B-1 became smaller than those of A-1. Therefore, the deflection of RC slabs subjected to repeated impact loading can be mitigated by increasing reinforcement ratio.

Both A-1 and B-1 reached the ultimate state when the impact velocity was 5.0m/s. Photograph 3 shows the damage state of the bottom surface of the slabs. Punching shear failure of RC slabs occurred regardless of the deflection state when the impact velocity was relatively large.

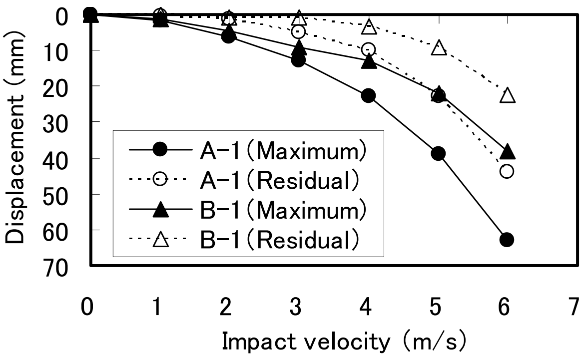

Figure 4: Impact velocity vs displacement of the slabs

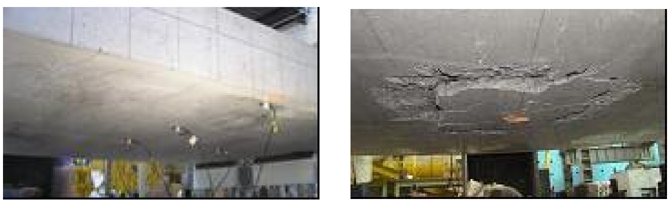

V = 1.0m/s *V = 6.0m/s*

(a) A-1

V = 1.0m/s *V = 6.0m/s*

(b) B-1

Photograph 3: Appearance of bottom surface of the slabs

3.2 Results of impact test by Loading Method II

All the test slabs showed the punching shear failure after yield of tensile reinforcement. Figure 5 shows the relationships between number of repetition of impact loading and displacement of the slab measured at the center of the bottom surface. The displacement of slabs increased remarkably at the stage of smaller numbers of repetition. Then after a slow progress, the displacement again increased acceleratedly with approaching the ultimate state. The whole tendency of the relationship drew an S-shaped curve. Figure 6 shows the crack patterns of the bottom surface of slabs for typical numbers of repetition. According to the observation of crack patterns of A-2, flexural cracks and radial cracks occurred at the bottom surface of the slab after the first impact loading and the amount of these cracks increased until about the 10th impact loading. Afterwards, these cracks did not increase so much until about the 25th impact loading. After about the

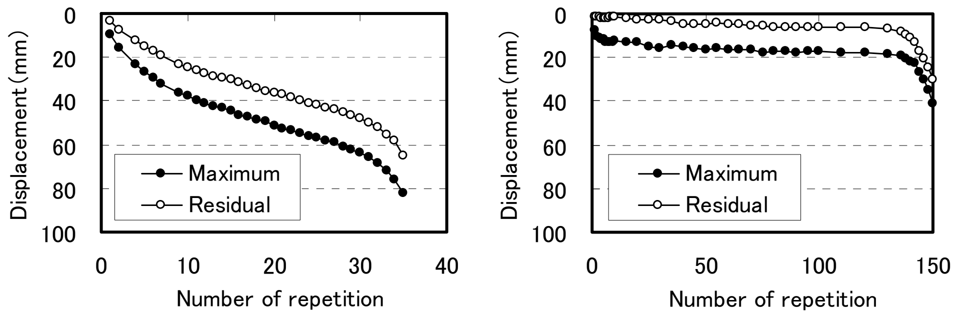

(a) A-2 *(b) B-2*

Figure 5: Number of repetition vs displacement of the slabs

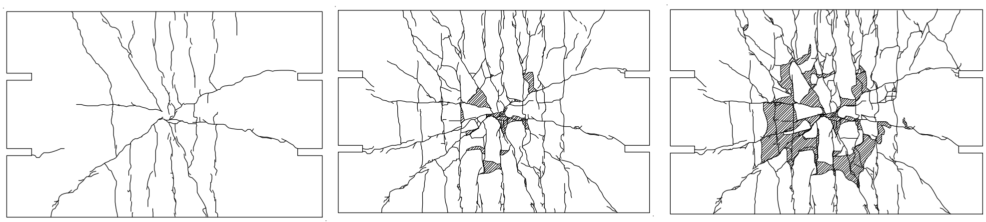

[1] *[25]* *[35]*

(a) A-2

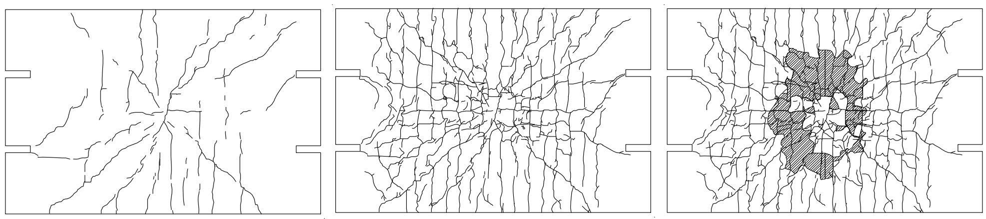

[1] *[100]* *[150]*

(b) B-2

[ ]; Number of repetition

Figure 6: Crack pattern of test slabs subjected to repeated impact loads

25th impact loading, punching shear cracks occurred. As shown in Figure 5 (a), the tendency of displacement progress was changed when the numbers of repetition were 10 and 25. Therefore, the tendency of displacement progress relates to the damage state of slab. It is supposed that the cause of rapid progress of the displacement until 10th impact loading was decrease in flexural rigidity of the slab due to increase in number and width of cracks. The cause of further progress of the displacement after 25th impact loading is considered that the punching shear capacity of the slab was declined by the occurrence of punching shear cracks.

In case of B-2, the whole tendency was similar to A-2 (S-shape curve). However, the amount of cracks of B-2 was much more than that of A-2. The number of repetition of B-2 until the ultimate state was about five times of A-2, and the displacement of B-2 until the ultimate state was about 1/3 of A-2. It was because that increase in reinforcement ratio caused improved flexural rigidity and punching shear capacity. Therefore, it is supposed that the number of repetition of impact loading until RC slabs reach punching shear failure can be increased by increasing reinforcement ratio when the impact velocity is relatively low, showing the possibility of improving the performance of port concrete structures against impulsive wave forces or impact forces due to collision of concrete blocks.

Figures 7 and 8 show the relationships between number of repetition of impact loading and maximum impact forces and maximum reaction forces measured by load cells mounted to the falling weight and supporting

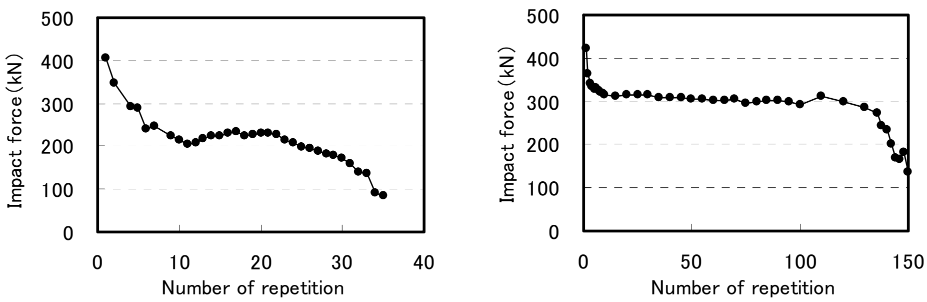

(a) A-2 (b) B-2

Figure 7: Number of repetition vs maximum impact force

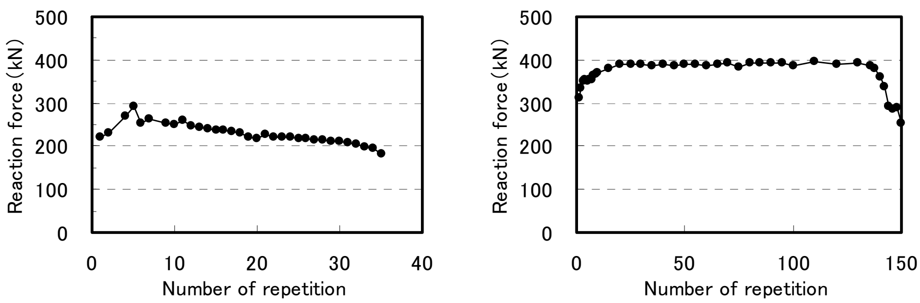

(a) A-2 (b) B-2

Figure 8: Number of repetition vs maximum reaction force

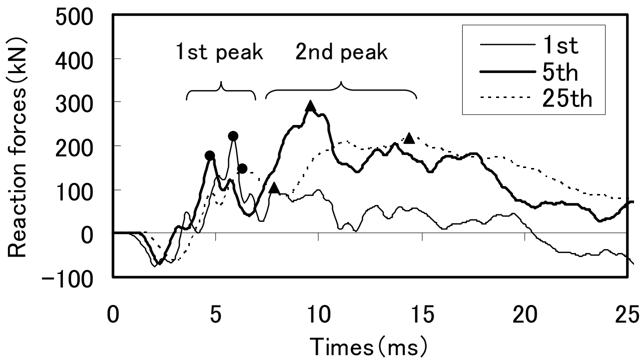

Figure 9: Time history of reaction forces (A-2)

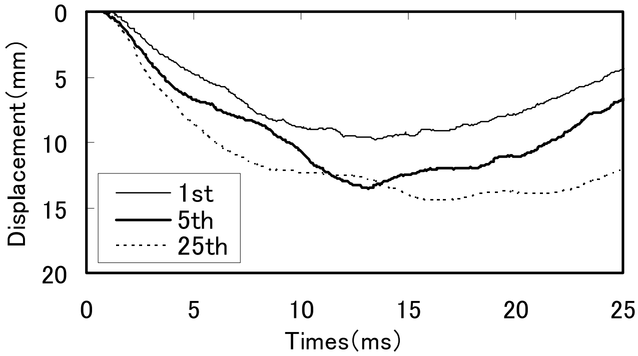

Figure 10: Time history of displacement (A-2)

devices. As for the maximum impact forces, the tendency of measured data was consistent with the tendency of displacement (S-shape curve), as shown in Figure 5. It is supposed that the decrease in flexural rigidity and declination of punching shear capacity of the slab influenced the impact force.

As for the maximum reaction forces, the tendency of measured data was not consistent with the tendency of displacement. Figure 9 shows time-history response of reaction force in case of A-2 for typical numbers of repetition. There are two kinds of peak in the waveform (first peak:●, second peak:▲). In case of the first impact loading, the first peak of reaction force was larger than the second one. In cases of the 5th and 25th impact loadings, the first peak was smaller than the second one. This phenomenon suggests that the factor to produce the maximum reaction force is different. Figure 10 shows time-history response of displacement of the slab measured at the center of the bottom surface in case of A-2. The first peak does not relate to the time when the displacement reached the maximum. The first peak decreases as the number of repetitions of the impact loading increases. Therefore, it is supposed that the reaction force at the first peak relates to the local damage of the slab at the impact point. The waveform including the second peak is roughly corresponding to the flexural deformation of the slab. Therefore, it is supposed that the second peak relates to the flexure of slab.

4. CONCLUSIONS

Based on the experimental results of repeated impact loading tests on one-way RC slabs, the following conclusions can be drawn:

- The deflection of RC slabs can be mitigated by increasing reinforcement ratio.
- Punching shear failure of RC slabs occurred regardless of the deflection state when the impact velocity is large.
- The number of repetition of impact loading until punching shear failure can be increased with increase in reinforcement ratio when the impact velocity is low.
- Increase in reinforcement ratio has the possibility of improving the structural performance of caisson-type breakwaters against impulsive wave forces or impact forces due to collision of concrete blocks.

REFERENCES

Arikawa, T., Ikebe, M., Osaki, N., Kuroda, T., Orita, T. and Shimosako, K., 2005. Study on punching shear failures of caisson wall caused by the impulsive force of dissipating blocks, *Report of the Port and Airport Research Institute*, V.44, No.1, 43-83. (in Japanese)

Chen Y. and May, I. M., 2009. Reinforced concrete members under drop-weight impacts, *Structures and Buildings*, V.162, Issue SBI, 45-56.

Hirayama, K., Minami, Y., Okuno, M., Minemura, K., Kawai, H., Hiraishi, T., 2005. Case study on wave disaster due to typhoons in 2004, *Technical Note of the Port and Airport Research Institute*, No.1101. (in Japanese)

Kishi, N., Mikami, H., Matsuoka, K.G. and Ando, T., 2002. Impact behavior of shear-failure-type RC beams without shear rebar, *International Journal of Impact Engineering*, V.27, 955-968.

Saatci, S. and Vecchio, F.J., 2009. Effects of Shear Mechanisms on Impact Behavior of Reinforced Concrete Beams, *ACI Structural Journal*, V.106, No.1, January-February, 78-86.

Standard Specifications for Concrete Structures-2007, *Design*, Japan Society of Civil Engineers, 2007. (in Japanese)

Technical Standards and Commentaries for Port and Harbour Facilities in Japan, Port and Harbor Association of Japan, 2007. (in Japanese)

A BASIC STUDY ON DEVELOPMENT OF NEW TRAINING SYSTEM FOR BUILDING DAMAGE ASSESSMENT

[1]MAKOTO FUJIU, [1]MIHO OHARA and [2]KIMIRO MEGURO
[1]Interfaculty Initiative in Information Studies,
The University of Tokyo, Japan
[2]ICUS, Institute of Industrial Science, The University of Tokyo, Japan
(fujiu, ohara, meguro)@iis.u-tokyo.ac.jp

ABSTRACT

Building damage assessment is necessary for governments to issue the Victim Certificates for residents who suffered housing damages. The process of assessment needs accuracy, quickness, objectivity and fairness because the results of assessment are used as criteria for providing public monetary supports for rebuilding their livelihood. In Japan, several big earthquakes are expected to occur in the near future. A lot of structural damages due to these earthquakes will cause enormous needs for building damage assessment. However, current number of human recourses who are trained with the procedure of building damage assessment is not enough. It is necessary to increase the number of investigators before a next event occurs. Moreover, recent experiences of assessment after past disasters pointed out several problems of the current system. Usually, investigators are consisted of non-experts of structural engineering such as general officials in local government, who were trained with the assessment procedure in a very short time after the disaster. Insufficient training led to the unequal personal skill of judgment and finally caused many misjudgments of housing damage. In order to achieve quick, accurate, objective and fair assessment, effective training system for building up qualified investigators who are familiar with the standard procedure before disasters is essential.

In this research, new training system for building damage assessment using virtual reality technology was proposed. First, problems of past building damage assessment were analyzed and applicability of new technologies including virtual reality for achieving ideal training system was discussed. Then, prototype images of new training system using virtual reality technology were developed based on the data of totally damaged houses due to the 2007 Niigata Chuetsu-oki earthquake in Japan.

1. INTRODUCTION

In Japan, several big earthquakes are expected to occur in the near future. A lot of structural damages due to these earthquakes will cause enormous needs for building damage assessment. Building damage assessment is necessary for governments to issue the Victim Certificates for residents who suffered housing damages. However, current number of human recourses who are trained with the procedure of building damage assessment is not enough. It is necessary to increase the number of inspectors before a next event occurs. The guidelines of general procedure for inspecting building damage and evaluating loss due to disasters were published by the Cabinet Office in 1968, 2001 and 2009. However, in past disasters, various problems of building damage assessment have been pointed out such as inspection accuracy, inspection quickness and lack of human recourses with sufficient skill of assessment.

In this research, new training system for simulating building damage assessment using virtual reality was proposed and prototype system was developed. Recently, several researches using virtual reality have been done in the field of disaster prevention, such as simulators for experiencing disaster (Doi, 2000) and fire drills (Masumura, 2001) etc. Virtual reality is defined as moving freely in the space using computer display, head mount display (HMD), screen, web site and so on. Virtual reality technology has high possibility for drastically enhancing people's response capacity to disasters.

2. PROBLEMS OF PAST BUILDING DAMAGE ASSESSMENTS

There are 3 inspection stages in building damage assessment such as "Primary Inspection", "Secondary Inspection" and "Issue of the Victim Certificates". Through these stages, damage levels of buildings are decided by visual inspection. The primary inspection evaluates the damages appeared on the exterior of a building. The secondary one evaluates not only the exterior damage but also the interior damage. The purpose of the secondary inspection is to provide the second opinion for the evaluation when the owner or resident of a damaged house does not accept the result of the primary one. Therefore, the primary inspection is carried out for all the damaged buildings, while the secondary inspection is usually carried out by request. Finally, Victim certificates for residents are issued from the local governments.

In past disasters, building damage assessments were carried out in Japan. However, various problems have been pointed out for the past building damage assessments. We reviewed literatures regarding past several building damage assessments such as Shigekawa (2005) and classified reported problems as shown in table 1. As a result, enormous problems in each inspection stage were obtained. The process of assessment needs accuracy, quickness, objectivity and fairness because the results of the assessments are used as criteria for providing public monetary supports for rebuilding their livelihood.

Table1: Problems of building damage assessment after past earthquakes

Flow of Inspection		2004 Niigata Chuetsu Earthquake	2007 Niigata Chuetsu-oki Earthquake
Ⅰ-Criteria	①Criteria	There is no standard to carry out the building damage assessment. Neither examination methods nor the inspection methods are clearly provided. Only guidelines were issued by the Cabinet Office. (Shigekawa,2005)	
Ⅱ-Training of Inspector	②Summon of Inspection	Insufficient number of assistant staff (Shigekawa,2005)	Difficulty in assemble of inspectors (Tanaka,2008)
	③Training	Because method of assessment is different in each local government, training is difficult. (Horie,2004)	−
	④Organize	Difficulty in gathering enough number of Inspectors and keeping inspection quality (Shigekawa,2005)	−
Ⅲ-Screening	⑤Screening	Limit in on-site inspection for lack of inspectors	
Ⅳ-Inspection	⑥Primary Inspection	Inspector's knowledge was insufficient. (Shigekawa,2005) Problem concerning inspection accuracy (Shigekawa,2005)	Difference between structural engineer's aspect and the Cabinet Office guideline (Tanaka,2008) Problem concerning inspection accuracy (Tanaka,2008)
	⑦Secondary Inspection	Difficulty in responding to residents who have dissatisfaction in inspection results (Shigekawa,2005)	Difficulty in predicting number of application (Tanaka,2008) Needs for assistant staff's (Tanaka,2008)
	⑧Victim Certificate	The efficiency of work was low, because the issue of enormous certificates was the first time for local governments. (Yoshitomi,2005)	−

3. PROPOSAL OF NEW TRAINING SYSTEM FOR BUILDIND DAMAGE ASSESSMENT

Based on the problems of past building damage assessments, we proposed solutions for improving each inspection stage using new technologies as shown in Table 2. In order to carry out ideal building damage assessment, all the stages in table 1 should be improved. Among all, this paper especially focused on the "II. Training of Inspector" stage.

In table 1, we proposed two types of training method. The first one is "a seminar for simulating assessment procedure on virtual reality space using head mount displays (HMDs)". Trainees experience building damage assessment of damaged houses using HMDs. On the simulator, damaged house are reproduced in the virtual reality space. Because a HMD is precious and the number of HMDs is limited, trainees are necessary to gather in the hall for using it. The second one is "Web based training". In "Web based training", we propose "training using web based simulation" and "training using web based simulation on virtual reality". There are a lot of advantages in web based simulation. For example, trainees can train at free time, a lot of people can participate in training at the same time, and it is easy to manage their results and abilities.

Figure 1 shows the concept of "training system using web based simulation training on virtual reality". Trainees access the Learning Management System (LMS) at free time for studying. Results and abilities of trainees are recorded in human resource database by the LMS. The manager can give inspection licenses according to their abilities in preparation for large-scale disasters. When a disaster occurs and building damage inspectors are needed, the managers can organize assessment teams using human resource database and dispatch them to the damaged area.

Table 2: Proposal of solutions using new technologies

Inspection Flow	New Technologies	
Ⅰ - Criteria	・Decision of new inspection standard ・Restructuring of new assessment procedure	
Ⅱ -Training of inspector	Seminar	・Simulation training on virtual reality space using Head Mount Display
	Web based training	・Web based simulation training ・Web based simulation training on virtual reality
Ⅲ - Screening	・Prior screening of severely damaged area by result of aerial survey ・Prior screening of severely damaged area using satellite photographs	
Ⅳ - Inspection	・Automatic inspection by image data processing of photographs of damaged buildings ・Remote inspection by forwarding damage photographs to specialists ・Automatic inspection using portable inspection devices ・Cut down of inspection procedures by using damage information by aerial survey ・Management of damage assessment data based on GIS mapping	

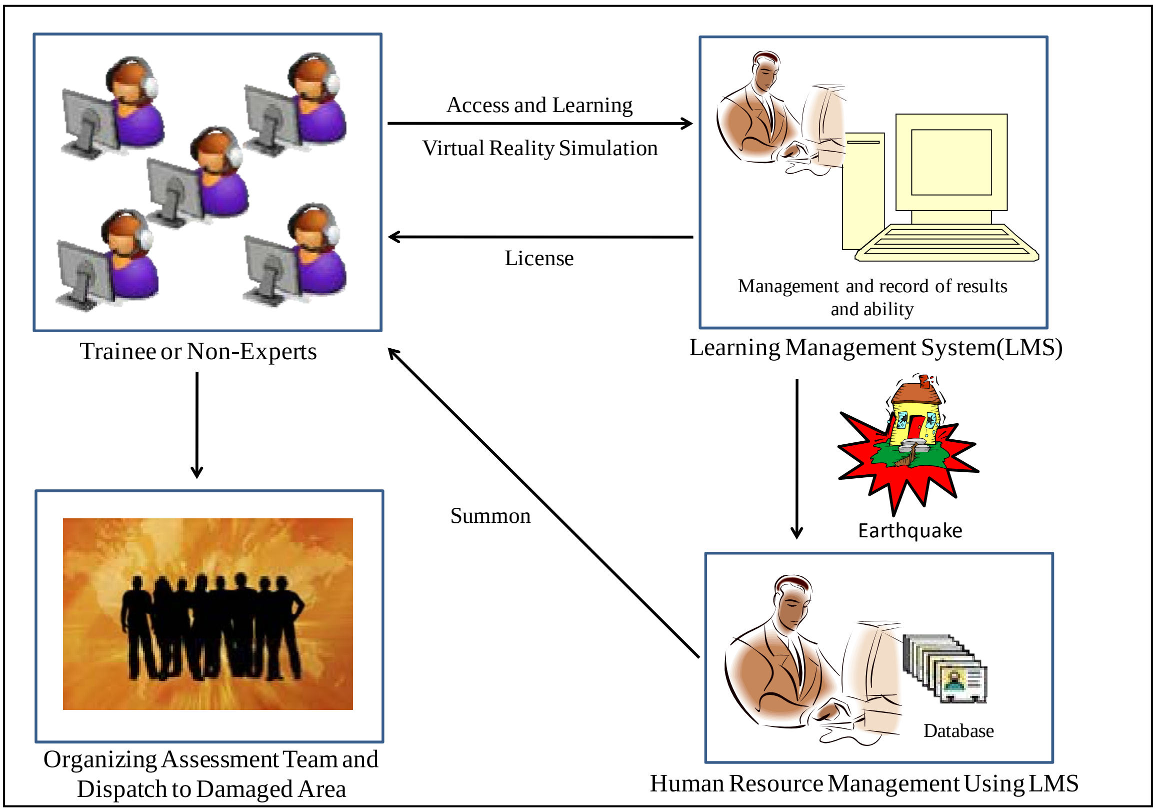

Figure 1: Concept of web based training system for building damage assessment

4. DEVELOPMENT OF PROTOTYPE TRAINING SYSTEM FOR BUILDIND DAMAGE ASSESSMENT

Here, prototype system of “training using web based simulation on virtual reality” was developed. As a part of the system, 3D houses were reproduced in the virtual reality space based on the data of totally damaged houses due to 2007 Niigata Chuetsu-oki earthquake such as external photographs, the indoor photographs and floor plans. Figure 2 shows a floor plan of the first and second floor of a modeled house.

Figures 3 and 4 show the prototype images of simulating building damage assessment of a model house. It is simulation of the primary inspection. Total damage level of a house is decided based on damage levels of three factors: externals, inclination and building element (roof, exterior wall and foundation). This system provides “walk through function”, and a trainee can move freely around a 3D house and inspect its damage in the virtual reality space on the website. A trainee can understand direction of his/her eye line in the right “View Direction Window” when they walk around a house. A trainee can answer the damage level of each building element by a quiz form and confirm their scores by “Your Record” window. In addition, when a trainee answers a question, they can get some hints. Their answers, scores and quickness of the building damage assessment are recorded by the LMS. The results of the study will be fed back to trainees.

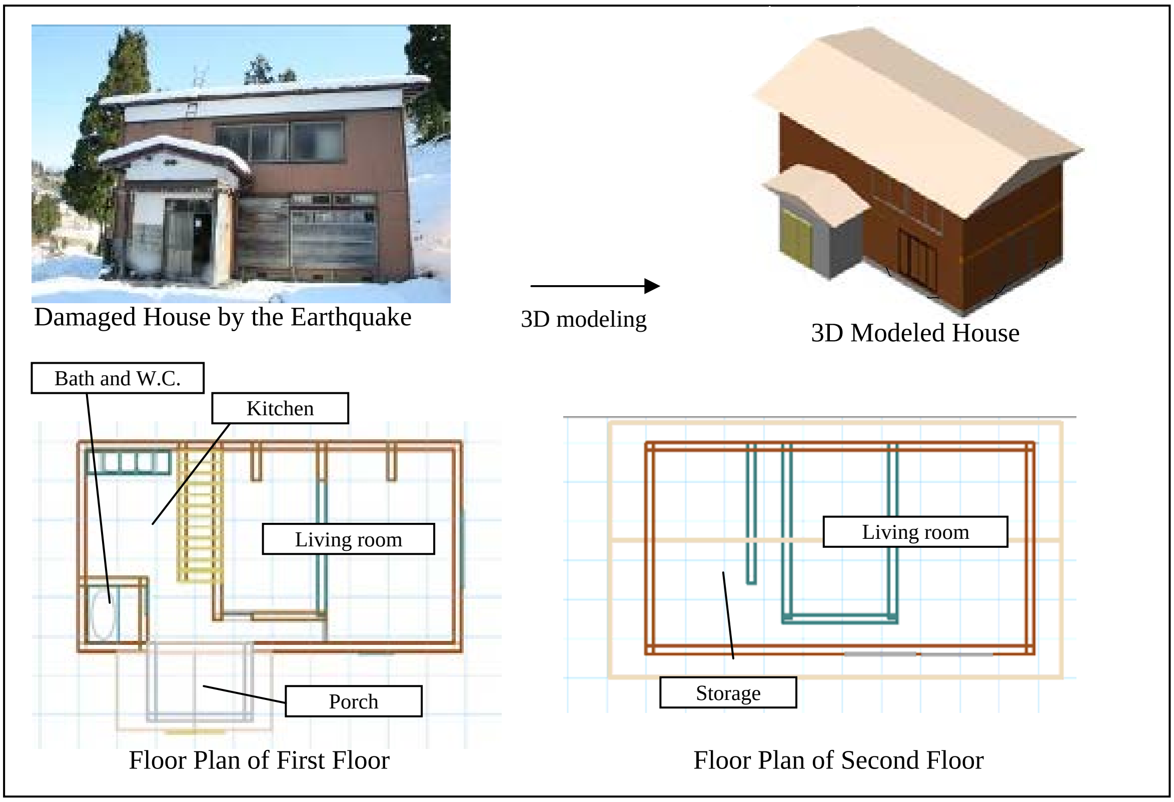

Figure 2: Overview of a 3D modeled house

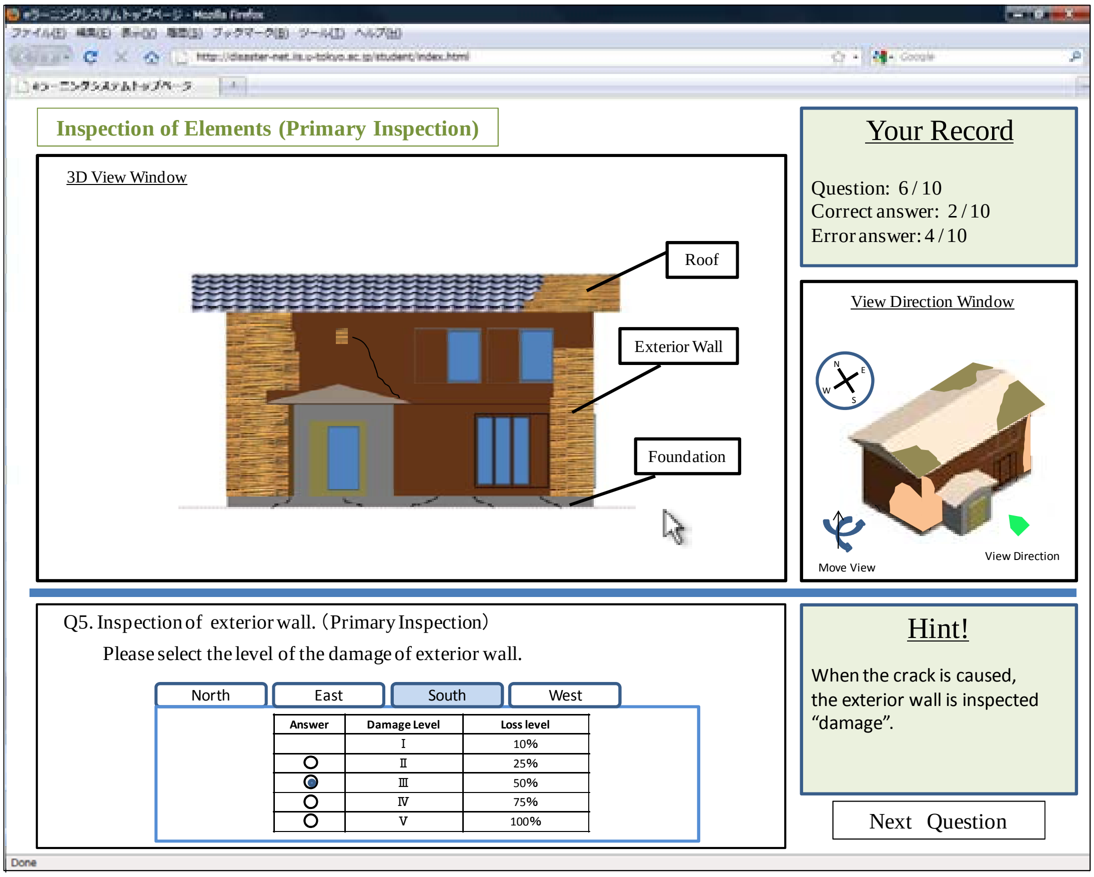

Figure 3: Prototype image of the proposed training system

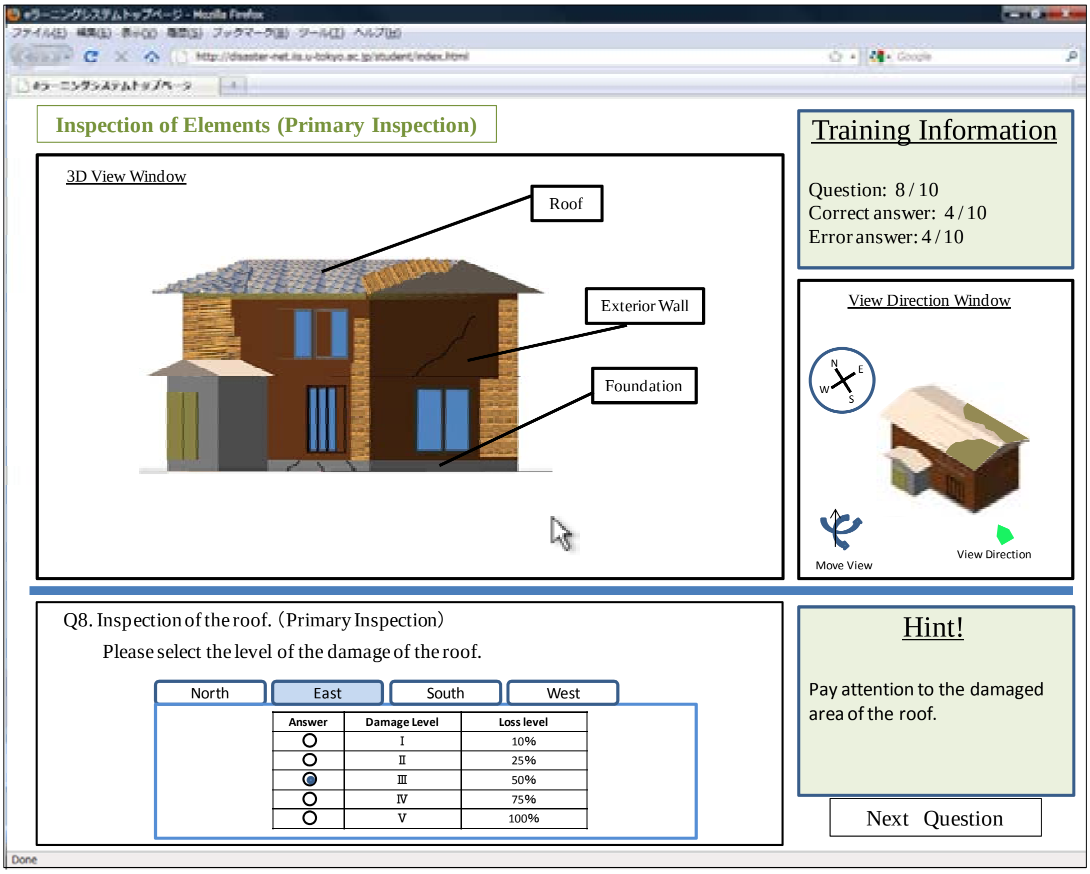

Figure 4: Prototype image of the training system (after 45 degree rotation)

5. CONCLUSIONS

In Japan, several big earthquakes are expected to occur in the near future. It is necessary to increase the number of building damage inspectors before a next event occurs. In this research, new training system for building damage assessment using virtual reality technology was proposed. First, problems of past building damage assessments were analyzed and applicability of new technologies including virtual reality for achieving ideal training system was discussed. Among these problems, this paper focused on the stage of "Training of inspector" and proposed new training system for building damage assessment using web based simulation on virtual reality.

The prototype images of simulating building damage assessment of model houses were developed based on the data of totally damaged houses due to 2007 Niigata Chuetsu-oki earthquake. 3D houses were reproduced in the virtual reality space and trainees can experience procedures of building assessment by walking around a model house. So far, developed system is prototype one with several model houses. In the future, we plan to improve the functions of the system and examine its effectiveness through experiments to several trainees.

6. REFERENCE

Doi, Satoru., Watanabe, S., Honma, M., Yoshino, S., and Oki, A., 2000. *Development of VR Simulator for Fire of Underground Markets : Part1 : Outline of the Simulator and Simulation of Smoke Diffusion,* Summaries of technical papers of Annual Meeting Architectural Institute of Japan, pp.395-396

Masumura, A., Tanaka, T., Ohnishi, N., 2001, *Extinguisher simulator with VR*, Proceedings of the Society Conference of IEICE, pp.265

Shigekawa, K., Tanaka, S., Horie, K., Hayashi, H., 2005, *Some Regulational Issues on Building Damage Assessment –A Case Study of Niigata-ken Chuetsu Earthquake*- , Journal of social Safety Science No.7, pp.133-140

Horie, K., Shigekawa, K., Maki, N., Tanaka, S., Hayashi, H., 2005, *Application of Damage Assessment Training (DATS) to Ojiya City following 2004 Niigata-ken Chuetsu Earthquake –Through a Disaster Response Support Activity for Issuing Victim Certificate*- , Journal of social Safety Science No.7, pp.123-132

Yoshitomi, N., Hayashi, H., Urakawa, G., Shigekawa, K., Tanaka, S., Horie, K., Matsuoka, K., 2005, *The Development of a Damage Certificate Issuing Support System –A new disaster response database schema created for the Niigata Chuetsu Earthquake*- , Journal of social Safety Science No.7, pp.141-150

Tanaka, S., 2008, *A Study on the Building Damage Assessment Processes for the 2007 Niigata Chuetsu Oki Earthquake Disaster : Kashiwazaki Case Study* , Proceedings of social Safety Science No.22, pp.35-38

PARALLEL SESSION 12

ANNUAL ENVIRONMENTAL CHANGES IN RUSSIA ANALYZED BY REMOTE SENSING DATA

HARUO SAWADA and YOSHITO SAWADA
International Center for Urban Safety Engineering
Institute of Industrial Science, University of Tokyo, Japan
{sawada, yoshitos}@iis.u-tokyo.ac.jp

ABSTRACT

Russia has about 800 million ha of forest land and not a few simulation studies show that the global environment change might affect them. However, there is not enough information which covers the whole area of vegetated area with the same accuracy. Satellite remote sensing of coarse resolution is considered effective to monitor large forest area because of their frequent observation capabilities. Phenological changes of ecosystem are greatly related to the changes of natural environment, such as water, temperature, soil and solar radiation. Growth condition of vegetation and soundness of ecosystem can be evaluated, if the seasonal changes of the photosynthesis are continuously monitored. Based on these ideas, we studied to get historical information about seasonal changes of Siberian forest by using remote sensing data.

After the LMF-KF processing to NOAA Pathfinder data for 20 years (1981-2001), we could get "clear" (cloud-free and noise-free) images with 10 days interval for both NDVI and LST (land surface temperature). The combination of NDVI (LMF-NDVI) and LST (LMF-LST) shows many possibilities to monitor environmental conditions in vegetated area. For example, the warm index is useful for zoning the eco-region in global scale and the freezing index has close relations with the distribution map of permafrost. The onset and offset day of vegetation growth of each pixel were also defined and the trends of both days for 20 years were obtained. The accumulation value of the NDVI between onset and offset, named NOOS index has high relation with a forest distribution map. The combination of LMF-NDVI and LMF-LST shows clear idea of the growing season and annual changes are also identified by various indices. The difference of maximum LMF-NDVI among 1981 to 2001 showed degraded vegetated areas.

The LMF-KL processing could successfully create noise free images of NDVI and LST with 10 days interval for 20 years from the NOAA Pathfinder data. The combination of NDVI and LST showed a unique and effective methodology for studying forest conditions in this region.

1. INTRODUCTION

Russia has about 800 million ha of forest land and not a few simulation studies show that the global environment change might affect them. However, there is not enough ground information which covers the whole area of vegetated area with the same accuracy. Therefore, satellite remote sensing with coarse resolution is considered effective to monitor large forest area because of their frequent observation capabilities.

Phenological changes of ecosystem are greatly related to the changes of natural environment, such as water, temperature, soil and solar radiation. Growth condition of vegetation and soundness of ecosystem can be evaluated, if the seasonal changes of the photosynthesis are continuously monitored. Based on these ideas, we studied to get historical information about seasonal changes of Siberian forest by using remote sensing technology.

Many researches utilize frequent observation satellite such as NOAA/AVHRR and SPOT/Vegetation for global environment study (Ricotta et al., 1999). In such researches, the "10-day composite images", which are created by choosing the best data in 10 days for each pixel, are often used to monitor seasonal changes of terrain conditions. The monthly composite data are not appropriate for monitoring phenological aspects because most of the seasonal changes of vegetation occur within a few weeks (Viovy et al., 1992). However, the influences of cloud, haze and system noises still remain in the 10-day composite data and that make difficult to monitor phenology with 10 days interval.

NOAA satellite has a long history of their observation of the Earth and there are data sets of 20 years of the globe. However, only the NDVI data are used and land surface temperature (LST) data were seldom processed, although temperature is well known as one of the most important environmental factors.

There are two difficulties for using these data in a long-term analysis. One is the differences of the radiometric characteristics of sensors on different NOAA satellites. The other difficulty is the algorithm to minimize both the atmospheric and systematic noises in NOAA data to observe the ground condition.

2. PROCESSSING METHODOLOGIES

Authors developed the processing method named LMF (Local Maximum and Fitting) and LMF-KF (Local Maximum and Kalman Fitting), which models the seasonal changes by time series satellite data for monitoring vegetation conditions.

2.1 LMF Processing

It is assumed that the seasonal change for each pixel is modeled by the sum of cyclic functions. It is also considered that model parameters are determined by the 10 day composite satellite data. Subsequently, the technique was developed to produce a new noise-free image using the models derived for each pixel with time-series data. We call this processing "the LMF model processing". The LMF model processing is composed of three steps as follows:

1) Revision of data by setting the adjacent maximum value;
2) Fitting with the time series model by a combination of cyclic functions;
3) Automatic decision to determine the optimum combination of the cyclic functions.

$$d'_t = Min\left[Max\left(d_{t-w+1}, d_{t-w+2}, \cdots, d_t\right), Max\left(d_t, d_{t+1}, \cdots, d_{t+w-1}\right)\right] \quad (1)$$

where d_t is the observed variable at the time t, w is the window size and d'_t is the modified variable at time t.

$$f_t = c_0 + c_1 t + \sum_{l=1}^{N}\left\{c_{2l}\sin\left(\frac{2\pi k_l t}{M}\right) + c_{2l+1}\cos\left(\frac{2\pi k_l t}{M}\right)\right\} \quad (2)$$

where c_i is a coefficient, t is time (the interval unit), N is the pair number of the cyclic function, M is the data number in a period (in case of NOAA 10 day composite products: M = 36), and k_l is the periodicity of each cyclic function in a period (in case of M = 36 , k_l = 1, 2, 3, 4, 6 and 12, meaning one year, a half year, 4 months, 3 months, 2 months and 1 month periods, respectively).

$$AIC = D\{\log(2\pi\sigma) + 1\} + 2(j+1) \quad (3)$$

where D is the number of data, j is a number of functions used and σ is the standard deviation of the residual.

2.2 LM-KF Model

In the LMF model processing, it is assumed that the seasonal changes can be expressed by a combination of linear and trigonometric functions like Eq. 2. Nishiyama (1991) reported that the discrete time variant NMR (Nuclear Magnetic Resonance) spectrum can be estimated when the frequency components of a signal are known. We applied his algorithm to the LMF model processing. When considering the set of coefficients {c0, c1,...,c2N+1} of Eq. 2 as the state vector of a state space model, their values can be estimated (state estimation) with a Kalman filter. The new methodology, LMF-KF model, was built in order to identify not only seasonal changes but also year-by-year fluctuations by considering the time dependency of each coefficient, although each coefficient of Eq. 2 is not a function of time (Sawada et al. 2005).

$$f_t = c_0(t) + \sum_{l=1}^{N}\left\{c_{2l}(t)\cdot\sin\left(\frac{2\pi k_l t}{M}\right) + c_{2l+1}(t)\cdot\cos\left(\frac{2\pi k_l t}{M}\right)\right\} \quad (2')$$

3. SATELLITE DATA PROCESSING

3.1 Result of LMF-KF Processing

The NOAA Pathfinder data from 1981 to 2001 were processed. On the NDVI data, the large fluctuations originated from noises have been removed by either method of LMF and LMF-KF. The LMF-KF model processing reveals the annual changes. As the LST data, we introduced the Channel 4 data of NOAA-AVHRR. The result of the LMF-KF model was well correspond to the meteorological data derived from AMeDAS in Japan.

3.2 Various Informative Data

After the LMF-KF processing to NOAA Pathfinder data for 20 years (1981-2001), we could get "clear" (cloud-free and noise-free) images with 10 days interval for both NDVI and LST. Because both the NDVI and LST are obtained from the LMF-KF processing, there are many possibilities to monitor environmental conditions in vegetated area.

The LST data is useful for understanding environmental condition of the terrain. One of the examples, is the warm index (the summation of temperature when it is higher than 5 degree C), which is considered useful for zoning the eco-region. LST makes us possible to monitor the condition of the annual changes of warm index in Russia, because the ground temperature is related to LST although ground coverage affects its value.

Table 1: Various indices derived from NDVI, LST and their combinations

Index	Meaning
NMXV, NMXD	Maximum NDVI, the day
NMNV,NMND	Minimum NDVI, the day
TMXV,TMXD	Maximum LST, the day
TMNV,TMND	Minimum LST, the day
T5S, T5D	Warm index, duration: LST > 5 C deg.
T00S, T00D	Freezing index, days: LST < 0 C deg.
NST5	ΣNDVI : LST >5 C dg.
MNV1	Minimum NDVI : LST>1C deg.
MXV1	Maximum NDVI: LST>1C deg.
NOND	Onset day : MNV1 to MAV1
NOFD	Offset day: MAV1 to MNV1
NOOD	Duration of growing season
NOOS	ΣNDVI during the NOOD

The LMF-KF processed images brought us the possibilities to develop further indices by the combination of NDVI and LST (Table 1), which could be useful for monitoring various phenological conditions of vegetated area.

4. ANALYSIS AND RESULTS

We, at first, checked the reliability of the LMF-KF processing methodology by the simulation data and found that it revealed the surface condition by minimizing the affects of clouds and system noises. After this evaluation, the 3-color composite images using NDVI and LST were created by our methodology. These color composite images of every 10 days (Fig.1) for 20 years (more than 720 scenes in total) show very clearly the global dynamics of surface conditions of Siberian forest.

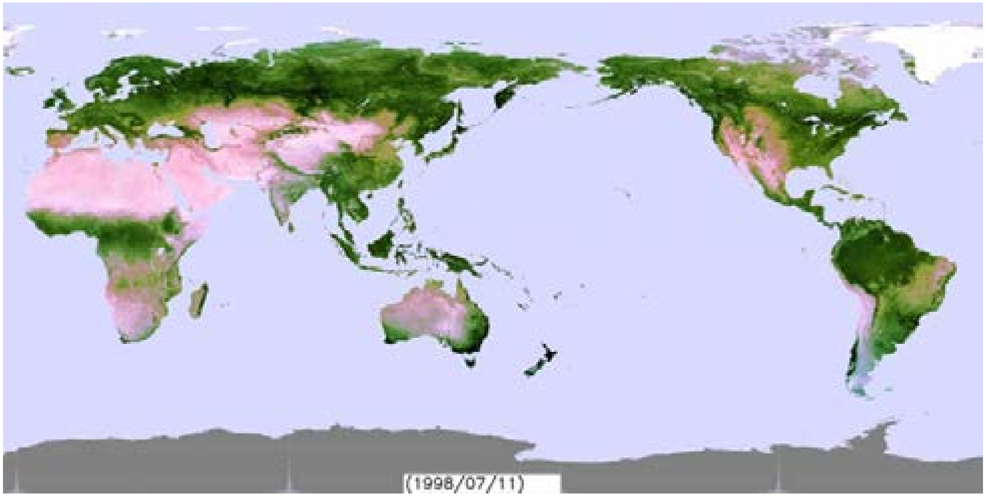

Figure 1: An example of the color composite image of NDVI and LST

4.1 NDVI and Thermal Data

The images of various indices, such as shown in Table 1, were created. The maximum NDVI of each year, for example, is considered as a good indicator for annual changes of vegetation condition as each NDVI shows the seasonal condition of vegetation coverage. The trend of annual maximum LST for 20 years is considered the average temperature changes of the surface, which must be related to the effect of global environmental and changes of ground coverage.

The onset day and offset day of vegetation growth of each pixel were defined from the maximum and minimum NDVI when the LST has greater than 1 degree C. The accumulation value of the NDVI between onset and offset is the NOOS index (Table 1). The NOOS has the highest relation with the forest distribution map which was reported by the International Institute for Applied Systems Analysis (IIASA). It seemed that the NOOS could be used as a good indicator for forest area.

We created the Freezing Index image of each year by using the LST data. The Mean Accumulated Freezing Index over 20 years (Fig.2) was compared to the permafrost extent map which had been created by IIASA. There were similar pattern and satellite information might have advantage over the map at its annual monitoring capability.

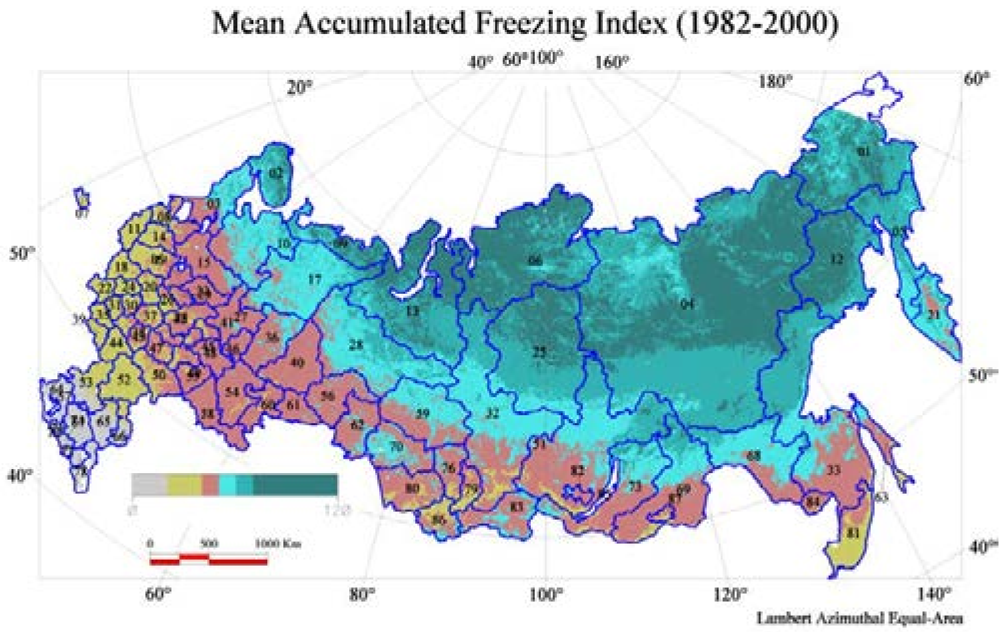

Figure 2: Mean Accumulated Freezing Index

4.2 Seasonal Changes

The seasonal changes are well observed on the NDVI and LST individually. However, the combination of NDVI and LST shows much clear idea of the growing season and the trend of vegetation condition of each pixel. We think that the LST greater than 5 degree C or 1 degree C is the growing season and the accumulation of the NDVI during the period is related to the vegetation growth, which means the CO2 uptake.

4.3 Annual Changes

The annual changes are also observed through the various indices presented on the Table 1 as well as the Freezing Index. Fig. 3 is one of such examples and it shows the difference of maximum NDVI between 1982 and 2000. The dark area indicates the degraded area. The changes are very much related to fire occurrence map in Far East. This fact means that the fire and forest logging are very much correlated each other in this region.

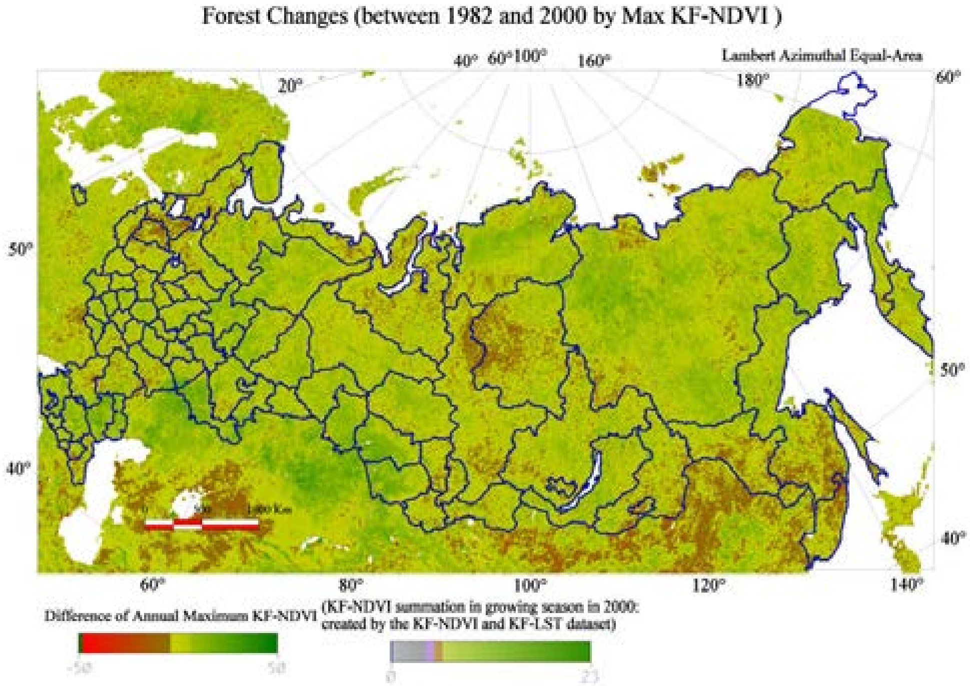

Figure 3: Forest changes between 1982 and 2000. The difference of the maximum NDVI of each pixel in both years is calculated. Dark are shows high degradation.

5. DISCUSSION

The LMF-KL processing could successfully create cloud and noise free images of NDVI and LST with 10 days interval for 20 years from the NOAA Pathfinder data. The combination of NDVI and LST is a unique and effective methodology for studying forest conditions in this region. These data can be used for further studies on carbon fixation, such as NPP estimation in this region.

ACKNOWLEDGMENTS

This report is a result of the Study on Estimation of Carbon Storage and Fixation in the Boreal Forest funded by the Global Environment Research Fund of Ministry of the Environment, Japan.

REFERENCES

Nishiyama, K., 1991. A method of Estimating Time-Varying Spectrum which includes Only Components with Known Frequencies. *IEICE Transactions*,Vol. J74-A, 916-918.8.
Ricotta, C., Avena, G. and De Palma, A. 1999. Mapping and monitoring net primary productivity with AVHRR NDVI time-series: statistical

equivalence of cumulative vegetation indices, *ISPRS Journal of Photogrammetric Engineering and Remote Sensing,* 54:325-331.

Sawada, Y., Mitsuzuka, No., Sawada, H. 2005. Development of a time-series model filter for high revisit satellite data. *Proc. the Second Int. VEGETATION User Conference,* pp.83-89

Viovy, N., Arino, O. and Belward, A. S. 1992. The Best Index Slope Extraction (BISE): A method for reducing noise in NDVI time-series. *I. J. Remote Sens*. 13:1585-1590

EFFECT OF CROWN PROPERTIES OF CHAMAECYPARIS OBTUSA TREE IN JAPAN FOR DEM CREATION

TAKAHIRO ENDO
ICUS, Institute of Industrial Science, The University of Tokyo, Japan
tendo@iis.u-tokyo.ac.jp
HARUO SAWADA
ICUS, Institute of Industrial Science, The University of Tokyo, Japan
sawada@iis.u-tokyo.ac.jp

ABSTRACT

A numerical simulation of airborne LiDAR (Light Detection and Ranging) measurement was conducted to clarify relationship between pulse density and tree crown properties from viewpoint of creation of Digital Elevation Model (DEM). The simulation was run in 3D Computer Graphics (3DCG) using a simulated tree which created full polygons using ray tracing technique. Initial parameters in the simulation were species, age of stand (size) and pulse density. Chamaecyparis obtusa, which is one of dominant spices of conifers in Japan, was selected. Tree ages were 25, 35, 45 and 60 years old. Pulse density was 1, 2, 4 and 8 points per square meters. As the result of analysis of relationship between pulse density and DEM creation, blank pixels which have no points on the ground decreased in proportion to pulse density. However, blank pixels remained around main stem of tree in spite of using high pulse density. Moreover, blank pixels existed around main stem in all cases with different ages. Configuration of structure of stems and branches around main stem was so complex that laser beam could not pass through a tree crown. This study concludes that high pulse density is needed for DEM creation, but space around main stem certainly become blank. It is important to use high pulse density for forest observation by LiDAR in order to create high accurate DEM.

1. INTRODUCTION

Recently in Japan, elevation has been measured increasingly by airborne LiDAR, because LiDAR measurement is becoming low cost and produces accurate spatial elevation maps directly with high efficiency in comparison to ground survey (Hirata, 2004). Then, DEM generated from LiDAR data is widely used for multiple purposes. However, still there is considerable difficulty in producing DEM in thickly forested area. Some researchers and survey companies pointed out the difficulty of creation of DEM under trees (Endo, 2009). For example, one case was to create DEM easily and the other case was difficult, when DEM was generated from LiDAR Data. This reason has not been made clear from viewpoint of quality yet. Because, we can not figure out true geographical position of a target laser beam hit. That is to say, there is unknown behavior between crown properties and laser pulse. Hence, a simulation system is needed to comprehend relationship between pulse density and crown properties. The objective of this study from viewpoint of DEM creation was to investigate relationship between pulse density and crown properties such as configuration of foliage, stems and branches using a numerical simulation system.

2. MATERIALS AND SIMULATION CONDITION

2.1 Test tree

A *Chamaecyparis obtusa* was simulated by a tree growth model (natFX) in the 3DCD software. The tree is one of dominants spices in Japan and is distributed almost throughout Japan. About 12％ Japanese forest area is covered by this tree (Forestry Agency). To investigate effect of crown properties such as size and branches, 25, 35, 45 and 60 years old tree were created. Figure 1 shows a simulated polygon of *Chamaecyparis obtusa* which is 60 years old.

2.2 Pulse density, emitting direction and diameter of foot print

Presently, 4 pulses per square meters is used in commercial operations. Pulse density will become 8 pulses per square meters in near future. Then, 1, 2, 4 and 8 pulses per square meters were used in the simulation to investigate an effect of pulse density by representing presently available data to the data available in near future. Emitting direction of Laser beam was vertical as in practical measurements. Also diameter of foot print was 0.2m to simulate practical measurement from 1000ｍ height and 0.2 mrad.

2.3 Points cloud simulation

Points cloud was simulated using a ray tracing method using tree polygon data in the 3DCG. A geographical positions of origin of ray tracing specific pulse density was created on a plane which was created on a upper polygon of tree. Points cloud was a geographical position where a ray intersected with the tree polygon. Figure 2 stands for the simulated points cloud generated from a tree polygon of 60 years old and 8 pulses per square meters.

2.4 DEM creation

DEM was created by a simple rasterization method with 1 meter mesh. Value of a specific mesh was number of points on the ground in the mesh. When no point existed in the mesh, value was 0. This case assumed that

DEM was not able to be created. Figure 3 stands for a result of DEM creation.

(a)

(b)

Figure 1: The simulated polygon of Chamaecyparis obtusa of 60 years old. (a) is perspective view and (b) is vertical view.

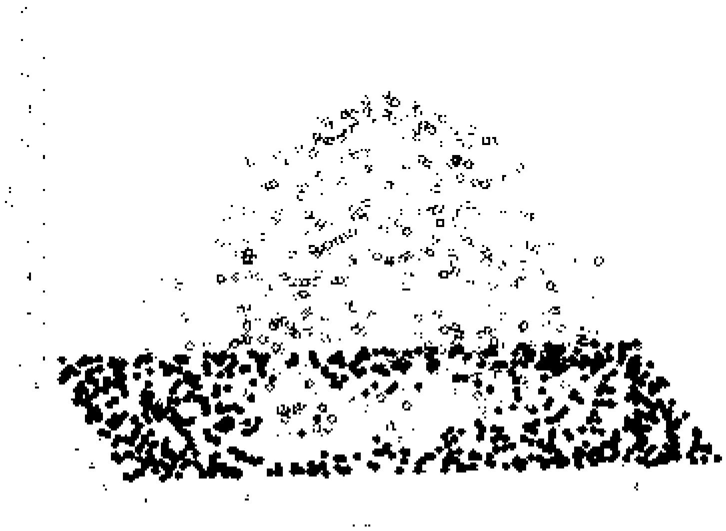

Figure 2: The simulated points cloud of 60 years old by 8 pulse per square meter density. Black colored circle are points cloud on a tree polygon. Black colored dot are points cloud on the ground.

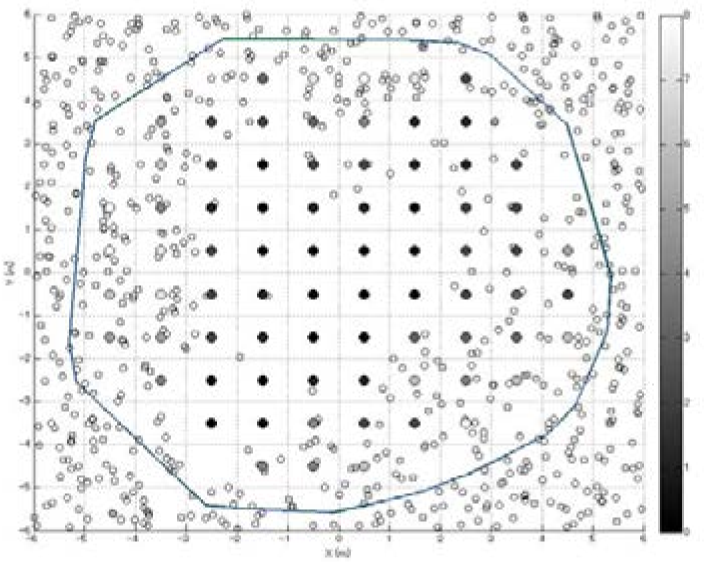

Figure 3: Potential of DEM creation. Black colored circle are points cloud on the ground. Gray colored circle are number of points cloud in the mesh. Black colored solid line is an edge of tree crown.

3. RESULTS AND DISCUSSION

3.1 Relationship between pulse density and DEM creation

Figure 4 shows relationship between ratio of creation of DEM and pulse density. Ratio of creation of DEM in any year old was increasing in proportion to pulse density. The relationship between the ratio and pulse density was a logarithmic function. The result indicates the ratio has upper limitation value.

3.2 Relationship between DEM and crown properties

To investigate the reason for the logarithmic function, number of points cloud on the ground within a circle with specific radius was analyzed. Radius in the analysis was from 1.0 to 5.0 meters at the interval of 0.5 meters. Figure 5 is relationship between number of points cloud on the ground.

Number of points cloud on the ground increased out of 2m range of radius. At the less than 1.5 m range, there was no point on the ground in any pulse densities. The reason was an effect of configuration of stem and branches, as the result of considerable analysis of structure of tree. The result indicates that there is no DEM area in case of measurement of conifer forest by LiDAR.

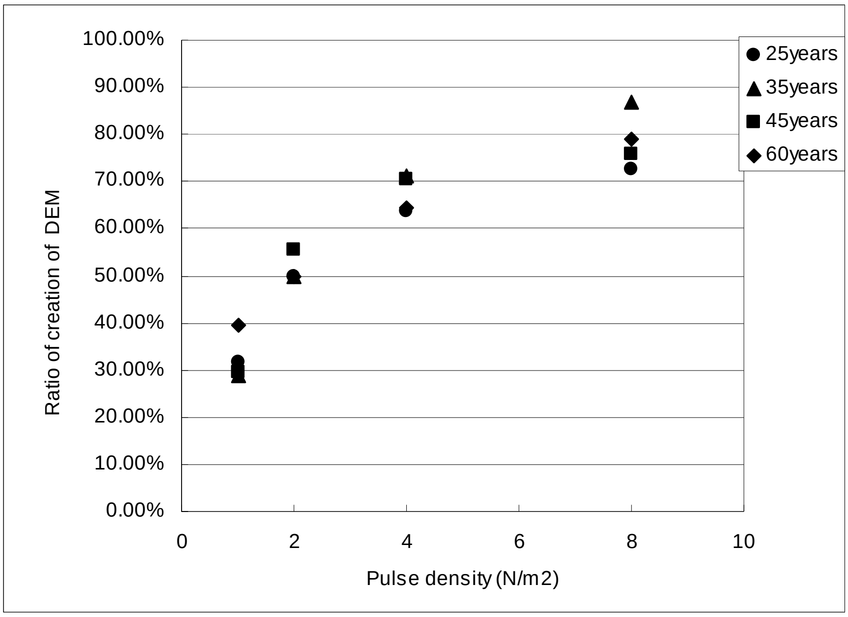

Figure 4: Relationship between ratio of creation of DEM and pulse density.

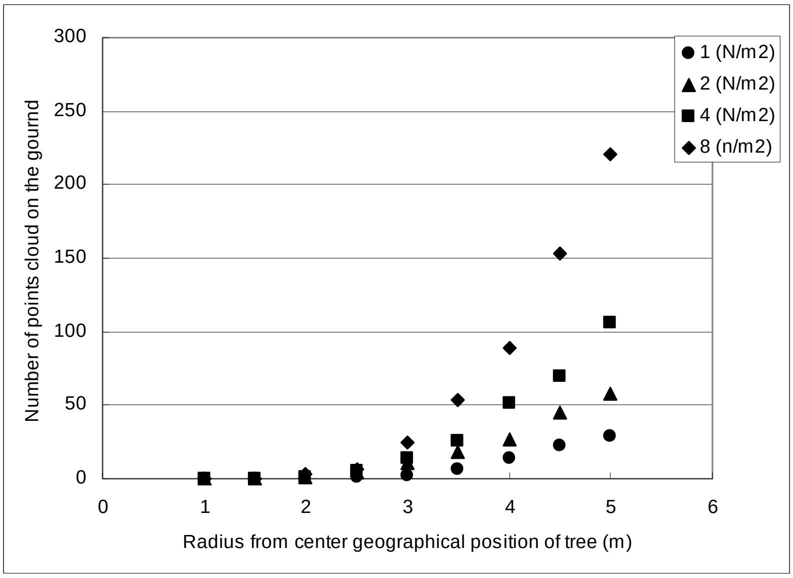

Figure 5: Relationship between number of points cloud on the ground within a circle with specific radius

4. CONCLUSIONS

This paper demonstrates that there is potential of estimating no creation area of DEM for analysis from the LiDAR simulation. In particular, this work provides the foundation for creation of DEM under forested area. Under trees, it is difficult to create DEM due to an effect of stem and branches around main stem. This study indicates that pulse density should be high to increase potential of DEM creation.

REFERENCES

Endo, T., 2009. A study on new analytical method by LiDAR for forest observation, PASUCO technical exhibition, Tokyo, 16 June, 2009.

Hirata, Y., 2004. The effects of footprint size and sampling density in airborne laser scanning to extract individual trees in mountainous terrain, International Achieves of Photogrammetry, Remote Sensing and Spatial Information, XXXVI-8/W2, 102-107.

Forestry Agency Statistics, http://www.rinya.maff.go.jp/j/kouhou/toukei/index.html , accessed on 25 August 2009.

SIMULATION OF EXPLOSION MODEL WITH GIS/RS DATA IN HILLY URBAN AREAS

EUNMI CHANG
Korean GeoSpatial Information and Communication, Korea
emchang21@gmail.com
HYUNGSUK KIM
Korean GeoSpatial Information and Communication, Korea
kimhs@ksic.net

ABSTRACT

Traditional Explosion Simulation studies assumed the flat environment and distance from the starting site have been regarded as a main parameter, so real GIS data and satellite data have not used frequently. Not only for the visualization but the actual estimation of damaged areas on real site, KOMPSAT 3, satellite imagery with 0.7meter resolution and detailed digital elevation data with less than 1 meter were modified and converted into Industrial Disaster Simulation System. Virtualization technology, such as SEDRIS standard, was adopted to set the object for terrain characteristics such as height, materials, and year of established and modified. All the data on the terrain objects were obtained through the Digital Terrain Map and sensor value of satellite imagery data.

Mega City with hilly mountainous areas, explosions in chemical plant may result in high casualty and loss in SOC. We used simple explosion model which is named as "TNT Equivalent Model" and applied the model for real GIS data. And then we got the result of representing the effect of real terrain data. In this research, we just focused on the integration of GIS and Remote Sensed data which have been collected for other purposes by using simple explosion model. The simulation result with API of SEDRIS viewer could give an outreach program for disaster prediction or estimation and preparedness for the managers of plants and city officers.

1. INTRODUCTION

An increase in oil and gas plants caused by development of process industry have brought into the increase in use of flammable and toxic materials in the complex process under high temperature and pressure. There is always possibility of fire and explosion of dangerous chemicals, which exists as raw materials, intermediates, and finished goods whether used or stored in the industrial plants. The scales of industrial and natural disasters in recent ten years are illustrated in Figure. 1.

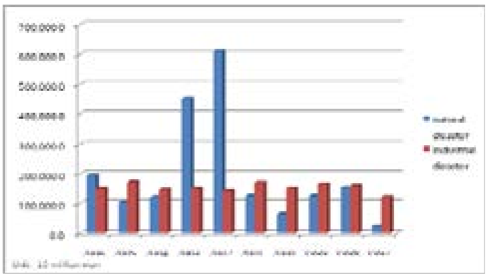

Figure 1: amount of damage in recent ten years

It shows industrial disaster was growing and its scale is as much as big. So, corresponding disaster prevention policy is needed. There are many cases of human cause and its damage range is predictable. So it is able to establish corresponding plan by prediction of accurate scale. Because past prevention policy of disaster was established without systematic analysis and survey, engineering simulations only performed. For simulation of industrial disaster, Phast Professional, commercial software, or CAMEO, EPA and NOAA made, has used in general condition. And the researches are active about relate part. But it is simple application of plain ground condition without considering Korean terrain environment. There are the necessities of simulation in real terrain condition.

For Quantitative Risk analyses, real terrain data is simulated by SEDRIS. To construct the target area’s terrain model with SEDRIS, we have to combine DEM(Digital Elevation Model) of high resolution satellite image and aerial photograph and SEDRIS with geographic data. And apply industrial disaster model with that result. This approach will show more accurate prediction of damage than past one.

2. SIMULATION METHODOLOGY OF INDUSTRIAL DISASTER

It is a UVCE which is frequently occurred explosion around chemical instruments.

The UVCE(Unconfined Vapor Cloud Explosion) is occurred through following 4 steps.

1. Leaking out flammable vapor or gas
2. Forming flammable vapor cloud by mixing leaked material and air
3. Igniting flammable vapor cloud compound
4. Propagating flame through vapor cloud in flammable concentration

It is seldom whole or almost vapor clouds explode. Flames propagate with chain detonation in many cases. Gas react rapidly seems to explode at a time. There are two cases Which One Flash Fire, flame propagate slowly Another UVCE, flame propagate rapidly, so it takes place a lot of over pressure.

If UVCE occurred, it companies big over pressure in conditions of turbulence flow and partial confinement or objection and explosion. In real UVCE, explosion over pressure can be 15 psi in stagnant area but 1.5 psi in not confinement condition. Using following equation 1, approximates the mass of TNT.

$$W = \frac{\eta M E_c}{E_{cTNT}} \quad \textbf{(1)}$$

where W = Equivalent mass of TNT[kg]
η = Empirical explosion yield[0.01~0.1]
M = Mass of flammable material released[kg]
E_c = Lower heating value of combustion of flammable gas[kJ/kg]
E_{cTNT} = Heat of combustion of TNT[4500kJ/kg]

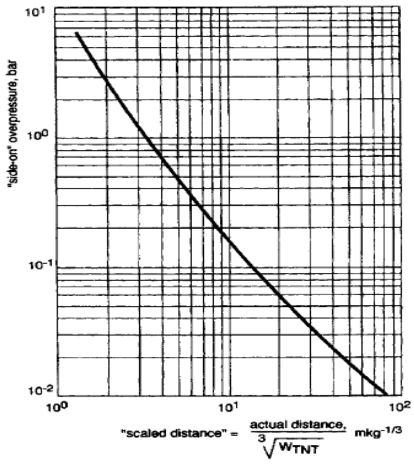

Figure 2: Overpressure due to explosions

The side-on blast overpressure at some real distance(R) of charge of mass of TNT, result of equation 1, is found by following equation.

$$R^* = \frac{R}{W_{TNT}^{1/3}} \quad \textbf{(2)}$$

where R^* = Hopkinson-scaled distance[m/kg1/3]
W_{TNT} = charge of weight of TNT[kg]
R = real distance from charge [m]

If the scaled distance is R* known, the corresponding side-on blast peak overpressure can be read from the chart in Figure 2. But Figure 2 about scalded distance vs. overpressure graph is non-linear. So regression equation is fitted as equation 3.

$$\log_{10} P^* = 1.052 - 2.158\log_{10}(R^*) + 0.3009\log_{10}(R^*)^2 \quad \textbf{(3)}$$

where P^* = explosion overpressure[bar]
R^* = Hopkinson-scaled distance[$m/kg^{1/3}$]

Damage amount of explosion area is estimated with above equations and chart. Whole flow chart for calculating explosion quantity is following.

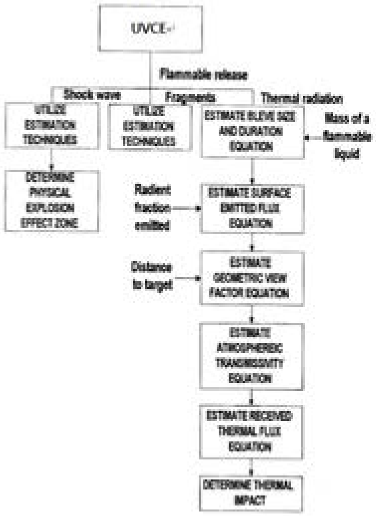

Figure 3: Logic Diagram for UVCE

3. CONSTRUCTION MODEL AND APPLICATION OF TERRAIN MODEL

Accurate and unambiguous representation of environmental data is an important part of many information technology applications. SEDRIS(Synthetic Environment Data Representation and Interchange Specification) permits representations of environmental data that can be described accurately, unambiguously, and precisely.

Authoritative representations of the environment are expected to be internally consistent and conform to physics-based principles. Furthermore, representations of environmental data shall contain an appropriate integration of terrain, ocean, atmosphere, and space domain data about a region of interest. SEDRIS supports the representation of the physical as well as the abstract aspects of each environmental domain. In addition, the actual reference objects being modeled or described can be either natural (e.g., some region of the Earth) or some constructed object. This latter capability is important in applications that evaluate the characteristics and performance of constructed objects with respect to environmental effects and impacts, prior to production (e.g., testing and evaluating land, water, air, and space vehicles).

SEDRIS also supports the representation of 3D models, including various articulations required to convey general system design characteristics, as well as data representation in the environmental domains of: Terrain, Ocean, Atmosphere, and Space.

A representation of the terrain domain includes data on the location and characteristics of a planetary surface, natural and permanent or semi-permanent constructed features, and related processes including seasonal and diurnal variation.

Figure 4: SEDRIS Environment domains

SEDRIS relies on its five core technology components. These are the SEDRIS Data Representation Model (DRM), the Environmental Data Coding Specification (EDCS), the Spatial Reference Model (SRM), the SEDRIS interface specification (API), and the SEDRIS Transmittal Format (STF).

Three of these (DRM, EDCS, and SRM) are used to achieve the unambiguous representation of environmental data. The combination of these three core components provides the mechanism for description of environmental data. In some respect, this capability within SEDRIS can be viewed as analogous to a language for describing data about the environment. The DRM, the EDCS, and the SRM enable us to capture and communicate meaning and semantics about environmental data. The SEDRIS API and the STF allow the efficient sharing and interchange of the environmental data represented by the other three components. In the following, each of these five components is briefly described.

4. SIMULATION RESULT

For performing simulation, explosion conditions are following.

Explosion in the LPG replenishment station case, Explosion Type : UVCE Explosion Material : LPG(Butane:C_4H_{10}) Released Mass : 10kg Empirical explosion yield : 0.04(4%)

Estimation result of UVCE model with plain terrain condition is illustrated in Figure 5. It shows explosion effect range is drawn by concentric circle. This result is obtained by not reflecting the geographical information in UVCE model. In plain ground case, a concentric circle indicating the pressure becomes a concentric circle.

If the explosion is simulated with three-dimensional model and non-existence of objection condition and reflecting the geographical information from DEM in UVCE model for hilly area, simulation result is represented by ellipsoidal shape according to the geography of the area. It is illustrated in Figure 6. This is the more correct result than application of plain ground and this can be used in planning for emergency fire escape.

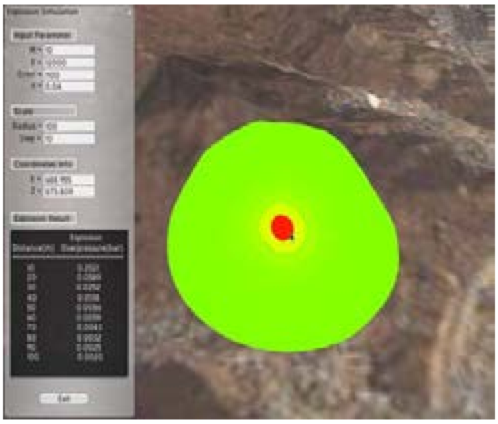

Figure 5: Explosion effect for plain ground

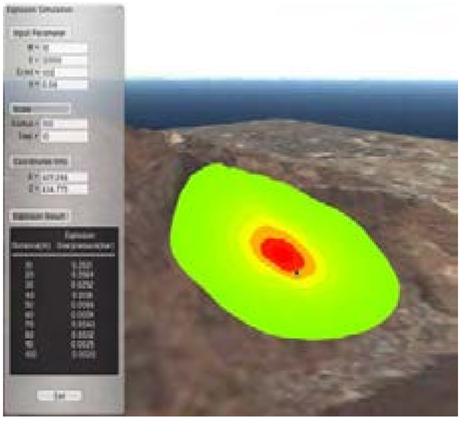

Figure 6: Explosion effect for hilly area

5. CONCLUSION

Today, not only the frequency of industry disaster has increased but also the scales of the disaster have enlarged and broaden due to the recent industrial development and constantly occurring accidents. Yet there is no disaster prediction system at present which is pointed out as the limitation to cope with disasters in scientific measures. Therefore, it is suggested to develop a disaster prediction system suitable for domestic terrain condition to establish a scientific disaster management system and an effective driving force in disaster prevention strategy and a disaster measure system. As a mean of status analysis study to predict disaster, this paper focuses on the application of the hilly area.

The result of the risk prediction made the two-dimensional damage prediction into a three-dimensional one. In other words, it can be used to predict possible damages more accurately and to make it possible to establish strategies for emergency evacuation. But on the other hand, due to the diversity of data on various subjects and in many different types, it is pointed out that standardization of the data types is highly required along with the articulated cooperation system for proper application for the sake of future damage prediction.

REFERENCES

AIChE-CCPS : Guidelines for Chemical Process Quantitative Risk Analysis, New York (1989)

Brasie, W. C., Simpson, D. W. : Guidelines for Estimating Damage Explosion, Dow Chemical Co., Midland. Mich (1990)

HyungSeok Kim : Study of 3D terrain information for risk assessment. In: 2008 fall academic Symposium on Korean Institute of Chemical Engineers Meetings, Busan(2008)

Kees van Wingerden : Predicting Blast Overpressure Caused by Vapor Cloud Explosions in the Vicinity of Control Rooms. Process Safety Progress, Vol. 18 , No. 1, pp 17-24 (1999)

SEDRIS – Environmental Data Representation & Interchange : http://www.sedris.org

IDENTIFICATION OF GROUNDWATER POTENTIAL ZONES IN KEN-BETWA RIVER LINKING AREA USING REMOTE SENSING AND GIS

RAM AVTAR[1], H. SAWADA[1], S. MUKHERJEE[2], C. K. Singh[2]
[1]Institute of Industrial Sciences, The University of Tokyo, Japan
[2]School of Environmental Sciences, Jawaharlal Nehru University, New Delhi, India
ram@iis.u-tokyo.ac.jp

ABSTRACT

The objective of this study is to identify the feasibility of the Ken-Betwa River link project in aspect of groundwater availability. This is done by studying the groundwater potential zonation (GWPZ) map of the project benefited area. Remote sensing data with other ancillary data in geographic information system (GIS) is useful to delineate GWPZ map of Ken-Betwa River linking area. Various thematic maps such as geomorphology, land use/land cover, lineament, drainage, soil, and slope were generated from Landsat (ETM+) satellite data of the year 2005, survey of India (SOI) topographic sheets, existing maps and SRTM DEM data. These themes were overlaid to generate GWPZ map of the area by using ranking and weight techniques. Groundwater level maps of the area were also generated by using interpolation of groundwater level data of the monitoring wells. The groundwater fluctuation during the monsoon season is due to the recharge from rain water. The GWPZ map of the area delineated from the overlay shows a strong correlation with the groundwater level maps. The final map of the area shows different zones of groundwater prospects, viz., good (5.22% of the area), moderate (65.83% of the area) poor (15.31% of the area) and very poor (13.64% of the area). This shows that supply of water through the link will be useful for the surrounding area but sometimes it will cause some problems like water logging.

1. INTRODUCTION

Water is the most precious and commonly used resource in nature, both surface and under groundwater. Groundwater is a dynamic resource which varies temporally as well as spatially. In a developing country like India where we have acute water problem, both in drinking and irrigation water, the nature, source and the availability of groundwater should be thoroughly studied and evaluation of groundwater potential is a very important issue.
Overexploitation of groundwater or monsoon failure results into inadequate recharge and depletion of groundwater table will cause hydro-meteorological hazards such as drought which is more frequent in the recent history of Bundelkhand (Bhagwat I. P., 2008).

The Ken-Betwa Link Project (KBLP) involves connecting the Ken and Betwa Rivers through the creation of a dam, reservoir, and canal to provide storage for excess rainfall during the monsoon season in the upper Ken basin and deliver this water for consumption and irrigation purposes to the upper Betwa basin (NWDA, 2007). The thematic layers like geology, geomorphology, lineament, drainage, soil type, land use/land cover, and slope were analyzed in GIS environment to generate GWPZ map of the study area (Krishnamurthy et al. 2000, Murthy 2000). Several studies (Jaiswal et al. 2003, Wolski and Gumbricht 2003) have demonstrated the use of remote sensing for groundwater zonation displaying the potential and limitations of this tool. Saaty (1994) proposed one of the most accepted quantitative method for assigning relative weights and rates for various themes is based on the multi-criteria evaluation for decision making. In this study an attempt was made to utilize similar method to identify feasibility of Ken-Betwa River linking project.

2. STUDY AREA

Most part of the study area lies in Bundelkhand which is divided between the states of Uttar Pradesh (UP) and Madhya Pradesh (MP). The command area of this link is bound between latitude $24^0$40’ E, $78^0$60’N to $25^0$65’E and longitude $78^0$40’N, $25^0$30’E to $80^0$00’N (figure 1). It covers approximately 61,750 km^2 of area spread in 17 administrative blocks.
Bundelkhand generally experiences a semi-arid climate, though this is highly variable depending on the region and the time of year. Indeed, the area is notorious for experiencing droughts in summer and disastrous floods during the monsoon. The monsoon brings over 90% of the annual rainfall between the months of June to September, with the highest precipitation occurring in July and August. The average annual rainfall varies from 75 to 125 cm. The dry plains in the north usually receive less rainfall while the southeast benefits from more. The area has average annual maximum and minimum temperature of 44.2^{0}C and 6.7^{0}C.

2.1 Geology of the area

The area contains three major groups of rock with high uncertain ages: the Bundelkhand complex (older than 2600 Million years) the Bijawar group (2600-2400 Million years), Vindhayan super group (1400-900 Million years) as shown in figure 2. The study area is predominantly made up of Bundelkhand Granite complex belonging to Bundelkhand Group. The Bijawar group of the area consists of terrigenous sequence of basal carbonates and shales with green schists or pillow basalts, chloritic shales, ferruginous quartzites and banded iron formations. Vindhayan super group are represented by red to greyish-white, medium to fine grained, compact and highly jointed sandstones all over the Vindhayan basin (Mallet, 1869).

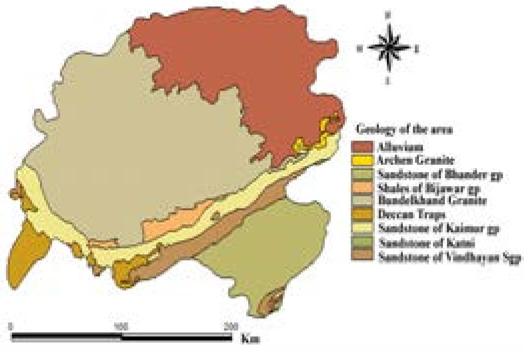

Figure 1: Location of the study area *Figure 2: Geology of the area*

3. MATERIALS AND METHODS

The methodology adopted for this study is given in the following flow chart (fig.3). Each thematic map was assigned a weight depending on its influence on the storage and movement of groundwater. The weight and rank of each layer is given in the table 1. The scored maps were overlaid by using spatial analyst tool of ArcGIS 9.3. The resultant map was classified into good, moderate and poor zones. The results were validated by using groundwater level data of the central groundwater board (CGWB).

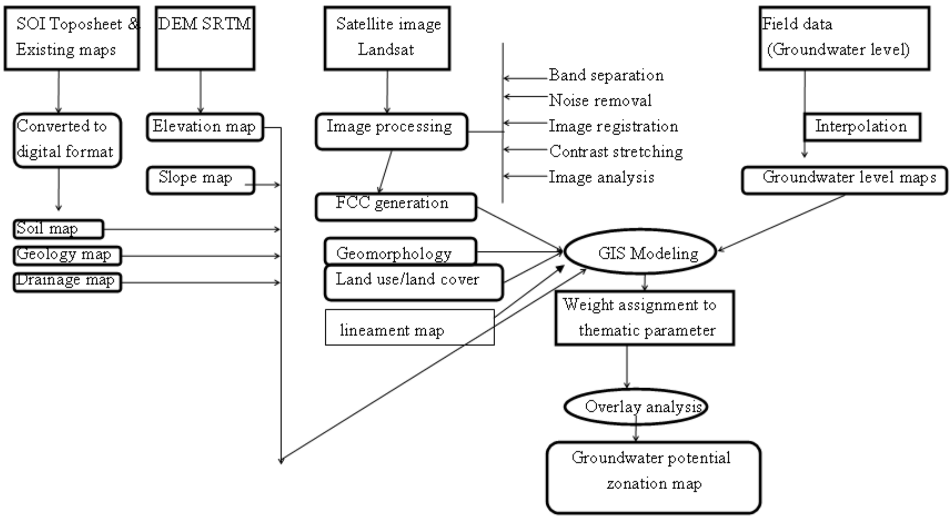

Figure 3: Methodology adopted for Groundwater potential zonation map

4. RESULTS AND DISCUSSION

4.1 Geomorphology of the area

Geomorphologically, the area depicts both erosional and depositional landforms as shown in figure 4. Geomorphology was assigned highest weight because it has a dominant role in the movement and storage of groundwater in the study area (Thomas B. C., 2009).

- **Erosional hills:** This represents the remnants of oldest planation surface marked by domes and ridges of Bundelkhand granite and gneiss. Because of high slope and relief they are not suitable for groundwater exploration.
- **River channel:** Ken, Betwa and Yamuna are main rivers along with number of tributaries, transporting a heavy amount of silt, clay and sand. These are considered as good zones for groundwater.
- **Flood Plain:** These are comparatively low-lying area, close to the river. The flood plain deposits are developed at the constructive side of river channels. They are considered as good zones for groundwater.
- **Alluvial plains:** The porosity and permeability of the alluvium are very high so they are considered as good zones for groundwater.
- **Ravines:** Most of the area of River Betwa, Dhasan and some area of Ken is covered by ravines. Ground water possibilities become less due to high run off and its impermeable nature.
- **Pediments:** Pediments are most prevalent in very arid environments. These are considered as poor to moderate for groundwater.

4.2 Lineament map of the area

Lineaments are the manifestation of linear features can play a major role in identifying suitable sites for groundwater recharge (Krishnamurthy J., 2000). Lineaments on the surface have been identified early as conduits for groundwater flow in fractured aquifers and hence targeted for locating production wells (Meijerink 1996). The purpose of the lineament density analysis is to calculate frequency of the lineaments per unit area (Greenbaum, 1985). Orientations of the lineaments are usually analyzed by rose diagrams. The rose diagram indicates that the most dominant fault direction is N30-40 degree and S210-220 degree (fig.5a, c). The lineament trends are predominantly along NNE-SSW, NNW and SSE. The lineament density is high in the southern and central part of study area (fig. 5b). Lineaments play important role in groundwater recharge in hard rock terrains (Koch and Mather 1997). Lineament-length density (Ld) is the total length of all delineated lineaments divided by the total area under consideration (Greenbaun, 1985):

$$Ld = \sum_{i=1}^{i=n} Li \Big/ A \quad (\mathrm{m}^{-1})$$

where $\sum_{i=1}^{i=n} Li$ = total length of all lineaments (m) and A= area (m^2).

4.3 Slope map of the area

Slope is a measurement of steepness from the ground surface. The slope map was generated from the DEM using Arc GIS 9.3 spatial analysis tool. Most parts of the study area have slope within the range of 39 to 57 degree. Southern part of the area exhibits steeper slope, where as the northern parts are associated with lower slopes. Alluvial region in the northern part shows that lower slope is good for groundwater recharge while hilly region of southern part shows that steeper slope is not good for groundwater recharge (fig. 6). The slope of the area has a large impact on the amount of water infiltration into the ground and amount of water lost as run off.

4.4 Soil map of the area

The climate, physiography and geology characterize soil and play important roles in groundwater recharge and run-off. The water holding capacity of the area depends upon the soil types and their permeability. Basically, the soil in this region is often divided into Clayed loam, Sandy loam, Loamy and Loamy sand. On the basis of soil texture, most of the part is covered by loamy soil (figure 5). The soil with poor water holding capacity like sandy loam is good for groundwater recharge.

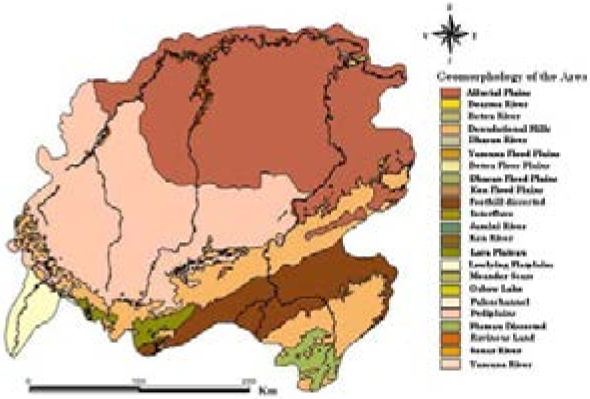

Figure 4: Geomorphology map

Figure 5(a): Lineament map

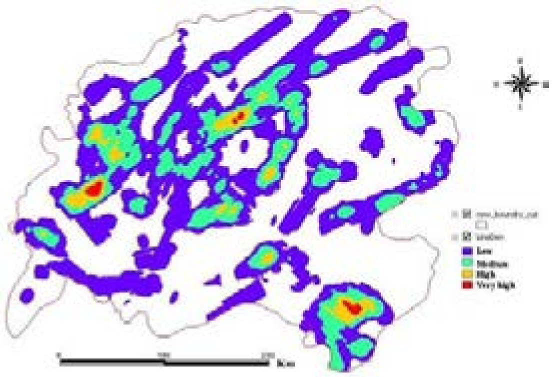

Figure5 (b): Lineament density map

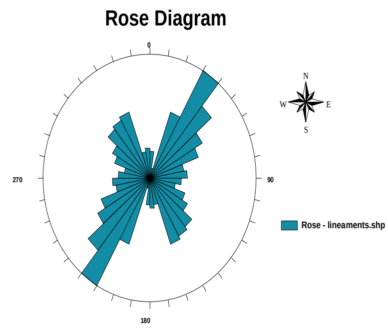

Figure5(c): Rose diagram

4.5 Drainage map of the area

Drainage map of the study area was generated from the vectorization of topographic sheet as well as satellite imagery, representing the network of main streams in the catchments, followed by the tributaries up to the last order. The drainage pattern in the area was dendritic, pinnate type (fig.8). Drainage density is the ratio of the total length of the stream to the area of the drainage basin. The southern part of the basin is associated with very high drainage density. About 40% of the area upstream of the ganagu weir shows medium drainage density. Some parts of the western and south-eastern of the catchment show low drainage density, this is due to high amount of vegetation and permeable nature of the soil (fig.9). Higher the drainage density lower is the infiltration and faster is the movement of the surface flow so less recharge (Pachauri et al. 1998).

4.6 Land use/Land cover map of the area

The land use/land cover map was generated by using unsupervised classification. Landsat ETM+ satellite data of year 2005 and topographic maps were used to prepare the land use map of the study area through image classification procedure. On this basis, the whole area was classified into 10 categories viz. water, dense forest, built up, current fallow/agricultural land, water logged, degraded forest, land with scrub, bare exposed rock, fallow

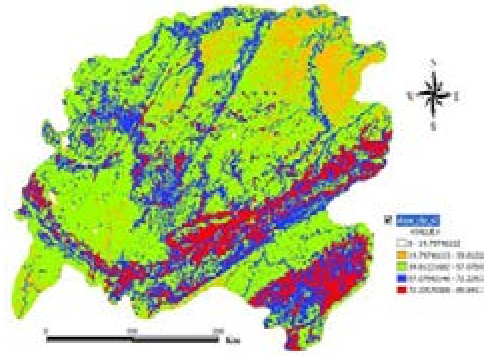

Figure6: Slope map

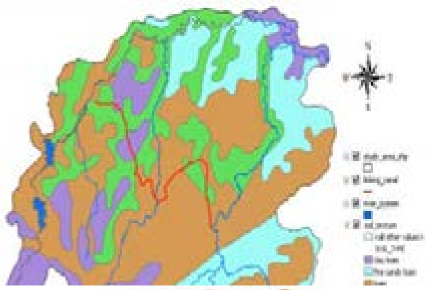

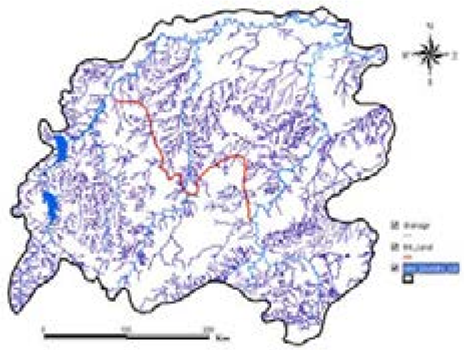

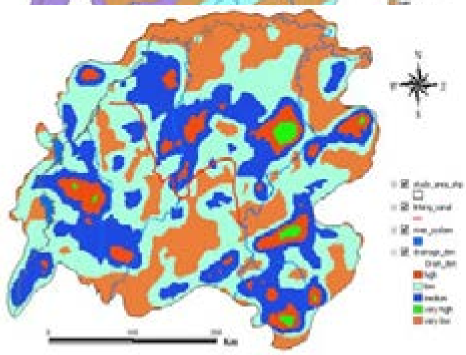

Figure 8: Drainage network map   *Figure 9: Drainage density map*

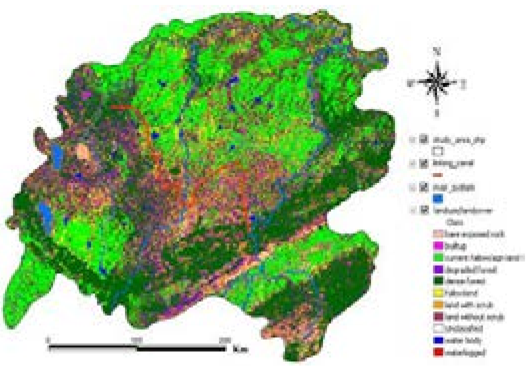

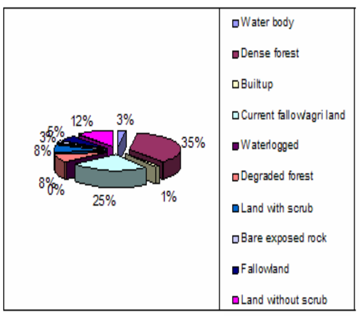

Figure 10: Land use/land cover map of the study area

land, and land without scrub (fig.10). Land use/land cover effect evapotranspiration, surface run-off, and groundwater recharge. Waterlogged area is good for groundwater recharge and fallow land is poor for it (Chowdary V. M., 2008).

4.7 Depth to water level

Ground water level data of 124 observation sites was collected from Central Ground Water Board (CGWB) for the year 1999 to 2004. The observation points originally expressed as geographic coordinates were converted to UTM projection system for interpolation (fig.9). Finally Interpolation of the ground water level was done by using Spline interpolator in Arc View 3.2a.

In the study area, as the precipitation is concentrated mainly in monsoon season, depth to ground water is generally reduced during monsoon and post-monsoon, whereas it gets deepened during pre-monsoon because discharge rates are greater than the recharge rates. Under natural conditions, depth to water-level is related to topography. The ground water depth is maximum in the northern portion of the study area, and minimum in the southern portion of the study area. The magnitude of seasonal fluctuation in water levels in response to monsoon recharge is related to aquifer porosity and storage. After recharge, the rise in water levels may be greater and sustained longer in aquifers with low permeability than in aquifers with high permeability (Sara M. N., 2003). The range of seasonal fluctuation generally varied from region by region of the study area, reflecting the different hydrogeological conditions and spatial variations in recharge rates or storage characteristics of the aquifer.

4.8 GIS modeling

These maps were superimposed on groundwater potential map and identify the area with water scarcity and it shows correlation with the groundwater potential zonation. The area around the rivers, alluvial plain, low slope, low drainage density, with high lineament density is good in groundwater prospects. The area with high slope, high drainage density, and ravenous, low lineaments are poor to very poor in groundwater prospects.

The linking canal will transfer water from Ken river to Betwa river is present in the very poor and poor zone of the GWPZ map so it will benefit enroute command area. This enroute command area covers Chhatarpur, Tikamgarh, Jhansi, Hamirpur district of Bundelkhand and these districts were severally affected by recent drought. So this link will help to solve water scarcity problems of these districts.

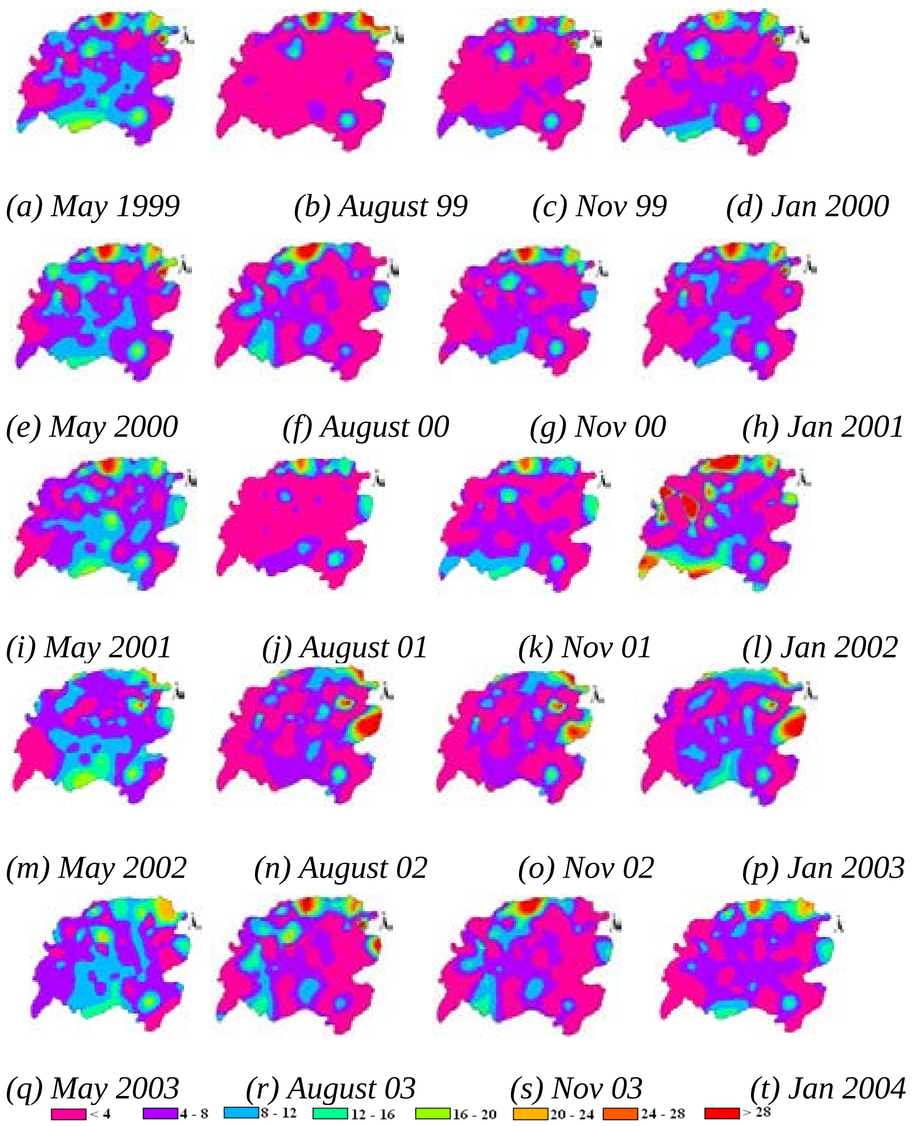

Figure 11: Interpolation maps of groundwater level

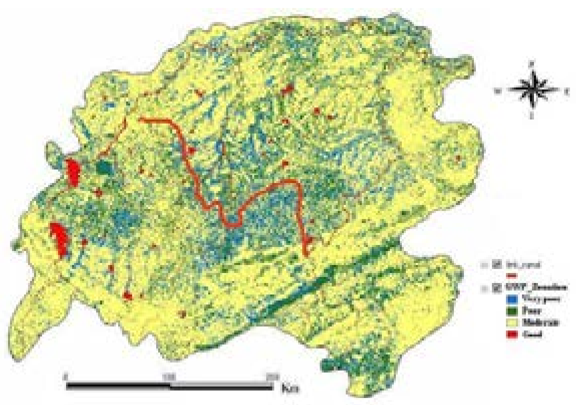

Figure 12: Groundwater potential zonation map of the area

Table1: Thematic map weight, feature and ranking for GWPZ

Theme	**Weight**	**Features**	**Rank**
Geomorphology	5	Flood plain Ravines Pediment Erosional hills Alluvial plain	5 1 2 2 3
Lineament density	4	High Medium Low Very low	4 3 2 1
Slope	3	>72 57-72 39-57 14-39 <14	1 2 3 4 5
Soil Cover	3	Clayed loam Sandy loam Loamy Loamy sand	1 4 2 3
Drainage Density	2	Very High High Medium Low Very Low	1 2 3 4 5
Land use/ land cover	1	Dense forest Land with scrub Agricultural land Degraded forest Land without scrub Fallow land	1 2 3 3 4 4

5. CONCLUSION

In the developing country like India, with weak infrastructure, low accessibility and data scarcity, utilization of remote sensing and GIS is a good tool for water resource management. GIS plays an important role in integrating all the data to generate groundwater potential zonation. This is useful in the study of feasibility of the Ken-Betwa River linking. The GWPZ map of the area shows a good correlation with the groundwater level data. This map will helps in planning strategies for effective management and distribution of water resources. The change in land use/land cover is the major threat to groundwater potential. In ancient time Bundelkhand area had lots of natural water bodies, which were a good source for groundwater recharge but due to population growth they disappeared. The water demand will increase with the increase in population. To solve this problem, river linking is a good solution. But the alternate techniques like rainwater harvesting, infiltration pits, reuse, recycle etc. are much more cost effective than such a huge project like linking river.

REFERENCES

Bhagwat I. P. 2008, Drought and Drinking Water Crisis in Bundelkhand, *Water aid India*, September 2008.
Chowdary V.M., Vinu Chandran R., Neeti N., Bothale R.V., Srivastava Y.K., Ingle P., Ramakrishnan D., Dutta D., Jeyaram A., Sharma J.R. and Singh R., 2008, Assessment of surface and sub-surface waterlogged areas in irrigation command areas of Bihar state using remote sensing and GIS. *Agricultural Water Management*, Volume 95, Issue 7, pp. 754-766.
Greenbaum, D., 1985, Review of remote sensing applications to groundwater exploration in basement and regolith, *Brit Geol Surv Rep* OD 85/8, 36 pp.
Jaiswal, R.K., Mukherjee, S., Krishnamurthy, J., and Saxena, R., 2003, Role of remote sensing and GIS techniques for generation of groundwater prospect zones towards rural development: an approach. *International Journal of Remote Sensing*, 24 (5), 993-1008.
Koch, M. and Mather, P. M., 1997, Lineament mapping for groundwater resource assessment: a comparison of digital Synthetic Aperture Radar (SAR) imagery and stereoscopic Large Format Camera (LFC) photographs in the Red Sea Hills, Sudan. *International Journal of Remote Sensing*, 18, 1465-1482.
Krishnamurthy, J., Mani, A., Jayaraman, V., and Manivel, M., 2000, Groundwater resources development in hard rock terrain: an approach using remote sensing and GIS techniques. *International Journal of Applied Earth Observation and Geoinformation*, 2 (3-4), 204-215.
Mallet, F. R. (1869), "Vindhayans of central provinces", *Memoir Geological Survey of India*, Vol. II, Part. I.
Meijerink AMJ, 1996, Remote sensing applications to hydrology: groundwater. *Hydrological Science Journal* 4:549–561
Murthy, K.S.R., 2000, Groundwater potential in a semi-arid region of Andhra Pradesh: a geographical information system approach. *International Journal of Remote Sensing*, 21, 1867-1884.
National Water Development Agency 2007, Ken-Betwa Link Project Feasibility Report,
Pachauri, A K, Gupta, P V, and Chander, R., 1998, Landslide zoning in a part of the Garwal Himalayas", *Environmental Geology*, Vol. 36, No. (3-4), pp. 325-34
Saaty, T.L. 1994, Highlights and critical points in the theory and application of the analytic hierarchy process, *European Journal of Operational Research*, Vol. 74 pp.426-47.
Sara M. N., 2003, Site assessment and remediation handbook. Lewis publishers.
Thomas B. C., Kuriakose S. L. and Jaydev S. K. 2009, A method for groundwater prospect zonation in data poor areas using remote sensing and GIS: a case study in Kalikavu Panchayath of Malappuram district, Kerala, India; *International Journal of Digital Earth*, Vol. 2, No.2, June 2009, pp. 155-170.

ESTIMATION OF LAND SURFACE WATER COVERAGE (LSWC) WITH OPTICAL VS. MICROWAVES

SHUMON MORI, WATARU TAKEUCHI and HARUO SAWADA
Institute of Industrial Science, The University of Tokyo
morishumon@gmail.com

ABSTRACT

This research focuses on estimation of land surface water coverage by using AMSR-E and MODIS sensors. The main point in this study is to calibrate the two data, NDPI (normalized difference polarization index) and LSWC (land surface water coverage) obtained by AMSR-E and NDWI (normalized difference water index) of MODIS respectively and finally we produced daily land surface water coverage map.

1. INTRODUCTION

In recent years, overpopulation, human activities and global warming are causing hydrological problems such as water shortage, increase of flood disasters. Then water cycle monitoring at different scales, from small catchments to large river basins, is important for drought analysis, crop yield forecasting, irrigation planning, floods and forest fire prediction (Teodosio, 2005).

In the past, many satellite techniques have been proposed to remotely map flooded areas and to monitor hydro-geophysical parameters. The main advantage of satellite remote sensing is the capability of monitoring large areas in temporal-spatial continuous record. Previous satellite techniques for monitoring the water cycle exploit the microwave data advantages. Microwave remote sensing can be used quite effectively to study seasonal inundation and flooding of rivers and swamps because microwave is unrestricted by cloud cover and can provide information about such hydrologic variables as soil wetness, seasonal inundation, vegetation, snow, wetness and its water equivalent and rainfall(Bhaskar, 1991).

In this study we used two sensors: AMSR-E as microwave sensor and MODIS as optical sensor. AMSR-E is a microwave sensor and its spatial resolution is in scale of kilometers, not high resolution, but it can observe the land surface with low cloud interruption (that means high temporal resolution). On the other hand MODIS sensor is an optical infrared sensor and its spatial resolution is in scale of hundreds meters (high spatial resolution) but its observation is frequently interrupted with cloud. In order to investigate the water cycle of the ground, high spatial-temporal resolution is required.

In previous research, Takeuchi (2006) focused on that optical and microwave sensors are in trade off relationship between spatial resolution and cloud interruption, then combined utilization of AMSR-E and MODIS has been conducted to enable us observing the water cycle with high spatial-temporal resolution. Takeuchi found the correspondence of water cycle between AMSR-E and MODIS. The data used were two indices, called NDPI (normalized difference polarization index) and NDWI (normalized difference polarization index) obtained from AMSR-E and MODIS respectively.

The objective of this study is to estimate land surface water coverage by using AMSR-E and MODIS sensors. In this study, the target area is located in Bangladesh, known as severe flood area. The footprint size of AMSR-E is 10 square km and that of MODIS is 2 km. It means that one footprint of AMSR-E includes 25 (5×5) footprints of MODIS. Then we counted the number of inundated footprints within these 25 footprints and calculated the land surface water coverage (LSWC [%]).

Here, AMSR-E gives us the index NDPI and MODIS gives us the LSWC. After getting these two data, NDPI and LSWC, we analyzed the relationship between them. This relationship enables us to estimate physical quantity - LSWC [%] everyday from index NDPI according to the feature of AMSR-E. By exploiting the relationship, finally we produced AMSR-E LSWC map.

2. METHODOLOGY

2.1. Flowchart to produce LSWC distribution map with AMSR-E and MODIS

Figure 1 shows a flowchart to produce land surface water coverage (denoted as LSWC) distribution map by combining AMSR-E and MODIS.

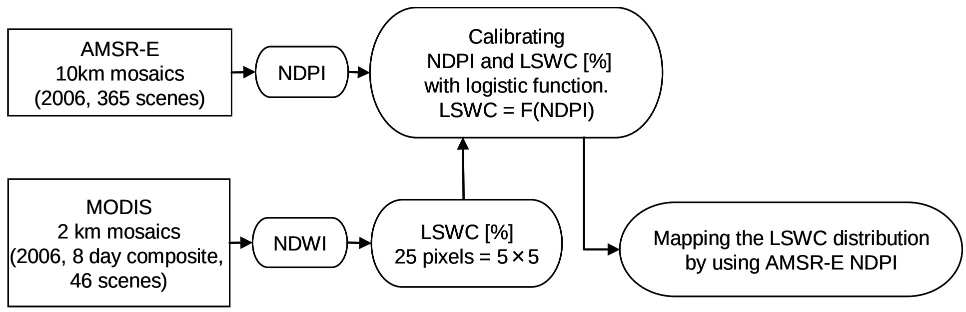

Figure1: Flowchart to produce LSWC distribution map by combining AMSR-E and MODIS

AMSR-E data was obtained from National Snow and Ice Data Center (NSIDC) in United States of America, and a series of preprocessing was carried out including radiance calibration, geometric correction, spatial mosaic and subset. Normalized difference polarization index (NDPI) was computed as shown in Equation (1).

$$NDPI = \frac{T_v - T_h}{T_v + T_h} \quad (1)$$

T_v : 36.5 GHz brightness temperature vertical
T_h : 36.5 GHz brightness temperature horizontal

MODIS data rebuilding was carried out by Linlle-University group (Dr. Louis Gonzalez, personal communication) based on NASA’s 8-day global mosaic composite product (MOD09A1). The idea is to remove clouds by spatio-temporal filtering technique on a footprint-basis processing. Normalized difference water index (NDWI) was computed as shown in Equation (2).

$$NDWI = \frac{VIS - SWIR}{VIS + SWIR} \qquad (2)$$

VIS : Reflectance of visible (630 nm, channel 1)
SWIR : Reflectance of short wave infrared (1620 nm, channel 6)

2.2. Study area

Figure 2 shows an area of interest in this study highlighted by red square, centered at latitude 54-17`59, 95”N, longitude 90-52`0.20”E. The area is 10,000 square kilometers (10x10 footprints) covered by seasonal dynamics of open water, natural wetlands and paddy fields. In this study, above ground vegetation contribution is neglected.

Figure2: Area of interest in this study is highlighted by red square, centered at latitude 54-17`59, 95”N, longitude 90-52`0.20”E and the area is 100 square kilometer known as open water area.

2.3. Setting the inundated footprint threshold

In this study land surface water coverage is strongly dependent on the inundated threshold. To estimate the precise inundated threshold we build the global land coverage histogram by utilizing MODIS NDWI images. After that, we simulated the histogram’s curve behavior with Gaussian function:

$$f(x) = \frac{a}{\sqrt{2\pi c^2}} \exp(-\frac{(x-b)^2}{2c^2}) \qquad (3)$$

The parameter ‘a’ expresses the height of the curve’s peak and ‘b’ expresses the center of curve’s peak and ‘c’ controls the width of peak. In this study we simulated 36 NDWI histograms.

Then we processed 3 steps:

First step is to classify the part of histogram such as vegetation, soil, and mixture of water and soil.

Second step is to confirm the dependence of temporal series of the threshold by verifying the fluctuation of the peaks.

Third step is to classify the distribution of inundated area in order to set the inundated threshold more precisely.

2.4. LSWC (Land Surface Water Coverage)

Figure 3 shows a schematic diagram between AMSR-E and MODIS footprints. One footprint of AMSR-E (10 square km) corresponds to the 5x5 block of MODIS footprints.

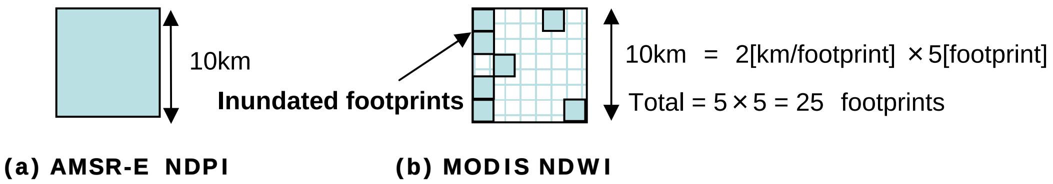

Figure 3: Spatial correspondence between AMSR-E and MODIS.

LSWC between AMSR-E and MODIS was estimated by following the three steps:

1. To select the threshold of MODIS NDWI images to distinguish between inundated and non-inundated footprints aided by histogram curve.

2. To produce the inundated distribution map in 2 km and spatially aggregate the inundated distribution map 2 km into the fractional coverage of land surface water coverage in 10 km (MODIS LSWC).

3. To find out the relationship between AMSR-E NDPI and MODIS LSWC. Logistic function as shown in Equation (4) is expected to fit well between those (Takeuchi, 2006). The coefficients a, b and c are estimated by using the least squares method.

$$LSWC = \frac{a}{1 + b \cdot \exp(-c \cdot NDPI)} \qquad (4)$$

3. RESULTS

3.1. Spatial correspondence between AMSR-E NDPI and MODIS NDWI

Figure 4 shows comparison of MODIS NDWI 2 km, MODIS LSW map 2 km, MODIS LSWC 10 km and AMSR-E NDPI 10 km. Brighter footprints indicate high abundance of inundated area.

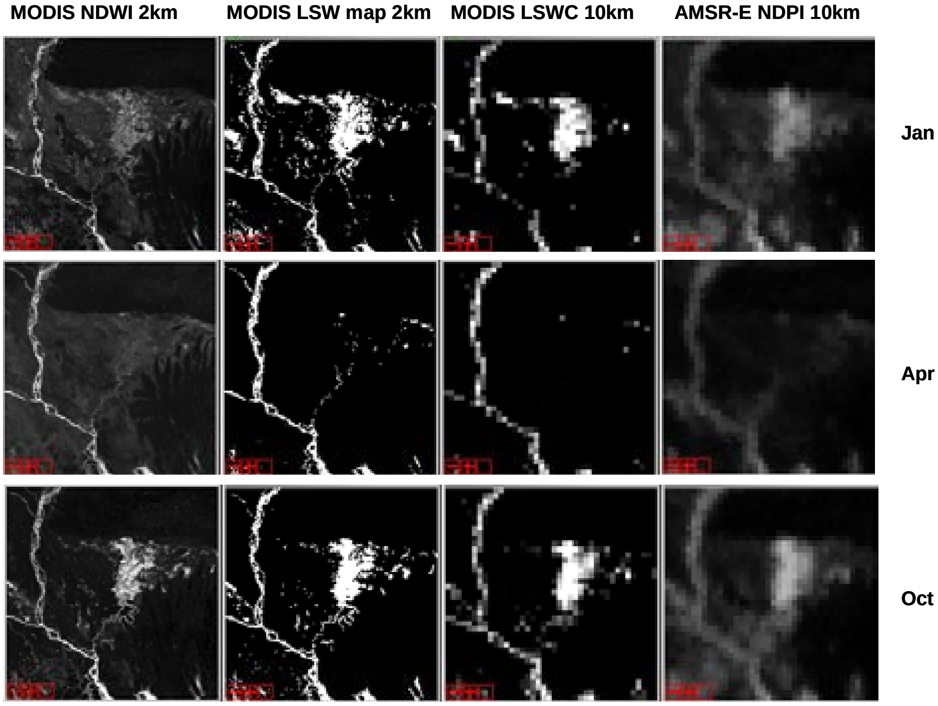

Figure 4: Comparison of MODIS NDWI 2km, MODIS LSW map 2km, MODIS LSWC 10 km and AMSR-E NDPI 10km. Brighter footprints indicate high abundance of inundated area.

3.2. Select the inundated threshold

Figure 5 shows a MODIS NDWI histogram in 2006 characterized by 4 peaks including vegetation (peak1), soil (peak2), mixture of soil and water (peak3), and water and snow (peak4).

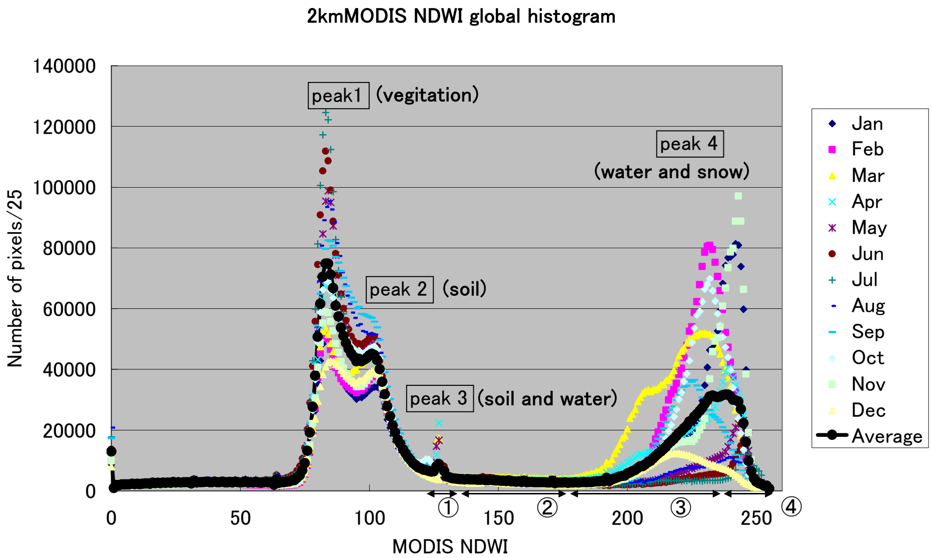

Figure 5 : MODIS NDWI histogram in 2006

In first step, we classified the peak1, 2 and 3 by matching the Gaussian function with them and we demonstrated approximately their land cover type according to NDWI values. Then, the result was that peak1 represents the vegetation area, that peak2 represents the soil area and that peak3 represents the mixture of soil and water area. The results are summarized in Table 1 and in Figure 6.

Table 1: details of 3 peaks

	averaged center of peak	S.D. of peak	S.D. of center
Peak1	83.0	5.2	0.7
Peak2	100.3	7.8	1
Peak3	126.8	3.3	1.5

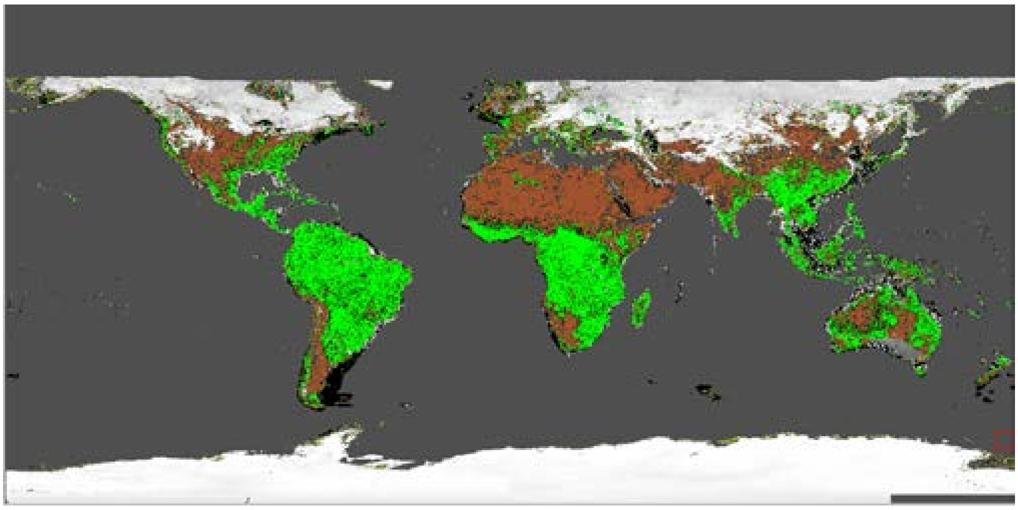

Figure 6: Global NDWI histogram mapping. The green footprints whose range o f [78, 81] shows vegetations, The brown footprints whose range of [92, 108] shows soils and the yellow footprints range of [123, 130].

In second step, we found the slight-fluctuation of the peaks as shown in Table 1 and in Figure 5. Therefore we suggested the independence of the inundated threshold on temporal series.

In third step, we investigated the inundated range, NDWI = [121, 255], to determine the precise inundated threshold by classifying the range to 4 areas, NDWI = [121, 136], [137, 178], [179, 239], [240, 255], as mentioned in the above Figure 5. The results are shown in the figure 7- (b).

Then we comprised the NDWI maps with MODIS visible map in Bangladesh and we determined that inundated threshold=121 represents the inundated areas most precisely as shown in MODIS visible image.

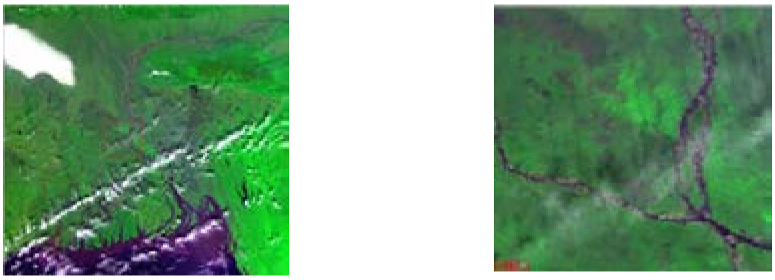

(a) MODIS visible image 20060106 as a reference

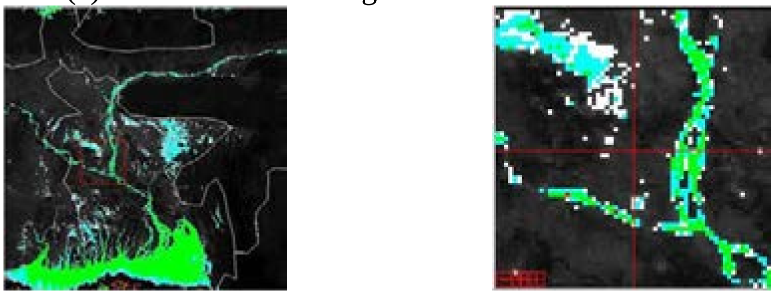

(b) MODIS NDWI image 20060101 (8 day composite) red footprints show range of [240, 255], green footprints show range of [179, 239], cyan footprints show range of [137, 178] and white footprints show range of [121, 136].

Figure 7: Comparison between MODIS visible image and MODIS NDWI image

3.3. Relationship between NDPI and LSWC

Figure 8 shows the scatter plot representing the relationship between AMSR-E NDPI and MODIS NDWI. We averaged the data collected from area mentioned above and after applying least squares method we received the following scatter plot, coefficients and standard deviation:

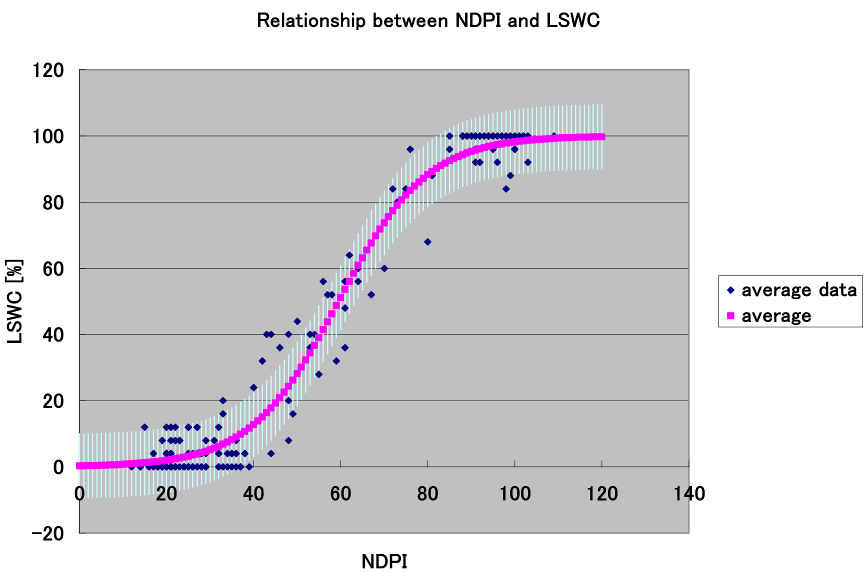

Figure 8 : Scatter plot representing the relation between AMSR-E NDPI and MODIS LSWC

Table 2 : Results of coefficients a, b, c and standard deviation after application of least method

a	100.0
b	353.5
c	0.1
S.D.	9.7

For your attention, the data is quantized to 4%. Then, the minimum standard error is 4 % (because MODIS image has 25 footprints in 10 square km area and then minimum scale of data is 4%).

We can find that the two regression curves are modeled similarly within the standard error 4%. Thus, we can hypothesize that theses regression curves represent precisely the LSWC in independent on temporal series.

3.4. Spatial correspondence between AMER-E NDPI LSWC distribution map and MODIS NDWI LSWC distribution map

Figure 9 shows the spatial correspondence between AMSR-E NDPI LSWC distribution map and MODIS NDWI LSWC distribution map. Brighter footprints indicate high abundance of inundated area. Although there is high correspondence between two maps as shown, we can find also a few difference in some places (indicated by red circle) due to above vegetation covers. We hypothesized that this difference is due to effects of above vegetation covers on microwaves and optical waves. AMSR-E using microwaves can detect the surface water covered by above vegetation as well as covered by cloud although MODIS using optical wavelength can't.

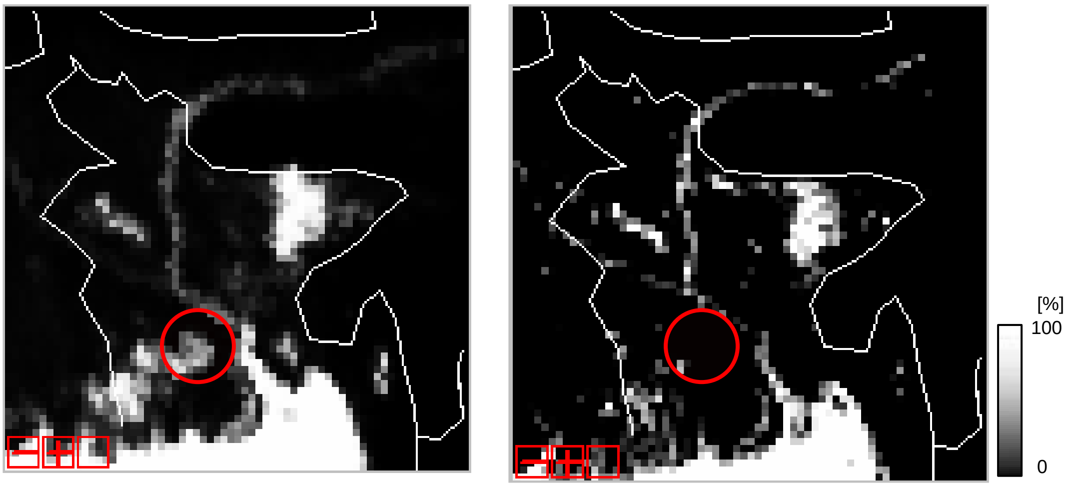

(a) LSWC distribution map of AMSR-E NDPI

(b) LSWC distribution map of MODIS NDWI

Figure 9 : Spatial correspondence of AMSR-E NDPI LSWC distribution map with MODIS NDWI LSWC distribution map

3.5. Land surface water coverage curve and map

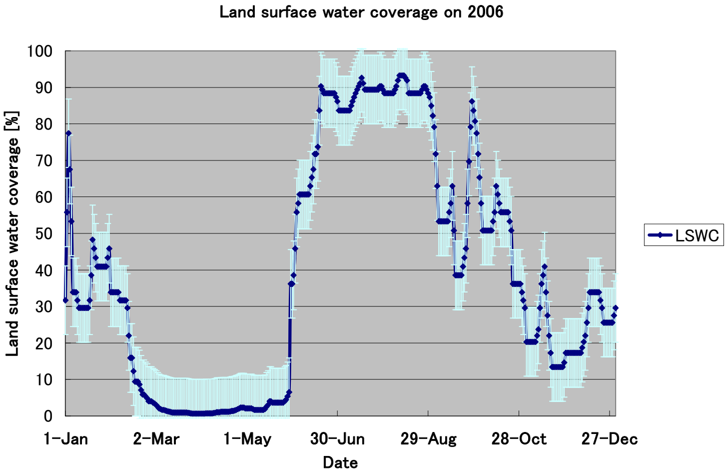

Figure10: Land surface water coverage curve in 2006 at Bangladesh.

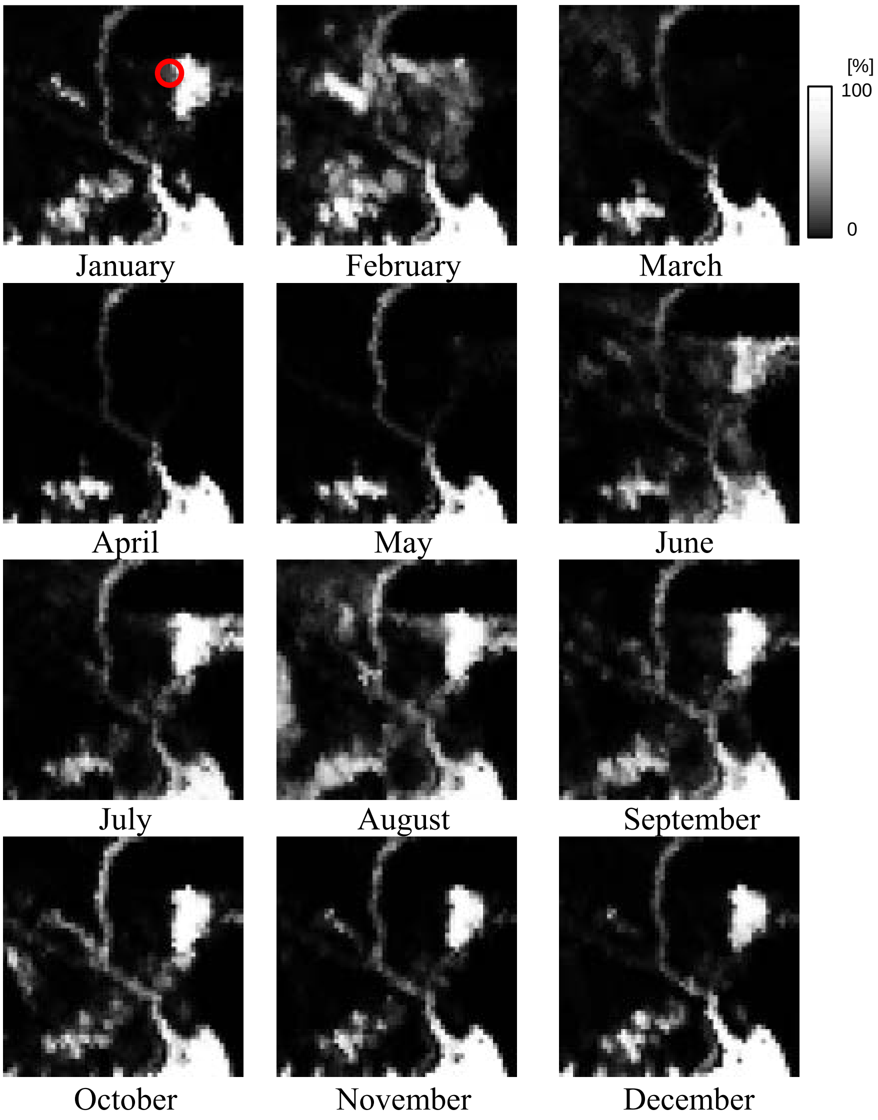

Figure 11: land surface water coverage map at Bangladesh in 2006.

Figure 10 and 11 shows LSWC curve (at location indicated by circle in Figure 11 on January) and maps respectively at Bangladesh monitored by AMSR-E. The brighter footprints indicate high abundance of inundated area in unit of water coverage [%]. Due to AMSR-E's high temporal resolution and non-cloud interruption ability, we can produce LSWC map for everyday.

4. CONCLUSION

In this study we built the NDWI histogram in global scale by MODIS 8-day composite data and we classified the main 3 peaks to assume the water-soil mixture NDWI range. Then, we classified more precisely the water NDWI range. Finally, we succeeded to hypothesize the inundated threshold with comparison of MODIS visible image.

Based on the threshold we processed the sub-footprint analysis in 10,000 square km open water area, and then we modeled the logistic regression curve by using 100 points data of this object area.

By comparing with two days regression curve, we found that their difference distance is closely 4% (the our data is quantized to 4% then the minimum standard error is 4 %) then we arrived to the conclusion that our logistic regression curve represent precisely and independently of temporal-series Land Surface Water Coverage in open water area..

Finally we produced the LSWC map monitored by AMSR-E. In this study we focus on only open water area. Then for the future work we need to investigate influences of above vegetation cover on microwaves and visible infrared waves to improve and apply the logistic regression curve for Amazon or other similar area and we should confirm the availability for application.

REFERENCES

Wataru Takeuchi, Daisuke Komori, Taikan Oki and Yoshifumi Yasuoka, 2006. An integrated approach on rice paddy irrigation pattern monitoring over Asia with MODIS and AMSR-E . American geophysical union fall meeting 2006 (AGU): San francisco, USA, 2006 Dec. 5.

Teodosio Lacava, Vincenzo Cuomo, Elena V.Di Leo, Nicola Pergola, Filomena Romano, Valerio Tramutoli, 2005. Improving soil wetness variations monitoring from passive microwave satellite data: The case of April 2000 Hungary flood, Remote Sensing of Environment 96 (2005) 135 – 148

Suzanne J. Sippel, Stephen K. Hamilton, John M. Melack and Bhaskar J. Choudhury, 1994. Determination of inundation area in the Amazon river flood plain using the SMMR 37 GHz Polarization difference, Remote Sens. Environ, 70-76, 48.

Bhaskar J., Choudhury, 1991. Passive microwave remote sensing contribution

M. Temimi, R. Leconte, F. Brissette, N. Chaouch, 2007. Flood and soil wetness monitoring over the Mckenzie River Basin using AMSR-E 37 GHz brightness temperature

REMOTELY SENSED SOIL MOISTURE CHARACTERIZATION WITH GROUND BASED MEASUREMENTS

HYUNJIN PARK[1], JIYE KANG[1], JONG AHN CHUN[2],
MINHA CHOI[1] and JONGKYU LEE[1]
[1] Department of Civil and Environmental Engineering, Hanyang University
hydro, newjiye, mchoi, leejk@hanyang.ac.kr
[2] U.S. Departement of Agriculture ARS
jongahn.chun@ars.usda.gov

ABSTRACT

Soil moisture is one of the most important key physical parameter in hydrologic processes. During past decade, remote sensing instruments have been widely used to provide mean surface soil moisture at large spatial scale because conventional ground based measurements are not always available and take time and cost. In this study, Soil moisture extracted from Advanced Microwave Scanning Radiometer E (AMSR-E) were compared with ground based measurements and water surface elevation of nearby station in a watershed scale in Korea.
Both soil moisture products from the AMSR-E and ground based stations were also examined whether the data has statistical correlations with measured water surface elevation for a watershed in the central Korea. The tendency between ground based soil moisture and water surface elevation was identified. Two factors were formed natural logarithm function and showed comparatively close correlation.
This type of work may provide an opportunity to examine operational utility of the remotely sensed soil moisture products as an alternative for the ground based measurements to understand hydrological science in Korea.

INTRODUCTION

Soil moisture is an important factor on the hydrological and ecological processes although the amount of water stored as soil moisture constitutes only a small proportion of freshwater on the Earth (Pachepsky. 2003) Since it is directly linked to various hydrological processes including rainfall, infiltration, and runoff in a watershed, it is a very important key parameter of hydrologic phenomena. In addition, soil moisture associated with evapotranspiration plays a great role in connection of the hydrologic cycle. It is generally required to obtain soil moisture data in widespread region and to analyze them to achieve further analyses for the relation between soil moisture data and water surface elevation time series from the watershed. An accurate evaluation of the spatial and temporal variation of soil moisture may be useful for improving the predictive capability of the runoff models. However, Ground based soil moisture is tedious and takes a lot of time to collect data (Hollinger and Isard, 1994; Rombach and Mauser, 1997).

Recently, Satellite instruments are available with advanced passive micro wave remote sensing of soil moisture. Microwave sensors have many advantages including the ability to directly measure soil moisture irrespective of weather conditions or time (Jackson.1995). Advanced Microwave Scanning Radiometer AMSR-E, which is instrument on the NASA EOS Aqua satellite provides global passive microwave measurements (Njoku, 2004).

The objective of this study is to develop the relationship among soil moisture from ground based data, remotely sensed data, and water surface elevation at downstream. The soil moisture from flux tower was continuously collected in the Wangsuk watershed. The relation between soil moisture and water surface elevation was investigated using in-situ and satellite soil moisture data.

1. STUDY AREA

1.1 Wangsuk watershed

The Wangsuk Stream watershed in the central Korea, where the Gwangneung flux tower was installed, was selected for this study. The annual air temperature of the watershed is 12.7 and average annual rainfall is 1381.2mm. Table 1 summarizes the geographic location, area, land use, and SCS type. Town/dryland account for 7.0% of the total watershed area followed by agriculture land (18.8%), forest (68.2%), Grassland (3.0%), Bare region (1.4%), and Waters (1.5%). SCS soil type A and B are predominant in the watershed.

Herbaceous plant, chestnut tree, white oak, pine tree and deciduous tree can be mainly found in the Wangsuk main stream. The watershed study consists of two 25 by 25km grids identified as 1 and 2 (Figure 1).

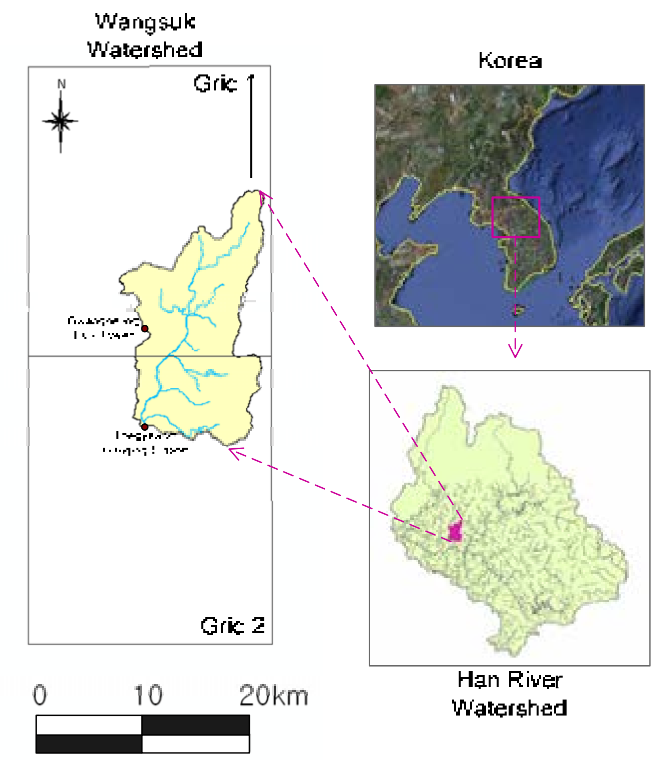

Figure 1: Wangsuk watershed, network sites, Grids

Table 1: Geographic locations, area, land use, and SCS type for the Wangsuk watershed

	Grid 1		**Grid 2**	
Coordinate of the Grid	37°57′14.76″ 127°01′40.08″	37°57′14.76″ 127°17′20.4″	37°42′24.84″ 127°01′40.08″	37°42′24.84″ 127°17′20.4″
	37°42′24.84″ 127°01′40.08	37°42′24.84″ 127°17′20.4″	37°27′37.8″ 127°01′40.08″	37°27′37.8″ 127°17′20.4″
Watershed area (% of grid cell)	$118.44km^2$ (18.8%)		$83.06\ km^2$ (13.2%)	
Land use				
Type	Area (km^2)		% of total area	
Town/Dryland	14.13		7.0	
Agriculture land	37.92		18.8	
Forest	137.52		68.2	
Grassland	6.06		3.0	
Swampy land	-		-	
Bare region	2.90		1.4	
Waters	2.97		1.5	
Soil Type				
SCS Type	Area (km^2)		% of total area	
A	100.71		50.0	
B	90.13		44.7	
C	6.28		3.1	
D	4.38		2.2	

1.2 Gwangneung site

The Gwangneung site which belongs to the Wangsuk watershed is located in the west-central part of the Korean peninsula (37°45′25.37″N, 127°09′11.62″E). As shown Figure 2, the site of flux tower is a typical montane landscape of the country. Annual air temperature is 11.5 , and average annual precipitation is 1,332mm. The slope of the hillside is 10-20°. Whole watershed is characterized by gneiss and schist (Kim et al, 2006).

1.3 Toegyewon gauging station

Toegyewon gauging station (37°38′50 ″N, 127°09′14 ″E) is located at the downstream of the Wangsuk stream. The station was installed at 21.930m of elevation.

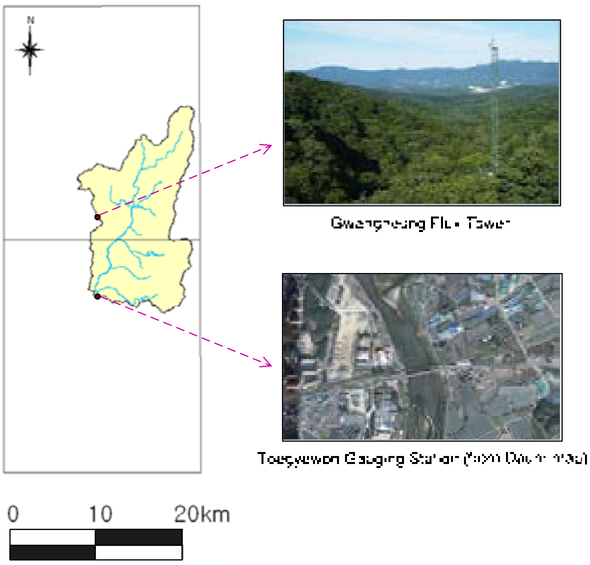

Figure 2: Location of Gwangneung flux tower and Toegyewon gauging station. Upper point is a position of Gwangneung flux tower and lower point is Toegyewon Gauging Station.

2. DATASETS

The study period was January 1, 2005 to December 31, 2006. During the study period, soil moisture data were obtained from Gwangneung flux tower (in-situ data) and satellite. Also, hydrologic data were available from Toegyewon gauging station

2.1 In-Situ Measurements

In-situ soil moisture data are obtained from Gwangneung flux tower which founded by KoFlux Program at Yonsei University (http://koflux.yonsei.ac.kr). The flux tower is continuously monitoring water, carbon and energy fluxes. In the Wangsuk stream, in-situ soil moisture data are obtained at a spot (Gwangneung site). In this study, we considered Gwangneung in-situ soil moisture data as representative values of total area. The Flux tower provides 8 different soil moisture values. The data were recorded at every 30 minute. There are missing periods (January 1 to March 15, 2005 and December 1 to December 31, 2006) due to unexpected malfunction of the instruments.

2.2 Satellite Observations

The satellite data were detected by AMSR-E(Advanced Microwave Scanning Radiometer) which is one of six sensors onboard Aqua satellite and obtained from NASA WIST (The Warehouse Inventory Search Tool, https://wist.echo.nasa.gov/~wist/api/imswelcome/). The AMSR-E sensor is a multi channel microwave image observation radiometer that observes 6~89GHz of microwave region. Generally, the sensor extracts various meteorological data such as rainfall, humidity, temperature of sea surface, and wind as well as physical earth surface data including soil moisture. Soil moisture values that detected by AMSR-E sensor were used for this study.

The Aqua satellite makes an orbit around polar with Sun-synchronous orbit and passes through Korea about 13:30 everyday. It provides daily data of 25 by 25km Grids. We used the processed data which weigh the watershed area.

2.3 Water Surface Elevation Measurements

Hydrologic data in downstream of Wangsuk watershed can be obtained from the Toegyewon gauging station. Thus, the Wangsuk watershed runoff has immediate connection with Toegyewon water surface elevation. Hourly water surface elevation data of the Toegyewon station used in this study were obtained from the Han-River Flood Control Office (http://www.hrfco.co.kr).

3. RESULT AND DISCUSSIONS

3.1 Time Series Analysis

Figure 3 and figure 4 show time series graphs of the water surface elevation, basin-averaged AMSR-E soil moisture and in-situ soil moisture for the study area in 2005 and 2006 respectively. In these figures, some spiking of the water surface elevation was detected. The research concentrated on the rainy seasons (July 1 to September 30). Time series of them in rainy seasons are shown in figure 3 (b), (d), figure 4 (b) and (d).

The comparisons between water surface elevation and basin-averaged AMSR-E soil moisture showed weak correlation. However, the comparisons between water surface elevation and in-situ soil moisture showed relatively strong correlation. As in-situ soil moisture increased, water surface elevation increased (figure 3 (d) and figure 4 (d)). While water surface elevation showed relatively abrupt temporal variations, in-situ soil moisture had somewhat weak temporal variability patterns with little antecedent peaks.

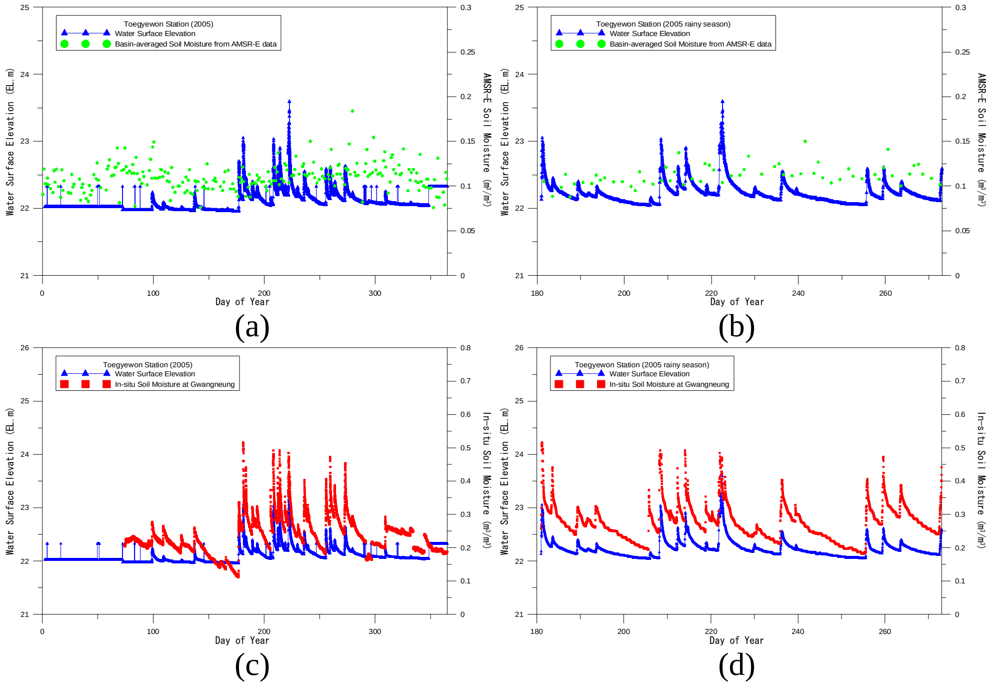

Figure 3: Time series of the Water surface elevation and AMSR-E soil moisture value for (a) 2005, (b) rainy season in 2005and Water surface elevation and the in-situ soil moisture values for (c) 2005, (d) rainy season in 2005.

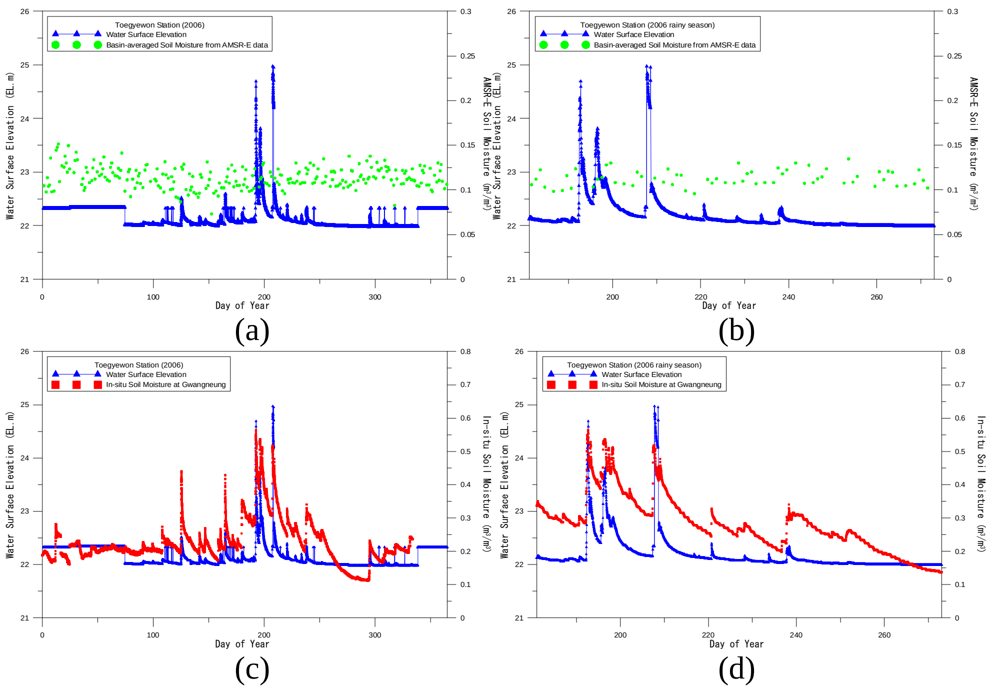

Figure 4: Time series of the Water surface elevation and AMSR-E soil moisture value for (a) 2006, (b) rainy season in 2006and Water surface elevation and the in-situ soil moisture values for (c) 2006, (d) rainy season in 2006.

3.2 Regression Analysis

Generally, runoff increases as soil moisture increases in the watershed. Figure 5 shows the relationship between the ground based soil moisture and the corrected water surface elevation values. As water surface increases, in-situ soil moisture also increases. The relation which assumes the form of natural logarithm function between soil moisture and water surface elevation was identified

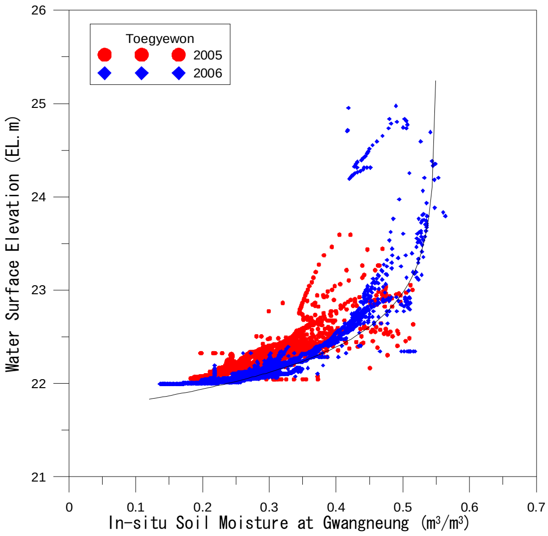

Figure 5: In-situ soil moisture and water surface elevation at the Toegyewon gauging station of the Wangsuk stream.

$$h(t) = 21.7 + 0.532 \ln \frac{0.55}{0.55 - SM(t)}, \quad R^2 = 0.724 \qquad (1)$$

$h(t)$: Water surface elevation (m) at time t
$SM(t)$: In-situ soil moisture (m^3/m^3) at time t

A regression analysis approach was used for rainy season. The result of regression analysis is equation 1 whose coefficient of determination (R^2) is 0.724.

4. CONCLUSION

In this study, we developed the relationship between in-situ soil moisture data and water surface elevation time series from the watershed.

Through the regression analysis the data was well fitted to natural logarithm. It is expected that the correlation between the corrected AMSR-E soil moisture data associated with in-situ soil moisture data and water surface elevation time series should be obtained.

Even if AMSR-E's grid may not provide enough the spatial resolution for the study watershed, the remotely sensed soil moisture data through the Cumulative Distribution Function (CDF) matching technique and Regional Statistics Method (RSM) may be improved to provide a unique relationship with water surface elevation at a watershed scale.

ACKNOWLEDGEMENTS

The data were provided by KoFlux from the projects funded by Ministry of Land, Transport and Maritime Affairs, the Korea Forest Research Institute , and the Korea Science and Engineering Foundation.

REFERENCES

Hollinger,S.E and Isard, S.A, *Soil Moisture Climatology of Illinois*,(1994) Journal of Climate, 7, 822-833

Jackson T.J., Le Vine D.M., Swift C.T., Schmugge T.J., and Schiebe F.R. 1995. *Large area mapping of soil moisture using th ESTAR passive microwave radiometer in Washita '92.* Remote Sens Environ. 53:27-37.

John R. J., 2007. *Remote Sensing of the Environment: An Earth Resource Perspective,* Second Edition, Prentice Hall.

Joon K., Dongho L., Jinkyu H., Sinkyu K., Su-Jin K., Sang-Ki M., Jong-Hwan L., Yowhan S., Jaeseok L., Sanghyun K., Namchil W., Kyongha K., Buyong L., Byong-Lyol L., and Sung K. 2006. *Hydro Korea and CarboKorea: cross-scal studies of ecohydrology and biogeochemistry in a heterogeneous and complex forest catchment of Korea.* The Ecological Society of Japan. 21: 881-889

Scipal K., Scheffler C., and Wagner W. 2005. *Soil moisture-runoff relation at the catchment scale as observed with coarse resolution microwave remote sensing.* Hydrology and Earth System Sciences, 9, 173-183

Minha C., and Jennifer M. J. 2008. *Tempoeal Variability Corrections for Advanced Microwave Scanning Radiometer E (AMSR-E) Surface Soil Moisture: Case Study in Little River Region, Georgia, U.S.* Sensors. 8, 2617-2627.

Pachepsky Y., Radcliffe D.E., and Selim H.M. 2003. *Scaling methods in soil physics.* CRC Press. 119 pp.

Rombach, M. and Mauser, W: *Multi-annual analysis of ERS surface soil moisture measurements of differents land uses*,1997, 3rd ERS Symposium on Space at the service of our Environment, Florence, Italy, 14-21 March, European Space Agency, SP-414, 27-34

ESTIMATION OF SEDIMENTS IN URBAN DRAINAGE AREAS AND RELATION ANALYSIS BETWEEN SEDIMENTS AND INUNDATION RISK USING GIS

[1]Moo-Jung PARK and [2]Hwan-Don JUN
[1]Dept of Civil Engineering, Hanseo University, Korea
mjpark@hanseo.ac.kr
[2]Dept of Civil Engineering, Seoul National University of Technology, Korea
hwandonjun@gmail.com

ABSTRACT

Sediments entering the sewer in urban areas reduce the conveyance in sewer pipes, which increases inundation risk. To estimate sediment yields, individual landuse areas in each sub-basin should be obtained. However, because of the complex nature of an urban area, this is almost impossible to obtain manually. Thus, a methodology to obtain individual landuse areas for each sub-basin has been suggested for estimating sediment yields. Using GIS, an urban area is divided into sub-basins with respect to the sewer layout, with the area of individual landuse estimated for each sub-basin. The sediment yield per unit area for each sub-basin is then calculated. The suggested method was applied to the GunJa basin in Seoul. For a relation analysis between sediments and inundation risk, sub-basins were ordered by the sediment yields per unit area and compared with historical inundation areas. From this analysis, sub-basins with higher order were found to match the historical inundation areas.

1. INTRODUCTION

Recently, rapid changes in the weather, such as flash floods in urban areas, frequently occur due to climate abnormalities over the world. For most urban watersheds, which have a large portion of impervious areas and short travel times, as a result of urbanization, the risk of inundation increases with the occurrence of flash floods or storms. Sewer systems, which play an important role in discharging storm flow to receiving waters, have experienced decreases in their conveyance due to the accumulation of sediments or solids in the sewer pipes. According to the USEPA report (EPA, 2004), the decreased conveyance increases the risk of inundation. However, insufficient attention has been paid to research on evaluating the effects of sediments or solids accumulation in sewer pipes on the increased risk of inundation. Thus, it is important to develop a methodology for evaluating the effect of reducing the risk of inundation in urban areas.

Most previous research associated with sediment yields from the overland surface has been made with regard to environmental characteristics.

However, various sediment sources, as well as the characteristics of sediments or solids, which occur from urban overland surfaces make the development of an efficient methodology for quantifying sediment yields and the evaluation of their effects difficult. One of the earliest examples of research on the subject, by Dalrymple et al. (1975), analyzed the distribution of the solid grain size (or accumulated sediments) collected from the inside of separate or combined sewer pipes with respect to the settlement characteristics. Klemetson et al. (1980) and Ashley et al. (2004) studied the characteristics of solids in combined sewer pipes and a method for their removal. However, their study only dealt with solids in sewer pipes, but not their various sources from overland surfaces. Brinkmann and Graham (2001) suggested a method for the removal of sediments from urban drainage areas, and Toy et al (2002) studied a mechanism and suggested a methodology for predicting soil loss. However, these studies were not suitable for application to soil loss in urban areas. Lee and Park (2006) reported their results of estimating sediment yields from urban overland surfaces and for the sediment loads inside the sewer pipes. In their method; however, they simplified the land use areas in each sub-basin to obtain parameters for the equations used to estimate the sediment yield; therefore, the accuracy of their model may not be high. Thus; in this study, a method for accurately and efficiently estimating sediment yields from various sources has been suggested and a relation analysis performed between sediment yields and the risk of inundation. For application of the method, a GIS is used to obtain the area of individual land use in each sub-basin, as well as data for urban drainage areas, which have complicated structures. An individual land use was categorized and built into the GIS data on the basis of the research of Lee et al. (2005) and Min and Kim (2006). Using the land use data and GIS, the suggested method was then applied to a real watershed in Seoul, Korea. As a result, it is possible to accurately estimate the amount of sediments compared to the field data and identify the potential inundation risk areas.

2. METHOD TO ESTIMATE SEDIMENT YIELDS IN URBAN DRAINAGE AREAS

The model suggested by the USEPA (EPA, 2004) was used to estimate the sediment yields from urban drainage areas, which is a grey-box model and; depending on the sediment sources, the sediment yields from each source can be estimated. The sources were divided into four categories, namely: Litter/Floatables, roadway sanding for snow/ice events, street dust and dirt, and soil erosion. The sediment yields were calculated for each source using relatively simple equations. The annual Litter/Floatables volume can be calculated using the equation suggested by Armitage and Rooseboom (2000), which was developed as an empirical equation relating to South Africa. An estimate of the roadway sanding used for snow/ice events was obtained using Guo’s equation (Guo, 1999). However, only a portion of the sand estimated by Guo’s equation can be consider a nonpoint source, as sand can be collected by road-cleaning vehicles or cleaning laborers after snow-melt. According to Guo (1999), about 30% of the total sand sprayed road surfaces are transported by storm runoff and collected in retention or detention basins. However, this will vary according to the condition and maintenance practice of a given watershed. To estimate the accumulation loading of dust and dirt, Hurber and Dickinson (1998) used three equations. Of these equations, the Michaelis-Menton equation was used in this study. The amount of soil erosion was estimated using the Revised Universal Soil Loss Equation (RUSLE). The details of each equation and their range of parameters are presented in the USEPA report (EPA, 2004)

3. APPLICATION OF GIS TO URBAN DRAINAGE AREAS

3.1 Classification of landuse

To estimate the sediment yields from urban drainage surfaces, it is necessary to divide the land use of urban areas into several classes, namely: high-density and low-density residential areas, schools, commercial areas, industrial areas, parks and roads, as the sources and sediment yields are determined by individual land use. Moreover, in the case of roads, one needs to measure road lengths to estimate the amount of dust/dirt, which can be facilitated using GIS.

3.2 Delineation of subbasins

In water resource engineering, most GIS applications are used for analyzing natural watersheds, especially their delineation. However, since urban drainage areas have a different structure from natural watersheds, i.e., stormflow runs through a man-made sewer system, sub-basins should be delineated along with the sewer pipeline. In addition, elevation of urban surfaces is another factor that has to be defined.

3.3 Data acquisition and Geoprocessing

To classify an individual land use, the CAD drawings established by the Sewer Division of Seoul Metropolitan Government were employed. In these drawings, individual land uses are stored in different “Layers”, so that each layer can be separately converted into a “shape file” format of ESRI. For the delineation of sub-basins, drawings of the sewer layout and the elevation data were used, the detail process of which is shown in Figure 1. Individual land use areas within each sub-basin were estimated by applying GeoProcessing functions, including “Intersect” and “Erase”.

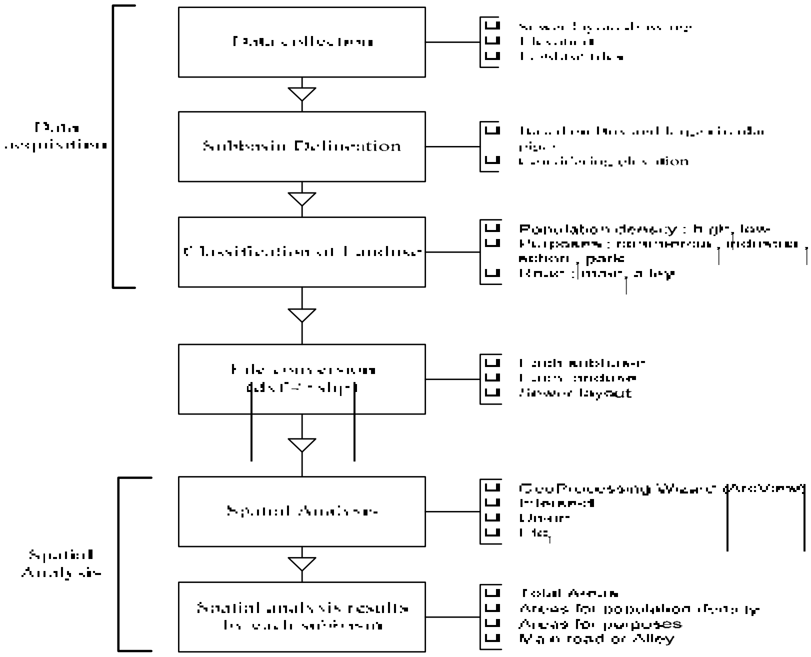

Figure 1: The process of data acquisition

These areas are the parameters used in the four equations to estimate the sediment yields. Estimating the “alley” areas for each sub-basin requires additional steps; whereas, the other land use areas for each sub-basin can be easily estimated, as is shown in Figure 2.

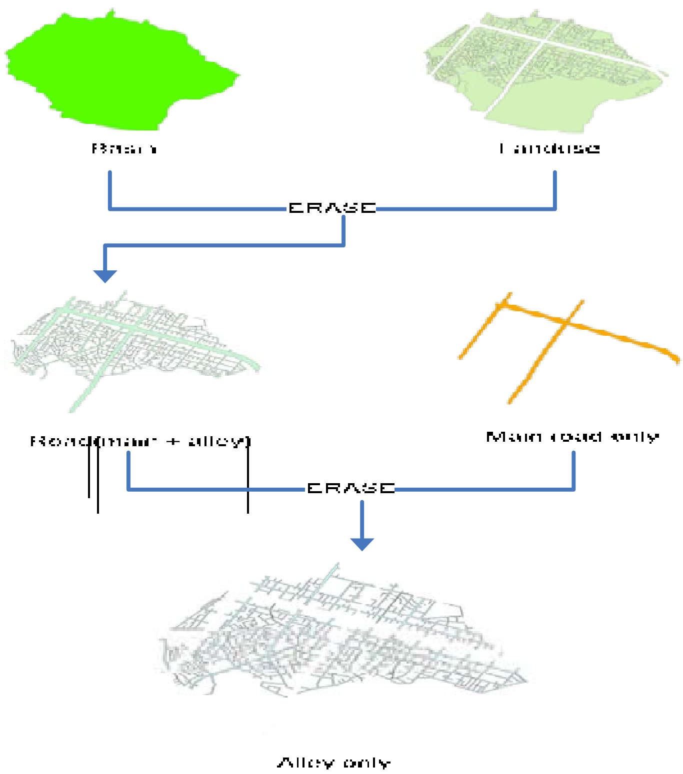

Figure 2: The process to obtain an “Alley”

4. REAL URBAN DRAINAGE AREA FOR APPLICATION OF THE SUGGESTED METHOD

4.1 The target area and individual landuse shape files

The urban drainage area, Gun Ja basin, where the suggested method was applied, is located in Seoul and has had some inundation events during the past decade. Its area of the GunJa basin is 193.62ha and divided into 26 subbasins. Of these, sub-basin “0” is part of the JoongRang stream, where no sediment is produced; therefore, it was not considered when estimating the sediment yields. The overall shapes of the area and files when converted from the CAD drawings from the application of the geoprocessing are shown in Figure 3.

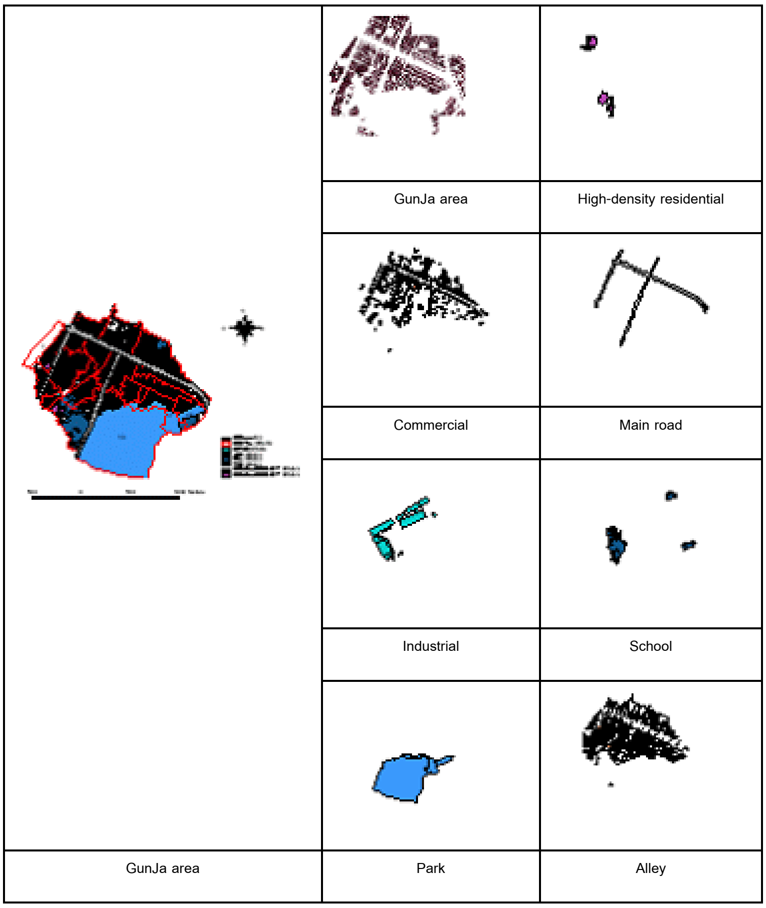

Figure 3: The shape files for individual land uses converted from CAD drawings

4.2 Determination of the parameters

To apply the four equations mentioned earlier, certain parameters have to be determined. Since the determination of these parameters is very difficult, requiring vast field surveys, which are a time- and cost-consuming task, the parameters were reasonably determined using the parameters suggested in the respective researches for the estimation of litter/floatables, roadway sanding for snow/ice events, and street dust and dirt. In the case of soil loss, the parameters used in a disaster analysis for a project to build an urban park in Seoul were substituted (Seoul Metropolitan Government, 2003). The determined parameters are shown in Table 1.

Table 1: Parameters for individual land use

Land use		Low-Density Residential	High-Density Residential	Commercial	Industrial	School	Park	Main Road	Alley
Litter/ Floatables	f_{sci}	1	1	1	1	1	1	1	1
	V_i (m^3/ha/yr)	0.02	0.02	0.03	0.03	0.03	0.01	N/A	N/A
	B_i (m^3/ha/yr)	0.01	0.02	1.2	0.8	0.02	0.5	N/A	N/A
Sanding	w_s(kg/m^2)	N/A	N/A	N/A	N/A	N/A	N/A	10	5
Dust/Dirt	DDLIM(g)	N/A	N/A	N/A	N/A	N/A	N/A	250	250
	DDFACT (day)	N/A	N/A	N/A	N/A	N/A	N/A	0.9	0.9
	T(day)	N/A	N/A	N/A	N/A	N/A	N/A	10	10
USLE	R (10^7/ha． mm/hr)	526	526	526	526	526	526	N/A	N/A
	K (tonnes/ha/R)	0.13	0.13	0.13	0.13	0.13	0.13	N/A	N/A
	LS	0.231	0.231	0.231	0.231	0.231	0.231	N/A	N/A
	C	0.1	0.1	0.1	0.1	0.1	0.1	N/A	N/A
	P	0.14	0.14	0.14	0.14	0.14	0.14	N/A	N/A

It should be noted that the amount of sediment from the urban drainage surface calculated using the stated equations, with the suggested parameters shown in Table 1, will be greater than the amount of sediment entering sewer pipes. In the case of litter/floatables, one of the parameters in the equation was the retrieving rate represented by a street cleaning factor for each land use (f_{sci}). However, for roadway sanding and dust/dirt, there is no retrieving rate in the equations. This means that all the solids calculated using the suggested equations will be considered as sediments entering sewer pipes. As mentioned earlier, for roadway sanding, Guo (Guo, 1999) reported that only 30% of sand sprayed road surfaces would enter the sewer pipes in the case of urban drainage areas. However, this may vary according to the condition of the urban drainage surface and maintenance practice, i.e. how many times cleaning vehicles are operated and the amount of snow. Therefore, a field survey is required to determine how much sand is retrieved by cleaning vehicles or other methods. In the case of the target area located in Seoul, the retrieving rate of roadway sand was less than 5% (Kim et al., 2004); therefore, the retrieving rates of roadway sanding and the wash-off of dust/dirt were assumed to be 0% and 0 g/curb-meter. To verify this assumption, the field survey data will be presented later.

4.3 Results of sediment yield estimation

Using the suggested method, the sediment yields from four sources were estimated, as shown in Table 2.

Table 2 : Results of estimated sediment yields by sub-basin

Sub-basin (ID)	*Litter/* Floatables(kg)	*Sand (kg)*	*DD (kg)*	*USLE (kg)*	*Area (m^2)*	*Sediment yield (kg)*	*S.Y. per unit area(kg/yr/m^2)*	*Order of S.Y. per unit area*
1	57.87	13,772.10	178.67	221.14	29,927.21	14,229.78	0.48	13
2	77.12	63,810.50	186.38	65.00	25,165.75	64,139.01	2.55	3
3	57.59	0.00	170.45	56.93	18,582.61	284.97	0.02	24
4	392.57	58,993.10	290.30	1638.22	151,969.89	61,314.19	0.40	14
5	141.21	0.00	359.66	467.82	62,903.62	968.70	0.02	23
6	472.42	110,500.10	924.60	578.41	124,918.75	112,475.54	0.90	11
7	175.88	90,557.10	230.41	195.09	42,119.43	91,158.48	2.16	4
8	0.00	51,724.80	17.98	0.00	5,172.48	51,742.78	10.00	1
9	259.59	74,698.30	310.78	330.92	56,580.07	75,599.59	1.34	10
10	271.89	118,874.30	390.32	285.46	60,858.94	119,821.97	1.97	6
11	181.81	57,683.00	199.40	196.00	36,578.89	58,260.21	1.59	8
12	140.60	84,571.90	263.87	202.98	41,534.09	85,179.34	2.05	5
13	669.98	201,412.10	782.99	944.37	151,810.93	203,809.44	1.34	9
14	0.74	256,298.60	88.08	0.52	25,670.12	256,387.94	9.99	2
15	246.99	0.00	198.92	812.14	64,921.36	1,258.05	0.02	20
16	116.29	0.00	392.92	455.85	63,431.44	965.06	0.02	25
17	457.82	0.00	258.91	1258.96	95,104.31	1,975.69	0.02	19
18	33.95	0.00	53.17	67.88	9,797.48	155.00	0.02	22
19	3,813.44	206,563.20	347.01	8935.07	545,278.35	219,658.71	0.40	15
20	124.35	0.00	264.80	347.77	42,225.10	736.91	0.02	21
21	385.49	228.00	217.89	412.87	52,082.64	1,244.26	0.02	18
22	238.40	137,716.80	481.77	437.65	77,640.44	138,874.62	1.79	7
23	430.60	62,111.70	371.88	554.38	77,044.94	63,468.56	0.82	12
24	98.04	14,112.80	206.36	297.45	48,833.61	14,714.66	0.30	16
25	199.05	0.00	285.76	177.92	29,814.31	662.72	0.02	17
Total	9,061.17	1,603,683.20	7,473.30	18,975.82	1,939,966.76	1,639,193.49	-	-

The total sediment yield was 1,639 ton/year, and that of roadway sanding was 1,603 ton/year, which were the dominant sediment sources, accounting for about 97% of the total sediment yields, which implies that for urban drainage areas, roadway sanding during the snow season is critical for reducing sediment yields. This result was compared with the data obtained from a field survey. The field survey was based on the dredging and road cleaning records of the local governments of Gwang Jin-gu and Seoung Dong-gu, Seoul, which are maintained for a three year period. The annual averages of each item were calculated, and are shown in Table 3.

Table 3 : Comparison between the estimated and surveyed sediment yields

Item	*Annual average (kg)*	*Remarks*
Roadway cleaning	70,230	By cleaning vehicles and labors
Dredging (sewer pipes)	1,290,600	Wet specific weight 1,800kg/m^3
Dredging (retention basins)	67,140	Wet specific weight 1,800kg/m^3
Total	1,427,970	-
Total sediment yields estimated	1,639,193	13.0% greater than the field survey

From a comparison, the estimated data were found to be 13% greater than those from the field survey. Taking into account the uncertainty in the determination of the parameters and assumptions, the sediment yields estimated can be considered reasonable estimations, with the suggested method using GIS adjudged to be applicable. However, further applications of the suggested method will be required to verify its applicability.

4.4 Inundation risk analysis

The sediment yields per sub-basin were estimated, and order the sub-basins according to the sediment yield per unit area. This was used to verify the relationship between the amount of sediments and the risk of inundation. Basically, sub-basins with a high ranking order according to the sediment yield per unit area were assumed to be vulnerable to inundation, as the conveyance of the sewer pipes may be reduced by the accumulation of sediments or solids. In the basin, the highest and second highest sub-basins were “8” and “14”, respectively, but contained main roads; thus, sub-basin “2” was the highest that contained sewer pipes. For this reason, sub-basins “2”, “3”, “4”, “5” and “6” were selected as expected inundation regions. The inundation records for 1998 were collected, and are displayed for those sub-basins. As shown in Figure 4, the expected and historical inundation regions matched. The same region had another inundation event in 2001. Interestingly, over the last decade, heavy snow events were recorded during 1998, 2001 and 2004. Two inundation events occurred during the rainy seasons in 1998 and 2001. Thus, a high risk of inundation may result from much sediment due to roadway sanding. Of course, it is obvious that many factors contribute to increase the risk of inundation, but according to our analysis, sediment yields also contributed to the increased risk of inundation.

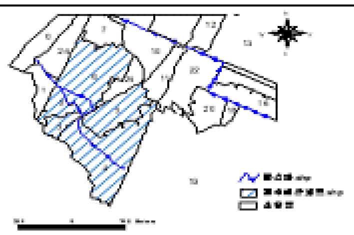

Expected inundation risk areas (subbasin 2,3,4,5, and 6)

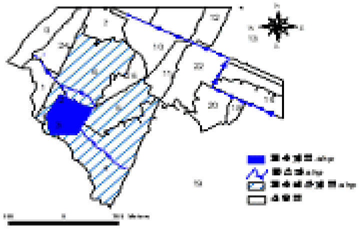

Comparison between historical inundation area (Filled in blue)

Figure 4: The expected and historical inundation risk areas

5. CONCLUSIONS

Due to the mixture of individual land uses in urban drainage areas, it is very difficult to estimate individual land use areas within each sub-basin, which is one of the basic parameters for estimating sediment yields, but using GIS, these can be easily and accurately estimated. To anticipate high inundation risk regions, the results of the sediment yield estimation were employed, and many sediment yields were found to increase the risk of inundation. It is obvious that further applications and comparisons will be required to confirm this conclusion, but the suggested method will be useful when performing additional research.

6. ACKNOWLEDGEMENTS

This study was supported by the 2003 Core Construction Technology Development Project (03-SANHAKYOUN-C01-01) through the Urban Flood Disaster Management Research Center in KICTTEP of MOCT Korea.

REFERENCES

Armitage, N. and Rooseboom, A. (2000). *The Removal of Urban Litter from Stormwater Conduits and Streams: The Quantities Involved and Catchment Litter Management Options*. Water South Africa, 26(2), 181.

Ashley, R. M., Bertrand-Krajewski, J. L., Hvitved-Jacobsen, T., and Verbanck, M. (2004), *Solid in Sewers*, IWA Pulishing.

Brinkmann, R. and Graham, T. (2001), *Urban Sediment Removal*. KLUWER ACADEMIC PUBLISHERS.

Dalrymple, R. J. Hodd, S. L., and Morin, D.C. (1975), *Physical and Settling Characteristics of Particulates in Storm and Sanitary Wastewaters*. Program Element No. 1BB034, U.S. Environmental Protection Agency, Cincinnati.

Guo, J. C-Y. (1999) *Sand Recovery for Highway Drainage Designs*. J. Irrig. & Drainag. Eng. 125(6).

Huber, W.C. and Dickinson, R.E. (1988) *Storm Water Management Model User's Manual, Version4*, EPA/600/3-88/001a; NTIS PB88-236641/AS, U.S. Environmental Protection Agency, Athens. GA.

Kim, J.H., Lee, J.S., Park, M.J., and Lee, S.Y. (2004), Technologies for operating and maintenance for urban sewer systems, project report, the Urban Flood Disaster Management Research Center.
Klemetson, S. L. Keefer, T. N., and. Simons, R.K. (1980), *Movement and Effects of combined Sewer Overflow Sediments in Receiving Waters*. Grant No. R806111, U.S. Environmental Protection Agency, Cincinnati.
Lee, J.I., Kang, Y.O., and Jeoung, M.Y (2005), *A research for establishing and applying landuse data of Seoul metropolitan*, Research report, Seoul Development Institute.
Lee, J.S. and Park. M.J. (2006), Estimation of Solid Sediments Load by Sewer and land Surface for Maintenance of Combined Sewer System, Journal of Korea Water Resources Association, Vol. 39, No. 6, pp 533-544.
Min, S.J. and Kim, G.H (2006), A Study on Utilizing 1:1,000 Digital Topographic Data for Urban Landuse Classification, Journal of Korean Society of Civil Engineers, Vol. 26, No. 1D, pp 149-156.
Park, J.H., Lee, K.S., and Lee, S.N. (2004), Runoff of an Small Urban Area Using DEM Accuracy Analysis, Journal of the Korean Association of Geographic Information Studies, Vol. 7, No. 1, pp 28-38.
Seoul Metropolitan Government (2003), *Disaster Analysis for a project to build an urban park in Seoul*, report.
Toy, T. J., Foster, G. R., and Renard, K. G. (2002), *Soil Errosion: Processes, Prediction, Measurement, and Control*, John Wiley and Son, Inc.
US EPA (2004) *Sewer Sediment and Control -A Management Practices Reference Guide-*. EPA/600/R-04-059, U.S. Environmental Protection Agency, Cincinnati.